VOLUME 29 / NUMBER 1
JANUARY 8, 1991
ACC. NOS. N91-10001 TO N91-10838

# STAR

AN ABSTRACT JOURNAL

# Scientific and Technical Aerospace Reports

PRODUCED BY THE
SCIENTIFIC AND TECHNICAL
INFORMATION
DIVISION

NASA

NATIONAL AERONAUTICS AND SPACE ADMINISTRATION

***Scientific and Technical Aerospace Reports* (*STAR*)** is an abstract journal that provides comprehensive coverage of worldwide aerospace-related reports. It is a major product of the International Aerospace Database managed by the NASA Scientific and Technical Information (STI) Program. The coverage includes reports on aeronautics, space, and supporting disciplines. *STAR* lists current, publicly available reports entered into the NASA STI Database during the 2-week period preceding publication. An explanation of items that appear in each citation is given on the last page of each volume.

NASA sponsors a companion journal, *International Aerospace Abstracts* (*IAA*), that lists abstracts of the open literature on aerospace subjects available worldwide. *IAA* is available through the American Institute of Aeronautics and Astronautics.

Entries found in *STAR* and *IAA* are available through NASA's online service, RECON, as the International Aerospace Database and through DIALOG as the Aerospace Database.

Information on aerospace and related subjects is gathered by the NASA STI Program through national and international agreements and exchanges and is made available to the NASA community as well as to the public in many forms through various outlets. The section on NASA STI Program Products and Services contains additional information.

**US ISSN 0036-8741**

*Volume 29 Number 1 / January 8, 1991*

# TABLE OF CONTENTS

## AERONAUTICS For related information see also *Astronautics.*

**01 AERONAUTICS (GENERAL)** .................... 1

**02 AERODYNAMICS** .................... 1
Includes aerodynamics of bodies, combinations, wings, rotors, and control surfaces; and internal flow in ducts and turbomachinery. For related information see also *34 Fluid Mechanics and Heat Transfer.*

**03 AIR TRANSPORTATION AND SAFETY** .................... 5
Includes passenger and cargo air transport operations; and aircraft accidents. For related information see also *16 Space Transportation* and *85 Urban Technology and Transportation.*

**04 AIRCRAFT COMMUNICATIONS AND NAVIGATION** .................... 6
Includes digital and voice communication with aircraft; air navigation systems (satellite and ground based); and air traffic control. For related information see also *17 Space Communications, Spacecraft Communications, Command and Tracking* and *32 Communications and Radar.*

**05 AIRCRAFT DESIGN, TESTING AND PERFORMANCE** .................... 7
Includes aircraft simulation technology. For related information see also *18 Spacecraft Design, Testing and Performance* and *39 Structural Mechanics.* For land transportation vehicles see *85 Urban Technology and Transportation.*

**06 AIRCRAFT INSTRUMENTATION** .................... 10
Includes cockpit and cabin display devices; and flight instruments. For related information see also *19 Space craft Instrumentation* and *35 Instrumentation and Photography.*

**07 AIRCRAFT PROPULSION AND POWER** .................... 10
Includes prime propulsion systems and systems components, e.g., gas turbine engines and compressors; and onboard auxiliary power plants for aircraft. For related information see also *20 Spacecraft Propulsion and Power, 28 Propellants and Fuels,* and *44 Energy Production and Conversion.*

**08 AIRCRAFT STABILITY AND CONTROL** .................... 13
Includes aircraft handling qualities; piloting; flight controls; and autopilots. For related information see also *05 Aircraft Design, Testing and Performance.*

**09 RESEARCH AND SUPPORT FACILITIES (AIR)** .................... 13
Includes airports, hangars and runways; aircraft repair and overhaul facilities; wind tunnels; shock tubes; and aircraft engine test stands. For related information see also *14 Ground Support Systems and Facilities (Space).*

## ASTRONAUTICS For related information see also *Aeronautics.*

**12 ASTRONAUTICS (GENERAL)** .................... 14
For extraterrestrial exploration see *91 Lunar and Planetary Exploration.*

**13 ASTRODYNAMICS** .................... 15
Includes powered and free-flight trajectories; and orbital and launching dynamics.

**14 GROUND SUPPORT SYSTEMS AND FACILITIES (SPACE)** .................... 15
Includes launch complexes, research and production facilities; ground support equipment, e.g., mobile transporters; and simulators. For related information see also *09 Research and Support Facilities (Air).*

**15 LAUNCH VEHICLES AND SPACE VEHICLES** .................... 16
Includes boosters; operating problems of launch/space vehicle systems; and reusable vehicles. For related information see also *20 Spacecraft Propulsion and Power.*

**16 SPACE TRANSPORTATION** .................... 16
Includes passenger and cargo space transportation, e.g., shuttle operations; and space rescue techniques. For related information see also *03 Air Transportation and Safety* and *18 Spacecraft Design, Testing and Performance.* For space suits see *54 Man/System Technology and Life Support.*

**17 SPACE COMMUNICATIONS, SPACECRAFT COMMUNICATIONS, COMMAND AND TRACKING** ... 16
Includes telemetry; space communications networks; astronavigation and guidance; and radio blackout. For related information see also *04 Aircraft Communications and Navigation* and *32 Communications and Radar.*

**N.A.—no abstracts were assigned to this category for this issue.**

**18 SPACECRAFT DESIGN, TESTING AND PERFORMANCE** ........ 17
Includes satellites; space platforms; space stations; spacecraft systems and components such as thermal and environmental controls; and attitude controls. For life support systems see *54 Man/System Technology and Life Support.* For related information see also *05 Aircraft Design, Testing and Performance, 39 Structural Mechanics,* and *16 Space Transportation.*

**19 SPACECRAFT INSTRUMENTATION** ........ 18
For related information see also *06 Aircraft Instrumentation* and *35 Instrumentation and Photography.*

**20 SPACECRAFT PROPULSION AND POWER** ........ 19
Includes main propulsion systems and components, e.g., rocket engines; and spacecraft auxiliary power sources. For related information see also *07 Aircraft Propulsion and Power, 28 Propellants and Fuels, 44 Energy Production and Conversion,* and *15 Launch Vehicles and Space Vehicles.*

## CHEMISTRY AND MATERIALS

**23 CHEMISTRY AND MATERIALS (GENERAL)** ........ 20

**24 COMPOSITE MATERIALS** ........ 21
Includes physical, chemical, and mechanical properties of laminates and other composite materials. For ceramic materials see *27 Nonmetallic Materials.*

**25 INORGANIC AND PHYSICAL CHEMISTRY** ........ 24
Includes chemical analysis, e.g., chromatography; combustion theory; electrochemistry; and photochemistry. For related information see also *77 Thermodynamics and Statistical Physics.*

**26 METALLIC MATERIALS** ........ 25
Includes physical, chemical, and mechanical properties of metals, e.g., corrosion; and metallurgy.

**27 NONMETALLIC MATERIALS** ........ 28
Includes physical, chemical, and mechanical properties of plastics, elastomers, lubricants, polymers, textiles, adhesives, and ceramic materials. For composite materials see *24 Composite Materials.*

**28 PROPELLANTS AND FUELS** ........ 31
Includes rocket propellants, igniters and oxidizers; their storage and handling procedures; and aircraft fuels. For related information see also *07 Aircraft Propulsion and Power, 20 Spacecraft Propulsion and Power,* and *44 Energy Production and Conversion.*

**29 MATERIALS PROCESSING** ........ 32
Includes space-based development of products and processes for commercial application. For biological materials see *55 Space Biology.*

## ENGINEERING For related information see also *Physics.*

**31 ENGINEERING (GENERAL)** ........ 32
Includes vacuum technology; control engineering; display engineering; cryogenics; and fire prevention.

**32 COMMUNICATIONS AND RADAR** ........ 33
Includes radar; land and global communications; communications theory; and optical communications. For related information see also *04 Aircraft Communications and Navigation* and *17 Space Communications, Spacecraft Communications, Command and Tracking.* For search and rescue see *03 Air Transportation and Safety,* and *16 Space Transportation.*

**33 ELECTRONICS AND ELECTRICAL ENGINEERING** ........ 36
Includes test equipment and maintainability; components, e.g., tunnel diodes and transistors; microminiaturization; and integrated circuitry. For related information see also *60 Computer Operations and Hardware* and *76 Solid-State Physics.*

**34 FLUID MECHANICS AND HEAT TRANSFER** ........ 39
Includes boundary layers; hydrodynamics; fluidics; mass transfer and ablation cooling. For related information see also *02 Aerodynamics* and *77 Thermodynamics and Statistical Physics.*

**35 INSTRUMENTATION AND PHOTOGRAPHY** ........ 44
Includes remote sensors; measuring instruments and gauges; detectors; cameras and photographic supplies; and holography. For aerial photography see *43 Earth Resources and Remote Sensing.* For related information see also *06 Aircraft Instrumentation* and *19 Spacecraft Instrumentation.*

**36 LASERS AND MASERS** ........ 46
Includes parametric amplifiers. For related information see also *76 Solid-State Physics.*

**37 MECHANICAL ENGINEERING** .......... **48**
Includes auxiliary systems (nonpower); machine elements and processes; and mechanical equipment.

**38 QUALITY ASSURANCE AND RELIABILITY** .......... **49**
Includes product sampling procedures and techniques; and quality control.

**39 STRUCTURAL MECHANICS** .......... **50**
Includes structural element design and weight analysis; fatigue; and thermal stress. For applications see *05 Aircraft Design, Testing and Performance* and *18 Spacecraft Design, Testing and Performance.*

## GEOSCIENCES For related information see also *Space Sciences.*

**42 GEOSCIENCES (GENERAL)** .......... **57**

**43 EARTH RESOURCES AND REMOTE SENSING** .......... **63**
Includes remote sensing of earth resources by aircraft and spacecraft; photogrammetry; and aerial photography. For instrumentation see *35 Instrumentation and Photography.*

**44 ENERGY PRODUCTION AND CONVERSION** .......... **63**
Includes specific energy conversion systems, e.g., fuel cells; global sources of energy; geophysical conversion; and windpower. For related information see also *07 Aircraft Propulsion and Power, 20 Spacecraft Propulsion and Power,* and *28 Propellants and Fuels.*

**45 ENVIRONMENT POLLUTION** .......... **65**
Includes atmospheric, noise, thermal, and water pollution.

**46 GEOPHYSICS** .......... **68**
Includes aeronomy; upper and lower atmosphere studies; ionospheric and magnetospheric physics; and geomagnetism. For space radiation see *93 Space Radiation.*

**47 METEOROLOGY AND CLIMATOLOGY** .......... **74**
Includes weather forecasting and modification.

**48 OCEANOGRAPHY** .......... **95**
Includes biological, dynamic, and physical oceanography; and marine resources. For related information see also *43 Earth Resources and Remote Sensing.*

## LIFE SCIENCES

**51 LIFE SCIENCES (GENERAL)** .......... **95**

**52 AEROSPACE MEDICINE** .......... **98**
Includes physiological factors; biological effects of radiation; and effects of weightlessness on man and animals.

**53 BEHAVIORAL SCIENCES** .......... **103**
Includes psychological factors; individual and group behavior; crew training and evaluation; and psychiatric research.

**54 MAN/SYSTEM TECHNOLOGY AND LIFE SUPPORT** .......... **103**
Includes human engineering; biotechnology; and space suits and protective clothing. For related information see also *16 Space Transportation.*

**55 SPACE BIOLOGY** .......... **N.A.**
Includes exobiology; planetary biology; and extraterrestrial life.

## MATHEMATICAL AND COMPUTER SCIENCES

**59 MATHEMATICAL AND COMPUTER SCIENCES (GENERAL)** .......... **103**

**60 COMPUTER OPERATIONS AND HARDWARE** .......... **104**
Includes hardware for computer graphics, firmware, and data processing. For components see *33 Electronics and Electrical Engineering.*

**61 COMPUTER PROGRAMMING AND SOFTWARE** .......... **104**
Includes computer programs, routines, algorithms, and specific applications, e.g., CAD/CAM.

**62 COMPUTER SYSTEMS** .......... **111**
Includes computer networks and special application computer systems.

**63 CYBERNETICS** ........ **112**
Includes feedback and control theory, artificial intelligence, robotics and expert systems. For related information see also *54 Man/System Technology and Life Support.*

**64 NUMERICAL ANALYSIS** ........ **112**
Includes iteration, difference equations, and numerical approximation.

**65 STATISTICS AND PROBABILITY** ........ **116**
Includes data sampling and smoothing; Monte Carlo method; and stochastic processes.

**66 SYSTEMS ANALYSIS** ........ **117**
Includes mathematical modeling; network analysis; and operations research.

**67 THEORETICAL MATHEMATICS** ........ **117**
Includes topology and number theory.

## PHYSICS

For related information see also *Engineering.*

**70 PHYSICS (GENERAL)** ........ **117**
For precision time and time interval (PTTI) see *35 Instrumentation and Photography;* for geophysics, astrophysics or solar physics see *46 Geophysics, 90 Astrophysics,* or *92 Solar Physics.*

**71 ACOUSTICS** ........ **118**
Includes sound generation, transmission, and attenuation. For noise pollution see *45 Environment Pollution.*

**72 ATOMIC AND MOLECULAR PHYSICS** ........ **119**
Includes atomic structure, electron properties, and molecular spectra.

**73 NUCLEAR AND HIGH-ENERGY PHYSICS** ........ **120**
Includes elementary and nuclear particles; and reactor theory. For space radiation see *93 Space Radiation.*

**74 OPTICS** ........ **121**
Includes light phenomena and optical devices. For lasers see *36 Lasers and Masers.*

**75 PLASMA PHYSICS** ........ **123**
Includes magnetohydrodynamics and plasma fusion. For ionospheric plasmas see *46 Geophysics.* For space plasmas see *90 Astrophysics.*

**76 SOLID-STATE PHYSICS** ........ **127**
Includes superconductivity. For related information see also *33 Electronics and Electrical Engineering* and *36 Lasers and Masers.*

**77 THERMODYNAMICS AND STATISTICAL PHYSICS** ........ **133**
Includes quantum mechanics; theoretical physics; and Bose and Fermi statistics. For related information see also *25 Inorganic and Physical Chemistry* and *34 Fluid Mechanics and Heat Transfer.*

## SOCIAL SCIENCES

**80 SOCIAL SCIENCES (GENERAL)** ........ **N.A.**
Includes educational matters.

**81 ADMINISTRATION AND MANAGEMENT** ........ **134**
Includes management planning and research.

**82 DOCUMENTATION AND INFORMATION SCIENCE** ........ **134**
Includes information management; information storage and retrieval technology; technical writing; graphic arts; and micrography. For computer documentation see *61 Computer Programming and Software.*

**83 ECONOMICS AND COST ANALYSIS** ........ **N.A.**
Includes cost effectiveness studies.

**84 LAW, POLITICAL SCIENCE AND SPACE POLICY** ........ **N.A.**
Includes NASA appropriation hearings; aviation law; space law and policy; international law; international cooperation; and patent policy.

**85 URBAN TECHNOLOGY AND TRANSPORTATION** ........ **136**
Includes applications of space technology to urban problems; technology transfer; technology assessment; and surface and mass transportation. For related information see *03 Air Transportation and Safety, 16 Space Transportation,* and *44 Energy Production and Conversion.*

## SPACE SCIENCES For related information see also *Geosciences.*

**88 SPACE SCIENCES (GENERAL)** .................... **N.A.**

**89 ASTRONOMY** .................... **136**
Includes radio, gamma-ray, and infrared astronomy; and astrometry.

**90 ASTROPHYSICS** .................... **137**
Includes cosmology; celestial mechanics; space plasmas; and interstellar and interplanetary gases and dust. For related information see also *75 Plasma Physics.*

**91 LUNAR AND PLANETARY EXPLORATION** .................... **139**
Includes planetology; and manned and unmanned flights. For spacecraft design or space stations see *18 Spacecraft Design, Testing and Performance.*

**92 SOLAR PHYSICS** .................... **140**
Includes solar activity, solar flares, solar radiation and sunspots. For related information see *93 Space Radiation.*

**93 SPACE RADIATION** .................... **142**
Includes cosmic radiation; and inner and outer earth's radiation belts. For biological effects of radiation see *52 Aerospace Medicine.* For theory see *73 Nuclear and High-Energy Physics.*

## GENERAL

Includes aeronautical, astronautical, and space science related histories, biographies, and pertinent reports too broad for categorization; histories or broad overviews of NASA programs.

**99 GENERAL** .................... **N.A.**

**SUBJECT INDEX** .................... **I-1**

**PERSONAL AUTHOR INDEX** .................... **I-55**

**CORPORATE SOURCE INDEX** .................... **I-63**

**CONTRACT NUMBER INDEX** .................... **I-73**

**REPORT/ACCESSION NUMBER INDEX** .................... **I-75**

**APPENDIX** .................... **A-1**

*VOLUME 29 NUMBER 1 / JANUARY 8, 1991*

# Scientific and Technical Aerospace Reports

*A Semimonthly Publication of the National Aeronautics and Space Administration*

## 01 AERONAUTICS (GENERAL)

**N91-10001#** Office of the Under Secretary of Defense (Acquisitions), Washington, DC.
**DOD RESPONSIBILITIES ON FEDERAL AVIATION AND NATIONAL AIRSPACE SYSTEM MATTERS**
R. Nakamura 22 Jun. 1989 9 p
(PB90-218827; DOD-D-5030.19) Avail: NTIS HC/MF A02
CSCL 01B

The directive reissues Department of Defense (DoD) Directive 5030.19 and supersedes DoD Directive 5030.17. It updates DoD policy and procedures to address peacetime, wartime, and emergency relationships between DoD, DoT, FAA, and other government agencies. The DoD organizational structure is described for interface with the DoT, FAA, and other agencies on air traffic control and airspace matters, NAS matters, joint system acquisitions, and oversight of airlift service provided to the DoD by civil air carriers. DoD policy and planning guidance is provided for comprehensive DoD airspace planning and the relationships between the DoD, DoT, FAA, other government agencies, state governments, and civil communities. Author

**N91-10002*** National Aeronautics and Space Administration, Washington, DC.
**AERONAUTICAL ENGINEERING: A CONTINUING BIBLIOGRAPHY WITH INDEXES (SUPPLEMENT 256)**
Sep. 1990 129 p
(NASA-SP-7037(256); NAS 1.21:7037(256)) Avail: NTIS HC A07; NTIS standing order as PB90-914100, $11.50 domestic, $23.00 foreign CSCL 01B

This bibliography lists 426 reports, articles, and other documents introduced into the NASA scientific and technical information system in August 1990. Subject coverage includes: design, construction and testing of aircraft and aircraft engines; aircraft components, equipment and systems; ground support systems; and theoretical and applied aspects of aerodynamics and general fluid dynamics. Author

## 02 AERODYNAMICS

Includes aerodynamics of bodies, combinations, wings, rotors, and control surfaces; and internal flow in ducts and turbomachinery.

For related information see also *34 Fluid Mechanics and Heat Transfer.*

**N91-10003** National Aerospace Lab., Tokyo (Japan).
**CHARACTERISTICS OF PIPING INTERFERENCE ELIMINATION UNIT USED IN THE HIGH-SPEED WIND TUNNEL TEST OF ASUKA SEVEN PERCENT SEMI-BORN PROTOTYPE [ASUKA NANA PASENTO HANSETSU MOKEI NO KOUSOKU FUUDOU SHIKEN NI MOCHIITAHAIKAN KANSHOU JOKYO SOUCHI NO TOKUSEI NI TSUITE]**
Nobuyuki Hosoe, Toshio Karasawa, Keisuke Asai, Syouji Suenaga, Yo Koike, Hirokazu Suzuki, Masayoshi Nakamura, and Susumu Mitsubori Jun. 1988 17 p In JAPANESE
(NAL-TM-588; ISSN-0452-2982; JTN-90-80015) Avail: NTIS HC/MF A03

In the high-speed aerodynamic test using a seven percent semiborne model for the low-noise STOL test aircraft, two TPS (Turbine Powered Simulators) were mounted for use in order to simulate the drive of an actual aircraft. In order to suppress the influence of the piping for supplying compressed air to the TPS measurement of air power by a balance of an external mount type (six percent balance), a unit for eliminating the influence of the piping was manufactured by way of trial. Factors which influence the piping measurement of air power are as follows: effect of air pressure in the piping, influence by the twisting and warping of the piping as a result of a change in the stance of the model, influence by the division of air power between the balance and the piping due rigidity of the piping itself, influence of thermal elongation and contraction of the piping, influence of the flow of compressed air in the piping. To minimize these influences, use was made of a combination of Zimbal bellow, high-pressure rubber hose, and apherical joint was made for eliminating the influence of the piping on an experimental basis which was checked for effect by conducting a wind-tunnel test with and without introduction of air. NASDA

**N91-10004#** Arnold Engineering Development Center, Arnold Air Force Station, TN.
**USER'S GUIDE TO CUNIFLOW Final Report, 1 Oct. 1981 - 30 Sep. 1988**
James T. Curtis Apr. 1989 118 p Prepared in cooperation with Calspan Field Services, Inc., Arnold AFS, TN
(AD-A207606; AEDC-TR-88-31) Avail: NTIS HC/MF A06
CSCL 01/2

CUNIFLOW is a fast, mature code for calculating the hypersonic flow of an inviscid reacting gas over an axisymmetric or planar body. The thermochemical model allows for the finite-rate chemical relaxation of an arbitrary mixture of perfect gases and the coupling of dissociation with nonequilibrium vibrational relaxation. Options for calculating the effects of radiant energy loss, of nonuniform free-stream conditions, and of boundary-layer displacement are available. A particular advantage of the code, in addition to its speed, is that it can often be made to complete a calculation for near-equilibrium situations where other reacting flow codes encounter difficulties. The thermophysical models and the computational methods embodied in the code are summarized and instructions for inputting a problem and interpreting the output are provided. The computational time for a standard configuration is plotted as a function of centerline velocity for various values of the binary scaling parameter. Author

**N91-10005#** Ballistic Research Labs., Aberdeen Proving Ground, MD.
**PREDICTION AND COMPARISON WITH MEASUREMENTS OF THE AERODYNAMIC CHARACTERISTICS OF FLARE-STABILIZED XM910 PROTOTYPES**
James E. Danberg, Asher Sigal, and Ilmars Celmins May 1989 12 p Prepared in cooperation with Technion-Israel Inst. of Tech., Haifa
(DA Proj. 1L1-62618-AH-80)
(AD-A208099; BRL-MR-3752) Avail: NTIS HC/MF A03 CSCL 01/1

A systematic study of a number of flare-stabilized projectile geometries has been undertaken at the U.S. Army Ballistic Research Laboratory (BRL). Ten projectile configurations having identical forebodies and a variety of flares were tested in the BRL Aerodynamics Ballistic Range and the results compared to numerical computations based on two design codes and a Parabolized Navier-Stokes (PNS) code. The design codes, in general, gave good results. The PNS code complemented these results by providing more details on the development of the aerodynamic forces. The results show the drag and stability trade-offs involved for the different configurations. This information can be used to tailor the flare geometry to meet future mission requirements. Author

**N91-10006** Georgia Inst. of Tech., Atlanta.
**APPLICATION OF A STATE-SPACE WAKE MODEL TO ELASTIC BLADE FLAPPING IN HOVER Ph.D. Thesis**
Ay Su 1989 145 p
Avail: Univ. Microfilms Order No. DA9014871

A finite-state inflow model is developed that models the three-dimensional rotor inflow in hover, axial flight, or forward flight. The basis of the model is an acceleration potential with a skewed cylindrical wake. The scope and objectives of the present research revolve around the development of this theoretical basis into a useful research and design tool for hover and axial flight. First, we establish the harmonic and radial convergence characteristics of the model. One-bladed and four-bladed rotors are used in this analysis. Second, this model is coupled with elastic-blade flap equations in hover and also in axial flight in order to determine its effect on aerodynamic damping. Third, the role of periodic coefficients in the dynamic response is investigated. A multi-blade coordinate transformation technique is used to transform the flap equations from the rotating to the nonrotating system. Similarly, the induced flow can be written in either the rotating or the nonrotating system. The effect of periodic coefficients is dependent upon which set of blade equations is coupled with which set of inflow equations. Fourth, we related the generalized forces in the inflow equations to the generalized forces already being used for structural response by constructing intermediate transformation matrices. Results obtained from these tasks show that the present model converges with 3 shape functions per harmonic and has high computational efficiency as compared to unsteady vortex-filament models. More importantly, results indicate that unsteady inflow is an important physical phenomenon that changes the qualitative nature of rotor dynamics in hover and in axial flight. Dissert. Abstr.

**N91-10007*#** National Aeronautics and Space Administration. Ames Research Center, Moffett Field, CA.
**TRANSONIC FLOW ANALYSIS FOR ROTORS. PART 3: THREE-DIMENSIONAL, QUASI-STEADY, EULER CALCULATION**
I-Chung Chang Jun. 1990 23 p
(NASA-TP-2375; A-86374-Pt-3; NAS 1.60:2375) Avail: NTIS HC/MF A03 CSCL 01A

A new method is presented for calculating the quasi-steady transonic flow over a lifting or non-lifting rotor blade in both hover and forward flight by using Euler equations. The approach is to solve Euler equations in a rotor-fixed frame of reference using a finite volume method. A computer program was developed and was then verified by comparison with wind-tunnel data. In all cases considered, good agreement was found with published experimental data. Author

**N91-10008#** Los Alamos National Lab., NM.
**OPTIMUM HYPERSONIC AIRFOIL WITH POWER LAW SHOCK WAVES**
B. A. Wagner 1990 10 p Presented at the 1st International Hypersonic Waverider Symposium, College Park, MD, Oct. 1990
(Contract W-7405-eng-36)
(DE90-014903; LA-UR-90-2437; CONF-9010154-1) Avail: NTIS HC/MF A03

The flow field over a class of 2-D lifting surfaces is examined from the viewpoint of inviscid, hypersonic small disturbance theory (HSDT). It is well known that a flow field in which the shock shape S(x) is similar to the body shape F(x) is only possible for F(x) = x sup k and the freestream Mach number M sub infinity = infinity. This self-similar flow has been studied for several decades as it represents one of the few existing exact solutions of the equations of HSDT. Detailed discussions are found for example in papers by Cole, Mirels, Chernyi and Gersten and Nicolai but they are limited to convex body shapes, that is, k less than or = 1. The only study of concave body shapes was attempted by Sullivan where only special cases were considered. The method used here shows that similarity also exists for concave shapes and a complete solution of the flow field for any k greater than 2/3 is given. The effect of varying k on C sub L sup 3/2 C sub D is then determined and an optimum shape is found. Furthermore, a wider class of lifting surfaces is constructed using the streamlines of the basic flow field and analysed with respect to the effect on C sub L sup 3/2 C sub D. DOE

**N91-10009*#** Institute for Computer Applications in Science and Engineering, Hampton, VA.
**BOUNDARY-LAYER RECEPTIVITY DUE TO A WALL SUCTION AND CONTROL OF TOLLMIEN-SCHLICHTING WAVES Final Report**
R. J. Bodonyi and P. W. Duck (Manchester Univ., England ) Sep. 1990 34 p Submitted for publication
(Contract NAS1-18605)
(NASA-CR-182103; NAS 1.26:182103; ICASE-90-62) Avail: NTIS HC/MF A03 CSCL 01A

A numerical study of the generation of Tollmien-Schlichting (T-S) waves due to the interaction between a small free-stream disturbance and a small localized suction slot on an otherwise flat surface was carried out using finite difference methods. The nonlinear steady flow is of the viscous-inviscid interactive type while the unsteady disturbed flow is assumed to be governed by the Navier-Stokes equations linearized about this flow. Numerical solutions illustrate the growth or decay of T-S waves generated by the interaction between the free-stream disturbance and the suction slot, depending on the value of the scaled Strouhal number. An important result of this receptivity problem is the numerical determination of the amplitude of the T-S waves and the demonstration of the possible active control of the growth of T-S waves. Author

**N91-10010*#** Institute for Computer Applications in Science and Engineering, Hampton, VA.
**TURBULENT FLOW CALCULATIONS USING UNSTRUCTURED AND ADAPTIVE MESHES Final Report**
Dimitri J. Mavriplis Sep. 1990 32 p Submitted for publication
(Contract NAS1-18605)
(NASA-CR-182102; NAS 1.26:182102; ICASE-90-61) Avail: NTIS HC/MF A03 CSCL 01A

A method of efficiently computing turbulent compressible flow over complex two dimensional configurations is presented. The method makes use of fully unstructured meshes throughout the entire flow-field, thus enabling the treatment of arbitrarily complex geometries and the use of adaptive meshing techniques throughout both viscous and inviscid regions of flow-field. Mesh generation is based on a locally mapped Delaunay technique in order to generate unstructured meshes with highly-stretched elements in the viscous regions. The flow equations are discretized using a finite element Navier-Stokes solver, and rapid convergence to steady-state is achieved using an unstructured multigrid algorithm. Turbulence modeling is performed using an inexpensive algebraic model, implemented for use on unstructured and adaptive meshes. Compressible turbulent flow solutions about multiple-element airfoil geometries are computed and compared with experimental data. Author

**N91-10011#** National Aerospace Lab., Tokyo (Japan). Aerodynamics Div.
**NUMERICAL SIMULATION OF HYPERSONIC FLOW AROUND A SPACE PLANE. PART 3: ANALYSIS OF AEROTHERMODYNAMIC HEATING**

Yukimitsu Yamamoto, Haruhiko Arakawa, and Ryuji Yoshida (Mitsubishi Heavy-Industries Ltd., Tokyo, Japan ) Aug. 1989 30 p
(NAL-TR-1027T; ISSN-0389-4010) Avail: NTIS HC/MF A03

The evaluation of hypersonic aerothermodynamic heating along the wing leading edge of the space plane is very important for preliminary aerothermal structural design, because severe local peak heating is caused there by recompression or shock impingement at low angles of attack. In the present numerical simulation, this local peak heating has been analyzed for the three space plane configurations proposed by the National Aerospace Laboratory (NAL). The proposed models have different wing leading edge sweep angles, and effects of the sweep angles on local peak heating were investigated in detail. In addition, two of the proposed configurations have tip fin controllers, and their heating characteristics were also investigated. As the numerical approach, a flux split upwind TVD scheme was adopted by using thin layer Navier-Stokes equations in a finite volume formulation. An implicit approximately factored ADI method has been used as the solution algorithm. Numerical computations were carried out at M(sub infinity) = 7.0 and Reynolds number of 4.4 x 10(exp 6) at angles of attack alpha = 0, 10, and 20 deg. Numerical results are compared with experimental heat transfer measurements by the infrared system developed in the hypersonic wind tunnel (HWT) at NAL. Author

**N91-10012#** National Aerospace Lab., Tokyo (Japan). Aerodynamics Div.
**COMPARISON BETWEEN THE NULL-COLLISION AND TIME COUNTER DIRECT-SIMULATION MONTE CARLO METHODS: LEADING-EDGE FLOW**
Katsuhisa Koura Feb. 1989 13 p
(NAL-TR-1016T; ISSN-0389-4010) Avail: NTIS HC/MF A03

A quantitative comparison between the null-collision (NC) and time-counter (TC) direct-simulation Monte Carlo methods is made in the leading-edge flow over a sharp flat plate for hard sphere molecules. The convergence of the Monte Carlo results due to the decrease in the time step and cell size and due to the increase in the number of simulation molecules is ascertained; the convergent NC and TC results are in good agreement. It is found that the NC method is stronger to the small number of simulation molecules than the TC method because of the accurate NC evaluation of the molecular collision number; the lower limit of the number of simulation molecules for the NC method is less than one third of that for the TC method. The computation time for the NC method is 10 to 15 percent larger than that for the TC method for the same number of simulation molecules (larger than the lower limit). The present NC and TC results are compared with the previous TC results and a considerable discrepancy is revealed. A possible source of the discrepancy is the insufficient number of simulation molecules (less than the lower limit) or convergence in the previous TC results. Author

**N91-10013*#** National Aeronautics and Space Administration. Ames Research Center, Moffett Field, CA.
**WAKE COUPLING TO FULL POTENTIAL ROTOR ANALYSIS CODE**
Francisco J. Torres, I-Chung Chang, and Byung K. Oh (Boeing Computer Services Co., Philadelphia, PA.) Aug. 1990 23 p
(NASA-TM-102805; A-90117; NAS 1.15:102805) Avail: NTIS HC/MF A03 CSCL 01A

The wake information from a helicopter forward flight code is coupled with two transonic potential rotor codes. The induced velocities for the near-, mid-, and far-wake geometries are extracted from a nonlinear rigid wake of a standard performance and analysis code. These, together with the corresponding inflow angles, computation points, and azimuth angles, are then incorporated into the transonic potential codes. The coupled codes can then provide an improved prediction of rotor blade loading at transonic speeds. Author

**N91-10014*#** National Aeronautics and Space Administration. Ames Research Center, Moffett Field, CA.
**EULER AND POTENTIAL EXPERIMENT/CFD CORRELATIONS FOR A TRANSPORT AND TWO DELTA-WING CONFIGURATIONS Technical Memorandum**
R. M. Hicks, S. E. Cliff, J. E. Melton, R. G. Langhi, A. M. Goodsell, D. D. Robertson, and S. A. Moyer Aug. 1990 180 p Original contains color illustrations
(NASA-TM-102208; A-89197; NAS 1.15:102208) Avail: NTIS HC/MF A09; 2 functional color pages CSCL 01A

A selection of successes and failures of Computational Fluid Dynamics (CFD) is discussed. Experiment/CFD correlations involving full potential and Euler computations of the aerodynamic characteristics of four commercial transport wings and two low aspect ratio, delta wing configurations are shown. The examples consist of experiment/CFD comparisons for aerodynamic forces, moments, and pressures. Navier-Stokes equations are not considered. Author

**N91-10015*#** National Aeronautics and Space Administration. Ames Research Center, Moffett Field, CA.
**APPLICATION OF CFD TO SONIC BOOM NEAR AND MID FLOW-FIELD PREDICTION**
Samson H. Cheung (MCAT Inst., San Jose, CA.), Thomas A. Edwards, and Scott L. Lawrence Aug. 1990 13 p Presented at the 13th AIAA Aeroacoustic Conference, Tallahassee, FL, 22-24 Oct. 1990
(NASA-TM-102867; A-90246; NAS 1.15:102867) Avail: NTIS HC/MF A03 CSCL 01A

A 3-D parabolized Navier-Stokes (PNS) code was used to calculate the supersonic overpressures from three different geometries at near- and mid-flow fields. Wind tunnel data is used for code validation. Comparison of the computed results with different grid refinements is shown. It is observed that a large number of grid points is needed to resolve the tail shock/expansion fan interaction. Therefore, an adaptive grid approach is employed to calculate the flow field. The agreement between the numerical results and the wind tunnel data confirms that computational fluid dynamics can be applied to the problem of sonic boom prediction. Author

**N91-10016#** Institut Franco-Allemand de Recherches, Saint-Louis (France).
**MODELING BLADE/VORTEX INTERACTIONS [MODELISATION D'INTERACTIONS PALE/TOURBILLON]**
P. Gnemmi, Jacques Haertig, and Ch. Johe 24 May 1989 43 p In FRENCH Original contains color illustrations
(ISL-R-107/89; ETN-90-97569) Avail: NTIS HC/MF A03

The development of an electron emitter based on a shallow pn-junction made of gallium arsenide is reported. Desirable properties of an electron gun are outlined and the attractive aspects and specific possibilities of the Avalanche Electron Emitting Diode (AEED) are discussed. Fabrication, including the self-made gold-germanium sputter and gold evaporation equipment, is explained. Ultrahigh vacuum measurement and cleaning setup and properties of the low energy argon ion sputter source and method of measurement are presented. Experimental results and theoretical calculations are given. The Ga AEED device is concluded to be of not good enough quality for fair comparison to the silicon AEED. ESA

**N91-10017#** Institut Franco-Allemand de Recherches, Saint-Louis (France).
**MEASUREMENT OF AIR ENTRAINMENT BY A FREE JET USING LASER VELOCIMETRY AND RAMAN SCATTERING [MESURE DE L'ENTRAINEMENT DE L'AIR PAR UN JET LIBRE AU MOYEN DE LA VELOCIMETRIE LASER ET DE LA DIFFUSION RAMAN SPONTANEE]**
L. Bobin and G. Brom 19 Jun. 1989 35 p In FRENCH
(Contract DRET-87-068)
(ISL-R-109/89; ETN-90-97570) Avail: NTIS HC/MF A03

The entrainment of ambient air by a free jet is studied using a measuring device combining laser velocimetry and Raman scattering. It is shown that the latter technique is particularly well adapted to study the phenomena of chemically inert gas mixtures. Local measurements of average speed and mean density are used to calculate the rate of entrainment. The empirical formulas are determined inadequate in predicting the entrainment by a free surface flow. It appears to be very sensitive to the confinement, but the evaluation of this is difficult. ESA

**N91-10018#** Institut Franco-Allemand de Recherches, Saint-Louis (France).

**ROTOR LOADS COMPUTATION USING SINGULARITY METHODS AND APPLICATION TO THE NOISE PREDICTION**

Martin Schaffar and Jacques Haertig 1990 13 p Presented at 3rd International Congress of Fluid Mechanics, Cairo, Egypt, 2-4 Jan. 1990

(ISL-PU-301/90; ETN-90-97577) Avail: NTIS HC/MF A03

In the two dimensional space, two singularity methods are described and applied to the profile/vortex interaction. The results show a good agreement with experiments in a water tunnel. In the three dimensional space, the vortex lattice method, with a local conformal mapping, is described and applied in order to predict the aerodynamic loads on a thick two bladed rotor. The pressure coefficients obtained for the thick rotor are fed into an acoustic code which is based on the Ffowcs-Williams-Hawkings equation. The results obtained with this method show the importance of the rotor and flight parameters. They are compared with results found for a two bladed rotor in hovering and advancing flight. The comparison shows a good agreement and shows that the cut off length used to smooth the singularity of the Biot and Savart law must be chosen carefully. ESA

**N91-10019*#** Iowa State Univ. of Science and Technology, Ames. Engineering Research Inst.

**NUMERICAL COMPUTATION OF VISCOUS FLOW ABOUT UNCONVENTIONAL AIRFOIL SHAPES Final Report**

S. Ahmed and J. C. Tannehill Oct. 1990 82 p

(Grant NAG1-645; ERI Proj. 1874)

(NASA-CR-187343; NAS 1.26:187343; ISU-ERI-Ames-91-110; CFD-24) Avail: NTIS HC/MF A05 CSCL 01A

A new two-dimensional computer code was developed to analyze the viscous flow around unconventional airfoils at various Mach numbers and angles of attack. The Navier-Stokes equations are solved using an implicit, upwind, finite-volume scheme. Both laminar and turbulent flows can be computed. A new nonequilibrium turbulence closure model was developed for computing turbulent flows. This two-layer eddy viscosity model was motivated by the success of the Johnson-King model in separated flow regions. The influence of history effects are described by an ordinary differential equation developed from the turbulent kinetic energy equation. The performance of the present code was evaluated by solving the flow around three airfoils using the Reynolds time-averaged Navier-Stokes equations. Excellent results were obtained for both attached and separated flows about the NACA 0012 airfoil, the RAE 2822 airfoil, and the Integrated Technology A 153W airfoil. Based on the comparison of the numerical solutions with the available experimental data, it is concluded that the present code in conjunction with the new nonequilibrium turbulence model gives excellent results. Author

**N91-10020*#** National Aeronautics and Space Administration. Langley Research Center, Hampton, VA.

**AEROELASTIC ANALYSIS OF WINGS USING THE EULER EQUATIONS WITH A DEFORMING MESH**

Brian A. Robinson, John T. Batina, and Henry T. Y. Yang (Purdue Univ., West Lafayette, IN.) Nov. 1990 11 p Presented at the AIAA/ASME/ASCE/AHS/ASC 31st Structures, Structural Dynamics, and Materials Conference, Long Beach, CA, 2-4 Apr. 1990 Previously announced in IAA as A90-29376

(NASA-TM-102733; NAS 1.15:102733; AIAA-90-1032) Avail: NTIS HC/MF A03 CSCL 01A

Modifications to the CFL3D three dimensional unsteady Euler/Navier-Stokes code for the aeroelastic analysis of wings are described. The modifications involve including a deforming mesh capability which can move the mesh to continuously conform to the instantaneous shape of the aeroelastically deforming wing, and including the structural equations of motion for their simultaneous time-integration with the governing flow equations. Calculations were performed using the Euler equations to verify the modifications to the code and as a first step toward aeroelastic analysis using the Navier-Stokes equations. Results are presented for the NACA 0012 airfoil and a 45 deg sweptback wing to demonstrate applications of CFL3D for generalized force computations and aeroelastic analysis. Comparisons are made with published Euler results for the NACA 0012 airfoil and with experimental flutter data for the 45 deg sweptback wing to assess the accuracy of the present capability. These comparisons show good agreement and, thus, the CFL3D code may be used with confidence for aeroelastic analysis of wings. Author

**N91-10021*#** Institute for Computer Applications in Science and Engineering, Hampton, VA.

**THE INVISCID SECONDARY INSTABILITY OF FULLY NONLINEAR LONGITUDINAL VORTEX STRUCTURES IN GROWING BOUNDARY LAYERS Final Report**

Philip Hall and Nicola J. Horseman (Exeter Univ., England ) Oct. 1990 41 p Submitted for publication Sponsored in part by Science Research Council and AF

(Contract NAS1-18605)

(NASA-CR-187455; NAS 1.26:187455; ICASE-90-71) Avail: NTIS HC/MF A03 CSCL 01A

The inviscid instability of a longitudinal vortex structure within a steady boundary layer is investigated. The instability has a wavelength comparable with the boundary layer thickness so that a quasi-parallel approach to the instability problem can be justified. The generalization of the Rayleigh equation to such a flow is obtained and solved for the case when the vortex structure is induced by curvature. Two distinct modes of instability are found; these modes correspond with experimental observations on the breakdown process for Goertler vortices. Author

**N91-10022*#** Institute for Computer Applications in Science and Engineering, Hampton, VA.

**VORTEX INSTABILITIES IN 3D BOUNDARY LAYERS: THE RELATIONSHIP BETWEEN GOERTLER AND CROSSFLOW VORTICES Final Report**

Andrew Bassom and Philip Hall (Exeter Univ., England ) Oct. 1990 76 p Submitted for publication Sponsored in part by Science Research Council and AF

(Contract NAS1-18605)

(NASA-CR-187456; NAS 1.26:187456; ICASE-90-72) Avail: NTIS HC/MF A05 CSCL 01A

The inviscid and viscous stability problems are addressed for a boundary layer which can support both Goertler and crossflow vortices. The change in structure of Goertler vortices is found when the parameter representing the degree of three-dimensionality of the basic boundary layer flow under consideration is increased. It is shown that crossflow vortices emerge naturally as this parameter is increased and ultimately become the only possible vortex instability of the flow. It is shown conclusively that at sufficiently large values of the crossflow there are no unstable Goertler vortices present in a boundary layer which, in the zero crossflow case, is centrifugally unstable. The results suggest that in many practical applications Goertler vortices cannot be a cause of transition because they are destroyed by the 3-D nature of the basic state. In swept wing flows the Goertler mechanism is probably not present for typical angles of sweep of about 20 degrees. Some discussion of the receptivity problem for vortex instabilities in weakly 3-D boundary layers is given; it is shown that inviscid modes have a coupling coefficient marginally smaller than those of the fastest growing viscous modes discussed recently by Denier, Hall, and Seddougui (1990). However the fact that the growth rates of the inviscid modes are the largest in most situations means that they are probably the most likely source of transition. Author

**N91-10023#** Helsinki Univ. Technology, Otaniemi (Finland). Aerodynamics Lab.
**THREE-DIMENSIONAL VISCOUS/INVISCID COUPLING IN SUBSONIC FLOW**
Ziquiang Zhu, Seppo Laine, and Esa Salminen 1990 27 p
(Rept-B-24; ISBN-951-22-0248-4; ISSN-0358-2620) Avail: NTIS HC/MF A03

Coupling MBB low-order panel code for three-dimensional compressible subsonic potential flow and Stock's boundary layer method for three-dimensional compressible laminar or turbulent flow is proposed. The resulting computer program is valid only for simple wings. The panel model may also contain body-like components, however. The friction drag of the wing is obtained as a result of the computations. The effect of the displacement thickness on the potential solution is simulated iteratively using a surface transpiration model. A comparison with experimental results shows that the method predicts the trend of the boundary layer effect correctly, although underestimates its magnitude. Author

**N91-10024#** Helsinki Univ. Technology, Otaniemi (Finland). Aerodynamics Lab.
**CALCULATION OF THREE-DIMENSIONAL VISCOUS/INVISCID INTERACTION IN SUBSONIC FLOW**
Ziqiang Zhu, Seppo Laine, and Esa Salminen 1990 36 p
(Rept-B-25; ISBN-951-22-0329-4; ISSN-0358-2620) Avail: NTIS HC/MF A03

The development of a method to obtain the subsonic viscous flow solution for three-dimensional geometries, using the viscous/inviscid interaction technique, is described. A 3-D panel method (MBB) for calculating three-dimensional inviscid flow is coupled iteratively with a two-dimensional, inverse integral boundary layer method, in which small separation bubbles can be handled. Cross flow is ignored in the boundary layer calculations, which are carried out along chordwise strips of the wing. The surface transpiration approach is used in the coupling. Numerical results indicate that good agreement with experimental data can be obtained up to an angle of attack near maximum lift. Author

**N91-10025#** Helsinki Univ. Technology, Otaniemi (Finland). Aerodynamics Lab.
**EVALUATION OF THE ZONA51D PROGRAM**
Kari Renko 1990 43 p
(Rept-B-28; ISBN-951-22-0398-7; ISSN-0358-2620) Avail: NTIS HC/MF A03

ZONA51D is a computer program which determines the unsteady aerodynamic forces acting on a lifting surface system in supersonic flow. The program is based on the harmonic gradient formulation. The ZONA51D code is installed into the IBM 3090-180E VF computer at the Helsinki University of Technology. Modifications are made to the code to ease its operation and the post-processing of the results. The proper operation of the code and the accuracy of the results is verified by running several test cases and comparing the results to analytical solutions, experimental results, and other representative computations. Author

**N91-10026#** Deutsche Forschungsanstalt fuer Luft- und Raumfahrt, Goettingen (Germany, F.R.). Abt. fuer Numerische Stroemungsmechanik.
**A CONTRIBUTION TO THE NUMERICAL SOLUTION OF TRANSONIC FLOW AROUND A DELTA WING BY SOLVING NAVIER-STOKES EQUATIONS Ph.D. Thesis - Karlsruhe Univ.**
Achim Hilgenstock Dec. 1989 101 p In GERMAN; ENGLISH summary Report will also be announced as translation (ESA-TT-1225) Original contains color illustrations
(DLR-FB-90-13; ISSN-0171-1342; ETN-90-97628) Avail: NTIS HC/MF A06; DLR, VB-OL-DO, Postfach 90 60 58, 5000 Cologne, Fed. Republic

The turbulent flow around a delta wing at incidence is simulated numerically using a finite volume Navier-Stokes method. The methods for selecting the optimal grid and the grid generation are outlined. The numerical simulation makes use of a simple algebraic turbulence model. Using a sharp leading edge delta wing, the influence of grid refinement is investigated. The realistic wing body configuration with round leading edge is used to discuss the influence of the position of the transition line. Experimental and numerical data are compared to validate the numerical method. The topological structure of the flow is interpreted. An explanation is given for the low particle density area close to the primary vortex as it is visualized by laser light sheet technique. The distribution of Mach number, velocity, temperature, pressure and total pressure is discussed in connection with the streamlines for the primary vortex. ESA

**N91-10027#** Deutsche Forschungsanstalt fuer Luft- und Raumfahrt, Cologne (Germany, F.R.). Hauptabt. Windkanaele.
**WIND TUNNEL INVESTIGATIONS OF THE APPEARANCE OF SHOCKS IN THE WINDWARD REGION OF BODIES WITH CIRCULAR CROSS SECTION AT ANGLE OF ATTACK**
Helmut Esch 15 Mar. 1990 63 p In GERMAN; ENGLISH summary Report will also be announced as translation (ESA-TT-1226)
(DLR-FB-90-15; ISSN-0171-1342; ETN-90-97629) Avail: NTIS HC/MF A04; DLR, VB-PL-DO, Postfach 90 60 58, 5000 Cologne, Fed. Republic

Conditions causing the primary embedded shock to deviate into the windward region of a circular cylinder at angle of attack were investigated by use of Schlieren photos, oil flow pictures, and surface pressure distribution measurements. The critical range of crossflow Mach number greater than or equal to 0.3 and less than or equal to 0.6 was covered at free stream Mach numbers between Ma = 1.25 and 2.5. Reynolds numbers based on body diameter varied between 3 x 10(exp 5) and 1.3 x 10(exp 6). ESA

# 03 AIR TRANSPORTATION AND SAFETY

Includes passenger and cargo air transport operations; and aircraft accidents.

For related information see also *16 Space Transportation* and *85 Urban Technology and Transportation.*

**N91-10028#** Federal Aviation Administration, Long Beach, CA. Northwest Mountain Region.
**SEAT DYNAMIC PERFORMANCE STANDARDS FOR A RANGE OF SIZES**
Stephen Soltis Aug. 1990 27 p
(DOT/FAA/CT-TN90/23) Avail: NTIS HC/MF A03

A summary is presented of the rationale that was used to determine the crash impact characteristics for a range of aircraft sizes and places emphasis on developing seat dynamic performance standards that might be used for commuter category size aircraft. The existing crash dynamics data base which includes twin engine general aviation aircraft, rotorcraft, narrow body and wide body transport aircraft were used in this study. The crash impact characteristic of typical airframe structure will be related to the geometric size of the airframe. Author

**N91-10029#** Federal Aviation Administration, Atlantic City, NJ.
**TESTS OF THE GENERAL FIRE SUPPRESSION CONCENTRATE PYROCAP B-136**
George B. Geyer, Joseph A. Wright, Dung Do, and Lawrence Hampton Aug. 1990 34 p
(DOT/FAA/CT-TN90/21) Avail: NTIS HC/MF A03

Fire extinguishing effectiveness of the general fire suppression concentrate identified as Pyrocap B-136 was determined by laboratory experiments and large-scale fire tests. This agent demonstrated strong emulsifying properties toward Jet A (kerosene fuel), JP-4 (kerosene and gasoline fuel blend), and avgas (aviation gasoline fuel). At 6 percent concentration, Pyrocap B-136 extinguished large Jet A fuel fires when applied at the rate of 0.052 gallon per minute per square foot. At 30 percent concentration, the agent was effective in extinguishing magnesium aircraft wheel fires at a low application rate. Author

# 04 AIRCRAFT COMMUNICATIONS AND NAVIGATION

Includes digital and voice communication with aircraft; air navigation systems (satellite and ground based); and air traffic control.

For related information see also *17 Space Communications, Spacecraft Communications, Command and Tracking* and *Communications and Radar.*

**N91-10030** National Aerospace Lab., Tokyo (Japan).
**THE ESTABLISHMENT AND PERFORMANCE TEST OF PAPI (PRECISION APPROACH PATH INDICATOR) SYSTEM FOR NAL STOL AIRCRAFT**
Yoshitaka Murakami, Yushi Terui, Takeshi Hanamatsu, Kenji Saito, Shintaro Yokoyama, and Toshiharu Inagaki Jan. 1988 48 p In JAPANESE; ENGLISH summary
(NAL-TM-579; ISSN-0452-2982; JTN-90-80007) Avail: NTIS HC/MF A03

Flight tests of NAL QSTOL experimental aircraft are being conducted at Gifu airfield. The PAPI (Precision Approach Path Indicator) system was placed at the left side of runway 28 at Gifu airfield as a visual approach guidance aid both STOL and CTOL landings. This system is composed of eight-light units arranged in a line perpendicular to the runway. The beam angle of four units is set at six degrees for STOL approach and that of the other four units is set at three degrees for CTOL approach. The establishment and performance test results of the PAPI system are summarized. NASDA

**N91-10031** National Aerospace Lab., Tokyo (Japan).
**APPLICATION OF FLIGHT PATH RECONSTRUCTION ALGORITHMS FOR FLIGHT DATA OF HELICOPTER**
Shuichi Sasaki Mar. 1988 25 p In JAPANESE; ENGLISH summary
(NAL-TM-582; ISSN-0452-2982; JTN-90-80010) Avail: NTIS HC/MF A03

The maximum-likelihood algorithm, the Kalman filter, and smoother algorithms were applied to real flight data from a CH-47 helicopter (two flights) to estimate motion (attitude, position, and velocity) and sensor parameters (gains and biases of the rate gyros and accelerometers) of the craft. Performances of the algorithms were compared. Some attempts were also made to estimate sensor noise parameters. NASDA

**N91-10032#** Federal Aviation Administration, Washington, DC.
**NATIONAL AIRSPACE SYSTEM: IN-FLIGHT ASSISTANCE OPERATIONAL CONCEPT**
27 Jul. 1989 38 p
(PB90-233115; NAS-SR-1328) Avail: NTIS HC/MF A03 CSCL 17G

This operational concept describes how in-flight assistance will be delivered in the National Airspace System (NAS). It is intended as a tool for systems designers, analysts, and operational test planners in determining if and how well the NAS design and its implementation meet the NAS requirements for in-flight assistance. In addition, management and technical personnel of the FAA and other involved organizations are provided with a general description of how the In-flight Assistance service of the NAS operates. Author

**N91-10033#** Federal Aviation Administration, Atlantic City, NJ.
**OPERATIONAL EVALUATION OF INITIAL DATA LINK AIR TRAFFIC CONTROL SERVICES. VOLUME 2: APPENDICES Final Report**
Nicholas J. Talotta, Clark Shingledecker, and Mike Reynolds (Midwest Systems Research, Inc., Dayton, OH.) Feb. 1990 207 p
(DOT/FAA/CT-90/1-Vol-2) Avail: NTIS HC/MF A10

The results of an operational evaluation of Initial Data Link Air Traffic Control (ATC) Services are detailed. The Operational Evaluation was conducted at the Federal Aviation Administration (FAA) Technical Center utilizing the Data Link test bed. Initial Data Link services were evaluated in order to identify service delivery methods which optimize controller acceptance, performance, and workload. Author

**N91-10034#** Federal Aviation Administration, Atlantic City, NJ.
**DIFFERENTIAL GLOBAL POSITIONING SYSTEM (DGPS) TEST PLAN Technical Report, Nov. 1989 - May 1990**
L. Frank Persello Aug. 1990 16 p
(DOT/FAA/CT-TN90/15) Avail: NTIS HC/MF A03

The Federal Aviation Administration (FAA) Technical Center will conduct Differential Global Positioning System (GPS) tests to address the demands for high levels of accuracy in the terminal area. The tests employed a Convair 580 (CV-580) and two Motorola Eagle Mini Rangers. With the advent of the maturing GPS constellation, the FAA is assuming a more intensive stance in addressing the many questions/problems associated with GPS. These Differential GPS tests investigate the obtainable accuracy under static and dynamic conditions. The static tests will employ surveyed points as a base line. The dynamic tests will incorporate terminal area flightpaths and non-precision approaches using a laser tracker as a base line. The Differential tests will be conducted in an effort to build an FAA Differential GPS data base to aid in addressing GPS questions/problems. Author

**N91-10035#** Oxford Univ. (England). Robotics Research Group.
**EXPERIMENTS AND THEORY WITH A 0.5 TON MOBILE ROBOT**
Barry Steer 1990 33 p Sponsored by Science Research Council, England and Royal Armament Research and Development Establishment, Chertsey, England
(OUEL-1807/90; ETN-90-97916) Avail: NTIS HC/MF A03

Autonomous navigation by an intelligent robot vehicle is studied. The process of navigation is the establishment (fixing) of the position and attitude of an object, in this case a terrestrial ground vehicle, relative to some reference system. The theory, hardware details, and experimental results obtained between 1980 and 1984 in the U.K. using data processing activities that were implemented on a 0.5 ton wheeled vehicle, equipped with four different types of sensors, and two computer controlled actuation systems that enabled it, among other things, to navigate autonomously, are described. ESA

**N91-10036#** Oxford Univ. (England). Robotics Research Group.
**DESIGN FOR NAVIGATION: USING ACOUSTIC CATS' EYES TO IMPROVE SONAR RANGE AND DIRECTION RANGE FINDING FOR INDUSTRIAL MOBILE ROBOTS AND AGV'S**
Barry Steer and Tim Atherton (Warwick Univ., Coventry, England ) 15 Oct. 1989 27 p
(OUEL-1812/90; ETN-90-97919) Avail: NTIS HC/MF A03

The specular reflection of sound from many surfaces makes the automatic construction of such accurate and truthful depth maps from time of flight acoustic rangers a surprisingly difficult task. A practical solution which overcomes the problem of specularity, and enables the standard Polaroid acoustic ranger with its standard electronics to accurately measure the range and direction to objects, is presented. To support this assertion, representative results obtained without innovation and with innovation are presented. The improvements in performance are dramatic and obvious. A visual comparison shows that the standard Polaroid ranger produces raw range scans which are (almost) as good as an architect's plan view of the same areas. While the technique has the merit of being low cost, it is also easy to apply in practice, and the computations needed to extract information concerning the location and number of walls and corners can be performed rapidly. ESA

**N91-10037#** Oxford Univ. (England). Robotics Research Group.
**REAL-TIME SAFETY ANALYSIS FOR AUTONOMOUS GUIDED VEHICLES**

Alan C. Brown May 1990 12 p
(OUEL-1833/90; ETN-90-97926) Avail: NTIS HC/MF A03

Unpredictable behavior in hard real time systems can have drastic consequences and the formal verification of system safety properties in this context is therefore particularly appropriate. Safety analysis is applied to the timing specification of a simple robot vehicle. The specification is given by a set of real time logic formulas (rules). A modified rule to permit the preemption of low priority real time processes is proposed. ESA

# 05 AIRCRAFT DESIGN, TESTING AND PERFORMANCE

Includes aircraft simulation technology.

For related information see also *18 Spacecraft Design, Testing and Performance* and *39 Structural Mechanics.*For land transportation vehicles see *85 Urban Technology and Transportation.*

**N91-10038** National Aerospace Lab., Tokyo (Japan). STOL Aircraft Project Group.
**THE ACTUATOR FOR THE LOW-NOISE STOL TEST PLANE FLIGHT CONTROL SYSTEM AND ITS DEVELOPMENT TEST [TEISOUON SUTORU JIKKENKI HIKOU SEIGYO SHISUTEMU YOU AKUCHUETA TO SONOKAIHATSU GIJUTSU SHIKEN]**
May 1987 172 p In JAPANESE
(NAL-TM-574; ISSN-0452-2892; JTN-90-80003) Copyright Avail: NTIS HC/MF A08

In total, 54 actuators (28 types) are used for the flight control system of the low-noise experimental STOL craft. Prior to application to the experimental craft, a development technology test was carried out on the parts other than the C-1 common parts of these actuators. The test was composed of a function and performance test which consisted in confirming the adaptability of the parts to the requirements of the craft on the one hand, and of a weather proofing test which consisted in verifying their adaptability to the operational circumstances of the craft on the other hand. This report explains the general characters of all the actuators used initially for the experimental STOL craft as well as the summary of the results of the development technology test carried out. NASDA

**N91-10039*#** College of William and Mary, Williamsburg, VA. Dept. of Computer Science.
**AUTOMATIC DETERMINATION OF FAULT EFFECTS ON AIRCRAFT FUNCTIONALITY Semiannual Progress Report, 17 Feb. - 17 Aug. 1989**
Stefan Feyock 1989 40 p
(Contract NCC1-122)
(NASA-CR-181352; NAS 1.26:181352) Avail: NTIS HC/MF A03 CSCL 01C

The problem of determining the behavior of physical systems subsequent to the occurrence of malfunctions is discussed. It is established that while it was reasonable to assume that the most important fault behavior modes of primitive components and simple subsystems could be known and predicted, interactions within composite systems reached levels of complexity that precluded the use of traditional rule-based expert system techniques. Reasoning from first principles, i.e., on the basis of causal models of the physical system, was required. The first question that arises is, of course, how the causal information required for such reasoning should be represented. The bond graphs presented here occupy a position intermediate between qualitative and quantitative models, allowing the automatic derivation of Kuipers-like qualitative constraint models as well as state equations. Their most salient feature, however, is that entities corresponding to components and interactions in the physical system are explicitly represented in the bond graph model, thus permitting systematic model updates to reflect malfunctions. Researchers show how this is done, as well as presenting a number of techniques for obtaining qualitative information from the state equations derivable from bond graph models. One insight is the fact that one of the most important advantages of the bond graph ontology is the highly systematic approach to model construction it imposes on the modeler, who is forced to classify the relevant physical entities into a small number of categories, and to look for two highly specific types of interactions among them. The systematic nature of bond graph model construction facilitates the process to the point where the guidelines are sufficiently specific to be followed by modelers who are not domain experts. As a result, models of a given system constructed by different modelers will have extensive similarities. Researchers conclude by pointing out that the ease of updating bond graph models to reflect malfunctions is a manifestation of the systematic nature of bond graph construction, and the regularity of the relationship between bond graph models and physical reality. Author

**N91-10040*#** Ohio State Univ., Columbus. Dept. of Aeronautical and Astronautical Engineering.
**PROJECT HyBuJET Final Report**
Tom Ramsay, Bill Collet, Karyn Igar, Dewayne Kendall, Dave Miklosovic, Robyn Reuss, Mark Ringer, and Tony Scheidt May 1990 166 p Prepared in cooperation with Universities Space Research Association, Houston, TX Sponsored by NASA
(NASA-CR-187011; NAS 1.26:187011) Avail: NTIS HC/MF A08 CSCL 01C

A conceptual Hypersonic Business Jet (HyBuJet) was examined. The main areas of concentration include: aerodynamics, propulsion, stability and control, mission profile, and atmospheric heating. In order to optimize for cruise conditions, a waverider configuration was chosen for the high lift drag ratio and low wave drag. The leading edge and lower surface of a waverider was mapped out from a known flow field and optimized for cruising at Mach 6 and at high altitudes. The shockwave generated by a waverider remains attached along the entire leading edge, allowing for a larger compression along the lower surface. Three turbofan ramjets were chosen as the propulsion of the aircraft due to the combination of good subsonic performance along with high speed propulsive capabilities. A combination of liquid silicon convective cooling for the leading edges with a highly radiative outer skin material was chosen to reduce the atmospheric heating to acceptable level. Author

**N91-10041*#** Ohio State Univ., Columbus. Dept. of Aeronautical and Astronautical Engineering.
**OVRhyp, SCRAMJET TEST AIRCRAFT Final Report**
J. Aslan, T. Bisard, S. Dallinga, K. Draper, G. Hufford, W. Peters, and J. Rogers May 1990 127 p Prepared in cooperation with Universities Space Research Association, Houston, TX Sponsored by NASA
(NASA-CR-187009; NAS 1.26:187009) Avail: NTIS HC/MF A07 CSCL 01C

A preliminary design for an unmanned hypersonic research vehicle to test scramjet engines is presented. The aircraft will be launched from a carrier aircraft at an altitude of 40,000 feet at Mach 0.8. The vehicle will then accelerate to Mach 6 at an altitude of 100,000 feet. At this stage the prototype scramjet will be employed to accelerate the vehicle to Mach 10 and maintain Mach 10 flight for 2 minutes. The aircraft will then decelerate and safely land. Author

**N91-10042#** Advisory Group for Aerospace Research and Development, Neuilly-Sur-Seine (France). Propulsion and Energetics Panel.
**ROTORCRAFT DRIVETRAIN LIFE SAFETY AND RELIABILITY**
Derek G. Astridge, ed. and M. Savage, ed. (Akron Univ., OH.) Jun. 1990 83 p
(AGARD-R-775; ISBN-92-835-0540-9) Copyright Avail: NTIS HC/MF A05; Non-NATO Nationals requests available only from AGARD/Scientific Publications Executive

This is a portion of a intended volume on Transmission Systems for Power Transfer in Helicopters and Turboprops. Lessons learned from accident data of large civil transport helicopters are examined, as are recent improvements in design and component technology, including recommendations and safety benefits achievable by monitoring systems. A statistical analysis was made of drive system life and reliability. A proper evaluation was made of drive systems design and the understanding and control of mean life and life scatter of a drive system at the design stage. For individual titles, see N91-10043 through N91-10044.

**N91-10043#** Astridge (Derek) and Associates, Langport (England).
**HELICOPTER TRANSMISSIONS: DESIGN FOR SAFETY AND RELIABILITY**
Derek G. Astridge *In* AGARD, Rotorcraft Drivetrain Life Safety and Reliability Jun. 1990 p 1-34 Previously announced in IAA as A90-20608 (For primary document see N91-10042 01-05)
Copyright Avail: NTIS HC/MF A05; Non-NATO Nationals requests available only from AGARD/Scientific Publications Executive

An analysis of the UK CAA's world wide helicopter accident data indicates that transmissions accounted for 22 percent of potentially airworthiness related accidents in civil helicopters of more than 4550 kg gross weight. An evaluation is made of design and technology advancements over the last decade which should benefit helicopter transmission safety and reliability. These encompass improved steels with superior fatigue performance, S/N curve refinement, computer aided design analysis systems, CAD/CAM, improved lubricants and filtration systems, and expert systems retaining a collective memory with regard to design practices' relationship to service experience. E.R.

**N91-10044#** Akron Univ., OH.
**DRIVE SYSTEM LIFE AND RELIABILITY**
M. Savage *In* AGARD, Rotorcraft Drivetrain Life Safety and Reliability Jun. 1990 p 35-71 (For primary document see N91-10042 01-05)
Copyright Avail: NTIS HC/MF A05; Non-NATO Nationals requests available only from AGARD/Scientific Publications Executive

Fuel efficiency is an important objective in aircraft propulsion. In design, the requirements of light weight and high reliability conflict. Designers use highly stressed, high quality alloy steels in the major load bearing components to resolve the conflict. One estimate for the service needs of a drive system comes from its life and reliability models. The design objectives of long life between repairs and high reliability are design goals. The statistics of drive system life and reliability are discussed. The statistics develop reliability models for repair prediction. The modes of failure which are the basis for these models are also discussed. Coverage of the two parameter Weibull distribution model for component and system life is detailed. Similar coverage is made of the Miner Palmgren load-life model. Based on this model, the theory of mission spectrum averaging is presented. Mission spectrum averaging determines the equivalent constant load which has the same life as the mission spectrum. Also the component life and reliability models for bearings and gears are described. On-board monitoring systems are described. Estimates of the drive system failure rate and replacement needs are still essential at the design stage. E.R.

**N91-10045*#** National Aeronautics and Space Administration. Ames Research Center, Moffett Field, CA.
**ROTOR SYSTEMS RESEARCH AIRCRAFT RISK-REDUCTION SHAKE TEST**
J. Brent Wellman Washington Aug. 1990 356 p
(NASA-TM-4186; A-88316; NAS 1.15:4186; AVSCOM-TR-88-A-003) Avail: NTIS HC/MF A16 CSCL 01C

A shake test and an extensive analysis of results were performed to evaluate the possibility of and the method for dynamically calibrating the Rotor Systems Research Aircraft (RSRA). The RSRA airframe was subjected to known vibratory loads in several degrees of freedom and the responses of many aircraft transducers were recorded. Analysis of the transducer responses using the technique of dynamic force determination showed that the RSRA, when used as a dynamic measurement system, could predict, a posteriori, an excitation force in a single axis to an accuracy of about 5 percent and sometimes better. As the analysis was broadened to include multiple degrees of freedom for the excitation force, the predictive ability of the measurement system degraded to about 20 percent, with the error occasionally reaching 100 percent. The poor performance of the measurement system is explained by the nonlinear response of the RSRA to vibratory forces and the inadequacy of the particular method used in accounting for this nonlinearity. Author

**N91-10046#** Oak Ridge National Lab., TN. Center for Transportation Analysis.
**ENERGY EFFICIENCY IMPROVEMENT POTENTIAL OF COMMERCIAL AIRCRAFT TO 2010**
David L. Greene Jun. 1990 42 p
(Contract DE-AC05-84OR-21400)
(DE90-014767; ORNL-6622) Avail: NTIS HC/MF A03

Aircraft are second only to motor vehicles in the use of motor fuels. Furthermore, air travel is growing twice as fast as highway travel. Clearly, the importance of energy use by commercial aircraft will continue to increase. Since 1970, air travel has more then tripled, but the growth of fuel use has been restrained by a near doubling of efficiency, from 26.2 seat miles per gallon (SMPG) in 1970 to about 49 SMPG in 1989. This paper explores the potential for future efficiency improvements via the replacement of existing aircraft with 1990's generation and post 2000 aircraft incorporating advances in engine and airframe technology. Today, new commercial passenger aircraft deliver 50 to 70 SMPG. New aircraft types scheduled for delivery in the early 1990's are expected to achieve 65 to 80 SMPG. Industry and government researchers have identified technologies capable of boosting aircraft efficiencies to the 100 to 150 SMPG range. Under current industry plans, which do not include a post-2000 generation of new aircraft, the total aircraft fleet should reach the vicinity of 65 SMPG by 2010. A new generation of 100 to 150 SMPG aircraft introduced in 2005 could raise the fleet average efficiency to 75 to 80 SMPG in 2010. In any case, fuel use will likely continue to grow at from 0.8 percent/y to 1.8 percent/y through 2010. DOE

**N91-10047*#** Georgia Inst. of Tech., Atlanta. School of Aerospace Engineering.
**NONLINEAR FEEDBACK CONTROL FOR HIGH ALPHA FLIGHT Final Report, Jan. 1989 - Apr. 1990**
Harold Stalford Apr. 1990 15 p
(Grant NAG1-959)
(NASA-CR-186545; NAS 1.26:186545) Avail: NTIS HC/MF A03 CSCL 01C

Analytical aerodynamic models are derived from a high alpha 6 DOF wind tunnel model. One detail model requires some interpolation between nonlinear functions of alpha. One analytical model requires no interpolation and as such is a completely continuous model. Flight path optimization is conducted on the basic maneuvers: half-loop, 90 degree pitch-up, and level turn. The optimal control analysis uses the derived analytical model in the equations of motion and is based on both moment and force equations. The maximum principle solution for the half-loop is poststall trajectory performing the half-loop in 13.6 seconds. The agility induced by thrust vectoring capability provided a minimum effect on reducing the maneuver time. By means of thrust vectoring control the 90 degrees pitch-up maneuver can be executed in a small place over a short time interval. The agility capability of thrust vectoring is quite beneficial for pitch-up maneuvers. The level turn results are based currently on only outer layer solutions of singular perturbation. Poststall solutions provide high turn rates but generate higher losses of energy than that of classical sustained solutions. Author

**N91-10048*#** National Aeronautics and Space Administration. Ames Research Center, Moffett Field, CA.
**INDUSTRY LIAISON SECTION IMPLEMENTATION PLAN**
Stephen Lakowske Sep. 1990 81 p
(Contract NAS2-11555)
(NASA-CR-177569; A-90303; NAS 1.26:177569) Avail: NTIS HC/MF A05 CSCL 01C

The Industry Liaison Section is a new function of the

Army/NASA Aircrew-Aircraft Integration (AAAI) Program that is intended to bridge an existing gap between Government developers (including contractors) and outside organizations who are potential users of products and services developed by the AAAI Program. Currently in its sixth year, the Program is experiencing considerable pull from industry and other government organizations to disseminate products. Since the AAAI Program's charter is exploratory and research in nature, and satisfying proper dissemination requirements is in conflict with the rapid prototyping approach utilized by the design team, the AAAI Program has elected to create an Industry Liaison Section (ILS) to serve as the Program's technology transfer focal point. The process by which the ILS may be established, organized and managed is described, including the baseline organizational structure, duties, functions, authority, responsibilities, relations and policies and procedures relevant to the conduct of the ILS. Author

**N91-10049*#** National Aeronautics and Space Administration. Ames Research Center, Moffett Field, CA.
**BODY WEIGHT OF HYPERSONIC AIRCRAFT, PART 1**
Mark D. Ardema Oct. 1988 62 p
(NASA-TM-101028; A-88279-Pt-1; NAS 1.15:101028) Avail: NTIS HC/MF A04 CSCL 01C

The load bearing body weight of wing-body and all-body hypersonic aircraft is estimated for a wide variety of structural materials and geometries. Variations of weight with key design and configuration parameters are presented and discussed. Both hot and cool structure approaches are considered in isotropic, organic composite, and metal matrix composite materials; structural shells are sandwich or skin-stringer. Conformal and pillow-tank designs are investigated for the all-body shape. The results identify the most promising hypersonic aircraft body structure design approaches and their weight trends. Geometric definition of vehicle shapes and structural analysis methods are presented in appendices. Author

**N91-10050#** Institut Franco-Allemand de Recherches, Saint-Louis (France).
**FAST STEERING OF THE ANGLE OF ATTACK: A CONTRIBUTION TO THE GUIDANCE OF HIGH VELOCITY PROJECTILES**
V. Fleck 20 Jun. 1989 22 p Presented at DEA-1060 Meeting, Unterluess, Fed. Republic of Germany, 16-19 May 1989
(ISL-CO-220/89; ETN-90-97573) Avail: NTIS HC/MF A03

A method for using fast jet actuators for steering the angle of attack of projectiles is described. In order to minimize the reaction time the response to pulse commands is analyzed. The conditions for inducing an angle of attack along a short flight path are defined. The cases of projectiles rotating slowly and fast, or not rotating at all, are examined. The shortest distance for achieving a flight path correction is the half wavelength of the pitching or yawing frequency of the projectile. To illustrate the ability of the method developed for solving interception problems, a test is carried out. The interception of an airplane maneuvering with 3 g by a guided projectile with a speed of 1800 m/s is analyzed. ESA

**N91-10051#** Federal Aviation Administration, Atlantic City, NJ.
**STRUCTURAL TESTS OF AIRCRAFT WINDOW ASSEMBLY EQUIPPED WITH SMOKE EVACUATION VALVE**
Anthony Wilson and William Cavage, Jr. Sep. 1990 20 p
(DOT/FAA/CT-TN89/44) Avail: NTIS HC/MF A03

The results of three tests performed on a window and window frame of a Boeing 707 are presented. The purpose of the test, conducted at the Federal Aviation Administration Technical Center, was to determine the maximum moment the window could withstand before becoming dislodged from its frame due to the failure of the window retention clips. The window assembly was modified to fit into a load machine. The loads were measured with a load cell and recorded on a Honeywell Test Management System. Author

**N91-10052#** Federal Aviation Administration, Atlantic City, NJ.
**AIRPLANE SYSTEMS MODIFICATIONS FOR IMPROVED CABIN SMOKE EVACUATION**
Thor I. Eklund Sep. 1990 20 p
(DOT/FAA/CT-TN90/24) Avail: NTIS HC/MF A03

Two concepts for improved aircraft in-flight smoke evacuation were analyzed and tested. The concept definition and evaluation efforts involved an additional ventilation outflow valve on the aircraft underside along with either increased ventilation air volume from the engine compressors or a supplemental ram air supply. Subsequent test aircraft modification involved addition of a pressure controlling outflow valve on the top of the fuselage and upgraded engine bleed air volume flow for cabin air-conditioning. Ground and flight tests were conducted on a test B757 with buoyant and nonbuoyant theatrical smokes generated continuously in various places in the passenger cabin. Buoyant smoke could be localized only when generated in the vicinity of the upper lobe outflow valve. Nonbuoyant smoke could be localized only when generated in the vicinity of an outflow valve, whether the valve was on the top or bottom of the fuselage. The buoyant smoke was formulated to have the same type flow behavior as a plume from the visible flames of a burning surface. The nonbuoyant smoke might be more representative of a smoldering material. Author

**N91-10053#** National Aerospace Lab., Tokyo (Japan).
**A CONSIDERATION ON FLIGHT PATHS FOR MICROWAVE-POWERED AIRPLANES**
Kingo Takasawa and Fumiko Itoh Jan. 1990 30 p In JAPANESE; ENGLISH summary
(NAL-TR-1051; ISSN-0389-4010) Avail: NTIS HC/MF A03

Flight paths for microwave-powered airplanes were investigated under uniform wind conditions. Some techniques for deducing flight paths are discussed. The loci of airspeed vectors which lead to preferable flight paths are sorted into four types. The effects of added higher harmonic components are discussed. For each type of airspeed vector loci, three kinds of solving methods are applied and 12 solutions are obtained. Examples of flight paths are illustrated with their mathematical expressions, and characteristics are discussed. Preferable flight paths from the view point of airplane design are described. Author

**N91-10054#** National Aerospace Lab., Tokyo (Japan).
**PRACTICAL FLIGHT PATHS FOR MICROWAVE-POWERED AIRPLANES**
Takeshi Ito Jan. 1990 15 p
(NAL-TR-1052T; ISSN-0389-4010) Avail: NTIS HC/MF A03

Although some types of closed flight paths have been proposed for microwave powered airplanes, they have unfavorable features from the viewpoint of airplane designers, especially under strong wind conditions. Here, by working out several methods of defining the airspeed vector, smooth practical periodic flight paths are deduced. Author

**N91-10055#** Messerschmitt-Boelkow-Blohm G.m.b.H., Munich (Germany, F.R.). Helicopter Div.
**MBB'S BO 108 DESIGN AND DEVELOPMENT**
Helmut B. Huber and Claus Schick May 1990 15 p Presented at 46th American Helicopter Society Annual Forum and Technology Display, Washington, DC, 21-23 May 1990
(MBB-UD-0568-90-PUB; ETN-90-97838; OTN-027636) Avail: NTIS HC/MF A03

The development by MBB of a new light twin, multipurpose helicopter, designated as the BO-108 is described. The design requirements and the technology advances in terms of the various components involved (rotor systems, drive system, anti-vibration system, control system, airframe, cockpit and cabin) are presented. An overview on the current status of bench and in-flight testing is given and the progress achieved in the fields of performance, flying qualities, noise and vibrations, weight, reliability and safety is assessed. Studies for increasing the aircraft's capabilities are described and a prospective about the future program plans is given. ESA

**N91-10056#** Rolls-Royce Ltd., Bristol (England).
**PROGRESS IN CERTIFYING F402-RR-408: THE IMPROVED PEGASUS ENGINE FOR AV-8B AND HARRIER 2 PLUS**
David J. Martin Derby, England 19 Sep. 1989 10 p Presented at Tactical V/STOL Aircraft, New Bern, NC, 19-21 Sep. 1989 Sponsored by Ministry of Defence, London, England
(PNR-90719; ETN-90-97945) Copyright Avail: NTIS HC/MF A02

The operational background of the Harrier/AV8 family of aircraft was used to define a demonstrator program for improved performance. The XG15 demonstrator program was completed in April 1988. The results formed the basis of the improved F402-RR-408 engine. The validation test program commenced with an engine roll out in June 1988 and is due for completion in May 1990. A summary of technical issues and program status is given. ESA

## 06 AIRCRAFT INSTRUMENTATION

Includes cockpit and cabin display devices; and flight instruments.

For related information see also *19 Spacecraft Instrumentation* and *35 Instrumentation and Photography.*

**N91-10057** National Aerospace Lab., Tokyo (Japan).
**WIND TUNNEL TEST OF REDUNDANT VANE-TYPE FLOW-DIRECTION SENSING SYSTEMS [YABANE O MOCHIITA JOUCHOUGATA KIRYUU HOUKOU SOKUTEI SOUCHI NO FUUDOUSHIKEN NI KANSURU HOUKOKU]**
Takeo Kimura, Minoru Takizawa, Tadao Uchida, Atsutoshi Fujieda, Akihito Iwasaki, Toshimi Fujita, and Teruo Someya Jul. 1988 41 p In JAPANESE
(NAL-TM-590; ISSN-0452-2982; JTN-90-80017) Avail: NTIS HC/MF A03

Trial fabrication of a triaxial sensor system, in which alpha is the front angle and beta is the side angles, and performance of wind tunnel tests are presented. An experiment based on the two-dimensional vector volume measurement method using a blast wind tunnel was performed to prove the measurement theory of the triaxial alpha/beta sensor system and to compare the measurement accuracy between the results obtained from a normally functioning sensor and a malfunctioning or out-of-order sensor. Values and errors were calculated from data obtained from three sensors under four different wind velocities of 10, 20, 30, and 40 m/s against a fixed air current of alpha zero beta zero in the wind tunnel. The accuracy of measurement was determined by comparing the measured data with the second and third sensor, first and third sensor, and first and second sensor. The results of the experiment indicated that the measurement of this system was extremely accurate. Even if one of the sensors becomes defective, the accuracy will not reduce the reliability limit as the other sensors functioned normally. Thus the feasibility of this system has been acknowledged. NASDA

**N91-10058*#** National Aeronautics and Space Administration. Langley Research Center, Hampton, VA.
**NASA TRANSPORT SYSTEMS RESEARCH VEHICLE B-737 DATA LINK SYSTEM AND DISPLAY FORMATS**
Charles E. Knox and Charles H. Scanlon Aug. 1990 22 p
(NASA-TM-102717; NAS 1.15:102717) Avail: NTIS HC/MF A03 CSCL 01C

A data link system was designed to support flight tests in the NASA Transport Systems Research Vehicle B-737 airplane. The purpose of the flight tests was to evaluate pilot acceptance of using data link as the primary source of communications for strategic and tactical air traffic control clearances, weather information, and company messages. The airborne functional operations of the data link system flight tested in 1990 are described. Author

## 07 AIRCRAFT PROPULSION AND POWER

Includes prime propulsion systems and systems components, e.g., gas turbine engines and compressors; and onboard auxilliary power plants for aircraft.

For related information see also *20 Spacecraft Propulsion and Power, 28 Propellants and Fuels,* and *44 Energy Production and Conversion.*

**N91-10059** National Aerospace Lab., Tokyo (Japan).
**EFFECTS OF COOLANT INJECTION ON TURBINE AERODYNAMIC CHARACTERISTICS. PART 1: TEST TURBINE AND APPARATUS**
Shigeo Inoue, Hiroshi Usui, Mitsuhiro Minoda, and Hiroyuki Nose May 1988 21 p In JAPANESE; ENGLISH summary
(NAL-TM-585-Pt-1; ISSN-0452-2982; JTN-90-80013) Avail: NTIS HC/MF A03

Effects of coolant injection on turbine aerodynamic characteristics were investigated with a test turbine. The main air flow was unheated and the temperature was about 100 C. The coolant (secondary air) temperature was kept at about 100 C, nearly the same as that of the main flow. The present investigation is concerned with effects of coolant injected from the following parts on turbine aerodynamic characteristics: (1) stator blades, (2) both stator and rotor blades, (3) stator casing, and (4) rotor casing (shroud ring). The test facility, the test turbine, and the measuring systems are described. NASDA

**N91-10060** National Aerospace Lab., Tokyo (Japan).
**EXPERIMENTAL INVESTIGATION ON THE EFFECT OF COOLANT INJECTION ON TURBINE AERODYNAMIC CHARACTERISTICS. PART 2: EFFECTS OF INJECTION FROM ROTOR CASING WITH 30 DEG SLANTED HOLES**
Hiroshi Usui, Shigeo Inoue, Mitsuhiro Minoda, and Hiroyuki Nouse Jun. 1988 25 p In JAPANESE; ENGLISH summary
(NAL-TM-587-Pt-2; ISSN-0452-2982; JTN-90-80014) Avail: NTIS HC/MF A03

Using a test turbine, the effect of coolant injection was investigated on turbine aerodynamic characteristics. The effects of the coolant injection from a rotor casing with 30 deg slanted holes are described. The discussed turbine efficiency introduced is based on torque, rotational speed, mass flow rate, and the radial and tangential distributions of total pressure and flow angles. It may be concluded that there are some reductions in total pressure losses and increases in outlet flow angles in the tip region caused by the coolant injection. NASDA

**N91-10061*#** Ohio State Univ., Columbus. Dept. of Aeronautical and Astronautical Engineering.
**SUPERSONIC COMBUSTION ENGINE TESTBED, HEAT LIGHTNING Final Report**
D. Hoying, C. Kelble, A. Langenbahn, M. Stahl, M. Tincher, M. Walsh, and S. Wisler May 1990 112 p Prepared in cooperation with Universities Space Research Association, Houston, TX Sponsored by NASA
(NASA-CR-187010; NAS 1.26:187010) Avail: NTIS HC/MF A06 CSCL 21E

The design of a supersonic combustion engine testbed (SCET) aircraft is presented. The hypersonic waverider will utilize both supersonic combustion ramjet (SCRAMjet) and turbofan-ramjet engines. The waverider concept, system integration, electrical power, weight analysis, cockpit, landing skids, and configuration modeling are addressed in the configuration considerations. The subsonic, supersonic and hypersonic aerodynamics are presented along with the aerodynamic stability and landing analysis of the aircraft. The propulsion design considerations include: engine selection, turbofan ramjet inlets, SCRAMjet inlets and the SCRAMjet diffuser. The cooling requirements and system are covered along with the topics of materials and the hydrogen fuel tanks and insulation system. A cost analysis is presented and the appendices include: information about the subsonic wind tunnel test, shock expansion calculations, and an aerodynamic heat flux program. M.G.

**N91-10062** Rensselaer Polytechnic Inst., Troy, NY.
**ANALYSIS OF PULSED LASER-GENERATED IMPULSE IN AN ADVANCED AIRBREATHING THRUSTER Ph.D. Thesis**
Jacques Constant Richard 1989 140 p
Avail: Univ. Microfilms Order No. DA9018446

An advanced beam-powered propulsion system, called an External Radiation-Heated (ERH) thruster is studied. The repetitively-pulsed, airbreathing engine develops thrust by expanding high pressure, radiation-heated gas over an annular shroud surface. The blast waves are generated by laser radiation heating of air using Laser Supported Detonation (LSD) waves. The phenomenology of LSD waves is described, as is the blast waves and resultant impulse they produce. Analytical simulation of the ERH thruster is accomplished with a one-dimensional model of blast waves propagating uniformly and radially outward from a laser-generated line source of high pressure, high temperature gas. Cylindrical blast wave scaling relationships developed by Sedov are employed in this model. The possibility of including other physical phenomena in the analysis are reviewed. The analyses for the ERH thruster model are performed for a sample vehicle point design. This vehicle, known as the Lightcraft Technology Demonstrator (LTD), may be constructed within the next five years to illustrate the potential of Earth-to-Orbit laser propulsion. The external flow over the LTD vehicle was analyzed to determine basic drag characteristics, inlet total pressure recovery and capture air mass flow rate. Dissert. Abstr.

**N91-10063#** Rolls-Royce Ltd., Derby (England).
**PARAMETRIC ASSESSMENT OF PROPULSION SYSTEM MASS FOR AIRBREATHING LAUNCHER CONFIGURATIONS**
F. A. Hewitt and Rainer R. Schwab (Motoren- und Turbinen-Union Muenchen G.m.b.H., Germany, F.R. ) 24 May 1989 7 p Presented at the 2nd Eurospace Aerospace Conference on Progress in Space Transportation, Bonn-Bad Godesberg, Fed. Republic of Germany, 22-24 May 1989 Previously announced as N90-16819 Sponsored in part by ESA
(PNR-90634; ETN-90-97142) Avail: NTIS HC/MF A02

Sensitivity of power plant mass to such variables as vehicle thrust requirements, precompression surface incidence, intake and nozzle designs and turbo machinery design constraints is described for an example of turboramjet power plant propelling the first stage of a two stage to orbit launcher. The propulsion system consisted of a turbojet engine behind a rectangular ramp intake with the reheat system operating as a ramjet burner for flight beyond approximately Mach 3. The core engine was isolated from the airflow at these conditions. Several of the aspects of overall vehicle performance are described where these interact with the power plant design, and the influence of mission definition on power plant optimization is discussed. ESA

**N91-10064#** Aeronautical Research Labs., Melbourne (Australia).
**FLIGHT TESTING OF TWO ALLISON T56 ENGINES MODIFIED TO THE ARL DEVELOPED LOW SMOKE CONFIGURATION**
P. N. Doogood Jun. 1990 19 p
(ARL-Prop-TM-449; AR-006-100) Avail: NTIS HC/MF A03

Two Allison T56 engines were modified to the ARL developed low smoke configuration and placed on wing of separate RAAF P-3C Orion aircraft for extensive flight testing. The initial tests are reported and it is concluded that the modification had no adverse effect on the performance of the engine. Author

**N91-10065*#** Hamilton Standard, Windsor Locks, CT.
**MEASUREMENT OF UNSTEADY BLADE SURFACE PRESSURE ON A SINGLE ROTATION LARGE SCALE ADVANCED PROP-FAN WITH ANGULAR AND WAKE INFLOW AT MACH NUMBERS FROM 0.02 TO 0.70 Final Report**
P. Bushnell, M. Gruber, and D. Parzych Oct. 1988 45 p MF as supplement
(Contract NAS3-23051)
(NASA-CR-182123; E-4137; NAS 1.26:182123) Avail: NTIS HC/MF A03 CSCL 21E

Unsteady blade surface pressure data for the Large-Scale Advanced Prop-Fan (LAP) blade operation with angular inflow, wake inflow and uniform flow over a range of inflow Mach numbers of 0.02 to 0.70 is provided. The data are presented as Fourier coefficients for the first 35 harmonics of shaft rotational frequency. Also presented is a brief discussion of the unsteady blade response observed at takeoff and cruise conditions with angular and wake inflow. Author

**N91-10066#** Rolls-Royce Ltd., Derby (England).
**AERO ENGINE DESIGN FACTORS FOR A LOW FUEL PRICE SCENARIO**
S. J. Hartropp 15 May 1989 20 p Presented at Canadian Aeronautics and Space Institute, Ottawa, Ontario, 15-17 May 1989
(PNR-90681; ETN-90-97928) Copyright Avail: NTIS HC/MF A03

The driving parameters for aero engine design were reassessed to account for the stabilization of fuel price in the vicinity of 50 cents per gallon. A program embracing studies in the fields of operating cost analysis, reliability research and engine specific thrust effects established principles reflecting the importance of engine direct operating cost. The same factors influence the aircraft life cycle cost, and as legislative compliance, operator acceptance and passenger appeal. The effect of applying these principles to a new powerplant and the ongoing development of current powerplants is evaluated. ESA

**N91-10067#** Rolls-Royce Ltd., Derby (England).
**THERMAL FATIGUE CYCLING IN TURBINE BLADES**
M. H. Coney 28 Sep. 1989 25 p Discussion held in Leatherhead, England, 28 Sep. 1989; sponsored by the Journal High Temperature Technology, CEGB Research Labs. Submitted for publication
(PNR-90682; ETN-90-97929) Copyright Avail: NTIS HC/MF A03

Thermal fatigue cycling in turbine blades under laboratory conditions is used to complement engine development testing and component theoretical lifting methods. The technique produced the required component temperatures by flame heating with a kerosene burning Dart engine combustor. The equipment improvements provide direct and gas bending load simulation and a high level of accuracy in cycle generation and control. Failure results show good agreement with those observed during engine service. ESA

**N91-10068#** Rolls-Royce Ltd., Derby (England).
**THE EVOLUTION OF THE BYPASS ENGINE**
G. M. Lewis 27 Oct. 1989 14 p Presented at DGLR Symposium on 50 Years of Jet-Powered Flight, Munich, Fed. Republic of Germany, 26-27 Oct. 1989
(PNR-90707; ETN-90-97939) Copyright Avail: NTIS HC/MF A03

The by-pass principle was understood in the early days of the jet engine. Exploitation of the known concepts progressed as the inherent design problems were solved. The advances which reduced the mechanical design problems of aircraft engines and components are summarized. Engine designs representing significant steps in the evolution of the by-pass engine are identified. ESA

**N91-10069#** Rolls-Royce Ltd., Coventry (England). Industrial and Marine.
**GAS TURBINES FOR MAIN PROPULSION AND AUXILIARY POWER SYSTEMS**
D. J. Pratley and D. A. Owen Derby, England 13 Jul. 1989 49 p Presented at West European Graduate Education Marine Technology 12th Graduate School Propulsion Systems, 10-13 Jul. 1989
(PNR-90709; ETN-90-97940) Copyright Avail: NTIS HC/MF A03

The warship machinery requirements concerning reliability, flexibility, maintenance time, service life, noise level, exhaust and infrared emission are discussed. The aero derivative gas turbines and the reasons for selecting gas turbines for marine propulsion are given. The characteristics of operation of several turbines and their installation in ships are described. Suggestions for turbine power increase are given. ESA

**N91-10070#** Rolls-Royce Ltd., Bristol (England).
**TECHNOLOGY UPDATE OF EARLY GAS TURBINE DESIGNS**
Alan Rhodes Derby, England 21 Sep. 1989 12 p Presented at Tactical V/STOL Aircraft Symposium, New Bern, NC, 19-21 Sep. 1989
(PNR-90710; ETN-90-97941) Copyright Avail: NTIS HC/MF A03

The power plant of the Pegasus gas turbine is described. The service hours of Pegasus from 1969 to 1989 in different countries are presented. The design evolution of several modules and subassemblies are shown. The improvements obtained by the total package of changes introduced through the Pegasus update program are summarized. The application of up to date technology to the system provides a cost effective way of bringing to the operator a competitive product. ESA

**N91-10071#** Rolls-Royce Ltd., Bristol (England).
**FUTURE SUPERSONIC TRANSPORT POPULSION OPTIMIZATION**
B. W. Lowrie Derby, England 8 Nov. 1989 8 p Presented ar European Symposium on Future Supersonic/Hypersonic Transport, Strasbourg, France, 8-9 Nov. 1989
(PNR-90737; ETN-90-97950) Copyright Avail: NTIS HC/MF A02

The interest in second generation supersonic transport is considered. The propulsion systems necessary for a commercially and environmentally acceptable aircraft are identified. It is shown that for an isolated installation the tandem fan concept is the best. A feature of most other systems is the increased installation cross section required at a cruise and this causes penalizing levels of ware drag of an isolated system. Typical weight penalities are found to be of less importance than the wave drag. The need to consider integrated rather than isolated installations is emphasized. ESA

**N91-10072#** Rolls-Royce Ltd., Bristol (England).
**APPLICATIONS OF THERMALLY SPRAYED COATING SYSTEMS IN AERO ENGINES**
T. N. Rhys-Jones Derby, England 15 Sep. 1989 16 p Presented at 12th International Conference on Thermal Spraying, London, England, 1989
(PNR-90750; ETN-90-97955) Copyright Avail: NTIS HC/MF A03

The principle thermal spray coating process used in aero engine applications are oultlined. Particular attention is given to high velocity combustion and plasma spray techniques. The use of coatings for wear resistance, clearance control, environmental degradation resistance and thermal barrier applications are described. The characteristics of the coatings exhibit a marked dependence on the thermal spray technique itself, the source of materials used and the spray process parameters. ESA

**N91-10073#** Rolls-Royce Ltd., Coventry (England). Advanced Technology Center.
**FABRICATION ASPECTS OF GLASS MATRIX COMPOSITES FOR GAS TURBINE APPLICATIONS**
David A. Clarke Derby, England 12 Apr. 1990 12 p Presented at Warwick University Institute of Physics Conference on New Materials and Their Applications, Coventry, England, 10-12 Apr. 1990
(PNR-90752; ETN-90-97956) Copyright Avail: NTIS HC/MF A03

The background to the development of Glass Matrix Composites (GMC's) including the basic fabrication methods is presented. Some of the key problems involved in manufacturing production quantities of GMC gas turbine components are described. The need for highly repeatable, and hence largely automated, processing methods are highlighted. Glass/glass-ceramic matrix composites have mechanical properties suitable for use in gas turbines. The requirement for reliable production process is the repeatability to ensure high quality and the minimum post-fabrication inspection. ESA

**N91-10074#** Rolls-Royce Ltd., Derby (England).
**HEAT TRANSFER IN AERO ENGINE GAS TURBINES, PART 1**
C. T. J. Scrivener 15 Jun. 1990 37 p Submitted for publication
(PNR-90754-Pt-1; ETN-90-97958) Copyright Avail: NTIS HC/MF A03

Some turbine blade designs, and some important aspects of airfoil internal heat transfer are described. The airfoil external heat transfer is discussed. For the rotor blades of high temperature gas turbines, modern multipass cooling configurations provide efficient effective cooling. They can provide low coolant flow, consistent with this high temperature capability. The heat transfer in airfoil internal passages is well understood. This includes both plain passages, and the characteristics of bends, and enhancement by ribs, pedestals and impingement. The areas where future heat transfer research is required, in order to understand the basic process involved, are summarized. ESA

**N91-10075#** Rolls-Royce Ltd., Derby (England).
**RE-ENGINING: REAL STAGE 3 COMPLIANCE PLUS OTHER BENEFITS**
K. Goddard 6 Apr. 1990 7 p Presented at Avmark Services Ltd. 1990 Update Aircraft Noise Attenuation Conference, 4-6 Apr. 1990
(PNR-90755; ETN-90-97959) Copyright Avail: NTIS HC/MF A02

A study to show that re-engining is the only satisfactory way in converting today's noisy stage 2 airliners to give stage 3 compliance with clear and comfortable margins, together with enhanced performance and improved fuel consumption is presented. The importance of eliminating stage 2 operations for the benefit of the community is summarized. The advantages and driving force behind previous post war re-engining programs are described. ESA

**N91-10076#** Rolls-Royce, Inc., Atlanta, GA.
**DESIGN/DEVELOPMENT ISSUES FOR HIGH BYPASS RATIO FANS**
R. R. Moritz and D. J. Nicholas (Rolls-Royce Ltd., Derby, England) Derby, England 15 May 1990 16 p Presented at 37th Annual General Meeting and 2nd Symposium on Propulsion, Toronto, Ontario, 15 May 1990
(PNR-90758; ETN-90-97960) Copyright Avail: NTIS HC/MF A03

Some of the lessons learned in the course of the generation of the RB211 series of engines are presented. The early stages of RB211 development are underlined. Recent experience from present day RB211 program staff is stressed. The RB211 family of engine is compared to other high bypass ratio civil engines. The most obvious differences is in its use of lower aspect ratio fan blades. This feature is credited with a wide range of benefits including better performance, durability and cost of ownership. These and other points are developed. ESA

## 08 AIRCRAFT STABILITY AND CONTROL

Includes aircraft handling qualities; piloting; flight controls; and autopilots.

For related information see also *05 Aircraft Design, Testing and Performance.*

**N91-10077** National Aerospace Lab., Tokyo (Japan). STOL Aircraft Project Group.
**THE FULL-BODY GROUND VIBRATION TESTS USING THE LOW-NOISE STOL TEST PLANE [TEISOUON SUTORU JIKKENKI NO ZENKI CHIJOU SHINDOU SHIKEN (SHINDOU DETA KANRISHISUTEMU)]**
Oct. 1987 30 p In JAPANESE
(NAL-TM-576; ISSN-0452-2982; JTN-90-80005) Avail: NTIS HC/MF A03

Experimental oscillation test equipment of NAL (National Aerospace Laboratory) was used for the whole-craft terrestrial oscillation test of the low-noise experimental STOL craft. The main components of the equipment include a system for analyzing multi-point applied oscillation, an oscillation data control system and a model analyzer. An oscillation test of the actual craft will need the exchange between several large scale or personal computers of the data obtained in the oscillation analyses and the experimental oscillation test. The oscillation control system assures the interexchange of data between different data types and the conversion of information media. This report presents the configuration and funtions of the system for analyzing multi-point applied oscillation and describes the role of the oscillation data control system in the whole-craft oscillation test. The report also described the developed software and its actual applications. NASDA

**N91-10078*#** National Aeronautics and Space Administration. Langley Research Center, Hampton, VA.
**DETERMINATION OF THE PRESSURE DRAG OF AIRFOILS BY INTEGRATION OF SURFACE PRESSURES**
William H. Phillips Oct. 1990 26 p
(NASA-TM-102722; NAS 1.15:102722) Avail: NTIS HC/MF A03 CSCL 01C

A study was conducted of the causes of pressure drag of subsonic airfoils. In a previous paper by the author, the pressure drag is obtained by calculating the total drag from the momentum defect in the boundary layer at the trailing edge and subtracting the friction drag obtained from integration of surface friction along the chord. Herein, the pressure drag is obtained by integrating the streamwise components of surface pressure around the airfoil. Studies were made to verify the accuracy of the integration procedure. The values of pressure drag were much smaller than those obtained by the previous method. This lack of agreement is attributed to the difficulty of calculating boundary layer conditions in the vicinity of the trailing edge and to the extreme sensitivity of the circulation and lift to the trailing edge conditions. The results of these studies are compared with those of previous investigations. Author

**N91-10079*#** National Aeronautics and Space Administration. Hugh L. Dryden Flight Research Facility, Edwards, CA.
**FLIGHT CHARACTERISTICS OF A MODIFIED SCHWEIZER SGS1-36 SAILPLANE AT LOW AND VERY HIGH ANGLES OF ATTACK**
Alex G. Sim Jul. 1990 48 p
(NASA-TP-3022; H-1563; NAS 1.60:3022) Avail: NTIS HC/MF A03 CSCL 01C

A manned flight research program using a modified sailplane was conducted to very high angles of attack at the NASA-Ames. Piloting techniques were established that enabled the pilot to attain and stabilize on an angle of attack in the 30 to 72 deg range. Aerodynamic derivatives were estimated from the flight data for both low and very high angles of attack and are compared to wind tunnel data. In addition, limited performance and trim data are presented. Author

## 09 RESEARCH AND SUPPORT FACILITIES (AIR)

Includes airports, hangars and runways; aircraft repair and overhaul facilities; wind tunnels; shock tubes; and aircraft engine test stands.

For related information see also *14 Ground Support Systems and Facilities (Space).*

**N91-10080** National Aerospace Lab., Tokyo (Japan).
**CONFIGURATION, FUNCTION AND PERFORMANCE OF THE FLIGHT SIMULATION TEST FACILITY AND ITS MOTION SIMULATION SYSTEM [HIKOU SHIMYURESHON SHIKEN SETSUBI MOSHON MOGI SOUCHI NO KOUSEI OYOBI KINOUSEINOU]**
Hiroyasu Kawahara, Masanori Okabe, Akira Watanabe, Toshio Bando, and Kaoru Wakairo Jun. 1987 38 p In JAPANESE
(NAL-TM-575; ISSN-0452-2982; JTN-90-80004) Avail: NTIS HC/MF A03

The National Aerospace Laboratory (NAL) has fixed the simulation control unit, the visual simulation unit and the motion simulation unit over a period of three years and four months since 1980. The present report explains the configuration, function, and capacity of the motion simulation unit. For multi-freedom-degree motion simulation units, various kinds of systems have been developed and are in use such as Zimbal method, joint-motion suspension method, joint-motion support method, and special drive method. The joint-motion six-freedom-degree support method was adopted. NASDA

**N91-10081** National Aerospace Lab., Tokyo (Japan).
**MODIFICATION IN THE MAIN AIR BLOWER UNIT FOR TWO METER TIMES TWO METER TRANSONIC WIND TUNNEL: PLAN AND CONFIGURATION [NI METORU KAKERU NI METORU SENONSOKU FUDOU SHU SOUFUUKI YOU KUDOUSETSUBI NO KOUSHIN (KEIKAKU TO KOUSEI NI TSUITE)]**
Masamitsu Suzuki, Nobuhiro Toda, Yukio Komatsu, and Toshio Karasawa Feb. 1988 27 p In JAPANESE
(NAL-TM-580; ISSN-0452-2982; JTN-90-80008) Avail: NTIS HC/MF A03

As a part of the improvement of the two meter times two meter Transonic Wind Tunnel, the National Aerospace Laboratory decide to modify the main air blower unit, which is located at the center of this tunnel. Repair of this unit was completed at the end of May, 1987. The improvement plan and modified unit configulation are described. NASDA

**N91-10082** National Aerospace Lab., Tokyo (Japan).
**FUNCTION AND PERFORMANCE OF VISUAL SIMULATION UNIT OF FLIGHT SIMULATION TEST FACILITY**
Kaoru Wakairo, Hiroyasu Kawahara, Akira Watanabe, and Masanori Okabe Feb. 1988 28 p In JAPANESE
(NAL-TM-581; ISSN-0452-2982; JTN-90-80009) Avail: NTIS HC/MF A03

The visual simulation unit with CGI (Computer Generated Imagery) enables a simulation of natural conditions by obtaining a wide view thanks to an increase in the number of display channels which catch sight of a wider range of flight. It is characterized by the ability to indicate an object in motion within sight as well as to add, delete, change, or otherwise revise the configuration of the ground or buildings generated as a simulated vision. The configuration, function, and capacity of the visual simulation unit with the CGI was introduced in consideration of the necessity to cope with a simulation test intended for the research and development of a new aircraft model including STOL at the National Aerospace Laboratory (NAL). Attention was paid in the designing of the unit to the ease of preparation of a three-dimensional visual model, the ability to simulate a daytime sight in color and nighttime lights of various kinds, the ability to easily simulate natural conditions and the ease of maintenance. NASDA

**N91-10083*#** Nevada Univ., Reno. Engineering Research and Development Center.
**NUMERICAL INVESTIGATIONS IN THREE-DIMENSIONAL INTERNAL FLOWS Semiannual Status Report, 1 Jan. - 30 Jun. 1990**
William C. Rose 11 Sep. 1990 29 p
(Contract NCC2-507)
(NASA-CR-186958; NAS 1.26:186958) Avail: NTIS HC/MF A03 CSCL 14B

The flow in the transonic test facility was investigated using the three dimensional computational fluid dynamics techniques. The application of the full Navier-Stokes three dimensional code to the flow qualities in the contraction section of transonic wind tunnel is discussed. Initially, two dimensional solutions indicated the possibility for large secondary flow to exist as a result of the asymmetries involved in the contraction section as it is constructed. The results of a full three dimensional solution indicate that only minor pressure variations actually occur in the contraction section within any given cross flow plane. Further analysis of the three dimensional solution indicated that these slight lateral pressure gradients lead to negligible secondary flows, except within a small region in the corners within the boundary layer. On the basis of present solution, it would not be expected that any flow asymmetries and/or secondary flow present within contraction section are associated with the methods by which the contraction is implemented in its present configuration. Author

**N91-10084#** Federal Aviation Administration, Atlantic City, NJ.
**FAA AIR TRAFFIC OPERATIONAL EVALUATION OF AUTOMATED SURFACE OBSERVING SYSTEM (ASOS)**
Elizabeth Turcich and Bruce E. Ware Oct. 1990 35 p
(DOT/FAA/CT-TN90/42) Avail: NTIS HC/MF A03

The results of the Federal Aviation Administration (FAA) Air Traffic Operational Evaluation of Automated Surface Observing System (ASOS) at the Tulsa International Airport, Oklahoma are detailed. The evaluation was conducted in order to obtain operational air traffic controller reaction to the AAI Corporation preproduction ASOS. The evaluation resulted in numerous recommendations to improve the ASOS prior to production. Author

**N91-10085*#** Essex Corp., Huntsville, AL. Space Systems Group.
**THE DESIGN AND FABRICATION OF THE CENTAUR NEUTRAL BUOYANCY TRAINER AND RELATED HARDWARE Final Report**
Alan S. Ware and Michael Hollingsworth 5 Apr. 1986 74 p
(Contract NAS9-17325)
(NASA-CR-171944; NAS 1.26:171944; H-86-04) Avail: NTIS HC/MF A04 CSCL 14B

Two full scale mockups of the Centaur upper stage were designed, fabricated and delivered to NASA. One was the Centaur Weightless Environment Training Facility (WETF) trainer and the other was the Centaur 1-G mockup. The Centaur upper stage booster is designed to carry the spacecraft Galileo to Jupiter, and the spacecraft Ulysses to an orbit around the Sun after launch from the Space Shuttle. The flight vehicle has several Extravehicular Activity (EVA) contingency tasks that require crew training. This need for crew training generated the requirement for the Centaur WETF crew trainer, which is high fidelity in areas of expected crew interface. During the production of the Centaur WETF crew trainer, the need for a jumper cable from Centaur to the Orbiter was identified. This EVA contingency task would be the installation of a cable from the Orbiter cargo bay sill to various command data boxes on Centaur to allow crew control deployment should a failure occur. This task required the upgrading of volumetric boxes on the trainer to a high fidelity configuration including electrical connector installation and cable routing. Author

**N91-10086#** Institut Franco-Allemand de Recherches, Saint-Louis (France).
**THE ISL HYPERSONIC SHOCK TUNNEL AND ITS INSTRUMENTATION**
G. Smeets 1 Jun. 1989 22 p Presented at VKI (AGARD Ad-Hoc Study Group on Hypersonic Technology-Subgroup on Hypersonic Wind Tunnel Instrumentation) Conference, 16 May 1989
(ISL-CO-213/89; ETN-90-97572) Avail: NTIS HC/MF A03

Th ISL hypersonic shock tunnel is described and the characteristics of hypersonic flows which can be produced in the shock tunnel are given. The five essential measuring techniques developed or collected during the last three decades when operating the tunnel, are presented: differential interferometry for flow vizualization and/or quantitative flow density measurements; laser differential interferometry for precise measurements of optical paths in a low density gas medium; heat flux measurements with thin film resistance thermometers; laser Doppler velocimetry; and the measurement of aerodynamic forces and moments in milliseconds. ESA

**N91-10087#** National Aerospace Lab., Tokyo (Japan).
**EVALUATION OF FLOW QUALITY IN NEWLY CONSTRUCTED LOW-TURBULENCE CALIBRATION WIND-TUNNEL FOR LASER VELOCIMETERS**
Shohei Takagi Feb. 1990 14 p In JAPANESE; ENGLISH summary
(NAL-TR-1054; ISSN-0389-4010) Avail: NTIS HC/MF A03

A low turbulence calibration wind tunnel for laser velocimeters was constructed at NAL. Detailed flow quality measurements in this facility were successively achieved to obtain a better understanding of the characteristics of facility disturbances and identification of their sources, using two hot-wire anemometers, a microphone and an accelerometer. Experimental results show that overall residual turbulence levels in free stream are 0.04 and 0.06 percent at fan speeds of 600 RPM and 1200 RPM, respectively. Extensive analyses of turbulence fluctuations show that the free stream velocity is unexpectedly contaminated by acoustic disturbances, which are regarded as non-vortical fluctuations generated by fan blades and vibratory resonance of a portion of the wind tunnel. Such pressure disturbances acoustically propagate into the flow direction. Cross correlation measurements between two distant anemometers indicate that the contamination level reaches 70 percent in the overall axial fluctuation energy at 600 RPM. It is estimated that the vortical turbulence level is about 0.022 percent at this speed. Author

## 12 ASTRONAUTICS (GENERAL)

For extraterrestrial exploration see *91 Lunar and Planetary Exploration.*

**N91-10088#** Joint Publications Research Service, Arlington, VA.
**JPRS REPORT: SCIENCE AND TECHNOLOGY. USSR: SPACE**
22 Sep. 1989 82 p Transl. into ENGLISH from various Russian articles
(JPRS-USP-89-009) Avail: NTIS HC/MF A05

Abstracts of Soviet literature in various areas of space sciences are compiled. The following subject areas are covered: manned missions; space sciences; interplanetary sciences; space engineering; space applications; and space policy and administration. M.G.

**N91-10089#** Joint Publications Research Service, Arlington, VA.
**JPRS REPORT: SCIENCE AND TECHNOLOGY. USSR: SPACE**
15 Mar. 1990 72 p Transl. into ENGLISH of various Russian documents
(JPRS-USP-90-001) Avail: NTIS HC/MF A04

A collection of short news articles, many of which appeared in U.S.S.R. newspapers, and abstracts of scientific articles is presented. Topics covered include manned space mission highlights, space science research, interplanetary sciences, life sciences, space engineering, space applications, and space policy and administration. Author

**N91-10090#** Joint Publications Research Service, Arlington, VA.
**JPRS REPORT: SCIENCE AND TECHNOLOGY. USSR: SPACE**
15 May 1990 65 p Transl. into ENGLISH from various Russian articles
(JPRS-USP-90-002) Avail: NTIS HC/MF A04

Abstracts of Soviet literature in various areas of the space sciences are compiled. The following subject areas are covered: manned missions; space sciences; interplanetary sciences; space engineering; space applications; and space policy and administration. M.G.

**N91-10091#** Messerschmitt-Boelkow-Blohm/Entwicklungspring Nord, Bremen (Germany, F.R.). Dienstleistungsbereich.
**COLUMBUS LOGISTICS SUPPORT. A CONCEPTIONAL DEFINITION OF THE OPERATIONAL PHASE**
H. J. C. Koopmann and Mike C. Attwood 1990 9 p
(MBB-UO-0093-90-PUB; ETN-90-97837; OTN-027616) Avail: NTIS HC/MF A02

In order to logistically support the systems included in the Columbus program, logistic support concepts and facilities are developed. The logistics support functions for the Columbus operational phase includes the identification of major facility requirements and recommendations for support of the implementation planning. These tasks have to be complemented by the definition and implementation of a logistics support system and its related facilities and proceedings. Emphasis is given to the logistics functions which drive facility requirements, on general considerations for a long term support program, e.g., centralization aspects, and on the intended implementation approach. ESA

**N91-10418#** Imperial Coll. of Science and Technology, London (England). Space and Atmospheric Physics Group.
**MULTISPACECRAFT MEASUREMENT AT VARYING SCALELENGTHS: THE CLUSTER/REGATTA OPPORTUNITY**
D. J. Southwood *In* ESA, Space Plasma Physics Investigation by Cluster and Regatta May 1990 p 1-5 (For primary document see N91-10417 01-46)
Copyright Avail: NTIS HC/MF A08; EPD, ESTEC, Noordwijk, Netherlands HC 40 Dutch guilders

# 13 ASTRODYNAMICS

Includes powered and free-flight trajectories; and orbital and launching dynamics.

**N91-10092*#** National Aeronautics and Space Administration. Marshall Space Flight Center, Huntsville, AL.
**LONG-TERM ORBITAL LIFETIME PREDICTIONS**
P. E. Dreher and A. T. Lyons Oct. 1990 26 p
(NASA-TP-3058; NAS 1.60:3058) Avail: NTIS HC/MF A03 CSCL 22A

Long-term orbital lifetime predictions are analyzed. Predictions were made for three satellites: the Solar Max Mission (SMM), the Long Duration Exposure Facility (LDEF), and the Pegasus Boiler Plate (BP). A technique is discussed for determining an appropriate ballistic coefficient to use in the lifetime prediction. The orbital decay rate should be monitored regularly. Ballistic coefficient updates should be done whenever there is a significant change in the actual decay rate or in the solar activity prediction. Author

**N91-10420#** Imperial Coll. of Science and Technology, London (England). Space and Atmospheric Physics Group.
**REVIEW OF THE CLUSTER ORBIT AND SEPARATION STRATEGY: CONSEQUENCE FOR MEASUREMENTS**
M. W. Dunlop *In* ESA, Space Plasma Physics Investigation by Cluster and Regatta May 1990 p 17-22 (For primary document see N91-10417 01-46)
Copyright Avail: NTIS HC/MF A08; EPD, ESTEC, Noordwijk, Netherlands HC 40 Dutch guilders

# 14 GROUND SUPPORT SYSTEMS AND FACILITIES (SPACE)

Includes launch complexes, research and production facilities; ground support equipment, e.g., mobile transporters; and simulators.

For related information see also *09 Research and Support Facilities (Air).*

**N91-10093#** National Oceanic and Atmospheric Administration, Washington, DC. National Environmental Satellite, Data, and Information Service.
**EDUCATOR'S GUIDE FOR BUILDING AND OPERATING ENVIRONMENTAL SATELLITE RECEIVING STATIONS**
R. Joe Summers (Chambersburg Area Senior High School, PA.) Feb. 1989 99 p Original contains color illustrations
(NOAA-TR-NESDIS-44) Avail: NTIS HC/MF A05

A great deal of meteorological and weather information is transmitted from satellites via direct readout to ground stations where it can be displayed and analyzed. This publication is designed to provide teachers with the basic information needed to operate a direct readout ground station so that they can introduce students to this new technology. With a direct readout ground station, every classroom can have access to millions of dollars of high tech equipment every day. Author

**N91-10094#** Department of Energy, Washington, DC.
**PREVENTION OF BREAKDOWN BEHIND RAILGUN PROJECTILES Patent Application**
Ronald S. Hawke, inventor (to DOE) (Lawrence Livermore National Lab., CA.) 20 Apr. 1989 18 p
(Contract W-7405-eng-48)
(DE90-014573; US-Patent-Appl-SN-341019; Patents-US-A7341019) Avail: NTIS HC/MF A03

An electromagnetic railgun accelerator system for accelerating projectiles by a plasma arc, introduces a breakdown inhibiting gas into the railgun chamber behind the accelerating projectile. The breakdown inhibiting gas, which absorbs electrons, is a halide or a halide compound such as fluorine or SF6. The gas is introduced between the railgun rails after the projectile has passed through inlets in the rails or the projectile; by coating the rails or the projectile with a material which releases the gas after the projectile passes over it; by fabricating the rails or the projectile or insulators out of a material which releases the gas into the portions of the chamber through which the projectile has traveled. The projectile may have a cavity at its rear to control the release of ablation products. DOE

**N91-10095#** Los Alamos National Lab., NM.
**RAILGUN RESTRIKE CONTROL Patent Application**
Jerald V. Parker, inventor (to DOE) 11 Apr. 1989 18 p
(Contract W-7405-eng-36)
(DE90-015108; US-Patent-Appl-SN-336377; Patents-US-A7336377) Avail: NTIS HC/MF A03

An electromagnetic railgun having electrically conductive segments overlying but insulated from the rails were designed. Switches are connected between each segment and its underlying rail. As a projectile and its plasma armature pass each segment, the switch associated with that segment opens, disconnecting the flow of current into the area behind the plasma armature. Without a source of current, parasitic current flow is prevented. DOE

**N91-10096#** Lawrence Livermore National Lab., CA.
**APPLICATION OF FABRY-PEROT VELOCIMETRY TO HYPERVELOCITY IMPACT EXPERIMENTS**
H. H. Chau and J. E. Osher Jun. 1990 10 p Presented at the SPIE 1990 International Symposium on Optical and Optoelectronic Applied Science and Engineering Exhibit, San Diego, CA, 8-13 Jul. 1990 Submitted for publication
(Contract W-7405-eng-48)
(DE90-015612; UCRL-102468; CONF-900756-26) Avail: NTIS HC/MF A02

The Fabry-Perot (F-P) velocimeter is our main diagnostic tool for hypervelocity impact experiments with the electric gun. Because of its immunity to electromagnetic interference, F-P velocimetry is well suited to studying the performance of flyers, providing data on velocity calibration, acceleration characteristics, and material erosion as well as spallation of various materials under high-velocity impact, measurement of impact pressure pulses, and Hugoniot measurements of composite materials. We present results and data from selected experiments and compare them with code predictions. DOE

## 15 LAUNCH VEHICLES AND SPACE VEHICLES

Includes boosters; operating problems of launch/space vehicle systems; and reusable vehicles.

For related information see also *20 Spacecraft Propulsion and Power.*

**N91-10097#** Bertin et Cie., Plaisir (France).
**TIME/FREQUENCY ANALYSIS OF VIBRO-ACOUSTIC BEHAVIOUR OF A LAUNCHER IN FLIGHT**
C. Fumoux and G. Marquette 1990 5 p Presented at Internoise 1990, Goteberg, Sweden, 13-18 Aug. 1990 Sponsored by CNES
(ETN-90-97584) Avail: NTIS HC/MF A01

A satellite placed under the cap of a space launcher is submitted to severe vibro-acoustic conditions especially during lift off and transonic phases. This high acoustic level field, which can be damaging for the satellite, is mainly nonstationary. Thus, caution must be taken about results produced by classical Fourier analysis, since they rely on strong stationary hypotheses. To characterize in an appropriate way nonstationary data, time frequency was analyzed by means of wavelet transform. Conceptually, the wavelet transform is similar to a Fourier transform, as there is convolution between the signal and an analyzing window, but it differs in that this window is frequency dependent, leading to a constant accuracy for all frequencies. In addition, the chosen wavelet, Morlet's wavelet, permits a direct reconstruction of the original time signature. This method was successfully applied to the analysis of the Ariane 4 launcher vibro-acoustic behavior. This study was based on real data, signals of transducers located at different places on the launcher and its proximity. Results show the interest of this technique for shock and transient analysis, nonstationarities, identification, and localization in the time/frequency plane. ESA

**N91-10098*#** George Washington Univ., Hampton, VA.
**FIRST EVALUATION OF THE MAIN PARAMETERS IN THE DYNAMICS OF THE SMALL EXPENDABLE DEPLOYER SYSTEM (SEDS) FOR A TETHERED SATELLITE Contractor Report, 4 Aug. - 2 Sep. 1988**
Luigi DeLuca Washington NASA Oct. 1990 18 p
(Contract NAS1-18458)
(NASA-CR-4319; NAS 1.26:4319) Avail: NTIS HC/MF A03
CSCL 22B

The dynamics of the motion of the Small Expendable Deployer System (SEDS) is studied by using a simplified model in which no external forces (except the gravity gradient field) are applied on the tethered body and the tether is assumed massless. The dynamics of SEDS operation is modeled as a sequence of two phases: the deployment phase and the swing phase. For the first one the velocity dependent forces are found to force the tether forward from the local vertical. When the deployment ends, Coriolis effects vanish and the swing phase begins, which is characterized by a wide free libration. The time duration as well as velocity, acceleration and tension of the tethered body are estimated for both deployment and swing phases. Author

**N91-10099#** National Aerospace Lab., Tokyo (Japan).
**VIBRATION TESTING OF A 1/5 SCALE MODEL OF H-2 LAUNCH VEHICLE**
Masakatsu Minegishi, Masaaki Sano, Keiji Komatsu, Toshiyuki Morita, Yoshiki Morino, Kenji Tomioka, and Isao Ujino Apr. 1990 156 p In JAPANESE; ENGLISH summary
(NAL-TR-1061; ISSN-0389-4010) Avail: NTIS HC/MF A08

A 1/5 scale replica model of the H-2 launch vehicle was constructed and tested for study of vehicle dynamics. This model was designed to duplicate, in miniature, as many of the full scale structural elements as was economically and technically feasible. A series of vibration tests, from the moving launcher phase to the second-state burn-out phase, were carried out, and resonant frequencies, mode shapes, and modal dampings were measured for each case. The test data verified the mathematical modeling techniques used for predicting the vibration characteristics of the various configurations of the H-2 launch vehicle. Author

## 16 SPACE TRANSPORTATION

Includes passenger and cargo space transportation, e.g., shuttle operations; and space rescue techniques.

For related information see also *03 Air Transportation and Safety* and *18 Spacecraft Design, Testing and Performance.* For space suits see *54 Man/System Technology and Life Support.*

**N91-10100*#** National Aeronautics and Space Administration, Washington, DC.
**NATIONAL SPACE TRANSPORTATION SYSTEM REFERENCE. VOLUME 2: OPERATIONS**
Sep. 1988 135 p
(NASA-TM-89785; NAS 1.15:89785) Avail: NTIS HC/MF A07
CSCL 22B

An overview of the Space Transportation System is presented in which aspects of the program operations are discussed. The various mission preparation and prelaunch operations are described including astronaut selection and training, Space Shuttle processing, Space Shuttle integration and rollout, Complex 39 launch pad facilities, and Space Shuttle cargo processing. Also, launch and flight operations and space tracking and data acquisition are described along with the mission control and payload operations control center. In addition, landing, postlanding, and solid rocket booster retrieval operations are summarized. Space Shuttle program management is described and Space Shuttle mission summaries and chronologies are presented. A glossary of acronyms and abbreviations are provided. M.G.

## 17 SPACE COMM., SPACECRAFT COMM., COMMAND & TRACKING

Includes telemetry; space communications networks; astronavigation and guidance; and radio blackout.

For related information see also *04 Aircraft Communications and Navigation* and *32 Communications and Radar.*

**N91-10345#** Meteorological Satellite Center, Tokyo (Japan).
**TELEMETRY SUBSYSTEM**
Saburo Takaku, Takeshi Yokoya, and Akihiko Tange *In its* Meteorological Satellite Center Technical Note. Special Issue (1989). Summary of GMS System. 1: Telecommunication System Mar. 1989 p 63-70 In JAPANESE; ENGLISH summary (For primary document see N91-10338 01-42)
Avail: NTIS HC/MF A08

# 18 SPACECRAFT DESIGN, TESTING AND PERFORMANCE

Includes satellites; space platforms; space stations; spacecraft systems and components such as thermal and environmental controls; and attitude controls.

For life support systems see *54 Man/System Technology and Life Support.* For related information see also *05 Aircraft Design, Testing and Performance, 39 Structural Mechanics,* and *16 Space Transportation.*

**N91-10101*#** Joint Oceanographic Inst., Inc., Washington, DC.
**THE SCIENTIFIC CASE FOR MAGNETIC FIELD SATELLITES Final Report**
George E. Backus, ed., Edward R. Benton, Christopher G. A. Harrison, and James R. Heirtzler (Woods Hole Oceanographic Inst., MA.) Sep. 1987 18 p
(Grant NAGw-856)
(NASA-CR-186532; NAS 1.26:186532) Avail: NTIS HC/MF A03 CSCL 22B

To make full use of modern magnetic data and the paleomagnetic record, we must greatly improve our understanding of how the geodynamo system works. It is clearly nonlinear, probably chaotic, and its dimensionless parameters cannot yet be reproduced on a laboratory scale. It is accessible only to theory and to measurements made at and above the earth's surface. These measurements include essentially all geophysical types. Gravity and seismology give evidence for undulations in the core-mantle boundary (CMB) and for temperature variations in the lower mantle which can affect core convection and hence the dynamo. VLBI measurements of the variations in the Chandler wobble and length of day are affected by, among other things, the electromagnetic and mechanical transfer of angular momentum across the CMB. Finally, measurements of the vector magnetic field, its intensity, or its direction, give the most direct access to the core dynamo and the electrical conductivity of the lower mantle. The 120 gauss coefficients of degrees up to 10 probably come from the core, with only modest interference by mantle conductivity and crustal magnetization. By contrast, only three angular accelerations enter the problem of angular momentum transfer across the CMB. Satellite measurements of the vector magnetic field are uniquely able to provide the spatial coverage required for extrapolation to the CMB, and to isolate and measure certain magnetic signals which to the student of the geodynamo represent noise, but which are of great interest elsewhere in geophysics. Here, these claims are justified and the mission parameters likely to be scientifically most useful for observing the geodynamo system are described. Author

**N91-10102*#** Draper (Charles Stark) Lab., Inc., Cambridge, MA.
**ENTRY VEHICLE PERFORMANCE ANALYSIS AND ATMOSPHERIC GUIDANCE ALGORITHM FOR PRECISION LANDING ON MARS M.S. Thesis - Massachusetts Inst. of Technology**
Todd A. Dieriam Jun. 1990 169 p
(Contract NAS9-18147)
(NASA-CR-185614; NAS 1.26:185614; CSDL-T-1053) Avail: NTIS HC/MF A08 CSCL 22B

Future missions to Mars may require pin-point landing precision, possibly on the order of tens of meters. The ability to reach a target while meeting a dynamic pressure constraint to ensure safe parachute deployment is complicated at Mars by low atmospheric density, high atmospheric uncertainty, and the desire to employ only bank angle control. The vehicle aerodynamic performance requirements and guidance necessary for 0.5 to 1.5 lift drag ratio vehicle to maximize the achievable footprint while meeting the constraints are examined. A parametric study of the various factors related to entry vehicle performance in the Mars environment is undertaken to develop general vehicle aerodynamic design requirements. The combination of low lift drag ratio and low atmospheric density at Mars result in a large phugoid motion involving the dynamic pressure which complicates trajectory control. Vehicle ballistic coefficient is demonstrated to be the predominant characteristic affecting final dynamic pressure. Additionally, a speed brake is shown to be ineffective at reducing the final dynamic pressure. An adaptive precision entry atmospheric guidance scheme is presented. The guidance uses a numeric predictor-corrector algorithm to control downrange, an azimuth controller to govern crossrange, and analytic control law to reduce the final dynamic pressure. Guidance performance is tested against a variety of dispersions, and the results from selected tests are presented. Precision entry using bank angle control only is demonstrated to be feasible at Mars. Author

**N91-10103*#** National Aeronautics and Space Administration. Marshall Space Flight Center, Huntsville, AL.
**SPACE STATION FREEDOM ENVIRONMENTAL CONTROL AND LIFE SUPPORT SYSTEM (ECLSS) PHASE 3 SIMPLIFIED INTEGRATED TEST TRACE CONTAMINANT CONTROL SUBSYSTEM PERFORMANCE**
J. L. Perry Washington Oct. 1990 30 p
(NASA-TM-4202; NAS 1.15:4202) Avail: NTIS HC/MF A03 CSCL 22B

Space Station Freedom environmental control and life support system testing has been conducted at Marshall Space Flight Center since 1986. The phase 3 simplified integrated test (SIT) conducted from July 30, 1989, through August 11, 1989, tested an integrated air revitalization system. During this test, the trace contaminant control subsystem (TCCS) was directly integrated with the bleed stream from the carbon dioxide reduction subsystem. The TCCS performed as expected with minor anomalies. The test set the basis for further characterizing the TCCS performance as part of advance air revitalization system configurations. Author

**N91-10104#** Pacific Northwest Lab., Richland, WA. Nuclear Systems and Concepts Dept.
**ADVANCED CERAMIC FABRIC BODY MOUNTED RADIATOR FOR SPACE STATION FREEDOM PHASE O DESIGN**
Brent J. Webb, Zen I. Antoniak, and Keith A. Pauley Jun. 1990 4 p Presented at the 5th AIAA/ASME Thermal Physics and Heat Transfer Conference, Seattle, WA, 18-20 Jun. 1990
(Contract DE-AC06-76RL-01830)
(DE90-016361; PNL-SA-17526; CONF-900619-7) Avail: NTIS HC/MF A01

A body mounted radiator concept constructed of advanced ceramic fabric materials for use with the Phase O design of Space Station Freedom is described. The radiator is expected to weigh between 1.4 and 3.5 kg/sq m of single sided radiating surface, use ammonia working fluid, be highly deployable, and exhibit good reliability characteristics. This compares well with the 11.8 kg/sq m for two sided radiators proposed for the current space station design. DOE

**N91-10105*#** Jet Propulsion Lab., California Inst. of Tech., Pasadena.
**A MOBILE SATELLITE EXPERIMENT (MSAT-X) NETWORK DEFINITION**
Charles C. Wang and Tsun-Yee Yan 15 Aug. 1990 56 p
(Contract NAS7-918)
(NASA-CR-187336; JPL-Publ-90-19; NAS 1.26:187336; MSAT-X-164) Avail: NTIS HC/MF A04 CSCL 22B

The network architecture development of the Mobile Satellite Experiment (MSAT-X) project for the past few years is described. The results and findings of the network research activities carried out under the MSAT-X project are summarized. A framework is presented upon which the Mobile Satellite Systems (MSSs) operator can design a commercial network. A sample network configuration and its capability are also included under the projected scenario. The Communication Interconnection aspect of the MSAT-X network is discussed. In the MSAT-X network structure two basic protocols are presented: the channel access protocol, and the link connection protocol. The error-control techniques used in the MSAT-X project and the packet structure are also discussed. A description of two testbeds developed for experimentally simulating the channel access protocol and link control protocol, respectively, is presented. A sample network configuration and some future network activities of the MSAT-X project are also presented. Author

**N91-10106*#** National Aeronautics and Space Administration. Langley Research Center, Hampton, VA.
**FILAMENT WOUND METAL LINED PROPELLANT TANKS FOR FUTURE EARTH-TO-ORBIT TRANSPORTS**
Ian O. MacConochie, Robert B. Davis, and William T. Freeman, Jr. Oct. 1988 32 p
(NASA-TM-100594; NAS 1.15:100594) Avail: NTIS HC/MF A03 CSCL 22B

For future Earth-to-orbit transport vehicles, reusability and lighter weights are sought for the main propellant tanks. To achieve this, a filament wound tank with a metal liner and an intermediate layer of foam-filled honeycomb is proposed. A hydrogen tank is used as an example. To accommodate mismatches in the expansion of liner and overwrap a design is proposed wherin the liner is configured so that the extension of the liner under pressure matches the expected contraction of the same liner due to the presence of a cryogen. In operation, the liner is pressurized at a rate such that the pressure strain matches the contraction due to decrease in temperature. As an alternate approach, compressive pre-stress is placed in the liner such that it will not separate from the overwrap. A finite element program is used to show stresses in the liner and overwrap for various tank pressures for the pre-stressed liner concept. A fracture mechanics analysis is made of the liners to determine tank life. The tank concept shown has a similar weight to the Shuttle external hydrogen tank, but the filament wound tank is expected to be reusable. Integration of the propellant tanks into a future transport vehicle is discussed. Author

**N91-10107#** Bertin et Cie., Plaisir (France).
**PRELIMINARY STUDIES BEFORE DEFINING A PAYLOAD ADAPTED TO THE PRIMATE MODEL**
Jean Boquet, Marc Aureille, and Claude Milhaud (Centre d'Etudes et de Recherches de Medecine Aerospatiale, Paris, France ) 1990 5 p
(ETN-90-97581) Avail: NTIS HC/MF A01

A preliminary study was carried out before a payload adapted to the primate model, to be flown onboard the RRS LIFESAT facility could be defined. With the prospect of an eight-week mission with a nominal load adapted to two adult Rhesus monkeys or four adult cynomolgus monkeys or eight adult squirrel monkeys, the purpose of this study was to determine: scientific objectives and constraints, animal maintenance conditions, functional specifications, preliminary technical specifications, safety specifications. The scientific value of this concept is confirmed and its agreement with research carried out on man or animal onboard manned spacecraft is shown. From a technical standpoint, compatibility with currently proposed LIFESAT program characteristics requires the nominal configuration to be reduced, limiting either the flight duration or the number of flown primates. ESA

**N91-10108#** Messerschmitt-Boelkow-Blohm/Entwicklungspring Nord, Bremen (Germany, F.R.). Dienstleistungsbereich.
**COLUMBUS ELEMENTS PROCESSING NEEDS AT KSC**
Dieter Husung 1990 10 p
(MBB-UO-0092-90-PUB; ETN-90-97836; OTN-027615) Avail: NTIS HC/MF A02

The Columbus Attached Laboratory will form an integral part of the Space Station Freedom and the Columbus Free Flying Laboratory will use the Space Station Freedom as a servicing base. The ground processing support for the initial delivery of the Columbus Attached Laboratory, payload outfitting launches, and the periodic resupply launches for both the Attached Laboratory and the Free Flyer is presented. The acceptance approach of flight hardware at the European facilities and the concepts for shipment to and essential processing at the launch site, are described. Primarily addressed is the intented use of the Space Station processing facility for these Columbus needs. A summary is presented in a scenario covering upload and download processing for the Columbus elements at KSC (Kennedy Space Center), Florida, U.S. ESA

**N91-10109#** Messerschmitt-Boelkow-Blohm G.m.b.H., Munich (Germany, F.R.). Integration Orbital Systems.
**OPTIMIZATION CRITERIA FOR THE DESIGN OF ORBITAL REPLACEMENT UNITS**
Manfred W. Schulze 1990 24 p Presented at the 17th International Symposium of Space Technology and Science, Tokyo, Japan, 21-25 May 1990 Prepared in cooperation with Erno Raumfahttechnik G.m.b.H.
(MBB-UO-0092-90-PUB; OTN-027668; ETN-90-97885) Avail: NTIS HC/MF A03

A reduction of life cycle costs of spacecraft or Space Station elements can be achieved by a modular build up which allows an in orbit replacement, maintenance, and service of functional units named Orbital Replacement Units (ORUs). The criteria for an optimal design for an ORU is presented. Requirements involving the user spacecraft configuration, the servicing vehicle, the handling by astronauts and remote manipulator system are considered. ESA

**N91-10423#** Academy of Sciences (USSR), Moscow. Space Research Inst.
**SMALL SPACE LAB AS A BASIC SPACECRAFT OF REGATTA PROJECT**
G. Avanesov, Ja. Ziman, A. Kogan, V. Kostenko, V. Fedotov, and V. Heifets *In* ESA, Space Plasma Physics Investigation by Cluster and Regatta May 1990 p 37-41 (For primary document see N91-10417 01-46)
Copyright Avail: NTIS HC/MF A08; EPD, ESTEC, Noordwijk, Netherlands HC 40 Dutch guilders

**N91-10576*#** National Aeronautics and Space Administration. Lyndon B. Johnson Space Center, Houston, TX.
**SPACE STATION**
Donald F. Stewart and Judith Hayes (Krug International, Houston, TX.) *In its* Workshop on Exercise Prescription for Long-Duration Space Flight Oct. 1989 p 15-18 (For primary document see N91-10574 01-52)
Avail: NTIS HC/MF A06 CSCL 22B

# 19 SPACECRAFT INSTRUMENTATION

For related information see also *06 Aircraft Instrumentation* and *35 Instrumentation and Photography.*

**N91-10110#** Centre National d'Etudes Spatiales, Toulouse (France).
**MAGNETIC SENSITIVITY OF ON-BOARD QUARTZ OSCILLATORS: STATE OF THE KNOWLEDGE**
Emmanuel Robert Dec. 1988 20 p In FRENCH; ENGLISH summary
(CNES-CT/DRT/TIT/TF-88/354; ETN-90-97812) Avail: NTIS HC/MF A03

The increasing accuracy of positioning systems, especially for space applications such as orbitography, requires better and better stability of the onboard oscillators. The magnetic environment, which can affect the onboard oscillator stability is investigated. The results of several experiments used in actual satellites are presented. Some explanations of the oscillator's sensitivity are proposed. A list of references reflecting the state of the knowledge is given. ESA

# 20 SPACECRAFT PROPULSION AND POWER

Includes main propulsion systems and components, e.g., rocket engines; and spacecraft auxilliary power sources.

For related information see also *07 Aircraft Propulsion and Power, 28 Propellants and Fuels, 44 Energy Production and Conversion,* and *15 Launch Vehicles and Space Vehicles.*

**N91-10111*#** General Dynamics Corp., San Diego, CA. Space Systems Div.
**HYBRID PROPULSION TECHNOLOGY PROGRAM: PHASE 1, VOLUME 1 Final Report, 6 Mar. - 20 Oct. 1989**
A. L. Schuler and D. R. Wiley 20 Nov. 1989 22 p
(Contract NAS8-37777)
(NASA-CR-183972; NAS 1.26:183972; GDSS-HPT-89-001-Vol-1)
Avail: NTIS HC/MF A03 CSCL 21H

A number of booster propulsion system concepts are being considered for the next generation of manned and unmanned space launch vehicles. The one propulsion system concept that has potential for reducing costs with increased safety, reliability, and performance is hybrid propulsion (HP). A HP system may be thought of as a liquid propulsion system with solid fuel or a solid propulsion system with a liquid oxidizer. The liquid propulsion features that are most attractive are the higher specific impulse, clean exhaust, separated propellants, and oxidizer loading just prior to launch. The most attractive solid propulsion features includes low life cycle costs, no rotating machinery, compact size, and a robust case. In addition, a HP system has a robust LO2 tank; provides thrust control for ignition, to alleviate flight loads, and for thrust termination; and uses an inert grain that is not sensitive to anomalies such as cracks, voids, and separations. The object is to develop the technology to enable the application of HP to manned and unmanned space launch vehicles. This program will identify the necessary technology, acquire that technology, and demonstrate that technology. This volume is the executive summary. E.R.

**N91-10112*#** General Dynamics Corp., San Diego, CA. Space Systems Div.
**HYBRID PROPULSION TECHNOLOGY PROGRAM: PHASE 1, VOLUME 2 Final Report, 6 Mar. - 30 Nov. 1989**
A. L. Schuler and D. R. Wiley 20 Nov. 1989 80 p
(Contract NAS8-37777)
(NASA-CR-183973; NAS 1.26:183973; GDSS-HPT-89-001-Vol-2)
Avail: NTIS HC/MF A05 CSCL 21H

The program objectives of developing hybrid propulsion technology (HPT) to enable its application for manned and unmanned high thrust, high performance space launch vehicles are examined. The studies indicate that the hybrid propulsion (HP) is very attractive, especially when applied to large boosters for programs such as the Advanced Launch System (ALS) and the second generation Space Shuttle. Some of the advantages of HP are identified. Space launch vehicles using HP are less costly than those flying today because their propellant and insulation costs are much less and there are fewer operational restraints due to reduced safety requirements. Boosters using HP have safety features that are highly desirable, particularly for manned flights. HP systems will have a clean exhaust and high performance. Boosters using HP readily integrate with launch vehicles and their launch operations, because they are very compact for the amount of energy contained. Hybrid propulsion will increase the probability of mission success. In order to properly develop the technologies of HP, preliminary HP concepts are evaluated. System analyses and trade studies were performed to identify technologies applicable to HP. E.R.

**N91-10113*#** General Dynamics Corp., San Diego, CA. Space Systems Div.
**HYBRID PROPULSION TECHNOLOGY PROGRAM: PHASE 1. VOLUME 3: THIOKOL CORPORATION SPACE OPERATIONS Final Report, 6 Mar. - 30 Nov. 1989**
A. L. Schuler and D. R. Wiley 1 Dec. 1989 99 p
(Contract NAS8-37777)
(NASA-CR-183974; NAS 1.26:183974) Avail: NTIS HC/MF A05 CSCL 21H

Three candidate hybrid propulsion (HP) concepts were identified, optimized, evaluated, and refined through an iterative process that continually forced improvement to the systems with respect to safety, reliability, cost, and performance criteria. A full scale booster meeting Advanced Solid Rocket Motor (ASRM) thrust-time constraints and a booster application for 1/4 ASRM thrust were evaluated. Trade studies and analyses were performed for each of the motor elements related to SRM technology. Based on trade study results, the optimum HP concept for both full and quarter sized systems was defined. The three candidate hybrid concepts evaluated are illustrated. Author

**N91-10114*#** Rockwell International Corp., Canoga Park, CA. Rocketdyne Div.
**HYBRID PROPULSION TECHNOLOGY PROGRAM: PHASE 1, VOLUME 4 Final Report, 6 Mar. - 30 Nov. 1989**
S. E. Claflin and A. W. Beckman 2 Oct. 1989 59 p
(Contract NAS8-37777)
(NASA-CR-183975; NAS 1.26:183975; RI/RD89-261-Vol-4)
Avail: NTIS HC/MF A04 CSCL 21H

The use of a liquid oxidizer-solid fuel hybrid propellant combination in booster rocket motors appears extremely attractive due to the integration of the best features of liquid and solid propulsion systems. The hybrid rocket combines the high performance, clean exhaust, and safety of liquid propellant engines with the low cost and simplicity of solid propellant motors. Additionally, the hybrid rocket has unique advantages such as an inert fuel grain and a relative insensitivity to fuel grain and oxidizer injection anomalies. The advantages mark the hybrid rocket as a potential replacement or alternative for current and future solid propellant booster systems. The issues are addressed and recommendations are made concerning oxidizer feed systems, injectors, and ignition systems as related to hybrid rocket propulsion. Early in the program a baseline hybrid configuration was established in which liquid oxygen would be injected through ports in a solid fuel whose composition is based on hydroxyl terminated polybutadiene (HTPB). Liquid oxygen remained the recommended oxidizer and thus all of the injector concepts which were evaluated assumed only liquid would be used as the oxidizer. E.R.

**N91-10115*#** Thiokol Corp., Brigham City, UT. Space Operations.
**FLIGHT SET 360L007 (STS-33R) FIELD JOINT PROTECTION SYSTEM, THERMAL PROTECTION SYSTEM, AND SYSTEMS TUNNEL COMPONENTS, VOLUME 7 Final Report**
Sep. 1990 36 p
(Contract NAS8-30490)
(NASA-CR-184026; NAS 1.26:184026; TWR-17546-Vol-7; Publ-91190) Avail: NTIS HC/MF A03 CSCL 21H

The performance of the thermal protection system, field joint protection system, and systems tunnel components of flight set 360L007 is presented as evaluated by postflight hardware inspection. The condition of both motors was similar to previous flights. Four aft edge strikes were noted on the ground environment instrumentation thermal protection system. The hits all left a clean substrate, indicating that the damage was caused by nozzle severance debris and/or water impact. No National Space Transportation System debris criteria for missing thermal protection system were violated. Two problem reports were written against the field joint protection system. The first concerned two cracks in the K5NA closeout over the trunnion/vent valve location on the left-hand aft field joint. A similar condition was observed on Flight 5 (360H005). The second problem report referred to a number of small surface cracks between two impact marks on the left-hand forward field joint. Neither area exhibited loose material or any abnormal heat effects, and they have no impact on flight safety. Author

**N91-10116*#** Rockwell International Corp., Downey, CA. Space Transportation Systems Div.
**INTEGRATED HYDROGEN/OXYGEN TECHNOLOGY APPLIED TO AUXILIARY PROPULSION SYSTEMS Final Report, Sep. 1990**
David L. Gerhardt Oct. 1990 104 p
(Contract NAS3-25643)
(NASA-CR-185289; NAS 1.26:185289) Avail: NTIS HC/MF A06 CSCL 21H

The purpose of the Integrated Hydrogen/Oxygen Technology (IHOT) study was to determine if the vehicle/mission needs and technology of the 1990's support development of an all cryogenic H2/O2 system. In order to accomplish this, IHOT adopted the approach of designing Integrated Auxiliary Propulsion Systems (IAPS) for a representative manned vehicle; the advanced manned launch system. The primary objectives were to develop IAPS concepts which appeared to offer viable alternatives to state-of-the-art (i.e., hypergolic, or earth-storable) APS approaches. The IHOT study resulted in the definition of three APS concepts; two cryogenic IAPS, and a third concept utilizing hypergolic propellants. Author

**N91-10117*#** National Aeronautics and Space Administration. Lewis Research Center, Cleveland, OH.
**ANALYSIS OF 5 KHz COMBUSTION INSTABILITIES IN 40K METHANE/LOX COMBUSTION CHAMBERS**
Kevin J. Breisacher and Richard J. Priem (Sverdrup Technology, Inc., Cleveland, OH.) 1988 12 p Presented at the 25th JANNAF Combustion Meeting, Huntsville, AL, 24-28 Oct. 1988
(Contract Sverdrup-5324-85)
(NASA-TM-101368; E-4407; NAS 1.15:101368) Avail: NTIS HC/MF A03 CSCL 21H

In 40K methane/LOX 5 KHz engine tests, (first transverse mode) combustion instabilities observed by Rocketdyne are analyzed using Heidmann and Wieber's vaporization model to include LOX flow oscillations. The LOX flow oscillations are determined by including acoustic waves in the feed system analysis. The major parameter controlling stability is the distance (or time delay) associated with atomizing the LOX stream in the coaxial injection system. Results of the analysis that show the influence of mixture ratio, oxidizer and fuel injection velocities, burning time and combustion chamber/injector dimensions on stability are used to explain the existing data. Calculated results to predict the influence of design changes being made for the next set of experiments are also presented. Author

**N91-10118*#** National Aeronautics and Space Administration. Lewis Research Center, Cleveland, OH.
**PERFORMANCE CHARACTERIZATION OF A SEGMENTED ANODE ARCJET THRUSTER**
Francis M. Curran, David H. Manzella (Sverdrup Technology, Inc., Brook Park, OH.), and Eric J. Pencil Jul. 1990 18 p Presented at the 21st International Electric Propulsion Conference, Orlando, FL, 18-20 Jul. 1990; sponsored in part by AIAA, DGLR, and JSASS
(NASA-TM-103227; E-5643; NAS 1.15:103227; AIAA-90-2582) Avail: NTIS HC/MF A03 CSCL 21H

A modular, 1 to 2 kW class arcjet thruster incorporating a segmented anode/nozzle was operated on a thrust stand to obtain performance characteristics of the device and further study its operating characteristics under a number of experimental conditions. The nozzle was composed of five axial conducting segments isolated from one another by boron nitride spacers. The electrical configuration allowed the current delivered to the arcjet to be collected at any combination of segments. Both the current collected by each segment, and the potential difference between the cathode and each segment were monitored throughout the test period. As in previous tests a similar device, current appeared to attach diffusely in the anode when all of the segments were allowed to conduct. Improvements to the device allowed long term (4 to 8 hour) operation at steady-state and operating characteristics were repeatable over extended periods. Performance characteristics indicated that the segmented anode reasonably simulates the behavior of solid anodes of similar geometry. Current distribution depended on flow rate as the arc attachment moved downstream in the nozzle with increases in the mass flow rate. The current level had little effect on current distribution on the anode segments. Thrust measurements indicated that the current distribution in the nozzle did not significantly affect performance of the device. Author

**N91-10119*#** National Aeronautics and Space Administration. Lewis Research Center, Cleveland, OH.
**DEVELOPMENTS IN REDES: THE ROCKET ENGINE DESIGN EXPERT SYSTEM**
Kenneth O. Davidian 1990 11 p Presented at the 27th JANNAF Combustion Meeting, Cheyenne, WY, 5-9 Nov. 1990
(NASA-TM-103657; E-5848; NAS 1.15:103657) Avail: NTIS HC/MF A03 CSCL 21H

The Rocket Engine Design Expert System (REDES) is being developed at the NASA-Lewis to collect, automate, and perpetuate the existing expertise of performing a comprehensive rocket engine analysis and design. Currently, REDES uses the rigorous JANNAF methodology to analyze the performance of the thrust chamber and perform computational studies of liquid rocket engine problems. The following computer codes were included in REDES: a gas properties program named GASP, a nozzle design program named RAO, a regenerative cooling channel performance evaluation code named RTE, and the JANNAF standard liquid rocket engine performance prediction code TDK (including performance evaluation modules ODE, ODK, TDE, TDK, and BLM). Computational analyses are being conducted by REDES to provide solutions to liquid rocket engine thrust chamber problems. REDES is built in the Knowledge Engineering Environment (KEE) expert system shell and runs on a Sun 4/110 computer. Author

# 23 CHEMISTRY AND MATERIALS (GENERAL)

**N91-10120#** National Inst. of Standards and Technology, Gaithersburg, MD.
**NIST (NATIONAL INSTITUTE OF STANDARDS AND TECHNOLOGY) STANDARD REFERENCE MATERIALS CATALOG, 1990-1991**
R. L. McKenzie Jan. 1990 169 p
(PB90-183310; NIST/SP-260) Avail: NTIS HC/MF A08; also available SOD HC $9.00 as 003-003-02994-7 CSCL 07A

The catalog describes the Standard Reference Materials (SRMs) currently available from the National Institute of Standards and Technology, lists those in preparation, and provides ordering information. The descriptions provide nominal values for these SRMs. Certified values are provided in the certificates that accompany each SRM. Price lists for SRMs are issued as separate supplements to the catalog and include new SRMs as they are issued. GRA

**N91-10121#** Wisconsin Univ., Madison.
**ORGANOMETALLIC CHEMISTRY OF BIMETALLIC COMPOUNDS Progress Report**
Charles P. Casey Aug. 1990 8 p
(Contract DE-FG02-85ER-13406)
(DE90-017601; DOE/ER-13406/5) Avail: NTIS HC/MF A02

This report briefly discusses past work on heterobimetallic dihydrides, early-late transition metal heterobimetallic compounds, and diphosphine chelates with natural bite angles near 120 degrees. DOE

# 24 COMPOSITE MATERIALS

Includes physical, chemical, and mechanical properties of laminates and other composite materials.
For ceramic materials see *27 Nonmetallic Materials.*

**N91-10122*#** Illinois Univ., Urbana. National Center for Composite Materials Research.
**ANALYSIS OF DELAMINATION IN FIBER COMPOSITE LAMINATES OUT-OF-PLANE UNDER BENDING Final Report**
S. S. Wang and F. G. Yuan 1990 47 p
(Grant NAG1-286)
(NASA-CR-186023; NAS 1.26:186023) Avail: NTIS HC/MF A03 CSCL 11D

Delamination in the form of cracking or separation between plies in an advanced fiber composite laminate is a problem of major concern. Both advanced analytical methods and advanced computational analyses are conducted to: (1) develop an asymptotic solution for a composite laminate subject to out-of-plane bending; (2) construct advanced singular finite elements in conjunction with the development of nonsingular elements for this bending problem; and (3) evaluate the delamination failure mechanics parameters and the subsequent modes of fracture. A parametric study was also conducted to evaluate the influences of various lamination parameters on the delaminated composites. Author

**N91-10123#** Pennsylvania State Univ., University Park. Materials Research Lab.
**NANO-COMPOSITE DESICCATION MATERIALS Final Report, Mar. 1987 - Feb. 1990**
S. Komarneni and R. Roy Jun. 1990 76 p
(Contract GRI-5087-260-1473)
(PB90-247388; GRI-90/0092) Avail: NTIS HC/MF A05 CSCL 11D

The objective was to make new desiccant materials involving nanocomposites of clays, zeolites, and gels for space cooling systems using gas energy. A montmorillonite clay was pillared with various thermally stable ceramic oxide pillars. Hydrophilic components were introduced into the hydrophobic alumina-pillared clay to achieve better water sorption properties. Pilaring of other smectite clays, such as nontronite, saponite, and hectorite exhibited various shapes of water isotherms (type I to type IV) as a result of the variation in their crystal chemistry. New types of silica gels were synthesized from hydrolysis of Si-methoxide with and without the use of catalysts. Some of the gels exhibited type IM isotherm shape. Natural zeolites exhibited extreme type I isotherms for water sorption with upward deviation of isotherm at higher relative pressures. Synthetic zeolites exchanged with various monovalent and divalent cations also produced extreme type I isotherms and the sorption capabilities increased with decreasing size of the exchanged cations. A proprietary process was developed which resulted in a reduction in the polarity of zeolite structure and yielded a desired isotherm shape. Author

**N91-10124#** Naval Ship Research and Development Center, Bethesda, MD. Ship Materials Engineering Dept.
**INFLUENCE OF EXPANDING MONOMER ON CARBON FIBER REINFORCED EPOXY COMPOSITES Research and Development Report, 10 Jan. 1988 - 11 Jan. 1989**
Barbara F. Howell Jun. 1990 25 p
(AD-A223277; DTRC/SME-90/20) Avail: NTIS HC/MF A03 CSCL 11/4

In this investigation it was confirmed that copolymerization of dinorbornene spiroorthocarbonate (DNSOC) with epoxy can eliminate sample shrinkage and even produce sample expansion. To maximize control of shrinkage, it is important to bring epoxy to the gel stage before the DNSOC begins to copolymerize. Embedded single filament tensile test results were compared for samples containing diglycidylether of bisphenol A (DGEBA)-epoxy cured with m-phenylene diamine (mPDA) with those for DNSOC-epoxy cured with m-phenylene diamene (mPDA) with those for DNSOC-epoxy samples cured with mPDA and BF3.diethylenetriamine for which BF3 was used to catalyze polymerization of the DNSOC. As compared with epoxy, the DNSOC sample showed ten-fold reductions in interfacial tensile stress, 10 C reduction in Tg (glass transition temperature), and 40 percent reduction in tensile strength. The tensile modulus was not reduced and the sample showed no shrinkage. No stress patterns were seen in the DNSOC-epoxy with a polarizing microscope. It is concluded that smaller amounts of DNSOC than 12 percent can be used to produce optimal effects on mechanical properties. GRA

**N91-10125#** Oak Ridge National Lab., TN.
**COMPOSITE HEAT DAMAGE. PART 1: MECHANICAL TESTING OF IM6/3501-6 LAMINATES. PART 2: NONDESTRUCTIVE EVALUATION STUDIES OF IM6/3501-6 LAMINATES**
B. J. Frame, C. J. Janke, W. A. Simpson, Jr., R. E. Ziegler, and H. E. Philpot (Oak Ridge Gaseous Diffusion Plant, TN.) May 1990 165 p
(Contract DE-AC05-84OR-21400)
(DE90-016207; ORNL/ATD-33) Avail: NTIS HC/MF A07

The matrix-dominated mechanical properties of heat-damaged and non-heat-damaged IM6/3501-6 laminates are presented in Part 1. Wet and dry preconditioned laminates were exposed on one side to temperatures ranging from room temperature to 750 F for 0 to 60 min and subsequently tested at ambient conditions in accordance with American Society for Testing and Materials (ASTM) standards, including compression -- ASTM D3410-87, flexure -- ASTM D790-87, short-beam shear -- ASTM D2344-84, and shore-D hardness -- ASTM D2240-86. Shore-D-hardness testing was a poor indicator of mechanical strength loss. Heat-damaged 0 degree compression specimens were the least sensitive to strength degradation compared with the other properties that were tested. Heat-damaged specimens that were tested in shear and flexure suffered significant strength reduction and degradation at exposure temperatures greater than or equal to 550 F for 5 to 60 min. The percent weight loss, micrometer measurements, and visual differences of IM6/3501-6 specimens as a function of elevated temperature exposure are reported. The results of heat-degradation effects on IM6/3501-6 specimens utilizing various nondestructive evaluation (NDE) techniques, including digital pulse (broadband), tone burst (monochromatic), ultrasonic color C scanning, and leaky Lamb waves are presented in Part 2. Preliminary results indicated that the leaky Lamb-wave technique appeared to be the most promising NDE tool for characterizing the level of heat damage in IM6/3501-6 laminates. This technique is capable of detecting relative changes in a given sample at a particular location; however, it does not appear to have the capability of providing absolute results on random samples. DOE

**N91-10126*#** Clemson Univ., SC. Dept. of Mechanical Engineering.
**MICRO-MECHANICAL ANALYSIS OF DAMAGE GROWTH AND FRACTURE IN DISCONTINUOUS FIBER REINFORCED METAL MATRIX COMPOSITES Semiannual Report**
James G. Goree and David E. Richardson 1990 16 p
(Grant NAG1-971)
(NASA-CR-187020; NAS 1.26:187020) Avail: NTIS HC/MF A03 CSCL 11D

The near-crack-tip stresses in any planar coupon of arbitrary geometry subjected to mode 1 loading may be equated to those in an infinite center-cracked panel subjected to the appropriate equivalent remote biaxial stresses (ERBS). Since this process can be done for all such mode 1 coupons, attention may be focused on the behavior of the equivalent infinite cracked panel. To calculate the ERBS, the constant term in the series expansion of the crack-tip stress must be retained. It is proposed that the ERBS may be used quantitatively to explain different fracture phenomena such as crack branching. Author

**N91-10127*#** National Aeronautics and Space Administration. Lewis Research Center, Cleveland, OH.
**STRUCTURAL PROPERTIES OF LAMINATED DOUGLAS FIR/EPOXY COMPOSITE MATERIAL**
David A. Spera, Jack B. Esgar, Meade Gougeon, and Michael D. Zuteck (Gougeon Bros., Inc., Bay City, MI.) May 1990 140 p
(Contracts NAS3-25266; DE-AI01-76ET-20320)
(NASA-RP-1236; E-4720; NAS 1.61:1236; DOE/NASA/20320-76)
Avail: NTIS HC/MF A07 CSCL 11D

This publication contains a compilation of static and fatigue strength data for laminated-wood material made from Douglas fir and epoxy. Results of tests conducted by several organizations are correlated to provide insight into the effects of variables such as moisture, size, lamina-to-lamina joint design, wood veneer grade, and the ratio of cyclic stress to steady stress during fatigue testing. These test data were originally obtained during development of wood rotor blades for large-scale wind turbines of the horizontal-axis (propeller) configuration. Most of the strength property data in this compilation are not found in the published literature. Test sections ranged from round cylinders 2.25 in. in diameter to rectangular slabs 6 by 24 in. in cross section and approximately 30 ft. long. All specimens were made from Douglas fir veneers 0.10 in. thick, bonded together with the WEST epoxy system developed for fabrication and repair of wood boats. Loading was usually parallel to the grain. Size effects (reduction in strength with increase in test volume) are observed in some of the test data, and a simple mathematical model is presented that includes the probability of failure. General characteristics of the wood/epoxy laminate are discussed, including features that make it useful for a wide variety of applications. Author

**N91-10128*#** National Aeronautics and Space Administration. Langley Research Center, Hampton, VA.
**A MACRO-MICROMECHANICS ANALYSIS OF A NOTCHED METAL MATRIX COMPOSITE**
C. A. Bigelow and R. A. Naik (Analytical Services and Materials, Inc., Hampton, VA.) Sep. 1990 33 p
(NASA-TM-102728; NAS 1.15:102728) Avail: NTIS HC/MF A03 CSCL 11D

A macro-micromechanics analysis was formulated to determine the matrix and fiber behavior near the notch tip in a center-notched metal matrix composite. Results are presented for a boron/aluminum monolayer. The macro-level analysis models the entire notched specimen using a three dimensional finite element program which uses the vanishing-fiber-diameter model to model the elastic-plastic behavior of the matrix and the elastic behavior of the fiber. The micro-behavior is analyzed using a Discrete Fiber-Matrix (DFM) model containing one fabric and the surrounding matrix. The dimensions of the DFM model were determined by the ply thickness and the fiber volume fraction and corresponded to the size of the notch-tip element in the macro-level analysis. The boundary conditions applied to the DFM model were determined from the macro-level analysis. Stress components within the DFM model were calculated and stress distributions are presented along selected planes and surfaces within the DFM model, including the fiber-matrix interface. Yielding in the matrix was examined at the notch tip in both the macro- and micro-level analyses. The DFM model predicted higher stresses (24 percent) in the fiber compared to the global analysis. In the notch-tip element, the interface stresses indicated that a multi-axial criterion may be required to predict interfacial failure. The DFM analysis predicted yielding to initiate in the notch-tip element at a stress level 28 percent lower than predicted by the global analysis. Author

**N91-10129#** California Univ., Berkeley. Lawrence Berkeley Lab. Center for X Ray Optics.
**MICROSTRUCTURAL AND PHASE STABILITY STUDIES OF NANOMETER PERIOD METAL/CARBON MULTILAYER STRUCTURES FOR X RAY OPTICS M.S. Thesis**
Tai D. Nguyen May 1990 97 p
(Contracts DE-AC03-76SF-00098; F49620-87-K-0001)
(DE90-015307; LBL-29206) Avail: NTIS HC/MF A05

Multilayer structures of W/C, WC/C, and Ru/C, of various periods were prepared by magnetron sputtering and studied by x ray diffraction and high-resolution transmission electron microscopy. Studies of microstructures and phases present inside the layers, interfaces, and stability of layered structures and period, of both as-prepared and annealed samples were made. Both as-prepared and annealed WC/C multilayers are predominantly amorphous, while the phases in the W/C depend on the periods. The 2 nm period W/C multilayer remains amorphous after annealing, and the longer periods recrystallize to form W2C. The layered structures of both W/C and WC/C systems are stable on annealing for periods equal to or larger than 2 nm, while the amorphous Ru-rich layers in the 2 nm period Ru/C multilayer agglomerate upon annealing to form elemental Ru crystallites. Annealing of 1 nm period W/C multilayer also leads to destruction of the layered structures. Longer period Ru/C multilayers show stable layered structures on annealing, and indicate elemental Ru in the Ru-rich layers. Crystalline planes extending into the amorphous layers and grain boundaries in the crystalline layers roughens the interfaces. X ray measurements show that the multilayer periods expand on annealing for all metal/C multilayers studied. Mechanisms for this expansion is not known, although it seems to be linked to the amorphous C-rich layers. DOE

**N91-10130#** Lawrence Livermore National Lab., CA.
**THE TRANSPORT PROPERTIES OF ACTIVATED CARBON FIBERS**
S. L. diVittorio, M. S. Dresselhaus, M. Endo, J.-P. Issi, and L. Piraux (Universite Catholique, Louvain, Belgium ) Jul. 1990 19 p
(Contract W-7405-eng-48)
(DE90-015910; UCRL-CR-104544) Avail: NTIS HC/MF A03

The transport properties of activated isotropic pitch-based carbon fibers with surface area 1000 sq m/g were investigated. Preliminary results are reported on the electrical conductivity, the magnetoresistance, the thermal conductivity and the thermopower of these fibers as a function of temperature. Comparisons are made to transport properties of other disordered carbons. DOE

**N91-10131*#** National Aeronautics and Space Administration. John F. Kennedy Space Center, Cocoa Beach, FL.
**EVALUATION OF COMPOSITE MATERIALS FOR USE ON LAUNCH COMPLEXES**
A. Finchum and Peter J. Welch Nov. 1989 27 p Original contains color illustrations
(NASA-TM-103809; MTB-402-89; NAS 1.15:103809) Avail: NTIS HC/MF A03; 5 functional color pages CSCL 11D

Commercially available composite structural shapes were evaluated for use. These composites, fiberglass-reinforced polyester and vinylester resin materials are being used extensively in the fabrication and construction of low maintenance, corrosion resistant structures. The evaluation found that in many applications these composite materials can be successfully used at the space center. These composite materials should not be used where they will be exposed to the hot exhaust plume/cloud of the launch vehicle during the liftoff, and caution should be taken in their use in areas where electrostatic discharge and hypergolic propellant compatibility are primary concerns. Author

**N91-10132#** Sandia National Labs., Albuquerque, NM.
**INFRARED ABSORPTION IN BORON CARBIDES: DEPENDENCE ON ISOTOPE AND CARBON CONCENTRATION**
Herman Stein, Terry Aselage, and David Emin 1990 4 p
Presented at the 10th International Symposium on Borron, Borides and Related Compounds, Albuquerque, NM, 27-30 Aug. 1990
(Contract DE-AC04-76DP-00789)
(DE90-017592; SAND-90-2060C; CONF-900870-4) Avail: NTIS HC/MF A01

Infrared reflectance and transmittance measurements between 500 and 1800 cm(-1) were obtained on boron carbides with between 10 and 20 atomic percent carbon. Measurements on both boron and carbon isotopically enriched samples indicate that all prominent modes involve boron motion, and that all but a mode near 950 cm(-1) involve carbon motion. Since the spectrum remains qualitatively unaltered as a function of carbon concentration, its prominent features must have a common structural origin. DOE

**N91-10133*#** California Univ., Santa Barbara.
**REDUCTION OF THERMAL STRESSES IN CONTINUOUS FIBER REINFORCED METAL MATRIX COMPOSITES WITH INTERFACE LAYERS Final Report**
S. Jansson and F. A. Leckie Oct. 1990 24 p
(Grant NAG3-894)
(NASA-CR-185302; NAS 1.26:185302) Avail: NTIS HC/MF A03 CSCL 11D

The potential of using an interface layer to reduce thermal stresses in the matrix of composites with a mismatch in coefficients of thermal expansion of fiber and matrix was investigated. It was found that compliant layers, with properties of readily available materials, do not have the potential to reduce thermal stresses significantly. However, interface layers with high coefficient of thermal expansion can compensate for the mismatch and reduce thermal stresses in the matrix significantly. Author

**N91-10134*#** National Aeronautics and Space Administration. Lewis Research Center, Cleveland, OH.
**INTERCALATED GRAPHITE FIBER COMPOSITES AS EMI SHIELDS IN AEROSPACE STRUCTURES**
James R. Gaier Nov. 1990 31 p Presented at the International Symposium on Carbon, Tsukubo, Japan, 4-8 Nov. 1990; sponsored in part by the Carbon Society of Japan
(NASA-TM-103632; E-5781; NAS 1.15:103632) Avail: NTIS HC/MF A03 CSCL 11D

The requirements for electromagnetic interference (EMI) shielding in aerospace structures are complicated over that of ground structures by their weight limitations. As a result, the best EMI shielding materials must blend low density, high strength, and high elastic modulus with high shielding ability. In addition, fabrication considerations including penetrations and joints play a major role. The EMI shielding properties are calculated for shields formed from pristine and intercalated graphite fiber/epoxy composites and compared to preliminary experimental results and to shields made from aluminum. Calculations indicate that EMI shields could be fabricated from intercalated graphite composites which would have less than 12 percent of the mass of conventional aluminum shields, based on mechanical properties and shielding properties alone. Author

**N91-10135#** Institut National des Sciences Appliquees de Lyon, Villeurbanne (France). Groupe d'Etudes de Metallurgie Physique et de Physique des Materiaux.
**STUDY OF THE MECHANISMS OF DAMAGE AND FAILURE OF FIBER AND CERAMIC MATRIX COMPOSITES Ph.D. Thesis [ETUDE DES MECANISMES D'ENDOMMAGEMENT ET DE RUPTURE DES MATERIAUX COMPOSITES A FIBRES ET A MATRICE CERAMIQUES]**
Gilles Alexandre Hen Navarre 1990 213 p In FRENCH
(ISAL-90-0026; ETN-90-97823) Avail: NTIS HC/MF A10

The role of several micromechanic parameters on the macroscopic behavior of ceramic matrix composites is discussed. Several approaches of fracture mechanics are described and applied to heterogeneous materials. The SiC/SiC and C/SiC materials are investigated. The experimental techniques applied are described and the results discussed. The failure characteristics of ceramic matrix composites and the properties of SiC/SiC and C/SiC, under several mechanic tests are summarized. ESA

**N91-10136#** Messerschmitt-Boelkow-Blohm G.m.b.H., Munich (Germany, F.R.).
**HOLOGRAPHIC EXAMINATION OF GREAT SURFACE FIBERBOUND COMPONENTS IN INDUSTRIAL CONDITIONS: RESUMES OF FINAL REPORTS, APRIL 1986 TO JUNE 1989 [HOLOGRAFISCHE PRUEFUNG VON GROSSFLAECHIGEN FASERVERBUNDBAUTEILEN UNTER INDUSTRIEBEDEDINGUNGEN: KURZFASSUNG DES ABSCHLUSSBERICHTES, APRIL 1986 BIS JUNI 1989]**
Helmar Langer 1989 22 p In GERMAN
(Contract BMFT-03-M-1012)
(MBB-Z-0306-90-PUB-Kurzfassung; ETN-90-97883; OTN-027462)
Avail: NTIS HC/MF A03

The Holographic Interferometry (HI) advantages are outlined. The fundamentals of the nondestructive examination process are described. The utilization of HI in industrial conditions offers no difficulty. Corresponding solutions for optical and mechanical constructions of movable holographic systems are demonstrated. The possibilities of using HI through new developments in the field of computerized evaluation will improve in the future. For example, it is to be expected that problems such as elimination of noncontrolable deformation will be automatically resolved. Henceforth, defect detection could be automatized. ESA

**N91-10137#** Rolls-Royce Ltd., Derby (England). Manufacturing Technology.
**FIBRE-MATRIX REACTION ZONES IN MODEL SILICON CARBIDE-TITANIUM ALUMINIDE METAL-MATRIX COMPOSITES**
D. R. Baker, P. J. Doorbar, and M. H. Loetto (Birmingham Univ., England ) 30 Aug. 1989 7 p Presented at MRS, Boston, MA, 1989
(PNR-90713; ETN-90-97942) Copyright Avail: NTIS HC/MF A02

The reactions between coated SiC continuous fibers and TiAl, Ti3Al, or Ti3Al + beta matrices are investigated. Optical metallography, scanning electron microscopy, and transmission electron microscopy, with chemical information obtained by energy dispersive x ray analysis and electron energy loss spectroscopy were applied. Similar sequences of phases were found in all the composites; carbides based on TiC and Ti sub x AlC (x = 2,3) and titanium silicides based on Ti5Si3 formed in narrow bands outside of the complex carbides. The occurrence of individual phases can be related to published phase diagram information. The sequences in which the reaction products occur within the reaction zones cannot be fully rationalized from the present results. ESA

**N91-10138#** Rolls-Royce Ltd., Derby (England).
**INDUSTRIAL APPLICATIONS AND MARKETS FOR CERAMIC MATRIX COMPOSITES**
David A. Clarke 28 Mar. 1990 31 p Presented at Short Course on Advanced Ceramic and Metallic Composites, Cambridge, England, 25-28 Mar. 1990
(PNR-90753; ETN-90-97957) Copyright Avail: NTIS HC/MF A03

An assessment of the ceramic matrix composites market is presented. The aim is focused on the use of particulate and fiber reinforced ceramics for cutting tools, space structures and heat engines. The types of materials in use and the reasons for their selection are discussed. An assessment of what industry must now do to realize the full potential of ceramic matrix composites materials in a wide range of market roles is presented. ESA

**N91-10139#** Rolls-Royce Ltd., Derby (England).
**MULTI INDUSTRY APPLICATION OF ADVANCED MATERIALS**
John F. Coplin 31 May 1989 20 p Presented in Japan, 31 May 1989
(PNR-90764; ETN-90-97963) Copyright Avail: NTIS HC/MF A03

Applications and market evolution of materials for aero engines are summarized. Early days market was provided by military engines. Civil airline market contributed to the market pull. Extra market pull can be provided by automotive industry. Technology developments, and production of high temperature/high resistance materials require new market pulls. At a time when military spending is going down in real money, and when a lower portion is going into aircraft and engines, it is found that lower cost machines made possible by ceramics and metal matrix developments can replace conventional concepts in the future. ESA

# 25 INORGANIC AND PHYSICAL CHEMISTRY

Includes chemical analysis, e.g., chromatography; combustion theory; electrochemistry; and photochemistry.

For related information see also *77 Thermodynamics and Statistical Physics.*.

**N91-10140#** SRI International Corp., Menlo Park, CA.
**ELECTROCHEMICAL OXIDATION OF METHANE AT METAL AND METAL OXIDE ELECTRODES Final Report, 1 Dec. 1986 - 1 Dec. 1989**
K. W. Frese and B. G. Pound 20 Mar. 1990 102 p
(Contract GRI-5086-260-1424)
(PB90-205196; SRI-PYU-2970; GRI-90/0026) Avail: NTIS HC/MF A06 CSCL 07D

An objective was to gain insight into the role of surface geometry, heat of reaction, force constants, and adsorption in the activated chemisorption of methane to adsorbed hydrogen and adsorbed methyl. The model successfully calculated the activation energy for abstraction of H from CH4 by O atoms in the gas phase. The results for two crystal planes of Ni were in good agreement with experimental findings and other calculations. For Ni(111) and Ni(110) Ea = 14 and 18 kcal/mol, respectively. The minimum electrode potential for adsorption of methane, OH, and O atoms on various metal electrodes was calculated. The open circuit decay method was employed to measure the rate of reaction between hydrocarbons including methane and adsorbed oxygen species on Pt, Pd, and Rh electrodes. Author

**N91-10141** Illinois Univ., Chicago.
**THE INSTABILITY OF COMBUSTION IN PROPULSION ENGINES Ph.D. Thesis**
Chun-Pao Kuo 1989 219 p
Avail: Univ. Microfilms Order No. DA9015753

The proposed theory provides a theoretical prediction of the aerothermochemical sources of acoustic excitation, growth of instability, propagation, and resonant pressure oscillation as well as the transition instability model. The thesis presents the description of four major aerothermochemical sources: (1) monopole; (2) dipole; (3) quadrupole sources, which are respectively due to the non-steady propellant vaporization, combustion, aerodynamic drag and turbulence; and (4) the mechanical dilation caused by the time dependent convective motion of multi-phase flow. This is followed by the presentation of comprehensive analytical techniques to predict the strength of each aerothermochemical source by the theoretical procedure devised in non-steady spray group combustion and acoustic response of propellant injection/atomization, and properties of propellant. The numerical simulation of the detailed development of engine start-up instability is presented to demonstrate the dynamic growth of instability sources and the corresponding evolution of an acoustic instability during the start-up of a liquid-gas propulsion engine. Dissert. Abstr.

**N91-10142#** Lawrence Livermore National Lab., CA. Chemistry and Materials Science Div.
**EQUAL EIGENVALUES IN MULTICOMPONENT DIFFUSION: THE EXTRACTION OF DIFFUSION COEFFICIENTS FROM EXPERIMENTAL DATA IN TERNARY SYSTEMS**
Donald G. Miller 2 May 1990 17 p Presented at the 29th Annual Conference of Metallurgists, Hamilton, Ontario, 26-30 Aug. 1990
(Contract W-7405-eng-48)
(DE90-012074; UCRL-JC-103247; CONF-9008106-1) Avail: NTIS HC/MF A03

There has been considerable theoretical and experimental work on ternary systems whose diffusion coefficient matrix has two distinct eigenvalues. This is the most common case. However, with the increasing number of ternary diffusion measurements in liquids, cases have arisen where the eigenvalues may be equal and where the usual equations do not apply. Little work has been done on the solution of the equal eigenvalues case, and none has been done on the connection of this solution to experimental data. This paper will present new explicit expressions connecting ternary diffusion coefficients to experimental data for the precise Gouy and Rayleigh optical methods. Some new results for the two 4-component cases will also be presented. DOE

**N91-10143#** Pacific Northwest Lab., Richland, WA.
**ADVANCED MATERIALS FOR HIGH-TEMPERATURE SOLID ELECTROLYTE APPLICATIONS**
J. L. Bates, L. A. Chick, W. J. Weber, and G. E. Youngblood May 1990 13 p Presented at the 4th Conference on Fossil Energy Materials, Oak Ridge, TN, 15-17 May 1990
(Contract DE-AC06-76RL-01830)
(DE90-016328; PNL-SA-18162; CONF-900546-13) Avail: NTIS HC/MF A03

Advanced materials for use as electrodes, interconnections, and electrolytes in high-temperature electrochemical applications are under investigation. The air sinterability of La(1-x)Sr(x)CrO3 is highly dependent upon a synergistic relationship between the (La + Sr)/Cr ratio, cation volatility, and second phase formation and transformation. Electrical conductivity in the ZrO2--Y2O3--CeO2 and ZrO2--Y2O3--TiO2 systems is highly dependent on composition and atmosphere. The electrochemical processes that occur at the solid-solid-gas interfaces in La(Sr)MnO3/ZrO2(Y2O3) have been studied using an unbonded interface cell and impedance spectroscopy. DOE

**N91-10144#** Ames Lab., IA.
**CHARACTERIZATION OF MONO- AND MULTI-MOLECULAR ASSEMBLIES AT GLASSY CARBON AND NOBLE METALS BY EX SITU AND IN SITU INFRARED EXTERNAL REFLECTION SPECTROSCOPY Ph.D. Thesis**
Scott M. Stole 23 Aug. 1990 199 p
(Contract W-7405-eng-82)
(DE90-016417; IS-T-1486) Avail: NTIS HC/MF A09

This dissertation describes the utilization of infrared external reflection spectroscopy (IR-ERS) as a means of elucidating many of the properties of polymer films and mono- and multimolecular films at both semiconducting glassy carbon and conducting noble metal surfaces. Infrared external reflection spectroscopy was utilized to monitor the hydrolysis of the film as the molecular composition changed from the acetate to the cellulosic form. The electrochemical measurements indicate a change in perselectivity as the hydrolysis proceeds. The effects of a variety of solvents on the integrity and orientation of an n-alkanethiol monolayer were studied by IR-ERS without the necessity for modulation methodologies. This dissertation reports the first in situ infrared external reflection spectra for an n-alkanethiol monolayer at Au and Ag in the presence of a variety of solvents without the need for potential or polarization modulation. Descriptions provided by such measurements promise to expand the understanding of the fundamental intermolecular forces that control the chemical and physical properties of these interfaces. Further, this technique has far-reaching applicability to a variety of other interfacial systems with varying properties. DOE

**N91-10145#** Oak Ridge Gaseous Diffusion Plant, TN. Enrichment Technical Operations Div.
**EVALUATION OF AVAILABLE PERFLUOROBUTANE DATA FOR SELECTED PHYSICAL PROPERTIES**
David Harkins Jan. 1990 16 p
(Contract DE-AC05-84OT-21400)
(DE90-016516; K/QT-331) Avail: NTIS HC/MF A03

A literature search was conducted, and available information accumulated on a short list of six properties of C4F10. These data were evaluated as to their applicability and accuracy, and the best results are presented in this report. In general, the properties included in this evaluation are known or approximated with an accuracy of 10 percent or better. DOE

**N91-10146#** Ames Lab., IA.
**DEVELOPMENT, CHARACTERIZATION, AND APPLICATIONS OF OPTICAL pH SENSORS SUPPORTED AT CELLULOSIC FILM Ph.D. Thesis**
Thomas P. Jones Aug. 1990 152 p
(Contract W-7405-eng-82)
(DE90-016416; IS-T-1484) Avail: NTIS HC/MF A08

Sensors for the determination of pH have been developed which are based on the immobilization of direct dyes at hydrolyzed cellulosic films. The performance and structural characteristics of the sensors were investigated by a variety of spectroscopic methods, and applications for remote sensing were developed. Films of cellulose acetate were base hydrolyzed in 0.07 M KOH to yield a porous support structure. The structural changes resulting from the hydrolysis on cellulose acetate were probed with infrared internal reflectance spectroscopy. The progress of the hydrolysis reaction was monitored by the changes in vibrational modes of the acetyl group, and other spectral changes indicated changes in film thickness as a result of solvent incorporation. Direct dyes, including Congo Red and C. I. Direct Blue 8, were then immobilized at these porous cellulosic films. The optical response characteristics of the Congo Red pH sensor were characterized, including the UV-visible absorption spectra as a function of pH, the response time as a function of ionic strength and ionic size of electrolyte, the long-term stability of the sensor, the effects of metal-ion interference, and the concentration of Congo Red in the polymer film. The structural characteristics of the sensor were investigated by internal reflectance spectroscopy and resonance-enhanced Raman spectroscopy, and the protonation sites were identified as the two azo groups of Congo Red. Infrared internal reflection spectra of immobilized Congo Red led to the development of a sensor for pH based on infrared spectroscopy. Finally, a two-wavelength fiber-optic photometer, which is based on solid-state sources and detectors, and a fiber-optic photometer, which is based on solid-state sources and detectors, and a fiber-optic probe were developed for pH determinations using Congo Red and C. I. Direct Blue 8 pH sensors. DOE

**N91-10147#** Fermi National Accelerator Lab., Batavia, IL.
**DIJET SPECTROSCOPY AT HIGH LUMINOSITY**
Dan Green Jul. 1990 21 p Presented at the 1990 DPF Summer Study on High Energy Physics, Snowmass, CO, 25 Jun. - 13 Jul. 1990
(Contract DE-AC02-76CH-03000)
(DE90-016901; FNAL/C-90/151; CONF-9006267-1) Avail: NTIS HC/MF A03

A study of the dijet mass resolution has been made appropriate to high luminosity operation. As a benchmark, the mass resolution of W (yields) jj for a Higgs boson of 800 GeV has been optimized for zero, eight, and sixteen overlapping minbias events. A factor of 2.5 degradation in M(sub jj) width is seen. DOE

**N91-10148#** National Aerospace Lab., Tokyo (Japan).
**SPECIFIC IMPULSE COMPARISON OF HIGH DENSITY HYDROCARBON FUEL BURNED WITH OXYGEN**
Tatsuo Kumagai, Shuichi Ueda, Masahiro Sato, Takayuki Sudo, Hiroshi Miyajima, Atsutaro Watanabe, and Masaki Yamakawa Feb. 1990 18 p In JAPANESE; ENGLISH summary
(NAL-TR-1053; ISSN-0389-4010) Avail: NTIS HC/MF A03

Performance tests of high density hydrocarbon fuel were conducted with a small rocket engine. The densities of the fuel examined, RJ-1J, HDF-1, and HDF-3 were 0.851, 0.996, and 1.006 respectively. The RJ-1J, which is used for the Japanese H-1 rocket, served as a reference for comparison. The thrust of the rocket engine was 490 N at a chamber pressure of 2.94 MPa and a nozzle area ratio of 5:1. The thrust chamber was water cooled, and gaseous oxygen was used as the oxidizer. To simulate a dual fuel condition, a small amount of gaseous hydrogen (2 percent of hydrocarbon fuel) was added to the combustion chamber. The effect of the amount of hydrogen addition on specific impulse was also tested. Measured peak vacuum specific impulses for RJ-1J, HDF-1, HDF-3 respectively were 291, 290, and 287 s, which is in qualitative accord with theoretical prediction. Specific impulse increased with the amount of hydrogen added as predicted. However, energy release efficiency was not affected appreciably, since it was very near to 100 percent at the conditions tested. It was concluded that two kinds of high density fuel tested have acceptable performance and properties for dual fuel engines. An engine specific impulse may be extrapolated from the present experiment to be 345 s at a 1000 kN thrust and 10 MPa chamber pressure level. Author

# 26 METALLIC MATERIALS

Includes physical, chemical, and mechanical properties of metals, e.g., corrosion; and metallurgy.

**N91-10149*#** National Aeronautics and Space Administration. Lewis Research Center, Cleveland, OH.
**HIGH TEMPERATURE CYCLIC OXIDATION DATA. PART 1: TURBINE ALLOYS**
Charles A. Barrett, Ralph G. Garlick, and Carl E. Lowell Oct. 1989 192 p Revised
(NASA-TM-83665; E-1499-Pt-1; NAS 1.15:83665) Avail: NTIS HC/MF A09 CSCL 11F

Specific-weight-change-versus-time data and x ray diffraction results are presented derived from high temperature cyclic tests on high temperature, high strength nickel-base gamma/gamma prime and cobalt-base turbine alloys. Each page of data summarizes a complete test on a given alloy sample. Author

**N91-10150*#** National Aeronautics and Space Administration. Lewis Research Center, Cleveland, OH.
**HIGH-TEMPERATURE CYCLIC OXIDATION DATA. PART 2: TURBINE ALLOYS**
Charles A. Barrett and Ralph G. Garlick Oct. 1989 462 p
(NASA-TM-101468; E-4263-Pt-2; NAS 1.15:101468) Avail: NTIS HC/MF A20 CSCL 11F

Specific-weight-change-versus-time data and x ray diffraction results are presented derived from high temperature cyclic tests on high temperature, high strength nickel-base gamma/gamma prime and cobalt-base turbine alloys. Each page of data summarizes a complete test on a given alloy sample. Author

**N91-10151#** National Aerospace Lab., Amsterdam (Netherlands). Structures and Materials Div.
**MECHANICAL PROPERTIES AND FRACTURE TOUGHNESS OF 8090-T651 PLATE AND 2091 AND 8090 SHEET**
W.G. T. Thart, L. Schra, D. S. McDarmaid, and M. Peters (Deutsche Forschungs- und Versuchsanstalt fuer Luft- und Raumfahrt, Cologne, Germany, F.R. ) 5 Aug. 1988 21 p Presented at AGARD Specialists Meeting on New Light Alloys, Mierlo, Netherlands, 3-5 Oct. 1988 Previously announced as N90-15188
(NRL-MP-88049-4; ETN-90-97188) Avail: NTIS HC/MF A03

The strength and thoughness properties of the medium Al-Li plate alloy 8090-T651 were determinated and compared to those of damage tolerant 2000 series plate alloys. For the LT and TL orientations similar K(sub Ic) values were obtained. Tensile tests through-the-thickness and with respect to rolling direction indicated considerable anisotropy. Residual strength tests were performed on center cracked sheet panels. The characteristics were analyzed using fractography and resulted in a better understanding of the fracture behavior of Al-Li alloys. Recrystallized Al-Li sheet in specific tempers achieved plane stress fracture toughness values similar to those of 2024-T3, but at lower yield strengths. ESA

**N91-10152#** Stanford Univ., CA. Dept. of Materials Science and Engineering.
**MECHANISMS OF HIGH TEMPERATURE CRACK GROWTH IN METALS AND ALLOYS Final Technical Report**
William D. Nix Jan. 1989 202 p
(Contract DE-FG03-84ER-45169)
(DE90-014934; DOE/ER-45169/T1) Avail: NTIS HC/MF A10

The high temperature creep crack growth behavior of pure Cu, Cu--Sn alloy, and predamaged Cu was investigated. The purposes were to understand the mechanisms of creep crack growth; to prove theoretical predictions with experimental studies; and eventually to predict the time to failure of high-temperature structural materials. High temperature crack growth experiments were conducted under various loading conditions with a computer-based data acquisition and control system. A model to describe creep crack growth in pre-damaged Cu was developed. It is based on cavity growth by coupled diffusional and creep processes under the damage-modified stress field. High temperature crack growth experiments were carried out under cyclic loading conditions. DOE

**N91-10153#** Sandia National Labs., Albuquerque, NM.
**WELDABILITY OF NICKEL AND IRON ALUMINIDES**
D. I. Ash, G. R. Edwards (Colorado School of Mines, Golden.), and M. C. Maguire 1990 6 p Presented at the ASM Fall Meeting, Detroit, MI, 6-12 Oct. 1990
(Contract DE-AC04-76DP-00789)
(DE90-013498; SAND-90-1694C; CONF-901095-2) Avail: NTIS HC/MF A02

The weldability of alloys based on Ni3Al and Fe3Al is discussed. Both of these ordered alloy systems may experience problems associated with welding. In the case of Ni3Al alloys, limited hot ductility contributes to heat-affected zone cracking. Fe3Al alloys experience similar difficulties in zone cracking. Fe3Al alloys experience similar difficulties in welding due to excessive grain embrittlement due to the presence of water vapor. Advances in both alloying and substructural refinement to improve the weldability are reviewed. DOE

**N91-10154#** Sandia National Labs., Albuquerque, NM.
**A WELDABILITY STUDY OF HAYNES ALLOY NO. 242**
M. C. Maguire and T. J. Headley 1990 7 p Presented at the ASM Fall Meeting, Detroit, MI, 6-12 Oct. 1990
(Contract DE-AC04-76DP-00789)
(DE90-013875; SAND-90-1693C; CONF-901095-3) Avail: NTIS HC/MF A02

The weldability of Haynes Alloy No. 242 (trademark), a new alloy derived from the Ni-Mo-Cr system, was investigated. Susceptibility to fusion zone hot cracking was determined by Varestraint testing, and hot ductility was characterized by Gleeble testing. Solidification phase transformation data was recorded with differential thermal analysis (DTA). Weld microstructures were characterized with scanning electron microscopy (SEM), analytical electron microscopy (AEM), and electron probe microanalysis (EPMA). The results of this study indicate that this alloy has better hot cracking resistance than high strength nickel base superalloy 718; however, it has lower resistance than other alloys derived from the Ni-Cr-Mo ternary such as the Hastelloy alloys B2, C-4, C-22, C-276, and W. Segregation patterns in weld microstructures agree well with established information concerning this family of alloys. Prediction of solidification products with the Ni-Mo-Cr phase diagram based on a chemical equivalence was unsuccessful due to the higher carbon content of this alloy which favors the formation of M6C. Solidification in Alloy 242 terminates with the formation of two eutectic-like constituents: a M6C/austenite eutectic, and a second eutectic with austenite and an undetermined phase. This latter phase has a composition similar to the M6C phase, but with a different crystal structure (cubic, ao = 6.6 A). DOE

**N91-10155#** Los Alamos National Lab., NM.
**BERYLLIUM WELDABILITY**
Mary Ann Hill, Brian K. Damkroger, Raymond D. Dixon, and Erica Robertson (Air Force Office of Scientific Research, Bolling AFB, Washington, DC.) 1990 11 p Presented at the ASM Fall Meeting, Detroit, MI, 6-12 Oct. 1990
(Contract W-7405-eng-36)
(DE90-014696; LA-UR-90-2516; CONF-901095-4) Avail: NTIS HC/MF A03

Welding processes and metallurgical considerations for beryllium welding are discussed. The primary difficulties of welding beryllium are hot cracking, cracking at defects, and ductility limitation or thermally induced cracking. Solutions to these welding problems include control of the Fe/Al ratio in the base metal to reduce hot cracking, minimization of the BeO content and starting grain size to limit cracking at defects and ductility limitation cracking, and optimization of the welding process and process variables. DOE

**N91-10156#** Oak Ridge National Lab., TN. Metals and Ceramics Div.
**ON THE EFFECTS OF MAGNETIC BONDING IN RARE EARTH TRANSITION METAL INTERMETALLICS**
R. Kumar, J. Bentley, and W. B. Yelon (Missouri Univ., Columbia.) 1990 8 p Presented at the Spring Meeting of the Materials Research Society, San Francisco, CA, 16-21 Apr. 1990
(Contract DE-AC05-84OR-21400)
(DE90-015800; CONF-900466-79) Avail: NTIS HC/MF A02

Neutron diffraction experiments on rare-earth transition metal magnetic alloys Er2, Fe14 B and Er2, Fe17 have been carried out at temperatures above and below the ordering temperature (Tc). An anomalously large magnetic moment is observed at the crystallographic j sub 2 site in Er2, Fe14 B which is the intersection point of the major ligand lines in the crystal structure. The interatomic Fe-Fe distances are in the range of strong ferromagnetic bonds (Ge 2.66 angstrom). The analogous f site in Er2 Fe17 does not develop as large a magnetic moment. In addition, the same sites show strong preference for Fe atoms in the respective substituted compounds. Due to poor phase stability of Er2, Co sub x Fe(sub 1 minus x) B-14 compounds, iron substitution has been studied in detail in Er2, Co sub x Fe(sub 1 minus x) sub 17 alloys for site specific order an lattice distortion effects. However, a nonlinear change in the c lattice parameter observed in the neutron diffraction results cannot be explained on the basis of site preference alone. The neutron refinement results indicate iron rich compositions in Er2, Co sub x Fe(sub 1 minus x) sub 17 materials, which is related to random substitution of Fe dumbbell pairs in the rare earth sites in the lattice. However, extensive electron microscopy (selected area electron diffraction and high resolution imaging) of Er2, Fe17 and Er2, Co sub .40 Fe sub .60 sub 17 failed to reveal any microscopic inhomogeneity. DOE

**N91-10157*#** National Aeronautics and Space Administration. John F. Kennedy Space Center, Cocoa Beach, FL.
**EVALUATION OF CANDIDATE ALLOYS FOR THE CONSTRUCTION OF METAL FLEX HOSES IN THE STS LAUNCH ENVIRONMENT**
Louis G. MacDowell, III and Cordelia Ontiveros Aug. 1988 90 p
(NASA-TM-103808; MTB-325-87A; NAS 1.15:103808) Avail: NTIS HC/MF A05 CSCL 11F

Various vacuum jacketed cryogenic supply lines at the Shuttle launch site use convoluted flexible expansion joints. The atmosphere at the launch site has a very high salt content, and during a launch fuel combustion products include hydrochloric acid. This extremely corrosive environment has caused pitting corrosion failure in the flex hoses, which were made out of 304L stainless steel. A search was done to find a more corrosion resistant replacement material. Nineteen metal alloys were tested. Tests which were performed include electrochemical corrosion testing, accelerated corrosion testing in a salt fog chamber, long term exposure at the beach corrosion testing site, and pitting corrosion tests in ferric chloride solution. Based on the results, the most corrosion resistant alloys were found to be, in order, Hastelloy C-22, Inconel 625, Hastelloy C-276, Hastelloy C-4, and Inco Alloy G-3. Of these top five alloys, the Hastelloy C-22 stands out as being the best of the alloys tested. Author

**N91-10158#** Los Alamos National Lab., NM.
**CONSTANT STRESS OF XD (TRADEMARK) TIAI CONTAINING NITROGEN**
Erica Robertson (Air Force Office of Scientific Research, Bolling AFB, Washington, DC.) and Patrick L. Martin 1990 9 p Presented at the Spring Meeting of the Materials Research Society,

San Francisco, CA, 16-20 Apr. 1990
(Contract W-7405-eng-36)
(DE90-011947; LA-UR-90-1552; CONF-900466-47) Avail: NTIS HC/MF A02

Ti-47 at percent Al+7vol percent (TiN+TiB2) alloys, produced by the Martin Marietta XD (trademark) process, were subjected to tensile constant stress creep deformation in the range 760 to 850 C temperature and 138 to 276 MPa stress. These alloys have a matrix of TiAl and Ti3Al initially containing 1 to 10 micron diameter equiaxed particles of TiB2 and Ti2AlN. Microstructures were examined using optical, scanning electron microscopy (SEM) and transmission electron microscopy (TEM) methods in an attempt to correlate the substructures with the property data. In particular, fine coherent particles were observed to decorate dislocations and the interior of TiAl grains. The presence of these particles is thought to explain the creep resistance of this alloy. DOE

**N91-10159#** Brookhaven National Lab., Upton, NY. Applied Physics Div.

**XAFS STUDIES OF INTERACTIONS AT TRANSITION-METAL/Al INTERFACES**

S. M. Heald and E. V. Barrera 1990 3 p Presented at the 6th International Conference on XAFS Meeting, York, England, 5-11 Aug. 1990
(Contracts DE-AC02-76CH-00016; DE-AS05-80ER-10742)
(DE90-016313; BNL-44434; CONF-9008141-1) Avail: NTIS HC/MF A01

X ray Absorption Fine Structure (XAFS) measurements on transition metal/Al interfaces were made using a combination of glancing angle and in-situ UHV techniques. Glancing angle methods provide depth dependent interface structural information for Al on metal bilayers, while SEXAFS methods were used for thin metal layers on Al substrates. In all cases studied (Ni, Cu, and Cr) interfacial O played a crucial role in determining the interface structure. DOE

**N91-10160#** Pacific Northwest Lab., Richland, WA.

**RADIATION-INDUCED MICROSTRUCTURAL DEVELOPMENT AND MICROCHEMICAL CHANGES IN Fe-Cr-Mn-Ni SOLUTE-BEARING ALLOYS**

H. Takahashi, S. Ohnuki, and F. Garner Jun. 1990 15 p Presented at the 15th Symposium on Effects of Radiation on Materials, Nashville, TN, 17-21 Jun. 1990
(Contract DE-AC06-76RL-01830)
(DE90-016359; PNL-SA-18229; CONF-900623-12) Avail: NTIS HC/MF A03

The density changes measured in three Fe--Cr--Mn--Ni solute-bearing austenitic alloys irradiated in the Fast-Flux Test Facility (FFTF) indicate that nickel additions do not decrease swelling as had been anticipated, but actually increase swelling initially. These data were confirmed by microscopy examination but are contrary to the behavior observed during electron irradiation of these same alloys. Nickel and commercially relevant solute additions also appear to suppress the formation of ferrite and sigma phases, which were observed in solute-free Fe--Cr--Mn ternary alloys irradiated in the same experiment. DOE

**N91-10161#** Lawrence Livermore National Lab., CA.

**HIGH STRAIN RATE DEFORMATION BEHAVIOR OF SHOCKED COPPER**

David H. Lassila, Mary LeBlanc, and George T. Gray, III (Los Alamos National Lab., NM.) Aug. 1990 9 p Presented at the International Conference on Shock Wave and High-Strain-Rate Phenomena in Materials, San Diego, CA, 12-17 Aug. 1990 Submitted for publication
(Contract W-7405-eng-48)
(DE90-016481; UCRL-JC-103469; CONF-900818-3) Avail: NTIS HC/MF A02

Uniaxial mechanical testing of shock-prestrained copper was performed over a range of strain rates from 10E-3 to 7x10E3 s-1 in tension and compression to study the effects of shock-induced substructure on constitutive behavior. For comparison, copper in the preshocked condition (annealed, 15 micron grain size) was also tested. Results of the study show that the post shock mechanical behavior of copper at high strain rates is similar to that previously reported at slow strain rates, i.e., the shocked copper had an increase in yield strength and a decrease in work hardening rate. The strain rate sensitivity of the shocked copper was found to be similar to that of the unshocked material. Tensile test results from both high and low strain rate tests are presented and show the elongation of the shocked material to be considerably less than that of the unshocked material. The effects of the constitutive behavior of the shocked and unshocked materials on elongation are discussed. DOE

**N91-10162#** Los Alamos National Lab., NM.

**MECHANICAL AND MICROSTRUCTURAL RESPONSE OF NI3AI AT HIGH STRAIN RATE AND ELEVATED TEMPERATURES**

H. W. Sizek and George T. Gray, III 1990 12 p Presented at the International Conference on Shock Wave and High-Strain-Rate Phenomena in Materials, San Diego, CA, 12-17 Aug. 1990
(Contract W-7405-eng-36)
(DE90-016489; LA-UR-90-2801; CONF-900818-4) Avail: NTIS HC/MF A03

The effect of strain rate and temperature on the substructure evolution and mechanical response of Ni3Al will be presented. The strain rate response of Ni3Al was studied at strain rates from 10(exp -3) s(exp -1) (quasi-static) to 10(exp 4) s(exp -1) using a Split Hopkinson Pressure Bar. The Hopkinson Bar tests were conducted at temperatures ranging from 77 to 1273 K. At high strain rates the flow strength increased significantly with increasing temperature, similar to the behavior observed at quasi-static rates. The work hardening rates increased with strain rate and varied with temperatures. The work hardening rates, appeared to be significantly higher than those found for Ni270. The substructure evolution was characterized utilizing TEM. The defect generation and rate sensitivity of Ni3Al are also discussed as a function of strain rate and temperature. DOE

**N91-10163#** Los Alamos National Lab., NM.

**TEXTURE-INDUCED ANISOTROPY AND HIGH-STRAIN RATE DEFORMATION IN METALS**

S. K. Schiferl and P. J. Maudlin 1990 17 p Presented at the Explomet 1990 Conference, San Diego, CA, 12-17 Aug. 1990 Sponsored in part by DARPA
(Contract W-7405-eng-36)
(DE90-016611; LA-UR-90-2679; CONF-9008125-8) Avail: NTIS HC/MF A03

Crystallographic texture calculations were used to model anisotropic yielding behavior for polycrystalline materials with strong preferred orientations and strong plastic anisotropy. Fitted yield surfaces were incorporated into an explicit Lagrangian finite-element code. Different anisotropic orientations were considered, as well as different yield-surface forms, for Taylor cylinder impacts of hcp metals such as titanium and zirconium. Some deformed shapes are intrinsic to anisotropic response. Also, yield surface curvature, as distinct from strength anisotropy, has a strong influence on plastic flow. DOE

**N91-10164#** Los Alamos National Lab., NM. Materials Science and Technology Div.

**THE INFLUENCE OF SHOCK PRE-STRAIN AND PEAK PRESSURE ON SPALL BEHAVIOR OF 4340 STEEL**

A. K. Zurek, Ch. E. Frantz, and George T. Gray, III 1990 10 p Presented at the Explomet 1990 International Conference on Shock-Wave and High-Strain-Rate Phenomena in Materials, San Diego, CA, 12-17 Aug. 1990
(Contract W-7405-eng-36)
(DE90-016612; LA-UR-90-2678; CONF-9008125-7) Avail: NTIS HC/MF A02

A fundamental study of the influence of peak stress amplitude and pre-strain on the spall fracture of pearlitic 4340 steel is presented. Spall tests were performed at projectile velocities to achieve approximately 5, 10, and 15 GPa peak stress amplitudes. Some spall tests were preceded by a pre-shock and recovery test at 10 and 15 GPa. Spall strength measurements suggest that there is a decrease in the spall strength of 4340 with an increase in the shock wave amplitude as the transition pressure of 13.1 GPa is approached. At this transition pressure, a substantial increase in the spall strength, as well as a change in a mode of fracture from brittle to ductile are observed, both attributed to the allotropic phase transformation at this amplitude. DOE

**N91-10165#** Los Alamos National Lab., NM. Physical Metallurgy Group.
**SHOCK EXPERIMENTS IN METALS AND CERAMICS**
George T. Gray, III 1990 15 p Presented at the Explomet 1990 Conference, San Diego, CA, 13-17 Aug. 1990
(Contract W-7405-eng-36)
(DE90-016613; LA-UR-90-2677; CONF-9008125-6) Avail: NTIS HC/MF A03

Shock recovery and spallation experiments, in which material structure/property effects are systematically varied and characterized quantitatively, offer two important experimental techniques to probe the physical mechanisms controlling shock processes and dynamic fracture. This paper highlights the current state of knowledge and principal challenges of the structure/property effects of shock-wave deformation on metals and ceramics. Recent shock-recovery and spallation experimental results on post-mortem material properties and fracture behavior in metals and ceramics are reviewed. Finally, the influence of shock-wave deformation on several intermetallics and a recent experiment examining the Bauschinger effect in Al-4 percent Cu during shock loading are presented. DOE

**N91-10166#** Pacific Northwest Lab., Richland, WA.
**STRENGTH AND TOUGHNESS OF SINGLE-PHASE AND DUAL-PHASE HIGH-TEMPERATURE INTERMETALLICS**
Stephen M. Bruemmer, John L. Brimhall, and Charles H. Henager, Jr. Apr. 1990 7 p Presented at the Spring Meeting of the Materials Research Society, San Francisco, CA, 16-21 Apr. 1990 Sponsored in part by ONR
(Contract DE-AC06-76RL-01830)
(DE90-017192; PNL-SA-17825; CONF-900466-82) Avail: NTIS HC/MF A02

The strength and toughness of several high temperature beryllium- niobium (Be12Nb and Be17Nb2) and iridium-niobium (Ir3Nb) intermetallic compounds were evaluated. Materials were prepared by high rate sputter deposition and characterized by x ray diffraction and analytical electron microscopy before and after heat treatment. As-sputtered microstructures were varied from amorphous to microcrystalline by control of substrate temperature. Grain size, degree of order, and second-phase distribution were modified by subsequent heat treatment. Strength as a function of temperature was assessed by hot hardness tests and toughness estimated from indentation-induced crack lengths. Intermetallics exhibited very high strength and low toughness up to temperatures of approx 1000 C. Mechanical behavior was a direct function of the microstructural parameters including matrix phase composition, second phase distribution, and degree of order. DOE

**N91-10167#** Oak Ridge National Lab., TN. Metals and Ceramics Div.
**BRITTLE FRACTURE AND DUCTILITY IMPROVEMENT IN NICKEL AND IRON ALUMINIDES**
E. P. George and C. T. Liu 1990 13 p Presented at the Meeting of the International Materials Research Society, Beijing, Peoples Rep. of China, 18-22 Jun. 1990
(Contract DE-AC05-84OR-21400)
(DE90-017319; CONF-900632-1) Avail: NTIS HC/MF A03

Nickel and iron aluminides are two potentially useful ordered intermetallic alloy systems that share a problem common to many ordered intermetallics, namely brittle fracture and poor ductility at room temperature. However, recent developments have shown that it is possible to overcome this problem and get significantly improved room-temperature ductilities in both these alloy systems by employing a combination of micro-and macro-alloying techniques. Concurrently, our understanding of the underlying causes of brittle fracture in ordered intermetallics has improved dramatically. We review here recent results related to the ductility and fracture behavior of two nickel aluminides (Ni3Al and NiAl), and two iron aluminides (FeAl, and Fe3Al). We will show that the major difference between Ni3Al and the two iron aluminides is the following: in the former, brittle fracture is a result of intrinsically weak grain boundaries, whereas in the latter, brittle fracture is a result of an extrinsic factor, namely moisture-induced environmental embrittlement. The brittleness of Ni3AL can be overcome by microalloying with boron and carefully controlling the alloy stoichiometry, whereas the ductilization of iron aluminides requires modification of their surface composition (or environment) to minimize the chemical reaction with moisture in air. NiAl also has weak grain boundaries (like Ni3Al), which can be strengthened by the addition of small amounts of boron. However, because of its other problems, like poor cleavage strength and insufficient number of deformation modes, the ductility of NiAl is not significantly improved even after intergranular fracture is totally suppressed. DOE

**N91-10168#** Rolls-Royce Ltd., Bristol (England).
**CASTING ALLOYS FOR THE JET AGE**
M. H. Griffiths Derby, England 22 Jun. 1989 10 p Presented at POS Jnl (IBF) Meeting, Stratford-upon-Avon, England, 22 Jun. 1989
(PNR-90723; ETN-90-97948) Copyright Avail: NTIS HC/MF A02

The historical development of casting alloys applied to jet aero engines is summarized. Special attention is given to nickel based superalloys. Relevant developments are discussed highlighting important milestones achieved in terms of the effects of alloying elements and their constituent phases. The investment casting route is described. References to the various processing techniques now employed are made. These include directional solidification, single crystals, heat treatment and ceramic core technology. Current limitations and future developments designed to improve foundry practices are underlined. ESA

## 27 NONMETALLIC MATERIALS

Includes physical, chemical, and mechanical properties of plastics, elastomers, lubricants, polymers, textiles, adhesives, and ceramic materials.
For composite materials see *24 Composite Materials.*

**N91-10169** United Kingdom Atomic Energy Authority, Harwell (England). Materials Development Div.
**ENVIRONMENTAL DEGRADATION OF MACRO DEFECT FREE CEMENTS. 1: MECHANICAL PROPERTIES INVESTIGATION**
I. Titchell 5 Dec. 1988 17 p
(AERE-R-13354-1; HL88-1003-1) Copyright Avail: Issuing Activity

Macro defect free (MDF) cements derive their name from the absence of the large scale (greater than 200 microns) porosity normally found in cement. This is achieved by a processing route which has a low water to cement ratio, a polymeric processing aid, and high shear mixing. The resulting material shows a considerable increase in flexural strength compared to the same cement produced by conventional techniques. In high alumina cement (HAC) MDF's the flexural strength is approx. 200 MPa compared to 20 to 30 MPa for a normal HAC. The exact cause of the enhanced strength is subject to debate, but it is clear that the MFD's represent a considerable advance in the search for high strength cements. Theoretically any hydraulic cement can be used to make an MDF. In practice it is found that some cements are very sensitive to the polymeric agent and before the MDF can be produced a suitable polymer needs to be found. For example, HAC produces MDF with polyvinyl alcohol/acetate (PVA), and an ordinary portland cement (OPC) MDF with PVA or hydroxy propyl methyl cellulose (HPMC) or polyacrylamide as the polymeric aid. The materials studied include: NIM 127 (HAC PVA based), NIM 125 (HAC PVA based), NIM 223 (with a heat treatment to remove the polymeric phase), an OPC based MDF (based on HPMC), and an OPC based MDF (with PVAL). The effects of heat, gamma radiation and immersion in water on these MDF's are explored. In particular, the role that the polymer and cement used to make the MDF play in determining the response of the material to its environment is explored. Author

**N91-10170*#** Southwest Texas State Coll., San Marcos. Dept. of Chemistry.
**TRIFLUOROMETHYL-SUBSTITUTED POLYMERS Semiannual Status Report, 1 Jan. - 30 Jun. 1990**
Patrick E. Cassidy 11 Sep. 1990 13 p
(Grant NAG1-631)
(NASA-CR-186955; NAS 1.26:186955) Avail: NTIS HC/MF A03 CSCL 11C

The synthesis of polymers is discussed. It includes: (1) the synthesis of fluorine-containing crosslinked poly(ether ketones); (2) the synthesis and characterization of poly(imide amides) and their N-methylated analogues; (3) the synthesis of fluorine-containing aromatic polyethers; (4) the synthesis of novel fluorine-containing aromatic polysiloxanes; and (5) the conversion of 6F-containing polythioethers to polysulfones. It is hoped that these polymers will find use as low dielectric materials in electronic applications, function as thermal control coatings, or be suitable elastomeric sealants for extreme service conditions. Author

**N91-10171#** Argonne National Lab., IL. Tribology Section.
**SELF-LUBRICATING BORIC ACID FILMS FOR TRIBOLOGICAL APPLICATIONS**
A. Erdemir, G. R. Fenske, F. A. Nichols, R. A. Erck, and D. E. Busch 1990 7 p Presented at the Japan International Tribology Conference, Nagoya, Japan, 29 Oct. - 1 Nov. 1990
(Contract W-31-109-eng-38)
(DE90-007805; CONF-901009-1) Avail: NTIS HC/MF A02

Because of its layered crystal structure, boric acid, has been found to be lubricious. Its self-lubricating mechanism is related to the easy shear of atomic layers over one another. Moreover, laser-Raman spectroscopy and electron microscopy analyses have confirmed that thin boric acid films can form on surfaces containing boron and boric oxides. To study the lubricity and self lubricating mechanism of boric acid, pin-on-disk tests were performed on pairs of boric acid compacts and steel disks, boric oxide films and steel pins, boron films and steel pins, and boron-implanted steel disks and steel pins. The mean steady-state friction coefficients of these tribosystems ranged from 0.04 to 0.12. DOE

**N91-10172#** Sandia National Labs., Albuquerque, NM.
**ANOMALOUS DISPERSION AS A PHASE-MATCHING TECHNIQUE FOR SECOND HARMONIC GENERATION**
P. A. Cahill and Kenneth D. Singer (Bell Telephone Labs., Inc., Princeton, NJ.) 1990 5 p Presented at the International Symposium on Nonlinear Optical Materials, El Paso, TX, 28 Oct. - 2 Nov. 1990
(Contract DE-AC04-76DP-00789)
(DE90-015696; SAND-90-2058C; CONF-9010170-1) Avail: NTIS HC/MF A01

Anomalous dispersion (the decrease in refractive index which is associated with absorption) can be used to produce a phase-matched condition for second harmonic generation. This process also gives rise to large increases in the useful second order hyperpolarizability. A new, soluble NLO dye with exceptionally low absorption near 400 nm has been used for anomalous dispersion phase-matching studies in thin films. DOE

**N91-10173#** Pacific Northwest Lab., Richland, WA.
**DESIGN CONSIDERATIONS FOR A CERAMIC FABRIC RADIATOR**
K. A. Pauley, B. J. Webb, and A. C. Klein (Oregon State Univ., Corvallis.) Apr. 1990 10 p Presented at the Engineering, Construction and Operations for Space, Albuquerque, NM, Apr. 1990
(Contract DE-AC06-76RL-01830)
(DE90-016342; PNL-SA-17201; CONF-900442-4) Avail: NTIS HC/MF A02

The design of an Advanced Ceramic Fabric (ACF) thermal management device for use in both interplanetary and near-earth space must consider several important aspects of the environment. First, the radiation field at various locations is dominated by a proton component which deposits its energy on the surface of the device. Second, the ACF materials, as well as pressure liner materials, must also be compatible with the working fluids selected for the system. Third, the fluid dynamics and heat transfer characteristics of this device should be adequately characterized. With the proper consideration of materials and operating conditions, the Bubble Membrane Radiator (BMR) may be utilized for several advanced space missions. DOE

**N91-10174#** Ames Lab., IA.
**MONOMOLECULAR AND THIN POLYMER FILMS: FABRICATION, CHARACTERIZATION, APPLICATIONS, AND MODELS OF WETTING Ph.D. Thesis**
Lai Kwan Chau 24 Aug. 1990 166 p
(Contract W-7405-eng-82)
(DE90-016415; IS-T-1487) Avail: NTIS HC/MF A08

A variety of chemically modified surfaces were synthesized and their molecular structures and reactivities were characterized. These interfaces include: (1) Monomolecular films of n-alkanoic acids (CH3(CH2)nCOOH) and n-perfluorocarboxylic acids (CF3(CF2)nCOOH) on silver; and (2) calcichrome immobilized at an anion exchange polymer film. The monomolecular films were fabricated by the self-assembly method and characterized by optical ellipsometry, infrared reflection spectroscopy, and contact angle measurements. A comparison is given of the properties of these films with regard to composition, defectiveness, intermolecular environment, molecular orientation, wettability, and formation thermodynamics. As it is relevant to monolayer formation thermodynamics, the isoelectric point of the surface of evaporated silver films was determined by contact angle titration. Potential applications of these films are discussed. Monomolecular films as models of wetting are also examined in terms of van der Waals interactions at the macroscopic interfaces. Theoretical considerations of the effects of intermolecular forces on depth sensitivity of wetting and limiting contact angles of various systems are assessed. One of the synthesized interfaces has been applied as a Ca(II) optical sensor. The sensor was fabricated by electrostatic immobilization of calcichrome at an anion exchange polymer film. The structure and reactivity of this interface was characterized by ultraviolet-visible diffuse reflectance spectroscopy and infrared photoacoustic spectroscopy. Equations to determine the metal complex formation constant and acid dissociation constants of the immobilized reagent form diffuse reflectance spectra are developed. Possible causes affecting the reactivity of an immobilized indicator are discussed. DOE

**N91-10175#** Oak Ridge Y-12 Plant, TN. Development Div.
**ANALYSIS OF ALUMINUM OXIDE CERAMIC**
D. A. Carpenter and C. E. Holcombe 29 Aug. 1990 12 p
(Contract DE-AC05-84OS-21400)
(DE90-016517; Y/DW-1008) Avail: NTIS HC/MF A03

Several aluminum oxide ceramic disks were received from Coors Ceramics for analysis of black spots occurring on some of the disks. The disks were analyzed by x ray fluorescence, using the x ray microprobe in the scanning mode, and by x ray diffraction. The elements (greater than Z=14) observed, listed in order of approximate concentration, were Zr (several percent), Fe, Ca, Ni, and Sr, (minor to trace amounts). X ray diffraction analysis revealed a major amount of Al2, O3 (corundum), a minor amount of ZrO2, and minor unidentified lines. Some of the unidentified lines could be accounted for by CaAl2, Si2, O8 and BaAl2, Si2, O8. There were no significant differences between the analyses of the rejected disks and those of the accepted ones. DOE

**N91-10176#** Los Alamos National Lab., NM. Materials Science and Technology Div.
**HIGH-STRAIN-RATE COMPRESSION AND FRACTURE OF B4C-ALUMINUM CERMETS**
William R. Blumenthal 1990 11 p Presented at the Explomet Conference, La Jolla, CA, 12-17 Aug. 1990
(Contract W-7405-eng-36)
(DE90-016568; LA-UR-90-2699; CONF-9008125-5) Avail: NTIS HC/MF A03

The compressive behavior of liquid-metal infiltrated boron carbide-aluminum cermets were studied as a function of strain rate, composition, and microstructure. Hopkinson split pressure bar (HSPB) and quasi-static compression tests were conducted using dumb-bell-shaped specimens. Results showed cermet compressive strength to be independent of loading rate. Strength was also found to be independent of the aluminum alloy used to infiltrate pre-sintered 65 vol percent B4C preforms. compositions with the smallest phase size displayed the best strength and ductility. DOE

**N91-10177#** Illinois Inst. of Tech., Chicago. Dept. of Chemical Engineering.
**CORROSION-RESISTANT COATINGS FOR HIGH-TEMPERATURE HIGH-SULFUR ACTIVITY APPLICATIONS**
J. Robert Selman Jun. 1990 18 p Prepared for Illinois Inst. of Tech., Chicago, IL
(Contracts DE-AC03-76SF-00098; LBL-4559910)
(DE90-016638; LBL-29138) Avail: NTIS HC/MF A03

The research described is intended to assist in developing the technology for the production of molybdenum, molybdenum carbide and titanium nitride coatings. These coatings have the potential to serve as an alternative to present methods of protecting the metal parts, at positive potential, of high temperature sulfur or sulfide batteries (e.g., chromizing). This research project was prompted by the observation that only very few materials are corrosion resistant in a high-temperature high sulfur activity environment containing polysulfide or FeS2. Among these materials only molybdenum has really satisfactory corrosion resistance. In LiCl-KCl eutectic containing FeS2, titanium nitride has also shown adequate corrosion resistance. In polysulfide melts chromium shows good corrosion resistance, and chromizing is presently used to protect the internal surface of the containers in the sodium-sulfur battery, as manufactured at Chloride Silent Power Ltd. It should be noted that the issue of an optimal coating for the sodium-sulfur battery container is somewhat clouded and may be resolved satisfactorily only when there is more information about the effect of very small amounts of dissolved metal, such as chromium or molybdenum, on the life of the sodium-beta-alumina electrolyte. Nevertheless, there is a clear incentive for exploring molybdenum, or molybdenum derivatives, and titanium nitride as alternative protecting materials. DOE

**N91-10178#** Oak Ridge National Lab., TN. Engineering Technology Div.
**DESIGN METHODOLOGY NEEDS FOR FIBER-REINFORCED CERAMIC HEAT EXCHANGERS**
J. J. Blass and M. B. Ruggles Aug. 1990 47 p
(Contract DE-AC05-84OR-21400)
(DE90-016659; ORNL/TM-11012) Avail: NTIS HC/MF A03

The purpose is to identify significant development and validation needs that must be satisfied to establish a viable design methodology for use of ceramic fiber reinforced, ceramic matrix composite materials in advanced heat exchangers for high temperature and high pressure applications. This is part of an initiative undertaken to foster the development and commercializaiton of high pressure heat exchange systems (HiPHES). Previous studies identified several industrial applications of HiPHES technology in which the use of fiber reinforced ceramic composites can provide very significant benefits. The studies resulted in a recommended development program that includes an early assessment of design methodology needs for these materials and applications. To provide this assessment, Oak Ridge National Laboratory (ORNL) assembled a panel of experts with government, university, and industrial affiliations. The present panel met in April 1988 for presentations and discussions related to structural design methodology for fiber reinforced ceramic heat exchanger components. DOE

**N91-10179#** Pacific Northwest Lab., Richland, WA. Materials and Chemical Sciences Center.
**OPTICAL PROPERTIES OF INORGANIC POLYMERS**
Kim F. Ferris and Steven M. Risser Nov. 1989 7 p Presented at the Materials Research Society Fall Meeting, Aberdeen, MD, 27 Nov. - 2 Dec. 1989
(Contract DE-AC06-76RL-01830)
(DE90-017143; PNL-SA-18059; CONF-891119-139) Avail: NTIS HC/MF A02

The electronic structure of organic and inorganic polymeric systems are well described by their molecular symmetry, even with the large bond polarity shown by such systems as polyphosphazenes. Calculations were performed using semi-empirical Hamiltonians to determine the electronic structure and optical nonlinearities for a series of model phosphonitrilic and organic compounds. The optical transition energies for phosphonitrilic compounds are greater than their organic counterparts as a result of in-plane pi' bonding interactions, and are modulated by the electronegativity of the substituent groups on the phosphorus atoms. Values are reported for the vertical ionization energy and electronic absorption wavelengths, and use molecular orbital contour analysis to show the effects of ligand electronegativity on the pi' network. Hyperpolarizabilities were calculated from third order perturbation theory for a series of phosphonitrilic compounds, (X sub 2 P-N) sub n, as a function of bond length alternation and ligand substitution. In contrast to organic polyenes, the difference in pi orbital energy between phosphorus and nitrogen is critical to determining the onset of saturation and the magnitude of the hyperpolarizability. DOE

**N91-10180#** Pacific Northwest Lab., Richland, WA. Materials and Chemical Sciences Center.
**EFFECTS OF IN-PLANE pi PRIME BONDING ON ELECTRONIC TRANSITION ENERGIES FOR INORGANIC POLYMERS**
Kim F. Ferris, Steven M. Risser, and Angela K. Hanson Mar. 1990 8 p Presented at the Materials Research Society Fall Meeting, Boston, MA, 27 Nov. - 2 Dec. 1989
(Contract DE-AC06-76RL-01830)
(DE90-017144; PNL-SA-17230; CONF-891119-138) Avail: NTIS HC/MF A02

The electronic structure of organic and inorganic polymeric systems are well described in terms of their molecular symmetry, even with the large bond polarity shown by such systems as polyphosphazenes. Calculations were performed using the semi-empirical (Complete Neglect of Differential Overlap) CNDO/1 method to determine the valence electronic structure for a series of model phosphonitrilic and organic compounds. The optical transition energies for phosphonitrilic compounds are greater than their organic counterparts as a result of in-plane pi' bonding interactions. The extent of these interactions is modulated by the electronegativity of the substituent groups on the phosphorus atoms. Values are reported for the vertical ionization energy and electronic absorption wavelengths, and use molecular orbital contour analysis to show the effects of ligand electronegativity on the pi' network. DOE

**N91-10181#** Oak Ridge National Lab., TN.
**MEETINGS ON THE STRUCTURE AND PROPERTIES OF IMPLANTED CERAMICS**
Carl J. McHargue and Linda L. Horton 1990 7 p
(Contract DE-AC05-84OR-21400)
(DE90-017313; ORNL/FTR-3720) Avail: NTIS HC/MF A02

The visit to the University Claude Bernard was for the purpose of analyzing data obtained there and at the Oak Ridge National Laboratory in a collaborative research program, to exchange samples, to plan further work, and to revise drafts of two manuscripts for publication. One of the travelers served on the

jury for the doctoral examination of E. Abonneau. The travelers also attended the NATO-ASI entitled, Diamond and Diamond-Like Films and Coatings, and served on the Organizing Committee.
DOE

**N91-10182*#** National Aeronautics and Space Administration. Langley Research Center, Hampton, VA.
**EVALUATION OF TWO BISIMIDE ADDITIVES IN LARC-TPI ADHESIVE**
Donald J. Progar and Terry L. StClair Nov. 1990 27 p
(NASA-TM-102742; NAS 1.15:102742) Avail: NTIS HC/MF A03 CSCL 11C

The processability of aromatic polyimides can be improved by the addition of bis (amide) acids or bisimides to LARC-TPI. These low molecular weight additives apparently lower the melt viscosity of aromatic polyimides without affecting the glass transition temperature. Well-consolidated, fiber reinforced composites were fabricated using this technology. LARC-TPI can be processed as a thermoplastic polyimide to form high strength bonds, however, this is generally accomplished by processing at relatively high bonding pressures. An adhesive investigation is presented on the effects of two bisimide additives to LARC-TPI in an attempt to improve the bonding process by lowering the viscosity of the material to achieve improved bond strength properties. Apparently, the high flow which is exhibited by the additives when they melt, tended to be masked by the more viscous LARC-TPI. Author

# 28 PROPELLANTS AND FUELS

Includes rocket propellants, igniters, and oxidizers; their storage and handling procedures; and aircraft fuels.

For related information see also *07 Aircraft Propulsion and Power, 20 Spacecraft Propulsion and Power,* and *44 Energy Production and Conversion.*

**N91-10183#** Sandia National Labs., Albuquerque, NM. Structural Physics and Shock Chemistry Div.
**THERMOCHEMISTRY OF SHOCK-INDUCED EXOTHERMIC REACTIONS IN SELECTED POROUS MIXTURES**
M. B. Boslough 1990 10 p Presented at the Explomet Conference, San Diego, CA, 12-17 Aug. 1990
(Contract DE-AC04-76DP-00789)
(DE90-016104; SAND-90-0647C; CONF-9008125-4) Avail: NTIS HC/MF A02

Steady detonation theory was used to describe shock induced chemical reactions in a variety of powder mixtures. By introducing a number of simplifications, pressure and temperature increases caused by a reaction can be estimated by considering only the initial powder density, porosity, heat of reaction and thermophysical properties of the product phases. For a given mixture, the pressure increase is greater for higher initial powder packing density. Materials with large volume increases associated with the reaction will demonstrate the largest pressure increases, as expected. Shock temperatures can be approximated by a linearly increasing function of pressure, where the zero-pressure intercept is the adiabatic reaction temperature and the slope depends on initial porosity, volume change and product specific heat. The approximation provides a means of characterizing shock induced chemical reactions in terms of zero-pressure material properties. DOE

**N91-10184#** Sandia National Labs., Albuquerque, NM.
**HYDROGEN-TRITIUM GETTERS AND THEIR APPLICATIONS**
Timothy J. Shepodd and Henry M. Smith (Allied-Signal Aerospace Co., Kansas City, MO.) Aug. 1990 6 p Presented at the Radioluminescent Technology Conference, Annapolis, MD, 25-26 Sep. 1990
(Contract DE-AC04-76DP-00613)
(DE90-016282; KCP-613-4410; CONF-9009201-4) Avail: NTIS HC/MF A02

The accumulation of hydrogen is usually an undesired event. Large leaks from hydrogen storage and handling facilities pose explosion hazards. Small amounts of hydrogen that may build up in sealed containers after long storage times can damage internal components. Any tritium leak is an immediate health hazard. Hydrogen scavengers or getters can avert all of these potential problems by irreversibly removing hydrogen from such environments. Early hydrogen getters were metals that, though effective, were sensitive to oxygen. More recent work with crystalline organic materials has yielded formulations that will scavenge hydrogen in the presence or absence of air. They commonly utilize a catalyst to add hydrogen across of carbon-carbon double or triple bond. Because of the instability of organic materials to ionizing radiation, a getter that will be stable after reaction with tritium is a further challenge. We will describe hydrogen getter materials and systems developed at Sandia National Laboratories and at Allied-Signal, Kansas City Division. These materials have the proven ability to scavenge and contain hydrogen and tritium. The technologies are based on the irreversible removal of hydrogen by catalytic hydrogenation of unsaturated organic compounds. DOE

**N91-10185#** Sandia National Labs., Albuquerque, NM.
**ORGANIC GETTER MATERIALS FOR THE REMOVAL OF HYDROGEN AND ITS ISOTOPES**
H. Mike Smith, Tim J. Shepodd, and Laura R. Gilliom (Allied-Signal Aerospace Co., Kansas City, MO.) Aug. 1990 12 p Presented at the 4th International Conference on Hydrogen Effects on Material Behavior, Jackson Hole, WY, 12-16 Sep. 1989
(Contract DE-AC04-76DP-00613)
(DE90-016284; KCP-613-4204; CONF-8909204-6) Avail: NTIS HC/MF A03

Hydrogen getter technologies are described which were developed at SNL and KCD over the past decade. The technologies are based on the irreversible removal of hydrogen by catalytic hydrogenation of unsaturated organic compounds. Different types have been developed: crystalline getters, dialkynes combined with heterogeneous catalysts; and a polymeric getter, a thermoplastic elastomer capable of reacting with hydrogen in the presence of oxygen without producing water. These materials can remove up to 300 cc (STP) of hydrogen per gram of material, and can maintain atmospheres of less than 10 ppM hydrogen. Crystalline getters for tritium and the combination hydrogen (tritium), water, and oxygen are described. The accumulation of hydrogen is usually an undesired event. Large leaks from hydrogen storage and handling facilities pose explosion hazards. Small amounts of hydrogen that may build up in sealed containers after long storage times can damage integral components. Any tritium leak is an immediate health hazard. Hydrogen scavengers or getters can avert all of these potential problems by irreversibly removing hydrogen from such environments. The development is described of two types of organic getters: the first is a new crystalline getter, based on 1,4-bis (phenylethynyl) benzene (5) (DEB); the second is a polymeric hydrogen getter, based on styrene-butadiene copolymer. DOE

**N91-10186#** Teledyne/McCormick Selph, Hollister, CA.
**VERY HIGH BURN RATE PROPELLANTS**
1990 76 p Prepared for LLNL, CA
(Contract W-7405-eng-48)
(DE90-016865; UCRL-CR-104639) Avail: NTIS HC/MF A05

Teledyne McCormick Selph has successfully completed the objectives of the program; the formulation, synthesis, and characterization of several cast solid propellants possessing very high burn rates (of the order of several meters per second) and suitable for incorporation as the propelling charge for a variety of modern gun systems of various calibers, and for potential rocket applications. More specifically, the tasks successfully accomplished include: (1) The selection of candidate propellant compositions based upon the practical factors of chemical stability and compatibility, density, heat of formation, availability and cost; (2) Theoretical thermochemical and ballistic evaluation and subsequent downselection; (3) Batch preparation of selected candidates and manufacturing process parameters studies; (4) Experimental determination of safety characteristics and ballistic evaluation (i.e., burn rate determination); and (5) Preliminary studies of grain designs and theoretical ballistic performance for gun applications. The results indicate substantial improvement in several current gun systems are achievable by incorporating the technology and propellants developed. DOE

**N91-10187#** Los Alamos National Lab., NM.
**TRANSITION STATE THEORY APPLYING TO THE STUDY OF REACTION PROCESSES IN DETONATION**
Pier K. Tang Jul. 1990 18 p
(Contract W-7405-eng-36)
(DE90-016558; LA-11903-MS) Avail: NTIS HC/MF A03

The presence of a nearly constant process time that characterizes the fast reaction portion found in the detonation of condensed high explosives can be explained by the transition state theory. Through hydrodynamic modeling, time is identified as the excitation time for the production of an energetic state that can go either forward to achieve decomposition or backward to the original unexcited state. The energetic state is a representation of a nonequilibrium condition that favors the chemical reaction, whereas the unexcited or equilibrium state does not. This process time is determined by matching the experimental interface velocimetry record, and its value is nearly constant over a wide range of conditions. DOE

**N91-10188#** Pennsylvania State Univ., University Park.
**THERMAL STABILITY OF JET FUEL Final Report, Sep. 1988 - Dec. 1989**
Semih Eser, Chunshan Song, Ronald M. Copenhaver, Janice Perison, and Harold H. Schobert 1990 125 p
(Contract DE-AC22-88PC-88827)
(DE90-016801; DOE/PC-88827/T5) Avail: NTIS HC/MF A06

The principal objectives of this study were to investigate the thermal stability of a suite of alkylated phenols as typical trace contaminants in jet fuels and to determine the thermal stability of various fractions of a coal-derived and a petroleum-derived JP-8 jet fuel as well as the thermal stability of the unfractionated fuels. The thermal treatment experiments were carried out in nitrogen and air atmospheres (100 psig cold) using 15 ml microautoclave reactors. The reactors were heated in a fluidized sand bath at temperatures ranging from 150 C to 450 C. The samples of the coal-derived and petroleum-derived jet fuels were separated into five distillate fractions and these fractions were characterized by high-resolution gas chromatography-mass spectrometry (GC-MS). The thermal treatment products from the alkylated phenols were analyzed by 1-H and 13-C Nuclear Magnetic Resonance spectroscopy and gas chromatography/mass spectroscopy. DOE

**N91-10189#** Institut Franco-Allemand de Recherches, Saint-Louis (France).
**COMBUSTION DIAGNOSTICS OF PROPELLANTS WITH SANDWICH STRUCTURE**
H. H. Licht 1 Jun. 1989 20 p Presented at DEA-1060 Meeting, Unterluess, Fed. Republic of Germany, 16-19 May 1989
(ISL-CO-212/89; ETN-90-97571) Avail: NTIS HC/MF A03

The combustion of gun propellants in flake geometry composed from several layers of different formulations was investigated. Although visual control and ballistic behavior exhibited a typical discontinuity due to the structure, the burning characteristics of these sandwich powders could be interpreted like that of a uniform propellant. The burning rate exponent of such sandwich flake, based upon nitramines, may be degressive or progressive dependent on the sequence of the layers. ESA

**N91-10190#** National Aerospace Lab., Tokyo (Japan).
**HOT GAS SIDE HEAT TRANSFER CHARACTERISTICS OF LOX/H2 AND LOX/HC TYPE PROPELLANTS**
Akinaga Kumakawa, Masaki Sasaki, Kazuo Sato, Hiroshi Tamura, Fumiei Ono, Hiroshi Sakamoto, and Nobuyuki Yatsuyanagi Apr. 1990 32 p
(NAL-TR-1062T; ISSN-0389-4010) Avail: NTIS HC/MF A03

Combustion tests were conducted using liquid oxygen (LOX)/gaseous hydrogen, LOX/gaseous methane, and LOX/RJ-1J as propellants. Two water-cooled calorimetric combustors and two types of injectors, i.e., a coaxial and impinging injector, were used. The maximum chamber pressure was 10 MPa and the heat flux reached 100 MW per sq m in the maximum. Heat flux values measured at the throat section were lower than those predicted by the simplified Bartz's equation. A modified Bartz's equation, which uses 0.023 as a coefficient (instead of 0.026 as in the original) and which takes into account the injector end effect as well as the film cooling effect, more accurately predicted the measured heat flux distribution of the coaxial type injector. With regard to LOX/RJ-1J propellants, an empirical correlation for the thermal resistance of the carbon layer deposited on the chamber wall was obtained. It was observed that the values of thermal resistance measured were a small percentage of the values found previously. Author

## 29 MATERIALS PROCESSING

Includes space-based development of products and processes for commercial applications.
For biological materials see *55 Space Biology.*

**N91-10191*#** National Aeronautics and Space Administration. Marshall Space Flight Center, Huntsville, AL.
**ANALYSIS TECHNIQUES FOR RESIDUAL ACCELERATION DATA**
Melissa J. B. Rogers, J. Iwan D. Alexander (Alabama Univ., Huntsville.), and Robert S. Snyder Jul. 1990 27 p
(NASA-TM-103507; NAS 1.15:103507) Avail: NTIS HC/MF A03 CSCL 22A

Various aspects of residual acceleration data are of interest to low-gravity experimenters. Maximum and mean values and various other statistics can be obtained from data as collected in the time domain. Additional information may be obtained through manipulation of the data. Fourier analysis is discussed as a means of obtaining information about dominant frequency components of a given data window. Transformation of data into different coordinate axes is useful in the analysis of experiments with different orientations and can be achieved by the use of a transformation matrix. Application of such analysis techniques to residual acceleration data provides additional information than what is provided in a time history and increases the effectiveness of post-flight analysis of low-gravity experiments. Author

## 31 ENGINEERING (GENERAL)

Includes vacuum technology; control engineering; display engineering; cryogenics; and fire prevention.

**N91-10192** Texas A&M Univ., College Station.
**SYSTEM ENGINEERING OF AEROSPACE AND ADVANCED TECHNOLOGY PROGRAMS AT AN ASTRONAUTICS COMPANY (RECORD OF STUDY) Ph.D. Thesis**
Mike O. Kennedy 1989 242 p
Avail: Univ. Microfilms Order No. DA9015434

An internship with the Martin Marietta Astronautics Group that was performed in partial fulfillment of the requirements for the Doctor of Engineering degree is documented. The internship included assignments with two Martin Marietta companies, on three different programs and in four areas of engineering. A first-hand look is taken at system engineering, SDI and advanced program management, and the way Martin Marietta conducts business. The five internship objectives were related to assignments in system modeling, system integration, engineering analysis and technical management: (1) The effects of thermally and mechanically induced mirror surface distortions upon the wavefront intensity field of a high energy laser beam passing through the optical train of a space-based laser system were modeled. (2) The restrictive as opposed to the broad interpretation of the 1972 ABM Treaty, and the capability of the Strategic Defense Initiative Zenith Star Program to comply with the Treaty were evaluated. (3) The capability of

Martin Marietta to develop an automated analysis system to integrate and analyze Superconducting Super Collider detector designs was investigated. (4) The thermal models that were developed in support of the Small Intercontinental Ballistic Missile flight tests were described. (5) The technical management role of the Product Integrity Engineer assigned to the Zenith Star spacecraft's Beam Control and Transfer Subsystem was discussed. The relationships between the engineering, business, security and social concerns associated with the practice of engineering and the management of programs by a major defense contractor are explored. Dissert. Abstr.

**N91-10193#** Worcester Polytechnic Inst., MA.
**TRANSIENT CHARACTERISTICS OF UNCONFINED FIRE PLUME-DRIVEN CEILING JETS Final Report, 1986-1989**
V. Motevalli and C. H. Marks May 1990 328 p Prepared in cooperation with Maryland Univ., College Park Sponsored by National Inst. of Standards and Technology, Gaithersburg, MD
(Grant NIST-NANB5H0551)
(PB90-227976; NIST/GCR-90/574) Avail: NTIS HC/MF A15
CSCL 21B

An extensive study of small-scale, unconfined, fire-induced ceiling jets was conducted under ceiling transient and steady state conditions. Detailed velocity and temperature measurements of the ceiling jet were made simultaneously using the cross-correlation velocimetry technique from the start of the fire until the ceiling reached steady state. Velocity and temperature profiles were obtained at several radial locations away from the plume impingement point. These measurements were made for transient and steady ceiling jet conditions in the case of the H=1.0 m. All the transient measurements in the H=0.5 m case were limited to temperature measurements. At steady state, however, both temperature and velocity measurements were obtained. GRA

**N91-10194*#** National Aeronautics and Space Administration. John F. Kennedy Space Center, Cocoa Beach, FL.
**PHYSICAL AND CHEMICAL TEST RESULTS OF ELECTROSTATIC SAFE FLOORING MATERIALS**
R. H. Gompf Apr. 1988 21 p
(NASA-TM-103501; MTB-316-87; NAS 1.15:103501) Avail: NTIS HC/MF A03 CSCL 13B

This test program was initiated because a need existed at the Kennedy Space Center (KSC) to have this information readily available to the engineer who must make the choice of which electrostatic safe floor to use in a specific application. The information, however, should be of value throughout both the government and private industry in the selection of a floor covering material. Included are the test results of 18 floor covering materials which by test evaluation at KSC are considered electrostatically safe. Tests were done and/or the data compiled in the following areas: electrostatics, flammability, hypergolic compatibility, outgassing, floor type, material thickness, and available colors. Each section contains the test method used to gather the data and the test results. Author

**N91-10195#** Oak Ridge National Lab., TN. Mathematical Sciences Section.
**ELECTROPLATING CORNERS**
L. J. Gray Feb. 1990 11 p Presented at the BETECH 1990, Newark, NJ, 10-12 Jul. 1990
(Contract DE-AC05-84OR-21400)
(DE90-017023; CONF-9007161-1) Avail: NTIS HC/MF A03

A recently proposed method for treating boundary corners is applied to a problem of practical interest, the simulation of an three-dimensional electrochemical plating process. At an edge point on the cathode surface there are two unknown flux (normal derivative) values, and the hypersingular integral equation for the boundary derivatives is employed to complete the linear system of equations. The additional complications arising in electroplating are the presence of singular solutions at a reentrant corner, nonlinear boundary conditions, and the close proximity of two different edges. Results for a realistic problem geometry are reported. DOE

**N91-10196#** Societe Europeenne de Propulsion, Vernon (France).
**INCORPORATION OF THE OPERATION SAFETY IN THE INDUSTRY AND IN A PRODUCT DEVELOPMENT PROCESS INDUCTING SUBCONTRACTORS [INTEGRATION DE LA SURETE DE FONCTIONNEMENT DANS L'ENTREPRISE ET DANS LE PROCESSUS DE DEVELOPPEMENT D'UN PRODUIT Y COMPRIS CHEZ LES COOPERANTS DE SOUS-TRAITANCE]**
Gerald Sciez, Bruno Majot, and Richard Vogin 1990 13 p In FRENCH Presented at 7th Colloque International de Fiabilite et de Maintenabilite, Brest, France, 18-22 Jun. 1990
(ETN-90-97822) Avail: NTIS HC/MF A03

The purpose of the work is to show how the activities concerning operation safety can be incorporated into the industries for reaching optimum quality. For constructing the operation safety, an accurate description of the basic requirements is needed. In a second step the means and the tools available in the industry have to be considered. It is shown that the operation safety is reliable when the utilization performances are included in the product quality control. ESA

**N91-10197#** Rolls-Royce Ltd., Derby (England).
**ENGINEERING DESIGN: A POWERFUL INFLUENCE ON THE BUSINESS SUCCESS ON MANUFACTURING INDUSTRY**
John F. Coplin 25 Aug. 1990 47 p Presented at I Mech E International Conference on Engineering Design, Harrogate, England, 22-25 Aug. 1989
(PNR-90763; ETN-90-97962) Copyright Avail: NTIS HC/MF A03

Engineering design, one of the most powerful forces in producing a package which matches market need, is discussed. It is essentially a detailed planning process backed by analysis and demonstration. The need for innovation to achieve competitive edge and profitability is considered. Innovation contains risk which must be controlled before substantial investment is made. The high rate of change of technology gives rise to the need for good training and retraining. Benefits which offsets costs at the time of occurring that cost are reached. ESA

**N91-10198#** Centre de Recherches Scientifiques et Techniques de l'Industrie des Fabrications Metalliques, Brussels (Belgium).
**[ACTIVITIES REPORT OF THE PERMANENT COMMITTEE OF THE GENERAL COUNCIL] Annual Report, 1989 [RAPPORT ANNUEL DU COMITE PERMANENT AU CONSEIL GENERAL DU 27 JUIN 1990]**
1990 67 p In FRENCH
(ISSN-0524-7705; ETN-90-97974) Avail: NTIS HC/MF A04

The 1989 progress report of the Scientific and Technical Research Center of the metal manufacturers industry is presented. The relevant investigation and results obtained in 1989 concern the following fields: foundry, metallic construction, forming and control of composites, welding techniques and materials, computer aided techniques in the industry, mechanical construction, transformation of plastic materials, surface protection, standardization and standards. ESA

# 32 COMMUNICATIONS AND RADAR

Includes radar; land and global communications; communications theory; and optical communications.

For related information see also *04 Aircraft Communications and Navigation* and *17 Space Communications, Spacecraft Communications, Command and Tracking.* For search and rescue see *03 Air Transportation and Safety,* and *16 Space Transportation.*

**N91-10199#** National Telecommunications and Information Administration, Annapolis, MD.
**HYDROLOGIC AND METEOROLOGICAL OPERATIONS IN THE 162-174 AND 406.1-420 MHz BANDS**
Cesar Filippi, Gary Patrick, Ernesto Cerezo, and Robert Wilson

Mar. 1990 125 p
(PB90-207820; NTIA-90-259) Avail: NTIS HC/MF A06 CSCL 17B

The report presents a detailed assessment of the hydrologic and meteorological operations in the 162 to 174 MHz (Very High Frequency) and 406.1 to 420 MHz (Ultra High Frequency) bands. The operations are currently supported by hydrologic and quasi-hydrologic channel assignments in these bands. There is a current need to jointly support hydrologic and nonhydrologic operations representing important national programs, and to develop solutions that alleviate spectral congestion and promote efficient spectrum utilization. The report identifies current regulations and channel usage, and analyzes the hydrologic emission characteristics to assess their bandwidth requirements and conservation alternatives. The current hydrologic channeling plans are also analyzed, and narrowband channeling options are assessed, along with the potential hydrologic service reaccommodation in current or other bands. All potential relocation and channeling options are explained and compared to illustrate their impact, tradeoffs, and compromises. The results of the study can serve to improve the spectral efficiency of hydrologic operations while remaining cost effective, and to conserve spectrum that can be made available for additional uses. GRA

**N91-10200** Princeton Univ., NJ.
**SIGNAL DETECTION IN NON-GAUSSIAN AND NON-WHITE NOISE Ph.D. Thesis**
Pamela Ann Nielsen 1990 186 p
Avail: Univ. Microfilms Order No. DA9014546

Emphasis is on the analysis and synthesis of different methods of detection when the noise distributions are not completely known. The work concentrates on noise sources whose distributions fail to satisfy some commonly held assumptions. In particular, the interest here is in non-stationary, non-Gaussian environments. Initially, statistical modeling of such a noise source is examined. It is later shown that even if a model appears to represent the empirical probability mass function well, if the model is used to design a detector, the resulting detector may not have a performance which is significantly better than the performance of a simpler structure. In particular, it is shown that if the data is highly correlated, incorporating the correlation into the structure of the detector may result in a substantial improvement in performance as compared to the performance of a detector which is derived using only the univariate characteristics. In addition, several different techniques for sub-optimal pre-whitening are discussed and their effect on the performance of a detector is examined. The performance of several non-parametric detectors is examined and they are compared for a wide range of acoustic environments. The effect on the performance is examined when the detector has available a noise reference channel. Finally, a new detector is proposed which is based on higher order moments. In particular, the detector is based on the bi-covariance function which is known to be identically zero for Gaussian noise. The asymptotic performance of the sensor outputs as compared to a linear detector is derived. Several sample bispectra are given, along with a detailed example for multivariate Gaussian noise. Dissert. Abstr.

**N91-10201*#** Michigan Univ., Ann Arbor. Radiation Lab.
**ELECTROMAGNETIC SCATTERING FROM TWO-DIMENSIONAL THICK MATERIAL JUNCTIONS Technical Report, Feb. - Sep. 1990**
M. A. Ricoy and John L. Volakis 1990 178 p
(Grant NAG2-541)
(NASA-CR-186976; NAS 1.26:186976; Rept-025921-14-T) Avail: NTIS HC/MF A09 CSCL 20N

Because material junction are commonplace in structures whose radar cross section is of interest, it is essential that their scattering properties be adequately characterized. To extend simple scattering models of material junctions with thin and/or high loss slabs to more general slabs, Generalized Impedance Boundary Conditions (GIBCs) and Generalized Sheet Transition Conditions (GSTCs) are proposed. The problem of the plane wave diffraction is examined by an arbitrary symmetric two-dimensional junction, where GIBCs and GSTCs are employed to simulate the slabs. GIBCs and GSTCs are constructed for multilayer planar slabs of arbitrary thickness and the resulting GIBC/GSTC reflection coefficients are compared with exact counterparts to evaluate the GIBCs/GSTCs. The plane wave diffraction by a multilayer material slab recessed in a perfectly conducting ground plane is formulated and solved via the generalized scattering matrix formulation in conjunction with the dual integral equation approach. Various scattering patterns are computed and validated with exact results where possible. The diffraction by a material discontinuity in a thick dielectric/ferrite slab is considered by modelling the constituent slabs with GSTCs. A non-unique solution in terms of unknown constants is obtained, and these constants are evaluated for the recessed slab geometry by comparison with the obtained solution. Several other simplified cases are also presented and discussed. Author

**N91-10202#** Sandia National Labs., Albuquerque, NM. Electromagnetic Testing Div.
**STATISTICAL CHARACTERIZATION OF A MODE-STIRRED CHAMBER**
J. G. Kostas and B. Boverie Jun. 1990 60 p
(Contract DE-AC04-76DP-00789)
(DE90-014860; SAND-90-1680) Avail: NTIS HC/MF A04

This report describes a statistical model for field amplitudes within a mode-stirred chamber. The parameters of the probability density function for field amplitudes are estimated by means of maximum likelihood. The accuracy of these parameters is specified as a function of the amount of data used. An experimental investigation of the possibility of using an existing electromagnetic shield room as a mode-stirred chamber is described. The physical alterations of the chamber and the instrumentation are summarized. Descriptions of the test results are reported. The tests were conducted to determine: the unloaded and loaded Q of the chamber, descriptive statistics of the electromagnetic fields, correlation distances of the fields in frequency, tuner angle, and spatial position, and the possibility of using frequency stirring as an alternative to mechanical stirring. DOE

**N91-10203#** California Univ., Berkeley. Lawrence Berkeley Lab.
**MODES OF ELLIPTICAL WAVEGUIDES: A CORRECTION**
D. A. Goldberg, L. J. Laslett, and R. A. Rimmer Mar. 1990 14 p
(Contract DE-AC03-76SF-00098)
(DE90-016647; LBL-28702) Avail: NTIS HC/MF A03

It is shown that the fields associated with the TM(sub 01) mode of an elliptical wave guide are qualitatively different from those which have appeared in the standard literature for the past fifty years, and that the original fields as plotted were also in qualitative disagreement with the analytic expressions which accompanied them. Nonetheless, the cutoff frequencies given for that mode, as well as for the five other modes described in those references, are exceedingly accurate (within roughly 1 percent) for elliptical eccentricities as large as 0.75; for eccentricities in excess of 0.9, the inaccuracy increases to from 5 to nearly 50 percent, depending on the mode in question. DOE

**N91-10204*#** Jet Propulsion Lab., California Inst. of Tech., Pasadena.
**SPACECRAFT HEALTH AUTOMATED REASONING PROTOTYPE (SHARP): THE FISCAL YEAR 1989 SHARP PORTABILITY EVALUATIONS TASK FOR NASA SOLAR SYSTEM EXPLORATION DIVISION'S VOYAGER PROJECT**
David J. Atkinson, Richard J. Doyle, Mark L. James, Tim Kaufman, and R. Gaius Martin 18 Aug. 1990 33 p
(Contract NAS7-918)
(NASA-CR-187338; JPL-Publ-90-20; NAS 1.26:187338) Avail: NTIS HC/MF A03 CSCL 17B

A Spacecraft Health Automated Reasoning Prototype (SHARP) portability study is presented. Some specific progress is described on the portability studies, plans for technology transfer, and potential applications of SHARP and related artificial intelligence technology to telescience operations. The application of SHARP to Voyager telecommunications was a proof-of-capability demonstration of artificial intelligence as applied to the problem of real time monitoring functions in planetary mission operations. An overview of the design and functional description of the SHARP system is also presented as it was applied to Voyager. Author

**N91-10205#** Institut Franco-Allemand de Recherches, Saint-Louis (France).
**NUMERICAL SIMULATION OF ELECTROMAGNETIC ACCELERATION BY INDUCTION. PART 1: THIN LOOPS [SIMULATION NUMERIQUE DE L'ACCELERATION ELECTROMAGNETIQUE PAR INDUCTION 1RE PARTIE: BOUCLES FILIFORMES]**
P. Raymond and A. Carriere 21 Feb. 1989 63 p In FRENCH
(ISL-R-102/89-Pt-1; ETN-90-97568) Avail: NTIS HC/MF A04

The physical modeling and numerical simulation of an electromagnetic accelerator composed of n fixed, coaxial coils accelerating a mobile coil are studied. All coils are supposed to be thin coils. This helps dimensioning of the electromagnetic device, in order to carry out the inverse ignition of a hollow charge (an active coil and a projectile ring), and to assess the necessary elements for studying an electromagnetic accelerator composed of n stages. ESA

**N91-10206#** Centre National d'Etudes Spatiales, Toulouse (France).
**INFLUENCE OF THE TELESCOPE DEPOINTING ON THE PERFORMANCES OF AN OPTICAL LINK. CORRELATION BETWEEN DEPOINTING LAW AND CODING, CONCERNING THE COMPUTATION OF MEAN BER**
S. Potteck 1 Feb. 1988 26 p In FRENCH; ENGLISH summary
(CNES-CT/DRT/TIT/TR-88/24-T; ETN-90-97805) Copyright Avail: NTIS HC/MF A03

On an optical link, the depointing of the telescopes induces rapid variations of the received power. The depointing probability law and the probability law of the received power as a function of the depointing are analyzed. The ways of computing the global performances of the link and the interaction of error correcting codes are discussed. A numerical application is described. ESA

**N91-10207#** Centre National d'Etudes Spatiales, Toulouse (France).
**PRINCIPLES OF LOCSTAR SYSTEM EXPERIMENTS**
S. Potteck 19 Dec. 1988 46 p In FRENCH; ENGLISH summary
(CNES-CT/DRT/TIT/TR-88/355; ETN-90-97807) Avail: NTIS HC/MF A03

The description of the LOCSTAR system experiments is provided. The aim of the work is to get results about the LOCSTAR spread spectrum return link (mobile towards station), and to test the equipment designed by CNES. The measurement system is described. The methods and program allowing discussion and exploitation of the measurements are included. ESA

**N91-10208*#** National Aeronautics and Space Administration. Lewis Research Center, Cleveland, OH.
**EFFECT OF SURFACE DEPOSITS ON ELECTROMAGNETIC WAVES PROPAGATING IN UNIFORM DUCTS**
Kenneth J. Baumeister Oct. 1990 13 p Presented at the 4th Biennial IEEE Conference on Electromagnetic Field Computation, Toronto, Ontario, 22-24 Oct. 1990
(NASA-TM-103282; E-5737; NAS 1.15:103282) Avail: NTIS HC/MF A03 CSCL 20N

A finite-element Galerkin formulation was used to study the effect of material surface deposits on the reflective characteristics of straight uniform ducts with PEC (perfectly electric conducting) walls. Over a wide frequency range, the effect of both single and multiple surface deposits on the duct reflection coefficient were examined. The power reflection coefficient was found to be significantly increased by the addition of deposits on the wall. Author

**N91-10209#** Consiglio Nazionale delle Ricerche, Frascati (Italy). Ist. di Fisica dello Spazio Interplanetario.
**FAST ESTIMATION OF THE VARIANCE OF A NARROWBAND PROCESS**
P. Astone, P. Bonifazi, and G. V. Pallottino Apr. 1990 25 p Submitted for publication
(IFSI-90-16; ETN-90-97798) Avail: NTIS HC/MF A03

Estimation of the variance of a narrowband stationary random process in the presence of wideband observation noise is discussed. Reduction of the measurement time required to obtain accurate estimates is the goal of the exercise. A solution, based on the Wiener-Kolmogoroff optimum filter is discussed. Two simple suboptimal techniques are proposed. Computational simulations and experimental results on the Brownian motion of a cryogenic gravitational wave detector with high Q value confirm the theoretical prediction that the variance of a narrowband process can be determined in a time smaller than the correlation time of the process. ESA

**N91-10210#** Ecole Centrale de Lyon (France).
**METHOD FOR SIMULATING LARGE DIMENSION DEVICES SUBMITTED TO ELECTROMAGNETIC PERTURBATIONS Ph.D. Thesis [UNE METHODE MIXTE POUR LA SIMULATION DES DISPOSITIFS DE GRANDES DIMENSIONS SOUMIS A DES PERTURBATIONS ELECTROMAGNETIQUES]**
Emmanuel Sabonnadiere 1990 154 p In FRENCH Original contains color illustrations
(ECL-90-10; ETN-90-97820) Avail: NTIS HC/MF A08

The electromagnetic compatibility of on-board electrical and electronic devices submitted to electromagnetic perturbation sources is investigated. The sources from the inside or outside of the spacecraft are considered. The coupling mechanisms between the sources and the devices are illustrated. A model allowing the description of electromagnetic compatibility is proposed. The frequency range from a few Hertz up to megaHertz is considered. ESA

**N91-10211#** Ecole Centrale de Lyon (France). Lab. d'Electrotechnique.
**CONTRIBUTION TO THE STUDY OF THE ELECTROMAGNETIC FIELD RADIATION CLOSE TO ELECTRONICS CIRCUITS Ph.D. Thesis [CONTRIBUTION A L'ETUDE DU RAYONNEMENT EN CHAMP ELECTROMAGNETIQUE PROCHE DES CIRCUITS EN ELECTRONIQUE DE PUISSANCE]**
Bei Lu 1990 151 p In FRENCH
(ECL-90-12; ETN-90-97821) Avail: NTIS HC/MF A08

The disturbances generated by power electronic circuits are investigated. The electric and the magnetic fields created by a 60 KVA power generator, using fast commutation semiconductor switches, are analyzed. The developed theoretical and experimental tools are described. The intensity and the configuration of the electric and magnetic fields are evaluated. The localization and modeling of the emitting sources is carried out. ESA

**N91-10339#** Meteorological Satellite Center, Tokyo (Japan).
**OUTLINE OF THE GMS TELECOMMUNICATION SYSTEM**
Masaru Fujimaki and Nobuyuki Taki *In its* Meteorological Satellite Center Technical Note. Special Issue (1989). Summary of GMS System. 1: Telecommunication System Mar. 1989 p 1-5 In JAPANESE; ENGLISH summary (For primary document see N91-10338 01-42)
Avail: NTIS HC/MF A08

**N91-10340#** Meteorological Satellite Center, Tokyo (Japan).
**OUTLINE OF CDAS TELECOMMUNICATION SYSTEM**
Kiyoshi Nakagawa, Tsutoya Abe, and Takao Suzuki *In its* Meteorological Satellite Center Technical Note. Special Issue (1989). Summary of GMS System. 1: Telecommunication System

Mar. 1989 p 7-9 In JAPANESE; ENGLISH summary (For primary document see N91-10338 01-42)
Avail: NTIS HC/MF A08

**N91-10341#** Meteorological Satellite Center, Tokyo (Japan).
**STATION CONTROL AND MONITOR SUBSYSTEM**
Yukio Sasaki and Hiroyuki Suzuki *In its* Meteorological Satellite Center Technical Note. Special Issue (1989). Summary of GMS System. 1: Telecommunication System Mar. 1989 p 11-20 In JAPANESE; ENGLISH summary (For primary document see N91-10338 01-42)
Avail: NTIS HC/MF A08

**N91-10342#** Meteorological Satellite Center, Tokyo (Japan).
**VISSR DEMODULATE AND PROCESSING SUBSYSTEM**
Toshiharu Tanaka and Akifumi Yamashita *In its* Meteorological Satellite Center Technical Note. Special Issue (1989). Summary of GMS System. 1: Telecommunication System Mar. 1989 p 21-45 In JAPANESE; ENGLISH summary (For primary document see N91-10338 01-42)
Avail: NTIS HC/MF A08

**N91-10343#** Meteorological Satellite Center, Tokyo (Japan).
**STRETCHED VISSR SUBSYSTEM**
Yoshikazu Mori *In its* Meteorological Satellite Center Technical Note. Special Issue (1989). Summary of GMS System. 1: Telecommunication System Mar. 1989 p 47-53 In JAPANESE; ENGLISH summary (For primary document see N91-10338 01-42)
Avail: NTIS HC/MF A08

**N91-10344#** Meteorological Satellite Center, Tokyo (Japan).
**IMAGE MONITOR**
Yukio Sasaki and Hiroyuki Suzuki *In its* Meteorological Satellite Center Technical Note. Special Issue (1989). Summary of GMS System. 1: Telecommunication System Mar. 1989 p 55-61 In JAPANESE; ENGLISH summary (For primary document see N91-10338 01-42)
Avail: NTIS HC/MF A08

**N91-10346#** Meteorological Satellite Center, Tokyo (Japan).
**COMMAND SUBSYSTEM**
Takeo Saito, Tatsuo Takahashi, and Masakazu Saito *In its* Meteorological Satellite Center Technical Note. Special Issue (1989). Summary of GMS System. 1: Telecommunication System Mar. 1989 p 71-77 In JAPANESE; ENGLISH summary (For primary document see N91-10338 01-42)
Avail: NTIS HC/MF A08

**N91-10347#** Meteorological Satellite Center, Tokyo (Japan).
**TRILATERATION RANGING SUBSYSTEM**
Shuji Naito, Kazuichirou Akimoto, and Masashi Morisaki *In its* Meteorological Satellite Center Technical Note. Special Issue (1989). Summary of GMS System. 1: Telecommunication System Mar. 1989 p 79-89 In JAPANESE; ENGLISH summary (For primary document see N91-10338 01-42)
Avail: NTIS HC/MF A08

**N91-10349#** Meteorological Satellite Center, Tokyo (Japan).
**FREQUENCY STANDARD UNIT**
Hirozou Nishida *In its* Meteorological Satellite Center Technical Note. Special Issue (1989). Summary of GMS System. 1: Telecommunication System Mar. 1989 p 97-99 In JAPANESE; ENGLISH summary (For primary document see N91-10338 01-42)
Avail: NTIS HC/MF A08

**N91-10350#** Meteorological Satellite Center, Tokyo (Japan).
**OPERATION CONSOLE**
Koji Sato and Shigeto Miura *In its* Meteorological Satellite Center Technical Note. Special Issue (1989). Summary of GMS System. 1: Telecommunication System Mar. 1989 p 101-111 In JAPANESE; ENGLISH summary (For primary document see N91-10338 01-42)
Avail: NTIS HC/MF A08

**N91-10351#** Meteorological Satellite Center, Tokyo (Japan).
**SYSTEM CONSOLE**
Yukio Sasaki and Hiroyuki Suzuki *In its* Meteorological Satellite Center Technical Note. Special Issue (1989). Summary of GMS System. 1: Telecommunication System Mar. 1989 p 113-117 In JAPANESE; ENGLISH summary (For primary document see N91-10338 01-42)
Avail: NTIS HC/MF A08

**N91-10352#** Meteorological Satellite Center, Tokyo (Japan).
**DCP SUBSYSTEM**
Masaaki Sugai, Kouzo Masubuchi, and Toshio Onigata *In its* Meteorological Satellite Center Technical Note. Special Issue (1989). Summary of GMS System. 1: Telecommunication System Mar. 1989 p 119-129 In JAPANESE; ENGLISH summary (For primary document see N91-10338 01-42)
Avail: NTIS HC/MF A08

**N91-10353#** Meteorological Satellite Center, Tokyo (Japan).
**WEFAX SUBSYSTEM**
Yoshiyuki Kanazawa *In its* Meteorological Satellite Center Technical Note. Special Issue (1989). Summary of GMS System. 1: Telecommunication System Mar. 1989 p 131-136 In JAPANESE; ENGLISH summary (For primary document see N91-10338 01-42)
Avail: NTIS HC/MF A08

**N91-10354#** Meteorological Satellite Center, Tokyo (Japan).
**DPC TELECOMMUNICATION SYSTEM**
Sadao Mita, Tsukasa Okazaki, and Ryoetsu Ansai *In its* Meteorological Satellite Center Technical Note. Special Issue (1989). Summary of GMS System. 1: Telecommunication System Mar. 1989 p 137-155 In JAPANESE; ENGLISH summary (For primary document see N91-10338 01-42)
Avail: NTIS HC/MF A08

**N91-10355#** Meteorological Satellite Center, Tokyo (Japan).
**MICROWAVE LINK**
Susumu Shinozuka *In its* Meteorological Satellite Center Technical Note. Special Issue (1989). Summary of GMS System. 1: Telecommunication System Mar. 1989 p 157-164 In JAPANESE; ENGLISH summary (For primary document see N91-10338 01-42)
Avail: NTIS HC/MF A08

# 33 ELECTRONICS AND ELECTRICAL ENGINEERING

Includes test equipment and maintainability; components, e.g., tunnel diodes and transistors; microminiaturization; and integrated circuitry.

For related information see also *60 Computer Operations and Hardware* and *76 Solid-State Physics.*

**N91-10212** Michigan Univ., Ann Arbor.
**THREE-DIMENSIONAL FULL-WAVE ANALYSIS OF SIGNAL COMMUNICATIONS IN ACTIVE INTEGRATED CIRCUITS USING A VARIABLE-MESH TLM METHOD Ph.D. Thesis**
Robert Heth Voelker 1989 237 p
Avail: Univ. Microfilms Order No. DA9014036

As the switching speed of digital integrated circuits (ICs) increases, detrimental effects such as signal crosstalk, propagation delay, attenuation, dispersion, and reflection become more important. At relatively low switching speeds, the signals have small bandwidth and thus quasi-static electromagnetic modeling methods are sufficient to analyze these effects. However, integrated circuits having high-speed, wide-bandwidth signals, where the signal wavelengths are comparable to the dimensions of the IC and package, must be analyzed with a full-wave electromagnetic field method. A three-dimensional variable-mesh transmission line matrix (TLM) method is developed for the full-wave time-domain simulation of the electromagnetic properties of ICs. This is made more computationally efficient by rewriting the TLM scattering matrices in the form of finite-differences, yielding the finite-difference transmission line matrix (FD-TLM) method. Models for lumped circuit components, such as resistors, capacitors, diodes, and GaAs metal-semiconductor field-effect transistors (MESFETs) are derived and incorporated into the FD-TLM method, allowing the three-dimensional full-wave electromagnetic field simulation of complete active ICs. Applications of the method are discussed. Dissert. Abstr.

**N91-10213#** Joint Publications Research Service, Arlington, VA.
**JPRS REPORT: SCIENCE AND TECHNOLOGY. USSR: ELECTRONICS AND ELECTRICAL ENGINEERING**
2 Jul. 1990 36 p Transl. into ENGLISH from various Russian articles
(JPRS-UEE-90-004) Avail: NTIS HC/MF A03

Abstracts of Soviet literature in various areas of the electronics and electrical engineering are compiled. The following subject areas are covered: broadcasting and consumer electronics; antennas and propagation; circuits and systems; computers; microwave theory and techniques; power engineering; quantum electronics and electro-optics; and solid state circuits. M.G.

**N91-10214#** Joint Publications Research Service, Arlington, VA.
**JPRS REPORT: SCIENCE AND TECHNOLOGY. USSR: ELECTRONICS AND ELECTRICAL ENGINEERING**
V. N. Akhtyrskiy and N. Ye. Fadeeva 17 Jul. 1990 24 p
(JPRS-UEE-90-006) Avail: NTIS HC/MF A03

A collection of abstracts of Soviet literature which deal in the fields of electronics and electrical engineering is presented. Areas of concentration include communication equipment, broadcasting, digital systems, rail transportation, and solid state devices. One particular abstract discusses infrared-system receiving devices and a description is presented for certain types of such systems for detection and recognition of objects based on their heat radiation. M.G.

**N91-10215#** Joint Publications Research Service, Arlington, VA.
**JPRS REPORT: SCIENCE AND TECHNOLOGY. USSR: ELECTRONICS AND ELECTRICAL ENGINEERING**
23 Jul. 1990 21 p Transl. into ENGLISH from various Russian articles
(JPRS-UEE-90-007) Avail: NTIS HC/MF A03

Abstracts of Soviet literature in various areas of electronics and electrical engineering are compiled. The following subject areas are covered: broadcasting and consumer electronics, circuits and systems, industrial electronics and control instrumentation, communications, and power engineering. M.G.

**N91-10216#** Joint Publications Research Service, Arlington, VA.
**JPRS REPORT: SCIENCE AND TECHNOLOGY. USSR: ELECTRONICS AND ELECTRICAL ENGINEERING**
2 Aug. 1990 35 p Transl. into ENGLISH from various Russian articles
(JPRS-UEE-90-008) Avail: NTIS HC/MF A03

Abstracts of Soviet literature in various areas of electronics and electrical engineering are compiled. The following subject areas are covered: broadcasting and consumer electronics, antennas and propagation, circuits and systems, transportation, industrial electronics and control instrumentation, power engineering, quantum electronics and electro-optics, and solid state circuits. M.G.

**N91-10217#** Joint Publications Research Service, Arlington, VA.
**JPRS REPORT: SCIENCE AND TECHNOLOGY. USSR: ELECTRONICS AND ELECTRICAL ENGINEERING**
8 Aug. 1990 26 p Transl. into ENGLISH from various Russian articles
(JPRS-UEE-90-009) Avail: NTIS HC/MF A03

Abstracts of Soviet literature in various areas of electronics and electrical engineering are compiled. The subject area is broadcasting and consumer electronics. M.G.

**N91-10218#** Sandia National Labs., Albuquerque, NM.
**MINIMIZING FREQUENCY PULLING OF QUARTZ OSCILLATORS DUE TO POWER SUPPLY VARIATIONS**
Kurt O. Wessendorf 1990 8 p Presented at the 12th Annual Piezoelectric Devices Conference, Kansas City, KS, 25-27 Sep. 1990
(Contract DE-AC04-76DP-00789)
(DE90-014566; SAND-90-1085C; CONF-9009220-1) Avail: NTIS HC/MF A02

When quartz controlled oscillators are required for use in applications demanding precision many factors will ultimately place limitations on the ability of the oscillator to remain at the desired frequency. These factors include temperature, resonator Q, pullability, radiation, output load variability, and the electronic components. This paper addresses the subject of frequency instability of oscillator circuits due to power supply voltage variations. In particular, the primary sources of this instability are described for a Pierce oscillator employing a bipolar transistor and design techniques are presented which minimize these frequency pulling effects. DOE

**N91-10219#** Lawrence Livermore National Lab., CA.
**AN X BAND BACKWARD-WAVE OSCILLATOR EXPERIMENT**
J. F. Camacho, E. T. Rosenbury, and B. R. Poole 1990 6 p Presented at the 5th National Conference on High-Power Microwave Technology, West Point, NY, 10-15 Jun. 1990
(Contract W-7405-eng-48)
(DE90-015119; UCRL-102625; CONF-9006179-5) Avail: NTIS HC/MF A02

A backward-wave oscillator (BWO) experiment is being conducted using a slow-wave structure which consists of a non-sinusoidal corrugated-wall waveguide with period z sub 0 = 1.67 cm, r sub min = 1.17 cm, r sub max = 1.97 cm, and length L = 15.03 cm (nine periods). An annular electron beam is injected with the following parameters: Phi sub cathode = 1 MV, 1 kA less than or = I sub beam less than or = 7 kA in 1 kA increments, r sub beam = 0.9 cm, and t sub pulse approx. 60 ns. The guiding axial magnetic field is varied from 0.6 T to 3.0 T in 0.4 T increments. The device is designed to operate at 8.0 GHz less than f less than 8.5 GHz in the lowest-order TM mode of the coupled beam-structure system. The experimental design and results are presented. In addition, the theoretical and modeling work is discussed. DOE

**N91-10220#** Argonne National Lab., IL.
**OVERDISCHARGE PROTECTION IN HIGH-TEMPERATURE CELLS AND BATTERIES Patent Application**
Laszlo Redey, inventor (to DOE) 25 Jul. 1989 29 p
(Contract W-31-109-eng-38)
(DE90-015180; US-Patent-Appl-SN-384604; Patents-US-A7384604) Avail: NTIS HC/MF A03

Overdischarge indication and protection is provided in a lithium alloy-metal sulfide, secondary electrochemical cell and batteries of such cells through use of a low lithium activity phase that ordinarily is not matched with positive electrode material. Low lithium activity phases such as Li(0.1)Al(0.9) and LiAlSi in correspondence with positive electrode material cause a downward gradient in cell voltage as an indication of overdischarge prior to damage to the cell. Moreover, the low lithium activity phase contributes lithium into the electrolyte and provides a lithium shuttling current as overdischarge protection after all of the positive electrode material is discharged. DOE

**N91-10221*#** National Aeronautics and Space Administration. Langley Research Center, Hampton, VA.
**AN ANALYSIS OF THE EFFECTS OF SECONDARY REFLECTIONS ON DUAL-FREQUENCY REFLECTOMETERS**
C. P. Hearn, C. R. Cockrell, and S. D. Harrah Oct. 1990 17 p

(NASA-TM-102709; NAS 1.15:102709) Avail: NTIS HC/MF A03 CSCL 09A

The error-producing mechanism involving secondary reflections in a dual-frequency, distance measuring reflectometer is examined analytically. Equations defining the phase, and hence distance, error are derived. The error-reducing potential of frequency-sweeping is demonstrated. It is shown that a single spurious return can be completely nullified by optimizing the sweep width. Author

**N91-10222*#** Jet Propulsion Lab., California Inst. of Tech., Pasadena.
**DESIGN AND APPLICATION OF GAS-GAP HEAT SWITCHES Final Report**
C. K. Chan and R. G. Ross, Jr. 15 Mar. 1990 62 p Prepared for Air Force Space Technology Center, Kirtland AFB, NM
(Contract NAS7-918)
(NASA-CR-187339; JPL-Publ-90-38; NAS 1.26:187339) Avail: NTIS HC/MF A04 CSCL 09C

Gas-gap heat switches can serve as an effective means of thermally disconnecting a standby cryocooler when the primary (operating) cooler is connected and vice versa. The final phase of the development and test of a cryogenic heat switch designed for loads ranging from 2 watts at 8 K, to 100 watts at 80 K are described. Achieved heat-switch on/off conductance ratio ranged from 11,000 at 8 K to 2200 at 80 K. A particularly challenging element of heat-switch design is achieving satisfactory operation when large temperatures differentials exist across the switch. A special series of tests and analyses was conducted and used in this Phase-2 activity to evaluate the developed switches for temperature differentials ranging up to 200 K. Problems encountered at the maximum levels are described and analyzed, and means of avoiding the problems in the future are presented. A comprehensive summary of the overall heat-switch design methodology is also presented with special emphasis on lessons learned over the course of the 4-year development effort. Author

**N91-10223#** Johns Hopkins Univ., Baltimore, MD. Dept. of Materials Science and Engineering.
**CORROSION, PASSIVITY, AND BREAKDOWN OF ALLOYS USED IN HIGH ENERGY DENSITY BATTERIES Final Report**
Jerome Kruger Jan. 1990 49 p Prepared for California Univ., Berkeley. Lawrence Berkeley Lab.
(Contracts DE-AC03-76SF-00098; LBL-4539610)
(DE90-016648; LBL-28515) Avail: NTIS HC/MF A04

The role of passive films in aqueous solutions has been studied extensively, yet the passivity of metals and alloys in non-aqueous solutions has received comparatively little attention despite its importance to such technologies as lithium batteries, chemical processing, and fuel processing. Long term integrity depends on the protective ability of the passive film in the non-aqueous electrolytes employed. By understanding the nature of passivity in non-aqueous solvents, and factors which cause its breakdown, improvements in the corrosive behavior of structural alloys and electrode materials in lithium batteries and other commercial applications in non-aqueous solutions can be made. The overall objective is to enhance the understanding of the major processes affecting corrosion in non-aqueous solvents: passivity and breakdown of passivity. Since passive layers control corrosion, the achievement of such an understanding especially in regards to how alloys composition affects these layers is crucial to the development of alloys more corrosion resistant in non-aqueous solvents. This research addresses the following fundamental questions: (1) Are the films found in organic solvents different from those produced in aqueous environments; (2) Can passive layers form on bare metals in the absence of water, and if they can, what is their nature; and (3) What are the kinetics of passive film formation, breakdown and repassivation. DOE

**N91-10224#** Oak Ridge National Lab., TN.
**THE GAMMASPHERE**
I-Yang Lee 1990 16 p Presented at the Nuclear Structure in the 1990's, Oak Ridge, TN, 23-27 Apr. 1990
(Contract DE-AC05-84OR-21400)
(DE90-016849; CONF-900450-10) Avail: NTIS HC/MF A03

GAMMASPHERE is one of a new generation of gamma ray detector arrays. It consists of 110 Compton-suppressed large volume Ge detectors. The design goal is to achieve high efficiency and peak-to-total value for four to five fold coincidence experiments. Such highfold coincidence capability will provide new physics opportunities in areas such as high spins, transfer reactions, giant resonances, and astrophysics. The design of the detector and shield has been developed through extensive simulation calculations and an electronic honeycomb design was chosen. The electronics and computer systems are capable of operating at 50,000 event/sec. The design and development tasks are being carried out at several laboratories in the U.S. The project is expected to be funded in the fall of 1990. The first experiment is planned in the summer of 1992. DOE

**N91-10225#** Technische Univ., Delft (Netherlands).
**AN AVALANCHE ELECTRON EMITTING DIODE IN GALLIUM ARSENIDE Ph.D. Thesis**
Tom vanZutphen 1990 122 p
(Contract STW-DTN33-467)
(ETN-90-97746) Avail: NTIS HC/MF A06

The development of an electron emitter based on a shallow pn-junction made of gallium arsenide is reported. Desirable properties of an electron gun are outlined and the attractive aspects and specific possibilities of the Avalanche Electron Emitting Diode (AEED) are discussed. Fabrication, including the self-made gold-germanium sputter and gold evaporation equipment, is explained. Ultrahigh vacuum measurement and cleaning setup and properties of the low energy argon ion sputter source and method of measurement are presented. Experimental results and theoretical calculations are given. The Ga AEED device is concluded to be of not good enough quality for fair comparison to the silicon AEED. ESA

**N91-10226#** Technische Univ., Delft (Netherlands).
**FIRST ORDER OSCILLATORS Ph.D. Thesis**
Christiaan Johannes Verhoeven 1990 200 p
(ETN-90-97758) Avail: NTIS HC/MF A09

The behavior of first order oscillators is studied in order to present the designer with the knowledge to change the oscillator properties. The understanding is based mainly on qualitative aspects. Regenerative and nonregenerative memory implementations for the binary memory function are discussed. The influence of noise is discussed. Electronic circuits which were integrated and verified experimentally are given. Bipolar technology was used. For exact numerical predictions of oscillator behavior, computer simulators such as SPICE can be used. ESA

**N91-10227#** Centre National d'Etudes Spatiales, Toulouse (France).
**MICROCHANNEL PLATE DETECTORS (MCP)**
Pierre Bricard 2 Dec. 1988 24 p In ENGLISH and FRENCH
(CNES-CT/DRT/TIT/OE-88/037-T; ETN-90-97810) Avail: NTIS HC/MF A02

The Micro Channel Plate (MCP) is a honeycomb of tiny tubular electron multipliers. Associated with a photocathode and a phosphor screen, it makes an image intensifier, tailored for the very weak illuminations. A description of the MCP and of a classical image intensifier, enlighting the way they work, are provided. The various structures used in applications are listed. The factors affecting the MCP intensifier lifetime are reviewed. ESA

**N91-10228#** Birmingham Univ. (England). Dept. of Engineering Production.
**AN EVALUATION OF THE PRODUCTION PROCESSES AND METHODS ASSOCIATED WITH CARELLO CELL AT RISTS, TELFORD M.S. Thesis**
Edward Connoly Sep. 1989 96 p
(ETN-90-97578) Avail: NTIS HC/MF A05

An evaluation of a small manufacturing unit, Carello Cell 1, a light leads assembly area at RISTS, Telford, is performed. The objectives are the followings: to examine the organization and tasking structure to evaluate the effectiveness of the manufacturing control procedures; to review the quality procedures and to comment their effectiveness; to assess machine utilization to identify potential problem areas; to investigate and to comment on machine serviceability, reliability, and maintainability; to identify factors to reduce machine down time and any other factors affecting production. Conclusions and recommendations are given, particularly concerning the needs of infrastructure of the factory, taking into account that it is in the process of major expansion. ESA

**N91-10229#** Oxford Univ. (England). Dept. of Engineering Science.
**APPLICATION OF GENERALIZED PREDICTIVE CONTROL TO A BOILER TURBINE UNIT FOR ELECTRICITY GENERATION**
J. A. Rossiter, B. Kouvaritakis, and R. M. Dunnett (Central Electricity Research Labs., Leatherhead, England ) 3 Apr. 1990 21 p
Sponsored by Central Electricity Generating Board and Science Research Council, England
(OUEL-1823/90; ETN-90-97921) Avail: NTIS HC/MF A03

The central task in power station control is to meet the system demand while minimizing state and input variations in the plant. In order to achieve good set point following, the control system must make good use of coupling between the different control loops and if possible use information about future set points to smooth out the control activity. Characteristic Generalized Predictive Control (GPC) sets out to achieve both these objectives and hence would seem ideally suited to power station control. The presence of some fast and slow dynamics implies that the boiler turbine system is in essence a stiff problem; the characteristic GPC algorithm is suitably extended to take direct account of this. Simulation results show that the characteristic GPC algorithm provides the systematic means of approaching the boiler-turbine problem and affords some improvements in performance over traditional proportional integral derivative control schemes. ESA

**N91-10348#** Meteorological Satellite Center, Tokyo (Japan).
**ANTENNA/TRANSMITTER CONTROL UNIT**
Seiji Kawabata and Masahiro Sasaki *In its* Meteorological Satellite Center Technical Note. Special Issue (1989). Summary of GMS System. 1: Telecommunication System Mar. 1989 p 91-95 In JAPANESE; ENGLISH summary (For primary document see N91-10338 01-42)
Avail: NTIS HC/MF A08

# 34 FLUID MECHANICS AND HEAT TRANSFER

Includes boundary layers; hydrodynamics; fluidics; mass transfer; and ablation cooling.

For related information see also *02 Aerodynamics* and *77 Thermodynamics and Statistical Physics.*

**N91-10230#** Ballistic Research Labs., Aberdeen Proving Ground, MD.
**LARGE BLAST AND THERMAL SIMULATOR ADVANCED CONCEPT DRIVER DESIGN BY COMPUTATIONAL FLUID DYNAMICS Final Report, 1987 - 1989**
Klaus O. Opalka Aug. 1989 12 p
(AD-A211364; BRL-TR-3026) Avail: NTIS HC/MF A03 CSCL 20/4

The construction of a large test facility is proposed for simulating the blast and thermal environment resulting from nuclear explosions. This facility would be used to test the survivability and vulnerability of military equipment such as trucks, tanks and helicopters in a simulated thermal and blast environment, and to perform research into nuclear blast phenomenology. The proposed advanced design concepts, heating of driver gas and fast-acting throat valves for wave shaping, are described and the results of CFD studies to advance these new technical concepts for simulating decaying blast waves are reported. Author

**N91-10231#** National Inst. of Standards and Technology, Gaithersburg, MD. Center for Chemical Engineering.
**MEASUREMENTS OF COEFFICIENTS OF DISCHARGE FOR CONCENTRIC FLANGE-TAPPED SQUARE-EDGED ORIFICE METERS IN NATURAL GAS OVER THE REYNOLDS NUMBER RANGE 25,000 TO 16,000,000 Final Report**
J. R. Whetstone, W. G. Cleveland, B. R. Bateman, and C. F. Sindt Sep. 1989 369 p Sponsored by American Petroleum Inst., Washington, DC
(PB90-219601; NIST/TN-1270) Avail: NTIS HC/MF A16; also available SOD HC $18.00 as 003-003-02974-2 CSCL 20D

The report describes the data acquisition systems and procedures used in the American Petroleum Institute (API)-sponsored orifice discharge coefficient project performed in natural gas flows and conducted at the test loop of the Natural Gas Pipeline Company of America (NGPL) in Joliet, Illinois. Measurements of orifice discharge coefficients for 6- and 10-inch diameter orifice meter runs were made using critical venturis for mass flowrate measurement with associated measurement of pressures and temperatures. Eleven venturis were calibrated at the Colorado Engineering Experiment Station, Inc. (CEESI). Measurements of absolute and differential pressure and temperature for venturi and orifice meter conditions were made using an automated data acquisition system. Temperature and pressure measurements were directly related to U.S. national measurement standards. Daily calibration of absolute and differential pressure transducers using pressure working standards was designed into the measurement procedures. Collected over a 2-year period, the database contains tests on 44 orifice plates in 8 beta ratios for two meter sizes (6- and 10-inches). The database contains 1,345 valid test points. GRA

**N91-10232#** National Aeronautical Lab., Bangalore (India). Computational and Theoretical Fluid Dynamics Div.
**WALL INTERFERENCE STUDIES Closing Report, Apr. 1983 - Jun. 1989**
R. Gopinath Jun. 1990 25 p
(PD-CF-9012) Avail: NTIS HC/MF A03

A closing report on the activity, Wall Interference Studies, is presented. Codes were developed to assess wall interference both for 2-D and 3-D cases, where the test section is ventilated, and validated. TSFOIL code was adapted for operation on the Univac computer. Instrumentation was developed for measuring the pressures on a control surface in the 1.2 m facility and once this is installed in the above facility, correcting the data from it for wall interference effects should be a routine affair. Author

**N91-10233** Rockefeller Univ., New York, NY.
**FAST SOUND PROPAGATION IN BINARY FLUID MIXTURES Ph.D. Thesis**
Alessandro Campa 1989 170 p
Univ. Microfilms Order No. DA9016118

The dynamical properties, at the molecular level, of binary fluid mixtures in equilibrium are studied; binary fluid mixtures are fluids consisting of two different components. As for simple fluids, the main experimental probes for the study of these properties of binary mixtures are light and neutron scattering. To connect the dynamics with scattering experiments the kinetic theory of fluids is used. The kinetic theory was applied to binary mixtures where the atomic masses of the molecules of the two components are very different. Both dilute (gaseous) mixtures and dense mixtures were studied. In the description of the dynamics of the fluid through the density-density correlation functions, one can introduce modes, which can be thought of as the different channels by which the correlations decay in time. Some modes are propagating, in the sense that they describe propagating, and damped, processes. Others are not propagating, and describe diffusive, purely damped processes. The results concern the appearance of a fast propagating mode, in disparate-mass binary mixtures, in a vast range of densities, from dilute gas mixtures to rather high (liquid) densities. This fast mode appears beyond the hydrodynamic regime. One can call this mode fast sound, because, like ordinary sound, it propagates, but it is faster. The most important point is that the fast sound is associated with dynamics of the light component only. How this phenomenon could be observed in light and neutron scattering experiments is explained. If it is detected in actual scattering experiments on disparate-mass binary mixtures it would be the first time that a non hydrodynamic mode in a fluid is clearly seen. Dissert. Abstr.

**N91-10234** Iowa State Univ. of Science and Technology, Ames.
**SIMULATION OF TIME-DEPENDENT COMPRESSIBLE VISCOUS FLOWS USING CENTRAL AND UPWIND-BIASED FINITE DIFFERENCE TECHNIQUES Ph.D. Thesis**
Edward Joseph Hall 1989 282 p
Avail: Univ. Microfilms Order No. DA9014903

Four time-dependent numerical algorithms for the prediction of unsteady, viscous compressible flows are compared. The analyses are based on the time-dependent Navier-Stokes equations expressed in a generalized curvilinear coordinate system. The methods tested include three traditional central-difference algorithms, and a new upwind-biased algorithm utilizing an implicit, time-marching relaxation procedure based on Newton iteration. Aerodynamic predictions are compared for internal duct-type flows and cascaded turbomachinery flows with spatial periodicity. Two-dimensional internal duct-type flow predictions are performed using an H-type grid system. Planar cascade flows are analyzed using a numerically generated, capped, body-centered, O-type grid system. Initial results are presented for critical and supercritical steady inviscid flow about an isolated cylinder. These predictions are verified by comparisons with published computational results from a similar calculation. Results from each method are then further verified by comparison with experimental data for the more demanding case of flow through a two-dimensional turbine cascade. Inviscid predictions are presented for two different transonic turbine cascade flows. Dissert. Abstr.

**N91-10235#** Michigan Univ., Ann Arbor. Dept. of Mechanical Engineering and Applied Mechanics.
**MASS TRANSFER IN OSCILLATING FLOWS: EFFICIENT DRYING VIA PULSE COMBUSTORS Annual Report, Jan. - Dec. 1989**
V. S. Arpaci, R. Gemmen, and A. Selamet Apr. 1990 96 p
(Contract GRI-5088-260-1686)
(PB90-242389; GRI-90/0135) Avail: NTIS HC/MF A05 CSCL 20D

Analytical and experimental methods are addressed for increasing industrial and home drying efficiency via pulse combustors. A fundamental scientific methodology is being developed for the momentum, heat, and mass transfer in oscillating (on the mean) turbulent flows. The approach follows the intuitive ideas of Taylor and Kolmogorov on the construction of microscales of turbulence. A parallel experimental program was carried out by the pulse combustor of the Continuous Combustion Lab of Sandia-Livermore National Labs. A droplet sizing technique and a quasi-steady computer model were developed. The unsteady analytical model determines the range of the quasi-steady model and provides also a mass transfer correlation beyond this range. The scales of mass transfer in oscillating turbulent flows were developed. A mass transfer correlation based on these scales was proposed. The correlation agrees well with the results so far obtained in the experimental program. Author

**N91-10236#** Argonne National Lab., IL. Materials and Components Technology Div.
**TWO-PHASE FLOW PATTERNS AND FRICTIONAL PRESSURE GRADIENTS IN A SMALL, HORIZONTAL, RECTANGULAR CHANNEL**
M. W. Wambsganss, J. A. Jendrzejczyk, D. M. France, and N. T. Obot (Clarkson Univ., Potsdam, NY.) May 1990 112 p
(Contract W-31-109-eng-38)
(DE90-014802; ANL-90/19) Avail: NTIS HC/MF A06

Two-phase flow patterns and frictional pressure gradients in flow in small, rectangular channels are being studies as part of a larger research program addressing phase change heat transfer of pure refrigerants and refrigerant mixtures in plate-fin heat exchangers. Small rectangular flow channels were selected as representative of plain fin geometries. The particular channel reported herein has dimensions of 19.05 x 3.18 mm. Adiabatic flows of air/water mixtures, with the flow channel horizontal and the channel exit at near-atmospheric conditions, were utilized in the experiments. Analysis and interpretation of the pressure data relative to observed flow pattern transitions led to an objective method for determining the plug/bubble-to-slug flow transition. This method, together with visual observations, supplemented with photographic data, was used to develop a flow pattern map. A comparison of existing flow pattern maps for circular pipes, capillary tubes, and larger rectangular channels led to the conclusion that, while qualitative agreement exists, these maps are not generally applicable on a quantitative basis to the subject small rectangular channel. Two state-of-the-art correlations for frictional pressure gradient were evaluated, with particular emphasis on the practically important ranges of total mass quality and mass flux, from the standpoint of plate-fin heat exchangers designed as evaporators. Neither correlation was in good agreement over the entire range of interest. A modified, semiempirical correlation was developed to predict, with satisfactory accuracy for design purposes, the measured data of these experiments. DOE

**N91-10237*#** Institute for Computer Applications in Science and Engineering, Hampton, VA.
**BOUNDED ENERGY STATES IN HOMOGENEOUS TURBULENT SHEAR FLOW: AN ALTERNATIVE VIEW Final Report**
Peter S. Bernard (Maryland Univ., College Park.) and Charles G. Speziale Oct. 1990 36 p Submitted for publication
(Contract NAS1-18605)
(NASA-CR-187439; NAS 1.26:187439; ICASE-90-66) Avail: NTIS HC/MF A03 CSCL 20D

The equilibrium structure of homogeneous turbulent shear flow is investigated from a theoretical standpoint. Existing turbulence models, in apparent agreement with physical and numerical experiments, predict an unbounded exponential time growth of the turbulent kinetic energy and dissipation rate; only the anisotropy tensor and turbulent time scale reach a structural equilibrium. It is shown that if vortex stretching is accounted for in the dissipation rate transport equation, then there can exist equilibrium solutions, with bounded energy states, where the turbulence production is balanced by its dissipation. Illustrative calculations are present for a k-epsilon model modified to account for vortex stretching. The calculations indicate an initial exponential time growth of the turbulent kinetic energy and dissipation rate for elapsed times that are as large as those considered in any of the previously conducted physical or numerical experiments on homogeneous shear flow. However, vortex stretching eventually takes over and forces a production-equals-dissipation equilibrium with bounded energy states. The validity of this result is further supported by an independent theoretical argument. It is concluded that the generally accepted structural equilibrium for homogeneous shear flow with unbounded component energies is in need of re-examination. Author

**N91-10238*#** Old Dominion Univ., Norfolk, VA. Dept. of Mechanical Engineering and Mechanics.
**INTERACTIVE REAL TIME FLOW SIMULATIONS Progress Report, period ending 30 Sep. 1990**
I. Sadrehaghighi and S. N. Tiwari Oct. 1990 47 p
(Contract NCC1-68)
(NASA-CR-187325; NAS 1.26:187325) Avail: NTIS HC/MF A03 CSCL 20D

An interactive real time flow simulation technique is developed for an unsteady channel flow. A finite-volume algorithm in conjunction with a Runge-Kutta time stepping scheme was developed for two-dimensional Euler equations. A global time step was used to accelerate convergence of steady-state calculations. A raster image generation routine was developed for high speed image transmission which allows the user to have direct interaction with the solution development. In addition to theory and results, the hardware and software requirements are discussed. Author

**N91-10239#** Los Alamos National Lab., NM.
**AFDM: AN ADVANCED FLUID-DYNAMICS MODEL. VOLUME 1: SCOPE, APPROACH, AND SUMMARY**
W. R. Bohl, F. R. Parker, D. Wilhelm, J. Berthier, L. Goutagny (Commissariat a l'Energie Atomique, Cadarache, France ), and H. Ninokata Sep. 1990 109 p
(Contract W-7405-eng-36)
(DE90-016723; LA-11692-MS-Vol-1) Avail: NTIS HC/MF A06

AFDM, or the Advanced Fluid-Dynamics Model, is a computer code that investigates new approaches simulating the multiphase-flow fluid-dynamics aspects of severe accidents in fast reactors. The AFDM formalism starts with differential equations similar to those in the SIMMER-II code. These equations are modified to treat three velocity fields and supplemented with a variety of new models. The AFDM code has 12 topologies describing what material contacts are possible depending on the presence or absence of a given material in a computational cell, on the dominant liquid, and on the continuous phase. Single-phase, bubbly, churn-turbulent, cellular, and dispersed flow regimes are permitted for the pool situations modeled. Virtual mass terms are included for vapor in liquid-continuous flow. Interfacial areas between the continuous and discontinuous phases are convected to allow some tracking of phenomenological histories. Interfacial areas are also modified by models of nucleation, dynamic forces, turbulence, flashing, coalescence, and mass transfer. Heat transfer is generally treated using engineering correlations. Liquid-vapor phase transitions are handled with the nonequilibrium, heat-transfer-limited model, whereas melting and freezing processes are based on equilibrium considerations. Convection is treated using a fractional-step method of time integration, including a semi-implicit pressure iteration. A higher-order differencing option is provided to control numerical diffusion. The Los Alamos SESAME equation-of-state has been implemented using densities and temperatures as the independent variables. DOE

**N91-10240#** Los Alamos National Lab., NM.
**AFDM: AN ADVANCED FLUID-DYNAMICS MODEL. VOLUME 4: THE AFDM HEAT- AND MASS-TRANSFER SOLUTION ALGORITHM**
W. R. Bohl, J. Berthier, L. Goutagny, and P. Schmuck Sep. 1990 46 p
(Contract W-7405-eng-36)
(DE90-017535; LA-11692-MS-Vol-4) Avail: NTIS HC/MF A04

This report gives the Advanced Fluid-Dynamics Model (AFDM) solution algorithm describing vaporization/condensation (V/C) and melting/freezing processes. The finite-difference equations used are derived from the general AFDM differential equations with convection ignored. In two-phase cells, V/C is determined by a simultaneous iterative solution. The objective is to retain stability and energy conservation with consistent interfacial and bulk conditions describing vapor/liquid densities and temperatures. Particular attention is given in the special cases required to obtain a solution. In single-phase cells, the heat transfer is determined first; then, a vapor composition is updated for the (alpha)(sub 0) volume based on the saturation pressures for the individual liquids. Melting/freezing rates are determined based on equilibrium considerations. Mass-transfer-induced velocity changes are calculated implicitly so as to conserve momentum. In addition to the treatment of the standard models, a description is provided on the energy transfers used for the simplified NOPHASE option. DOE

**N91-10241#** Los Alamos National Lab., NM.
**AFDM: AN ADVANCED FLUID-DYNAMICS MODEL**
W. R. Bohl Sep. 1990 127 p
(Contract W-7405-eng-36)
(DE90-017536; LA-11692-MS-Vol-5) Avail: NTIS HC/MF A07

This report gives the details for the convection of mass, momentum, and energy in the Advanced Fluid-Dynamics Model (AFDM) code. Steps 2 to 4 of the AFDM algorithm are described. Step 2 explicitly convects the results of Step 1 intracell transfers. Step 3 performs an iteration to obtain consistent end-of-time-step cell-edge velocities and cell-centered pressures. Step 4 convects all cell variables with converged Step 3 velocities and includes the effects of interfacial dissipation. The unique AFDM higher-order spatial differencing format and the iterative solution for velocities based on three-field momentum coupling coefficients are described. The rationale for the momentum convection relationships selected is discussed. Details are provided on the linear equation-solver options available to treat the five-diagonal pressure-coefficient matrix formulated in the Step 3 iteration. DOE

**N91-10242#** Los Alamos National Lab., NM.
**AFDM: AN ADVANCED FLUID-DYNAMICS MODEL**
J. Berthier, D. Wilhelm, and W. R. Bohl Sep. 1990 85 p
(Contract W-7405-eng-36)
(DE90-017537; LA-11692-MS-Vol-3) Avail: NTIS HC/MF A05

This report consists of three parts. First, for the standard Advanced Fluid-Dynamics Model (AFDM), heat-transfer coefficients between components are worked out, depending on the different possible topologies. Conduction, convection, and radiative heat-transfer mechanisms are modeled. For solid particles, discontinuous phases that obey a rigid model, and components lacking relative motion, heat transfer is by conduction. Convection is represented for fluids in motion inside circulating bubbles and/or droplets. Radiation is considered between droplets in vapor continuous flow. In addition, a film-boiling model has been formulated, where radiation provides the lower limit on the fuel-to-coolant heat-transfer coefficient. Second, the momentum-exchange coefficients are defined for the standard AFDM. Between a continuous and discontinuous phase, the model consists of both laminar and turbulent terms. The most important feature is the drag coefficient in the turbulent term. It is calculated by a drag similarity hypothesis with limits for large Reynolds numbers, distorted particles, and churn-turbulent flow. A unique hysteresis algorithm exists to treat the liquid continuous to vapor continuous transition. Two discontinuous components are coupled using a turbulent term with an input drag coefficient. Fluid structure momentum exchange is represented with a standard friction-factor correlation. Third, the formulas used for the AFDM simplified Step 1 models are discussed. These include the heat-transfer coefficients, the momentum-exchange functions, and the manner in which interfacial areas are determined from input length scales. The simplified modeling uses steady-state engineering correlations, as in SIMMER-II. DOE

**N91-10243#** Los Alamos National Lab., NM.
**AFDM: AN ADVANCED FLUID-DYNAMICS MODEL**
F. R. Parker Sep. 1990 133 p
(Contract W-7405-eng-36)
(DE90-017538; LA-11692-MS-Vol-8) Avail: NTIS HC/MF A07

The T6P postprocessor analyzes data from TAPE6 and TAPE36. The processor calculates new variables, integrates variables over regions of the mesh, compares values of a variable of a given problem at selected times, compares values of a variable at selected times between problems for parameter studies, calculates derivatives of a variable with respect to time or another variable, and traces a variable at a requested location in the mesh over time. The data are presented to the user graphically, using two-dimensional graphs and three-dimensional perspective or contour plots. Interactive graphic techniques may be used with perspective plots. DOE

**N91-10244#** Los Alamos National Lab., NM.
**AFDM: AN ADVANCED FLUID-DYNAMICS MODEL**
F. R. Parker, W. R. Bohl, and R. J. Henninger Sep. 1990 202 p
(Contract W-7405-eng-36)
(DE90-017539; LA-11692-MS-Vol-7) Avail: NTIS HC/MF A10

The Advanced Fluid-Dynamics Model (AFDM) computer code is designed to test advanced fluid-dynamics models. The programming objectives in writing AFDM were: (1) to produce a code in which all computational loops were vectorized, and (2) to produce an exportable code. To accomplish these objectives, we used gather/scatter and vector-merge techniques and shorter, more managable DO loops. We also reduced the number of DO loops over a computational mesh to one. The disadvantage of having only one DO loop was the need to recalculate a small set of boundary cells. The gather/scatter process divides the computational mesh into classes such as two-phase and single-phase cells. The scattered data then are gathered, the computation is executed by a high-speed vectorized loop, and the results are scattered again. Vector merges use a truth vector to choose the needed results; however, all results for both sides of the truth vector must be calculated. A small test code using these features shows efficiency improvements of a factor of 5 to 10 over nonvectorized codes. The AFDM input is completely free form. The variables were divided into classes, and each variable was given a unique name in that class to allow the input deck to be edited by a variable name. The AFDM output can be text or plot output. The text output goes to printers and will not include plots. The plot output goes to a plotting medium that also can include the text. DOE

**N91-10245*#** National Aeronautics and Space Administration. Langley Research Center, Hampton, VA.

### MEASURED AND PREDICTED SHOCK SHAPES FOR AFE CONFIGURATION AT MACH 6 IN AIR AND IN CF4

William L. Wells and Alan M. Franks Oct. 1988 56 p
(NASA-TM-100660; NAS 1.15:100660) Avail: NTIS HC/MF A04
CSCL 20D

Shock shapes and stand-off distances were obtained for the Aeroassist Flight Experiment configuration from Mach 6 tests in air and in CF4. Results were plotted for an angle-of attack range from -10 to 10 degrees and comparisons were made at selected angles with inviscid-flow predictions. Tests were performed in the Langley Research Center (LaRC) 20 inch Mach 6 Tunnel (air) at unit free-stream Reynolds numbers (N sub Re, infinity) of 2 million/ft and 0.6 million/ft and in the LaRC Hypersonic CF4 Tunnel at N sub Re, infinity = 0.5 million/ft and 0.3 million/ft. Within the range of these tests, N sub Re, infinity did not affect the shock shape or stand off distance, and the predictions were in good agreement with the measurements. The shock stand-off distance in CF4 was approximately half of that in air. This effect resulted from the differences in density ratio across the normal shock, which was approximately 12 in CF4 and 5 in air. In both test gases, the shock lay progressively closer to the body as angle of attack decreased. Author

**N91-10246#** Institut Franco-Allemand de Recherches, Saint-Louis (France).

### TURBULENT BOUNDARY LAYERS IN HIGH ENTHALPY FLOWS. NUMERICAL CODE VALIDATION BY SHOCK TUBE EXPERIMENTS

G. Smeets 10 Jul. 1989 17 p Presented at 17th International Symposium on Shock Waves and Shock Tubes, Bethlehem, PA, 17-21 Jul. 1989
(ISL-CO-221/89; ETN-90-97574) Avail: NTIS HC/MF A03

Departing from Prandtl's mixing length concept, Van Driest in 1951 derived a differential equation describing the mean velocity profile of a compressible boundary layer near the wall. The solution of this equation contained a complex integral which could at that time only be approximated by a series expansion. A more general solution of Van Driest's differential equation is given, describing both the near wall and the outer velocity profiles. A closed set of general equations containing three free parameters is established. The parameters are then determined by fitting the theoretical predictions to reliable experimental data for incompressible boundary layers. By comparing with a great deal of data on two dimensional compressible turbulent boundary layers, all received with shock tube experiments, it is shown that this theoretical scheme also gives correct predictions in the case of high stagnation enthalpy flows up to 2000 K stagnation temperature. ESA

**N91-10247#** Institut Franco-Allemand de Recherches, Saint-Louis (France).

### VELOCITY MEASUREMENTS IN PISTON-INDUCED TURBULENT BOUNDARY LAYERS IN A SHOCK TUBE

F. Seiler 5 Oct. 1989 18 p Presented at 13th International Congress on Instrumentation in Aerospace Simulation Facilities, Goettingen, Fed. Republic of Germany, 18-21 Sep. 1989
(Contract BMVg-T/R-760/H-0003/H-1763)
(ISL-CO-235/89; ETN-90-97576) Avail: NTIS HC/MF A03

Velocity measurements using the laser Doppler velocimeter were performed in a shock tube to obtain information about the behavior of piston induced turbulent boundary layers. The velocity distributions behind a shock accelerated piston inside the turbulent boundary layer were investigated at different distances from the tube wall surface. A comparison is made between the experimental data and theoretical calculations. The experimentally determined velocity profiles were found to be in good agreement with the theory applied for the piston boundary layer formation. ESA

**N91-10248#** Bertin et Cie., Plaisir (France).

### A KNUDSEN LAYER THEORY FOR LATTICE GASES

R. Cornubert, D. dHumieres, and D. Levermore (Arizona Univ., Tucson.) 1990 23 p Presented at the Workshop on Lattice Gas Methods for PDE's: Theory, Application, and Hardware, Los Alamos, NM, 6-9 Sep. 1989 Submitted for publication
(Grant NSF DMS-89-14420)
(ETN-90-97583) Avail: NTIS HC/MF A03

A Knudsen layer theory is presented for lattice gases with arbitrary boundariy conditions. Analytical results are carried out for two special orientations; these exhibit anisotropic Kundsen layers provided that suitable conditions are satisfied. However, the standard boundary conditions used in previous simulations are shown to be isotropic, the bulk steady state extending everywhere in the gas. This theory allows a more accurate localization of the obstacle with respect to the lattice nodes. These results are in good agreement with the numerical simulations. ESA

**N91-10249*#** National Aeronautics and Space Administration. Lewis Research Center, Cleveland, OH.

### A THREE-DIMENSIONAL TURBULENT HEAT TRANSFER ANALYSIS FOR ADVANCED TUBULAR ROCKET THRUST CHAMBERS

Kenneth J. Kacynski Oct. 1990 10 p Presented at the JANNAF Propulsion Conference, Anaheim, CA, 3-5 Oct. 1990
(NASA-TM-103293; E-5753; NAS 1.15:103293) Avail: NTIS HC/MF A02 CSCL 20D

Heat transfer was analyzed in the throat region of a plug and spool rocket engine for both smooth and corrugated walls. A three-dimensional, Navier-Stokes code was used for the analysis. The turbulence model in the code was modified to handle turbulence suppression in the crevice region of the corrugated wall. The overall heat transfer at the throat for the corrugated wall was 34 percent higher than it was for the smooth wall for comparable rocket flow conditions. Author

**N91-10250*#** Institute for Computer Applications in Science and Engineering, Hampton, VA.

### THE 'OPTIMUM' UPWIND ADVECTION ON A TRIANGULAR MESH Final Report

P. L. Roe (Michigan Univ., Ann Arbor.) Oct. 1990 23 p Submitted for publication
(Contract NAS1-18605)
(NASA-CR-187459; NAS 1.26:187459; ICASE-90-75) Avail: NTIS HC/MF A03 CSCL 20D

For advection schemes based on fluctuation splitting, a design criterion of optimizing the time step leads to linear schemes that coincide with those designed for least truncation error. A further stage of optimizing the time step using a nonlinear positivity criterion, leads to considerable further gains in resolution. Author

**N91-10251*#** Institute for Computer Applications in Science and Engineering, Hampton, VA.
**QUADRATURE IMPOSITION OF COMPATIBILITY CONDITIONS IN CHEBYSHEV METHODS Final Report**
D. Gottlieb (Brown Univ., Providence, RI.) and C. L. Streett Oct. 1990 21 p Submitted for publication
(Contracts NAS1-18107; NAS1-18605)
(NASA-CR-187458; ICASE-90-74; NAS 1.26:187458) Avail: NTIS HC/MF A03 CSCL 20D

Often, in solving an elliptic equation with Neumann boundary conditions, a compatibility condition has to be imposed for well-posedness. This condition involves integrals of the forcing function. When pseudospectral Chebyshev methods are used to discretize the partial differential equation, these integrals have to be approximated by an appropriate quadrature formula. The Gauss-Chebyshev (or any variant of it, like the Gauss-Lobatto) formula can not be used here since the integrals under consideration do not include the weight function. A natural candidate to be used in approximating the integrals is the Clenshaw-Curtis formula, however it is shown that this is the wrong choice and it may lead to divergence if time dependent methods are used to march the solution to steady state. The correct quadrature formula is developed for these problems. This formula takes into account the degree of the polynomials involved. It is shown that this formula leads to a well conditioned Chebyshev approximation to the differential equations and that the compatibility condition is automatically satisfied. Author

**N91-10252*#** National Aeronautics and Space Administration. Ames Research Center, Moffett Field, CA.
**A ONE-EQUATION TURBULENCE TRANSPORT MODEL FOR HIGH REYNOLDS NUMBER WALL-BOUNDED FLOWS**
Barrett S. Baldwin and Timothy J. Barth Aug. 1990 23 p
(NASA-TM-102847; A-90231; NAS 1.15:102847) Avail: NTIS HC/MF A03 CSCL 20D

A one-equation turbulence model that avoids the need for an algebraic length scale is derived from a simplified form of the standard k-epsilon model equations. After calibration based on well established properties of the flow over a flat plate, predictions of several other flows are compared with experiment. The preliminary results presented indicate that the model has predictive and numerical properties of sufficient interest to merit further investigation and refinement. The one-equation model is also analyzed numerically and robust solution methods are presented. Author

**N91-10253#** Helsinki Univ. Technology, Otaniemi (Finland). Aerodynamics Lab.
**MULTIGRID SOLUTION FOR THE EULER EQUATIONS IN AXISYMMETRIC FLOW**
Jaakko Hoffren and Timo Siikonen 1989 34 p
(Rept-B-17; ISBN-951-754-987-3; ISSN-0358-2620) Avail: NTIS HC/MF A03

A two-dimensional multigrid method for Euler equations is extended to a three-dimensional axisymmetric case. The basic features of the original method, such as finite volume form and flux vector splitting, are retained, and so too is the implicit time integration scheme with a multigrid algorithm. Several test cases are studied in various flow regimes, and the results are compared with references. The performance of the extended code is found to be fair, but the convergence is degraded compared to the original two-dimensional code. Author

**N91-10254#** Helsinki Univ. Technology, Otaniemi (Finland). Aerodynamics Lab.
**COMPUTATION OF BOUNDARY LAYER FLOW USING THIN-LAYER NAVIER-STOKES EQUATIONS WITH FLUX-VECTOR SPLITTING**
Huachen Pan, Timo Siikonen, and Seppo Laine 1989 31 p
(Rept-B-21; ISBN-951-22-0117-8; ISSN-0358-2620) Avail: NTIS HC/MF A03

The thin-layer compressible Navier-Stokes equations are used for the calculation of boundary layer flows. A flux-vector splitting technique is applied for the convective parts of the fluxes, the viscous parts are centrally differenced. The computed flow cases include flat plate boundary layer flows with free stream Mach numbers of 0.3 (nearly incompressible) and 4, and the flow of shock and boundary layer interaction with the free stream Mach number of 2. The calculations are compared with theoretical and experimental results. Author

**N91-10255#** Universiteit Twente, Enschede (Netherlands).
**DYNAMICS OF GAS BUBBLES MOVING THROUGH LIQUID Ph.D. Thesis**
Jacobus Bernardus Wi Kok 1989 125 p
(ETN-90-97760) Avail: NTIS HC/MF A06

The flow of mixtures of liquid and gas bubbles and dynamics of gas bubbles moving through liquid are addressed. Kinetic energy and added mass of hydrodynamically interacting gas bubbles in liquid are investigated and results compare well with those in the literature. The dynamics of pairs gas bubbles moving through liquid are studied. Experiments on a pair of air bubbles rising at moderate Reynolds number in water are described. The bubble trajectories were measured with high accuracy using multiple exposure photographic techniques and detailed conclusions are presented. Equations of motion for a pair of bubbles moving through a perfect liquid, the deflection of the bubble paths in an encounter and the collision cross section of two colliding bubbles are investigated. ESA

**N91-10256#** Kaiserslautern Univ. (Germany, F.R.). Arbeitsgruppe Technomathematik.
**COMPUTATIONAL METHODS FOR THE BOLTZMANN EQUATION**
F. Gropengiesser, H. Neunzert, and J. Struckmeier Feb. 1990 36 p Submitted for publication
(Br-43; ETN-90-97865) Avail: NTIS HC/MF A03

The basic ideas and practical aspects for numerical methods for solving the Boltzmann equation are presented. The main field of application considered is the reentry of the Space Shuttle in the transition from free molecular flow to continuum flow. The method used is called Finite Pointset Method (FPM) approximating the solution by finite sets of particles. Convergence results and practical aspects of the algorithm are emphasized. Ideas for the transition to the Navier-Stokes domain are discussed. ESA

**N91-10257#** Kaiserslautern Univ. (Germany, F.R.). Fachbereich Mathematik.
**ON THE CONVERGENCE AT INFINITY, RATE OF CONVERGENCE AND UNIQUENESS OF SOLUTIONS WITH FINITE DIRICHLET INTEGRAL TO THE EXTERIOR DIRICHLET PROBLEM FOR THE STEADY PLANE NAVIER-STOKES SYSTEM OF EQUATIONS**
Dan Socolescu Oct. 1989 53 p
(Preprint-166; ETN-90-97866) Avail: NTIS HC/MF A04

The Navier-Stokes equation, the continuity equation, and the boundary conditions describing a steady flow of a viscous incompressible fluid past on obstacle with uniform velocity are discussed. The solutions constructed for the exterior Dirichlet problem are analyzed. The convergence and the rate of convergence at infinity of a solution with finite Dirichlet integral of the velocity are detailed. The uniqueness in the Leray class of solutions with finite Dirichlet integral of the velocity is proved. ESA

**N91-10258#** Erlangen-Nuremberg Univ. (Germany, F.R.). Lehrstuhl fuer Stroemungsmechanik.
**CORIOLIS-EFFECT IN MASS FLOW METERING**
H. Raszillier and F. Durst 1989 50 p
(LSTM-266/T/89; ETN-90-97889) Avail: NTIS HC/MF A03

The physical background for the so-called Coriolis mass flow meter is described. The vibration modes of a fluid conveying straight pipe segment are analyzed. These modes deviate in shape from those appearing in the absence of fluid motion. The effect of fluid inertia may be exploited for the purpose of flow measurement. The analysis is performed under a simplifying approximation: the pipe is considered as a beam, the fluid as a moving string. The equations describing the vibrations are derived variationally, with the constraint of a common vibration amplitude of both fluid and pipe. The Lagrange multiplier associated with the constraint gives the interaction force between pipe and fluid. The modes are determined by a perturbation procedure. The analysis shows how the time delay between the vibrations of two appropriately chosen points of the pipe may serve to determine the mass flow rate of the fluid. The precise role of the Coriolis force is considered. The improvements of the used approximation are discussed. ESA

**N91-10259#** Rolls-Royce Ltd., Derby (England). Theoretical Science Group.
**NUMERICAL SOLUTIONS OF ROTATING DISC FLOWS USING A NON-LINEAR MULTIGRID ALGORITHM**
C. M. Vaughan, S. Gilham (Sussex Univ., Brighton, England ), and J. W. Chew 15 Jul. 1989 12 p Presented at the 6th International Conference on Numerical Methods in Laminar and Turbulent Flow, Swansea, England, Jul. 1989 Sponsored by Ruston's Gas Turbines Ltd., and Science Research Council, England
(PNR-90679; ETN-90-97927) Copyright Avail: NTIS HC/MF A03

A finite difference solution algorithm incorporating a multigrid acceleration technique is presented. Applications to rotating disc flows are included. Comparisons to a one grid algorithm are made. The multigrid scheme is shown to be efficient over a wide range of test cases, including fully turbulent compressible non isothermal flow at high rotational speed. Comparisons with previous numerical and experimental results confirm the accuracy of the current code. ESA

**N91-10260#** Rolls-Royce Ltd., Derby (England).
**DETAILED HEAT TRANSFER MEASUREMENTS IN NOZZLE GUIDE VANE PASSAGES IN LINEAR AND ANNULAR CASCADES IN THE PRESENCE OF SECONDARY FLOWS**
N. W. Harvey, Z. Wang, P. T. Ireland, and T. V. Jones (Oxford Univ., England ) 1 Sep. 1989 13 p Presented at AGARD PEP 74th Secondary Flow in Turbomachines, Luxembourg, Luxembourg, 30 Aug. - 1 Sep. 1989 Sponsored by Ministry of Defence Procurement Executive, London, England
(PNR-90706; ETN-90-97938) Copyright Avail: NTIS HC/MF A03

Two transient techniques, used to measure to heat transfer coefficient distributions in nozzle guide vane passages, are described. The first employs liquid crystal methods in a cold heat transfer tunnel and examines the flow in a two dimensional cascade. The second uses localized thin film heat transfer gauges within an annular cascade at engine representative Mach numbers and Reynolds numbers. The resulting heat transfer coefficient distributions are interpreted in terms of the secondary flows and vortex structures. Typical heat transfer distributions are presented over the endwalls and blade surfaces. The endwall heat transfer results are analyzed for the annular cascade. ESA

**N91-10261#** Rolls-Royce Ltd., Derby (England). Advanced Research Lab.
**FLOW MEASUREMENTS IN TURBOMACHINERY USING LASER ANEMOMETRY AND HOLOGRAPHY**
D. G. Jones, R. J. Parker, and S. S. Wiseall Derby, England 26 Sep. 1989 37 p Presented at the 3rd International Conference on Laser Anemometry: Advances and Applications, Wales, 26-29 Sep. 1989; sponsored by University College of Swansea; I Mech E; and BHRA Sponsored in part by Ministry of Defence Procurement Agency, London, England
(PNR-90717; ETN-90-97944) Copyright Avail: NTIS HC/MF A03

The optical techniques of holography and laser anemometry are powerful and complementary methods of non-intrusively probing flows in turbomachinery. Some factors and conflicting constraints which need to shape the design of optical techniques are discussed. The use of double pulsed holographic interferometry for flow visualization in transonic fans is described. The value of the technique for diagnosing and verifying the influence of design changes of fan performance is emphasized. The principle factors which influence the design and choice of the anomometer are analyzed. Some lasers transit anemometer measurements within the blade row of a rotating wide chord fan are presented. For measurements in a compressor, a Doppler difference anemometer with burst correlation processing was used. The advantages of conditional correlation for flare rejection when working close to surfaces are described, and measurements for radial and circumferential traverses are presented. ESA

**N91-10262#** Rolls-Royce Ltd., Bristol (England).
**AN INVESTIGATION OF SECONDARY FLOWS IN NOZZLE GUIDE VANES**
R. G. Dominy (Durham Univ., England ) and S. C. Harding Derby, England 28 Aug. 1989 14 p Presented at AGARD PEP 74th Secondary Flows in Turbomachines, Luxembourg, Luxembourg, 28 Aug. - 1 Sep. 1989 Sponsored by Science Research Council, England
(PNR-90739; ETN-90-97951) Copyright Avail: NTIS HC/MF A03

Most of the energy loss in turbine nozzles is associated with 3-D secondary flows that result from the interaction between the surface boundary layers and the nozzle row with its associated pressure field. Three alternative nozzles with differences in their designs to control secondary flows are studied. These chosen nozzle guide vanes are representative of the current generation of high hub-tip ratio aero engine nozzles. A computational analysis of all three nozzles is presented including predictions from three alternative viscous, 3-D methods. These detailed measurements and predictions demonstrate the influence of the vane geometries on the magnitude and the distribution of the secondary losses. ESA

**N91-10263#** Swedish Defence Research Establishment, Umea.
**PRESSURE MEASUREMENTS ON THE RELEASE SYSTEM AND DETERMINATION OF JET MOMENTUM IN THE PROJECT BA PROPANE FIELD TESTS 1989**
Kenneth Nyren and Stellan Winter Mar. 1990 22 p Sponsored by the Swedish Fire Research Board
(FOA-E-40044-4.5; ISSN-0281-9945; ETN-90-97988) Avail: NTIS HC/MF A03; Swedish Defence Research Establishment, S-901 82 Umea, Sweden,

The results of the pressure measurements, conducted on the pipeline before the nozzle and on the nozzle itself, are discussed. Using these measured data, the mass flow rate and jet momentum were calculated. It appeared that stagnation pressures 2.5 to 4 bars higher than the saturation pressure gave rise to pure liquid flow all the way up to the exhaust plane, where the pressure was equal to the saturation pressure. The experiment with the 15 mm nozzle showed that the jet momentum could be calculated with the flow rate equation presented with good accuracy. ESA

## 35 INSTRUMENTATION AND PHOTOGRAPHY

Includes remote sensors; measuring instruments and gages; detectors; cameras and photographic supplies; and holography.

For aerial photography see *43 Earth Resources and Remote Sensing.* For related information see also *06 Aircraft Instrumentation,* and *19 Spacecraft Instrumentation.*

**N91-10264#** Amptek, Inc., Bedford, MA.
**PROTOTYPE INSTRUMENTATION AND DESIGN STUDIES**
**Scientific Report No. 1**
Alan C. Huber, John O. McGarity, John A. Pantazis, A. Wallace Everest, III, David J. Sperry, and Scott J. Moran 5 Apr. 1989 12 p
(Contract F19628-87-C-0094)
(AD-A211566; GL-TR-89-0098) Avail: NTIS HC/MF A03 CSCL 14/2

Flight prototype sensor systems using spherical sections and electrostatic deflection are being developed, fabricated, tested and calibrated. The detectors will measure the flux of ions and electrons over a 100 degree x 10 degree angular fan and in 32 discrete energy levels from 10 eV to 10 KeV. This report describes the sensor system design for an instrument package for shuttle flight as well as studies being performed investigating the feasibility of using strip detectors to produce a multiangular solid state detector for high energy particles and the use of time of flight techniques for mass determination and a correlator to look for wave-particle interactions. Author

**N91-10265** Wisconsin Univ., Madison.
**THIN FILM THERMOMETERS AND FLOWMETERS FOR APPLICATIONS IN LIQUID HELIUM Ph.D. Thesis**
Douglas Scott Holmes 1989 275 p
Avail: Univ. Microfilms Order No. DA9013348

A flowmeter design was developed and investigated for the metering of liquid He II bulk flows in small channels. The flowmeter consists of a thin film heater with thin film temperature sensors located upstream and downstream from the heater. Thin film temperature sensors were developed based on amorphous semiconductor-metal alloys. The amorphous films were deposited by dc magnetron sputtering in an argon plasma. The thin film heaters and sensors can be placed on the inside walls of a flow channel and do not restrict the flow or cause cavitation as do venturi or turbine flowmeters. One mode of flowmeter operation is to pulse the heater, creating second sound pulses which travel upstream and downstream to the temperature sensors. The Doppler shift in the pulse arrival times can be related to the bulk flow velocity. A second mode of operation requires a continuous sinusoidal driving current supplied to the heater to produce second sound and a lock-in amplifier to detect the resulting signal at a temperature sensor either upstream or downstream from the heater. The phase shift of the received signal is related to the bulk flow velocity. The resolution and accuracy of second sound based flowmeters are shown to depend on channel size and heater-to-detector distance, bulk flow velocity, a maximum allowable heat flux from the heater to the He II, and attenuation of second sound by quantum turbulence in the flowing He II. Doppler shift flowmeter operation was successful. Phase shift flowmeter operation was unreliable, probably as a result of unfavorable geometry. Dissert. Abstr.

**N91-10266#** Los Alamos National Lab., NM.
**AN IMAGING X-RAY MICROSCOPE USING A LASER PLASMA SOURCE AND A SCHWARZCHILD OBJECTIVE**
H. K. Pew and G. L. Stradling 1990 16 p Presented at the X Ray Microscopy Conference, London, England, 3-7 Sep. 1990
(Contract W-7405-eng-36)
(DE90-016432; LA-UR-90-2915; CONF-9009235-1) Avail: NTIS HC/MF A03

This paper presents some design considerations for an imaging x-ray microscope to be used in the 'water window' region of the spectrum. The usefulness of such an instrument is discussed. The suitability of current soft x-ray sources and optics are discussed, and the selection of a laser plasma source and a multilayer coated Schwarzchild objective is justified. Also, problems associated with the production of figured multilayer coatings for the 'water window' region are discussed. DOE

**N91-10267#** Lawrence Livermore National Lab., CA. Field Test Systems Div.
**A NEW METHOD FOR DOING FLAT-FIELD INTENSITY CALIBRATIONS OF MULTIPLEXED ITT STREAK CAMERAS**
K. F. Hugenberg 18 Jun. 1990 8 p Presented at the SPIE's International Symposium on Optical and Optoelectronic Applied Science and Engineering Exhibit, San Diego, CA, 8-13 Jul. 1990
(Contract W-7405-eng-48)
(DE90-016475; UCRL-JC-104336; CONF-900756-37) Avail: NTIS HC/MF A02

The flat-field intensity calibrations of ITT downhole streak cameras were previously done with a bandpass filtered flashlamp/integrating sphere combination. However, this system had several problems when characterizing ITT streak cameras that were spatially multiplexed. The main problem, simply stated, was that there was excessive charge build-up on the phosphor screen of the microchannel plate image intensifier (MCPII) before the sweep of the streak camera started. Consequently, the swept CCD image has as many as twenty rows of saturated pixels. In addition, contamination or charge spillover into other rows of the CCD readout became an issue. This article outlines a better approach for doing flat-field calibrations which avoids the CCD saturation problem. DOE

**N91-10268*#** National Aeronautics and Space Administration. Ames Research Center, Moffett Field, CA.
**A LASER-SHEET FLOW VISUALIZATION TECHNIQUE FOR THE LARGE WIND TUNNELS OF THE NATIONAL FULL-SCALE AERODYNAMICS COMPLEX**
M. S. Reinath and J. C. Ross Sep. 1990 15 p
(NASA-TM-102793; A-90082; NAS 1.15:102793) Avail: NTIS HC/MF A03 CSCL 14B

A flow visualization technique for the large wind tunnels of the National Full Scale Aerodynamics Complex (NFAC) is described. The technique uses a laser sheet generated by the NFAC Long Range Laser Velocimeter (LRLV) to illuminate a smoke-like tracer in the flow. The LRLV optical system is modified slightly, and a scanned mirror is added to generate the sheet. These modifications are described, in addition to the results of an initial performance test conducted in the 80- by 120-Foot Wind Tunnel. During this test, flow visualization was performed in the wake region behind a truck as part of a vehicle drag reduction study. The problems encountered during the test are discussed, in addition to the recommended improvements needed to enhance the performance of the technique for future applications. Author

**N91-10269#** Ceramphysics, Inc., Westerville, OH.
**A MINIATURE INEXPENSIVE, OXYGEN SENSING ELEMENT Quarterly Report No. 8, 30 Apr. - 31 Jul. 1990**
R. W. Arenz 31 Jul. 1990 8 p
(Contract DE-FG01-88CE-15401)
(DE90-014080; DOE/CE-15401/T8) Avail: NTIS HC/MF A02

This paper is a progress report by: Ceramphysics, Inc. on the design, fabrication and testing of a miniature, inexpensive, oxygen sensing element. Four tasks are discussed. The first is the choice of ceramics, development of a sealing technique and the design of a heating element; the second is preliminary fabrication; the third the testing of prototypes and final fabrication; and the fourth is the preparation of the final report. DOE

**N91-10270#** Physical Optics Corp., Torrance, CA.
**HOLOGRAPHIC RUGATE STRUCTURES FOR X RAY OPTICS APPLICATIONS Final Report**
Tomasz Jannson and Gajendra Savant 19 Mar. 1990 160 p
(Contract DE-FG03-86ER-13600)
(DE90-017103; DOE/ER-13600/T1) Avail: NTIS HC/MF A08

A novel approach to x ray optics was proposed and investigated, based on the well established technologies in volume holography and holographic materials. With these technologies, a majority of conventional XUV optical elements, such as uniform and nonuniform gratings/multilayers, lenses, slanted (non-Snellian) mirrors, Fresnel zone-plates, concentrators/collimators, beam splitters, Fabry-Perot etalons, and binary optical elements, can be fabricated using a unified, low cost process. Furthermore, volume holography offer nonconventional optical elements, such as x ray holographic optical elements (HOEs) with any desirable wavefront formation characteristics and multiple gratings multiplexed in the same volume to perform different operations for different wavelengths, that are difficult or even impossible to produce with the existing technologies. DOE

**N91-10271*#** National Aeronautics and Space Administration. Lewis Research Center, Cleveland, OH.
**PARTICLE DISPLACEMENT TRACKING FOR PIV**
Mark P. Wernet Sep. 1990 25 p

(NASA-TM-103288; E-5507-1; NAS 1.15:103288) Avail: NTIS HC/MF A03 CSCL 14B

A new Particle Imaging Velocimetry (PIV) data acquisition and analysis system, which is an order of magnitude faster than any previously proposed system has been constructed and tested. The new Particle Displacement Tracing (PDT) system is an all electronic technique employing a video camera and a large memory buffer frame-grabber board. Using a simple encoding scheme, a time sequence of single exposure images are time coded into a single image and then processed to track particle displacements and determine velocity vectors. Application of the PDT technique to a counter-rotating vortex flow produced over 1100 velocity vectors in 110 seconds when processed on an 80386 PC. Author

**N91-10272#** Oxford Univ. (England). Dept. of Engineering Science.

**A FACILITY FOR CALIBRATING CALORIMETER GAUGES AT HIGH RATES OF CONVECTIVE HEAT TRANSFER**

Z. Wang and P. T. Ireland Apr. 1990 16 p
(OUEL-1825/90; ETN-90-97922) Avail: NTIS HC/MF A03

A method of calibrating calorimeter gauges at high rates convective heating was developed. The method calibrates the voltage produced by the thermocouple embedded in the gauge to the heat flux measured by a thin film gauge. The extremely high rates of heat transfer are produced by an acetylene flame. The gauges were also calibrated at lower heat fluxes using a butane flame. The gauge calibration coefficient was found to be sensibly insensitive to the heat transfer rate. ESA

**N91-10484*#** Colorado State Univ., Fort Collins. Dept. of Atmospheric Science.

**TEMPERATURE SENSITIVITY OF EPPLEY BROADBAND RADIOMETERS**

William L. Smith, Jr. and Stephen K. Cox *In* NASA, Langley Research Center, FIRE Science Results 1988 Jul. 1990 p 183-186 (For primary document see N91-10448 01-47)
(Grants NAG1-554; NSF ATM-85-21214)
Avail: NTIS HC/MF A17 CSCL 14B

**N91-10532*#** National Aeronautics and Space Administration. Goddard Space Flight Center, Greenbelt, MD.

**COMPARISON AND CALIBRATION OF NCAR ELECTRA INSTRUMENTS: JULY 5 AND 7, 1987**

Philip H. Austin and Reinout Boers *In* NASA, Langley Research Center, FIRE Science Results 1988 Jul. 1990 p 425-427 (For primary document see N91-10448 01-47)
Avail: NTIS HC/MF A17 CSCL 14B

# 36 LASERS AND MASERS

Includes parametric amplifiers.
For related information see also *76 Solid-State Physics.*

**N91-10273#** Texas A&M Univ., College Station. Dept. of Mechanical Engineering.

**THE 3-D LASER ANEMOMETER STUDY OF COMPRESSIBLE FLOW THROUGH ORIFICE PLATES Annual Report, Sep. 1988 - Oct. 1989**

Gerald L. Morrison, Kenneth R. Hall, and James C. Holste Nov. 1989 141 p
(Contract GRI-5086-260-1340)
(PB90-216771; GRI-90/0036) Avail: NTIS HC/MF A07 CSCL 20E

Two experimental facilities were constructed, one for the measurement of the pressure distributions on the pipe wall upstream and downstream of the orifice plate and on the orifice plate surface. The other for use with a laser Doppler anemometer (LDA) system to measure the complex flow field inside the orifice run. Pressure measurements for Beta = 0.50 and 0.75 have been performed at Reynolds numbers from 18,400 to 122,800. These results show the influence of the orifice plate extending less than 0.5 diameters upstream. On the upstream surface of the orifice plate the pressure remains constant over the outer regions of the plate then decreases rapidly near the hole. The pressure remains constant on the downstream face of the orifice plate. The pressure recovery on the pipe wall downstream of the orifice plate is characterized by a minimum pressure occurring at X/R = 1.0 for Beta = 0.50 and X/R approx. 0 for Beta = 0.75 and the distance required for full pressure recovery is approximately four pipe diameters. The 3-D LDA flow field measurements have been performed upstream and downstream of the orifice plate for Beta = 0.50 at Reynolds numbers of 18,400, 54,700 and 91,100. These data include the mean velocity vector field and contour plots of the axial and radial mean velocities, and the entire Reynolds stress tensor. These data show the vena contracta, the primary recirculation zone downstream of the orifice plate, a secondary recirculation zone at the downstream base of the orifice plate, a small recirculation zone on the upstream face of the orifice plate at the pipe wall, and the development of the flow into fully developed pipe flow downstream of the orifice plate. GRA

**N91-10274#** Lawrence Livermore National Lab., CA.

**THE 1987 STRATEGIC DEFENSE INITIATIVE ORGANIZATION (SDIO) WORKSHOP ON LASER PROPULSION**

Jordin T. Kare, ed. 1 Mar. 1990 252 p Workshop held in Los Alamos, NM, 14-18 Oct. 1987
(Contract W-7405-eng-48)
(DE90-013484; CONF-8710452) Avail: NTIS HC/MF A12

Two dimensional effects on laser propulsion performance were studied analytically using an ideal gas model. The two processes considered for an axially symmetric detonation wave are the effect of radial expansion within the detonation reaction layer and the effect of radial expansion in the region between the detonation wave and the base plate. In both cases, the two dimensional effects cause the reduction of the base pressure and the total thrust. The amount of reductions of base pressures are calculated and are plotted as functions of the reaction length/beam radius and beam radius/detonation were travel distance, respectively. Each report will be individually cataloged. DOE

**N91-10275#** Sandia National Labs., Albuquerque, NM.

**SODIUM-NEON RESONANT PHOTOEXCITATION SOFT X RAY LASER EXPERIMENTS ON SATURN**

John Porter, Rick Spielman, Keith Matzen, Gene McGuire, and Tom Hussey 1990 16 p Presented at the SDIO/T/IS Ultra Short Wavelength Laser Briefing, Washington, DC, Aug. 1990
(Contract DE-AC04-76DP-00789)
(DE90-014946; SAND-90-1944C; CONF-9008128-1) Avail: NTIS HC/MF A03

Progress made at Sandia Laboratories on x ray lasers is summarized. Experiments have demonstrated two main requirements necessary for constructing a radiation pumped soft x ray laser: (1) a source of sufficient intensity to produce high grain, and (2) creation of a significant population of neon ions close to the pump. DOE

**N91-10276#** Los Alamos National Lab., NM. Laser and Optical Sciences Group.

**RECENT ADVANCES IN EXCIMER LASER TECHNOLOGY AT LOS ALAMOS**

Irving J. Bigio, Steven J. Czuchlewski, Andrew W. McCown, and Antoinette J. Taylor 1990 8 p Presented at the 8th Biennial International Symposium on Gas Flow and Chemical Lasers, Madrid, Spain, 10-14 Sep. 1990
(Contract W-7405-eng-36)
(DE90-016441; LA-UR-89-2875; CONF-900953-1) Avail: NTIS HC/MF A02

Current research in excimer laser technology at Los Alamos progresses in two major areas: in the Bright Source program, the development of ultra-high brightness (sub-picosecond) laser systems, based on discharge-pumped excimer laser amplifiers, continues. Rigorous measurements were made of the saturation parameter for ultra-short pulses. In the laser fusion program, implementation of the large KrF laser fusion amplifiers were accompanied by numerous studies of the laser physics and kinetics of large e-beam pumped devices. DOE

**N91-10277#** Los Alamos National Lab., NM. Laser Science and Applications Group.
**BIOMEDICAL APPLICATIONS ON LASER TECHNOLOGY AT LOS ALAMOS**
Irving J. Bigio and Thomas R. Loree 1990 6 p Presented at the International Conference on Laser Applications in Life Sciences, Moscow, USSR, 27-31 Aug. 1990
(Contract W-7405-eng-36)
(DE90-016447; LA-UR-90-2854; CONF-9008142-1) Avail: NTIS HC/MF A02

Los Alamos has a long history of research in laser technology, and over the past few years a program was begun directing some of that technology to a variety of applications in biology and medicine. As examples, two of these activities are described: the use of a laser interferometer to measure the microwave absorption spectrum of DNA, and spectral measurements of the secondary light produced during laser corneal ablation. DOE

**N91-10278#** Lawrence Livermore National Lab., CA.
**DAMAGE ASSESSMENT AND POSSIBLE DAMAGE MECHANISMS TO 1-METER DIAMETER NOVA TURNING MIRRORS**
G. Edwards, J. Campbell, R. Wolfe, and E. Lindsey Aug. 1990 14 p Presented at the 1989 Boulder Damage Symposium, Boulder, CO, 1-3 Nov. 1989
(Contract W-7405-eng-48)
(DE90-016473; UCRL-101768; CONF-8911192-6) Avail: NTIS HC/MF A03

A major concern in the operation of the LLNL 120 kJ Nova laser system is damage to the nominal l-meter diameter mirrors (i.e., HR coatings). The damage appears to originate from microscopic defects that vary in size up to approximately 30 (mu)m in diameter. These defects produce damage sites up to 250 microns and, in some cases, covering 20 percent or more of the mirror surface. Defects due to particulates that are in or under the coating are highly unlikely due to the fact that coating thickness is only 5 microns thick and particles up to 30 microns would produce surface roughness that could be easily detected. Consequently, the defects must be plate-like (i.e., 2-D) in nature. A by-product of the damage is a haze left on the surface of the mirror. This haze is analyzed and shown to be blown-off particles of ZrO2/SiO2 coating material. The particle morphology suggests nucleation from a vapor phase which implies localized heating in the coating to temperatures on the order of 3000 K. Some possible damage mechanisms are also explored. DOE

**N91-10279#** Los Alamos National Lab., NM.
**CUMULATIVE BEAM BREAKUP OF THE GROUND-BASED-FREE-ELECTRON LASER**
K. C. D. Chan and G. Spalek Aug. 1990 15 p Presented at the 12th International Free Electron Laser Conference, Paris, France, 17-21 Sep. 1990
(Contract W-7405-eng-36)
(DE90-016485; LA-UR-90-2845; CONF-9009166-1) Avail: NTIS HC/MF A03

Strategies employed by the Ground-Based Free Electron Laser system to maintain beam stability in its RF linac against cumulative beam breakup is described. These strategies include a proper choice of cavity shape and the use of staggered tuning. Simulations show that the growths of effective transverse emittance due to cumulative beam breakup can be limited to 10 percent. DOE

**N91-10280#** Los Alamos National Lab., NM.
**INEX MODELING OF THE BOEING RING OPTICAL RESONATOR FREE-ELECTRON LASER**
J. C. Goldstein, R. L. Tokar, B. D. McVey, C. J. Elliott, D. H. Dowell, M. L. Laucks, and A. R. Lowrey (Boeing Aerospace Co., Seattle, WA.) 1990 24 p Presented at the 12th International Free Electron Laser Conference, Paris, France, 17-21 Sep. 1990
(Contract W-7405-eng-36)
(DE90-016488; LA-UR-90-2809; CONF-9009166-2) Avail: NTIS HC/MF A03

New results are presented from the integrated numerical model of the accelerator/beam transport system and ring optical resonator of the Boeing free electron laser experiment. Modifications of the electron beam transport have been included in a previously developed PARMELA model and are shown to reduce dramatically emittance growth in the 180 deg bend. The new numerically generated electron beam is used in the 3-D FEL simulation code FELEX to calculate expected laser characteristics with the ring optical resonator and the 5-m untapered THUNDER wiggler. Gain, extraction efficiency, and optical power are compared with experimental data. Performance sensitivity to optical cavity misalignments is studied. DOE

**N91-10281#** Fermi National Accelerator Lab., Batavia, IL.
**SSC DIPOLE MAGNET MEASUREMENT AND ALIGNMENT USING LASER TECHNOLOGY**
A. Lipski, J. A. Carson, and W. F. Robotham Jun. 1990 9 p Presented at the 2nd International Industrial Symposium on the Super Collider, Miami, FL, 14-16 Mar. 1990
(Contract DE-AC02-76CH-03000)
(DE90-014881; FNAL-TM-1671; CONF-900348-13) Avail: NTIS HC/MF A02

Advancing into the prototype production stage of the Superconducting Super Collider (SSC) dipole magnets has introduced the need for a reliable, readily available, accurate alignment measuring system which gives results in real time. Components and subassemblies such as the cold mass and vacuum vessel are being measured for various geometric conditions such as straightness and twist. Variations from nominal dimensions are also being recorded so they can be compensated for during the final assembly process. Precision laser alignment takes specific advantages of the greatest accuracy. When combined with an optically produced perpendicular plane, this results in a system of geometric references of unparalleled accuracy. This paper describes the geometric requirements for SSC dipole magnet components, sub and final assemblies as well as the use of laser technology for surveying as part of the assembly process. DOE

**N91-10282#** Lawrence Livermore National Lab., CA.
**KrF LASER PATH TO HIGH GAIN ICF (INERTIAL CONFINEMENT FUSION) LABORATORY MICROFUSION FACILITY**
David B. Harris, J. Al Sullivan, Joseph F. Figueiro, David C. Cartwright, Thomas E. McDonald, Allan A. Hauer, Stephen V. Coggeshall, and Stephen M. Younger 1990 6 p Presented at the 16th Symposium on Fusion Technology, London, England, 3-7 Sep. 1990
(Contract W-7405-eng-36)
(DE90-016439; LA-UR-90-2887; CONF-900918-3) Avail: NTIS HC/MF A02

The krypton-fluoride laser has many desirable features for inertial confinement fusion. Because it is a gas laser capable of operation with high efficiency, it is the only known laser candidate capable of meeting the driver requirements for inertial fusion energy (IFE) production. Los Alamos National Laboratory has defined a program plan to develop KrF lasers for IFE production. This plan develops the KrF laser and demonstrates the target performance in single-pulse facilities. A 100-kJ Laser Target Test Facility (LTTF) is proposed as the next step, to be followed by a 3 to 10-MJ Laboratory Microfusion Facility (LMF). The LTTF will resolve many target physics issues and accurately define the driver energy required for the LMF. It is also proposed that the technology development for IFE, such as the high-efficiency, high-reliability, repetitively pulsed driver, the reactor, mass production of targets, and the mechanism of injecting targets be developed in parallel with the single-pulse facilities. DOE

**N91-10283#** Institut Franco-Allemand de Recherches, Saint-Louis (France).
**INVESTIGATION OF PULSED LASER TARGET INTERACTION PROCESSES BY HIGH-SPEED DIAGNOSTIC TECHNIQUES**
Manfred Hugenschmidt 29 Sep. 1989 13 p Presented at 18th International Congress on High-Speed Photography and Photonics, Xian, Shaanxi, China, 29 Aug. - 2 Sep. 1988
(ISL-CO-234/89; ETN-90-97575) Avail: NTIS HC/MF A03

The application of laser power densities above the plasma ignition threshold to any dielectric, semiconducting, or metallic target material is capable of providing a most efficient energy transfer by an enhanced coupling mechanism. Experimental investigations of pulsed laser target interaction phenomena in a medium power density range below air breakdown threshold are described. When infrared lasers are considered, these values are in the range of some hundreds MW/sq cm or even below, for UV-lasers these values may be higher by one or two orders of magnitude. This range is of particular interest, as plasma induced thermomechanical processes are governing and improving the energy transfer. The most interesting features are occurring, however, if trains of pulses are applied, thereby building up high average power densities so that target effects are integrated temporally. These effects are then increasing rapidly giving rise to fast heating, melting, vaporization and subsequent ablation, including thermally induced chemical reactions. An overview on current research in the above mentioned field is given and recent measurements are described. ESA

**N91-10284#** Centre National d'Etudes Spatiales, Toulouse (France).
**HYDROGEN MASER: RESULTS OF EVALUATIONS DONE BY THE CNES FROM MAY 1986 TO DECEMBER 1987**
Jean-Bernard Laporte 6 Dec. 1988 48 p In FRENCH; ENGLISH summary
(CNES-DRT/TIT/TF-88/338-T; ETN-90-97811) Avail: NTIS HC/MF A03

The performances of two hydrogen masers are evaluated. The system can be used in space applications such as orbitography. High stability of the quartz oscillators, is required. In order to precisely measure these oscillators, references such as hydrogen masers are needed. Using different measurement sets, the two masers were tested in different time domains exhibiting excellent short term performances (for counting time from 100 to 10,000 seconds). ESA

**N91-10285#** Universiteit Twente, Enschede (Netherlands).
**LASER DOPPLER VELOCIMETRY USING DIODE LASERS Ph.D. Thesis**
Hendrik Willem Jentink 1989 145 p Sponsored by Netherlands Foundation for Technical Research
(ISBN-90-9002803-X; ETN-90-97771) Avail: NTIS HC/MF A07

The development of very small velocimeters for biomedical and industrial applications with emphasis on instrumentation and theory for skin blood flow measurements is addressed. Characteristics of the diode lasers used in the velocimeters are presented and discussed. The problems of tissue perfusion measurements are discussed. The optical probe of a developed differential laser Doppler velocimeter is described and is smaller than any gas laser equipped equivalent. The practical realization and theoretical description of a developed self mixing velocimeter is studied. Demands of temporal coherence on spectral characteristics of the diode laser and spatial coherence determination of signal magnitudes in correlation with detection sizes and detector positions in the various velocimeters are considered. ESA

**N91-10286#** Karlsruhe Univ. (Germany, F.R.). Sonderforschungsbereich 210.
**DISTORTION OF LDA FRINGE PATTERN BY TRACER PERTICLES**
B. Ruck Mar. 1990 20 p
(SFB-210/E/59; ETN-90-97876) Avail: NTIS HC/MF A03

For precise flow velocity measurements Laser Doppler Anemometry (LDA) is used. The LDA method has the advantage not to be intrusive and to be able to discriminate between forward and reverse velocities. Experimental investigations which show that the particle passage through the laser beams shortly before the point of superposition yields a distorted LDA fringe pattern are summarized. The period length of an individual LDA burst-passing the center of the measuring volume at the same time varies according to the distortion of the fringe spacing. ESA

## 37 MECHANICAL ENGINEERING

Includes auxiliary systems (nonpower); machine elements and processes; and mechanical equipment.

**N91-10287** Pennsylvania Univ., Philadelphia.
**REDUNDANCY CONTROL OF A ROBOT MANIPULATOR USING A SYSTOLIC ARRAY PROCESSOR Ph.D. Thesis**
Yehong Zhang 1989 140 p
Avail: Univ. Microfilms Order No. DA9015189

An approach is provided to the solution of a number of key problems in robotics, namely planning, force and motion control of a highly redundant manipulator system by means of a special computer architecture. Robotic control is a computationally intensive task. The real time requirement makes many control formulations impractical. In particular, planning and redundancy control require so much computation that they are performed off-line. Planning algorithms are global in nature and are carried out before motion starts. Redundancy control involves the computation of a pseudoinverse of a 6 x n matrix which is computationally expensive and thus real time control is very difficult. The motion and force control of a highly redundant robotic system is studied. A local, time optimal planning algorithm is formulated to provide the robot with a time optimal trajectory. A hybrid motion/force control method for a highly redundant system using joint space partition and compensation is also presented. At the same time, a special purpose Systolic Array Processor is studied and its applications in robotics are explored. Because of the matrix nature of control formulations, a matrix engine based on the systolic computational structure greatly enhances the computational power of the robot controller making real time planning and control possible. Dissert. Abstr.

**N91-10288#** Caterpillar Tractor Co., Peoria, IL.
**HEAVY DUTY LIQUID AND GASEOUS FUEL EMISSIONS DATABASE TEST RESULTS FROM FOUR ALTERNATIVE FUEL CONFIGURATIONS OF THE CATERPILLAR 3406 ENGINE**
D. J. Waldman Jun. 1990 68 p Prepared for ORNL, TN
(Contract DE-AC05-84OR-21400)
(DE90-014783; ORNL/Sub-86-SB195/1) Avail: NTIS HC/MF A04

Through the cooperation of several organizations including the Oak Ridge National Laboratory (ORNL) acting under the auspices of the DOE Alternative Fuels Utilization Program, heavy duty transient and steady-state emissions tests were conducted on four alternative fuel configurations of the Caterpillar 3406 engine. These included a diesel baseline, glow plug ignited methanol (diesel cycle), lean-burn spark ignited natural gas, and dual fuel (diesel pilot ignited natural gas). Results indicated methanol and natural gas both show excellent potential for low NOx and low particulate emissions. With these fuels however, unburned fuel emissions were much higher, especially in the dual fuel case, than the diesel baseline. Particulate emissions from the methanol and lean burn gas engines are thought to be almost entirely lube oil sourced. All of the configurations will require significant reduction in hydrocarbon and/or particulate emissions in order to meet the 1994 EPA emissions standards for heavy duty truck engines. DOE

**N91-10289#** Oak Ridge National Lab., TN. Fusion Energy Div.
**MODELING OF HYDROCARBON FUELING**
J. T. Hogan and A. Pospieszczyk (Kernforschungsanlage, Juelich, Germany, F.R.) Jul. 1990 18 p Presented at the 7th American

Physical Society Topical Conference on Atomic Processes in Plasmas, Gaithersburg, MD, 2 Oct. 1990
(Contract DE-AC05-84OR-21400)
(DE90-014790; ORNL/TM-11542; CONF-901099-1) Avail: NTIS HC/MF A03

A database of rate coefficients for CH4 was compared with experiments on PISCES-A to understand the role of carbon-based impurities in determining the fueling profile of carbon-dominated machines. A three-dimensional Monte Carlo model that embodies the Ehrhardt-Langer CH4 breakup scheme has been developed. The model was compared with spectroscopic observations of the spatial variation of the hydrocarbon product decay rates, and reasonable agreement was found. The comparison is sensitive to the non-Maxwellian electron distribution and to observed spatial inhomogeneities in the electron density and temperature profiles. Applications of the model to parameters characteristic of the tokamak scrape-off layer are presented. DOE

**N91-10290#** Universiteit Twente, Enschede (Netherlands). Dept. of Applied Mathematics.
**ELASTOHYDRODYNAMIC LUBRICATION: A DYNAMIC VARIATION METHOD Ph.D. Thesis**
Roeland Wilhemus Car Verstappen 1989 194 p
(ISBN-90-9003079-4; ETN-90-97776) Avail: NTIS HC/MF A09

Applications of the method of variations in elastohydrodynamic lubrication theory to describe the fully lubricated line contact between a rotating, deformable cylinder and a rigid surface as well as to obtain efficient numerical methods are presented. The equations for the deformation of the elastic material and for the flow of the viscous fluid are assumed to be determined by an elastic energy and a power functional. It is shown that a variational formulation of an elastic-fluid contact can be given. The expressions that result when elastohydrodynamically lubricated line contact is considered, are simplified. The performance of the proposed dynamic algorithm is improved by utilizing both continuation and preconditionning techniques. ESA

**N91-10291#** Institut National Polytechnique, Grenoble (France). Lab. d'Informatique Fondamentale et d'Intelligence Artificielle.
**PLANNING OF THE PATHS FOR MANIPULATION ROBOTS Ph.D. Thesis [PLANIFICATION DE TRAJECTOIRES POUR UN ROBOT MANIPULATEUR]**
Michel Pasquier 1989 209 p In FRENCH; ENGLISH summary Sponsored by ADI; Direction des Recherches Etudes et Techniques; and ADR
(ETN-90-97826) Avail: NTIS HC/MF A10

The problem of planning collision free paths for manipulator robots is discussed. The robotic context of the work and the general system for automatic robot programming are presented. The needs in geometric modeling for the reasoning techniques particular to the motion planning problem, and the representations implemented are reported. A path planning system for a robot arm is presented. A global method, aimed at planning a trajectory in a completely mapped configuration space is included. A hybrid method which realizes a synthesis of these complementary approaches, giving algorithms, experimental results and improvements is described. ESA

**N91-10292#** Oxford Univ. (England). Robotics Research Group.
**PROTECTIVE AUTONOMY: EMBEDDING SENSOR-BASED SAFETY AND PROTECTION MECHANISMS INTO THE MOTION CONTROL OF MOBILE AND TELE-OPERATED ROBOTS**
Barry Steer 17 Dec. 1988 25 p Sponsored by Royal Armament Research and Development Establishment, Chetsey, England
(OUEL-1808/90; ETN-90-97917) Avail: NTIS HC/MF A03

The flow of information and the implementation of processes that aim to provide a mobile robot with the autonomous sensor-based competence to protect itself and its local environment while being directed to move by some other agent are examined. To endow the robot with protective autonomy it is proposed that local observations of the relative range to objects (using active sensors) coupled with an implementation of spatio-temporal filters designed to obtain relative velocity estimates, can be used to form the ratio range/range-rate. This ratio, the time-to-arrival, can be used to guide the robot tactically relative to its local environment. In the simplest case of straight ahead motion, the simple law output = gain constant/time-to-arrival may be used to back-off the main control signal into the drive systems of a mobile or tele-operated robot. ESA

# 38 QUALITY ASSURANCE AND RELIABILITY

Includes product sampling procedures and techniques; and quality control.

**N91-10293*#** Washington Univ., Saint Louis, MO. Lab. for Ultrasonics.
**PHYSICAL INTERPRETATION AND APPLICATION OF PRINCIPLES OF ULTRASONIC NONDESTRUCTIVE EVALUATION OF HIGH-PERFORMANCE MATERIALS**
**Semiannual Progress Report, 15 Mar. - 14 Sep. 1990**
James G. Miller 1990 33 p
(Grant NsG-1601)
(NASA-CR-180489; NAS 1.26:180489) Avail: NTIS HC/MF A03 CSCL 14D

An ultrasonic measurement system employed in the experimental interrogation of the anisotropic properties (through the measurement of the elastic stiffness constants) of the uniaxial graphite-epoxy composites is presented. The continuing effort for the development of improved visualization techniques for physical parameters is discussed. The background is set for the understanding and visualization of the relationship between the phase and energy/group velocity for propagation in high-performance anisotropic materials by investigating the general requirements imposed by the classical wave equation. The consequences are considered when the physical parameters of the anisotropic material are inserted into the classical wave equation by a linear elastic model. The relationship is described between the phase velocity and the energy/group velocity three dimensional surfaces through graphical techniques. Author

**N91-10294*#** National Aeronautics and Space Administration. Marshall Space Flight Center, Huntsville, AL.
**EDDY CURRENT INSPECTION OF GRAPHITE FIBER COMPONENTS**
G. L. Workman (Alabama Univ., Huntsville.) and C. C. Bryson Oct. 1990 52 p
(NASA-TM-103514; NAS 1.15:103514) Avail: NTIS HC/MF A04 CSCL 09D

The recognition of defects in materials properties still presents a number of problems for nondestructive testing in aerospace systems. This project attempts to utilize current capabilities in eddy current instrumentation, artificial intelligence, and robotics in order to provide insight into defining geometrical aspects of flaws in composite materials which are capable of being evaluated using eddy current inspection techniques. The unique capabilities of E-probes and horseshoe probes for inspecting probes for inspecting graphite fiber materials were evaluated and appear to hold great promise once the technology development matures. The initial results are described of modeling eddy current interactions with certain flaws in graphite fiber samples. Author

**N91-10295#** Pacific Northwest Lab., Richland, WA.
**A REPRESENTATION SCHEME FOR FAULT DIAGNOSIS OF PHYSICAL SYSTEMS**
Rex C. Stratton Jun. 1990 6 p Presented at the Advances in Human Factors Research on Man-computer Interactions: Nuclear and Beyond, Nashville, TN, 10-15 Jun. 1990
(Contract DE-AC06-76RL-01830)
(DE90-016362; PNL-SA-17302; CONF-900607-6) Avail: NTIS HC/MF A02

For the most part operators of simple machines do so in a run-till-breakdown mode. But, because of safety and and economic concerns, society cannot afford to operate complex machines in this run-till-breakdown mode. An alternate to operating in this mode is the predictive-corrective mode. A principal element in the predictive-corrective mode is the determination of system behavior and the analysis of the implications of that behavior. A representation scheme used to model and execute knowledge for reasoning about fault behavior in physical systems is discussed. The representation scheme consists of a function hierarchy of the physical system, object hierarchies of components found in physical systems, a generalized inference methodology for determining component and system performance, and a task control scheme that allows concurrent and integrated reasoning during fault diagnosis. DOE

**N91-10296#** Westinghouse Hanford Co., Richland, WA. Analytical Systems Labs.
**STRUCTURAL INTEGRITY ASSESSMENT OF CONCRETE SLABS BY NONDESTRUCTIVE EXAMINATION AND FOURIER TRANSFORM-INFRARED METHODS**
T. V. Rebagay and D. A. Dodd Jul. 1990 7 p Presented at the Rocky Mountain Conference on Analytical Chemistry, Denver, CO, 28 Jul. - 2 Aug. 1990
(Contract DE-AC06-87RL-10930)
(DE90-017233; WHC-SA-0872; CONF-9007109-2) Avail: NTIS HC/MF A02

A nitric acid spill occurred in a chemical preparation room causing reaction of the concrete floor with the acid. To assess the structural integrity of the reacted concrete and to define the extent of needed repairs, a nondestructive evaluation (NDE) using pulse echo method and a Fourier transform infrared (FT-IR) spectrometric method was employed. DOE

**N91-10297#** Rolls-Royce Ltd., Derby (England).
**INTRODUCTION: NEEDS AND APPROACHES TO RELIABILITY AND QUALITY ASSURANCE IN DESIGN AND MANUFACTURE**
A. C. Pickard 6 Oct. 1989 8 p Presented at AGARD Damage Tolerance Concept Review Conference, Brussels, Belgium, 1-6 Oct. 1989
(PNR-90683; ETN-90-97930) Copyright Avail: NTIS HC/MF A02

In the damage tolerance approach, for improving the integrity of aero engines, reliability, and quality assurance issues are discussed. The implications of the following aspects on the damage tolerance concept are investigated: component material specifications and standards, controls on manufacturing processes, design systems and quality assurance. The subjects reviewed in the workshop on reliability and quality assurance are given. ESA

**N91-10298#** Rolls-Royce Ltd., Derby (England).
**TOTAL QUALITY MANAGEMENT AT ROLLS-ROYCE PLC**
R. H. Wedge 15 Sep. 1990 10 p Submitted for publication
(PNR-90759; ETN-90-97961) Copyright Avail: NTIS HC/MF A02

The Rolls-Royce concept concerning quality and quality management is reviewed. The work is focused on the business associated with aircraft gas turbine manufacture. The reasons for the adoption of quality assurance methods and the company's targets are justified. The distribution of responsibilities and tasks in the quality assurance chain is explained. Resulting from the management plans, more effort is accorded to elimination and prevention, so that less time is spent on detection and correction. ESA

# 39 STRUCTURAL MECHANICS

Includes structural element design and weight analysis; fatigue; and thermal stress.

For applications see *05 Aircraft Design, Testing and Performance* and *18 Spacecraft Design, Testing and Performance.*

**N91-10299** National Aerospace Lab., Tokyo (Japan).
**AXIAL COMPRESSION BUCKLING TEST ON CFRP SURFACE PLATE/ALUMINUM HONEYCOMB SANDWICHED CURVED SURFACE PLATE [SHI EFU ARU PI MENBAN/ARUMI HANIKAMU SANDOICCHI KYOKUMENBAN NO JIKUASSHUKU ZAKUTSU SIKEN]**
Shuji Endo, Yoshio Noguchi, Kunihiko Otake, Koichi Ono, and Yukio Fukushima Mar. 1988 40 p In JAPANESE
(NAL-TM-584; ISSN-0452-2982; JTN-90-80012) Avail: NTIS HC/MF A03

The National Aerospace Laboratory (NASDA) is considering adopting the sandwich structure to make an aluminum surface plate and an aluminum honeycomb core which was adopted as the standard fairing of the H-2 Launch Vehicle and satellite fairing. Buckling strength is an essential structure design requirement, because the satellite fairing is a large-scale shell structure. There have been, however, very few sandwich structure-type buckling tests performed to date, which leaves little test data as a reference. Tests on buckling by axial compression of the surface plates made of three kinds of carbon fiber reinforced plastics (CFRP), which were laminated in 60/0/-60 degrees, plain fabrics 0/90/-4, and plain fabrics + or - 45 deg, respectively and a surface plate of sandwich structure comprising 2.3-1/4-5056-.001 density (pcf) - cell size (in.) - material quality - foil thickness (in.) - aluminum honey comb core of the same specifications as the CFRP. The plain fabrics + or - 45 degree sample fell apart at the center as a result of the total buckling. Other samples cracked by wrinkling under low levels of stress which was produced by local bending in the upper or lower corner areas near the plastic reinforced edges. NASDA

**N91-10300#** Ballistic Research Labs., Aberdeen Proving Ground, MD.
**A SIMPLE SCREW THREAD MODEL FOR USE IN FINITE ELEMENT STRESS ANALYSIS Technical Report, Sep.-Dec. 1988**
J. M. Bender Jul. 1989 12 p
(DA Proj. 1L6-62618-AH-80)
(AD-A210233; BRL-MR-3773) Avail: NTIS HC/MF A03 CSCL 13/8

A technique for modeling screw threads, such as those found on artillery projectiles, was developed. The model employs a matrix of gap elements which are easier to use and require less computation time than the current method of modelling actual threads with material elements. A comparison of this new method to the current method illustrates that there is no tradeoff of accuracy. Author

**N91-10301*#** National Aeronautics and Space Administration. Langley Research Center, Hampton, VA.
**RESEARCH IN STRUCTURES, STRUCTURAL DYNAMICS AND MATERIALS, 1990**
Jean-Francois M. Barthelemy, comp. and Ahmed K. Noor, comp. (George Washington Univ., Hampton, VA.) Washington Mar. 1990 283 p The 31st conference was held in Long Beach, CA, 2-4 Apr. 1990; sponsored by AIAA, ASME, ASCE, AHS, and ASC
(NASA-CP-3064; L-16735; NAS 1.55:3064) Avail: NTIS HC/MF A13 CSCL 20K

The Structural Dynamics and Materials (SDM) Conference was held on April 2 to 4, 1990 in Long Beach, California. This publication is a compilation of presentations of the work-in-progress sessions and does not contain papers from the regular sessions since those papers are published by AIAA in the conference proceedings. For individual titles, see N91-10302 through N91-10322.

**N91-10302*#** Rohr Industries, Inc., San Diego, CA.

**TEST/SEMI-EMPIRICAL ANALYSIS OF A CARBON/EPOXY FABRIC STIFFENED PANEL**

E. E. Spier and J. A. Anderson *In* NASA, Langley Research Center, Research in Structures, Structural Dynamics, and Materials, 1990 Mar. 1990 p 3-35 (For primary document see N91-10301 01-39)

Avail: NTIS HC/MF A13 CSCL 20K

The purpose of this work-in-progress is to present a semi-empirical analysis method developed to predict the buckling and crippling loads of carbon/epoxy fabric blade stiffened panels in compression. This is a hand analysis method comprised of well known, accepted techniques, logical engineering judgements, and experimental data that results in conservative solutions. In order to verify this method, a stiffened panel was fabricated and tested. Both the best and analysis results are presented. Author

**N91-10303*#** Technion - Israel Inst. of Tech., Haifa. Faculty of Aerospace Engineering.

**REPEATED BUCKLING OF COMPOSITE SHEAR PANELS**

Josef Singer and Tanchum Weller *In* NASA, Langley Research Center, Research in Structures, Structural Dynamics and Materials, 1990 Mar. 1990 p 37-42 (For primary document see N91-10301 01-39)

Avail: NTIS HC/MF A13 CSCL 20K

Failures in service of aerospace structures and research at the Technion Aircraft Structures Laboratory have revealed that repeatedly buckled stiffened shear panels might be susceptible to premature fatigue failures. Extensive experimental and analytical studies have been performed at Technion on repeated buckling, far in excess of initial buckling, for both metal and composite shear panels with focus on the influence of the surrounding structure. The core of the experimental investigation consisted of repeated buckling and postbuckling tests on Wagner beams in a three-point loading system under realistic test conditions. The effects of varying sizes of stiffeners, of the magnitude of initial buckling loads, of the panel aspect ratio and of the cyclic shearing force, V sub cyc, were studied. The cyclic to critical shear buckling ratios, (V sub cyc/V sub cr) were on the high side, as needed for efficient panel design, yet all within possible flight envelopes. The experiments were supplemented by analytical and numerical analyses. For the metal shear panels the test and numerical results were synthesized into prediction formulas, which relate the life of the metal shear panels to two cyclic load parameters. The composite shear panels studied were hybrid beams with graphite/epoxy webs bonded to aluminum alloy frames. The test results demonstrated that composite panels were less fatigue sensitive than comparable metal ones, and that repeated buckling, even when causing extensive damage, did not reduce the residual strength by more than 20 percent. All the composite panels sustained the specified fatigue life of 250,000 cycles. The effect of local unstiffened holes on the durability of repeatedly buckled shear panels was studied for one series of the metal panels. Tests on 2024 T3 aluminum panels with relatively small unstiffened holes in the center of the panels demonstrated premature fatigue failure, compared to panels without holes. Preliminary tests on two graphite epoxy shear panels with small holes in the center showed no similar fatigue life degradation and no shift in failure mode. Further tests on the effect of holes are in progress. Author

**N91-10304*#** Illinois Univ. at Urbana-Champaign, Savoy. National Center for Composite Materials Research.

**COMPRESSIVE FAILURE OF THICK-SECTION COMPOSITE LAMINATES WITH AND WITHOUT CUTOUTS SUBJECTED TO BIAXIAL LOADING**

L. Rouxel and S. S. Wang *In* NASA, Langley Research Center, Research in Structures, Structural Dynamics and Materials, 1990 Mar. 1990 p 43-54 (For primary document see N91-10301 01-39)

Avail: NTIS HC/MF A13 CSCL 20K

The composites studied are fiber composite laminate plates made of carbon fibers and a thermoplastic matrix material. Tests and results are given for: the solution convergence for transverse shear in a clamped plate without cutout under compression; the effects of cutout and laminate thickness on maximum shear in buckling and postbuckling response of a clamped plate under biaxial compression; the effects of cutout and laminate thickness on maximum shear in buckling and postbuckling response of a clamped plate under biaxial compression; and the effects of laminate thickness and cutout of the lowest three eigenvalues of a clamped plate under biaxial compression. Additional test results are given. Author

**N91-10305*#** Texas A&M Univ., College Station. Dept. of Aerospace Engineering.

**AN ANALYTICAL SOLUTION FOR THE ELASTOPLASTIC RESPONSE OF A CONTINUOUS FIBER COMPOSITE UNDER UNIAXIAL LOADING**

Jong-Won Lee and David H. Allen *In* NASA, Langley Research Center, Research in Structures, Structural Dynamics and Materials, 1990 Mar. 1990 p 55-66 (For primary document see N91-10301 01-39)

Avail: NTIS HC/MF A13 CSCL 20K

A continuous fiber composite is modelled by a two-element composite cylinder in order to predict the elastoplastic response of the composite under a monotonically increasing tensile loading parallel to fibers. The fibers and matrix are assumed to be elastic-perfectly plastic materials obeying Hill's and Tresca's yield criteria, respectively. Here, the composite behavior when the fibers yield prior to the matrix is investigated. Author

**N91-10306*#** Rutgers - The State Univ., Piscataway, NJ. Dept. of Mechanics and Materials Science.

**THE LOOPED ADHESIVE STRIP: AN EXAMPLE OF COPLANAR DELAMINATION INTERACTION**

W. J. Bottega *In* NASA, Langley Research Center, Research in Structures, Structural Dynamics and Materials, 1990 Mar. 1990 p 67-83 (For primary document see N91-10301 01-39)

Avail: NTIS HC/MF A13 CSCL 20K

The phenomenon of peeling and debonding of thin layers is a subject of interest to those concerned with adhesives, thin films, and layered materials. In recent years much attention has been focused on such problems as a result of increased interest and application of advanced composites and thin film coatings. A related problem which is of interest for its own sake but also represents a simple example of a tangled adhesive strip and of coplanar delamination interaction, is the problem of a looped adhesive strip. This is the subject of the present study. Researchers consider here the problem of an elastic strip which possesses an adherend on (at least) one of its surfaces. If the strip is deformed so that two portions of such a surface are brought into contact, a position of the strip becomes bonded and a loop is formed. Researchers are interested in determining the equilibrium configuration of such a strip and investigating the behavior of the strip when its edges are pulled apart. The problem is approached as a moving interior boundary problem in the calculus of variations with the strip modeled as an inextensible elastica and the bond strength characterized by its surface energy. A Griffith type energy criterion is employed for debonding, and solutions corresponding to the problem of interest obtained. The solution obtained will be seen to predict the interesting phenomenon of bond point propagation, as well as the more standard peeling type behavior. Numerical results demonstrating the phenomena of interest are presented as well and will be seen to reveal both stable and unstable propagation of the boundaries of the bonded portion of the strip, depending upon the loading conditions. Author

**N91-10307*#** California Univ., San Diego, La Jolla.

**A NEW BEAM THEORY USING FIRST-ORDER WARPING FUNCTIONS**

C. A. Ie and J. B. Kosmatka *In* NASA, Langley Research Center, Research in Structures, Structural Dynamics and Materials, 1990 Mar. 1990 p 85-102 (For primary document see N91-10301 01-39)

Avail: NTIS HC/MF A13 CSCL 20K

Due to a certain type of loading and geometrical boundary conditions, each beam will respond differently depending on its geometrical form of the cross section and its material definition. As an example, consider an isotropic rectangular beam under pure bending. Plane sections perpendicular to the longitudinal axis of the beam will remain plane and perpendicular to the deformed axis after deformation. However, due to the Poisson effect, particles in the planes will move relative to each other resulting in a form of anticlastic deformation. In other words, even in pure bending of an isotropic beam, each cross section will deform in the plane. If the material of the beam above is replaced by a generally anisotropic material, then the cross sections will not only deform in the plane, but also out of plane. Hence, in general, both in-plane deformation and out-of-plane warping will exist and depend on the geometrical form and material definition of the cross sections and also on the loadings. For the purpose of explanation, an analogy is made. The geometrical forms of the bodies of each individual are unique. Hence, different sizes of clothes are needed. Finding the sizes of clothes for individuals is like determining the warping functions in beams. A new beam theory using first-order warping functions is introduced. Numerical examples will be presented for an isotropic beam with rectangular cross section. The theory can be extended for composite beams. Author

**N91-10308*#** EQE Engineering, Inc., Costa Mesa, CA.
**PROBABILISTIC STRUCTURAL ANALYSIS BY EXTREMUM METHODS**
Avinash M. Nafday *In* NASA, Langley Research Center, Research in Structures, Structural Dynamics, and Materials, 1990 Mar. 1990 p 103-113 (For primary document see N91-10301 01-39)
Avail: NTIS HC/MF A13 CSCL 20K

The objective is to demonstrate discrete extremum methods of structural analysis as a tool for structural system reliability evaluation. Specifically, linear and multiobjective linear programming models for analysis of rigid plastic frames under proportional and multiparametric loadings, respectively, are considered. Kinematic and static approaches for analysis form a primal-dual pair in each of these models and have a polyhedral format. Duality relations link extreme points and hyperplanes of these polyhedra and lead naturally to dual methods for system reliability evaluation. Author

**N91-10309*#** Jet Propulsion Lab., California Inst. of Tech., Pasadena.
**PROBABILISTIC FAILURE ASSESSMENT WITH APPLICATION TO SOLID ROCKET MOTORS**
Darrell L. Jan, Barry D. Davidson, and Nicholas R. Moore *In* NASA, Langley Research Center, Research in Structures, Structural Dynamics and Materials, 1990 Mar. 1990 p 115-121 Sponsored in part by Air Force Astronautics Lab., Edwards AFB, CA (For primary document see N91-10301 01-39)
Avail: NTIS HC/MF A13 CSCL 20K

A quantitative methodology is being developed for assessment of risk of failure of solid rocket motors. This probabilistic methodology employs best available engineering models and available information in a stochastic framework. The framework accounts for incomplete knowledge of governing parameters, intrinsic variability, and failure model specification error. Earlier case studies have been conducted on several failure modes of the Space Shuttle Main Engine. Work in progress on application of this probabilistic approach to large solid rocket boosters such as the Advanced Solid Rocket Motor for the Space Shuttle is described. Failure due to debonding has been selected as the first case study for large solid rocket motors (SRMs) since it accounts for a significant number of historical SRM failures. Impact of incomplete knowledge of governing parameters and failure model specification errors is expected to be important. Author

**N91-10310*#** Iowa Univ., Iowa City. Optimal Design Lab.
**GLOBAL OPTIMIZATION METHODS FOR ENGINEERING DESIGN**
Jasbir S. Arora *In* NASA, Langley Research Center, Research in Structures, Structural Dynamics and Materials, 1990 Mar. 1990 p 123-135 (For primary document see N91-10301 01-39)
Avail: NTIS HC/MF A13 CSCL 20K

The problem is to find a global minimum for the Problem P. Necessary and sufficient conditions are available for local optimality. However, global solution can be assured only under the assumption of convexity of the problem. If the constraint set S is compact and the cost function is continuous on it, existence of a global minimum is guaranteed. However, in view of the fact that no global optimality conditions are available, a global solution can be found only by an exhaustive search to satisfy Inequality. The exhaustive search can be organized in such a way that the entire design space need not be searched for the solution. This way the computational burden is reduced somewhat. It is concluded that zooming algorithm for global optimizations appears to be a good alternative to stochastic methods. More testing is needed; a general, robust, and efficient local minimizer is required. IDESIGN was used in all numerical calculations which is based on a sequential quadratic programming algorithm, and since feasible set keeps on shrinking, a good algorithm to find an initial feasible point is required. Such algorithms need to be developed and evaluated. Author

**N91-10311*#** Pennsylvania State Univ., University Park. Dept. of Mechanical Engineering.
**EXPONENTIAL APPROXIMATIONS IN OPTIMAL DESIGN**
A. D. Belegundu, S. D. Rajan, and J. Rajgopal (Pittsburgh Univ., PA.) *In* NASA, Langley Research Center, Research in Structures, Structural Dynamics and Materials, 1990 Mar. 1990 p 137-150 (For primary document see N91-10301 01-39)
Avail: NTIS HC/MF A13 CSCL 20K

One-point and two-point exponential functions have been developed and proved to be very effective approximations of structural response. The exponential has been compared to the linear, reciprocal and quadratic fit methods. Four test problems in structural analysis have been selected. The use of such approximations is attractive in structural optimization to reduce the numbers of exact analyses which involve computationally expensive finite element analysis. Author

**N91-10312*#** California Univ., Los Angeles.
**CONSERVATIVE BUFFERING OF APPROXIMATE NONLINEAR CONSTRAINTS**
H. L. Thomas and L. A. Schmit *In* NASA, Langley Research Center, Research in Structures, Structural Dynamics and Materials, 1990 Mar. 1990 p 151-158 (For primary document see N91-10301 01-39)
(Grant NsG-1490)
Avail: NTIS HC/MF A13 CSCL 20K

In engineering design practice behavior is usually predicted based on some known nominal design. However, when the design is fabricated it will differ from the nominal design because of manufacturing tolerances. In order to generate nominal designs that will still satisfy behavior constraints in the presence of manufacturing tolerances, engineers resort to the use of safety factors, over and above those introduced to account for other uncertainties (e.g., in load conditions, material properties, analysis modeling). The accurate selection of the values of these manufacturing tolerances safety factors is dependent on the capability of the engineer to determine the sensitivity of the critical constraints to changes in the design variables. This process usually leads to overly conservative designs. The task of choosing safety factors is much more difficult in structural synthesis because: (1) it is not known which constraints will be active at the final design, (2) as the design changes during the synthesis process the sensitivities of the constraints with respect to the design variables also change, and (3) the imposition of the safety factors themselves may change the set of critical constraints. These difficulties can be overcome with the approximation concepts approach to structural synthesis by buffering the approximate constraints with quantities that are related to the design variable tolerances and the accurate sensitivities of the constraints with respect to the design variable. Designs generated by this approach tend to be feasible but not overly conservative. Author

**N91-10313*#** Technion - Israel Inst. of Engineering, Haifa. Faculty of Aerospace Engineering.

### EVALUATION OF ALTERNATIVES FOR BEST-FIT PARABOLOID FOR DEFORMED ANTENNA SURFACES

Menahem Baruch and Raphael T. Haftka (Virginia Polytechnic Inst. and State Univ., Blacksburg.) *In* NASA, Langley Research Center, Research in Structures, Structural Dynamics and Materials, 1990 Mar. 1990 p 159-176 (For primary document see N91-10301 01-39)
(Grant NAG1-224)
Avail: NTIS HC/MF A13 CSCL 20K

Paraboloid antenna surfaces suffer performance degradation due to structural deformation. A first step in the prediction of the performance degradation is to find the best-fit paraboloid to the deformed surface. Examined here is the question of whether rigid body translations perpendicular to the axis of the paraboloid should be included in the search for the best-fit paraboloid. It is shown that if these translations are included the problem is ill-conditioned, and small structural deformation can result in large translations of the best-fit paraboloid with respect to the original surface. The magnitude of these translations then requires nonlinear analysis for finding the best-fit paraboloid. On the other hand, if these translations are excluded, or if they are limited in magnitude, the errors with respect to the restricted not-so-best-fit paraboloid can be much greater than the errors with respect to the true best-fit paraboloid. Author

**N91-10314*#** Michigan Univ., Ann Arbor. Dept. of Aerospace Engineering.

### COMBINED DESIGN OF STRUCTURES AND CONTROLLERS FOR OPTIMAL MANEUVERABILITY

Jer Ling, Pierre Kabamba, and John Taylor *In* NASA, Langley Research Center, Research in Structures, Structural Dynamics and Materials, 1990 Mar. 1990 p 179-192 (For primary document see N91-10301 01-39)
Avail: NTIS HC/MF A13 CSCL 20K

Approaches to the combined design of structures and controllers for achieving optimal maneuverability are presented. A maneuverability index which directly reflects the minimum time required to perform a given set of maneuvers is introduced. By designing the flexible appendages, the maneuver time of the spacecraft is minimized under the constraints of structural properties, and post maneuver spillover is kept within a specified bound. The spillover reduction is achieved by making use of an appropriate reduced order model. The distributed parameter design problem is approached using assumed shape functions, and finite element analysis with dynamic reduction. Solution procedures have been investigated. Approximate design methods have been developed to overcome the computational difficulties. Some new constraints on the modal frequencies of the spacecraft are introduced in the original optimization problem to facilitate the solution process. It is shown that the global optimal design may be obtained by tuning the natural frequencies to satisfy specific constraints. Researchers quantify the difference between a lower bound to the solution for maneuver time associated with the original problem and the estimate obtained from the modified problem, for a specified application requirement. Numerical examples are presented to demonstrate the capability of this approach. Author

**N91-10315*#** General Dynamics Corp., San Diego, CA. Space Systems Div.

### GROUND TEST PROGRAM FOR NEW ATLAS PAYLOAD FAIRINGS

Michael J. Robbins *In* NASA, Langley Research Center, Research in Structures, Structural Dynamics and Materials, 1990 Mar. 1990 p 193-205 (For primary document see N91-10301 01-39)
Avail: NTIS HC/MF A13 CSCL 20K

To establish the competitiveness of the revitalized family of Atlas launch vehicles (I, II, IIA, and IIAS) a new series of payload fairings, an 11-foot and a 14-foot diameter version, were designed to accommodate the widest possible variety of satellites. Because these aluminum fairings are new designs, the plant at which they are produced is new, and launch customers are very anxious to fly their payloads, an ambitious and efficient test program is essential. Five major tests have been planned for completion within the span of one calendar year. One of these has been completed, with every indication that it was a success, one is currently under way, and two more are scheduled to start in the month of April. Through effective use of test assets, facilities, and personnel, all testing will be completed, allowing the fairing design to be completely characterized and then qualified through analysis prior to first launch of each of the fairings. Author

**N91-10316*#** National Aeronautics and Space Administration. Langley Research Center, Hampton, VA.

### DIRECT USE OF LINEAR TIME-DOMAIN AERODYNAMICS IN AEROSERVOELASTIC ANALYSIS: AERODYNAMIC MODEL

J. A. Woods and Michael G. Gilbert *In its* Research in Structures, Structural Dynamics and Materials, 1990 Mar. 1990 p 207-220 (For primary document see N91-10301 01-39)
Avail: NTIS HC/MF A13 CSCL 20K

The work presented here is the first part of a continuing effort to expand existing capabilities in aeroelasticity by developing the methodology which is necessary to utilize unsteady time-domain aerodynamics directly in aeroservoelastic design and analysis. The ultimate objective is to define a fully integrated state-space model of an aeroelastic vehicle's aerodynamics, structure and controls which may be used to efficiently determine the vehicle's aeroservoelastic stability. Here, the current status of developing a state-space model for linear or near-linear time-domain indicial aerodynamic forces is presented. Author

**N91-10317*#** National Aeronautics and Space Administration. Langley Research Center, Hampton, VA.

### COMPUTATION OF MAXIMUM GUST LOADS IN NONLINEAR AIRCRAFT USING A NEW METHOD BASED ON THE MATCHED FILTER APPROACH AND NUMERICAL OPTIMIZATION

Anthony S. Pototzky (Lockheed Engineering and Sciences Co., Hampton, VA.), Jennifer Heeg, and Boyd Perry, III *In its* Research in Structures, Structural Dynamics and Materials, 1990 Mar. 1990 p 221-229 (For primary document see N91-10301 01-39)
Avail: NTIS HC/MF A13 CSCL 20K

Time-correlated gust loads are time histories of two or more load quantities due to the same disturbance time history. Time correlation provides knowledge of the value (magnitude and sign) of one load when another is maximum. At least two analysis methods have been identified that are capable of computing maximized time-correlated gust loads for linear aircraft. Both methods solve for the unit-energy gust profile (gust velocity as a function of time) that produces the maximum load at a given location on a linear airplane. Time-correlated gust loads are obtained by re-applying this gust profile to the airplane and computing multiple simultaneous load responses. Such time histories are physically realizable and may be applied to aircraft structures. Within the past several years there has been much interest in obtaining a practical analysis method which is capable of solving the analogous problem for nonlinear aircraft. Such an analysis method has been the focus of an international committee of gust loads specialists formed by the U.S. Federal Aviation Administration and was the topic of a panel discussion at the Gust and Buffet Loads session at the 1989 SDM Conference in Mobile, Alabama. The kinds of nonlinearities common on modern transport aircraft are indicated. The Statical Discrete Gust method is capable of being, but so far has not been, applied to nonlinear aircraft. To make the method practical for nonlinear applications, a search procedure is essential. Another method is based on Matched Filter Theory and, in its current form, is applicable to linear systems only. The purpose here is to present the status of an attempt to extend the matched filter approach to nonlinear systems. The extension uses Matched Filter Theory as a starting point and then employs a constrained optimization algorithm to attack the nonlinear problem. Author

**N91-10318*#** Aerostructures, Inc., Arlington, VA.

**PIEZOELECTRICALLY FORCED VIBRATIONS OF ELECTRODED DOUBLY ROTATED QUARTZ PLATES BY STATE SPACE METHOD**

R. Chander *In* NASA, Langley Research Center, Research in Structures, Structural Dynamics and Materials, 1990 Mar. 1990 p 231-238 (For primary document see N91-10301 01-39)
Avail: NTIS HC/MF A13 CSCL 20K

The purpose of this investigation is to develop an analytical method to study the vibration characteristics of piezoelectrically forced quartz plates. The procedure can be summarized as follows. The three dimensional governing equations of piezoelectricity, the constitutive equations and the strain-displacement relationships are used in deriving the final equations. For this purpose, a state vector consisting of stresses and displacements are chosen and the above equations are manipulated to obtain the projection of the derivative of the state vector with respect to the thickness coordinate on to the state vector itself. The solution to the state vector at any plane is then easily obtained in a closed form in terms of the state vector quantities at a reference plane. To simplify the analysis, simple thickness mode and plane strain approximations are used. Author

**N91-10319*#** Jet Propulsion Lab., California Inst. of Tech., Pasadena.

**ANALYSIS OF ELASTICALLY TAILORED VISCOELASTIC DAMPING MEMBER**

G.-S. Chen and B. P. Dolgin *In* NASA, Langley Research Center, Research in Structures, Structural Dynamics and Materials, 1990 Mar. 1990 p 239-247 (For primary document see N91-10301 01-39)
Avail: NTIS HC/MF A13 CSCL 20K

For more than two decades, viscoelastic materials have been commonly used as a passive damping source in a variety of structures because of their high material loss factors. In most of the applications, viscoelastic materials are used either in series with or parallel to the structural load path. The latter is also known as the constrained-layer damping treatment. The advantage of the constrained-layer damping treatment is that it can be incorporated without loss in structural integrity, namely, stiffness and strength. However, the disadvantages are that: (1) it is not the most effective use of the viscoelastic material when compared with the series-type application, and (2) weight penalty from the stiff constraining layer requirement can be excessive. To overcome the disadvantages of the constrained-layer damping treatment, a new approach for using viscoelastic material in axial-type structural components, e.g., truss members, was studied in this investigation. Author

**N91-10320*#** National Aeronautics and Space Administration. Langley Research Center, Hampton, VA.

**STATIC AND DYNAMIC AEROELASTIC CHARACTERIZATION OF AN AERODYNAMICALLY HEATED GENERIC HYPERSONIC AIRCRAFT CONFIGURATION**

Jennifer Heeg, Michael G. Gilbert, and Anthony S. Pototzky *In its* Research in Structures, Structural Dynamics and Materials, 1990 Mar. 1990 p 249-261 (For primary document see N91-10301 01-39)
Avail: NTIS HC/MF A13 CSCL 20K

This work-in-progress presentation describes an ongoing research activity at the NASA Langley Research Center to develop analytical methods for the prediction of aerothermoelastic stability of hypersonic aircraft including active control systems. The objectives of this research include application of aerothermal loads to the structural finite element model, determination of the thermal effects on flutter, and assessment of active controls technology applied to overcome any potential adverse aeroelastic stability or response problems due to aerodynamic heating- namely flutter suppression and ride quality improvement. For this study, a generic hypersonic aircraft configuration was selected which incorporates wing flaps, ailerons and all-moveable fins to be used for active control purposes. The active control systems would use onboard sensors in a feedback loop through the aircraft flight control computers to move the surfaces for improved structural dynamic response as the aircraft encounters atmospheric turbulence. Author

**N91-10321*#** McDonnell Aircraft Co., Saint Louis, MO. Structural Research Div.

**STRUCTURAL RISK ASSESSMENT AND AIRCRAFT FLEET MAINTENANCE**

Herb Smith, Jr., C. R. Saff, and Tom F. Christian (Air Force Logistics Command, Robins AFB, GA.) *In* NASA, Langley Research Center, Research in Structures, Structural Dynamics and Materials, 1990 Mar. 1990 p 263-274 (For primary document see N91-10301 01-39)
Avail: NTIS HC/MF A13 CSCL 20K

In the present analysis, deterministic flaw growth analysis is used to project the failure distributions from inspection data. Inspection data is reported for each critical point in the aircraft. The data will indicate either a crack of a specific size or no crack. The crack length may be either less than, equal to, or greater than critical size for that location. Non-critical length cracks are projected to failure using the crack growth characteristics for that location to find the life when it will be at critical length. Greater-than-critical length cracks are projected back to determine the life at failure, that is, when it was at critical length. The same process is used as in the case of a non-critical crack except that the projection goes the other direction. These points, along with the critical length cracks are used to determine the failure distribution. To be able to use data from different aircraft to build a common failure distribution, a consistent life variable must be used. Aircraft life varies with the severity of the usage; therefore the number of flight hours for a particular aircraft must be modified by its usage factor to obtain a normalized life which can be compared with that from other aircraft. Author

**N91-10322*#** Minnesota Univ., Saint Paul. Dept. of Forest Products.

**DEVELOPING A FRAMEWORK FOR QUALITATIVE ENGINEERING: RESEARCH IN DESIGN AND ANALYSIS OF COMPLEX STRUCTURAL SYSTEMS**

Bruno M. Franck *In* NASA, Langley Research Center, Research in Structures, Structural Dynamics and Materials, 1990 Mar. 1990 p 275-288 (For primary document see N91-10301 01-39)
Avail: NTIS HC/MF A13 CSCL 20K

The research is focused on automating the evaluation of complex structural systems, whether for the design of a new system or the analysis of an existing one, by developing new structural analysis techniques based on qualitative reasoning. The problem is to identify and better understand: (1) the requirements for the automation of design, and (2) the qualitative reasoning associated with the conceptual development of a complex system. The long-term objective is to develop an integrated design-risk assessment environment for the evaluation of complex structural systems. The scope of this short presentation is to describe the design and cognition components of the research. Design has received special attention in cognitive science because it is now identified as a problem solving activity that is different from other information processing tasks (1). Before an attempt can be made to automate design, a thorough understanding of the underlying design theory and methodology is needed, since the design process is, in many cases, multi-disciplinary, complex in size and motivation, and uses various reasoning processes involving different kinds of knowledge in ways which vary from one context to another. The objective is to unify all the various types of knowledge under one framework of cognition. This presentation focuses on the cognitive science framework that we are using to represent the knowledge aspects associated with the human mind's abstraction abilities and how we apply it to the engineering knowledge and engineering reasoning in design. Author

**N91-10323** Wisconsin Univ., Madison.
**ANALYSIS OF MOVING STRONG DISCONTINUITY SURFACES IN ELASTIC-PLASTIC SOLIDS INCLUDING EFFECTS OF INERTIA AND FINITE STRAIN Ph.D. Thesis**
Yinong Shen 1989 127 p
Avail: Univ. Microfilms Order No. DA9010331

The determination of conditions governing the existence and character of propagating surfaces of strong discontinuity (shock waves) is a fundamental problem of plasticity theory. For a large class of purely mechanical constitutive models, restrictions on shock waves are derived, within both small and large displacement-gradient formulations, and for quasi-static and dynamic deformations. For general dynamic three dimensional deformations within a small-deformation-gradient formulation, the Drugan and Rice (1984) direct integration approach is extended for quasi-static deformations, a necessary condition on moving strong discontinuities in the form of an inequality in terms of stress components. Material elastic moduli are obtained for general elastic-plastic deformation. This inequality strengthens to an equality when the material is elastic-ideally plastic. This is accomplished by applying the continuum mechanical requirements of geometrical compatibility, conservation of mass and momentum and the constitutive assumptions that the elastic part of the response is hyperelastic while the plastic part is constrained only by the maximum plastic work inequality. Another general restriction for materials possessing smooth yielding surfaces is derived by seeking the non-trivial solution of the explicit incremental stress strain equations across a shock front. Explicit restrictions on shock waves are also obtained for finite deformations through the same continuum mechanical requirements and similar material constitutive assumptions appropriately generalized to finite deformations, which are in broad agreement with experimental results and subsume many specific large deformation models. The cases for quasi-static deformations and for dynamic deformations are treated separately. Dissert. Abstr.

**N91-10324** Iowa State Univ. of Science and Technology, Ames.
**STUDY OF MIXED MODE STRESS INTENSITY FACTOR USING THE EXPERIMENTAL METHOD OF TRANSMITTED CAUSTICS Ph.D. Thesis**
Nasser Soltani 1989 139 p
Avail: Univ. Microfilms Order No. DA9014957

A convenient, new experimental technique for estimating both mode 1 and mode 2 stress intensity factors using the method of caustics is described and demonstrated. The use of transmitted caustics was thought to have limited potential and for this reason and others, the method was almost forgotten. One of the problems with the transmitted caustic was that the information gained seemed to be limited. But now with available least square techniques, which was modified to be used with transmitted caustics, transmitted caustics can be used to solve many different mixed mode fracture problems. As one of the first steps in bringing up the almost forgotten method of transmitted caustics, stress intensity factors were determined using this method. Twelve sets of specimens with double edge cracks were examined. The models for this experiment were from a thin plate of transparent material, plexiglas. Two edge cracks were machined into one of the long edges of the plate 9.5 in long, 1.8 in wide, and 1/8 in thick. The straight cracks were positioned perpendicular to the edge of the plate with various lengths and distances with respect to each other. The models were subjected to a uniaxial tension. The caustic curves were photographed with a 35-mm camera, at different loading conditions, during the test. Measurement of the photographs gave caustic dimensions as a function of applied load. Different cases of interaction between two edge cracks have been studied. The results compared well with experimental method of reflected caustics and a numerical method. The reliability of the method of transmitted caustic is established. Dissert. Abstr.

**N91-10325** Texas A&M Univ., College Station.
**AN EXPERIMENTAL AND ANALYTICAL STUDY OF STRUCTURAL IDENTIFICATION Ph.D. Thesis**
George Henry James, III 1989 175 p
Avail: Univ. Microfilms Order No. DA9015518

A start to finish study of structural identification was performed. All phases of the problem (mathematical modeling, testing, modal identification, and structural identification) were studied. An optical sensor system and conventional strain gauges were used to generate a data set from both free and forced response tests. An expanded version of the Creamer/Junkins method was used to upgrade the model using both types of data from both types of sensors. A monolithic grid, instrumented with fiber optic targets, strain gauges, and reaction wheels was used as the test article. Resection techniques with planar control points were developed for static calibration of cameras. The efficiency of the optical data reduction was increased through the use of a non-real time video processor. Statistical information was propagated through the resection and triangulation processes. The System Equivalent Reduction and Expansion Process (SEREP) was used to estimate unmeasured degrees of freedom. The Eignesystem Realization Algorithm (ERA) was used as the primary means of modal identification. Real and imaginary parts of the frequency response function were used in the forced response analysis based on a proportional damping model. Dissert. Abstr.

**N91-10326** Cranfield Inst. of Tech., Bedford (England).
**STATIC AND DYNAMIC FINITE ELEMENT STRESS ANALYSIS OF LAYERED COMPOSITE PLATES AND SHELLS Ph.D. Thesis**
Rashid Mahmood 1989 330 p
Avail: Univ. Microfilms Order No. BRDX88642

An attempt was made to develop theories for finite element static and dynamic stress analysis tailored for use with composite layered plates and shells. It was hoped to provide accurate values of the stresses particularly transverse shear stresses through the thickness and to perform accurate natural frequency analysis by including non-linear effects such as centrifugal stiffening. Initial derivations were based upon first order facet shell element analysis and first order curved shell element analysis. Subsequently, derivations were produced for higher order element analysis. A programming package was developed based upon the above derivations, containing a banded solver as well as a frontal solver, capable of analyzing structures build up from uniform or variable thickness layers, and with a multiple number of layers having constant or variable dimension. Results obtained with the aid of the present package were compared with results derived from experimental work as well as with results derived from available analytical solutions. Investigations were carried out for existing compressor blades, made of isotropic material and layered composite material, respectively. The results obtained from the package were compared with available experimental results produced by RR or carried out at Cranfield. It was shown that the above mentioned derivations produce comparable results and that the package was reliable and accurate. Dissert. Abstr.

**N91-10327#** Laboratorio de Computacao Cientifica, Rio de Janeiro (Brazil).
**FINITE ELEMENT ANALYSIS OF NONLINEAR CREEPING FLOWS**
Abinmael F. D. Loula and Joao Nisan C. Guerreiro Dec. 1988 36 p
(DE90-627189; LNCC-044/88; ISSN-0101-6113) Avail: NTIS (US Sales Only) HC/MF A03

Steady state creep problems with monotone constitutive laws are studied. Finite element approximations are constructed based on mixed Petrov-Galerkin formulations for constrained problems. Stability, convergence and a priori error estimates are proved for equal-order discontinuous stress and continuous velocity interpolations. Numerical results are presented confirming the rates of convergence predicted in the analysis and the good performance of this formulation. DOE

**N91-10328*#** National Aeronautics and Space Administration. Hugh L. Dryden Flight Research Facility, Edwards, CA.
**DESIGN OF CONTROL LAWS FOR FLUTTER SUPPRESSION BASED ON THE AERODYNAMIC ENERGY CONCEPT AND COMPARISONS WITH OTHER DESIGN METHODS**
Eli Nissim (Technion - Israel Inst. of Tech., Haifa.) Oct. 1990 59 p Previously anounced in IAA as A89-31100
(NASA-TP-3056; H-1549; NAS 1.60:3056; AIAA-89-1212) Avail: NTIS HC/MF A04 CSCL 20K

The aerodynamic energy method is used to synthesize control laws for NASA's drone for aerodynamic and structural testing-aerodynamic research wing 1 (DAST-ARW1) mathematical model. The performance of these control laws in terms of closed-loop flutter dynamic pressure, control surface activity, and robustness is compared with other control laws that relate to the same model. A control law synthesis technique that makes use of the return difference singular values is developed. It is based on the aerodynamic energy approach and is shown to yield results that are superior to those results given in the literature and are based on optimal control theory. Nyquist plots are presented, together with a short discussion regarding the relative merits of the minimum singular value as a measure of robustness as compared with the more traditional measure involving phase and gain margins. Author

**N91-10329#** Sandia National Labs., Albuquerque, NM.
**DEVELOPMENT OF THE FORCE ENVELOPE FOR AN ACCELERATION/FORCE EXTREMAL CONTROLLED VIBRATION TEST**
David O. Smallwood 1990 10 p Presented at the 61st Shock and Vibration Symposium, Pasadena, CA, 16-18 Oct. 1990
(Contract DE-AC04-76DP-00789)
(DE90-015712; SAND-90-1583C; CONF-9010172-1) Avail: NTIS HC/MF A02

A method is presented for determining the force spectral density function for a vibration test where a combination of force and acceleration is used for control. First the acceleration spectral density is established based on an envelope of the interface motion between the test item and the mounting structure (the base) in the use (field) environment. The driving point accelerance (acceleration/force) of the test item is measured at the mounting interface. The force required to drive the test item in an acceleration controlled test is then estimated. A force spectral density is then established using the estimated motion controlled force, and a derived force reduction factor. An extremal control vibration test is then performed based on which parameter (input force or input acceleration) reaches based on which parameter (input force or input acceleration) reaches its envelope first. DOE

**N91-10330#** Oak Ridge Y-12 Plant, TN. Development Div.
**EVALUATION OF NONDESTRUCTIVE EVALUATION TECHNIQUES FOR DETERMINATION OF FLAWED CONDITIONS AND THE EFFECTS OF FLAWS ON THE BURST PRESSURE IN KEVLAR-EPOXY FILAMENT-WOUND SPHERICAL TEST SPECIMENS**
W. D. Brosey, M. T. Calfee, J. W. Whittaker, D. A. Waldrop, E. G. Henneke, D. Post, K. L. Reifsnider, and R. A. Blake (Delaware Univ., Newark.) Dec. 1989 92 p
(Contract DE-AC05-84OS-21400)
(DE90-014839; Y-2428) Avail: NTIS HC/MF A05

A study of nondestructive evaluation techniques on spherical filament-wound Kevlar-epoxy test specimens has been performed, and the results are presented. The objectives of the study were (1) to determine the sensitivity of several NDE techniques for the detection of a series of flaw conditions in an enclosed geometry, and (2) to determine which flaw conditions affected the mechanical strength of the composite specimens. Seventy spherical specimens were made. Ten of the specimens contained one of seven defect conditions which simulated manufacturing or handling defects. Defect conditions involving delaminations, voids, inclusions, loss of fiber, loss of matrix, reduced fiber modulus, or matrix cracking were readily detectable with one or more inspection techniques. Specimens with fiber tension variation could not be distinguished from standard no-defect specimens with the inspection techniques used in this study. It was found that nominal defects introduced during the manufacturing or handling process do not significantly reduce the ultimate burst strength of the composite material in this geometry; however, impact damage was found to significantly affect burst pressure and location. Acousto-ultrasonic and acoustic emission techniques were found to be predictive of burst pressure for specimens with a normal matrix. Low-epoxy matrix specimens were found to sustain more damage for a given impact energy than specimens containing a normal matrix. DOE

**N91-10331#** Lawrence Livermore National Lab., CA.
**DESIGN OF A TRIAXIAL RESIDUAL STRESS MEASUREMENT SYSTEM USING HIGH-ENERGY X RAY DIFFRACTION Final Report**
J. F. Shackelford, B. D. Brown, and J. S. Park 1989 7 p
(Contract W-7405-eng-48)
(DE90-016212; UCRL-CR-104574) Avail: NTIS HC/MF A02

Previous design studies in developing concepts for residual stress measurement in engineering materials have been extended. A pre-prototype energy dispersive x ray diffraction (EDXRD) system has been fabricated. A 300 kV radiography source is used in conjunction with an intrinsic germanium detector and a MacII/LabVIEW data acquisition system. Specimens up to 25mm equivalent steel thickness (and one meter gross dimensions) can now be evaluated. The pre-prototype system serves as the hard x ray, bulk stress measurement component of the previously reported hybrid stress measuring system (which would include a traditional multi-angle surface measurement system using soft x rays). In addition, a detailed study of residual stress analytical equations has been completed and applied to various metallic and ceramic materials. During the grant period, related studies were completed on stress measurement using synchrotron radiation and on a critical review of the residual stress literature. DOE

**N91-10332*#** National Aeronautics and Space Administration. Lewis Research Center, Cleveland, OH.
**CALCULATION OF WEIBULL STRENGTH PARAMETERS, BATDORF FLAW DENSITY CONSTANTS AND RELATED STATISTICAL QUANTITIES USING PC-CARES**
Steven A. Szatmary, John P. Gyekenyesi, and Noel N. Nemeth (Aerospace Design and Fabrication, Inc., Brook Park, OH.) Oct. 1990 111 p
(NASA-TM-103247; E-5674; NAS 1.15:103247) Avail: NTIS HC/MF A06 CSCL 20K

This manual describes the operation and theory of the PC-CARES (Personal Computer-Ceramic Analysis and Reliability Evaluation of Structures) computer program for the IBM PC and compatibles running PC-DOS/MS-DOR OR IBM/MS-OS/2 (version 1.1 or higher) operating systems. The primary purpose of this code is to estimate Weibull material strength parameters, the Batdorf crack density coefficient, and other related statistical quantities. Included in the manual is the description of the calculation of shape and scale parameters of the two-parameter Weibull distribution using the least-squares analysis and maximum likelihood methods for volume- and surface-flaw-induced fracture in ceramics with complete and censored samples. The methods for detecting outliers and for calculating the Kolmogorov-Smirnov and the Anderson-Darling goodness-of-fit statistics and 90 percent confidence bands about the Weibull line, as well as the techniques for calculating the Batdorf flaw-density constants are also described. Author

**N91-10333*#** California Univ., San Diego, La Jolla. Dept. of Applied Mechanics and Engineering Sciences.
**COMPARISON OF NASTRAN ANALYSIS WITH GROUND VIBRATION RESULTS OF UH-60A NASA/AEFA TEST CONFIGURATION Final Report**
Florentino Idosor and Frieder Seible Sep. 1990 101 p Original contains color illustrations
(Contract NCC2-598)
(NASA-CR-184565; NAS 1.26:184565; SSRP-90/03) Avail: NTIS HC/MF A06; 4 functional color pages CSCL 20K

Preceding program flight tests, a ground vibration test and modal test analysis of a UH-60A Black Hawk helicopter was conducted by Sikorsky Aircraft to complement the UH-60A test plan and NASA/ARMY Modern Technology Rotor Airloads Program. The 'NASA/AEFA' shake test configuration was tested for modal frequencies and shapes and compared with its NASTRAN finite element model counterpart to give correlative results. Based upon previous findings, significant differences in modal data existed and were attributed to assumptions regarding the influence of secondary structure contributions in the preliminary NASTRAN modeling. An analysis of an updated finite element model including several secondary structural additions has confirmed that the inclusion of specific secondary components produces a significant effect on modal frequency and free-response shapes and improves correlations at lower frequencies with shake test data. Author

**N91-10334*#** Florida Atlantic Univ., Boca Raton. Dept. of Ocean Engineering.
**MOBILITY POWER FLOW ANALYSIS OF AN L-SHAPED PLATE STRUCTURE SUBJECTED TO DISTRIBUTED LOADING**
J. M. Cuschieri and B. Cimmerman 1990 10 p
(Grant NAG1-685)
(NASA-CR-187353; NAS 1.26:187353) Avail: NTIS HC/MF A02 CSCL 20K

An analytical investigation based in the Mobility Power Flow (MPF) method is presented for the determination of the vibrational response and power flow for two coupled flat plate structures in an L-shaped configuration, subjected to distributed excitation. The principle of the MPF method consists of dividing the global structure into a series of subsystems coupled together using mobility functions. Each separate subsystem is analyzed independently to determine the structural mobility functions for the junction and excitation locations. The mobility functions, together with the characteristics of the junction between the subsystems, are then used to determine the response of the global structure and the MPF. In the considered coupled plate structure, MPF expressions are derived for distributed mechanical excitation which is independent of the structure response. However using a similar approach with some modifications excitation by an acoustic plane wave can be considered. Some modifications are required to deal with the latter case are necessary because the forces (acoustic pressure) acting on the structure are dependent on the response of the structure due to the presence of the scattered pressure. Author

**N91-10335*#** Florida Atlantic Univ., Boca Raton. Dept. of Ocean Engineering.
**EXPERIMENTAL MEASUREMENT OF STRUCTURAL POWER FLOW ON AN AIRCRAFT FUSELAGE Progress Report**
J. M. Cuschieri Jun. 1989 29 p
(Grant NAG1-685)
(NASA-CR-187352; NAS 1.26:187352) Avail: NTIS HC/MF A03 CSCL 20K

An experimental technique is used to measure the structural power flow through an aircraft fuselage with the excitation near the wing attachment location. Because of the large number of measurements required to analyze the whole of an aircraft fuselage, it is necessary that a balance be achieved between the number of measurement transducers, the mounting of these transducers, and the accuracy of the measurements. Using four transducers mounted on a bakelite platform, the structural intensity vectors at locations distributed throughout the fuselage are measured. To minimize the errors associated with using a four transducers technique the measurement positions are selected away from bulkheads and stiffeners. Because four separate transducers are used, with each transducer having its own drive and conditioning amplifiers, phase errors are introduced in the measurements that can be much greater than the phase differences associated with the measurements. To minimize these phase errors two sets of measurements are taken for each position with the orientation of the transducers rotated by 180 deg and an average taken between the two sets of measurements. Results are presented and discussed. Author

**N91-10336#** Rolls-Royce Ltd., Derby (England). Advanced Research Lab.
**VIBRO-ACOUSTIC EMISSION RUBBING SOURCES**
John R. Webster 20 Mar. 1989 5 p Presented at World Conference on Acoustic Emission, Charlotte, NC, 20-23 Mar. 1989
(PNR-90730; ETN-90-97949) Copyright Avail: NTIS HC/MF A01

Fundamental studies of two basic Vibro-Acoustic Emission (VAE) source categories of impacts and rubbing are summarized. The effects of the main parameters on these sources were modeled. The feasibility of measuring relative levels of energy dissipation at a rubbing source was demonstrated. The evaluation or prediction of wear rates can be performed. Signal detection and analysis methods were developed to allow qualitative VAE measurements to be made in real structures. VAE was successfully demonstrated for the three application areas of defect detection, failure analysis and mechanism investigations. ESA

**N91-10337#** Rolls-Royce Ltd., Derby (England).
**FATIGUE CRACK PROPAGATION OF COPLANAR SEMI-ELLIPTICAL CRACKS IN PURE BENDING**
W. O. Soboyejo, M. J. Walsh, K. R. Cropper, and J. F. Knott (Cambridge Univ., England ) 1 May 1990 51 p Submitted for publication Sponsored in part by Admiralty Research Establishment
(PNR-90742; ETN-90-97952) Copyright Avail: NTIS HC/MF A04

Stress intensity factor solutions for coalescing coplanar semi-elliptical cracks subjected to pure bending are presented. Crack shapes of beach marked test pieces were modeled using a finite element method. Stress intensity factors were obtained using an elastic strain energy method and a displacement extrapolation method. The results of the fatigue propagation of coplanar semi-elliptical cracks are discussed. Fatigue tests were carried out for stress ratios of 0.2, 0.5, and 0.7, and for initial crack separations of 4 mm, 8 mm, and 16 mm. Several models are employed for the prediction of fatigue crack growth of coalescing coplanar cracks. The implications for fatigue life assessment are discussed. ESA

## 42 GEOSCIENCES (GENERAL)

**N91-10338#** Meteorological Satellite Center, Tokyo (Japan).
**METEOROLOGICAL SATELLITE CENTER TECHNICAL NOTE. SPECIAL ISSUE (1989). SUMMARY OF GMS SYSTEM. 1: TELECOMMUNICATION SYSTEM**
Mar. 1989 157 p In ENGLISH and JAPANESE
Avail: NTIS HC/MF A08

The Geostationary Meteorological Satellite System (GMSS) is discussed. The station control and monitoring subsystem, the visible infrared spin scan radiometer (VISSR) demodulation and processing system, the telemetry subsystem, and the antenna/transmitter subsystem are among the topics covered. For individual titles, see N91-10339 through N91-10355.

**N91-10339#** Meteorological Satellite Center, Tokyo (Japan).
**OUTLINE OF THE GMS TELECOMMUNICATION SYSTEM** c32
Masaru Fujimaki and Nobuyuki Taki *In its* Meteorological Satellite Center Technical Note. Special Issue (1989). Summary of GMS System. 1: Telecommunication System Mar. 1989 p 1-5 In JAPANESE; ENGLISH summary (For primary document see N91-10338 01-42)
Avail: NTIS HC/MF A08

The Geostationary Meteorological Satellite (GMS) ground telecommunication facilities of the Japanese Meteorological Agency (JMA) consist of the Command and Data Acquisition (CDAS) system and DPC (MSC) system. The primary role of the CDAS is to make a communication between the GMS spacecraft/other ground facilities and itself. The DPC communication system is the important center between the CDAS and the computer system. It works as the window of the DPC. The ground telecommunication system was partly renovated in 1987. That system is mainly described here. The following are the main results of renovation and improvement of the CDAS system: (1) adopting a homemade machine as Visible Infrared Spin-Scan Radiometer (VISSR) equipment, which is the mainstay of atmospheric observation service; (2) dissemination of stretched VISSR data, to make hourly observation available; and (3) an automated system with centralized control and status monitoring is available for reliable operation by minicomputer system. The renovated DPC telecommunication system has centralized control and status monitoring by a micro-computer system. FAX image films for archive are processed automatically without a darkroom. Author

**N91-10340#** Meteorological Satellite Center, Tokyo (Japan).
**OUTLINE OF CDAS TELECOMMUNICATION SYSTEM** c32
Kiyoshi Nakagawa, Tsutoya Abe, and Takao Suzuki *In its* Meteorological Satellite Center Technical Note. Special Issue (1989). Summary of GMS System. 1: Telecommunication System Mar. 1989 p 7-9 In JAPANESE; ENGLISH summary (For primary document see N91-10338 01-42)
Avail: NTIS HC/MF A08

The new telecommunication system is designed to have a dual system for matching the multipurpose operation, e.g., telemetry, command and Visible Infrared Spin-Scan Radiometer (VISSR), etc. The new system is mainly controlled by a pair of computer systems constituted hot-standby. The computer systems are able to support the operation of the Command and Data Acquisition Station (CDAS) telecommunication equipment with high reliability. Major functions of the improved CDAS system are as follows: (1) to process the raw VISSR data and generate the stretched VISSR data for transmission both to DPC and the satellite; and (2) to centralize the main function of station operation. Author

**N91-10341#** Meteorological Satellite Center, Tokyo (Japan).
**STATION CONTROL AND MONITOR SUBSYSTEM** c32
Yukio Sasaki and Hiroyuki Suzuki *In its* Meteorological Satellite Center Technical Note. Special Issue (1989). Summary of GMS System. 1: Telecommunication System Mar. 1989 p 11-20 In JAPANESE; ENGLISH summary (For primary document see N91-10338 01-42)
Avail: NTIS HC/MF A08

The station control and monitor subsystem consists of a monitor and control unit, a data interface unit and an operating console unit. A pair of minicomputers is installed at the Command and Data Acquisition Station (CDAS). These computers monitor and control communication equipment in CDAS. The computer system in always in dual operation in order to prevent the system shutting down. Operation of the Geostationary Meteorological Satellite System (GMSS) is achieved almost automatically under an intensive control system. Author

**N91-10342#** Meteorological Satellite Center, Tokyo (Japan).
**VISSR DEMODULATE AND PROCESSING SUBSYSTEM** c32
Toshiharu Tanaka and Akifumi Yamashita *In its* Meteorological Satellite Center Technical Note. Special Issue (1989). Summary of GMS System. 1: Telecommunication System Mar. 1989 p 21-45 In JAPANESE; ENGLISH summary (For primary document see N91-10338 01-42)
Avail: NTIS HC/MF A08

The Visible Infrared Spin-Scan Radiometer (VISSR) demodulation and processing subsystem receives Geostationary Meteorological Satellite (GMS) wind-band VISSR data and demodulates it to digital image data. This subsystem consists of demodulator unit, line-frame sync unit and data processing unit. The wide band VISSR signal is demodulated and synchronized. Author

**N91-10343#** Meteorological Satellite Center, Tokyo (Japan).
**STRETCHED VISSR SUBSYSTEM** c32
Yoshikazu Mori *In its* Meteorological Satellite Center Technical Note. Special Issue (1989). Summary of GMS System. 1: Telecommunication System Mar. 1989 p 47-53 In JAPANESE; ENGLISH summary (For primary document see N91-10338 01-42)
Avail: NTIS HC/MF A08

The stretched Visible Infrared Spin-Scan Radiometer (S-VISSR) data of the Geostationary Meteorological Satellite (GMS) system is the digital image data originated by raw VISSR data from the GMS. Raw VISSR data are demodulated and reconstructed by the ground system in order to reduce data rate. Then these processed data are retransmitted to the medium scale data utilization station (MDUS) via the GMS during VISSR observation. Stretched VISSR dissemination has started as new service instead of HR-FAX since January 5, 1989. MDUS shall be adopted for new service with modification according to the transmission characteristics of the S-VISSR. Author

**N91-10344#** Meteorological Satellite Center, Tokyo (Japan).
**IMAGE MONITOR** c32
Yukio Sasaki and Hiroyuki Suzuki *In its* Meteorological Satellite Center Technical Note. Special Issue (1989). Summary of GMS System. 1: Telecommunication System Mar. 1989 p 55-61 In JAPANESE; ENGLISH summary (For primary document see N91-10338 01-42)
Avail: NTIS HC/MF A08

The image monitor is a part of the station control and monitor subsystem. The purpose of this system is to monitor the stretched Visible Infrared Spin-Scan Radiometer (S-VISSR) signal which transmits the signal to the Geostationary Meteorological Satellite (GMS) and receives it at CDAS. Monitor methods are as follows: (1) make an image from S-VISSR data and display it on CRT terminal; (2) monitor and inspect S-VISSR signal condition; and (3) transmit these data to the central processing unit and operating console. Author

**N91-10345#** Meteorological Satellite Center, Tokyo (Japan).
**TELEMETRY SUBSYSTEM** c17
Saburo Takaku, Takeshi Yokoya, and Akihiko Tange *In its* Meteorological Satellite Center Technical Note. Special Issue (1989). Summary of GMS System. 1: Telecommunication System Mar. 1989 p 63-70 In JAPANESE; ENGLISH summary (For primary document see N91-10338 01-42)
Avail: NTIS HC/MF A08

This equipment demodulates the received Geostationary Meteorological Satellite's (GMS) telemetry signal and devides it into two kinds of data signals, so-called Pulse Code Modulation (PCM) telemetry and real time telemetry. These data are distributed to the CRT monitor display, penrecorder, command subsystem, Visible Infrared Spin-Scan Radiometer (VISSR) subsystem, and the central processing unit. This section deals with such equipment, data format, etc. Author

**N91-10346#** Meteorological Satellite Center, Tokyo (Japan).
**COMMAND SUBSYSTEM** c32
Takeo Saito, Tatsuo Takahashi, and Masakazu Saito *In its* Meteorological Satellite Center Technical Note. Special Issue (1989). Summary of GMS System. 1: Telecommunication System Mar. 1989 p 71-77 In JAPANESE; ENGLISH summary (For primary document see N91-10338 01-42)
Avail: NTIS HC/MF A08

Here, researchers describe the command subsystem. This subsystem generates command pulses and sends them to the Geostationary Meteorological Satellite (GMS) in order to change its operation mode or to do its house keeping. The command subsystem is normally under control of the DPC computer system and it can be controlled by the Command and Data Acquisition Station (CDAS) itself. This subsystem is connected to the Station Control and Monitor Unit (SCMU) and cooperates with the telemetry subsystem, Visible Infrared Spin-Scan Radiometer (VISSR) processing subsystem and other equipment in CDAS. Author

**N91-10347#** Meteorological Satellite Center, Tokyo (Japan).
**TRILATERATION RANGING SUBSYSTEM** c32
Shuji Naito, Kazuichirou Akimoto, and Masashi Morisaki *In its*

Meteorological Satellite Center Technical Note. Special Issue (1989). Summary of GMS System. 1: Telecommunication System Mar. 1989 p 79-89 In JAPANESE; ENGLISH summary (For primary document see N91-10338 01-42)
Avail: NTIS HC/MF A08

The trilateration ranging system provides data which are used in determining the orbit of the Geostationary Meteorological Satellite (GMS). The GMS system employed a trilateration ranging technique wherein a near simultaneous measurement of three range vectors are obtained from the Command and Data Acquisition Station (CDAS) and two Turn-Around Ranging Stations (TARS) which are located on Ishigaki Is., Japan, and on Crib Point, Australia. Author

**N91-10348#** Meteorological Satellite Center, Tokyo (Japan).
**ANTENNA/TRANSMITTER CONTROL UNIT** c33
Seiji Kawabata and Masahiro Sasaki *In its* Meteorological Satellite Center Technical Note. Special Issue (1989). Summary of GMS System. 1: Telecommunication System Mar. 1989 p 91-95 In JAPANESE; ENGLISH summary (For primary document see N91-10338 01-42)
Avail: NTIS HC/MF A08

The primary function of the antenna control unit is control of the Command and Data Acquisition Station (CDAS) 18 m phi antenna driver, and part of its function is performed by a central monitoring and control central processing unit (CPU) board. These units are connected to the station control and monitor unit (Mini computer system) via process I/O unit. Each transmitter system control unit (Tx. Cont) is composed of the Equivalent Isotropically Radiated Power (EIRP) control unit and HPA control unit. The Tx. cont units adjust the output signal level of each transmitter, and have a safety function that prevents radiation of unnecessary power. The function, performance and operation of the renovated unit are explained. Author

**N91-10349#** Meteorological Satellite Center, Tokyo (Japan).
**FREQUENCY STANDARD UNIT** c32
Hirozou Nishida *In its* Meteorological Satellite Center Technical Note. Special Issue (1989). Summary of GMS System. 1: Telecommunication System Mar. 1989 p 97-99 In JAPANESE; ENGLISH summary (For primary document see N91-10338 01-42)
Avail: NTIS HC/MF A08

A frequency standard unit supplies a high precision signal and accurate clock timing for communication units in the Command and Data Acquisition Station (CDAS). This unit has a 5 MHz stabilized crystal oscillator and synthesizes some standard frequency signals. These signals are calibrated by standard wave transmissions of 40 KHz VLF (JG 2 AS). And clock timing is also calibrated by a JJY standard wave with accuracy of better than plus or minus 2.5 msec. After renewal of this unit, duplex operation ensures reliable operations. Author

**N91-10350#** Meteorological Satellite Center, Tokyo (Japan).
**OPERATION CONSOLE** c32
Koji Sato and Shigeto Miura *In its* Meteorological Satellite Center Technical Note. Special Issue (1989). Summary of GMS System. 1: Telecommunication System Mar. 1989 p 101-111 In JAPANESE; ENGLISH summary (For primary document see N91-10338 01-42)
Avail: NTIS HC/MF A08

The operation console is a part of a Station Control and Monitor Unit (SCMU). With this console, operators can perform various operations with the Geostationary Meteorological Satellite System (GMSS) which depend on man-machine interface. For reliable operation, the operation console has a dual system in accordance with the SCMU. Author

**N91-10351#** Meteorological Satellite Center, Tokyo (Japan).
**SYSTEM CONSOLE** c32
Yukio Sasaki and Hiroyuki Suzuki *In its* Meteorological Satellite Center Technical Note. Special Issue (1989). Summary of GMS System. 1: Telecommunication System Mar. 1989 p 113-117 In JAPANESE; ENGLISH summary (For primary document see N91-10338 01-42)
Avail: NTIS HC/MF A08

The system console is a part of the station control and monitor subsystem. This system consists of keyboard/display, serial-printer and line-printer. The system console works as a man-machine interface unit. The Station Control and Monitor Unit (SCMU) is under the control of the system console. Author

**N91-10352#** Meteorological Satellite Center, Tokyo (Japan).
**DCP SUBSYSTEM** c32
Masaaki Sugai, Kouzo Masubuchi, and Toshio Onigata *In its* Meteorological Satellite Center Technical Note. Special Issue (1989). Summary of GMS System. 1: Telecommunication System Mar. 1989 p 119-129 In JAPANESE; ENGLISH summary (For primary document see N91-10338 01-42)
Avail: NTIS HC/MF A08

There are many data collection stations in the coverage area of the Geostationary Meteorological Satellite (GMS) that are called Data Collection Platforms (DCP). Each station collects environmental data and sends it to DPC computer systems. DCP reported data is sended by UHF transmitter equipment after reception of the interrogation signal from DPC. The UHF signal is received at GMS and converted to an S-band down-link signal to sent to the Command and Data Acquisition Station (CDAS). The GMS UHF receiver and transmitter is cross-strapped to S-band communication equipment. The CDAS receiver equipment demodulates the S-band down link signal and discrimination to 133 channel data. Frequency drift in the satellite will be corrected by the DCP standard equipment in the CDAS. Author

**N91-10353#** Meteorological Satellite Center, Tokyo (Japan).
**WEFAX SUBSYSTEM** c32
Yoshiyuki Kanazawa *In its* Meteorological Satellite Center Technical Note. Special Issue (1989). Summary of GMS System. 1: Telecommunication System Mar. 1989 p 131-136 In JAPANESE; ENGLISH summary (For primary document see N91-10338 01-42)
Avail: NTIS HC/MF A08

This subsystem consists of subcarrier modulators, carrier modulators and demodulators. WEFAX signal generated by DPC computer system and sent to the Command and Data Acquisition Station (CDAS), is modulated by this subsystem and retransmitted to a Secondary Data Users' Station (SDUS) via the Geostationary Meteorological Satellite (GMS). The WEFAX signal relayed to GMS, is received and demodulated by this subsystem in order to monitor the operational condition. Author

**N91-10354#** Meteorological Satellite Center, Tokyo (Japan).
**DPC TELECOMMUNICATION SYSTEM** c32
Sadao Mita, Tsukasa Okazaki, and Ryoetsu Ansai *In its* Meteorological Satellite Center Technical Note. Special Issue (1989). Summary of GMS System. 1: Telecommunication System Mar. 1989 p 137-155 In JAPANESE; ENGLISH summary (For primary document see N91-10338 01-42)
Avail: NTIS HC/MF A08

This system is composed of the Visible Infrared Spin-Scan Radiometer (VISSR) interface unit, monitor and control unit, automatic image recorder and other units, monitored by a microprocessor. The system processes the image data and various other signals which are sent from the Command and Data Acquisition Station (CDAS) via the microwave link to DPC. These signals are transmited to the DPC computer system and processed. Others are transmitted to the Geostationary Meteorological Satellite (GMS) via CDAS. Furthermore, WEFAX is transmitted by land line to domestic users. Author

**N91-10355#** Meteorological Satellite Center, Tokyo (Japan).
**MICROWAVE LINK** c32
Susumu Shinozuka *In its* Meteorological Satellite Center Technical Note. Special Issue (1989). Summary of GMS System. 1: Telecommunication System Mar. 1989 p 157-164 In

JAPANESE; ENGLISH summary (For primary document see N91-10338 01-42)
Avail: NTIS HC/MF A08

This is the circuit between the Japan Meteorological Agency (JMA) and the DPC (via Tukuba). This microwave link is to transmit and receive the 7.5 MHz band signals. Space diversity reception is adopted to improve circuit dependability. Channel capacity is 6.312 Mbps. HR-FAX and WEFAX are transmitted from DPC to JMA. Author

**N91-10356#** Meteorological Satellite Center, Tokyo (Japan).
**METEOROLOGICAL SATELLITE CENTER TECHNICAL NOTE. SPECIAL ISSUE (1989). SUMMARY OF GMS SYSTEM. 2: DATA PROCESSING**
Mar. 1989 170 p In ENGLISH and JAPANESE Original contains color illustrations
Avail: NTIS HC/MF A08

The Japanese Meteorological Satellite Center (MSC) is discussed. The computer system, image data processing, data processing of raw images and pre-processed images, as well as the processing of Visible Infrared Spin Scan Radiometer (VISSR) histogram and cloud grid data are among the topics covered. For individual titles, see N91-10357 through N91-10375.

**N91-10357#** Meteorological Satellite Center, Tokyo (Japan).
**COMPUTER SYSTEM** **c60**
Shigenori Naito *In its* Meteorological Satellite Center Technical Note. Special Issue (1989). Summary of GMS System. 2: Data Processing Mar. 1989 p 1-35 In JAPANESE; ENGLISH summary (For primary document see N91-10356 01-42)
Avail: NTIS HC/MF A08

The new computer system (second generation) at the Japanese Meteorological Satellite Center (JMSC) has been working since May, 1987. Various new products were developed and put into routine operation. Buy adopting the new computer technology, researchers have improved operation efficiency without missing reliability. An outline of the new computer system and some essential points to be understood are given. Author

**N91-10358#** Meteorological Satellite Center, Tokyo (Japan).
**GENERAL FLOW OF IMAGE DATA PROCESSING** **c60**
Taichi Takahashi *In its* Meteorological Satellite Center Technical Note. Special Issue (1989). Summary of GMS System. 2: Data Processing Mar. 1989 p 37-38 In JAPANESE; ENGLISH summary (For primary document see N91-10356 01-42)
Avail: NTIS HC/MF A08

Since the operation of Geostationary Meteorological Satellite (GMS) and meteorological data processing were started in April 1978, many products have been added. On replacing the Meteorological Satellite Center's (MSC) computer system in 1987, overlapping processes of these products were integrated into one (so called the Basic Data Processing). This consists of pre-processing of image data, Visible Infrared Spin-Scan Radiometer (VISSR) histogram processing, and cloud grid data processing. MSC's products are derived using both raw VISSR data and the results of these three processings. Author

**N91-10359#** Meteorological Satellite Center, Tokyo (Japan).
**IMAGE MAPPING** **c61**
Mitsuo Nesasa *In its* Meteorological Satellite Center Technical Note. Special Issue (1989). Summary of GMS System. 2: Data Processing Mar. 1989 p 39-43 In JAPANESE; ENGLISH summary (For primary document see N91-10356 01-42)
Avail: NTIS HC/MF A08

Mapping (to make each pixel of Visible Infrared Spin Scan Radiometer (VISSR) image data correspond to the longitude and latitude of the earth) is one of the most important processing steps for analyzing Geostationary Meteorological Satellite (GMS) VISSR image data. The VISSR misalignment is used at the Meteorological Center (MSC) for mapping. This value changes nominally according to diurnal changes of the internal temperature of the satellite, and this change lowers the accuracy of the mapping. To prevent this, the value is corrected in the mapping by detection of the earth's edge. Author

**N91-10360#** Meteorological Satellite Center, Tokyo (Japan).
**CALIBRATION** **c61**
Masayuki Sasaki *In its* Meteorological Satellite Center Technical Note. Special Issue (1989). Summary of GMS System. 2: Data Processing Mar. 1989 p 45-51 In JAPANESE; ENGLISH summary (For primary document see N91-10356 01-42)
Avail: NTIS HC/MF A08

Visible Infrared Spin-Scan Radiometer (VISSR) data are used for facsimile pictures production and derivation of meteorological parameters such as sea surface temperature, cloud amount, and cloud motion wind. Prior to processing, VISSR calibration is necessary. VISSR calibration determines the relationship between brightness level and radiation energy (albedo or temperature). In addition, the relationship is used for stretched-VISSR data production. Author

**N91-10361#** Meteorological Satellite Center, Tokyo (Japan).
**FAX IMAGE PROCESSING** **c43**
Yoshishige Shirakawa *In its* Meteorological Satellite Center Technical Note. Special Issue (1989). Summary of GMS System. 2: Data Processing Mar. 1989 p 53-65 In JAPANESE; ENGLISH summary (For primary document see N91-10356 01-42)
Avail: NTIS HC/MF A08

The facsimile image data are produced in several kinds of format useful for meteorological and oceanographic analysis on the basis of the Visible Infrared Spin-Scan Radiometer (VISSR) image data. Facsimiles were added and modified at the replacement of Meteorological Satellite Center (MSC) computer system. The Sea Surface Temperature facsimile (SST-FAX) is produced from VISSR infrared image data to draw the contour of sea surface temperature. The Sea-ice FAX is produced from VISSR visible image data and NOAA Advanced Very High Resolution Radiometer (AVHRR) infrared image data to watch the sea-ice in Okhostk Sea and Pohai Bay. The archiving FAX archives VISSR image as pictures for meteorological analysis. The Weather facsimile (WEFAX) is renamed from Low-Resolution facsimile (LR-FAX) in October 1988. The H,I,J pictures of WEFAX is modified from sectorized pictures to polar-stereographic pictures covering the Far East, including Japan. Author

**N91-10362#** Meteorological Satellite Center, Tokyo (Japan).
**SATELLITE-DERIVED INDEX OF PRECIPITATION INTENSITY** **c47**
Kazufumi Suzuki *In its* Meteorological Satellite Center Technical Note. Special Issue (1989). Summary of GMS System. 2: Data Processing Mar. 1989 p 67-74 In JAPANESE; ENGLISH summary (For primary document see N91-10356 01-42)
Avail: NTIS HC/MF A08

Satellite-derived Index of precipitation intensity (SI) is designed to estimate precipitation intensity from Geostationary Meteorological Satellite (GMS) data. SI is calculated on every 5 km grid and is graded in 16 intensity levels corresponding to radar echo intensity level. The calculated region consists of 700 x 300 grids covering the whole of the Japanese islands. SI is automatically processed hourly according to the schedule and is disseminated to the Forecast Division of the Japanese Meteorological Agency (JMA) within a few minutes after the satellite observations. Estimation formula of SI is a polynomial equation determined by multiple regression analysis of GMS data and composite digital radar data. After the latest GMS data are converted to 5 km x 5 km grid value, the SI is obtained by substituting the GMS grid data into a polynomial equation which had been obtained by previous multiple regression analysis. Both VIS and IR channels data are available in the daytime and only IR channel data in the nighttime. Author

**N91-10363#** Meteorological Satellite Center, Tokyo (Japan).
**ISCCP DATA PROCESSING** **c61**
Saya Kondo *In its* Meteorological Satellite Center Technical Note. Special Issue (1989). Summary of GMS System. 2: Data

Processing Mar. 1989 p 75-78 In JAPANESE; ENGLISH summary Original contains color illustrations (For primary document see N91-10356 01-42)
Avail: NTIS HC/MF A08

The International Satellite Cloud Climatology Project (ISCCP) began on 1 July 1983 as the first element of the World Climate Research Program (WCRP). This project aims to develop a global data set of calibrated radiances by the international network of operational geostationary and polar orbiting meteorological satellites for climatological research. The Geostationary Meteorological Satellite (GMS) image data are processed at the Meteorological Satellite Center (MSC) and provided to the ISCCP on a routine basis. Author

**N91-10364#** Meteorological Satellite Center, Tokyo (Japan).
**PRE-PROCESSING OF IMAGE DATA** **c61**
Shinichi Miyatake and Takashi Ohshima *In its* Meteorological Satellite Center Technical Note. Special Issue (1989). Summary of GMS System. 2: Data Processing Mar. 1989 p 79-83 In JAPANESE; ENGLISH summary (For primary document see N91-10356 01-42)
Avail: NTIS HC/MF A08

Two kinds or pre-processed image data are routinely produced. The earth disc image and the polar-stereographic image are provided in order to shorten the access time on the Image Display Unit. These data are treated as a Image Data Set of the Relational Date Base (RDB), so that a large amount of image data can be searched and handled easily. The pre-processed image data files are commonly used by the successive processings: derivation of cloud motion winds, manual processing of satellite cloud information charts, analysis of tropical cyclones, editing of image movies on video tape recorders, and extraction of landmark. Author

**N91-10365#** Meteorological Satellite Center, Tokyo (Japan).
**CLOUD MOTION WIND** **c47**
Takashi Ohshima *In its* Meteorological Satellite Center Technical Note. Special Issue (1989). Summary of GMS System. 2: Data Processing Mar. 1989 p 85-102 In JAPANESE; ENGLISH summary (For primary document see N91-10356 01-42)
Avail: NTIS HC/MF A08

Cloud motion winds are derived four times per day, 00UT, 06UT, 12UT and 18UT at the Meteorological Satellite Center (MSC). Two types of cloud motion winds are derived at MSC. One is cumulus level or low-level cloud motion wind which is derived through automatical process, and another is cirrus level or high-level cloud motion wind which is derived through combined processes, the automatical process and the man-machine interactive process. In the automatical process, the cloud height information is used for selection of suitable target clouds to be tracked. The tracking is performed by a pattern matching technique. In the manual process, an operator selects and tracks suitable targets on an animated movie loop of the image display unit. Both types of winds are assigned to certain levels and quality-checked manually and automatically. The extracted winds are coded into World Meteorological Organization (WMO) formats (SATOB) and transmitted to the Forecast Department of the Japanese Meteorological Agency (JMA) via ADESS within three hours after Visible Infrared Spin-Scan Radiometer (VISSR) observation. These winds are used as the initial data for numerical weather prediction and also used as the basic data for typhoon analysis, and are transmitted to world-wide users via Global Telecommunications System (GTS). The details of the current cloud motion wind derivation system at the MSC are described. Author

**N91-10366#** Meteorological Satellite Center, Tokyo (Japan).
**TYPHOON INFORMATION** **c47**
Hiroyuki Koba *In its* Meteorological Satellite Center Technical Note. Special Issue (1989). Summary of GMS System. 2: Data Processing Mar. 1989 p 103-108 In JAPANESE; ENGLISH summary Original contains color illustrations (For primary document see N91-10356 01-42)
Avail: NTIS HC/MF A08

Three types of information on tropical cyclones are extracted from Geostationary Meteorological Satellite (GMS) images by using man-machine interactive processing in Meteorological Satellite Center (MSC) computer system. First is center information with the center position, movement and accuracy; second is intensity information with CI number and size of cloud system; and last is cloud parameter of the tropical cyclone corresponding to the gale force area (wind speed more than 30 knots) and the storm force area (wind speed more than 50 knots). The information corresponding to center and intensity of tropical cyclones are reported by SAREP (WMO international codes FM85-IX) on the Global Telecommunications System (GTS). The cloud parameters of tropical cyclone are reported to the Japanese Meteorological Agency (JMA) forecast division via facsimile telegraph. Author

**N91-10367#** Meteorological Satellite Center, Tokyo (Japan).
**VTR LOOP MOVIE** **c47**
Tokuei Uchiyama *In its* Meteorological Satellite Center Technical Note. Special Issue (1989). Summary of GMS System. 2: Data Processing Mar. 1989 p 109-111 In JAPANESE; ENGLISH summary (For primary document see N91-10356 01-42)
Avail: NTIS HC/MF A08

Sequestial cloud images are recorded periodically on video tape for archiving and nephanalysis. Three kinds of hourly IR images are recorded on video tapes: full disk image, partial enlargement of full disk image in Northern Hemisphere, and polar-stereographic image in Northern Hemisphere. Analysts can watch cloud image animation repeatedly for nephanalysis by replaying video tape. Cloud images copied in cassette tape from archiving video tape are used widely for long range forecast and research. Author

**N91-10368#** Meteorological Satellite Center, Tokyo (Japan).
**VISSR HISTOGRAM DATA** **c46**
Hideyuki Sasaki *In its* Meteorological Satellite Center Technical Note. Special Issue (1989). Summary of GMS System. 2: Data Processing Mar. 1989 p 113-115 In JAPANESE; ENGLISH summary (For primary document see N91-10356 01-42)
Avail: NTIS HC/MF A08

Visible Infrared Spin-Scan Radiometer (VISSR) histogram data, which consists of a one-dimensional histogram of IR or VIS radiance, is the primary earth-located VISSR data. The processed area is from 60 degrees N to 60 degrees S and from 80 degrees E to 160 degrees W. The VISSR image in the processed area is divided into 230,400 (480 x 480) segments with the regular intervals of 0.25 degrees latitude and 0.25 degrees longitude. The maximum level, the minimum level, and each pixel between the minimum and maximum level are calculated at each segment. The 480 histograms of the same latitude are ordered from west to east and the same latitudinal histograms are ordered from north to south. Author

**N91-10369#** Meteorological Satellite Center, Tokyo (Japan).
**BRIGHTNESS TEMPERATURE DISTRIBUTION** **c46**
Kazuhiro Oosawa *In its* Meteorological Satellite Center Technical Note. Special Issue (1989). Summary of GMS System. 2: Data Processing Mar. 1989 p 117-119 In JAPANESE; ENGLISH summary (For primary document see N91-10356 01-42)
Avail: NTIS HC/MF A08

The radiation with a wave-length of 3 to 100 microns emitted from the earth-atmosphere system is called Outgoing Longwave Radiation (OLR) and imparts useful information to evaluate the earth's radiation budget. While the radiation observed by the Geostationary Meteorological Satellite (GMS) is limited in the infrared window region (10.5 to 12.5 microns), it is impossible to determine the OLR flux exactly. Brightness temperature represents approximately OLR flux. Meterological Satellite Center (MSC) calculates average brightness temperature in every 2.5 degrees on the latitude/longitude grid. The contour maps of 5-day, monthly and past 3-month mean brightness temperature are produced and disseminated to the Long-range Forecast Division of the Japanese Meteorological Agency (JMA) via ADESS. Author

**N91-10370#** Meteorological Satellite Center, Tokyo (Japan).
**GPCP DATA PROCESSING c46**
Kazuhiro Oosawa *In its* Meteorological Satellite Center Technical Note. Special Issue (1989). Summary of GMS System. 2: Data Processing Mar. 1989 p 121-122 In JAPANESE; ENGLISH summary (For primary document see N91-10356 01-42)
Avail: NTIS HC/MF A08

It has been well recognized that latent heat with condensation of water vapor plays an important role in large scale atmospheric circulations. The Global Precipitation Climatology Project (GPCP) was planned as a part of the World Climate Research Program (WCRP) in 1984, and aims to estimate the spatial and temporal average of global precipitation. MSC has been producing the histogram data sets of Geostationary Meteorological Satellite (GMS) infrared radiance and their statistics since March 1984 and has been providing those data to the GPCP on a routine basis since March 1987. The data are sent to Geostationary Satellite Precipitation Data Center (GSPDC) to produce estimates of area-averaged monthly precipitation totals. Author

**N91-10371#** Meteorological Satellite Center, Tokyo (Japan).
**CLOUD GRID DATA c47**
Hideyuki Sasaki *In its* Meteorological Satellite Center Technical Note. Special Issue (1989). Summary of GMS System. 2: Data Processing Mar. 1989 p 123-139 In JAPANESE; ENGLISH summary (For primary document see N91-10356 01-42)
Avail: NTIS HC/MF A08

The cloud algorithm, which consists of clear sky radiance retrieval and cloud parameter retrieval, is based on Visible Infrared Spin-Scan Radiometer (VISSR) histogram data and clear sky radiance data which are produced at 0.25 degrees latitude by 0.25 degrees longitude segment in the area from 60 degrees N to 60 degrees S and 80 degrees E to 160 degrees W. Two correlative data are used. One is the modified profile of temperature which is theoretically calculated from output data of the numerical prediction model. Another is surface type classification data which is produced from the one year's data set of clear sky brightness temperatures from November 1984 to October 1985. The retrieved parameters (clear sky radiance, cloud amount and cloud top height), statistics of radiance data (mean, standard deviation, maximum, minimum, and mode of brightness temperature and albedo), and other data (the output code of the retrieval, land/sea flag, viewing geometry of a satellite and the sun) are stored in the cloud grid data. Author

**N91-10372#** Meteorological Satellite Center, Tokyo (Japan).
**SEA SURFACE TEMPERATURE c48**
Hideyuki Sasaki *In its* Meteorological Satellite Center Technical Note. Special Issue (1989). Summary of GMS System. 2: Data Processing Mar. 1989 p 141-145 In JAPANESE; ENGLISH summary (For primary document see N91-10356 01-42)
Avail: NTIS HC/MF A08

Sea Surface Temperature (SST) is theoretically estimated from the analyzed clear sky brightness temperature by the following steps. The first step is to correct an atmospheric attenuation from output data of the numerical prediction model using a radiative transfer model. This step is processed at 0.25 degrees latitude by 0.25 degrees longitude segment with 3-hour interval. The second step is to calculate 5-day or 10-day mean SST at 1 degree latitude by 1 degree longitude segment from SST of the first step. The third step is to check the quality of 5-day or 10-day mean SST using climatical SST. The last step is to produce the monthly mean SST from 10-day mean SST. Author

**N91-10373#** Meteorological Satellite Center, Tokyo (Japan).
**CLOUD AMOUNT DISTRIBUTION c47**
Kazuhiro Oosawa *In its* Meteorological Satellite Center Technical Note. Special Issue (1989). Summary of GMS System. 2: Data Processing Mar. 1989 p 147-154 In JAPANESE; ENGLISH summary (For primary document see N91-10356 01-42)
Avail: NTIS HC/MF A08

High (less than or equal to 400 mb), low (greater than 400 mb) and total cloud amount are derived operationally from the Geostationary Meteorological Satellite (GMS) infrared data in every 1 degree latitude/longitude grid. Anomaly of cloud amount was calculated from the normal value based on 9-years of GMS cloud amount data since July 1988. The contour maps of 5-day, monthly and past 3-month mean cloud amount and cloud amount anomaly are produced and disseminated. These data impart useful information for watching the climate system. Author

**N91-10374#** Meteorological Satellite Center, Tokyo (Japan).
**SATELLITE CLOUD INFORMATION CHART c43**
Tadashi Aso *In its* Meteorological Satellite Center Technical Note. Special Issue (1989). Summary of GMS System. 2: Data Processing Mar. 1989 p 155-163 In JAPANESE; ENGLISH summary (For primary document see N91-10356 01-42)
Avail: NTIS HC/MF A08

The Satellite Cloud Information Chart (SCIC) is designed to represent horizontal and vertical cloud distribution for domestic users. This is mainly used for short-range weather forecasting and aviational forecasting. SCIC is calculated by using Geostationary Meteorological Satellite (GMS) infrared data. There are two kinds of SCIC: one is the Satellite Cloud Information Chart in the Vicinity of Japan (SCIC-VJ); and the other is the Satellite Cloud Information Chart Far East (SCIC-FE). Cloud distribution in the SCIC-VJ is depicted with the combination of the mean Tbb contour lines, the hatched patterns of the maximum or minimum Tbb values. Symbols representing cloud types, developing/weakening and movement of cloud systems, and cloud patterns are added by man-machine interactive operation. SCIC-VJ is a chart of polar stereographic projection around Japan and the scale of mapping is 1/10,000,000. SCIC-VJ is disseminated 3-hourly to the Japanese Meteorological Agency (JMA) meteorological observatories and relevant institutions within 45 minutes after the satellite observations by the coded digital facsimile (CDF). Cloud distribution in the SCIC-FE is depicted with the cloud top height contour lines in feet and the hatched patterns of the categorized cloud area. SCIC-FE is a chart of Mercator projection and covers an area from equator to 60 degrees N and from 90 degree E to 170 degrees W. The scale of mapping is 1/25,000,000. SCIC-FE is disseminated 3-hourly within 50 minutes after the satellite observations by CDF. Author

**N91-10375#** Meteorological Satellite Center, Tokyo (Japan).
**DCP DATA PROCESSING c61**
Motoyasu Satoh *In its* Meteorological Satellite Center Technical Note. Special Issue (1989). Summary of GMS System. 2: Data Processing Mar. 1989 p 165-176 In JAPANESE; ENGLISH summary (For primary document see N91-10356 01-42)
Avail: NTIS HC/MF A08

The DCS is one of the Missions of the Geostationary Meteorological Satellite (GMS). This is the system which collects the environmental data on a real-time basis from Data Collection Platforms (DCP) installed at remote stations, ships, buoys and aircraft under wide ratio view of GMS. The data collected by the system are utilized in the Japanese Meteorological Agency (JMA) and in other domestic organizations, and are distributed to worldwide users through the Global Telecommunications System (GTS). The other Geostationary Satellites, namely, GOES East/West (U.S.A.) and METEOSAT (E.S.A) also collect the environmental data from their areas of responsibility. The international coordination between each satellite's data collection service are made at the conference of, The Coordination on Geostationary Meteorological Satellites (CGMS), which will be held each year. Here, the methods of DCP data processing at the Meteorological Satellite Center (MSC), are explained, and developments of DCS/DCP with their recent trends are introduced. Author

**N91-10376#** Joint Publications Research Service, Arlington, VA.
**JPRS REPORT: SCIENCE AND TECHNOLOGY. USSR: EARTH SCIENCES**
19 Mar. 1990 98 p Transl. into ENGLISH from various Russian articles
(JPRS-UES-90-006-L) Avail: NTIS HC/MF A05

Soviet reports in various areas of the earth sciences are compiled. The following subject areas are covered: geology and atmospheric physics. M.G.

**N91-10377#** Joint Publications Research Service, Arlington, VA.
**JPRS REPORT: SCIENCE AND TECHNOLOGY. USSR: EARTH SCIENCES**
27 Jul. 1990 20 p Transl. into ENGLISH from various Russian articles
(JPRS-UES-90-007) Avail: NTIS HC/MF A03

Abstracts of Soviet literature in various areas of the Earth sciences are compiled. The following subject areas are covered: Arctic and Antarctic research, oceanography, atmospheric physics, and ecology. M.G.

## 43 EARTH RESOURCES AND REMOTE SENSING

Includes remote sensing of earth resources by aircraft and spacecraft; photogrammetry; and aerial photography.

For instrumentation see *35 Instrumentation and Photography.*

**N91-10378*#** National Aeronautics and Space Administration. Goddard Space Flight Center, Greenbelt, MD.
**THE 1990 REFERENCE HANDBOOK: EARTH OBSERVING SYSTEM**
1990 154 p
(NASA-TM-102910; NAS 1.15:102910) Avail: NTIS HC/MF A08 CSCL 05B

An overview of the Earth Observing System (EOS) including goals and requirements is given. Its role in the U.S. Global Change Research Program and the International--Biosphere Program is addressed. The EOS mission requirements, science, fellowship program, data and information systems architecture, data policy, space measurement, and mission elements are presented along with the management of EOS. Descriptions of the facility instruments, instrument investigations, and interdisciplinary investigations are also present. The role of the National Oceanic and Atmospheric Administration in the mission is mentioned. M.G.

**N91-10379*#** Delaware Univ., Newark. College of Marine Studies.
**DOCUMENTATION FOR PROGRAM SOILSIM: A COMPUTER PROGRAM FOR THE SIMULATION OF HEAT AND MOISTURE FLOW IN SOILS AND BETWEEN SOILS, CANOPY AND ATMOSPHERE**
Richard T. Field 30 May 1990 50 p
(Grant NAG5-915)
(NASA-CR-186953; NAS 1.26:186953) Avail: NTIS HC/MF A03 CSCL 08B

SOILSIM, a digital model of energy and moisture fluxes in the soil and above the soil surface, is presented. It simulates the time evolution of soil temperature and moisture, temperature of the soil surface and plant canopy the above surface, and the fluxes of sensible and latent heat into the atmosphere in response to surface weather conditions. The model is driven by simple weather observations including wind speed, air temperature, air humidity, and incident radiation. The model intended to be useful in conjunction with remotely sensed information of the land surface state, such as surface brightness temperature and soil moisture, for computing wide area evapotranspiration. Author

**N91-10380#** Centre National d'Etudes Spatiales, Toulouse (France).
**GEOID AND DOPPLER INDUCED ERRORS ON THE ALTIMETER MEASUREMENT AND THEIR CORRECTION**
M. Dorrer and P. Raizonville 29 Aug. 1988 12 p
(CNES-CT/DRT/TIT/RL-88/226; ETN-90-97808) Avail: NTIS HC/MF A03

Doppler induced bias on altimetric measurement is studied. The Doppler effect is due to the relative velocity between the satellite and the points observed at the sea surface. A frame is defined and the radial velocities are computed. The effect of the measurement is estimated. The geometric effect and the Doppler effect are calculated. Corrections of errors are proposed. It is shown that the Doppler effect requires only the knowledge of the height derivative which is provided by the altimeter tracker. The geometric effect related to the geoid slopes can be large and requires the knowledge of the total slope of the geoid versus the ellipsoid, as well as a precise satellite horizontal localization. ESA

**N91-10361#** Meteorological Satellite Center, Tokyo (Japan).
**FAX IMAGE PROCESSING**
Yoshishige Shirakawa *In its* Meteorological Satellite Center Technical Note. Special Issue (1989). Summary of GMS System. 2: Data Processing Mar. 1989 p 53-65 In JAPANESE; ENGLISH summary (For primary document see N91-10356 01-42)
Avail: NTIS HC/MF A08

**N91-10374#** Meteorological Satellite Center, Tokyo (Japan).
**SATELLITE CLOUD INFORMATION CHART**
Tadashi Aso *In its* Meteorological Satellite Center Technical Note. Special Issue (1989). Summary of GMS System. 2: Data Processing Mar. 1989 p 155-163 In JAPANESE; ENGLISH summary (For primary document see N91-10356 01-42)
Avail: NTIS HC/MF A08

## 44 ENERGY PRODUCTION AND CONVERSION

Includes specific energy conversion systems, e.g., fuel cells; global sources of energy; geophysical conversion; and windpower.

For related information see also *07 Aircraft Propulsion and Power, 20 Spacecraft Propulsion and Power,* and *28 Propellants and Fuels.*

**N91-10381#** Eltron Research, Inc., Aurora, IL.
**METHANE CONVERSION BY SOLID ELECTROLYTE MEMBRANES Annual Report, 1 Jan. - 31 Dec. 1989**
Anthony F. Sammells, Ronald L. Cook, and Wayne L. Worrel (Pennsylvania Univ., Philadelphia.) Apr. 1990 34 p
(Contract GRI-5089-260-1824)
(PB90-226341; GRI-90/0136) Avail: NTIS HC/MF A03 CSCL 10A

The work has resulted in the identification of a new strategy for predicting perovskite solid electrolytes with the potential for achieving high ionic conductivities at intermediate temperatures. This approach is based in part upon identification of a clear relationship between the activation energy for ionic conduction in perovskite solid electrolytes and the free volume of their lattice structures, where free volume is defined as the difference between the volume of the perovskite crystallographic unit cell and the volumes occupied by the constituent ions resident at lattice sites. Other restrictions incorporated towards selection of perovskite solid electrolytes included: avoiding ionic radii mismatch between dopants and the ionic species they replace, and ensuring that the aliovalent dopant concentration within the perovskite lattice is below a level where introduced lattice vacancies become ordered, resulting in a decrease in ionic conductivity. This has resulted in the fabrication and preliminary testing of fuel cells operating at intermediate temperatures. GRA

**N91-10382#** Los Alamos National Lab., NM.
**THE PHYSICAL AND CHEMICAL STATE OF WESTINGHOUSE PHOSPHORIC ACID FUEL CELL ASSEMBLIES AFTER LONG TERM OPERATION: SURFACE AND NEAR-SURFACE ANALYSIS**
M. T. Paffett, W. Hutchinson, J. D. Farr, P. Papin, J. G. Beery, S. Gottesfeld, and J. Feret (Westinghouse Electric Corp., Pittsburgh, PA.) 1990 37 p Presented at the 178th Meeting of

Electrochemical Society, Inc., Seattle, WA, 14-19 Oct. 1990
(Contract W-7405-eng-36)
(DE90-015055; LA-UR-90-2538; CONF-901073-6) Avail: NTIS HC/MF A03

An attempt was made to correlate performance losses with materials compatibility and compositional changes in Phosphoric Acid Fuel Cell (PAFC) electrode assemblies as a function of operation time. Westinghouse PAFC stacks were run under a constant operating regime and portions of some of the single cells were analysed after stack operation for 5000 and 16,000 hrs along with appropriate reference samples. The PAFC assemblies were disassembled, sectioned where appropriate and analyzed using scanning and transmission electron microscopy (SEM and TEM), Rutherford backscattering spectroscopy (RBS), electron microprobe analysis (EMP), and x ray photoelectron spectroscopy (XPS). The profiles of the Pt catalyst in both the anode and the cathode layer did not show any preferential loss or peaking. The most pronounced change in cell composition detected following stack operation for 5000 and 16,000 hours was the increase in Pt/C ratio, that was related to loss of carbon from the cathode electrocatalyst. In contrast, the anode catalyst layer maintains the same ratio of Pt/C following 16,000 hours of operation. The loss of carbon is thought to occur by an electrochemical mechanism and is enhanced at the higher potentials experienced by the air cathode in the fuel cell. In addition, TEM results clearly demonstrate the well recognized phenomenon of Pt particle agglomeration in the cathode catalyst layer, which is seen to be quite substantial after 5000 hours of stack operation. The mechanical integrity of the assemblies was found to be quite satisfactory after 5000 hours, but much less so after 16,000 hours. Questions regarding carbon and Pt corrosion, Pt migration, and the mechanical and physical integrity of the PAFC structures are addressed and are all postulated to be contributing to the observed cell performance losses. DOE

**N91-10383#** GA Technologies, Inc., San Diego, CA.
**THERMIONIC CONVERTER EMITTER SUPPORT ARRANGEMENT Patent Application**
Daniel T. Allen, inventor (to DOE) Jul. 1989 18 p
(Contract DE-AC03-86SF-16298)
(DE90-015132; US-Patent-Appl-SN-376071; Patents-US-A7376071) Avail: NTIS HC/MF A03

A support is discussed which was provided for use in a thermionic converter to support an end of an emitter to keep it out of contact with a surrounding collector while allowing the emitter end to move axially as its temperature changes. The emitter end is supported by a spring structure that includes a pair of Belleville springs, and the spring structure is supported by a support structure fixed to the housing that includes the collector. The support structure is in the form of a sandwich with a small metal spring-engaging element at the front end, a larger metal main support at the rear end that is attached to the housing, and with a ceramic layer between them that is bonded by hot isostatic pressing to the metal element and metal main support. The spring structure can include a loose wafer captured between the Belleville springs. DOE

**N91-10384#** Midwest Research Inst., Golden, CO.
**MATERIALS ANALYSIS AND DEVICE OPTIMIZATION OF CuInSe2 SOLAR CELLS Technical Report, 16 Jan. 1987 - 15 Jan. 1989**
B. N. Baron, R. W. Birkmire, B. E. McCandless, M. Roy, J. E. Phillips, and W. N. Shafarman Jul. 1990 46 p Prepared in cooperation with Delaware Univ., Newark, DE
(Contract DE-AC02-83CH-10093)
(DE90-000365; SERI/TP-211-3896) Avail: NTIS HC/MF A04

This report presents results and conclusions from the two-year research program on CuInSe2 thin-film solar cells. The research was carried out in two integrated tasks: materials preparation and analysis, and high-efficiency solar cell fabrication and analysis. CuInSe2 thin-films were prepared by vacuum evaporation of elemental Cu, In, and Se onto heated substrates. Systematic studies of the effects of incident flux and substrate temperature on CuInSe2 film composition and morphology are presented. Mirror smooth CuInSe2 films are prepared using a newly developed aqueous bromine solution as a chemical polishing etch, and heterojunction photovoltaic devices with (CdZn)S, ITO/(CdZn)S, ZnO, and ZnO/(CdZn) window layer are fabricated and analyzed. The dominant recombination mechanism in high-efficiency CuInSe2 devices are found to be space-charge recombination in the CuInSe2. Optimized one-square-centimeter CuInSe2/(CdZn)S solar cells are fabricated with efficiencies over 10 percent. DOE

**N91-10385#** Argonne National Lab., IL.
**PROCEEDINGS OF THE 8TH SYMPOSIUM ON ENERGY ENGINEERING SCIENCES: MICRO/MACRO STUDIES OF MULTIPHASE MEDIA**
1990 254 p Symposium held in Argonne, IL, 9-11 May 1990
(Contract W-31-109-eng-38)
(DE90-014844; CONF-9005183) Avail: NTIS HC/MF A12

These proceedings include the program, list of participants, and the papers that were presented during the eight technical sessions. The central theme of this year's meeting was micro/macro studies of multiphase media and related topics. Each year a group of selected researchers in the DOE/BES Engineering Research Program are invited to present their research findings in such an open forum. By organizing around a central theme, principal investigators, their associates, and other interested parties are able to engage in discussions and share thoughts on subjects of common interests. To achieve these goals, the Engineering Research Program supports about one hundred and ten research projects covering a wide spectrum of topics cutting across traditional engineering disciplines with a focus on the following three areas: (1) mechanical sciences; (2) control systems and instrumentation; and (3) engineering data and analysis. The Eighth Symposium on Energy Engineering Sciences covered the review of approximately one-fourth of the total activities sponsored by the DOE/BES Engineering Research Program. DOE

**N91-10386#** Central Research Inst. of Electric Power Industry, Tokyo (Japan).
**BASIC STUDY OF SOLID OXIDE FUEL CELLS**
N. Mori, T. Hisamatsu, I. Yuri, T. Abe, and H. Ishikawa Nov. 1989 27 p In JAPANESE; ENGLISH summary
(DE90-517069; CRIE-W-89011) Avail: NTIS (US Sales Only) HC/MF A03

Together with prototypical making of cell and test unit of solid oxide fuel cell (SOFC), basic study was made about the development of cell. High temperature test portion proper, heat resistant property and high temperature strength being taken into consideration, was made of Si3N4. The cell was fixed and sealed at the fore end of support part, made of ZrO2, and inserted into the test portion proper. As a result of experiment, using hydrogen as fuel, the test unit was confirmed to be able to safely and simply test air and fuel at the SOFC operation range of temperature, 800 to 1100 centigrade. Cell, prototypically made by dipping is not good because electrolyte has open air holes having crossleak occur. Cell which is tape formed by doctor blade or press formed of partially stabilized zirconia, coprecipitated has small contact area between collecting electrode and electrode, and is so small in output power that further heightening is necessary in performance. DOE

**N91-10387#** New Energy Development Organization, Tokyo (Japan).
**SURVEY OF POSSIBILITY FOR VOLCANIC ENERGY DEVELOPMENT**
Mar. 1990 315 p In JAPANESE; ENGLISH summary
(DE90-517230; NEDO-P-8912) Avail: NTIS (US Sales Only) HC/MF A14

Volcanic areas, clarification of heat source structure, evaluation of resources and problems on utilization techniques were arranged to search the possibility of future volcanic heat source. It is necessary to improve the exploration accuracy by combining geophysical exploration with geological and geochemical surveys in order to explorate a magma reservoir. Especially, seismic exploration is effective. The surveying procedure is as follows: confirmation of magma existence and grasping the whole image, evaluation of resources, clarification of three-dimensional distribution of magma in a promising area, and heat structure survey by heat flow measurement and others to construct more accurate model for resources. This model is verified finally by practical drilling. Promising areas which are worthy of development, are active volcanic areas in Kyushu, Hakkoda nad Hokkaido. It is desirable to make drilling to the depth of 3 km or magma reservoir to develop the future heat source. It is also required to improve the thermal resistance and corrosion resistance of materials to be used. Heat extraction by a single well is most realistic and the closed coaxial double pipe heat exchanger or open heat exchanger in the well will be used to improve the extraction. DOE

**N91-10388#** Pacific Northwest Lab., Richland, WA.
**THERMAL ENERGY STORAGE FOR POWER GENERATION APPLICATIONS**
M. K. Drost, Zen I. Antoniak, and D. R. Brown Mar. 1990 7 p
Presented at the American Power Conference, Chicago, IL, 23-25 Apr. 1990
(Contract DE-AC06-76RL-01830)
(DE90-016539; PNL-SA-17992; CONF-9004133-4) Avail: NTIS HC/MF A02

Studies strongly indicate that the United States will face widespread electrical power constraints in the 1990s. In many cases, the demand for increased power will occur during peak and intermediate demand periods. While natural gas is currently plentiful and economically attractive for meeting peak and intermediate loads, the development of a coal-fired peaking option would give utilities insurance against unexpected supply shortages or cost increases. This paper discusses a conceptual evaluation of using thermal energy storage (TES) to improve the economics of coal-fired peak and intermediate load power generation. The use of TES can substantially improve the economic attractiveness of meeting peak and intermediate loads with coal-fired power generation. In this case, conventional pulverized coal combustion equipment is continuously operated to heat molten nitrate salt, which is then stored. During peak demand periods, hot salt is withdrawn from storage and used to generate steam for a Rankine steam power cycle. This allows the coal-fired salt heater to be approximately one-third the size of a coal-fired boiler in a conventional cycling plant. The general impact is to decouple the generation of thermal energy from its conversion to electricity. The present study compares a conventional cycling pulverized coal-fired power plant to a pulverized coal-fired plant using nitrate salt TES. The study demonstrates that a coal-fired salt heater is technically feasible and should be less expensive than a similar coal-fired boiler. The results show the use of nitrate salt TES reduced the levelized cost of power by between 5 and 24 percent, depending on the operating schedule. DOE

**N91-10389#** National Aerospace Lab., Tokyo (Japan).
**A SYSTEM DESIGN AND DEMONSTRATIVE FIELD TEST OF WIND TURBINE WITH A 14 m DIAMETER ROTOR**
Masataka Hashidate, Tadashi Ito, Asao Hanzawa, Osamu Nonaka, Tosio Nohara, Yukio Komatsu, and Hiroshi Endo Feb. 1990 41 p In JAPANESE; ENGLISH summary
(NAL-TR-1056; ISSN-0389-4010) Avail: NTIS HC/MF A03

The National Aerospace Laboratory participated in a comprehensive program for developing the technology for conversion and storage of wind energy which was promoted by the Science and Technology Agency of Japan, undertaking the research and development of a horizontal axis type wind turbine with a 14 m dia. rotor. The system design, the ground-based hybrid dynamic simulation, and the demonstrative field test of the 14 m Wind Turbine is described. The test results confirm the following characteristics: (1) The minimum operational wind speed is as low as 3 m/s; (2) The rotational speed is kept almost constant within the accuracy of + or -4/min; (3) The output-power is 22 kW on the rotor axis at the rated wind speed of 8 m/s; (4) The maximum aerodynamics power coefficient is about 48 percent at the operational pitch angle; and (5) The maximum rate of heat generation is 5.2 x 10(exp 4) kJ/hr at a wind speed of 10 m/s. Author

**N91-10390#** Deutsche Forschungsanstalt fuer Luft- und Raumfahrt, Stuttgart (Germany, F.R.). Fachgruppe Solare Energietechnik.
**DESIGN OF HIGHLY CONCENTRATING SOLAR COLLECTORS AND SOLAR COLLECTOR SYSTEMS**
Rainer Koehne Mar. 1990 61 p In GERMAN; ENGLISH summary Report will also be announced as translation (ESA-TT-1224)
(DLR-FB-90-11; ISSN-0171-1342; ETN-90-97626) Avail: NTIS HC/MF A04; DLR, VB-PL-DO, Postfach 90 60 58, 5000 Cologne, Fed. Republic

The influence of the configuration of symmetric and unsymmetric concentration solar collector systems and of their optical quality on the maximum obtainable thermal efficiency was investigated. The optimization is made in relation to the aperture diameter and shape of the cavity. Receiver codes CIRCE and CAV2 are used in a parameter study. Efficiencies of 70 percent are obtained at absorber temperatures between 800 to 1000 C with a single dish of systems composed of many dishes. At higher temperatures, only the single dish is suitable. Optimized receiver aperture diameters can increase the efficiency by 5 to 10 percent. ESA

# 45 ENVIRONMENT POLLUTION

Includes atmospheric, noise, thermal, and water pollution.

**N91-10391#** Environmental Protection Agency, Annapolis, MD. Chesapeake Bay Program.
**CHESAPEAKE BAY BASIN MONITORING PROGRAM ATLAS. VOLUME 1: WATER QUALITY AND OTHER PHYSIOCHEMICAL MONITORING PROGRAMS**
Patricia Heasly, Susan Pultz, and Richard Batiuk Aug. 1989 434 p
(PB90-147935; CBP/TRS-34/89-Vol-1) Avail: NTIS HC/MF A19 CSCL 13B

The Monitoring Program Atlas provides an overview of current long term environmental monitoring programs in the Chesapeake Bay Basin. The Atlas covers a wide scope of program types, ranging from water quality, living resources, toxics, and physical processes to air quality, acid deposition, and climate monitoring programs. The two volume publication is intended to facilitate coordination and integration of environmental monitoring programs and to encourage the collection of comparable monitoring data basinwide. Author

**N91-10392#** Environmental Protection Agency, Annapolis, MD. Chesapeake Bay Program.
**CHESAPEAKE BAY BASIN MONITORING PROGRAM ATLAS. VOLUME 2: BIOLOGICAL AND LIVING RESOURCE MONITORING PROGRAMS**
Patricia Heasly, Susan Pultz, and Richard Batiuk Aug. 1989 334 p
(PB90-147943; CBP/TRS-35/89-Vol-2) Avail: NTIS HC/MF A15 CSCL 13B

The Monitoring Atlas provides an overview of current long term environmental monitoring programs in the Chesapeake Bay Basin. The Atlas covers a wide scope of program types, ranging from water quality, living resources, toxics, and physical processes to air quality, acid deposition, and climate monitoring program. This volume of the two volume set covers bacteriology, phytoplankton, zooplankton, benthos, aquatic vegetation, shellfish, finfish, and waterfowls and other birds. Author

**N91-10393*#** National Aeronautics and Space Administration, Washington, DC.

**ATMOSPHERIC OZONE 1985: ASSESSMENT OF OUR UNDERSTANDING OF THE PROCESSES CONTROLLING ITS PRESENT DISTRIBUTION AND CHANGE, VOLUME 3**

1990 558 p Prepared in cooperation with World Meteorological Organization, Geneva, Switzerland; FAA, Washington, DC; NOAA, Rockville, MD; and United Nations Environment Program, New York Original contains color illustrations
(NASA-TM-103462; NAS 1.15:103462; PB90-181504; WMO-16-Vol-3) Avail: NTIS HC/MF A24 CSCL 13B

The types of atmospheric models used in the assessment of possible chemical perturbations to the stratosphere are reviewed. The status of photochemical modelling efforts, trends in the ozone and atmospheric temperature, and a hierarchy of tests for photochemical models are presented. Several one-dimensional model predictions for scenarios in steady-state or time dependent approximations are examined, and calculations for a small number of two-dimensional steady-state predictions for a limited number of scenarios are performed. Greenhouse forcing of the climate system due to the growth of a number of trace gases is discussed. This phenomenon is quantitatively illustrated by estimating the decadal increment in greenhouse forcing for several trace gases and comparing this with the forcing due to increasing CO2 in the same decade. Several appendices included in the document are kinetics and photochemical data base, spectroscopic data base--infrared to microwave, instrument intercomparisons and assessments, monthly mean distribution of ozone and temperature, chemical formulas and nomenclature, and a pressure-altitude chart. M.G.

**N91-10394#** Environmental Protection Agency, Washington, DC. Office of Policy, Planning, and Evaluation.

**POTENTIAL EFFECTS OF GLOBAL CLIMATE CHANGE ON THE UNITED STATES. APPENDIX C: AGRICULTURE, VOLUME 1 Final Report**

Joel B. Smith, ed. and Dennis A. Tirpak, ed. May 1989 302 p
(PB90-171588; EPA/230/05-89/053-App-C-Vol-1) Avail: NTIS HC/MF A14 CSCL 13B

Back-up research studies are presented for the Potential Effects of Global Climate Change on the United States report for Congress (1989). Volume 1 of the studies presents simulated potential effects of global climate change on agriculture in the Great Lakes Region, the Southeastern United States, California, and the Great Plains States. Economic and water irrigation effects for particular regions are included. Author

**N91-10395#** Environmental Protection Agency, Washington, DC. Office of Policy, Planning, and Evaluation.

**POTENTIAL EFFECTS OF GLOBAL CLIMATE CHANGE ON THE UNITED STATES. APPENDIX A: WATER RESOURCES Final Report**

Joel B. Smith, ed. and Dennis A. Tirpak, ed. May 1989 333 p
(PB90-171968; EPA/230/05-89/051-App-A) Avail: NTIS HC/MF A15 CSCL 13B

Areas of discussion are: interpretation of hydrologic effects of climate change in the Sacramento-San Joaquin River Basin, methods for evaluating the potential impacts of global climate change in California and Georgia; impacts of climate change on the salinity of San Francisco Bay; effects of climate changes on the Laurentian Great Lakes levels; the impact of global warming on the Great Lakes' ice cycles; potential climate changes to the Lake Michigan thermal structure; effects of climate warming on Lake Erie water quality; impacts of global warming on runoff in the upper Chattahoochee River Basin; and potential impacts of climate change on the Tennessee Valley Authority Reservoir System. Author

**N91-10396#** Environmental Protection Agency, Washington, DC. Office of Policy, Planning, and Evaluation.

**POTENTIAL EFFECTS OF GLOBAL CLIMATE CHANGE ON THE UNITED STATES. APPENDIX B: SEA LEVEL RISE Final Report**

Joel B. Smith, ed. and Dennis A. Tirpak, ed. May 1989 274 p
(PB90-172628; EPA/230/05-89/052-App-B) Avail: NTIS HC/MF A12 CSCL 13B

Back-up research studies are presented for the Potential Effects of Global Climate Change on the United States report for Congress (1989). The following topics are discussed: the effects of sea level rise on U.S. Coastal Wetlands; a national assessment of beach nourishment requirements associated with accelerated sea level rise; the cost of defending developed shorelines along sheltered waters of the United States from a two meter rise in mean sea level; and the cost of not holding back the sea (phase 1 economic vulnerability). An overview of the nationwide impacts of sea level rise is presented. Author

**N91-10397#** Environmental Protection Agency, Washington, DC. Office of Policy, Planning, and Evaluation.

**POTENTIAL EFFECTS OF GLOBAL CLIMATE CHANGE ON THE UNITED STATES. APPENDIX C: AGRICULTURE, VOLUME 2 Final Report**

Joel B. Smith, ed. and Dennis A. Tirpak, ed. May 1989 236 p
(PB90-171596; EPA/230/05-89/053-App-C-Vol-2) Avail: NTIS HC/MF A11 CSCL 13B

Back-up research studies are presented for the Potential Effects of Global Climate Change on the United States report for Congress (1989). Volume 2 of the studies includes effects of climate changes on agriculture. The studies include: direct (physiological) effects of increasing CO2 on crop plants and their interactions with indirect (climatic) effects; potential effects of climate change on plant-pest interactions; impacts of climate change on the transport of agricultural chemicals across the USA Great Plains and Central Prairie; farm-level adjustments by Illinois corn producers to climate change; changing animal disease patterns induced by the greenhouse effect; the effect of climatic warming on populations of the horn fly with associated impact on weight gain and milk production in cattle; and the agricultural policies for climate changes induced by greenhouse gases. Author

**N91-10398#** Environmental Protection Agency, Washington, DC. Office of Policy, Planning, and Evaluation.

**POTENTIAL EFFECTS OF GLOBAL CLIMATE CHANGE ON THE UNITED STATES. APPENDIX D: FORESTS Final Report**

Joel B. Smith, ed. and Dennis A. Tirpak, ed. May 1989 235 p
(PB90-173238; EPA/230/05-89/054-App-D) Avail: NTIS HC/MF A11 CSCL 13B

Back-up research studies are presented for the Potential Effects of Global Climate Change on the United States report for Congress (1989). The studies include: assessment of the response of vegetation to future climate change through ecological response surfaces and paleoecological model validation; the effects of climate change on the forests of the Great Lakes Region, California, and the Southeastern United States; and ancient analogs for greenhouse warming of central California. Author

**N91-10399#** Environmental Protection Agency, Washington, DC. Office of Policy, Planning, and Evaluation.

**POTENTIAL EFFECTS OF GLOBAL CLIMATE CHANGE ON THE UNITED STATES. APPENDIX E: AQUATIC RESOURCES Final Report**

Joel B. Smith, ed. and Dennis A. Tirpak, ed. May 1989 182 p
(PB90-172297; EPA/230/05-89/055-App-E) Avail: NTIS HC/MF A09 CSCL 13B

Back-up research studies are presented for the Potential Effects of Global Climate Change on the United States report for Congress (1989). The studies include: the effects of global climate change on the water quality of mountain lakes and streams; potential responses of Great Lakes' fishes and their habitat to global climate warming; ecological effects of global climate change and the wetland resources of San Francisco Bay; and the projected changes in estuarine conditions based on models of long-term atmospheric alteration. Author

**N91-10400#** Environmental Protection Agency, Washington, DC. Office of Policy, Planning, and Evaluation.
**POTENTIAL EFFECTS OF GLOBAL CLIMATE CHANGE ON THE UNITED STATES. APPENDIX F: AIR QUALITY Final Report**
Joel B. Smith, ed. and Dennis A. Tirpak, ed. May 1989 209 p
(PB90-172230; EPA/230/05-89/056-App-F) Avail: NTIS HC/MF A10 CSCL 13B

Back-up research studies are presented for the Potential Effects of Global Climate Change on the United States report for Congress (1989). The studies included are climate change and its interactions with air chemistry, and sensitivity of a regional oxidant model to variations in climate parmeters. Author

**N91-10401#** Environmental Protection Agency, Washington, DC. Office of Policy, Planning, and Evaluation.
**POTENTIAL EFFECTS OF GLOBAL CLIMATE CHANGE ON THE UNITED STATES. APPENDIX G: HEALTH Final Report**
Joel B. Smith, ed. and Dennis A. Tirpak, ed. May 1989 109 p
(PB90-173881; EPA/230/05-89/057-App-G) Avail: NTIS HC/MF A06 CSCL 13B

Health research studies are given for the Potential Effects of Global Climate Change on the United States report for Congress (1989). The studies include: the impact of CO2 and trace gas-induced climate changes upon human mortality; computer simulation of the effects of changes in weather patterns on vector-borne disease transmission; and the potential impact of climate change on patterns of infectious disease in the United States. Author

**N91-10402#** Environmental Protection Agency, Washington, DC. Office of Policy, Planning, and Evaluation.
**POTENTIAL EFFECTS OF GLOBAL CLIMATE CHANGE ON THE UNITED STATES. APPENDIX H: INFRASTRUCTURE Final Report**
Joel B. Smith, ed. and Dennis A. Tirpak, ed. May 1989 179 p
(PB90-172313; EPA/230/05-89/058-App-H) Avail: NTIS HC/MF A09 CSCL 13B

Back-up research studies are presented for the Potential Effects of Global Climate Change on the United States report for Congress (1989). The studies include: the potential effects of climate change on regional and national demands for electricity; impact of global climate change on urban infrastructure; impacts of extremes in Lake Michigan levels along Illinois shoreline low levels; and the effect of climate change on shipping within Lake Superior and Lake Erie. Author

**N91-10403#** Environmental Protection Agency, Washington, DC. Office of Policy, Planning, and Evaluation.
**POTENTIAL EFFECTS OF GLOBAL CLIMATE CHANGE ON THE UNITED STATES. APPENDIX I: VARIABILITY Final Report**
Joel B. Smith, ed. and Dennis A. Tirpak, ed. May 1989 110 p
(PB90-173899; EPA/230/05-89/059-App-I) Avail: NTIS HC/MF A06 CSCL 13B

Weather variability research studies are presented for the Potential Effects of Global Climate Change on the United States report for Congress (1989). The studies include: an analysis of climate variability in general circulation models, comparison with observations and changes in variability in 2 x CO2 experiments, and the change in climate variability in the 21st century. Author

**N91-10404#** Environmental Protection Agency, Washington, DC. Office of Policy, Planning, and Evaluation.
**POTENTIAL EFFECTS OF GLOBAL CLIMATE CHANGE ON THE UNITED STATES. APPENDIX J: POLICY Final Report**
Joel B. Smith, ed. and Dennis A. Tirpak, ed. May 1989 190 p
(PB90-173188; EPA/230/05-89/060-App-J) Avail: NTIS HC/MF A09 CSCL 13B

Back-up research studies are presented for the Potential Effects of Global Climate Change on the United States report for Congress (1989). The studies include: societal responses to regional climate change (forecasting by analogy); climate change perceptions among natural resource decision-makers in the case of water supply managers; applicability of Federal long-range planning and environmental impact statement processes to global climate change issues; climate change and water resources in the Sacramento-San Joaquin region of California (policy adjustment options); effects of global warming on the implications for policies and institutions in the Great Lakes Region; policy implications of global climate change impacts upon the Tennessee Valley Authority Reservoir System, Apalachicola River esturary and bay, and South Florida. Author

**N91-10405#** Council on Environmental Quality, Washington, DC.
**NATIONAL ACID PRECIPITATION ASSESSMENT PROGRAM. REPORT TO THE PRESIDENT AND CONGRESS Annual Report, 1988**
13 Jan. 1989 98 p
(PB90-185646) Avail: NTIS HC/MF A05 CSCL 13B

The Acid Precipitation Act of 1980 established the Interagency Task Force on Acid Precipitation to develop and implement the National Acid Precipitation Assessment Program (NAPAP). The purpose of NAPAP is to increase the authors understanding of the causes and effects of acidic deposition, and to produce scientific information to support decision making regarding acidic deposition control and abatement strategies. The report, the Program's seventh, is divided into three major sections. The first section described the Program's organizational structure, external coordination activities, peer reviews, and budgetary status. It also includes a discussion of the NAPAP assessment process, and provides a synopsis of NAPAP's plan and schedule for 1989 and 1990 assessment reports. Author

**N91-10406#** Oak Ridge National Lab., TN. Energy Div.
**SHORT-ROTATION WOODY CROP OPPORTUNITIES TO MITIGATE CARBON DIOXIDE BUILDUP**
L. L. Wright, R. L. Graham, and A. F. Turhollow 1990 19 p
Presented at the North American Conference on Forestry Responses to Climate Change, Washington, DC, 15-17 May 1990
(Contract DE-AC05-84OR-21400)
(DE90-016526; CONF-9005261-1) Avail: NTIS HC/MF A03

Short-rotation woody crops (SRWC) have a significant potential for permanently mitigating carbon dioxide buildup in the atmosphere. The greatest benefit can be derived from growing large amounts of woody crops dedicated to substitute for fossil energy resources. Assuming current production and conversion technologies and a conservative estimate of the viable U.S. land base (35 million acres), SRWC energy could displace 34 to 67 million tons of fossil carbon releases, 3 to 5 percent of current annual U.S. emissions. Assuming predicted technology advancements and a high estimate of the U.S. land base available for SRWC (103 million acres), SRWC energy could displace 272 to 470 million tons of annual fossil fuel carbon releases. The carbon mitigation potential of SRWC-based electricity production would be equivalent to about 7.5 percent of current global fossil fuel emissions and 35 percent of current total U.S. fossil fuel emissions. This document discusses the strategies to mitigate carbon dioxide in the atmosphere. Topics include planting new trees, managing forests, improving forest utilization and using wood as a renewable energy source to replace fossil fuels. DOE

**N91-10407#** Brookhaven National Lab., Upton, NY. Environmental Chemistry Div.
**GLOBAL AND REGIONAL ENVIRONMENTAL ATMOSPHERIC CHEMISTRY**
Leonard Newman, comp. and ed., Wenxing Wang, comp. and ed., and C. S. Kiang, comp. and ed. (Georgia Inst. of Tech., Atlanta.) Aug. 1990 773 p Presented at the International Conference on Global and Regional Environmental Atmospheric Chemistry, Beijing, China, 3-10 May 1989
(Contract DE-AC02-76CH-00016)
(DE90-016693; CONF-890525) Avail: NTIS HC/MF A99

More than two hundred fifty scientists from eighteen different countries attended the first International Conference on Global and Regional Environmental Atmospheric Chemistry in the Science Hall of Friendship Hotel at Beijing, May 3 to 10, 1989. This volume documents the proceedings of this historical event. Following the meeting, some 173 papers were submitted for this publication. When follow up papers were not submitted the original abstract is presented. Also included are abstracts of the posters presented by the Chinese participants who could not be accommodated during the more formal sessions. We might add that this more informal session was particularly useful for the exchange of ideas and information between east and west. Indeed, the conference overall certainly provided an enthusiastic platform for interactions among scientists from around the world. It is our hope that these proceedings will serve as a vehicle to further enhance collaboration for joint studies of the changes in the global environment. DOE

**N91-10408#** Oak Ridge National Lab., TN.
**RESEARCH ON CLIMATE CHANGE**
Tommy Ray Nelson 23 Aug. 1990 5 p Presented at the International Symposium on Climate Change with the Academy of Sciences, Beijing, Peoples Rep. of China, 8-13 Aug. 1990
(Contract DE-AC05-84OR-21400)
(DE90-016726; ORNL/FTR-3714) Avail: NTIS HC/MF A01

The objective of the August 8 to 13 visit to Beijing, People's Republic of China (PRC), was to assist with research under the joint U.S. Department of Energy (DOE)/PRC Academia Sinica agreement ANNEX 3 to the Protocol on Fossil Energy Research and Development on Cooperation in the Field of Atmospheric Trace Gases, Article 3 — Means of Cooperation, signed August 19, 1987, on carbon dioxide and climate research. Assistance was given in the form of technical expertise in the design and implementation of data acquisition, certification, and analysis systems. These systems consisted of personal computers running database management software, FORTRAN, and graphics software. This report gives relevant background information and summarizes the traveler's activities as they relate to the installation of the computer systems in Beijing. DOE

**N91-10409#** Lawrence Livermore National Lab., CA.
**GLOBAL TROPOSPHERIC CHEMISTRY MODELING**
Joyce E. Penner Aug. 1990 8 p Presented at the National Academy of Sciences Committee on Atmospheric Change, Washington, DC, 25-26 Sep. 1990 Submitted for publication
(Contract W-7405-eng-48)
(DE90-015908; UCRL-JC-104734; CONF-9009240-1) Avail: NTIS HC/MF A02

To build a National Energy Strategy that is respectful of the environment, the effects of fossil fuel emissions on atmospheric chemistry and climate must be understood. Because many of the important effects involve species whose lifetimes are short compared to mixing times in the atmosphere, the further advancement of our understanding of the effects of these species requires the development of three-dimensional models. The development of 3-D models has been limited because of the lack of computer resources, the lack of relevant observations, and the lack of funding. However, with the development of the U.S. Global Change Program and with the increased speed and availability of today's computers it is now possible to build models capable of describing the effects of these shorter-lived pollutants on a global basis. The Atmospheric Microphysics and Chemistry group has focussed on the development of three-dimensional Lagrangian models capable of running in a coupled mode with a climate model, as a tool for understanding the atmospheric cycles of these species. We have developed a Lagrangian chemistry model that is capable of running interactively with a global general circulation model. Distinct versions of the Lagrangian model with varying degrees of sophistication have been used to treat different chemical cycles. Additional funding is needed to extend capabilities to treat the full suite of species necessary to understand ambient aerosol concentrations and the effects of aerosols on climate. DOE

# 46 GEOPHYSICS

Includes aeronomy; upper and lower atmosphere studies; ionospheric and magnetospheric physics; and geomagnetism.

For space radiation see *93 Space Radiation.*

**N91-10410** Utah State Univ., Logan.
**STUDIES OF THE SYSTEM-ENVIRONMENT INTERACTION BY ELECTRON BEAM EMISSION FROM A SOUNDING ROCKET PAYLOAD IN THE IONOSPHERE Ph.D. Thesis**
Neil Brubaker Myers 1989 176 p
Avail: Univ. Microfilms Order No. DA9015024

The CHARGE-2 sounding rocket payload was designed to measure the transient and steady-state electrical charging of a space vehicle at low-Earth-orbit altitudes during the emission of a low-power electron beam from the vehicle. In addition to the electron gun, the payload contained several diagnostics to monitor plasma and waves resulting from the beam/space/vehicle interaction. The payload was separated into two sections, the larger section carried a 1-keV electron gun and was referred to as the mother vehicle. The smaller section, referred to as the daughter, was connected to the mother by an insulated, conducting tether and was deployed to a distance of up to 426 m across the geomagnetic field. Payload stabilization was obtained using thrusters that released cold nitrogen gas. In addition to performing electron beam experiments, the mother vehicle contained a high-voltage power supply capable of applying up to +450 V and 28 mA to the daughter through the tether. Steady-state potentials of up to 560 V were measured for the mother vehicle. The daughter attained potentials of up to 1000 V relative to the background ionosphere and collected currents up to 6.5 mA. Thruster firings increased the current collection to the vehicle firing the thrusters and resulted in neutralization of the payload. The CHARGE-2 experiment was unique in that for the first time a comparison was made of the current collection between an electron beam-emitting vehicle and a non-emitting vehicle at high potential.
Dissert. Abstr.

**N91-10411#** National Geophysical Data Center, Boulder, CO.
**SOLAR-GEOPHYSICAL DATA NUMBER 548, APRIL 1990. PART 1: (PROMPT REPORTS). DATA FOR MARCH, FEBRUARY 1990, AND LATE DATA**
H. E. Coffey Apr. 1990 160 p
(PB90-226028; SGD-548-Pt-1) Avail: NTIS HC/MF A08 CSCL 04A

A detailed index is presented for 1989 and 1990. Data for March 1990 include: Solar terrestrial environment; IUWDS alert periods (advance and worldwide); Solar activity indices; Solar flares; Solar radio emission; and Stanford mean solar magnetic field. Data for February include: Solar active regions; Sudden ionospheric disturbances; Solar radio spectral observations; Cosmic ray measurements by neutron counter; and Geomagnetic indices. Late data include: Solar radio emission for Feb. 1990; Cosmic rays Climax and Huancayo for Jan. 1990; Printer's error for Nov. and Dec. 1989; and Data reprint of Halftone images of Kitt Peak solar magnetic field synoptic charts rotations 1822 and 1823. Author

**N91-10412#** National Geophysical Data Center, Boulder, CO.
**SOLAR-GEOPHYSICAL DATA NUMBER 548, APRIL 1990. PART 2: (COMPREHENSIVE REPORTS). DATA FOR OCTOBER 1989 AND MISCELLANEOUS**
H. E. Coffey Apr. 1990 99 p
(PB90-226036; SGD-548-Pt-2) Avail: NTIS HC/MF A05 CSCL 04A

A detailed index is presented for 1989 and 1990. Data for October 1898 include: Solar flares; Solar radio bursts at fixed frequencies; Solar x ray radiation from GOES satellite; Mass ejections from the sun; and Active prominences and filaments. Miscellaneous data include: Meudon carte synoptique Carrington rotation 1819 Aug. 1989; Active regions and filaments; and Synoptic solar map. Author

**N91-10413#** National Oceanic and Atmospheric Administration, Boulder, CO. Wave Propagation Lab.

**MODEL OF GRAVITY-WAVE-INDUCED VARIABILITY AND TURBULENCE IN THE STRATIFIED FREE ATMOSPHERE**

C. W. Fairall Apr. 1990 70 p
(PB90-235482; NOAA-TM-ERL-WPL-179) Avail: NTIS HC/MF A04 CSCL 04A

The consequences are examined of using a vertical wavenumber spectral model to describe variations of vertical profiles of atmospheric variables (horizontal and vertical wind, temperature, and other scalars) about a mean profile. At high wavenumbers the model exhibits a wavenumber to the -3 dependence, which is characteristic of a continuum of internal gravity waves whose amplitudes are controlled by a breaking process. By employing a random phase between wavenumber amplitude components, a reverse Fourier transform of the spectrum yields simulated profiles of velocity and thermal variability as well as shear and Brunt-Vaisala frequency variability. The horizontal wind components of shear and the Brunt-Vaisala frequency exhibit Gaussian distributions. For a typical tropospheric condition, the average turbulent layer thickness turns out to be about 35 m and about 20 percent of the troposphere appears to be actively turbulent. The majority of the turbulent layers appear to be due to autoconvective overturning instead of Kelvin-Helmholtz dynamic instability. Author

**N91-10414#** National Weather Service, Fort Worth, TX.

**Q-VECTORS: A NEW APPROACH TO AN OLD PROBLEM**

E. T. Prater May 1990 23 p
(PB90-235490; NOAA-TM-NWS-SR-129) Avail: NTIS HC/MF A03 CSCL 04A

Many forecasters infer synoptic-scale vertical motion from the traditional form of the quasi-geostrophic omega equation, which relates vertical motion to fields of thickness and vorticity advection. The brief paper discusses the weaknesses typically involved in real-time interpretation of this form of the equation and acquaints the reader with an alternative form which greatly simplifies the task of inferring synoptic-scale vertical motion. GRA

**N91-10415#** Transportation Research Board, Washington, DC.

**GEOTECHNICAL ENGINEERING, 1989**

R. J. Fragaszy, D. Argo, and J. D. Higgins 1989 192 p
(PB90-222159; TRB/TRR-1219; LC-90-5427; ISBN-0-309-04815-X) Avail: NTIS HC/MF A09 CSCL 08G

The 16 papers in the report deal with the following areas: Comparison of Formula Predictions with Pile Load Tests; Study of Dynamic Methods of Predicting Pile Axial Load Capacity by Louisiana Department of Transportation and Development; Analysis of Drilled Piers Used for Slope Stabilization; Analytical Study of Laterally Loaded Cast-in-Drilled-Hole Piles; Bolted Connections of Rib-Plate Structures; Validation of Correlations Between a Number of Penetration Tests and In Situ California Bearing Ratio Tests: Class C Fly Ash as a Full or Partial Replacement for Portland Cement or Lime; Accelerated Curing of Fly Ash-Lime Soil Mixtures; Frost Resistance of Lime-Stabilized Clay Soil; Stabilization of Expansive Clay Soils; Expansion of Cement-Stabilized Minestone due to the Oxidation of Pyrite; Field Measurement of Shrinkage Crack Depth in Expansive Soils; Evaluation of AGWA-II Thermal Conductivity Sensors for Soil Suction Measurement; Pore Fluid Effects on the Fabric and Hydraulic Conductivity of Laboratory-Compacted Clay; Organically Modified Clays; and Diffusion of Contaminants Through Waste Containment Barriers. GRA

**N91-10416#** Environmental Protection Agency, Research Triangle Park, NC. Atmospheric Research and Exposure Assessment Lab.

**THE INTERNATIONAL SODAR INTERCOMPARISON EXPERIMENT**

J. E. Gaynor, C. B. Baker, and J. C. Kaimal (National Oceanic and Atmospheric Administration, Boulder, CO.) 1990 11 p
(PB90-246224; EPA/600/D-90/069) Avail: NTIS HC/MF A03 CSCL 04A

Preliminary results are presented from the International Sodar Intercomparison Experiment (ISIE). Twenty-minute mean wind speeds and directions from a variety of sodar systems compare well with measurements on the 300 m BAO tower, as they did in an earlier comparison experiment at the site. The vertical velocity standard deviations compare better than they did before, but the horizontal wind standard deviations showed no improvement. Author

**N91-10417#** European Space Agency, Paris (France).

**SPACE PLASMA PHYSICS INVESTIGATIONS BY CLUSTER AND REGATTA**

E. J. Rolfe, ed. May 1990 165 p International workshop held in Graz, Austria, 20-22 Feb. 1990; sponsored by Academy of Sciences, Graz, Austria; ESTEC, Noordwijk, Netherlands; Academy of Sciences (USSR), Moscow; Intercosmos Council; and Technical Univ., Graz, Austria
(ESA-SP-306; ISBN-92-9092-066-1; ISSN-0379-6566; ETN-90-97587) Copyright Avail: NTIS HC/MF A08; EPD, ESTEC, Noordwijk, Netherlands HC 40 Dutch guilders

Space plasma measurements to be undertaken by the Cluster/Regatta mission are addressed. Specific studies relate to shocks, turbulence studies and waves (sheath, solar wind, foreshock), cusp, magnetopause and boundary layers, magnetotail and plasma sheet, and radiowave remote sensing. Reference is made to data obtained from AMPTE (Active Magnetospheric Particle Tracer Explorer) satellites and ISEE (International Sun Earth Explorers). For individual titles, see N91-10418 through N91-10439.

**N91-10418#** Imperial Coll. of Science and Technology, London (England). Space and Atmospheric Physics Group.

**MULTISPACECRAFT MEASUREMENT AT VARYING SCALELENGTHS: THE CLUSTER/REGATTA OPPORTUNITY**

**c12**

D. J. Southwood *In* ESA, Space Plasma Physics Investigation by Cluster and Regatta May 1990 p 1-5 (For primary document see N91-10417 01-46)
Copyright Avail: NTIS HC/MF A08; EPD, ESTEC, Noordwijk, Netherlands HC 40 Dutch guilders

The opportunities offered by the addition of a fifth spacecraft, Regatta, to fly in a coordinated way with ESA Cluster spacecraft, is reviewed. The aim is to outline a rationale for such a coordinated international activity and at the same time to define what should be the goals and strategies of such a program. The addition of the Regatta spacecraft to the Cluster mission requires thorough planning but the opportunities gives possibilities of substantially enhancing the Cluster program. ESA

**N91-10419#** Academy of Sciences (USSR), Moscow. Space Research Inst.

**SPECIFIC TASKS OF MULTIPLE SCALE PLASMA MEASUREMENTS IN REGATTA-CLUSTER SYSTEM**

S. P. Savin, L. M. Zelenyi, and V. I. Prokhorenko *In* ESA, Space Plasma Physics Investigation by Cluster and Regatta May 1990 p 7-16 (For primary document see N91-10417 01-46)
Copyright Avail: NTIS HC/MF A08; EPD, ESTEC, Noordwijk, Netherlands HC 40 Dutch guilders

Appropriate options for separation strategy are discussed. Specific purposes of Regatta A measurements in the Regatta-Cluster missions are addressed: measurements on the scales several times larger than the distance between the Cluster spacecraft in the magnetotail, cusp, magnetopause, and bow shock will allow the simultaneous study of the structure of characteristic magnetospheric regions, their surrounding and their thin boundaries; providing of the background conditions for the measurements of fine structures by Cluster system; extension of the capabilities for the comprehensive study of local processes, including vector measurements of localized electric fields and currents; extension of the capabilities of three dimensional measurements at the auroral field lines and in the inner regions where the Cluster spacecrafts will be distributed mainly along the orbit, not forming a tetrahedron. ESA

**N91-10420#** Imperial Coll. of Science and Technology, London (England). Space and Atmospheric Physics Group.
**REVIEW OF THE CLUSTER ORBIT AND SEPARATION STRATEGY: CONSEQUENCE FOR MEASUREMENTS** **c13**
M. W. Dunlop *In* ESA, Space Plasma Physics Investigation by Cluster and Regatta May 1990 p 17-22 (For primary document see N91-10417 01-46)
Copyright Avail: NTIS HC/MF A08; EPD, ESTEC, Noordwijk, Netherlands HC 40 Dutch guilders

The spatial orientation of simulated orbits, together with the associated separation scenarios, in relation to key physical features are reviewed using three dimensional graphical display. Various three dimensional surface boundaries in the near Earth plasma environment, together with a time dependent field model, are used to model each plasma region physically. The consequences for science investigations are considered in terms of feasibility of the proposed measurements. It is noted that the dayside orbit does not pass through the position of the exterior cusp for the field model used. The separation strategy chosen, which was optimized for fuel on each of four maneuvers, would result in poor science performance as a result of extreme distortion of the tetrahedron. A more scientifically optimized strategy, which regulates tetrahedral shape at some cost in fuel per maneuver is recommended. ESA

**N91-10421#** Imperial Coll. of Science and Technology, London (England). Space and Atmospheric Physics Group.
**CONFIGURATIONAL SENSITIVITY OF MULTIPOINT MAGNETIC FIELD MEASUREMENTS**
M. W. Dunlop, A. Balogh, D. J. Southwood, R. C. Elphic, K.-H. Glassmeier, and F. M. Neubauer (Cologne Univ., Germany, F.R. ) *In* ESA, Space Plasma Physics Investigation by Cluster and Regatta May 1990 p 23-28 (For primary document see N91-10417 01-46)
Copyright Avail: NTIS HC/MF A08; EPD, ESTEC, Noordwijk, Netherlands HC 40 Dutch guilders

A computational calibration model which can access the error budget for these measurements at all system levels is reported. The model is parametric since the total error contribution can be treated as an error function for the derived quantity, dependent on the various error sources. The possible measurement errors for the derived quantities to be critical at current mission specifications are found. Typical hard error sources, which are likely to remain following standard interspacecraft calibration, are identified. Orbit strategy, in particular, imposes constraints at the four spacecraft level. The sensitivity of the error functions to spacecraft configuration is investigated. The determination of the vector curl of the magnetic field is taken as a model measurement and the role of the divergence of the field for this quantity is discussed. ESA

**N91-10422#** Centre de Recherches en Physique de l'Environnement Terrestre et Planetaire, Orleans (France).
**ACCURACY OF THE ESTIMATE OF J VIA MULTIPOINT MEASUREMENTS**
P. Robert and A. Roux *In* ESA, Space Plasma Physics Investigation by Cluster and Regatta May 1990 p 29-35 (For primary document see N91-10417 01-46)
Copyright Avail: NTIS HC/MF A08; EPD, ESTEC, Noordwijk, Netherlands HC 40 Dutch guilders

A numerical model is carried out to estimate the accuracy of the determination of the current density via measurements of the magnetic field at four locations. Three potential sources of error are investigated: the error associated with the nonhomogeneity of the current density profile over the volume defined by the four Cluster spacecraft; the error associated with the natural noise or the noise in the electronics of the magnetometer; and the error related to the uncertainty in the determination of the distances between the spacecraft. The latter two errors are modelled by random perturbations applied to the 4 by 3 magnetic waveforms. ESA

**N91-10423#** Academy of Sciences (USSR), Moscow. Space Research Inst.
**SMALL SPACE LAB AS A BASIC SPACECRAFT OF REGATTA PROJECT** **c18**
G. Avanesov, Ja. Ziman, A. Kogan, V. Kostenko, V. Fedotov, and V. Heifets *In* ESA, Space Plasma Physics Investigation by Cluster and Regatta May 1990 p 37-41 (For primary document see N91-10417 01-46)
Copyright Avail: NTIS HC/MF A08; EPD, ESTEC, Noordwijk, Netherlands HC 40 Dutch guilders

A small low cost satellite named Small Space Lab (SSL) is a principal element of the Regatta project including two branches. One of them is dedicated to explorations of interplanetary plasma and its interaction with the terrestrial magnetosphere. Another one envisages a wide program of spaceborne astrometrical observations. A description of SSL, mainly relating to its plasmophysical version, is presented. ESA

**N91-10424#** Cologne Univ. (Germany, F.R.). Inst. fuer Geophysik und Meteorologie.
**CLUSTER AS A WAVE TELESCOPE** **c89**
F. M. Neubauer, K.-H. Glassmeier, R. Walter, and M. W. Dunlop (Imperial Coll. of Science and Technology, London, England ) *In* ESA, Space Plasma Physics Investigation by Cluster and Regatta May 1990 p 51-55 Sponsored by BMFT and United Kingdom Science and Engineering Research Council (For primary document see N91-10417 01-46)
Copyright Avail: NTIS HC/MF A08; EPD, ESTEC, Noordwijk, Netherlands HC 40 Dutch guilders

The use of the four satellite configuration of the Cluster mission as a frequency dependent phased array is proposed in order to obtain not only a frequency spectrum of complex electromagnetic plasma wave fields in the magnetosphere, magnetosheath, and solar wind but also directional information and mode discrimination. This formulation is shown to be equivalent to a most general linear filter formulation described by a suitable set of transfer functions. The combination of the four satellites and an appropriate set of transfer functions is called a wave telescope. A transmission function to characterize a telescope is introduced. As an example, a special filter to separate waves propagating parallel and antiparallel to a background magnetic field is designed. Application to a complex simulated magnetohydrodynamic wave field illustrates the wave telescope. ESA

**N91-10425#** Centre National de la Recherche Scientifique, Orleans (France). Lab. de Physique et Chimie de l'Environment.
**EXPERIMENTAL CONSTRAINTS IN THE CHARACTERIZATION OF A TURBULENT FIELD FROM SEVERAL SATELLITES**
J. L. Pincon, F. Lefeuvre, and M. Parrot *In* ESA, Space Plasma Physics Investigation by Cluster and Regatta May 1990 p 57-67 (For primary document see N91-10417 01-46)
Copyright Avail: NTIS HC/MF A08; EPD, ESTEC, Noordwijk, Netherlands HC 40 Dutch guilders

The best method for defining an electrostatic or an electromagnetic turbulence in a space plasma, based on the simultaneous measurement of several wave-field components at several points in space is sought. The turbulent field is supposed to be stationary in time and homogeneous. An estimate of the field-energy distribution, which specifies how the field energy is distributed with regard to the angular frequency and to the wave-number, is derived from a generalization of the Capon high resolution method. Applications to the Cluster and Regatta missions are discussed from the analysis of simulated data. Experimental constraints are examined, particularly the number of satellites, the measure field components, and the accuracy in the measurements (distance between satellites, time synchronization). ESA

**N91-10426#** Sheffield Univ. (England).
**PLASMA WAVE MEASUREMENTS ON THE DAYSIDE: SCALE SIZES AND OBSERVATIONAL REQUIREMENTS**
H. St. C. Alleyne, M. A. Balikhin, S. I. Klimov, V. V. Krasnoselskikh (Academy of Sciences, USSR, Troitsk ), S. N. Walker, and L. J. C. Woolliscroft *In* ESA, Space Plasma Physics Investigation by

Cluster and Regatta May 1990 p 69-74 Sponsored by British National Space Center; United Kingdom Science and Engineering Research Council; and Sheffield Univ. Funding Council (For primary document see N91-10417 01-46)
Copyright Avail: NTIS HC/MF A08; EPD, ESTEC, Noordwijk, Netherlands HC 40 Dutch guilders

Observation from the AMPTE (Active Magnetospheric Particle Tracer Explorers) spacecraft and published data are used to review the various scale sizes of structures and plasma wave phenomena. Scientific problems which can be tackled at various scale sizes are identified. The advantages of combining data from the Cluster and Regatta spacecraft are concluded to outweigh the technical difficulties in achieving compatible datasets. ESA

**N91-10427#** Polish Academy of Sciences, Warsaw. Space Research Centre.

**PLASMA WAVES AS A SIGNATURE OF FLUX TRANSFER EVENTS**

J. Blecki, M. Denis, K. Kossacki, Jr., and L. J. C. Woolliscroft (Sheffield Univ., England ) *In* ESA, Space Plasma Physics Investigation by Cluster and Regatta May 1990 p 75-78 Sponsored in part by United Kingdom Science and Engineering Research Council (For primary document see N91-10417 01-46)
Copyright Avail: NTIS HC/MF A08; EPD, ESTEC, Noordwijk, Netherlands HC 40 Dutch guilders

The observations of plasma waves made in Flux Transfer Events (FTE's) by the Prognoz-8 and AMPTE-UKS satellites are studied. Wide band emissions are found to be associated with the boundaries of these regions. Some characteristic features of the spectra were determined. Phenomena similar to FTE's were observed by Prognoz-8 near the nightside magnetopause. These observations illustrate that plasma wave data can provide high time resolution information on plasma structures. ESA

**N91-10428#** Academy of Sciences (USSR), Troitsk. Inst. of Terrestrial Magnetism and Radio Wave Propagation.

**ON THE POSSIBILITY TO SUPPORT MULTISATELLITE MEASUREMENTS OF THE CLUSTER MISSION BY SINGLE SATELLITE MEASUREMENTS IN THE REGATTA-CLUSTER PROJECT**

V. V. Krasnoselskikh, A. M. Natanzon, A. E. Reznikov, A. Yu. Schyokotov, S. I. Klimov, A. E. Kruglyi, and L. J. C. Woolliscroft (Sheffield Univ., England ) *In* ESA, Space Plasma Physics Investigation by Cluster and Regatta May 1990 p 79-82 (For primary document see N91-10417 01-46)
Copyright Avail: NTIS HC/MF A08; EPD, ESTEC, Noordwijk, Netherlands HC 40 Dutch guilders

The main objective of the Cluster mission is to provide spatially separated measurements so as to help distinguish between spatial and temporal variations. A crucial aspect of this procedure is the estimate of the spatial derivatives of the vector field. To solve this it is necessary to equip all four Cluster satellites with identical instruments. This technique permits the analysis of phenomena with scale size greater than the inter-satellite separation. It is proposed that these measurements be supported by the direct measurement of the CurlB vector onboard the Regatta-Cluster single satellite using three component Rogovskii coil instruments. These measurements, together with the simultaneous vector B measurements in the same frequency range, make it possible to reconstruct the wave vector of the single plane wave or several first moments of the wave-vector distribution in a more general case. The scales of the phenomena to be studied by this technique are much smaller than those to be investigated by the Cluster mission but still they can give complementary information. ESA

**N91-10429#** Academy of Sciences, Berlin (German D.R.). Space Research Inst.

**MULTIPLE-ION WAVES BEHIND SHOCKS**

K. Sauer and U. Motschmann *In* ESA, Space Plasma Physics Investigation by Cluster and Regatta May 1990 p 83-86 (For primary document see N91-10417 01-46)
Copyright Avail: NTIS HC/MF A08; EPD, ESTEC, Noordwijk, Netherlands HC 40 Dutch guilders

The properties of multiple-ion shocks and related waves are studied by both multifluid theories and hybrid code simulations. Under the assumption of predominant electron heating, generalized Rankine-Hugoniot relations are derived which indicate that the velocity jump of the heavier ions is much less than that of the protons. The wave length of the associated multiple-ion waves in dependence of the basic plasma parameters follows from simple dispersion relations. The perspectives from which to study the fine-structure of the Earth bow shock by the Cluster/Regatta instruments are discussed. ESA

**N91-10430#** Centre de Recherches en Physique de l'Environnement Terrestre et Planetaire, Orleans (France).

**NON-LINEAR EVOLUTION OF THE KELVIN-HELMHOLTZ INSTABILITY: CONSTRAINTS ON MULTIPOINT MEASUREMENTS**

G. Chanteur and G. Belmont *In* ESA, Space Plasma Physics Investigation by Cluster and Regatta May 1990 p 91-94 (For primary document see N91-10417 01-46)
Copyright Avail: NTIS HC/MF A08; EPD, ESTEC, Noordwijk, Netherlands HC 40 Dutch guilders

A bidimensional magnetohydrodynamic simulation is used in a first attempt to estimate the optimal separations of the Cluster Regatta spacecraft, for the study of the Kelvin-Helmholtz instability at the magnetopause. A small separation of the Cluster spacecraft (approximately 200 km) is concluded to be adaptable to resolve the current layer and to study the small scale turbulence which may provide the macroscopic equivalent. However, a remote spacecraft is necessary at a distance of 1 R sub E to unambiguously study the propagation of the waves and their nonlinear evolution. ESA

**N91-10431#** Academy of Sciences (USSR), Moscow. Space Research Inst.

**PROBLEMS OF COLD PLASMA MEASUREMENTS ON THE REGATTA-A SPACECRAFT**

Yu. I. Galperin and B. A. Whalen (Herzberg Inst. of Astrophysics, Ottawa, Ontario ) *In* ESA, Space Plasma Physics Investigation by Cluster and Regatta May 1990 p 95-102 (For primary document see N91-10417 01-46)
Copyright Avail: NTIS HC/MF A08; EPD, ESTEC, Noordwijk, Netherlands HC 40 Dutch guilders

General physical processes and models which govern the thermal plasma number density distribution, field aligned flows and perpendicular drifts in the magnetosphere are outlined. The decisive role of the spacecraft electric potential and the Debye length for the thermal ion measurements onboard are considered. An approach to evaluate experimentally the necessary corrections to the three dimensional ion measurements is described. Cold electron distributions in the auroral environment are considered and their relation to the spacecraft potential in rarified plasmas is discussed. Advantages of the proposed Regatta A instrumentation are presented. ESA

**N91-10432#** Centre de Recherches en Physique de l'Environnement Terrestre et Planetaire, Orleans (France).

**MULTIPOINT STUDY OF SMALL-SCALE STRUCTURES AT THE MAGNETOPAUSE**

L. Rezeau, A. Roux, and N. Cornilleau-Wehrlin *In* ESA, Space Plasma Physics Investigation by Cluster and Regatta May 1990 p 103-108 (For primary document see N91-10417 01-46)
Copyright Avail: NTIS HC/MF A08; EPD, ESTEC, Noordwijk, Netherlands HC 40 Dutch guilders

Preliminary results from a study conducted on the basis of ISEE (International Sun Earth Explorers) 1 and 2 data are presented. Different methods are proposed for studying small structures with a set of four spacecraft. In order to illustrate these methods the ideal case of a uniformly moving current tube is considered. It is emphasized that a small interspacecraft distance (150 km) is needed to characterize the strong fluctuations of interest. It is also pointed out that the interpretation of small scale structures implies the knowledge of larger ones, for example: are there Kelvin-Helmholtz instabilities that may develop small scale structures. This question is proposed as one of the main goals of a joint Regatta Cluster mission. ESA

**N91-10433#** Ceskoslovenska Akademie Ved, Ondrejov. Astronomical Inst.

**THE IMPORTANCE OF SIMULTANEOUS MONITORING OF SOLAR ACTIVITY FOR THE INTERPRETATION OF SOLAR PLASMA PHENOMENA** **c92**

B. Valnicek *In* ESA, Space Plasma Physics Investigation by Cluster and Regatta May 1990 p 109-111 (For primary document see N91-10417 01-46)

Copyright Avail: NTIS HC/MF A08; EPD, ESTEC, Noordwijk, Netherlands HC 40 Dutch guilders

Studying solar wind and magnetospheric phenomena requires some fundamental data of the solar activity, and the registration of essential solar data onboard the same spacecraft is the most favorable way to obtain fundamental data needed for comparison. The easiest is the registration of x ray integral flux in more energetic channels. Complex information can be obtained in the combination of x ray integral flux and weak x ray imaging telescope onboard. With this object, such a registration of the solar activity is proposed for Cluster and Regatta. ESA

**N91-10434#** Academy of Sciences, Potsdam (German D.R.). Central Inst. for Astrophysics.

**ENERGETIC PARTICLES IN THE EARTH'S MAGNETOTAIL OR: CLUSTER AND REGATTA AS A DISPERSIOMETER**

J. Buechner *In* ESA, Space Plasma Physics Investigation by Cluster and Regatta May 1990 p 117-125 (For primary document see N91-10417 01-46)

Copyright Avail: NTIS HC/MF A08; EPD, ESTEC, Noordwijk, Netherlands HC 40 Dutch guilders

Energetic particles in the Earth's magnetotail carry information about the site and origin of their acceleration, i.e., about the dynamics of the main magnetospheric plasma reservoir. Despite several previous attempts to use this information, a separation of temporal and spatial effects in energetic particle observations was almost impossible. The multi-satellite Cluster and Regatta A missions will provide a new chance to solve this problem, if their relative positions in the tail are chosen appropriately. If so, the combination of Cluster and Regatta A energetic particle analyzers may act as a dispersiometer. To prepare its data interpretation, theoretical models of magnetotail particle acceleration are discussed with the two main sources, the more or less stationary dawn-dusk electric field, induced by the flowing solar wind and impulsive fields, related to fast changes in the tail magnetic field. ESA

**N91-10435#** European Space Agency. European Space Research and Technology Center, ESTEC, Noordwijk (Netherlands). Space Science Dept.

**FEATURES OF MID-TAIL ION TRAJECTORIES DURING SUBSTORMS**

D. C. Delcourt *In its* Space Plasma Physics Investigation by Cluster and Regatta May 1990 p 127-136 (For primary document see N91-10417 01-46)

Copyright Avail: NTIS HC/MF A08; EPD, ESTEC, Noordwijk, Netherlands HC 40 Dutch guilders

The storm time transport of ions originating from the high latitude ionosphere is examined by means of three dimensional particle codes. It is shown that tail-like to dipole-like reconfigurations of the geomagnetic field yield rapid injections of ions travelling in the mid-tail into closer L-shells. It is demonstrated that the particle motion is controlled, to a major extent, by drifts that are negligible in steady state. For singly charged and heavy ions such as $O+$, the simulations reveal intense energization (possibly a factor 1000 in relative magnitude) and pitch angle diffusion, which relate to the violation of the first adiabatic invariant. In view of these results, it is argued that the left fountain is a potential plasma source for the ring current. ESA

**N91-10436#** Academy of Sciences (USSR), Moscow. Space Research Inst.

**SPECIFIC TASKS OF REGATTA-E MEASUREMENTS CORRELATED WITH CLUSTER/REGATTA-A IN THE ISTP AND REGATTA PROGRAMMES**

A. P. Remizov, K. I. Gringauz, and V. S. Bassolo *In* ESA, Space Plasma Physics Investigation by Cluster and Regatta May 1990 p 137-140 (For primary document see N91-10417 01-46)

Copyright Avail: NTIS HC/MF A08; EPD, ESTEC, Noordwijk, Netherlands HC 40 Dutch guilders

Perspectives of the magnetosphere studies aboard the Regatta E spacecraft are discussed, including the scientific objectives and payload proposals. This new Soviet near equatorial spacecraft is to be launched at the end of 1994 for a five year period overlapping with operation of Regatta Astro, Regatta A and ISTP, providing coordinated measurements of fields and particles. ESA

**N91-10437#** Academy of Sciences (USSR), Moscow. Space Research Inst.

**POSSIBILITIES OF CHARGED PARTICLE INJECTION FROM SPACECRAFT FOR ACTIVE DIAGNOSTICS OF THE SURROUNDING PLASMA AND ACTIVE SPACECRAFT POTENTIAL CONTROL**

G. G. Managadze, W. Riedler, T. I. Gagua, M. Friedrich, K. Torkar (Academy of Sciences, Graz, Austria ), and N. A. Leonov *In* ESA, Space Plasma Physics Investigation by Cluster and Regatta May 1990 p 141-142 (For primary document see N91-10417 01-46)

Copyright Avail: NTIS HC/MF A08; EPD, ESTEC, Noordwijk, Netherlands HC 40 Dutch guilders

An active experiment utilizing energetic electrons and lithium ions is proposed for the Regatta spacecraft. The possibilities for active experiments onboard Regatta A are discussed. The importance of providing normal functioning of the instrumentation is stressed. A fully conductive surface of the spacecraft will have to be maintained irrespective of the type of individual experiment. ESA

**N91-10438#** Academy of Sciences (USSR), Moscow. Space Research Inst.

**THE POSSIBILITY OF MAKING FAST MEASUREMENTS OF ION DISTRIBUTION FUNCTIONS**

O. L. Vaisberg, A. O. Fedorov, A. Johnstone (Mullard Space Science Lab., Dorking, England ), E. I. Kolesnikova, A. I. Kozhukhovsky, and V. M. Balebanov *In* ESA, Space Plasma Physics Investigation by Cluster and Regatta May 1990 p 143-148 (For primary document see N91-10417 01-46)

Copyright Avail: NTIS HC/MF A08; EPD, ESTEC, Noordwijk, Netherlands HC 40 Dutch guilders

Measurements of the ion velocity distribution function, with mass selection, requires four dimensional measurements. Existing three dimensional plasma analyzers have to scan sequentially in at least two of these dimensions, leading to relatively long sampling times and the time-aliasing of measurements. An approach in which the proposed ion spectrometer consists of an array of many energy-mass analyzers, each one performing measurements within a specific solid angle was developed. The value of this solid angle can be set quite arbitrarily and the total angular coverage can be made about 4 pi steradians. This instrument is able to make truly simultaneous measurements of the complete three dimensional distribution functions of several ions. The sensitivity is large enough to provide temporal resolution as short as 0.1 sec. ESA

**N91-10439*#** Iowa Univ., Iowa City. Dept. of Physics and Astronomy.

**RADIO WAVE REMOTE SENSING BY CLUSTER AND REGATTA** **c89**

Donald A. Gurnett *In* ESA, Space Plasma Physics Investigation by Cluster and Regatta May 1990 p 153-158 (For primary document see N91-10417 01-46)

(Contracts NAS5-30365; NAS5-30730)

Copyright Avail: NTIS HC/MF A08; EPD, ESTEC, Noordwijk, Netherlands HC 40 Dutch guilders CSCL 03A

A coordinated Cluster/Regatta mission provides unique opportunities for remote sensing studies of terrestrial radio emissions. The scientific questions that can be addressed by remote radio measurements from Cluster and Regatta are described and the technical issues involved are discussed. The radio emission of primary interest is Auroral Kilometric Radiation (AKR) which is a powerful radio emission generated over the Earth's auroral zones at frequencies from 100 to 500 kHz. ESA

**N91-10440#** Pacific Northwest Lab., Richland, WA.
**THE EFFECTS OF CRITICAL LAYERS ON ATMOSPHERIC CNOIDAL WAVES**
E. D. Skyllingstad Mar. 1989 3 p Presented at the 4th Conference on Mesoscale Processes and Mountain Meteorology, Boulder, CO, 25-29 Jun. 1990
(Contract DE-AC06-76RL-01830)
(DE90-016540; PNL-SA-17988; CONF-9006111-7) Avail: NTIS HC/MF A01

The topic of atmospheric cnoidal and solitary waves has received considerable attention in recent years. These waves are of interest because of their strength, permanence of form, and ability to travel long distances with minimal decrease in amplitude. Observations of solitary waves have identified two classes of disturbances. The first wave type, known as a wave of depression, extends through the depth of the atmosphere and is noticeable as a trough of low pressure at the surface. These waves are commonly observed downstream from regions of strong cyclogenesis suggesting a generation mechanism of convection, frontogenesis, or other mesoscale instability. The second wave type, known as a wave of elevation, propagates along a surface inversion and is identified by a high-pressure spike. Waves of elevation are formed by the intrusion of a gust front or sea breeze beneath an existing inversion. This interaction leads to the formation of a bore or jump in the inversion height, that eventually develops undulations or cnoidal waves under the proper atmospheric conditions. A numerical model is used to study critical levels as possible trapping mechanisms for cnoidal waves. DOE

**N91-10441*#** National Aeronautics and Space Administration. Marshall Space Flight Center, Huntsville, AL.
**PROPERTIES OF LARGE SCALE PLASMA FLOW DURING THE EARLY STAGE OF THE PLASMASPHERIC REFILLING**
Nagendra Singh, P. Craven, D. G. Torr, and P. G. Richards (Alabama Univ., Huntsville.) 1990 38 p
(NASA-TM-103446; NAS 1.15:103446) Avail: NTIS HC/MF A03 CSCL 04A

The objective is to better characterize the macroscopic properties of the interhemisphere plasma flow by solving a more complete set of hydrodynamic equations than that solved previously. Specifically, the ion continuity, momentum and energy equations were solved for the plasma flow along the closed magnetic field lines. During the initial stage of the supersonic outflow in the equatorial region, the ions cool substantially. Using the hydrodynamic model for the large-scale plasma flow, the dynamics of shocks was examined which form in the geomagnetic flux tubes during the early stages of refilling. These shocks are more like those forming in neutral gases than the electrostatic shocks driven by microinstabilities involving ion-ion interaction. Therefore, the shocks seen in the hydrodynamic model are termed as hydrodynamic shocks. Such shocks are generally unsteady and therefore the usual shock jump conditions given by Rankine-Hugoniot relations are not strictly applicable to them. The density, flow velocity and temperature structures associated with the shocks are examined for both asymmetrical and symmetrical flows. In the asymmetrical flow the outflow from one of two conjugate ionospheres is dominant. On the other hand, in the symmetrical case outflows from the two ionospheric sources are identical. Both cases are treated by a two-stream model. In the late type of flow, the early-time refilling shows a relaxation type of oscillation, which is driven by the large-scale interactions between the two identical streams. After this early stage, the resulting temperature structure shows some interesting features. In the equatorial region the streams are isothermal, but in the off-equatorial regions the streams have quite different temperatures, and also densities and flow velocities. The dense and slow stream is found to be warmer than the low-density fast stream. In the late stage of refilling, the temperature is found to steadily increase from the conjugate ionospheres towards the equator; the equatorial temperature is found to be as high as about 8000 K compared to the ionospheric temperature of 3600 K. Author

**N91-10442*#** Bionetics Corp., Cocoa Beach, FL.
**GEOLOGY, GEOHYDROLOGY, AND SOILS OF NASA, KENNEDY SPACE CENTER: A REVIEW**
Paul A. Schmalzer and C. Ross Hinkle 15 Aug. 1990 49 p
(Contract NAS10-11624)
(NASA-TM-103813; NAS 1.15:103813; BIO-2) Avail: NTIS HC/MF A03 CSCL 08G

Sediments underlying Kennedy Space Center (KSC) have accumulated in alternating periods of deposition and erosion since the Eocene. Surface sediments are of Pleistocene and Recent ages. Fluctuating sea levels with the alternating glacial-interglacial cycles have shaped the formation of the barrier island. Merritt Island is an older landscape whose formation may have begun as much as 240,000 years ago, although most of the surface sediments are not that old. Cape Canaveral probably dates from less than 7,000 years B.P. (before present) as does the barrier strip separating Mosquito Lagoon from the Atlantic Ocean. Merritt Island and Cape Canaveral have been shaped by progradational processes but not continuously so, while the Mosquito Lagoon barrier has been migrating landward. Deep acquifers beneath KSC are recharged inland but are highly mineralized in the coastal region and interact little with surface vegetation. The Surficial acquifer has formed in the Pleistocene and Recent deposits and is recharged by local rainfall. Sand ridges in the center of Merritt Island are important to its recharge. Author

**N91-10443#** Universiteit Twente, Enschede (Netherlands).
**THE NUMERICAL SIMULATION OF NONLINEAR GRAVITY WAVES IN THREE DIMENSIONS USING A HIGHER ORDER PANEL METHOD Ph.D. Thesis**
Johan Egbert Romate 1989 228 p
(Grants STW-CWI44-0632; STW-CWI47-0632)
(ISBN-90-9002667-23; ETN-90-97767) Avail: NTIS HC/MF A11

A numerical model for the simulation of these nonlinear free surface waves in three dimensions is described. This model uses a boundary integral equation method for discretization in space, and an ordinary differential equation solver (4th order Runge-Kutta) for the development in time. The formulation of absorbing boundary conditions is considered. A literature survey of numerical solution procedures is presented. The various parts of the proposed numerical method are discussed. Discretizations of the time independent problems show the accuracy and efficiency of the method. Tests with the linearized free surface equations confirm theoretical results obtained. Both first and second order absorbing boundary conditions can be used. The method is applied to some nonlinear (cross) wave phenomena in a numerical wave tank. ESA

**N91-10368#** Meteorological Satellite Center, Tokyo (Japan).
**VISSR HISTOGRAM DATA**
Hideyuki Sasaki *In its* Meteorological Satellite Center Technical Note. Special Issue (1989). Summary of GMS System. 2: Data Processing Mar. 1989 p 113-115 In JAPANESE; ENGLISH summary (For primary document see N91-10356 01-42)
Avail: NTIS HC/MF A08

**N91-10369#** Meteorological Satellite Center, Tokyo (Japan).
**BRIGHTNESS TEMPERATURE DISTRIBUTION**
Kazuhiro Oosawa *In its* Meteorological Satellite Center Technical Note. Special Issue (1989). Summary of GMS System. 2: Data Processing Mar. 1989 p 117-119 In JAPANESE; ENGLISH summary (For primary document see N91-10356 01-42)
Avail: NTIS HC/MF A08

**N91-10370#** Meteorological Satellite Center, Tokyo (Japan).
**GPCP DATA PROCESSING**
Kazuhiro Oosawa *In its* Meteorological Satellite Center Technical Note. Special Issue (1989). Summary of GMS System. 2: Data Processing Mar. 1989 p 121-122 In JAPANESE; ENGLISH summary (For primary document see N91-10356 01-42)
Avail: NTIS HC/MF A08

# 47 METEOROLOGY AND CLIMATOLOGY

Includes weather forecasting and modification.

**N91-10444#** World Meteorological Organization, Geneva (Switzerland).
**ANALYZING LONG TIME SERIES OF HYDROLOGICAL DATA WITH RESPECT TO CLIMATE VARIABILITY: PROJECT DESCRIPTION**
Feb. 1988 37 p
(WCAP-3; WMO/TD-224) Avail: NTIS HC/MF A03

Two projects are to be undertaken within the water-related activities of the World Climate Program (WCP-Water). Project A.1 is analyzing historical hydrological and related information with respect to climate change, and project A.2 is analyzing long time series of hydrological data and indices with respect to climate variability. To ensure uniformity within the WCP, the concepts of the variability and change in hydrology and climate are defined. In addition, the selection of the time series of data and the analysis of variability are discussed. The appendices contain a description of the projects, information required for each station, and a list of the projects' statistical formulas. M.G.

**N91-10445#** World Meteorological Organization, Geneva (Switzerland).
**PROCEEDINGS OF THE WMO REGION 3/4 TRAINING SEMINAR ON CLIMATE DATA MANAGEMENT AND USER SERVICES**
1989 86 p Seminar held in Barbados, 22-26 Sep. 1986, and in Panama, 29 Sep. - 3 Oct. 1986
(WCDP-1; WMO/TD-227) Avail: NTIS HC/MF A05

Papers presented at the Training Seminar in Climate Data Management and User Services are presented. The following subject areas are covered: climate data management and standard user services; simple climate data applications such as the analysis of rainfall data to assist agricultural planning and decision making; and advanced climate data applications using climate and other geographical data for natural resource management and modelling. Author

**N91-10446#** National Oceanic and Atmospheric Administration, Washington, DC. Office of Research and Applications.
**GEOGRAPHIC DISPLAY OF CIRCULATION MODEL DATA**
Kurt W. Hess and Peter J. Pytlowany (National Oceanographic Data Center, Washington, DC.) Aug. 1989 49 p Original contains color illustrations
(NOAA-NESDIS-27) Avail: NTIS HC/MF A03

Circulation models of coastal area data can potentially be integrated with geographic locations, satellite data, and other types of information and used for analysis, prediction, and verification. The goal is to put circulation model data into a geographic mode for display in combination with other data fields. The satellite image display software allows for overlaying several planes of different types of data on top of a gridded field in geographic format, so the software is essentially a geographic information system. The satellite image processing system was used to analyze the NOAA polar orbiter's Advanced Very High Resolution Radiometer (AVHRR) data, including sea surface temperature, chlorophyll, and sediment concentration. The data are displayed with a geographic orientation using a matrix to hold data for a selected area of the earth surface. Compound images showing several data types result from overlaying the AVHRR field with other fields such as coastline geography, land masks, and scale bars. Author

**N91-10447#** National Oceanographic Data Center, Washington, DC.
**MARINERS WEATHER LOG, VOLUME 33, NUMBER 1, WINTER, 1989 Quarterly Report**
R. M. DeAngelis 1989 73 p
(PB90-179987) Avail: NTIS HC/MF A04 CSCL 04B

This volume of the journal contains articles on these topics: Whale diary; Malstrom, the legend and the reality; Avoid the typhoon; Whale oil and wicks; Beyond the rainbow; Editor's desk; Marine observation program; Radio officer tips; Hurricane alley; North Atlantic Ocean; North Pacific Ocean; and Track charts and tables. Author

**N91-10448*#** National Aeronautics and Space Administration. Langley Research Center, Hampton, VA.
**FIRE SCIENCE RESULTS 1988**
David S. McDougal, ed. and H. Scott Wagner, ed. Washington Jul. 1990 394 p Workshop held in Vail, CO, 11-15 Jul. 1988; sponsored in cooperation with NASA, NSF, ONR, DOE, AFGL, and NOAA
(NASA-CP-3083; L-16814; NAS 1.55:3083) Avail: NTIS HC/MF A17 CSCL 04B

FIRE (First ISCCP Regional Experiment) is a U.S. cloud-radiation program that seeks to address the issues of a basic understanding and parameterizations of cirrus and marine stratocumulus cloud systems and ISCCP data products. The papers describe research analysis of data collected at the 1986 Cirrus Intensive Field Observations (IFO), the 1987 Marine Stratocumulus IFO, and the Extended Time Observations. The papers are grouped into sessions on satellite studies, lidar/radiative properties/microphysical studies, radiative properties, thermodynamic and dynamic properties, case studies, and large scale environment and modeling studies. For individual titles, see N91-10449 through N91-10535.

**N91-10449*#** National Aeronautics and Space Administration. Goddard Space Flight Center, Greenbelt, MD.
**SYNOPTIC CONDITIONS PRODUCING CIRRUS DURING THE FIRE CIRRUS IFO**
David OC. Starr and Donald P. Wylie (Wisconsin Univ., Madison.) *In* NASA, Langley Research Center, FIRE Science Results 1988 Jul. 1990 p 3-10 (For primary document see N91-10448 01-47)
Avail: NTIS HC/MF A17 CSCL 04B

Although direct observations of cirrus clouds by the FIRE research aircraft were usually confined to the area of Intensive Field Observation (IFO) surface network, these cirrus were generally part of a more extensive zone of upper level cloudiness. It is these large scale patterns of cirriform cloud and their relationship to the corresponding synoptic environment which are the prime focus. Three conceptual models are presented and each of the individual cases are classified into one of these categories. Although the cases manifest significant differences in intensity and small scale structure, it is believed that they are best viewed in this unified context. The descriptions given are mostly qualitative, however, quantitative descriptions of the synoptic control and its relationship to cloud structure for all the IFO cases are summarized. The synoptic situations in which extensive cirriform clouds were observed are classified into three basic types: warm front cases, cold front cases, and closed low aloft cases. A simplified summary of each type of situation is presented. Author

**N91-10450*#** Wisconsin Univ., Madison. Space Science and Engineering Center.
**WHERE ARE CIRRUS CLOUDS AND WHY ARE THEY THERE**
Donald P. Wylie *In* NASA, Langley Research Center, FIRE Science Results 1988 Jul. 1990 p 11-16 (For primary document see N91-10448 01-47)
Avail: NTIS HC/MF A17 CSCL 04B

The cirrus cloud climatology of Wylie and Menzel (1988) and some ancillary studies of cirrus clouds that have been made using the same data are summarized. The Wylie and Menzel climatology is a data set of cloud statistics extracted from the GOES/VAS satellite. With these data the geographical distributions of clouds,

the seasonal changes, some diurnal changes, and also what atmospheric conditions cause the clouds can be described.
Author

**N91-10451*#** National Aeronautics and Space Administration. Goddard Inst. for Space Studies, New York, NY.
**ISCCP RESULTS FOR THE FIRE IFO REGIONS AND TIMES Abstract Only**
William B. Rossow *In* NASA, Langley Research Center, FIRE Science Results 1988 Jul. 1990 p 17 (For primary document see N91-10448 01-47)
Avail: NTIS HC/MF A17 CSCL 04B

The ISCCP analysis of cloud conditions during and in the vicinity of the FIRE cirrus and marine stratus Intensive Field Observations (IFOs) is presented in two forms: the standard climatology product, which is averaged to a nominal 250 km resolution and a pixel-by-pixel version that samples the original data at about 30 km spacing every three hours. These results are based on NOAA-9 and GOES-6 images covering October to November 1986 and July 1987 for the FIRE Extended Area. Comparisons of these results with other FIRE observations will serve to check the accuracy of the clear sky radiances inferred by the ISCCP analysis, which determines the accuracy of the cloud detections. Of more interest is the exploration of the dependence of the inferred cloud properties for direct evaluation of the role of small scale variability of cloud properties on the radiation field. This is illustrated by preliminary results obtained for the scales contained in the ISCCP data. The ISCCP analysis also sets the larger scale context of the FIRE data: (1) comparisons of the clouds occurring in the FIRE IFOs with nearby locations and times are presented, and (2) comparisons of the cloud conditions for the same month in other years are shown. Author

**N91-10452*#** Colorado Univ., Boulder. Cooperative Inst. for Research in Environmental Sciences.
**CLOUD INFORMATION FOR FIRE FROM SURFACE WEATHER REPORTS**
Carole J. Hahn, Stephen G. Warren (Washington Univ., Seattle.), and Julius London *In* NASA, Langley Research Center, FIRE Science Results 1988 Jul. 1990 p 19-23 (For primary document see N91-10448 01-47)
(Grant NAG2-206)
Avail: NTIS HC/MF A17 CSCL 04B

Surface weather observations of clouds were analyzed to obtain a global cloud climatology (Warren et al, 1986; 1988). The form of the synoptic weather code limits the types of cloud information which are available from these reports. Comparison of surface weather reports with instrumental observations during the FIRE field experiments can help to clarify the operational definitions which were made in the climatology because of the nature of the synoptic code. The long-term climatology from surface weather observations is also useful background for planning the location and timing of intensive field experiments. Author

**N91-10453*#** National Aeronautics and Space Administration. Goddard Space Flight Center, Greenbelt, MD.
**CIRRUS CLOUD MODEL PARAMETERIZATIONS: INCORPORATING REALISTIC ICE PARTICLE GENERATION**
Kenneth Sassen, G. C. Dodd (Utah Univ., Salt Lake City.), and David OC. Starr *In* NASA, Langley Research Center, FIRE Science Results 1988 Jul. 1990 p 25-27 (For primary document see N91-10448 01-47)
(Grant NSF ATM-85-13975)
Avail: NTIS HC/MF A17 CSCL 04B

Recent cirrus cloud modeling studies have involved the application of a time-dependent, two dimensional Eulerian model, with generalized cloud microphysical parameterizations drawn from experimental findings. For computing the ice versus vapor phase changes, the ice mass content is linked to the maintenance of a relative humidity with respect to ice (RHI) of 105 percent; ice growth occurs both with regard to the introduction of new particles and the growth of existing particles. In a simplified cloud model designed to investigate the basic role of various physical processes in the growth and maintenance of cirrus clouds, these parametric relations are justifiable. In comparison, the one dimensional cloud microphysical model recently applied to evaluating the nucleation and growth of ice crystals in cirrus clouds explicitly treated populations of haze and cloud droplets, and ice crystals. Although these two modeling approaches are clearly incompatible, the goal of the present numerical study is to develop a parametric treatment of new ice particle generation, on the basis of detailed microphysical model findings, for incorporation into improved cirrus growth models. For example, the relation between temperature and the relative humidity required to generate ice crystals from ammonium sulfate haze droplets, whose probability of freezing through the homogeneous nucleation mode are a combined function of time and droplet molality, volume, and temperature. As an example of this approach, the results of cloud microphysical simulations are presented showing the rather narrow domain in the temperature/humidity field where new ice crystals can be generated. The microphysical simulations point out the need for detailed CCN studies at cirrus altitudes and haze droplet measurements within cirrus clouds, but also suggest that a relatively simple treatment of ice particle generation, which includes cloud chemistry, can be incorporated into cirrus cloud growth. Author

**N91-10454*#** Colorado State Univ., Fort Collins. Dept. of Atmospheric Science.
**EVIDENCE FOR ASYMMETRIC INERTIAL INSTABILITY IN THE FIRE SATELLITE DATASET**
Duane E. Stevens and Paul E. Ciesielski *In* NASA, Langley Research Center, FIRE Science Results 1988 Jul. 1990 p 29-33 (For primary document see N91-10448 01-47)
(Grant NSF ATM-83-52205)
Avail: NTIS HC/MF A17 CSCL 04B

One of the main goals of the First ISCCP Regional Experiment (FIRE) is obtaining the basic knowledge to better interpret satellite image of clouds on regional and smaller scales. An analysis of a mesoscale circulation phenomenon as observed in hourly FIRE satellite images is presented. Specifically, the phenomenon of interest appeared on satellite images as a group of propagating cloud wavelets located on the edge of a cirrus canopy on the anticylonic side of a strong, upper-level subtropical jet. These wavelets, which were observed between 1300 and 2200 GMT on 25 February 1987, are seen most distinctly in the GOES-West infrared satellite picture at 1800 GMT. The purpose is to document that these wavelets were a manifestation of asymmetric inertial instability. During their lifetime, the wavelets were located over the North American synoptic sounding network, so that the meteorological conditions surrounding their occurrence could be examined. A particular emphasis of the analysis is on the jet streak in which the wavelets were imbedded. The characteristics of the wavelets are examined using hourly satellite imagery. The hypothesis that inertial instability is the dynamical mechanism responsible for generating the observed cloud wavelets was examined. To further substantiate this contention, the observed characteristics of the wavelets are compared to, and found to be consistent with, a theoretical model of inertia instability by Stevens and Ciesielski. Author

**N91-10455*#** National Aeronautics and Space Administration. Goddard Space Flight Center, Greenbelt, MD.
**CLIMATE DATA SYSTEM SUPPORTS FIRE**
Lola M. Olsen, Dominick Iascone, and Mary G. Reph *In* NASA, Langley Research Center, FIRE Science Results 1988 Jul. 1990 p 35-37 (For primary document see N91-10448 01-47)
Avail: NTIS HC/MF A17 CSCL 04B

The NASA Climate Data System (NCDS) at Goddard Space Flight Center is serving as the FIRE Central Archive, providing a centralized data holding and data cataloging service for the FIRE project. NCDS members are carrying out their responsibilities by holding all reduced observations and data analysis products submitted by individual principal investigators in the agreed upon format, by holding all satellite data sets required for FIRE, by providing copies of any of these data sets to FIRE investigators, and by producing and updating a catalog with information about the FIRE holdings. FIRE researchers were requested to provide their reduced data sets in the Standard Data Format (SDF) to the FIRE Central Archive. This standard format is proving to be of value. An improved SDF document is now available. The document provides an example from an actual FIRE SDF data set and clearly states the guidelines for formatting data in SDF. NCDS has received SDF tapes from a number of investigators. These tapes were analyzed and comments provided to the producers. One product which is now available is William J. Syrett's sodar data product from the Stratocumulus Intensive Field Observation. Sample plots from all SDF tapes submitted to the archive will be available to FSET members. Related cloud products are also available through NCDS. Entries describing the FIRE data sets are being provided for the NCDS on-line catalog. Detailed information for the Extended Time Observations is available in the general FIRE catalog entry. Separate catalog entries are being written for the Cirrus Intensive Field Observation (IFO) and for the Marine Stratocumulus IFO. Short descriptions of each FIRE data set will be installed into the NCDS Summary Catalog. Author

**N91-10456*#** Colorado State Univ., Fort Collins. Dept. of Atmospheric Science.

**THE EFFECTS OF CLOUD RADIATIVE FORCING ON AN OCEAN-COVERED PLANET**

David A. Randall *In* NASA, Lahgley Research Center, FIRE Science Results 1988 Jul. 1990 p 39-43 Sponsored by NASA, Ames Research Center (For primary document see N91-10448 01-47)
Avail: NTIS HC/MF A17 CSCL 04B

Cumulus anvil clouds, whose importance has been emphasized by observationalists in recent years, exert a very powerful influence on deep tropical convection by tending to radiatively destabilize the troposphere. In addition, they radiatively warm the column in which they reside. Their strong influence on the simulated climate argues for a much more refined parameterization in the General Circulation Model (GCM). For Seaworld, the atmospheric cloud radiative forcing (ACRF) has a powerful influence on such basic climate parameters as the strength of the Hadley circulation, the existence of a single narrow InterTropical Convergence Zone (ITCZ), and the precipitable water content of the atmosphere. It seems likely, however, that in the real world the surface CRF feeds back negatively to suppress moist convection and the associated cloudiness, and so tends to counteract the effects of the ACRF. Many current climate models have fixed sea surface temperatures but variable land-surface temperatures. The tropical circulations of such models may experience a position feedback due to ACRF over the oceans, and a negative or weak feedback due to surface CRF over the land. The overall effects of the CRF on the climate system can only be firmly established through much further analysis, which can benefit greatly from the use of a coupled ocean-atmospheric model. Author

**N91-10457*#** National Aeronautics and Space Administration. Langley Research Center, Hampton, VA.

**A SYNOPSIS OF LANGLEY RESEARCH CENTER'S LIDAR EFFORT FOR THE 1986 FIRE IFO Abstract Only**

Jose M. Alvarez, M. P. McCormick, J. D. Moore, W. H. Hunt (Wyle Labs., Inc., Hampton, VA.), B. R. Rouse, L. R. Poole, and B. D. Poole *In its* FIRE Science Results 1988 Jul. 1990 p 47 (For primary document see N91-10448 01-47)
Avail: NTIS HC/MF A17 CSCL 04B

The lidar data obtained by the Langley Aircraft Lidar in October 1986 in Wisconsin is being reduced in a transparent, simple fashion and will be published in its reduced form in a NASA Reference Publication (RP). This reduced data will also be submitted to the FIRE data archives. Some of this reduced data will be presented at the FIRE FSET Workshop to acquaint the science team with the data format to be used in the archive and the upcoming catalog contained in the RP. A new method was utilized in Wisconsin for obtain the depolarization ratio of aerosols. This method involves using a half-wave plate to calibrate the lidar under field conditions. The theory behind this technique will be presented at this workshop as well as some of the lidar calibration results. The lidar calibration will be utilized in interpreting some of the dual polarization lidar data obtained during the IFO in Wisconsin. Some of these data are also discussed. A continuous wave laser lab-type lidar simulator was constructed during the previous year. One of the primary reasons for the construction of the simulator was to attempt dual-polarization lidar-like calibrations under laboratory, rather than field conditions. The data collected by this system was used to experimentally check and thus, inspire confidence in the algorithms being used to interpret the lidar data obtained in the field. A computer program which simulates noisy lidar data was used as a part of this effort in order to obtain some feel for the noise in the inversion parameters as a function of noise in the actual measurements. The lidar simulation will be described in addition to presenting some of the lab-generated calibration data. Author

**N91-10458*#** Wisconsin Univ., Madison. Dept. of Meteorology.

**OPTICAL AND MORPHOLOGICAL PROPERTIES OF CIRRUS CLOUDS DETERMINED BY THE HIGH SPECTRAL RESOLUTION LIDAR DURING FIRE**

Christian John Grund and Edwin W. Eloranta *In* NASA, Langley Research Center, FIRE Science Results 1988 Jul. 1990 p 49-53 (For primary document see N91-10448 01-47)
(Contract N00014-85-K-0581; DAAG29-84-K-0069)
Avail: NTIS HC/MF A17 CSCL 04B

Cirrus clouds reflect incoming solar radiation and trap outgoing terrestrial radiation; therefore, accurate estimation of the global energy balance depends upon knowledge of the optical and physical properties of these clouds. Scattering and absorption by cirrus clouds affect measurements made by many satellite-borne and ground based remote sensors. Scattering of ambient light by the cloud, and thermal emissions from the cloud can increase measurement background noise. Multiple scattering processes can adversely affect the divergence of optical beams propagating through these clouds. Determination of the optical thickness and the vertical and horizontal extent of cirrus clouds is necessary to the evaluation of all of these effects. Lidar can be an effective tool for investigating these properties. During the FIRE cirrus IFO in Oct. to Nov. 1986, the High Spectral Resolution Lidar (HSRL) was operated from a rooftop site on the campus of the University of Wisconsin at Madison, Wisconsin. Approximately 124 hours of fall season data were acquired under a variety of cloud optical thickness conditions. Since the IFO, the HSRL data set was expanded by more than 63.5 hours of additional data acquired during all seasons. Measurements are presented for the range in optical thickness and backscattering phase function of the cirrus clouds, as well as contour maps of extinction corrected backscatter cross sections indicating cloud morphology. Color enhanced images of range-time indicator (RTI) displays a variety of cirrus clouds with approximately 30 sec time resolution are presented. The importance of extinction correction on the interpretation of cloud height and structure from lidar observations of optically thick cirrus are demonstrated. Author

**N91-10459*#** National Center for Atmospheric Research, Boulder, CO.

**HYDROMETEOR DEVELOPMENT IN COLD CLOUDS IN FIRE**

Andrew J. Heymsfield, Nancy C. Knight, and Kenneth Sassen (Utah Univ., Salt Lake City.) *In* NASA, Langley Research Center, FIRE Science Results 1988 Jul. 1990 p 55-59 (For primary document see N91-10448 01-47)
(Grant NASA Order L-98100-B; NSF ATM-85-13975)
Avail: NTIS HC/MF A17 CSCL 04B

The role of cirrus clouds, particularly in weather and climate processes, has been increasingly investigated. Numerical models have demonstrated the importance of the solar reflectivity and infrared radiation of cirrus clouds in the Earth's radiation budget and climate. These properties depend upon the cloud microphysical characteristics, density, and altitude and hence justify investigation. The results reported were obtained from cold clouds (-20 to -46 C) in the mid to upper troposphere during ten flights of the NCAR King Air as part of the First ISCCP Research Experiment (FIRE) in Wisconsin. Author

**N91-10460*#** Utah Univ., Salt Lake City. Dept. of Meteorology.
**LIDAR AND AIRCRAFT STUDIES OF DEEP CIRRUS SYSTEMS FROM THE 1986 FIRE IFO**
Kenneth Sassen, Andrew J. Heymsfield, and Nancy C. Knight (National Center for Atmospheric Research, Boulder, CO.) *In* NASA, Langley Research Center, FIRE Science Results 1988 Jul. 1990 p 61-65 (For primary document see N91-10448 01-47)
(Grant NASA Order L-08100-B; NSF ATM-85-13975)
Avail: NTIS HC/MF A17 CSCL 04B

Several NCAR King Air flight missions were conducted during the Wisconsin FIRE IFO experiment in support of the University of Utah polarization lidar observations of deep cirrus cloud systems at the Wausau ground site. Data collected from four cirrus systems are included in this analysis, including those of 22 and 28 October, and 1 and 2 November. Lidar data were generally obtained at 2 min intervals in the zenith direction over observation periods that ranged from approximately 4 to 10 h, bracketing the aircraft missions. The data were processed to yield height-time (HTI) displays of lidar linear depolarization ratio sigma and relative range-normalized return power P. King Air operations consisted of a combination of rapid profiling and Lagrangian spiral descents and stacked racetrack patterns in the vicinity of the field site. From the spiral descents are constructed vertical profiles of ice particle concentration N(sub i) and ice mass content IWC derived from PMS 2-D probe imagery and, when detected, FSSP cloud droplet concentration N(sub W) and liquid water content, LWC. Aircraft flight leg data are presented for the vertical velocity W and the same ice and water cloud content parameters. In addition, aerosol particle concentrations obtained with the ASAS probe are examined, and photographs of ice particles collected in-situ on oil-coated slides are presented to illustrate ice particle habit. Author

**N91-10461*#** National Center for Atmospheric Research, Boulder, CO.
**VERTICAL VELOCITIES WITHIN A CIRRUS CLOUD FROM DOPPLER LIDAR AND AIRCRAFT MEASUREMENTS DURING FIRE: IMPLICATIONS FOR PARTICLE GROWTH**
Ismail Gultepe and Andrew J. Heymsfield *In* NASA, Langley Research Center, FIRE Science Results 1988 Jul. 1990 p 67-71 Sponsored in part by NSF (For primary document see N91-10448 01-47)
Avail: NTIS HC/MF A17 CSCL 04B

A large and comprehensive data set taken by the NOAA CO2 Doppler lidar, the NCAR King Air, and rawinsondes on 31 October 1986 during the FIRE (First ISCCP Regional Experiment) field program which took place in Wisconsin are presented. Vertical velocities are determined from the Doppler lidar data, and are compared with velocities derived from the aircraft microphysical data. The data are used for discussion of particle growth and dynamical processes operative within the cloud. Author

**N91-10462*#** Colorado State Univ., Fort Collins. Dept. of Atmospheric Science.
**RADIATIVE PROPERTIES OF VISIBLE AND SUBVISIBLE CIRRUS: SCATTERING ON HEXAGONAL ICE CRYSTALS**
Piotr J. Flatau, Graeme L. Stephens, and Bruce T. Draine (Princeton Univ., NJ.) *In* NASA, Langley Research Center, FIRE Science Results 1988 Jul. 1990 p 75-80 (For primary document see N91-10448 01-47)
(Grants AF-AFOSR-0143-88; NSF AST-86-12013; NSF ATM-85-19160)
Avail: NTIS HC/MF A17 CSCL 04B

One of the main objectives of the First International Satellite Cloud Climatology Project (ISCCP) Regional Experiment (FIRE) is to provide a better understanding of the physics of upper level clouds. The focus is on just one specific aspect of cirrus physics, namely on characterizing the radiative properties of single, nonspherical ice particles. The basis for further more extensive studies of the radiative transfer through upper level clouds is provided. Radiation provides a potential mechanism for strong feedback between the divergence of in-cloud radiative flux and the cloud microphysics and ultimately on the dynamics of the cloud. Some aspects of ice cloud microphysics that are relevant to the radiation calculations are described. Next, the Discrete Dipole Approximation (DDA) is introduced and some new results of scattering by irregular crystals are presented. The Anomalous Diffraction Theory (ADT) was adopted to investigate the scattering properties of even larger crystals. In this way the scattering properties of nonspherical particles were determined over a range of particle sizes. Author

**N91-10463*#** National Aeronautics and Space Administration. Ames Research Center, Moffett Field, CA.
**CIRRUS MICROPHYSICS AND RADIATIVE TRANSFER: A CASE STUDY**
Stefan A. Kinne, Thomas P. Ackerman, and Andrew J. Heymsfield (National Center for Atmospheric Research, Boulder, CO.) *In* NASA, Langley Research Center, FIRE Science Results 1988 Jul. 1990 p 81-83 (For primary document see N91-10448 01-47)
Avail: NTIS HC/MF A17 CSCL 04B

During the Cirrus Intensive Field Operations of FIRE, data collected by the NCAR King Air in the vicinity of Wausau, WI on October 28 were selected to study the influence of cirrus cloud microphysics on radiative transfer and the role of microphysical approximations in radiative transfer models. The instrumentation of the King Air provided, aside from temperature and wind data, up-and downwelling broadband solar and infrared fluxes as well as detailed microphysical data. The aircraft data, supplied every second, are averaged over the 7 legs to represent the properties for that altitude. The resulting vertical profiles, however, suffer from the fact that each leg represents a different cloud column path. Based on the measured microphysical data particle size distributions of equivalent spheres for each cloud level are developed. Accurate radiative transfer calculations are performed, incorporating atmospheric and radiative data from the ground and the stratosphere. Comparing calculated to the measured up- and downwelling fluxes at the seven cloud levels for both the averaged and the three crossover data will help to assess the validity of particle size and shape approximation as they are frequently used to model cirrus clouds. Once agreement is achieved the model results may be applied to determine, in comparison to a cloudfree case, the influence of this particular cirrus on the radiation budget of the earth atmosphere system. Author

**N91-10464*#** Utah Univ., Salt Lake City. Dept. of Meteorology.
**SUBVISUAL CIRRUS CLOUD PROPERTIES DERIVED FROM A FIRE IFO CASE STUDY**
Kenneth Sassen, M. K. Griffin, and G. C. Dodd *In* NASA, Langley Research Center, FIRE Science Results 1988 Jul. 1990 p 85-88 (For primary document see N91-10448 01-47)
(Grants NAG1-686; NAG1-718; NSF ATM-85-13975)
Avail: NTIS HC/MF A17 CSCL 04B

From the central Wisconsin IFO field at Wausau, the Mobile Polarization Lidar and a surface radiation station from the Lamont-Doherty Geological Observatory observed two very tenuous cirrus clouds on 21 October 1986. The clouds were present just below the height of the tropopause, between -60 to -70 C. The first cloud was not detected visually, and is classified as subvisual cirrus. The second, a relatively narrow cloud band that was probably the remnants of an aircraft contrail, can be termed zenith-subvisual since, although it was invisible in the zenith direction, it could be discerned when viewed at lower elevation angles and also due to strong solar forward-scattering and corona effects. The observations provide an opportunity to assess the threshold cloud optical thickness associated with cirrus cloud visibility. Ruby lidar backscattered signals were converted to isotropic volume backscatter coefficients by applying the pure-molecular scattering assumption just below the cloud base. The backscattering coefficient due to the cloud is then obtained and expressed in relation to the molecular backscattering coefficient in terms of the scattering ratio R. The linear depolarization ratio for the cloud is computed after removing the essentially parallel-polarized scattering contribution from air molecules. The values are also applied to determine the cloud optical thickness through the use of backscatter-to-extinction ratio, and the concentration of cloud particles using the backscattering gain, and the effective diameter of the particles obtained from the analysis of solar corona photographs. The sizes of the particles generating the corona are related to the angular separations between the centers of the red bands and the sun, yielding diameters of approximately 25 microns. The direct and diffuse components of shortwave radiation fluxes, measured by full hemispheric pyranometers, were used to compute the nadir optical thickness of the total atmosphere. Author

**N91-10465*#** Wisconsin Univ., Madison. Cooperative Inst. for Meteorological Satellite Studies.
**MULTI-SPECTRAL WINDOW RADIANCE OBSERVATIONS OF CIRRUS FROM SATELLITE AND AIRCRAFT, NOVEMBER 2, 1986 PROJECT FIRE**
William L. Smith, H. E. Revercomb, H. B. Howell, and M.-X. Lin (National Meteorological Bureau, Beijing, China ) *In* NASA, Langley Research Center, FIRE Science Results 1988 Jul. 1990 p 89-93 (For primary document see N91-10448 01-47)
(Contract NAS1-18272)
Avail: NTIS HC/MF A17 CSCL 04B

High resolution infrared radiance spectra achieved from the NASA ER2 airborne HIS experiment are used to analyze the spectral emissivity properties of cirrus clouds within the 8 to 12 micron atmospheric window region. Observations show that the cirrus emissivity generally decreases with increasing wavenumber (i.e., decreasing wavelength) within this band. A very abrupt decrease in emissivity (increase in brightness temperature) exists between 930/cm (10.8 microns) and 1000/cm (10.0 microns), the magnitude of the change being associated with the cirrus optical thickness as observed by lidar. The HIS observations are consistent with theoretical calculations of the spectral absorption coefficient for ice. The HIS observations imply that cirrus clouds can be detected unambiguously from the difference in brightness temperatures observed within the 8.2 and 11.0 micron window regions of the HIRS sounding radiometer flying on the operational NOAA satellites. This ability is demonstrated using simultaneous 25 km resolution HIRS observations and 1 km resolution AVHRR imagery achieved from the NOAA-9 satellite. Finally, the cirrus cloud location estimates combined with the 6.7 micron channel moisture imagery portray the boundaries of the ice/vapor phase of the upper troposphere moisture. This phase distinction is crucial for infrared radiative transfer considerations for weather and climate models, since upper tropospheric water vapor has little effect on the Earth's outgoing radiation whereas cirrus clouds have a very large attenuating effect. Author

**N91-10466*#** National Aeronautics and Space Administration. Ames Research Center, Moffett Field, CA.
**CIRRUS CLOUD STATISTICS: TEMPERATURES AND OPTICAL DEPTHS**
Francisco P. J. Valero, Thomas P. Ackerman (Pennsylvania State Univ., University Park.), and Warren J. Y. Gore *In* NASA, Langley Research Center, FIRE Science Results 1988 Jul. 1990 p 95-98 (For primary document see N91-10448 01-47)
Avail: NTIS HC/MF A17 CSCL 04B

Measurements of the upwelling infrared radiance at 10.5 and 6.5 microns were obtained during the FIRE cirrus Intensive Field Observations using a radiometer with a 15 deg cone nadir field-of-view flown on the NASA Ames ER-2. Data are recorded at a frequency of 1 Hz and the radiometer is continuously calibrated with a liquid nitrogen blackbody source, thereby providing a large number of very accurate radiance values during the course of a several hour flight. For this study, the focus is on the statistical properties of the cirrus deck as deduced from the radiance data. The data acquired on 28 October 1986 is stressed, but some data from the other flights are also shown for comparison purposes. Author

**N91-10467*#** National Aeronautics and Space Administration. Ames Research Center, Moffett Field, CA.
**THE RADIATION BUDGET OF A CIRRUS LAYER DEDUCED FROM SIMULTANEOUS AIRCRAFT OBSERVATIONS AND MODEL CALCULATIONS Abstract Only**
Thomas P. Ackerman, Stefan A. Kinne, Andrew J. Heymsfield (National Center for Atmospheric Research, Boulder, CO.), and Francisco P. J. Valero *In* NASA, Langley Research Center, FIRE Science Results 1988 Jul. 1990 p 99 (For primary document see N91-10448 01-47)
Avail: NTIS HC/MF A17 CSCL 04B

Several aircraft were employed during the FIRE Cirrus IFO in order to make nearly simultaneous observations of cloud properties and fluxes. A segment of the flight data collected on 28 October 1988 during which the NASA Ames ER-2 overflew the NCAR King Air was analyzed. The ER-2 flew at high altitude making observations of visible and infrared radiances and infrared flux and cloud height and thickness. During this segment, the King Air flew just above the cloud base making observations of ice crystal size and shape, local meteorological variables, and infrared fluxes. While the two aircraft did not collect data exactly coincident in space and time, they did make observations within a few minutes of each other. For this case study, the infrared radiation balance of the cirrus layer is of primary concern. Observations of the upwelling 10 micron radiance, made from the ER-2, can be used to deduce the 10 micron optical depth of the layer. The upwelling broadband infrared flux is also measured from the ER-2. At the same time, the upwelling and downwelling infrared flux at the cloud base is obtained from the King Air measurements. Information on cloud microphysics is also available from the King Air. Using this data in conjunction with atmospheric temperature and humidity profiles from local radiosondes, the necessary inputs for an infrared radiative transfer model can be developed. Infrared radiative transfer calculations are performed with a multispectral two-stream model. The model fluxes at the cloud base and at 19 km are then compared with the aircraft observations to determine whether the model is performing well. Cloud layer heating rates can then be computed from the radiation exchange. Author

**N91-10468*#** National Aeronautics and Space Administration. Goddard Space Flight Center, Greenbelt, MD.
**LIDAR AND RADIOMETER RESULTS FROM THE ER-2 FOR THE FIRE FIELD EXPERIMENTS**
James D. Spinhirne *In* NASA, Langley Research Center, FIRE Science Results 1988 Jul. 1990 p 101-104 (For primary document see N91-10448 01-47)
Avail: NTIS HC/MF A17 CSCL 04B

The airborne lidar and radiometers which were flown during the FIRE cirrus and marine stratus field experiments had multiple objectives. Cloud parameters of direct interest, such as cirrus infrared emittance or convective scales for marine stratus, may be derived from the observations and analyzed along with the available cloud physics and meteorological observations. Additionally however a stated goal of the FIRE studies was to validate satellite cloud retrievals. To this end a number of derived products are to be available from the basic lidar and radiometer observations. The characteristics of the derived products are described, and in addition analysis results for cloud radiometric and structure parameters are presented. This extended abstract will be used to describe the available data products and the associated presentation will emphasize case study analysis results. Author

**N91-10469*#** Rutgers - The State Univ., New Brunswick, NJ. Dept. of Geography.
**IDENTIFICATION OF CIRRUS OVER WAUSAU DURING THE 1986 FIRE IFO FROM GROUND-BASED RADIOMETER DATA**
David A. Robinson and Allan Frei (Lamont-Doherty Geological Observatory, Palisades, NY.) *In* NASA, Langley Research Center, FIRE Science Results 1988 Jul. 1990 p 105-109 (For primary document see N91-10448 01-47)
(Grant NAG1-653)
Avail: NTIS HC/MF A17 CSCL 04B

The potential of using irradiation data to indicate episodes of cirrus cloudiness during the daylight hours is explored. Thresholds separating cirrus from other clouds and clear skies are determined using four days of irradiation data, hourly weather observations, sky photographs, sky video, and occasional lidar observations.

Data were gathered during the First International Satellite Cloud Climatology Program (ISCCP) Regional Experiment (FIRE) Intensive Field Observations (IFO) cirrus project. Thresholds are tested using data from the remaining 17 days of the IFO. Cirrus episodes are defined as intervals when the sky cover is primarily cirrus. Measurements of incoming shortwave and near infrared full hemispheric and diffuse irradiation, and atmospheric infrared irradiation were made at Wausau, Wisconsin Municipal Airport. Data were collected between October 13 and November 2, 1986 and are one minute averages of ten second samples. Data from October 23 and from October 27 to 29 were used for threshold determination. Using weather observations, lidar output, photographs and video, sky conditions were grouped into three categories: noncirrus cloudy, cirrus, and clear. Irradiation data from all periods falling under each of the sky categories were then examined and thresholds denoting a change from one sky category to another were determined. Variables with only a small amount of overlap between sky categories were selected as key indicators. Author

**N91-10470*#** Utah Univ., Salt Lake City.
**INTERPRETATION OF SATELLITE-MEASURED BIDIRECTIONAL REFLECTANCE FROM CIRRUS CLOUDY ATMOSPHERES**
Y. Takano, K. N. Liou, and Patrick Minnis (National Aeronautics and Space Administration. Langley Research Center, Hampton, VA.) *In* NASA, Langley Research Center, FIRE Science Results 1988 Jul. 1990 p 111-113 (For primary document see N91-10448 01-47)
Avail: NTIS HC/MF A17 CSCL 04B

The interpretation of the observed bidirectional reflectance from cirrus cloudy atmospheres is presented. A theoretical model was developed for the computation of the transfer of solar radiation in an anisotropic medium with particular applications to oriented ice crystals in cirrus clouds. In this model, the adding principle for radiative transfer was used with modifications to account for the anisotropy of scattering particles and the associated scattering phase matrix. The single-scattering properties, including the phase function, single-scattering albedo, and extinction cross sections, were used for randomly and horizontally oriented hexagonal ice crystals in radiative transfer computations. The radiative transfer model developed for the cirrus clouds was modified to account for the scattering contributions from the atmosphere and the surface. In order to test the relevance and significance of the ice crystal model for the interpretation of observed bidirectional reflectance from satellites, visible radiances collected on the half hour by the GOES series were selected. The data are calibrated and corrected with the proper filter functions, then navigated to match selected landmark data. A number of clear and cloudy cases during the cirrus IFO of the Fire experiment were chosen for theoretical analyses. The cloud particle shape and size distributions that were taken during satellite overpasses are used in radiative transfer calculations. The sensitivities of the shape, orientation, and size distribution of ice crystals on the reflected intensities at the top of the atmosphere are investigated. Finally, the relative importance of these cloud microphysical properties in the interpretation of satellite bidirectional reflectance are assessed and presented. Author

**N91-10471*#** Wisconsin Univ., Madison. Cooperative Inst. for Meteorological Satellite Studies.
**COMPARISON OF NOAA-9 ERBE MEASUREMENTS WITH CIRRUS IFO SATELLITE AND AIRCRAFT MEASUREMENTS**
Steven A. Ackerman, Hyosang Chung, Stephen K. Cox (Colorado State Univ., Fort Collins.), Leroy Herman, William L. Smith, and Donald P. Wylie *In* NASA, Langley Research Center, FIRE Science Results 1988 Jul. 1990 p 117-121 (For primary document see N91-10448 01-47)
Avail: NTIS HC/MF A17 CSCL 04B

Earth Radiation Budget Experiment (ERBE) measurements onboard the NOAA-9 are compared for consistency with satellite and aircraft measurements made during the Cirrus Intensive Field Observation (IFO) of October 1986. ERBE scene identification is compared with NOAA-9 TIROS Operational Vertical Sounder (TOVS) cloud retrievals; results from the ERBE spectral inversion algorithms are compared with High resolution Interferometer Sounder (HIS) measurements; and ERBE radiant existance measurements are compared with aircraft radiative flux measurements. Author

**N91-10472*#** National Aeronautics and Space Administration. Langley Research Center, Hampton, VA.
**ERBE AND AVHRR CIRRUS CLOUD FIRE STUDY**
Edwin F. Harrison, Patrick Minnis, Bruce A. Wielicki, Patrick W. Heck, S. K. Gupta, David F. Young, and G. G. Gibson (Planning Research Corp., Hampton, VA.) *In its* FIRE Science Results 1988 Jul. 1990 p 123-127 (For primary document see N91-10448 01-47)
Avail: NTIS HC/MF A17 CSCL 04B

Understanding the impact of cirrus clouds on the global radiation budget is essential to determining the role of clouds in the process of climate change. The ongoing Earth Radiation Budget Experiment (ERBE) is charged with measuring the global radiation balance at the top of the atmosphere. The International Satellite Cloud Climatology Project (ISCCP) is measuring global cloud amounts and properties over a time frame similar to ERBE. Specific cloud properties are absent from the ERBE program, while ISCCP lacks the broadband radiances necessary to determine the total radiation fields. Together, results from these two global programs have the potential for improving the knowledge of the relationship between cirrus clouds and the Earth radiation balance. The First ISCCP Regional Experiment (FIRE), especially its cirrus Intensive Field Observations (IFO), provides opportunities for studying radiation measurements from the ERBE taken over areas with known cirrus cloud properties. Satellite measurements taken during the IFO are used to determine the broadband radiation fields over cirrus clouds and to examine the relationship between narrowband and broadband radiances over various known scenes. The latter constitutes the link between the ERBE and the ISCCP. Author

**N91-10473*#** National Aeronautics and Space Administration. Langley Research Center, Hampton, VA.
**CLOUD PARAMETERS FROM GOES VISIBLE AND INFRARED RADIANCES DURING THE FIRE CIRRUS IFO, OCTOBER 1986**
Patrick W. Heck, David F. Young (Planning Research Corp., Hampton, VA.), Patrick Minnis, and Edwin F. Harrison *In its* FIRE Science Results 1988 Jul. 1990 p 129-133 (For primary document see N91-10448 01-47)
Avail: NTIS HC/MF A17 CSCL 04B

Visible (VIS, 0.65 micron) and infrared (IR, 10.5 microns) channels on geostationary satellites are the key elements of the International Satellite Cloud Climatology Project (ISCCP). All daytime ISCCP cloud parameters are derived from a combination of VIS and IR data. Validation and improvement of the ISCCP and other cloud retrieval algorithms are important components of the First ISCCP Regional Experiment (FIRE) Intensive Field Observations (IFO). Data from the Cirrus IFO (October 19 to November 2, 1986) over Wisconsin are available for validating cirrus cloud retrievals from satellites. The Geostationary Operational Environmental Satellite (GOES) located over the Equator at approximately 100 deg W provided nearly continuous measurements of VIS and IR radiances over the IFO areas. The preliminary results of cloud parameters derived from the IFO GOES data are presented. Cloud attitudes are first derived using an algorithms without corrections for cloud emissivity. These same parameters will then be computed from the same data relying on an emissivity correction algorithm based on correlative data taken during the Cirrus IFO. Author

**N91-10474*#** Wisconsin Univ., Madison. Cooperative Inst. for Meteorological Satellite Studies.
**CLOUD ALTITUDE DETERMINATION FROM INFRARED SPECTRAL RADIANCES**
William L. Smith and Richard Frey *In* NASA, Langley Research Center, FIRE Science Results 1988 Jul. 1990 p 135-139 (For

primary document see N91-10448 01-47)
(Contract NAS1-18272)
Avail: NTIS HC/MF A17 CSCL 04B

The CO2 slicing method is generally recognized as the most accurate means of inferring cloud altitude from passive infrared radiance observations. The method is applicable to semi-transparent and broken clouds. During the cirrus FIRE and COHMEX field experiments, CO2 channel radiance data suitable for cloud altitude specification were achieved from moderate spectral resolution satellite sounders (NOAA-TOVS and GOES-VAS) and from a High spectral resolution Interferometer Spectrometer (HIS) flown on the NASA U2/ER2 aircraft. Also aboard the ER2 was a down-looking active lidar unit capable of providing cloud top pressure verifications with high accuracy. A third instrument, the Multispectral Atmospheric Mapping Sensor (MAMS) provided 50 meter resolution infrared window data which is used wtih radiosonde data to verify the heights of middle and low level clouds. Comparisons of lidar and MAMS/radiosonde ground truth cloud heights are made with those determined from: high resolution (0.5/cm) HIS spectra, HIS spectra degraded to the moderate resolution (15/cm) of the VAS/TOVS instruments, and spectrally averaged HIS radiances for individual pairs of VAS spectral channels. The results show that the best results are achieved from high resolution spectra; the RMS difference with the ground truth is 23 mb. The RMS differences between the infrared radiance determination and ground truth increase by 35 percent when the spectral resolution is degraded to the moderate spectral resolution of the VAS/TOVS instruments and by 52 to 183 percent, depending upon channel combinations, when only two spectral channels at VAS/TOVS spectral resolution are used.
Author

**N91-10475*#** National Aeronautics and Space Administration. Langley Research Center, Hampton, VA.
**AVHRR AND VISSR SATELLITE INSTRUMENT CALIBRATION RESULTS FOR BOTH CIRRUS AND MARINE STRATOCUMULUS IFO PERIODS**
C. H. Whitlock, W. F. Staylor, John T. Suttles, G. Smith, R. Levin, R. Frouin, C. Gautier, P. M. Teillet, P. N. Slater, and Y. J. Kaufman (National Aeronautics and Space Administration. Goddard Space Flight Center, Greenbelt, MD.) et al *In its* FIRE Science Results 1988 Jul. 1990 p 141-145 (For primary document see N91-10448 01-47)
Avail: NTIS HC/MF A17 CSCL 04B

Accurate characterizations of some cloud parameters are dependent upon the absolute accuracy of satellite radiance measurements. Visible wavelength measurements from both the AVHRR and VISSR instruments are often used to study cloud characteristics. Both of these instruments were radiometrically calibrated prior to launch, but neither has an onboard device to monitor degradation after launch. During the FIRE/SRB cirrus Intensive Field Operation (IFO), a special effort was made to monitor calibration of these two instruments onboard the NOAA-9 and GOES-6 spacecraft. In addition, several research groups have combined their efforts to assess the long-term performance of both instruments. These results are presented, and a limited comparison is made with the ERBE calibration standard. Author

**N91-10476*#** National Aeronautics and Space Administration. Langley Research Center, Hampton, VA.
**CIRRUS CLOUD PROPERTIES DERIVED FROM COINCIDENT GOES AND LIDAR DATA DURING THE 1986 FIRE CIRRUS INTENSIVE FIELD OBSERVATIONS (IFO)**
Patrick Minnis, Jose M. Alvarez, David F. Young, Patrick W. Heck, and Kenneth Sassen (Utah Univ., Salt Lake City.) *In its* FIRE Science Results 1988 Jul. 1990 p 147-151 (For primary document see N91-10448 01-47)
Avail: NTIS HC/MF A17 CSCL 04B

One of the main difficulties in detecting cirrus clouds and determining their correct altitude using satellite measurements is their nonblackness. In the present algorithm (Rossow et al., 1985) used by the International Satellite Cloud Climatology Project (ISCCP), the cirrus cloud emissivity is estimated from the derived cloud reflectance using a theoretical model relating visible (VIS, 0.65 micron) optical depth to infrared (IR, 10.5 micron) emissivity. At this time, it is unknown how accurate this approach is or how the derived cloud altitude relates to the physical properties of the cloud. The First ISCCP Regional Experiment (FIRE) presents opportunities for determining how the observed radiances depend on the cloud properties. During the FIRE Cirrus Intensive Field Observations (IFO, see Starr, 1987), time series of cloud thickness, height, and relative optical densities were measured from several surface-based lidars. Cloud microphysics and radiances at various wavelengths were also measured simultaneously over these sites from aircraft at specific times during the IFO (October 19 to November 2, 1986). Satellite-observed radiances taken simultaneously can be matched with these data to determine their relationships to the cirrus characteristics. The first step is taken toward relating all of these variables to the satellite observations. Lidar-derived cloud heights are used to determine cloud temperatures which are used to estimate cloud emissivities from the satellite IR radiances. These results are then correlated to the observed VIS reflectances for various solar zenith angles.
Author

**N91-10477*#** National Aeronautics and Space Administration. Goddard Space Flight Center, Greenbelt, MD.
**OVERVIEW OF THE 27-28 OCTOBER FIRE CIRRUS IFO CASE: METEOROLOGY AND CLOUD FIELDS Abstract Only**
David OC. Starr and Donald P. Wylie (Wisconsin Univ., Madison.) *In* NASA, Langley Research Center, FIRE Science Results 1988 Jul. 1990 p 155 (For primary document see N91-10448 01-47)
Avail: NTIS HC/MF A17 CSCL 04B

A detailed description of the meteorology of the 27 and 28 October FIRE Cirrus IFO case is presented. The progression of synoptic scale events over the region is reviewed including the evolution of surface and upper air features, i.e., the surface cyclone that formed to the west over Montana on the 27th and moved through Wisconsin late on the 28th and the associated short wave ridge aloft. A summary of the corresponding cloud conditions observed over the area of aircraft operations is given including characterization of the cloud forms and cloud heights based on information derived from debriefings of the aircrews, surface observations, airborne (ER-2) and surface lidars observations and satellite imagery (GOES). The correspondence between the resolved meteorological features (subsynoptic rawinsonde network) and the development of cloud layers is illustrated. In particular, the discussion emphasizes the relationship between vertical thermodynamic structure and the character and vertical structure of the cloud fields. The role of the larger scale in maintaining the observed vertical structure is quantified both with respect to its control via forced ascent and advective processes. Based on results of these analyses, conclusions are drawn with respect to the design of future field missions. Author

**N91-10478*#** National Aeronautics and Space Administration. Langley Research Center, Hampton, VA.
**A FOUR-LIDAR VIEW OF CIRRUS FROM THE FIRE IFO: 27-28 OCTOBER 1986**
Kenneth Sassen, Christian John Grund, Jose M. Alvarez, and Freeman F. Hall (National Oceanic and Atmospheric Administration, Boulder, CO.) *In its* FIRE Science Results 1988 Jul. 1990 p 157-158 (For primary document see N91-10448 01-47)
(Contract N00014-85-K-0581; NSF ATM-85-13975; DAAG29-84-K-0069)
Avail: NTIS HC/MF A17 CSCL 04B

The four ground-based lidar systems that participated in the 1986 FIRE IFO were configured in a diamond-shaped array across central and southern Wisconsin. Data were generally collected in the zenith pointing mode, except for the Doppler lidar, which regularly operated in a scanning mode with intermittent zenith observations. As a component of the cirrus case study of 27 and 28 October 1986 selected for initial analysis, data collected by the remote sensor ensemble from 1600 (on the 27th) to 2400 UTC (on the 28th) is described and compared. In general, the cirrus studied on the 27th consisted of intermittent layers of thin and subvisual cirrus clouds. Particularly at Wausau, subvisual cirrus was detected from 11.0 to 11.5 km MSL, just below the tropopause. At lower levels, occasional cirrus clouds between approx. 8.0 to 9.5 km were detected from all ground sites. Preliminary analysis of the four-lidar dataset reveals the passage of surprisingly consistent cloud features across the experiment area. A variety of types and amounts of middle and high level clouds occurred, ranging from subvisual cirrus to deep cloud bands. It is expected that the ground-based lidar measurements from this case study, as well as the airborne observations, will provide an excellent data base for comparison to satellite observations. Author

**N91-10479*#** Colorado State Univ., Fort Collins. Dept. of Atmospheric Science.

**RADIATIVE PROPERTIES OF CIRRUS CLOUDS: FIRE IFO CASE OCTOBER 28, 1986**

Paul F. Hein, William L. Smith, Jr., and Stephen K. Cox *In* NASA, Langley Research Center, FIRE Science Results 1988 Jul. 1990 p 159-162 (For primary document see N91-10448 01-47)

(Grants NAG1-554; NSF ATM-85-21214)

Avail: NTIS HC/MF A17 CSCL 04B

A description of the radiative properties of two cirrus clouds sampled on 10/28/88 in the FIRE cirrus IFO is presented. The clouds are characterized in terms of the broadband infrared effective emittance, cloud fractional absorptance, shortwave heating rate, cloud albedo and vertical velocity. The broadband fluxes used in these calculations were obtained from measurements made by pyranometers and pyrgeometers. The shortwave irradiances were corrected to a horizontal plane and normalized to the same time by taking into account Sabreliner flight information (i.e., pitch, roll, heading and angle of attack), as well as sun-earth geometry considerations. Since only one aircraft was used, broadband fluxes at different levels in the cloud were not measured simultaneously. As a result, sampling errors may occur due to the nonsteady state of the cloud field or due to the possibility that the flight legs were not flown directly above or below each other. To minimize these errors and to simplify the analysis, the necessary variables were averaged and the averages used in the calculations. The downwelling shortwave and longwave irradiances were used as selection criteria to remove cloud free data encountered along the data sampling leg. Author

**N91-10480*#** National Aeronautics and Space Administration. Langley Research Center, Hampton, VA.

**FIRE CIRRUS ON OCTOBER 28, 1986: LANDSAT; ER-2; KING AIR; THEORY**

Bruce A. Wielicki, John T. Suttles, Andrew J. Heymsfield, Ronald M. Welch, James D. Spinhirne, Lindsay Parker, and Robert F. Arduini (Planning Research Corp., Hampton, VA.) *In its* FIRE Science Results 1988 Jul. 1990 p 163-168 (For primary document see N91-10448 01-47)

Avail: NTIS HC/MF A17 CSCL 04B

A simultaneous examination was conducted of cirrus clouds in the FIRE Cirrus IFO-I on 10/28/86 using a multitude of remote sensing and in-situ measurements. The focus is cirrus cloud radiative properties and their relationship to cloud microphysics. A key element is the comparison of radiative transfer model calculations and varying measured cirrus radiative properties (emissivity, reflectance vs. wavelength, reflectance vs. viewing angle). As the number of simultaneously measured cloud radiative properties and physical properties increases, more sharply focused tests of theoretical models are possible. Author

**N91-10481*#** National Aeronautics and Space Administration. Langley Research Center, Hampton, VA.

**SURFACE RADIATION OBSERVATIONS FOR OCTOBER 27-28, 1986 DURING THE WISCONSIN FIRE/SRB EXPERIMENT**

C. H. Whitlock, L. R. Poole, S. R. LeCroy, and D. A. Robinson (Rutgers - The State Univ., New Brunswick, NJ.) *In its* FIRE Science Results 1988 Jul. 1990 p 169-172 (For primary document see N91-10448 01-47)

Avail: NTIS HC/MF A17 CSCL 04B

A portion of both the shortwave and longwave surface radiation data is presented which was measured during the combined FIRE (First ISCCP Regional Experiment) and SRB (Surface Radiation Budget) experiments conducted in central Wisconsin from October 14 to November 2, 1988. The time periods from which high quality measurement values were obtained are summarized. Data gaps exist because of either equipment malfunctions or electrical power failures. Intercomparison of pre-experiment measurements by the various organizations involved suggests that all stations are accurate (relative to each other) to within about 10 W/m(sup -2) on a 24-hour daily average basis. Most of the instruments were calibrated by the National Radiation Centers in either the U.S. (National Oceanic and Atmospheric Administration) or Canada (Atmospheric Environment Service). October 27 and 28, 1986 were selected for detailed case study because a large amount of cirrus clouds existed over the experiment region on those days. Downwelled irradiance values are shown at each surface station at the time of afternoon NOAA-9 overpasses. Values shown are 10-minute averages centered about each overpass time, but minute-average data are available. Author

**N91-10482*#** National Aeronautics and Space Administration. Langley Research Center, Hampton, VA.

**THE NEW FIRE CLOUD LIDAR AT LANGLEY RESEARCH CENTER Abstract Only**

Jose M. Alvarez, M. P. McCormick, M. A. Vaughn, G. Kent, W. H. Hunt, W. H. Fuller, B. R. Rouse, and R. Dubinsky (Science and Technology Corp., Hampton, VA.) *In its* FIRE Science Results 1988 Jul. 1990 p 175 (For primary document see N91-10448 01-47)

Avail: NTIS HC/MF A17 CSCL 04B

Using the Langley Aircraft Lidar for cirrus cloud observations at Langley Research Center in Hampton, Virginia is overkill both in terms of the actual lidar and the people required to run the system. A small lidar system to be used specifically for cloud probing was designed and constructed at Langley in 1987. This lidar is presently being used to collect the FIRE ETO (Extended Time Observation) data at Langley. A description of the new FIRE Cloud Lidar System is presented. The data collected by this lidar is discussed as well as some of the cloud statistics emerging from the data. A brief synopsis of system performance is also given. Author

**N91-10483*#** Wisconsin Univ., Madison. Dept. of Meteorology.

**INTERPRETATION OF THE OPTICAL AND MORPHOLOGICAL PROPERTIES OF CIRRUS CLOUDS FROM LIDAR MEASUREMENTS**

Christian John Grund and Edwin W. Eloranta *In* NASA, Langley Research Center, FIRE Science Results 1988 Jul. 1990 p 177-181 (For primary document see N91-10448 01-47)

(Contract N00014-85-K-0581; DAAG29-84-K-0069)

Avail: NTIS HC/MF A17 CSCL 04B

Lidar measurements can provide a great deal of information about the structure, location, and scattering properties of cirrus clouds. However, caution must be used when interpreting raw lidar backscatter profiles in terms of relative or absolute extinction distribution, internal cloud structure, and, at times, cloud location. The problem arises because the signal measured from a range by any monostatic lidar system depends on the backscatter cross section at that range and the 2-way optical thickness to the scattering volume. Simple lidar systems, however, produce only one measurement of attenuated backscatter from each range. The general FIRE research community is given aid in interpretation of lidar measurements, and the special capabilities of the High Spectral Resolution Lidar (HSRL) is explained. Some examples are given of conditions under which direct interpretation of cirrus cloud morphology from simple lidar profiles could be misleading. Author

**N91-10484*#** Colorado State Univ., Fort Collins. Dept. of Atmospheric Science.
**TEMPERATURE SENSITIVITY OF EPPLEY BROADBAND RADIOMETERS** c35
William L. Smith, Jr. and Stephen K. Cox *In* NASA, Langley Research Center, FIRE Science Results 1988 Jul. 1990 p 183-186 (For primary document see N91-10448 01-47)
(Grants NAG1-554; NSF ATM-85-21214)
Avail: NTIS HC/MF A17 CSCL 14B

Broadband radiometers manufactured by Eppley Laboratories Inc. are commonly used to measure irradiance from both ground-based and aircraft platforms. Namely, the pyranometer (Model PSP) measures irradiance in the .3 to 3.0 micron spectral region while the pyrgeometer (Model PIR) senses energy in the 4 to 50 micron region. The two instruments have a similar thermopile construction but different filters to achieve the appropriate spectral selection. During the fall of 1986, the First ISCCP (International Satellite Cloud Climatology Project) Regional Experiment (FIRE) commenced with the first cirrus Intensive Field Observation (IFO) conducted in Central Wisconsin. Due to the nature of this field project, pyranometers and pyrgeometers manufactured by Eppley were flown on NCAR's high altitude research aircraft, the Sabreliner. Inherent in the construction of these radiometers is temperature compensation circuitry designed to make the instrument sensitivity nominally constant over a temperature range from -20 to +40 C. Because the Sabreliner flew at high altitudes where temperatures were as cold as -70 C, it was necessary to determine the radiometers relative sensitivity to temperatures below -20 C and apply appropriate corrections to the FIRE radiation data set. A procedure to perform this calibration is outlined. It is meant to serve as a supplement to calibration procedures. Author

**N91-10485*#** Wisconsin Univ., Madison. Space Science and Engineering Center.
**BOTH SIDES NOW**
Donald P. Wylie *In* NASA, Langley Research Center, FIRE Science Results 1988 Jul. 1990 p 187-190 (For primary document see N91-10448 01-47)
Avail: NTIS HC/MF A17 CSCL 04B

On November 2, 1986 of the cirrus Intensive Field Observations, cirrus clouds were observed from both ground-based and aircraft lidar. The NASA ER2 aircraft carrying a lidar, crossed Madison three times and Wausau five times during its mission. Ground-based lidars from the University of Wisconsin in Madison and the University of Utah in Wausau were operating during the ER2 overpasses. This gave FIRE unique lidar observations of cirrus clouds from both sides. This lidar data are presented and analyzed. Author

**N91-10486*#** Georgia Inst. of Tech., Atlanta. School of Geophysical Sciences.
**SUB-VISUAL CIRRUS DETECTION AND CHARACTERIZATION**
E. Schmidt, G. Grams, and E. Patterson *In* NASA, Langley Research Center, FIRE Science Results 1988 Jul. 1990 p 191-192 (For primary document see N91-10448 01-47)
Avail: NTIS HC/MF A17 CSCL 04B

Analysis of archived cold optics (COR) radiometer data is yielding useful information on the diurnal, geographic, seasonal and altitude variability of atmospheric background radiance levels in the 11 micron window region. This database is a compilation of Kuiper Infrared Technology Experiment (KITE) and Atmospheric Radiance Study (ARS) observations under a wide variety of conditions. Correlating the measurements from these two studies with the LOWTRAN model code has revealed several important results. First, the 11 micron window appears to be filled-in, i.e., the troughs on either side of the nitric acid peak are shallower than expected. Second, the amplitude of the background radiances measured exceeds the model predictions by a factor of 2 to 3 or more. This is thought to be due to the existence of thin, high altitude cirrus clouds (sub-visual cirrus) above the sensor platform. These high background levels are observed under quiescent conditions in the South Pacific (Marshall Islands), as well as over the continental United States (the West Coast). In the tropics, there appears to be little diurnal variability, a plausible seasonal variation and a linear dependence between 7.2 and 11.4 micron band data, indicating possible multi-spectral approaches to detection of sub-visual cirrus clouds. Theoretical analysis of the magnitude of the effects of a sub-visual cirrus cloud on atmospheric background radiances measured by a near-horizontal sensor is in progress. Author

**N91-10487*#** National Aeronautics and Space Administration. Goddard Space Flight Center, Greenbelt, MD.
**CLOUD ATLAS FOR THE FIRE CIRRUS INTENSIVE FIELD OBSERVATION (IFO)**
Albert Arking, Jeffrey D. Childs, John H. Merritt, and Sharen L. Williams (Applied Research Corp., Landover, MD.) *In* NASA, Langley Research Center, FIRE Science Results 1988 Jul. 1990 p 193-196 (For primary document see N91-10448 01-47)
Avail: NTIS HC/MF A17 CSCL 04B

An Intensive Field Observation (IFO) of cirrus clouds was conducted over the mid-western U.S. during the period October 13 to November 2, 1986. This activity, part of the First ISCCP Regional Experiment (FIRE), included measurements made from specially deployed instruments on the ground, balloons, and aircraft as well as observations from existing operational and experimental satellites. One of the sets of satellite observations was the radiance measurements made with the 5-channel AVHRR radiometer on the NOAA 9 polar orbiting meteorological satellite. The ground resolution of the measurements at nadir is approx. 1 km. It is these measurements, made once each day at approximately 2:30 p.m. local time, that were used in determining the present cloud atlas. The area covered by the atlas is slightly larger than the area specified for the IFO, in order to be in alignment with the grid that will be used in a forthcoming atlas for the larger, ETO region. The atlas contains four pages of information for each satellite pass. The 1st page of each group shows the distribution of measured radiances in channel 1 (normalized to the incoming solar flux multiplied by the cosine of the solar zenith angle) and in channel 4 for the area as a whole and for each analysis box. The 2nd page shows the images in: channels 1 and 2, channel 3R; and channel 4. The 3rd page shows the retrieved parameters in graphical form for the region as a whole and for each analysis box, where cloud fraction appears as a contour plot with respect to optical thickness and cloudtop temperature. The 4th page provides a statistical summary of the retrieved parameters in numerical form for each analysis box. Author

**N91-10488*#** National Aeronautics and Space Administration. Langley Research Center, Hampton, VA.
**EXTENDED TIME OBSERVATIONS OF CALIFORNIA MARINE STRATOCUMULUS CLOUDS FROM GOES FOR JULY 1983-1987**
Patrick Minnis, Edwin F. Harrison, and David F. Young (Planning Research Corp., Hampton, VA.) *In its* FIRE Science Results 1988 Jul. 1990 p 201-205 (For primary document see N91-10448 01-47)
Avail: NTIS HC/MF A17 CSCL 04B

One of the goals of the First ISCCP Regional Experiment (FIRE) is to relate the relatively small scale (spatial and temporal) Intensive Field Observations (IFO) to larger time and space domains embodied in the Extended Time Observations (ETO) phase of the experiment. The data analyzed as part of the ETO are to be used to determine some climatological features of the limited area which encompasses the Marine Stratocumulus IFO which took place between 29 June and 19 July 1987 off the coast of southern California. Author

**N91-10489*#** Wisconsin Univ., Madison.
**THE RELATIONSHIP OF MARINE STRATUS TO SYNOPTIC CONDITIONS**
Donald P. Wylie, Barry Hinton, Peter Grimm, and Kevin A. Kloesel (Pennsylvania State Univ., University Park.) *In* NASA, Langley Research Center, FIRE Science Results 1988 Jul. 1990 p 207-211 (For primary document see N91-10448 01-47)
Avail: NTIS HC/MF A17 CSCL 04B

The marine stratus which persistently covered most of the eastern Pacific Ocean, had large clear areas during the FIRE Intensive Field Operations (IFO) in 1987. Clear zones formed inside the large oceanic cloud mass on almost every day during the IFO. The location and size of the clear zones varied from day to day implying that they were related to dynamic weather conditions and not to oceanic conditions. Forecasting of cloud cover for aircraft operations during the IFO was directed towards predicting when and where the clear and broken zones would form inside the large marine stratus cloud mass. The clear zones often formed to the northwest of the operations area and moved towards it. However, on some days the clear zones appeared to form during the day in the operations area as part of the diurnal cloud burn off. The movement of the clear zones from day to day were hard to follow because of the large diurnal changes in cloud cover. Clear and broken cloud zones formed during the day only to distort in shape and fill during the following night. The field forecasters exhibited some skill in predicting when the clear and broken cloud patterns would form in the operations area. They based their predictions on the analysis and simulations of the models run by NOAA's Numeric Meteorological Center. How the atmospheric conditions analyzed by one NOAA/NMC model related to the cloud cover is discussed. Author

**N91-10490*#** Betts (Alan K.), Middlebury, VT.

**ANALYSIS OF DIURNAL VARIATION OF SCu LAYER USING 2 DAYS OF CLASS SOUNDINGS ON SAN NICOLAS ISLAND Abstract Only**

Alan K. Betts *In* NASA, Langley Research Center, FIRE Science Results 1988 Jul. 1990 p 213 (For primary document see N91-10448 01-47)

(Contract NAS5-28800; NSF ATM-87-05403)

Avail: NTIS HC/MF A17 CSCL 04B

Sixty-nine soundings were taken at San Nicolas Island during the FIRE marine stratocumulus experiment. The archived thermodynamic data at 5mb vertical resolution were reduced to 25mb vertical resolution by averaging. Ceilometer data showed the time variation of cloud-base. A subset of 20 soundings taken during a 2 day period of light winds were analyzed. The soundings are grouped into 6 hr. averages (with 5 soundings in each category) to examine the diurnal variation of the thermodynamic structure. Consistent with the solar heating during the daytime, cloud-base rises during the daytime hours and the cloud layer thins. The subcloud layer also becomes more stable, suggesting some uncoupling of the cloud layer from the surface. Author

**N91-10491*#** McGill Univ., Montreal (Quebec). Dept. of Meteorology.

**DIURNAL VARIATION OF MARINE STRATOCUMULUS OVER SAN NICOLAS ISLAND DURING THE FIRE IFO**

R. Davies and M. Blaskovic *In* NASA, Langley Research Center, FIRE Science Results 1988 Jul. 1990 p 215-219 Sponsored in part by NSERC, and AES (For primary document see N91-10448 01-47)

(Grant NAG1-552)

Avail: NTIS HC/MF A17 CSCL 04B

Preliminary analysis was made of data collected at San Nicolas Island during the Intensive Field Observation (IFO) phase of the First International Satellite Cloud Climatology Program's Regional Experiment (FIRE). Of particular interest was an examination of a distinct diurnal variation in the cloud properties, despite an apparent absence of diurnal forcing from the surface. Direct or indirect radiative modulation of such clouds, as proposed by Fravalo at el. (1981) and Turton and Nicholls (1987) indeed seems likely. Preliminary observational evidence for diurnal change in the marine stratocumulus adjacent to San Nicolas Island is presented. A comparison is then made between the observed behavior and predictions from theoretical models of the interactive effect of radiation on boundary layer clouds. Author

**N91-10492*#** Colorado State Univ., Fort Collins. Dept. of Atmospheric Science.

**ANALYSIS OF TETHERED BALLOON, CEILOMETER AND CLASS SOUNDING DATA TAKEN ON SAN NICOLAS ISLAND DURING THE FIRE PROJECT**

Wayne H. Schubert, Paul E. Ciesielski, Thomas A. Guinn, Stephen K. Cox, and Thomas B. McKee *In* NASA, Langley Research Center, FIRE Science Results 1988 Jul. 1990 p 221-223 (For primary document see N91-10448 01-47)

(Contract NAG1-554; N000014-87-K-0228)

Avail: NTIS HC/MF A17 CSCL 04B

During the FIRE Marine Stratocumulus Program on San Nicolas Island, Colorado State University (CSU) and the British Meteorological Office (BMO) operated separate instrument packages on the NASA tethered balloon. The CSU package contained instrumentation for the measurement of temperature, pressure, humidity, cloud droplet concentration, and long and short wave radiation. Eight research flights, performed between July 7 and July 14, are summarized. An analysis priority to the July 7, 8 and 11 flights was assigned for the purposes of comparing the CSU and BMO data. Results are presented. In addition, CSU operated a laser ceilometer for the determination of cloud base, and a CLASS radiosonde site which launched 69 sondes. Data from all of the above systems are being analyzed. Author

**N91-10493*#** Betts (Alan K.), Middlebury, VT.

**RADIATIVE CONTROL ON TROPICAL CONVECTIVE BOUNDARY LAYER EQUILIBRIUM Abstract Only**

Alan K. Betts and W. Ridgway (Applied Research Corp., Landover, MD.) *In* NASA, Langley Research Center, FIRE Science Results 1988 Jul. 1990 p 225 (For primary document see N91-10448 01-47)

(Contract NAS5-28800; NSF ATM-87-05403)

Avail: NTIS HC/MF A17 CSCL 04B

How the near-balance between the radiative cooling and the surface fluxes in the tropics controls boundary layer, the height of cloud-base and the top of the convective boundary layer over the tropical oceans is discussed. The impact of boundary layer cloudiness and upper level moisture on the equilibrium solutions is explored. Author

**N91-10494*#** National Center for Atmospheric Research, Boulder, CO.

**A GCM PARAMETERIZATION FOR THE SHORTWAVE RADIATIVE PROPERTIES OF WATER CLOUDS Abstract Only**

A. Slingo *In* NASA, Langley Research Center, FIRE Science Results 1988 Jul. 1990 p 227 Sponsored in part by NSF (For primary document see N91-10448 01-47)

Avail: NTIS HC/MF A17 CSCL 04B

A new parameterization was developed for predicting the shortwave radiative properties of water clouds, suitable for inclusion in general circulation models (GCMs). The parameterization makes use of the simple relationships found by Slingo and Schrecker, giving the three input parameters required to calculate the cloud radiative properties (the optical depth, single scatter albedo and asymmetry parameter) in terms of the liquid water path and equivalent radius of the drop size distribution. The input parameters are then used to derive the cloud radiative properties, using standard two-stream equations for a single layer. The relationships were originally derived for fairly narrow spectral bands but it was found that it is possible to average the coefficients so as to use a much smaller number of bands, without sacrificing accuracy in calculating the cloud radiative properties. This makes the parameterization fast enough to be included in GCMs. The parameterization was programmed into the radiation scheme used in the U.K. Meteorological Office GCM. This scheme and the 24 band Slingo/Schrecker scheme were compared with each other and with observations, using a variety of published datasets. There is good agreement between the two schemes for both cloud albedo and absorption, even when only four spectral bands are employed in the GCM. Author

**N91-10495*#** Meteorological Office, London (England). Cloud Physics Branch.

**PRELIMINARY MIXED-LAYER MODEL RESULTS FOR FIRE MARINE STRATOCUMULUS IFO CONDITIONS Abstract Only**

R. Barlow and S. Nicholls *In* NASA, Langley Research Center, FIRE Science Results 1988 Jul. 1990 p 229 (For primary document see N91-10448 01-47)

Avail: NTIS HC/MF A17 CSCL 04B

Some preliminary results from the Turton and Nicholls mixed layer model using typical FIRE boundary conditions are presented. The model includes entrainment and drizzle parametrizations as well as interactive long and shortwave radiation schemes. A constraint on the integrated turbulent kinetic energy balance ensures that the model remains energetically consistent at all times. The preliminary runs were used to identify the potentially important terms in the heat and moisture budgets of the cloud layer, and to assess the anticipated diurnal variability. These are compared with typical observations from the C130. Sensitivity studies also revealed the remarkable stability of these cloud sheets: a number of negative feedback mechanisms appear to operate to maintain the cloud over an extended time period. These are also discussed. The degree to which such a modelling approach can be used to explain observed features, the specification of boundary conditions and problems of interpretation in non-horizontally uniform conditions is also raised. Author

**N91-10496*#** Washington Univ., Seattle. Dept. of Applied Mathematics.

**SIMULATIONS AND OBSERVATIONS OF CLOUDTOP PROCESSES**

S. T. Siems, C. S. Bretherton, and M. B. Baker *In* NASA, Langley Research Center, FIRE Science Results 1988 Jul. 1990 p 231-235 (For primary document see N91-10448 01-47) (Grant NSF ATM-86-20165)

Avail: NTIS HC/MF A17 CSCL 04B

Turbulent entrainment at zero mean shear stratified interfaces has been studied extensively in the laboratory and theoretically for the classical situation in which density is a passive tracer of the mixing and the turbulent motions producing the entrainment are directed toward the interface. It is the purpose of the numerical simulations and data analysis to investigate these processes and, specifically, to focus on the following questions: (1) Can local cooling below cloudtop play an important role in setting up convective circulations within the cloud, and bringing about entrainment; (2) Can Cloudtop Entrainment Instability (CEI) alone lead to runaway entrainment under geophysically realistic conditions; and (3) What are the important mechanisms of entrainment at cloudtop under zero or low mean shear conditions. Author

**N91-10497*#** Colorado Univ., Boulder. Cooperative Inst. for Research in Environmental Sciences.

**A CLOUD CLASSIFICATION SCHEME APPLIED TO THE BREAKUP REGION OF MARINE STRATOCUMULUS**

Siri Jodha Singh Khalsa and Catherine Gautier (Scripps Institution of Oceanography, La Jolla, CA.) *In* NASA, Langley Research Center, FIRE Science Results 1988 Jul. 1990 p 237-242 Sponsored in part by Navy (For primary document see N91-10448 01-47)

Avail: NTIS HC/MF A17 CSCL 04B

A major goal of the marine stratocumulus (MSc) segment of FIRE is to describe and explain the temporal and spatial variability in fractional cloud cover. The challenge from a theoretical standpoint is to correctly represent the mechanisms leading to the transitions between solid stratus, stratocumulus and trade wind cumulus. The development and testing of models accounting for fractional cloudiness require an observational data base that will come primarily from satellites. This, of course, is one of the missions of the ISCCP. There are a number of satellite cloud analysis programs that are being undertaken as part of FIRE. One that has already produced data from the FIRE MSc experiment is the spatial coherence method (COAKLEY and Baldwin, 1984). This method produces information on fractional cloud coverage and cloud heights. It may be possible, however, to extract more information on cloud structure from satellite data that might be of use in describing the transitions in the marine stratocumulus cloud deck. Potential applications are explored of a cloud analysis scheme relying on more detailed analysis of visible and infrared cloud radiance statistics. For this preliminary study, data is examined from three days during the 1987 FIRE MSc field work. These case studies provide a basis for comparison and evaluation of the technique. Author

**N91-10498*#** Colorado State Univ., Fort Collins. Dept. of Atmospheric Science.

**FRACTIONAL CLOUDINESS IN SHALLOW CUMULUS LAYERS**

David A. Randall *In* NASA, Langley Research Center, FIRE Science Results 1988 Jul. 1990 p 243-247 Sponsored by NASA (For primary document see N91-10448 01-47)

Avail: NTIS HC/MF A17 CSCL 04B

Fractional cloudiness influences the planetary boundary layer (PBL) by controlling the cloud-top radiative cooling rate, and regulating the buoyant production and consumption of turbulence kinetic energy. Betts, Hanson, and Albrecht have modeled partly cloudy PBLs by assuming a single family of convective circulations. The same idealized model has been used in observational studies, based on conditional sampling and/or joint distribution functions, by Lenschow, Albrecht, and others. This approach is extended. None of these authors has proposed a method to determine the fractional area covered by rising motion; finding such a method was a key objective of the present study. Author

**N91-10499*#** National Center for Atmospheric Research, Boulder, CO.

**STUDYING MARINE STRATUS WITH LARGE EDDY SIMULATION Abstract Only**

Chin-Hoh Moeng *In* NASA, Langley Research Center, FIRE Science Results 1988 Jul. 1990 p 249-250 Sponsored in part by NSF (For primary document see N91-10448 01-47)

Avail: NTIS HC/MF A17 CSCL 04B

Data sets from field experiments over the stratocumulus regime may include complications from larger scale variations, decoupled cloud layers, diurnal cycle, or entrainment instability, etc. On top of the already complicated turbulence-radiation-condensation processes within the cloud-topped boundary layer (CTBL), these complexities may sometimes make interpretation of the data sets difficult. To study these processes, a better understanding is needed of the basic processes involved in the prototype CTBL. For example, is cloud top radiative cooling the primary source of the turbulent kinetic energy (TKE) within the CTBL. Historically, laboratory measurements have played an important role in addressing the turbulence problems. The CTBL is a turbulent field which is probably impossible to generate in laboratories. Large eddy simulation (LES) is an alternative way of 'measuring' the turbulent structure under controlled environments, which allows the systematic examination of the basic physical processes involved. However, there are problems with the LES approach for the CTBL. The LES data need to be consistent with the observed data. The LES approach is discussed, and results are given which provide some insights into the simulated turbulent flow field. Problems with this approach for the CTBL and information from the FIRE experiment needed to justify the LES results are discussed. Author

**N91-10500*#** National Aeronautics and Space Administration. Goddard Space Flight Center, Greenbelt, MD.

**CLOUD SPATIAL STRUCTURE DURING THE FIRE MS IFO**

Robert F. Cahalan *In* NASA, Langley Research Center, FIRE Science Results 1988 Jul. 1990 p 253-257 (For primary document see N91-10448 01-47)

Avail: NTIS HC/MF A17 CSCL 04B

The fractal properties of clouds observed during the FIRE Marine Stratocumulus Intensive Field Observations (MS IFO) and their effects on the large scale radiative properties of the atmosphere are examined. This involves three states: (1) analysis of LANDSAT Thematic Mapper (TM) cloud data to determine the scaling properties associated with various cloud types; (2) simulation of fractal clouds with realistic scaling properties; and (3) computation of mean radiative properties of fractal clouds as a function of their scaling properties. Thirty-three LANDSAT scenes were acquired as part of the FIRE Marine Stratocumulus IFO in July 1987. They exhibit a wide variety of stratocumulus structures. Analysis has so far focused upon the July 7 scene, in which the NASA ER-2, the BMO C130 and the NCAR Electra repeatedly gathered data across a stratocumulus-fair weather cumulus transition. Author

**N91-10501*#** National Center for Atmospheric Research, Boulder, CO.

**REFLECTIVITIES OF UNIFORM AND BROKEN MARINE STRATIFORM CLOUDS**

James A. Coakley, Jr. *In* NASA, Langley Research Center, FIRE Science Results 1988 Jul. 1990 p 259-263 Sponsored in part by AF (For primary document see N91-10448 01-47) (NASA Order L-79877-B)

Avail: NTIS HC/MF A17 CSCL 04B

Plane-parallel radiative transfer models are often used to estimate the effects of clouds on the earth's energy budget and to retrieve cloud properties from satellite observations. An attempt is made to assess the performance of such models by using AVHRR data collected during the FIRE MARINE Stratus IFO to determine the reflectivities and, in particular, the anisotropy of the reflected radiances for the clouds observed during the field experiment. The intent is to determine the anisotropy for conditions that are overcast and to compare this anisotropy with that produced by the same cloud when broken. The observations are used to quantify aspects of the differences between reflection by plane-parallel clouds and non-planar clouds expected on the basis of theoretical studies. Author

**N91-10502*#** Naval Postgraduate School, Monterey, CA. Dept. of Meteorology.

**MARINE STRATOCUMULUS CLOUD CHARACTERISTICS FROM MULTICHANNEL SATELLITE MEASUREMENTS**

Philip A. Durkee and Gary M. Mineart *In* NASA, Langley Research Center, FIRE Science Results 1988 Jul. 1990 p 265-269 (For primary document see N91-10448 01-47)

Avail: NTIS HC/MF A17 CSCL 04B

Understanding the effects of aerosols on the microphysical characteristics of marine stratocumulus clouds, and the resulting influence on cloud radiative properties, is a primary goal of FIRE. The potential for observing variations of cloud characteristics that might be related to variations of available aerosols is studied. Some results from theoretical estimates of cloud reflectance are presented. Also presented are the results of comparisons between aircraft measured microphysical characteristics and satellite detected radiative properties of marine stratocumulus clouds. These results are extracted from Mineart where the analysis procedures and a full discussion of the observations are presented. Only a brief description of the procedures and the composite results are presented. Author

**N91-10503*#** Ecole Polytechnique, Paris (France).

**STRUCTURES OBSERVED ON THE SPOT RADIANCE FIELDS DURING THE FIRE EXPERIMENT**

Genevieve Seze, Leonard Smith (Cambridge Univ., England ), and Michel Desbois *In* NASA, Langley Research Center, FIRE Science Results 1988 Jul. 1990 p 271-275 (For primary document see N91-10448 01-47)

Avail: NTIS HC/MF A17 CSCL 04B

Three Spot images taken during the FIRE experiment on stratocumulus are analyzed. From this high resolution data detailed observations of the true cloud radiance field may be made. The structure and inhomogeneity of these radiance fields hold important implications for the radiation budget, while the fine scale structure in radiance field provides information on cloud dynamics. Wieliki and Welsh, and Parker et al., have quantified the inhomogeneities of the cumulus clouds through a careful examination of the distribution of cloud (and hole) size as functions of an effective cloud diameter and radiance threshold. Cahalan (1988) has compared for different cloud types of (stratocumulus, fair weather cumulus, convective clouds in the ITCZ) the distributions of clouds (and holes) sizes, the relation between the size and the perimeter of these clouds (and holes), and examining the possibility of scale invariance. These results are extended from LANDSAT resolution (57 m and 30 m) to the Spot resolution (10 m) resolution in the case of boundary layer clouds. Particular emphasis is placed on the statistics of zones of high and low reflectivity as a function of a threshold reflectivity. Author

**N91-10504*#** South Dakota School of Mines and Technology, Rapid City. Inst. of Atmospheric Sciences.

**ANALYSIS OF STRATOCUMULUS CLOUD FIELDS USING LANDSAT IMAGERY: SIZE DISTRIBUTIONS AND SPATIAL SEPARATIONS Abstract Only**

R. M. Welch, S. K. Sengupta, and D. W. Chen *In* NASA, Langley Research Center, FIRE Science Results 1988 Jul. 1990 p 277 (For primary document see N91-10448 01-47)

Avail: NTIS HC/MF A17 CSCL 04B

Stratocumulus cloud fields in the FIRE IFO region are analyzed using LANDSAT Thematic Mapper imagery. Structural properties such as cloud cell size distribution, cell horizontal aspect ratio, fractional coverage and fractal dimension are determined. It is found that stratocumulus cloud number densities are represented by a power law. Cell horizontal aspect ratio has a tendency to increase at large cell sizes, and cells are bi-fractal in nature. Using LANDSAT Multispectral Scanner imagery for twelve selected stratocumulus scenes acquired during previous years, similar structural characteristics are obtained. Cloud field spatial organization also is analyzed. Nearest-neighbor spacings are fit with a number of functions, with Weibull and Gamma distributions providing the best fits. Poisson tests show that the spatial separations are not random. Second order statistics are used to examine clustering. Author

**N91-10505*#** National Aeronautics and Space Administration. Langley Research Center, Hampton, VA.

**CLOUD PARAMETERS DERIVED FROM GOES DURING THE 1987 MARINE STRATOCUMULUS FIRE INTENSIVE FIELD OBSERVATION (IFO) PERIOD**

David F. Young (Planning Research Corp., Hampton, VA.), Patrick Minnis, and Edwin F. Harrison *In its* FIRE Science Results 1988 Jul. 1990 p 279-283 (For primary document see N91-10448 01-47)

Avail: NTIS HC/MF A17 CSCL 04B

The Geostationary Operational Environmental Satellite (GOES) is well suited for observations of the variations of clouds over many temporal and spatial scales. For this reason, GOES data taken during the Marine Stratocumulus Intensive Field Observations (IFO) (June 29 to July 19, 1987, Kloessel et al.) serve several purposes. One facet of the First ISCCP Regional Experiment (FIRE) is improvement of the understanding of cloud parameter retrievals from satellite-observed radiances. This involves comparisons of coincident satellite cloud parameters and high resolution data taken by various instruments on other platforms during the IFO periods. Another aspect of FIRE is the improvement of both large- and small-scale models of stratocumulus used in general circulation models (GCMs). This may involve, among other studies, linking the small-scale processes observed during the IFO to the variations in large-scale cloud fields observed with the satellites during the IFO and Extended Time Observation (ETO) periods. Preliminary results are presented of an analysis of GOES data covering most of the IFO period. The large scale cloud-field characteristics are derived, then related to a longer period of measurements. Finally, some point measurements taken from the surface are compared to regional scale cloud parameters derived from satellite radiances. Author

**N91-10506*#** Desert Research Inst., Reno, NV.

**AEROSOL MEASUREMENTS IN THE STRATOCUMULUS PROJECT**

James G. Hudson *In* NASA, Langley Research Center, FIRE

Science Results 1988 Jul. 1990 p 287-290 (For primary document see N91-10448 01-47)
Avail: NTIS HC/MF A17 CSCL 04B

Cloud Condensation Nuclei (CCN) and Condensation Nuclei (CN) were measured from the National Center for Atmospheric Research (NCAR) Electra throughout the marine stratocumulus project. The total particle concentration was measured with a condensation nucleus counter. The CCN were measured with the Desert Research Institute (DRI) instantaneous CCN spectrometer. This instrument simultaneously measures the concentration of aerosol active at up to 100 different critical supersaturations (Sc). This is accomplished by exposing the sample to a fixed supersaturation field and using the size of the droplets produced in this cloud chamber to deduce the Sc of the nuclei upon which they have grown. Droplet size is associated with Sc through a calibration which is accomplished by passing soluble aerosols of known size and composition through the cloud chamber. This procedure results in a calibration curve of Sc vs. droplet size. This then allows the channel number to be directly associated with Sc. Thus, number concentration vs. Sc is obtained and this is a CCN spectrum. Since the instrument operates continuously, the measurements at all Sc's are available simultaneously. Samples are drawn directly from the ambient air and data is displayed in nearly real time. Samples were integrated over times of about 10 seconds so that substantial spatial resolution is available. Calibrations were performed once or twice a day and were found to be consistent. Preliminary results are shown. Author

**N91-10507*#** Washington Univ., Seattle. Dept. of Atmospheric Sciences.
**IN SITU MEASUREMENTS OF SHIP TRACKS**
Lawrence F. Radke, Jamie H. Lyons, Peter V. Hobbs, and James E. Coakley (National Center for Atmospheric Research, Boulder, CO.) *In* NASA, Langley Research Center, FIRE Science Results 1988 Jul. 1990 p 291-293 (For primary document see N91-10448 01-47)
(Grant NSF ATM-86-15344)
Avail: NTIS HC/MF A17 CSCL 04B

It has long been known that cloud droplet concentrations are strongly influenced by cloud condensation nuclei (CCN) and that anthropogenic sources of pollution can affect CCN concentrations. More recently it has been suggested that CCN may play an important role in climate through their effect on cloud albedo. A interesting example of the effect of anthropogenic CCN on cloud albedo is the so-called 'ship track' phenomenon. Ship tracks were first observed in satellite imagery when the ship's emissions were evidently needed for the formation of a visible cloud. However, they appear more frequently in satellite imagery as modifications to existing stratus and stratocumulus clouds. The tracks are seen most clearly in satellite imagery by comparing the radiance at 3.7 microns with that at 0.63 and 11 microns. To account for the observed change in radiance, droplet concentrations must be high, and the mean size of the droplets small, in ship tracks. Researchers describe what they believe to be the first in situ measurements in what appears to have been a ship track. Author

**N91-10508*#** National Oceanic and Atmospheric Administration, Boulder, CO.
**ESTIMATED ACCURACY OF GROUND-BASED LIQUID WATER MEASUREMENTS DURING FIRE**
Jack B. Snider *In* NASA, Langley Research Center, FIRE Science Results 1988 Jul. 1990 p 295-298 Sponsored in part by Navy, and by Colorado State Univ. (For primary document see N91-10448 01-47)
Avail: NTIS HC/MF A17 CSCL 04B

Since on goal of the First ISCCP Regional Experiment (FIRE) project is to improve our understanding of the relationships between cloud microphysics and cloud reflectivity, it is important that the accuracy of remote liquid measurements by microwave radiometry be thoroughly understood. The question is particularly relevant since the uncertainty in the absolute value of the radiometric liquid measurement is greatest at low liquid water contents (less than 0.1 mm). However it should be stressed that although uncertainty exists in the absolute value of liquid, it is well known that the observed radiometric signal is proportional to the amount of liquid in the antenna beam. As a result, changes in amounts of liquid are known to greater accuracy than the absolute value, which may contain a bias. Here, an assessment of the liquid measurement accuracy attained at San Nicolas Island (SNI) is presented. The vapor and liquid water data shown were computed from the radiometric brightness temperatures using statistical retrieval algorithms. The retrieval coefficients were derived from the 69 soundings made by Colorado State University during the SNI observations. Sources of error in the vapor and liquid measurements include cross-talk in the retrieval algorithms (not a factor at low liquid contents), uncertainties in the brightness temperature measurement, and uncertainties in the vapor and liquid attenuation coefficients. The relative importance of these errors is discussed. For the retrieval of path-integrated liquid water, the greatest uncertainty is caused by the temperature dependence of the absorption at microwave frequencies. As a result, the accuracy of statistical retrieval of liquid depends to large measure upon how representative the a priori radiosonde data are of the conditions prevailing during the measurements. The microwave radiometer measurements at SNI were supplemented by an infrared (IR) radiometer modified for measurement of cloud-base temperature. Thus, the IR system provides the means to incorporate continuous measurements of the liquid temperature into the retrieval process. Author

**N91-10509*#** Naval Research Lab., Washington, DC.
**NRL TETHERED BALLOON MEASUREMENTS AT SAN NICOLAS ISLAND DURING FIRE IFO 1987**
Hermann Gerber, Stuart Gathman, Jeffrey James, Mike Smith, Ian Consterdine, and Scott Brandeki (Denver Univ., CO.) *In* NASA, Langley Research Center, FIRE Science Results 1988 Jul. 1990 p 299-303 (For primary document see N91-10448 01-47)
Avail: NTIS HC/MF A17 CSCL 04B

An overview is given of the tethered balloon measurements made during the First ISCCP Regional Experiment (FIRE) marine stratocumulus intensive field observations (IFO) at San Nicolas Island in 1987. The instrument utilized on the balloon flights, the 17 flights over a 10 day period, the state of the data analysis, and some preliminary results are described. A goal of the measurements with the Naval Research Laboratory (NRL) balloon was to give a unique and greatly improved look at the microphysics of the clear and cloud-topped boundary layer. For this goal, collocated measurements were made of turbulence, aerosol, cloud particles, and meteorology. Two new instruments which were expected to make significant contributions to this effort were the saturation hygrometer, capable of measuring 95 percent less than RH 105 percent (with an accuracy of 0.05 percent near 100 percent) and used for the first time in clouds; and the forward scatter meter which gives in situ LWC measurements at more than 10 Hz. The data set, while unfortunately only partially simultaneous with the bulk of the FIRE stratocumulus observations, is unique and worthwhile in its own right. For the first time accurate RH measurements near 100 percent have been made in-cloud; although, the use of the saturation hygrometer reflected a learning experience which will result is substantially better performance the next time. These measurements were made in conjunction with other microphysical measurements such as aerosol and cloud droplet spectra, and perhaps most important of all, they were all collocated with bivane turbulence measurements thus permitting flux calculations. Thus the analysis of this data set, which consisted of about 50 percent stratocumulus cases including increasing and decreasing partial cloud cover, should lead to new insights on the physical mechanisms which drive the boundary-layer/cloud/turbulence system. Author

**N91-10510*#** Pennsylvania State Univ., University Park. Dept. of Meteorology.
**ESTIMATING INTEGRATED CLOUD LIQUID WATER FROM EXTENDED TIME OBSERVATIONS OF SOLAR IRRADIANCE**
C. W. Fairall, Raja El-Salem Rabadi, and Jack B. Snider (National Oceanic and Atmospheric Administration, Boulder, CO.) *In* NASA,

Langley Research Center, FIRE Science Results 1988 Jul. 1990 p 307-312 (For primary document see N91-10448 01-47)
Avail: NTIS HC/MF A17 CSCL 04B

An analysis technique used to estimate the integrated liquid water content (LWC) from the measured solar irradiance is described. The cloud transmittance is computed by dividing the irradiance measured at some time by a clear sky value obtained at the same time on a cloudless day. From the transmittance and the zenith angle, the cloud LWC is computed using the radiative transfer parameterizations of Stephens et al., (1984). The results are compared with 17 days of mm-wave (20.6 and 31.65 GHz) radiometer measurements made during the First ISCCP Regional Experiment (FIRE) Intensive Field Observation (IFO) in July of 1987. Author

**N91-10511*#** National Center for Atmospheric Research, Boulder, CO.

**A STUDY OF MARINE STRATOCUMULUS USING LIDAR AND OTHER FIRE AIRCRAFT OBSERVATIONS**

Jorgen B. Jensen and Donald H. Lenschow *In* NASA, Langley Research Center, FIRE Science Results 1988 Jul. 1990 p 313-317 Sponsored in part by NSF (For primary document see N91-10448 01-47)
Avail: NTIS HC/MF A17 CSCL 04B

The National Center for Atmospheric Research (NCAR) airborne infrared lidar system (NAILS) used in the 1987 First ISCCP Regional Experiment (FIRE) off the coast of California is a 10.6 microns wavelength carbon dioxide lidar system constructed by Ron Schwiesow and co-workers at NCAR. The lidar is particularly well suited for detailed observations of cloud shapes; i.e., height of cloud top (when flying above cloud and looking down) and cloud base (when flying below cloud and looking up) along the flight path. A brief summary of the lidar design characteristics is given. The lidar height resolution of plus or minus 3 m allows for the distance between the aircraft and cloud edge to be determined with this accuracy; however, the duration of the emitted pulse is approximately 3 microseconds, which corresponds to a 500 m pulse length. Therefore, variations in backscatter intensities within the clouds can normally not be resolved. Hence the main parameter obtainable from the lidar is distance to cloud; in some cases the cloud depth can also be determined. During FIRE the lidar was operational on 7 of the 10 Electra flights, and data were taken when the distance between cloud and aircraft (minimum range) was at least 500 m. The lidar was usually operated at 8 Hz, which at a flight speed of 100 m s(-1) translates into a horizontal resolution of about 12 m. The backscatter as function of time (equivalent to distance) for each laser pulse is stored in digital form on magnetic tape. Currently, three independent variables are available to the investigators on the FIRE Electra data tapes: lidar range to cloud, strength of return (relative power), and pulse width of return, which is related to penetration depth. Author

**N91-10512*#** National Aeronautics and Space Administration. Goddard Space Flight Center, Greenbelt, MD.

**CLOUD ABSORPTION PROPERTIES AS DERIVED FROM AIRBORNE MEASUREMENTS OF SCATTERED RADIATION WITHIN CLOUDS**

Michael D. King, Teruyuki Nakajima, Lawrence F. Radke, and Peter V. Hobbs (Washington Univ., Seattle.) *In* NASA, Langley Research Center, FIRE Science Results 1988 Jul. 1990 p 319-325 (For primary document see N91-10448 01-47)
Avail: NTIS HC/MF A17 CSCL 04B

Researchers briefly review the diffusion domain method for deriving the cloud similarity parameter and present preliminary analyses of the results thus far obtained. The presentation concentrates on the following points: (1) intercomparison of calibrated reflected intensities between the cloud absorption radiometer and the U.K. multispectral cloud radiometer; (2) quality control tests required to select those portions of an aircraft flight for which measurements are obtained within the diffusion domain; (3) case studies of the spectral similarity parameter of marine stratocumulus clouds; and comparisons of the experimentally-derived similarity parameter spectrum with that expected theoretically from the cloud droplet size distribution obtained from in situ observations. Author

**N91-10513*#** National Aeronautics and Space Administration. Goddard Space Flight Center, Greenbelt, MD.

**CLOUD OPTICAL PARAMETERS AS DERIVED FROM THE MULTISPECTRAL CLOUD RADIOMETER**

Eruyuki Nakajima and Michael D. King *In* NASA, Langley Research Center, FIRE Science Results 1988 Jul. 1990 p 327-332 (For primary document see N91-10448 01-47)
Avail: NTIS HC/MF A17 CSCL 04B

Here, researchers analyze the data taken in the marine stratocumulus intensive field observation component of the First ISCCP Regional Experiment (FIRE), conducted off the California coast in July, 1987 using the Multispectral Cloud Radiometer (MCR). Researchers installed an efficient retrieval scheme for deriving the cloud optical thickness and droplet mode radius, and have described the behavior of the retrieval error. Generally the scheme can retrieve the optical thickness and mode radius adequately unless they are too small; the use of the forward scattering region is more sound than the use of the backscattering portion. Applying the method to real data, researchers derived the two-dimensional distribution of optical thickness and mode radius for a portion of one of the FIRE marine stratocumulus missions. In this case study, the droplet size showed a more uniform distribution than optical thickness with some correlation between large droplet size and small optical thickness. Although researchers can find microphysical reasons for these tendencies, they suspect that the remotely sensed droplet size may be overestimated. As a future problem, they will compare results with in situ data of the droplet size distribution. Also it will be very important to check several reasons why the droplet radius might be overestimated, e.g., soot contamination, effect of escaping photons from the lateral sides of broken clouds, and so on. Author

**N91-10514*#** Pennsylvania State Univ., University Park. Dept. of Meteorology.

**AIRCRAFT MEASUREMENTS OF THE MEAN AND TURBULENT STRUCTURE OF MARINE STRATOCUMULUS CLOUDS DURING FIRE Abstract Only**

Bruce A. Albrecht, Kevin A. Kloesel, Kerry A. Moyer, Jefferey J. Nucciarone, and George Young *In* NASA, Langley Research Center, FIRE Science Results 1988 Jul. 1990 p 335 (For primary document see N91-10448 01-47)
Avail: NTIS HC/MF A17 CSCL 04B

The mean and turbulent structure of marine stratocumulus clouds is defined from data that were collected from 10 flights made with the National Center for Atmospheric Research (NCAR) Electra during the First ISCCP Regional Experiment (FIRE). The number of cases sampled is sufficiently large that researchers can compare the boundary layer structure obtained (1) for solid and broken cloud conditions, (2) for light and strong surface wind conditions, (3) for different sea-surface temperatures, and (4) on day and night flights. Researchers will describe the cloud and synoptic conditions present at the time of the Electra flights and show how those flights were coordinated with the operations of other aircraft and with satellite overpasses. Mean thermodynamic and wind profiles and the heat, moisture, and momentum fluxes obtained from data collected during these flights will be compared. Variations in the cloud-top structure will be quantified using LIDAR data collected during several of the Electra flights. The spatial structure of cloud-top height and the cloud-base height will be compared with the turbulent structure in the boundary layer as defined by spectra and cospectra of the wind, temperature, and moisture. Author

**N91-10515*#** Pennsylvania State Univ., University Park. Dept. of Meteorology.

**CLOUD AND BOUNDARY LAYER STRUCTURE OVER SAN NICOLAS ISLAND DURING FIRE**

Bruce A. Albrecht, Christopher W. Fairall, William J. Syrett, Wayne H. Schubert, and Jack B. Snider (National Oceanic and Atmospheric

Administration, Boulder, CO.) *In* NASA, Langley Research Center, FIRE Science Results 1988 Jul. 1990 p 337-338 (For primary document see N91-10448 01-47)
Avail: NTIS HC/MF A17 CSCL 04B

The temporal evolution of the structure of the marine boundary layer and of the associated low-level clouds observed in the vicinity of the San Nicolas Island (SNI) is defined from data collected during the First ISCCP Regional Experiment (FIRE) Marine Stratocumulus Intense Field Observations (IFO) (July 1 to 19). Surface, radiosonde, and remote-sensing measurements are used for this analysis. Sounding from the Island and from the ship Point Sur, which was located approximately 100 km northwest of SNI, are used to define variations in the thermodynamic structure of the lower-troposphere on time scales of 12 hours and longer. Time-height sections of potential temperature and equivalent potential temperature clearly define large-scale variations in the height and the strength of the inversion and periods where the conditions for cloud-top entrainment instability (CTEI) are met. Well defined variations in the height and the strength of the inversion were associated with a Cataline Eddy that was present at various times during the experiment and with the passage of the remnants of a tropical cyclone on July 18. The large-scale variations in the mean thermodynamic structure at SNI correlate well with those observed from the Point Sur. Cloud characteristics are defined for 19 days of the experiment using data from a microwave radiometer, a cloud ceilometer, a sodar, and longwave and shortwave radiometers. The depth of the cloud layer is estimated by defining inversion heights from the sodar reflectivity and cloud-base heights from a laser ceilometer. The integrated liquid water obtained from NOAA's microwave radiometer is compared with the adiabatic liquid water content that is calculated by lifting a parcel adiabatically from cloud base. In addition, the cloud structure is characterized by the variability in cloud-base height and in the integrated liquid water. Author

**N91-10516*#** National Aeronautics and Space Administration. Goddard Space Flight Center, Greenbelt, MD.

**THERMODYNAMIC STRUCTURE OF THE STRATOCUMULUS-CAPPED BOUNDARY LAYER ON 5 JULY 1987 Abstract Only**

Philip H. Austin, Reinout Boers, and Alan K. Betts (Betts, Alan K., Middlebury, VT ) *In* NASA, Langley Research Center, FIRE Science Results 1988 Jul. 1990 p 339 (For primary document see N91-10448 01-47)
Avail: NTIS HC/MF A17 CSCL 04B

The National Center for Atmospheric Research (NCAR) Electra flew a single aircraft mission on July 5 in comparatively uniform stratocumulus cloud (80 to 100 percent cloud coverage). The flight pattern, a series of north-south doglegs centered at (32N, -122W), included 15 full or partial soundings to examine layer vertical structure between altitudes of 150 and 5000 m. The air below the inversion was well-mixed in moist static energy, total water, and ozone. The inversion base measured by the aircraft ranged from 920 to 938 hPa, while the thickness of the cloud layer varied between 30 and 10 hPa. Maximum cloud liquid water contents approached 0.3 g kg(-1) (as measured by the Johnson-Williams and King probes). Comparison of soundings made in the same location show a strengthening of the inversion and increasing shear at cloud top over the observation period (16:50 to 00:22 UT). Typical windspeeds below the inversion were approximately 10 m s(-1) decreasing to 6 m s(-1) 8 hPa above cloud top. A thermodynamic budget for this case is in preparation; it will provide a comparison and contrast with the more complicated July 7 case. Author

**N91-10517*#** Colorado State Univ., Fort Collins. Dept. of Atmospheric Science.

**ANALYSIS OF TETHERED BALLOON DATA FROM SAN NICOLAS ISLAND ON 8 JULY 1987**

Stephen K. Cox, David P. Duda, Thomas A. Guinn, Christopher M. Johnson-Pasqua, Wayne H. Schubert, and Jack B. Snider (National Oceanic and Atmospheric Administration, Boulder, CO.) *In* NASA, Langley Research Center, FIRE Science Results 1988 Jul. 1990 p 341-356 (For primary document see N91-10448 01-47)
(Contract NAG1-554; N00014-87-K-0228)
Avail: NTIS HC/MF A17 CSCL 04B

Analysis of the 8 July 1987 (Julian Day 189) tethered balloon flight from San Nicolas Island is summarized. The flight commenced at about 14:30 UTC (7:30 Pacific Daylight Time) and lasted six and one-half hours. The position of the Colorado State University (CSU) instrument package as a function of time is shown. For the purpose of presentation of results, researchers divided the flight into 13 legs. These legs consist of 20 minute constant level runs, with the exception of leg 1, which is a sounding from the surface to just above 930 mb. The laser ceilometer record of cloud base is also shown. The cloud base averaged around 970 mb during much of the flight but was more variable near the end. Before the tethered balloon flight commenced, a Communications Link Analysis and Simulation System (CLASS) sounding was released at 12:11 UTC (5:11 PDT). Temperature and moisture data below 927 mb for this sounding is shown. The sounding indicates a cloud top around 955 mb at this time. Author

**N91-10518*#** Royal Air Force, Cardington (England). Meteorological Research Unit.

**TURBULENCE MEASUREMENTS USING TETHERED BALLOON INSTRUMENTATION DURING FIRE 1987 Abstract Only**

Phillip Hignett *In* NASA, Langley Research Center, FIRE Science Results 1988 Jul. 1990 p 357 (For primary document see N91-10448 01-47)
Avail: NTIS HC/MF A17 CSCL 04B

As part of the surface-based observations conducted on San Nicolas Island, the U.K. Meteorological Office operated a set of turbulence probes attached to a balloon tether cable. Typically six probes were used, each capable of measuring momentum, heat, and humidity fluxes. Two probes were fitted with net radiometers, one positioned above cloud and the other below; a third probe carried a Lyman-alpha hygrometer fitted with a pre-heater for the measurement of total water content. Some preliminary results are presented from the 14th July describing the variation in structure of the cloudy boundary layer during the daytime. This day was characterized by a complete cloud cover, an inversion height of approximately 600 m. and north-westerly winds of approximately 6 m.s(-1). As an illustration the equivalent potential temperature derived from a profile ascent made between approximately 0830 and 0930 (PDT) is shown. The data has been smoothed to a height resolution of about 4 metres. At this time the cloud base was approximately 200 m. and very light drizzle was reaching the surface. The vertical velocity variance and potential temperature flux for two periods are shown; the first (shown by full lines) immediately follows the profile and the second (shown by dashed lines) is central around 1400 (PDT). The data have been normalized by their maximum values in the first period. Cloud base has now risen to approximately 300 m. There is a marked variation during the morning, particularly in sigma w. The net radiative flux above cloud top has by now reached its maximum value. Author

**N91-10519*#** National Aeronautics and Space Administration. Langley Research Center, Hampton, VA.

**HORIZONTAL VARIABILITY OF THE MARINE BOUNDARY LAYER STRUCTURE UPWIND OF SAN NICOLAS ISLAND DURING FIRE, 1987**

Douglas R. Jensen *In* NASA, Langley Research Center, FIRE Science Results, 1988 Jul. 1990 p 359-363 (For primary document see N91-10448 01-47)
Avail: NTIS HC/MF A17 CSCL 04B

During the months of June and July 1987, the Marine Stratocumulus Intensive Field Observation Experiment of First ISCCP Regional Experiment (FIRE) was conducted in the Southern California offshore area in the vicinity of San Nicolas Island (SNI). The Naval Ocean Systems Center (NOSC) airborne platform was utilized during FIRE to investigate the upwind low level horizontal variability of the marine boundary layer structure to determine the representativeness of SNI-based measurements to upwind open ocean conditions. The NOSC airborne meteorological platform made three flights during FIRE, two during clear sky conditions (19 and 23 July), and one during two stratus conditions (15 July). The boundary layer structure variations associated with the stratus clouds of 15 July 1987 are discussed. Profiles of air temperature (AT) and relative humidity (RH) taken 'at' and 'upwind' of SNI do show differences between the so-called open ocean conditions and those taken near the island. However, the observed difference cannot be uniquely identified to island effects, especially since the upwind fluctuations of AT and RH bound the SNI measurements. Total optical depths measures at SNI do not appear to be greatly affected by any surface based aerosol effects created by the island and could therefore realistically represent open ocean conditions. However, if one were to use the SNI aerosol measurements to predict ship to ship EO propagation conditions, significant errors could be introduced due to the increased number of surface aerosols observed near SNI which may not be, and were not, characteristic of open ocean conditions. Sea surface temperature measurements taken at the island will not, in general, represent those upwind open ocean conditions. Also, since CTT's varied appreciably along the upwind radials, measurements of CTT over the island may not be representative of actual open ocean CTT's. Author

**N91-10520*#** Meteorological Office, London (England). Cloud Physics Branch.

**AN OVERVIEW OF UK C130 OBSERVATIONS FROM THE FIRE MARINE STRATOCUMULUS IFO Abstract Only**

S. Nicholls, J. Leighton, and R. Barlow *In* NASA, Langley Research Center, FIRE Science Results 1988 Jul. 1990 p 365 (For primary document see N91-10448 01-47)
Avail: NTIS HC/MF A17 CSCL 04B

An overview of the characteristics of the ten flights made by the C130 during the Intensive Field Observations (IFO) are presented. An indication of data quality is given. Comparisons of the carbon dioxide radiation thermometer and the Rosemount suggest there may be potentially serious wetting problems with the latter, especially close to cloud base. The main features of the cloud layers sampled by the C130 are summarized, including microphysical parameters. Many of the results shown are derived from a first order analysis of turbulence quantities. The gross vertical variation of heat, vapor, and liquid water fluxes from case to case, together with the observed vertical velocity variance, a good indicator of convective activity, are discussed. Preliminary results suggest that the different cases can be usefully categorized using these data. The relationship between these and the measured boundary conditions is mentioned. Similarities and differences between the various cases are highlighted, and interpreted in terms of the researchers' current understanding of stratocumulus. Attention is given to particular features of the various flights which may deserve more intensive study. Author

**N91-10521*#** Pennsylvania State Univ., University Park. Dept. of Meteorology.

**BOUNDARY LAYER ROLL CIRCULATIONS DURING FIRE**

Hampton N. Shirer and Tracy Haack *In* NASA, Langley Research Center, FIRE Science Results 1988 Jul. 1990 p 367-370 (For primary document see N91-10448 01-47)
(Contract N00014-86-K-06880; NSF ATM-86-19854)
Avail: NTIS HC/MF A17 CSCL 04B

The probable mechanism underlying the development of boundary layer roll circulations are studied using wind and temperature profiles measured by the National Center for Atmospheric Research (NCAR) Electra during the stratocumulus phase of the First ISCCP Regional Experiment (FIRE). The expected, or preferred, roll orientations, horizontal wavelengths, and propagation periods are determined by finding the minimum values of the dynamic and thermodynamic forcing parameters, which here are the eddy Reynolds number (Re) and moist Rayleigh number (Ra sub m). These minimum values depend on the height z sub T of the capping temperature inversion and on the values of the Fourier coefficients of the background height-dependent vector wind profile. As input to our nonlinear spectral model, descent and ascent runs by the Electra provide for initial estimates of the inversion height and the wind profiles. In the first phase of the investigation presented here, a mechanism is said to be a probable contributor to the development of roll circulations within the stratocumulus-topped boundary layer if the modeled roll orientation and wavelengths agree with their observed values. Preliminary results using the 14-coefficient model of Haack-Hirschberg (1988) are discussed for the 7 July 1987 Electra Mission 188-A (Flight 5). This mission was flown across a sharp cloud boundary that was within a LANDSAT/SPOT scene. The stratocumulus deck was relatively solid in the eastern part of the scene, while there was a rapid decrease in cloud cover to scattered cumulus clouds aligned in streets to the west. These cloud streets were oriented nearly parallel to the mean wind direction in the layer, which was approximately 340 degrees. The hypothesis that roll circulations occurred in both the relatively clear and the cloudy regions is investigated using as model input a descent profile obtained in the relatively clear air and an ascent profile obtained in the cloudy air. Initial results for the clear air case are that the pure inflection point mode is not possible and the pure thermal mode was oriented 35 degrees to the right of the mean wind direction. The origin of this unacceptably large discrepancy between the observed and modeled results will be investigated further and the conclusions reported at the next FIRE workshop. Author

**N91-10522*#** Pennsylvania State Univ., University Park. Dept. of Meteorology.

**WINDS AND TURBULENCE ABOVE SAN NICOLAS ISLAND DURING FIRE Abstract Only**

Allen B. White, William J. Syrett, Christopher W. Fairall, and Dennis W. Thomson *In* NASA, Langley Research Center, FIRE Science Results 1988 Jul. 1990 p 371 (For primary document see N91-10448 01-47)
Avail: NTIS HC/MF A17 CSCL 04B

Winds and turbulence above San Nicolas Island (SNI) were continuously monitored during the First ISCCP Regional Experiment (FIRE) with a Doppler sodar (1600 Hz) and an ultrahigh frequencies (UHF) (400 MHz) wind profiler. Individual profiles were logged from 1 through 19 July 1987 at 30 sec to 2 min intervals; preliminary processing of hourly averaged winds from 100 to 2300 m is complete. These wind profiles have been combined with intermittent radiosonde profiles to construct time-height sections of parameters such as the Richardson Number. Analysis now in progress includes interpretation of the sodar (C 2/T) and profiler (C 2/N, C 2/q) reflectivity profiles. These profiles are being combined with radiometric and ceilometer data for investigations of vertical transport and cloud base/top entrainment processes. Finally, by using the SNI data in conjunction with soundings made from the research vessel Pt. Sur, the relationship between changes in the SNI winds and mesoscale and synoptic-scale weather features is being investigated. Author

**N91-10523*#** National Aeronautics and Space Administration. Goddard Space Flight Center, Greenbelt, MD.

**ER-2 LIDAR MEASUREMENTS OF STRATOCUMULUS CLOUD TOP STRUCTURE ON JULY 14, 1987**

Reinout Boers and James D. Spinhirne *In* NASA, Langley Research Center, FIRE Science Results 1988 Jul. 1990 p 375-376 (For primary document see N91-10448 01-47)
Avail: NTIS HC/MF A17 CSCL 04B

On July 14, 1987 NASA's ER-2 high altitude aircraft flew a mission to measure the structure of stratocumulus clouds off the coast of California. A flight pattern was executed so that the two-dimensional variability of the clouds could be detected. The technique of analysis of the lidar data to measure cloud tops follows. First each signal is searched for its maximum in return strength. This maximum is caused by scattering of the laser light off cloud particles or from the ocean surface. Next the variance of the signal return above the level of maximum backscatter is determined. Cloud top is assigned to a level (above the level of maximum backscatter) where the backscatter exceeds the average variance. This two-step process is necessary because the level of maximum backscatter does not correspond to the cloud top. Ocean surface returns are easily separated from cloud returns in this process, described in detail by Boers, Spinhirne, and Hart (1988). Analysis of the data so far has shown that there were very few breaks in the clouds. Furthermore the layer top was very flat with local oscillations not exceeding 30 m. Such small cloud top variations are still well within the range of detectability, because the precision of this technique of cloud top detection has previously been established to be 13 to 15 m. Data are presently being analyzed to compute cloud top distributions and fractional cloudiness. The aim of this research is to relate the fractional cloudiness to the mean thermodynamic structure of the boundary layer. Researchers plan to compute spectral scales of the cloud top variability in two dimensions to determine the orientation of the clouds with respect to the mean wind. Furthermore the lidar derived cloud top distribution will be used in the computation of the thermodynamic and radiation budget of the boundary layer. Author

**N91-10524*#** National Center for Atmospheric Research, Boulder, CO.

**DEPENDENCE OF MARINE STRATOCUMULUS REFLECTIVITIES ON LIQUID WATER PATHS**

James A. Coakley, Jr. and Jack B. Snider (National Oceanic and Atmospheric Administration, Boulder, CO.) *In* NASA, Langley Research Center, FIRE Science Results 1988 Jul. 1990 p 377-381 Sponsored in part by AF and Navy (For primary document see N91-10448 01-47)
(NASA Order L-79877-B)
Avail: NTIS HC/MF A17 CSCL 04B

Simple parameterizations that relate cloud liquid water content to cloud reflectivity are often used in general circulation climate models to calculate the effect of clouds in the earth's energy budget. Such parameterizations have been developed by Stephens (1978) and by Slingo and Schrecker (1982) and others. Here researchers seek to verify the parametric relationship through the use of simultaneous observations of cloud liquid water content and cloud reflectivity. The column amount of cloud liquid was measured using a microwave radiometer on San Nicolas Island following techniques described by Hogg et al., (1983). Cloud reflectivity was obtained through spatial coherence analysis of Advanced Very High Resolution Radiometer (AVHRR) imagery data (Coakley and Beckner, 1988). They present the dependence of the observed reflectivity on the observed liquid water path. They also compare this empirical relationship with that proposed by Stephens (1978). Researchers found that by taking clouds to be isotropic reflectors, the observed reflectivities and observed column amounts of cloud liquid water are related in a manner that is consistent with simple parameterizations often used in general circulation climate models to determine the effect of clouds on the earth's radiation budget. Attempts to use the results of radiative transfer calculations to correct for the anisotropy of the AVHRR derived reflectivities resulted in a greater scatter of the points about the relationship expected between liquid water path and reflectivity. The anisotropy of the observed reflectivities proved to be small, much smaller than indicated by theory. To critically assess parameterizations, more simultaneous observations of cloud liquid water and cloud reflectivities and better calibration of the AVHRR sensors are needed. Author

**N91-10525*#** Royal Aircraft Establishment, Farnborough (England). Meteorological Research Flight.

**NEAR INFRARED RADIANCES OBSERVED BY THE UK C130 MULTI-CHANNEL RADIOMETER DURING THE MARINE STRATOCUMULUS IFO AND PRELIMINARY COMPARISON WITH MODEL CALCULATIONS**

J. S. Foot *In* NASA, Langley Research Center, FIRE Science Results 1988 Jul. 1990 p 383-392 (For primary document see N91-10448 01-47)
Avail: NTIS HC/MF A17 CSCL 04B

A preliminary analysis of some of the narrow band radiance data measured on the U.K. Meteorological Office's C130 aircraft during the marine stratocumulus intensive field observation of First ISCCP Regional Experiment (FIRE), San Diego 29 June to 18 July 1987, is presented. The data are compared with Monte Carlo calculations of the reflectance and transmittance of the cloud based upon the observed droplet size distribution. The main scientific question being addressed is whether there is any evidence of anomalous absorption within the cloud which had been observed in similar measurements (Rozenberg et al., 1974; Twomey and Cocks, 1982; Foot, 1988). The measurements also indicate the potential for remotely sensing cloud properties. The data and method of presentation discussed here clearly separates out clouds in terms of the size of the cloud droplets. All of the daytime C130 FIRE flights have been studied and are consistent with the data presented here. There appears to be no peculiarities that might arise, for example if pollution were to be a significant factor in determining cloud absorption. Variation in the inferred size parameters, r sub e, along runs are also very small. Author

**N91-10526*#** National Oceanic and Atmospheric Administration, Boulder, CO. Cooperative Inst. for Research in Environmental Sciences.

**PLUME MECHANICS AND STRATOCUMULUS CONVECTION**

Howard P. Hanson *In* NASA, Langley Research Center, FIRE Science Results 1988 Jul. 1990 p 393-396 (For primary document see N91-10448 01-47)
(Contract NAG1-651; N00014-84-K-0405)
Avail: NTIS HC/MF A17 CSCL 04B

The First ISCCP Regional Experiment (FIRE) marine stratocumulus Intensive Field Observation (IFO) held in July, 1987 produced a data set that is far more comprehensive than data sets from previous stratocumulus experiments. One exciting new development was the use of the 10.6 micron lidar system for cloud-top mapping that was available on the National Center for Atmospheric Research (NCAR) Electra. This system provided a unique look at the small scales of the turbulence in the clouds, images of the turbulent structures that are quantitatively revealed by conditional sampling (e.g., Khalsa and Greenhut, 1987). The behavior of these updrafts and downdrafts is central to the dynamics of the stratocumulus-topped marine boundary layer. FIRE's objectives of understanding cloud dynamics and how they affect the cloud optical depth - which, in turn, is the crucial factor in determining the clouds' albedo - therefore require the investigation of these drafts. Given here are initial results from a simple model capable of simulating moist, entraining plumes that are subject to water phase changes and radiative heating and cooling. These results correspond, therefore, to the 'dry cloud' case discussed by Lilly and Schubert (1980). The model's simplicity limits the realism of the results - the plumes are assumed not to interact, for example - but the role of radiative processes in influencing the plume dynamics is clear. Also revealed is the role the plumes play is maintaining the cloud-top inversion. The model equations and methodology used, and qualitative results are given. Author

**N91-10527*#** Rutgers - The State Univ., New Brunswick, NJ. Dept. of Geography.

**FIRE EXTENDED TIME/LIMITED AREA OBSERVATIONS AT PALISADES, NEW YORK**

David A. Robinson, George Kukla, and Alan Frei (Lamont-Doherty Geological Observatory, Palisades, NY.) *In* NASA, Langley Research Center, FIRE Science Results 1988 Jul. 1990 p 397-401 (For primary document see N91-10448 01-47)
(Grant NAG1-653)
Avail: NTIS HC/MF A17 CSCL 04B

Downwelling shortwave and longwave irradiation are being continuously monitored at Palisades, New York as part of the First International Satellite Cloud Climatology Project (ISCCP) Regional Experiment (FIRE) Extended Time/Limited Area Initiative. In addition, fisheye (180 degree) sky photographs are taken at the times of NOAA 9 and LANDSAT satellite overpasses on select days, particularly when cirrus clouds are present. Measurements of incoming shortwave (0.28 to 2.80 microns) hemispheric and diffuse, hemispheric near infrared (0.7 to 2.80 microns), and downwelling hemispheric infrared (4.0 to 50.0 microns) irradiation have been made from a rooftop location on the grounds of the Lamont-Doherty Geological Observatory since December 1986. The three Eppley Precision Spectral Pyranometers and the Eppley Pyrgeometer used to measure these variables were calibrated with Colorado State University instruments at Madison, Wisconsin as part of the FIRE Intensive Laboratory. Pyrgeometer output contains an adjustment for body temperature but not for dome temperature. Data are transmitted to a Campbell CR-21 Digital Recorder, where one minute averages of ten second samples are stored and subsequently dumped to a cassette recorder. Using a Campbell C-20 Cassette Interface, these data are transferred to an Apple Macintosh computer for analysis and for archiving on floppy disks. In addition to the raw irradiances collected, variables derived from these data are generated and stored. These include: the ratio of near infrared irradiation to visible irradiation and the fraction of the full shortwave irradiation which is diffuse; and will soon include: shortwave transmissivity and optical depth in the shortwave. Sky photographs are taken with an Olympus OM2-N 35 mm camera and are timed to be coincident with overpassing NOAA and LANDSAT satellites. Palisades is within the field of view of the NOAA 9 daily in the middle to late afternoon. The satellite viewing angle is within 45 degrees of nadir over Palisades on approximately half of the passes. Author

**N91-10528*#** Washington Univ., Seattle.

### MEASUREMENTS OF THE LIGHT-ABSORBING MATERIAL INSIDE CLOUD DROPLETS AND ITS EFFECT ON CLOUD ALBEDO

C. H. Twohy, A. D. Clarke (Hawaii Univ., Honolulu.), Stephen G. Warren, L. F. Radke, and R. J. Charleson *In* NASA, Langley Research Center, FIRE Science Results 1988 Jul. 1990 p 403-407 Prepared in cooperation with Sandia National Labs., Albuquerque, NM; and National Center for Atmospheric Research, Boulder, CO Submitted for publication (For primary document see N91-10448 01-47)
(Grants NSF ATM-86-07377; NSF ATM-86-05134)
Avail: NTIS HC/MF A17 CSCL 04B

Most of the measurements of light-absorbing aerosol particles made previously have been in non-cloudy air and therefore provide no insight into aerosol effects on cloud properties. Here, researchers describe an experiment designed to measure light absorption exclusively due to substances inside cloud droplets, compare the results to related light absorption measurements, and evaluate possible effects on the albedo of clouds. The results of this study validate those of Twomey and Cocks and show that the measured levels of light-absorbing material are negligible for the radiative properties of realistic clouds. For the measured clouds, which appear to have been moderately polluted, the amount of elemental carbon (EC) present was insufficient to affect albedo. Much higher contaminant levels or much larger droplets than those measured would be necessary to significantly alter the radiative properties. The effect of the concentrations of EC actually measured on the albedo of snow, however, would be much more pronounced since, in contrast to clouds, snowpacks are usually optically semi-infinite and have large particle sizes. Author

**N91-10529*#** National Aeronautics and Space Administration. Ames Research Center, Moffett Field, CA.

### PRELIMINARY RESULTS OF RADIATION MEASUREMENTS FROM THE MARINE STRATUS FIRE EXPERIMENT

Francisco P. J. Valero, Philip D. Hammer, Thomas P. Ackerman (Pennsylvania State Univ., University Park.), Warren J. Y. Gore, and Melinda L. Weil *In* NASA, Langley Research Center, FIRE Science Results 1988 Jul. 1990 p 409-410 (For primary document see N91-10448 01-47)
Avail: NTIS HC/MF A17 CSCL 04B

During the marine stratocumulus phase of the First International Satellite Cloud Climatology Regional Experiment (FIRE) in July 1987, researchers acquired radiative flux data from a variety of instruments which were flown on the ER-2 high altitude aircraft. The spectral coverage ranged from the near UV to beyond 40 microns. A survey and selected preliminary analyses of these measurements are presented. The specific instruments used in the experiment were chosen primarily for measuring quantities of specific interest for marine stratocumulus fields. However, testing and evaluation of instrumentation and techniques to be used in the future inland cirrus experiment was also an important consideration. Details of the instruments and the significance of what they measure are given. Author

**N91-10530*#** Colorado State Univ., Fort Collins. Cooperative Inst. for Research in the Atmosphere.

### THIRD GENERATION EARTH RADIATION BUDGET MEASUREMENTS; ERBE IN THE CONTEXT OF EARLIER SYSTEMS

Thomas H. VonderHaar *In* NASA, Langley Research Center, FIRE Science Results 1988 Jul. 1990 p 411-415 (For primary document see N91-10448 01-47)
Avail: NTIS HC/MF A17 CSCL 04B

The Earth Radiation Budget Experiment (ERBE) observations are just becoming available for scientific use. These represent the third generation of measurements with steadily improving accuracy and resolution. Beginning in the 1960's observations by spherical detectors established the mean albedo of the Earth near 30 percent in substantial variance from presatellite estimates. The Nimbus 6 and 7 wide field of view ERB measurements represent a long-term climatology of measurements at 1000 km resolution. The ERBE measurements introduce higher accuracy and higher space and time resolution result. Comparisons will be presented of several April ERB measurements to illustrate what this improvement in resolution and accuracy can yield. Simultaneous ERBE and Nimbus 7 measurements for April 1985 show nearly identical results on the large scale. Comparison of measurements of direct solar energy from ERBE, Solar Max Mission and Nimbus 7 suggest a 'solar constant' value of 1368 w/sq m for the 1979 to 1986 period. The long-term record of earth radiation budget (Aprils from 1976 to 1985) over large regions is shown to have interannual variation of plus or minus 20 to 30 w/sq. m. The new ERBE data will allow this climate record measurement to continue. Author

**N91-10531*#** Colorado State Univ., Fort Collins. Dept. of Atmospheric Science.

### SAN NICOLAS ISLAND SURFACE RADIATION-METEOROLOGY DATA

Christopher M. Johnson-Pasqua and Stephen K. Cox *In* NASA, Langley Research Center, FIRE Science Results 1988 Jul. 1990 p 417-422 (For primary document see N91-10448 01-47)
(Contract NAG1-554; N00014-87-K-0228)
Avail: NTIS HC/MF A17 CSCL 04B

A summary of the surface data collected by Colorado State University (CSU) on San Nicolas Island during the First ISCCP Regional Experiment (FIRE) from 30 June (Julian Day 181) through 19 July (Julian Day 200) is given. The data are available in two formats: hard copy graphs, and processed data on floppy disk. Author

**N91-10532*#** National Aeronautics and Space Administration. Goddard Space Flight Center, Greenbelt, MD.

### COMPARISON AND CALIBRATION OF NCAR ELECTRA INSTRUMENTS: JULY 5 AND 7, 1987 c35

Philip H. Austin and Reinout Boers *In* NASA, Langley Research Center, FIRE Science Results 1988 Jul. 1990 p 425-427 (For primary document see N91-10448 01-47)
Avail: NTIS HC/MF A17 CSCL 14B

Measurements of temperature, water vapor, cloud liquid water, and lidar cloud height taken by the National Center for Aeronautical Research (NCAR) Electra are analyzed for two days of the First ISCCP Regional Experiment (FIRE) stratocumulus field program. Examination of instrument time series, correlations between sensors, soundings through the layer, and lidar measurements of cloud base height are used to correct sensor offset problems, check for probe wetting, and choose the most accurate measurements of temperature, humidity, and cloud liquid water. Author

**N91-10533*#** National Aeronautics and Space Administration. Goddard Space Flight Center, Greenbelt, MD.
**THERMODYNAMIC STRUCTURE OF THE STRATOCUMULUS-CAPPED BOUNDARY LAYER ON 7 JULY, 1987**
Reinout Boers, Alan K. Betts (Betts, Alan K., Middlebury, VT ), and Philip H. Austin *In* NASA, Langley Research Center, FIRE Science Results 1988 Jul. 1990 p 429-436 (For primary document see N91-10448 01-47)
Avail: NTIS HC/MF A17 CSCL 04B

As part of project First ISCCP Regional Experiment (FIRE), a mission was carried out on 7 July 1987 to study the thermodynamic structure of a boundary layer which is in transition from a clear to a cloudy state. The National Center for Aeronautical Research (NCAR) Electra flew a pattern in tight coordination with the NASA ER-2 aircraft near 122 West, 31.6 North off the coast of California. A description is given here of the thermodynamic structure. The purpose is to derive the entrainment rate and the fluxes of the thermodynamic variables. To this end researchers represent the data in conserved variable diagrams. Author

**N91-10534*#** National Aeronautics and Space Administration. Langley Research Center, Hampton, VA.
**AIRCRAFT/ISLAND/SHIP/SATELLITE INTERCOMPARISON: PRELIMINARY RESULTS FROM JULY 16, 1987**
Howard P. Hanson, Ken Davidson, Herman Gerber, Siri Jodha Singh Khalsa, Kevin A. Kloesel, Ronald Schwiesow, Jack B. Snider, Bruce M. Wielicki, and Donald P. Wylie (Wisconsin Univ., Madison.) *In its* FIRE Science Results 1988 Jul. 1990 p 433-436 Sponsored in part by various agencies involved in First ISCCP Regional Experiment (FIRE) (For primary document see N91-10448 01-47)
Avail: NTIS HC/MF A17 CSCL 04B

The First ISCCP Regional Experiment (FIRE) objective of validating and improving satellite algorithms for inferring cloud properties from satellite radiances was one of the central motivating factors in the design of the specific field experimental strategies used in the July, 1987 marine stratocumulus intensive field observations (IFO). The in situ measuring platforms were deployed to take maximum advantage of redundant measurements (for intercomparison of the in situ sensors) and to provide optimal coverage within satellite images. One of the most ambitious of these strategies was the attempt to coordinate measurements from San Nicolas Island (SNI), the R/V Pt. Sur, the meteorological aircraft, and the satellites. For the most part, this attempt was frustrated by flight restrictions in the vicinity of SNI. The exception was the mission of July 16, 1987, which achieved remarkable success in the coordination of the platforms. This presentation concerns operations conducted by the National Center for Atmospheric Research (NCAR) Electra and how data from the Electra can be integrated with and compared to data from the Pt. Sur, SNI, and the satellites. The focus is on the large-scale, integrated picture of the conditions on July 16 from the perspective of the Electra's flight operations. Author

**N91-10535*#** Meteorological Office, London (England). Cloud Physics Branch.
**A PRELIMINARY ANALYSIS OF LANDSAT AND UK C130 DATA FROM MISSION 197-A, ON 16 JULY 1987 Abstract Only**
S. Nicholls *In* NASA, Langley Research Center, FIRE Science Results 1988 Jul. 1990 p 437 (For primary document see N91-10448 01-47)
Avail: NTIS HC/MF A17 CSCL 04B

The co-ordinated LANDSAT-aircraft mission flown on 16 July to the west of San Nicolas Island shows a number of interesting features. There is considerable structure in the Band 4 (0.76 to 0.90 microns) reflectance on km to 10 km scales in otherwise complete cloud cover. In extremely light winds, the C130 performed a series of runs throughout the boundary layer and above for a period of approximately 90 mins on either side of the LANDSAT overpass time. Because of the light winds, the same features can be recognized on the various aircraft penetrations and composited. Furthermore, the accurate renavigation of the aircraft positions enables these to be unambiguously related to the features seen on the LANDSAT image. Early indications suggest that the reflectance features are related to local thickenings on the cloud layer, associated with slightly deeper convection rising into the overlying stratiform deck. If this is true, then LANDSAT images could possibly be used to remotely infer aspects of the convective regime within the boundary layer. In addition, the LANDSAT images also display a quasi-linear feature extending for some 50 km, although only a km or so wide. This feature was, in fact, photographed from the C130 flying just above cloud top and termed a 'cloud-cliff'. It is clearly a rapid and sizeable local change in cloud top height and is therefore presumably a propagating feature. An explanation is still outstanding, but it appears to resemble an undular bore. Further descriptions of this unexpected feature, and its possible origin will be discussed. Author

**N91-10536** Princeton Univ., NJ.
**THE STATIONARY WAVE RESPONSE TO TROPICAL AND MIDLATITUDE SST ANOMALIES Ph.D. Thesis**
Mingfang Ting 1990 210 p
Avail: Univ. Microfilms Order No. DA9014550

The atmospheric stationary wave responses to tropical and mid-latitude sea surface temperature (SST) anomalies are examined with an idealized general circulation model (GCM) as well as steady linear and nonlinear models. The control climate of the GCM is zonally symmetric; this symmetric climate is then perturbed by a dipolar SST anomaly centered at the equator in the tropical anomaly experiment, and by a monopole SST anomaly centered at 40 deg N in the mid-latitude anomaly experiment. Two tropical experiments, with anomaly amplitudes differing by a factor of two, were conducted. The response is linear in the amplitude of the SST anomaly. The linear model simulates the GCM's stationary wave reasonably well when it is forced by anomalous heating as well as anomalous transients. A steady nonlinear model is also used to evaluate the importance of transients, and confirms the diagnosis based on the linear model. Two mid-latitude anomaly experiments, with anomalies of opposite sign, were conducted. The stationary response is again roughly linear in the sign of the SST anomaly. The same linear model, when forced by anomalous heating and the transients, reproduces the GCM's stationary response even better than in the tropical anomaly case. Dissert. Abstr.

**N91-10537#** National Oceanographic Data Center, Washington, DC.
**MARINERS WEATHER LOG, VOLUME 34, NUMBER 2, SPRING 1990 Quarterly Report**
R. M. DeAngelis 1990 93 p
(PB90-222324) Avail: NTIS HC/MF A05; also available SOD HC $3.50 as 703-029-00022-1 CSCL 04B

This document contains the following: Hurricanes Haunt our History; I Remember Camille; North Atlantic Tropical Cyclones, 1989; Eastern North Pacific Tropical Cyclones, 1989; Central North Pacific Tropical Cyclones, 1989; Western North Pacific Tropical Cyclones, 1989; North Atlantic Ocean; North Pacific Ocean; Track Charts; and Tables. GRA

**N91-10538#** National Oceanic and Atmospheric Administration, Boulder, CO. Air Resources Lab.
**GEOPHYSICAL MONITORING FOR CLIMATIC CHANGE Summary Report, 1988**
J. W. Elkins and R. M. Rosson Dec. 1989 152 p
(PB90-222126; GMCC-17) Avail: NTIS HC/MF A08 CSCL 04B

Reports are presented from the following groups and offices: Observatory reports; Aerosols and radiation monitoring group; Carbon cycle group; Ozone group; Acquisition and data management group; Air quality group; Nitrous oxide and halocarbon group; Directors Office; and Cooperative programs. Author

**N91-10539#** Department of Energy, New York, NY. Environmental Measurements Lab.

**Rn222, Rn222 PROGENY AND Rn220 PROGENY AS ATMOSPHERIC TRACERS OF AIR MASSES AT THE MAUNO LOA OBSERVATORY**

Adam R. Hutter, Andreas C. George, Mark L. Maiello, Isabel M. Fisenne, Richard J. Larsen, Harold L. Beck, and Frederick C. Wilson Mar. 1990 26 p
(DE90-014872; EML-522) Avail: NTIS HC/MF A03

Rn-222, Rn-222 progeny, and Rn-220 Rn progeny concentrations in air were measured at the Mauna Loa Observatory (MLO) in Hawaii during March 1989 in order to investigate the feasibility of using them as atmospheric tracers to help determine local air mass flow patterns. Charcoal traps, cooled to dry ice temperatures, were used to collect Rn-222, which was subsequently measured in pulse ionization chambers at the Environmental Measurements Laboratory (EML). Rn-222 progeny and Rn-220 progeny for 37 samples were measured at the Observatory by sampling high volumes of air through filters, which were counted for up to 11 h in alpha scintillation counters. Individual progeny concentrations were calculated using both least squares and maximum likelihood techniques. In general, Rn-222 progeny and Rn-220 progeny concentrations were low when free tropospheric air was present (downslope and tradewind conditions), and consistently higher when surface air from the island broke through the trade wind inversion layer (upslope conditions). The data suggest that Rn-222, Rn-222 progeny, or Rn-220 progeny monitoring may provide new and useful information to help indicate the different air flow patterns present at MLO. DOE

**N91-10540** Royal Netherlands Meteorological Inst., De Bilt.

**ABOUT THE POSSIBILITIES OF USING AN AIR MASS TRANSFORMATION MODEL IN TAIYUAN, SHANXI PROVINCE, CHINA**

J. Reiff, Li Tao-Guang, and Gao Kang (Meteorological Bureau of Shanxi Province, Taiyuan, China ) 1990 21 p
(KNMI-TR-120; ISSN-0169-1708; ETN-90-97649) Avail: Royal Netherlands Meteorological Inst., P.O. Box 201, 3730 AE De Bilt, Wilhelminalaan 10, Netherlands

The AMT (Air Mass Transformation) model is tested for trajectories arriving in Taiyuan to study the possibilities of using it in Taiyuan, People's Republic of China. The sensitivity of the model for the different processes was studied. Some parameters of the model were modified for the purpose of forecasting in specific mountainous terrain and dry climate conditions. Results of examples which were worked for Taiyuan circumtances for the periods of July (Summer) 1985 and January (Winter) 1986, show that the 12 hour runs of the AMT model are able to reproduce (on historical data) the sounding of Taiyuan. The AMT model contribute fruitfully to short range weather forecasts (12 to 36 hoours ahead) during periods of severe air pollution and when cold waves occur. ESA

**N91-10541#** Pacific Northwest Lab., Richland, WA.

**TERRAIN-INDUCED MESOSCALE CIRCULATIONS IN THE COLUMBIA BASIN**

E. D. Skyllingstad and J. C. Doran Jun. 1990 20 p Presented at the Conference on Mesoscale Processes and Mountain Meteorology, Boulder, CO, 25-29 Jun. 1990
(Contract DE-AC06-76RL-01830)
(DE90-016338; PNL-SA-17987; CONF-9006111-4) Avail: NTIS HC/MF A03

Mountain basins present a difficult problem for the analysis and prediction of local temperature and wind structure. The flow complexity is compounded by the formation of mountain gravity waves and subsequent downslope winds and increased mixing. The influence of the basin topography often leads to widely varying stability and surface winds. Basin meteorology is also strongly tied to the strength of solar heating and vertical structure of the local air column. Stagnation and strong inversions, resulting from weak flow aloft and low solar heating, are common in mountain basins and have a large impact on the transport and diffusion of atmospheric contaminants. As in many atmospheric flow problems, studying the structure of basin flow is hampered by the high cost of extensive field programs. Another option is the use of numerical models to supplement a limited observation program. Models can provide a reasonable diagnostic tool at low cost for gaining insight on the dynamics of geophysical fluid problems. Here, we examine the characteristics of a particular flow pattern that is common in the Columbia Basin located in south-central Washington State. This preliminary case study is performed using a combination of surface observations and vertical soundings and a data set generated by a hydrostatic numerical model. Our intent is to demonstrate the importance of terrain blocking and channeling on the circulation and trapping of cool air within a partially closed mountain basin. DOE

**N91-10542#** Pacific Northwest Lab., Richland, WA.

**ENERGETICS OF VALLEY AND BASIN ATMOSPHERES DURING THE EVENING TRANSITION AND NIGHTTIME PERIODS**

C. D. Whiteman Mar. 1990 8 p Presented at the Conference on Mesoscale Processes and Mountain Meteorology, Boulder, CO, 25-29 Jun. 1990
(Contract DE-AC06-76RL-01830)
(DE90-016356; PNL-SA-17536; CONF-9006111-6) Avail: NTIS HC/MF A02

In recent years there have been several attempts to calculate individual components of the heat budgets of various valleys and basins. The impetus for this work has generally been the desire to gain a better understanding of the role of the valley's heat budget in generating local thermally driven circulations. Methods for the calculation of such heat budgets are in an early state of development, and investigators have had difficulty in getting the heat budgets to close. The purpose of this paper is to present a conceptual framework for such calculations, to compare individual terms in several valleys and basins where bulk budget terms have been estimated, and to draw conclusions regarding the meteorology of valley and basin atmospheres during the evening transition and nighttime periods. We begin by developing a mathematical framework that allows the calculation of individual heat budget terms in individual valleys and allows intercomparions between various valleys and basins. We then evaluate the change of heat storage term in a single valley to illustrate the effects of valley topography on the interpretation of this term. Finally, we evaluate the heat budgets for three different valleys and basins and consider the possible reasons for the poor closure of the budgets. DOE

**N91-10543*#** National Aeronautics and Space Administration. Goddard Space Flight Center, Greenbelt, MD.

**NEUTRAL WINDS DERIVED FROM IRI PARAMETERS AND FROM THE HWM87 WIND MODEL FOR THE SUNDIAL CAMPAIGN OF SEPTEMBER, 1986**

K. L. Miller, A. E. Hedin, P. J. Wilkinson, D. G. Torr, and P. G. Richards (Alabama Univ., Huntsville.) 1990 40 p Previously announced in IAA as A90-21571
(NASA-TM-103445; NAS 1.15:103445) Avail: NTIS HC/MF A03 CSCL 04B

Meridional neutral winds derived from the height of the maximum ionization of the F2 layer are compared with values from results of the HWM87 empirical neutral wind model. The time period considered is the SUNDIAL-2 campaign, 21 Sept. through 5 Oct. 1986. Winds were derived from measurements by a global network of ionosondes, as well as from similar quantities generated by the International Reference Ionosphere. Global wind patterns from the three sources are similar. Differences tend to be the result of local or transient phenomena that are either too rapid to be described by the order of harmonics of the empirical models, or are the result of temporal changes not reproduced by models based on average conditions. Author

**N91-10544#** Beleidscommissie Remote Sensing, Delft (Netherlands).

**IMPACT OF SASS WIND DATA ON ANALYSES AND FORECASTS OF A FINE MESH LIMITED AREA MODEL**

A. C. M. Stoffelen, G. Cats, L. M. Hafkenscheid, and A. P. M.

Baede (Royal Netherlands Meteorological Inst., The Hague.) Feb. 1990 82 p
(BCRS-89-38; ETN-90-97687) Avail: NTIS HC/MF A05

The impact of SEASAT/SASS (SEASAT-A Scatterometer System) data on analyses and forecasts was studied in preparation for the use of ERS-1 scatterometer winds in a Limited Area Model (LAM). With the LAM, parallel runs are carried out with and without these winds. The resulting analyses and forecasts are evaluated. A case study on the QE2 storm is performed. It is concluded that maximum positive impact of single level RS surface data possibly relies on the availability of upper air data, and on the development of optimal assimilation techniques for this type of highly correlated and spatially dense satellite data. ESA

**N91-10545** Royal Netherlands Meteorological Inst., De Bilt. Afdeling Oceanografisch Onderzoek.
**VERIFICATION OF GONO WAVE PREDICTIONS FOR THE PERIOD OCTOBER 1987 TO APRIL 1988 [VERIFICATIE VAN GONO GOLFVERWACHTING OVER DE PERIODE OKTOBER 1987 - APRIL 1988]**
R. A. vanMoerkerken 1989 83 p In DUTCH; ENGLISH summary
(KNMI-TR-118; ISSN-0169-1708; ETN-90-97647) Copyright
Avail: Royal Netherlands Meteorological Inst., P.O. Box 201, 3730 AE De Bilt, Wilhelminalaan 10, Netherlands

Wave heights predicted by an operational wave model (GONO) and wind fields derived from an atmospheric fine mesh model (GONO wind) were compared with observations. The comparison was made for wind direction, wind speed, wave height, and low frequency wave height for the locations EPF, YMUIDEN and K-13 the southern North Sea, AVK in the central North Sea, and Brent in the northern North Sea. It is shown that there is a quite strong correlation between errors in the GONO wind and errors in the calculated wave height. The correlation coefficient at the coastal stations is about 0.7 and at the stations in open sea about 0.5. ESA

**N91-10546** Royal Netherlands Meteorological Inst., De Bilt. Afdeling Fysische Meteorologie.
**SPECTRA AND GRADIENTS OF STORMY WINDS AT CABAUW, NETHERLANDS, UP TO 200 METERS HIGH Thesis - Tech. Univ. Delft**
R. W. M. Meijer 1989 178 p In DUTCH; ENGLISH summary
(KNMI-TR-119; ISSN-0169-1708; ETN-90-97648) Copyright
Avail: Royal Netherlands Meteorological Inst., P.O. Box 201, 3730 AE De Bilt, Willhelminalaan 10, Netherlands

Atmospheric turbulence data, collected in 1986 at the 213 m Cabauw mast in stormy weather, were analyzed. The theory on the subject is discussed. Experimental situation, instrumentation, and data evaluation procedures are described. Fifteen selected 30 minute runs were analyzed in similitary form, including dimensionless wind speed gradients as well as horizontal wind spectra. The uncertainties about the quality of the local scales are discussed. It is shown that Sorbjan's assumption for the dimensionless wind velocity gradient in the stable boundary layer does not agree well with the Cabauw data. The horizontal wind velocity spectra are markedly influenced by the propellor vanes used. There are not enough published turbulence data above 100 m available to check the reliability of various models. ESA

**N91-10547#** World Meteorological Organization, Geneva (Switzerland).
**[ACTIVITIES REPORT OF THE WORLD METEOROLOGICAL ORGANIZATION] Annual Report, 1989**
1990 63 p
(WMO-734; ISBN-92-63-10734-9; ETN-90-97973) Copyright
Avail: NTIS HC/MF A04

The research and technical activities and observations of the global environment are reported. The Earth global climate in 1989 is summarized. The program performed in the following fields are included: world weather, applications of meteorology, hydrology and water resources, education, training and regional programs. Published papers, conferences, and staff are listed. ESA

**N91-10548*#** Electro Magnetic Applications, Inc., Denver, CO.
**DEVELOPMENT AND APPLICATION OF LINEAR AND NONLINEAR METHODS FOR INTERPRETATION OF LIGHTNING STRIKES TO IN-FLIGHT AIRCRAFT Final Report**
Terence Rudolph, Rodney A. Perala, Calvin C. Easterbrook, and Steven L. Parker Sep. 1986 441 p
(Contract NAS1-17748)
(NASA-CR-3974; NAS 1.26:3974; EMA-85-R-37) Avail: NTIS HC/MF A19 CSCL 04B

Since 1980, NASA has been collecting direct strike lightning data by flying an instrumented F-106B aircraft into thunderstorms. The continuing effort to interpret the measured data is reported here. Both linear and nonlinear finite difference modeling techniques are applied to the problem of lightning triggered by an aircraft in a thunderstorm. Five different aircraft are analyzed to determine the effect of aircraft size and shape on lightning triggering. The effect of lightning channel impedance on aircraft response is investigated. The particle environment in thunderstorms and electric field enhancements by typical ice particles is also investigated. Author

**N91-10362#** Meteorological Satellite Center, Tokyo (Japan).
**SATELLITE-DERIVED INDEX OF PRECIPITATION INTENSITY**
Kazufumi Suzuki *In its* Meteorological Satellite Center Technical Note. Special Issue (1989). Summary of GMS System. 2: Data Processing Mar. 1989 p 67-74 In JAPANESE; ENGLISH summary (For primary document see N91-10356 01-42)
Avail: NTIS HC/MF A08

**N91-10365#** Meteorological Satellite Center, Tokyo (Japan).
**CLOUD MOTION WIND**
Takashi Ohshima *In its* Meteorological Satellite Center Technical Note. Special Issue (1989). Summary of GMS System. 2: Data Processing Mar. 1989 p 85-102 In JAPANESE; ENGLISH summary (For primary document see N91-10356 01-42)
Avail: NTIS HC/MF A08

**N91-10366#** Meteorological Satellite Center, Tokyo (Japan).
**TYPHOON INFORMATION**
Hiroyuki Koba *In its* Meteorological Satellite Center Technical Note. Special Issue (1989). Summary of GMS System. 2: Data Processing Mar. 1989 p 103-108 In JAPANESE; ENGLISH summary Original contains color illustrations (For primary document see N91-10356 01-42)
Avail: NTIS HC/MF A08

**N91-10367#** Meteorological Satellite Center, Tokyo (Japan).
**VTR LOOP MOVIE**
Tokuei Uchiyama *In its* Meteorological Satellite Center Technical Note. Special Issue (1989). Summary of GMS System. 2: Data Processing Mar. 1989 p 109-111 In JAPANESE; ENGLISH summary (For primary document see N91-10356 01-42)
Avail: NTIS HC/MF A08

**N91-10371#** Meteorological Satellite Center, Tokyo (Japan).
**CLOUD GRID DATA**
Hideyuki Sasaki *In its* Meteorological Satellite Center Technical Note. Special Issue (1989). Summary of GMS System. 2: Data Processing Mar. 1989 p 123-139 In JAPANESE; ENGLISH summary (For primary document see N91-10356 01-42)
Avail: NTIS HC/MF A08

**N91-10373#** Meteorological Satellite Center, Tokyo (Japan).
**CLOUD AMOUNT DISTRIBUTION**
Kazuhiro Oosawa *In its* Meteorological Satellite Center Technical Note. Special Issue (1989). Summary of GMS System. 2: Data Processing Mar. 1989 p 147-154 In JAPANESE; ENGLISH summary (For primary document see N91-10356 01-42)
Avail: NTIS HC/MF A08

# 48 OCEANOGRAPHY

Includes biological, dynamic, and physical oceanography; and marine resources.

For related information see also *43 Earth Resources and Remote Sensing.*

**N91-10549#** Technische Univ., Delft (Netherlands). Fluid Mechanics Group.
**DIRECTIONAL RESPONSE OF WIND WAVES TO TURNING WINDS Ph.D. Thesis**
Gerbrant Philippus vanVledder 1990 266 p Sponsored by Netherlands Technology Foundation
(Rept-90-2; ETN-90-97755) Avail: NTIS HC/MF A12

The directional response of wind generated waves to turning winds was studied theoretically by using an advanced numerical wave prediction model, and empirically by using the results of directional wave measurements in the open ocean. The shape of the two-dimensional spectra and physical processes during responses of the waves, and the relation between the time scale of the directional response and local wind and wave parameters were studied. Results obtained show that for the relatively small wind shifts up to 45 deg the shapes of the two-dimensional spectrum and corresponding source function remain almost unchanged, and symmetric around the (turning) mean wave direction. For the larger wind shifts of 60 and 90 deg the spectrum and source function become strongly skewed. In all sudden wind shift cases a second spectral peak develops initially, but for relatively small wind shift this second peak is rapidly absorbed. ESA

**N91-10550#** Technische Univ., Delft (Netherlands). Fluid Mechanics Group.
**WIND WAVE PROPAGATION IN TIDAL SEAS Ph.D. Thesis**
Hendrik Lieuwe Tolman 1990 188 p
(Rept-90-1; ETN-90-97756) Avail: NTIS HC/MF A09

The effects of tides and storm surges on wind waves in shelf seas are assessed using analytical and numerical approaches for several academic cases and by hindcasting three storm cases on the North Sea. The results of the hindcast are compared with observed wave data using a developed wave model which incorporates all relevant effects of tides and surges on wind waves. It is shown that tides and storm surges should be considered as an instationary medium for wind wave propagation in shelf seas. For such conditions the commonly applied quasi-stationary approximation to wave current interactions cannot be used. It is shown that interactions are predominantly caused by currents; effects of mean surface level variations contribute significantly in storm surge conditions only. The hindcasts for the North Sea show relatively small tide and surge induced modulation of mean wave parameters such as the significant wave height or the mean wave period (typically 5 to 10 percent). The magnitude of these modulations decreases with increasing severity of wind and wave conditions. Modulations of the spectral density of the wave spectrum can be of the order of 50 percent. Observed modulations of mean wave parameters in the storm cases considered here appear to be for the most part wind induced. ESA

**N91-10372#** Meteorological Satellite Center, Tokyo (Japan).
**SEA SURFACE TEMPERATURE**
Hideyuki Sasaki *In its* Meteorological Satellite Center Technical Note. Special Issue (1989). Summary of GMS System. 2: Data Processing Mar. 1989 p 141-145 In JAPANESE; ENGLISH summary (For primary document see N91-10356 01-42)
Avail: NTIS HC/MF A08

# 51 LIFE SCIENCES (GENERAL)

**N91-10551#** Joint Publications Research Service, Arlington, VA.
**JPRS REPORT: SCIENCE AND TECHNOLOGY. USSR: LIFE SCIENCES**
6 Jan. 1990 80 p Transl. into ENGLISH from various Russian articles
(JPRS-ULS-90-001) Avail: NTIS HC/MF A05

Abstracts of Soviet literature in various areas of the life sciences are compiled. The following subject areas are covered: aerospace medicine, agriculture, biochemistry, biophysics, epidemiology, genetics, immunology, industrial medicine, laser bioeffects, medicine, nonionizing radiation effects, pharmacology and toxicology, physiology, public health, radiobiology, veterinary medicine, and virology. M.G.

**N91-10552#** Joint Publications Research Service, Arlington, VA.
**JPRS REPORT: SCIENCE AND TECHNOLOGY. USSR: LIFE SCIENCES**
26 Jul. 1990 40 p Transl. into ENGLISH from various Russian articles
(JPRS-ULS-90-013) Avail: NTIS HC/MF A03

Abstracts of Soviet literature in various areas of the life sciences are compiled. The following subject areas are covered: aerospace medicine, agriculture, biochemistry, biotechnology, epidemiology, genetics, immunology, laser bioeffects, medicine, microbiology, molecular biology, nonionizing radiation effects, pharmacology and toxicology, physiology, public health, radiobiology, and virology. For individual titles, see N91-10553 through N91-10555.

**N91-10553#** Joint Publications Research Service, Arlington, VA.
**MORPHOLOGICAL EXAMINATION OF RAT ADRENAL GLANDS FOLLOWING FLIGHT ABOARD BIOSPUTNIK KOSMOS-1667 Abstract Only**
N. G. Prodan and V. Baranska *In its* JPRS Report: Science and Technology. USSR: Life Sciences 26 Jul. 1990 p 2 Transl. into ENGLISH from Kosmicheskaya Biologiya I Aviakosmicheskaya Meditsina, Moscow (USSR), v. 23, no. 6, Nov. - Dec. 1989 p 27-30 (For primary document see N91-10552 01-51)
Avail: NTIS HC/MF A03

Histological examinations were performed on the adrenal glands of seven male Wistar rats after a 7-days flight aboard biosatellite Cosmos-1667. The studies were conducted 4 to 6 hours after landing to assess the effects of weightlessness. The weight of the glands and the volume of cortical and medullary tissue were not affected. The general architectonics of the glands were within normal limits, although the width of the zona glomerulosa was somewhat narrowed. In the zona glomerulosa the nuclei:cytoplasm ratio remained normal, although the cytoplasm and nuclear volumes in the experimental animals were expanded. The ratio was increased in the zona fasciculata due to an increase in the nuclear volume. The zona reticularis remained unaffected. The entire cortex was hyperemic, while the presence of numerous cytoplasmic vacuoles indicated lipid depletion. Increased vacuolization of medullary cells and diminished area of epinephrine- and norepinephrine-producing cells were interpreted to reflect gravitational stress. The findings suggested diminished medullary function and attenuation of the sympathetic system during space flight. Author

**N91-10554#** Joint Publications Research Service, Arlington, VA.
**CENTRAL AND REGIONAL HEMODYNAMICS IN PROLONGED SPACE FLIGHTS Abstract Only** c52
V. F. Turchaninova, A. D. Yegorov, and M. V. Domracheva *In its* JPRS Report: Science and Technology. USSR: Life Sciences 26 Jul. 1990 p 2 Transl. into ENGLISH from Kosmicheskaya Biologiya I Aviakosmicheskaya Meditsina, Moscow (USSR), v. 23, no. 6, Nov. - Dec. 1989 p 19-26 (For primary document see N91-10552 01-51)
Avail: NTIS HC/MF A03

An analysis was conducted on changes in central and regional hemodynamics on cosmonauts during ten short-term (7 days) and nine long-term (65 to 237 days) on Salyut 6-Soyuz and Salyut 7-Soyuz space flights using tetrapolar rheography. Hemodynamic monitoring, in conjunction with stress-testing and negative pressure on the lower part of the body, demonstrates that under conditions of weightlessness the increase in the activity of the vasomotor center and enhanced adrenergic mechanisms was due to a major blood volume shift to the lower extremities from the cardiopulmonary compartment. In short-term flights the heart rate remained essentially unchanged, while the stroke volume and minute volume diminished by 8 and 13 percent, respectively. In long-term flights the heart rate increased slightly, while the stroke and minutes volumes remained unaltered. The hemodynamic changes were interpreted to reflect ongoing adaptation and adjustment to weightlessness, a process that has been demonstrated to function for at least 237 days. Author

**N91-10555#** Joint Publications Research Service, Arlington, VA.
**PROTECTIVE FUNCTIONS OF SKIN Abstract Only** c52
O. V. Ignatova, A. A. Berlin, Z. P. Pak, and I. G. Popov *In its* JPRS Report: Science and Technology. USSR: Life Sciences 26 Jul. 1990 p 1 Transl. into ENGLISH from Kosmicheskaya Biologiya I Aviakosmicheskaya Meditsina, Moscow (USSR), v. 23, no. 6, Nov. - Dec. 1989 p 15-19 (For primary document see N91-10552 01-51)
Avail: NTIS HC/MF A03

A brief review is presented of changes in the protective functions of the skin under conditions of space flight. In general, confinement aboard space ships has been accompanied by loss of bactericidal properties and changes in the normal skin flora, changes that have been reported to persist for prolonged periods of time. It is generally accepted that the microclimatic conditions lead to functional changes in the skin that alter the normal pH, fatty acid, and amino acid profiles. The net change is a reduction in the bactericidal potency of the skin, and a change in the skin flora. Changes in bacterial flora in themselves eliminate normal bacterial antagonism. Finally, morphological changes in the epidermis further compromise the barrier function of the skin. Author

**N91-10556#** Joint Publications Research Service, Arlington, VA.
**JPRS REPORT: SCIENCE AND TECHNOLOGY. USSR: LIFE SCIENCES**
16 Jul. 1990 48 p Transl. into ENGLISH from various Russian articles
(JPRS-ULS-90-012) Avail: NTIS HC/MF A03

Abstracts of Soviet literature in various areas of the life sciences are compiled. The following subject areas are covered: aerospace medicine, biochemistry, epidemiology, immunology, medicine, military medicine, molecular biology, pharmacology and toxicology, physiology, and public health. For individual titles, see N91-10557 through N91-10564.

**N91-10557#** Joint Publications Research Service, Arlington, VA.
**DIAGNOSTIC POSSIBILITIES OF INFLIGHT EKG MONITORING OF FLIGHT CREW Abstract Only** c52
V. M. Kondrakov and V. I. Sinopalnikov *In its* JPRS Report: Science and Technology. USSR: Life Sciences 16 Jul. 1990 p 1 Transl. into ENGLISH from Voyenno-Meditsinskiy (Moscow, USSR), no. 5 May 1989 p 57-59 (For primary document see N91-10556 01-51)
Avail: NTIS HC/MF A03

Ambulatory inflight electrocardiography (EKG) monitoring was carried out on 22 pilots, ranging in age from 35 to 45 years, to evaluate this method for pilot health screening. The results disclosed that the use of the Soviet Lenta-MT monitor facilitated diagnosis of latent forms of coronary heart disease, arrhythmia, and conductive disorders in 15 of the subjects. All had previously passed fitness certification after conventional stress testing, which points to the utility of the ambulatory inflight monitoring in uncovering potential health problems in pilots. Author

**N91-10558#** Joint Publications Research Service, Arlington, VA.
**EFFECTS OF ROLLING MOTION ON THE CIRCADIAN RHYTHM OF SINOATRIAL NODE Abstract Only** c52
A. M. Marchenko *In its* JPRS Report: Science and Technology. USSR: Life Sciences 16 Jul. 1990 p 1 Transl. into ENGLISH from Voyenno-Meditsinskiy (Moscow, USSR), no. 5, May 1989 p 59-61 (For primary document see N91-10556 01-51)
Avail: NTIS HC/MF A03

Electrocardiography (EKG) studies were performed on 33 healthy sailors with a mean age of 37.5 years to assess the effects of seasickness on circadian rhythm of the sinoatrial node. The results demonstrate considerable individual variability in susceptibility to desynchronization of the self-excitation pattern and attendant deterioration of capacity for work. In individuals regarded as well adapted, usually with a work history of 10 to 15 years at sea, the changes were less pronounced and recovery was more rapid. This approach was felt to provide an objective assessment of the severity of seasickness, an important factor in determining occupational fitness and health status. Author

**N91-10559#** Joint Publications Research Service, Arlington, VA.
**PROBABILTY OF DECOMPRESSION SICKNESS DURING SPACE SUIT TESTING Abstract Only** c52
S. N. Filipenkov *In its* JPRS Report: Science and Technology. USSR: Life Sciences 16 Jul. 1990 p 1 Transl. into ENGLISH from Kosmicheskaya Biologiya i Aviakosmicheskaya Meditsina (Moscow, USSR), v. 23, no. 3, May - Jun. 1989 p 53-58 (For primary document see N91-10556 01-51)
Avail: NTIS HC/MF A03

The results are presented derived from an extensive series of trials conducted on space suits and decompression procedures to assess their efficacy in prevention of Decompression Sickness (DS). The studies involved 193 volunteers with good tolerance of moderate hypoxia and low barometric pressure. The data demonstrated that with long physical exertions and in-suit pressures of 105 to 320 mm Hg, commonly employed decompression procedures are effective in preventing DS with the probability of 0.75 to 0.9 after 1 to 2 hours of oxygen inhalation under terrestrial-equivalent conditions. A probability of 0.9 to 0.98 for the prevention of DS was theoretically attainable with a short period of decompression for several minutes with a coefficient if supersaturation of 3.5 to 5.4. However, with a coefficient of supersaturation of 1.9 to 2.1 success in prevention DS with a probability of 0.98 to 0.99 was shown to require oxygen breathing for 0.5 to 1 hour. Author

**N91-10560#** Joint Publications Research Service, Arlington, VA.
**CHANGES IN MAXIMUM ALLOWABLE SUPERSATURATION COEFFICIENT IN HIGH-ALTITUDE DECOMPRESSION Abstract Only** c52
V. I. Chadov and L. R. Iseyev *In its* JPRS Report: Science and Technology. USSR: Life Sciences 16 Jul. 1990 p 1 Transl. into ENGLISH from Kosmicheskaya Biologiya i Aviakosmicheskaya Meditsina (Moscow, USSR), v. 23, no. 3, May - Jun. 1989 p 58-62 (For primary document see N91-10556 01-51)
Avail: NTIS HC/MF A03

Male volunteers were used in pressure chamber studies designed to assess in the Maximum Allowable Coefficient of Supersaturation (MACS) in relation to pressure after decomposition, in order to assess the safety of high-altitude decompression procedures. The 70 volunteers ranged in age from 21 to 47 years underwent a total of 383 measurements that simulated transition from an orbital station to a space suit at reduced oxygen tension. MACS values were seen to decrease from 1.661 at 452 kPa (6300 m, 339 mm Hg), to 1.608 at 467 kPa (6080 m, 350 mm Hg), to 1.55 at 268 kPa (201 mm Hg), and 1.24 at 240 kPa (180 mm Hg). In practical terms the plots of coefficient of supersaturation vs. pressure after decompression demonstrated that MACS does not change significantly over an altitude range of 6100 to 9300 m, retaining value of essentially 1.6. Accordingly, this figure provides an acceptable margin of safety for prevention of decompression sickness. Author

**N91-10561#** Joint Publications Research Service, Arlington, VA.
**EFFECTS OF PROLONGED EXPOSURE TO ACETIC ACID VAPORS ON ACID-BASE BALANCE IN HUMANS Abstract Only** c52
L. Kh. Bragin *In its* JPRS Report: Science and Technology. USSR: Life Sciences 16 Jul. 1990 p 2 Transl. into ENGLISH from Kosmicheskaya Biologiya i Aviakosmicheskaya Meditsina (Moscow, USSR), v. 23, no. 3, May - Jun. 1989 p 65-68 (For

primary document see N91-10556 01-51)
Avail: NTIS HC/MF A03

Acid-base monitoring and determination of blood gases were conducted on 8 healthy males, 25 to 44 years old, to assess the physiological effects of prolonged exposure to 15 or 25 mg per cu m acetic acid vapors. Acetic acid was selected for the study because it is one of the key body surface metabolites and has previously been shown to be innocuous in concentrations of 10 mg per cu m. The experimental conditions utilized exposure for 20 days, with the temperature elevated to 33 C from day 16 through day 19 in one set of experiments and from day 6 to day 9 in another. The blood chemistries demonstrated that the low exposure level was innocuous in the long run, with any changes that were observed of limited duration. Data on the higher dosage showed more pronounced alteration in acid-base equilibrium, but again within physiological limits and without long-term sequels. Nevertheless, a concentration of 25 mg per cu m was felt to represent the upper limit of physiologically tolerable acetic acid concentration in the environment. Author

**N91-10562#** Joint Publications Research Service, Arlington, VA.
**EFFECTS OF TAURINE ON CYTOGENETIC CORNEAL DISTURBANCES INDUCED IN MICE BY 9 GeV PROTONS Abstract Only**
S. V. Vorozhtsova and Ye. I. Yartsev *In its* JPRS Report: Science and Technology. USSR: Life Sciences 16 Jul. 1990 p 2 Transl. into ENGLISH from Kosmicheskaya Biologiya i Aviakosmicheskaya Meditsina (Moscow, USSR), v. 23, no. 3, May - Jun. 1989 p 86-89 (For primary document see N91-10556 01-51)
Avail: NTIS HC/MF A03

The fact that protons account for some 80 percent of cosmic radiation led to a more detailed analysis on the efficiency of taurine drops on mitigating proton-induced cytogenetic damage to the cornea. The experiments were performed with mice irradiated with 9 GeV protons in doses ranging from 0.25 to 7.0 Gy. Certain animals were treated with 2 drops of 4 percent taurine solution in each eye five times before or after irradiation. Corneal monitoring at 24 and 72 hours demonstrated that proton irradiation led to a reduction in mitotic activity, an increase in the number of cells with chromosomal abnormalities, and cell depletion. These changes were essentially dose-dependent. Treatment with taurine reduced the number of cells with chromosomal abnormalities by two- to fivefold and was effective when administered both before and after irradiation. The effects of taurine were attributed to the fact that it had an inhibitory effect on mitosis, limiting thereby the extent of primary radiation damage and, consequently, postradiation damage to the genome. Author

**N91-10563#** Joint Publications Research Service, Arlington, VA.
**COMBINED EFFECTS OF ELEVATED CONCENTRATIONS OF CARBON DIOXIDE AND AMBIENT TEMPERATURE ON THERMAL STATE OF HUMANS IN CLOSED CHAMBERS Abstract Only** c52
A. V. Sosnovskiy *In its* JPRS Report: Science and Technology. USSR: Life Sciences 16 Jul. 1990 p 2 Transl. into ENGLISH from Kosmicheskaya Biologiya i Aviakosmicheskaya Meditsina (Moscow, USSR), v. 23, no. 3, May - Jun. 1989 p 89-90 (For primary document see N91-10556 01-51)
Avail: NTIS HC/MF A03

An analysis was conducted on the thermal state of 10 males exposed to elevated carbon dioxide concentrations and temperatures in 50 cu m closed chambers for 5 days. The experimental parameters were as follows: 26 to 28 C, 70 to 85 percent rel. humidity, 740 to 770 mm Hg barometric pressure, 3 to 3.5 percent CO2, 20 to 21 percent O2, and N2 to make 100 percent gas mixture. Physiological monitoring showed that mean body temperature remained unaffected as a result of elevation of the skin temperature by 0.7 C and a reduction in rectal temperature by 0.5 C. However, both the respiratory and heart rates were significantly increased. On balance, the data indicated that the level of discomfort and changes in body temperature regulation under the combined effect of elevated concentrations of carbon dioxide and ambient temperature serve to diminish work performance. Author

**N91-10564#** Joint Publications Research Service, Arlington, VA.
**PSYCHOPHYSIOLOGICAL ASSESSMENT OF PILOTING MOTOR HABITS IN PILOT RETRAINING Abstract Only** c53
N. N. Frolov and A. S. Kuzmin *In its* JPRS Report: Science and Technology. USSR: Life Sciences 16 Jul. 1990 p 2 Transl into ENGLISH from Voyenno-Meditsinskiy (Moscow, USSR), no. 1, Jan. 1989 p 54-57 (For primary document see N91-10556 01-51)
Avail: NTIS HC/MF A03

An analysis was conducted on the motor activity of pilots undergoing retraining on single-seat airplanes during landing maneuvers. The study was performed with 56 pilots during 290 flights. In general, as the pilots gained familiarity and experience with the new planes there was a gradual reduction in the number of control column movements and their amplitudes. Correspondingly, the quality of landings improved. The reduction in the incidence of control and adjustment movements was accompanied by an increase in the number of fine feedback movements. Readjustment of pilot to new airplanes appears to involve fine-tuning of established habituated movements rather than a fundamental reconstructing of underlying motor activity inherent in piloting skills. Consequently, fine feedback movements that appear as second nature and represent a form of international automation may be used to assess the degree of piloting habituation. Author

**N91-10565#** Joint Publications Research Service, Arlington, VA.
**JPRS REPORT: SCIENCE AND TECHNOLOGY. USSR: LIFE SCIENCES**
11 Jul. 1990 18 p Transl. into ENGLISH from various Russian articles
(JPRS-ULS-90-011) Avail: NTIS HC/MF A03

Abstracts of Soviet literature in various areas of the life sciences are compiled. The following subject areas are covered: aerospace medicine, epidemiology, pharmacology and toxicology, and public health. For individual titles, see N91-10566 through N91-10567.

**N91-10566#** Joint Publications Research Service, Arlington, VA.
**REQUIREMENTS FOR AN IDEAL DRUG FOR PREVENTING SPACE MOTION SICKNESS** c52
N. N. Karkishchenko *In its* JPRS Report: Science and Technology. USSR: Life Sciences 11 Jul. 1990 p 1-3 Transl. into ENGLISH from Kosmicheskaya Biologiya I Aviakosmicheskaya Meditsina, Moscow (USSR), v. 23, no. 6 Nov. - Dec. 1989 p 33-36 (For primary document see N91-10565 01-51)
Avail: NTIS HC/MF A03

The imperfect state of medical protection against Space Motion Sickness (SMS) is largely due to insufficient study of the mechanisms underlying this syndrome and the lack of theoretical approaches that could be used to formulate the property requirements of an ideal drug and produce highly effective prescriptions. The existing pharmacological methods are insufficiently effective. The action of existing agents is chiefly aimed at suppressing the central links of vestibular reflexes by acting upon the chemoreceptor trigger zone and vestibular nuclei. However, the onset of intensive vestibular-autonomic disturbances during motion sickness is associated with the generalized propagation of stimulation along Central Nervous System (CNS) structures that originated from the vestibular apparatus. In this connection, the use of anti-epileptic agents that affect the intercentral reciprocal relationships in the CNS to restrict such stimulation may be quite promising. At the same time, the generalized propagation of stimulation along the CNS structures during which typical SMS disturbances occur in the sensory, motor, and autonomic areas is a result of the excessively pronounced vestibular asymmetry that occurs in microgravity. The use of adaptive agents that stimulate the synthesis of nucleic acids and protein and that activate energy metabolism must be conducive to the formation of adaptive changes in vestibular analyzer function and asymmetry compensation. The research was undertaken with the purpose of identifying and substantiating the range of effects and action mechanisms of drugs that might be used to produce a powerful, low-toxic drug to prevent SMS. Author

**N91-10567#** Joint Publications Research Service, Arlington, VA.
**EFFECT OF SINGLE IMPACTS OF HEAVY IONS OF GALACTIC COSMIC RAYS ON LACTUCA SATIVA SEEDS EXPOSED ON SALYUT-6 AND SALYUT-7 STATIONS** c52
L. V. Nevzgodina, Ye. N. Maksimova, and Ye. V. Kaminskaya *In its* JPRS Report: Science and Technology. USSR: Life Sciences 11 Jul. 1990 p 3-7 Transl. into ENGLISH from Kosmicheskaya Biologiya I Aviakosmicheskaya Meditsina, Moscow (USSR), v. 23, no. 6, Nov. - Dec. 1989 p 66-70 (For primary document see N91-10565 01-51)
Avail: NTIS HC/MF A03

In spite of the comparatively low doses of total ionizing radiation received during space flights, radiation alterations did take place in biological test objects. Such changes can be induced by protons and gamma rays at doses 100 or 1000 higher than the doses received in flight. Therefore, the results of the space flight experiments cannot be easily associated with protons. It would seem more probable that the observed alterations are associated with the passage of some heavy ions (HI) of galactic cosmic rays (GCR) through the biological object. Calculations have shown that when HI pass through biological tissue in a 2 to 20 nm radius track area, the energy released is equivalent to a dose of several hundred rads. Inasmuch as the HI energy transfer is markedly localized, the observed effects may result from the impact of these particles in the region of certain sensitive cellular structures. The effect of single HI of GCR was studied during extensive flights on the orbiting manned stations Salyut. Air-dried Lactuca sativa lettuce seeds were employed as the biological test object. Author

**N91-10568#** Joint Publications Research Service, Arlington, VA.
**JPRS REPORT: SCIENCE AND TECHNOLOGY. USSR: LIFE SCIENCES**
A. P. Dmitriyev 2 Jul. 1990 74 p
(JPRS-ULS-90-010) Avail: NTIS HC/MF A04

Abstracts of Soviet literature in various areas of the life sciences are compiled. The following subject areas are covered: agriculture, biochemistry, biophysics, biotechnology, epidemiology, immunology, laser bioeffects, microbiology, pharmacology and toxicology, physiology, public health, and veterinary medicine. M.G.

**N91-10569#** Joint Publications Research Service, Arlington, VA.
**JPRS REPORT: SCIENCE AND TECHNOLOGY. USSR: LIFE SCIENCES**
A. N. Palilova 9 Jul. 1990 79 p
(JPRS-ULS-90-009) Avail: NTIS HC/MF A05

Abstracts of Soviet literature in various areas of the life sciences are compiled. The following subject areas are covered: biophysics, epidemiology, genetics, medicine, molecular biology, physiology, and public health. M.G.

**N91-10570#** Joint Publications Research Service, Arlington, VA.
**JPRS REPORT: SCIENCE AND TECHNOLOGY. USSR: LIFE SCIENCES**
Ye. A. Kovalenko 27 Jun. 1990 82 p
(JPRS-ULS-90-008) Avail: NTIS HC/MF A05

Abstracts of Soviet literature in various areas of the life sciences are compiled. The following subject areas are covered: aerospace medicine, agriculture, biochemistry, epidemiology, genetics, laser bioeffects, microbiology, pharmacology and toxicology, physiology, radiobiology, and public health. M.G.

**N91-10571#** Joint Publications Research Service, Arlington, VA.
**JPRS REPORT: SCIENCE AND TECHNOLOGY. USSR: LIFE SCIENCES**
A. V. Ovsyannikov 18 Jun. 1990 56 p
(JPRS-ULS-90-006) Avail: NTIS HC/MF A04

Abstracts of Soviet literature in various areas of the life sciences are compiled. The following subject areas are covered: agriculture, biochemistry, biotechnology, immunology, laser bioeffects, microbiology, pharmacology and toxicology, physiology, public health, radiobiology, veterinary medicine, and virology. M.G.

**N91-10572#** Joint Publications Research Service, Arlington, VA.
**JPRS REPORT: SCIENCE AND TECHNOLOGY. USSR: LIFE SCIENCES**
14 Jun. 1990 40 p Transl. into ENGLISH from various Russian articles
(JPRS-ULS-90-005) Avail: NTIS HC/MF A03

Abstracts of Soviet literature in various areas of the life sciences are compiled. The following subject areas are covered: aerospace medicine, biochemistry, epidemiology, genetics, immunology, industrial medicine, laser bioeffects, medicine, microbiology, military medicine, nonionizing radiation effects, pharmacology and toxicology, physiology, and virology. M.G.

**N91-10573#** Pacific Northwest Lab., Richland, WA.
**ELF (EXTREMELY-LOW-FREQUENCY): EXPOSURE LEVELS, BIOEFFECTS, AND EPIDEMIOLOGY**
Larry E. Anderson Jun. 1990 18 p Presented at the 1990 Health Physics Society Meeting, Anaheim, CA, 18-22 Jun. 1990
(Contract DE-AC06-76RL-01830)
(DE90-016554; PNL-SA-18314; CONF-900679-7) Avail: NTIS HC/MF A03

Extremely-low-frequency (ELF) electromagnetic fields arise from a variety of sources including power distribution networks, public transportation systems, electrical appliances and motors, electrically heated beds and blankets, etc. In fact, in an industrialized society, people and animals are bathed in complex milieu of elevated electromagnetic fields. The ways in which exposure to these ELF electric and magnetic fields may affect biological systems are not obvious. Ionizing radiation can interact with neutral molecules to form chemically reactive radical or ionic species; however, ELF radiation transfers energy to tissues at a level lower than is already present in the form of thermal energy. ELF electromagnetic fields, nonetheless, appear to interact with tissue, and in particular with neural tissue in some whole-animal and cellular systems. This paper evaluates possible interactions between the contemporary electromagnetic environment and living organisms, and whether such influences are temporary or long lasting, beneficial or harmful. In studies on electric and magnetic fields, a broad range of exposure levels has been employed from a few volts/meter to more than 100 kV/m, and from 0.01 to 30 millitessla. A equally wide span of biological endpoints have been evaluated for possible response to ELF fields. DOE

## 52 AEROSPACE MEDICINE

Includes physiological factors; biological effects of radiation; and effects of weightlessness on man and animals.

**N91-10574*#** National Aeronautics and Space Administration. Lyndon B. Johnson Space Center, Houston, TX.
**WORKSHOP ON EXERCISE PRESCRIPTION FOR LONG-DURATION SPACE FLIGHT**
Bernard A. Harris, Jr., ed. and Donald F. Stewart, ed. Washington Oct. 1989 125 p Workshop held in Houston, TX, 1986
(NASA-CP-3051; S-597; NAS 1.55:3051) Avail: NTIS HC/MF A06 CSCL 06P

The National Aeronautics and Space Administration has a dedicated history of ensuring human safety and productivity in flight. Working and living in space long term represents the challenge of the future. Our concern is in determining the effects on the human body of living in space. Space flight provides a powerful stimulus for adaptation, such as cardiovascular and musculoskeletal deconditioning. Extended-duration space flight will influence a great many systems in the human body. We must understand the process by which this adaptation occurs. The NASA is agressively involved in developing programs which will act as a foundation for this new field of space medicine. The hallmark of these programs deals with prevention of deconditioning, currently referred to as countermeasures to zero g. Exercise appears to be most effective in preventing the cardiovascular and musculoskeletal degradation of microgravity. For individual titles, see N91-10575 through N91-10588.

**N91-10575*#** Methodist Hospital, Indianapolis, IN. Dept. of Medical Research.

**US SPACE FLIGHT EXPERIENCE. PHYSICAL EXERTION AND METABOLIC DEMAND OF EXTRAVEHICULAR ACTIVITY: PAST, PRESENT, AND FUTURE**

Thomas P. Moore *In* NASA, Johnson Space Center, Workshop on Exercise Prescription for Long-Duration Space Flight Oct. 1989 p 3-13 (For primary document see N91-10574 01-52)
Avail: NTIS HC/MF A06 CSCL 06P

A review of physical exertion and metabolic demands of extravehicular activity (EVA) on U.S. astronauts is given. Information is given on EVA during Gemini, Apollo and Skylab missions. It is noted that nominal EVA's should not be overstressful from a cardiovascular standpoint; that manual-intensive EVA's such as are planned for the construction phase of the Space Station can and will be demanding from a muscular standpoint, primarily for the upper extremities; that off-nominal unplanned EVA's can be physically demanding both from an endurance and from a muscular standpoint; and that crewmembers should be physically prepared and capable of performing these EVA's at any time during the mission. Author

**N91-10576*#** National Aeronautics and Space Administration. Lyndon B. Johnson Space Center, Houston, TX.

**SPACE STATION** c18

Donald F. Stewart and Judith Hayes (Krug International, Houston, TX.) *In its* Workshop on Exercise Prescription for Long-Duration Space Flight Oct. 1989 p 15-18 (For primary document see N91-10574 01-52)
Avail: NTIS HC/MF A06 CSCL 22B

The history of American space flight indicates that a space station is the next logical step in the scientific pursuit of greater knowledge of the universe. The Space Station and its complement of space vehicles, developed by NASA, will add new dimensions to an already extensive space program in the United States. The Space Station offers extraordinary benefits for a comparatively modest investment (currently estimated at one-ninth the cost of the Apollo Program). The station will provide a permanent multipurpose facility in orbit necessary for the expansion of space science and technology. It will enable significant advancements in life sciences research, satellite communications, astronomy, and materials processing. Eventually, the station will function in support of the commercialization and industrialization of space. Also, as a prerequisite to manned interplanetary exploration, the long-duration space flights typical of Space Station missions will provide the essential life sciences research to allow progressively longer human staytime in space. Author

**N91-10577*#** Methodist Hospital, Indianapolis, IN.

**THE HISTORY OF IN-FLIGHT EXERCISE IN THE US MANNED SPACE PROGRAM**

Thomas P. Moore *In* NASA, Johnson Space Center, Workshop on Exercise Prescription for Long-Duration Space Flight Oct. 1989 p 19-21 (For primary document see N91-10574 01-52)
Avail: NTIS HC/MF A06 CSCL 06P

A historical perspective on in-flight exercise in the U.S. manned space program is given. We have learned a great deal in the 25 years since the inception of Project Mercury. But, as we look forward to a Space Station and long-duration space flight, we must recognize the challenge that lies ahead. The importance of maintenance of the crewmember's physical condition during long stays in weightlessness is a prime concern that should not be minimized. The challenge lies in the design and development of exercise equipment and protocols that will prevent or minimize the deleterious sequelae of long-duration space flight while maximizing valuable on-orbit crew time. Author

**N91-10578*#** National Aeronautics and Space Administration. Lyndon B. Johnson Space Center, Houston, TX.

**WORK, EXERCISE, AND SPACE FLIGHT. 1: OPERATIONS, ENVIRONMENT, AND EFFECTS OF SPACEFLIGHT**

William Thornton *In its* Workshop on Exercise Prescription for Long-Duration Space Flight Oct. 1989 p 23-30 (For primary document see N91-10574 01-52)
Avail: NTIS HC/MF A06 CSCL 06P

The selection, training, and operations of space flight impose significant physical demands which seem to be adequately met by the existing physical training facilities and informal individual exercise programs. The professional astronaut population has, by selection, better than average health and physical capacity. The essentials of life on earth are adequately met by the spacecraft. However, as the human body adapts to weightlessness, it is compromised for the usual life on earth, but readaptation is rapid. Long term flight without countermeasures will produce major changes in the cardiovascular, respiratory, musculoskeletal and neuromuscular systems. There is strong theoretical and experimental evidence from 1-g studies and limited in-flight evidence to believe that exercise is a key counter-measure to many of these adaptations. Author

**N91-10579*#** National Aeronautics and Space Administration. Lyndon B. Johnson Space Center, Houston, TX.

**WORK, EXERCISE, AND SPACE FLIGHT. 3: EXERCISE DEVICES AND PROTOCOLS**

William Thornton *In its* Workshop on Exercise Prescription for Long-Duration Space Flight Oct. 1989 p 31-42 (For primary document see N91-10574 01-52)
Avail: NTIS HC/MF A06 CSCL 06P

Preservation of locomotor capacity by earth equivalent, exercise in space is the crucial component of inflight exercise. At this time the treadmill appears to be the only way possible to do this. Work is underway on appropriate hardware but this and a proposed protocol to reduce exercise time must be tested. Such exercise will preserve muscle, bone Ca(++) and cardiovascular-respiratory capacity. In addition, reasonable upper body exercise can be supplied by a new force generator/measurement system-optional exercise might include a rowing machine and bicycle ergometer. A subject centered monitoring-evaluation program will allow real time adjustments as required. Absolute protection for any astronaut will not be possible and those with hypertrophied capacities such as marathoners or weight lifters will suffer significant loss. However, the program described should return the crew to earth with adequate capacity of typical activity on earth including immediate ambulation and minimal recovery time and without permanent change. An understanding of the practical mechanics and biomechanics involved is essential to a solution of the problem. Author

**N91-10580*#** National Aeronautics and Space Administration. Lyndon B. Johnson Space Center, Houston, TX.

**SPACE MEDICINE CONSIDERATIONS: SKELETAL AND CALCIUM HOMEOSTASIS**

Victor B. Schneider *In its* Workshop on Exercise Prescription for Long-Duration Space Flight Oct. 1989 p 47-52 (For primary document see N91-10574 01-52)
Avail: NTIS HC/MF A06 CSCL 06P

Based on the information obtained from space missions, particularly Skylab and the longer Salyut missions, it is clear that bone and mineral metabolism is substantially altered during space flight. Calcium balance becomes increasingly more negative throughout the flight, and the bone mineral content of the os calcis declines. The major health hazards associated with skeletal changes include the signs and symptoms of hypercalcemia with rapid bone turnover, the risk of kidney stones because of hypercalciuria, the lengthy recovery of lost bone mass after flight, the possibility of irreversible bone loss (particularly the trabecular bone), the possible effects of metastated calcification in the soft tissues, and the possible increase in fracture potential. For these reasons, major efforts need to be directed toward elucidating the fundamental mechanisms by which bone is lost in space and developing more effective countermeasures to prevent both short-term and long-term complications. Author

**N91-10581*#** Creighton Univ., Omaha, NE.
**CHANGES IN MINERAL METABOLISM WITH IMMOBILIZATION/SPACE FLIGHT**
J. C. Gallagher *In* NASA, Johnson Space Center, Workshop on Exercise Prescription for Long-Duration Space Flight Oct. 1989 p 53-55 (For primary document see N91-10574 01-52)
Avail: NTIS HC/MF A06 CSCL 06P

Researchers are still unsure of the accuracy of previous bone density measurements of their significance following a period of weightlessness. Rapid technological advances in the measurement of bone density will enable us now to measure bone density accurately at multiple sites in the skeleton with doses of radiation less than that given by a spine x ray. It may not be possible to obtain this type of information before the next series of space flights take place, although the bed-rest model may provide supporting information. Extensive testing of bone density on every astronaut should be performed before and after the space flight. Prevention and treatment can only be undertaken after gathering sufficient baseline information. The use of exercise in preventing bone loss is still highly speculative, but represents a relatively easy approach to the problem in terms of study. Author

**N91-10582*#** West Virginia Univ., Morgantown. Dept. of Physiology and Neurology
**A UNIQUE PROBLEM OF MUSCLE ADAPTATION FROM WEIGHTLESSNESS: THE DECELERATION DEFICIENCY**
William T. Stauber *In* NASA, Johnson Space Center, Workshop on Exercise Prescription for Long-Duration Space Flight Oct. 1989 p 57-59 (For primary document see N91-10574 01-52)
Avail: NTIS HC/MF A06 CSCL 06P

Decelerator problems of the knee are emphasized since the lower leg musculature is known to atrophy in response to weightlessness. However, other important decelerator functions are served by the shoulder muscles, in particular the rotator cuff muscles. Problems in these muscles often result in tears and dislocations as seen in baseball pitchers. It is noteworthy that at least one device currently exists that can measure concentric and eccentric muscle loading including a submaximal simulated free weight exercise (i.e., force-controlled) and simultaneously record integrated EMG analysis appropriate for assessment of all muscle functional activities. Studies should be undertaken to provide information as to the performance of maximal and submaximal exercise in space travelers to define potential problems and provide rationale for prevention. Author

**N91-10583*#** Pennsylvania State Univ., University Park. Center for Locomotion Studies.
**BIOMEDICAL PERSPECTIVES ON LOCOMOTION IN NULL GRAVITY**
Peter R. Cavanagh *In* NASA, Johnson Space Center, Workshop on Exercise Prescription for Long-Duration Space Flight Oct. 1989 p 61-67 (For primary document see N91-10574 01-52)
Avail: NTIS HC/MF A06 CSCL 06P

A number of important features of various locomotor activities are discussed, and approaches to the study of these activities in the context of space flight are suggested. In particular, the magnitude of peak forces and the rates of change of force during terrestrial cycling, walking, and running are compared. It is shown that subtle changes in the conditions and techniques of locomotion can have a major influence on the biomechanical consequences to the skeleton. The various hypotheses that identify locomotor exercise as a countermeasure to bone demineralization during weightlessness deserve to be tested with some degree of biomechanical rigor. Various approaches for achieving such scrutiny are discussed. Author

**N91-10584*#** California Univ., Los Angeles. Dept. of Kinesiology.
**EXERCISE ISSUES RELATED TO THE NEUROMUSCULAR FUNCTION AND ADAPTATION TO MICROGRAVITY**
Reggie Edgerton *In* NASA, Johnson Space Center, Workshop on Exercise Prescription for Long-Duration Space Flight Oct. 1989 p 77-78 (For primary document see N91-10574 01-52)
Avail: NTIS HC/MF A06 CSCL 06P

Explored here is the question of whether astronauts can perform extravehicular activities effectively, efficiently, and productively. The loss of muscle mass, movement control, central nervous system function, muscle atrophy and fatigue, all consequent to weightlessness exposure, are discussed. The author recommends more research in these areas. Author

**N91-10585*#** Bionetics Corp., Cocoa Beach, FL. Biomedical Operations and Research Office.
**CONSIDERATIONS FOR AN EXERCISE PRESCRIPTION**
Victor A. Convertino *In* NASA, Johnson Space Center, Workshop on Exercise Prescription for Long-Duration Space Flight Oct. 1989 p 99-105 (For primary document see N91-10574 01-52)
Avail: NTIS HC/MF A06 CSCL 06P

A number of past and most recent research findings that describe some of the physiological responses to exercise in man and their relationship with exposure to various gravitational environments are discussed. Most of the data pertain to adaptations of the cardiovascular and body fluid systems. It should be kept in mind that the data from studies on microgravity simulation in man include exposures of relatively short duration (5 hours to 14 days). However, it is argued that the results may provide important guidelines for the consideration of many variables which are pertinent to the development of exercise prescription for long-duration space flight. The following considerations for exercise prescriptions during long-duration space flight are noted: (1) Relatively high aerobic fitness and strength, especially of the upper body musculature, should be a criterion for selection of astronauts who will be involved in EVA, since endurance and strength appear to be predominant characteristics for work performance. (2) Some degree of upper body strength will probably be required for effective performance of EVA. However, the endurance and strength required by the upper body for EVA can probably be obtained through preflight exercise prescription which involves swimming. (3) Although some degree of arm exercise may be required to maintain preflight endurance and strength, researchers propose that regular EVA will probably be sufficient to maintain the endurance and strength required to effectively perform work tasks during space flight. (4) A minimum of one maximal aerobic exercise every 7 to 10 days during space flight may be all that is necessary for maintenance of normal cardiovascular responsiveness and replacement of body fluids for reentry following prolonged space flight. (5) The possible reduction in the amount of exercise required for maintenance of cardiovascular system and body fluids in combination with the use of electromyostimulation (EMS) or methods other than conventional exercise for maintaining size and strength of muscles and bones needs great consideration for further research. These approaches represent a potential solution to the problem of compromising valuable time for exercise that is needed for daily operations. Author

**N91-10586*#** National Aeronautics and Space Administration. Lyndon B. Johnson Space Center, Houston, TX.
**WORK, EXERCISE, AND SPACE FLIGHT. 2: MODIFICATION OF ADAPTATION BY EXERCISE (EXERCISE PRESCRIPTION)**
William Thornton *In its* Workshop on Exercise Prescription for Long-Duration Space Flight Oct. 1989 p 107-115 (For primary document see N91-10574 01-52)
Avail: NTIS HC/MF A06 CSCL 06P

The fundamentals of exercise theory on earth must be rigorously understood and applied to prevent adaptation to long periods of weightlessness. Locomotor activity, not weight, determines the capacity or condition of the largest muscles and bones in the body and usually also determines cardio-respiratory capacity. Absence of this activity results in rapid atrophy of muscle, bone, and cardio-respiratory capacity. Upper body muscle and bone are less affected depending upon the individual's usual, or 1-g, activities. Methodology is available to prevent these changes but space operations demand that it be done in the most efficient fashion, i.e., shortest time. At this point in time we can reasonably select the type of exercise and methods of obtaining it, but additional work in 1-g will be required to optimize the time. Author

**N91-10587*#** Texas Univ. Health Science Center, Dallas. Div. of Cardiology.
**CARDIOVASCULAR GROUP**
Gunnar Blomqvist *In* NASA, Johnson Space Center, Workshop on Exercise Prescription for Long-Duration Space Flight Oct. 1989 p 117-123 (For primary document see N91-10574 01-52)
Avail: NTIS HC/MF A06 CSCL 06P

As a starting point, the group defined a primary goal of maintaining in flight a level of systemic oxygen transport capacity comparable to each individual's preflight upright baseline. The goal of maintaining capacity at preflight levels would seem to be a reasonable objective for several different reasons, including the maintenance of good health in general and the preservation of sufficient cardiovascular reserve capacity to meet operational demands. It is also important not to introduce confounding variables in whatever other physiological studies are being performed. A change in the level of fitness is likely to be a significant confounding variable in the study of many organ systems. The principal component of the in-flight cardiovascular exercise program should be large-muscle activity such as treadmill exercise. It is desirable that at least one session per week be monitored to assure maintenance of proper functional levels and to provide guidance for any adjustments of the exercise prescription. Appropriate measurements include evaluation of the heart-rate/workload or the heart-rate/oxygen-uptake relationship. Respiratory gas analysis is helpful by providing better opportunities to document relative workload levels from analysis of the interrelationships among VO2, VCO2, and ventilation. The committee felt that there is no clear evidence that any particular in-flight exercise regimen is protective against orthostatic hypotension during the early readaptation phase. Some group members suggested that maintenance of the lower body muscle mass and muscle tone may be helpful. There is also evidence that late in-flight interventions to reexpand blood volume to preflight levels are helpful in preventing or minimizing postflight orthostatic hypotension. Author

**N91-10588*#** National Aeronautics and Space Administration. Lyndon B. Johnson Space Center, Houston, TX.
**SUMMARY AND RECOMMENDATIONS FOR INITIAL EXERCISE PRESCRIPTION**
Donald F. Stewart and Bernard A. Harris, Jr. (Space Biomedical Research Inst., Houston, TX.) *In its* Workshop on Exercise Prescription for Long-Duration Space Flight Oct. 1989 p 125-130 (For primary document see N91-10574 01-52)
Avail: NTIS HC/MF A06 CSCL 06P

The recommendations summarized herein constitute a basis on which an initial exercise prescription can be formulated. It is noteworthy that any exercise program designed currently would be an approximation. Examination of the existing space-flight data reveals a scarcity of in-flight data on which to rigorously design an exercise program. The relevant experience within the U.S. space program (with regard to long-duration space flight) is limited to the Skylab Program. Lessons learned from Skylab are relevant to the design of a Space Station exercise program, especially with regard to the total length of exercise time required, cardiovascular (CV) deconditioning/reconditioning, and bone loss. Certain observations of the U.S.S.R. exercise activities can also contribute to the formulation of an exercise prescription of Space Station. Reportedly, the U.S.S.R. uses both a bicycle ergometer and a treadmill device on long-duration missions with some degree of success. Using the third crew of Salyut 6, which was a 175-day stay, as a representative mission, the typical time dedicated to exercise varies from 2 to 3 hours per day. In addition, the cosmonauts wear an elasticized suit, called a penquin suit, for time periods ranging from 12 to 16 hours per day. This device provides a load across the axial skeleton against which the wearer must exert himself. Despite these extensive countermeasures, the effects of adaptation are not totally prevented. Author

**N91-10589#** Joint Publications Research Service, Arlington, VA.
**JPRS REPORT: SCIENCE AND TECHNOLOGY. USSR: LIFE SCIENCES**
13 Jun. 1989 38 p Transl. into ENGLISH from various Russian articles
(JPRS-ULS-89-008) Avail: NTIS HC/MF A03

Abstracts of Soviet literature in various areas of the life sciences are compiled. The following areas are covered: biophysics; laser bioeffects; medicine; pharmacology and toxicology; physiology; public health; and virology. M.G.

**N91-10590#** Joint Publications Research Service, Arlington, VA.
**JPRS REPORT: SCIENCE AND TECHNOLOGY. USSR: LIFE SCIENCES**
29 Sep. 1989 43 p Transl. into ENGLISH from various Russian articles
(JPRS-ULS-89-010) Avail: NTIS HC/MF A03

Abstracts of Soviet literature in various areas of the life sciences are compiled. The following subject areas are covered: agriculture; biochemistry; microbiology; nonionizing radiation effects; pharmacology and toxicology; physiology; public health; and psychology. M.G.

**N91-10591*#** Good Samaritan Hospital and Medical Center, Portland, OR. Neurological Sciences Inst.
**ROLE OF ORIENTATION REFERENCE SELECTION IN MOTION SICKNESS Semiannual Status Report**
Robert J. Peterka and F. Owen Black Sep. 1990 37 p
(Grant NAG9-117)
(NASA-CR-186612; NAS 1.26:186612) Avail: NTIS HC/MF A03 CSCL 06E

Three areas related to human orientation control are investigated: (1) reflexes associated with the control of eye movements and posture; (2) the perception of body rotation and position with respect to gravity; and (3) the strategies used to resolve sensory conflict situations which arise when different sensory systems provide orientation cues which are not consistent with one another or with previous experience. Of particular interest is the possibility that a subject may be able to ignore an inaccurate sensory modality in favor of one or more other sensory modalities which do provide accurate orientation reference information. This process is referred as sensory selection. This proposal will attempt to quantify subject's sensory selection abilities and determine if this ability confers some immunity to the development of motion sickness symptoms. Author

**N91-10592#** Pacific Northwest Lab., Richland, WA.
**INTERACTION OF EXTREMELY LOW-FREQUENCY ELECTROMAGNETIC FIELDS WITH HUMANS**
T. S. Tenforde Apr. 1990 3 p Presented at the Annual Meeting of the Division of Physics of Beams of the American Physical Society, Washington, DC, 16-19 Apr. 1990
(Contract DE-AC06-76RL-01830)
(DE90-017190; PNL-SA-17819; CONF-900495-2) Avail: NTIS HC/MF A01

Public concern has grown in recent years concerning the possible health effects of extremely low frequency (ELF) electromagnetic fields to which we are exposed in all aspects of everyday life. By definition ELF refers to the range of electromagnetic field frequencies below 300 Hz, which includes the power transmission and distribution frequencies used throughout the world. In materials with the electrical and magnetic properties of living tissues, these fields have a long wavelength (5000 m) and skin depth (150 m). As a consequence, in their interactions with humans and other living organisms ELF fields behave as though they are composed of independent electric and magnetic fields components. ELF fields and their interactions with humans and other living organisms as well as their biological effects are discussed. DOE

**N91-10593#** Pacific Northwest Lab., Richland, WA.
**STATISTICAL METHODS FOR ANALYZING AND COMBINING DATA ON LOW-LEVEL EXPOSURES TO IONIZING RADIATION**
Ethel S. Gilbert Jul. 1990 5 p Presented at the American Statistical Association Conference on Radiation and Health, Copper Mountain, CO, 8-13 Jul. 1990
(Contract DE-AC06-76RL-01830)
(DE90-017193; PNL-SA-18391; CONF-9007165-2) Avail: NTIS HC/MF A01

Occupational studies of workers who have been exposed to radiation provide a direct assessment of low level radiation risks, and can serve as a check on estimates obtained through extrapolation from studies of populations exposed at high levels. Several studies of workers involved in the production of both defense materials and nuclear power in the United States, Great Britain, and Canada are being conducted. If the current risk estimates are correct, these studies have very low power for detecting risks, but can be used to provide useful upper limits on risks. If the current risk estimates are too low, the studies are adequate to detect large departures from these estimates. A broad assessment based on the totality of evidence from all occupational studies is obviously desirable, and such an assessment can be best accomplished by analyzing combined data from all studies. Plans for international combined analyses are underway, and combined analyses on a national scale are also being conducted. In the U.S., results based on combined data on male workers at the Hanford Site, Oak Ridge National Laboratory (ORNL), and Rocky Flats Weapons Plant have been published, and are used in this presentation to illustrate the application of various statistical procedures. DOE

**N91-10594*** National Aeronautics and Space Administration, Washington, DC.
**AEROSPACE MEDICINE AND BIOLOGY: A CONTINUING BIBLIOGRAPHY WITH INDEXES (SUPPLEMENT 341)**
Oct. 1990 50 p
(NASA-SP-7011(341); NAS 1.21:7011(341)) Avail: NTIS HC A03; NTIS standing order as PB90-912300, $11.50 domestic, $23.00 foreign CSCL 06E

This bibliography lists 133 reports, articles and other documents introduced into the NASA Scientific and Technical Information System during September 1990. Subject coverage includes: aerospace medicine and psychology, life support systems and controlled environments, safety equipment, exobiology and extraterrestrial life, and flight crew behavior and performance. Author

**N91-10554#** Joint Publications Research Service, Arlington, VA.
**CENTRAL AND REGIONAL HEMODYNAMICS IN PROLONGED SPACE FLIGHTS Abstract Only**
V. F. Turchaninova, A. D. Yegorov, and M. V. Domracheva *In its* JPRS Report: Science and Technology. USSR: Life Sciences 26 Jul. 1990 p 2 Transl. into ENGLISH from Kosmicheskaya Biologiya I Aviakosmicheskaya Meditsina, Moscow (USSR), v. 23, no. 6, Nov. - Dec. 1989 p 19-26 (For primary document see N91-10552 01-51)
Avail: NTIS HC/MF A03

**N91-10555#** Joint Publications Research Service, Arlington, VA.
**PROTECTIVE FUNCTIONS OF SKIN Abstract Only**
O. V. Ignatova, A. A. Berlin, Z. P. Pak, and I. G. Popov *In its* JPRS Report: Science and Technology. USSR: Life Sciences 26 Jul. 1990 p 1 Transl. into ENGLISH from Kosmicheskaya Biologiya I Aviakosmicheskaya Meditsina, Moscow (USSR), v. 23, no. 6, Nov. - Dec. 1989 p 15-19 (For primary document see N91-10552 01-51)
Avail: NTIS HC/MF A03

**N91-10557#** Joint Publications Research Service, Arlington, VA.
**DIAGNOSTIC POSSIBILITIES OF INFLIGHT EKG MONITORING OF FLIGHT CREW Abstract Only**
V. M. Kondrakov and V. I. Sinopalnikov *In its* JPRS Report: Science and Technology. USSR: Life Sciences 16 Jul. 1990 p 1 Transl. into ENGLISH from Voyenno-Meditsinskiy (Moscow, USSR), no. 5 May 1989 p 57-59 (For primary document see N91-10556 01-51)
Avail: NTIS HC/MF A03

**N91-10558#** Joint Publications Research Service, Arlington, VA.
**EFFECTS OF ROLLING MOTION ON THE CIRCADIAN RHYTHM OF SINOATRIAL NODE Abstract Only**
A. M. Marchenko *In its* JPRS Report: Science and Technology. USSR: Life Sciences 16 Jul. 1990 p 1 Transl. into ENGLISH from Voyenno-Meditsinskiy (Moscow, USSR), no. 5, May 1989 p 59-61 (For primary document see N91-10556 01-51)
Avail: NTIS HC/MF A03

**N91-10559#** Joint Publications Research Service, Arlington, VA.
**PROBABILTY OF DECOMPRESSION SICKNESS DURING SPACE SUIT TESTING Abstract Only**
S. N. Filipenkov *In its* JPRS Report: Science and Technology. USSR: Life Sciences 16 Jul. 1990 p 1 Transl. into ENGLISH from Kosmicheskaya Biologiya i Aviakosmicheskaya Meditsina (Moscow, USSR), v. 23, no. 3, May - Jun. 1989 p 53-58 (For primary document see N91-10556 01-51)
Avail: NTIS HC/MF A03

**N91-10560#** Joint Publications Research Service, Arlington, VA.
**CHANGES IN MAXIMUM ALLOWABLE SUPERSATURATION COEFFICIENT IN HIGH-ALTITUDE DECOMPRESSION Abstract Only**
V. I. Chadov and L. R. Iseyev *In its* JPRS Report: Science and Technology. USSR: Life Sciences 16 Jul. 1990 p 1 Transl. into ENGLISH from Kosmicheskaya Biologiya i Aviakosmicheskaya Meditsina (Moscow, USSR), v. 23, no. 3, May - Jun. 1989 p 58-62 (For primary document see N91-10556 01-51)
Avail: NTIS HC/MF A03

**N91-10561#** Joint Publications Research Service, Arlington, VA.
**EFFECTS OF PROLONGED EXPOSURE TO ACETIC ACID VAPORS ON ACID-BASE BALANCE IN HUMANS Abstract Only**
L. Kh. Bragin *In its* JPRS Report: Science and Technology. USSR: Life Sciences 16 Jul. 1990 p 2 Transl. into ENGLISH from Kosmicheskaya Biologiya i Aviakosmicheskaya Meditsina (Moscow, USSR), v. 23, no. 3, May - Jun. 1989 p 65-68 (For primary document see N91-10556 01-51)
Avail: NTIS HC/MF A03

**N91-10563#** Joint Publications Research Service, Arlington, VA.
**COMBINED EFFECTS OF ELEVATED CONCENTRATIONS OF CARBON DIOXIDE AND AMBIENT TEMPERATURE ON THERMAL STATE OF HUMANS IN CLOSED CHAMBERS Abstract Only**
A. V. Sosnovskiy *In its* JPRS Report: Science and Technology. USSR: Life Sciences 16 Jul. 1990 p 2 Transl. into ENGLISH from Kosmicheskaya Biologiya i Aviakosmicheskaya Meditsina (Moscow, USSR), v. 23, no. 3, May - Jun. 1989 p 89-90 (For primary document see N91-10556 01-51)
Avail: NTIS HC/MF A03

**N91-10566#** Joint Publications Research Service, Arlington, VA.
**REQUIREMENTS FOR AN IDEAL DRUG FOR PREVENTING SPACE MOTION SICKNESS**
N. N. Karkishchenko *In its* JPRS Report: Science and Technology. USSR: Life Sciences 11 Jul. 1990 p 1-3 Transl. into ENGLISH from Kosmicheskaya Biologiya I Aviakosmicheskaya Meditsina, Moscow (USSR), v. 23, no. 6 Nov. - Dec. 1989 p 33-36 (For primary document see N91-10565 01-51)
Avail: NTIS HC/MF A03

**N91-10567#** Joint Publications Research Service, Arlington, VA.
**EFFECT OF SINGLE IMPACTS OF HEAVY IONS OF GALACTIC COSMIC RAYS ON LACTUCA SATIVA SEEDS EXPOSED ON SALYUT-6 AND SALYUT-7 STATIONS**
L. V. Nevzgodina, Ye. N. Maksimova, and Ye. V. Kaminskaya *In its* JPRS Report: Science and Technology. USSR: Life Sciences 11 Jul. 1990 p 3-7 Transl. into ENGLISH from Kosmicheskaya Biologiya I Aviakosmicheskaya Meditsina, Moscow (USSR), v. 23, no. 6, Nov. - Dec. 1989 p 66-70 (For primary document see N91-10565 01-51)
Avail: NTIS HC/MF A03

## 53 BEHAVIORAL SCIENCES

Includes psychological factors; individual and group behavior; crew training and evaluation; and psychiatric research.

**N91-10595*#** Houston Univ., TX. Dept. of Psychology.
**THE EFFECTS OF OUTCOME AND PROCESS FEEDBACK**
Debra Steele Johnson 25 Oct. 1990 82 p
(Grant NAG9-398)
(NASA-CR-187332; NAS 1.26:187332) Avail: NTIS HC/MF A05 CSCL 05I

A study was conducted to examine the effects of process and outcome feedback on performance during a skill acquisition phase and a transfer test phase. The research also examined the role of two moderators: self-efficacy and intrinsic motivation. Subjects were college students participating for course credit. The task involved using a computerized simulation of the Space Shuttle's Remote Manipulation System (RMS). Results provided evidence of the beneficial effects of process feedback during skill acquisition. Results also provided evidence that self-efficacy and intrinsic motivation moderate the effects of feedback type on performance. Author

**N91-10564#** Joint Publications Research Service, Arlington, VA.
**PSYCHOPHYSIOLOGICAL ASSESSMENT OF PILOTING MOTOR HABITS IN PILOT RETRAINING Abstract Only**
N. N. Frolov and A. S. Kuzmin *In its* JPRS Report: Science and Technology. USSR: Life Sciences 16 Jul. 1990 p 2 Transl into ENGLISH from Voyenno-Meditsinskiy (Moscow, USSR), no. 1, Jan. 1989 p 54-57 (For primary document see N91-10556 01-51)
Avail: NTIS HC/MF A03

## 54 MAN/SYSTEM TECHNOLOGY AND LIFE SUPPORT

Includes human engineering; biotechnology; and space suits and protective clothing.

For related information see also *16 Space Transportation.*

**N91-10596#** Technische Univ., Delft (Netherlands).
**TECHNIQUE FOR HUMAN-ERROR SEQUENCE IDENTIFICATION AND SIGNIFICATION Ph.D. Thesis**
Gerben Heslinga 1988 161 p Submitted for publication Sponsored by Dutch Electricity Supply Companies, Arnhem, Netherlands
(ISBN-90-353-10144; ETN-90-97757) Avail: NTIS HC/MF A08

The human factor influence on the safety of complex installations was addressed. An event tree technique was adapted to the study: Technique for Human Error Sequence Identification and Signification (THESIS). The THESIS event trees, appear to present problems if they are applied to human performance instead of technical systems. These problems, referred to as the 'man-related features' of THESIS, are: the human capability to choose among several procedures, the ergonomics of the panel layout, human actions of a continuous nature, dependence between human errors, human capability to recover possible errors, the influence of memory during the recovery attempt, variability in human performance and correlations between human error probabilities. The influence of these problems on the applicability of THESIS was assessed by means of mathematical analyses, field studies and laboratory experiments. The main conclusion is that, with certain limitations, event trees can be used to predict sequences of human errors if procedural actions are performed. ESA

**N91-10597#** Universiteit Twente, Enschede (Netherlands).
**MODELS OF THE HUMAN OBSERVER AND CONTROLLER OF A DYNAMIC SYSTEM Ph.D. Thesis**
Paulus Heinrich Wewerinke 1989 205 p
(ETN-90-97759) Avail: NTIS HC/MF A10

Human functioning and its interaction with a dynamic system are studied. The total Man Machine System (MMS) is described in precise terms resulting in mathematical models. By comparing model results with results of experiments, the correspondence of the models with reality is investigated. Models relating to the human observer and controller, human regulator control, visual scene perception and the human observer and decision maker are described. Detailed conclusions and recommendations for future work are given. ESA

## 55 SPACE BIOLOGY

Includes exobiology; planetary biology; and extraterrestrial life.

No abstracts in this category.

## 59 MATHEMATICAL AND COMPUTER SCIENCES (GENERAL)

**N91-10598#** National Academy of Sciences - National Research Council, Washington, DC. Board on Mathematical Sciences.
**[ACTIVITIES OF THE BOARD ON MATHEMATICAL SCIENCES] Annual Report**
1990 13 p
(Contract DE-FG05-89ER-25080)
(DE90-015118; DOE/ER-25080/1) Avail: NTIS HC/MF A03

The DOE and other member agencies of the Interagency Committee on Extramural Mathematics Programs (ICEMAP) established levels of total ICEMAP core support for the Board over the referenced three-year period and corresponding levels of total support and support by year from the six participating ICEMAP agencies (AFOSR, ARO, DOE, NSA, NSF, and ONR). The amount requested herein and the activities proposed for the coming second year of support correspond to those set in 1989 during deliberations on the three-year proposal. As this request is for the second year of funding for activities covered by a three-year proposal and award, this report is limited to an update of progress over the first year and plans for the second year. As the original proposal provided a progress report through calendar year 1988 and plans for calendar year 1989, the progress is presented for 1989 to March 1990, and plans for 1990 to 1991. The Board, with its committees and panels, expended considerable energy along several fronts in 1989. This will result in the release of 18 publications, in addition to the anticipated start-up of five new studies leading to reports. DOE

**N91-10599*#** Institute for Computer Applications in Science and Engineering, Hampton, VA.
**A MANUAL FOR PARTI RUNTIME PRIMITIVES Interim Report**
Harry Berryman and Joel Saltz (Yale Univ., New Haven, CT.) Sep. 1990 27 p

(Contract NAS1-18605; NSF ASC-88-19374)
(NASA-CR-187442; NAS 1.26:187442; ICASE-IR-13) Avail: NTIS HC/MF A03 CSCL 12A

Primitives are presented that are designed to help users efficiently program irregular problems (e.g., unstructured mesh sweeps, sparse matrix codes, adaptive mesh partial differential equations solvers) on distributed memory machines. These primitives are also designed for use in compilers for distributed memory multiprocessors. Communications patterns are captured at runtime, and the appropriate send and receive messages are automatically generated. Author

**N91-10600*#** Institute for Computer Applications in Science and Engineering, Hampton, VA.
**MULTIPROCESSORS AND RUNTIME COMPILATION Final Report**
Joel Saltz, Harry Berryman, and Janet Wu Sep. 1990 24 p
Submitted for publication
(Contract NAS1-18605)
(NASA-CR-182100; ICASE-90-59; NAS 1.26:182100) Avail: NTIS HC/MF A03 CSCL 12A

Runtime preprocessing plays a major role in many efficient algorithms in computer science, as well as playing an important role in exploiting multiprocessor architectures. Examples are given that elucidate the importance of runtime preprocessing and show how these optimizations can be integrated into compilers. To support the arguments, transformations implemented in prototype multiprocessor compilers are described and benchmarks from the iPSC2/860, the CM-2, and the Encore Multimax/320 are presented. Author

## 60 COMPUTER OPERATIONS AND HARDWARE

Includes hardware for computer graphics, firmware, and data processing.

For components see *33 Electronics and Electrical Engineering.*

**N91-10601** National Aerospace Lab., Tokyo (Japan).
**ARCHITECTURE SIMULATOR OF PARALLEL COMPUTER [HEIRETSU KEISANKI NO AKITEKUCHA SHIMYURETA]**
Koichi Harada Mar. 1988 18 p In JAPANESE
(NAL-TM-583; ISSN-0452-2982; JTN-90-80011) Avail: NTIS HC/MF A03

A parallel computer is assumed as one of the future-oriented computer models. To prove its usefulness for clarifying the physical and engineering phenomena in aerospace, an architecture simulator is used which simulates movements of a parallel computer to verify the state of competition in the demand for reading/writing and the operation condition of the arithmetic operating unit and to evaluate the capacity of the computer. The architecture to be used in the project is presented. NASDA

**N91-10602#** Department of Energy, Washington, DC.
**MULTIPLE CHANNEL PROGRAMMABLE COINCIDENCE COUNTER Patent Application**
Gaetano J. Arnone, inventor (to DOE) (Los Alamos National Lab., NM.) 27 Feb. 1989 20 p
(Contract W-7405-eng-36)
(DE90-014681; US-Patent-Appl-SN-315871; Patents-US-A7315871) Avail: NTIS HC/MF A03

A programmable digital coincidence counter having multiple channels and featuring minimal dead time is disclosed. Neutron detectors supply electrical pulses to a synchronizing circuit which in turn inputs derandomized pulses to an adding circuit. A random access memory circuit connected as a programmable length shift register receives and shifts the sum of the pulses, and outputs to a serializer. A counter is input by the adding circuit and downcounted by the serializer, one pulse at a time. The decoded contents of the counter after each decrement is output to scalers. DOE

**N91-10603#** Argonne National Lab., IL.
**ULTRA-THIN VERTICAL MAGNETO-OPTICAL MEDIA AND SYSTEM FOR USING SAME Patent Application**
Samuel D. Bader, inventor (to DOE) and Chian Liu, inventor (to DOE) 26 May 1989 25 p
(Contract W-31-109-eng-38)
(DE90-014589; US-Patent-Appl-SN-357246; Patents-US-A7357246) Avail: NTIS HC/MF A03

A high density information storage medium utilizing the properties of an ultrathin film was invented. The present invention includes an information storage medium comprised of an ultrathin film capable of possessing vertical magnetic orientation. The present invention also includes methods for the storage, retrieval of and erasure of data on the ultrathin film medium utilizes the temperature dependent magnetic coercivity of the ultrathin film medium. The retrieval of information from the ultrathin film medium is based on the Kerr effect property of the ultrathin film and employs detection of the rotation of a beam of polarized light. The invention also includes the beneficial utilization of the reflection of the laser from the underlying metallic substrate back through the magnetic film to enhance the rotation and reflectivity characteristics of the signal. DOE

**N91-10357#** Meteorological Satellite Center, Tokyo (Japan).
**COMPUTER SYSTEM**
Shigenori Naito *In its* Meteorological Satellite Center Technical Note. Special Issue (1989). Summary of GMS System. 2: Data Processing Mar. 1989 p 1-35 In JAPANESE; ENGLISH summary (For primary document see N91-10356 01-42)
Avail: NTIS HC/MF A08

**N91-10358#** Meteorological Satellite Center, Tokyo (Japan).
**GENERAL FLOW OF IMAGE DATA PROCESSING**
Taichi Takahashi *In its* Meteorological Satellite Center Technical Note. Special Issue (1989). Summary of GMS System. 2: Data Processing Mar. 1989 p 37-38 In JAPANESE; ENGLISH summary (For primary document see N91-10356 01-42)
Avail: NTIS HC/MF A08

## 61 COMPUTER PROGRAMMING AND SOFTWARE

Includes computer programs, routines, alogorithms, and specific applications, e.g., CAD/CAM.

**N91-10604** National Aerospace Lab., Tokyo (Japan).
**FUNCTION LIBRARY USING APL FOR TIME SERIES ANALYSIS AND SYSTEM IDENTIFICATION IN STRUCTURES [KOUZOUBUTSU NO JIKEIRETSU BUNSEKI TO SHISUTEMU DOUTEI NO TAMENOEI PI ERU NIYORU KANSUU RAIBURARI]**
Keiji Komatsu Nov. 1987 31 p In JAPANESE
(NAL-TM-578; ISSN-0452-2982; JTN-90-80006) Avail: NTIS HC/MF A03

The influence of the digital signal processing technology on the theoretical and experimetal aspects of the study on dynamic characteristics is becoming stronger day by day.The National Aerospace Laboratory (NAL) in these circumstances has written down and completed a basic library which makes it possible to easily conduct a time series analysis of structures and a numerical simulation with a fixed system using the programming language APL. APL was adopted since it has for its proceeding basis an array of interpreting methods capable of interactively executing a simulation and using a subroutine structure with the help of a functional language, which is characterized by the possibility of a clarifying algorithm with the aid of a short program list adapted to a time series handling. The beta method of Newmark is explained for the preparation of time series data on a structure, the program for plate bending, and three-dimensional beam by finite element method which forms its basis for inputting, the occurrence of M-series as external forces and the program for generating a random wave by combining sinus curves as external force and noise. In addition, the power spectrum/frequency response function is explained with FFT as a basis. The low-pass, high-pass and bandpass digital filter; the autocorrelation function; the spectral analysis by maximum entrop method; and the program for free attenuation wave extraction from random data by random deck are explained. NASDA

**N91-10605** National Aerospace Lab., Tokyo (Japan).
**SOFTWARE PACKAGE FOR 2-DIMENSIONAL GRAPHIC DISPLAY UNIT [NIJIGEN GURAFIKKU DISUPUREI SOUCHI YOU SOFUTO UEA PAKKEJI]**
Kazuyo Suematsu and Toshio Isobe Jun. 1988 39 p In JAPANESE
(NAL-TM-589; ISSN-0452-2982; JTN-90-80016) Avail: NTIS HC/MF A03

In the National Aerospace Laboratory's NS system, some graphics processers are introduced. In order to assist in the use of those processors, graphics output libraries are provided in each processor. The user must learn those graphic output libraries for the various function of the processors and develop a drawing program for each piece of equipment used. In order to decrease the user's burden and to assist in the development efficiency of numerical simulation programs, the original library, the GCP library, was developed and improved. The functions of the software package and the program structure are explained in detail. NASDA

**N91-10606*#** National Aeronautics and Space Administration. Goddard Space Flight Center, Greenbelt, MD.
**PROCEEDINGS OF THE THIRTEENTH ANNUAL SOFTWARE ENGINEERING WORKSHOP**
Nov. 1988 363 p Workshop held in Greenbelt, MD, 30 Nov. 1988
(NASA-TM-103314; SEL-88-004; NAS 1.15:103314) Avail: NTIS HC/MF A16 CSCL 09B

Topics covered in the workshop included studies and experiments conducted in the Software Engineering Laboratory (SEL), a cooperative effort of NASA Goddard Space Flight Center, the University of Maryland, and Computer Sciences Corporation; software models; software products; and software tools. For individual titles, see N91-10607 through N91-10617.

**N91-10607*#** National Aeronautics and Space Administration. Goddard Space Flight Center, Greenbelt, MD.
**EVOLVING IMPACT OF Ada ON A PRODUCTION SOFTWARE ENVIRONMENT**
F. McGarry, L. Esker, and K. Quimby (Computer Sciences Corp., Greenbelt, MD.) *In its* Proceedings of the Thirteenth Annual Software Engineering Workshop Nov. 1988 31 p (For primary document see N91-10606 01-61)
Avail: NTIS HC/MF A16 CSCL 09B

Many aspects of software development with Ada have evolved as our Ada development environment has matured and personnel have become more experienced in the use of Ada. The Software Engineering Laboratory (SEL) has seen differences in the areas of cost, reliability, reuse, size, and use of Ada features. A first Ada project can be expected to cost about 30 percent more than an equivalent FORTRAN project. However, the SEL has observed significant improvements over time as a development environment progresses to second and third uses of Ada. The reliability of Ada projects is initially similar to what is expected in a mature FORTRAN environment. However, with time, one can expect to gain improvements as experience with the language increases. Reuse is one of the most promising aspects of Ada. The proportion of reusable Ada software on our Ada projects exceeds the proportion of reusable FORTRAN software on our FORTRAN projects. This result was noted fairly early in our Ada projects, and experience shows an increasing trend over time. Author

**N91-10608*#** Maryland Univ., College Park. Inst. for Advanced Computer Studies.
**TOWARDS A COMPREHENSIVE FRAMEWORK FOR REUSE: A REUSE-ENABLING SOFTWARE EVOLUTION ENVIRONMENT**
V. R. Basili and H. D. Rombach *In* NASA, Goddard Space Flight Center, Proceedings of the Thirteenth Annual Software Engineering Workshop Nov. 1988 45 p (For primary document see N91-10606 01-61)
(Contracts NsG-5123; N00014-87-K-0307; DE-AC05-84OR-21400)
(UMIACS-TR-88-92; CS-TR-2158) Avail: NTIS HC/MF A16 CSCL 09B

Reuse of products, processes and knowledge will be the key to enable the software industry to achieve the dramatic improvement in productivity and quality required to satisfy the anticipated growing demand. Although experience shows that certain kinds of reuse can be successful, general success has been elusive. A software life-cycle technology which allows broad and extensive reuse could provide the means to achieving the desired order-of-magnitude improvements. The scope of a comprehensive framework for understanding, planning, evaluating and motivating reuse practices and the necessary research activities is outlined. As a first step towards such a framework, a reuse-enabling software evolution environment model is introduced which provides a basis for the effective recording of experience, the generalization and tailoring of experience, the formalization of experience, and the (re-)use of experience. Author

**N91-10609*#** National Aeronautics and Space Administration. Goddard Space Flight Center, Greenbelt, MD.
**THE SOFTWARE MANAGEMENT ENVIRONMENT (SME)**
Jon D. Valett, William Decker, and John Buell (Computer Sciences Corp., Greenbelt, MD.) *In its* Proceedings of the Thirteenth Annual Software Engineering Workshop Nov. 1988 20 p (For primary document see N91-10606 01-61)
Avail: NTIS HC/MF A16 CSCL 09B

The Software Management Environment (SME) is a research effort designed to utilize the past experiences and results of the Software Engineering Laboratory (SEL) and to incorporate this knowledge into a tool for managing projects. SME provides the software development manager with the ability to observe, compare, predict, analyze, and control key software development parameters such as effort, reliability, and resource utilization. The major components of the SME, the architecture of the system, and examples of the functionality of the tool are discussed. Author

**N91-10610*#** Jet Propulsion Lab., California Inst. of Tech., Pasadena.
**A COMMUNICATION CHANNEL MODEL OF THE SOFTWARE PROCESS**
Robert C. Tausworthe *In* NASA, Goddard Space Flight Center, Proceedings of the Thirteenth Annual Software Engineering Workshop Nov. 1988 40 p (For primary document see N91-10606 01-61)
Avail: NTIS HC/MF A16 CSCL 09B

Beginning research into a noisy communication channel analogy of software development process productivity, in order to establish quantifiable behavior and theoretical bounds is discussed. The analogy leads to a fundamental mathematical relationship between human productivity and the amount of information supplied by the developers, the capacity of the human channel for processing and transmitting information, the software product yield (object size) the work effort, requirements efficiency, tool and process efficiency, and programming environment advantage. An upper bound to productivity is derived that shows that software reuse is the only means that can lead to unbounded productivity growth; practical considerations of size and cost of reusable components may reduce this to a finite bound. Author

**N91-10611*#** International Business Machines Corp., Houston, TX.
**KNOWLEDGE-BASED ASSISTANCE IN COSTING THE SPACE STATION DMS**

Troy Henson and Kyle Rone *In* NASA, Goddard Space Flight Center, Proceedings of the Thirteenth Annual Software Engineering Workshop Nov. 1988 18 p (For primary document see N91-10606 01-61)
Avail: NTIS HC/MF A16 CSCL 09B

The Software Cost Engineering (SCE) methodology developed over the last two decades at IBM Systems Integration Division (SID) in Houston is utilized to cost the NASA Space Station Data Management System (DMS). An ongoing project to capture this methodology, which is built on a foundation of experiences and lessons learned, has resulted in the development of an internal-use-only, PC-based prototype that integrates algorithmic tools with knowledge-based decision support assistants. This prototype Software Cost Engineering Automation Tool (SCEAT) is being employed to assist in the DMS costing exercises. At the same time, DMS costing serves as a forcing function and provides a platform for the continuing, iterative development, calibration, and validation and verification of SCEAT. The data that forms the cost engineering database is derived from more than 15 years of development of NASA Space Shuttle software, ranging from low criticality, low complexity support tools to highly complex and highly critical onboard software. Author

**N91-10612*#** Martin Marietta Aerospace, Denver, CO. Astronautics Group.

**SOFTWARE SIZING, COST ESTIMATION AND SCHEDULING**

William G. Cheadle *In* NASA, Goddard Space Flight Center, Proceedings of the Thirteenth Annual Software Engineering Workshop Nov. 1988 28 p (For primary document see N91-10606 01-61)
Avail: NTIS HC/MF A16 CSCL 09B

The Technology Implementation and Support Section at Martin Marietta Astronautics Group Denver is tasked with software development analysis, data collection, software productivity improvement and developing and applying various computerized software tools and models. The computerized tools are parametric models that reflect actuals taken from the large data base of completed software development projects. Martin Marietta's data base consists of over 300 completed projects and hundreds of cost estimating relationships (CERs) that are used in sizing, costing, scheduling and productivity improvement equations, studies, models and computerized tools. Author

**N91-10613*#** Jet Propulsion Lab., California Inst. of Tech., Pasadena.

**Ada SOFTWARE PRODUCTIVITY PROTOTYPES: A CASE STUDY**

Jairus M. Hihn, Hamid Habib-agahi, and Shan Malhotra *In* NASA, Goddard Space Flight Center, Proceedings of the Thirteenth Annual Software Engineering Workshop Nov. 1988 31 p (For primary document see N91-10606 01-61)
Avail: NTIS HC/MF A16 CSCL 09B

A case study of the impact of Ada on a Command and Control project completed at the Jet Propulsion Laboratory (JPL) is given. The data for this study was collected as part of a general survey of software costs and productivity at JPL and other NASA sites. The task analyzed is a successful example of the use of rapid prototyping as applied to command and control for the U.S. Air Force and provides the U.S. Air Force Military Airlift Command with the ability to track aircraft, air crews and payloads worldwide. The task consists of a replicated database at several globally distributed sites. The local databases at each site can be updated within seconds after changes are entered at any one site. The system must be able to handle up to 400,000 activities per day. There are currently seven sites, each with a local area network of computers and a variety of user displays; the local area networks are tied together into a single wide area network. Using data obtained for eight modules, totaling approximately 500,000 source lines of code, researchers analyze the differences in productivities between subtasks. Factors considered are percentage of Ada used in coding, years of programmer experience, and the use of Ada tools and modern programming practices. The principle findings are the following. Productivity is very sensitive to programmer experience. The use of Ada software tools and the use of modern programming practices are important; without such use Ada is just a large complex language which can cause productivity to decrease. The impact of Ada on development effort phases is consistent with earlier reports at the project level but not at the module level. Author

**N91-10614*#** Martin Marietta Aerospace, Denver, CO. Astronautics Group.

**EXPERIENCES WITH Ada IN AN EMBEDDED SYSTEM**

Robert J. LaBaugh *In* NASA, Goddard Space Flight Center, Proceedings of the Thirteenth Annual Software Engineering Workshop Nov. 1988 18 p (For primary document see N91-10606 01-61)
Avail: NTIS HC/MF A16 CSCL 09B

Recent experiences with using Ada in a real time environment are described. The application was the control system for an experimental robotic arm. The objectives of the effort were to experiment with developing embedded applications in Ada, evaluating the suitability of the language for the application, and determining the performance of the system. Additional objectives were to develop a control system based on the NASA/NBS Standard Reference Model for Telerobot Control System Architecture (NASREM) in Ada, and to experiment with the control laws and how to incorporate them into the NASREM architecture. Author

**N91-10615*#** Unisys Corp., Houston, TX. Operations Div.

**A PRACTICAL APPROACH TO OBJECT BASED REQUIREMENTS ANALYSIS**

Daniel W. Drew and Michael Bishop *In* NASA, Goddard Space Flight Center, Proceedings of the Thirteenth Annual Software Engineering Workshop Nov. 1988 30 p (For primary document see N91-10606 01-61)
Avail: NTIS HC/MF A16 CSCL 09B

Presented here is an approach developed at the Unisys Houston Operation Division, which supports the early identification of objects. This domain oriented analysis and development concept is based on entity relationship modeling and object data flow diagrams. These modeling techniques, based on the GOOD methodology developed at the Goddard Space Flight Center, support the translation of requirements into objects which represent the real-world problem domain. The goal is to establish a solid foundation of understanding before design begins, thereby giving greater assurance that the system will do what is desired by the customer. The transition from requirements to object oriented design is also promoted by having requirements described in terms of objects. Presented is a five step process by which objects are identified from the requirements to create a problem definition model. This process involves establishing a base line requirements list from which an object data flow diagram can be created. Entity-relationship modeling is used to facilitate the identification of objects from the requirements. An example is given of how semantic modeling may be used to improve the entity-relationship model and a brief discussion on how this approach might be used in a large scale development effort. Author

**N91-10616*#** General Electric Co., Philadelphia, PA. Ada Core Team.

**A MODERNIZED PDL APPROACH FOR Ada SOFTWARE DEVELOPMENT**

Paul Usavage, Jr. *In* NASA, Goddard Space Flight Center, Proceedings of the Thirteenth Annual Software Engineering Workshop Nov. 1988 21 p (For primary document see N91-10606 01-61)
Avail: NTIS HC/MF A16 CSCL 09B

The desire to integrate newly available, graphically-oriented Computed Aided Software Engineering (CASE) tools with existing software design approaches is changing the way Program Design Language (PDL) or Process Description Language is used for large system development. In the approach documented here, Software Engineers use graphics tools to model the problem and to describe high level software design in diagrams. An Ada-based PDL is used to document low level design. Some results are provided along with an analysis for each of three smaller General Electric (GE) Ada development projects that utilized variations on this approach. Finally some considerations are identified for larger scale implementation. Author

**N91-10617*#** Software Development Concepts, MD.
**REPRESENTING OBJECT ORIENTED SPECIFICATIONS AND DESIGNS WITH EXTENDED DATA FLOW NOTATIONS**
Jon Franklin Buser and Paul T. Ward *In* NASA, Goddard Space Flight Center, Proceedings of the Thirteenth Annual Software Engineering Workshop Nov. 1988 20 p (For primary document see N91-10606 01-61)
Avail: NTIS HC/MF A16 CSCL 09B

The issue of using extended data flow notations to document object oriented designs and specifications is discussed. Extended data flow notations, for the purposes here, refer to notations that are based on the rules of Yourdon/DeMarco data flow analysis. The extensions include additional notation for representing real-time systems as well as some proposed extensions specific to object oriented development. Some advantages of data flow notations are stated. How data flow diagrams are used to represent software objects are investigated. Some problem areas with regard to using data flow notations for object oriented development are noted. Some initial solutions to these problems are proposed. Author

**N91-10618*#** Alabama Univ., Huntsville.
**NETWORK, SYSTEM, AND STATUS SOFTWARE ENHANCEMENTS FOR THE AUTONOMOUSLY MANAGED ELECTRICAL POWER SYSTEM BREADBOARD. VOLUME 1: PROJECT SUMMARY Research Report, Jun. 1988 - May 1990**
James W. McKee 1990 19 p
(Grant NAG8-720)
(NASA-CR-185880; NAS 1.26:185880; Rept-90-18-Vol-1) Avail: NTIS HC/MF A03 CSCL 09B

This volume (1 of 4) gives a summary of the original AMPS software system configuration, points out some of the problem areas in the original software design that this project is to address, and in the appendix collects all the bimonthly status reports. The purpose of AMPS is to provide a self reliant system to control the generation and distribution of power in the space station. The software in the AMPS breadboard can be divided into three levels: the operating environment software, the protocol software, and the station specific software. This project deals only with the operating environment software and the protocol software. The present station specific software will not change except as necessary to conform to new data formats. E.R.

**N91-10619*#** Alabama Univ., Huntsville.
**NETWORK, SYSTEM, AND STATUS SOFTWARE ENHANCEMENTS FOR THE AUTONOMOUSLY MANAGED ELECTRICAL POWER SYSTEM BREADBOARD. VOLUME 2: PROTOCOL SPECIFICATION Research Report, Jun. 1988 - May 1990**
James W. McKee 1990 119 p
(Grant NAG8-720)
(NASA-CR-185881; NAS 1.26:185881; Rept-90-18-Vol-2) Avail: NTIS HC/MF A06 CSCL 09B

This volume (2 of 4) contains the specification, structured flow charts, and code listing for the protocol. The purpose of an autonomous power system on a spacecraft is to relieve humans from having to continuously monitor and control the generation, storage, and distribution of power in the craft. This implies that algorithms will have been developed to monitor and control the power system. The power system will contain computers on which the algorithms run. There should be one control computer system that makes the high level decisions and sends commands to and receive data from the other distributed computers. This will require a communications network and an efficient protocol by which the computers will communicate. One of the major requirements on the protocol is that it be real time because of the need to control the power elements. E.R.

**N91-10620*#** Alabama Univ., Huntsville.
**NETWORK, SYSTEM, AND STATUS SOFTWARE ENHANCEMENTS FOR THE AUTONOMOUSLY MANAGED ELECTRICAL POWER SYSTEM BREADBOARD. VOLUME 3: COMMANDS SPECIFICATION Research Report, Jun. 1988 - May 1990**
James W. McKee 1990 15 p
(Grant NAG8-720)
(NASA-CR-185882; NAS 1.26:185882; Rept-90-18-Vol-3) Avail: NTIS HC/MF A03 CSCL 09B

This volume (3 of 4) contains the specification for the command language for the AMPS system. The volume contains a requirements specification for the operating system and commands and a design specification for the operating system and command. The operating system and commands sits on top of the protocol. The commands are an extension of the present set of AMPS commands in that the commands are more compact, allow multiple sub-commands to be bundled into one command, and have provisions for identifying the sender and the intended receiver. The commands make no change to the actual software that implement the commands. E.R.

**N91-10621*#** Alabama Univ., Huntsville.
**NETWORK, SYSTEM, AND STATUS SOFTWARE ENHANCEMENTS FOR THE AUTONOMOUSLY MANAGED ELECTRICAL POWER SYSTEM BREADBOARD. VOLUME 4: GRAPHICAL STATUS DISPLAY Research Report, Jun. 1988 - May 1990**
James W. McKee 1990 56 p
(Grant NAG8-720)
(NASA-CR-185879; NAS 1.26:185879; Rept-90-18-Vol-4) Avail: NTIS HC/MF A04 CSCL 09B

This volume (4 of 4) contains the description, structured flow charts, prints of the graphical displays, and source code to generate the displays for the AMPS graphical status system. The function of these displays is to present to the manager of the AMPS system a graphical status display with the hot boxes that allow the manager to get more detailed status on selected portions of the AMPS system. The development of the graphical displays is divided into two processes; the creation of the screen images and storage of them in files on the computer, and the running of the status program which uses the screen images. E.R.

**N91-10622#** National Oceanic and Atmospheric Administration, Boulder, CO. Wave Propagation Lab.
**CONVERTING FROM VMS TO ULTRIX**
M. K. Goldstein Feb. 1990 27 p
(PB90-220310; NOAA-TM-ERL-WPL-176) Avail: NTIS HC/MF A03 CSCL 09B

Over the next couple of years, Wave Propagation Laboratory (WPL) is making the transition from several different operating systems on its various platforms to UNIX, which is fast becoming the computer industry standard. The report records many of the tasks involved in converting from DEC's VMS (Virtual Memory System) operating system to ULTRIX on one of WPL's micro VAX's. It emphasizes the user's perspective and, thus, avoids most of the system-level work. It should, as a result, serve as a handy reference manual for those making the transition from VMS to ULTRIX. GRA

**N91-10623*#** Michigan Univ., Ann Arbor. Radiation Lab.
**USERS MANUAL FOR AUTOMESH-2D: A PROGRAM OF AUTOMATIC MESH GENERATION FOR TWO-DIMENSIONAL SCATTERING ANALYSIS BY THE FINITE ELEMENT METHOD**
Chongyu Hua and John L. Volakis 5 Aug. 1990 42 p
(Grant NAG2-541)
(NASA-CR-186929; NAS 1.26:186929; Rept-025921-15-T) Avail: NTIS HC/MF A03 CSCL 09B

AUTOMESH-2D is a computer program specifically designed as a preprocessor for the scattering analysis of two dimensional bodies by the finite element method. This program was developed due to a need for reproducing the effort required to define and check the geometry data, element topology, and material

properties. There are six modules in the program: (1) Parameter Specification; (2) Data Input; (3) Node Generation; (4) Element Generation; (5) Mesh Smoothing; and (5) Data File Generation.
Author

**N91-10624#** NSI Technology Services Corp., Corvallis, OR.
**CONFIDENCE INTERVALS AND CURVATURE MEASURES IN NONLINEAR REGRESSION USING THE IML AND NLIN PROCEDURES IN SAS(TM) SOFTWARE**
D. L. Kugler and E. H. Lee 1990 8 p Presented at the SAS(tm) Users Group International Conference, Nashville, TN, 1-4 Apr. 1990 Sponsored by Corvallis Environmental Research Lab.
(PB90-246398; EPA/600/D-90/077) Avail: NTIS HC/MF A02 CSCL 09B

Interval estimates for nonlinear parameters using the linear approximation are sensitive to parameter curvature effects. The adequacy of the linear approximation interval is determined using the nonlinearity measures of Bates and Watts, and Clarke, and the profile t plots of Bates and Watts. These curvature measures and profile t plot calculations are implemented using the SAS/IML and SAS/NLIN procedures. Author

**N91-10625#** National Aeronautical Lab., Bangalore (India). Structural Sciences Div.
**SCRIPT: GENERAL PURPOSE GRAPHICS PROGRAM; USER'S MANUAL**
G. A. Nirmala Apr. 1990 10 p
(PD-ST-9027) Avail: NTIS HC/MF A02

The user's manual to a general purpose graphics software program Script is presented. The main aim of developing this software is efficient documentation of results. With Script software it is possible to decide about the plot by looking at the screen. The changes could be made till the plot is satisfactory. The final plot then could be obtained on the plotter. Script is user interactive. Author

**N91-10626#** Lawrence Livermore National Lab., CA. Prompt Diagnostics Group.
**CVMAC 2D PROGRAM: A METHOD OF CONVERTING 3D TO 2D**
Joe Lown 20 Jun. 1990 14 p Presented at the 12th Annual International Computervision User Conference, Nashville, TN, 30 Sep. - 3 Oct. 1990
(Contract W-7405-eng-48)
(DE90-015147; UCRL-JC-104204; CONF-9009225-1) Avail: NTIS HC/MF A03

The user is presented with a method of converting a 3-D wire frame model into a technical illustration, detail, or assembly drawing. By using the 2D Program, entities can be mapped from 3-D model space into two-dimensional model space, as if they are being traced. Selected entities to be mapped can include circles, arcs, lines, and points. This program prompts the user to digitize the view to be mapped, specify the layers in which the new 2-D entities will reside, and select the entities, either by digitizing or windowing. The new 2-D entities are displayed in a small view which the program creates in the lower left corner of the drawing.
DOE

**N91-10627#** Finnish Academy of Technical Sciences, Helsinki.
**SOFTWARE INTEGRATION TECHNOLOGIES IN INDUSTRIAL APPLICATIONS Ph.D. Thesis - Helsinki Univ. of Technol.**
Tapani Savolainen (Hewlett-Packard Oy, Espoo, Finland ) 1990 129 p Sponsored in part by Helsinki Univ. of Technol., Finland; and CEE
(Ma-55; ISBN-951-666-304-4; ISSN-0355-2713; ETN-90-97631) Avail: NTIS HC/MF A07

Two CASE (Computer Assisted Software Engineering) tools for CIM (Computer Integrated Manufacturing) are defined: CIMVIEW for high level, functional, top-down integration, company specific analysis and modeling, and CIMGLUE for low level, bottom-up integration, interfacing of existing applications. A method, STIF, is defined for interface program design to reduce the need to change the interface during the normal evolution of the applications. In CIMVIEW the user builds interactively a SA/SD data flow model of the functions of the company being examined. CIMGLUE, is a general tool to build conversion programs between almost any software packages a and b. The conversion program is built interactively utilizing example of package a's output and package b's input. Both CIMGLUE and CIMVIEW tools are described generally for different types of implementations. A CIMVIEW prototype was implemented based on common lisp and common windows. In the STIF (Semantically Transparent Interfacing) method the variable definitions of transferred items are isolated as much outside the interface as possible instead of using cross references inside the interface. This is done by embedding some elements of the definition language of package 1 into the definition language of package 2. Two example cases in which the method was applied are described. The interfaces are in use in practical industrial applications. ESA

**N91-10628*#** Institute for Computer Applications in Science and Engineering, Hampton, VA.
**CONSERVATIVE PARALLEL SIMULATION OF PRIORITY CLASS QUEUEING NETWORKS Final Report**
David M. Nicol (College of William and Mary, Williamsburg, VA.) Sep. 1990 24 p Submitted for publication
(Contract NAS1-18605)
(NASA-CR-187438; ICASE-90-64; NAS 1.26:187438) Avail: NTIS HC/MF A03 CSCL 09B

A conservative synchronization protocol is described for the parallel simulation of queueing networks having C job priority classes, where a job's class is fixed. This problem has long vexed designers of conservative synchronization protocols because of its seemingly poor ability to compute lookahead: the time of the next departure. For, a job in service having low priority can be preempted at any time by an arrival having higher priority and an arbitrarily small service time. The solution is to skew the event generation activity so that the events for higher priority jobs are generated farther ahead in simulated time than lower priority jobs. Thus, when a lower priority job enters service for the first time, all the higher priority jobs that may preempt it are already known and the job's departure time can be exactly predicted. Finally, the protocol was analyzed and it was demonstrated that good performance can be expected on the simulation of large queueing networks. Author

**N91-10629*#** Institute for Computer Applications in Science and Engineering, Hampton, VA.
**A CONSERVATIVE APPROACH TO PARALLELIZING THE SHARKS WORLD SIMULATION Final Report**
David M. Nicol and Scott E. Riffe Oct. 1990 15 p Submitted for publication
(Contract NAS1-18605; NAG1-1060; NSF ASC-88-19373)
(NASA-CR-187440; NAS 1.26:187440; ICASE-90-67) Avail: NTIS HC/MF A03 CSCL 09B

Parallelizing a benchmark problem for parallel simulation, the Sharks World, is described. The described solution is conservative, in the sense that no state information is saved, and no 'rollbacks' occur. The used approach illustrates both the principal advantage and principal disadvantage of conservative parallel simulation. The advantage is that by exploiting lookahead an approach was found that dramatically improves the serial execution time, and also achieves excellent speedups. The disadvantage is that if the model rules are changed in such a way that the lookahead is destroyed, it is difficult to modify the solution to accommodate the changes.
Author

**N91-10630#** Sandia National Labs., Albuquerque, NM.
**SOFTWARE SAFETY WORKSHOP PROBLEM**
1990 7 p Presented at the Workshop on Design and Assurance for Software Safety, Las Cruces, NM, 16-18 Oct. 1990
(Contract DE-AC04-76DP-00789)
(DE90-016222; SAND-90-2255C; CONF-9010171-2) Avail: NTIS HC/MF A02

More than 20 years ago, a philosophy was developed for the design and analysis of hardware systems to ensure that they would perform in a predictably safe manner, even in severe abnormal environments. This philosophy has been scrutinized and tested during the intervening years, and has proved successful in practice. A requirement guiding the development of the philosophy was that the resulting design must be simple enough to be amenable to analysis. The inherent simplicity is a safety attribute, because complex analyses, such as those represented by fault trees containing hundreds of branches, are extremely susceptible to error. There are many examples where such errors led analysts to believe systems were safe when they were not, with disastrous consequences. The purpose of this workshop problem is to determine whether the principles developed to ensure hardware safety are applicable in any way to safety-critical software systems. It is possible that hardware associations with software will need to be considered, but whether or not this is true is left as an aspect of the investigation. In order to put the ground rules in perspective, it will be necessary to establish some framework. DOE

**N91-10631#** Pacific Northwest Lab., Richland, WA.
**A REPRESENTATION SCHEME FOR FAULT DIAGNOSIS**
Rex C. Stratton Jul. 1990 12 p Presented at the 8th AAAI '90 National Conference on Artificial Intelligence, Boston, MA, 17 Jul. - 3 Aug. 1990
(Contract DE-AC06-76RL-01830)
(DE90-016291; PNL-SA-18090; CONF-900793-4) Avail: NTIS HC/MF A03

Subsequent to developing the conceptual description of a intelligent software system a representation scheme is selected. The knowledge representation scheme constrains the way in which knowledge is represented and executed in a software system. The representation scheme consists of methods for writing down information, organizing information, controlling software execution, and performing inference. This paper discusses a knowledge representation scheme that we are developing for use in building intelligent systems that assist in physical system fault diagnosis. This scheme consists of function and object hierarchies, generalized inference methodologies, and a control scheme that allows for concurrent reasoning during fault diagnosis. DOE

**N91-10632#** Allied-Signal Aerospace Co., Kansas City, MO.
**BIDIRECTIONAL TRANSLATOR BETWEEN DXF AND IGES FORMATS Final Report**
J. R. Bradford Aug. 1990 46 p
(Contract DE-AC04-76DP-00613)
(DE90-016430; KCP-613-4172) Avail: NTIS HC/MF A03

Software was conceived that provided two-way CAD data exchange between AotCAD's DXF format and the IGES format. Obstacles were found with a newly emerging DXF format, and enhancements were added to accommodate multiple DXF forms. Successful code was written using the C programming language, thus providing portability to other hardware. Future enhancements to the code were identified. DOE

**N91-10633*#** Cornell Univ., Ithaca, NY. Dept. of Computer Science.
**DESIGNING APPLICATION SOFTWARE IN WIDE AREA NETWORK SETTINGS**
Mesaac Makpangou and Ken Birman Oct. 1990 27 p
(Contract NAG2-593; MDA972-88-C-0024)
(NASA-CR-187333; NAS 1.26:187333; TR-90-1165) Avail: NTIS HC/MF A03 CSCL 09B

Progress in methodologies for developing robust local area network software has not been matched by similar results for wide area settings. The design of application software spanning multiple local area environments is examined. For important classes of applications, simple design techniques are presented that yield fault tolerant wide area programs. An implementation of these techniques as a set of tools for use within the ISIS system is described. Author

**N91-10634#** Bertin et Cie., Plaisir (France).
**PROTHE: A SOFTWARE AS A HELP FOR THE STUDIES IN INDUSTRIAL THERMAL ENGINEERING [PROTHE: LOGICIEL D'AIDE A L'ETUDE EN THERMIQUE INDUSTRIELLE]**
P. Carette 25 Jan. 1990 9 p In FRENCH
(ETN-90-97582) Avail: NTIS HC/MF A02

The PROTHE software presented aims to give a data processing aid to the industry which provides a better management of their technical knowledge, and offers simultaneous good conditions for filing, accessing, consulting, and increasing the data base. It takes part in the dissemination of the results of scientific research within companies in the thermal engineering field. The data base is situated in the central part of the software. It is divided into libraries, each of them being dedicated to a specific technical theme. The industry will also be able to acquire libraries prepared by scientific bodies, such as laboratories and technical centers. Such a library is being developed under the theme of heat exchange thermal engineering. ESA

**N91-10635#** Center for Mathematics and Computer Science, Amsterdam (Netherlands). Dept. of Operations Research, Statistics, and System Theory.
**OPTIMIZATION OF POLLING SYSTEMS**
O. J. Boxma, H. Levy, and J. A. Westrate (Tiburg Univ., Netherlands) Dec. 1989 20 p
(CWI-BS-R8932; ETN-90-97665) Copyright Avail: NTIS HC/MF A03

The issue of deriving efficient operational rules for polling systems with switch-over periods is addressed. The static optimization problem of determining the server visit order (polling table) that minimizes the mean total workload is studied. This problem is strongly related with, and in many applications coincides with, that of minimizing the overall mean customer delay in the system. A heuristic approach to the polling table problem is presented, using the exact solution of a related problem, specifically that of determining those server routing probabilities in a random polling system, that lead to the minimal mean total workload. Numerical experiments show that this heuristic approach yields excellent results. ESA

**N91-10636#** Technische Univ., Delft (Netherlands). Faculty of Technical Mathematics and Informatics.
**A POTENTIAL REDUCTION METHOD FOR A CLASS OF SMOOTH CONVEX PROGRAMMING PROBLEMS**
D. denHertog, C. Roos, and T. Terlaky (Eoetvoes Lorand Univ., Budapest, Hungary ) 9 Jan. 1990 26 p
(Rept-90-01; ISSN-0922-5641; ETN-90-97698) Copyright Avail: NTIS HC/MF A03

A potential reduction method for smooth convex programming is proposed. It is assumed that the objective and constraint functions fulfill the so called relative Lipschitz condition, with Lipschitz constant M greater than 0. A great advantage of the method, above the existing path following methods, is that the steps can be made long by performing linesearches. In the method linesearches are done along the Newton direction with respect to a strictly convex potential function when far away from the central path. When sufficiently close to this path, a lower bound is updated for the optimal value. The number of iterations required by the algorithm to converge to an epsilon optimal solution 0((1+(M squared)) square root of(n)ln epsilon) or 0((1+(M squared)) n ln epsilon), dependent on the updating scheme for the lower bound. ESA

**N91-10637#** Technische Univ., Delft (Netherlands). Faculty of Technical Mathematics and Informatics.
**ON THE ROTATION INTERPOLATION AND ANIMATION PROBLEMS IN COMPUTER GRAPHICS**
J. E. Mebius 1990 18 p
(Rept-90-08; ISSN-0922-5641; ETN-90-97704) Copyright Avail: NTIS HC/MF A03

A new technique for performing three-dimensional rotation interpolation and animation is explained. Its advantages and disavantages are pointed out. The mathematics underlying three-dimensional rotations is presented as a piece of Lie group theory. Existing work is analyzed within this framework. ESA

**N91-10638#** Technische Univ., Delft (Netherlands). Faculty of Technical Mathematics and Informatics.

**AUTOMATED SUPPORT OF THE MODELLING PROCESS: A VIEW BASED ON EXPERIMENTS WITH EXPERT INFORMATION ENGINEERS**

G. M. Winters 1990 22 p Sponsored in part by Dutch User Group of Structured Development Methods; BSO, Rotterdam, Netherlands; Hightech Automation; Nixdorf Computer; and Unisys Corp.

(Rept-90-09; ISSN-0922-5641; ETN-90-97705) Copyright Avail: NTIS HC/MF A03

A trend can be discerned clearly indicating that today's developments in methodologies concentrate on an ongoing structuring and integration of modeling techniques. Automated support is the prime mover of this trend. An argument that a lack of explicit knowledge about the process of model construction has resulted in problems with computer aided software engineering tools concerning adequate support in the form of verification and navigation is given. Important aspects of the modeling process deduced from the analysis of experiments with expert information engineers are presented. Some of the important notions are strategy, refinement, division and integration as far as the process of model construction is concerned, and the notions of natural level of consistency and finer categorization of concepts as far as the model constructs themselves are concerned. An architecture of modeling support systems and a corresponding prototype, that are able to reflect the mentioned aspects of modeling processes, are described. ESA

**N91-10639#** Royal Signals and Radar Establishment, Malvern (England).

**SILAGE TO ELLA TRANSLATION**

M. G. Hill and E. V. Whiting Apr. 1990 25 p

(RSRE-Memo-4385; BR114304; ETN-90-97609) Copyright Avail: NTIS HC/MF A03

SILAGE is an applicative behavioral specification language especially suited for digital signal processing (DSP) applications. A study of the translation of SILAGE circuits to ELLA is carried out. The ELLA system is an integrated hardware design tool set, which comprises the ELLA language compiler, the ELLA application support environment, the ELLA simulator, and the ELLANET procedural interface. A series of ELLA macrofunctions which could be combined into a library for use in the translation of SILAGE circuits is outlined. ESA

**N91-10640#** Leiden Univ. (Netherlands). Div. of Applied Mathematics.

**DISCOUNTED DYNAMIC PROGRAMMING. PART 3: SUCCESSIVE APPROXIMATION**

A. Hordijk and L. C. M. Kallenberg Dec. 1989 26 p

(TW-89-14-Pt-3; ETN-90-97727) Avail: NTIS HC/MF A03

The Markov decision theory, with emphasis on theory and methods, was studied. In the method of successive approximation the value vector is approximated by a sequence which converges to it. A nearly optimal policy is determined. The algorithm is presented. Exclusion of suboptimal actions and advanced algorithms are considered. ESA

**N91-10641#** Leiden Univ. (Netherlands). Div. of Applied Mathematics.

**DISCOUNTED DYNAMIC PROGRAMMING. PART 4: ACCELERATED SUCCESSIVE APPROXIMATION**

A. Hordijk and L. C. M. Kallenberg Jan. 1990 35 p

(TW-90-03-Pt-4; ETN-90-97729) Avail: NTIS HC/MF A03

The Markov decision theory, with emphasis on theory and methods, was studied. Some variants of the successive approximation iterative procedure to solve the functional equation $Ux = x$ are discussed. The pre-Gauss-Seidel, Gauss-Seidel, and the successive over-relaxation techniques are presented and these variants are generalized by using stopping times. All variants are based on contraction mappings and may be considered as an acceleration of the basic algorithm. ESA

**N91-10642#** Leiden Univ. (Netherlands). Dept. of Mathematics and Computer Science.

**DISCOUNTED DYNAMIC PROGRAMMING. PART 5: MODIFIED POLICY ITERATION**

A. Hordijk and L. C. M. Kallenberg Jan. 1990 25 p

(TW-90-04-Pt-5; ETN-90-97730) Avail: NTIS HC/MF A03

The Markov decision theory, with emphasis on theory and methods was studied. An algorithm for policy improvement was discussed. The algorithm is presented. The convergence rate is examined and bounds on the value vector are given in order to exclude suboptimal actions. ESA

**N91-10643#** Universiteit Twente, Enschede (Netherlands). Tele-Informatics Group.

**TEST CASE DERIVATION FROM LOTOS SPECIFICATIONS**

Jan Tretmans Apr. 1990 17 p Sponsored by EEC and Netherlands Ministry of Education

(Memo-INF-90-21; ISSN-0923-1714; ETN-90-97731) Avail: NTIS HC/MF A03

Test cases are derived from LOTOS behavior expressions. Starting point is the conformance relation 'conf' and the related theory to derive canonical testers for testing conformance of implementations to specifications. This theory is applicable to formalisms that have labelled transition systems with internal steps as a model. The algorithm for the derivation of canonical testers was already applied to basic LOTOS. Here it is adapted in order to derive test cases from full LOTOS expressions, i.e., LOTOS expressions with data-value communication. In order to apply the derived algorithm, value communication is interpreted as infinite choice over all possible values of the communication. Examples of test cases for simple expressions are given, together with problems and (im)possibilities in this approach. ESA

**N91-10644#** Oxford Univ. (England). Dept. of Engineering Science.

**CASUAL EIGENVECTOR FUNCTION APPROXIMATIONS AND THE PROBLEM OF SCALING: AN ALGORITHM**

J. A. Rossiter and B. Kouvaritakis 3 Apr. 1990 19 p

(OUEL-1822/90; ETN-90-97920) Avail: NTIS HC/MF A03

Eigenvector scaling implies the existence of degrees of freedom in the power series approximations of the eigenvector and dual eigenvector functions of discrete time transfer function matrix. An earlier study gave consideration to the anticlockwise winding associated with anti-causality and proposed an algorithm which scaled eigenvectors with a view to reducing their anti-causal component. A different algorithm is proposed which, although still formulated in the frequency domain, places a direct penalty on the time domain anti-causal component of the eigenvector sequences and avoids some of the aliasing difficulties that could arise in connection with the earlier algorithm. The new algorithm also provides the systematic means of reducing the length of the causal component of the associated vector sequences and results in better eigenvector approximations, as illustrated by means of two numerical examples. ESA

**N91-10645#** Oxford Univ. (England). Dept. of Engineering Science.

**SOME DEFECTS IN FINITE-DIFFERENCE EDGE FINDERS**

Margaret M. Fleck 1990 27 p Sponsored by British Petroleum Co. Ltd.

(OUEL-1826/90; ETN-90-97923) Avail: NTIS HC/MF A03

A study of how performance of finite difference edge finders varies with which order differences they use and how they combine differences taken in different directions is presented. Five algorithms are considered: Canny's, Boie and Cox's, and three variations on Marr and Hildreth's. These algorithms were re-implemented using a uniform method of noise suppression and a uniform output representation. Small problems in the original designs or published descriptions are identified and repaired. All the algorithms produce artifacts on simple test patterns which contains features such as sharp corners, junctions, and intensity slopes. The artifacts include gaps in boundaries, spurious boundaries, and deformation of region shape. They also differ in their ability to distinguish faint features from noise. Differences not previously reported are described, previous discussion where it exits is collated and places where current beliefs may be inaccurate are identified. ESA

**N91-10646#** Oxford Univ. (England). Dept. of Engineering Science.
**MULTIPLE WIDTHS YIELD RELIABLE FINITE DIFFERENCES**
Margaret M. Fleck 1990 39 p Sponsored by British Petroleum Co. Ltd.
(OUEL-1827/90; ETN-90-97924) Avail: NTIS HC/MF A03

Algorithms for suppressing the effects of image noise on differences for edge finding and image description are addressed. The study proposes that finite differences be computed using a range of operator widths. Although narrow operators are best for describing detailed texture, wide operators report low amplitude responses more reliably. Thus, if wide operators are used to fill gaps in narrow operator responses, each operator can be restricted to report only statistically reliable responses without losing many real features. This sharply reduces the noise in the final output. Theoretical bounds on spurious responses in the finite difference outputs, given only weak assumptions about the signal and noise, are presented. The expected response of the edge finder to an ideal straight step edge is analyzed. These performance measures are compared to those for an algorithm based on smoothing and an algorithm that also considers the spatial structure of noise. Empirical results including measurements of noise in real camera images are presented. ESA

**N91-10647#** Rolls-Royce Ltd., Bristol (England).
**FULLY AUTOMATIC ANALYSIS IN AN INDUSTRIAL ENVIRONMENT**
I. Armstrong and T. Edmunds Derby, England 15 May 1989 12 p Presented at 2nd International Conference on Quality Assurance and Standards in Finite Elements Analysis, May 1989
(PNR-90722; ETN-90-97947) Copyright Avail: NTIS HC/MF A03

Part of the Computer Aided Engineering and Manufacturing (CAEM) project is described. The objective of CAEM is to halve the time between commitment to an engine and entry into service. A two dimensional automatic finite element analysis facility is described. This is designed to contribute to the CAEM project objective by reducing the elapsed time to perform a high quality finite element analysis of the circumferentially averaged response of main engine rotor systems. This allows these analyses to be performed earlier in a design's evolution and increases confidence in the design prior to commitment to manufacture. ESA

**N91-10359#** Meteorological Satellite Center, Tokyo (Japan).
**IMAGE MAPPING**
Mitsuo Nesasa *In its* Meteorological Satellite Center Technical Note. Special Issue (1989). Summary of GMS System. 2: Data Processing Mar. 1989 p 39-43 In JAPANESE; ENGLISH summary (For primary document see N91-10356 01-42)
Avail: NTIS HC/MF A08

**N91-10360#** Meteorological Satellite Center, Tokyo (Japan).
**CALIBRATION**
Masayuki Sasaki *In its* Meteorological Satellite Center Technical Note. Special Issue (1989). Summary of GMS System. 2: Data Processing Mar. 1989 p 45-51 In JAPANESE; ENGLISH summary (For primary document see N91-10356 01-42)
Avail: NTIS HC/MF A08

**N91-10363#** Meteorological Satellite Center, Tokyo (Japan).
**ISCCP DATA PROCESSING**
Saya Kondo *In its* Meteorological Satellite Center Technical Note. Special Issue (1989). Summary of GMS System. 2: Data Processing Mar. 1989 p 75-78 In JAPANESE; ENGLISH summary Original contains color illustrations (For primary document see N91-10356 01-42)
Avail: NTIS HC/MF A08

**N91-10364#** Meteorological Satellite Center, Tokyo (Japan).
**PRE-PROCESSING OF IMAGE DATA**
Shinichi Miyatake and Takashi Ohshima *In its* Meteorological Satellite Center Technical Note. Special Issue (1989). Summary of GMS System. 2: Data Processing Mar. 1989 p 79-83 In JAPANESE; ENGLISH summary (For primary document see N91-10356 01-42)
Avail: NTIS HC/MF A08

**N91-10375#** Meteorological Satellite Center, Tokyo (Japan).
**DCP DATA PROCESSING**
Motoyasu Satoh *In its* Meteorological Satellite Center Technical Note. Special Issue (1989). Summary of GMS System. 2: Data Processing Mar. 1989 p 165-176 In JAPANESE; ENGLISH summary (For primary document see N91-10356 01-42)
Avail: NTIS HC/MF A08

## 62 COMPUTER SYSTEMS

Includes computer networks and special application computer systems.

**N91-10648#** Department of Energy, Washington, DC.
**MASSIVELY PARALLEL COMPUTING SYSTEM Patent Application**
Robert E. Benner, inventor (to DOE), John L. Gustafson, inventor (to DOE), and Gary R. Montry, inventor (to DOE) (Sandia National Labs., Albuquerque, NM.) 1 Mar. 1989 57 p
(Contract DE-AC04-76DP-00789)
(DE90-014683; US-Patent-Appl-SN-317389; Patents-US-A7317389) Avail: NTIS HC/MF A04

A parallel computing system and method having improved performance is disclosed. A program is concurrently run on a plurality of nodes for reducing total processing time, each node having a processor, a memory, and a predetermined number of communication channels connected to the node and independently connected directly to other nodes. The present invention improves performance of the parallel computing system by providing a system which can provide efficient communication between the processors and between the system and input and output devices. A method is also disclosed which can locate defective nodes with the computing system. DOE

**N91-10649#** Sandia National Labs., Albuquerque, NM.
**PERFORMANCE AND OPERATIONAL CHARACTERISTICS OF A FIBER DISTRIBUTED DATA INTERFACE (FDDI) RING**
Nicholas Testi and Steven A. Gossage 1990 27 p Presented at the 23d NEXUS Conference, Orlando, FL, 11-14 Sep. 1990
(Contract DE-AC04-76DP-00789)
(DE90-016103; SAND-90-2066C; CONF-9009232-2) Avail: NTIS HC/MF A03

Sandia National Laboratories is in the process of upgrading the Central Computing Network, which is a large heterogeneous network providing scientific computing, file storage, output services, and remote access to network resources. The migration from the present HYPERchannel-50 technology to HYPERchannel-100 is currently in progress and plans to migrate to the Fiber Distributed Data Interface (FDDI) token ring architecture are being considered. A migration from a variety of proprietary protocols to a primarily TCP/IP environment is also in progress. In order to test the feasibility of the Network Systems Corporation FDDI technology platform, two test rings were constructed. Ring A consists of nine dual attached Data Exchange Units (DXUs) and ring B consists of two dual attached DXUs. The rings are linked together using N715 DXUs. Other DXU models (with associated host computers where applicable) include N130s, an N220, N400s, and FE640 IP routers. Test data on fault isolation and recovery mechanisms, performance, IP routing (within and between rings), and monitor capabilities is presented. Interoperability data based on tests between DXUs and Sun FDDI workstations is also presented. DOE

**N91-10650#** Lawrence Livermore National Lab., CA.
**WORKSHOP ON MASSIVELY PARALLEL COMPUTING IN MAGNETIC FUSION ENERGY**
A. A. Mirin, comp. Aug. 1990 28 p Workshop held in Williamsburg, VA, 25-26 Apr. 1990
(Contract W-7405-eng-48)
(DE90-018009; UCRL-JC-104774; CONF-9004240-Summ) Avail: NTIS HC/MF A03

This paper discusses the following topics: Parallel computing at Oak Ridge National Laboratory (ORNL); massive parallelization of fluid plasma turbulence computations; a parallel implementation of the reduced MHD equations; massively parallel Fokker-Planck calculations; massively parallel Fokker-Planck calculations via Monte-Carlo; gyrokinetic calculations on the connection machine; a parallel 2D electrostatic PIC code for the Mark III Hypercube; particle simulation on the NCUBE concurrent multiprocessor; gyrokinetic simulations on massively parallel computers; and, numerical study of collisionless magnetic reconnection on the connection machine. DOE

**N91-10651#** Technische Univ., Delft (Netherlands). Faculty of Technical Mathematics and Informatics.
**LABELING PROBLEMS IN TRUTH MAINTENANCE SYSTEMS**
Cees Witteveen and Luc Stakenborg 1989 27 p
(Rept-89-90; ISSN-0922-5641; ETN-90-97697) Copyright Avail: NTIS HC/MF A03

Along with a new and simple NP-completeness proof of the general labeling problem for Truth Maintenance Systems (TMS), some special cases are discussed and some methods to determine an upperbound for the possible number of labelings for a given TMS are given. Efficient algorithms to estimate this number are used and these algorithms are expected to be used in relabeling TMS networks. ESA

**N91-10652#** Institut National Polytechnique, Grenoble (France). Lab. d'Informatique Fondamentale et d'Intelligence Artificielle.
**PARALLEL INFERENCE AND COMMUNICATION PROCESS FOR HORN CLAUSE. FIRST ORDER EXTENSION BY CONNECTION METHOD Ph.D. Thesis [INFERENCE PARELLELE ET PROCESSUS COMMUNICANTS POUR LES CLAUSES DE HORN. EXTENSION AU PREMIER ORDRE PAR LA METHODE DE CONNEXION]**
Maria-Blanca Ibanez-Espiga 1990 253 p In FRENCH; ENGLISH summary Sponsored by CROUS, France and CONICIT, Venezuela
(ETN-90-97825) Avail: NTIS HC/MF A12

An OR-parallel inference machine for Horn clause processing is described. This machine is formed by a network of processes ressembling the syntactic structure of the logic program and it uses resolution as its inference mechanism. The FP2 language is used for describing the machine. The communication capabilities of this language are applied for implementing the basic operation in inference: unification. When proving a Horn clause using resolution, the search space contains the axioms of the proof and the current resolvent. This search space is not enough when proving a first order logic formula using Bibel's connection method. At each step, the set of pairs of literals (connections) has to be resolved. This set is called the spanning set of connections. The specification of a correct method for calculating spanning sets of connections is presented. ESA

## 63 CYBERNETICS

Includes feedback and control theory, artificial intelligence, robotics and expert systems.

For related information see also *54 Man/System Technology and Life Support.*

**N91-10653#** Oak Ridge National Lab., TN.
**ARTIFICIAL INTELLIGENCE, HUMAN FACTORS, ROBOTICS, AND COMPUTER SIMULATION**
Philip F. Spelt Sep. 1990 22 p
(Contract DE-AC05-84OR-21400)
(DE90-016866; ORNL/FTR-3715) Avail: NTIS HC/MF A03

Traveler was invited to participate in information exchange between Oak Ridge National Laboratory (ORNL) and CISC/Japan Atomic Energy Research Institute (JAERI) on four topics: Artificial Intelligence, Human Factors, robotics, and computer simulation. This exchange took the form of 9 (2-hour) lectures presented by traveler on work done in CS and HF Group, and four presentations by Japanese for traveler's edification. Seven of traveler's lectures were to CISC/JAERI, one to Toshiba Corporation, and one to the AI Steering Committee of JAERI. There was also a presentation by Toshiba Corporation on high frequency work connected with their Boiling Water Reactor (BWR) control room. Final discussion between traveler and JAERI personnel concerned an umbrella agreement with the U.S. Department of Energy (DOE) permitting researcher exchange similar to nuclear researchers. Conclusions are: the U.S. has definite advantages in most areas of AI progress; the Japanese are creating a Monte Carlo radiation dose calculation simulation which will operate at the level of radiating particles (neutrons) with doses calculated for all major organ systems of humans, and major circuits for robots; they are gaining experience in creating major integrated simulations of human/robot activity in a nuclear reactor; and that it would be advantageous for us to have a formal agreement permitting scientists to visit there for more than 15 days at a time. DOE

**N91-10654#** Oxford Univ. (England). Robotics Research Group.
**IMAGE MOTION EXPERIMENTS WITH THE OXFORD AGV**
Barry Steer Aug. 1989 32 p Sponsored by Royal Armament Research and Development Establishment, Chetsey, England
(OUEL-1809/90; ETN-90-97918) Avail: NTIS HC/MF A03

The theory, hardware details, and experiments carried out with transputers controlling the motion of the Oxford AGV (a robotic rover type vehicle), and using Datacube image processing to acquire a sequence of images as the vehicle was moved at different speeds, are described. Techniques to interpret visual motion, including differential camera motion, widely separated views, integrating information along the camera path and techniques not requiring correspondence are reviewed. Basic equations describing optic flow are introduced. Results include an initial view from the vehicle, four translational sequences superimposed on the first frame, and each result shows image features trucked across the sequence when the camera was moved in a straight line. To minimize the effect of rotation the camera should be placed as far back towards the differential point consistent with preserving the required field of view. ESA

## 64 NUMERICAL ANALYSIS

Includes iteration, difference equations, and numerical approximation.

**N91-10655#** Sydney Univ. (Australia). School of Civil and Mining Engineering.
**SOME RECENT APPLICATIONS OF NUMERICAL METHODS TO GEOTECHNICAL ANALYSIS**
J. R. Booker, J. P. Carter, J. C. Small, P. T. Brown, and H. G. Poulos May 1989 37 p
(PB90-201229; R-598) Avail: NTIS HC/MF A03 CSCL 12A

In geotechnical engineering it is often important to take into account construction path, constitutive modelling and three dimensional effects. In such cases the use of the most complicated form of analysis may not be feasible and it is necessary to adopt simpler approaches which recognize the most important geotechnical aspects of the situation. GRA

**N91-10656#** International Centre for Theoretical Physics, Trieste (Italy).
**THE COUSIN PROBLEMS IN THE VIEWPOINT OF PARTIAL DIFFERENTIAL EQUATIONS**
Le Hung Son (Polytechnical Univ., Hanoi, Vietnam ) Jan. 1990 18 p Submitted for publication
(DE90-627172; IC-90/9) Avail: NTIS (US Sales Only) HC/MF A03

The Cousin problems for overdetermined systems of partial differential equations, which are generalizations of the Cauchy-Riemann system are considered. The general methods for solving these problems are given. Applying the given methods the Cousin problems are solved for many important systems in theoretical physics. DOE

**N91-10657#** International Centre for Theoretical Physics, Trieste (Italy).
**OPERATOR FORMALISM OF MULTI-POLE VIRASORO ALGEBRA ON RIEMANN SPHERE**
Zhe Chang, Han-Ying Guo, Jian-Min Shen, Shi-Kun Wang, Ke Wu (Academia Sinica, Beijing, China ), and Kei-Wen Xu Jan. 1990 11 p Prepared in cooperation with Zhejiang Univ., Peoples Rep. of China
(DE90-627217; IC-90/20) Avail: NTIS (US Sales Only) HC/MF A03

It is shown that the multi-pole Virasoro algebra on Riemann sphere can be obtained from operator product expansion of the stress-energy tensors in conformal field theory with modified definition of the vacua and other states and the BRST formalism of the algebra can also be constructed. The implications of the symmetry in string theory and in conformal theory are briefly mentioned. DOE

**N91-10658** Politecnico di Milano (Italy). Dipt. di Elettronica.
**TABU-SEARCH AND SIMULATED ANNEALING FOR THE QUADRATIC ASSIGNMENT PROBLEM [TABU-SEARCH E SIMULATED ANNEALING PER IL PROBLEMA DI ASSEGNAMENTO QUADRATICO]**
F. Maffioli and M. T. Galli (AGIP S.p.A., Milan, Italy ) 1989 63 p In ITALIAN Sponsored by Italian Ministry of Public Education
(Rept-89-028; ETN-90-97360) Avail: Politecnico di Milano, Piazza Leonardo da Vinci 32, 20133 Milan, Italy

The simulated annealing and the Tabu-search heuristic algorithms are evaluated for the solution of a combinatory optimization problem. The experimental results show a slight advantage to the simulated annealing procedure, due to a better use of the additional computing times to obtain increasingly better results. ESA

**N91-10659#** Clarkson Univ., Potsdam, NY. Dept. of Physics.
**PATH INTEGRAL ASYMPTOTICS IN THE ABSENCE OF CLASSICAL PATHS**
L. S. Schulman and R. W. Ziolkowski (Lawrence Livermore National Lab., CA.) Jul. 1990 26 p Presented at the 3d Path Integrals from MeV to MeV Conference, Bangkok, Thailand, Jan. 1989 Sponsored in part by NSF
(Contract W-7405-eng-48)
(DE90-016213; UCRL-CR-104583) Avail: NTIS HC/MF A03

When a boundary value problem in classical mechanics has no solution, the corresponding quantum propagator may be asymptotically dominated by locally flawed classical paths. It is indicated how this assertion can be made precise and it is shown how the propagator is calculated under these circumstances. The essential tools in the arguments will be the use of neutralizers and the path decomposition formula for path integrals. With this method the propagator for barrier penetration is expressed as an integral over real tunneling time, defined as the interval between first striking the barrier and last emerging from it. DOE

**N91-10660#** Stanford Univ., CA. Systems Optimization Lab.
**PSEUDO-MONOTONE COMPLEMENTARITY PROBLEMS IN HILBERT SPACE**
Richard W. Cottle and Jen-Chih Yao Jul. 1990 19 p
(Contracts DE-FG03-87ER-25028; N00014-89-J-1659; NSF DMS-89-13089)
(DE90-016310; SU-SOL-90-10) Avail: NTIS HC/MF A03

Some existence results for a nonlinear complementarity problem involving a pseudo-monotone mapping over an arbitrary closed convex cone in a real Hilbert space are established. In particular, some known existence results for a nonlinear complementarity problem in a finite-dimensional Hilbert space are generalized to infinite-dimensional real Hilbert space. Applications to a class of nonlinear complementarity problems and the study of the post-critical equilibrium state of thin elastic plate subjected to unilateral conditions are given. DOE

**N91-10661#** Lawrence Livermore National Lab., CA.
**DOMAIN DECOMPOSITION: AN INSTRUMENT OF ASYMPTOTIC-NUMERICAL METHODS**
R. C. Y. Chin and G. W. Hedstrom 1 Aug. 1990 27 p Presented at the Workshop on Asymptotic Analysis and Numerical Solution of Partial Differential Equations, Argonne, IL, 26-28 Feb. 1990
(Contract W-7405-eng-48)
(DE90-016478; UCRL-JC-104693; CONF-9002131-2) Avail: NTIS HC/MF A03

Several examples were given showing the use of asymptotic analysis in the construction of numerical methods based on domain decomposition. Many of the examples come from singularly-perturbed convection-diffusion equations with boundary and internal layers. The final example is less standard in that it deals with the numerical generation of orthogonal polynomials. DOE

**N91-10662#** Los Alamos National Lab., NM. Theoretical Div.
**STABILITY OF SOME STATIONARY SOLUTIONS FOR THE FORCED KdV EQUATION**
Roberto Camassa and T. Yao-Tsu Wu (California Inst. of Tech., Pasadena.) 1990 17 p Presented at the 10th Annual Conference on Nonlinear Science: The Next Decade, Los Alamos, NM, 21-25 May 1990
(Contract W-7405-eng-36)
(DE90-016506; LA-UR-90-2744; CONF-9005237-4) Avail: NTIS HC/MF A03

The forced KdV (fKdV) equation has been established by recent studies as a simple mathematical model capable of describing the physics of a shallow layer of fluid subject to external forcing. For a particular one-parameter family of forcings which is characterized by a wave amplitude parameter for supercritical forcing distributions, exact stationary solutions are known. The stability of these solutions was studied as the parameter varies. The linear stability analysis is first carried out, and the structure of the spectrum of the associated eigenvalue problem is discussed using a perturbation approach, about isolated parameter values where eigenfunctions can be expressed in closed form and are the fixed-point solutions of the fKdV equation corresponding to zero eigenvalues. The results identify a set of intervals in the parameter space corresponding to different types of manifestation of instability. In the region of the parameter space where the linear stability analysis fails to provide an answer, a nonlinear analysis was developed to provide a sufficient condition for stability. DOE

**N91-10663#** Los Alamos National Lab., NM.
**LOBE AREA IN ADIABATIC HAMILTONIAN SYSTEMS**
Tasso J. Kaper and Stephen Wiggins (California Inst. of Tech., Pasadena.) 1990 22 p Presented at the 10th Annual Conference on Nonlinear Science: The Next Decade, Los Alamos, NM, 21-25 May 1990

(Contract W-7405-eng-36)
(DE90-016566; LA-UR-90-2714; CONF-9005237-6) Avail: NTIS HC/MF A03

An analytically computable formula, based on the adiabatic Melnikov function, is established for lobe area in one-degree-of-freedom Hamiltonian systems depending on a parameter which varies slowly in time. This lobe area result is illustrated on a slowly parametrically forced pendulum, a paradigm problem for adiabatic chaos. The analysis unties the theory of action from classical mechanics with the theory of the adiabatic Melnikov function from the field of global bifurcation theory. DOE

**N91-10664*#** Institute for Computer Applications in Science and Engineering, Hampton, VA.
**SPECTRAL METHODS FOR TIME DEPENDENT PROBLEMS Interim Report**
Eitan Tadmor Sep. 1990 67 p
(Contract NAS1-18605)
(NASA-CR-187443; ICASE-IR-14; NAS 1.26:187443) Avail: NTIS HC/MF A04 CSCL 12A

Spectral approximations are reviewed for time dependent problems. Some basic ingredients from the spectral Fourier and Chebyshev approximations theory are discussed. A brief survey was made of hyperbolic and parabolic time dependent problems which are dealt with by both the energy method and the related Fourier analysis. The ideas presented above are combined in the study of accuracy stability and convergence of the spectral Fourier approximation to time dependent problems. Author

**N91-10665#** Louisiana State Univ., Baton Rouge. Dept. of Physics and Astronomy.
**CONVERGENCE OF LANGEVIN SIMULATION FOR COMPLEX GAUSSIAN INTEGRALS**
R. W. Haymaker and Yingcai Peng 1990 2 p Presented at the DPF Summer Study on High Energy Physics, Snowmass, 25 Jun. - 13 Jul. 1990
(Contract DE-AS05-77ER-05490)
(DE90-017402; DOE/ER-05490/111; CONF-9006267-2) Avail: NTIS HC/MF A01

The convergence of complex Langevin simulations was studied for simple Gaussian integrals analytically, and obtained the eigenvalues and eigenfunctions of the corresponding Fokker-Planck equations. This shows the convergence explicitly. DOE

**N91-10666#** Technische Univ., Delft (Netherlands). Faculty of Technical Mathematics and Informatics.
**ON q-ANALOGUES OF THE FOURIER AND HANKEL TRANSFORMS**
Tom H. Koornwinder (Center for Mathematics and Computer Science, Amsterdam, Netherlands ) and Rene F. Swarttouw 1989 19 p
(Rept-89-89; ISSN-0922-5641; ETN-90-97696) Copyright Avail: NTIS HC/MF A03

Symmetry and orthogonality for q-Bessel functions are studied. Some limit transitions are considered. A q-analog of Graf's addition formula and q-analogs of the Fourier cosine and sine transforms are given. Rigorous proofs of some limit results are included. Exton's functions are considered to be more suitable than Jackson's q-Bessel functions for harmonic analysis, both within and outside the context of quantum groups, and within the study, Exton's notation is preserved and the results in terms of a given q-hypergeometric function are stated. ESA

**N91-10667#** Technische Univ., Delft (Netherlands). Faculty of Technical Mathematics and Informatics.
**EXISTENCE OF AT MOST TWO LIMIT CYCLES FOR THE SYSTEM OF DIFFERENTIAL EQUATIONS: dx/dt = a + SUMMATION FOR i+j = 2 OF (a SUB ij) (x SUP i) (y SUP j) AND dy/dt =b + SUMMATION FOR i+j = 2 OF (b SUB ij) (x SUP i) (y SUP j)**
Suo Guangjian 1990 9 p Transl. into ENGLISH from Kexue Tongbao, no. 24, 1981 p 1481-1482
(Rept-90-03; ISSN-0922-5641; ETN-90-97700) Copyright Avail: NTIS HC/MF A02

The number of limit cycles for a quadratic system of differential equations with the following real coefficients is given: dx/dt = a + (a sub 20)(x squared) + (a sub 11)(xy) + (a sub 02)(y squared) = P(x,y); dy/dt = b + (b sub 20)(x squared) + (b sub 11)(xy) + (b sub 02)(y squared) = Q(x,y). The number of limit cycles for quadratic symmetric vector fields was shown to be at least two. It is proved that the system has at most two limit cycles. ESA

**N91-10668#** Technische Univ., Delft (Netherlands). Faculty of Technical Mathematics and Informatics.
**THE DIGITAL REGULATOR AND TRACKER FOR DETERMINISTIC CONTINUOUS-TIME LINEAR TIME-VARYING SYSTEMS**
L. G. vanWilligenburg and W. L. deKoning 1990 28 p
(Rept-90-05; ISSN-0922-5641; ETN-90-97702) Copyright Avail: NTIS HC/MF A03

The regulator and tracking problem are solved for deterministic continuous time linear time varying systems with complete state information at the sampling instants and piecewise constant control. The solutions are in feedback form and generated by a Riccati type recursion which runs backwards in time. In case of the tracking problem the feedforward control component is also generated by a recursion that runs backwards in time. Both recursions can be calculated off line. ESA

**N91-10669#** Technische Univ., Delft (Netherlands). Faculty of Technical Mathematics and Informatics.
**RELATIVE POSITION OF THE CRITICAL POINTS OF A CERTAIN CUBIC SYSTEM AND A GENERALIZATION OF THE BENDIXSON INDEX FORMULA**
Ye Yanqian (Nanjing Univ., China ) 1990 29 p
(Rept-90-23; ISSN-0922-5641; ETN-90-97716) Copyright Avail: NTIS HC/MF A03

The configuration of saddle points on a cubic system are investigated. It is proved for a specific case that they cannot lie on a straight line. A configuration 3-3+3 and 4-3+2 is investigated. A generalization of the Bendixson formula is obtained. Using numerical calculation on a computer, a phase portrait with seven finite critical points is shown. ESA

**N91-10670#** Technische Univ., Delft (Netherlands). Faculty of Technical Mathematics and Informatics.
**INVARIANT MEASURES EXIST UNDER A SUMMABILITY CONDITION FOR UNIMODAL MAPS**
Tomasz Nowicki (Warsaw Univ., Poland ) and Sebastian vanStrien 1990 23 p Sponsored in part by Netherlands Organization for Scientific Research
(Rept-90-36; ISSN-0922-5641; ETN-90-97717) Copyright Avail: NTIS HC/MF A03

For unimodal maps with negative Schwarzian derivative a sufficient condition for the existence of an invariant measure, absolutely continuous with respect to Lebesgue measure, is given. Namely the derivatives of the iterations of the map in the (unique) critical value must be so large that sum of (some root of) the inverses is finite. ESA

**N91-10671#** Technische Univ., Delft (Netherlands). Faculty of Technical Mathematics and Informatics.
**STRONG MAXIMUM PRINCIPLES FOR SYSTEMS**
Guido Sweers 1990 25 p Sponsored in part by Netherlands Organization for Scientific Research
(Rept-90-37; ISSN-0922-5641; ETN-90-97718) Copyright Avail: NTIS HC/MF A03

Necessary and sufficient conditions for linear elliptic and parabolic systems are considered such that these systems satisfy a strong maximum principle. Partial results when one of the conditions fails are obtained. ESA

**N91-10672#** Universiteit Twente, Enschede (Netherlands). Dept. of Applied Mathematics.
**AN INTRODUCTION TO ULTRAFUNCTIONS**
Martin Damsma Feb. 1990 25 p
(MEMO-841; ISSN-0169-2690; ETN-90-97732) Avail: NTIS HC/MF A03

A simplified form of Colombean's theory of new generalized functions and multiplication of distributions is presented. The algebra G of the ultrafunctions is defined as a sheaf and D prime is embedded as a subsheaf. The algebra is made appropriate for Fourier transform and an example from field theory is given as an application. ESA

**N91-10673#** Universiteit Twente, Enschede (Netherlands). Faculty of Applied Mathematics.
**APPROXIMATION AND GEOMETRIC MODELING WITH SIMPLEX B-SPLINES ASSOCIATED WITH IRREGULAR TRIANGLES**
S. Auerbach, R. H. J. GmeligMeyling, M. Neamtu, and H. Schaeben (Bonn Univ., Germany, F.R. ) Mar. 1990 38 p Sponsored by DFG and Dutch Science Foundation
(MEMO-842; ISSN-0169-2690; ETN-90-97733) Avail: NTIS HC/MF A03

Bivariate quadratic simplicial B-splines defined by their corresponding set of knots derived from a (suboptimal) constrained Delaunay triangulation of the domain are employed to obtain a C1-smooth surface. The generation of triangle vertices is adjusted to the areal distribution of the data in the domain. It is emphasized that the vertices of the triangles initially define the knots of the B-splines and do generally not coincide with the abscissae of the data. Thus, this approach is well suited to process scattered data. An example for least squares approximation with simplex splines is presented. ESA

**N91-10674#** Universiteit Twente, Enschede (Netherlands). Faculty of Applied Mathematics.
**SYMMETRIES OF THE THREE BODY PROBLEM**
Theo vanBemmelen Mar. 1990 41 p
(MEMO-843; ISSN-0169-2690; ETN-90-97734) Avail: NTIS HC/MF A03

A lot of insight into the three body problem for equal mass particles in a plane was evolved by the discovery of a remarkable symmetry which straightens out the problem. A study where all infinitesimal symmetries of the transformed and original three body problem are determined using computer algebra is presented. ESA

**N91-10675#** Universiteit Twente, Enschede (Netherlands). Faculty of Applied Mathematics.
**A MARKOV RENEWAL APPROACH TO AN APPORTUNISTIC REPLACEMENT MODEL IN CONTINUOUS TIME**
Dirk P. Kroese and Erhan Cinlar (Princeton Univ., NJ.) Mar. 1990 19 p Sponsored by Netherlands Organization for Applied Scientific Research TNO, Delft
(MEMO-844; ISSN-0169-2690; ETN-90-97735) Avail: NTIS HC/MF A03

Most multi-component replacement models are formulated in discrete time and require dynamic programming techniques to obtain the optimal replacement policy. Some models however, admit an optimal policy that is characterized by only a few constants. A continuous time replacement model in which the simple structure of the replacement rule is exploited, using embedding techniques and Marko renewal theory, is considered. ESA

**N91-10676#** Universiteit Twente, Enschede (Netherlands). Dept. of Applied Mathematics.
**LONG CYCLES, DEGREE SUMS, AND NEIGHBORHOOD UNIONS**
H. J. Broersma, J. vandenHeuvel, and H. J. Veldman 25 Jun. 1990 24 p
(MEMO-851; ISSN-0169-2690; ETN-90-97738) Avail: NTIS HC/MF A03

Graphs with defined parameters and independent sets of vertices are examined. Least cycle lengths of 1-tough graphs are determined. Analogous results for 2-connected graphs are established. ESA

**N91-10677#** Universiteit Twente, Enschede (Netherlands). Faculty of Applied Mathematics.
**CHEBYSHEV APPROXIMATION BY SPLINE FUNCTIONS WITH FREE KNOTS**
B. Mulansky (Technische Univ., Dresden, German D.R. ) Apr. 1990 20 p
(MEMO-853; ISSN-0169-2690; ETN-90-97739) Avail: NTIS HC/MF A03

The Chebyshev approximation of real continuous functions from the class (S sub n,k) of polynomial spline functions of degree n with k free knots is addressed. Using the notion of the tangent cone and a new sign rule for spline functions a necessary alternant condition for local best approximations from (S sub n,k) is derived. It shows that the corresponding error function must have an alternant of a certain length with a prescribed sign on a subinterval. This condition improves results by Braess and Cromme. A characterization of best approximations by fixed knots splines with coefficient constraints is obtained. ESA

**N91-10678#** Universiteit Twente, Enschede (Netherlands). Faculty of Applied Mathematics.
**GENERATING ALL 3-CONNECTED 4-REGULAR PLANAR GRAPHS FROM THE OCTAHEDRON GRAPH**
H. J. Broersma, A. J. W. Duijvestijn, and F. Goebel Apr. 1990 12 p
(MEMO-854; ISSN-0169-2690; ETN-90-97740) Avail: NTIS HC/MF A03

A proof that all 3-connected 4-regular planar graphs can be generated from the octahedron graph, using three operations is presented. These graphs are generated up to 15 vertices inclusive. By including a fourth operation, an alternative to a procedure by Lehel to generate all connected 4-regular planar graphs from the octahedron graph is obtained. ESA

**N91-10679#** National Aerospace Lab., Tokyo (Japan).
**OPTIMUM ORIENTATIONS OF THE OBSERVATION AXES FOR 2-DIMENSIONAL VECTOR SENSING UNDER CONSIDERATION OF BIAS ERRORS**
Takeo Kimura Feb. 1990 21 p In JAPANESE; ENGLISH summary
(NAL-TR-1055; ISSN-0389-4010) Avail: NTIS HC/MF A03

In a previous investigation it was shown that the determinant of a covariance matrix should be recognized as a reasonable criterion for comparing the quality of observation systems, and the determinant criterion was applied to find the optimum observation systems for two-dimensional vector sensing in cases where the observation errors were not correlated with each other and were normally distributed with zero means and equal variances. In the present investigation the determinant method is applied to cases where the observation errors contain not only random errors but also bias errors, provided that the values of these are mutually equal in each measuring instrument. The general properties of the optimum orientations are also shown. Furthermore the investigation is extended to include cases where some of the measuring instruments are out of order, as well as cases where there are misalignment errors in the configuration of the measuring instruments. Author

**N91-10680#** Leiden Univ. (Netherlands). Div. of Applied Mathematics.
**GEOMETRIC ERGODICITY OF THE ALOHA-SYSTEM AND A COUPLED PROCESSORS MODEL**
Flos M. Spieksma 1990 26 p Sponsored by Netherlands Organization for Scientific Research
(TW-90-01-B; ETN-90-97728) Avail: NTIS HC/MF A03

Mu-geometric recurrence of two two dimensional queueing models with mu a productform vector that increases exponentially fast with increasing states are illustrated. The mu-geometric ergodicity is implied. The first model is a time-slotted ALOHA-type system with general but stationary arrival distributions in each time-slot. Ergodicity together with convergence of the Laplace-Stieltjes transforms of the arrival distributions in a small disk around 0 are necessary and sufficient conditions for mu-geometric recurrence. The second is an exponential coupled processors model, for which only ergodicity is required to establish the results. ESA

**N91-10681#** Universiteit Twente, Enschede (Netherlands). Faculty of Applied Mathematics.
**ON BAECKLUND TRANSFORMATIONS AND IDENTITIES IN BILINEAR FORM**
G. Post May 1990 14 p
(MEMO-856; ISSN-0169-2690; ETN-90-97742) Avail: NTIS HC/MF A03

For bilinear equations of the form P(D)f.f = 0, all possibilities of rewriting (g squared)P(D)f.f - (f squared) P(D)g.g = 0 in the form Q(D)f.g = 0 are found. This is the first step in finding a Baecklund transformation. ESA

**N91-10682#** Universiteit Twente, Enschede (Netherlands). Faculty of Applied Mathematics.
**A REMARK ON THE CONVEXITY OF PIECEWISE POLYNOMIAL FUNCTIONS ON TRIANGULATIONS**
Bernd Mulansky (Technische Univ., Dresden, German D.R. ) May 1990 13 p
(MEMO-857; ISSN-0169-2690; ETN-90-97743) Avail: NTIS HC/MF A03

The restrictivity of the combination of the C1 smoothness conditions and of the convexity of the B-net for splines on certain triangulations is considered. It is pointed out that a negative result stated by Grandine does not hold for adjacent triangles forming a degenerate quadrilateral. This implies that some configurations do admit nonplanar convex B-nets satisfying the C1 conditions in contrast to the statements by Grandine. As an example, C1 piecewise quadratics on a Powel-Sabin-split are considered in more detail. ESA

**N91-10683#** Oxford Univ. (England). Dept. of Engineering Science.
**BOUNDED-ERROR DATA, AND FREQUENCY RESPONSE DESIGN**
B. Kouvaritakis and M. S. Trimboli 1989 16 p
(OUEL-1766/89; ETN-90-97912) Avail: NTIS HC/MF A03

The presence of bounded noise in identification data implies uncertainty in the parameters of system models. Earlier results provide analytical means for determining optimal ellipsoidal regions that bound the vector of parameters. Parameter space information however is only of secondary interest in frequency response design when the main preoccupation is with the bounding of Nyquist diagrams. The projection of ellipsoidal regions from parameter space to the Nyquist plane are considered and results which are optimal from a frequency response point of view are obtained. As an illustration of the potential use for frequency response bounding regions, consideration is given to the problem of multivariable robust frequency response design and a numerical example is discussed. ESA

**N91-10684#** Oxford Univ. (England). Dept. of Engineering Science.
**H 2 AND H INFINITY APPROXIMATIONS FOR EIGENVALUE/VECTOR FUNCTIONS OF TRANSFER MATRICES**
B. Kouvaritakis, J. A. Rossiter, and M. S. Trimboli 1989 43 p
Previously announced in IAA as A90-34733
(OUEL-1778/89; ETN-90-97913) Avail: NTIS HC/MF A03

H2 and H(infinity) weighting sequence approximations to rational and rational functions and techniques combining inverse discrete Fourier transforms with what amounts to H2 approximations are addressed. The theoretical background is discussed and new H2 and H(infinity) techniques are developed. The resulting algorithms can be applied to general (rational/irrational) function and vector function approximation problems, but are shown to be particularly effective in the approximation of eigenvalue/vector functions of transfer function matrices; as such the derived techniques provide some very useful tools for the characteristic locus design method. ESA

**N91-10685#** Oxford Univ. (England). Dept. of Engineering Science.
**ROBUSTNESS EFFECTS OF A PREFILTER IN GENERALIZED PREDICTIVE CONTROL**
B. D. Robinson and D. W. Clarke 27 Oct. 1989 30 p
(OUEL-1799/89; ETN-90-97914) Avail: NTIS HC/MF A03

Simple stability bounds for closed-loop robustness in the presence of modeling errors are presented in terms of the steady state gain of the model. The effects of user specified prefilters upon these bounds are discussed, leading to guidelines for selection of the filters. This allows commissioning of the adaptive controller to be done on the basis of the robustness of the nominal closed loop to modeling errors, based only upon the estimated model and the particular control strategy to be employed. ESA

# 65 STATISTICS AND PROBABILITY

Includes data sampling and smoothing; Monte Carlo method; and stochastic processes.

**N91-10686#** Xerox Palo Alto Research Center, CA.
**DENSITY ESTIMATION USING OPTIMALLY QUANTIZED HISTOGRAMS**
L. D. Wilcox Dec. 1989 48 p
(PB90-190588; PARC-EDL-89-4) Avail: NTIS HC/MF A03 CSCL 12A

A method is derived for obtaining an optimal histogram estimate of a multivariate probability density function. In an optimal histogram, the location, shape, and size of each of the bins for the histogram are chosen to minimize the integrated mean square error to the density estimate. The mean square error is shown to be the sum of a variance term, which is proportional to the number of bins in the histogram divided by the sample size used for the estimate, and a bias term, which depends on the number of histogram bins and on their location, shape, and size. The bias can be expressed as a weighted Euclidean distance, with weighting matrix equal to the outer product of the gradient of the density. It shows that a local minimum of the bias term can be obtained with the k-means clustering algorithm used in vector quantization. Thus the optimal histogram is formed by vector quantizing the feature vector using the Euclidean distortion measure, and estimating the value of the density on the resulting quantization regions. The optimal number of bins for the density estimate is determined by minimizing an approximation to the integrated mean square error of the estimate, and is expressed in terms of the sample size and number of features. Author

**N91-10687#** Technische Univ., Delft (Netherlands). Faculty of Technical Mathematics and Informatics.
**THE GENERALIZED MODUS PONENS CONSIDERED AS A FUZZY RELATION**
Hans Hellendoorn 1990 35 p
(Rept-90-02; ISSN-0922-5641; ETN-90-97699) Copyright Avail: NTIS HC/MF A03

The generalized modus ponens in fuzzy logic is studied. The scheme of the inference rule is given. Basic assumptions for dealing with it are given. A number of theorems are shown to be incompatible with these. It is shown that it is arduous to construct an implication rule to meet two of the conditions, and a way to alter them which restores this is shown. ESA

**N91-10688#** Technische Univ., Delft (Netherlands). Faculty of Technical Mathematics and Informatics.
**MULTIVARIATE TAU-ESTIMATORS FOR LOCATION AND SCATTER Ph.D. Thesis**
Hendrik P. Lopuhaa 1990 33 p

(Grant NWO-10-62-10)
(Rept-90-04; ISSN-0922-5641; ETN-90-97701) Copyright Avail: NTIS HC/MF A03

The robustness and asymptotic behavior of tau-estimators for multivariate location and scatter are discussed. Estimators are shown to correspond with multivariate M-estimators defined by a weighted average of redescending psi functions, where the weights are adaptive. The study proves consistency and asymptotic normality under weak assumptions on the underlying distribution P, shows that tau-estimators have a high breakdown point, and obtains the influence function at general distributions P. In the special case of a location-scatter family tau-estimators are asymptotically equivalent to multivariate S-estimators defined by means of a weighted rho function. This enables a high breakdown point and bounded influence to be combined with good asymptotic efficiency for the location and covariance estimator. ESA

**N91-10689#** Technische Univ., Delft (Netherlands). Faculty of Technical Mathematics and Informatics.
**THE DIGITAL REGULATOR AND TRACKER FOR STOCHASTIC CONTINUOUS-TIME LINEAR TIME-VARYING SYSTEMS**
L. G. vanWilligenburg and W. L. deKoning 1990 26 p
(Rept-90-06; ISSN-0922-5641; ETN-90-97703) Copyright Avail: NTIS HC/MF A03

The regulator and tracking problem are solved for continuous time linear time varying systems disturbed by additive white noise, with incomplete state information at the sampling instants corrupted by additive white Gaussian noise, and piecewise constant control. Both the regulator and tracking problem turn out to be certainty equivalent. The solutions to both the regulator and tracking problem therefore consist to the well known discrete time Kalman filter, and a feedback generated by a Riccati type recursion that runs backwards in time. In case of the tracking problem the feed forward is also generated by a recursion that runs backwards in time. Both recursions can be calculated off line. Explicit expressions for the minimum cost of both problems are derived. ESA

**N91-10690#** Universiteit Twente, Enschede (Netherlands). Faculty of Applied Mathematics.
**THE DIFFERENCE OF TWO RENEWAL PROCESSES: LEVEL CROSSING AND THE INFIMUM**
D. P. Kroese Mar. 1990 34 p
(MEMO-845; ISSN-0169-2690; ETN-90-97736) Avail: NTIS HC/MF A03

The difference process N of two renewal processes studied by Kroese and Kallengerg (1989) is considered. First and second order approximations to the distribution function of the time that process N crosses level n, as n approaches infinity, are compared to simulation or exact results. Numerical results confirm that second order approximations give considerable improvement on known first order results. Direct application of the second order approximation is complicated by the occurrence of the term EM = E inf N(t) (t is greater than or = 0). Considerable attention is paid to the derivation of EM for important special cases. Earlier results on the sum and difference process are stated in more general form. M.G.

**N91-10691#** Centre National d'Etudes Spatiales, Toulouse (France).
**MODELIZATION OF LOCSTAR SYNCHRONISATION SYSTEM. COMPUTATION OF NON DETECTION AND FALSE ALARM PROBABILITIES. REFLECTIONS ON THRESHOLD ADJUSTMENT AND CORRELATOR STRUCTURE**
S. Potteck 14 Apr. 1988 47 p In FRENCH; ENGLISH summary
(CNES-CT/DRT/TIT/TR-88/060; ETN-90-97806) Avail: NTIS HC/MF A03

A modelization of the LOCSTAR synchronization system, working on a binary phase shift keying signal is described. False alarms probability due to barker pulses are computed. First reflections about the threshold control and optimization are presented. Proposals concerning the improvement of the correlator structure are induded. The results show that computerized simulation is required to support LOCSTAR tests, in order to avoid measurements in each new case. ESA

## 66 SYSTEMS ANALYSIS

Includes mathematical modeling; network analysis; and operations research.

**N91-10692#** Universiteit Twente, Enschede (Netherlands). Faculty of Applied Mathematics.
**THE CORE AND THE TAU-VALUE FOR COOPERATIVE GAMES WITH COALITION STRUCTURES**
T. S. H. Driessen and S. H. Tijs (Catholic Univ., Nijmegen, Netherlands ) Apr. 1990 23 p
(MEMO-848; ISSN-0169-2690; ETN-90-97737) Avail: NTIS HC/MF A03

Solution concepts for cooperative games with coalition structures are studied. The tau-value concept for such games is introduced as an equitable compromise between a lower bound and an upper bound for the core. Several properties for the tau-value are presented. The determination of both the core and the tau-value is carried out for convex and 1-convex games with coalition structures. ESA

## 67 THEORETICAL MATHEMATICS

Includes topology and number theory.

**N91-10693#** International Centre for Theoretical Physics, Trieste (Italy).
**CONTINUUM STATES OF THE KLEIN-GORDON EQUATIONS FOR VECTOR AND SCALAR INTERACTIONS**
B. Talukdar, A. Yunus, and M. R. Amin (Saint Andrew's Univ., Scotland ) Nov. 1989 7 p Submitted for publication
(DE90-627178; IC-89/277) Avail: NTIS (US Sales Only) HC/MF A02

The scattering states solutions of the s-wave Klein-Gordon equation with vector and scalar Hulthen type potentials are obtained both for regular and irregular boundary conditions. The Coulomb limit of these results is examined and the s-wave Hulthen problem is related to the l-wave Coulomb problem. Explicit expressions are constructed for the associated Jost functions, which play a role in determining the redundant states of the S matrix. DOE

## 70 PHYSICS (GENERAL)

For precision time and time interval (PTTI) see *35 Instrumentation and Photography;* for geophysics, astrophysics or solar physics see *46 Geophysics, 90 Astrophysics,* or *92 Solar Physics.*

**N91-10694#** Joint Publications Research Service, Arlington, VA.
**JPRS REPORT: SCIENCE AND TECHNOLOGY. USSR: PHYSICS AND MATHEMATICS**
30 Jul. 1990 57 p Transl. into ENGLISH from various Russian articles
(JPRS-UPM-90-003) Avail: NTIS HC/MF A04

Abstracts of Soviet literature in various areas of physics and mathematics are compiled. The following subject areas are covered: acoustics; crystals, laser glasses, and semiconductors; fluid dynamics; lasers; magnetohydrodynamics; nuclear physics; optics and spectroscopy; plasma physics; superconductivity; and numerical analysis and algorithms. M.G.

**N91-10695*#** Fermi National Accelerator Lab., Batavia, IL.
**FALSE-VACUUM DECAY IN GENERALIZED EXTENDED INFLATION**
Richard Holman, Edward W. Kolb, Sharon L. Vadas, and Yun Wang (Carnegie-Mellon Univ., Pittsburgh, PA.) Jul. 1990 12 p

(Grant NAGw-1340)
(NASA-CR-186419; NAS 1.26:186419; CMU-HEP90-13; FNAL-PUB-90/147-A) Avail: NTIS HC/MF A03 CSCL 20C

False-vacuum decay was studied in context of generalized extended inflationary theories, and the bubble nucleation rates was computed for these theories in the limit of G(sub N) yields 0. It was found that the time dependence of the nucleation rate can be exponentially strong through the time dependence of the Jordan-Brans-Dicke field. This can have a pronounced effect on whether extended inflation can be successfully implemented. Author

**N91-10696#** Sandia National Labs., Albuquerque, NM.
**INTRINSIC (?) REFERENCE STANDARDS**
R. P. Reed 1990 12 p Presented at the 1990 National Conference of Standards Laboratories (NCSL) Symposium and Workshop, Washington, DC, 19-23 Aug. 1990
(Contract DE-AC04-76DP-00789)
(DE90-015714; SAND-89-2877C; CONF-9008134-2) Avail: NTIS HC/MF A03

The term Intrinsic refers to something that is inherent in the nature of a thing. With regard to metrologic references, it usually concerns a characteristic property of a natural material or process. International standard scales, such as those for time, dimension, temperature, voltage, and resistance, are increasingly based on intrinsic natural properties rather than on physical artifacts. The objective is to provide accurate and reliable fiducials that are themselves reproducible independent of place, time, or observer. A distinction must be made, however, between intrinsic properties on which measurement scales are based and physical realizations of particular values of those intrinsic properties in actual reference devices used for practical calibration. Ideally, intrinsic references are not subject to calibration as they represent quantities that are exact by definition. It is sometimes asserted, for example, that such references do not require calibration traceability to a national laboratory. But, it must not be casually assumed that a calibration device that employs a class of natural phenomenon does, in fact, necessarily impose the standardized value on a calibration subject. Some of the problems associated with the practical use of so-called intrinsic standard references in industrial measurement practice are considered. In particular, distinctions between validation, qualification, and calibration are discussed in relation to intrinsic reference standards and measurement quality assurance. DOE

**N91-10697#** Los Alamos National Lab., NM. Applied Theoretical Physics Div.
**PREDICTION AND CONTROL OF CHAOTIC PROCESSES USING NONLINEAR ADAPTIVE NETWORKS**
R. D. Jones, C. W. Barnes, G. W. Flake, K. Lee, P. S. Lewis, M. K. ORouke, and S. Qian 1990 9 p Presented at the Summer Workshop on Nonlinear and Chaotic Phenomena in Plasmas, Solids, and Fluids, Edmonton, Alberta, 23-27 Jul. 1990 Prepared in cooperation with Maryland Univ., College Park
(Contract W-7405-eng-36)
(DE90-016505; LA-UR-90-2755; CONF-9007136-3) Avail: NTIS HC/MF A02

We present the theory of nonlinear adaptive networks and discuss a few applications. In particular, we review the theory of feedforward backpropagation networks. We then present the theory of the Connectionist Normalized Linear Spline network in both its feedforward and iterated modes. Also, we briefly discuss the theory of stochastic cellular automata. We then discuss applications to chaotic time series, tidal prediction in Venice lagoon, finite differencing, sonar transient detection, control of nonlinear processes, control of a negative ion source, balancing a double inverted pendulum and design advice for free electron lasers and laser fusion targets. DOE

# 71 ACOUSTICS

Includes sound generation, transmission and attenuation.
For noise pollution see *45 Environmental Pollution.*

**N91-10698#** Massachusetts Inst. of Tech., Cambridge.
**STRUCTURAL ACOUSTICS: AN APPLIED SCIENCE WITH MANY APPLICATIONS**
1990 24 p Presented at the MIT/Marine Industry Collegium, Cambridge, MA, 9 Jan. 1990
(Contract NA86AA-D-SG089)
(PB90-183633; MITSG-89-33; OB-56) Avail: NTIS HC/MF A03 CSCL 20A

The Massachusetts Institute of Technology (MIT) Sea Grant Marine Industry Collegium joined with the MIT-Industry Program in Structural Acoustics to sponsor a one-day workshop, on January 9, 1990. The workshop addressed current research efforts and provided an opportunity for attendees to actively interact through their questions and comments. Presentations covered such topics as the transmission properties of fluid storage tanks within vessels, recent developments in analytical models of machine systems for noise and vibration minimization, techniques to combine analytically and experimentally derive acoustic parameters for model definition, and the application of active and passive control techniques to minimize structural acoustic wave propagation. GRA

**N91-10699*#** National Aeronautics and Space Administration. Langley Research Center, Hampton, VA.
**HELICOPTER FAR-FIELD ACOUSTIC LEVELS AS A FUNCTION OF REDUCED MAIN-ROTOR ADVANCING BLADE-TIP MACH NUMBER**
Arnold W. Mueller, Charles D. Smith, and Philip LeMasurier (Sikorsky Aircraft, Stratford, CT.) Jul. 1990 28 p
(NASA-TM-102684; NAS 1.15:102684) Avail: NTIS HC/MF A03 CSCL 20A

During the design of a helicopter, the weight, engine, rotor speed, and rotor geometry are given significant attention when considering the specific operations for which the helicopter will be used. However, the noise radiated from the helicopter and its relationship to the design variables is currently not well modeled with only a limited set of full-scale field test data to study. In general, limited field data have shown that reduced main-rotor advancing blade-tip Mach numbers result in reduced far-field noise levels. The status of a recent helicopter noise research project is reviewed. It is designed to provide flight experimental data which may be used to further understand helicopter main-rotor advancing blade-tip Mach number effects on far-field acoustic levels. Preliminary results are presented relative to tests conducted with a Sikorsky S-76A helicopter operating with both the rotor speed and the flight speed as the control variable. The rotor speed was operated within the range of 107 to 90 percent NR at nominal forward speeds of 35, 100, and 155 knots. Author

**N91-10700#** Sandia National Labs., Albuquerque, NM. Applied Mechanics Div.
**PREGO: A SIMULATION CODE FOR ONE-DIMENSIONAL VISCOELASTIC ACOUSTICS**
Daniel J. Segalman Jul. 1990 34 p
(Contract DE-AC04-76DP-00789)
(DE90-014859; SAND-90-0593) Avail: NTIS HC/MF A03

A computer code, PREGO, has been developed to perform calculations for three related problems: reflection of an acoustic wave against a layered viscoelastic medium: (water/medium); transmission of an acoustic wave through such a medium (water/medium/water); and radiation of an acoustic wave through such a medium: (medium/water). This code draws on experience gained in writing and using a predecessor code, IMPEDE, which was devised to calculate the steady state reflection of an acoustic wave impinging on a layered substrate of elastic or viscoelastic materials. That code employed a finite element formulation to discretize the complex-valued, second order ordinary differential equations for monochromatic steady state acoustics. The principles of numerical analysis that underlie PREGO are different and less subject to discretization error than those used in IMPEDE. The formulation used in PREGO is similar to that of higher dimensional boundary integral formulations in that it uses closed form expressions for the complex velocity fields in each layer, given in terms of the velocities at the boundary of that layer. The solutions for each layer are coupled together by requiring that stresses and velocities be continuous across interfaces. DOE

**N91-10701#** Technical Research Centre of Finland, Espoo. Safety Engineering Lab.

**PROPERTIES OF ACOUSTIC ENERGY QUANTITIES**

Seppo Uosukainen Sep. 1989 233 p
(DE90-518714; VTT-TUTK-656) Avail: NTIS (US Sales Only) HC/MF A11

The sound power of a source is shown to depend on other sources and environment through the coherent and incoherent interaction and on the mounting conditions of the source. The conditions for a source to be a constant power source (being a rare exception amoung sound sources) are defined. A new quantity semianalytic intensity is defined. By its help the mean value, time-dependent, active and reactive intensity are defined in general time-dependent fields. In time harmonic fields the active part of the mean value intensity is rotational. The rotationality is proportional to the polarization vector of particle velocity, the polarization being elliptical in general. The changes of sound field are shown to generate rotationality in all intensity components. The negative pl-indicator is shown to be a possible indication of the rotationality of intensity. Fundamental intensity vortices are defined. The size of the lowest order vortices is of the order of 0.5 to 0.7 (Lambda). A modified J.M.C. method is developed for the basis of the vector and dyadic weighting, the former of which weights the sound pressure and particle velocity differently, and the latter also changes the polarization (or direction) of the particle velocity. Theoretical possibilities of general field modifications and acoustic sink optimization based on these new field reshapers are presented. A new field indicator for intensity measurements is defined. It can be used as a measure of the diffuseness and reactivity as a function of time and observation direction. DOE

**N91-10702*#** National Aeronautics and Space Administration. Langley Research Center, Hampton, VA.

**THE DEVELOPMENT OF INTERIOR NOISE AND VIBRATION CRITERIA**

J. D. Leatherwood, S. A. Clevenson, and D. G. Stephens Oct. 1990 30 p Presented at the International Symposium on Subjective Responses Under Simultaneous Exposures to Noise and Vibration, Tampere, Finland, 6-8 Jun. 1990, and at the 120th Meeting of the Acoustical Society of America, San Diego, CA, 26-30 Nov. 1990
(NASA-TM-102736; NAS 1.15:102736) Avail: NTIS HC/MF A03 CSCL 20A

A generalized model was developed for estimating passenger discomfort response to combined noise and vibration. This model accounts for broadband noise and vibration spectra and multiple axes of vibration as well as the interactive effects of combined noise and vibration. The model has the unique capability of transforming individual components of noise/vibration environment into subjective comfort units and then combining these comfort units to produce a total index of passenger discomfort and useful sub-indices that typify passenger comfort within the environment. An overview of the model development is presented including the methodology employed, major elements of the model, model applications, and a brief description of a commercially available portable ride comfort meter based directly upon the model algorithms. Also discussed are potential criteria formats that account for the interactive effects of noise and vibration on human discomfort response. Author

**N91-10703*#** National Aeronautics and Space Administration. Lewis Research Center, Cleveland, OH.

**AEROACOUSTIC EFFECTS OF REDUCED AFT TIP SPEED AT CONSTANT THRUST FOR A MODEL COUNTERROTATION TURBOPROP AT TAKEOFF CONDITIONS**

Richard P. Woodward and Christopher E. Hughes Oct. 1990 21 p Presented at the 13th Aeroacoustics Conference, Tallahassee, FL, 22-24 Oct. 1990; sponsored in part by AIAA
(NASA-TM-103608; E-5732; NAS 1.15:103608; AIAA-90-3933) Avail: NTIS HC/MF A03 CSCL 20A

A model high-speed, advanced counterrotation propeller, F7/A7, was tested in the anechoic wind tunnel at simulated takeoff and approach conditions of Mach 0.2. The propeller was operated in a baseline configuration with the forward and aft rotor blade setting angles and forward and aft rotational speeds essentially equal. Two additional configurations were tested with the aft rotor at increased blade setting angles and the rotational speed reduced to achieve overall performance similar to that of the baseline configuration. Acoustic data were taken with an axially translating microphone probe that was attached to the tunnel floor. Concurrent aerodynamic data were taken to define propeller operating conditions. Author

**N91-10704#** Rolls-Royce Ltd., Derby (England).

**DO WE REALLY NEED 57 WAYS OF RATING AIRCRAFT NOISE**

M. J. T. Smith 13 Aug. 1990 5 p Presented at the 1990 International Conference on Noise Control Engineering, Goteberg, Sweden, 13-15 Aug. 1990
(PNR-90720; ETN-90-97946) Copyright Avail: NTIS HC/MF A01

The difficulties encountered for measuring and quantifying the effects of aircraft noise are analyzed. The impact of the noise measurement results on the air transport business community is discussed. The common elements between all noise measurements and control methodologies are given. The relationship between absolute level and footprint area of constant noise level is presented. The noise certification standards are determined. ESA

# 72 ATOMIC AND MOLECULAR PHYSICS

Includes atomic structure, electron properties, and molecular spectra.

**N91-10705#** Lund Univ. (Sweden). Dept. of Physics.

**PRE-EQUILIBRIUM EMISSION AND MULTIFRAGMENTATION IN HEAVY ION COLLISIONS**

B. Jakobsson and M. Berk 1989 15 p Presented at the 27th International Winter Meeting on Nuclear Physics, Bormio, Italy, 23-27 Jan. 1989
(LUIP-8902; LUNFD6/(NFFK-7098)1-14(1988); ISSN-0348-9329) Avail: NTIS HC/MF A03

The strong affection of the dynamical evolution from pre-equilibrium processes was pointed out from measurements of high energy protons and pions. The proton emission source velocity at 35A MeV indicates a strong equal participation component (nucleon-nucleon scattering or a very early participant source of some other kind). Pion production in coincidence with projectile-like fragment measurements at 85A MeV - well below the nucleon-nucleon production threshold - indicates that central collisions are favored when a high energy (density) concentration is required. In spite of these energy consuming pre-equilibrium process multifragmentation-like breakup channels are found already for energies greater than or equal to 50A MeV even in asymmetric reactions. No direct indication of a critical behavior is however observed. Author

**N91-10706#** Lawrence Livermore National Lab., CA.

**THEORETICAL STUDIES OF HIGH ENERGY DENSITY MATTER (HEDM) MOLECULES**

Byron H. Lengsfield, III and Stephen Rogers (Air Force Astronautics Lab., Edwards AFB, CA.) Mar. 1990 29 p
(Contract W-7405-eng-48)
(DE90-014831; UCRL-ID-103344) Avail: NTIS HC/MF A03

This research effort consisted of two tasks. The first task was to improve and document the MESA series of electronic structure codes. The second task was to carry out theoretical studies of the molecules B2H2 and Be2H2 in order to assess their potential as high energy density materials. A summary is given of the progress attained on each of the tasks. In these sections, the arguments used to motivate support for this work will be repeated so that the results attained in this study can measured against the goals put forth in the funding proposal. Then, a detailed description of the B2H2 and Be2H2 calculations is provided. A concluding section follows which concisely reviews the progress attained to date and suggests areas which merit further study. Finally, the MESA documentation is included as an appendix. DOE

**N91-10707*#** Oregon Univ., Eugene. Inst. of Chemical Physics.
**COLLISION-INDUCED GAS PHASE DISSOCIATION RATES Final Report, Sep. 1989 - Aug. 1990**
C. Frederick Hansen Aug. 1990 27 p
(Grant NAG1-1046)
(NASA-CR-185874; NAS 1.26:185874) Avail: NTIS HC/MF A03
CSCL 20H

The Landau-Zener theory of reactive cross sections was applied to diatomic molecules dissociating from a ladder of vibrational states. The result predicts a dissociation rate that is quite well duplicated by an Arrhenius function having a preexponential temperature dependence of about T(sub -1/2), at least for inert collision partners. This relation fits experimental data reasonably well. The theory is then used to calculate the effect of vibrational nonequilibrium on dissociation rate. For Morse oscillators, the results are about the same as given by Hammerling, Kivel, and Teare in their analytic approximation for harmonic oscillators, though at very high temperature a correction for the partition function limit is included. The empirical correction for vibration nonequilibrium proposed by Park, which is a convenient algorithm for CFD calculations, is modified to prevent a drastic underestimation of dissociation rates that occurs with this method when vibrational temperature is much smaller than the kinetic temperature of the gas. Author

**N91-10708#** Louisiana State Univ., Baton Rouge.
**RESEARCH IN ELEMENTARY PARTICLE PHYSICS Progress Report**
Lai-Him Chan, Richard Haymaker, Richard Imlay, Roger McNeil, and William Metcalf 1990 112 p
(Contract DE-AS05-77ER-05490)
(DE90-017278; DOE/ER-05490/123) Avail: NTIS HC/MF A06

Theoretical work is described on effective action expansion of an effective low energy theory of hadrons, dynamical symmetry breaking, and lattice gauge theories. The high energy experimental group finished taking data on a neutrino oscillation experiment at LAMPF in 1989 and expects to complete the data analysis soon. LSU is also participating on an electron-positron experiment, AMY, that is running at TRISTAN in Japan. The plans are to leave on March 1, 1990 to concentrate on ZEUS and SSC activities. For ZEUS we are presently building the EMC waveshifters for the barrel calorimeter and participating on the calorimeter beam tests at Fermilab. DOE

**N91-10709#** Virginia Polytechnic Inst. and State Univ., Blacksburg.
**THEORETICAL STUDIES IN FEW-BODY INTERMEDIATE ENERGY PHYSICS Progress Report, 1 Nov. 1989 - 31 Aug. 1990**
T. Mizutani Aug. 1990 3 p
(Contract DE-FG05-84ER-40143)
(DE90-017279; DOE/ER-40143/7) Avail: NTIS HC/MF A01

Theoretical studies were in the following areas: pp yields pi (+)np reactions at T sub lab sup p = 800 MeV; NN yields N Delta reactions; N Delta phase shifts; and low energy elastic K(-) d scattering. DOE

**N91-10710#** Auburn Univ., AL. Dept. of Physics.
**THEORETICAL ATOMIC PHYSICS FOR FUSION Annual Report, 1990**
Michael S. Pindzola, J. Ivan Legg, Joseph D. Perez, and Paul F. Parks Aug. 1990 11 p
(Contract DE-FG05-86ER-53217)
(DE90-017280; DOE/ER-53217/4) Avail: NTIS HC/MF A03

The understanding of electron-ion collision processes in high temperature plasmas remains a key factor in the ultimate development of nuclear fusion as a viable energy source for the nation. The 1990 to 1992 research proposal delineated excitation, ionization and dielectronic recombination as the main areas of research in electron-ion scattering theory. The 1990 efforts in each of these research areas are summarized. DOE

**N91-10711#** Amsterdam Univ. (Netherlands).
**PROMPT LEPTON PRODUCTION IN A PROTON BEAMDUMP EXPERIMENT Ph.D. Thesis**
Felix Bergsma 1990 131 p Sponsored by Stichting voor Fundamenteel Onderzoek der Materie
(ETN-90-97750) Avail: NTIS HC/MF A07

The results of a 400 GeV proton on copper beam dump experiment concerning the production of prompt neutrinos and muons are described. The CHARM-1 neutrino detector, a fine grained sampling calorimeter with large fiducial mass, was used to record neutrino interactions. The muon energy spectrum was determined by measuring the muon flux at several depths in an iron muon shield just downstream of the dump. The prompt event rates were separated from the conventional event rates by the technique of extrapolation to 'infinite' target density. Two targets of different density were used, one made of solid copper and a copper/air segmented one, with one third density of the first. The distance between dump and neutrino detector was 490 m. The amount of protons on the high density target was 13.26 times 10(exp 17) and on the low density target 6.35 times 10(exp 17). ESA

**N91-10712#** National Aerospace Lab., Tokyo (Japan).
**A SENSITIVE TEST FOR ACCURACY IN EVALUATION OF MOLECULAR COLLISION NUMBER IN THE DIRECT-SIMULATION MONTE CARLO METHOD**
Katsuhisa Koura Jan. 1990 9 p
(NAL-TR-1050T; ISSN-0389-4010) Avail: NTIS HC/MF A02

A sensitive test is proposed for accuracy in the evaluation of molecular collision number in the direct-simulation Monte Carlo method. It is shown that the translational relaxation in a spatially homogeneous box, which is divided into a number of cells where the simulation of molecular collisions is carried out, is a simple but sensitive test problem for the evaluation of the lower limit of mean molecular number per cell and the computation time, as well as for the check of the accuracy in the evaluation of collision number. It is verified from the test that the lower limit of mean molecular number per cell for the (modified) null-collision technique is about 1 but that for the (modified) time-counter technique is about 30. The computation time for the (modified) null-collision technique is about 10 to 30 percent larger than that for the (modified) time-counter technique in the simulation with the same molecular number. Author

## 73 NUCLEAR AND HIGH-ENERGY PHYSICS

Includes elementary and nuclear particles; and reactor theory.

For space radiation see *93 Space Radiation.*

**N91-10713#** Sandia National Labs., Albuquerque, NM.
**NUMERICAL MODELS OF BEAM DYNAMICS IN ION INDUCTION LINACS**
John R. Freeman and John S. Wagner 1990 4 p Presented at the 1990 LINAC Conference, Albuquerque, NM, 10-14 Sep. 1990 Sponsored in part by the Navy and DARPA
(Contract DE-AC04-76DP-00789)
(DE90-017043; SAND-90-1491C; CONF-9009200-10) Avail: NTIS HC/MF A01

A numerical simulation code was written to study beam dynamics in ion induction linear accelerators. The code is used to study axial beam expansion for a particular example. Voltage ramping of the gap reduces the expansion. The code is also used to study the longitudinal instability. The instability grows and saturates after increasing the axial divergence. DOE

**N91-10714#** Leiden Univ. (Netherlands).
**THE TECHNIQUE OF CERENKOV RING IMAGE DETECTION Ph.D. Thesis**
Dirk Langerveld 1990 126 p Sponsored by Stichting voor Fundamenteel Onderzoek der Materie
(ETN-90-97747) Avail: NTIS HC/MF A07

The method of particle identification using Ring Imaging Cerenkov (RICH) detectors and its application in the DELPHI barrel RICH detector in the LEP accelerator are addressed. The drift properties of electrons in gases and over long distances are examined. Several wire chamber prototypes were tested, and the gating system was shown to be satisfactory. An efficient photon detection is shown and an accurate localization of the photon conversion points is shown possible. For the working conditions of the barrel RICH vector the average spatial resolution for the x, y, and z coordinates of the Cerenkov photon conversion points is 0.9, 1.8, and 1.5 mm respectively. ESA

# 74 OPTICS

Includes light phenomena; and optical devices.
For lasers see *36 Lasers and Masers.*

**N91-10715#** Los Alamos National Lab., NM. Center for Nonlinear Studies.
**POLARIZATION MODULATED SOLITARY WAVES IN AN OPTICAL FIBER**
D. David and M. V. Tratnik 1990 15 p Presented at the 10th Annual Conference on Nonlinear Science: The Next Decade, Los Alamos, NM, 21-25 May 1990
(Contract W-7405-eng-36)
(DE90-015034; LA-UR-90-2272; CONF-9005237-3) Avail: NTIS HC/MF A03

A family of solitary waves is found which satisfy the coupled nonlinear Schroedinger equations governing optical pulse propagation in an elliptical core optical fiber. These are polarization modulated pulses which are bound states of two solitons which when decoupled have constant and uniform orthogonal linear polarizations. The information of these bound states is possible only above a minimum energy threshold determined by the ellipticity of the fiber. DOE

**N91-10716#** Oak Ridge National Lab., TN.
**NONLINEAR OPTICS AND NONLINEAR DYNAMICS**
C. H. Chen 28 Aug. 1990 6 p
(Contract DE-AC05-84OR-21400)
(DE90-015975; ORNL/FTR-3709) Avail: NTIS HC/MF A02

The author was invited by the Institute of Atomic and Molecular Sciences, Academia Sinica, in Taiwan to give six lectures on nonlinear optics. The participants included graduate students, postdoctoral fellows, research staff, and professors from several research organizations and universities. Extensive discussion followed each lecture. Since both the Photophysics Group at Oak Ridge National Laboratory (ORNL) and Institute of Atomic and Molecular Sciences in Taiwan have been actively participating in nonlinear optics research, the discussions are very beneficial to ORNL programs. The author also visited several laboratories at IAMS to exchange research ideas on nonlinear optics. DOE

**N91-10717#** Los Alamos National Lab., NM.
**HIGH-ORDER OPTICS OF MULTIPOLE MAGNETS**
Peter Walstrom, Feri Neri, and Tom Mottershead 1990 4 p Presented at the 1990 LINAC Conference, Los Alamos, NM, 9-14 Sep. 1990
(Contract W-7405-eng-36)
(DE90-016438; LA-UR-90-2888; CONF-9009200-5) Avail: NTIS HC/MF A01

A new capability was developed to compute third and fifth order Lie algebraic transfer maps for a family of realistic multipole magnets, including dipoles. The general Hamiltonian is expanded symbolically to arbitrary order. The vector potential off axis, for a given multipole symmetry, is determined from the appropriate magnetic field gradients and their longitudinal derivatives on axis. Subroutines to compute the required gradients are available for Halbach REC quadrupoles, and for general multipoles, with the current distribution on a cylindrical surface specified by a shape function. This function can be supplied by the user, or selected from internal options. Both the reference trajectory, and the map about it are calculated by numerical integration through the general magnetic field, using modular GENMAP software. This allows the calculation of curved reference trajectories in a general dipole magnet, as well as offset reference trajectories needed for misalignment tolerance studies. These new calculational capabilities were added to the MARYLIE Lie Algebraic beam optics design code. DOE

**N91-10718#** Lawrence Livermore National Lab., CA.
**DEPOSITION CONTROLLED UNIFORMITY OF MULTILAYER MIRRORS**
A. F. Jankowski, D. M. Makowiecki, R. G. Patterson, M. A. McKernan, and R. J. Foreman Jun. 1990 9 p Presented at the SPIE 1990 International Symposium on Optical and Optoelectric Applied Science and Engineering, San Diego, CA, 8-13 Jul. 1990 Submitted for publication
(Contract W-7405-eng-48)
(DE90-015906; UCRL-102583; CONF-900756-38) Avail: NTIS HC/MF A02

The widely used physical vapor deposition techniques to produce multilayer x ray optics with uniform layer pair spacings (less than 1 percent variation) over large areas (greater than 10 cm x 10 cm) have all been limited by the geometry of the vapor source. Magnetron sputtering sources, geometrically a convolution of point sources in a circular or rectangular array, provide uniformly thick regions of coating only within the boundaries of the erosion track. To maximize uniformity over large regions requires target materials equally as large, proving a costly proposition. Electron beam or molecular beam sources are similarly limited by the size of the melt pool or effusion cell diameter. For ion beam deposition, spatial divergence from typical ion sources results in coating thickness variations of 5 percent or more for large areas as previously described. To minimize the ultimate expense of designing a necessarily large, single deposition source to provide a small thickness variation (without the use of compensating substrate motion or elaborate shielding over the deposition sources), several small sources arranged in an appropriate array may provide a viable alternative. To this end, the use of linear array of one-inch magnetron sources has proven effective. Material has been deposited within the limitations of 1.5 percent thickness variation, along the axis of a linear gun array, over 15 cm in length. The feasibility of using two linear arrays of magnetron sources is investigated to prepare large area multilayer mirrors with minimal layer pair spacing variations. Such a deposition system also allows for gradually varying the layer pair spacings across the surface of an optic, in a designed manner, which proves useful for focusing applications. DOE

**N91-10719#** Lawrence Livermore National Lab., CA.
**DIAMOND TURNING OF OPTICAL CRYSTALS**
T. T. Saito, C. K. Syn, B. A. Fuchs, and S. P. Velsko Mar. 1990 4 p Presented at the Optical Fabrication and Testing Workshop, Monterey, CA, 12-14 Jun. 1990 Submitted for publication
(Contract W-7405-eng-48)
(DE90-015909; UCRL-102807; CONF-9006265-1) Avail: NTIS HC/MF A01

Diamond turning (DT) has proven to be a cost effective optical fabrication technique for both aspherical and spherical/flat figures when precise geometrical tolerances are important. We are interested in the DT of crystals for several reasons. DT has been very effective to insure requisite accurate geometrical orientation of optical surfaces to crystalline axes for frequency conversion applications. Also, DT can achieve figure up to the edge of the crystal. Another key DT benefit is enhanced laser damage threshold, which we feel in part is due to the freedom of the surface from polishing impurities. Several important issues for diamond turning optical crystals are the tool wear, associated surface finish, and laser damage properties. We have found that careful selection and control of diamond turning parameters can yield production techniques for crystals previously considered incompatible with diamond turning. DOE

**N91-10720#** Lawrence Livermore National Lab., CA.
**DESIGN, PERFORMANCE, AND CALIBRATION OF THE ALEXIS ULTRASOFT X-RAY TELESCOPES**
Jeffrey J. Bloch, Frank Ameduri, William C. Priedhorsky, Diane Roussel-Dupre, Barham W. Smith, Oswald H. W. Siegmund, Scott Cully, John Warren, and Geoffrey A. Gaines (California Univ., Berkeley.) 1990 12 p Presented at the SPIE Conference on EUX X Ray and Gamma Ray Instrumentation for Astronomy, San Diego, CA, 8-13 Jul. 1990 Submitted for publication
(Contract W-7405-eng-36)
(DE90-016483; LA-UR-90-2851; CONF-9007157-1) Avail: NTIS HC/MF A03

The Array of Low Energy X-ray Imaging Sensors (ALEXIS) experiment consists of six wide angle extreme ultraviolet (EUV)/ultrasoft x-ray telescopes utilizing normal incidence multilayer mirrors, flown on a miniature satellite to map out the sky in three narrow bandpasses around 66, 71, and 95 eV. The 66 and 71 eV bandpasses are centered on intense Fe emission lines which are characteristic of million degree plasmas such as the one thought to produce the soft x-ray background. The 95 eV bandpass has a higher throughput and is more sensitive to continuum sources. The mission will be launched into orbit on the Pegasus Air Launched Vehicle in mid-1991. We will present the details of the ALEXIS telescope optical design, initial characterizations of the first flight mirrors and detectors, and the current schemes for characterizing and calibrating the completed telescope assemblies. We will also discuss the details of a novel 'wavetrap' feature incorporated into the multilayer mirror structure to greatly reduce the mirror's reflectivity at 304 (angstrom), a major background contamination flux of He II emission from the geocorona. DOE

**N91-10721#** Los Alamos National Lab., NM. Theoretical Div.
**ORDER AND CHAOS IN POLARIZED NONLINEAR OPTICS**
Darryl D. Holm 1990 19 p Presented at the Chaos Down Under Conference, Sydney, Australia, Feb. 1990 Submitted for publication
(Contract W-7405-eng-36)
(DE90-016717; LA-UR-90-2660; CONF-9002140-1) Avail: NTIS HC/MF A03

Methods for investigating temporal complexity in Hamiltonian systems are applied to the dynamics of a polarized optical laser beam propagating as a travelling wave in a medium with cubically nonlinear polarizability (i.e., a Kerr medium). The theory of Hamiltonian systems with symmetry is used to study the geometry of phase space for the optical problem, transforming from C sup 2 to S sup 2 x (J, theta), where (J, theta) is a symplectic action-angle pair. The bifurcations of the phase portraits of the Hamiltonian motion on S sup 2 are classified and shown graphically. These bifurcations create various saddle connections on S sup 2 as either J (the beam intensity), or the optical parameters of the medium are varied. After this bifurcation analysis, the Melnikov method is used to demonstrate analytically that the saddle connections break and intersect transversely in a Poincare map under spatially periodic perturbations of the optical parameters of the medium. These transverse intersections in the Poincare map imply intermittent polarization switching with extreme sensitivity to initial conditions characterized by a Smale horseshoe construction for the travelling waves of a polarized optical laser pulse. The resulting chaotic behavior in the form of sensitive dependence on initial conditions may have implications for the control and predictability of nonlinear optical polarization switching in birefringent media. DOE

**N91-10722#** Colorado Univ., Boulder. Dept. of Astrophysics and Biochemistry.
**TIME-RESOLVED FTIR (FOURIER TRANSFORM INFRARED) EMISSION STUDIES OF LASER PHOTOFRAGMENTATION AND CHAIN REACTIONS Progress Report, 15 Sep. 1987 - 15 Sep. 1990**
Stephen R. Leone 1990 36 p
(Contract DE-FG02-88ER-13860)
(DE90-017223; DOE/ER-13860/3) Avail: NTIS HC/MF A03

Recent progress is described resulting from the studies of combustion-related photofragmentation dynamics, energy transfer, and reaction processes using a time resolved Fourier transform infrared (FTIR) emission technique. The FTIR is coupled to a high repetition rate excimer laser which produces radicals by photolysis to obtain novel, high resolution measurements on vibrational and rotational state dynamics. The results are important for the study of numerous radical species relevant to combustion processes. The method was applied to the detailed study of photofragmentation dynamics in systems such as acetylene, which produces C2H; chlorofluoroethylene to study the HF product channel; vinyl chloride and dichloroethylene, which produce HCl; acetone, which produces CO and CH3; and ammonia, which produces NH2. In addition, the use was demonstrated of the FTIR technique for preliminary studies of energy transfer events under near single collision conditions, radical-radical reactions, and laser-initiated chain reaction processes. DOE

**N91-10723#** Ecole Centrale de Lyon (France). Lab. de Mecanique des Fluides.
**MARKOV MODEL OF THE PROPAGATION OF A LIGHT WAVE IN A HEATED TURBULENT MEDIA Ph.D. Thesis [MODELISATION MARKOVIENNE DE LA PROPAGATION D'UNE ONDE LUMINEUSE DANS UN MILIEU TURBULENT CHAUFFE]**
Elkana Pemha 1990 162 p In FRENCH
(ECL-90-06; ETN-90-97818) Avail: NTIS HC/MF A08

The purpose of the study is the obtention of the scattering coefficient relating to the fluctuations of the refraction index in the jet. Theoretical results on the directional fluctuations of the incident wave are reviewed. The Einstein-Fokker-Planck-Kolmogorov equation, which regulates the Markov process, is demonstrated. The different steps of the calculation code and the obtention of the scattering coefficient are presented. The experiments performed are described. ESA

**N91-10724#** Helsinki Univ. of Technology, Espoo (Finland). Dept. of Technical Physics.
**VARIABLE-COHERENCE BEAM OPTICS Ph.D. Thesis**
Jari Turunen 1990 65 p Sponsored by Academy of Finland and by Jenny and Antii Wihuri Foundation
(ISBN-952-90-1784-7; ETN-90-97978) Avail: NTIS HC/MF A04

The generation, propagation, and applications of highly directional light beams with variable spatial coherence properties are studied. The propagation of so-called Gaussian Schell Model (GSM) beams in arbitrary diffraction limited optical systems is analyzed. The main results are verified experimentally. A novel algorithm to determine the transverse mode structure of a laser from spatial coherence measurements is proposed, and applied to a multimode He-Ne laser. A new concept of a synthetic acousto-optic hologram is introduced, and a method based on this device is presented. The light fields that propagate in free space without modification are discussed. A holographic technique for generating coherent diffraction free wavefields is proposed and demonstrated. A new class of partially coherent fields with a propagation invariant cross spectral density function is introduced. The relationship between the concepts of nonmodified propagation and self imaging is discussed. ESA

# 75 PLASMA PHYSICS

Includes magnetohydrodynamics and plasma fusion.

For ionospheric plasmas see *46 Geophysics.* For space plasmas see *90 Astrophysics.*

**N91-10725#** Ceskoslovenska Akademie Ved, Prague. Inst. of Plasma Physics.

**ON LOWER HYBRID WAVE SCATTERING BY PLASMA DENSITY FLUCTUATION NONLINEAR REFLECTION COEFFICIENT OF THE FAST MAGNETOACOUSTIC WAVE**

V. Petrzilka May 1988 15 p
(IPPCZ-281) Avail: NTIS HC/MF A03

Plasma density fluctuations at the plasma boundary were observed and studied on many tokamaks. The presence of turbulent boundary layers is closely related to the anomalous transport problems. Furthermore, lower hybrid waves radiated by grill scatter on plasma density fluctuations. This may be very important for noninductive current drive in tokamaks. The dependence of lower hybrid wave scattering on the plasma density is discussed and the dependence of the wave scattering on the safety factor is presented. Author

**N91-10726#** Ceskoslovenska Akademie Ved, Prague. Inst. of Plasma Physics.

**COMMENTS ON EDGE TURBULENCE DURING LOWER HYBRID CURRENT DRIVE EXPERIMENT ON CASTOR TOKAMAK**

J. Stoeckel, L. Kryska, F. Zacek, and S. Nanobashvili (Academy of Sciences of the Georgian SSR, Tbilisi.) Mar. 1988 23 p
(IPPCZ-279) Avail: NTIS HC/MF A03

In present day tokamaks, the experimentally determined electron confinement time is roughly two orders of magnitude lower than the neoclassical prediction. A recent review of turbulence and anomalous transport identified both magnetic and electrostatic turbulence as candidates for inducing anomalous transport, but also concluded that their relative importance is unknown up to now. The preliminary measurements of the plasma edge fluctuations on the CASTOR tokamak are presented. Description of experiment including the discussion of Langmuir probe diagnostics is also presented. The preliminary experimental results concerning with some characteristic features on the edge electrostatic turbulence in Ohmical Heating (OH) regimes are compared with that of Lower Hybrid Current Drive (LHCD)/OH plasmas. The level of the edge turbulence was found sufficiently high to explain anomalous particle losses in the OH-discharge in tokamak and it decreases appreciably during the combined LHCD/OH regimes. This fact indicates an improvement of the particle confinement. Author

**N91-10727** Wisconsin Univ., Madison.

**TWO-DIMENSIONAL MAGNETOHYDRODYNAMIC EQUILIBRIA WITH FLOW AND STUDIES OF EQUILIBRIUM FLUCTUATIONS Ph.D. Thesis**

Yusuf Ziya Agim 1989 144 p
Avail: Univ. Microfilms Order No. DA9006866

A set of reduced ideal MHD (magnetohydrodynamic) equations is derived to investigate equilibria of plasmas with mass flow in general two-dimensional geometry. These equations provide a means of investigating the effects of flow on self-consistent equilibria in a number of new two-dimensional configurations such as helically symmetric configurations with helical axis, which are relevant to stellarators, as well as axisymmetric configurations. In the second part, magnetic fluctuations due to the thermally excited MHD waves are investigated using fluid and kinetic models to describe a stable, uniform, compressible plasma in the range above the drift wave frequency and below the ion cyclotron frequency. Dissert. Abstr.

**N91-10728** Wisconsin Univ., Madison.

**SELF-CONSISTENT FIELD ERROR EFFECTS IN REVERSED FIELD PINCH PLASMAS Ph.D. Thesis**

Kenneth Lee Sidikman 1990 291 p
Avail: Univ. Microfilms Order No. DA9013369

Magnetic field perturbations induced inside a reversed field pinch (RFP) plasma by field errors at the plasma edge are examined. Such perturbations can have an important effect on the plasma behavior. Some of the key features of the RFP depend upon an edge region of reversed toroidal field. Perturbations with poloidal mode number (m) equal to zero resonate with the plasma at the field reversal point and threaten to disrupt this region. Perturbations with m = 1 can influence the instabilities that play a role in maintaining the RFP state. In assessing these effects, it must be remembered that interaction with the plasma can also alter the perturbations. Such a calculation was undertaken, combining a field error model with a model of the RFP equilibrium and allowing their interaction to be computed via the three-dimensional magnetohydrodynamic (3-D MHD) equations. Realistic plasma features, such as a partially-relaxed equilibrium were incorporated. In addition, the use of a set of dynamical equations allowed perturbed flow and finite resistivity eta and viscosity (nu sub 0) to come into play. It is shown that all of these have measurable effects. Numerical simulations of the 3-D MHD equations were performed using a static equilibrium. An analytic investigation was performed to clarify the roles of finite grad-lambda and finite eta, nu(sub 0) in the plasma-perturbation interaction. Numerical simulations with an evolving equilibrium were also performed. Dissert. Abstr.

**N91-10729** California Univ., Los Angeles.

**PLASMA WAKEFIELD EXCITATION BY CHARGE PARTICLE BEAMS Ph.D. Thesis**

Jao-Jang Su 1990 159 p
Avail: Univ. Microfilms Order No. DA9016117

Electron plasma waves excited by a charge bunch are studied analytically and via computer simulations in full generality. Analytic results of plasma wakefield excitation are compared with particle-in-cell computer simulations both qualitatively and quantitatively. Doppler shifts and the nonlinear properties of plasma waves are included. One of the major goals is to study plasma applications to high energy physics. Accelerator physics issues, such as the transformer ratio, energy extraction efficiency, quality of the accelerated beam and the stability of the acceleration scheme, are discussed extensively. Simulations demonstrate 1 giga electron volt energy gain of a test particle in a short distance. A comparison of a computer simulation with a plasma wakefield experiment is given. Instabilities of the driving beam in the plasma wakefield accelerator are investigated. High luminosity is a major challenge for future colliders. The idea of focusing two colliding beams by thin plasma slabs is proposed. Dissert. Abstr.

**N91-10730** Wisconsin Univ., Madison.

**A COMPUTATIONAL MODEL FOR z-PINCH PLASMA CHANNELS Ph.D. Thesis**

Osman Yasar 1989 261 p
Avail: Univ. Microfilms Order No. DA9010339

An adaptive grid finite difference scheme was derived for simulating non-linear and unsteady one dimensional (planar, cylindrical and spherical) fluid flow by adapting to steep gradients in different physical quantities. The scheme is applied to z-pinch plasma channels that are used for ion beam transport in Light Ion Beam Fusion Reactor designs. The radiation emitted by the plasma seems to be vitally important for analyzing the formation of channels, requiring accurate methods that treat radiative transfer coupled to magnetohydrodynamics. The channel formation and ion beam injection is studied by simulations with a 1-D Adaptive Radiation Magnetohydrodynamics (ARMHD) computer code developed for the purpose of this thesis research. ARMHD models the plasma with single-fluid MHD equations, and solves for the radiation field intensity through the radiative transfer equation using a multi-group discrete ordinate S(sub N) method. The governing equations are hyperbolic conservation laws transformed to an adaptive grid reference frame that moves in time to follow the high gradients in the solutions. An explicit procedure based on the equidistribution principle is used to move the grid system to avoid the implicit coupling between the physical equations and the grid system. Adaptive gridding seems to be most effective in

flows with high gradient regions. For z-pinch plasma channel simulations, the adaption on temperature-momentum proves to be good in terms of the high mesh concentration it provides throughout the channel, where other quantities besides the temperature and momentum are also varying. Applications of ARMHD indicate the feasibility of using argon and nitrogen for plasma channels.
Dissert. Abstr.

**N91-10731#** International Centre for Theoretical Physics, Trieste (Italy).
**TEMPORAL BEHAVIOUR OF SELF GENERATED MAGNETIC FIELD AND ITS INFLUENCE ON INHIBITION OF THERMAL FLUX IN ICF PLASMA**
L. N. Jha (Tribhuvan Univ., Tripureswar, Nepal ) Jun. 1989 12 p Sponsored in part by Swedish Academy of Sciences and RONAST
(DE90-627478; IC-89/144) Avail: NTIS (US Sales Only) HC/MF A03

The self generated magnetic field of megagauss order is reported to play a crucial role in Inertial Confinement Fusion (ICF) target designs because of its strong influence on the transport of energy from the critical density region to the ablation layer. The inhibition of the thermal flux due to such a field, thus, affects the whole of the other phenomenon of ICF. The knowledge of the proper variation of the magnetic field may help in assigning the existing controversial value of flux limit, f. Many papers dealing with the spatial variation of such a field exist and are well documented but the study on the variation of self generated field with time is rare. Here, the spatial variation of the megagauss field generated in the corona of a wire target irradiated by a laser as well as a model to study the temporal nature of the B-field at the peak were obtained by solving the self inhibited diffusion which is regarded as the most dominant mechanism by which the thermal transport is influenced. The field exists for about ten nanoseconds even after the laser is switched off. The ratio of the two components of the thermal conductivity is also plotted against time and shows the inhibition. So, a track on the B-field variation both in space and time is necessary to keep for at least a few nanoseconds for computation of f. DOE

**N91-10732#** Lawrence Livermore National Lab., CA.
**A DISTRIBUTED CONTROL AND MONITOR SYSTEM USED IN LASER FUSION RESEARCH**
Bobby A. Jones and Nicholas J. Selchow May 1990 10 p Presented at the International Conference and Exhibition of the Instrument Society of America, New Orleans, LA, 14-19 Oct. 1990 Revised
(Contract W-7405-eng-48)
(DE90-013478; UCRL-101945-Rev-2; CONF-901017-1-Rev-2)
Avail: NTIS HC/MF A02

Laser Fusion research experiments require very low pressure environments to properly diagnose the plasma physics phenomena occurring during laser fusion reactions. Target chambers with very large and complex pumping systems are required to achieve and maintain these extremely low pressures. This paper describes a recently installed distributed control and monitoring system that automates the operation of these pumping systems. Through automation, this system is providing an enhanced shot rate by reducing the manpower required to ready the system for a target shot while increasing the overall safety of the system. DOE

**N91-10733#** Lawrence Livermore National Lab., CA.
**ELECTROMAGNETIC PARTICLE CODES ON UNSTRUCTURED GRIDS**
John J. Ambrosiano, Scott T. Brandon, and Rainald Loehner (George Washington Univ., Washington, DC.) Jun. 1990 10 p Presented at the Free Lagrange Conference, Jackson Lake, WY, 3-7 Jun. 1990
(Contract W-7405-eng-48)
(DE90-015187; UCRL-JC-104241; CONF-9006195-7) Avail: NTIS HC/MF A02

The most widely used computational model of collisionless plasmas is the Lagrangian-Eulerian hybrid technique known as particle-in-cell or PIC. In the electromagnetic version, Maxwell's equations are solved on an Eulerian grid and electromagnetic forces are interpolated from the grid to particle locations. Particles are then moved in Lagrangian fashion while their currents are interpolated back onto the grid to provide sources for the fields on the next cycle. There are many applications where one needs to model plasmas and electromagnetic waves inside regions of complicated shape. Traditional methods for solving Maxwell's equations employ finite differences on regular grids to replace differential operators. These methods are awkward for complicated boundary shapes, often replacing smoothly curved or slanted boundaries with stairsteps. The desire to incorporate realistic boundaries into plasma simulations is motivated by a host of situations in which proper representation of the boundary shape is expected to be critical. The approach to solving this problem is to design electromagnetic particle codes based on the use of unstructured grids. The arbitrary connectivity of unstructured grids provides the flexibility to place nodes wherever needed to fit the most complex boundary shapes. The most significant problems that must be addressed as a result of this strategy are grid generation, field solution, and particle tracking. The solutions to these problems, along with a few preliminary results, are presented. DOE

**N91-10734*#** Cornell Univ., Ithaca, NY. Lab. of Plasma Studies.
**A MATHEMATICAL MODEL OF THE STRUCTURE AND EVOLUTION OF SMALL SCALE DISCRETE AURORAL ARCS**
C. E. Seyler Jan. 1990 41 p
(Grants NAGw-1581; NSF ATM-89-00357)
(NASA-CR-187238; NAS 1.26:187238; LPS-90-1) Avail: NTIS HC/MF A03 CSCL 20I

A three dimensional fluid model which includes the dispersive effect of electron inertia is used to study the nonlinear macroscopic plasma dynamics of small scale discrete auroral arcs within the auroral acceleration zone and ionosphere. The motion of the Alfven wave source relative to the magnetospheric and ionospheric plasma forms an oblique Alfven wave which is reflected from the topside ionosphere by the negative density gradient. The superposition of the incident and reflected wave can be described by a steady state analytical solution of the model equations with the appropriate boundary conditions. This two dimensional discrete auroral arc equilibrium provides a simple explanation of auroral acceleration associated with the parallel electric field. Three dimensional fully nonlinear numerical simulations indicate that the equilibrium arc configuration evolves three dimensionally through collisionless tearing and reconnection of the current layer. The interaction of the perturbed flow and the transverse magnetic field produces complex transverse structure that may be the origin of the folds and curls observed to be associated with small scale discrete arcs. Author

**N91-10735*#** Hampton Inst., VA. Dept. of Physics.
**PLASMA PUFF INITIATION OF HIGH COULOMB TRANSFER SWITCHES Annual Progress Report, 1 Oct. 1989 - 30 Sep. 1990**
D. D. Venable and E. H. Choi 30 Sep. 1990 48 p
(Grant NAG1-970)
(NASA-CR-187024; NAS 1.26:187024) Avail: NTIS HC/MF A03 CSCL 20I

The plasma-puff triggering mechanism based on a hypocycloidal pinch geometry was investigated to determine the optimal operating conditions for the azimuthally uniform surface flashover which initiates plasma-puff under wide range of fill gas pressure of Ar, He and N2. The optimal fill gas pressure for the azimuthally uniform plasma-puff was about 120 mTorr and 450 Torr for He and N2, and between 120 mTorr and 5 Torr for Ar. The inverse pinch switch was triggered with the plasma-puff and the switching capability under various electrical parameters and working gas pressures of Ar, He and N2 was determined. It was also shown that the azimuthally uniform switching discharges were dependent on the type of fill gas and its fill pressure. A new concept of plasma-focus driven plasma-puff was also discussed in comparison with the hypocycloidal pinch plasma-puff triggering. The main discharge of inverse pinch switch with plasma-focus driven plasma-puff trigger is found to be more azimuthally uniform than that with hypocycloidal pinch plasma-puff trigger in a gas pressure region between 80 mTorr and 1 Torr. Author

**N91-10736#** Sandia National Labs., Albuquerque, NM.
**A REFRACTIVE INDEX GRADIENT (RING) DIAGNOSTIC FOR TRANSIENT DISCHARGES OR EXPANSIONS OF VAPOR OR PLASMAS**
M. E. Cuneo, T. R. Lockner, G. S. Tisone, K. W. Bieg, R. W. Stinnett, and J. R. Chavez (Ktech Corp., Albuquerque, NM.) 1990 8 p Presented at the 14th International Symposium on Discharges and Electrical Insulation in Vacuum, Santa Fe, NM, 17-20 Sep. 1990
(Contract DE-AC04-76DP-00789)
(DE90-015840; SAND-90-1002C; CONF-9009192-12) Avail: NTIS HC/MF A02

The use of lasers to measure plasma properties is well known. Common methods include interferometry (density), Schlieren (gradient of density), and shadowgraphy (derivative of gradient). The diagnostic described uses a fast silicon photodiode quadrant detector with a differential amplifier to temporally detect the refraction of a CW laser by transient discharges or expansions of vapor, gas or plasma. The laser beam is refracted by the gradient of the total index of refraction due to neutral and ionized atoms (positive index) and electrons (negative index) in those discharges. The output of the circuit is a voltage proportional to the deflection angle of the laser beam through the discharge. The method is a time-resolved, quantitative, species discriminating (i.e., atoms or electrons) Schlieren technique. The diagnostic is easy to field, sensitive 1.3 + or - 0.1 to 3.3 + or - 0.1 mv/mrad depending on laser power, divergence, moment arm and circuit gain) and fast (rise time = 11 (+ or -) 1 to 24 (+ or -) 1 ns depending on various circuit parameters). Diagnostic theory, and circuit design and performance is discussed. This Refractive INdex Gradient (RING) diagnostic was applied to measurements on several ion sources under development at Sandia for use on intense applied-B ion diodes in the light ion fusion program. Sources studied include different types of flashboards, a thermal evaporation lithium ion source, and a laser produced ion source. To illustrate the utility of this technique, examples of measurements on LEVIS (Laser EVaporation Ion Source), a laser produced active lithium ion source is given. Measured properties include vapor/plasma production thresholds, expansion velocities, some species information, gradient profiles, and estimates of density profiles. DOE

**N91-10737#** Sandia National Labs., Albuquerque, NM.
**THEORETICAL ANALYSIS OF A RUNAWAY ELECTRON SUPPRESSION DEVICE**
K. A. Niemer, J. G. Gilligan, C. D. Croessmann, and A. C. England (Oak Ridge National Lab., TN.) 1990 12 p Presented at the 16th Symposium on Fusion Technology, London, England, 3-7 Sep. 1990
(Contracts DE-AC04-76DP-00789; DE-AC05-84OR-21400)
(DE90-015992; SAND-90-2018C; CONF-900918-1) Avail: NTIS HC/MF A03

A new runaway electron suppression paddle was designed with the PTA code package to reduce the runaway electron population in the Advanced Toroidal Facility (ATF), Oak Ridge National Laboratory. The PTA code package is a unique application of PATRAN, the Integrated TIGER Series, and ABAQUS for modeling high energy electron impact on magnetic fusion components and materials. By its nature, ATF is susceptible to runaway electron formation and confinement resulting in the production of a high level of hard x rays near the machine. Four previous stainless steel paddles proved effective in reducing the runaway electron population; however, electrons above 15 MeV have still been observed. Melting and bending were observed in each of the previous paddles, reducing their effectiveness. Scoping experiments are under way to further characterize the runaway electrons in ATF. Data from these experiments will provide insight into runaway electron damage mechanisms. Proposals for the insertion of a new paddle in ATF are being considered. These analyses add to the knowledge of runaway electron damage and will aid in the design of future components to withstand runaway electron discharges in all magnetic fusion devices, including tokamaks. DOE

**N91-10738#** Washington Univ., Seattle.
**EXPERIMENTS ON LINEAR HIGH BETA HELICAL AXIS STELLARATORS TO STUDY SIMULATED TOROIDAL EFFECTS AND ALFVEN-WAVE HEATING Progress Report No. 4, 16 Jul. - 15 Nov. 1989**
F. L. Ribe and B. A. Nelson 1989 52 p
(Contract DE-FG06-87ER-53242)
(DE90-016122; DOE/ER-53242/4; UWAERP-23) Avail: NTIS HC/MF A04

Some of the experiments are as follows: induced axial current studies in a hardcore Theta Pinch; nonaxisymmetric RF heating of a high Beta plasma column; formation of Axisymmetric hardcore theta pinches with notched hardcore current; and externally driven till made experiments on the high beta Q machine field reversed configuration. DOE

**N91-10739#** Los Alamos National Lab., NM.
**CONFINEMENT STUDIES IN THE ZT-40M REVERSED FIELD PINCH**
Paul G. Weber, Kurt F. Schoenberg, John C. Ingraham, Guthrie Miller, Ronald W. Moses, Carter P. Munson, Richard A. Nebel, Mark M. Pickrell, Glen A. Wurden, and Hermann Y. W. Tsui (Texas Univ., Austin.) et al 1990 9 p Presented at the 13th International Conference on Plasma Physics and Controlled Nuclear Fusion Research, Washington, DC, 1-6 Oct. 1990
(Contract W-7405-eng-36)
(DE90-016442; LA-UR-90-2868; CONF-901025-3; IAEA-CN-53/C-2-2(1)) Avail: NTIS HC/MF A02

Measurement of electrostatic and magnetic fluctuations in the ZT-40M Reversed Field Pinch (RFP) are used to estimate fluctuation driven transport. Edge electrostatic fluctuations appear to explain edge particle transport, analogously to some tokamak and stellarator observations. However, in contrast to tokamaks, electrostatic fluctuations do not explain the heat flux through the edge. Instead, transport of suprathermal electrons along fluctuating magnetic field lines constitute the major electron heat loss. Ion losses in ZT-40M appear to be dominated by charge exchange. DOE

**N91-10740#** Los Alamos National Lab., NM.
**TILT STABILITY AND COMPRESSION HEATING STUDIES OF FIELD-REVERSED CONFIGURATIONS**
D. J. Rej, M. Tuszewski, D. C. Barnes, G. A. Barnes, R. E. Chrien, R. E. Siemon, D. P. Taggart, R. B. Webster, B. L. Wright, and R. D. Milroy (Spectra Technology, Inc., Bellevue, WA.) et al 1990 7 p Presented at the 13th International Conference on Plasma Physics and Controlled Nuclear Fusion Research, Washington, DC, 1-6 Oct. 1990
(Contract W-7405-eng-36)
(DE90-016443; LA-UR-90-2864; CONF-901025-2; IAEA-CN-53/C-4-4) Avail: NTIS HC/MF A02

The first observations of internal tilt instabilities in field-reversed configurations (FRCs) are reported. Detailed comparisons with theory establish that data from an array of external magnetic probes are signatures of these destructive plasma instabilities. Theory and experiments are reconciled which suggests that grossly stable FRCs are restricted to very kinetic and elongated plasmas. Self-consistent 3-D numerical simulations demonstrate tilt stabilization by the addition of a beam ion component. High power compression heating experiments with stable equilibrium FRCs are also reported. Plasmas formed in a tapered theta-pinch coil were translated along a guide magnetic field into a new single-turn compression coil where the external field is increased up to 7 times the initial value in 55 microsecs. Substantial heating is observed accompanied by a decrease in confinement time. DOE

**N91-10741#** Wisconsin Univ., Madison. Dept. of Nuclear Engineering.
**MODELS OF PLASMA CONFINEMENT AND HEATING IN TOKAMAKS**
J. D. Callen Sep. 1989 193 p
(Contract DE-FG02-86ER-5321)
(DE90-016671; UWPR-89-2) Avail: NTIS HC/MF A09

This report discusses the following topics: introduction to fusion and tokamaks; tokamak equilibria; ideal magnetohydrodynamic (MHD) stability; resistive MHD instabilities; particle orbits; classical transport in magnetized plasmas; neoclassical transport; models of anomalous transport; auxiliary heating and current-drive; plasma modelling; and tokamak fusion reactor issues and summary. DOE

**N91-10742#** Oak Ridge National Lab., TN.
**PELLET INJECTOR DEVELOPMENT AT ORNL (OAK RIDGE NATIONAL LABORATORY)**
M. J. Gouge, B. E. Argo, L. R. Baylor, S. K. Combs, D. T. Fehling, P. W. Fisher, C. A. Foster, C. R. Foust, S. L. Milora, and A. L. Qualls et al 1990 6 p Presented at the 16th Symposium on Fusion Technology, London, England, 3-7 Sep. 1990
(Contract DE-AC05-84OR-21400)
(DE90-017024; CONF-900918-4) Avail: NTIS HC/MF A02

Advanced plasma fueling systems for magnetic confinement experiments are under development at Oak Ridge National Laboratory (ORNL). The general approach is that of producing and accelerating frozen hydrogenic pellets to speeds in the kilometer-per-second range by either pneumatic (light-gas gun) or mechanical (centrifugal force) techniques. ORNL has recently provided a centrifugal pellet injector for the Tore Supra tokamak and a new, simplified, eight-shot pneumatic injector for the Advanced Toroidal Facility stellarator at ORNL. Hundreds of tritium and DT pellets were accelerated at the Tritium Systems Test Assembly facility at Los Alamos in 1988 to 1989. These experiments, done in a single-shot pipe-gun system, demonstrated the feasibility of forming and accelerating tritium pellets at low (sup 3)He levels. A new, tritium-compatible extruder mechanism is being designed for longer-pulse DT applications. Two-stage light-gas guns and electron beam rocket accelerators for speeds of the order of 2 to 10 km/s are also under development. Recently, a repeating, two-stage light-gas gun accelerated 10 surrogate pellets at a 1-Hz repetition rate to speeds in the range of 2 to 3 km/s; and the electron beam rocket accelerator completed initial feasibility and scaling experiments. ORNL has also developed conceptual designs of advanced plasma fueling systems for the Compact Ignition Tokamak and the International Thermonuclear Experimental Reactor. DOE

**N91-10743#** Texas Univ., Austin. Inst. for Fusion Studies.
**TEARING MODES IN TOKAMAKS WITH LOWER HYBRID CURRENT DRIVE**
X. Q. Xu and M. N. Rosenbluth (California Univ., San Diego, La Jolla.) Aug. 1990 22 p
(Contract DE-FG05-80ET-53088)
(DE90-017090; DOE/ET-53088/444; IFSR-444) Avail: NTIS HC/MF A03

The effect of current drive on the tearing modes in the semi-collisional regime is analyzed using the drift-kinetic equation. A collisional operator is developed to model electron parallel conductivity. For the pure tearing modes the linear and quasilinear growth rates in the Rutherford regimes were found to have roughly the same forms with a modified resistivity as without current drive. One interesting result is the prediction of a new instability. This instability, driven by the current gradient inside the tearing mode layer, is possibly related to MHD behavior observed in these experiments. DOE

**N91-10744#** Texas Univ., Austin. Inst. for Fusion Studies.
**UNIFIED THEORY OF BALLOONING INSTABILITIES AND TEMPERATURE GRADIENT DRIVEN TRAPPED ION MODES**
X. Q. Xu and M. N. Rosenbluth (California Univ., San Diego, La Jolla.) Aug. 1990 24 p
(Contract DE-FG05-80ET-53088)
(DE90-017091; DOE/ET-53088/443; IFSR-443) Avail: NTIS HC/MF A03

A unified theory of temperature gradient driven trapped ion modes and ballooning instabilities is developed using kinetic theory in banana regimes. All known results, such as electrostatic and purely magnetic trapped particle modes and ideal MHD ballooning modes (or shear Alfven waves) are readily derived from the single general dispersion relation. Several new results from ion-ion collision and trapped particle modification of ballooning modes are derived and discussed and the interrelationship between those modes is established. DOE

**N91-10745#** Texas Univ., Austin. Inst. for Fusion Studies.
**NUMERICAL SIMULATION OF ION TEMPERATURE GRADIENT DRIVEN MODES IN THE PRESENCE OF ION-ION COLLISIONS**
X. Q. Xu and M. N. Rosenbluth (California Univ., San Diego, La Jolla.) Aug. 1990 51 p
(Contracts DE-FG05-80ET-53088; DE-FG03-88ER-53275)
(DE90-017092; DOE/ET-53088/445; IFSR-445) Avail: NTIS HC/MF A04

Ion temperature gradient driven modes in the presence of ion-ion collisions in a toroidal geometry with trapped ions were studied by using a 1 2/2 d linearized gyro-kinetic particle simulation code in the electrostatic limit. The purpose is to try to understand the physics of flat density discharges, in order to test the marginal stability hypothesis. Results giving threshold conditions of L sub Ti/R sub 0, an upper bound on k sub chi, and linear growth rates and mode frequencies over all wavelengths for the collisionless ion temperature gradient driven modes are obtained. The behavior of ion temperature gradient driven instabilities in the transition from slab to toroidal geometry, with trapped ions, is shown. A Monte Carlo scheme for the inclusion of ion-ion collisions, in which ions can undergo Coulomb collisional dynamical friction, velocity space diffusion and random walk of guiding centers, was constructed. The effects of ion-ion collisions on the long wave length limit of the ion modes is discussed. DOE

**N91-10746#** New York Univ., New York. Inst. of Mathematical Sciences.
**PLASMA PROPERTIES Progress Report**
1990 15 p
(Contract DE-FG02-86ER-53223)
(DE90-017256; DOE/ER-53223/145) Avail: NTIS HC/MF A03

The confinement of fusion plasma by strong magnetic fields is discussed. The effects of MHD instabilities and charged particle transport are investigated. DOE

**N91-10747#** Wisconsin Univ., Madison. Dept. of Physics.
**THEORETICAL STUDIES OF TURBULENCE AND ANOMALOUS TRANSPORT IN TOROIDAL CONFINEMENT DEVICES**
P. W. Terry 1990 11 p
(Contract DE-FG02-89ER-53291)
(DE90-017606; DOE/ER-53291/1) Avail: NTIS HC/MF A03

The research performed under this grant during the current year has focused on key issues with respect to turbulence and transport in toroidal confinement devices. This work includes theoretical and computational studies of electron thermal confinement which have concentrated on the role of sheared poloidal flow in suppressing turbulence and transport, trapped ion convective cell turbulence and microtearing turbulence; analytical studies of anomalous particle transport and pinch mechanisms, and comparison with experimental measurement; development of the theory of self-consistent radial transport of field-aligned momentum in the tokamak and reverse-field pinch (RFP); and work on other topics (ion temperature gradient driven turbulence, RFP fluctuation theory, coherent structures). Progress and publications in these areas are briefly summarized in this report. DOE

**N91-10748#** Wisconsin Univ., Madison.
**STELLARATOR THEORY**

1990 6 p
(Contract DE-FG02-85ER-53201)
(DE90-017607; DOE/ER-53201/T5) Avail: NTIS HC/MF A02

This report is principally concerned with explaining the progress which has been made in developing and applying our kinetic plasma model, in sufficient detail to demonstrate the main issues involved. At the end of this paper we briefly discuss work we have done in other areas of stellarator theory. DOE

**N91-10749#** National Inst. for Fusion Science, Nagoya (Japan).
**THEORY OF LONGITUDINAL ADIABATIC INVARIANT IN THE HELICAL TORUS**
Jiro Todoroki Aug. 1990 35 p
(NIFS-37; ISSN-0915-633X) Avail: NTIS HC/MF A03

The theory on the longitudinal adiabatic invariant valid for the helical magnetic field is developed on the basis of the variable transformation from the guiding center variables to the new adiabatic variables. The theory uses the Hamiltonian formalism with non canonical variables. Under the assumption that the rotational transform per period is small, the adiabatic invariant is defined by integral along the toroidal direction, not along the field line. The transition between the passing and the ripple trapped states is investigated; the jump of adiabatic invariant and other variables in the transition process is evaluated. The change of distribution function in the variable transformation is also discussed. Author

**N91-10750#** National Inst. for Fusion Science, Nagoya (Japan).
**RF HELICITY INJECTION AND CURRENT DRIVE**
K. Hamamatsu, A. Fukuyama, S.-I. Itoh, K. Itoh, and M. Azumi (Japan Atomic Energy Research Inst., Naka.) Jul. 1990 37 p
(NIFS-34; ISSN-0915-633X) Avail: NTIS HC/MF A03

The relation between (Range of Frequency) RF-driven current and wave helicity is analytically and numerically studied for tokamak plasma. The helicity conversion coefficient from the wave to the plasma is generally obtained and numerically examined for the waves in the range of ion cyclotron frequency. The wave propagation equation is solved as a boundary-value problem with one-dimensional inhomogeneities. It is shown that the wave helicity well satisfies the continuity equation. It was confirmed that the RF-helicity injection is not an identical phenomenon of the reduction of the one turn loop voltage due to the RF-driven current. Author

**N91-10751#** National Inst. for Fusion Science, Nagoya (Japan).
**DIRECT EXTRACTION OF A Na(-) BEAM FROM A SODIUM PLASMA**
Mamiko Sasao, Hitoshi Yamaoka, Motoi Wada, and Junji Fujita (Doshisha Univ., Kyoto, Japan ) Jul. 1990 18 p
(NIFS-35; ISSN-0915-633X) Avail: NTIS HC/MF A03

Negative sodium ions Na(-) were extracted from a small multi-cusp ion source. A steady state sodium plasma was produced by primary electrons in a sodium gas evaporating from a metal sample placed in the discharge chamber. The Na(-) current density of 1.5 microA/sq cm was obtained from a single aperture of 1.5 mm at relatively low discharge power of about 0.4 W and filament power of 50 W. Extraction characteristics were studied by changing the plasma electrode bias. The extracted Na(-) current showed dependence on the bias voltage similar to that of H(-) or Li(-) volume production. Author

**N91-10752#** National Inst. for Fusion Science, Nagoya (Japan).
**ANOMALOUS VISCOSITY DUE TO DRIFT WAVE TURBULENCE**
S.-I. Itoh Jun. 1990 25 p Sponsored by Grant-in-Aid for Scientific Research for MoE, Japan
(NIFS-33; ISSN-0915-633X) Avail: NTIS HC/MF A03

Anomalous ion, electron viscosities and off-diagonal elements of transport matrix in the presence of low frequency microturbulence are calculated. Quasilinear theory is used in the electrostatic limit. Symmetric matrix is obtained including the off-diagonal terms. The electron and ion components in transport matrix apparently decouple in the drift wave approximation. Particle, momentum and energy fluxes are presented in terms of three thermodynamical forces, where the gradient of parallel flow is included. Particle and energy fluxes are driven by density gradient, temperature gradient, radial electric field and convection due to the fluctuations. Anomalous electron viscosity is found to be very small. Ion anomalous viscosity, heat conductivity and off-diagonal elements are comparable to the coefficients for electrons. The transport equations of ions show that off-diagonal element reduces the heat conductivity and even causes the anomalous heat pinch effect. Anomalous viscosity gives rise to additional heating on ions due to viscous damping. Author

**N91-10753** Max-Planck-Inst. fuer Physik und Astrophysik, Garching (Germany, F.R.). Inst. fuer Extraterrestrische Physik.
**EXAMINATION OF ION ACCELERATION IN THE PLASMA LAYER DURING MAGNETOSPHERIC PARTIAL GALES [UNTERSUCHUNGEN ZUR BESCHLEUNIGUNG VON IONEN IN DER PLASMASCHICHT WAEHREND MAGNETOSPHAERISCHER TEILSTUERME]**
Doris Sachsenweger Feb. 1990 177 p In GERMAN
(MPE-218; ISSN-0178-0719; ETN-90-97871) Copyright Avail: Fachinformationszentrum Karlsruhe, 7514 Eggenstein-Leopoldshafen 2, Fed. Republic of Germany

The existing acceleration and heating process of ions, and the modification of the relative contributions of the two sources of the plasma layer, solar wind and ionosphere, depending on the magnetic activity, are investigated. To this aim, measurements of loading and mass structure and the spectra of superthermic ions in the plasma layer are evaluated. They were taken in detail with the flying time spectrometer SULEICA on the AMPTE/IRM satellite. Two partial gale events are examined. The observations are compared to a model, in which the ions are accelerated through electric fields. The computations and the numerical calculations show that the flow variations observed through an acceleration in electric fields, either together with a scattering of Alfven wave high amplitude, or in the case of ion beams in the boundary layer, can be explained under the form of a flow layer acceleration. ESA

**N91-10754#** Oxford Univ. (England). Dept. of Engineering Science.
**PASSIVE-FILTERED AND ACTIVE-DRIVEN PROBES FOR RF PLASMAS**
B. M. Annaratone and N. S. J. Braithwaite 1989 8 p
(OUEL-1806/89; ETN-90-97915) Avail: NTIS HC/MF A02

The use of electrostatic probes in processing plasmas which are generated by RF (13.56 MHz) excitation is addressed. The chief problems for probes in these plasmas arises from the RF fluctuations of space potential. At this operating frequency cable capacitance is a considerable load. Owing to the nonlinear nature of the probe characteristic the averaging process distorts the data. The favored solution is to ensure that the RF component of the potential between the plasma and the probe circuit is prevented from appearing across the sheath around the probe tip and also from charging the cable capacitance. Two differently designed probes were tested simultaneously in the same RF plasma discharge, and the performances are analyzed. ESA

## 76 SOLID-STATE PHYSICS

Includes superconductivity.

For related information, see also *33 Electronics and Electrical Engineering* and *36 Lasers and Masers.*

**N91-10755*#** Alabama Univ., Huntsville.
**THE GROWTH OF ZINC SELENIDE SINGLE CRYSTALS BY PHYSICAL VAPOR TRANSPORT IN MICROGRAVITY**
**Semiannual Status Report No. 2, 1 Nov. 1989 - 31 Mar. 1990**
Elmer E. Anderson, Franz E. Rosenberger, and Hai-Yuin Cheng
5 Jun. 1990 23 p Original contains color illustrations
(Grant NAG8-767)

(NASA-CR-180428; NAS 1.26:180428) Avail: NTIS HC/MF A03; 4 functional color pages CSCL 20L

Growth and characterization studies will be performed on zinc selenide single crystals. The high temperature outgassing behavior of the silica ampoule material will be studied in order to develop a cleaning and bake-out procedure that will minimize the amount of impurities introduced into the vapor from the ampoule materials and in particular during the seal-off procedure. The outgassing behavior of the ZnSe starting material will be studied during high vacuum refinement at elevated temperatures in order to develop a temperature pressure program that will optimize the removal of impurities while minimizing a shift in stoichiometry due to preferred evaporation of the higher fugacity component. The mass spectrometer system was completed, and after calibration, will be used to perform the above tasks. The system and its operation is described in detail. E.R.

**N91-10756#** Midwest Research Inst., Golden, CO. Solar Energy Research Inst.

**ION-ASSISTED DOPING OF 2-6 COMPOUNDS DURING PHYSICAL VAPOR DEPOSITION**

R. H. Bube, A. L. Farenbruch, A. Lopez-Otero, K.-F. Chien, M. Grimbergen, D. Kim, and P. Sharps Jul. 1990 85 p
(Contract DE-AC02-83CH-10093)
(DE90-000358; SERI/TP-211-3907) Avail: NTIS HC/MF A05

This report describes a research program to (1) investigate ion-assisted doping during chemical vapor deposition of CdTe and (2) determine the influence of co-depositing ionized dopant atoms in the growth and structural and photoelectronic properties of the deposited films. In p-CdTe homo-epitaxial films, we controlled doping up to about 6 x 10(exp 16) cm(exp-3) and 2 x 10(exp 17) cm(exp-3) or ion-assisted depositions with As and P ions, respectively. At a growth rate of approximately 0.1 microns/min., a substrate temperature of 400 C, and ion energy of 60 eV, a maximum doping density was found near an ion current of 0.6 microamps/cm(exp 2). Related studies included elucidating the role of low-energy ion damage in the ion-assisted doping process, and investigating the decrease in carrier density near the surface of p-CdTe upon heating in vacuum, H(sub 2), or Ar. We demonstrate the ability to make carrier density profiles and to grade junctions, and we present preliminary results from polycrystalline p-CdTe films grown on graphite and alumina substrates. We also present solar cells prepared using the p-CdTe as the collector area and n-CdS as the window layer, and we examine their photovoltaic parameters for different carrier densities and configurations in p-CdTe. DOE

**N91-10757#** Argonne National Lab., IL.

**HIGH-TEMPERATURE SUPERCONDUCTORS: THEIR POTENTIAL FOR UTILITY APPLICATIONS**

R. F. Giese, T. P. Sheahen, A. M. Wolsky, and D. K. Sharma (Electric Power Research Inst., Palo Alto, CA.) 1990 7 p Presented at the 1st Joint IEEE/PES International Power Meeting, New Delhi, India, 28 Oct. - 1 Nov. 1990
(Contract W-31-109-eng-38)
(DE90-009704; CONF-901062-1) Avail: NTIS HC/MF A02

A number of proposed applications of superconductivity for the electric utility sector are described, the current status of their development is summarized, and the potential impact of successful development of high-temperature superconductors (HTSC's) is discussed. Performance goals for development of HTSCs are presented and compared with the current status of development of HTSCs. Applications discussed include large-scale generators, motors, transmission lines, magnetic storage, transformers, power electronics, and fault-current limiters. DOE

**N91-10758#** Oak Ridge National Lab., TN.

**PREPARATION OF SUPERCONDUCTING WIRE BY DEPOSITION OF YBa2Cu3O(x) ONTO FIBERS**

W. J. Lackey, J. A. Hanigofsky, M. J. Shapiro, W. B. Carter, D. N. Hill, E. K. Barefield, E. A. Judson, D. F. OBrien, Y. S. Chung, and T. S. Moss et al 1990 16 p Presented at the 11th International Conference on Chemical Vapor Deposition, Seattle, WA, 14-19 Oct. 1990 Prepared in cooperation with Georgia Inst. of Tech., Atlanta Sponsored in part by DARPA and Navy
(Contract DE-AC05-84OR-21400)
(DE90-013380; CONF-901088-3) Avail: NTIS HC/MF A03

A controllable process was developed for chemical vapor deposition of superconducting YBa2Cu3O(x). The process relies on feeding and transport of a finely ground powder mixture of Y, Ba, and Cu tetramethylheptanedionates into a CVD furnace. X ray diffraction, scanning electron microscopy, analytical electron microscopy, analytical electron microscopy, resistance versus temperature, and critical current measurements have been used to characterize the films. The optimum processing parameters were determined using parametric studies involving temperature, pressure, reagent feed rate and composition, and coating time. Extensive c-axis orientation was observed using x ray diffraction and transmission electron microscopy. The presence of impurity phases and substrate coating interaction layers were observed. YBa2Cu3O(x) coatings on MgO (100) single crystal substrates exhibited critical currents of 2 x 10(exp 4) A sq cm at 77 K, 0 Tesla, with critical temperatures of 86 K. Deposition of the YBa2Cu3O(x) material onto several fibrous substrates was achieved, and a continuous fiber coating furnace is in operation. DOE

**N91-10759#** Argonne National Lab., IL. Materials and Components Technology Div.

**IMPACT OF HIGH-CRITICAL-TEMPERATURE SUPERCONDUCTORS ON ELECTROMAGNETIC PUMP APPLICATIONS**

J. L. Krazinski, R. E. Holtz, and R. A. Jaross May 1990 48 p Sponsored in part by Electric Power Research Inst.
(Contract W-31-109-eng-38)
(DE90-014809; ANL/MCT-90/1) Avail: NTIS HC/MF A04

The impact is studied of the development of practical, high critical temperature superconducting materials on applications involving electromagnetic (EM) pumping. Potential improvements in the operating characteristics of EM pumps were examined for current pump technology. In addition, the study addressed whether the development of high (Tc) superconductors could enable the implementation of EM pumps in applications where it has not been previously feasible. This assessment focused on two specific types of EM pumps: helical rotor pumps with rotating field coils and EM thruster pumps for ship propulsion. The design and performance of helical rotor pumps were analyzed for both liquid metals and nonmetallic fluids. For liquid metals, the impact of superconductors on the pump size, mass, and efficiency was examined for EM pumps operating at relatively lower magnetic field strengths. For nonmetallic fluids, the study investigated whether the use of high magnetic field strengths, in conjunction with high (Tc) superconductors, could enable the pumping of these fluids with EM pumps of reasonable size and efficiency. The impact of high (Tc) superconducting materials on the reliability and economics of EM pumps was also examined. In addition, the study assessed the impact of high field strength, superconducting magnets on the feasibility of using EM thrusters for ship propulsion. Parametric studies were conducted on the effects of magnetic field strength, thruster size, vessel speed, and vessel size on the predicted thruster efficiencies. The results were compared with these of earlier studies on electromagnetic propulsion that incorporated both superconducting and nonsuperconducting magnet designs. DOE

**N91-10760#** Brookhaven National Lab., Upton, NY. Dept. of Physics.

**MUON SR AND HIGH T(SUB c) SUPERCONDUCTIVITY**

V. J. Emery 1990 13 p Presented at the 5th International Conference on Muon Spin Rotation, Relaxation and Resonance, Oxford, England, 9-12 Apr. 1990
(Contract DE-AC02-76CH-00016)
(DE90-015089; BNL-44819; CONF-900489-2) Avail: NTIS HC/MF A03

Some implications of Muon Spin Rotation experiments on high temperature superconductors are discussed. The possible relationship between the observation of spin freezing and the tendency of mobile holes to phase separate is considered. Measurements of the magnetic penetration depth as a function of doping are shown to imply that a non-retarded, or high energy scale pairing interaction is responsible for high temperature superconductivity. The depression of the transition temperature at high doping is associated with a crossover away from the regime in which a charge transfer gap is relevant. DOE

**N91-10761#** Oak Ridge National Lab., TN. Solid State Div.
**RADIATION DAMAGE IN Al2O3 CRYSTALS IMPLANTED WITH 3.8 MeV Fe(2+)**
Y. Chen, M. M. Abraham, and D. F. Pedraza 1990 14 p
Presented at the 7th International Conference on Ion Beam Modification of Materials, Knoxville, TN, 9-14 Sep. 1990
(Contract DE-AC05-84OR-21400)
(DE90-016038; CONF-900936-1) Avail: NTIS HC/MF A03

Sapphire alpha Al2, O3 crystals were implanted with 3.8 MeV Fe(2+) ions to fluences of 0.5 times 10 to the 16th power and 2 times 10 to the 16th power cm(-2). The sample face was perpendicular to the c-axis. The radiation damage produced by the implantation was investigated using optical and electron paramagnetic resonance (EPR) techniques. The former encompassed optical absorption and luminescence. The predominant defect detected optically was the oxygen vacancy with two electrons (F center), identified by an absorption peak at 6.2 eV (approximately 200 nm). The paramagnetic oxygen vacancy with one electron (F(sup plus) center) absorbs at 4.8 eV (approximately 260 nm) and was identified by EPA. Divacancies in various charge states were present in much lower concentrations and could not be unambiguously identified by optical absorption. Instead, they were detected by the highly sensitive luminescence measurements. Upon isochronal annealing between 500 and 1200 K, the concentration of the F center decreased monotonically. No evidence of the F(+)-center found after annealing at 800 K. On the other hand, the concentration of the higher order defects initially increased, presumably at the expense of the oxygen vacancies, and subsequently also decreased. DOE

**N91-10762#** Sandia National Labs., Albuquerque, NM.
**MEASURED SILICON DISPLACEMENT DAMAGE RATIOS SUPPORT THE NEED TO REPLACE THE ASTM E-722 DAMAGE FUNCTION WITH THE NJOY CALCULATED FUNCTION**
J. G. Kelly and P. J. Griffin 1990 10 p Presented at the 7th ASTM-Euratom Symposium on Reactor Dosimetry, Strasbourg, France, 27-31 Aug. 1990
(Contract DE-AC04-76DP-00789)
(DE90-016225; SAND-89-2284C; CONF-900814-8) Avail: NTIS HC/MF A02

Experiments with discrete silicon bipolar transistors exposed to 14 MeV neutrons and Sandia Pulsed Reactor (SPR III) fission type neutrons demonstrate that the silicon damage function listed in ASTM standard E-722 needs to be replaced by the NJOY calculated function to ensure simulation fidelity in testing for transient radiation effects in electronic devices. An annealing procedure applied between exposures ensured accurate damage comparisons between the two environments. Re-evaluation of the dosimetry foil cross sections and fluence determination methodology was also necessary to ensure that damage per neutron/sq cm could be evaluated properly. The results provide a clear distinction between the two damage predictions and show that the NJOY function is the one of choice. DOE

**N91-10763*#** Howard Univ., Washington, DC. Dept. of Physics.
**EVALUATION, DEVELOPMENT, AND CHARACTERIZATION OF SUPERCONDUCTING MATERIALS FOR SPACE APPLICATIONS Semiannual Report**
Arthur N. Thorpe Sep. 1990 29 p
(Grant NAG5-1017)
(NASA-CR-187017; NAS 1.26:187017) Avail: NTIS HC/MF A03
CSCL 20L

The anisotropic electromagnetic features of a grain-aligned YBa2Cu3O(x) bulk sample derived from a process of long-time partial melt growth were investigated by the measurements of direct current magnetization (at 77 K) and alternating current susceptibility as a function of temperature, with the fields applied parallel and perpendicular to the c axis, respectively. The extended Bean model was further studied and applied to explain the experimental results. Upon comparison of the grain-aligned sample with pure single crystal materials, it is concluded that because of the existence of more effective pinning sites in the grain-aligned sample, not only its critical current density perpendicular to the c axis is improved, but the one parallel to the c axis is improved even more significantly. The anisotropy in the critical current densities in the grain-aligned sample at 77 K is at least one to two orders of magnitude smaller than in the pure single crystal. The measurement of anisotropy of alternating current susceptibility as a function of temperature, especially its imaginary part, shows that there are still some residues of interlayer weak links in the grain-aligned samples, but they are quite different from and far less serious than the weak links in the sintered sample. Author

**N91-10764#** Colorado School of Mines, Golden. Dept. of Physics.
**PHYSICAL AND ELECTRONIC STRUCTURE OF THE ELECTROLYTE-SOLID INTERFACE THROUGH OPTICAL PHENOMENA Progress Report, 1 Jan. 1989 - 30 Jun. 1990**
T. E. Furtak Jul. 1990 26 p
(Contract DE-FG02-86ER-45253)
(DE90-015935; DOE/ER-45253/5) Avail: NTIS HC/MF A03

The goal was to develop and exploit new techniques, primarily optical, which can be used to reveal the microscopic details of the electrolyte-solid interface. The most significant recent advance was in the area of second harmonic reflectance spectroscopy. Initial studies were completed of the Ag(111) electrode in which the anisotropic character of the second order effect was used to extract the essential susceptibility contributions as a function of the incident photon energy. Other studies along this direction include an in-depth treatment of Cd on Ag(111). In summary, the goal was reached of establishing a multi-technique approach to the study of elementary excitations as the electrolyte-solid interface. Several central phenomena involving these probes were explored and good progress was made toward understanding the optical interactions with a detail not previously achieved. DOE

**N91-10765#** Sandia National Labs., Albuquerque, NM. Solid State Theory Div.
**RENORMALIZATION FROM DENSITY FUNCTIONAL THEORY STRONG COUPLING MODELS FOR THE ELECTRONIC STRUCTURE OF La2CuO4**
Mark S. Hybertsen, Michael Schluter (Bell Telephone Labs., Inc., Murray Hill, NJ.), E. B. Stechel, and D. R. Jennison 1989 9 p
Presented at the Materials Research Society Fall Meeting, Boston, MA, 27 Nov. - 2 Dec. 1989
(Contract DE-AC04-76DP-00789)
(DE90-015990; SAND-89-2771C; CONF-891119-136) Avail: NTIS HC/MF A02

Strong coupling models for the electronic structure of La2CuO4 are derived in two successive stages of renormalization. First, a three-band Hubbard model is derived using a constrained density functional approach. Second, exact diagonalization studies of finite clusters within the three band Hubbard model are used to select and map the low energy spectra onto effective one-band Hamiltonians. At each stage, some observables are calculated and found to be in quantitative agreement with experiment. The final results suggest the given models to be adequate descriptions of the low energy scale dynamics. DOE

**N91-10766#** Pacific Northwest Lab., Richland, WA.
**PROPERTIES OF REACTIVELY-DEPOSITED SiC AND GeC ALLOYS**
P. M. Martin, J. W. Johnston, and W. D. Bennett Jun. 1990 8 p Presented at the SPIE's International Symposium on Optical and Optoelectronic Applied Science and Engineering Exhibit, San Diego, CA, 8-13 Jul. 1990

(Contract DE-AC06-76RL-01830)
(DE90-016363; PNL-SA-17876; CONF-900756-35) Avail: NTIS HC/MF A02

Thin-film silicon carbide, Si(x)C(1-x) and germanium carbon, Ge(x)C(1-x), alloy coatings with low infrared optical absorption have been fabricated by dc- and rf-reactive magnetron sputtering. The optical and mechanical properties of the coatings depend on composition determined by deposition conditions. The refractive index and optical absorption coefficient of Si(x)C(1-x) alloys were varied from those of amorphous Si to those near diamond-like carbon (DLC) by increasing C content. The band edge shifted below 1.2 eV with C content as high as 0.8. The useful range of the Si(x)C(1-x) coatings was extended to wavelengths as low as 1 micron. The useful transparency range of Ge(x)C(1-x) coatings is from 3 to 12 microns. The refractive index of Ge(x)C(1-x) coatings was varied from 4.2 of amorphous Ge to near 3.4 by increasing x from 0 to 0.5. The optical absorption coefficient was a complex function of composition and C-H, Ge-H, and Ge-C bonding. Mechanical stress in both materials was generally moderate, and increased with increasing C content for the GeC alloys and decreased with increasing C or the SiC alloys. The wide range of optical properties obtainable for both coating types makes them useful in many types of multilayer designs. Abrasion-resistant infrared (IR) multispectral antireflection coatings on zinc sulfide (ZnS) were demonstrated using Ge0.9C0.1 and DLC layers. DOE

**N91-10767#** Los Alamos National Lab., NM.
**NONLINEAR OPTICAL ABSORPTION IN INTRINSIC STARK EFFECT SUPERLATTICES**
B. K. Laurich, D. L. Smith, D. E. Watkins, I. Sela, H. Kroemer, and S. Subbanna (California Univ., Santa Barbara.) 1990 12 p Presented at the Superlattices and Microstructures, Berlin, Fed. Republic of Germany, 13-16 Aug. 1990
(Contract W-7405-eng-36)
(DE90-016466; LA-UR-90-2632; CONF-9008143-1) Avail: NTIS HC/MF A03

We have investigated the nonlinear optical properties of a new class of strained-layer superlattices, the intrinsic Stark effect superlattices (ISES). The superlattices consisted of GaInAs/GaAs grown along the (211)B direction. We observed a shift of the excitonic absorption to higher energies (blue shift) with increasing intensity of the transmitted beam. The observed optical nonlinearity was one order of magnitude stronger than the one due to excitonic screening in the (100) oriented reference material. This effect is attributed to the screening of the internal electric fields by photogenerated carriers. DOE

**N91-10768#** Los Alamos National Lab., NM.
**COPPER NMR AND HOLE DEPLETION IN THE NORMAL STATE OF Y(1-x)Pr(x)Ba2Cu3O7**
D. E. MacLaughlin, A. P. Reyes, M. Takigawa, P. C. Hammel, R. H. Heffner, J. D. Thompson, and J. E. Crow (Temple Univ., Philadelphia, PA.) 1990 26 p Presented at the 6th International Conference on Valence Fluctuations, Rio de Janeiro, Brazil, 9-13 Jul. 1990 Submitted for publication Sponsored in part by University of California Riverside Academic Senate Committee on Research and University of California INCOR Program in High-Temperature Superconductivity
(Contract W-7405-eng-36; NSF DMR-88-14783; NSF DMR-88-02401)
(DE90-016468; LA-UR-90-2623; CONF-900751-3) Avail: NTIS HC/MF A03

Normal-state copper NMR spectra and spin-lattice relaxation rates 1/T(sub 1) have been measured in the planar cuprate system YBa2Cu3O7. With Pr doping the Knight shift K decreases and develops a temperature dependence at both plane and chain sites. Analysis of the bulk susceptibility and NMR data indicate that pair breaking and hole depletion both take part in the suppression of the superconducting transition temperature (Tc). The Knight shift behavior resembles that in oxygen-deficient YBa2Cu3O(7-y), as does the temperature dependence of 1/T(sub 1) for plane Cu sites and magnetic field perpendicular to the c axis. This agreement leads to a consistent picture of the role of antiferromagnetic fluctuations in these materials. An analysis of the data in the framework of the phenomenological theory of Millis, Monien, and Pines is given. In the end compound PrBa2Cu3O7 the NMR signal from plane Cu sites indicates antiferromagnetic (AF) ordering at a Neel temperature approximately 280 K, and in the AF state yields an internal field similar to those found in AF YBa2Cu3O6 and La2CuO4. DOE

**N91-10769#** Los Alamos National Lab., NM.
**SUPERCONDUCTING BORIDES**
Z. Fisk 1990 11 p Presented at the 10th International Symposium on Boron, Borides and Related Compounds, Albuquerque, NM, 27-30 Aug. 1990 Submitted for publication
(Contract W-7405-eng-36)
(DE90-016484; LA-UR-90-2847; CONF-900870-3) Avail: NTIS HC/MF A03

A number of superconductors are found among binary and ternary boride compounds. The highest (Tc)'s are often found near a limiting composition for the compound's stability. Ternary borides have been a fertile area for exploring the interaction between superconductivity and magnetism, and appear to be the area in which further aspects of boride superconductivity will be pursued. DOE

**N91-10770#** Los Alamos National Lab., NM. Center for Materials Research.
**CALCULATION OF THE STATIC MAGNETISM OF METAMAGNETIC La2CuO4**
Dermot Coffey 1990 13 p Presented at the Conference on Magnetism and Magnetic Materials, San Diego, CA, 29 Oct. - 1 Nov. 1990
(Contract W-7405-eng-36)
(DE90-016490; LA-UR-90-2799; CONF-901004-1) Avail: NTIS HC/MF A03

Interactions in La2CuO4 are predominantly antiferromagnetic. However a strong field induced transition is seen in the static magnetic susceptibility which points to the existence of a net ferromagnetic moment in the CuO layers. Here, this net ferromagnetic moment is incorporated into a description of the CuO layers by the inclusion of a modified Dzyaloshinskii-Moriya term in the Hamiltonian. The spin wave spectrum in the presence of an applied field is calculated with this Hamiltonian and the ground state is determined as a function of applied field from the free energy. A calculation of the static magnetization as a function applied field perpendicular to the CuO layers is used to determine the parameters of the model. Comparison is made with experiment. DOE

**N91-10771#** Los Alamos National Lab., NM.
**ELECTRONIC, STRUCTURAL AND TRANSPORT PROPERTIES OF (ALMOST) RARE-EARTH-LIKE ACTINIDE HYDRIDES**
John W. Ward, Barbara Cort, Joyce A. Goldstone, Andrew C. Lawson, Lawrence E. Cox, and Richard G. Haire (Oak Ridge National Lab., TN.) 1990 21 p Presented at the 200th American Chemical Society National Meeting, Washington, DC, 26-31 Aug. 1990
(Contract W-7405-eng-36)
(DE90-016491; LA-UR-90-2792; CONF-900802-5) Avail: NTIS HC/MF A03

By the virtue of broadband, hybridized 5f-electron behavior, the hydride systems for Pa and U exhibit unique properties and structures, the actinide metal atoms existing in different states. A sudden change at Np to more rare earth-like behavior implies a major change in electronic structure. There are both many parallels but also enigmas for the Np + H and Pu + H systems. Electrical resistivities are large and complex with temperature. Low temperature structural transitions as studied by neutron diffraction help elucidate some of these effects. Phonon spectra are quite rare earth-like, and XPS data imply a metal atom with mostly d-screened core levels. Then it is at americium, where fully localized and corelike 5f electrons are found, that we look finally for true rare earth-like behavior, which should include a large drop in electrical resistivity. DOE

**N91-10772#** Oak Ridge National Lab., TN. Solid State Div.
**SUBSTRATE TEMPERATURE EFFECTS ON (CUBIC X CUBIC LATTICE) R 30 DEG DOMAIN GROWTH OF Ag ON Si(111) SURFACE**
J. K. Zuo and J. F. Wendelken Aug. 1990 9 p Presented at the 5th International Conference on Solid Films and Surfaces, Providence, RI, 13-17 Aug. 1990
(Contract DE-AC05-84OR-21400)
(DE90-016527; CONF-900830-1) Avail: NTIS HC/MF A02

High-resolution low-energy electron diffraction (LEED) angular profiles associated with (square root of 3 x square root of 3) R30(degree) domain growth of Ag on Si(111) were analyzed following Ag deposition as a function of substrate temperature. We found that the square root of 3 domain size distribution has the same Gamma distribution at different coverages and substrate temperatures. However, at higher substrate temperatures the square root of 3 structure grows with coverage primarily by domain coalescence as indicated by the considerable increase in the mean and width of the size distribution. As a result, scaling, i.e., self-similar domain growth, is observed. At lower substrate temperatures the square root of 3 structure grows with coverage by simply increasing the number of small, randomly nucleated domains. Hence, the domain size distribution at low temperatures is narrow and varies little with coverage. DOE

**N91-10773#** Los Alamos National Lab., NM.
**COMPUTATION OF SUPERCONDUCTOR CRITICAL CURRENT DENSITIES AND MAGNETIZATION CURVES**
Marion L. Hodgdon 1990 17 p Presented at the Conference on Magnetism and Magnetic Materials, San Diego, CA, 29 Oct. - 1 Nov. 1990
(Contract W-7405-eng-36)
(DE90-016567; LA-UR-90-2708; CONF-901004-2) Avail: NTIS HC/MF A03

Using a constitutive law for superconductor hysteresis and the ideas of the critical state model, a system of equations is developed for the critical current density J(sub c), the equilibrium magnetization M(sub e), the upper and lower portions, M(sub U) and M(sub L), of the major hysteresis loop, and their derivatives with respect to the applied field. The constitutive law consists of a differential equation relating the time rate of change of the flux density B to that of the applied field, dB/dt = alpha(H) times the absolute value of dH/dt (f(H) - B) + dH/dt g(H), and a rule governing the abrupt changes observed at the turning points of H. For the case presented here in which f, g, and alpha have analytic forms, the constitutive law yields an easily differentiable expression for the major loop. Hysteresis curves computed from this constitutive law are shown to be in good agreement with experiments. Calculations of the critical current densities and equilibrium magnetization for the case in which the derivatives are neglected, i.e., the Bean model with J(sub c) proportional to M(sub U) - M(sub L) and M(sub e) proportional to M(sub U) + M(sub L), are compared with J(sub c) and M(sub e) computed using a system of equations that takes into account the first two derivatives of all quantities. Exponential approximations are given for the critical current densities of several samples of Y-Ba-Cu-O at temperatures between 5 and 60 K. DOE

**N91-10774#** Los Alamos National Lab., NM. Physics Div.
**Fe SITE OCCUPANCY AND SUPERCONDUCTIVITY IN Y(1-z)Ca(z)Ba(z) (Cu(1-x)Fe(x))3O(6+y)**
M. G. Smith, R. D. Taylor, and H. Oesterreicher (California Univ., San Diego, La Jolla.) 2 Aug. 1990 12 p Presented at the 35th Annual Conference on Magnetism and Magnetic Materials, San Diego, CA, 29 Oct. - 1 Nov. 1990
(Contract W-7405-eng-36)
(DE90-016614; LA-UR-90-2671; CONF-901004-4) Avail: NTIS HC/MF A03

X ray diffraction and Fe-57 Moessbauer spectroscopy studies show that partial substitution of Ca for Y in Y(1-z)Ca(z)Ba2(Cu(1-x)Fe(x))3O(6+y) (0.05 (le) z (le) 0.15,0.003 (le) x (le) 0.20) result in increased Fe solubility and a larger percentage of Fe occupancy of the Cu(2) plane site (prepared conventionally). Materials with z (gt) 0.00 have a slightly depressed superconducting transition onset temperature (Tc) relative to the z = 0.00 compounds. It is also shown that Fe occupancy of the Cu(2) site in Y(1-z)Ca(z)Ba2 (Cu(1-x)Fe(x))3O(6+y) can be substantially increased when these materials are treated at high temperatures in inert atmospheres followed by oxygenation at low temperatures. T(sub c) decreases more rapidly in these latter materials compared to the conventionally prepared ones. Implications concerning ordered Fe cluster formation and superconducting pair breaking in the Cu(2) site are drawn. DOE

**N91-10775#** California Univ., Berkeley. Lawrence Berkeley Lab. Materials and Chemical Sciences Div.
**A CORRELATION BETWEEN T(SUB 3) AND ELECTRONEGATIVITY DIFFERENCE IN HIGH-TEMPERATURE SUPERCONDUCTORS**
Chengfong Joseph Jou (Ecole Polytechnique, Palaiseau, France ) and J. Washburn Apr. 1990 7 p
(Contract DE-AC03-76SF-00098)
(DE90-016640; LBL-28993) Avail: NTIS HC/MF A02

For compound superconductors a correlation is found between superconducting critical temperature. Tc is greater than or equal to 10 K and difference in Pauling's electronegativity, delta N, between certain elements in the structure. For all the high-(Tc) oxide layer-structure compounds, (Tc) increases linearly with delta N with the (Tc) corresponding to the extrapolation to delta N = 0 being approximately 30 K. For all others, the more three-dimensional structures, Tc also appears to be related to delta N but forms a completely separate correlation curve at lower values of Tc. DOE

**N91-10776#** Los Alamos National Lab., NM.
**XAFS ANALYSIS IN THE ANHARMONIC LIMIT: APPLICATION TO HI-Tc SUPERCONDUCTORS AND FERROSILICATES**
J. MustredeLeon and S. D. Conradson 1990 5 p Presented at the 6th International Conference on X Ray Absorption Fine Structure, York, England, 5-11 Aug. 1990
(Contract W-7405-eng-36)
(DE90-016720; LA-UR-90-2633; CONF-9008141-2) Avail: NTIS HC/MF A01

The effect of lattice vibrations in x ray absorption fine structure (XAFS), reflected in the relative motion of atomic pairs, is usually taken into account by the use of a harmonic Debye-Waller factor. However such treatment is known to be invalid in several situations of interest e.g., superionic conductors metals near the melting point, etc. The use of a harmonic treatment in these situations leads to results in conflict with those obtained using diffraction techniques. The effect of small anharmonicity has been discussed by several authors, finding that in some cases the correction of the harmonic Debye-Waller factor by the first few cumulant expression terms suffices to reconcile XAFS and diffraction results. However, even in situations where anharmonicity is moderate or when the single particle potentials used to describe the lattice dynamics of the system exhibit nearby minima the cumulant expansion breaks down. In order to treat the problem of high anharmonicity, we have generalized the formulation for the exact XAFS thermal average in terms of a RDF, to the quantum mechanical regime, and implemented this formulation in the fitting of XAFS data. This approach permits the treatment of highly anharmonic motion that can not analyzed using cumulant expansion of the Debye-Waller factor. DOE

**N91-10777#** Los Alamos National Lab., NM.
**RADIATION-INDUCED NOISE IN CHARGE-COUPLED DEVICE (CCD) AND CHARGE-INJECTION DEVICE (CID) IMAGERS**
George J. Yates and Bojan T. Turko (California Univ., Berkeley. Lawrence Berkeley Lab.) Aug. 1990 24 p
(Contract W-7405-eng-36)
(DE90-016724; LA-11706-MS) Avail: NTIS HC/MF A03

Measurements of radiation sensitivity for interline transfer charge-coupled devices (CCDs) and charge-injection devices (CIDs) from irradiation with high-energy photons (CO-60 gammas and 3-to 5-MeV end-point Bremsstrahlung) and 14-MeV neutrons are presented to establish imager susceptibility in such environments. Results from electric clearing techniques designed for quick (approximately 300 microseconds for the CCDs and approximately 10 microseconds for CIDs) removal (or dumping) of radiation-induced charge from prompt sources are discussed. Application of the techniques coupled with long (microsecond to millisecond) persistence radiation-to-light converters for image retention is described. Typical data illustrating the effectiveness of charge clearing in removal of radiation noise are included for nanosecond duration pulsed x ray/gamma-ray doses (50 millirad to 5-rad range) and microsecond duration neutron fluences approaching 10(exp 8) n/sq cm. DOE

**N91-10778#** Pacific Northwest Lab., Richland, WA. Materials and Chemical Sciences Center.

**THEORETICAL CALCULATIONS OF THE NONLINEAR DIELECTRIC FUNCTION OF INHOMOGENEOUS THIN FILMS**

Steven M. Risser and Kim F. Ferris Nov. 1989 8 p Presented at the Materials Research Society Fall Meeting, Boston, MA, 27 Nov. - 2 Dec. 1989
(Contract DE-AC06-76RL-01830)
(DE90-017186; PNL-SA-17225; CONF-891119-137) Avail: NTIS HC/MF A02

The dielectric function of inhomogeneous materials is composed of linear and nonlinear responses which are sensitive to the film microstructure as well as the intrinsic properties of the materials. A method was developed to self-consistently determine the linear and non-linear contributions to the dielectric function of films with random microstructure. This method is based upon a numerical solution of the general electrostatic equations and is applicable to arbitrary shapes and orientations of model defects. This method provides near exact solutions to the linear response of the dielectric function. It was shown that the nonlinear part of the dielectric function is extremely sensitive to the void shape and void fraction. DOE

**N91-10779#** Dartmouth Coll., Hanover, NH. Dept. of Physics.

**EXCITONS IN SEMICONDUCTING SUPERLATTICES, QUANTUM WELLS, AND TERNARY ALLOYS Progress Report, 15 Sep. 1988 - 14 Sep. 1990**

M. D. Sturge, R. E. Nahory, and M. C. Tamargo (Bell Communications Research, Inc., Red Bank, NJ.) 22 Aug. 1990 20 p
(Contract DE-FG02-87ER-45330)
(DE90-017287; DOE/ER-45330/2) Avail: NTIS HC/MF A03

It is now possible to fabricate semiconducting layered structures with precisely defined layer thicknesses of a few atomic diameters. Examples are the quantum well and the superlattice structures, in which semiconductors with different band gaps are interleaved. Microstructures can be produced from this material by patterning and etching them on a small (approx. 10 nm) scale. Their electronic properties are quite different from those of the constituents and offer interesting new possibilities both in device design and in basic physics. This proposal aims to improve the understanding of optically excited states (excitons and electron-hole plasmas) in these structures. Work will also continue on ternary alloys, primarily to establish if the alloy disorder produces a mobility edge for excitons, and on II-VI compounds, where the principal interest at present is in the nature of the exciton-phonon coupling. DOE

**N91-10780*#** National Aeronautics and Space Administration. Lewis Research Center, Cleveland, OH.

**DETERMINATION OF SURFACE RESISTANCE AND MAGNETIC PENETRATION DEPTH OF SUPERCONDUCTING YBa2Cu3O(7-DELTA) THIN FILMS BY MICROWAVE POWER TRANSMISSION MEASUREMENTS**

K. B. Bhasin, J. D. Warner, F. A. Miranda, W. L. Gordon, and H. S. Newman (Naval Research Lab., Washington, DC.) Sep. 1990 7 p Presented at the Applied Superconductivity Conference, Aspen, CO, 24-28 Sep. 1990; sponsored in part by IEEE
(NASA-TM-103616; E-5743; NAS 1.15:103616) Avail: NTIS HC/MF A02 CSCL 20L

A novel waveguide power transmission measurement technique was developed to extract the complex conductivity of superconducting thin films at microwave frequencies. The microwave conductivity was taken of two laser ablated YBa2Cu3O(7-delta) thin films on LaAlO3 with transition temperatures of approx. 86.3 and 82 K, respectively, in the temperature range 25 to 300 K. From the conductivity values, the penetration depth was found to be approx. 0.54 and 0.43 micron, and the surface resistance (R sub s) to be approx. 24 and 36 micro-Ohms at 36 GHz and 76 K for the two films under consideration. The R sub s values were compared with those obtained from the change in the Q-factor of a 36 GHz Te sub 011-mode (OFHC) copper cavity by replacing one of its end walls with the superconducting sample. This technique allows noninvasive characterization of high transition temperature superconducting thin films at microwave frequencies. Author

**N91-10781#** West Virginia Univ., Morgantown. Dept. of Chemical Engineering.

**REACTION KINETICS OF THE Ca-SO2 SYSTEM IN ABSENCE OF INTER-GRAIN PORE DIFFUSION Annual Report**

H. Kono Apr. 1990 17 p
(Contract DE-FC21-87MC-24207)
(DE90-009672; DOE/MC-24207/2857) Avail: NTIS HC/MF A03

Effective removal of SO2 released due to the combustion of coal is of primary concern and of vital importance in fluidized bed combustion technology. Utilization of limestone, as a sorbent in FBC, to remove SO(x) is an attractive and promising technique. However, the incomplete utilization of limestone causes an increase in limestone usage and bed spent materials. In order to improve the limestone utilization, one must understand the fundamental rate-limiting step and particle deactivation mechanism during CaO-SO2 reaction. The aim of this work is to better understand the CaO-SO2 reaction, particularly in terms of its intrinsic kinetics, rate-limiting steps, and particle deactivation mechanisms. The proposed approach involves the reaction of a single flat plate CaO crystal with SO2 in a thermogravimetric analyzer. Appropriate experimental equipment was installed and the methodology to derive the related parameters has been established. Based on the mathematical mode, the effect of diffusion rate, chemical reaction rate and reaction time on the reaction conversion were preliminarily obtained numerically and experimentally. Thus, the reliable experimental data of the gas diffusion coefficient in the product layer of CaSO4 was obtained for the first time in open literature. DOE

**N91-10782#** Argonne National Lab., IL. Materials and Components Technology Div.

**YBa2Cu3O(x) COMPOSITES WITH IMPROVED TOUGHNESS AND STRENGTH**

J. P. Singh, H. J. Leu, M. L. Kullberg, R. B. Poeppel, and K. C. Goretta Apr. 1990 15 p Presented at the ASME Winter Annual Meeting, Dallas, TX, 25-30 Nov. 1990
(Contract W-31-109-eng-38; NSF STC-88-09854)
(DE90-011180; CONF-901109-4) Avail: NTIS HC/MF A03

Composite YBa2Cu3O(x)/Ag superconductors were cast into thin tapes. Tapes containing 15 volume percent Ag were 2 to 2.5 times stronger than monolithic YBa2Cu3O(x) tapes and had higher fracture toughnesses. The tapes containing Ag flakes were stronger than those containing Ag powder, possibly because of effects of preferred orientation. The superconducting properties of the tapes were not appreciably affected by Ag addition. Composite bars of YBa2Cu3O(x) and 10 mole percent ZrO2 coated with Y2BaCuO5 were found to have double the fracture toughness of unreinforced YBa2Cu3O(x). Strength was unaffected by ZrO2 addition, however, because of differences in flaw populations. DOE

**N91-10783#** California Univ., Berkeley. Lawrence Berkeley Lab. Dept. of Materials Science and Chemical Engineering.
**IN SITU TRANSMISSION ELECTRON MICROSCOPY AND COMPUTER SIMULATION STUDY OF THE KINETICS OF OXYGEN LOSS IN YBa2Cu3O(z)**
C. P. Burmester, R. Gronsky, L. T. Wille, B. T. Ahn, V. Y. Lee, R. Beyers, T. M. Guer, and R. A. Huggins (Stanford Univ., CA.) Jul. 1990 4 p Presented at the Fall Meeting of the Materials Research Society, Boston, MA, 26 Nov. - 1 Dec. 1990
(Contracts DE-AC03-76SF-00098; MDA972-88-J-1006)
(DE90-014508; LBL-27358; CONF-901105-2) Avail: NTIS HC/MF A01

High resolution transmission electron microscopy during in situ quenching of YBa2Cu3O(z) is used to study the kinetics of microdomain formation during oxygen loss in this system. Image simulations based on atomic models of oxygen vacancy order in the basal plane of this material generated by Monte Carlo calculations are used to interpret high resolution micrographs of the structures obtained by quenching. The observed domain structures agree well with those obtained from the simualtions. DOE

**N91-10784#** Universiteit Twente, Enschede (Netherlands).
**ABOUT ANTIFERROMAGNETIC HEISENBERG MODELS Ph.D. Thesis**
Paul-Louis Iske 1989 216 p
(ETN-90-97768) Avail: NTIS HC/MF A10

Phase transitions and magnetism are addressed. Focus on the (antiferromagnetic) Heisenberg model, a quantum mechanical model for describing (anti)ferromagnetic systems. Classical statistical lattice models, including the Ising model, are compared with models in which the constituting particles are treated as quantum mechanical objects. The resonating valence bonds method, by which the antiferromagnetic ground state may be described, is discussed. The Hubbard model is proposed as suitable for describing the characteristics of the high-T (sub c) superconductors. An estimate of the gap in the energy spectrum of the spin-1 antiferromagnetic Heisenberg chain (Haldane conjecture), which was proved for the valence bond solids chain, is made. ESA

**N91-10785#** Ecole Centrale de Lyon (France). Lab. d'Electrique, Automatique et Mesures Electriques.
**CONTRIBUTION TO THE STUDY OF MOS STRUCTURES AGEING Ph.D. Thesis [CONTRIBUTION A L'ETUDE DU VIEILLISSEMENT DES STRUCTURES MOS]**
Hussein Nabha 1990 116 p In FRENCH Sponsored in part by Foundation Hariri
(ECL-90-04; ETN-90-97819) Avail: NTIS HC/MF A06

The physical mechanisms responsible for the deterioration of electrical characteristics of metal oxide semiconductors (MOS) structures are investigated. The use of silicon compounds and refractory metals in MOS technology are discussed. The experimental techniques of characterization by inner photoemission and for electrical characteristics analysis are described. The results of the WSi2-polySi/SiO2/Si and Al/SiO2/Si structures submitted to electrical constraints are analyzed. The creation of interface states in MOS transistors, submitted to hole and electrons injections, is discussed. ESA

# 77 THERMODYNAMICS AND STATISTICAL PHYSICS

Includes quantum mechanics; theoretical physics; and Bose and Fermi statistics.

For related information see also *25 Inorganic and Physical Chemistry* and *34 Fluid Mechanics and Heat Transfer.*

**N91-10786#** Instituto de Fisica Teorica, Sao Paulo (Brazil).
**ON THE STRUCTURE OF QUANTUM PHASE SPACE**
R. Aldrovandi and D. Galetti 1989 44 p Sponsored in part by FINEP; and by CNPq
(DE90-627185; IFT-P-29/89) Avail: NTIS (US Sales Only) HC/MF A03

The space of labels characterizating the elements of Schwinger's basis for unitary quantum operators is endowed with a structure of symplectic type. This structure is embodied in a certain algebric cocycle, whose main features are inherited by the symplectic form of classical phase space. In consequence, the label space may be taken as the Quantum Phase Space: it plays, in the quantum case, the same role played by phase in classical mechanics, some differences coming inevitably from its nonlinear character. DOE

**N91-10787#** Central Inst. of Physics, Bucharest (Romania). Inst. of Physics and Nuclear Engineering.
**LOCALIZABILITY IN THE HAMILTONIAN FORMALISM AND IN QUANTUM-MECHANICS**
R. D. Grigore Jan. 1989 29 p
(DE90-628368; IFIN-FT-346-1989) Avail: NTIS (US Sales Only) HC/MF A03

The problem of localizability is studied in the framework of Hamiltonian formalism. Only the systems of nonzero mass and any spin, and of zero mass and zero helicity are localizable for the Poincare group. These results suggest a possible solution for the problem of localizability of the photon in quantum mechanics. It is proved that the photon is localizable in the sense of Wightman, on the manifold of bidimensional planes in R(sup 3). So the photon must be considered as a bidimensional object: the plane wave. DOE

**N91-10788#** Central Inst. of Physics, Bucharest (Romania). Inst. of Physics and Nuclear Engineering.
**COHOMOLOGY FOR LAGRANGIAN SYSTEMS AND NOETHERIAN SYMMETRIES**
O. T. Popp Jun. 1989 47 p
(DE90-628371; IFIN-FT-357-1989) Avail: NTIS (US Sales Only) HC/MF A03

Using the theory of sheaves, some exact sequences describing the locally Lagrangian systems were found. Using cohomology theory of groups with coefficients in sheaves, some exact sequences describing the Noetherian symmetries were obtained. It is shown how the results can be used to find all locally Lagrangian dynamics Noetherian invariant with respect to a given group of kinematical symmetries. DOE

**N91-10789#** Stanford Linear Accelerator Center, CA.
**DISCRETE GRAVITY**
H. Pierre Noyes Jul. 1990 21 p Presented at the 2nd Physical Interpretations of Relativity Theory, London, England, 3-8 Sep. 1990
(Contract DE-AC03-76SF-00515)
(DE90-014808; SU-SLAC-PUB-5218; CONF-9009227-1) Avail: NTIS HC/MF A03

The following areas are discussed: constructing a bit-string universe; quantized space-time; combinatorial hierarchy labels; gravitational stabilization of the proton; quantum geons; cosmological consequences; the proton-electron mass ratio, weak electromagnetic unification; and sewgut. DOE

**N91-10790#** Stanford Linear Accelerator Center, CA.
**DISCRETIZED LIGHT-CONE QUANTIZATION: APPLICATION TO QUANTUM ELECTRODYNAMICS Ph.D. Thesis**
Andrew C. Tang Jun. 1990 225 p
(Contract DE-AC03-76SF-00515)
(DE90-014832; SU-SLAC-351) Avail: NTIS HC/MF A11

A general method for solving quantum field theories, Discretized Light-Cone Quantization (DLCQ), is presented. The method is very straightforward and essentially consists of diagonalizing the light-cone Hamiltonian matrix for the mass spectrum and wavefunctions. This method was applied successfully in the past to various one space, one time dimensional theories. In each of these past applications, the mass spectrum and wave functions were successfully obtained, and all results agree with previous analytical and numerical work. The success of DLCQ in 1 + 1 dimensions provides the hope of solving theories in three space and one time dimensions. The application to higher dimensions is much more involved than in 1 + 1 dimensions due to the need to introduce ultraviolet and infrared regulators, and invoke a renormalization scheme consistent with gauge invariance and Lorentz invariance. This is in addition to the extra work involved implementing two extra dimensions with their added degrees of freedom. The application is presented of DLCQ to 3 + 1 dimensional Quantum Electrodynamics. DOE

**N91-10791#** IIT Research Inst., Bartlesville, OK.
**DETERMINATION OF IDEAL-GAS ENTHALPIES OF FORMATION FOR KEY COMPOUNDS: THE 1988 PROJECT RESULTS**
W. V. Steele, R. D. Chirico, A. Nguyen, I. A. Hossenlopp, and N. K. Smith Jul. 1990 46 p
(Contract DE-FC22-83FE-60149)
(DE90-000247; NIPER-422) Avail: NTIS HC/MF A04

The results of a study aimed at improvement of group contribution methodology for estimation of thermodynamic properties of organic substances are reported. Specific weakness where particular group-contribution terms were unknown, or estimated because of lack of experimental data, are addressed by experimental studies of enthalpies of combustion in the condensed phase and vapor pressure measurements. Ideal-gas enthalpies of formation are reported for 3-methylbuta 1,2-diene; 2,5-dimethylhexa 2,4-diene; acetaldoxime; N,N-diethyl hydroxylamine; 1-methylpyrrolidin-2-one; and phenanthrene. Solid and liquid phase enthalpies of formation at 298.15 K are determined for benzamide. Ring corrections, group terms, and next-nearest-neighbor interaction terms useful in the application of group contribution correlations are derived. DOE

**N91-10792#** State Univ. of New York, Albany.
**THERMOPHYSICAL PROPERTIES OF FLUIDS AND FLUID MIXTURES Progress Report**
George Stell Jul. 1990 11 p
(Contract DE-FG02-88ER-13850)
(DE90-016306; DOE/ER-13850/15) Avail: NTIS HC/MF A03

This progress report, written in July 1990, plays a dual role of annual progress report and the component of the renewal proposal package that provides in detail the necessary background for the thermophysical research proposed therein. Because of its second role, some overall Grant aims and overall accomplishments, are summarized stressing the progress that has been made over the last year. DOE

## 80 SOCIAL SCIENCES (GENERAL)

Includes educational matters.

No abstracts in this category.

## 81 ADMINISTRATION AND MANAGEMENT

Includes management planning and research.

**N91-10793*#** Houston Univ., Clear Lake, TX. Research Inst. for Computing and Information Systems.
**THE INTEGRATED SCHEDULING SYSTEM: A CASE STUDY IN PROJECT MANAGEMENT**
Peter C. Bishop, David B. Learned, and Cissy A. Yoes Oct. 1989 117 p
(Contract NCC9-16)
(NASA-CR-187261; NAS 1.26:187261) Avail: NTIS HC/MF A06 CSCL 05A

A prototype project management system was developed for the Level III Project Office for the Space Station Freedom. The main goal was to establish a framework for the Space Station Project Office whereby Project and Office Managers can jointly establish and review scheduled milestones and activities. The objective was to assist office managers in communicating their objectives, milestones, schedules, and other project information more effectively and efficiently. Consideration of sophisticated project management systems was included, but each of the systems had limitations in meeting the stated objectives. Author

**N91-10794*#** Houston Univ., Clear Lake, TX. Research Inst. for Computing and Information Systems.
**APPLIED TECHNOLOGY CENTER BUSINESS PLAN AND MARKET SURVEY**
Robert F. Hodgin and Roberto Marchesini [1990] 68 p
(Contract NCC9-16)
(NASA-CR-187259; NAS 1.26:187259) Avail: NTIS HC/MF A04 CSCL 05B

Business plan and market survey for the Applied Technology Center (ATC), computer technology transfer and development non-profit corporation, is presented. The mission of the ATC is to stimulate innovation in state-of-the-art and leading edge computer based technology. The ATC encourages the practical utilization of late-breaking computer technologies by firms of all variety. Author

**N91-10795*#** Houston Univ., Clear Lake, TX. Research Inst. for Computing and Information Systems.
**SPACE MARKET MODEL SPACE INDUSTRY INPUT-OUTPUT MODEL**
Robert F. Hodgin and Roberto Marchesini Mar. 1987 39 p
(Contract NCC9-16)
(NASA-CR-187252; NAS 1.26:187252) Avail: NTIS HC/MF A03 CSCL 05A

The goal of the Space Market Model (SMM) is to develop an information resource for the space industry. The SMM is intended to contain information appropriate for decision making in the space industry. The objectives of the SMM are to: (1) assemble information related to the development of the space business; (2) construct an adequate description of the emerging space market; (3) disseminate the information on the space market to forecasts and planners in government agencies and private corporations; and (4) provide timely analyses and forecasts of critical elements of the space market. An Input-Output model of market activity is proposed which are capable of transforming raw data into useful information for decision makers and policy makers dealing with the space sector. Author

## 82 DOCUMENTATION AND INFORMATION SCIENCE

Includes information management; information storage and retrieval technology; technical writing; graphic arts; and micrography.

For computer documentation see *61 Computer Programming and Software.*

**N91-10796#** National Telecommunications and Information Administration, Boulder, CO. Inst. for Telecommunication Sciences.
**IMAGE DATA COMPRESSION OVERVIEW: ISSUES AND PARTIAL SOLUTIONS**
M. Nesenbergs Oct. 1989 65 p Sponsored by Naval Sea Systems Command, Washington, DC
(PB90-172008; NTIA-89-252) Avail: NTIS HC/MF A04 CSCL 05B

The report presents an overview of moving image (video) data compression. Because the report deals with a subtask of a major program, a limited number of the most pertinent topics and issues have been addressed. The topics include a listing of human perception effects and parameters for visual information; theoretical aspects of image data compression; a selective review of compression techniques; a closer look at motion detection, prediction and compensation; and a start to survey existing systems and their capabilities. Finally a multipage bibliography, while not exhaustive in any sense, shows the depth and breadth of the rapidly growing technology of image data compression. GRA

**N91-10797#** Government Printing Office, Washington, DC. Cataloging Branch.
**US CONGRESSIONAL SERIAL SET CATALOG: NUMERICAL LISTS AND SCHEDULE OF VOLUMES; 99TH CONGRESS: 1985-1986: ENTRIES AND INDEXES**
1989 672 p
(PB90-171737; GP-3.34:85-86) Avail: NTIS HC/MF A99
CSCL 05B

The catalog is a finding aid for the reports and documents of the 99th Congress, 1st and 2nd Sessions. The report has been prepared by the staff of the Cataloging Branch, Library Programs Service, under the direction of the Joint Committee on Printing, pursuant to Section 1710, Title 44, United States Code. Through the 96th Congress, the index had been issued as the Numerical Lists and Schedule of Volumes. In 1985, the title for the records of the 97th Congress was changed to Monthly Catalog-U.S. Congressional Serial Set Supplement and made part of the Monthly Catalog. Catalog entries may be accessed by the following indexes: Author, Title, Subject, Series/report, and Bill number. GRA

**N91-10798*#** National Aeronautics and Space Administration. Lewis Research Center, Cleveland, OH.
**BIBLIOGRAPHY OF LEWIS RESEARCH CENTER TECHNICAL PUBLICATIONS ANNOUNCED IN 1989**
May 1990 399 p
(NASA-TM-102542; E-5352; NAS 1.15:102542) Avail: NTIS HC/MF A17 CSCL 05B

This compilation of abstracts describes and indexes the technical reporting that resulted from the scientific and engineering work performed and managed by the Lewis Research Center in 1989. All the publications were announced in the 1989 issues of STAR (Scientific and Technical Aerospace Reports) and/or IAA (International Aerospace Abstracts). Included are research reports, journal articles, conference presentations, patents and patent applications, and theses. Author

**N91-10799#** National Oceanic and Atmospheric Administration, Washington, DC. Data and Information Management Program Office.
**EARTH SYSTEM MONITOR, VOLUME 1, NUMBER 1, JUNE 1990**
A. H. Horvitz Jun. 1990 8 p
(PB90-215146) Avail: NTIS HC/MF A02 CSCL 05B

The Earth Systems Monitor, issued 2 to 3 times a year as developments warrent, will contain current information on NOAA's Earth System Data and Information Management program. It is needed to inform sector users of improvements in vital environmental science and prediction services through the rapidly evolving developments in NOAA's data and information management systems. Audience includes NOAA employees, other Govt. agencies and outside community involved in data management program in NOAA. Author

**N91-10800#** National Inst. of Standards and Technology, Gaithersburg, MD.
**NIST RESEARCH REPORTS, MAY 1990**
May 1990 37 p
(PB90-244435; NIST/SP-783) Avail: NTIS HC/MF A03; also available SOD HC $1.75 as 003-003-03020-1 CSCL 05B

A collection of research reports and updates from the National Institute of Standards and Technology (NIST) is presented. The titles of the reports included are Lyons New Head of NIST, President Boosts for NIST in 1991, Milestones--500 Very Good Ideas, Looking for Good Vibrations, Measuring in the Lilliputian World of Semiconductors, Loma Prieta--A Primer for Public Policy, More than Just for Saftey's Sake, and Stress and Strain on the Railroad Train. A few topics covered are the use of pulsed lasers in the study of reaction kinetics, energy-related invention development and marketing aid from NIST and DOE, chipmaking technology, earthquake resistant structures, the economic motivation for reliable and safe construction, and more reliable and efficient ways to detect high stress level and cracks in railroad wheels. Also, two short articles of the Hubble Space Telescope are included among the topics in the research update section. M.G.

**N91-10801#** China Nuclear Information Centre, Beijing.
**DIGITAL IMAGE INTEGRATION TECHNIQUE OF MULTIPLE GEOSCIENCE INFORMATION SYSTEM AND ITS APPLICATION**
Dechang Liu, Jingke Zou, Maorong Sun, and Guo-Juan Wang (Beijing Uranium Geology Research Inst., China ) 1988 11 p
In CHINESE; ENGLISH summary
(DE90-627893; CNIC-00257; BUGRI-0005) Avail: NTIS (US Sales Only) HC/MF A03

By using the computer integration technique, the multiple geoscience information such as geological, remote sensing, hydrogeological, geophysical and geochemical information is comprehensively processed. The technique consists of the data input, registration, interpolation, and the enhancement, decomposition, abstraction, classification, overlay and combination process procedures. This technique was tested on six promising areas and one testing area where the geological environment had been known. In the testing area, the distribution pattern of U, Th and K as well as their geological significance were analyzed. On the basis of compositing and abstracting the prospecting criteria, the target areas were preliminarily selected. The information classification technique was used for the general evaluation of uranium resource. Finally, on the tested results a multiple geological information image system for uranium resource evaluation was established. DOE

**N91-10802#** Lawrence Livermore National Lab., CA.
**TECHNICAL ABSTRACTS: MECHANICAL ENGINEERING**
J. Bruner, ed. 1989 60 p
(Contract W-7405-eng-48)
(DE90-014797; UCRL-ID-103495-89) Avail: NTIS HC/MF A04

A compilation is presented of the published, unclassified abstracts produced by mechanical engineers at Lawrence Livermore National Laboratory (LLNL) during the calendar year 1989. Many abstracts summarize work completed and published in report form. These are UCRL-90,000 and 100,000 series documents, which include the full text of articles to be published in journals and of papers to be presented at meetings, and UCID reports, which are informal documents. Not all UCIDs contain abstracts: short summaries were generated when abstracts were not included. Technical abstracts also provides descriptions of those documents assigned to the MISC (miscellaneous) category. These are generally viewgraphs or photographs presented at meetings. DOE

**N91-10803#** Los Alamos National Lab., NM.
**AN INTERPERSONAL MULTIMEDIA VISUALIZATION SYSTEM**
Richard L. Phillips 1990 4 p Presented at the Visualization '90, San Francisco, CA, 23-26 Oct. 1990
(Contract W-7405-eng-36)
(DE90-014974; LA-UR-90-2614; CONF-901089-2) Avail: NTIS HC/MF A01

MediaView is a computer program that provides a generic infrastructure for authoring and interacting with multimedia documents. Among its many applications is the ability to furnish a user with a comprehensive environment for analysis and visualization. With MediaView the user produces a document that contains mathematics, datasets and associated visualizations. From the dataset or embedded mathematics animated sequences can be produced in situ. The mathematical content of the document can be explored through manipulation with Mathematica (trademark). Since the document is all digital, it can be shared with a co-worker on a local network or mailed electronically to a colleague at a distant site. Animations and any other substructure of the document persist through the mailing process and can be awakened at the destination by the recipient. DOE

**N91-10804*#** National Aeronautics and Space Administration, Washington, DC.
**NASA THESAURUS SUPPLEMENT: A FOUR PART CUMULATIVE SUPPLEMENT TO THE 1988 EDITION OF THE NASA THESAURUS (SUPPLEMENT 4) Semiannual Report**
Sep. 1990 26 p
(NASA-SP-7064-Suppl-4; NAS 1.21:7064-Suppl-4) Avail: NTIS HC/MF A03 CSCL 05B

The four-part cumulative supplement to the 1988 edition of the NASA Thesaurus includes the Hierarchical Listing (Part 1), Access Vocabulary (Part 2), Definitions (Part 3), and Changes (Part 4). The semiannual supplement gives complete hierarchies and accepted upper/lowercase forms for new terms. Author

## 83 ECONOMICS AND COST ANALYSIS

Includes cost effectiveness studies.

No abstracts in this category.

## 84 LAW, POLITICAL SCIENCE AND SPACE POLICY

Includes NASA appropriation hearings; aviation law; space law and policy; international law; international cooperation; and patent policy.

No abstracts in this category.

## 85 URBAN TECHNOLOGY AND TRANSPORTATION

Includes applications of space technology to urban problems; technology transfer; technology assessment; and surface and mass transportation.

For related information see also *03 Air Transportation and Safety, 16 Space Transportation,* and *44 Energy Production and Conversion.*

**N91-10805#** Federal Lab. Consortium, Washington, DC.
**PUTTING TECHNOLOGY TO WORK, 1990. EXAMPLES OF INDUSTRY-LABORATORY COOPERATION CONTRIBUTING TO OUR NATION'S ECONOMIC STRENGTH**
Apr. 1990 94 p
(PB90-215187) Avail: NTIS HC/MF A05 CSCL 05A

The report was compiled and produced by the Federal Laboratory Consortium, which works to improve and promote technology transfer by assisting businesses and others to identify the 'right' federal laboratory contacts in their fields of infrastructure for cooperation. The document is also a collection of examples from 14 laboratories representing 6 government agencies. A similar document was issued in 1988 and is available through the National Technical Information Service. Both sets of examples are indicative of the full potential for industry-laboratory cooperation to contribute to the nation's economic strength. GRA

## 88 SPACE SCIENCES (GENERAL)

No abstracts in this category.

## 89 ASTRONOMY

Includes radio, gamma-ray, and infrared astronomy, and astrometry.

**N91-10806** Arizona Univ., Tucson.
**ESTIMATION OF ASTRONOMICAL IMAGES FROM THE BISPECTRUM OF ATMOSPHERICALLY DISTORTED INFRARED DATA Ph.D. Thesis**
Jonathan Dennis Freeman 1989 164 p
Avail: Univ. Microfilms Order No. DA9014668

The uses of the bispectrum for recovering the images of one-dimensional infrared astronomical speckle data are examined. An analytic model for the bispectral transfer function, the variance, and the covariance of the bispectrum are developed. The models are evaluated by Monte Carlo integration and the results are compared to sample estimates of the same quantities obtained from simulated data. For comparison, the same sample quantities are computed from observed data. The bispectrum is shown to be useful for determining estimates of the object phase. A recursive method which is used to obtain the object phase estimates is introduced. Since the bispectrum provides multiple estimates of each object phase, a number of methods for combining the multiple estimates are developed and compared. Many techniques were proposed to determine the phase of images which were atmospherically distorted. Among these techniques are the Knox-Thompson, and the Simple Shift-and-Add algorithms. These methods are compared to the bispectrum via an objective measure which is developed. Optimization techniques are used to great success. A model for the bispectrum of a binary star is developed and fit to the image bispectrum by the Levenberg-Marquardt algorithm for non-linear least squares. The ability of the algorithm to determine binary star parameters from the bispectrum is tested with both simulated and observed data. Since the bispectrum may not always be available, a method is developed which determines binary star parameters from the image Fourier transform. The full set of object phases and moduli are determined by use of the conjugate gradient and conjugate direction algorithms. Two starting points for each algorithm are employed. The first starting point uses the estimates of the object phases obtained from the recursive bispectrum technique. The second assumes no information is known about the object. The speed of convergence of each algorithm is analyzed and recommendations are made for future use. Dissert. Abstr.

**N91-10807** Iowa State Univ. of Science and Technology, Ames.
**TESTS AND APPLICATIONS OF CHERENKOV IMAGING IN TEV ASTRONOMY Ph.D. Thesis**
Daryl Jack Macomb 1989 179 p
Avail: Univ. Microfilms Order No. DA9014926

The use of Cherenkov imaging for background reduction in TeV Astronomy is described. The technique of measuring the angular distribution of Cherenkov light from air showers as a means of identifying the primary particle type has been predicted to lead to a significant increase in the sensitivity for ground-based gamma ray telescopes. The hardware test of imaging successfully finds the Cherenkov light patterns from local cosmic ray particles using the Whipple Observatory collaboration's air Cherenkov telescope. This shows that a Whipple type imaging detector is sensitive to subtle images and therefore suitable for such a technique. A Monte Carlo simulation test confirms the current knowledge of the angular distribution of Cherenkov light expected from gamma ray induced air showers. The search for TeV photons from two massive x-ray binaries, 4U0115+63 and VO332+53, using both uncut and image selected data sets shows little evidence for emission from either source. Dissert. Abstr.

**N91-10808** Max-Planck-Inst. fuer Physik und Astrophysik, Garching (Germany, F.R.). Inst. fuer Extraterrestrische Physik.
**BICOLORED PHOTOMETRY AND SPECTRAL ACCOMMODATION IN X-RAY REGION OF MASS IMPREGNATED STELLAR X-RAY BINARIES Thesis - Ludwig-Maximilians-Univ. [ZWEIFARBENPHOTOMETRIE UND SPEKTRALE ANPASSUNG IM ROENTGENBEREICH AN MASSEARMEN ROENTGENDOPPELSTERNEN]**
Norbert S. Schulz Mar. 1990 166 p In GERMAN
(MPE-219; ISSN-0178-0719; ETN-90-97872) Copyright Avail: Fachinformationszentrum Karlsruhe, 7514 Eggenstein-Leopoldshafen 2, Fed. Republic of Germany

From June 1983 to April 1986 onwards, a great number of light galactic X-ray sources were observed several times at long intervals at the EXOSAT European X-ray Observatory. Among the lightest of these sources , the so called mass-impregnated X-ray binaries (LMXBs) are found. LMXBs are semi-separated contact systems composed of a neutron star and of a mass-impregnated satellite star. The neutron star receives substance from its satellite star, thus developing an accretion disk. The liberated gravitational energy is observed at collision on the neutron star surface under the form of X-ray radiation. Among the most well known subjects of this system are Sco X-1, Cyg X-2 and the light sources of the galactic bulge. They are the lightest extrasolar X-ray sources. A model of energy spectrum is used for the examination of a number of LMXB, with these radiation characteristics. Their most important physical properties are considered. The EXOSAT X-ray satellite and the MEAR-experiments are described. The methods of data reduction and the observation catalog are presented. ESA

**N91-10809#** European Southern Observatory, Garching (Germany, F.R.).
**[ACTIVITIES REPORT OF THE EUROPEAN SOUTHERN OBSERVATORY] Annual Report, 1989**
1990 128 p In ENGLISH, FRENCH, and GERMAN
(ISSN-0531-4496; ETN-90-97875) Avail: NTIS HC/MF A07

The work carried out by the several divisions, the observations performed, the staff international cooperation activities and conferences of the European Southern Observatory (ESO) are reported. The ESO's actions and achievements involving La Silla Observatory and efforts to finish the New Technology Telescope are underlined. The SN1987A observations are summarized. The activities of the European Coordination Facility for the Space Telescope are included. Researches on image processing and sky surveys are described. ESA

**N91-10424#** Cologne Univ. (Germany, F.R.). Inst. fuer Geophysik und Meteorologie.
**CLUSTER AS A WAVE TELESCOPE**
F. M. Neubauer, K.-H. Glassmeier, R. Walter, and M. W. Dunlop (Imperial Coll. of Science and Technology, London, England ) *In* ESA, Space Plasma Physics Investigation by Cluster and Regatta May 1990 p 51-55 Sponsored by BMFT and United Kingdom Science and Engineering Research Council (For primary document see N91-10417 01-46)
Copyright Avail: NTIS HC/MF A08; EPD, ESTEC, Noordwijk, Netherlands HC 40 Dutch guilders

**N91-10439*#** Iowa Univ., Iowa City. Dept. of Physics and Astronomy.
**RADIO WAVE REMOTE SENSING BY CLUSTER AND REGATTA**
Donald A. Gurnett *In* ESA, Space Plasma Physics Investigation by Cluster and Regatta May 1990 p 153-158 (For primary document see N91-10417 01-46)
(Contracts NAS5-30365; NAS5-30730)
Copyright Avail: NTIS HC/MF A08; EPD, ESTEC, Noordwijk, Netherlands HC 40 Dutch guilders CSCL 03A

## 90 ASTROPHYSICS

Includes cosmology; celestial mechanics; space plasmas; and interstellar and interplanetary gases and dust.
For related information see also *75 Plasma Physics.*

**N91-10810*#** Maryland Univ., College Park. Dept. of Physics and Astronomy.
**THE JOINT NASA/GODDARD-UNIVERSITY OF MARYLAND RESEARCH PROGRAM IN CHARGED PARTICLE AND HIGH ENERGY PHOTON DETECTOR TECHNOLOGY Final Report**
F. M. Ipavich May 1990 14 p
(Grant NGR-21-002-316)
(NASA-CR-180335; NAS 1.26:180335) Avail: NTIS HC/MF A03 CSCL 03B

The Univ. of Maryland portion investigated the following areas. The Space Physics Group performed studies of data from the AMPTE/CCE spacecraft CHEM experiment and found that the ratio of solar wind to photospheric abundances decreased rather smoothly with the first ionization potential (FIP) of the ion with the low FIP ion being about a factor of two overabundant. Carbon and hydrogen fit this trend particularly well. Several occurrences were analyzed of field aligned beams observed when CCE was upstream of the Earth's bow shock. Also using CHEM data, ring current intensity and composition changes during the main and recovery phases of the great geomagnetic storm that occurred in February 1986 was examined in detail. Still using CHEM data, ring current characteristics were examined in a survey of 20 magnetic storms ranging in size from -50 nT to -312 nT. A study was done of energetic ion anisotropy characteristics in the Earth's magnetosheath region using data from the UMD/MPE experiment on ISEE-1. The properties were analyzed of approx. 30 to 130 keV/e protons and alpha particles upstream of six quasi-parallel interplanetary shocks that passed by the ISEE-3 spacecraft during 1978 to 1979. Work from NASA-Goddard include studies from the High Energy Cosmic Ray Group, Low Energy Cosmic Ray Group, Low Energy Gamma Ray Group, High Energy Astrophysics Theory Group, and the X ray Astronomy Group. E.R.

**N91-10811** Yale Univ., New Haven, CT.
**COSMOLOGICAL SINGULARITIES IN ELECTROVACUUM SPACETIMES WITH TWO-PARAMETER SPACELIKE ISOMETRY GROUPS Ph.D. Thesis**
Philip Andrew Mansfield 1989 128 p
Avail: Univ. Microfilms Order No. DA9015837

The big bang singularities occurring in an infinite-dimensional class of solutions to the source-free Einstein-Maxwell equations are presented. These solutions are essentially Gowdy three-torus universes (not necessarily polarized) with electromagnetic radiation added. The problem is reformulated in terms of complex potentials analogous to those used by Ernst in the study of stationary axisymmetric metrics. It is shown that in these new variables the problem admits a harmonic map formulation. Its general solution is written as a perturbation series, where the background solutions being perturbed are a special class of real analytic functions obtained by evolving analytic data specified right at the singularity. The perturbation problem is solved to all orders, and terms which dominate as the singularity is approached are identified at each order. It is possible to sum the dominant terms, and thereby obtain explicit expressions representing the asymptotic structure of the singularities. This representation of asymptotic structure is developed into a simple geometric model. Specializing to the case of no electromagnetic fields, the model is then used to determine asymptotic metric and curvature properties in Gowdy spacetimes. The Gowdy metrics are Kasner-like near their singularity, which is generically a curvature singularity. Curvature-nonsingular solutions can be constructed, and extended into the past beyond a Cauchy horizon. However, such solutions are unstable, a fact which is consistent with Strong Cosmic Censorship. Dissert. Abstr.

**N91-10812** Cornell Univ., Ithaca, NY.
**LARGE SCALE STRUCTURES IN NONZERO LAMBDA FRIEDMANN UNIVERSES Ph.D. Thesis**

Hugo Martel 1990 191 p
Avail: Univ. Microfilms Order No. DA9018044

Several theoretical and observational arguments suggest the existence of a nonzero cosmological constant Lambda. Since the presence of such constant would affect the growth of gravitational instabilities leading to the formation of large scale structures, detailed observations of these structures, combined with theoretical models, might help to determine, or rule out, the existence of the cosmological constant. The results of a detailed study of the formation and evolution of large scale structures in Friedmann models composed of non-relativistic, pressureless matter and a nonzero cosmological constant are presented. The main objective was to determine how large scale structures are affected by the presence of the cosmological constant, and whether introducing a nonzero Lambda in the model improves the fit to the observations. The results can help to decide which observational tests are most likely to yield a determination the value of Lambda. The main approach consists of deriving relations among various quantities characterizing the large scale structures and the Friedmann background, and to study the dependence of these relations upon the value of the cosmological constant. Analytical approximations are described. Linear perturbation theory for Lambda models is rederived, and a simple relation between the peculiar velocity field, the density parameter, and the cosmological constant is obtained. The properties of spherically symmetric systems in nonzero Lambda models are described. Analytical expressions for the density enhancement inside halos for zero and nonzero Lambdas are derived. Numerical simulations of cosmic voids are presented. The relation between density contrast, peculiar velocity field, initial perturbation, and the cosmological parameters is discussed in great detail. N body simulations of galaxy clustering in nonzero Lambda models are presented. The dependence of the two-point correlation function upon the cosmological constant is discussed. All results lead to the conclusion that studying the large scale structures is unlikely to provide definitive information on the value of the cosmological constant. Dissert. Abstr.

**N91-10813** Michigan Univ., Ann Arbor.
**INVESTIGATION OF MARKARIAN GALAXIES WITH MULTIPLE NUCLEI Ph.D. Thesis**
Joseph Michael Mazzarella 1989 421 p
Avail: Univ. Microfilms Order No. DA9013968

Optical CCD images, long-slit spectroscopic data, coadded IRAS fluxes, and global H I line profiles are analyzed for a sample of 125 Markarian galaxies reported earlier to possess multiple optical nuclei or extreme morphological peculiarities. Twenty-six objects are isolated which display the strongest evidence for ongoing mergers between disk galaxies; the remainder consist of separated interacting systems, single late-type galaxies with multiple giant H II regions, plus a few ambiguous objects. The merger candidates are involved in low velocity encounters. H alpha and far-infrared luminosities indicate star formation rates that are an average of 3 to 10 times higher than in isolated disk galaxies. The presence of 8 Seyfert nuclei and 5 LINERs among 52 merger nuclei indicates a higher incidence of AGNs compared to isolated spirals at a significance level of 99.9 percent, and there is a higher fraction of AGN pairs than would be expected if the merger process did not induce Seyfert-like activity. Evidence for coupling between the ionization levels of the paired nuclei suggests either mixing by gas transfer between the components, or a selection bias towards pairs of galaxies with similar mass and metal abundances. Correlations between nuclear emission-line properties and global FIR properties indicate that the nuclei and giant H II regions are responsible for the bulk of the FIR luminosity. Radio continuum maps and optical images of Markarian 266 reveal the presence of a strong synchrotron source located between the active nuclei. This is interpreted as shock-induced acceleration of cosmic rays during the ongoing merger of two disk galaxies. Large scale shocking of the interstellar medium may also trigger star formation and destroy large dust grains, resulting in warm far-infrared emission which characterizes colliding disk galaxies. Dissert. Abstr.

**N91-10814** Edinburgh Univ. (Scotland).
**VIGOROUS STAR FORMATION IN GALACTIC NUCLEI Ph.D. Thesis**
Philip John Puxley 1988 232 p
Avail: Univ. Microfilms Order No. BRD-88486

Vigorous star formation in the nuclei of nearby galaxies is studied. A variety of techniques were employed to investigate several aspects of this phenomenon. Analysis of mid- and far-infrared data, taken by the Infrared Astronomical Satellite, suggests that among nearby spiral galaxies the presence of a stellar bar is a necessary condition for the existence of vigorous star-formation activity. Such regions contribute, on average, one third of the luminosity of the host galaxy. Medium-resolution radio continuum observations show that active star formation occurs in the central regions of galaxies, supporting the hypothesis that it is caused by a bar-driven inflow of disk material. Near-infrared spectrophotometry was used to study several of these highly dust-obscured regions in greater detail. Detection of the hydrogen recombination line Br gamma, which arises in photoionized gas, is further evidence for the presence of a population of massive stars. Measurements of molecular hydrogen lines demonstrate that this gas is also photoexcited, in contrast with previous studies. Models of the gas excitation in star-forming regions are constructed and comparison of the predicted line intensities with observations yields information regarding the gas density and structure of the complexes. The ionized gas in the archetypal starburst galaxy M82 is examined in greater detail through measurements made in mm-wavelength recombination lines (H40 and H53 alpha). These observations avoid the problems which occur when shorter-wavelength lines are employed since they are unaffected by dust attenuation. The ionization state of the gas and the total luminosity are used to infer the range of stellar masses present in this galaxy. This range may be very narrow. Dissert. Abstr.

**N91-10815** Alabama Univ., Huntsville.
**PARAMETERIZATION OF COSMOLOGICAL SCALE FACTOR DURING INFLATIONARY TIMES Ph.D. Thesis**
Renee Raouf Wahba 1989 96 p
Avail: Univ. Microfilms Order No. DA9015924

The inflationary period is modeled by generating a cosmological function, lambda(t), that depends on a period of exponential growth followed by a period of exponential decay. The model is equivalent to a single thermodynamic phase change and exhibits all the required features of an inflationary period such as exponential growth of the scale factor plus a natural relaxation (graceful exit) of lambda to the present day cosmological constant. After constraining the model to conditions imposed, by the inflationary hypothesis, a numerical computation is performed over the time period from the Planck time to the beginning of the radiation era. As a result of the constraints on the model, the presence of a very large negative Planckian cosmological constant was found. It was also found that the present-day value of this function, albeit small, is nevertheless positive. Using this model, the growth of the cosmological scale factor R(lambda) was found as a parameterized function of the cosmological function. It is shown that the numerical integration is greatly simplified if the multivalued function is solved. Not only does this greatly simplify the calculation, it shows that the parameterization of the scale factor in terms of the cosmological function is useful. Results are presented in a series of graphs. How the model could be related to either a Grand Unified theory or a quantum mechanical model of inflation in terms of the rate of production and decay of a (massive) X particle created by the initial instability of the vacuum at the planck time is discussed. It is further suggested that the cosmological function provides direct information about the decay rate (and hence the mass) of this X particle. Dissert. Abstr.

**N91-10816*#** National Aeronautics and Space Administration. Goddard Space Flight Center, Greenbelt, MD.
**ACCELERATION BY PULSAR WINDS IN BINARY SYSTEMS**
Alice K. Harding and T. K. Gaisser (Delaware Univ., Newark.) 30 Jan. 1990 43 p Submitted for publication

(NASA-TM-103451; NAS 1.15:103451; PB90-233305) Avail: NTIS HC/MF A03 CSCL 03B

In the absence of accretion torques, a pulsar in a binary system will spin down due to electromagnetic dipole radiation and the spin-down power will drive a wind of relativistic electron-positron pairs. Winds from pulsars with short periods will prevent any subsequent accretion but may be confined by the companion star atmosphere, wind, or magnetosphere to form a standing shock. The authors investigate the possibility of particle acceleration at such a pulsar wind shock and the production of very high energy (VHE) and ultra high energy (UHE) gamma rays from interactions of accelerated protons in the companion star's wind or atmosphere. They find that in close binaries containing active pulsars, protons will be shock accelerated to a maximum energy dependent on the pulsar spin-down luminosity. If a significant fraction of the spin-down power goes into particle acceleration, these systems should be sources of VHE and possibly UHE gamma rays. The authors discuss the application of the pulsar wind model to binary sources such as Cygnus X-3, as well as the possibility of observing VHE gamma-rays from known binary radio pulsar systems. GRA

**N91-10817#** Los Alamos National Lab., NM.
**A SEMI-ANALYTICAL MODEL OF STELLAR FLARES**
Roger A. Kopp and Giannina Poletto (Osservatorio Astrofisico di Arcetri, Florence, Italy ) 1990 4 p Presented at the Armagh International Colloquium on Surface Inhomogenities, Armagh, Ireland, 24-27 Jul. 1990 Submitted for publication Sponsored in part by Consiglio Nazionale delle Ricerche; Florence Univ., Italy; and Italian Space Agency
(Contract W-7405-eng-36)
(DE90-016434; LA-UR-90-2903; CONF-9007158-1) Avail: NTIS HC/MF A01

We present a simplified 'point' model to describe the hydrodynamic response of coronal loop plasma to the sudden release of energy which occurs at the time of a flare. Our simplification allows the full set of partial differential equations for energy, momentum, and mass conservation to be replaced by a corresponding set of ordinary differential equations for the plasma properties averaged over the loop volume. The temporal profiles of plasma temperature, density, and velocity are calculated over a time interval long enough to ensure that pre-flare conditions are re-established. The model is used for the interpretation of stellar flare data. In particular, we derive a set of representative loop geometries and flare energy inputs which allows us to reproduce the high emission measures typically inferred from observations of stellar flares. DOE

**N91-10818#** Los Alamos National Lab., NM. Theoretical Div.
**NUCLEAR STRUCTURE CALCULATIONS FOR ASTROPHYSICAL APPLICATIONS**
Peter Moeller, J. Rayford Nix, Karl-Ludwig Kratz, and W. Michael Howard (Lawrence Livermore National Lab., CA.) 15 Aug. 1990 12 p Presented at the International Symposium on Nuclear Astrophysics: Nuclei in the Cosmos, Vienna, Austria, 18-22 Jun. 1990 Submitted for publication
(Contract W-7405-eng-36)
(DE90-016433; LA-UR-90-2909; CONF-9006212-2) Avail: NTIS HC/MF A03

Relative to other fields of physics, astrophysics is probably unique in its requirement that a very large number of physical environments be modeled to achieve a satisfactory description of the phenomena under study. The dynamics of the cosmos is governed by interactions that span a vast range, from subnucleon, nucleon and nuclear distances to distances affected by the gravitational interactions, which extend over the width of a galaxy and beyond, to the edge of the universe. It is the nuclear processes that provide much of the energy that drives the macroscopic behavior of the cosmos. Through this energy release the behavior on the very small scale is coupled to the very large-scale behavior. On the nuclear level, cross sections, nuclear decay energies and nuclear decay paths are but a few examples of quantities that are of paramount importance in astrophysical models. Because nuclei of extreme composition, quite different from what can be studied on earth, exist in stellar environments, an understanding of the nuclear structure properties of these nuclei can only be obtained through theoretical means. This presents a continuing, stimulating challenge to the nuclear-physics community. Here we present calculated results on such diverse properties as nuclear energy levels, ground-state masses and shapes, (beta)-decay properties and fission-barrier heights. Our approach to these calculations is to use a unified theoretical framework within which the above properties can all be studied. The results are obtained in the macroscopic-microscopic approach in which a microscopic nuclear-structure single-particle model with extensions is combined with a macroscopic model, such as the liquid-drop model. DOE

**N91-10819#** Consiglio Nazionale delle Ricerche, Frascati (Italy). Ist. di Fisica dello Spazio Interplanetario.
**UV OBSERVATIONS OF HERBIG-HARO OBJECTS ASSOCIATED WITH BIPOLAR MOLECULAR OUTFLOWS: HH 7, HH 11 AND HH 29**
Murray Cameron (University Coll., London, England ) and Rene Liseau Apr. 1990 44 p Submitted for publication Sponsored in part by Swedish Board for Space Activities; Deutche Akademie der Wissenschaften; and Royal Society
(IFSI-90-9; ETN-90-97792) Avail: NTIS HC/MF A03

Observations carried out by the International Ultraviolet Explorer (IUE) of the shock exited nebulae HH 7, HH 11 and HH 29 are presented. The individual UV observations of these objects appear very faint. An alternative extraction method different from that commonly used for the reduction of IUE data is described. The method is applied to the data in image space therefore not distorting the photometry. The reliability of this method is demonstrated. Data from the observation of the Herbig-Haro stars is presented and discussed. ESA

**N91-10820#** Consiglio Nazionale delle Ricerche, Frascati (Italy). Ist. di Fisica dello Spazio Interplanetario.
**THE EMPIRICAL GEOMAGNETIC PARAMETER INFER NEAR-EARTH INTERPLANETARY SHOCKS**
A. Felici and M. Storini Apr. 1990 17 p
(IFSI-90-14; ETN-90-97796) Avail: NTIS HC/MF A03

The interaction of an interplanetary shock with the terrestrial magnetic field produces geomagnetic sudden storm commencements. Rapid variations observed in terrestrial magnetographs recorded from 1975 to 1986 are collected. They are to be used in a preliminary evaluation of the sudden storm commencement event which occurred during solar cycle N.21. The data is useful for studies connected to solar-terrestrial physics in the absence of solar wind measurements. ESA

# 91 LUNAR AND PLANETARY EXPLORATION

Includes planetology; and manned and unmanned flights. For spacecraft design or space stations see *18 Spacecraft Design, Testing and Performance.*

**N91-10821** Toledo Univ., OH.
**FUNDAMENTAL PROPERTIES AND MASS LOSS IN HOT, NEAR-MAIN SEQUENCE STARS Ph.D. Thesis**
James A. Grigsby 1989 559 p
Avail: Univ. Microfilms Order No. DA9015889

By obtaining spectra of 33 O9-B2 near-main sequence stars, and by calculating a grid of theoretical stellar atmospheres, the fundamental properties were determined and mass loss was examined in a select sample of stars. Most stars are cluster members and photometrically constant; all are single stars and none exhibit emission lines. The optical observations were made with the coude spectrograph at the 2.1 m and coude feed telescopes at Kitt Peak National Observatory; the data have a signal-to-noise ratio of around 100, and resolutions ranging from .11 to .5 A. High dispersion ultraviolet observations were made with the IUE satellite; additional data were obtained from the IUE archives. Effective temperatures, surface gravities, and projected rotational velocities in the program stars were determined by comparing selected lines of H, He I, and Mg II with a grid of models calculated with a non-LTE, line-blanketed code (Anderson, 1985, 1989). The code was updated to include bound-bound and bound-free transitions of H, He I and II, C II-III, N II-IV, O II-IV, and Mg II. A method of opacity sampling was developed to account for blanketing due to the elements with atomic numbers 21 to 28. Mass loss was characterized by a parameter describing the asymmetry of the C IV doublet. Roughly half the program stars show evidence of a wind-winds appear to switch on at around 26000 to 27000 K at a log g of 4, where the equivalent width of the model C IV doublet is 2.5 to 3 A. The degree of asymmetry of the C IV doublet shows a clear monotonic increase with temperature; it also shows a monotonic trend with luminosity. No abundance anomalies in He, N, and C are apparent. Dissert. Abstr.

# 92 SOLAR PHYSICS

Includes solar activity, solar flares, solar radiation and sunspots.

For related information see *93 Space Radiation.*

**N91-10822#** National Geophysical Data Center, Boulder, CO.
**SOLAR-GEOPHYSICAL DATA NUMBER 545, JANUARY 1990. PART 1 (PROMPT REPORTS). DATA FOR DECEMBER, NOVEMBER 1989 AND LATE DATA**
Helen E. Coffey, ed. Jan. 1990 154 p
(PB90-182338; SGD-545-Pt-1; ISSN-0038-0911; LC-79-640375)
Avail: NTIS HC/MF A08 CSCL 03B

A detailed index for 1989 is presented. Data for December 1989 include: solar-terrestrial environment, IUWDS alert periods (advance and worldwide), solar activity indices, solar flares, solar radio emission, and Stanford mean solar magnetic field. Data for November 1989 include: solar active regions, sudden ionospheric disturbances, solar radio spectral observations, cosmic ray measurements by neutron monitor, and geomagnetic indices. Late Data of geomagnetic indices from September to October 1989 include: solar active regions-Carrington Rotation 1821 October 1989. Author

**N91-10823#** National Geophysical Data Center, Boulder, CO.
**SOLAR-GEOPHYSICAL DATA NUMBER 546, FEBRUARY 1990. PART 1: (PROMPT REPORTS). DATA FOR JANUARY 1990, DECEMBER 1989, AND LATE DATA**
H. E. Coffey Feb. 1990 164 p
(PB90-195363; SGD-546-Pt-1) Avail: NTIS HC/MF A08 CSCL 09B

A detailed index is presented for 1989 and 1990. Data for January 1990 include: Solar terrestrial environment; IUWDS alert periods (advance and worldwide); Solar activity indices; Solar flares; Solar radio emission, and Stanford mean solar magnetic field. Data for December 1989 include: Solar active regions; Sudden ionospheric disturbances; Solar radio spectral observations; Cosmic ray measurements by neutron monitor; and Geomagnetic indices. Late data include: Cosmic ray measurements by neutron monitor; and Reprint of Halftone page Kitt Peak solar magnetic field synoptic chart for Nov. 1989. Author

**N91-10824#** National Geophysical Data Center, Boulder, CO.
**SOLAR-GEOPHYSICAL DATA NUMBER 546, FEBRUARY 1990. PART 2: (COMPREHENSIVE REPORTS). DATA FOR AUGUST 1989 AND MISCELLANEOUS**
H. E. Coffey Feb. 1990 184 p
(PB90-195371; SGD-546-Pt-2) Avail: NTIS HC/MF A09 CSCL 03B

A detailed index is presented for 1989 and 1990. Data for August 1989 include: Solar flares; solar radio bursts at fixed frequencies; Solar x ray radiation from GOES satellite; Mass ejections from the sun; and Active prominences and filaments. Miscellaneous data include: Meudon carte synoptique Carrington rotations 1816 and 1817 for June 1989; and Interplanetary solar particles. Author

**N91-10825#** National Geophysical Data Center, Boulder, CO.
**SOLAR-GEOPHYSICAL DATA NUMBER 547, MARCH 1990. PART 1: (PROMPT REPORTS). DATA FOR FEBRUARY, JANUARY 1990, AND LATE DATA**
H. E. Coffey Mar. 1990 153 p
(PB90-208877; SGD-547-Pt-1) Avail: NTIS HC/MF A08 CSCL 03B

A detailed index is presented for 1989 and 1990. Data for February 1990 include: Solar terrestrial environment; IUWDS alert periods (advance and worldwide); Solar activity indices; Solar flares; Solar radio emission; and Stanford mean solar magnetic field. Data for January 1990 include: Solar active regions; Sudden ionospheric disturbances; Solar radio spectral observations; Cosmic ray measurements by neutron monitor; and Geomagnetic indices. Late data include: Solar radio emission January 1990; Geomagnetic indices Oct. to Nov. 1989; and Solar geophysical data questionnaire results. Author

**N91-10826#** National Geophysical Data Center, Boulder, CO.
**SOLAR-GEOPHYSICAL DATA NUMBER 547, MARCH 1990. PART 2: (COMPREHENSIVE REPORTS). DATA FOR SEPTEMBER 1989 AND MISCELLANEOUS**
H. E. Coffey Mar. 1990 147 p
(PB90-208885; SGD-547-Pt-2) Avail: NTIS HC/MF A07 CSCL 03B

A detail index is presented for 1989 and 1990. Data for September 1989 include: Solar flares; Solar radio bursts at fixed frequencies; Solar x ray radiation from GOES satellite; Mass ejections from the sun; and Active prominences and filaments. Miscellaneous data include: Meudon carte synoptique; Carrington rotation 1818 July 1989; Solar proton events affecting the Earth's environment (GOES satellites) Jan. 1976 to Jan. 1990; and Solar geophysical data questionnaire results. Author

**N91-10827** Arizona Univ., Tucson.
**THE DEVELOPMENT OF THE CONTINUOUS ORTHONORMALIZATION AND ADJOINT METHODS FOR SOLAR SEISMOLOGY: EIGENFREQUENCY COMPUTATION AND SENSITIVITY ANALYSIS FOR DIRECT AND INVERSE PROBLEMS Ph.D. Thesis**
Ross Debner Rosenwald 1989 461 p
Avail: Univ. Microfilms Order No. DA9014679

Two new analysis methods for solar seismology are developed. Called the continuous orthonormalization (CON) and adjoint methods, their use enables both solar eigenfrequencies and eigenfrequency sensitivities to be computed more accurately and efficiently than with existing methods. The CON method integrates an eighth-order nonlinear system of ordinary differential equations (ODEs) which defines the linear adiabatic nonradial oscillation modes of the Sun. All normal modes of oscillation are treated identically, regardless of their type or their predominant location inside the Sun. The adjoint method integrates a related eighth-order linear inhomogeneous system of ODEs. From the resultant solution, an eigenfrequency's partial derivatives with respect to an extensive set of solar model parameters may be computed simultaneously. Extensive numerical tests confirm the validity of the two new methods. Eigenfrequencies obtained via the CON method have seven significant digits and match within 1 percent the eigenfrequencies obtained via finite difference or mesh approaches. Eigenfrequency sensitivities obtained via the adjoint method match with 2 percent the results obtained by explicitly perturbing the solar model parameters and recomputing the eigenfrequencies. The usefulness and power of the two new methods are demonstrated by applying them to the solution of an elementary solar inversion problem. A sample solar model's f-mode frequencies are iteratively driven into agreement with an observed set of f-mode frequencies. Adjoint sensitivity results are used to alter solar model parameters within hundreds of radial bins. Dissert. Abstr.

**N91-10828#** National Center for Atmospheric Research, Boulder, CO.

### SYNTHESIS AND INVERSION OF STOKES SPECTRAL PROFILES

G. A. Murphy 1990 341 p Prepared in cooperation with Sydney Univ., Australia
(Grant NSF ATM-87-09659)
(PB90-214487; NCAR/CT-124) Avail: NTIS HC/MF A15
CSCL 03B

Observations of Stokes spectral profiles enable the magnetic fields on the Sun's surface to be determined. Inversion is the process whereby the profiles are reduced to magnetic field vectors. One of the most robust, accurate, and rapid methods available for inversion uses the least squares fitting of analytical Stokes profiles. As this technique is suitable for the automated reduction of large sets of data, it was adopted for use with the Advanced Stokes Polarimeter, presently under development. The limitations of inversion by analytical profile fitting were not firmly established. Confident analysis of magnet field vectors depends upon the precise interpretation of reduced data. A framework is introduced which allows such an assessment to be made. The magnetofluid-static sunspon models presented provide a self-consistent range of physical conditions similar to those in sunspots. Inversion can then be carried out on Stokes profiles synthesized from these known realistic conditions. Author

**N91-10829*#** Jet Propulsion Lab., California Inst. of Tech., Pasadena.

### SOLAR EMISSION LEVELS AT LOW RADIO FREQUENCIES

W. C. Erickson (Maryland Univ., College Park.) 1 Oct. 1990 41 p
(Contract NAS7-918)
(NASA-CR-187337; JPL-Publ-90-34; NAS 1.26:187337) Avail: NTIS HC/MF A03 CSCL 03B

Solar radio emission could seriously interfere with observations made by a low frequency (1 to 10 MHz) array in space. International Sun-Earth Explorer (ISEE-3) radio data were used to determine solar emission level. The results indicate that solar emission should seriously disturb less than ten percent of the data, even during the years of solar maximum. Thus it appears that solar emission should not cause a disastrous loss of data. The information needed to design procedures to excise solar interference from the data produced by any low-frequency array is provided. Author

**N91-10830#** Lawrence Livermore National Lab., CA.

### CORONAL HEATING BY NANOFLARES: PLASMA DYNAMICS OF ELEMENTARY EVENTS

Roger A. Kopp and Giannina Poletto (Osservatorio Astrofisico di Arcetri, Florence, Italy ) 1990 4 p Presented at the Mechanisms of Chromospheric and Coronal Heating, Heidelberg, Fed. Republic of Germany, 5-8 Jun. 1990 Sponsored in part by Consiglio Nazionale delle Richerche; Florence Univ, Italy; and Italian Space Agency
(Contract W-7405-eng-36)
(DE90-016495; LA-UR-90-2764; CONF-9006261-1) Avail: NTIS HC/MF A01

It has been suggested by Parker Sturrock et al., and others that the corona may be stochastically heated, on spatial scales at or below current instrumental resolution limits, by a continuous succession of many small flarelike events commonly referred to as nanoflares. In this paper we extend a semi-analytical point model developed previously for solar compact flares, to include gravitational plasma downfall during the late decay phase. Applying the model to conditions representative of nanoflares allows us to predict the temporal variation of average plasma properties in such events and should ultimately facilitate a calculation of the spectral characteristics of a nanoflare-heated corona. DOE

**N91-10831#** Texas Univ., Austin.

### PROPAGATION OF MAGNETOACOUSTIC WAVES IN THE SOLAR ATMOSPHERE WITH RANDOM INHOMOGENEITIES OF DENSITY AND MAGNETIC FIELDS

M. Ryutova (Academy of Sciences, USSR, Novosibirsk ), M. Kaisig, and T. Tajima Aug. 1990 18 p
(Contract DE-FG05-80ET-53088)
(DE90-017616; DOE/ET-53088/446; IFSR-446) Avail: NTIS HC/MF A03

Effects of strong and random inhomogeneities of the magnetic fields, plasma density, and temperature in the solar atmosphere on the properties of magnetoacoustic waves of arbitrary amplitudes are studied. The procedure which allows one to obtain the averaged equation containing the nonlinearity of a wave, dispersion properties of a system, and dissipative effects is described. It is shown that depending on the statistical properties of the medium, different scenarios of wave propagation arise: in the predominance of dissipative effects the primary wave is damped away in the linear stage and the efficiency of heating due to inhomogeneities is much greater than that in homogeneous medium. Depending on the interplay of nonlinear and dispersion effects, the process of heating can be afforded through the formation of shocks or through the storing of energy in a system of solitons which are later damped away. Our computer simulation supports and extends the above theoretical investigations. In particular the enhanced dissipation of waves due to the strong and random inhomogeneities is observed and this is more pronounced for shorter waves. DOE

**N91-10832*#** National Aeronautics and Space Administration. Marshall Space Flight Center, Huntsville, AL.

### COALIGNED OBSERVATIONS OF SOLAR MAGNETIC FIELDS AT DIFFERENT HEIGHTS: MSFC CENTER DIRECTOR'S DISCRETIONARY FUND FINAL REPORT (PROJECT NO. 88-10)

M. J. Hagyard, E. A. West, G. A. Gary, and J. E. Smith Sep. 1990 36 p
(NASA-TM-103516; NAS 1.15:103516) Avail: NTIS HC/MF A03
CSCL 03B

The objective was to develop the capability for and coaligned observations of the structure and evolution of the Sun's magnetic field at two different heights in the solar atmosphere: the photosphere, which is the lowest region observable with optical telescopes; and the chromosphere, which lies just above the photosphere and is the region where the magnetic field dominates the gas motion so that a well-ordered structure governed by the field is observed. By obtaining this three-dimensional picture of the solar magnetic field, a better understanding can be developed of the magnetic forces that produce and control the dynamic, high-energy phenomena occurring in the solar atmosphere that can affect the entire heliosphere, including the terrestrial environment. Author

**N91-10833#** Consiglio Nazionale delle Ricerche, Rome (Italy). Ist. di Fisica dello Spazio Interplanetario.

### PLOTS OF THE 5-MINUTE NEUTRON MONITOR INTENSITY AND MULTIPLICITIES RECORDED BY THE ROME 17-NM64, MARCH 1990

G. Villoresi, F. Re, F. Signoretti, N. L. Zangrilli, and N. Iucci (Rome Univ., Italy ) Frascati, Italy Apr. 1990 67 p
(IFSI-90-15; ETN-90-97797) Avail: NTIS HC/MF A04

The preliminary five minute pressure corrected data of total neutron intensity and of the intensities of multiplicities one to greater than or equal to eight are presented in the form of daily plots. The data was recorded during March 1990 by the Rome 17-NM-64. Ways in which the data can be used during the forthcoming solar activity maximum are discussed. For each monitor section the various multiplicities are measured in a gate time of 1200 microseconds. The attenuation coefficients for atmospheric pressure change correction are given. ESA

**N91-10834#** Consiglio Nazionale delle Ricerche, Rome (Italy). Ist. di Fisica dello Spazio Interplanetario.

### PLOTS OF THE 5-MINUTE NEUTRON MONITOR INTENSITY AND MULTIPLICITIES RECORDED BY THE ROME 17-NM64, APRIL 1990

G. Villoresi, F. Re, F. Signoretti, N. L. Zangrilli, and N. Iucci (Rome Univ., Italy ) Frascati, Italy May 1990 63 p
(IFSI-90-18; ETN-90-97800) Avail: NTIS HC/MF A04

The preliminary five minute pressure corrected data of total neutron intensity and of the intensities of multiplicities one to greater than or equal to eight are presented in the form of daily plots. The data was recorded during April 1990 by the Rome 17-NM-64. Ways in which this data could be used during the forthcoming solar activity maximum are discussed. For each monitor section the various multiplicities are measured in a gate time of 1200 microseconds. The attenuation coefficients for atmospheric pressure change correction are given. ESA

**N91-10433#** Ceskoslovenska Akademie Ved, Ondrejov. Astronomical Inst.
**THE IMPORTANCE OF SIMULTANEOUS MONITORING OF SOLAR ACTIVITY FOR THE INTERPRETATION OF SOLAR PLASMA PHENOMENA**
B. Valnicek *In* ESA, Space Plasma Physics Investigation by Cluster and Regatta May 1990 p 109-111 (For primary document see N91-10417 01-46)
Copyright Avail: NTIS HC/MF A08; EPD, ESTEC, Noordwijk, Netherlands HC 40 Dutch guilders

# 93 SPACE RADIATION

Includes cosmic radiation; and inner and outer earth's radiation belts.

For biological effects of radiation see *52 Aerospace Medicine.* For theory see *73 Nuclear and High-Energy Physics.*

**N91-10835** Manchester Univ. (England).
**CORE-DOMINATED RADIO SOURCES AND THE UNIFIED SCHEME Ph.D. Thesis**
David W. Murphy 1988 284 p
Avail: Univ. Microfilms Order No. BRD-88730

The radio properties of a complete sample of 94 core-dominated radio sources, observed with the VLA, are examined to determine whether these properties are consistent with the hypothesis, known as the unified scheme, that core-dominated quasars are intrinsically the same object as lobe-dominated quasars, but just viewed with their radio jets oriented closer to the line of sight. High dynamic range maps are produced by combining data sets from different VLA arrays, frequencies and epochs. Various distributions of parameters are compared with the predictions of the relativistic beaming models. In particular it is found that the data cannot be fitted with a single relativistic jet velocity but require a large dispersion in this parameter. This dispersion only agrees with VLBI data on transverse motions if Hubble's constant is nearer to 100 than 50 km s(exp-1) Mpc(exp-1). Furthermore the large projected linear sizes of the quasars cannot be explained by large intrinsic bend angles but require that these sources have large intrinsic linear sizes. Evidence is also found from the radio properties of the BL Lacs in the sample that they are not quasars oriented with their radio jets at very small angles to the line of sight, as has been proposed by various authors. The radio morphology and spectra of the empty field sources indicate that they may belong to the 'compact VLBI double' class of radio source. Finally published optical and x-ray data on quasars are examined and evidence is found for the existence of a beamed component in radio sources which exhibits itself in all wavebands from the radio to the x-ray regime. The presence of such a component has obvious repercussions for understanding of Active Galactic Nuclei. Dissert. Abstr.

**N91-10836#** Los Alamos National Lab., NM.
**INTRINSIC NEUTRINO PROPERTIES: AS DEDUCED FROM COSMOLOGY, ASTROPHYSICS, ACCELERATOR, AND NON-ACCELERATOR EXPERIMENTS**
S. P. Rosen 25 Jul. 1990 17 p Presented at the 1st International Symposium on Particles, Strings, and Cosmology, Boston, MA, 27-31 Mar. 1990 Submitted for publication
(Contract W-7405-eng-36)
(DE90-016467; LA-UR-90-2631; CONF-900367-2) Avail: NTIS HC/MF A03

Intrinsic properties of neutrinos as deduced from cosmological, astrophysical, and laboratory experiments are reviewed. Bounds on magnetic moments and theoretical models which yield large moments but small masses are briefly discussed. The MSW solution to the solar neutrino problem is reviewed in light of the existing data from the Cl-37 and Kamiokande II experiments. The combined data disfavor the adiabatic solution and tend to support either the large angle solution or the nonadiabatic one. In the former case the Ga-71 signal will be suppressed by the same factor as for Cl-37, and in the latter case the suppression factor could be as large as 10 or more. DOE

**N91-10837#** Consiglio Nazionale delle Ricerche, Rome (Italy). Ist. di Fisica dello Spazio Interplanetario.
**ON THE AUTOREGRESSION METHODS APPLIED TO THE HOURLY NUCLEONIC-COMPONENT RECORDS**
S. Pase, M. Parisi, S. Sparnocchia (Rome Univ., Italy ), E. Salusti, and M. Storini Frascati, Italy Oct. 1989 29 p
(IFSI-89-19; ETN-90-97780) Avail: NTIS HC/MF A03

Application of autoregressive methods to temporal variations of the cosmic ray nucleonic component is presented. The hourly data registered in Rome (Italy) in the NM-64 detector with a threshold rigidity of 6.2 GV during the period 1977 to 1982 is examined. The results obtained through analysis of two Forbush decreases are discussed in detail. These events on February 14, 1978 and July 10, 1982 are shown to be best analyzed using a nonlinear autoregressive model rather than a linear model. The decrease amplitude and temporal recovery phase are easily reconstructed without the aid of external physical parameters. ESA

**N91-10838#** Consiglio Nazionale delle Ricerche, Rome (Italy). Ist. di Fisica dello Spazio Interplanetario.
**COSMIC-RAY INTENSITY INCREASE OBSERVED ON SEPTEMBER 29, 1989: THE CHILEAN NEUTRON MONITOR DATA (BRIEF REPORT)**
E. G. Cordado, N. Iucci (Rome Univ., Italy ), and M. Storini Frascati, Italy Feb. 1990 12 p
(IFSI-90-4; ETN-90-97787) Avail: NTIS HC/MF A03

Data obtained in Chile with the standard neutron monitor are reported. The Santiago 6NM-64 monitor has a geomagnetic cut-off rigidity of about 11 GV. A ground-level solar cosmic ray event registered on September 29, 1989 is analyzed in detail. Possible studies connected with such a rare event are suggested. The importance of such studies in developing a better understanding of solar-interplanetary-terrestrial relations is stressed. Comparisons between the readings recorded at the Rome and Japan based stations are presented. ESA

# 99 GENERAL

No abstracts in this category.

# SUBJECT INDEX

## Typical Subject Index Listing

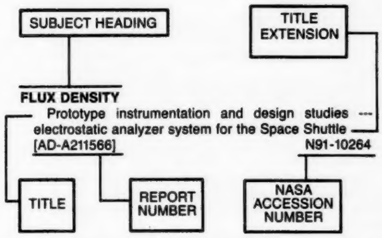

The subject heading is a key to the subject content of the document. Titles, report numbers, and accession numbers of pertinent documents are provided under each subject heading. When the title is insufficiently descriptive of the document content, a title extension has been added, separated from the title by three hyphens. The report number helps to indicate the type of document cited (e.g., NASA report, NASA translation, NASA contractor report). The NASA accession number is the number by which the document abstracts are arranged in this journal and by which the document is sold or requested. The titles, with title extensions if present, are arranged under each subject heading in ascending accession number order. The subject headings have been selected from the latest revision of the *NASA Thesaurus* (NASA SP-7064).

## A

**ABILITIES**
The effects of outcome and process feedback [NASA-CR-187332] N91-10595

**ABLATION**
Prevention of breakdown behind railgun projectiles [DE90-014573] N91-10094

**ABSORPTION SPECTRA**
Infrared absorption in boron carbides: Dependence on isotope and carbon concentration [DE90-017592] N91-10132
Recent advances in excimer laser technology at Los Alamos [DE90-016441] N91-10276
Biomedical applications on laser technology at Los Alamos [DE90-016447] N91-10277
Nonlinear optical absorption in intrinsic Stark effect superlattices [DE90-016466] N91-10767

**ABSORPTION SPECTROSCOPY**
Measurements of the light-absorbing material inside cloud droplets and its effect on cloud albedo N91-10528

**ABSORPTIVITY**
Multi-spectral window radiance observations of Cirrus from satellite and aircraft, November 2, 1986 Project FIRE N91-10465

**ABSTRACTS**
JPRS report: Science and technology. USSR: Space [JPRS-USP-89-009] N91-10088
JPRS report: Science and technology. USSR: Space [JPRS-USP-90-001] N91-10089
JPRS report: Science and technology. USSR: Space [JPRS-USP-90-002] N91-10090
JPRS report: Science and technology. USSR: Electronics and electrical engineering [JPRS-UEE-90-004] N91-10213
JPRS report: Science and technology. USSR: Electronics and electrical engineering [JPRS-UEE-90-007] N91-10215
JPRS report: Science and technology. USSR: Electronics and electrical engineering [JPRS-UEE-90-008] N91-10216
JPRS report: Science and technology. USSR: Electronics and electrical engineering [JPRS-UEE-90-009] N91-10217
JPRS report: Science and technology. USSR: Earth sciences [JPRS-UES-90-007] N91-10377
JPRS report: Science and technology. USSR: Life sciences [JPRS-ULS-90-001] N91-10551
JPRS report: Science and technology. USSR: Life sciences [JPRS-ULS-90-013] N91-10552
JPRS report: Science and technology. USSR: Life sciences [JPRS-ULS-90-012] N91-10556
JPRS report: Science and technology. USSR: Life sciences [JPRS-ULS-90-011] N91-10565
JPRS Report: Science and technology. USSR: Life sciences [JPRS-ULS-90-010] N91-10568
JPRS Report: Science and technology. USSR: Life sciences [JPRS-ULS-90-009] N91-10569
JPRS Report: Science and technology. USSR: Life sciences [JPRS-ULS-90-008] N91-10570
JPRS Report: Science and technology. USSR: Life sciences [JPRS-ULS-90-006] N91-10571
JPRS report: Science and technology. USSR: Life sciences [JPRS-ULS-90-005] N91-10572
JPRS report: Science and technology. USSR: Life sciences [JPRS-ULS-89-008] N91-10589
JPRS report: Science and technology. USSR: Life sciences [JPRS-ULS-89-010] N91-10590
JPRS report: Science and technology. USSR: Physics and mathematics [JPRS-UPM-90-003] N91-10694
Technical Abstracts: Mechanical engineering [DE90-014797] N91-10802

**ABUNDANCE**
The Joint NASA/Goddard-University of Maryland Research Program in Charged Particle and High Energy Photon Detector Technology [NASA-CR-180335] N91-10810

**ACCELERATION (PHYSICS)**
Analysis techniques for residual acceleration data [NASA-TM-103507] N91-10191
Development of the force envelope for an acceleration/force extremal controlled vibration test [DE90-015712] N91-10329

**ACCESS CONTROL**
Optimization of polling systems [CWI-BS-R8932] N91-10635

**ACCURACY**
Intrinsic (?) reference standards [DE90-015714] N91-10696

**ACETIC ACID**
Effects of prolonged exposure to acetic acid vapors on acid-base balance in humans N91-10561

**ACID BASE EQUILIBRIUM**
Effects of prolonged exposure to acetic acid vapors on acid-base balance in humans N91-10561

**ACID RAIN**
National acid precipitation assessment program. Report to the President and Congress [PB90-185646] N91-10405

**ACOUSTIC EMISSION**
Vibro-acoustic emission rubbing sources [PNR-90730] N91-10336

**ACOUSTIC EXCITATION**
The instability of combustion in propulsion engines N91-10141

**ACOUSTIC PROPAGATION**
Structural acoustics: An applied science with many applications [PB90-183633] N91-10698

**ACOUSTIC PROPERTIES**
Properties of acoustic energy quantities [DE90-518714] N91-10701

**ACOUSTICAL HOLOGRAPHY**
Variable-coherence beam optics [ISBN-952-90-1784-7] N91-10724

**ACOUSTICS**
Time/frequency analysis of vibro-acoustic behaviour of a launcher in flight [ETN-90-97584] N91-10097
PREGO: A simulation code for one-dimensional viscoelastic acoustics [DE90-014859] N91-10700
Properties of acoustic energy quantities [DE90-518714] N91-10701

**ACTIVATED CARBON**
The transport properties of activated carbon fibers [DE90-015910] N91-10130

**ACTIVATION ENERGY**
Reaction kinetics of the Ca-SO2 system in absence of inter-grain pore diffusion [DE90-009672] N91-10781

**ACTIVE CONTROL**
Computation of maximum gust loads in nonlinear aircraft using a new method based on the matched filter approach and numerical optimization N91-10317
Static and dynamic aeroelastic characterization of an aerodynamically heated generic hypersonic aircraft configuration N91-10320
A distributed control and monitor system used in laser fusion research [DE90-013476] N91-10732

**ACTUATORS**
The actuator for the low-noise STOL test plane flight control system and its development test [NAL-TM-574] N91-10038
Plasma puff initiation of high Coulomb transfer switches [NASA-CR-187024] N91-10735

**ADA (PROGRAMMING LANGUAGE)**
Proceedings of the Thirteenth Annual Software Engineering Workshop [NASA-TM-103314] N91-10606
Evolving impact of Ada on a production software environment N91-10607
Ada software productivity prototypes: A case study N91-10613
Experiences with Ada in an embedded system N91-10614
A modernized PDL approach for Ada software development N91-10616

**ADAPTATION**
Work, exercise, and space flight. 1: Operations, environment, and effects of spaceflight N91-10578
A unique problem of muscle adaptation from weightlessness: The deceleration deficiency N91-10582
Work, exercise, and space flight. 2: Modification of adaptation by exercise (exercise prescription) N91-10586
Cardiovascular group N91-10587

**ADDING CIRCUITS**
Multiple channel programmable coincidence counter [DE90-014681] N91-10602

**ADDITIVES**
Specific impulse comparison of high density hydrocarbon fuel burned with oxygen [NAL-TR-1053] N91-10148
Radiation-induced microstructural development and microchemical changes in Fe-Cr-Mn-Ni solute-bearing alloys [DE90-016359] N91-10160
Evaluation of two bisimide additives in LARC-TPI adhesive [NASA-TM-102742] N91-10182

**ADHESIVES**
Evaluation of two bisimide additives in LARC-TPI adhesive
[NASA-TM-102742] N91-10182
The looped adhesive strip: An example of coplanar delamination interaction N91-10306
**ADIABATIC EQUATIONS**
Theory of longitudinal adiabatic invariant in the helical torus
[NIFS-37] N91-10749
**ADRENAL GLAND**
Morphological examination of rat adrenal glands following flight aboard Biosputnik Kosmos-1667
N91-10553
**ADSORPTION**
Nano-composite desiccation materials
[PB90-247388] N91-10123
**ADVANCED VERY HIGH RESOLUTION RADIOMETER**
FAX image processing N91-10361
ERBE and AVHRR Cirrus cloud fire study N91-10472
AVHRR and VISSR satellite instrument calibration results for both Cirrus and marine stratocumulus IFO periods N91-10475
**ADVECTION**
The 'optimum' upwind advection on a triangular mesh
[NASA-CR-187459] N91-10250
Q-vectors: A new approach to an old problem
[PB90-235490] N91-10414
Energetics of valley and basin atmospheres during the evening transition and nighttime periods
[DE90-016356] N91-10542
**AERODYNAMIC CHARACTERISTICS**
Euler and potential experiment/CFD correlations for a transport and two delta-wing configurations
[NASA-TM-102206] N91-10014
Application of flight path reconstruction algorithms for flight data of helicopter
[NAL-TM-582] N91-10031
Nonlinear feedback control for high alpha flight
[NASA-CR-186545] N91-10047
Effects of coolant injection on turbine aerodynamic characteristics. Part 1: Test turbine and apparatus
[NAL-TM-585-PT-1] N91-10059
Experimental investigation on the effect of coolant injection on turbine aerodynamic characteristics. Part 2: Effects of injection from rotor casing with 30 deg slanted holes
[NAL-TM-587-PT-2] N91-10060
The evolution of the bypass engine
[PNR-90707] N91-10068
Entry vehicle performance analysis and atmospheric guidance algorithm for precision landing on Mars
[NASA-CR-185614] N91-10102
Aeroacoustic effects of reduced aft tip speed at constant thrust for a model counterrotation turboprop at takeoff conditions
[NASA-TM-103608] N91-10703
**AERODYNAMIC CONFIGURATIONS**
Euler and potential experiment/CFD correlations for a transport and two delta-wing configurations
[NASA-TM-102206] N91-10014
Project HyBuJET
[NASA-CR-187011] N91-10040
Body weight of hypersonic aircraft, part 1
[NASA-TM-101028] N91-10049
The evolution of the bypass engine
[PNR-90707] N91-10068
Design/development issues for high bypass ratio fans
[PNR-90758] N91-10076
**AERODYNAMIC FORCES**
Evaluation of the ZONA51D program
[REPT-B-28] N91-10025
Direct use of linear time-domain aerodynamics in aeroservoelastic analysis: Aerodynamic model
N91-10316
**AERODYNAMIC INTERFERENCE**
Wall interference studies
[PD-CF-9012] N91-10232
**AERODYNAMIC STABILITY**
Prediction and comparison with measurements of the aerodynamic characteristics of flare-stabilized XM910 prototypes
[AD-A208099] N91-10005
Flight characteristics of a modified Schweizer SGS1-36 sailplane at low and very high angles of attack
[NASA-TP-3022] N91-10079
**AERODYNAMICS**
Aeronautical engineering: A continuing bibliography with indexes (supplement 256)
[NASA-SP-7037(256)] N91-10002
Energy efficiency improvement potential of commercial aircraft to 2010
[DE90-014767] N91-10046
Measurement of unsteady blade surface pressure on a single rotation large scale advanced prop-fan with angular and wake inflow at Mach numbers from 0.02 to 0.70
[NASA-CR-182123] N91-10065
**AEROELASTIC RESEARCH WINGS**
Design of control laws for flutter suppression based on the aerodynamic energy concept and comparisons with other design methods
[NASA-TP-3056] N91-10328
**AEROELASTICITY**
Aeroelastic analysis of wings using the Euler equations with a deforming mesh
[NASA-TM-102733] N91-10020
Evaluation of the ZONA51D program
[REPT-B-28] N91-10025
Direct use of linear time-domain aerodynamics in aeroservoelastic analysis: Aerodynamic model
N91-10316
Static and dynamic aeroelastic characterization of an aerodynamically heated generic hypersonic aircraft configuration N91-10320
**AERONAUTICAL ENGINEERING**
Aeronautical engineering: A continuing bibliography with indexes (supplement 256)
[NASA-SP-7037(256)] N91-10002
Bibliography of Lewis Research Center technical publications announced in 1989
[NASA-TM-102542] N91-10798
**AEROSOLS**
A synopsis of Langley Research Center's lidar effort for the 1986 FIRE IFO N91-10457
Lidar and aircraft studies of deep Cirrus systems from the 1986 FIRE IFO N91-10460
Marine stratocumulus cloud characteristics from multichannel satellite measurements N91-10502
Aerosol measurements in the stratocumulus project
N91-10506
NRL tethered balloon measurements at San Nicolas Island during FIRE IFO 1987 N91-10509
Horizontal variability of the marine boundary layer structure upwind of San Nicolas Island during FIRE, 1987 N91-10519
Measurements of the light-absorbing material inside cloud droplets and its effect on cloud albedo
N91-10528
**AEROSPACE ENGINEERING**
JPRS report: Science and technology. USSR: Space
[JPRS-USP-90-001] N91-10089
Bibliography of Lewis Research Center technical publications announced in 1989
[NASA-TM-102542] N91-10798
**AEROSPACE INDUSTRY**
Total quality management at Rolls-Royce PLC
[PNR-90759] N91-10298
Space market model space industry input-output model
[NASA-CR-187252] N91-10795
**AEROSPACE MEDICINE**
Aerospace medicine and biology: A continuing bibliography with indexes (supplement 341)
[NASA-SP-7011(341)] N91-10594
**AEROSPACE PLANES**
Numerical simulation of hypersonic flow around a space plane. Part 3: Analysis of aerothermodynamic heating
[NAL-TR-1027T] N91-10011
**AEROSPACE SCIENCES**
JPRS report: Science and technology. USSR: Space
[JPRS-USP-89-009] N91-10088
JPRS report: Science and technology. USSR: Space
[JPRS-USP-90-002] N91-10090
Bibliography of Lewis Research Center technical publications announced in 1989
[NASA-TM-102542] N91-10798
NASA Thesaurus supplement: A four part cumulative supplement to the 1988 edition of the NASA Thesaurus (supplement 4)
[NASA-SP-7064-SUPPL-4] N91-10804
**AEROTHERMOCHEMISTRY**
User's guide to CUNIFLOW
[AD-A207606] N91-10004
The instability of combustion in propulsion engines
N91-10141
**AEROTHERMODYNAMICS**
Numerical simulation of hypersonic flow around a space plane. Part 3: Analysis of aerothermodynamic heating
[NAL-TR-1027T] N91-10011
Static and dynamic aeroelastic characterization of an aerodynamically heated generic hypersonic aircraft configuration N91-10320
**AEROTHERMOELASTICITY**
Static and dynamic aeroelastic characterization of an aerodynamically heated generic hypersonic aircraft configuration N91-10320
**AGING (MATERIALS)**
Contribution to the study of MOS structures ageing
[ECL-90-04] N91-10785
**AGRICULTURE**
Potential effects of global climate change on the United States. Appendix C: Agriculture, volume 1
[PB90-171588] N91-10394
Potential effects of global climate change on the United States. Appendix C: Agriculture, volume 2
[PB90-171596] N91-10397
**AIR**
Measured and predicted shock shapes for AFE configuration at Mach 6 in air and in CF4
[NASA-TM-100660] N91-10245
**AIR BREATHING ENGINES**
Analysis of pulsed laser-generated impulse in an advanced airbreathing thruster N91-10062
**AIR FLOW**
Measurement of air entrainment by a free jet using laser velocimetry and Raman scattering
[ISL-R-109/89] N91-10017
Effects of coolant injection on turbine aerodynamic characteristics. Part 1: Test turbine and apparatus
[NAL-TM-585-PT-1] N91-10059
Experimental investigation on the effect of coolant injection on turbine aerodynamic characteristics. Part 2: Effects of injection from rotor casing with 30 deg slanted holes
[NAL-TM-587-PT-2] N91-10060
Terrain-induced mesoscale circulations in the Columbia Basin
[DE90-016338] N91-10541
**AIR JETS**
Transient characteristics of unconfined fire plume-driven ceiling jets
[PB90-227976] N91-10193
**AIR MASSES**
Rn222, Rn222 progeny and Rn220 progeny as atmospheric tracers of air masses at the Mauno Loa Observatory
[DE90-014872] N91-10539
About the possibilities of using an air mass transformation model in Taiyuan, Shanxi Province, China
[KNMI-TR-120] N91-10540
**AIR POLLUTION**
National acid precipitation assessment program. Report to the President and Congress
[PB90-185646] N91-10405
**AIR QUALITY**
Chesapeake Bay Basin Monitoring Program Atlas. Volume 1: Water quality and other physiochemical monitoring programs
[PB90-147935] N91-10391
Potential effects of global climate change on the United States. Appendix F: Air quality
[PB90-172230] N91-10400
Geophysical monitoring for climatic change
[PB90-222126] N91-10538
**AIR TRAFFIC CONTROL**
DOD responsibilities on Federal aviation and national airspace system matters
[PB90-218827] N91-10001
National airspace system: In-flight assistance operational concept
[PB90-233115] N91-10032
Operational evaluation of initial data link air traffic control services. Volume 2: Appendices
[DOT/FAA/CT-90/1-VOL-2] N91-10033
FAA air traffic operational evaluation of Automated Surface Observing System (ASOS)
[DOT/FAA/CT-TN90/42] N91-10084
**AIR TRANSPORTATION**
Ada software productivity prototypes: A case study
N91-10613
**AIR WATER INTERACTIONS**
Cloud and boundary layer structure over San Nicolas Island during FIRE N91-10515
Horizontal variability of the marine boundary layer structure upwind of San Nicolas Island during FIRE, 1987 N91-10519
Plume mechanics and stratocumulus convection
N91-10526
**AIRBORNE EQUIPMENT**
Lidar and aircraft studies of deep Cirrus systems from the 1986 FIRE IFO N91-10460
A study of marine stratocumulus using lidar and other FIRE aircraft observations N91-10511
Cloud absorption properties as derived from airborne measurements of scattered radiation within clouds
N91-10512
**AIRBORNE/SPACEBORNE COMPUTERS**
Static and dynamic aeroelastic characterization of an aerodynamically heated generic hypersonic aircraft configuration N91-10320

**AIRCRAFT CONFIGURATIONS**

Re-engining: Real stage 3 compliance plus other benefits
[PNR-90755] N91-10075

Static and dynamic aeroelastic characterization of an aerodynamically heated generic hypersonic aircraft configuration N91-10320

**AIRCRAFT CONTROL**

Computation of maximum gust loads in nonlinear aircraft using a new method based on the matched filter approach and numerical optimization N91-10317

**AIRCRAFT DESIGN**

Project HyBuJET
[NASA-CR-187011] N91-10040

OVRhyp, scramjet test aircraft
[NASA-CR-187009] N91-10041

Body weight of hypersonic aircraft, part 1
[NASA-TM-101028] N91-10049

Supersonic combustion engine testbed, heat lightning
[NASA-CR-187010] N91-10061

Computation of maximum gust loads in nonlinear aircraft using a new method based on the matched filter approach and numerical optimization N91-10317

**AIRCRAFT ENGINES**

Progress in certifying F402-RR-408: The improved Pegasus engine for AV-8B and Harrier 2 plus
[PNR-90719] N91-10056

Aero engine design factors for a low fuel price scenario
[PNR-90681] N91-10066

The evolution of the bypass engine
[PNR-90707] N91-10068

Applications of thermally sprayed coating systems in aero engines
[PNR-90750] N91-10072

Casting alloys for the jet age
[PNR-90723] N91-10168

Total quality management at Rolls-Royce PLC
[PNR-90759] N91-10298

**AIRCRAFT EQUIPMENT**

The actuator for the low-noise STOL test plane flight control system and its development test
[NAL-TM-574] N91-10038

**AIRCRAFT FUELS**

Tests of the general fire suppression concentrate Pyrocap B-136
[DOT/FAA/CT-TN90/21] N91-10029

**AIRCRAFT INSTRUMENTS**

Automatic determination of fault effects on aircraft functionality
[NASA-CR-181352] N91-10039

**AIRCRAFT MAINTENANCE**

Structural risk assessment and aircraft fleet maintenance N91-10321

**AIRCRAFT NOISE**

Re-engining: Real stage 3 compliance plus other benefits
[PNR-90755] N91-10075

Do we really need 57 ways of rating aircraft noise
[PNR-90720] N91-10704

**AIRCRAFT POWER SUPPLIES**

Practical flight paths for microwave-powered airplanes
[NAL-TR-1052T] N91-10054

**AIRCRAFT SAFETY**

Development and application of linear and nonlinear methods for interpretation of lightning strikes to in-flight aircraft
[NASA-CR-3974] N91-10548

**AIRCRAFT STABILITY**

Static and dynamic aeroelastic characterization of an aerodynamically heated generic hypersonic aircraft configuration N91-10320

**AIRCRAFT STRUCTURES**

Seat dynamic performance standards for a range of sizes
[DOT/FAA/CT-TN90/23] N91-10028

Introduction: Needs and approaches to reliability and quality assurance in design and manufacture
[PNR-90683] N91-10297

Repeated buckling of composite shear panels
N91-10303

Computation of maximum gust loads in nonlinear aircraft using a new method based on the matched filter approach and numerical optimization N91-10317

**AIRCRAFT WAKES**

Application of a state-space wake model to elastic blade flapping in hover N91-10006

**AIRFOIL OSCILLATIONS**

Aeroelastic analysis of wings using the Euler equations with a deforming mesh
[NASA-TM-102733] N91-10020

**AIRFOIL PROFILES**

Optimum hypersonic airfoil with power law shock waves
[DE90-014903] N91-10008

Modeling blade/vortex interactions
[ISL-R-107/89] N91-10016

Determination of the pressure drag of airfoils by integration of surface pressures
[NASA-TM-102722] N91-10078

**AIRFOILS**

Numerical computation of viscous flow about unconventional airfoil shapes
[NASA-CR-187343] N91-10019

Heat transfer in aero engine gas turbines, part 1
[PNR-90754-PT-1] N91-10074

**AIRFRAMES**

Rotor systems research aircraft risk-reduction shake test
[NASA-TM-4186] N91-10045

**AIRPORT TOWERS**

FAA air traffic operational evaluation of Automated Surface Observing System (ASOS)
[DOT/FAA/CT-TN90/42] N91-10084

**AIRSPEED**

A consideration on flight paths for microwave-powered airplanes
[NAL-TR-1051] N91-10053

**ALBEDO**

Measurements of the light-absorbing material inside cloud droplets and its effect on cloud albedo
N91-10528

**ALGORITHMS**

Application of flight path reconstruction algorithms for flight data of helicopter
[NAL-TM-582] N91-10031

Simulation of time-dependent compressible viscous flows using central and upwind-biased finite difference techniques N91-10234

AFDM: An Advanced Fluid-Dynamics Model. Volume 4: The AFDM heat- and mass-transfer solution algorithm
[DE90-017535] N91-10240

AFDM: An Advanced Fluid-Dynamics Model
[DE90-017536] N91-10241

Global optimization methods for engineering design
N91-10310

An experimental and analytical study of structural identification N91-10325

Cloud grid data N91-10371

Where are cirrus clouds and why are they there
N91-10450

Cloud parameters from GOES visible and infrared radiances during the FIRE Cirrus IFO, October 1986
N91-10473

Multiprocessors and runtime compilation
[NASA-CR-182100] N91-10600

Network, system, and status software enhancements for the autonomously managed electrical power system breadboard. Volume 2: Protocol specification
[NASA-CR-185881] N91-10619

Discounted dynamic programming. Part 5: Modified policy iteration
[TW-90-04-PT-5] N91-10642

Casual eigenvector function approximations and the problem of scaling: An algorithm
[OUEL-1822/90] N91-10644

Some defects in finite-difference edge finders
[OUEL-1826/90] N91-10645

Labeling problems in truth maintenance systems
[REPT-89-90] N91-10651

Tabu-search and simulated annealing for the quadratic assignment problem
[REPT-89-028] N91-10658

Domain decomposition: An instrument of asymptotic-numerical methods
[DE90-016478] N91-10661

Density estimation using optimally quantized histograms
[PB90-190588] N91-10686

Collision-induced gas phase dissociation rates
[NASA-CR-185874] N91-10707

**ALIGNMENT**

SSC dipole magnet measurement and alignment using laser technology
[DE90-014881] N91-10281

**ALKALIES**

Study of mixed mode stress intensity factor using the experimental method of transmitted caustics
N91-10324

**ALOHA SYSTEM**

Geometric ergodicity of the ALOHA-system and a coupled processors model
[TW-90-01-B] N91-10680

**ALPHA JET AIRCRAFT**

Nonlinear feedback control for high alpha flight
[NASA-CR-186545] N91-10047

**ALUMINIDES**

Weldability of nickel and iron aluminides
[DE90-013498] N91-10153

Brittle fracture and ductility improvement in nickel and iron aluminides
[DE90-017319] N91-10167

**ALUMINUM**

XAFS studies of interactions at transition-metal/Al interfaces
[DE90-016313] N91-10159

**ALUMINUM ALLOYS**

Mechanical properties and fracture toughness of 8090-T651 plate and 2091 and 8090 sheet
[NRL-MP-88049-4] N91-10151

Constant stress of XD (trademark) TiAl containing nitrogen
[DE90-011947] N91-10158

Mechanical and microstructural response of Ni3Al at high strain rate and elevated temperatures
[DE90-016489] N91-10162

Axial compression buckling test on CFRP surface plate/aluminum honeycomb sandwiched curved surface plate
[NAL-TM-584] N91-10299

**ALUMINUM BORON COMPOSITES**

A macro-micromechanics analysis of a notched metal matrix composite
[NASA-TM-102728] N91-10128

**ALUMINUM OXIDES**

Analysis of aluminum oxide ceramic
[DE90-016517] N91-10175

Radiation damage in Al2O3 crystals implanted with 3.8 MeV Fe(2+)
[DE90-016038] N91-10761

**AMBIENT TEMPERATURE**

Combined effects of elevated concentrations of carbon dioxide and ambient temperature on thermal state of humans in closed chambers N91-10563

**AMIDES**

Evaluation of two bisimide additives in LARC-TPI adhesive
[NASA-TM-102742] N91-10182

**AMPLIFICATION**

Minimizing frequency pulling of quartz oscillators due to power supply variations
[DE90-014566] N91-10218

**AMPS (SATELLITE PAYLOAD)**

Network, system, and status software enhancements for the autonomously managed electrical power system breadboard. Volume 1: Project summary
[NASA-CR-185880] N91-10618

**ANALOGIES**

A communication channel model of the software process N91-10610

**ANALYTIC FUNCTIONS**

The cousin problems in the viewpoint of partial differential equations
[DE90-627172] N91-10656

**ANALYZERS**

Prototype instrumentation and design studies — electrostatic analyzer system for the Space Shuttle
[AD-A211566] N91-10264

**ANGLE OF ATTACK**

Fast steering of the angle of attack: A contribution to the guidance of high velocity projectiles
[ISL-CO-220/89] N91-10050

Flight characteristics of a modified Schweizer SGS1-36 sailplane at low and very high angles of attack
[NASA-TP-3022] N91-10079

**ANGULAR ACCELERATION**

The scientific case for magnetic field satellites
[NASA-CR-186532] N91-10101

**ANGULAR DISTRIBUTION**

The possibility of making fast measurements of ion distribution functions N91-10438

Tests and applications of Cherenkov imaging in TeV astronomy N91-10807

**ANISOTROPY**

Texture-induced anisotropy and high-strain rate deformation in metals
[DE90-016611] N91-10163

Physical interpretation and application of principles of ultrasonic nondestructive evaluation of high-performance materials
[NASA-CR-180489] N91-10293

Evaluation, development, and characterization of superconducting materials for space applications
[NASA-CR-187017] N91-10763

**ANNEALING**

Fe site occupancy and superconductivity in Y(1-z)Ca(z)Ba(z) (Cu(1-x)Fe(x))3O(6+y)
[DE90-016614] N91-10774

**ANNULAR FLOW**

Detailed heat transfer measurements in nozzle guide vane passages in linear and annular cascades in the presence of secondary flows
[PNR-90706] N91-10260

**ANODES**
Performance characterization of a segmented anode arcjet thruster
[NASA-TM-103227] N91-10118
The physical and chemical state of Westinghouse Phosphoric Acid Fuel Cell assemblies after long term operation: Surface and near-surface analysis
[DE90-015055] N91-10382
**ANOMALIES**
Space Station Freedom Environmental Control and Life Support System (ECLSS) phase 3 simplified integrated test trace contaminant control subsystem performance
[NASA-TM-4202] N91-10103
Anomalous dispersion as a phase-matching technique for second harmonic generation
[DE90-015696] N91-10172
The stationary wave response to tropical and midlatitude SST anomalies N91-10536
Fundamental properties and mass loss in hot, near-main sequence stars N91-10821
**ANTENNA RADIATION PATTERNS**
Contribution to the study of the electromagnetic field radiation close to electronics circuits
[ECL-90-12] N91-10211
**ANTENNAS**
Antenna/transmitter control unit N91-10348
**ANTIFERROMAGNETISM**
Calculation of the static magnetism of metamagnetic La2CuO4
[DE90-016490] N91-10770
About antiferromagnetic Heisenberg models
[ETN-90-97768] N91-10784
**ANTIREFLECTION COATINGS**
Damage assessment and possible damage mechanisms to 1-meter diameter Nova turning mirrors
[DE90-016473] N91-10278
Properties of reactively-deposited SiC and GeC alloys
[DE90-016363] N91-10766
**ANVIL CLOUDS**
The effects of cloud radiative forcing on an ocean-covered planet N91-10456
**APERTURES**
Design of highly concentrating solar collectors and solar collector systems
[DLR-FB-90-11] N91-10390
**APL (PROGRAMMING LANGUAGE)**
Function library using APL for time series analysis and system identification in structures
[NAL-TM-578] N91-10604
**APPENDAGES**
Combined design of structures and controllers for optimal maneuverability N91-10314
**APPLICATIONS PROGRAMS (COMPUTERS)**
User's guide to CUNIFLOW
[AD-A207606] N91-10004
Static and dynamic finite element stress analysis of layered composite plates and shells N91-10326
Designing application software in wide area network settings
[NASA-CR-187333] N91-10633
**APPROACH CONTROL**
Differential Global Positioning System (DGPS) test plan
[DOT/FAA/CT-TN90/15] N91-10034
**APPROXIMATION**
Exponential approximations in optimal design N91-10311
Conservative buffering of approximate nonlinear constraints N91-10312
Discounted dynamic programming. Part 3: Successive approximation
[TW-89-14-PT-3] N91-10640
Discounted dynamic programming. Part 4: Accelerated successive approximation
[TW-90-03-PT-4] N91-10641
Discounted dynamic programming. Part 5: Modified policy iteration
[TW-90-04-PT-5] N91-10642
Casual eigenvector function approximations and the problem of scaling: An algorithm
[OUEL-1822/90] N91-10644
Path integral asymptotics in the absence of classical paths
[DE90-016213] N91-10659
Approximation and geometric modeling with simplex B-splines associated with irregular triangles
[MEMO-842] N91-10673
H 2 and H infinity approximations for eigenvalue/vector functions of transfer matrices
[OUEL-1778/89] N91-10684
The difference of two renewal processes: Level crossing and the infimum
[MEMO-845] N91-10690
**ARC JET ENGINES**
Performance characterization of a segmented anode arcjet thruster
[NASA-TM-103227] N91-10118
**ARCHITECTURE (COMPUTERS)**
AFDM: An Advanced Fluid-Dynamics Model
[DE90-017538] N91-10243
AFDM: An Advanced Fluid-Dynamics Model
[DE90-017539] N91-10244
A representation scheme for fault diagnosis of physical systems
[DE90-016362] N91-10295
Multiprocessors and runtime compilation
[NASA-CR-182100] N91-10600
Architecture simulator of parallel computer
[NAL-TM-583] N91-10601
Experiences with Ada in an embedded system N91-10614
A representation scheme for fault diagnosis
[DE90-016291] N91-10631
Bidirectional translator between DXF and IGES formats
[DE90-016430] N91-10632
Designing application software in wide area network settings
[NASA-CR-187333] N91-10633
Massively parallel computing system
[DE90-014683] N91-10648
Performance and operational characteristics of a Fiber Distributed Data Interface (FDDI) ring
[DE90-016103] N91-10649
**AROMATIC COMPOUNDS**
Trifluoromethyl-substituted polymers
[NASA-CR-186955] N91-10170
**ARTIFICIAL INTELLIGENCE**
Experiments and theory with a 0.5 ton mobile robot
[OUEL-1807/90] N91-10035
Spacecraft Health Automated Reasoning Prototype (SHARP): The fiscal year 1989 SHARP portability evaluations task for NASA Solar System Exploration Division's Voyager project
[NASA-CR-187338] N91-10204
A representation scheme for fault diagnosis of physical systems
[DE90-016362] N91-10295
Developing a framework for qualitative engineering: Research in design and analysis of complex structural systems N91-10322
A representation scheme for fault diagnosis
[DE90-016291] N91-10631
Artificial intelligence, human factors, robotics, and computer simulation
[DE90-016866] N91-10653
**ARTIFICIAL SATELLITES**
Examination of ion acceleration in the plasma layer during magnetospheric partial gales
[MPE-218] N91-10753
**ASPECT RATIO**
Analysis of stratocumulus cloud fields using LANDSAT imagery: Size distributions and spatial separations N91-10504
**ASSESSMENTS**
Structural risk assessment and aircraft fleet maintenance N91-10321
**ASTRONAUTS**
US space flight experience. Physical exertion and metabolic demand of extravehicular activity: Past, present, and future N91-10575
Work, exercise, and space flight. 1: Operations, environment, and effects of spaceflight N91-10578
Work, exercise, and space flight. 3: Exercise devices and protocols N91-10579
Exercise issues related to the neuromuscular function and adaptation to microgravity N91-10584
Considerations for an exercise prescription N91-10585
**ASTRONOMICAL MODELS**
Large scale structures in nonzero Lambda Friedmann universes N91-10812
**ASTRONOMICAL OBSERVATORIES**
Activities report of the European Southern Observatory
[ISSN-0531-4496] N91-10809
**ASTROPHYSICS**
Nuclear structure calculations for astrophysical applications
[DE90-016433] N91-10818
Intrinsic neutrino properties: As deduced from cosmology, astrophysics, accelerator, and non-accelerator experiments
[DE90-016467] N91-10836
**ASYMMETRY**
Evidence for asymmetric inertial instability in the FIRE satellite dataset N91-10454
Fundamental properties and mass loss in hot, near-main sequence stars N91-10821
**ASYMPTOTIC METHODS**
Path integral asymptotics in the absence of classical paths
[DE90-016213] N91-10659
Domain decomposition: An instrument of asymptotic-numerical methods
[DE90-016478] N91-10661
**ATLAS LAUNCH VEHICLES**
Ground test program for new Atlas payload fairings N91-10315
**ATMOSPHERIC ATTENUATION**
Sea surface temperature N91-10372
**ATMOSPHERIC BOUNDARY LAYER**
Diurnal variation of marine stratocumulus over San Nicolas Island during the FIRE IFO N91-10491
Radiative control on tropical convective boundary layer equilibrium N91-10493
Studying marine stratus with large eddy simulation N91-10499
Cloud and boundary layer structure over San Nicolas Island during FIRE N91-10515
Horizontal variability of the marine boundary layer structure upwind of San Nicolas Island during FIRE, 1987 N91-10519
Plume mechanics and stratocumulus convection N91-10526
**ATMOSPHERIC CHEMISTRY**
Atmospheric ozone 1985: Assessment of our understanding of the processes controlling its present distribution and change, volume 3
[NASA-TM-103462] N91-10393
Global and regional environmental atmospheric chemistry
[DE90-016693] N91-10407
Global tropospheric chemistry modeling
[DE90-015908] N91-10409
**ATMOSPHERIC CIRCULATION**
Q-vectors: A new approach to an old problem
[PB90-235490] N91-10414
Synoptic conditions producing cirrus during the FIRE cirrus IFO N91-10449
Terrain-induced mesoscale circulations in the Columbia Basin
[DE90-016338] N91-10541
**ATMOSPHERIC COMPOSITION**
Geophysical monitoring for climatic change
[PB90-222126] N91-10538
**ATMOSPHERIC ENTRY**
Entry vehicle performance analysis and atmospheric guidance algorithm for precision landing on Mars
[NASA-CR-185614] N91-10102
**ATMOSPHERIC GENERAL CIRCULATION MODELS**
Potential effects of global climate change on the United States. Appendix I: Variability
[PB90-173899] N91-10403
A GCM parameterization for the shortwave radiative properties of water clouds N91-10494
Cloud parameters derived from GOES during the 1987 marine stratocumulus FIRE Intensive Field Observation (IFO) period N91-10505
**ATMOSPHERIC MODELS**
Atmospheric ozone 1985: Assessment of our understanding of the processes controlling its present distribution and change, volume 3
[NASA-TM-103462] N91-10393
Model of gravity-wave-induced variability and turbulence in the stratified free atmosphere
[PB90-235482] N91-10413
The effects of critical layers on atmospheric cnoidal waves
[DE90-016540] N91-10440
Synoptic conditions producing cirrus during the FIRE cirrus IFO N91-10449
Cirrus cloud model parameterizations: Incorporating realistic ice particle generation N91-10453
The effects of cloud radiative forcing on an ocean-covered planet N91-10456
Cirrus microphysics and radiative transfer: A case study N91-10463
Multi-spectral window radiance observations of Cirrus from satellite and aircraft, November 2, 1986 Project FIRE N91-10465
The relationship of marine stratus to synoptic conditions N91-10489
The stationary wave response to tropical and midlatitude SST anomalies N91-10536
**ATMOSPHERIC MOISTURE**
Analysis of tethered balloon data from San Nicolas Island on 8 July 1987 N91-10517
**ATMOSPHERIC PHYSICS**
The Joint NASA/Goddard-University of Maryland Research Program in Charged Particle and High Energy Photon Detector Technology
[NASA-CR-180335] N91-10810

**ATMOSPHERIC RADIATION**
The radiation budget of a Cirrus layer deduced from simultaneous aircraft observations and model calculations N91-10467
Comparison of NOAA-9 ERBE measurements with Cirrus IFO satellite and aircraft measurements N91-10471
ERBE and AVHRR Cirrus cloud fire study N91-10472
Surface radiation observations for October 27-28, 1986 during the Wisconsin FIRE/SRB experiment N91-10481
Third generation earth radiation budget measurements; ERBE in the context of earlier systems N91-10530

**ATMOSPHERIC SOUNDING**
Comparison of NOAA-9 ERBE measurements with Cirrus IFO satellite and aircraft measurements N91-10471
Cloud altitude determination from infrared spectral radiances N91-10474
Analysis of diurnal variation of SCu layer using 2 days of CLASS soundings on San Nicolas Island N91-10490

**ATMOSPHERIC TEMPERATURE**
Model of gravity-wave-induced variability and turbulence in the stratified free atmosphere [PB90-235482] N91-10413
Cloud and boundary layer structure over San Nicolas Island during FIRE N91-10515
Analysis of tethered balloon data from San Nicolas Island on 8 July 1987 N91-10517
Turbulence measurements using tethered balloon instrumentation during FIRE 1987 N91-10518
Horizontal variability of the marine boundary layer structure upwind of San Nicolas Island during FIRE, 1987 N91-10519
Boundary layer roll circulations during FIRE N91-10521

**ATMOSPHERIC TURBULENCE**
Simulations and observations of cloudtop processes N91-10496
Fractional cloudiness in shallow cumulus layers N91-10498
Turbulence measurements using tethered balloon instrumentation during FIRE 1987 N91-10518
Winds and turbulence above San Nicolas Island during FIRE N91-10522

**ATMOSPHERIC WINDOWS**
Multi-spectral window radiance observations of Cirrus from satellite and aircraft, November 2, 1986 Project FIRE N91-10465

**ATOMIC STRUCTURE**
Optical properties of inorganic polymers [DE90-017143] N91-10179
Theoretical studies of High Energy Density Matter (HEDM) molecules [DE90-014831] N91-10706
Physical and electronic structure of the electrolyte-solid interface through optical phenomena [DE90-015935] N91-10764
Renormalization from density functional theory strong coupling models for the electronic structure of La2CuO4 [DE90-015990] N91-10765
Electronic, structural and transport properties of (almost) rare-earth-like actinide hydrides [DE90-016491] N91-10771
Fundamental properties and mass loss in hot, near-main sequence stars N91-10821

**ATROPHY**
Work, exercise, and space flight. 2: Modification of adaptation by exercise (exercise prescription) N91-10586

**ATTITUDE CONTROL**
Application of flight path reconstruction algorithms for flight data of helicopter [NAL-TM-582] N91-10031

**ATTITUDE INDICATORS**
Wind tunnel test of redundant vane-type flow-direction sensing systems [NAL-TM-590] N91-10057

**AUDIO FREQUENCIES**
Do we really need 57 ways of rating aircraft noise [PNR-90720] N91-10704

**AURORAL ARCS**
A mathematical model of the structure and evolution of small scale discrete auroral arcs [NASA-CR-187238] N91-10734

**AURORAL IRRADIATION**
Radio wave remote sensing by Cluster and Regetta N91-10439

**AURORAL ZONES**
Radio wave remote sensing by Cluster and Regetta N91-10439
A mathematical model of the structure and evolution of small scale discrete auroral arcs [NASA-CR-187238] N91-10734

**AUTOMATIC CONTROL**
Automatic determination of fault effects on aircraft functionality [NASA-CR-181352] N91-10039
Planning of the paths for manipulation robots [ETN-90-97826] N91-10291

**AUTOMATIC WEATHER STATIONS**
FAA air traffic operational evaluation of Automated Surface Observing System (ASOS) [DOT/FAA/CT-TN90/42] N91-10084

**AUTONOMOUS NAVIGATION**
Experiments and theory with a 0.5 ton mobile robot [OUEL-1807/90] N91-10035
Design for navigation: Using acoustic cats' eyes to improve sonar range and direction range finding for industrial mobile robots and AGV's [OUEL-1812/90] N91-10036
Real-time safety analysis for autonomous guided vehicles [OUEL-1833/90] N91-10037

**AUTONOMY**
Protective autonomy: Embedding sensor-based safety and protection mechanisms into the motion control of mobile and tele-operated robots [OUEL-1808/90] N91-10292
Network, system, and status software enhancements for the autonomously managed electrical power system breadboard. Volume 1: Project summary [NASA-CR-185880] N91-10618
Automated support of the modelling process: A view based on experiments with expert information engineers [REPT-90-09] N91-10638
Image motion experiments with the Oxford AGV [OUEL-1809/90] N91-10654

**AUTOREGRESSIVE PROCESSES**
On the autoregression methods applied to the hourly nucleonic-component records [IFSI-89-19] N91-10837

**AUXILIARY PROPULSION**
Integrated hydrogen/oxygen technology applied to auxiliary propulsion systems [NASA-CR-185289] N91-10116

**AVALANCHE DIODES**
An avalanche electron emitting diode in gallium arsenide [ETN-90-97746] N91-10225

**AXIAL COMPRESSION LOADS**
Axial compression buckling test on CFRP surface plate/aluminum honeycomb sandwiched curved surface plate [NAL-TM-584] N91-10299

**AXIAL LOADS**
Compressive failure of thick-section composite laminates with and without cutouts subjected to biaxial loading N91-10304

**AXISYMMETRIC FLOW**
Multigrid solution for the Euler equations in axisymmetric flow [REPT-B-17] N91-10253

## B

**B STARS**
Fundamental properties and mass loss in hot, near-main sequence stars N91-10821

**BACKSCATTERING**
Subvisual Cirrus cloud properties derived from a FIRE IFO case study N91-10464
ER-2 lidar measurements of stratocumulus cloud top structure on July 14, 1987 N91-10523

**BACKWARD WAVE TUBES**
An x band backward-wave oscillator experiment [DE90-015119] N91-10219

**BACKWARD WAVES**
An x band backward-wave oscillator experiment [DE90-015119] N91-10219

**BACTERIA**
Protective functions of skin N91-10555

**BACTERIOLOGY**
Chesapeake Bay Basin Monitoring Program Atlas. Volume 2: Biological and living resource monitoring programs [PB90-147943] N91-10392

**BALLOON FLIGHT**
NRL tethered balloon measurements at San Nicolas Island during FIRE IFO 1987 N91-10509

**BALLOON SOUNDING**
Analysis of tethered balloon, ceilometer and class sounding data taken on San Nicolas Island during the FIRE project N91-10492
NRL tethered balloon measurements at San Nicolas Island during FIRE IFO 1987 N91-10509

**BALLOONING MODES**
Unified theory of ballooning instabilities and temperature gradient driven trapped ion modes [DE90-017091] N91-10744

**BARIUM OXIDES**
Preparation of superconducting wire by deposition of YBa2Cu3O(x) onto fibers [DE90-013380] N91-10758
Evaluation, development, and characterization of superconducting materials for space applications [NASA-CR-187017] N91-10763
Copper NMR and hole depletion in the normal state of Y(1-x)Pr(x)Ba2Cu3O7 [DE90-016468] N91-10768
YBa2Cu3O(x) composites with improved toughness and strength [DE90-011180] N91-10782

**BEAMS (SUPPORTS)**
Research in Structures, Structural Dynamics and Materials, 1990 [NASA-CP-3064] N91-10301

**BEND TESTS**
Environmental degradation of macro defect free cements. 1: Mechanical properties investigation [AERE-R-13354-1] N91-10169

**BENDING**
Analysis of delamination in fiber composite laminates out-of-plane under bending [NASA-CR-186023] N91-10122
A new beam theory using first-order warping functions N91-10307
Fatigue crack propagation of coplanar semi-elliptical cracks in pure bending [PNR-90742] N91-10337

**BERYLLIUM**
Beryllium weldability [DE90-014696] N91-10155

**BERYLLIUM ALLOYS**
Strength and toughness of single-phase and dual-phase high-temperature intermetallics [DE90-017192] N91-10166

**BERYLLIUM HYDRIDES**
Theoretical studies of High Energy Density Matter (HEDM) molecules [DE90-014831] N91-10706

**BERYLLIUM OXIDES**
Beryllium weldability [DE90-014696] N91-10155

**BESSEL FUNCTIONS**
On q-analogues of the Fourier and Hankel transforms [REPT-89-89] N91-10666

**BIAS**
Geoid and Doppler induced errors on the altimeter measurement and their correction [CNES-CT/DRT/TIT/RL-88/226] N91-10380
Optimum orientations of the observation axes for 2-dimensional vector sensing under consideration of bias errors [NAL-TR-1055] N91-10679

**BIBLIOGRAPHIES**
Aeronautical engineering: A continuing bibliography with indexes (supplement 256) [NASA-SP-7037(256)] N91-10002
Aerospace medicine and biology: A continuing bibliography with indexes (supplement 341) [NASA-SP-7011(341)] N91-10594
US Congressional serial set catalog: Numerical lists and schedule of volumes; 99th Congress: 1985-1986: Entries and indexes [PB90-171737] N91-10797
Bibliography of Lewis Research Center technical publications announced in 1989 [NASA-TM-102542] N91-10798

**BIDIRECTIONAL REFLECTANCE**
Interpretation of satellite-measured bidirectional reflectance from Cirrus cloudy atmospheres N91-10470

**BIG BANG COSMOLOGY**
Large scale structures in nonzero Lambda Friedmann universes N91-10812

**BIMETALS**
Organometallic chemistry of bimetallic compounds [DE90-017601] N91-10121

**BINARY FLUIDS**
Fast sound propagation in binary fluid mixtures N91-10233

**BINARY MIXTURES**
Fast sound propagation in binary fluid mixtures N91-10233

**BINARY STARS**
Acceleration by pulsar winds in binary systems [NASA-TM-103451] N91-10616

**BIOASTRONAUTICS**
Aerospace medicine and biology: A continuing bibliography with indexes (supplement 341) [NASA-SP-7011(341)] N91-10594

**BIODYNAMICS**
Work, exercise, and space flight. 3: Exercise devices and protocols N91-10579
Biomedical perspectives on locomotion in null gravity N91-10583

**BIOLOGICAL EFFECTS**
ELF (extremely-low-frequency): Exposure levels, bioeffects, and epidemiology
[DE90-016554] N91-10573
Interaction of extremely low-frequency electromagnetic fields with humans
[DE90-017190] N91-10592
Aerospace medicine and biology: A continuing bibliography with indexes (supplement 341)
[NASA-SP-7011(341)] N91-10594
**BIOMAGNETISM**
Interaction of extremely low-frequency electromagnetic fields with humans
[DE90-017190] N91-10592
**BIOMASS ENERGY PRODUCTION**
Short-rotation woody crop opportunities to mitigate carbon dioxide buildup
[DE90-016526] N91-10406
**BIOPHYSICS**
Statistical methods for analyzing and combining data on low-level exposures to ionizing radiation
[DE90-017193] N91-10593
**BIOSATELLITES**
Preliminary studies before defining a payload adapted to the primate model
[ETN-90-97581] N91-10107
**BLADE-VORTEX INTERACTION**
Modeling blade/vortex interactions
[ISL-R-107/89] N91-10016
**BLOOD VOLUME**
Cardiovascular group N91-10587
**BLOWERS**
Modification in the main air blower unit for two meter times two meter transonic wind tunnel: Plan and configuration
[NAL-TM-580] N91-10081
**BLUNT BODIES**
User's guide to CUNIFLOW
[AD-A207606] N91-10004
**BODY FLUIDS**
Considerations for an exercise prescription
N91-10585
**BODY-WING CONFIGURATIONS**
A contribution to the numerical solution of transonic flow around a delta wing by solving Navier-Stokes equations
[DLR-FB-90-13] N91-10026
**BOEING 737 AIRCRAFT**
NASA transport systems research vehicle B-737 data link system and display formats
[NASA-TM-102717] N91-10058
**BOILER PLATE**
Long-term orbital lifetime predictions
[NASA-TP-3058] N91-10092
**BOLTZMANN TRANSPORT EQUATION**
Computational methods for the Boltzmann equation
[BR-43] N91-10256
**BOND GRAPHS**
Automatic determination of fault effects on aircraft functionality
[NASA-CR-181352] N91-10039
**BONE DEMINERALIZATION**
Workshop on Exercise Prescription for Long-Duration Space Flight
[NASA-CP-3051] N91-10574
Space medicine considerations: Skeletal and calcium homeostasis N91-10580
Changes in mineral metabolism with immobilization/space flight N91-10581
Biomedical perspectives on locomotion in null gravity
N91-10583
Summary and recommendations for initial exercise prescription N91-10588
**BONE MINERAL CONTENT**
Space medicine considerations: Skeletal and calcium homeostasis N91-10580
**BONES**
Space medicine considerations: Skeletal and calcium homeostasis N91-10580
Changes in mineral metabolism with immobilization/space flight N91-10581
Considerations for an exercise prescription
N91-10585
**BOOSTER ROCKET ENGINES**
Hybrid propulsion technology program: Phase 1, volume 4
[NASA-CR-183975] N91-10114
Integrated hydrogen/oxygen technology applied to auxiliary propulsion systems
[NASA-CR-185289] N91-10116
**BORIC ACIDS**
Self-lubricating boric acid films for tribological applications
[DE90-007605] N91-10171
**BORIDES**
Superconducting borides
[DE90-016484] N91-10769
**BORON ALLOYS**
Constant stress of XD (trademark) TiAl containing nitrogen
[DE90-011947] N91-10158
**BORON CARBIDES**
Infrared absorption in boron carbides: Dependence on isotope and carbon concentration
[DE90-017592] N91-10132
High-strain-rate compression and fracture of B4C-aluminum cermets
[DE90-016568] N91-10176
**BOUNDARIES**
The scientific case for magnetic field satellites
[NASA-CR-186532] N91-10101
Boundary layer roll circulations during FIRE
N91-10521
Bounded-error data, and frequency response design
[OUEL-1766/89] N91-10683
**BOUNDARY CONDITIONS**
Electromagnetic scattering from two-dimensional thick material junctions
[NASA-CR-186976] N91-10201
Multigrid solution for the Euler equations in axisymmetric flow
[REPT-B-17] N91-10253
On the convergence at infinity, rate of convergence and uniqueness of solutions with finite Dirichlet integral to the exterior Dirichlet problem for the steady plane Navier-Stokes system of equations
[PREPRINT-166] N91-10257
A new beam theory using first-order warping functions
N91-10307
Preliminary mixed-layer model results for FIRE marine stratocumulus IFO conditions N91-10495
An overview of UK C130 observations from the FIRE marine stratocumulus IFO N91-10520
**BOUNDARY ELEMENT METHOD**
Some recent applications of numerical methods to geotechnical analysis
[PB90-201229] N91-10655
**BOUNDARY INTEGRAL METHOD**
The numerical simulation of nonlinear gravity waves in three dimensions using a higher order panel method
[ISBN-90-9002667-23] N91-10443
**BOUNDARY LAYER FLOW**
Boundary-layer receptivity due to a wall suction and control of Tollmien-Schlichting waves
[NASA-CR-182103] N91-10009
Determination of the pressure drag of airfoils by integration of surface pressures
[NASA-TM-102722] N91-10078
Numerical investigations in three-dimensional internal flows
[NASA-CR-186958] N91-10083
A one-equation turbulence transport model for high Reynolds number wall-bounded flows
[NASA-TM-102847] N91-10252
Computation of boundary layer flow using thin-layer Navier-Stokes equations with flux-vector splitting
[REPT-B-21] N91-10254
**BOUNDARY LAYER PLASMAS**
Plasma waves as a signature of flux transfer events
N91-10427
**BOUNDARY LAYER STABILITY**
The inviscid secondary instability of fully nonlinear longitudinal vortex structures in growing boundary layers
[NASA-CR-187455] N91-10021
Vortex instabilities in 3D boundary layers: The relationship between Goertler and crossflow vortices
[NASA-CR-187456] N91-10022
**BOUNDARY LAYERS**
The inviscid secondary instability of fully nonlinear longitudinal vortex structures in growing boundary layers
[NASA-CR-187455] N91-10021
A Knudsen layer theory for lattice gases
[ETN-90-97583] N91-10248
Computation of boundary layer flow using thin-layer Navier-Stokes equations with flux-vector splitting
[REPT-B-21] N91-10254
NRL tethered balloon measurements at San Nicolas Island during FIRE IFO 1987 N91-10509
Cloud and boundary layer structure over San Nicolas Island during FIRE N91-10515
Thermodynamic structure of the stratocumulus-capped boundary layer on 5 July 1987 N91-10516
Turbulence measurements using tethered balloon instrumentation during FIRE 1987 N91-10518
Boundary layer roll circulations during FIRE
N91-10521
ER-2 lidar measurements of stratocumulus cloud top structure on July 14, 1987 N91-10523
Thermodynamic structure of the stratocumulus-capped boundary layer on 7 July, 1987 N91-10533
A preliminary analysis of LANDSAT and UK C130 data from Mission 197-A, on 16 July 1987 N91-10535
**BOUNDARY VALUE PROBLEMS**
An analytical solution for the elastoplastic response of a continuous fiber composite under uniaxial loading
N91-10305
Path integral asymptotics in the absence of classical paths
[DE90-016213] N91-10659
**BOW WAVES**
Specific tasks of multiple scale plasma measurements in Regatta-Cluster system N91-10419
**BRIGHTNESS TEMPERATURE**
Brightness temperature distribution N91-10369
Cloud grid data N91-10371
Sea surface temperature N91-10372
Multi-spectral window radiance observations of Cirrus from satellite and aircraft, November 2, 1986 Project FIRE N91-10465
Cirrus cloud statistics: Temperatures and optical depths N91-10466
**BRISTOL-SIDDELEY BS 53 ENGINE**
Progress in certifying F402-RR-408: The improved Pegasus engine for AV-8B and Harrier 2 plus
[PNR-90719] N91-10056
Technology update of early gas turbine designs
[PNR-90710] N91-10070
**BRITTLENESS**
Brittle fracture and ductility improvement in nickel and iron aluminides
[DE90-017319] N91-10167
**BROADBAND**
VISSR demodulate and processing subsystem
N91-10342
**BROADCASTING**
JPRS report: Science and technology. USSR: Electronics and electrical engineering
[JPRS-UEE-90-006] N91-10214
**BUBBLES**
Dynamics of gas bubbles moving through liquid
[ETN-90-97760] N91-10255
False-vacuum decay in generalized extended inflation
[NASA-CR-186419] N91-10695
**BUCKLING**
Axial compression buckling test on CFRP surface plate/aluminum honeycomb sandwiched curved surface plate
[NAL-TM-584] N91-10299
Research in Structures, Structural Dynamics and Materials, 1990
[NASA-CP-3064] N91-10301
Test/semi-empirical analysis of a carbon/epoxy fabric stiffened panel N91-10302
Repeated buckling of composite shear panels
N91-10303
Compressive failure of thick-section composite laminates with and without cutouts subjected to biaxial loading N91-10304
**BUFFETING**
Computation of maximum gust loads in nonlinear aircraft using a new method based on the matched filter approach and numerical optimization N91-10317
**BURNING RATE**
Very high burn rate propellants
[DE90-016865] N91-10186
**BUTANES**
Evaluation of available perfluorobutane data for selected physical properties
[DE90-016516] N91-10145
**BYPASS RATIO**
The evolution of the bypass engine
[PNR-90707] N91-10068
Design/development issues for high bypass ratio fans
[PNR-90758] N91-10076

## C

**CADMIUM SULFIDES**
Ion-assisted doping of 2-6 compounds during physical vapor deposition
[DE90-000358] N91-10756
**CADMIUM TELLURIDES**
Ion-assisted doping of 2-6 compounds during physical vapor deposition
[DE90-000358] N91-10756
**CALCIUM OXIDES**
Reaction kinetics of the Ca-SO2 system in absence of inter-grain pore diffusion
[DE90-009672] N91-10781
**CALCULUS OF VARIATIONS**
Pseudo-monotone complementarity problems in Hilbert space
[DE90-016310] N91-10660
**CALIBRATING**
Rotor systems research aircraft risk-reduction shake test
[NASA-TM-4186] N91-10045

A new method for doing flat-field intensity calibrations of multiplexed ITT streak cameras
[DE90-016475] N91-10267

A facility for calibrating calorimeter gauges at high rates of convective heat transfer
[OUEL-1825/90] N91-10272

Calibration N91-10360

Materials analysis and device optimization of CuInSe2 solar cells
[DE90-000365] N91-10384

Configurational sensitivity of multipoint magnetic field measurements N91-10421

A synopsis of Langley Research Center's lidar effort for the 1986 FIRE IFO N91-10457

AVHRR and VISSR satellite instrument calibration results for both Cirrus and marine stratocumulus IFO periods N91-10475

Temperature sensitivity of Eppley broadband radiometers N91-10484

Comparison and calibration of NCAR electra instruments: July 5 and 7, 1987 N91-10532

Intrinsic (?) reference standards
[DE90-015714] N91-10696

Design, performance, and calibration of the ALEXIS ultrasoft x-ray telescopes
[DE90-016483] N91-10720

**CALORIMETERS**

A facility for calibrating calorimeter gauges at high rates of convective heat transfer
[OUEL-1825/90] N91-10272

**CANTILEVER BEAMS**

A new beam theory using first-order warping functions
N91-10307

**CARBON**

Microstructural and phase stability studies of nanometer period metal/carbon multilayer structures for x ray optics
[DE90-015307] N91-10129

Characterization of mono- and multi-molecular assemblies at glassy carbon and noble metals by ex situ and in situ infrared external reflection spectroscopy
[DE90-016417] N91-10144

**CARBON DIOXIDE**

Short-rotation woody crop opportunities to mitigate carbon dioxide buildup
[DE90-016526] N91-10406

Research on climate change
[DE90-016726] N91-10408

Combined effects of elevated concentrations of carbon dioxide and ambient temperature on thermal state of humans in closed chambers N91-10563

**CARBON FIBER REINFORCED PLASTICS**

Influence of expanding monomer on carbon fiber reinforced epoxy composites
[AD-A223277] N91-10124

Study of the mechanisms of damage and failure of fiber and ceramic matrix composites
[ISAL-90-0026] N91-10135

Axial compression buckling test on CFRP surface plate/aluminum honeycomb sandwiched curved surface plate
[NAL-TM-584] N91-10299

**CARBON FIBERS**

The transport properties of activated carbon fibers
[DE90-015910] N91-10130

Compressive failure of thick-section composite laminates with and without cutouts subjected to biaxial loading N91-10304

**CARBON TETRAFLUORIDE**

Measured and predicted shock shapes for AFE configuration at Mach 6 in air and in CF4
[NASA-TM-100660] N91-10245

**CARDIOVASCULAR SYSTEM**

Central and regional hemodynamics in prolonged space flights N91-10554

Workshop on Exercise Prescription for Long-Duration Space Flight
[NASA-CP-3051] N91-10574

US space flight experience. Physical exertion and metabolic demand of extravehicular activity: Past, present, and future N91-10575

Considerations for an exercise prescription
N91-10585

Cardiovascular group N91-10587

Summary and recommendations for initial exercise prescription N91-10588

**CASTING**

Casting alloys for the jet age
[PNR-90723] N91-10168

**CATALOGS (PUBLICATIONS)**

NIST (National Institute of Standards and Technology) standard reference materials catalog, 1990-1991
[PB90-183310] N91-10120

Climate data system supports FIRE N91-10455

A synopsis of Langley Research Center's lidar effort for the 1986 FIRE IFO N91-10457

US Congressional serial set catalog: Numerical lists and schedule of volumes; 99th Congress: 1985-1986: Entries and indexes
[PB90-171737] N91-10797

**CATHODES**

The physical and chemical state of Westinghouse Phosphoric Acid Fuel Cell assemblies after long term operation: Surface and near-surface analysis
[DE90-015055] N91-10382

**CAUCHY PROBLEM**

The cousin problems in the viewpoint of partial differential equations
[DE90-627172] N91-10656

**CAVITATION FLOW**

Thin film thermometers and flowmeters for applications in liquid helium N91-10265

**CAVITY RESONATORS**

Statistical characterization of a mode-stirred chamber
[DE90-014860] N91-10202

Cumulative beam breakup of the ground-based-free-electron laser
[DE90-016485] N91-10279

INEX modeling of the Boeing ring optical resonator free-electron laser
[DE90-016488] N91-10280

**CEILINGS (ARCHITECTURE)**

Transient characteristics of unconfined fire plume-driven ceiling jets
[PB90-227976] N91-10193

**CEILINGS (METEOROLOGY)**

Cloud altitude determination from infrared spectral radiances N91-10474

Cirrus cloud properties derived from coincident GOES and lidar data during the 1986 FIRE Cirrus Intensive Field Observations (IFO) N91-10476

**CEMENTS**

Environmental degradation of macro defect free cements. 1: Mechanical properties investigation
[AERE-R-13354-1] N91-10169

**CENTAUR LAUNCH VEHICLE**

The design and fabrication of the Centaur neutral buoyancy trainer and related hardware
[NASA-CR-171944] N91-10085

**CENTRAL NERVOUS SYSTEM**

Requirements for an ideal drug for preventing space motion sickness N91-10566

Exercise issues related to the neuromuscular function and adaptation to microgravity N91-10584

**CENTRAL PROCESSING UNITS**

Image monitor N91-10344

Telemetry subsystem N91-10345

Antenna/transmitter control unit N91-10348

**CERAMIC FIBERS**

Design methodology needs for fiber-reinforced ceramic heat exchangers
[DE90-016659] N91-10178

**CERAMIC MATRIX COMPOSITES**

Fabrication aspects of glass matrix composites for gas turbine applications
[PNR-90752] N91-10073

Study of the mechanisms of damage and failure of fiber and ceramic matrix composites
[ISAL-90-0026] N91-10135

Industrial applications and markets for ceramic matrix composites
[PNR-90753] N91-10138

Design methodology needs for fiber-reinforced ceramic heat exchangers
[DE90-016659] N91-10178

**CERAMICS**

Advanced ceramic fabric body mounted radiator for Space Station Freedom Phase O design
[DE90-016361] N91-10104

Shock experiments in metals and ceramics
[DE90-016613] N91-10165

Design considerations for a ceramic fabric radiator
[DE90-016342] N91-10173

Analysis of aluminum oxide ceramic
[DE90-016517] N91-10175

Meetings on the structure and properties of implanted ceramics
[DE90-017313] N91-10181

Calculation of Weibull strength parameters, Batdorf flaw density constants and related statistical quantities using PC-CARES
[NASA-TM-103247] N91-10332

**CERENKOV COUNTERS**

The technique of Cerenkov ring image detection
[ETN-90-97747] N91-10714

**CERMETS**

High-strain-rate compression and fracture of B4C-aluminum cermets
[DE90-016568] N91-10176

**CH-47 HELICOPTER**

Application of flight path reconstruction algorithms for flight data of helicopter
[NAL-TM-582] N91-10031

**CHANNEL FLOW**

Statistical characterization of a mode-stirred chamber
[DE90-014860] N91-10202

Two-phase flow patterns and frictional pressure gradients in a small, horizontal, rectangular channel
[DE90-014802] N91-10236

Interactive real time flow simulations
[NASA-CR-187325] N91-10238

A computational model for z-pinch plasma channels
N91-10730

**CHANNEL NOISE**

Signal detection in non-Gaussian and non-white noise
N91-10200

**CHANNELS (DATA TRANSMISSION)**

Hydrologic and meteorological operations in the 162-174 and 406.1-420 MHz bands
[PB90-207820] N91-10199

A communication channel model of the software process N91-10610

**CHAOS**

Prediction and control of chaotic processes using nonlinear adaptive networks
[DE90-016505] N91-10697

Order and chaos in polarized nonlinear optics
[DE90-016717] N91-10721

**CHARACTERIZATION**

Monomolecular and thin polymer films: Fabrication, characterization, applications, and models of wetting
[DE90-016415] N91-10174

**CHARGE COUPLED DEVICES**

Radiation-induced noise in Charge-Coupled Device (CCD) and Charge-Injection Device (CID) imagers
[DE90-016724] N91-10777

**CHARGE EXCHANGE**

Confinement studies in the ZT-40M reversed field pinch
[DE90-016442] N91-10739

**CHARGE INJECTION DEVICES**

Radiation-induced noise in Charge-Coupled Device (CCD) and Charge-Injection Device (CID) imagers
[DE90-016724] N91-10777

**CHARGED PARTICLES**

Theoretical studies of turbulence and anomalous transport in toroidal confinement devices
[DE90-017606] N91-10747

**CHARTS**

Satellite cloud information chart N91-10374

**CHEBYSHEV APPROXIMATION**

Quadrature imposition of compatibility conditions in Chebyshev methods
[NASA-CR-187458] N91-10251

Spectral methods for time dependent problems
[NASA-CR-187443] N91-10664

Chebyshev approximation by spline functions with free knots
[MEMO-853] N91-10677

**CHEMICAL ANALYSIS**

Structural integrity assessment of concrete slabs by nondestructive examination and Fourier transform-infrared methods
[DE90-017233] N91-10296

**CHEMICAL BONDS**

On the effects of magnetic bonding in rare earth transition metal intermetallics
[DE90-015800] N91-10156

Effects of in-plane pi prime bonding on electronic transition energies for inorganic polymers
[DE90-017144] N91-10180

**CHEMICAL COMPOSITION**

Very high burn rate propellants
[DE90-016865] N91-10186

Corrosion, passivity, and breakdown of alloys used in high energy density batteries
[DE90-016648] N91-10223

**CHEMICAL EXPLOSIONS**

Transition state theory applying to the study of reaction processes in detonation
[DE90-016558] N91-10187

**CHEMICAL REACTIONS**

Transition state theory applying to the study of reaction processes in detonation
[DE90-016558] N91-10187

**CHEMICAL TESTS**

Physical and chemical test results of electrostatic safe flooring materials
[NASA-TM-103501] N91-10194

**CHEMISORPTION**

Electrochemical oxidation of methane at metal and metal oxide electrodes
[PB90-205196] N91-10140

**CHESAPEAKE BAY (US)**
Chesapeake Bay Basin Monitoring Program Atlas. Volume 1: Water quality and other physiochemical monitoring programs [PB90-147935] N91-10391
Chesapeake Bay Basin Monitoring Program Atlas. Volume 2: Biological and living resource monitoring programs [PB90-147943] N91-10392
**CHINA**
About the possibilities of using an air mass transformation model in Taiyuan, Shanxi Province, China [KNMI-TR-120] N91-10540
**CHROMIUM OXIDES**
Advanced materials for high-temperature solid electrolyte applications [DE90-016328] N91-10143
**CHROMOSPHERE**
Coaligned observations of solar magnetic fields at different heights: MSFC Center director's discretionary fund final report (Project No. 88-10) [NASA-TM-103516] N91-10632
**CIRCADIAN RHYTHMS**
Effects of rolling motion on the circadian rhythm of sinoatrial node N91-10558
**CIRCUITS**
Microwave link N91-10355
**CIRCULAR CYLINDERS**
Wind tunnel investigations of the appearance of shocks in the windward region of bodies with circular cross section at angle of attack [DLR-FB-90-15] N91-10027
An analytical solution for the elastoplastic response of a continuous fiber composite under uniaxial loading N91-10305
**CIRRUS CLOUDS**
Cloud motion wind N91-10365
FIRE Science Results 1988 [NASA-CP-3083] N91-10448
Synoptic conditions producing cirrus during the FIRE cirrus IFO N91-10449
Where are cirrus clouds and why are they there N91-10450
ISCCP results for the FIRE IFO regions and times N91-10451
Cloud information for FIRE from surface weather reports N91-10452
Cirrus cloud model parameterizations: Incorporating realistic ice particle generation N91-10453
Climate data system supports FIRE N91-10455
Optical and morphological properties of Cirrus clouds determined by the high spectral resolution lidar during FIRE N91-10458
Hydrometeor development in cold clouds in FIRE N91-10459
Lidar and aircraft studies of deep Cirrus systems from the 1986 FIRE IFO N91-10460
Vertical velocities within a Cirrus cloud from Doppler lidar and aircraft measurements during FIRE: Implications for particle growth N91-10461
Radiative properties of visible and subvisible Cirrus: Scattering on hexagonal ice crystals N91-10462
Cirrus microphysics and radiative transfer: A case study N91-10463
Subvisual Cirrus cloud properties derived from a FIRE IFO case study N91-10464
Multi-spectral window radiance observations of Cirrus from satellite and aircraft, November 2, 1986 Project FIRE N91-10465
Cirrus cloud statistics: Temperatures and optical depths N91-10466
The radiation budget of a Cirrus layer deduced from simultaneous aircraft observations and model calculations N91-10467
Identification of Cirrus over Wausau during the 1986 FIRE IFO from ground-based radiometer data N91-10469
Interpretation of satellite-measured bidirectional reflectance from Cirrus cloudy atmospheres N91-10470
ERBE and AVHRR Cirrus cloud fire study N91-10472
Cloud parameters from GOES visible and infrared radiances during the FIRE Cirrus IFO, October 1986 N91-10473
Cirrus cloud properties derived from coincident GOES and lidar data during the 1986 FIRE Cirrus Intensive Field Observations (IFO) N91-10476
Overview of the 27-28 October FIRE Cirrus IFO case: Meteorology and cloud fields N91-10477
A four-lidar view of Cirrus from the FIRE IFO: 27-28 October 1986 N91-10478
Radiative properties of Cirrus clouds: FIRE IFO case October 28, 1986 N91-10479
FIRE Cirrus on October 28, 1986: LANDSAT; ER-2; King Air; theory N91-10480
Surface radiation observations for October 27-28, 1986 during the Wisconsin FIRE/SRB experiment N91-10481
The new FIRE cloud lidar at Langley Research Center N91-10482
Interpretation of the optical and morphological properties of Cirrus clouds from lidar measurements N91-10483
Both sides now N91-10485
Sub-visual Cirrus detection and characterization N91-10486
Cloud atlas for the FIRE Cirrus Intensive Field Observation (IFO) N91-10487
FIRE extended time/limited area observations at Palisades, New York N91-10527
**CIVIL AVIATION**
DOD responsibilities on Federal aviation and national airspace system matters [PB90-218827] N91-10001
National airspace system: In-flight assistance operational concept [PB90-233115] N91-10032
**CLASSICAL MECHANICS**
On the structure of quantum phase space [DE90-627185] N91-10786
**CLAYS**
Nano-composite desiccation materials [PB90-247388] N91-10123
**CLEAR AIR TURBULENCE**
Model of gravity-wave-induced variability and turbulence in the stratified free atmosphere [PB90-235482] N91-10413
**CLIMATE**
ISCCP data processing N91-10363
GPCP data processing N91-10370
Cloud amount distribution N91-10373
Chesapeake Bay Basin Monitoring Program Atlas. Volume 2: Biological and living resource monitoring programs [PB90-147943] N91-10392
Research on climate change [DE90-016726] N91-10408
Proceedings of the WMO Region 3/4 Training Seminar on Climate Data Management and User Services [WCDP-1] N91-10445
Climate data system supports FIRE N91-10455
The effects of cloud radiative forcing on an ocean-covered planet N91-10456
Hydrometeor development in cold clouds in FIRE N91-10459
Multi-spectral window radiance observations of Cirrus from satellite and aircraft, November 2, 1986 Project FIRE N91-10465
Third generation earth radiation budget measurements; ERBE in the context of earlier systems N91-10530
**CLIMATE CHANGE**
Atmospheric ozone 1985: Assessment of our understanding of the processes controlling its present distribution and change, volume 3 [NASA-TM-103462] N91-10393
Potential effects of global climate change on the United States. Appendix C: Agriculture, volume 1 [PB90-171588] N91-10394
Potential effects of global climate change on the United States. Appendix A: Water resources [PB90-171968] N91-10395
Potential effects of global climate change on the United States. Appendix B: Sea level rise [PB90-172628] N91-10396
Potential effects of global climate change on the United States. Appendix C: Agriculture, volume 2 [PB90-171596] N91-10397
Potential effects of global climate change on the United States. Appendix D: Forests [PB90-173238] N91-10398
Potential effects of global climate change on the United States. Appendix E: Aquatic resources [PB90-172297] N91-10399
Potential effects of global climate change on the United States. Appendix F: Air quality [PB90-172230] N91-10400
Potential effects of global climate change on the United States. Appendix G: Health [PB90-173881] N91-10401
Potential effects of global climate change on the United States. Appendix H: Infrastructure [PB90-172313] N91-10402
Potential effects of global climate change on the United States. Appendix I: Variability [PB90-173899] N91-10403
Potential effects of global climate change on the United States. Appendix J: Policy [PB90-173188] N91-10404
Research on climate change [DE90-016726] N91-10408
Analyzing long time series of hydrological data with respect to climate variability: Project description [WCAP-3] N91-10444
ERBE and AVHRR Cirrus cloud fire study N91-10472
Geophysical monitoring for climatic change [PB90-222126] N91-10538
**CLIMATOLOGY**
ISCCP data processing N91-10363
GPCP data processing N91-10370
FIRE Science Results 1988 [NASA-CP-3083] N91-10448
Where are cirrus clouds and why are they there N91-10450
ISCCP results for the FIRE IFO regions and times N91-10451
Cloud information for FIRE from surface weather reports N91-10452
Evidence for asymmetric inertial instability in the FIRE satellite dataset N91-10454
Hydrometeor development in cold clouds in FIRE N91-10459
Vertical velocities within a Cirrus cloud from Doppler lidar and aircraft measurements during FIRE: Implications for particle growth N91-10461
Radiative properties of visible and subvisible Cirrus: Scattering on hexagonal ice crystals N91-10462
Identification of Cirrus over Wausau during the 1986 FIRE IFO from ground-based radiometer data N91-10469
ERBE and AVHRR Cirrus cloud fire study N91-10472
Cloud parameters from GOES visible and infrared radiances during the FIRE Cirrus IFO, October 1986 N91-10473
Cirrus cloud properties derived from coincident GOES and lidar data during the 1986 FIRE Cirrus Intensive Field Observations (IFO) N91-10476
Surface radiation observations for October 27-28, 1986 during the Wisconsin FIRE/SRB experiment N91-10481
Temperature sensitivity of Eppley broadband radiometers N91-10484
Extended time observations of California marine stratocumulus clouds from GOES for July 1983-1987 N91-10488
Estimated accuracy of ground-based liquid water measurements during FIRE N91-10508
NRL tethered balloon measurements at San Nicolas Island during FIRE IFO 1987 N91-10509
A study of marine stratocumulus using lidar and other FIRE aircraft observations N91-10511
Cloud optical parameters as derived from the multispectral cloud radiometer N91-10513
Cloud and boundary layer structure over San Nicolas Island during FIRE N91-10515
Horizontal variability of the marine boundary layer structure upwind of San Nicolas Island during FIRE, 1987 N91-10519
Boundary layer roll circulations during FIRE N91-10521
Winds and turbulence above San Nicolas Island during FIRE N91-10522
Near infrared radiances observed by the UK C130 multi-channel radiometer during the marine stratocumulus IFO and preliminary comparison with model calculations N91-10525
Plume mechanics and stratocumulus convection N91-10526
FIRE extended time/limited area observations at Palisades, New York N91-10527
Preliminary results of radiation measurements from the marine stratus FIRE experiment N91-10529
Third generation earth radiation budget measurements; ERBE in the context of earlier systems N91-10530
San Nicolas Island surface radiation-meteorology data N91-10531
Comparison and calibration of NCAR electra instruments: July 5 and 7, 1987 N91-10532
Thermodynamic structure of the stratocumulus-capped boundary layer on 7 July, 1987 N91-10533
Aircraft/island/ship/satellite intercomparison: Preliminary results from July 16, 1987 N91-10534
**CLOCKS**
Frequency standard unit N91-10349
**CLOSED CYCLES**
Application of generalized predictive control to a boiler turbine unit for electricity generation [OUEL-1823/90] N91-10229
**CLOSURE LAW**
Numerical computation of viscous flow about unconventional airfoil shapes [NASA-CR-187343] N91-10019
**CLOUD COVER**
The effects of cloud radiative forcing on an ocean-covered planet N91-10456

The radiation budget of a Cirrus layer deduced from simultaneous aircraft observations and model calculations N91-10467

Identification of Cirrus over Wausau during the 1986 FIRE IFO from ground-based radiometer data N91-10469

Overview of the 27-28 October FIRE Cirrus IFO case: Meteorology and cloud fields N91-10477

A four-lidar view of Cirrus from the FIRE IFO: 27-28 October 1986 N91-10478

Radiative properties of Cirrus clouds: FIRE IFO case October 28, 1986 N91-10479

Both sides now N91-10485

Cloud atlas for the FIRE Cirrus Intensive Field Observation (IFO) N91-10487

The relationship of marine stratus to synoptic conditions N91-10489

Analysis of diurnal variation of SCu layer using 2 days of CLASS soundings on San Nicolas Island N91-10490

Radiative control on tropical convective boundary layer equilibrium N91-10493

Preliminary mixed-layer model results for FIRE marine stratocumulus IFO conditions N91-10495

A cloud classification scheme applied to the breakup region of marine stratocumulus N91-10497

Fractional cloudiness in shallow cumulus layers N91-10498

Studying marine stratus with large eddy simulation N91-10499

Cloud spatial structure during the FIRE MS IFO N91-10500

Reflectivities of uniform and broken marine stratiform clouds N91-10501

Analysis of stratocumulus cloud fields using LANDSAT imagery: Size distributions and spatial separations N91-10504

Cloud parameters derived from GOES during the 1987 marine stratocumulus FIRE Intensive Field Observation (IFO) period N91-10505

Cloud and boundary layer structure over San Nicolas Island during FIRE N91-10515

Thermodynamic structure of the stratocumulus-capped boundary layer on 5 July 1987 N91-10516

Turbulence measurements using tethered balloon instrumentation during FIRE 1987 N91-10518

An overview of UK C130 observations from the FIRE marine stratocumulus IFO N91-10520

Boundary layer roll circulations during FIRE N91-10521

A preliminary analysis of LANDSAT and UK C130 data from Mission 197-A, on 16 July 1987 N91-10535

**CLOUD HEIGHT INDICATORS**

Cloud motion wind N91-10365

Cloud grid data N91-10371

Satellite cloud information chart N91-10374

Analysis of tethered balloon, ceilometer and class sounding data taken on San Nicolas Island during the FIRE project N91-10492

Analysis of tethered balloon data from San Nicolas Island on 8 July 1987 N91-10517

Winds and turbulence above San Nicolas Island during FIRE N91-10522

ER-2 lidar measurements of stratocumulus cloud top structure on July 14, 1987 N91-10523

Comparison and calibration of NCAR electra instruments: July 5 and 7, 1987 N91-10532

A preliminary analysis of LANDSAT and UK C130 data from Mission 197-A, on 16 July 1987 N91-10535

**CLOUD PHYSICS**

Synoptic conditions producing cirrus during the FIRE cirrus IFO N91-10449

ISCCP results for the FIRE IFO regions and times N91-10451

Cloud information for FIRE from surface weather reports N91-10452

Cirrus cloud model parameterizations: Incorporating realistic ice particle generation N91-10453

Optical and morphological properties of Cirrus clouds determined by the high spectral resolution lidar during FIRE N91-10458

Hydrometeor development in cold clouds in FIRE N91-10459

Radiative properties of visible and subvisible Cirrus: Scattering on hexagonal ice crystals N91-10462

Cirrus microphysics and radiative transfer: A case study N91-10463

Subvisual Cirrus cloud properties derived from a FIRE IFO case study N91-10464

Lidar and radiometer results from the ER-2 for the FIRE field experiments N91-10468

Interpretation of satellite-measured bidirectional reflectance from Cirrus cloudy atmospheres N91-10470

Cirrus cloud properties derived from coincident GOES and lidar data during the 1986 FIRE Cirrus Intensive Field Observations (IFO) N91-10476

FIRE Cirrus on October 28, 1986: LANDSAT; ER-2; King Air; theory N91-10480

A GCM parameterization for the shortwave radiative properties of water clouds N91-10494

Cloud spatial structure during the FIRE MS IFO N91-10500

Marine stratocumulus cloud characteristics from multichannel satellite measurements N91-10502

Estimated accuracy of ground-based liquid water measurements during FIRE N91-10508

Cloud absorption properties as derived from airborne measurements of scattered radiation within clouds N91-10512

Winds and turbulence above San Nicolas Island during FIRE N91-10522

ER-2 lidar measurements of stratocumulus cloud top structure on July 14, 1987 N91-10523

Near infrared radiances observed by the UK C130 multi-channel radiometer during the marine stratocumulus IFO and preliminary comparison with model calculations N91-10525

Measurements of the light-absorbing material inside cloud droplets and its effect on cloud albedo N91-10528

Aircraft/island/ship/satellite intercomparison: Preliminary results from July 16, 1987 N91-10534

**CLOUDS (METEOROLOGY)**

ISCCP data processing N91-10363

Cloud grid data N91-10371

Cloud amount distribution N91-10373

Evidence for asymmetric inertial instability in the FIRE satellite dataset N91-10454

Surface radiation observations for October 27-28, 1986 during the Wisconsin FIRE/SRB experiment N91-10481

The new FIRE cloud lidar at Langley Research Center N91-10482

Temperature sensitivity of Eppley broadband radiometers N91-10484

Cloud atlas for the FIRE Cirrus Intensive Field Observation (IFO) N91-10487

Extended time observations of California marine stratocumulus clouds from GOES for July 1983-1987 N91-10488

Estimated accuracy of ground-based liquid water measurements during FIRE N91-10508

NRL tethered balloon measurements at San Nicolas Island during FIRE IFO 1987 N91-10509

Aircraft measurements of the mean and turbulent structure of marine stratocumulus clouds during FIRE N91-10514

Boundary layer roll circulations during FIRE N91-10521

Winds and turbulence above San Nicolas Island during FIRE N91-10522

Plume mechanics and stratocumulus convection N91-10526

FIRE extended time/limited area observations at Palisades, New York N91-10527

San Nicolas Island surface radiation-meteorology data N91-10531

Comparison and calibration of NCAR electra instruments: July 5 and 7, 1987 N91-10532

Aircraft/island/ship/satellite intercomparison: Preliminary results from July 16, 1987 N91-10534

A preliminary analysis of LANDSAT and UK C130 data from Mission 197-A, on 16 July 1987 N91-10535

**CLUSTER MISSION**

Space Plasma Physics Investigations by Cluster and Regatta
[ESA-SP-306] N91-10417

Multispacecraft measurement at varying scalelengths: The Cluster/Regatta opportunity N91-10418

Specific tasks of multiple scale plasma measurements in Regatta-Cluster system N91-10419

Review of the Cluster orbit and separation strategy: Consequence for measurements N91-10420

Configurational sensitivity of multipoint magnetic field measurements N91-10421

Accuracy of the estimate of J via multipoint measurements N91-10422

Small Space Lab as a basic spacecraft of Regatta project N91-10423

Cluster as a wave telescope N91-10424

Experimental constraints in the characterization of a turbulent field from several satellites N91-10425

Plasma wave measurements on the dayside: Scale sizes and observational requirements N91-10426

Plasma waves as a signature of flux transfer events N91-10427

On the possibility to support multisatellite measurements of the Cluster mission by single satellite measurements in the Regatta-Cluster project N91-10428

Multiple-ion waves behind shocks N91-10429

Non-linear evolution of the Kelvin-Helmholtz instability: Constraints on multipoint measurements N91-10430

Problems of cold plasma measurements on the Regatta-A spacecraft N91-10431

The importance of simultaneous monitoring of solar activity for the interpretation of solar plasma phenomena N91-10433

Energetic particles in the Earth's magnetotail or: Cluster and Regatta as a dispersiometer N91-10434

Features of mid-tail ion trajectories during substorms N91-10435

Specific tasks of Regatta-E measurements correlated with Cluster/Regatta-A in the ISTP and Regatta programmes N91-10436

Possibilities of charged particle injection from spacecraft for active diagnostics of the surrounding plasma and active spacecraft potential control N91-10437

Radio wave remote sensing by Cluster and Regatta N91-10439

**CNOIDAL WAVES**

The effects of critical layers on atmospheric cnoidal waves
[DE90-016540] N91-10440

**COAL**

Thermal energy storage for power generation applications
[DE90-016539] N91-10388

**COASTAL WATER**

Potential effects of global climate change on the United States. Appendix B: Sea level rise
[PB90-172628] N91-10396

**COATINGS**

Self-lubricating boric acid films for tribological applications
[DE90-007805] N91-10171

Meetings on the structure and properties of implanted ceramics
[DE90-017313] N91-10181

Evaluation of nondestructive evaluation techniques for determination of flawed conditions and the effects of flaws on the burst pressure in Kevlar-epoxy filament-wound spherical test specimens
[DE90-014839] N91-10330

Preparation of superconducting wire by deposition of YBa2Cu3O(x) onto fibers
[DE90-013380] N91-10758

Properties of reactively-deposited SiC and GeC alloys
[DE90-016363] N91-10766

**COAXIAL CABLES**

Numerical simulation of electromagnetic acceleration by induction. Part 1: Thin loops
[ISL-R-102/89-PT-1] N91-10205

**COBALT ALLOYS**

High temperature cyclic oxidation data. Part 1: Turbine alloys
[NASA-TM-83665] N91-10149

High-temperature cyclic oxidation data. Part 2: Turbine alloys
[NASA-TM-101468] N91-10150

**COERCIVITY**

Ultra-thin vertical magneto-optical media and system for using same
[DE90-014589] N91-10603

**COGNITION**

Developing a framework for qualitative engineering: Research in design and analysis of complex structural systems N91-10322

**COHERENT ELECTROMAGNETIC RADIATION**

Variable-coherence beam optics
[ISBN-952-90-1784-7] N91-10724

**COLD PLASMAS**

Problems of cold plasma measurements on the Regatta-A spacecraft N91-10431

**COLLISIONLESS PLASMAS**

Electromagnetic particle codes on unstructured grids
[DE90-015187] N91-10733

**COLLISIONS**

Collision-induced gas phase dissociation rates
[NASA-CR-185874] N91-10707

**COLUMBIA RIVER BASIN (ID-OR-WA)**

Terrain-induced mesoscale circulations in the Columbia Basin
[DE90-016338] N91-10541

**COLUMBUS SPACE STATION**

Columbus logistics support. A conceptional definition of the operational phase
[MBB-UO-0093-90-PUB] N91-10091

Columbus elements processing needs at KSC
[MBB-UO-0092-90-PUB] N91-10108

**COMBINATIONS (MATHEMATICS)**

Long cycles, degree sums, and neighborhood unions
[MEMO-851] N91-10676

**COMBINATORIAL ANALYSIS**

Tabu-search and simulated annealing for the quadratic assignment problem
[REPT-89-028] N91-10658

**COMBUSTIBLE FLOW**
Transient characteristics of unconfined fire plume-driven ceiling jets
[PB90-227976] N91-10193
**COMBUSTION**
Airplane systems modifications for improved cabin smoke evacuation
[DOT/FAA/CT-TN90/24] N91-10052
**COMBUSTION CHAMBERS**
Analysis of 5 KHz combustion instabilities in 40K methane/LOX combustion chambers
[NASA-TM-101368] N91-10117
**COMBUSTION PRODUCTS**
Time-resolved FTIR (Fourier Transform Infrared) emission studies of laser photofragmentation and chain reactions
[DE90-017223] N91-10722
**COMBUSTION STABILITY**
Analysis of 5 KHz combustion instabilities in 40K methane/LOX combustion chambers
[NASA-TM-101368] N91-10117
The instability of combustion in propulsion engines
N91-10141
**COMFORT**
The development of interior noise and vibration criteria
[NASA-TM-102736] N91-10702
**COMMAND AND CONTROL**
Meteorological Satellite Center Technical Note. Special Issue (1989). Summary of GMS System. 1: Telecommunication System N91-10338
Command subsystem N91-10346
Models of the human observer and controller of a dynamic system
[ETN-90-97759] N91-10597
Ada software productivity prototypes: A case study
N91-10613
**COMMAND GUIDANCE**
Command subsystem N91-10346
**COMMAND LANGUAGES**
Network, system, and status software enhancements for the autonomously managed electrical power system breadboard. Volume 3: Commands specification
[NASA-CR-185882] N91-10620
**COMMERCE**
Applied technology center business plan and market survey
[NASA-CR-187259] N91-10794
**COMMERCIAL AIRCRAFT**
Energy efficiency improvement potential of commercial aircraft to 2010
[DE90-014767] N91-10046
**COMMUNICATION EQUIPMENT**
JPRS report: Science and technology. USSR: Electronics and electrical engineering
[JPRS-UEE-90-006] N91-10214
Station control and monitor subsystem N91-10341
Frequency standard unit N91-10349
DCP subsystem N91-10352
Massively parallel computing system
[DE90-014683] N91-10648
**COMMUNICATION NETWORKS**
A Mobile Satellite Experiment (MSAT-X) network definition
[NASA-CR-187336] N91-10105
Principles of LOCSTAR system experiments
[CNES-CT/DRT/TIT/TR-88/355] N91-10207
**COMMUNICATION SATELLITES**
A Mobile Satellite Experiment (MSAT-X) network definition
[NASA-CR-187336] N91-10105
**COMPILERS**
A manual for PARTI runtime primitives
[NASA-CR-187442] N91-10599
**COMPLEX SYSTEMS**
Developing a framework for qualitative engineering: Research in design and analysis of complex structural systems N91-10322
**COMPONENT RELIABILITY**
Drive system life and reliability N91-10044
**COMPOSITE MATERIALS**
Nano-composite desiccation materials
[PB90-247388] N91-10123
Composite heat damage. Part 1: Mechanical testing of IM6/3501-6 laminates. Part 2: Nondestructive evaluation studies of IM6/3501-6 laminates
[DE90-016207] N91-10125
Holographic examination of great surface fiberbound components in industrial conditions: Resumes of final reports, April 1986 to June 1989
[MBB-Z-0306-90-PUB-KURZFASSUNG] N91-10136
Fibre-matrix reaction zones in model silicon carbide-titanium aluminide metal-matrix composites
[PNR-90713] N91-10137
Multi industry application of advanced materials
[PNR-90764] N91-10139
Evaluation of nondestructive evaluation techniques for determination of flawed conditions and the effects of flaws on the burst pressure in Kevlar-epoxy filament-wound spherical test specimens
[DE90-014839] N91-10330
**COMPOSITE STRUCTURES**
Structural properties of laminated Douglas fir/epoxy composite material
[NASA-RP-1236] N91-10127
Research in Structures, Structural Dynamics and Materials, 1990
[NASA-CP-3064] N91-10301
Repeated buckling of composite shear panels
N91-10303
Static and dynamic finite element stress analysis of layered composite plates and shells N91-10326
**COMPRESSIBILITY**
Compressive failure of thick-section composite laminates with and without cutouts subjected to biaxial loading N91-10304
**COMPRESSIBLE FLOW**
Turbulent flow calculations using unstructured and adaptive meshes
[NASA-CR-182102] N91-10010
The 3-D laser anemometer study of compressible flow through orifice plates
[PB90-216771] N91-10273
**COMPRESSING**
Composite heat damage. Part 1: Mechanical testing of IM6/3501-6 laminates. Part 2: Nondestructive evaluation studies of IM6/3501-6 laminates
[DE90-016207] N91-10125
**COMPRESSION LOADS**
Test/semi-empirical analysis of a carbon/epoxy fabric stiffened panel N91-10302
**COMPRESSION TESTS**
Axial compression buckling test on CFRP surface plate/aluminum honeycomb sandwiched curved surface plate
[NAL-TM-584] N91-10299
**COMPUTATION**
Rotor loads computation using singularity methods and application to the noise prediction
[ISL-PU-301/90] N91-10018
**COMPUTATIONAL ASTROPHYSICS**
Configurational sensitivity of multipoint magnetic field measurements N91-10421
Cluster as a wave telescope N91-10424
**COMPUTATIONAL FLUID DYNAMICS**
User's guide to CUNIFLOW
[AD-A207606] N91-10004
Prediction and comparison with measurements of the aerodynamic characteristics of flare-stabilized XM910 prototypes
[AD-A208099] N91-10005
Application of a state-space wake model to elastic blade flapping in hover N91-10006
Euler and potential experiment/CFD correlations for a transport and two delta-wing configurations
[NASA-TM-102208] N91-10014
Application of CFD to sonic boom near and mid flow-field prediction
[NASA-TM-102867] N91-10015
Aeroelastic analysis of wings using the Euler equations with a deforming mesh
[NASA-TM-102733] N91-10020
Three-dimensional viscous/inviscid coupling in subsonic flow
[REPT-B-24] N91-10023
Numerical investigations in three-dimensional internal flows
[NASA-CR-186958] N91-10083
Evaluation of flow quality in newly constructed low-turbulence calibration wind-tunnel for laser velocimeters
[NAL-TR-1054] N91-10087
Large blast and thermal simulator advanced concept driver design by computational fluid dynamics
[AD-A211364] N91-10230
AFDM: An Advanced Fluid-Dynamics Model. Volume 1: Scope, approach, and summary
[DE90-016723] N91-10239
AFDM: An Advanced Fluid-Dynamics Model. Volume 4: The AFDM heat- and mass-transfer solution algorithm
[DE90-017535] N91-10240
AFDM: An Advanced Fluid-Dynamics Model
[DE90-017536] N91-10241
Computation of boundary layer flow using thin-layer Navier-Stokes equations with flux-vector splitting
[REPT-B-21] N91-10254
Computational methods for the Boltzmann equation
[BR-43] N91-10256
Collision-induced gas phase dissociation rates
[NASA-CR-185874] N91-10707
**COMPUTATIONAL GRIDS**
Turbulent flow calculations using unstructured and adaptive meshes
[NASA-CR-182102] N91-10010
Application of CFD to sonic boom near and mid flow-field prediction
[NASA-TM-102867] N91-10015
Numerical investigations in three-dimensional internal flows
[NASA-CR-186958] N91-10083
The 'optimum' upwind advection on a triangular mesh
[NASA-CR-187459] N91-10250
Multigrid solution for the Euler equations in axisymmetric flow
[REPT-B-17] N91-10253
A manual for PARTI runtime primitives
[NASA-CR-187442] N91-10599
A computational model for z-pinch plasma channels
N91-10730
Electromagnetic particle codes on unstructured grids
[DE90-015187] N91-10733
**COMPUTER AIDED DESIGN**
Developments in REDES: The rocket engine design expert system
[NASA-TM-103657] N91-10119
Developing a framework for qualitative engineering: Research in design and analysis of complex structural systems N91-10322
Software integration technologies in industrial applications
[MA-55] N91-10627
Bidirectional translator between DXF and IGES formats
[DE90-016430] N91-10632
PROTHE: A software as a help for the studies in industrial thermal engineering
[ETN-90-97582] N91-10634
Automated support of the modelling process: A view based on experiments with expert information engineers
[REPT-90-09] N91-10638
Fully automatic analysis in an industrial environment
[PNR-90722] N91-10647
An interpersonal multimedia visualization system
[DE90-014974] N91-10803
**COMPUTER AIDED MANUFACTURING**
Activities report of the Permanent Committee of the General Council
[ISSN-0524-7705] N91-10198
Software integration technologies in industrial applications
[MA-55] N91-10627
Fully automatic analysis in an industrial environment
[PNR-90722] N91-10647
**COMPUTER ANIMATION**
On the rotation interpolation and animation problems in computer graphics
[REPT-90-08] N91-10637
**COMPUTER ASSISTED INSTRUCTION**
Automated support of the modelling process: A view based on experiments with expert information engineers
[REPT-90-09] N91-10638
**COMPUTER GRAPHICS**
AFDM: An Advanced Fluid-Dynamics Model
[DE90-017538] N91-10243
Research on climate change
[DE90-016726] N91-10408
Software package for 2-dimensional graphic display unit
[NAL-TM-589] N91-10605
Network, system, and status software enhancements for the autonomously managed electrical power system breadboard. Volume 4: Graphical status display
[NASA-CR-185879] N91-10621
Script: General purpose graphics program; user's manual
[PD-ST-9027] N91-10625
CVMAC 2D Program: A method of converting 3D to 2D
[DE90-015147] N91-10626
An interpersonal multimedia visualization system
[DE90-014974] N91-10803
**COMPUTER NETWORKS**
Ada software productivity prototypes: A case study
N91-10613
Network, system, and status software enhancements for the autonomously managed electrical power system breadboard. Volume 1: Project summary
[NASA-CR-185880] N91-10618
Network, system, and status software enhancements for the autonomously managed electrical power system breadboard. Volume 2: Protocol specification
[NASA-CR-185881] N91-10619
Network, system, and status software enhancements for the autonomously managed electrical power system breadboard. Volume 3: Commands specification
[NASA-CR-185882] N91-10620

Software safety workshop problem
[DE90-016222] N91-10630
Designing application software in wide area network settings
[NASA-CR-187333] N91-10633
PROTHE: A software as a help for the studies in industrial thermal engineering
[ETN-90-97582] N91-10634
Optimization of polling systems
[CWI-BS-R8932] N91-10635
Performance and operational characteristics of a Fiber Distributed Data Interface (FDDI) ring
[DE90-016103] N91-10649
Labeling problems in truth maintenance systems
[REPT-89-90] N91-10651
An interpersonal multimedia visualization system
[DE90-014974] N91-10803

**COMPUTER PROGRAMMING**
AFDM: An Advanced Fluid-Dynamics Model
[DE90-017538] N91-10243
Function library using APL for time series analysis and system identification in structures
[NAL-TM-578] N91-10604
Proceedings of the Thirteenth Annual Software Engineering Workshop
[NASA-TM-103314] N91-10606
Evolving impact of Ada on a production software environment N91-10607
The Software Management Environment (SME) N91-10609
A communication channel model of the software process N91-10610
Software sizing, cost estimation and scheduling N91-10612
Ada software productivity prototypes: A case study N91-10613
A modernized PDL approach for Ada software development N91-10616
Software safety workshop problem
[DE90-016222] N91-10630
Optimization of polling systems
[CWI-BS-R8932] N91-10635
Test case derivation from LOTOS specifications
[MEMO-INF-90-21] N91-10643

**COMPUTER PROGRAMS**
Transonic flow analysis for rotors. Part 3: Three-dimensional, quasi-steady, Euler calculation
[NASA-TP-2375] N91-10007
Wake coupling to full potential rotor analysis code
[NASA-TM-102805] N91-10013
Application of CFD to sonic boom near and mid flow-field prediction
[NASA-TM-102867] N91-10015
Numerical computation of viscous flow about unconventional airfoil shapes
[NASA-CR-187343] N91-10019
Aeroelastic analysis of wings using the Euler equations with a deforming mesh
[NASA-TM-102733] N91-10020
Three-dimensional viscous/inviscid coupling in subsonic flow
[REPT-B-24] N91-10023
Calculation of three-dimensional viscous/inviscid interaction in subsonic flow
[REPT-B-25] N91-10024
Evaluation of the ZONA51D program
[REPT-B-28] N91-10025
Developments in REDES: The rocket engine design expert system
[NASA-TM-103657] N91-10119
Wall interference studies
[PD-CF-9012] N91-10232
Interactive real time flow simulations
[NASA-CR-187325] N91-10238
AFDM: An Advanced Fluid-Dynamics Model
[DE90-017537] N91-10242
Turbulent boundary layers in high enthalpy flows. Numerical code validation by shock tube experiments
[ISL-CO-221/89] N91-10246
INEX modeling of the Boeing ring optical resonator free-electron laser
[DE90-016488] N91-10280
Calculation of Weibull strength parameters, Batdorf flaw density constants and related statistical quantities using PC-CARES
[NASA-TM-103247] N91-10332
Documentation for Program SOILSIM: A computer program for the simulation of heat and moisture flow in soils and between soils, canopy and atmosphere
[NASA-CR-186953] N91-10379
A synopsis of Langley Research Center's lidar effort for the 1986 FIRE IFO N91-10457
Multiple channel programmable coincidence counter
[DE90-014681] N91-10602
Function library using APL for time series analysis and system identification in structures
[NAL-TM-578] N91-10604
Software package for 2-dimensional graphic display unit
[NAL-TM-589] N91-10605
Proceedings of the Thirteenth Annual Software Engineering Workshop
[NASA-TM-103314] N91-10606
Towards a comprehensive framework for reuse: A reuse-enabling software evolution environment
[UMIACS-TR-88-92] N91-10608
A communication channel model of the software process N91-10610
Software sizing, cost estimation and scheduling N91-10612
Network, system, and status software enhancements for the autonomously managed electrical power system breadboard. Volume 1: Project summary
[NASA-CR-185880] N91-10618
Network, system, and status software enhancements for the autonomously managed electrical power system breadboard. Volume 2: Protocol specification
[NASA-CR-185881] N91-10619
Network, system, and status software enhancements for the autonomously managed electrical power system breadboard. Volume 3: Commands specification
[NASA-CR-185882] N91-10620
Network, system, and status software enhancements for the autonomously managed electrical power system breadboard. Volume 4: Graphical status display
[NASA-CR-185879] N91-10621
Confidence intervals and curvature measures in nonlinear regression using the IML and NLIN procedures in SAS(tm) software
[PB90-246398] N91-10624
CVMAC 2D Program: A method of converting 3D to 2D
[DE90-015147] N91-10626
Software safety workshop problem
[DE90-016222] N91-10630
A representation scheme for fault diagnosis
[DE90-016291] N91-10631
Bidirectional translator between DXF and IGES formats
[DE90-016430] N91-10632
PROTHE: A software as a help for the studies in industrial thermal engineering
[ETN-90-97582] N91-10634
Theoretical studies of High Energy Density Matter (HEDM) molecules
[DE90-014831] N91-10706
Numerical models of beam dynamics in ion induction linacs
[DE90-017043] N91-10713
High-order optics of multipole magnets
[DE90-016438] N91-10717
Theoretical analysis of a runaway electron suppression device
[DE90-015992] N91-10737
An interpersonal multimedia visualization system
[DE90-014974] N91-10803

**COMPUTER STORAGE DEVICES**
Ultra-thin vertical magneto-optical media and system for using same
[DE90-014589] N91-10603

**COMPUTER SYSTEMS DESIGN**
Computer system N91-10357
Architecture simulator of parallel computer
[NAL-TM-583] N91-10601

**COMPUTER SYSTEMS PERFORMANCE**
The full-body ground vibration tests using the low-noise STOL test plane
[NAL-TM-576] N91-10077
Software package for 2-dimensional graphic display unit
[NAL-TM-589] N91-10605
Performance and operational characteristics of a Fiber Distributed Data Interface (FDDI) ring
[DE90-016103] N91-10649

**COMPUTER SYSTEMS PROGRAMS**
The Software Management Environment (SME) N91-10609

**COMPUTER SYSTEMS SIMULATION**
Architecture simulator of parallel computer
[NAL-TM-583] N91-10601

**COMPUTER TECHNIQUES**
A representation scheme for fault diagnosis
[DE90-016291] N91-10631
Digital image integration technique of multiple geoscience information system and its application
[DE90-627893] N91-10801

**COMPUTER VISION**
Function and performance of visual simulation unit of flight simulation test facility
[NAL-TM-581] N91-10082

**COMPUTERIZED SIMULATION**
Comparison between the null-collision and time counter direct-simulation Monte Carlo methods: Leading-edge flow
[NAL-TR-1016T] N91-10012
Function and performance of visual simulation unit of flight simulation test facility
[NAL-TM-581] N91-10082
First evaluation of the main parameters in the dynamics of the Small Expendable Deployer System (SEDS) for a tethered satellite
[NASA-CR-4319] N91-10098
Analysis of delamination in fiber composite laminates out-of-plane under bending
[NASA-CR-186023] N91-10122
Electroplating corners
[DE90-017023] N91-10195
Method for simulating large dimension devices submitted to electromagnetic perturbations
[ECL-90-10] N91-10210
Simulation of time-dependent compressible viscous flows using central and upwind-biased finite difference techniques N91-10234
Interactive real time flow simulations
[NASA-CR-187325] N91-10238
AFDM: An Advanced Fluid-Dynamics Model. Volume 1: Scope, approach, and summary
[DE90-016723] N91-10239
Documentation for Program SOILSIM: A computer program for the simulation of heat and moisture flow in soils and between soils, canopy and atmosphere
[NASA-CR-186953] N91-10379
Architecture simulator of parallel computer
[NAL-TM-583] N91-10601
Software sizing, cost estimation and scheduling N91-10612
CVMAC 2D Program: A method of converting 3D to 2D
[DE90-015147] N91-10626
A conservative approach to parallelizing the Sharks World simulation
[NASA-CR-187440] N91-10629
Artificial intelligence, human factors, robotics, and computer simulation
[DE90-016866] N91-10653
PREGO: A simulation code for one-dimensional viscoelastic acoustics
[DE90-014859] N91-10700
Numerical models of beam dynamics in ion induction linacs
[DE90-017043] N91-10713
Plasma wakefield excitation by charge particle beams N91-10729
A computational model for z-pinch plasma channels N91-10730
In situ transmission electron microscopy and computer simulation study of the kinetics of oxygen loss in YBa2Cu3O(z)
[DE90-014508] N91-10783

**COMPUTERS**
Outline of CDAS telecommunication system N91-10340
Research on climate change
[DE90-016726] N91-10408
Architecture simulator of parallel computer
[NAL-TM-583] N91-10601
Applied technology center business plan and market survey
[NASA-CR-187259] N91-10794

**CONCRETES**
Structural integrity assessment of concrete slabs by nondestructive examination and Fourier transform-infrared methods
[DE90-017233] N91-10296

**CONDENSATION NUCLEI**
Aerosol measurements in the stratocumulus project N91-10506
In situ measurements of ship tracks N91-10507

**CONDENSING**
AFDM: An Advanced Fluid-Dynamics Model. Volume 4: The AFDM heat- and mass-transfer solution algorithm
[DE90-017535] N91-10240

**CONFERENCES**
Research in Structures, Structural Dynamics and Materials, 1990
[NASA-CP-3064] N91-10301
Proceedings of the 8th Symposium on Energy Engineering Sciences: Micro/Macro Studies of Multiphase Media
[DE90-014844] N91-10385
Global and regional environmental atmospheric chemistry
[DE90-016693] N91-10407
Proceedings of the WMO Region 3/4 Training Seminar on Climate Data Management and User Services
[WCDP-1] N91-10445

FIRE Science Results 1988 [NASA-CP-3083] N91-10448
Proceedings of the Thirteenth Annual Software Engineering Workshop [NASA-TM-103314] N91-10606

**CONFIDENCE**
Confidence intervals and curvature measures in nonlinear regression using the IML and NLIN procedures in SAS(tm) software [PB90-246398] N91-10624

**CONGRESSIONAL REPORTS**
US Congressional serial set catalog: Numerical lists and schedule of volumes; 99th Congress: 1985-1986: Entries and indexes [PB90-171737] N91-10797

**CONSECUTIVE EVENTS**
Technique for human-error sequence identification and signification [ISBN-90-353-10144] N91-10596

**CONSERVATION LAWS**
Analysis of moving strong discontinuity surfaces in elastic-plastic solids including effects of inertia and finite strain N91-10323

**CONSOLES**
Station control and monitor subsystem N91-10341
Image monitor N91-10344
Operation console N91-10350
System console N91-10351

**CONSTRUCTION INDUSTRY**
Activities report of the Permanent Committee of the General Council [ISSN-0524-7705] N91-10198

**CONTACT RESISTANCE**
Determination of surface resistance and magnetic penetration depth of superconducting YBa2Cu3O(7-delta) thin films by microwave power transmission measurements [NASA-TM-103616] N91-10780

**CONTINUOUS WAVE LASERS**
A synopsis of Langley Research Center's lidar effort for the 1986 FIRE IFO N91-10457

**CONTINUUM FLOW**
Computational methods for the Boltzmann equation [BR-43] N91-10256

**CONTINUUMS**
Continuum states of the Klein-Gordon equations for vector and scalar interactions [DE90-627178] N91-10693

**CONTROL EQUIPMENT**
Station control and monitor subsystem N91-10341
Antenna/transmitter control unit N91-10348
DPC telecommunication system N91-10354

**CONTROL STABILITY**
Application of generalized predictive control to a boiler turbine unit for electricity generation [OUEL-1823/90] N91-10229
Bounded-error data, and frequency response design [OUEL-1766/89] N91-10683
Robustness effects of a prefilter in generalized predictive control [OUEL-1799/89] N91-10685

**CONTROL SURFACES**
Project HyBuJET [NASA-CR-187011] N91-10040
Wall interference studies [PD-CF-9012] N91-10232

**CONTROL SYSTEMS DESIGN**
Space Station Freedom Environmental Control and Life Support System (ECLSS) phase 3 simplified integrated test trace contaminant control subsystem performance [NASA-TM-4202] N91-10103
Research in Structures, Structural Dynamics and Materials, 1990 [NASA-CP-3064] N91-10301
Combined design of structures and controllers for optimal maneuverability N91-10314
Design of control laws for flutter suppression based on the aerodynamic energy concept and comparisons with other design methods [NASA-TP-3056] N91-10328
Proceedings of the 8th Symposium on Energy Engineering Sciences: Micro/Macro Studies of Multiphase Media [DE90-014844] N91-10385

**CONTROL THEORY**
Design of control laws for flutter suppression based on the aerodynamic energy concept and comparisons with other design methods [NASA-TP-3056] N91-10328
Experiences with Ada in an embedded system N91-10614
Prediction and control of chaotic processes using nonlinear adaptive networks [DE90-016505] N91-10697

**CONTROLLED FUSION**
KrF laser path to high gain ICF (inertial confinement fusion) laboratory microfusion facility [DE90-016439] N91-10282
Models of plasma confinement and heating in tokamaks [DE90-016671] N91-10741
Pellet injector development at ORNL (Oak Ridge National Laboratory) [DE90-017024] N91-10742

**CONTROLLERS**
Numerical simulation of hypersonic flow around a space plane. Part 3: Analysis of aerothermodynamic heating [NAL-TR-1027T] N91-10011
Combined design of structures and controllers for optimal maneuverability N91-10314

**CONVECTION**
AFDM: An Advanced Fluid-Dynamics Model [DE90-017536] N91-10241
The effects of cloud radiative forcing on an ocean-covered planet N91-10456
Plume mechanics and stratocumulus convection N91-10526
A preliminary analysis of LANDSAT and UK C130 data from Mission 197-A, on 16 July 1987 N91-10535

**CONVECTION CLOUDS**
Radiative control on tropical convective boundary layer equilibrium N91-10493
Simulations and observations of cloudtop processes N91-10496
Structures observed on the spot radiance fields during the FIRE experiment N91-10503

**CONVECTIVE FLOW**
Radiative control on tropical convective boundary layer equilibrium N91-10493

**CONVECTIVE HEAT TRANSFER**
A facility for calibrating calorimeter gauges at high rates of convective heat transfer [OUEL-1825/90] N91-10272

**CONVERGENCE**
Interactive real time flow simulations [NASA-CR-187325] N91-10238
On the convergence at infinity, rate of convergence and uniqueness of solutions with finite Dirichlet integral to the exterior Dirichlet problem for the steady plane Navier-Stokes system of equations [PREPRINT-166] N91-10257
Finite element analysis of nonlinear creeping flows [DE90-627189] N91-10327
Convergence of Langevin simulation for complex Gaussian integrals [DE90-017402] N91-10665

**CONVEXITY**
A remark on the convexity of piecewise polynomial functions on triangulations [MEMO-857] N91-10682

**COOLERS**
Design and application of gas-gap heat switches [NASA-CR-187339] N91-10222

**COORDINATION**
DCP data processing N91-10375

**COPOLYMERIZATION**
Influence of expanding monomer on carbon fiber reinforced epoxy composites [AD-A223277] N91-10124

**COPPER**
High strain rate deformation behavior of shocked copper [DE90-016481] N91-10161

**COPPER ALLOYS**
Mechanisms of high temperature crack growth in metals and alloys [DE90-014934] N91-10152

**COPPER OXIDES**
Preparation of superconducting wire by deposition of YBa2Cu3O(x) onto fibers [DE90-013380] N91-10758
Evaluation, development, and characterization of superconducting materials for space applications [NASA-CR-187017] N91-10763
Renormalization from density functional theory strong coupling models for the electronic structure of La2CuO4 [DE90-015990] N91-10765
Copper NMR and hole depletion in the normal state of Y(1-x)Pr(x)Ba2Cu3O7 [DE90-016468] N91-10768
Calculation of the static magnetism of metamagnetic La2CuO4 [DE90-016490] N91-10770
Determination of surface resistance and magnetic penetration depth of superconducting YBa2Cu3O(7-delta) thin films by microwave power transmission measurements [NASA-TM-103616] N91-10780
YBa2Cu3O(x) composites with improved toughness and strength [DE90-011180] N91-10782
In situ transmission electron microscopy and computer simulation study of the kinetics of oxygen loss in YBa2Cu3O(z) [DE90-014508] N91-10783

**COPPER SELENIDES**
Materials analysis and device optimization of CuInSe2 solar cells [DE90-000365] N91-10384

**CORIOLIS EFFECT**
First evaluation of the main parameters in the dynamics of the Small Expendable Deployer System (SEDS) for a tethered satellite [NASA-CR-4319] N91-10098
Coriolis-effect in mass flow metering [LSTM-266/T/89] N91-10258

**CORNEA**
Effects of taurine on cytogenetic corneal disturbances induced in mice by 9 GeV protons N91-10562

**CORNERS**
Electroplating corners [DE90-017023] N91-10195

**CORONAL LOOPS**
A semi-analytical model of stellar flares [DE90-016434] N91-10817

**CORRELATION**
Euler and potential experiment/CFD correlations for a transport and two delta-wing configurations [NASA-TM-102208] N91-10014
Statistical characterization of a mode-stirred chamber [DE90-014860] N91-10202
Comparison and calibration of NCAR electra instruments: July 5 and 7, 1987 N91-10532

**CORRELATION DETECTION**
Prototype instrumentation and design studies — electrostatic analyzer system for the Space Shuttle [AD-A211566] N91-10264
Modelization of LOCSTAR synchronisation system. Computation of non detection and false alarm probabilities. Reflections on threshold adjustment and correlator structure [CNES-CT/DRT/TIT/TR-88/060] N91-10691

**CORRELATORS**
Modelization of LOCSTAR synchronisation system. Computation of non detection and false alarm probabilities. Reflections on threshold adjustment and correlator structure [CNES-CT/DRT/TIT/TR-88/060] N91-10691

**CORROSION RESISTANCE**
Evaluation of candidate alloys for the construction of metal flex hoses in the STS launch environment [NASA-TM-103808] N91-10157
Corrosion-resistant coatings for high-temperature high-sulfur activity applications [DE90-016638] N91-10177
Corrosion, passivity, and breakdown of alloys used in high energy density batteries [DE90-016648] N91-10223

**COSMIC RAYS**
The Joint NASA/Goddard-University of Maryland Research Program in Charged Particle and High Energy Photon Detector Technology [NASA-CR-180335] N91-10810
On the autoregression methods applied to the hourly nucleonic-component records [IFSI-89-19] N91-10837
Cosmic-ray intensity increase observed on September 29, 1989: The Chilean neutron monitor data (brief report) [IFSI-90-4] N91-10838

**COSMOLOGY**
False-vacuum decay in generalized extended inflation [NASA-CR-186419] N91-10695
Cosmological singularities in electrovacuum spacetimes with two-parameter spacelike isometry groups N91-10811
Parameterization of cosmological scale factor during inflationary times N91-10815

**COSMONAUTS**
Summary and recommendations for initial exercise prescription N91-10588

**COST ANALYSIS**
Aero engine design factors for a low fuel price scenario [PNR-90681] N91-10066

**COST ESTIMATES**
Knowledge-based assistance in costing the space station DMS N91-10611
Software sizing, cost estimation and scheduling N91-10612

**COST REDUCTION**
Optimization criteria for the design of orbital replacement units [MBB-UO-0092-90-PUB] N91-10109

**COSTS**
Knowledge-based assistance in costing the space station DMS N91-10611
Ada software productivity prototypes: A case study N91-10613
**COUNTER ROTATION**
Aeroacoustic effects of reduced aft tip speed at constant thrust for a model counterrotation turboprop at takeoff conditions
[NASA-TM-103608] N91-10703
**COUNTERFLOW**
Statistical characterization of a mode-stirred chamber
[DE90-014860] N91-10202
**COUNTERMEASURES**
Work, exercise, and space flight. 1: Operations, environment, and effects of spaceflight N91-10578
Summary and recommendations for initial exercise prescription N91-10588
**COUNTERS**
Aerosol measurements in the stratocumulus project N91-10506
**COUPLING**
Wake coupling to full potential rotor analysis code
[NASA-TM-102805] N91-10013
Three-dimensional viscous/inviscid coupling in subsonic flow
[REPT-B-24] N91-10023
Mobility power flow analysis of an L-shaped plate structure subjected to distributed loading
[NASA-CR-187353] N91-10334
**COVARIANCE**
Optimum orientations of the observation axes for 2-dimensional vector sensing under consideration of bias errors
[NAL-TR-1055] N91-10679
**CRACK GEOMETRY**
Fatigue crack propagation of coplanar semi-elliptical cracks in pure bending
[PNR-90742] N91-10337
**CRACK PROPAGATION**
Micro-mechanical analysis of damage growth and fracture in discontinuous fiber reinforced metal matrix composites
[NASA-CR-187020] N91-10126
Mechanisms of high temperature crack growth in metals and alloys
[DE90-014934] N91-10152
High-strain-rate compression and fracture of B4C-aluminum cermets
[DE90-016568] N91-10176
Structural risk assessment and aircraft fleet maintenance N91-10321
Fatigue crack propagation of coplanar semi-elliptical cracks in pure bending
[PNR-90742] N91-10337
**CRACKS**
Micro-mechanical analysis of damage growth and fracture in discontinuous fiber reinforced metal matrix composites
[NASA-CR-187020] N91-10126
Structural risk assessment and aircraft fleet maintenance N91-10321
Calculation of Weibull strength parameters, Batdorf flaw density constants and related statistical quantities using PC-CARES
[NASA-TM-103247] N91-10332
**CRASHES**
Seat dynamic performance standards for a range of sizes
[DOT/FAA/CT-TN90/23] N91-10028
**CREEP STRENGTH**
Constant stress of XD (trademark) TiAl containing nitrogen
[DE90-011947] N91-10158
**CRITERIA**
Optimization criteria for the design of orbital replacement units
[MBB-UO-0092-90-PUB] N91-10109
**CRITICAL POINT**
Relative position of the critical points of a certain cubic system and a generalization of the Bendixson index formula
[REPT-90-23] N91-10669
**CRITICAL TEMPERATURE**
A correlation between T(sub 3) and electronegativity difference in high-temperature superconductors
[DE90-016640] N91-10775
**CROPS**
Short-rotation woody crop opportunities to mitigate carbon dioxide buildup
[DE90-016526] N91-10406
**CROSS FLOW**
Vortex instabilities in 3D boundary layers: The relationship between Goertler and crossflow vortices
[NASA-CR-187456] N91-10022
**CRYOGENIC EQUIPMENT**
Fast estimation of the variance of a narrowband process
[IFSI-90-16] N91-10209
**CRYOGENICS**
Design and application of gas-gap heat switches
[NASA-CR-187339] N91-10222
**CRYSTAL DEFECTS**
Radiation damage in Al2O3 crystals implanted with 3.8 MeV Fe(2+)
[DE90-016038] N91-10761
**CRYSTAL GROWTH**
Ion-assisted doping of 2-6 compounds during physical vapor deposition
[DE90-000358] N91-10756
**CRYSTAL LATTICES**
Methane conversion by solid electrolyte membranes
[PB90-226341] N91-10381
Fe site occupancy and superconductivity in Y(1-z)Ca(z)Ba(z) (Cu(1-x)Fe(x))3O(6+y)
[DE90-016614] N91-10774
**CRYSTAL OSCILLATORS**
Magnetic sensitivity of on-board quartz oscillators: State of the knowledge
[CNES-CT/DRT/TIT/TF-88/354] N91-10110
Hydrogen maser: Results of evaluations done by the CNES from May 1986 to December 1987
[CNES-DRT/TIT/TF-88/338-T] N91-10284
**CRYSTAL STRUCTURE**
On the effects of magnetic bonding in rare earth transition metal intermetallics
[DE90-015800] N91-10156
Constant stress of XD (trademark) TiAl containing nitrogen
[DE90-011947] N91-10158
Texture-induced anisotropy and high-strain rate deformation in metals
[DE90-016611] N91-10163
Strength and toughness of single-phase and dual-phase high-temperature intermetallics
[DE90-017192] N91-10166
Superconducting borides
[DE90-016484] N91-10769
Substrate temperature effects on (cubic x cubic lattice) R 30 deg domain growth of Ag on Si(111) surface
[DE90-016527] N91-10772
Fe site occupancy and superconductivity in Y(1-z)Ca(z)Ba(z) (Cu(1-x)Fe(x))3O(6+y)
[DE90-016614] N91-10774
**CRYSTALLOGRAPHY**
Texture-induced anisotropy and high-strain rate deformation in metals
[DE90-016611] N91-10163
**CRYSTALS**
Cirrus cloud model parameterizations: Incorporating realistic ice particle generation N91-10453
Radiative properties of visible and subvisible Cirrus: Scattering on hexagonal ice crystals N91-10462
Interpretation of satellite-measured bidirectional reflectance from Cirrus cloudy atmospheres N91-10470
Diamond turning of optical crystals
[DE90-015909] N91-10719
Radiation damage in Al2O3 crystals implanted with 3.8 MeV Fe(2+)
[DE90-016038] N91-10761
**CUBIC EQUATIONS**
Relative position of the critical points of a certain cubic system and a generalization of the Bendixson index formula
[REPT-90-23] N91-10669
**CUMULATIVE DAMAGE**
Study of the mechanisms of damage and failure of fiber and ceramic matrix composites
[ISAL-90-0026] N91-10135
**CUMULUS CLOUDS**
Cloud motion wind N91-10365
The effects of cloud radiative forcing on an ocean-covered planet N91-10456
Fractional cloudiness in shallow cumulus layers N91-10498
Structures observed on the spot radiance fields during the FIRE experiment N91-10503
Boundary layer roll circulations during FIRE N91-10521
**CURING**
Influence of expanding monomer on carbon fiber reinforced epoxy composites
[AD-A223277] N91-10124
**CURL (VECTORS)**
On the possibility to support multisatellite measurements of the Cluster mission by single satellite measurements in the Regatta-Cluster project N91-10428
**CURRENT DENSITY**
Railgun restrike control
[DE90-015108] N91-10095
Accuracy of the estimate of J via multipoint measurements N91-10422
Computation of superconductor critical current densities and magnetization curves
[DE90-016567] N91-10773
**CURVATURE**
Confidence intervals and curvature measures in nonlinear regression using the IML and NLIN procedures in SAS(tm) software
[PB90-246398] N91-10624
**CYCLES**
Existence of at most two limit cycles for the system of differential equations: dx/dt = a + summation for i+j = 2 of (a sub ij) (x sup i) (y sup j) and dy/dt =b + summation for i+j = 2 of (b sub ij) (x sup i) (y sup j)
[REPT-90-03] N91-10667
Long cycles, degree sums, and neighborhood unions
[MEMO-851] N91-10676
**CYCLIC LOADS**
Repeated buckling of composite shear panels N91-10303
**CYCLONES**
Pre-processing of image data N91-10364
Typhoon information N91-10366
Mariners Weather Log, Volume 34, Number 2, Spring 1990
[PB90-222324] N91-10537
**CYCLOTRON FREQUENCY**
RF helicity injection and current drive
[NIFS-34] N91-10750

## D

**DAMAGE**
Flight set 360L007 (STS-33R) field joint protection system, thermal protection system, and systems tunnel components, volume 7
[NASA-CR-184026] N91-10115
Micro-mechanical analysis of damage growth and fracture in discontinuous fiber reinforced metal matrix composites
[NASA-CR-187020] N91-10126
Damage assessment and possible damage mechanisms to 1-meter diameter Nova turning mirrors
[DE90-016473] N91-10278
Evaluation of nondestructive evaluation techniques for determination of flawed conditions and the effects of flaws on the burst pressure in Kevlar-epoxy filament-wound spherical test specimens
[DE90-014839] N91-10330
Theoretical analysis of a runaway electron suppression device
[DE90-015992] N91-10737
**DAMAGE ASSESSMENT**
Composite heat damage. Part 1: Mechanical testing of IM6/3501-6 laminates. Part 2: Nondestructive evaluation studies of IM6/3501-6 laminates
[DE90-016207] N91-10125
Damage assessment and possible damage mechanisms to 1-meter diameter Nova turning mirrors
[DE90-016473] N91-10278
Measured silicon displacement damage ratios support the need to replace the ASTM E-722 damage function with the NJOY calculated function
[DE90-016225] N91-10762
**DAMPING**
An experimental and analytical study of structural identification N91-10325
**DATA ACQUISITION**
Meteorological Satellite Center Technical Note. Special Issue (1989). Summary of GMS System. 1: Telecommunication System N91-10338
Outline of CDAS telecommunication system N91-10340
Command subsystem N91-10346
Trilateration ranging subsystem N91-10347
Antenna/transmitter control unit N91-10348
Frequency standard unit N91-10349
DCP subsystem N91-10352
WEFAX subsystem N91-10353
DPC telecommunication system N91-10354
DCP data processing N91-10375
Research on climate change
[DE90-016726] N91-10408
**DATA BASE MANAGEMENT SYSTEMS**
The full-body ground vibration tests using the low-noise STOL test plane
[NAL-TM-576] N91-10077
Research on climate change
[DE90-016726] N91-10408
PROTHE: A software as a help for the studies in industrial thermal engineering
[ETN-90-97582] N91-10634

Earth System Monitor, Volume 1, Number 1, June 1990
[PB90-215146] N91-10799
**DATA BASES**
Seat dynamic performance standards for a range of sizes
[DOT/FAA/CT-TN90/23] N91-10028
Heavy duty liquid and gaseous fuel emissions database test results from four alternative fuel configurations of the Caterpillar 3406 engine
[DE90-014783] N91-10288
Knowledge-based assistance in costing the space station DMS N91-10611
Software sizing, cost estimation and scheduling N91-10612
Ada software productivity prototypes: A case study N91-10613
**DATA COLLECTION PLATFORMS**
DCP subsystem N91-10352
DCP data processing N91-10375
**DATA COMPRESSION**
Image data compression overview: Issues and partial solutions
[PB90-172006] N91-10796
**DATA CONVERSION ROUTINES**
Software package for 2-dimensional graphic display unit
[NAL-TM-589] N91-10605
**DATA CONVERTERS**
The full-body ground vibration tests using the low-noise STOL test plane
[NAL-TM-576] N91-10077
**DATA CORRELATION**
Analyzing long time series of hydrological data with respect to climate variability: Project description
[WCAP-3] N91-10444
**DATA FLOW ANALYSIS**
A practical approach to object based requirements analysis N91-10615
Representing object oriented specifications and designs with extended data flow notations N91-10617
**DATA LINKS**
Operational evaluation of initial data link air traffic control services. Volume 2: Appendices
[DOT/FAA/CT-90/1-VOL-2] N91-10033
NASA transport systems research vehicle B-737 data link system and display formats
[NASA-TM-102717] N91-10058
Influence of the telescope depointing on the performances of an optical link. Correlation between depointing law and coding, concerning the computation of mean BER
[CNES-CT/DRT/TIT/TR-88/24-T] N91-10206
Principles of LOCSTAR system experiments
[CNES-CT/DRT/TIT/TR-88/355] N91-10207
**DATA MANAGEMENT**
Proceedings of the WMO Region 3/4 Training Seminar on Climate Data Management and User Services
[WCDP-1] N91-10445
Knowledge-based assistance in costing the space station DMS N91-10611
**DATA PROCESSING**
Experiments and theory with a 0.5 ton mobile robot
[OUEL-1807/90] N91-10035
Meteorological Satellite Center Technical Note. Special Issue (1989). Summary of GMS System. 1: Telecommunication System N91-10338
Stretched VISSR subsystem N91-10343
DPC telecommunication system N91-10354
Meteorological Satellite Center Technical Note. Special Issue (1989). Summary of GMS System. 2: Data Processing N91-10356
General flow of image data processing N91-10358
Pre-processing of image data N91-10364
VISSR histogram data N91-10368
GPCP data processing N91-10370
DCP data processing N91-10375
Plasma wave measurements on the dayside: Scale sizes and observational requirements N91-10426
**DATA PROCESSING EQUIPMENT**
VISSR demodulate and processing subsystem N91-10342
**DATA PROCESSING TERMINALS**
Software package for 2-dimensional graphic display unit
[NAL-TM-589] N91-10605
**DATA REDUCTION**
An experimental and analytical study of structural identification N91-10325
Stretched VISSR subsystem N91-10343
Multispacecraft measurement at varying scalelengths: The Cluster/Regatta opportunity N91-10418
Climate data system supports FIRE N91-10455
A synopsis of Langley Research Center's lidar effort for the 1986 FIRE IFO N91-10457
**DATA SYSTEMS**
DCP data processing N91-10375
Climate data system supports FIRE N91-10455
**DATA TRANSMISSION**
Operational evaluation of initial data link air traffic control services. Volume 2: Appendices
[DOT/FAA/CT-90/1-VOL-2] N91-10033
Hydrologic and meteorological operations in the 162-174 and 406.1-420 MHz bands
[PB90-207820] N91-10199
Image monitor N91-10344
**DAYTIME**
Aircraft measurements of the mean and turbulent structure of marine stratocumulus clouds during FIRE N91-10514
**DEBYE LENGTH**
Problems of cold plasma measurements on the Regatta-A spacecraft N91-10431
**DECELERATION**
A unique problem of muscle adaptation from weightlessness: The deceleration deficiency N91-10582
**DECISION MAKING**
Models of the human observer and controller of a dynamic system
[ETN-90-97759] N91-10597
Knowledge-based assistance in costing the space station DMS N91-10611
**DECISION THEORY**
Discounted dynamic programming. Part 3: Successive approximation
[TW-89-14-PT-3] N91-10640
Discounted dynamic programming. Part 4: Accelerated successive approximation
[TW-90-03-PT-4] N91-10641
Discounted dynamic programming. Part 5: Modified policy iteration
[TW-90-04-PT-5] N91-10642
**DECOMPOSITION**
Domain decomposition: An instrument of asymptotic-numerical methods
[DE90-016478] N91-10661
**DECOMPRESSION SICKNESS**
Probability of decompression sickness during space suit testing N91-10559
Changes in maximum allowable supersaturation coefficient in high-altitude decompression N91-10560
**DECONDITIONING**
Workshop on Exercise Prescription for Long-Duration Space Flight
[NASA-CP-3051] N91-10574
**DEFECTS**
Structural risk assessment and aircraft fleet maintenance N91-10321
Calculation of Weibull strength parameters, Batdorf flaw density constants and related statistical quantities using PC-CARES
[NASA-TM-103247] N91-10332
Massively parallel computing system
[DE90-014683] N91-10648
**DEFENSE PROGRAM**
DOD responsibilities on Federal aviation and national airspace system matters
[PB90-218827] N91-10001
System engineering of aerospace and advanced technology programs at an astronautics company (record of study) N91-10192
**DEFORMATION**
High strain rate deformation behavior of shocked copper
[DE90-016481] N91-10161
The looped adhesive strip: An example of coplanar delamination interaction N91-10306
A new beam theory using first-order warping functions N91-10307
Evaluation of alternatives for best-fit paraboloid for deformed antenna surfaces N91-10313
**DEGASSING**
Hydrogen-tritium getters and their applications
[DE90-016282] N91-10184
**DEGENERATION**
First order oscillators
[ETN-90-97758] N91-10226
**DEGRADATION**
Environmental degradation of macro defect free cements. 1: Mechanical properties investigation
[AERE-R-13354-1] N91-10169
**DELAMINATING**
Analysis of delamination in fiber composite laminates out-of-plane under bending
[NASA-CR-186023] N91-10122
The looped adhesive strip: An example of coplanar delamination interaction N91-10306
**DELTA WINGS**
A contribution to the numerical solution of transonic flow around a delta wing by solving Navier-Stokes equations
[DLR-FB-90-13] N91-10026
**DEMODULATION**
VISSR demodulate and processing subsystem N91-10342
Stretched VISSR subsystem N91-10343
WEFAX subsystem N91-10353
**DEMODULATORS**
VISSR demodulate and processing subsystem N91-10342
WEFAX subsystem N91-10353
**DENSITY MEASUREMENT**
Changes in mineral metabolism with immobilization/space flight N91-10581
**DEOXYGENATION**
In situ transmission electron microscopy and computer simulation study of the kinetics of oxygen loss in YBa2Cu3O(z)
[DE90-014508] N91-10783
**DEPLETION**
Copper NMR and hole depletion in the normal state of Y(1-x)Pr(x)Ba2Cu3O7
[DE90-016468] N91-10768
**DEPLOYMENT**
First evaluation of the main parameters in the dynamics of the Small Expendable Deployer System (SEDS) for a tethered satellite
[NASA-CR-4319] N91-10098
**DEPOLARIZATION**
A synopsis of Langley Research Center's lidar effort for the 1986 FIRE IFO N91-10457
Lidar and aircraft studies of deep Cirrus systems from the 1986 FIRE IFO N91-10460
**DEPOSITION**
Deposition controlled uniformity of multilayer mirrors
[DE90-015906] N91-10718
**DEPOSITS**
Effect of surface deposits on electromagnetic waves propagating in uniform ducts
[NASA-TM-103282] N91-10208
**DEPTH**
Determination of surface resistance and magnetic penetration depth of superconducting YBa2Cu3O(7-delta) thin films by microwave power transmission measurements
[NASA-TM-103616] N91-10780
**DESICCANTS**
Nano-composite desiccation materials
[PB90-247388] N91-10123
**DESIGN ANALYSIS**
The GAMMASPHERE
[DE90-016849] N91-10224
Global optimization methods for engineering design N91-10310
Conservative buffering of approximate nonlinear constraints N91-10312
**DESTABILIZATION**
The effects of cloud radiative forcing on an ocean-covered planet N91-10456
**DETECTION**
MicroChannel Plate detectors (MCP)
[CNES-CT/DRT/TIT/OE-88/037-T] N91-10227
A miniature inexpensive, oxygen sensing element
[DE90-014080] N91-10269
Some defects in finite-difference edge finders
[OUEL-1826/90] N91-10645
**DETERMINANTS**
Optimum orientations of the observation axes for 2-dimensional vector sensing under consideration of bias errors
[NAL-TR-1055] N91-10679
**DETONATION**
Thermochemistry of shock-induced exothermic reactions in selected porous mixtures
[DE90-016104] N91-10183
Transition state theory applying to the study of reaction processes in detonation
[DE90-016558] N91-10187
**DETONATION WAVES**
Analysis of pulsed laser-generated impulse in an advanced airbreathing thruster N91-10062
**DIAGNOSIS**
Diagnostic possibilities of inflight EKG monitoring of flight crew N91-10557
**DIAMONDS**
Meetings on the structure and properties of implanted ceramics
[DE90-017313] N91-10181
Diamond turning of optical crystals
[DE90-015909] N91-10719
**DIELECTRIC PROPERTIES**
Theoretical calculations of the nonlinear dielectric function of inhomogeneous thin films
[DE90-017186] N91-10778

**DIFFERENCES**
The difference of two renewal processes: Level crossing and the infimum
[MEMO-845] N91-10690
**DIFFERENTIAL EQUATIONS**
Existence of at most two limit cycles for the system of differential equations: dx/dt = a + summation for i+j = 2 of (a sub ij) (x sup i) (y sup j) and dy/dt =b + summation for i+j = 2 of (b sub ij) (x sup i) (y sup j)
[REPT-90-03] N91-10667
Computation of superconductor critical current densities and magnetization curves
[DE90-016567] N91-10773
**DIFFRACTION**
Radiative properties of visible and subvisible Cirrus: Scattering on hexagonal ice crystals N91-10462
**DIFFRACTION PATTERNS**
Distortion of LDA fringe pattern by tracer perticles
[SFB-210/E/59] N91-10286
Variable-coherence beam optics
[ISBN-952-90-1784-7] N91-10724
**DIFFUSION**
Equal eigenvalues in multicomponent diffusion: The extraction of diffusion coefficients from experimental data in ternary systems
[DE90-012074] N91-10142
Cloud absorption properties as derived from airborne measurements of scattered radiation within clouds
N91-10512
Thermophysical properties of fluids and fluid mixtures
[DE90-016306] N91-10792
**DIFFUSION COEFFICIENT**
Reaction kinetics of the Ca-SO2 system in absence of inter-grain pore diffusion
[DE90-009672] N91-10781
**DIFFUSIVITY**
Fast sound propagation in binary fluid mixtures
N91-10233
**DIGITAL COMPUTERS**
Computer system N91-10357
**DIGITAL DATA**
Digital image integration technique of multiple geoscience information system and its application
[DE90-627893] N91-10801
**DIGITAL ELECTRONICS**
Three-dimensional full-wave analysis of signal communications in active integrated circuits using a variable-mesh TLM method N91-10212
**DIGITAL RADAR SYSTEMS**
Satellite-derived index of precipitation intensity
N91-10362
**DIGITAL SYSTEMS**
An interpersonal multimedia visualization system
[DE90-014974] N91-10803
**DIMENSIONAL ANALYSIS**
Numerical investigations in three-dimensional internal flows
[NASA-CR-186958] N91-10083
**DIRICHLET PROBLEM**
Analysis techniques for residual acceleration data
[NASA-TM-103507] N91-10191
On the convergence at infinity, rate of convergence and uniqueness of solutions with finite Dirichlet integral to the exterior Dirichlet problem for the steady plane Navier-Stokes system of equations
[PREPRINT-166] N91-10257
**DISCHARGE COEFFICIENT**
Measurements of coefficients of discharge for concentric flange-tapped square-edged orifice meters in natural gas over the Reynolds number range 25,000 to 16,000,000
[PB90-219601] N91-10231
**DISCONTINUITY**
Analysis of moving strong discontinuity surfaces in elastic-plastic solids including effects of inertia and finite strain N91-10323
**DISEASES**
Potential effects of global climate change on the United States. Appendix G: Health
[PB90-173881] N91-10401
**DISK GALAXIES**
Investigation of Markarian galaxies with multiple nuclei
N91-10813
**DISPERSING**
Energetic particles in the Earth's magnetotail or: Cluster and Regatta as a dispersiometer N91-10434
**DISPLACEMENT**
Particle displacement tracking for PIV
[NASA-TM-103288] N91-10271
Measured silicon displacement damage ratios support the need to replace the ASTM E-722 damage function with the NJOY calculated function
[DE90-016225] N91-10762
**DISPLAY DEVICES**
NASA transport systems research vehicle B-737 data link system and display formats
[NASA-TM-102717] N91-10058
Function and performance of visual simulation unit of flight simulation test facility
[NAL-TM-581] N91-10082
FAA air traffic operational evaluation of Automated Surface Observing System (ASOS)
[DOT/FAA/CT-TN90/42] N91-10084
Pre-processing of image data N91-10364
Software package for 2-dimensional graphic display unit
[NAL-TM-589] N91-10605
**DISSOCIATION**
Collision-induced gas phase dissociation rates
[NASA-CR-185874] N91-10707
**DISTANCE MEASURING EQUIPMENT**
An analysis of the effects of secondary reflections on dual-frequency reflectometers
[NASA-TM-102709] N91-10221
**DISTORTION**
Estimation of astronomical images from the bispectrum of atmospherically distorted infrared data N91-10806
**DISTRIBUTED PARAMETER SYSTEMS**
A distributed control and monitor system used in laser fusion research
[DE90-013478] N91-10732
**DISTRIBUTED PROCESSING**
A manual for PARTI runtime primitives
[NASA-CR-187442] N91-10599
Performance and operational characteristics of a Fiber Distributed Data Interface (FDDI) ring
[DE90-016103] N91-10649
**DISTRIBUTION FUNCTIONS**
An introduction to ultrafunctions
[MEMO-841] N91-10672
**DIURNAL VARIATIONS**
Image mapping N91-10359
Sub-visual Cirrus detection and characterization
N91-10486
Analysis of diurnal variation of SCu layer using 2 days of CLASS soundings on San Nicolas Island N91-10490
Diurnal variation of marine stratocumulus over San Nicolas Island during the FIRE IFO N91-10491
**DOMAINS**
Domain decomposition: An instrument of asymptotic-numerical methods
[DE90-016478] N91-10661
**DOPED CRYSTALS**
Methane conversion by solid electrolyte membranes
[PB90-226341] N91-10381
Ion-assisted doping of 2-6 compounds during physical vapor deposition
[DE90-000358] N91-10756
Fe site occupancy and superconductivity in Y(1-z)Ca(z)Ba(z) (Cu(1-x)Fe(x))3O(6+y)
[DE90-016614] N91-10774
**DOPPLER EFFECT**
Thin film thermometers and flowmeters for applications in liquid helium N91-10265
Plasma wakefield excitation by charge particle beams
N91-10729
**DOPPLER RADAR**
Vertical velocities within a Cirrus cloud from Doppler lidar and aircraft measurements during FIRE: Implications for particle growth N91-10461
A four-lidar view of Cirrus from the FIRE IFO: 27-28 October 1986 N91-10478
**DOUBLE BASE ROCKET PROPELLANTS**
Specific impulse comparison of high density hydrocarbon fuel burned with oxygen
[NAL-TR-1053] N91-10148
**DOWNLINKING**
DCP subsystem N91-10352
**DROP SIZE**
Cloud absorption properties as derived from airborne measurements of scattered radiation within clouds
N91-10512
Cloud optical parameters as derived from the multispectral cloud radiometer N91-10513
**DROPS (LIQUIDS)**
Aerosol measurements in the stratocumulus project
N91-10506
In situ measurements of ship tracks N91-10507
Cloud optical parameters as derived from the multispectral cloud radiometer N91-10513
Near infrared radiances observed by the UK C130 multi-channel radiometer during the marine stratocumulus IFO and preliminary comparison with model calculations
N91-10525
Measurements of the light-absorbing material inside cloud droplets and its effect on cloud albedo
N91-10528
**DRUGS**
Requirements for an ideal drug for preventing space motion sickness N91-10566
**DRYING**
Nano-composite desiccation materials
[PB90-247388] N91-10123
Mass transfer in oscillating flows: Efficient drying via pulse combustors
[PB90-242389] N91-10235
**DUCTILITY**
Weldability of nickel and iron aluminides
[DE90-013496] N91-10153
A weldability study of Haynes Alloy no. 242
[DE90-013875] N91-10154
**DUCTS**
Effect of surface deposits on electromagnetic waves propagating in uniform ducts
[NASA-TM-103282] N91-10208
**DURABILITY**
Repeated buckling of composite shear panels
N91-10303
**DYES**
Anomalous dispersion as a phase-matching technique for second harmonic generation
[DE90-015696] N91-10172
**DYNAMIC CHARACTERISTICS**
The 1987 Strategic Defense Initiative Organization (SDIO) Workshop on Laser Propulsion
[DE90-013484] N91-10274
Nonlinear optics and nonlinear dynamics
[DE90-015975] N91-10716
**DYNAMIC LOADS**
Development of the force envelope for an acceleration/force extremal controlled vibration test
[DE90-015712] N91-10329
**DYNAMIC MODELS**
Elastohydrodynamic lubrication: A dynamic variation method
[ISBN-90-9003079-4] N91-10290
**DYNAMIC PRESSURE**
Entry vehicle performance analysis and atmospheric guidance algorithm for precision landing on Mars
[NASA-CR-185614] N91-10102
**DYNAMIC PROGRAMMING**
Discounted dynamic programming. Part 3: Successive approximation
[TW-89-14-PT-3] N91-10640
Discounted dynamic programming. Part 4: Accelerated successive approximation
[TW-90-03-PT-4] N91-10641
Discounted dynamic programming. Part 5: Modified policy iteration
[TW-90-04-PT-5] N91-10642
**DYNAMIC RESPONSE**
Research in Structures, Structural Dynamics and Materials, 1990
[NASA-CP-3064] N91-10301
Static and dynamic aeroelastic characterization of an aerodynamically heated generic hypersonic aircraft configuration N91-10320
Directional response of wind waves to turning winds
[REPT-90-2] N91-10549
**DYNAMIC STRUCTURAL ANALYSIS**
Research in Structures, Structural Dynamics and Materials, 1990
[NASA-CP-3064] N91-10301
**DYNAMIC TESTS**
Differential Global Positioning System (DGPS) test plan
[DOT/FAA/CT-TN90/15] N91-10034
**DYNAMICAL SYSTEMS**
Models of the human observer and controller of a dynamic system
[ETN-90-97759] N91-10597
**DYNAMO THEORY**
The scientific case for magnetic field satellites
[NASA-CR-186532] N91-10101

**E**

**EARTH (PLANET)**
JPRS report: Science and technology. USSR: Earth sciences
[JPRS-UES-90-006-L] N91-10376
JPRS report: Science and technology. USSR: Earth sciences
[JPRS-UES-90-007] N91-10377
**EARTH ALBEDO**
Third generation earth radiation budget measurements; ERBE in the context of earlier systems N91-10530
**EARTH CRUST**
The scientific case for magnetic field satellites
[NASA-CR-186532] N91-10101

**EARTH ENVIRONMENT**
Earth System Monitor, Volume 1, Number 1, June 1990
[PB90-215146] N91-10799
**EARTH IONOSPHERE**
Features of mid-tail ion trajectories during substorms
N91-10435
**EARTH MAGNETOSPHERE**
Space Plasma Physics Investigations by Cluster and Regatta
[ESA-SP-306] N91-10417
Energetic particles in the Earth's magnetotail or: Cluster and Regatta as a dispersiometer N91-10434
Specific tasks of Regatta-E measurements correlated with Cluster/Regatta-A in the ISTP and Regatta programmes N91-10436
**EARTH OBSERVING SYSTEM (EOS)**
The 1990 Reference Handbook: Earth Observing System
[NASA-TM-102910] N91-10378
**EARTH RADIATION BUDGET**
Reflectivities of uniform and broken marine stratiform clouds N91-10501
Structures observed on the spot radiance fields during the FIRE experiment N91-10503
Third generation earth radiation budget measurements; ERBE in the context of earlier systems N91-10530
**EARTH RADIATION BUDGET EXPERIMENT**
Comparison of NOAA-9 ERBE measurements with Cirrus IFO satellite and aircraft measurements N91-10471
ERBE and AVHRR Cirrus cloud fire study N91-10472
Third generation earth radiation budget measurements; ERBE in the context of earlier systems N91-10530
**EARTH SURFACE**
Geographic display of circulation model data
[NOAA-NESDIS-27] N91-10446
**EARTHQUAKE RESISTANT STRUCTURES**
NIST research reports, May 1990
[PB90-244435] N91-10800
**ECOLOGY**
Potential effects of global climate change on the United States. Appendix E: Aquatic resources
[PB90-172297] N91-10399
**ECONOMIC ANALYSIS**
Energy efficiency improvement potential of commercial aircraft to 2010
[DE90-014767] N91-10046
Space market model space industry input-output model
[NASA-CR-187252] N91-10795
**EDDY CURRENTS**
Eddy current inspection of graphite fiber components
[NASA-TM-103514] N91-10294
**EDGE DETECTION**
Multiple widths yield reliable finite differences
[OUEL-1827/90] N91-10646
**EDGES**
Some defects in finite-difference edge finders
[OUEL-1826/90] N91-10645
**EDUCATION**
Educator's guide for building and operating environmental satellite receiving stations
[NOAA-TR-NESDIS-44] N91-10093
Proceedings of the WMO Region 3/4 Training Seminar on Climate Data Management and User Services
[WCDP-1] N91-10445
Activities of the Board on Mathematical Sciences
[DE90-015118] N91-10598
**EIGENVALUES**
Equal eigenvalues in multicomponent diffusion: The extraction of diffusion coefficients from experimental data in ternary systems
[DE90-012074] N91-10142
Casual eigenvector function approximations and the problem of scaling: An algorithm
[OUEL-1822/90] N91-10644
H 2 and H infinity approximations for eigenvalue/vector functions of transfer matrices
[OUEL-1778/89] N91-10684
**EIGENVECTORS**
Casual eigenvector function approximations and the problem of scaling: An algorithm
[OUEL-1822/90] N91-10644
H 2 and H infinity approximations for eigenvalue/vector functions of transfer matrices
[OUEL-1778/89] N91-10684
**ELASTIC DAMPING**
Application of a state-space wake model to elastic blade flapping in hover N91-10006
**ELASTIC DEFORMATION**
Elastohydrodynamic lubrication: A dynamic variation method
[ISBN-90-9003079-4] N91-10290
**ELASTIC PROPERTIES**
Analysis of delamination in fiber composite laminates out-of-plane under bending
[NASA-CR-186023] N91-10122
Physical interpretation and application of principles of ultrasonic nondestructive evaluation of high-performance materials
[NASA-CR-180489] N91-10293
**ELASTIC SCATTERING**
Theoretical studies in few-body intermediate energy physics
[DE90-017279] N91-10709
**ELASTOHYDRODYNAMICS**
Elastohydrodynamic lubrication: A dynamic variation method
[ISBN-90-9003079-4] N91-10290
**ELECTRIC BATTERIES**
Corrosion, passivity, and breakdown of alloys used in high energy density batteries
[DE90-016648] N91-10223
**ELECTRIC DISCHARGES**
Overdischarge protection in high-temperature cells and batteries
[DE90-015180] N91-10220
Development and application of linear and nonlinear methods for interpretation of lightning strikes to in-flight aircraft
[NASA-CR-3974] N91-10548
**ELECTRIC FIELDS**
Contribution to the study of the electromagnetic field radiation close to electronics circuits
[ECL-90-12] N91-10211
**ELECTRIC GENERATORS**
Application of generalized predictive control to a boiler turbine unit for electricity generation
[OUEL-1823/90] N91-10229
**ELECTRIC POWER PLANTS**
Thermal energy storage for power generation applications
[DE90-016539] N91-10388
**ELECTRIC POWER TRANSMISSION**
High-temperature superconductors: Their potential for utility applications
[DE90-009704] N91-10757
**ELECTRIC ROCKET ENGINES**
Performance characterization of a segmented anode arcjet thruster
[NASA-TM-103227] N91-10118
**ELECTRIC SWITCHES**
Plasma puff initiation of high Coulomb transfer switches
[NASA-CR-187024] N91-10735
**ELECTRICAL ENGINEERING**
JPRS report: Science and technology. USSR: Electronics and electrical engineering
[JPRS-UEE-90-004] N91-10213
JPRS report: Science and technology. USSR: Electronics and electrical engineering
[JPRS-UEE-90-006] N91-10214
JPRS report: Science and technology. USSR: Electronics and electrical engineering
[JPRS-UEE-90-007] N91-10215
JPRS report: Science and technology. USSR: Electronics and electrical engineering
[JPRS-UEE-90-008] N91-10216
JPRS report: Science and technology. USSR: Electronics and electrical engineering
[JPRS-UEE-90-009] N91-10217
**ELECTRICAL PROPERTIES**
Materials analysis and device optimization of CuInSe2 solar cells
[DE90-000365] N91-10384
Contribution to the study of MOS structures ageing
[ECL-90-04] N91-10785
**ELECTRICAL RESISTIVITY**
Railgun restrike control
[DE90-015108] N91-10095
The transport properties of activated carbon fibers
[DE90-015910] N91-10130
Design and application of gas-gap heat switches
[NASA-CR-187339] N91-10222
Electronic, structural and transport properties of (almost) rare-earth-like actinide hydrides
[DE90-016491] N91-10771
**ELECTROCARDIOGRAPHY**
Diagnostic possibilities of inflight EKG monitoring of flight crew N91-10557
Effects of rolling motion on the circadian rhythm of sinoatrial node N91-10558
**ELECTROCATALYSTS**
The physical and chemical state of Westinghouse Phosphoric Acid Fuel Cell assemblies after long term operation: Surface and near-surface analysis
[DE90-015055] N91-10382
**ELECTROCHEMICAL CORROSION**
Evaluation of candidate alloys for the construction of metal flex hoses in the STS launch environment
[NASA-TM-103808] N91-10157
Corrosion-resistant coatings for high-temperature high-sulfur activity applications
[DE90-016638] N91-10177
**ELECTROCHEMICAL OXIDATION**
Electrochemical oxidation of methane at metal and metal oxide electrodes
[PB90-205196] N91-10140
**ELECTRODE MATERIALS**
Electrochemical oxidation of methane at metal and metal oxide electrodes
[PB90-205196] N91-10140
Overdischarge protection in high-temperature cells and batteries
[DE90-015180] N91-10220
**ELECTROLYTES**
Physical and electronic structure of the electrolyte-solid interface through optical phenomena
[DE90-015935] N91-10764
**ELECTROLYTIC CELLS**
Advanced materials for high-temperature solid electrolyte applications
[DE90-016328] N91-10143
Basic study of solid oxide fuel cells
[DE90-517069] N91-10386
**ELECTROMAGNETIC ABSORPTION**
Measurements of the light-absorbing material inside cloud droplets and its effect on cloud albedo
N91-10528
**ELECTROMAGNETIC ACCELERATION**
Numerical simulation of electromagnetic acceleration by induction. Part 1: Thin loops
[ISL-R-102/89-PT-1] N91-10205
**ELECTROMAGNETIC COMPATIBILITY**
Hydrologic and meteorological operations in the 162-174 and 406.1-420 MHz bands
[PB90-207820] N91-10199
Method for simulating large dimension devices submitted to electromagnetic perturbations
[ECL-90-10] N91-10210
**ELECTROMAGNETIC FIELDS**
Railgun restrike control
[DE90-015108] N91-10095
Statistical characterization of a mode-stirred chamber
[DE90-014860] N91-10202
Interaction of extremely low-frequency electromagnetic fields with humans
[DE90-017190] N91-10592
Cosmological singularities in electrovacuum spacetimes with two-parameter spacelike isometry groups
N91-10811
**ELECTROMAGNETIC INTERACTIONS**
Interaction of extremely low-frequency electromagnetic fields with humans
[DE90-017190] N91-10592
Discrete gravity
[DE90-014808] N91-10789
**ELECTROMAGNETIC INTERFERENCE**
Intercalated graphite fiber composites as EMI shields in aerospace structures
[NASA-TM-103632] N91-10134
Contribution to the study of the electromagnetic field radiation close to electronics circuits
[ECL-90-12] N91-10211
**ELECTROMAGNETIC NOISE**
Radiation-induced noise in Charge-Coupled Device (CCD) and Charge-Injection Device (CID) imagers
[DE90-016724] N91-10777
**ELECTROMAGNETIC NOISE MEASUREMENT**
Method for simulating large dimension devices submitted to electromagnetic perturbations
[ECL-90-10] N91-10210
**ELECTROMAGNETIC PROPERTIES**
Three-dimensional full-wave analysis of signal communications in active integrated circuits using a variable-mesh TLM method N91-10212
**ELECTROMAGNETIC PROPULSION**
Impact of high-critical-temperature superconductors on electromagnetic pump applications
[DE90-014809] N91-10759
**ELECTROMAGNETIC PUMPS**
Impact of high-critical-temperature superconductors on electromagnetic pump applications
[DE90-014809] N91-10759
**ELECTROMAGNETIC RADIATION**
Characterization of mono- and multi-molecular assemblies at glassy carbon and noble metals by ex situ and in situ infrared external reflection spectroscopy
[DE90-016417] N91-10144
Effect of surface deposits on electromagnetic waves propagating in uniform ducts
[NASA-TM-103282] N91-10208

Cosmological singularities in electrovacuum spacetimes with two-parameter spacelike isometry groups
N91-10811

**ELECTROMAGNETIC SCATTERING**
Electromagnetic scattering from two-dimensional thick material junctions
[NASA-CR-186976] N91-10201

**ELECTROMAGNETIC SHIELDING**
Intercalated graphite fiber composites as EMI shields in aerospace structures
[NASA-TM-103632] N91-10134

**ELECTROMAGNETIC WAVE TRANSMISSION**
Method for simulating large dimension devices submitted to electromagnetic perturbations
[ECL-90-10] N91-10210

**ELECTRON AVALANCHE**
An avalanche electron emitting diode in gallium arsenide
[ETN-90-97746] N91-10225

**ELECTRON BEAMS**
An x band backward-wave oscillator experiment
[DE90-015119] N91-10219
INEX modeling of the Boeing ring optical resonator free-electron laser
[DE90-016488] N91-10280
Studies of the system-environment interaction by electron beam emission from a sounding rocket payload in the ionosphere N91-10410

**ELECTRON FLUX DENSITY**
Prototype instrumentation and design studies --- electrostatic analyzer system for the Space Shuttle
[AD-A211566] N91-10264

**ELECTRON GUNS**
An avalanche electron emitting diode in gallium arsenide
[ETN-90-97746] N91-10225

**ELECTRON MICROSCOPY**
In situ transmission electron microscopy and computer simulation study of the kinetics of oxygen loss in YBa2Cu3O(z)
[DE90-014508] N91-10783

**ELECTRON PLASMA**
Plasma wakefield excitation by charge particle beams
N91-10729

**ELECTRON RUNAWAY (PLASMA PHYSICS)**
Theoretical analysis of a runaway electron suppression device
[DE90-015992] N91-10737

**ELECTRON TRANSFER**
Theoretical atomic physics for fusion
[DE90-017280] N91-10710

**ELECTRON-POSITRON PLASMAS**
Research in elementary particle physics
[DE90-017278] N91-10708

**ELECTRONIC EQUIPMENT**
JPRS report: Science and technology. USSR: Electronics and electrical engineering
[JPRS-UEE-90-007] N91-10215
JPRS report: Science and technology. USSR: Electronics and electrical engineering
[JPRS-UEE-90-008] N91-10216
JPRS report: Science and technology. USSR: Electronics and electrical engineering
[JPRS-UEE-90-009] N91-10217

**ELECTRONICS**
JPRS report: Science and technology. USSR: Electronics and electrical engineering
[JPRS-UEE-90-006] N91-10214

**ELECTRONS**
Possibilities of charged particle injection from spacecraft for active diagnostics of the surrounding plasma and active spacecraft potential control N91-10437
Direct extraction of a Na(-) beam from a sodium plasma
[NIFS-35] N91-10751

**ELECTROPLATING**
Electroplating corners
[DE90-017023] N91-10195

**ELECTROSTATIC PROBES**
Passive-filtered and active-driven probes for RF plasmas
[OUEL-1806/89] N91-10754

**ELECTROSTATICS**
Physical and chemical test results of electrostatic safe flooring materials
[NASA-TM-103501] N91-10194
Comments on edge turbulence during lower hybrid current drive experiment on CASTOR tokamak
[IPPCZ-279] N91-10726

**ELLIPSES**
Modes of elliptical waveguides: A correction
[DE90-016647] N91-10203

**ELLIPSOIDS**
Bounded-error data, and frequency response design
[OUEL-1766/89] N91-10683

**ELLIPTIC DIFFERENTIAL EQUATIONS**
Strong maximum principles for systems
[REPT-90-37] N91-10671

**EMBEDDING**
Experiences with Ada in an embedded system
N91-10614
A Markov renewal approach to an apportunistic replacement model in continuous time
[MEMO-844] N91-10675

**EMBRITTLEMENT**
Weldability of nickel and iron aluminides
[DE90-013498] N91-10153

**EMISSION**
Global tropospheric chemistry modeling
[DE90-015908] N91-10409

**EMISSION SPECTRA**
Vibro-acoustic emission rubbing sources
[PNR-90730] N91-10336
Time-resolved FTIR (Fourier Transform Infrared) emission studies of laser photofragmentation and chain reactions
[DE90-017223] N91-10722

**EMISSIVITY**
Multi-spectral window radiance observations of Cirrus from satellite and aircraft, November 2, 1986 Project FIRE N91-10465
Cloud parameters from GOES visible and infrared radiances during the FIRE Cirrus IFO, October 1986
N91-10473
Cirrus cloud properties derived from coincident GOES and lidar data during the 1986 FIRE Cirrus Intensive Field Observations (IFO) N91-10476

**EMITTANCE**
Brightness temperature distribution N91-10369

**EMULSIONS**
Tests of the general fire suppression concentrate Pyrocap B-136
[DOT/FAA/CT-TN90/21] N91-10029

**ENERGY BUDGETS**
The radiation budget of a Cirrus layer deduced from simultaneous aircraft observations and model calculations N91-10467
Comparison of NOAA-9 ERBE measurements with Cirrus IFO satellite and aircraft measurements N91-10471
ERBE and AVHRR Cirrus cloud fire study N91-10472
Third generation earth radiation budget measurements; ERBE in the context of earlier systems N91-10530

**ENERGY CONSERVATION**
Energy efficiency improvement potential of commercial aircraft to 2010
[DE90-014767] N91-10046

**ENERGY CONVERSION**
A system design and demonstrative field test of wind turbine with a 14 m diameter rotor
[NAL-TR-1056] N91-10389

**ENERGY CONVERSION EFFICIENCY**
High-temperature superconductors: Their potential for utility applications
[DE90-009704] N91-10757

**ENERGY DISSIPATION**
Vibro-acoustic emission rubbing sources
[PNR-90730] N91-10336

**ENERGY DISTRIBUTION**
Experimental constraints in the characterization of a turbulent field from several satellites N91-10425

**ENERGY LEVELS**
Nuclear structure calculations for astrophysical applications
[DE90-016433] N91-10818

**ENERGY METHODS**
Design of control laws for flutter suppression based on the aerodynamic energy concept and comparisons with other design methods
[NASA-TP-3056] N91-10328

**ENERGY SPECTRA**
Bicolored photometry and spectral accommodation in X-ray region of mass impregnated stellar X-ray binaries
[MPE-219] N91-10808

**ENERGY STORAGE**
Thermal energy storage for power generation applications
[DE90-016539] N91-10388
A system design and demonstrative field test of wind turbine with a 14 m diameter rotor
[NAL-TR-1056] N91-10389

**ENERGY TECHNOLOGY**
Research on climate change
[DE90-016726] N91-10408
NIST research reports, May 1990
[PB90-244435] N91-10800

**ENERGY TRANSFER**
AFDM: An Advanced Fluid-Dynamics Model
[DE90-017536] N91-10241
Damage assessment and possible damage mechanisms to 1-meter diameter Nova turning mirrors
[DE90-016473] N91-10278

Time-resolved FTIR (Fourier Transform Infrared) emission studies of laser photofragmentation and chain reactions
[DE90-017223] N91-10722
Temporal behaviour of self generated magnetic field and its influence on inhibition of thermal flux in ICF plasma
[DE90-627478] N91-10731

**ENGINE DESIGN**
Energy efficiency improvement potential of commercial aircraft to 2010
[DE90-014767] N91-10046
Parametric assessment of propulsion system mass for airbreathing launcher configurations
[PNR-90634] N91-10063
Aero engine design factors for a low fuel price scenario
[PNR-90681] N91-10066
Design/development issues for high bypass ratio fans
[PNR-90758] N91-10076
A three-dimensional turbulent heat transfer analysis for advanced tubular rocket thrust chambers
[NASA-TM-103293] N91-10249
Introduction: Needs and approaches to reliability and quality assurance in design and manufacture
[PNR-90683] N91-10297

**ENGINE TESTS**
OVRhyp, scramjet test aircraft
[NASA-CR-187009] N91-10041
Flight testing of two Allison T56 engines modified to the ARL developed low smoke configuration
[ARL-PROP-TM-449] N91-10064
Analysis of 5 KHz combustion instabilities in 40K methane/LOX combustion chambers
[NASA-TM-101368] N91-10117

**ENGINEERING DRAWINGS**
Engineering design: A powerful influence on the business success on manufacturing industry
[PNR-90763] N91-10197

**ENTHALPY**
Turbulent boundary layers in high enthalpy flows. Numerical code validation by shock tube experiments
[ISL-CO-221/89] N91-10246

**ENTRAINMENT**
Measurement of air entrainment by a free jet using laser velocimetry and Raman scattering
[ISL-R-109/89] N91-10017
Preliminary mixed-layer model results for FIRE marine stratocumulus IFO conditions N91-10495
Simulations and observations of cloudtop processes
N91-10496
Thermodynamic structure of the stratocumulus-capped boundary layer on 7 July, 1987 N91-10533

**ENVIRONMENT EFFECTS**
Potential effects of global climate change on the United States. Appendix C: Agriculture, volume 1
[PB90-171588] N91-10394
Potential effects of global climate change on the United States. Appendix A: Water resources
[PB90-171968] N91-10395
Potential effects of global climate change on the United States. Appendix B: Sea level rise
[PB90-172628] N91-10396
Potential effects of global climate change on the United States. Appendix C: Agriculture, volume 2
[PB90-171596] N91-10397
Potential effects of global climate change on the United States. Appendix D: Forests
[PB90-173238] N91-10398
Potential effects of global climate change on the United States. Appendix E: Aquatic resources
[PB90-172297] N91-10399
Potential effects of global climate change on the United States. Appendix F: Air quality
[PB90-172230] N91-10400
Potential effects of global climate change on the United States. Appendix H: Infrastructure
[PB90-172313] N91-10402
Potential effects of global climate change on the United States. Appendix I: Variability
[PB90-173899] N91-10403
Potential effects of global climate change on the United States. Appendix J: Policy
[PB90-173188] N91-10404
Work, exercise, and space flight. 1: Operations, environment, and effects of spaceflight N91-10578

**ENVIRONMENT SIMULATORS**
Large blast and thermal simulator advanced concept driver design by computational fluid dynamics
[AD-A211364] N91-10230

**ENVIRONMENTAL CHEMISTRY**
Global and regional environmental atmospheric chemistry
[DE90-016693] N91-10407

**ENVIRONMENTAL CONTROL**
Space Station Freedom Environmental Control and Life Support System (ECLSS) phase 3 simplified integrated test trace contaminant control subsystem performance
[NASA-TM-4202] N91-10103

**ENVIRONMENTAL MONITORING**
Chesapeake Bay Basin Monitoring Program Atlas. Volume 2: Biological and living resource monitoring programs
[PB90-147943] N91-10392
National acid precipitation assessment program. Report to the President and Congress
[PB90-185646] N91-10405
Geophysical monitoring for climatic change
[PB90-222126] N91-10538
Activities report of the World Meteorological Organization
[WMO-734] N91-10547

**ENVIRONMENTAL TESTS**
The actuator for the low-noise STOL test plane flight control system and its development test
[NAL-TM-574] N91-10038
Environmental degradation of macro defect free cements. 1: Mechanical properties investigation
[AERE-R-13354-1] N91-10169

**EPIDEMIOLOGY**
ELF (extremely-low-frequency): Exposure levels, bioeffects, and epidemiology
[DE90-016554] N91-10573

**EPOXY MATRIX COMPOSITES**
Influence of expanding monomer on carbon fiber reinforced epoxy composites
[AD-A223277] N91-10124
Test/semi-empirical analysis of a carbon/epoxy fabric stiffened panel N91-10302
Evaluation of nondestructive evaluation techniques for determination of flawed conditions and the effects of flaws on the burst pressure in Kevlar-epoxy filament-wound spherical test specimens
[DE90-014839] N91-10330

**EPOXY RESINS**
Structural properties of laminated Douglas fir/epoxy composite material
[NASA-RP-1236] N91-10127
Repeated buckling of composite shear panels
N91-10303

**EQUATIONS OF MOTION**
Dynamics of gas bubbles moving through liquid
[ETN-90-97760] N91-10255

**EQUATIONS OF STATE**
AFDM: An Advanced Fluid-Dynamics Model
[DE90-017539] N91-10244

**EQUILIBRIUM**
Bounded energy states in homogeneous turbulent shear flow: An alternative view
[NASA-CR-187439] N91-10237

**EQUIPMENT SPECIFICATIONS**
Effects of coolant injection on turbine aerodynamic characteristics. Part 1: Test turbine and apparatus
[NAL-TM-585-PT-1] N91-10059
Configuration, function and performance of the flight simulation test facility and its motion simulation system
[NAL-TM-575] N91-10080
Modification in the main air blower unit for two meter times two meter transonic wind tunnel: Plan and configuration
[NAL-TM-580] N91-10081

**ERGODIC PROCESS**
Geometric ergodicity of the ALOHA-system and a coupled processors model
[TW-90-01-B] N91-10680

**ERGOMETERS**
Work, exercise, and space flight. 3: Exercise devices and protocols N91-10579

**ERROR ANALYSIS**
A representation scheme for fault diagnosis of physical systems
[DE90-016362] N91-10295
Configurational sensitivity of multipoint magnetic field measurements N91-10421
Accuracy of the estimate of J via multipoint measurements N91-10422
Software safety workshop problem
[DE90-016222] N91-10630
A representation scheme for fault diagnosis
[DE90-016291] N91-10631
Self-consistent field error effects in reversed field pinch plasmas N91-10728

**ERROR CORRECTING CODES**
Influence of the telescope depointing on the performances of an optical link. Correlation between depointing law and coding, concerning the computation of mean BER
[CNES-CT/DRT/TIT/TR-88/24-T] N91-10206

**ERRORS**
An analysis of the effects of secondary reflections on dual-frequency reflectometers
[NASA-TM-102709] N91-10221
SSC dipole magnet measurement and alignment using laser technology
[DE90-014881] N91-10281
Technique for human-error sequence identification and signification
[ISBN-90-353-10144] N91-10596
Self-consistent field error effects in reversed field pinch plasmas N91-10728

**ESTIMATES**
Fast estimation of the variance of a narrowband process
[IFSI-90-16] N91-10209

**ESTIMATING**
Study of mixed mode stress intensity factor using the experimental method of transmitted caustics
N91-10324
Sea surface temperature N91-10372
Cirrus cloud properties derived from coincident GOES and lidar data during the 1986 FIRE Cirrus Intensive Field Observations (IFO) N91-10476
Estimated accuracy of ground-based liquid water measurements during FIRE N91-10508

**ETHYL ALCOHOL**
Short-rotation woody crop opportunities to mitigate carbon dioxide buildup
[DE90-016526] N91-10406

**EULER EQUATIONS OF MOTION**
Transonic flow analysis for rotors. Part 3: Three-dimensional, quasi-steady, Euler calculation
[NASA-TP-2375] N91-10007
Multigrid solution for the Euler equations in axisymmetric flow
[REPT-B-17] N91-10253

**EUTECTIC ALLOYS**
A weldability study of Haynes Alloy no. 242
[DE90-013875] N91-10154

**EVAPORATION**
Mass transfer in oscillating flows: Efficient drying via pulse combustors
[PB90-242389] N91-10235

**EVOLUTION (DEVELOPMENT)**
The evolution of the bypass engine
[PNR-90707] N91-10068
Towards a comprehensive framework for reuse: A reuse-enabling software evolution environment
[UMIACS-TR-88-92] N91-10608

**EXCIMER LASERS**
Recent advances in excimer laser technology at Los Alamos
[DE90-016441] N91-10276

**EXCITONS**
Excitons in semiconducting superlattices, quantum wells, and ternary alloys
[DE90-017287] N91-10779

**EXERCISE PHYSIOLOGY**
Workshop on Exercise Prescription for Long-Duration Space Flight
[NASA-CP-3051] N91-10574
US space flight experience. Physical exertion and metabolic demand of extravehicular activity: Past, present, and future N91-10575
Work, exercise, and space flight. 3: Exercise devices and protocols N91-10579
Exercise issues related to the neuromuscular function and adaptation to microgravity N91-10584
Considerations for an exercise prescription
N91-10585
Work, exercise, and space flight. 2: Modification of adaptation by exercise (exercise prescription)
N91-10586
Cardiovascular group N91-10587
Summary and recommendations for initial exercise prescription N91-10588

**EXHAUST EMISSION**
Flight testing of two Allison T56 engines modified to the ARL developed low smoke configuration
[ARL-PROP-TM-449] N91-10064
Heavy duty liquid and gaseous fuel emissions database test results from four alternative fuel configurations of the Caterpillar 3406 engine
[DE90-014783] N91-10288

**EXOBIOLOGY**
Aerospace medicine and biology: A continuing bibliography with indexes (supplement 341)
[NASA-SP-7011(341)] N91-10594

**EXOSAT SATELLITE**
Bicolored photometry and spectral accommodation in X-ray region of mass impregnated stellar X-ray binaries
[MPE-219] N91-10808

**EXOTHERMIC REACTIONS**
Thermochemistry of shock-induced exothermic reactions in selected porous mixtures
[DE90-016104] N91-10183

**EXPERIMENT DESIGN**
Preliminary studies before defining a payload adapted to the primate model
[ETN-90-97581] N91-10107

**EXPERT SYSTEMS**
Automatic determination of fault effects on aircraft functionality
[NASA-CR-181352] N91-10039
Developments in REDES: The rocket engine design expert system
[NASA-TM-103657] N91-10119
Eddy current inspection of graphite fiber components
[NASA-TM-103514] N91-10294

**EXPONENTIAL FUNCTIONS**
Exponential approximations in optimal design
N91-10311

**EXPOSURE**
Effects of prolonged exposure to acetic acid vapors on acid-base balance in humans N91-10561
ELF (extremely-low-frequency): Exposure levels, bioeffects, and epidemiology
[DE90-016554] N91-10573

**EXTRATERRESTRIAL RADIATION**
Effect of single impacts of heavy ions of galactic cosmic rays on lactuca sativa seeds exposed on Salyut-6 and Salyut-7 stations N91-10567

**EXTRAVEHICULAR ACTIVITY**
The design and fabrication of the Centaur neutral buoyancy trainer and related hardware
[NASA-CR-171944] N91-10085
US space flight experience. Physical exertion and metabolic demand of extravehicular activity: Past, present, and future N91-10575
Exercise issues related to the neuromuscular function and adaptation to microgravity N91-10584

**EXTREMELY LOW FREQUENCIES**
ELF (extremely-low-frequency): Exposure levels, bioeffects, and epidemiology
[DE90-016554] N91-10573

**EXTREMUM VALUES**
Probabilistic structural analysis by extremum methods
N91-10308

## F

**F 2 REGION**
Neutral winds derived from IRI parameters and from the HWM87 wind model for the sundial campaign of September, 1986
[NASA-TM-103445] N91-10543

**F-106 AIRCRAFT**
Development and application of linear and nonlinear methods for interpretation of lightning strikes to in-flight aircraft
[NASA-CR-3974] N91-10548

**FABRICATION**
Fabrication aspects of glass matrix composites for gas turbine applications
[PNR-90752] N91-10073
Prevention of breakdown behind railgun projectiles
[DE90-014573] N91-10094
Structural properties of laminated Douglas fir/epoxy composite material
[NASA-RP-1236] N91-10127
A miniature inexpensive, oxygen sensing element
[DE90-014080] N91-10269

**FABRICS**
Advanced ceramic fabric body mounted radiator for Space Station Freedom Phase O design
[DE90-016361] N91-10104
Design considerations for a ceramic fabric radiator
[DE90-016342] N91-10173
Test/semi-empirical analysis of a carbon/epoxy fabric stiffened panel N91-10302

**FABRY-PEROT INTERFEROMETERS**
Application of Fabry-Perot velocimetry to hypervelocity impact experiments
[DE90-015612] N91-10096

**FACSIMILE COMMUNICATION**
FAX image processing N91-10361
Typhoon information N91-10366

**FAILURE**
Test/semi-empirical analysis of a carbon/epoxy fabric stiffened panel N91-10302
Repeated buckling of composite shear panels
N91-10303
Compressive failure of thick-section composite laminates with and without cutouts subjected to biaxial loading N91-10304
Probabilistic failure assessment with application to solid rocket motors N91-10309

**FAILURE ANALYSIS**

Structural tests of aircraft window assembly equipped with smoke evacuation valve
[DOT/FAA/CT-TN89/44] N91-10051

Study of the mechanisms of damage and failure of fiber and ceramic matrix composites
[ISAL-90-0026] N91-10135

A representation scheme for fault diagnosis of physical systems
[DE90-016362] N91-10295

Probabilistic failure assessment with application to solid rocket motors N91-10309

**FAILURE MODES**

Probabilistic failure assessment with application to solid rocket motors N91-10309

**FAINT OBJECTS**

UV observations of Herbig-Haro objects associated with bipolar molecular outflows: HH 7, HH 11 and HH 29
[IFSI-90-9] N91-10819

**FAIRINGS**

Ground test program for new Atlas payload fairings N91-10315

**FAN BLADES**

Design/development issues for high bypass ratio fans
[PNR-90758] N91-10076

**FAR FIELDS**

Contribution to the study of the electromagnetic field radiation close to electronics circuits
[ECL-90-12] N91-10211

Helicopter far-field acoustic levels as a function of reduced main-rotor advancing blade-tip Mach number
[NASA-TM-102684] N91-10699

**FAST NUCLEAR REACTORS**

AFDM: An Advanced Fluid-Dynamics Model. Volume 1: Scope, approach, and summary
[DE90-016723] N91-10239

**FATIGUE (MATERIALS)**

Fatigue crack propagation of coplanar semi-elliptical cracks in pure bending
[PNR-90742] N91-10337

**FATIGUE LIFE**

Repeated buckling of composite shear panels N91-10303

**FAULT TOLERANCE**

Designing application software in wide area network settings
[NASA-CR-187333] N91-10633

**FAULT TREES**

Software safety workshop problem
[DE90-016222] N91-10630

**FEASIBILITY ANALYSIS**

Survey of possibility for volcanic energy development
[DE90-517230] N91-10387

Rn222, Rn222 progeny and Rn220 progeny as atmospheric tracers of air masses at the Mauno Loa Observatory
[DE90-014872] N91-10539

**FEEDBACK**

The effects of outcome and process feedback
[NASA-CR-187332] N91-10595

The digital regulator and tracker for stochastic continuous-time linear time-varying systems
[REPT-90-06] N91-10689

**FEEDBACK CONTROL**

Nonlinear feedback control for high alpha flight
[NASA-CR-186545] N91-10047

A Markov renewal approach to an apportunistic replacement model in continuous time
[MEMO-844] N91-10675

**FEEDFORWARD CONTROL**

Prediction and control of chaotic processes using nonlinear adaptive networks
[DE90-016505] N91-10697

**FIBER COMPOSITES**

Analysis of delamination in fiber composite laminates out-of-plane under bending
[NASA-CR-186023] N91-10122

Evaluation of composite materials for use on launch complexes
[NASA-TM-103809] N91-10131

Reduction of thermal stresses in continuous fiber reinforced metal matrix composites with interface layers
[NASA-CR-185302] N91-10133

Intercalated graphite fiber composites as EMI shields in aerospace structures
[NASA-TM-103632] N91-10134

Industrial applications and markets for ceramic matrix composites
[PNR-90753] N91-10138

Design methodology needs for fiber-reinforced ceramic heat exchangers
[DE90-016659] N91-10178

Eddy current inspection of graphite fiber components
[NASA-TM-103514] N91-10294

Compressive failure of thick-section composite laminates with and without cutouts subjected to biaxial loading N91-10304

An analytical solution for the elastoplastic response of a continuous fiber composite under uniaxial loading N91-10305

**FIBER OPTICS**

An experimental and analytical study of structural identification N91-10325

Performance and operational characteristics of a Fiber Distributed Data Interface (FDDI) ring
[DE90-016103] N91-10649

**FIBERS**

Reduction of thermal stresses in continuous fiber reinforced metal matrix composites with interface layers
[NASA-CR-185302] N91-10133

Holographic examination of great surface fiberbound components in industrial conditions: Resumes of final reports, April 1986 to June 1989
[MBB-Z-0306-90-PUB-KURZFASSUNG] N91-10136

**FIELD ALIGNED CURRENTS**

Problems of cold plasma measurements on the Regatta-A spacecraft N91-10431

**FIELD THEORY (ALGEBRA)**

An introduction to ultrafunctions
[MEMO-841] N91-10672

**FIELD THEORY (PHYSICS)**

Operator formalism of multi-pole Virasoro algebra on Riemann sphere
[DE90-627217] N91-10657

Research in elementary particle physics
[DE90-017278] N91-10708

Discretized light-cone quantization: Application to quantum electrodynamics
[DE90-014832] N91-10790

**FILAMENT WINDING**

Filament wound metal lined propellant tanks for future Earth-to-orbit transports
[NASA-TM-100594] N91-10106

Evaluation of nondestructive evaluation techniques for determination of flawed conditions and the effects of flaws on the burst pressure in Kevlar-epoxy filament-wound spherical test specimens
[DE90-014839] N91-10330

**FILM THICKNESS**

Deposition controlled uniformity of multilayer mirrors
[DE90-015906] N91-10718

**FINE STRUCTURE**

XAFS studies of interactions at transition-metal/Al interfaces
[DE90-016313] N91-10159

Multiple-ion waves behind shocks N91-10429

Structures observed on the spot radiance fields during the FIRE experiment N91-10503

XAFS analysis in the anharmonic limit: Application to HI-Tc superconductors and ferrosilicates
[DE90-016720] N91-10776

**FINITE DIFFERENCE THEORY**

Three-dimensional full-wave analysis of signal communications in active integrated circuits using a variable-mesh TLM method N91-10212

Simulation of time-dependent compressible viscous flows using central and upwind-biased finite difference techniques N91-10234

AFDM: An Advanced Fluid-Dynamics Model. Volume 4: The AFDM heat- and mass-transfer solution algorithm
[DE90-017535] N91-10240

AFDM: An Advanced Fluid-Dynamics Model
[DE90-017536] N91-10241

Numerical solutions of rotating disc flows using a non-linear multigrid algorithm
[PNR-90679] N91-10259

Some defects in finite-difference edge finders
[OUEL-1826/90] N91-10645

Multiple widths yield reliable finite differences
[OUEL-1827/90] N91-10646

A computational model for z-pinch plasma channels N91-10730

**FINITE ELEMENT METHOD**

Effect of surface deposits on electromagnetic waves propagating in uniform ducts
[NASA-TM-103282] N91-10208

A simple screw thread model for use in finite element stress analysis
[AD-A210233] N91-10300

Static and dynamic finite element stress analysis of layered composite plates and shells N91-10326

Finite element analysis of nonlinear creeping flows
[DE90-627189] N91-10327

Comparison of NASTRAN analysis with ground vibration results of UH-60A NASA/AEFA test configuration
[NASA-CR-184565] N91-10333

Some recent applications of numerical methods to geotechnical analysis
[PB90-201229] N91-10655

**FINITE VOLUME METHOD**

Transonic flow analysis for rotors. Part 3: Three-dimensional, quasi-steady, Euler calculation
[NASA-TP-2375] N91-10007

**FIRE CONTROL**

Railgun restrike control
[DE90-015108] N91-10095

**FIRE EXTINGUISHERS**

Tests of the general fire suppression concentrate Pyrocap B-136
[DOT/FAA/CT-TN90/21] N91-10029

**FIRES**

Transient characteristics of unconfined fire plume-driven ceiling jets
[PB90-227976] N91-10193

**FLAME TEMPERATURE**

Transient characteristics of unconfined fire plume-driven ceiling jets
[PB90-227976] N91-10193

**FLAMMABILITY**

Physical and chemical test results of electrostatic safe flooring materials
[NASA-TM-103501] N91-10194

**FLARED BODIES**

Prediction and comparison with measurements of the aerodynamic characteristics of flare-stabilized XM910 prototypes
[AD-A208099] N91-10005

**FLASHOVER**

Plasma puff initiation of high Coulomb transfer switches
[NASA-CR-187024] N91-10735

**FLAT PLATES**

Static and dynamic finite element stress analysis of layered composite plates and shells N91-10326

Mobility power flow analysis of an L-shaped plate structure subjected to distributed loading
[NASA-CR-187353] N91-10334

**FLAT SURFACES**

Boundary-layer receptivity due to a wall suction and control of Tollmien-Schlichting waves
[NASA-CR-182103] N91-10009

**FLEXIBILITY**

Evaluation of candidate alloys for the construction of metal flex hoses in the STS launch environment
[NASA-TM-103808] N91-10157

**FLIGHT CHARACTERISTICS**

Application of flight path reconstruction algorithms for flight data of helicopter
[NAL-TM-582] N91-10031

Flight characteristics of a modified Schweizer SGS1-36 sailplane at low and very high angles of attack
[NASA-TP-3022] N91-10079

**FLIGHT CONTROL**

The actuator for the low-noise STOL test plane flight control system and its development test
[NAL-TM-574] N91-10038

Static and dynamic aeroelastic characterization of an aerodynamically heated generic hypersonic aircraft configuration N91-10320

**FLIGHT CREWS**

Diagnostic possibilities of inflight EKG monitoring of flight crew N91-10557

**FLIGHT INSTRUMENTS**

NASA transport systems research vehicle B-737 data link system and display formats
[NASA-TM-102717] N91-10058

**FLIGHT MANAGEMENT SYSTEMS**

Differential Global Positioning System (DGPS) test plan
[DOT/FAA/CT-TN90/15] N91-10034

**FLIGHT OPERATIONS**

National airspace system: In-flight assistance operational concept
[PB90-233115] N91-10032

National Space Transportation System Reference. Volume 2: Operations
[NASA-TM-89785] N91-10100

**FLIGHT OPTIMIZATION**

Practical flight paths for microwave-powered airplanes
[NAL-TR-1052T] N91-10054

**FLIGHT PATHS**

The establishment and performance test of PAPI (Precision Approach Path Indicator) System for NAL STOL aircraft
[NAL-TM-579] N91-10030

Application of flight path reconstruction algorithms for flight data of helicopter
[NAL-TM-582] N91-10031

A consideration on flight paths for microwave-powered airplanes
[NAL-TR-1051] N91-10053

Practical flight paths for microwave-powered airplanes
[NAL-TR-1052T] N91-10054

A study of marine stratocumulus using lidar and other FIRE aircraft observations N91-10511

**FLIGHT SIMULATION**
Configuration, function and performance of the flight simulation test facility and its motion simulation system
[NAL-TM-575] N91-10080
Function and performance of visual simulation unit of flight simulation test facility
[NAL-TM-581] N91-10082

**FLIGHT SIMULATORS**
Configuration, function and performance of the flight simulation test facility and its motion simulation system
[NAL-TM-575] N91-10080
Function and performance of visual simulation unit of flight simulation test facility
[NAL-TM-581] N91-10082

**FLIGHT TESTS**
OVRhyp, scramjet test aircraft
[NASA-CR-187009] N91-10041
Airplane systems modifications for improved cabin smoke evacuation
[DOT/FAA/CT-TN90/24] N91-10052
NASA transport systems research vehicle B-737 data link system and display formats
[NASA-TM-102717] N91-10058
Flight testing of two Allison T56 engines modified to the ARL developed low smoke configuration
[ARL-PROP-TM-449] N91-10064
Development and application of linear and nonlinear methods for interpretation of lightning strikes to in-flight aircraft
[NASA-CR-3974] N91-10548

**FLOORS**
Physical and chemical test results of electrostatic safe flooring materials
[NASA-TM-103501] N91-10194

**FLORIDA**
Geology, geohydrology, and soils of NASA, Kennedy Space Center: A review
[NASA-TM-103813] N91-10442

**FLOW CHARACTERISTICS**
Comparison between the null-collision and time counter direct-simulation Monte Carlo methods: Leading-edge flow
[NAL-TR-1016T] N91-10012
Experimental investigation on the effect of coolant injection on turbine aerodynamic characteristics. Part 2: Effects of injection from rotor casing with 30 deg slanted holes
[NAL-TM-587-PT-2] N91-10060

**FLOW CHARTS**
Representing object oriented specifications and designs with extended data flow notations N91-10617
Network, system, and status software enhancements for the autonomously managed electrical power system breadboard. Volume 2: Protocol specification
[NASA-CR-185881] N91-10619
Network, system, and status software enhancements for the autonomously managed electrical power system breadboard. Volume 4: Graphical status display
[NASA-CR-185879] N91-10621

**FLOW DIRECTION INDICATORS**
Wind tunnel test of redundant vane-type flow-direction sensing systems
[NAL-TM-590] N91-10057

**FLOW DISTRIBUTION**
Optimum hypersonic airfoil with power law shock waves
[DE90-014903] N91-10008
Turbulent flow calculations using unstructured and adaptive meshes
[NASA-CR-182102] N91-10010
Application of CFD to sonic boom near and mid flow-field prediction
[NASA-TM-102867] N91-10015
Experimental investigation on the effect of coolant injection on turbine aerodynamic characteristics. Part 2: Effects of injection from rotor casing with 30 deg slanted holes
[NAL-TM-587-PT-2] N91-10060
Determination of the pressure drag of airfoils by integration of surface pressures
[NASA-TM-102722] N91-10078
Numerical investigations in three-dimensional internal flows
[NASA-CR-186958] N91-10083
Evaluation of flow quality in newly constructed low-turbulence calibration wind-tunnel for laser velocimeters
[NAL-TR-1054] N91-10087
Two-phase flow patterns and frictional pressure gradients in a small, horizontal, rectangular channel
[DE90-014802] N91-10236
A one-equation turbulence transport model for high Reynolds number wall-bounded flows
[NASA-TM-102847] N91-10252
A laser-sheet flow visualization technique for the large wind tunnels of the National Full-Scale Aerodynamics Complex
[NASA-TM-102793] N91-10268
The 3-D laser anemometer study of compressible flow through orifice plates
[PB90-216771] N91-10273
Studying marine stratus with large eddy simulation N91-10499

**FLOW EQUATIONS**
Image motion experiments with the Oxford AGV
[OUEL-1809/90] N91-10654

**FLOW GEOMETRY**
Calculation of three-dimensional viscous/inviscid interaction in subsonic flow
[REPT-B-25] N91-10024
An investigation of secondary flows in nozzle guide vanes
[PNR-90739] N91-10262
Two-dimensional magnetohydrodynamic equilibria with flow and studies of equilibrium fluctuations N91-10727

**FLOW MEASUREMENT**
Measurements of coefficients of discharge for concentric flange-tapped square-edged orifice meters in natural gas over the Reynolds number range 25,000 to 16,000,000
[PB90-219601] N91-10231
Coriolis-effect in mass flow metering
[LSTM-266/T/89] N91-10258
Detailed heat transfer measurements in nozzle guide vane passages in linear and annular cascades in the presence of secondary flows
[PNR-90706] N91-10260
Flow measurements in turbomachinery using laser anemometry and holography
[PNR-90717] N91-10261
Experimental measurement of structural power flow on an aircraft fuselage
[NASA-CR-187352] N91-10335
Turbulence measurements using tethered balloon instrumentation during FIRE 1987 N91-10518

**FLOW STABILITY**
Two-dimensional magnetohydrodynamic equilibria with flow and studies of equilibrium fluctuations N91-10727

**FLOW VELOCITY**
Performance characterization of a segmented anode arcjet thruster
[NASA-TM-103227] N91-10118
Transient characteristics of unconfined fire plume-driven ceiling jets
[PB90-227976] N91-10193
Measurements of coefficients of discharge for concentric flange-tapped square-edged orifice meters in natural gas over the Reynolds number range 25,000 to 16,000,000
[PB90-219601] N91-10231
Coriolis-effect in mass flow metering
[LSTM-266/T/89] N91-10258
Thin film thermometers and flowmeters for applications in liquid helium N91-10265

**FLOW VISUALIZATION**
Detailed heat transfer measurements in nozzle guide vane passages in linear and annular cascades in the presence of secondary flows
[PNR-90706] N91-10260
A laser-sheet flow visualization technique for the large wind tunnels of the National Full-Scale Aerodynamics Complex
[NASA-TM-102793] N91-10268

**FLOWMETERS**
Measurements of coefficients of discharge for concentric flange-tapped square-edged orifice meters in natural gas over the Reynolds number range 25,000 to 16,000,000
[PB90-219601] N91-10231
Thin film thermometers and flowmeters for applications in liquid helium N91-10265

**FLUID DYNAMICS**
AFDM: An Advanced Fluid-Dynamics Model
[DE90-017537] N91-10242

**FLUID FLOW**
AFDM: An Advanced Fluid-Dynamics Model. Volume 4: The AFDM heat- and mass-transfer solution algorithm
[DE90-017535] N91-10240
AFDM: An Advanced Fluid-Dynamics Model
[DE90-017536] N91-10241
AFDM: An Advanced Fluid-Dynamics Model
[DE90-017537] N91-10242
AFDM: An Advanced Fluid-Dynamics Model
[DE90-017538] N91-10243
AFDM: An Advanced Fluid-Dynamics Model
[DE90-017539] N91-10244
Dynamics of gas bubbles moving through liquid
[ETN-90-97760] N91-10255
Numerical solutions of rotating disc flows using a non-linear multigrid algorithm
[PNR-90679] N91-10259

**FLUID MECHANICS**
Design considerations for a ceramic fabric radiator
[DE90-016342] N91-10173
AFDM: An Advanced Fluid-Dynamics Model
[DE90-017539] N91-10244
Proceedings of the 8th Symposium on Energy Engineering Sciences: Micro/Macro Studies of Multiphase Media
[DE90-014844] N91-10385

**FLUIDS**
Thermophysical properties of fluids and fluid mixtures
[DE90-016306] N91-10792

**FLUORINE**
Prevention of breakdown behind railgun projectiles
[DE90-014573] N91-10094

**FLUOROHYDROCARBONS**
Evaluation of available perfluorobutane data for selected physical properties
[DE90-016516] N91-10145

**FLUOROPOLYMERS**
Trifluoromethyl-substituted polymers
[NASA-CR-186955] N91-10170

**FLUTTER**
Static and dynamic aeroelastic characterization of an aerodynamically heated generic hypersonic aircraft configuration N91-10320

**FLUTTER ANALYSIS**
Design of control laws for flutter suppression based on the aerodynamic energy concept and comparisons with other design methods
[NASA-TP-3056] N91-10328

**FLUX (RATE)**
Anomalous viscosity due to drift wave turbulence
[NIFS-33] N91-10752

**FLUX DENSITY**
Prototype instrumentation and design studies — electrostatic analyzer system for the Space Shuttle
[AD-A211566] N91-10264

**FLUX TRANSFER EVENTS**
Plasma waves as a signature of flux transfer events N91-10427

**FLUX VECTOR SPLITTING**
Multigrid solution for the Euler equations in axisymmetric flow
[REPT-B-17] N91-10253
Computation of boundary layer flow using thin-layer Navier-Stokes equations with flux-vector splitting
[REPT-B-21] N91-10254

**FOKKER-PLANCK EQUATION**
Convergence of Langevin simulation for complex Gaussian integrals
[DE90-017402] N91-10665

**FORBUSH DECREASES**
On the autoregression methods applied to the hourly nucleonic-component records
[IFSI-89-19] N91-10837

**FORCED VIBRATION**
Piezoelectrically forced vibrations of electroded doubly rotated quartz plates by state space method N91-10318

**FORECASTING**
Atmospheric ozone 1985: Assessment of our understanding of the processes controlling its present distribution and change, volume 3
[NASA-TM-103462] N91-10393

**FOREST MANAGEMENT**
Short-rotation woody crop opportunities to mitigate carbon dioxide buildup
[DE90-016526] N91-10406

**FORESTS**
Potential effects of global climate change on the United States. Appendix D: Forests
[PB90-173238] N91-10398

**FORMALISM**
Test case derivation from LOTOS specifications
[MEMO-INF-90-21] N91-10643
Localizability in the Hamiltonian formalism and in quantum-mechanics
[DE90-628368] N91-10787

**FORMING TECHNIQUES**
Activities report of the Permanent Committee of the General Council
[ISSN-0524-7705] N91-10198

**FORTRAN**
Evolving impact of Ada on a production software environment N91-10607

**FORWARD SCATTERING**
Subvisual Cirrus cloud properties derived from a FIRE IFO case study N91-10464

**FOSSIL FUELS**
Research on climate change
[DE90-016726] N91-10408

Global tropospheric chemistry modeling [DE90-015908] N91-10409

**FOURIER ANALYSIS**

Analysis techniques for residual acceleration data [NASA-TM-103507] N91-10191

Spectral methods for time dependent problems [NASA-CR-187443] N91-10664

**FOURIER SERIES**

Computation of maximum gust loads in nonlinear aircraft using a new method based on the matched filter approach and numerical optimization N91-10317

**FOURIER TRANSFORMATION**

Structural integrity assessment of concrete slabs by nondestructive examination and Fourier transform-infrared methods [DE90-017233] N91-10296

On q-analogues of the Fourier and Hankel transforms [REPT-89-89] N91-10666

Time-resolved FTIR (Fourier Transform Infrared) emission studies of laser photofragmentation and chain reactions [DE90-017223] N91-10722

Estimation of astronomical images from the bispectrum of atmospherically distorted infrared data N91-10806

**FRACTURE MECHANICS**

High-strain-rate compression and fracture of B4C-aluminum cermets [DE90-016568] N91-10176

**FRACTURE STRENGTH**

Study of the mechanisms of damage and failure of fiber and ceramic matrix composites [ISAL-90-0026] N91-10135

Mechanical properties and fracture toughness of 8090-T651 plate and 2091 and 8090 sheet [NRL-MP-88049-4] N91-10151

Strength and toughness of single-phase and dual-phase high-temperature intermetallics [DE90-017192] N91-10166

Environmental degradation of macro defect free cements. 1: Mechanical properties investigation [AERE-R-13354-1] N91-10169

YBa2Cu3O(x) composites with improved toughness and strength [DE90-011180] N91-10782

**FRACTURING**

Micro-mechanical analysis of damage growth and fracture in discontinuous fiber reinforced metal matrix composites [NASA-CR-187020] N91-10126

Brittle fracture and ductility improvement in nickel and iron aluminides [DE90-017319] N91-10167

Calculation of Weibull strength parameters, Batdorf flaw density constants and related statistical quantities using PC-CARES [NASA-TM-103247] N91-10332

**FRAGMENTATION**

The influence of shock pre-strain and peak pressure on spall behavior of 4340 steel [DE90-016612] N91-10164

Pre-equilibrium emission and multifragmentation in heavy ion collisions [LUIP-8902] N91-10705

**FRAMES**

Structural tests of aircraft window assembly equipped with smoke evacuation valve [DOT/FAA/CT-TN89/44] N91-10051

**FREE ELECTRON LASERS**

Cumulative beam breakup of the ground-based-free-electron laser [DE90-016485] N91-10279

INEX modeling of the Boeing ring optical resonator free-electron laser [DE90-016488] N91-10280

Prediction and control of chaotic processes using nonlinear adaptive networks [DE90-016505] N91-10697

**FREE FLOW**

User's guide to CUNIFLOW [AD-A207606] N91-10004

Boundary-layer receptivity due to a wall suction and control of Tollmien-Schlichting waves [NASA-CR-182103] N91-10009

**FREE JETS**

Measurement of air entrainment by a free jet using laser velocimetry and Raman scattering [ISL-R-109/89] N91-10017

**FREE MOLECULAR FLOW**

Computational methods for the Boltzmann equation [BR-43] N91-10256

**FREEZING**

AFDM: An Advanced Fluid-Dynamics Model. Volume 4: The AFDM heat- and mass-transfer solution algorithm [DE90-017535] N91-10240

**FREQUENCY ASSIGNMENT**

Hydrologic and meteorological operations in the 162-174 and 406.1-420 MHz bands [PB90-207820] N91-10199

**FREQUENCY CONTROL**

Hydrologic and meteorological operations in the 162-174 and 406.1-420 MHz bands [PB90-207820] N91-10199

**FREQUENCY RANGES**

Bounded-error data, and frequency response design [OUEL-1766/89] N91-10683

**FREQUENCY STABILITY**

Hydrogen maser: Results of evaluations done by the CNES from May 1986 to December 1987 [CNES-DRT/TIT/TF-88/338-T] N91-10284

**FREQUENCY STANDARDS**

Frequency standard unit N91-10349

Do we really need 57 ways of rating aircraft noise [PNR-90720] N91-10704

**FRICTION FACTOR**

Two-phase flow patterns and frictional pressure gradients in a small, horizontal, rectangular channel [DE90-014802] N91-10236

**FUEL CELLS**

Methane conversion by solid electrolyte membranes [PB90-226341] N91-10381

Basic study of solid oxide fuel cells [DE90-517069] N91-10386

**FUEL COMBUSTION**

Determination of ideal-gas enthalpies of formation for key compounds: The 1988 project results [DE90-000247] N91-10791

**FUEL CONSUMPTION**

Energy efficiency improvement potential of commercial aircraft to 2010 [DE90-014767] N91-10046

**FUEL PRODUCTION**

Short-rotation woody crop opportunities to mitigate carbon dioxide buildup [DE90-016526] N91-10406

**FUEL TESTS**

Heavy duty liquid and gaseous fuel emissions database test results from four alternative fuel configurations of the Caterpillar 3406 engine [DE90-014783] N91-10288

**FULL SCALE TESTS**

Helicopter far-field acoustic levels as a function of reduced main-rotor advancing blade-tip Mach number [NASA-TM-102684] N91-10699

**FUNCTIONS (MATHEMATICS)**

The possibility of making fast measurements of ion distribution functions N91-10438

The core and the tau-value for cooperative games with coalition structures [MEMO-848] N91-10692

**FUSELAGES**

Airplane systems modifications for improved cabin smoke evacuation [DOT/FAA/CT-TN90/24] N91-10052

Experimental measurement of structural power flow on an aircraft fuselage [NASA-CR-187352] N91-10335

**FUSION (MELTING)**

AFDM: An Advanced Fluid-Dynamics Model. Volume 4: The AFDM heat- and mass-transfer solution algorithm [DE90-017535] N91-10240

**FUZZY SYSTEMS**

The generalized modus ponens considered as a fuzzy relation [REPT-90-02] N91-10687

## G

**GALACTIC BULGE**

Bicolored photometry and spectral accommodation in X-ray region of mass impregnated stellar X-ray binaries [MPE-219] N91-10808

**GALACTIC CLUSTERS**

Large scale structures in nonzero Lambda Friedmann universes N91-10812

**GALACTIC COSMIC RAYS**

Effect of single impacts of heavy ions of galactic cosmic rays on lactuca sativa seeds exposed on Salyut-6 and Salyut-7 stations N91-10567

**GALACTIC EVOLUTION**

Large scale structures in nonzero Lambda Friedmann universes N91-10812

**GALACTIC NUCLEI**

Vigorous star formation in galactic nuclei N91-10814

**GALERKIN METHOD**

Effect of surface deposits on electromagnetic waves propagating in uniform ducts [NASA-TM-103282] N91-10208

Finite element analysis of nonlinear creeping flows [DE90-627189] N91-10327

**GALLIUM ARSENIDES**

An avalanche electron emitting diode in gallium arsenide [ETN-90-97746] N91-10225

**GAME THEORY**

The core and the tau-value for cooperative games with coalition structures [MEMO-848] N91-10692

**GAMMA RAY ASTRONOMY**

Tests and applications of Cherenkov imaging in TeV astronomy N91-10807

**GAMMA RAY SPECTROMETERS**

The GAMMASPHERE [DE90-016849] N91-10224

**GAMMA RAYS**

The GAMMASPHERE [DE90-016849] N91-10224

Effect of single impacts of heavy ions of galactic cosmic rays on lactuca sativa seeds exposed on Salyut-6 and Salyut-7 stations N91-10567

Radiation-induced noise in Charge-Coupled Device (CCD) and Charge-Injection Device (CID) imagers [DE90-016724] N91-10777

Acceleration by pulsar winds in binary systems [NASA-TM-103451] N91-10816

**GAS ANALYSIS**

Cardiovascular group N91-10587

**GAS DYNAMICS**

Dynamics of gas bubbles moving through liquid [ETN-90-97760] N91-10255

**GAS FLOW**

Measurements of coefficients of discharge for concentric flange-tapped square-edged orifice meters in natural gas over the Reynolds number range 25,000 to 16,000,000 [PB90-219601] N91-10231

Turbulent boundary layers in high enthalpy flows. Numerical code validation by shock tube experiments [ISL-CO-221/89] N91-10248

**GAS MIXTURES**

Fast sound propagation in binary fluid mixtures N91-10233

**GAS PRESSURE**

Plasma puff initiation of high Coulomb transfer switches [NASA-CR-187024] N91-10735

**GAS TURBINE ENGINES**

Heat transfer in aero engine gas turbines, part 1 [PNR-90754-PT-1] N91-10074

**GAS TURBINES**

Effects of coolant injection on turbine aerodynamic characteristics. Part 1: Test turbine and apparatus [NAL-TM-585-PT-1] N91-10059

Experimental investigation on the effect of coolant injection on turbine aerodynamic characteristics. Part 2: Effects of injection from rotor casing with 30 deg slanted holes [NAL-TM-587-PT-2] N91-10060

Gas turbines for main propulsion and auxiliary power systems [PNR-90709] N91-10069

Fabrication aspects of glass matrix composites for gas turbine applications [PNR-90752] N91-10073

Total quality management at Rolls-Royce PLC [PNR-90759] N91-10298

**GAS-LIQUID INTERACTIONS**

False-vacuum decay in generalized extended inflation [NASA-CR-186419] N91-10695

**GASEOUS FUELS**

Heavy duty liquid and gaseous fuel emissions database test results from four alternative fuel configurations of the Caterpillar 3406 engine [DE90-014783] N91-10288

**GAUGE INVARIANCE**

Discretized light-cone quantization: Application to quantum electrodynamics [DE90-014832] N91-10790

**GAUGE THEORY**

Research in elementary particle physics [DE90-017278] N91-10708

**GEOGRAPHIC INFORMATION SYSTEMS**

Geographic display of circulation model data [NOAA-NESDIS-27] N91-10446

**GEOIDS**

Geoid and Doppler induced errors on the altimeter measurement and their correction [CNES-CT/DRT/TIT/RL-88/226] N91-10380

**GEOMAGNETIC TAIL**

Energetic particles in the Earth's magnetotail or: Cluster and Regatta as a dispersiometer N91-10434

Features of mid-tail ion trajectories during substorms N91-10435

**GEOMAGNETISM**
Studies of the system-environment interaction by electron beam emission from a sounding rocket payload in the ionosphere N91-10410
Solar-geophysical data number 548, April 1990. Part 1: (Prompt reports). Data for March, February 1990, and late data
[PB90-226028] N91-10411
Solar-geophysical data number 545, January 1990. Part 1 (Prompt reports). Data for December, November 1989 and late data
[PB90-182338] N91-10822
Solar-geophysical data number 546, February 1990. Part 1: (Prompt reports). Data for January 1990, December 1989, and late data
[PB90-195363] N91-10823
Solar-geophysical data number 547, March 1990. Part 1: (Prompt reports). Data for February, January 1990, and late data
[PB90-208877] N91-10825
**GEOMETRY**
Geometric ergodicity of the ALOHA-system and a coupled processors model
[TW-90-01-B] N91-10680
**GEOPHYSICS**
The scientific case for magnetic field satellites
[NASA-CR-186532] N91-10101
Solar-geophysical data number 548, April 1990. Part 1: (Prompt reports). Data for March, February 1990, and late data
[PB90-226028] N91-10411
Solar-geophysical data number 548, April 1990. Part 2: (Comprehensive reports). Data for October 1989 and miscellaneous
[PB90-226036] N91-10412
Geophysical monitoring for climatic change
[PB90-222126] N91-10538
Solar-geophysical data number 546, February 1990. Part 1: (Prompt reports). Data for January 1990, December 1989, and late data
[PB90-195363] N91-10823
Solar-geophysical data number 546, February 1990. Part 2: (Comprehensive reports). Data for August 1989 and miscellaneous
[PB90-195371] N91-10824
Solar-geophysical data number 547, March 1990. Part 1: (Prompt reports). Data for February, January 1990, and late data
[PB90-208877] N91-10825
Solar-geophysical data number 547, March 1990. Part 2: (Comprehensive reports). Data for September 1989 and miscellaneous
[PB90-208885] N91-10826
**GEOTECHNICAL ENGINEERING**
Geotechnical Engineering, 1989
[PB90-222159] N91-10415
Some recent applications of numerical methods to geotechnical analysis
[PB90-201229] N91-10655
**GEOTHERMAL RESOURCES**
Survey of possibility for volcanic energy development
[DE90-517230] N91-10387
**GEOTHERMAL TECHNOLOGY**
Survey of possibility for volcanic energy development
[DE90-517230] N91-10387
**GERMANIUM ALLOYS**
Properties of reactively-deposited SiC and GeC alloys
[DE90-016363] N91-10766
**GETTERS**
Hydrogen-tritium getters and their applications
[DE90-016282] N91-10184
Organic getter materials for the removal of hydrogen and its isotopes
[DE90-016284] N91-10185
**GLASS FIBER REINFORCED PLASTICS**
Fabrication aspects of glass matrix composites for gas turbine applications
[PNR-90752] N91-10073
Evaluation of composite materials for use on launch complexes
[NASA-TM-103809] N91-10131
**GLASSY CARBON**
Characterization of mono- and multi-molecular assemblies at glassy carbon and noble metals by ex situ and in situ infrared external reflection spectroscopy
[DE90-016417] N91-10144
**GLIDERS**
Flight characteristics of a modified Schweizer SGS1-36 sailplane at low and very high angles of attack
[NASA-TP-3022] N91-10079
**GLOBAL POSITIONING SYSTEM**
Differential Global Positioning System (DGPS) test plan
[DOT/FAA/CT-TN90/15] N91-10034
**GLOBAL WARMING**
Potential effects of global climate change on the United States. Appendix C: Agriculture, volume 1
[PB90-171588] N91-10394
Potential effects of global climate change on the United States. Appendix A: Water resources
[PB90-171968] N91-10395
Potential effects of global climate change on the United States. Appendix B: Sea level rise
[PB90-172628] N91-10396
Potential effects of global climate change on the United States. Appendix C: Agriculture, volume 2
[PB90-171596] N91-10397
Potential effects of global climate change on the United States. Appendix D: Forests
[PB90-173238] N91-10398
Potential effects of global climate change on the United States. Appendix E: Aquatic resources
[PB90-172297] N91-10399
Potential effects of global climate change on the United States. Appendix F: Air quality
[PB90-172230] N91-10400
Potential effects of global climate change on the United States. Appendix G: Health
[PB90-173881] N91-10401
Potential effects of global climate change on the United States. Appendix H: Infrastructure
[PB90-172313] N91-10402
Potential effects of global climate change on the United States. Appendix I: Variability
[PB90-173899] N91-10403
Potential effects of global climate change on the United States. Appendix J: Policy
[PB90-173188] N91-10404
**GOERTLER INSTABILITY**
The inviscid secondary instability of fully nonlinear longitudinal vortex structures in growing boundary layers
[NASA-CR-187455] N91-10021
Vortex instabilities in 3D boundary layers: The relationship between Goertler and crossflow vortices
[NASA-CR-187456] N91-10022
**GOVERNMENT/INDUSTRY RELATIONS**
Industry liaison section implementation plan
[NASA-CR-177569] N91-10048
Putting technology to work, 1990. Examples of industry-laboratory cooperation contributing to our nation's economic strength
[PB90-215187] N91-10805
**GRADIENTS**
Spectra and gradients of stormy winds at Cabauw, Netherlands, up to 200 meters high
[KNMI-TR-119] N91-10546
**GRAIN BOUNDARIES**
Mechanisms of high temperature crack growth in metals and alloys
[DE90-014934] N91-10152
XAFS studies of interactions at transition-metal/Al interfaces
[DE90-016313] N91-10159
**GRAIN SIZE**
Beryllium weldability
[DE90-014696] N91-10155
**GRAND UNIFIED THEORY**
Parameterization of cosmological scale factor during inflationary times N91-10815
**GRANTS**
Activities of the Board on Mathematical Sciences
[DE90-015118] N91-10598
**GRAPHITE**
Eddy current inspection of graphite fiber components
[NASA-TM-103514] N91-10294
Repeated buckling of composite shear panels
N91-10303
**GRAPHITE-EPOXY COMPOSITES**
Intercalated graphite fiber composites as EMI shields in aerospace structures
[NASA-TM-103632] N91-10134
Physical interpretation and application of principles of ultrasonic nondestructive evaluation of high-performance materials
[NASA-CR-180489] N91-10293
Repeated buckling of composite shear panels
N91-10303
**GRAPHS (CHARTS)**
Long cycles, degree sums, and neighborhood unions
[MEMO-851] N91-10676
Generating all 3-connected 4-regular planar graphs from the octahedron graph
[MEMO-854] N91-10678
Solar-geophysical data number 545, January 1990. Part 1 (Prompt reports). Data for December, November 1989 and late data
[PB90-182338] N91-10822
**GRATINGS (SPECTRA)**
Holographic rugate structures for x ray optics applications
[DE90-017103] N91-10270
**GRAVITATION**
The scientific case for magnetic field satellites
[NASA-CR-186532] N91-10101
Biomedical perspectives on locomotion in null gravity
N91-10583
Discrete gravity
[DE90-014808] N91-10789
**GRAVITATIONAL PHYSIOLOGY**
Morphological examination of rat adrenal glands following flight aboard Biosputnik Kosmos-1667
N91-10553
Central and regional hemodynamics in prolonged space flights N91-10554
**GRAVITATIONAL WAVE ANTENNAS**
Fast estimation of the variance of a narrowband process
[IFSI-90-16] N91-10209
**GRAVITY WAVES**
Model of gravity-wave-induced variability and turbulence in the stratified free atmosphere
[PB90-235482] N91-10413
The numerical simulation of nonlinear gravity waves in three dimensions using a higher order panel method
[ISBN-90-9002667-23] N91-10443
**GREEN'S FUNCTIONS**
Path integral asymptotics in the absence of classical paths
[DE90-016213] N91-10659
**GREENHOUSE EFFECT**
Atmospheric ozone 1985: Assessment of our understanding of the processes controlling its present distribution and change, volume 3
[NASA-TM-103462] N91-10393
Potential effects of global climate change on the United States. Appendix C: Agriculture, volume 1
[PB90-171588] N91-10394
Potential effects of global climate change on the United States. Appendix A: Water resources
[PB90-171968] N91-10395
Potential effects of global climate change on the United States. Appendix B: Sea level rise
[PB90-172628] N91-10396
Potential effects of global climate change on the United States. Appendix C: Agriculture, volume 2
[PB90-171596] N91-10397
Potential effects of global climate change on the United States. Appendix D: Forests
[PB90-173238] N91-10398
Potential effects of global climate change on the United States. Appendix E: Aquatic resources
[PB90-172297] N91-10399
Potential effects of global climate change on the United States. Appendix F: Air quality
[PB90-172230] N91-10400
Potential effects of global climate change on the United States. Appendix G: Health
[PB90-173881] N91-10401
Potential effects of global climate change on the United States. Appendix H: Infrastructure
[PB90-172313] N91-10402
Potential effects of global climate change on the United States. Appendix I: Variability
[PB90-173899] N91-10403
Potential effects of global climate change on the United States. Appendix J: Policy
[PB90-173188] N91-10404
Global and regional environmental atmospheric chemistry
[DE90-016693] N91-10407
Global tropospheric chemistry modeling
[DE90-015908] N91-10409
**GRID GENERATION (MATHEMATICS)**
Turbulent flow calculations using unstructured and adaptive meshes
[NASA-CR-182102] N91-10010
Aeroelastic analysis of wings using the Euler equations with a deforming mesh
[NASA-TM-102733] N91-10020
The numerical simulation of nonlinear gravity waves in three dimensions using a higher order panel method
[ISBN-90-9002667-23] N91-10443
Users manual for AUTOMESH-2D: A program of automatic mesh generation for two-dimensional scattering analysis by the finite element method
[NASA-CR-186929] N91-10623
**GROUND STATIONS**
Educator's guide for building and operating environmental satellite receiving stations
[NOAA-TR-NESDIS-44] N91-10093
Meteorological Satellite Center Technical Note. Special Issue (1989). Summary of GMS System. 1: Telecommunication System N91-10338

Station control and monitor subsystem N91-10341

Stretched VISSR subsystem N91-10343

Image monitor N91-10344

System console N91-10351

**GROUND SUPPORT SYSTEMS**

National Space Transportation System Reference. Volume 2: Operations
[NASA-TM-89785] N91-10100

**GROUND TESTS**

Airplane systems modifications for improved cabin smoke evacuation
[DOT/FAA/CT-TN90/24] N91-10052

The full-body ground vibration tests using the low-noise STOL test plane
[NAL-TM-576] N91-10077

Ground test program for new Atlas payload fairings
N91-10315

Comparison of NASTRAN analysis with ground vibration results of UH-60A NASA/AEFA test configuration
[NASA-CR-184565] N91-10333

**GROUND TRUTH**

Cloud altitude determination from infrared spectral radiances N91-10474

**GROUP THEORY**

On the rotation interpolation and animation problems in computer graphics
[REPT-90-08] N91-10637

**GUIDANCE (MOTION)**

Real-time safety analysis for autonomous guided vehicles
[OUEL-1833/90] N91-10037

Fast steering of the angle of attack: A contribution to the guidance of high velocity projectiles
[ISL-CO-220/89] N91-10050

**GUIDANCE SENSORS**

Protective autonomy: Embedding sensor-based safety and protection mechanisms into the motion control of mobile and tele-operated robots
[OUEL-1808/90] N91-10292

**GUIDE VANES**

An investigation of secondary flows in nozzle guide vanes
[PNR-90739] N91-10262

**GUN PROPELLANTS**

Very high burn rate propellants
[DE90-016865] N91-10186

**GUST LOADS**

Computation of maximum gust loads in nonlinear aircraft using a new method based on the matched filter approach and numerical optimization N91-10317

## H

**H I REGIONS**

Investigation of Markarian galaxies with multiple nuclei
N91-10813

**H II REGIONS**

Investigation of Markarian galaxies with multiple nuclei
N91-10813

**HABITS**

Psychophysiological assessment of piloting motor habits in pilot retraining N91-10564

**HADRONS**

Research in elementary particle physics
[DE90-017278] N91-10708

**HALIDES**

Prevention of breakdown behind railgun projectiles
[DE90-014573] N91-10094

**HAMILTONIAN FUNCTIONS**

Lobe area in adiabatic Hamiltonian systems
[DE90-016566] N91-10663

Order and chaos in polarized nonlinear optics
[DE90-016717] N91-10721

Localizability in the Hamiltonian formalism and in quantum-mechanics
[DE90-628368] N91-10787

**HANDBOOKS**

The 1990 Reference Handbook: Earth Observing System
[NASA-TM-102910] N91-10378

**HANKEL FUNCTIONS**

On q-analogues of the Fourier and Hankel transforms
[REPT-89-89] N91-10666

**HARDNESS**

Strength and toughness of single-phase and dual-phase high-temperature intermetallics
[DE90-017192] N91-10166

**HARMONIC GENERATIONS**

Anomalous dispersion as a phase-matching technique for second harmonic generation
[DE90-015696] N91-10172

**HARMONIC OSCILLATION**

Properties of acoustic energy quantities
[DE90-518714] N91-10701

**HARMONIC OSCILLATORS**

XAFS analysis in the anharmonic limit: Application to HI-Tc superconductors and ferrosilicates
[DE90-016720] N91-10776

**HARRIER AIRCRAFT**

Progress in certifying F402-RR-408: The improved Pegasus engine for AV-8B and Harrier 2 plus
[PNR-90719] N91-10056

**HASTELLOY (TRADEMARK)**

Evaluation of candidate alloys for the construction of metal flex hoses in the STS launch environment
[NASA-TM-103808] N91-10157

**HAWAII**

Rn222, Rn222 progeny and Rn220 progeny as atmospheric tracers of air masses at the Mauno Loa Observatory
[DE90-014872] N91-10539

**HEALTH**

Potential effects of global climate change on the United States. Appendix G: Health
[PB90-173881] N91-10401

Work, exercise, and space flight. 1: Operations, environment, and effects of spaceflight N91-10578

**HEALTH PHYSICS**

Potential effects of global climate change on the United States. Appendix G: Health
[PB90-173881] N91-10401

**HEAT BUDGET**

Energetics of valley and basin atmospheres during the evening transition and nighttime periods
[DE90-016356] N91-10542

**HEAT EXCHANGERS**

Design methodology needs for fiber-reinforced ceramic heat exchangers
[DE90-016659] N91-10178

**HEAT MEASUREMENT**

A facility for calibrating calorimeter gauges at high rates of convective heat transfer
[OUEL-1825/90] N91-10272

**HEAT OF FORMATION**

Determination of ideal-gas enthalpies of formation for key compounds: The 1988 project results
[DE90-000247] N91-10791

**HEAT RADIATORS**

Advanced ceramic fabric body mounted radiator for Space Station Freedom Phase O design
[DE90-016361] N91-10104

Design considerations for a ceramic fabric radiator
[DE90-016342] N91-10173

**HEAT RESISTANT ALLOYS**

High temperature cyclic oxidation data. Part 1: Turbine alloys
[NASA-TM-83665] N91-10149

High-temperature cyclic oxidation data. Part 2: Turbine alloys
[NASA-TM-101468] N91-10150

Mechanisms of high temperature crack growth in metals and alloys
[DE90-014934] N91-10152

**HEAT STORAGE**

Thermal energy storage for power generation applications
[DE90-016539] N91-10388

**HEAT TRANSFER**

Numerical simulation of hypersonic flow around a space plane. Part 3: Analysis of aerothermodynamic heating
[NAL-TR-1027T] N91-10011

Heat transfer in aero engine gas turbines, part 1
[PNR-90754-PT-1] N91-10074

Design considerations for a ceramic fabric radiator
[DE90-016342] N91-10173

Hot gas side heat transfer characteristics of LOX/H2 and LOX/HC type propellants
[NAL-TR-1062T] N91-10190

Two-phase flow patterns and frictional pressure gradients in a small, horizontal, rectangular channel
[DE90-014802] N91-10236

AFDM: An Advanced Fluid-Dynamics Model. Volume 1: Scope, approach, and summary
[DE90-016723] N91-10239

Detailed heat transfer measurements in nozzle guide vane passages in linear and annular cascades in the presence of secondary flows
[PNR-90706] N91-10260

Thermal energy storage for power generation applications
[DE90-016539] N91-10388

**HEAT TRANSFER COEFFICIENTS**

Detailed heat transfer measurements in nozzle guide vane passages in linear and annular cascades in the presence of secondary flows
[PNR-90706] N91-10260

**HEAT TRANSMISSION**

PROTHE: A software as a help for the studies in industrial thermal engineering
[ETN-90-97582] N91-10634

**HEATING**

Numerical simulation of hypersonic flow around a space plane. Part 3: Analysis of aerothermodynamic heating
[NAL-TR-1027T] N91-10011

Markov model of the propagation of a light wave in a heated turbulent media
[ECL-90-06] N91-10723

Coronal heating by nanoflares: Plasma dynamics of elementary events
[DE90-016495] N91-10830

**HEAVY IONS**

Effect of single impacts of heavy ions of galactic cosmic rays on lactuca sativa seeds exposed on Salyut-6 and Salyut-7 stations N91-10567

Pre-equilibrium emission and multifragmentation in heavy ion collisions
[LUIP-8902] N91-10705

**HEISENBERG THEORY**

About antiferromagnetic Heisenberg models
[ETN-90-97768] N91-10784

**HELICAL WINDINGS**

Theory of longitudinal adiabatic invariant in the helical torus
[NIFS-37] N91-10749

**HELICOPTER CONTROL**

Rotor loads computation using singularity methods and application to the noise prediction
[ISL-PU-301/90] N91-10018

**HELICOPTER DESIGN**

Helicopter transmissions: Design for safety and reliability N91-10043

MBB'S BO 108 design and development
[MBB-UD-0568-90-PUB] N91-10055

Helicopter far-field acoustic levels as a function of reduced main-rotor advancing blade-tip Mach number
[NASA-TM-102684] N91-10699

**HELICOPTER PERFORMANCE**

Rotorcraft drivetrain life safety and reliability
[AGARD-R-775] N91-10042

MBB'S BO 108 design and development
[MBB-UD-0568-90-PUB] N91-10055

**HELICOPTER PROPELLER DRIVE**

Rotorcraft drivetrain life safety and reliability
[AGARD-R-775] N91-10042

Helicopter transmissions: Design for safety and reliability N91-10043

**HELICOPTER WAKES**

Wake coupling to full potential rotor analysis code
[NASA-TM-102805] N91-10013

**HELICOPTERS**

MBB'S BO 108 design and development
[MBB-UD-0568-90-PUB] N91-10055

**HELIOSEISMOLOGY**

The development of the continuous orthonormalization and adjoint methods for solar seismology: Eigenfrequency computation and sensitivity analysis for direct and inverse problems N91-10827

**HELIOSPHERE**

Coaligned observations of solar magnetic fields at different heights: MSFC Center director's discretionary fund final report (Project No. 88-10)
[NASA-TM-103516] N91-10832

**HELIUM ISOTOPES**

Fundamental properties and mass loss in hot, near-main sequence stars N91-10821

**HEMODYNAMIC RESPONSES**

Central and regional hemodynamics in prolonged space flights N91-10554

**HERBIG-HARO OBJECTS**

UV observations of Herbig-Haro objects associated with bipolar molecular outflows: HH 7, HH 11 and HH 29
[IFSI-90-9] N91-10619

**HETEROJUNCTIONS**

Materials analysis and device optimization of CuInSe2 solar cells
[DE90-000365] N91-10384

**HEURISTIC METHODS**

Optimization of polling systems
[CWI-BS-R8932] N91-10635

Tabu-search and simulated annealing for the quadratic assignment problem
[REPT-89-028] N91-10658

**HIGH ALTITUDE**

Changes in maximum allowable supersaturation coefficient in high-altitude decompression N91-10560

**HIGH ENERGY INTERACTIONS**

Pre-equilibrium emission and multifragmentation in heavy ion collisions
[LUIP-8902] N91-10705

Research in elementary particle physics
[DE90-017278] N91-10708

Plasma wakefield excitation by charge particle beams
N91-10729

**HIGH FREQUENCIES**
Hydrologic and meteorological operations in the 162-174 and 406.1-420 MHz bands
[PB90-207820] N91-10199
**HIGH RESOLUTION**
Cloud altitude determination from infrared spectral radiances N91-10474
**HIGH SPEED PHOTOGRAPHY**
Investigation of pulsed laser target interaction processes by high-speed diagnostic techniques
[ISL-CO-234/89] N91-10283
**HIGH STRENGTH ALLOYS**
High temperature cyclic oxidation data. Part 1: Turbine alloys
[NASA-TM-83665] N91-10149
High-temperature cyclic oxidation data. Part 2: Turbine alloys
[NASA-TM-101468] N91-10150
**HIGH TEMPERATURE ENVIRONMENTS**
Heat transfer in aero engine gas turbines, part 1
[PNR-90754-PT-1] N91-10074
Corrosion-resistant coatings for high-temperature high-sulfur activity applications
[DE90-016638] N91-10177
**HIGH TEMPERATURE GASES**
Hot gas side heat transfer characteristics of LOX/H2 and LOX/HC type propellants
[NAL-TR-1062T] N91-10190
**HIGH TEMPERATURE PLASMAS**
The possibility of making fast measurements of ion distribution functions N91-10438
**HIGH TEMPERATURE SUPERCONDUCTORS**
High-temperature superconductors: Their potential for utility applications
[DE90-009704] N91-10757
Impact of high-critical-temperature superconductors on electromagnetic pump applications
[DE90-014809] N91-10759
Muon SR and high T(sub c) superconductivity
[DE90-015089] N91-10760
Computation of superconductor critical current densities and magnetization curves
[DE90-016567] N91-10773
A correlation between T(sub 3) and electronegativity difference in high-temperature superconductors
[DE90-016640] N91-10775
Determination of surface resistance and magnetic penetration depth of superconducting YBa2Cu3O(7-delta) thin films by microwave power transmission measurements
[NASA-TM-103616] N91-10780
YBa2Cu3O(x) composites with improved toughness and strength
[DE90-011180] N91-10782
In situ transmission electron microscopy and computer simulation study of the kinetics of oxygen loss in YBa2Cu3O(z)
[DE90-014506] N91-10783
About antiferromagnetic Heisenberg models
[ETN-90-97768] N91-10784
**HILBERT SPACE**
Pseudo-monotone complementarity problems in Hilbert space
[DE90-016310] N91-10660
**HISTOGRAMS**
General flow of image data processing N91-10358
VISSR histogram data N91-10368
GPCP data processing N91-10370
Cloud grid data N91-10371
Density estimation using optimally quantized histograms
[PB90-190588] N91-10686
**HISTOLOGY**
Morphological examination of rat adrenal glands following flight aboard Biosputnik Kosmos-1667
N91-10553
**HISTORIES**
The history of in-flight exercise in the US manned space program N91-10577
**HOLES (ELECTRON DEFICIENCIES)**
Copper NMR and hole depletion in the normal state of Y(1-x)Pr(x)Ba2Cu3O7
[DE90-016468] N91-10768
**HOLOGRAPHIC INTERFEROMETRY**
Holographic examination of great surface fiberbound components in industrial conditions: Resumes of final reports, April 1986 to June 1989
[MBB-Z-0306-90-PUB-KURZFASSUNG] N91-10136
Flow measurements in turbomachinery using laser anemometry and holography
[PNR-90717] N91-10261
**HOLOGRAPHY**
Flow measurements in turbomachinery using laser anemometry and holography
[PNR-90717] N91-10261
Holographic rugate structures for x ray optics applications
[DE90-017103] N91-10270
**HOMEOSTASIS**
Space medicine considerations: Skeletal and calcium homeostasis N91-10580
**HOMOGENEOUS TURBULENCE**
Bounded energy states in homogeneous turbulent shear flow: An alternative view
[NASA-CR-187439] N91-10237
**HOMOLOGY**
Cohomology for Lagrangian systems and Noetherian symmetries
[DE90-628371] N91-10788
**HOMOMORPHISMS**
An introduction to ultrafunctions
[MEMO-841] N91-10672
**HONEYCOMB CORES**
Axial compression buckling test on CFRP surface plate/aluminum honeycomb sandwiched curved surface plate
[NAL-TM-584] N91-10299
**HORIZONTAL FLIGHT**
Application of a state-space wake model to elastic blade flapping in hover N91-10006
**HOSES**
Evaluation of candidate alloys for the construction of metal flex hoses in the STS launch environment
[NASA-TM-103808] N91-10157
**HOT STARS**
Fundamental properties and mass loss in hot, near-main sequence stars N91-10821
**HOVERING**
Application of a state-space wake model to elastic blade flapping in hover N91-10006
**HUMAN FACTORS ENGINEERING**
A representation scheme for fault diagnosis of physical systems
[DE90-016362] N91-10295
Models of the human observer and controller of a dynamic system
[ETN-90-97759] N91-10597
Artificial intelligence, human factors, robotics, and computer simulation
[DE90-016866] N91-10653
Image data compression overview: Issues and partial solutions
[PB90-172008] N91-10796
**HUMAN PERFORMANCE**
The effects of outcome and process feedback
[NASA-CR-187332] N91-10595
Technique for human-error sequence identification and signification
[ISBN-90-353-10144] N91-10596
**HUMIDITY**
Cirrus cloud model parameterizations: Incorporating realistic ice particle generation N91-10453
Turbulence measurements using tethered balloon instrumentation during FIRE 1987 N91-10518
Horizontal variability of the marine boundary layer structure upwind of San Nicolas Island during FIRE, 1987 N91-10519
**HURRICANES**
Mariners Weather Log, Volume 34, Number 2, Spring 1990
[PB90-222324] N91-10537
**HYBRID PROPULSION**
Hybrid propulsion technology program: Phase 1, volume 1
[NASA-CR-183972] N91-10111
Hybrid propulsion technology program: Phase 1, volume 2
[NASA-CR-183973] N91-10112
Hybrid propulsion technology program: Phase 1. Volume 3: Thiokol Corporation Space Operations
[NASA-CR-183974] N91-10113
Hybrid propulsion technology program: Phase 1, volume 4
[NASA-CR-183975] N91-10114
**HYDRIDES**
Organometallic chemistry of bimetallic compounds
[DE90-017601] N91-10121
Electronic, structural and transport properties of (almost) rare-earth-like actinide hydrides
[DE90-016491] N91-10771
**HYDROCARBON FUELS**
Specific impulse comparison of high density hydrocarbon fuel burned with oxygen
[NAL-TR-1053] N91-10148
Modeling of hydrocarbon fueling
[DE90-014790] N91-10289
**HYDROCARBONS**
Modeling of hydrocarbon fueling
[DE90-014790] N91-10289
**HYDRODYNAMIC EQUATIONS**
Properties of large scale plasma flow during the early stage of the plasmaspheric refilling
[NASA-TM-103446] N91-10441
**HYDRODYNAMICS**
Transition state theory applying to the study of reaction processes in detonation
[DE90-016558] N91-10187
Fast sound propagation in binary fluid mixtures
N91-10233
Dynamics of gas bubbles moving through liquid
[ETN-90-97760] N91-10255
Properties of large scale plasma flow during the early stage of the plasmaspheric refilling
[NASA-TM-103446] N91-10441
**HYDROGEN**
Specific impulse comparison of high density hydrocarbon fuel burned with oxygen
[NAL-TR-1053] N91-10148
Hydrogen-tritium getters and their applications
[DE90-016282] N91-10184
Organic getter materials for the removal of hydrogen and its isotopes
[DE90-016284] N91-10185
Hot gas side heat transfer characteristics of LOX/H2 and LOX/HC type propellants
[NAL-TR-1062T] N91-10190
**HYDROGEN EMBRITTLEMENT**
Brittle fracture and ductility improvement in nickel and iron aluminides
[DE90-017319] N91-10167
**HYDROGEN ISOTOPES**
Organic getter materials for the removal of hydrogen and its isotopes
[DE90-016284] N91-10185
**HYDROGEN MASERS**
Hydrogen maser: Results of evaluations done by the CNES from May 1986 to December 1987
[CNES-DRT/TIT/TF-88/338-T] N91-10284
**HYDROGEN OXYGEN ENGINES**
Integrated hydrogen/oxygen technology applied to auxiliary propulsion systems
[NASA-CR-185289] N91-10116
**HYDROGEN RECOMBINATIONS**
Vigorous star formation in galactic nuclei N91-10814
**HYDROGENATION**
Organic getter materials for the removal of hydrogen and its isotopes
[DE90-016284] N91-10185
**HYDROGEOLOGY**
Geology, geohydrology, and soils of NASA, Kennedy Space Center: A review
[NASA-TM-103813] N91-10442
**HYDROLOGICAL CYCLE**
Analyzing long time series of hydrological data with respect to climate variability: Project description
[WCAP-3] N91-10444
**HYDROMETEOROLOGY**
Analyzing long time series of hydrological data with respect to climate variability: Project description
[WCAP-3] N91-10444
Hydrometeor development in cold clouds in FIRE
N91-10459
**HYDROTHERMAL SYSTEMS**
Survey of possibility for volcanic energy development
[DE90-517230] N91-10387
**HYGROMETERS**
NRL tethered balloon measurements at San Nicolas Island during FIRE IFO 1987 N91-10509
Turbulence measurements using tethered balloon instrumentation during FIRE 1987 N91-10518
**HYPERBOLIC DIFFERENTIAL EQUATIONS**
Spectral methods for time dependent problems
[NASA-CR-187443] N91-10664
**HYPERSONIC AIRCRAFT**
Body weight of hypersonic aircraft, part 1
[NASA-TM-101028] N91-10049
Supersonic combustion engine testbed, heat lightning
[NASA-CR-187010] N91-10061
Static and dynamic aeroelastic characterization of an aerodynamically heated generic hypersonic aircraft configuration N91-10320
**HYPERSONIC FLOW**
User's guide to CUNIFLOW
[AD-A207606] N91-10004
Optimum hypersonic airfoil with power law shock waves
[DE90-014903] N91-10008
Numerical simulation of hypersonic flow around a space plane. Part 3: Analysis of aerothermodynamic heating
[NAL-TR-1027T] N91-10011
The ISL hypersonic shock tunnel and its instrumentation
[ISL-CO-213/89] N91-10086

**HYPERSONIC VEHICLES**
Project HyBuJET
[NASA-CR-187011] N91-10040
OVRhyp, scramjet test aircraft
[NASA-CR-187009] N91-10041
**HYPERSONIC WIND TUNNELS**
Characteristics of piping interference elimination unit used in the high-speed wind tunnel test of ASUKA seven percent semi-born prototype
[NAL-TM-588] N91-10003
Modification in the main air blower unit for two meter times two meter transonic wind tunnel: Plan and configuration
[NAL-TM-580] N91-10081
The ISL hypersonic shock tunnel and its instrumentation
[ISL-CO-213/89] N91-10086
**HYPERSONICS**
Prediction and comparison with measurements of the aerodynamic characteristics of flare-stabilized XM910 prototypes
[AD-A208099] N91-10005
**HYPERVELOCITY IMPACT**
Application of Fabry-Perot velocimetry to hypervelocity impact experiments
[DE90-015612] N91-10096
**HYPERVELOCITY PROJECTILES**
Prediction and comparison with measurements of the aerodynamic characteristics of flare-stabilized XM910 prototypes
[AD-A208099] N91-10005
Fast steering of the angle of attack: A contribution to the guidance of high velocity projectiles
[ISL-CO-220/89] N91-10050
Application of Fabry-Perot velocimetry to hypervelocity impact experiments
[DE90-015612] N91-10096
**HYPOXIA**
Probabilty of decompression sickness during space suit testing N91-10559
**HYSTERESIS**
AFDM: An Advanced Fluid-Dynamics Model
[DE90-017537] N91-10242
Computation of superconductor critical current densities and magnetization curves
[DE90-016567] N91-10773

**I**

**ICE**
Cirrus cloud model parameterizations: Incorporating realistic ice particle generation N91-10453
Lidar and aircraft studies of deep Cirrus systems from the 1986 FIRE IFO N91-10460
Radiative properties of visible and subvisible Cirrus: Scattering on hexagonal ice crystals N91-10462
**ICE CLOUDS**
Cirrus cloud model parameterizations: Incorporating realistic ice particle generation N91-10453
Lidar and aircraft studies of deep Cirrus systems from the 1986 FIRE IFO N91-10460
Interpretation of satellite-measured bidirectional reflectance from Cirrus cloudy atmospheres N91-10470
**IDEAL GAS**
Determination of ideal-gas enthalpies of formation for key compounds: The 1988 project results
[DE90-000247] N91-10791
**IGNITION**
The 1987 Strategic Defense Initiative Organization (SDIO) Workshop on Laser Propulsion
[DE90-013484] N91-10274
**IMAGE CONVERTERS**
Radiation-induced noise in Charge-Coupled Device (CCD) and Charge-Injection Device (CID) imagers
[DE90-016724] N91-10777
**IMAGE ENHANCEMENT**
Digital image integration technique of multiple geoscience information system and its application
[DE90-627893] N91-10801
**IMAGE INTENSIFIERS**
MicroChannel Plate detectors (MCP)
[CNES-CT/DRT/TIT/OE-88/037-T] N91-10227
**IMAGE PROCESSING**
Function and performance of visual simulation unit of flight simulation test facility
[NAL-TM-581] N91-10082
Particle displacement tracking for PIV
[NASA-TM-103288] N91-10271
Meteorological Satellite Center Technical Note. Special Issue (1989). Summary of GMS System. 2: Data Processing N91-10356
General flow of image data processing N91-10358
FAX image processing N91-10361
Pre-processing of image data N91-10364
Geographic display of circulation model data
[NOAA-NESDIS-27] N91-10446
Image data compression overview: Issues and partial solutions
[PB90-172008] N91-10796
Digital image integration technique of multiple geoscience information system and its application
[DE90-627893] N91-10801
Estimation of astronomical images from the bispectrum of atmospherically distorted infrared data N91-10806
**IMAGERY**
Lidar and aircraft studies of deep Cirrus systems from the 1986 FIRE IFO N91-10460
**IMAGES**
Evaluation of nondestructive evaluation techniques for determination of flawed conditions and the effects of flaws on the burst pressure in Kevlar-epoxy filament-wound spherical test specimens
[DE90-014839] N91-10330
FAX image processing N91-10361
**IMAGING TECHNIQUES**
A new method for doing flat-field intensity calibrations of multiplexed ITT streak cameras
[DE90-016475] N91-10267
Particle displacement tracking for PIV
[NASA-TM-103288] N91-10271
Distortion of LDA fringe pattern by tracer perticles
[SFB-210/E/59] N91-10286
Where are cirrus clouds and why are they there
N91-10450
Image motion experiments with the Oxford AGV
[OUEL-1809/90] N91-10654
Image data compression overview: Issues and partial solutions
[PB90-172008] N91-10796
Tests and applications of Cherenkov imaging in TeV astronomy N91-10807
**IMPACT DAMAGE**
Seat dynamic performance standards for a range of sizes
[DOT/FAA/CT-TN90/23] N91-10028
**IMPEDANCE**
Electromagnetic scattering from two-dimensional thick material junctions
[NASA-CR-186976] N91-10201
PREGO: A simulation code for one-dimensional viscoelastic acoustics
[DE90-014859] N91-10700
**IMPLOSIONS**
Sodium-neon resonant photoexcitation soft x ray laser experiments on Saturn
[DE90-014946] N91-10275
**IMPULSES**
Analysis of pulsed laser-generated impulse in an advanced airbreathing thruster N91-10062
**IMPURITIES**
The growth of zinc selenide single crystals by physical vapor transport in microgravity
[NASA-CR-180428] N91-10755
**IN-FLIGHT MONITORING**
Spacecraft Health Automated Reasoning Prototype (SHARP): The fiscal year 1989 SHARP portability evaluations task for NASA Solar System Exploration Division's Voyager project
[NASA-CR-187338] N91-10204
Diagnostic possibilities of inflight EKG monitoring of flight crew N91-10557
**INDEXES (DOCUMENTATION)**
Aeronautical engineering: A continuing bibliography with indexes (supplement 256)
[NASA-SP-7037(256)] N91-10002
Aerospace medicine and biology: A continuing bibliography with indexes (supplement 341)
[NASA-SP-7011(341)] N91-10594
US Congressional serial set catalog: Numerical lists and schedule of volumes; 99th Congress: 1985-1986: Entries and indexes
[PB90-171737] N91-10797
Bibliography of Lewis Research Center technical publications announced in 1989
[NASA-TM-102542] N91-10798
NASA Thesaurus supplement: A four part cumulative supplement to the 1988 edition of the NASA Thesaurus (supplement 4)
[NASA-SP-7064-SUPPL-4] N91-10804
**INDIUM COMPOUNDS**
Materials analysis and device optimization of CuInSe2 solar cells
[DE90-000365] N91-10384
**INDUSTRIAL MANAGEMENT**
Engineering design: A powerful influence on the business success on manufacturing industry
[PNR-90763] N91-10197
**INDUSTRIAL SAFETY**
Incorporation of the operation safety in the industry and in a product development process inducting subcontractors
[ETN-90-97822] N91-10196
**INDUSTRIES**
Holographic examination of great surface fiberbound components in industrial conditions: Resumes of final reports, April 1986 to June 1989
[MBB-Z-0306-90-PUB-KURZFASSUNG] N91-10136
An evaluation of the production processes and methods associated with Carello Cell at RISTS, Telford
[ETN-90-97578] N91-10228
**INERTIAL CONFINEMENT FUSION**
Recent advances in excimer laser technology at Los Alamos
[DE90-016441] N91-10276
Temporal behaviour of self generated magnetic field and its influence on inhibition of thermal flux in ICF plasma
[DE90-627478] N91-10731
Confinement studies in the ZT-40M reversed field pinch
[DE90-016442] N91-10739
**INERTIAL FUSION (REACTOR)**
KrF laser path to high gain ICF (inertial confinement fusion) laboratory microfusion facility
[DE90-016439] N91-10282
**INFERENCE**
Parallel inference and communication process for Horn clause. First order extension by connection method
[ETN-90-97825] N91-10652
The generalized modus ponens considered as a fuzzy relation
[REPT-90-02] N91-10687
**INFLATING**
False-vacuum decay in generalized extended inflation
[NASA-CR-186419] N91-10695
Parameterization of cosmological scale factor during inflationary times N91-10815
**INFORMATION FLOW**
A practical approach to object based requirements analysis N91-10615
Representing object oriented specifications and designs with extended data flow notations N91-10617
**INFORMATION MANAGEMENT**
Earth System Monitor, Volume 1, Number 1, June 1990
[PB90-215146] N91-10799
**INFORMATION RETRIEVAL**
NASA Thesaurus supplement: A four part cumulative supplement to the 1988 edition of the NASA Thesaurus (supplement 4)
[NASA-SP-7064-SUPPL-4] N91-10804
**INFORMATION SYSTEMS**
Automated support of the modelling process: A view based on experiments with expert information engineers
[REPT-90-09] N91-10638
Earth System Monitor, Volume 1, Number 1, June 1990
[PB90-215146] N91-10799
Digital image integration technique of multiple geoscience information system and its application
[DE90-627893] N91-10801
**INFORMATION TRANSFER**
Space market model space industry input-output model
[NASA-CR-187252] N91-10795
**INFRARED ABSORPTION**
Infrared absorption in boron carbides: Dependence on isotope and carbon concentration
[DE90-017592] N91-10132
**INFRARED ASTRONOMY**
Estimation of astronomical images from the bispectrum of atmospherically distorted infrared data N91-10806
Vigorous star formation in galactic nuclei N91-10814
**INFRARED IMAGERY**
FAX image processing N91-10361
VTR loop movie N91-10367
**INFRARED RADAR**
A study of marine stratocumulus using lidar and other FIRE aircraft observations N91-10511
**INFRARED RADIATION**
Infrared absorption in boron carbides: Dependence on isotope and carbon concentration
[DE90-017592] N91-10132
Image mapping N91-10359
GPCP data processing N91-10370
Cloud amount distribution N91-10373
Cloud parameters from GOES visible and infrared radiances during the FIRE Cirrus IFO, October 1986
N91-10473
Radiative properties of Cirrus clouds: FIRE IFO case October 28, 1986 N91-10479
Sub-visual Cirrus detection and characterization
N91-10486

A cloud classification scheme applied to the breakup region of marine stratocumulus N91-10497

**INFRARED RADIOMETERS**

Command subsystem N91-10346

Calibration N91-10360

FAX image processing N91-10361

VISSR histogram data N91-10368

**INFRARED REFLECTION**

Characterization of mono- and multi-molecular assemblies at glassy carbon and noble metals by ex situ and in situ infrared external reflection spectroscopy [DE90-016417] N91-10144

**INFRARED SPECTRA**

Characterization of mono- and multi-molecular assemblies at glassy carbon and noble metals by ex situ and in situ infrared external reflection spectroscopy [DE90-016417] N91-10144

Structural integrity assessment of concrete slabs by nondestructive examination and Fourier transform-infrared methods [DE90-017233] N91-10296

Radiative properties of Cirrus clouds: FIRE IFO case October 28, 1986 N91-10479

Time-resolved FTIR (Fourier Transform Infrared) emission studies of laser photofragmentation and chain reactions [DE90-017223] N91-10722

**INFRARED SPECTROSCOPY**

Development, characterization, and applications of optical pH sensors supported at cellulosic film [DE90-016416] N91-10146

**INFRARED STARS**

UV observations of Herbig-Haro objects associated with bipolar molecular outflows: HH 7, HH 11 and HH 29 [IFSI-90-9] N91-10819

**INJECTION**

RF helicity injection and current drive [NIFS-34] N91-10750

**INJECTORS**

Pellet injector development at ORNL (Oak Ridge National Laboratory) [DE90-017024] N91-10742

**INLAND WATERS**

Potential effects of global climate change on the United States. Appendix E: Aquatic resources [PB90-172297] N91-10399

**INSPECTION**

Structural risk assessment and aircraft fleet maintenance N91-10321

Evaluation of nondestructive evaluation techniques for determination of flawed conditions and the effects of flaws on the burst pressure in Kevlar-epoxy filament-wound spherical test specimens [DE90-014839] N91-10330

**INSTRUMENT ERRORS**

Wind tunnel test of redundant vane-type flow-direction sensing systems [NAL-TM-590] N91-10057

**INTAKE SYSTEMS**

Parametric assessment of propulsion system mass for airbreathing launcher configurations [PNR-90634] N91-10063

**INTEGRAL EQUATIONS**

Convergence of Langevin simulation for complex Gaussian integrals [DE90-017402] N91-10665

**INTEGRALS**

Quadrature imposition of compatibility conditions in Chebyshev methods [NASA-CR-187458] N91-10251

Convergence of Langevin simulation for complex Gaussian integrals [DE90-017402] N91-10665

**INTEGRATED CIRCUITS**

Three-dimensional full-wave analysis of signal communications in active integrated circuits using a variable-mesh TLM method N91-10212

**INTERACTIONAL AERODYNAMICS**

Modeling blade/vortex interactions [ISL-R-107/89] N91-10016

**INTERCALATION**

Intercalated graphite fiber composites as EMI shields in aerospace structures [NASA-TM-103632] N91-10134

**INTERFACES**

Microstructural and phase stability studies of nanometer period metal/carbon multilayer structures for x ray optics [DE90-015307] N91-10129

Monomolecular and thin polymer films: Fabrication, characterization, applications, and models of wetting [DE90-016415] N91-10174

**INTERFERENCE IMMUNITY**

Characteristics of piping interference elimination unit used in the high-speed wind tunnel test of ASUKA seven percent semi-born prototype [NAL-TM-588] N91-10003

**INTERMETALLICS**

On the effects of magnetic bonding in rare earth transition metal intermetallics [DE90-015800] N91-10156

Shock experiments in metals and ceramics [DE90-016613] N91-10165

**INTERNATIONAL SUN EARTH EXPLORERS**

Multipoint study of small-scale structures at the magnetopause N91-10432

**INTERPLANETARY SPACE**

JPRS report: Science and technology. USSR: Space [JPRS-USP-90-001] N91-10089

Design considerations for a ceramic fabric radiator [DE90-016342] N91-10173

**INTERPOLATION**

Approximation and geometric modeling with simplex B-splines associated with irregular triangles [MEMO-842] N91-10673

**INTERVALS**

Confidence intervals and curvature measures in nonlinear regression using the IML and NLIN procedures in SAS(tm) software [PB90-246398] N91-10624

**INVARIANCE**

Invariant measures exist under a summability condition for unimodal maps [REPT-90-36] N91-10670

**INVENTIONS**

Massively parallel computing system [DE90-014683] N91-10648

**INVERSIONS**

Turbulence measurements using tethered balloon instrumentation during FIRE 1987 N91-10518

The development of the continuous orthonormalization and adjoint methods for solar seismology: Eigenfrequency computation and sensitivity analysis for direct and inverse problems N91-10827

**INVISCID FLOW**

User's guide to CUNIFLOW [AD-A207606] N91-10004

The inviscid secondary instability of fully nonlinear longitudinal vortex structures in growing boundary layers [NASA-CR-187455] N91-10021

Three-dimensional viscous/inviscid coupling in subsonic flow [REPT-B-24] N91-10023

Calculation of three-dimensional viscous/inviscid interaction in subsonic flow [REPT-B-25] N91-10024

**ION ACCELERATORS**

Examination of ion acceleration in the plasma layer during magnetospheric partial gales [MPE-218] N91-10753

**ION ACOUSTIC WAVES**

Multiple-ion waves behind shocks N91-10429

**ION BEAMS**

Tilt stability and compression heating studies of field-reversed configurations [DE90-016443] N91-10740

**ION CONCENTRATION**

Features of mid-tail ion trajectories during substorms N91-10435

**ION CURRENTS**

RF helicity injection and current drive [NIFS-34] N91-10750

**ION CYCLOTRON RADIATION**

RF helicity injection and current drive [NIFS-34] N91-10750

**ION DISTRIBUTION**

The possibility of making fast measurements of ion distribution functions N91-10438

**ION EXCHANGE MEMBRANE ELECTROLYTES**

Methane conversion by solid electrolyte membranes [PB90-226341] N91-10381

**ION IMPLANTATION**

Meetings on the structure and properties of implanted ceramics [DE90-017313] N91-10181

Radiation damage in Al2O3 crystals implanted with 3.8 MeV Fe(2+) [DE90-016038] N91-10761

**ION SOURCES**

Direct extraction of a Na(-) beam from a sodium plasma [NIFS-35] N91-10751

**ION TEMPERATURE**

Numerical simulation of ion temperature gradient driven modes in the presence of ion-ion collisions [DE90-017092] N91-10745

**IONIC COLLISIONS**

Numerical simulation of ion temperature gradient driven modes in the presènce of ion-ion collisions [DE90-017092] N91-10745

**IONIZATION CROSS SECTIONS**

Theoretical atomic physics for fusion [DE90-017280] N91-10710

**IONIZING RADIATION**

Effect of single impacts of heavy ions of galactic cosmic rays on lactuca sativa seeds exposed on Salyut-6 and Salyut-7 stations N91-10567

Statistical methods for analyzing and combining data on low-level exposures to ionizing radiation [DE90-017193] N91-10593

**IONOSPHERIC ION DENSITY**

Neutral winds derived from IRI parameters and from the HWM87 wind model for the sundial campaign of September, 1986 [NASA-TM-103445] N91-10543

**IONOSPHERIC SOUNDING**

Neutral winds derived from IRI parameters and from the HWM87 wind model for the sundial campaign of September, 1986 [NASA-TM-103445] N91-10543

**IONOSPHERIC STORMS**

Features of mid-tail ion trajectories during substorms N91-10435

**IRON**

Brittle fracture and ductility improvement in nickel and iron aluminides [DE90-017319] N91-10167

Fe site occupancy and superconductivity in Y(1-z)Ca(z)Ba(z) (Cu(1-x)Fe(x))3O(6+y) [DE90-016614] N91-10774

XAFS analysis in the anharmonic limit: Application to Hi-Tc superconductors and ferrosilicates [DE90-016720] N91-10776

**IRON ALLOYS**

Weldability of nickel and iron aluminides [DE90-013498] N91-10153

**IRRADIANCE**

Temperature sensitivity of Eppley broadband radiometers N91-10484

Estimating integrated cloud liquid water from extended time observations of solar irradiance N91-10510

**IRRADIATION**

Radiation-induced microstructural development and microchemical changes in Fe-Cr-Mn-Ni solute-bearing alloys [DE90-016359] N91-10160

Identification of Cirrus over Wausau during the 1986 FIRE IFO from ground-based radiometer data N91-10469

FIRE extended time/limited area observations at Palisades, New York N91-10527

ELF (extremely-low-frequency): Exposure levels, bioeffects, and epidemiology [DE90-016554] N91-10573

Statistical methods for analyzing and combining data on low-level exposures to ionizing radiation [DE90-017193] N91-10593

Measured silicon displacement damage ratios support the need to replace the ASTM E-722 damage function with the NJOY calculated function [DE90-016225] N91-10762

Radiation-induced noise in Charge-Coupled Device (CCD) and Charge-Injection Device (CID) imagers [DE90-016724] N91-10777

**ISLANDS**

San Nicolas Island surface radiation-meteorology data N91-10531

**ITERATION**

Discounted dynamic programming. Part 4: Accelerated successive approximation [TW-90-03-PT-4] N91-10641

**ITERATIVE SOLUTION**

AFDM: An Advanced Fluid-Dynamics Model. Volume 4: The AFDM heat- and mass-transfer solution algorithm [DE90-017535] N91-10240

**IUE**

UV observations of Herbig-Haro objects associated with bipolar molecular outflows: HH 7, HH 11 and HH 29 [IFSI-90-9] N91-10819

**J**

**JET ENGINE FUELS**

Tests of the general fire suppression concentrate Pyrocap B-136 [DOT/FAA/CT-TN90/21] N91-10029

Thermal stability of jet fuel [DE90-016801] N91-10188

**JET ENGINES**

The evolution of the bypass engine [PNR-90707] N91-10068

**JET FLOW**

Pressure measurements on the release system and determination of jet momentum in the project BA propane field tests 1989 [FOA-E-40044-4.5] N91-10263

**JOINTS (JUNCTIONS)**
Flight set 360L007 (STS-33R) field joint protection system, thermal protection system, and systems tunnel components, volume 7
[NASA-CR-184026] N91-10115
Evaluation of candidate alloys for the construction of metal flex hoses in the STS launch environment
[NASA-TM-103808] N91-10157

**K**

**K-EPSILON TURBULENCE MODEL**
Bounded energy states in homogeneous turbulent shear flow: An alternative view
[NASA-CR-187439] N91-10237
A one-equation turbulence transport model for high Reynolds number wall-bounded flows
[NASA-TM-102847] N91-10252
**KALMAN FILTERS**
The digital regulator and tracker for stochastic continuous-time linear time-varying systems
[REPT-90-06] N91-10689
**KELVIN-HELMHOLTZ INSTABILITY**
Non-linear evolution of the Kelvin-Helmholtz instability: Constraints on multipoint measurements N91-10430
Multipoint study of small-scale structures at the magnetopause N91-10432
**KERNEL FUNCTIONS**
Bounded-error data, and frequency response design
[OUEL-1766/89] N91-10683
**KERR MAGNETOOPTICAL EFFECT**
Ultra-thin vertical magneto-optical media and system for using same
[DE90-014589] N91-10603
**KEVLAR (TRADEMARK)**
Evaluation of nondestructive evaluation techniques for determination of flawed conditions and the effects of flaws on the burst pressure in Kevlar-epoxy filament-wound spherical test specimens
[DE90-014839] N91-10330
**KILOMETRIC WAVES**
Radio wave remote sensing by Cluster and Regatta
N91-10439
**KINEMATICS**
Probabilistic structural analysis by extremum methods
N91-10308
**KINETIC ENERGY**
Bounded energy states in homogeneous turbulent shear flow: An alternative view
[NASA-CR-187439] N91-10237
**KINETIC EQUATIONS**
Tearing modes in tokamaks with lower hybrid current drive
[DE90-017090] N91-10743
**KINETIC FRICTION**
Vibro-acoustic emission rubbing sources
[PNR-90730] N91-10336
**KINETICS**
Stellarator theory
[DE90-017607] N91-10748
**KNOWLEDGE BASES (ARTIFICIAL INTELLIGENCE)**
Knowledge-based assistance in costing the space station DMS N91-10611
**KNOWLEDGE REPRESENTATION**
A representation scheme for fault diagnosis
[DE90-016291] N91-10631
**KNUDSEN FLOW**
A Knudsen layer theory for lattice gases
[ETN-90-97583] N91-10248
**KORTEWEG-DEVRIES EQUATION**
Stability of some stationary solutions for the forced KdV equation
[DE90-016506] N91-10662
**KRYPTON FLUORIDE LASERS**
KrF laser path to high gain ICF (inertial confinement fusion) laboratory microfusion facility
[DE90-016439] N91-10282

**L**

**LABORATORIES**
Putting technology to work, 1990. Examples of industry-laboratory cooperation contributing to our nation's economic strength
[PB90-215187] N91-10805
**LAGRANGE COORDINATES**
Cohomology for Lagrangian systems and Noetherian symmetries
[DE90-628371] N91-10788
**LAMINATES**
Analysis of delamination in fiber composite laminates out-of-plane under bending
[NASA-CR-186023] N91-10122
Structural properties of laminated Douglas fir/epoxy composite material
[NASA-RP-1236] N91-10127
Microstructural and phase stability studies of nanometer period metal/carbon multilayer structures for x ray optics
[DE90-015307] N91-10129
Compressive failure of thick-section composite laminates with and without cutouts subjected to biaxial loading N91-10304
Deposition controlled uniformity of multilayer mirrors
[DE90-015906] N91-10718
**LANDSAT SATELLITES**
A preliminary analysis of LANDSAT and UK C130 data from Mission 197-A, on 16 July 1987 N91-10535
**LANGUAGE PROGRAMMING**
SILAGE to ELLA translation
[RSRE-MEMO-4385] N91-10639
**LANTHANUM COMPOUNDS**
Advanced materials for high-temperature solid electrolyte applications
[DE90-016328] N91-10143
Renormalization from density functional theory strong coupling models for the electronic structure of La2CuO4
[DE90-015990] N91-10765
**LANTHANUM OXIDES**
Calculation of the static magnetism of metamagnetic La2CuO4
[DE90-016490] N91-10770
**LARGE SPACE STRUCTURES**
Combined design of structures and controllers for optimal maneuverability N91-10314
**LASER ANEMOMETERS**
Flow measurements in turbomachinery using laser anemometry and holography
[PNR-90717] N91-10261
The 3-D laser anemometer study of compressible flow through orifice plates
[PB90-216771] N91-10273
**LASER BEAMS**
Order and chaos in polarized nonlinear optics
[DE90-016717] N91-10721
Variable-coherence beam optics
[ISBN-952-90-1784-7] N91-10724
**LASER DOPPLER VELOCIMETERS**
Measurement of air entrainment by a free jet using laser velocimetry and Raman scattering
[ISL-R-109/89] N91-10017
Evaluation of flow quality in newly constructed low-turbulence calibration wind-tunnel for laser velocimeters
[NAL-TR-1054] N91-10087
Application of Fabry-Perot velocimetry to hypervelocity impact experiments
[DE90-015612] N91-10096
Flow measurements in turbomachinery using laser anemometry and holography
[PNR-90717] N91-10261
A laser-sheet flow visualization technique for the large wind tunnels of the National Full-Scale Aerodynamics Complex
[NASA-TM-102793] N91-10268
Laser Doppler velocimetry using diode lasers
[ISBN-90-9002803-X] N91-10285
Distortion of LDA fringe pattern by tracer perticles
[SFB-210/E/59] N91-10286
**LASER FUSION**
KrF laser path to high gain ICF (inertial confinement fusion) laboratory microfusion facility
[DE90-016439] N91-10282
A distributed control and monitor system used in laser fusion research
[DE90-013478] N91-10732
**LASER INTERFEROMETRY**
Biomedical applications on laser technology at Los Alamos
[DE90-016447] N91-10277
**LASER MICROSCOPY**
An imaging x-ray microscope using a laser plasma source and a Schwarzchild objective
[DE90-016432] N91-10266
**LASER PLASMAS**
An imaging x-ray microscope using a laser plasma source and a Schwarzchild objective
[DE90-016432] N91-10266
A refractive index gradient (RING) diagnostic for transient discharges or expansions of vapor or plasmas
[DE90-015840] N91-10736
**LASER PROPULSION**
Analysis of pulsed laser-generated impulse in an advanced airbreathing thruster N91-10062
The 1987 Strategic Defense Initiative Organization (SDIO) Workshop on Laser Propulsion
[DE90-013484] N91-10274
**LASER PUMPING**
Sodium-neon resonant photoexcitation soft x ray laser experiments on Saturn
[DE90-014946] N91-10275
**LASER STABILITY**
Cumulative beam breakup of the ground-based-free-electron laser
[DE90-016485] N91-10279
**LASER TARGET INTERACTIONS**
Investigation of pulsed laser target interaction processes by high-speed diagnostic techniques
[ISL-CO-234/89] N91-10283
**LASER TARGETS**
Prediction and control of chaotic processes using nonlinear adaptive networks
[DE90-016505] N91-10697
Temporal behaviour of self generated magnetic field and its influence on inhibition of thermal flux in ICF plasma
[DE90-627478] N91-10731
**LASERS**
SSC dipole magnet measurement and alignment using laser technology
[DE90-014881] N91-10281
**LATENT HEAT**
Documentation for Program SOILSIM: A computer program for the simulation of heat and moisture flow in soils and between soils, canopy and atmosphere
[NASA-CR-186953] N91-10379
**LATTICE PARAMETERS**
A Knudsen layer theory for lattice gases
[ETN-90-97583] N91-10248
**LAUNCH VEHICLES**
Vibration testing of a 1/5 scale model of H-2 launch vehicle
[NAL-TR-1061] N91-10099
Hybrid propulsion technology program: Phase 1, volume 1
[NASA-CR-183972] N91-10111
Hybrid propulsion technology program: Phase 1, volume 2
[NASA-CR-183973] N91-10112
Hybrid propulsion technology program: Phase 1. Volume 3: Thiokol Corporation Space Operations
[NASA-CR-183974] N91-10113
**LAUNCHERS**
Parametric assessment of propulsion system mass for airbreathing launcher configurations
[PNR-90634] N91-10063
Time/frequency analysis of vibro-acoustic behaviour of a launcher in flight
[ETN-90-97584] N91-10097
**LAUNCHING**
The 1987 Strategic Defense Initiative Organization (SDIO) Workshop on Laser Propulsion
[DE90-013484] N91-10274
**LAUNCHING BASES**
Evaluation of composite materials for use on launch complexes
[NASA-TM-103809] N91-10131
**LAUNCHING SITES**
Evaluation of candidate alloys for the construction of metal flex hoses in the STS launch environment
[NASA-TM-103808] N91-10157
**LEADING EDGE SWEEP**
Numerical simulation of hypersonic flow around a space plane. Part 3: Analysis of aerothermodynamic heating
[NAL-TR-1027T] N91-10011
**LEADING EDGES**
Comparison between the null-collision and time counter direct-simulation Monte Carlo methods: Leading-edge flow
[NAL-TR-1016T] N91-10012
Project HyBuJET
[NASA-CR-187011] N91-10040
**LEARNING**
The effects of outcome and process feedback
[NASA-CR-187332] N91-10595
**LEAST SQUARES METHOD**
Synthesis and inversion of Stokes spectral profiles
[PB90-214487] N91-10828
**LEBESGUE THEOREM**
Invariant measures exist under a summability condition for unimodal maps
[REPT-90-36] N91-10670
**LEPTONS**
Prompt lepton production in a proton beamdump experiment
[ETN-90-97750] N91-10711
**LIE GROUPS**
On the rotation interpolation and animation problems in computer graphics
[REPT-90-08] N91-10637
High-order optics of multipole magnets
[DE90-016438] N91-10717

**LIFE SCIENCES**
JPRS report: Science and technology. USSR: Life sciences
[JPRS-ULS-90-001] N91-10551
JPRS report: Science and technology. USSR: Life sciences
[JPRS-ULS-90-013] N91-10552
JPRS report: Science and technology. USSR: Life sciences
[JPRS-ULS-90-012] N91-10556
JPRS report: Science and technology. USSR: Life sciences
[JPRS-ULS-90-011] N91-10565
JPRS Report: Science and technology. USSR: Life sciences
[JPRS-ULS-90-010] N91-10568
JPRS Report: Science and technology. USSR: Life sciences
[JPRS-ULS-90-009] N91-10569
JPRS Report: Science and technology. USSR: Life sciences
[JPRS-ULS-90-008] N91-10570
JPRS Report: Science and technology. USSR: Life sciences
[JPRS-ULS-90-006] N91-10571
JPRS report: Science and technology. USSR: Life sciences
[JPRS-ULS-90-005] N91-10572
JPRS report: Science and technology. USSR: Life sciences
[JPRS-ULS-89-008] N91-10589
JPRS report: Science and technology. USSR: Life sciences
[JPRS-ULS-89-010] N91-10590

**LIFE SUPPORT SYSTEMS**
Space Station Freedom Environmental Control and Life Support System (ECLSS) phase 3 simplified integrated test trace contaminant control subsystem performance
[NASA-TM-4202] N91-10103

**LIFT DRAG RATIO**
Entry vehicle performance analysis and atmospheric guidance algorithm for precision landing on Mars
[NASA-CR-185614] N91-10102

**LIFTING BODIES**
Evaluation of the ZONA51D program
[REPT-B-28] N91-10025

**LIFTING ROTORS**
Transonic flow analysis for rotors. Part 3: Three-dimensional, quasi-steady, Euler calculation
[NASA-TP-2375] N91-10007

**LIFTOFF (LAUNCHING)**
Time/frequency analysis of vibro-acoustic behaviour of a launcher in flight
[ETN-90-97584] N91-10097
Evaluation of composite materials for use on launch complexes
[NASA-TM-103809] N91-10131

**LIGANDS**
Effects of in-plane pi prime bonding on electronic transition energies for inorganic polymers
[DE90-017144] N91-10180

**LIGHT BEAMS**
Tests and applications of Cherenkov imaging in TeV astronomy N91-10807

**LIGHT GAS GUNS**
Pellet injector development at ORNL (Oak Ridge National Laboratory)
[DE90-017024] N91-10742

**LIGHT SCATTERING**
Fast sound propagation in binary fluid mixtures N91-10233
Markov model of the propagation of a light wave in a heated turbulent media
[ECL-90-06] N91-10723

**LIGHT-CONE EXPANSION**
Discretized light-cone quantization: Application to quantum electrodynamics
[DE90-014832] N91-10790

**LIGHTNING**
Development and application of linear and nonlinear methods for interpretation of lightning strikes to in-flight aircraft
[NASA-CR-3974] N91-10548

**LIMITS (MATHEMATICS)**
Existence of at most two limit cycles for the system of differential equations: dx/dt = a + summation for i+j = 2 of (a sub ij) (x sup i) (y sup j) and dy/dt =b + summation for i+j = 2 of (b sub ij) (x sup i) (y sup j)
[REPT-90-03] N91-10667

**LINEAR ACCELERATORS**
Cumulative beam breakup of the ground-based-free-electron laser
[DE90-016485] N91-10279

**LINEAR EQUATIONS**
On Baecklund transformations and identities in bilinear form
[MEMO-856] N91-10681

**LINEAR FILTERS**
Cluster as a wave telescope N91-10424
Robustness effects of a prefilter in generalized predictive control
[OUEL-1799/89] N91-10685

**LINEAR PROGRAMMING**
Probabilistic structural analysis by extremum methods N91-10308
A potential reduction method for a class of smooth convex programming problems
[REPT-90-01] N91-10636

**LINEAR SYSTEMS**
The digital regulator and tracker for deterministic continuous-time linear time-varying systems
[REPT-90-05] N91-10668
Strong maximum principles for systems
[REPT-90-37] N91-10671

**LININGS**
Filament wound metal lined propellant tanks for future Earth-to-orbit transports
[NASA-TM-100594] N91-10106

**LIPSCHITZ CONDITION**
A potential reduction method for a class of smooth convex programming problems
[REPT-90-01] N91-10636

**LIQUID FUELS**
Heavy duty liquid and gaseous fuel emissions database test results from four alternative fuel configurations of the Caterpillar 3406 engine
[DE90-014783] N91-10288

**LIQUID HELIUM**
Thin film thermometers and flowmeters for applications in liquid helium N91-10265

**LIQUID OXYGEN**
Analysis of 5 KHz combustion instabilities in 40K methane/LOX combustion chambers
[NASA-TM-101368] N91-10117
Hot gas side heat transfer characteristics of LOX/H2 and LOX/HC type propellants
[NAL-TR-1062T] N91-10190

**LIQUID PROPELLANT ROCKET ENGINES**
Developments in REDES: The rocket engine design expert system
[NASA-TM-103657] N91-10119
The instability of combustion in propulsion engines N91-10141

**LITHIUM ALLOYS**
Mechanical properties and fracture toughness of 8090-T651 plate and 2091 and 8090 sheet
[NRL-MP-88049-4] N91-10151
Overdischarge protection in high-temperature cells and batteries
[DE90-015180] N91-10220

**LITHIUM SULFUR BATTERIES**
Overdischarge protection in high-temperature cells and batteries
[DE90-015180] N91-10220

**LOAD TESTS**
Test/semi-empirical analysis of a carbon/epoxy fabric stiffened panel N91-10302

**LOADS (FORCES)**
Seat dynamic performance standards for a range of sizes
[DOT/FAA/CT-TN90/23] N91-10028
Research in Structures, Structural Dynamics and Materials, 1990
[NASA-CP-3064] N91-10301
Study of mixed mode stress intensity factor using the experimental method of transmitted caustics N91-10324
Experimental measurement of structural power flow on an aircraft fuselage
[NASA-CR-187352] N91-10335
Summary and recommendations for initial exercise prescription N91-10588

**LOCI**
A consideration on flight paths for microwave-powered airplanes
[NAL-TR-1051] N91-10053

**LOCOMOTION**
Biomedical perspectives on locomotion in null gravity N91-10583

**LOGIC CIRCUITS**
Three-dimensional full-wave analysis of signal communications in active integrated circuits using a variable-mesh TLM method N91-10212

**LOGIC PROGRAMMING**
Real-time safety analysis for autonomous guided vehicles
[OUEL-1833/90] N91-10037
Parallel inference and communication process for Horn clause. First order extension by connection method
[ETN-90-97825] N91-10652

**LONG DURATION EXPOSURE FACILITY**
Long-term orbital lifetime predictions
[NASA-TP-3058] N91-10092

**LONG DURATION SPACE FLIGHT**
Central and regional hemodynamics in prolonged space flights N91-10554
Workshop on Exercise Prescription for Long-Duration Space Flight
[NASA-CP-3051] N91-10574
Considerations for an exercise prescription N91-10585

**LONG TERM EFFECTS**
Long-term orbital lifetime predictions
[NASA-TP-3058] N91-10092

**LOOPS**
Numerical simulation of electromagnetic acceleration by induction. Part 1: Thin loops
[ISL-R-102/89-PT-1] N91-10205

**LOSSES**
Fundamental properties and mass loss in hot, near-main sequence stars N91-10821

**LOW FREQUENCIES**
Anomalous viscosity due to drift wave turbulence
[NIFS-33] N91-10752
Solar emission levels at low radio frequencies
[NASA-CR-187337] N91-10829

**LOWER BODY NEGATIVE PRESSURE**
Central and regional hemodynamics in prolonged space flights N91-10554

**LUBRICANT TESTS**
Self-lubricating boric acid films for tribological applications
[DE90-007805] N91-10171

**LUBRICATION**
Elastohydrodynamic lubrication: A dynamic variation method
[ISBN-90-9003079-4] N91-10290

**LUMINESCENCE**
Radiation damage in Al2O3 crystals implanted with 3.8 MeV Fe(2+)
[DE90-016038] N91-10761

**M**

**MACH NUMBER**
Prediction and comparison with measurements of the aerodynamic characteristics of flare-stabilized XM910 prototypes
[AD-A208099] N91-10005

**MACHINE TOOLS**
Diamond turning of optical crystals
[DE90-015909] N91-10719

**MACHINING**
Diamond turning of optical crystals
[DE90-015909] N91-10719

**MAGNESIUM**
Tests of the general fire suppression concentrate Pyrocap B-136
[DOT/FAA/CT-TN90/21] N91-10029

**MAGNETIC COILS**
Numerical simulation of electromagnetic acceleration by induction. Part 1: Thin loops
[ISL-R-102/89-PT-1] N91-10205

**MAGNETIC COMPRESSION**
Tilt stability and compression heating studies of field-reversed configurations
[DE90-016443] N91-10740

**MAGNETIC DIPOLES**
SSC dipole magnet measurement and alignment using laser technology
[DE90-014881] N91-10281
High-order optics of multipole magnets
[DE90-016438] N91-10717

**MAGNETIC EFFECTS**
Magnetic sensitivity of on-board quartz oscillators: State of the knowledge
[CNES-CT/DRT/TIT/TF-88/354] N91-10110

**MAGNETIC FIELD CONFIGURATIONS**
Tilt stability and compression heating studies of field-reversed configurations
[DE90-016443] N91-10740
Theory of longitudinal adiabatic invariant in the helical torus
[NIFS-37] N91-10749

**MAGNETIC FIELD INVERSIONS**
Synthesis and inversion of Stokes spectral profiles
[PB90-214487] N91-10828

**MAGNETIC FIELDS**
Contribution to the study of the electromagnetic field radiation close to electronics circuits
[ECL-90-12] N91-10211

Configurational sensitivity of multipoint magnetic field measurements N91-10421
Accuracy of the estimate of J via multipoint measurements N91-10422
Properties of large scale plasma flow during the early stage of the plasmaspheric refilling
[NASA-TM-103446] N91-10441
Workshop on Massively Parallel Computing in Magnetic Fusion Energy
[DE90-018009] N91-10650
High-order optics of multipole magnets
[DE90-016438] N91-10717
Temporal behaviour of self generated magnetic field and its influence on inhibition of thermal flux in ICF plasma
[DE90-627478] N91-10731
Experiments on linear high beta helical axis stellarators to study simulated toroidal effects and Alfven-wave heating
[DE90-016122] N91-10738
Theoretical studies of turbulence and anomalous transport in toroidal confinement devices
[DE90-017606] N91-10747
Computation of superconductor critical current densities and magnetization curves
[DE90-016567] N91-10773
Propagation of magnetoacoustic waves in the solar atmosphere with random inhomogeneities of density and magnetic fields
[DE90-017616] N91-10831

**MAGNETIC FILMS**
Ultra-thin vertical magneto-optical media and system for using same
[DE90-014589] N91-10603

**MAGNETIC FLUX**
Properties of large scale plasma flow during the early stage of the plasmaspheric refilling
[NASA-TM-103446] N91-10441
Examination of ion acceleration in the plasma layer during magnetospheric partial gales
[MPE-218] N91-10753

**MAGNETIC INDUCTION**
Numerical simulation of electromagnetic acceleration by induction. Part 1: Thin loops
[ISL-R-102/89-PT-1] N91-10205

**MAGNETIC MATERIALS**
On the effects of magnetic bonding in rare earth transition metal intermetallics
[DE90-015800] N91-10156

**MAGNETIC MOMENTS**
Calculation of the static magnetism of metamagnetic La2CuO4
[DE90-016490] N91-10770
Intrinsic neutrino properties: As deduced from cosmology, astrophysics, accelerator, and non-accelerator experiments
[DE90-016467] N91-10836

**MAGNETIC PERMEABILITY**
Calculation of the static magnetism of metamagnetic La2CuO4
[DE90-016490] N91-10770

**MAGNETIC POLES**
High-order optics of multipole magnets
[DE90-016438] N91-10717

**MAGNETIC PROPERTIES**
On the effects of magnetic bonding in rare earth transition metal intermetallics
[DE90-015800] N91-10156

**MAGNETIC SIGNALS**
The scientific case for magnetic field satellites
[NASA-CR-186532] N91-10101

**MAGNETIC SIGNATURES**
Plasma waves as a signature of flux transfer events N91-10427
Solar-geophysical data number 545, January 1990. Part 1 (Prompt reports). Data for December, November 1989 and late data
[PB90-182338] N91-10822

**MAGNETIC STORAGE**
Ultra-thin vertical magneto-optical media and system for using same
[DE90-014589] N91-10603

**MAGNETIC STORMS**
The empirical geomagnetic parameter infer near-Earth interplanetary shocks
[IFSI-90-14] N91-10820
On the autoregression methods applied to the hourly nucleonic-component records
[IFSI-89-19] N91-10837

**MAGNETIZATION**
The scientific case for magnetic field satellites
[NASA-CR-186532] N91-10101
Computation of superconductor critical current densities and magnetization curves
[DE90-016567] N91-10773

**MAGNETOACOUSTIC WAVES**
On lower hybrid wave scattering by plasma density fluctuation nonlinear reflection coefficient of the fast magnetoacoustic wave
[IPPCZ-281] N91-10725
Propagation of magnetoacoustic waves in the solar atmosphere with random inhomogeneities of density and magnetic fields
[DE90-017616] N91-10831

**MAGNETOHYDRODYNAMIC FLOW**
Multipoint study of small-scale structures at the magnetopause N91-10432
Properties of large scale plasma flow during the early stage of the plasmaspheric refilling
[NASA-TM-103446] N91-10441
A computational model for z-pinch plasma channels N91-10730

**MAGNETOHYDRODYNAMIC STABILITY**
Multipoint study of small-scale structures at the magnetopause N91-10432
Tilt stability and compression heating studies of field-reversed configurations
[DE90-016443] N91-10740
Tearing modes in tokamaks with lower hybrid current drive
[DE90-017090] N91-10743
Unified theory of ballooning instabilities and temperature gradient driven trapped ion modes
[DE90-017091] N91-10744
Numerical simulation of ion temperature gradient driven modes in the presence of ion-ion collisions
[DE90-017092] N91-10745
Plasma properties
[DE90-017256] N91-10746

**MAGNETOHYDRODYNAMIC TURBULENCE**
Non-linear evolution of the Kelvin-Helmholtz instability: Constraints on multipoint measurements N91-10430

**MAGNETOHYDRODYNAMIC WAVES**
Cluster as a wave telescope N91-10424
Two-dimensional magnetohydrodynamic equilibria with flow and studies of equilibrium fluctuations N91-10727
A mathematical model of the structure and evolution of small scale discrete auroral arcs
[NASA-CR-187238] N91-10734

**MAGNETOHYDRODYNAMICS**
Workshop on Massively Parallel Computing in Magnetic Fusion Energy
[DE90-018009] N91-10650
Two-dimensional magnetohydrodynamic equilibria with flow and studies of equilibrium fluctuations N91-10727
Self-consistent field error effects in reversed field pinch plasmas N91-10728
Models of plasma confinement and heating in tokamaks
[DE90-016671] N91-10741

**MAGNETOPAUSE**
Specific tasks of multiple scale plasma measurements in Regatta-Cluster system N91-10419
Non-linear evolution of the Kelvin-Helmholtz instability: Constraints on multipoint measurements N91-10430
Multipoint study of small-scale structures at the magnetopause N91-10432

**MAGNETORESISTIVITY**
The transport properties of activated carbon fibers
[DE90-015910] N91-10130

**MAGNETOSPHERIC ION DENSITY**
Problems of cold plasma measurements on the Regatta-A spacecraft N91-10431

**MAGNETRON SPUTTERING**
Deposition controlled uniformity of multilayer mirrors
[DE90-015906] N91-10718

**MAGSAT SATELLITES**
The scientific case for magnetic field satellites
[NASA-CR-186532] N91-10101

**MAINTENANCE**
Columbus logistics support. A conceptional definition of the operational phase
[MBB-UO-0093-90-PUB] N91-10091
Prevention of breakdown behind railgun projectiles
[DE90-014573] N91-10094
Structural properties of laminated Douglas fir/epoxy composite material
[NASA-RP-1236] N91-10127

**MALFUNCTIONS**
Automatic determination of fault effects on aircraft functionality
[NASA-CR-181352] N91-10039

**MAN MACHINE SYSTEMS**
FAA air traffic operational evaluation of Automated Surface Observing System (ASOS)
[DOT/FAA/CT-TN90/42] N91-10084
System console N91-10351
Technique for human-error sequence identification and signification
[ISBN-90-353-10144] N91-10596

**MANAGEMENT INFORMATION SYSTEMS**
The integrated scheduling system: A case study in project management
[NASA-CR-187261] N91-10793

**MANAGEMENT PLANNING**
The integrated scheduling system: A case study in project management
[NASA-CR-187261] N91-10793

**MANAGEMENT SYSTEMS**
Operational evaluation of initial data link air traffic control services. Volume 2: Appendices
[DOT/FAA/CT-90/1-VOL-2] N91-10033
Structural tests of aircraft window assembly equipped with smoke evacuation valve
[DOT/FAA/CT-TN89/44] N91-10051
Knowledge-based assistance in costing the space station DMS N91-10611
The integrated scheduling system: A case study in project management
[NASA-CR-187261] N91-10793

**MANEUVERABILITY**
Nonlinear feedback control for high alpha flight
[NASA-CR-186545] N91-10047
Combined design of structures and controllers for optimal maneuverability N91-10314

**MANIPULATORS**
Redundancy control of a robot manipulator using a systolic array processor N91-10287

**MANNED ORBITAL LABORATORIES**
Columbus elements processing needs at KSC
[MBB-UO-0092-90-PUB] N91-10108

**MANNED SPACE FLIGHT**
JPRS report: Science and technology. USSR: Space
[JPRS-USP-90-001] N91-10089

**MANUALS**
A manual for PARTI runtime primitives
[NASA-CR-187442] N91-10599

**MANUFACTURING**
Casting alloys for the jet age
[PNR-90723] N91-10168
Engineering design: A powerful influence on the business success on manufacturing industry
[PNR-90763] N91-10197

**MAPPING**
Image mapping N91-10359

**MAPS**
High-order optics of multipole magnets
[DE90-016438] N91-10717

**MARINE BIOLOGY**
Chesapeake Bay Basin Monitoring Program Atlas. Volume 2: Biological and living resource monitoring programs
[PB90-147943] N91-10392

**MARINE ENVIRONMENTS**
Mariners Weather Log, Volume 33, Number 1, Winter, 1989
[PB90-179987] N91-10447

**MARINE METEOROLOGY**
FIRE Science Results 1988
[NASA-CP-3083] N91-10448
ISCCP results for the FIRE IFO regions and times N91-10451
Climate data system supports FIRE N91-10455
Lidar and radiometer results from the ER-2 for the FIRE field experiments N91-10468
AVHRR and VISSR satellite instrument calibration results for both Cirrus and marine stratocumulus IFO periods N91-10475
Extended time observations of California marine stratocumulus clouds from GOES for July 1983-1987 N91-10486
The relationship of marine stratus to synoptic conditions N91-10489
Analysis of diurnal variation of SCu layer using 2 days of CLASS soundings on San Nicolas Island N91-10490
Diurnal variation of marine stratocumulus over San Nicolas Island during the FIRE IFO N91-10491
Analysis of tethered balloon, ceilometer and class sounding data taken on San Nicolas Island during the FIRE project N91-10492
Preliminary mixed-layer model results for FIRE marine stratocumulus IFO conditions N91-10495
A cloud classification scheme applied to the breakup region of marine stratocumulus N91-10497
Studying marine stratus with large eddy simulation N91-10499
Cloud spatial structure during the FIRE MS IFO N91-10500
Reflectivities of uniform and broken marine stratiform clouds N91-10501
Marine stratocumulus cloud characteristics from multichannel satellite measurements N91-10502
Cloud parameters derived from GOES during the 1987 marine stratocumulus FIRE Intensive Field Observation (IFO) period N91-10505

A study of marine stratocumulus using lidar and other FIRE aircraft observations N91-10511
Cloud absorption properties as derived from airborne measurements of scattered radiation within clouds N91-10512
Cloud optical parameters as derived from the multispectral cloud radiometer N91-10513
Aircraft measurements of the mean and turbulent structure of marine stratocumulus clouds during FIRE N91-10514
Cloud and boundary layer structure over San Nicolas Island during FIRE N91-10515
Horizontal variability of the marine boundary layer structure upwind of San Nicolas Island during FIRE, 1987 N91-10519
An overview of UK C130 observations from the FIRE marine stratocumulus IFO N91-10520
Dependence of marine stratocumulus reflectivities on liquid water paths N91-10524
Near infrared radiances observed by the UK C130 multi-channel radiometer during the marine stratocumulus IFO and preliminary comparison with model calculations N91-10525
Plume mechanics and stratocumulus convection N91-10526
Preliminary results of radiation measurements from the marine stratus FIRE experiment N91-10529
Aircraft/island/ship/satellite intercomparison: Preliminary results from July 16, 1987 N91-10534
Mariners Weather Log, Volume 34, Number 2, Spring 1990 [PB90-222324] N91-10537

**MARINE TECHNOLOGY**
Structural acoustics: An applied science with many applications [PB90-183633] N91-10698

**MARKARIAN GALAXIES**
Investigation of Markarian galaxies with multiple nuclei N91-10813

**MARKET RESEARCH**
Industrial applications and markets for ceramic matrix composites [PNR-90753] N91-10138
Multi industry application of advanced materials [PNR-90764] N91-10139
Applied technology center business plan and market survey [NASA-CR-187259] N91-10794
Space market model space industry input-output model [NASA-CR-187252] N91-10795

**MARKOV PROCESSES**
A Markov renewal approach to an apportunistic replacement model in continuous time [MEMO-844] N91-10675
Markov model of the propagation of a light wave in a heated turbulent media [ECL-90-06] N91-10723

**MARS ATMOSPHERE**
Entry vehicle performance analysis and atmospheric guidance algorithm for precision landing on Mars [NASA-CR-185614] N91-10102

**MARS LANDING**
Entry vehicle performance analysis and atmospheric guidance algorithm for precision landing on Mars [NASA-CR-185614] N91-10102

**MASS FLOW**
Coriolis-effect in mass flow metering [LSTM-266/T/89] N91-10258
Pressure measurements on the release system and determination of jet momentum in the project BA propane field tests 1989 [FOA-E-40044-4.5] N91-10263
Two-dimensional magnetohydrodynamic equilibria with flow and studies of equilibrium fluctuations N91-10727

**MASS FLOW RATE**
Performance characterization of a segmented anode arcjet thruster [NASA-TM-103227] N91-10118

**MASS RATIOS**
Parametric assessment of propulsion system mass for airbreathing launcher configurations [PNR-90634] N91-10063

**MASS SPECTRA**
Discretized light-cone quantization: Application to quantum electrodynamics [DE90-014832] N91-10790

**MASS SPECTROMETERS**
The growth of zinc selenide single crystals by physical vapor transport in microgravity [NASA-CR-180428] N91-10755

**MASS TRANSFER**
Mass transfer in oscillating flows: Efficient drying via pulse combustors [PB90-242389] N91-10235
AFDM: An Advanced Fluid-Dynamics Model [DE90-017536] N91-10241

**MASSIVELY PARALLEL PROCESSORS**
Workshop on Massively Parallel Computing in Magnetic Fusion Energy [DE90-018009] N91-10650

**MATCHED FILTERS**
Computation of maximum gust loads in nonlinear aircraft using a new method based on the matched filter approach and numerical optimization N91-10317

**MATHEMATICAL MODELS**
Application of a state-space wake model to elastic blade flapping in hover N91-10006
Optimum hypersonic airfoil with power law shock waves [DE90-014903] N91-10008
Turbulent flow calculations using unstructured and adaptive meshes [NASA-CR-182102] N91-10010
Numerical computation of viscous flow about unconventional airfoil shapes [NASA-CR-187343] N91-10019
Drive system life and reliability N91-10044
Analysis of pulsed laser-generated impulse in an advanced airbreathing thruster N91-10062
Vibration testing of a 1/5 scale model of H-2 launch vehicle [NAL-TR-1061] N91-10099
Structural properties of laminated Douglas fir/epoxy composite material [NASA-RP-1236] N91-10127
Reduction of thermal stresses in continuous fiber reinforced metal matrix composites with interface layers [NASA-CR-185302] N91-10133
Mechanisms of high temperature crack growth in metals and alloys [DE90-014934] N91-10152
Transition state theory applying to the study of reaction processes in detonation [DE90-016558] N91-10187
Signal detection in non-Gaussian and non-white noise N91-10200
Electromagnetic scattering from two-dimensional thick material junctions [NASA-CR-186976] N91-10201
An analysis of the effects of secondary reflections on dual-frequency reflectometers [NASA-TM-102709] N91-10221
Simulation of time-dependent compressible viscous flows using central and upwind-biased finite difference techniques N91-10234
Mass transfer in oscillating flows: Efficient drying via pulse combustors [PB90-242389] N91-10235
AFDM: An Advanced Fluid-Dynamics Model. Volume 4: The AFDM heat- and mass-transfer solution algorithm [DE90-017535] N91-10240
AFDM: An Advanced Fluid-Dynamics Model [DE90-017536] N91-10241
Modeling of hydrocarbon fueling [DE90-014790] N91-10289
A simple screw thread model for use in finite element stress analysis [AD-A210233] N91-10300
Direct use of linear time-domain aerodynamics in aeroservoelastic analysis: Aerodynamic model N91-10316
Analysis of moving strong discontinuity surfaces in elastic-plastic solids including effects of inertia and finite strain N91-10323
An experimental and analytical study of structural identification N91-10325
Comparison of NASTRAN analysis with ground vibration results of UH-60A NASA/AEFA test configuration [NASA-CR-184565] N91-10333
Mobility power flow analysis of an L-shaped plate structure subjected to distributed loading [NASA-CR-187353] N91-10334
The effects of critical layers on atmospheric cnoidal waves [DE90-016540] N91-10440
Evidence for asymmetric inertial instability in the FIRE satellite dataset N91-10454
Hydrometeor development in cold clouds in FIRE N91-10459
The radiation budget of a Cirrus layer deduced from simultaneous aircraft observations and model calculations N91-10467
Interpretation of satellite-measured bidirectional reflectance from Cirrus cloudy atmospheres N91-10470
Cirrus cloud properties derived from coincident GOES and lidar data during the 1986 FIRE Cirrus Intensive Field Observations (IFO) N91-10476
FIRE Cirrus on October 28, 1986: LANDSAT; ER-2; King Air; theory N91-10480
Fractional cloudiness in shallow cumulus layers N91-10498
About the possibilities of using an air mass transformation model in Taiyuan, Shanxi Province, China [KNMI-TR-120] N91-10540
Verification of GONO wave predictions for the period October 1987 to April 1988 [KNMI-TR-118] N91-10545
Directional response of wind waves to turning winds [REPT-90-2] N91-10549
Statistical methods for analyzing and combining data on low-level exposures to ionizing radiation [DE90-017193] N91-10593
Models of the human observer and controller of a dynamic system [ETN-90-97759] N91-10597
Activities of the Board on Mathematical Sciences [DE90-015118] N91-10598
Some recent applications of numerical methods to geotechnical analysis [PB90-201229] N91-10655
Stability of some stationary solutions for the forced KdV equation [DE90-016506] N91-10662
Geometric ergodicity of the ALOHA-system and a coupled processors model [TW-90-01-B] N91-10680
Properties of acoustic energy quantities [DE90-518714] N91-10701
Numerical models of beam dynamics in ion induction linacs [DE90-017043] N91-10713
Polarization modulated solitary waves in an optical fiber [DE90-015034] N91-10715
A mathematical model of the structure and evolution of small scale discrete auroral arcs [NASA-CR-187238] N91-10734
Models of plasma confinement and heating in tokamaks [DE90-016671] N91-10741
Substrate temperature effects on (cubic x cubic lattice) R 30 deg domain growth of Ag on Si(111) surface [DE90-016527] N91-10772
Reaction kinetics of the Ca-SO2 system in absence of inter-grain pore diffusion [DE90-009672] N91-10781
About antiferromagnetic Heisenberg models [ETN-90-97768] N91-10784
Estimation of astronomical images from the bispectrum of atmospherically distorted infrared data N91-10806
A semi-analytical model of stellar flares [DE90-016434] N91-10817

**MATHEMATICS**
Activities of the Board on Mathematical Sciences [DE90-015118] N91-10598
JPRS report: Science and technology. USSR: Physics and mathematics [JPRS-UPM-90-003] N91-10694

**MATRICES (MATHEMATICS)**
Tabu-search and simulated annealing for the quadratic assignment problem [REPT-89-028] N91-10658
Optimum orientations of the observation axes for 2-dimensional vector sensing under consideration of bias errors [NAL-TR-1055] N91-10679
H 2 and H infinity approximations for eigenvalue/vector functions of transfer matrices [OUEL-1778/89] N91-10684
Anomalous viscosity due to drift wave turbulence [NIFS-33] N91-10752

**MATRIX MATERIALS**
Reduction of thermal stresses in continuous fiber reinforced metal matrix composites with interface layers [NASA-CR-185302] N91-10133
Compressive failure of thick-section composite laminates with and without cutouts subjected to biaxial loading N91-10304

**MATRIX METHODS**
Three-dimensional full-wave analysis of signal communications in active integrated circuits using a variable-mesh TLM method N91-10212

**MAXIMUM LIKELIHOOD ESTIMATES**
Calculation of Weibull strength parameters, Batdorf flaw density constants and related statistical quantities using PC-CARES [NASA-TM-103247] N91-10332

**MAXIMUM PRINCIPLE**
Strong maximum principles for systems [REPT-90-37] N91-10671

**MAXWELL EQUATION**
Electromagnetic particle codes on unstructured grids [DE90-015187] N91-10733

**MEASURING INSTRUMENTS**
Characteristics of piping interference elimination unit used in the high-speed wind tunnel test of ASUKA seven percent semi-born prototype
[NAL-TM-588] N91-10003
Wind tunnel test of redundant vane-type flow-direction sensing systems
[NAL-TM-590] N91-10057
Effects of coolant injection on turbine aerodynamic characteristics. Part 1: Test turbine and apparatus
[NAL-TM-585-PT-1] N91-10059
The ISL hypersonic shock tunnel and its instrumentation
[ISL-CO-213/89] N91-10086
A miniature inexpensive, oxygen sensing element
[DE90-014080] N91-10269
**MECHANICAL DRIVES**
Drive system life and reliability N91-10044
**MECHANICAL ENGINEERING**
Technical Abstracts: Mechanical engineering
[DE90-014797] N91-10802
**MECHANICAL PROPERTIES**
Composite heat damage. Part 1: Mechanical testing of IM6/3501-6 laminates. Part 2: Nondestructive evaluation studies of IM6/3501-6 laminates
[DE90-016207] N91-10125
A macro-micromechanics analysis of a notched metal matrix composite
[NASA-TM-102728] N91-10128
Mechanical properties and fracture toughness of 8090-T651 plate and 2091 and 8090 sheet
[NRL-MP-88049-4] N91-10151
A weldability study of Haynes Alloy no. 242
[DE90-013875] N91-10154
Axial compression buckling test on CFRP surface plate/aluminum honeycomb sandwiched curved surface plate
[NAL-TM-584] N91-10299
Calculation of Weibull strength parameters, Batdorf flaw density constants and related statistical quantities using PC-CARES
[NASA-TM-103247] N91-10332
Properties of reactively-deposited SiC and GeC alloys
[DE90-016363] N91-10786
**MECHANICAL SHOCK**
Wind tunnel investigations of the appearance of shocks in the windward region of bodies with circular cross section at angle of attack
[DLR-FB-90-15] N91-10027
**MEDICAL ELECTRONICS**
Biomedical applications on laser technology at Los Alamos
[DE90-016447] N91-10277
**MEMORY (COMPUTERS)**
Multiple channel programmable coincidence counter
[DE90-014681] N91-10602
**MEROMORPHIC FUNCTIONS**
Operator formalism of multi-pole Virasoro algebra on Riemann sphere
[DE90-627217] N91-10657
**MESOMETEOROLOGY**
Winds and turbulence above San Nicolas Island during FIRE N91-10522
**MESOSCALE PHENOMENA**
The effects of critical layers on atmospheric cnoidal waves
[DE90-016540] N91-10440
Evidence for asymmetric inertial instability in the FIRE satellite dataset N91-10454
Winds and turbulence above San Nicolas Island during FIRE N91-10522
Terrain-induced mesoscale circulations in the Columbia Basin
[DE90-016338] N91-10541
**METABOLISM**
Requirements for an ideal drug for preventing space motion sickness N91-10566
**METAL BONDING**
On the effects of magnetic bonding in rare earth transition metal intermetallics
[DE90-015800] N91-10156
**METAL FILMS**
Deposition controlled uniformity of multilayer mirrors
[DE90-015906] N91-10718
**METAL IONS**
Direct extraction of a Na(-) beam from a sodium plasma
[NIFS-35] N91-10751
**METAL MATRIX COMPOSITES**
Micro-mechanical analysis of damage growth and fracture in discontinuous fiber reinforced metal matrix composites
[NASA-CR-187020] N91-10126
A macro-micromechanics analysis of a notched metal matrix composite
[NASA-TM-102728] N91-10128
Reduction of thermal stresses in continuous fiber reinforced metal matrix composites with interface layers
[NASA-CR-185302] N91-10133
Fibre-matrix reaction zones in model silicon carbide-titanium aluminide metal-matrix composites
[PNR-90713] N91-10137
An analytical solution for the elastoplastic response of a continuous fiber composite under uniaxial loading
N91-10305
**METAL OXIDE SEMICONDUCTORS**
Contribution to the study of MOS structures ageing
[ECL-90-04] N91-10785
**METAL OXIDES**
Electrochemical oxidation of methane at metal and metal oxide electrodes
[PB90-205196] N91-10140
**METAL PLATES**
Axial compression buckling test on CFRP surface plate/aluminum honeycomb sandwiched curved surface plate
[NAL-TM-584] N91-10299
**METAL SURFACES**
Characterization of mono- and multi-molecular assemblies at glassy carbon and noble metals by ex situ and in situ infrared external reflection spectroscopy
[DE90-016417] N91-10144
**METAL WORKING**
Casting alloys for the jet age
[PNR-90723] N91-10168
**METALLIC PLASMAS**
Direct extraction of a Na(-) beam from a sodium plasma
[NIFS-35] N91-10751
**METALS**
Filament wound metal lined propellant tanks for future Earth-to-orbit transports
[NASA-TM-100594] N91-10106
Shock experiments in metals and ceramics
[DE90-016613] N91-10165
**METEOROLOGICAL CHARTS**
Satellite cloud information chart N91-10374
Mariners Weather Log, Volume 34, Number 2, Spring 1990
[PB90-222324] N91-10537
**METEOROLOGICAL PARAMETERS**
Lidar and radiometer results from the ER-2 for the FIRE field experiments N91-10468
**METEOROLOGICAL SATELLITES**
Educator's guide for building and operating environmental satellite receiving stations
[NOAA-TR-NESDIS-44] N91-10093
Meteorological Satellite Center Technical Note. Special Issue (1989). Summary of GMS System. 1: Telecommunication System N91-10338
Outline of the GMS telecommunication system
N91-10339
Station control and monitor subsystem N91-10341
VISSR demodulate and processing subsystem
N91-10342
Stretched VISSR subsystem N91-10343
Image monitor N91-10344
Telemetry subsystem N91-10345
Command subsystem N91-10346
Trilateration ranging subsystem N91-10347
Operation console N91-10350
DCP subsystem N91-10352
WEFAX subsystem N91-10353
DPC telecommunication system N91-10354
Meteorological Satellite Center Technical Note. Special Issue (1989). Summary of GMS System. 2: Data Processing N91-10356
Computer system N91-10357
General flow of image data processing N91-10358
Image mapping N91-10359
FAX image processing N91-10361
Satellite-derived index of precipitation intensity
N91-10362
ISCCP data processing N91-10363
Cloud motion wind N91-10365
Typhoon information N91-10366
Brightness temperature distribution N91-10369
GPCP data processing N91-10370
Cloud amount distribution N91-10373
Satellite cloud information chart N91-10374
DCP data processing N91-10375
Aircraft/island/ship/satellite intercomparison: Preliminary results from July 16, 1987 N91-10534
**METEOROLOGY**
Educator's guide for building and operating environmental satellite receiving stations
[NOAA-TR-NESDIS-44] N91-10093
Meteorological Satellite Center Technical Note. Special Issue (1989). Summary of GMS System. 2: Data Processing N91-10356
Image mapping N91-10359
FAX image processing N91-10361
Satellite-derived index of precipitation intensity
N91-10362
Typhoon information N91-10366
Brightness temperature distribution N91-10369
Satellite cloud information chart N91-10374
DCP data processing N91-10375
Where are cirrus clouds and why are they there
N91-10450
NRL tethered balloon measurements at San Nicolas Island during FIRE IFO 1987 N91-10509
Near infrared radiances observed by the UK C130 multi-channel radiometer during the marine stratocumulus IFO and preliminary comparison with model calculations
N91-10525
Energetics of valley and basin atmospheres during the evening transition and nighttime periods
[DE90-016356] N91-10542
**METHANE**
Analysis of 5 KHz combustion instabilities in 40K methane/LOX combustion chambers
[NASA-TM-101368] N91-10117
Electrochemical oxidation of methane at metal and metal oxide electrodes
[PB90-205196] N91-10140
Hot gas side heat transfer characteristics of LOX/H2 and LOX/HC type propellants
[NAL-TR-1062T] N91-10190
Methane conversion by solid electrolyte membranes
[PB90-226341] N91-10381
**METHYL COMPOUNDS**
Electrochemical oxidation of methane at metal and metal oxide electrodes
[PB90-205196] N91-10140
**METROLOGY**
Intrinsic (?) reference standards
[DE90-015714] N91-10696
**MICE**
Effects of taurine on cytogenetic corneal disturbances induced in mice by 9 GeV protons N91-10582
**MICROCHANNEL PLATES**
MicroChannel Plate detectors (MCP)
[CNES-CT/DRT/TIT/OE-88/037-T] N91-10227
**MICROCLIMATOLOGY**
Protective functions of skin N91-10555
**MICROMECHANICS**
Micro-mechanical analysis of damage growth and fracture in discontinuous fiber reinforced metal matrix composites
[NASA-CR-187020] N91-10126
A macro-micromechanics analysis of a notched metal matrix composite
[NASA-TM-102728] N91-10128
Study of the mechanisms of damage and failure of fiber and ceramic matrix composites
[ISAL-90-0026] N91-10135
**MICROSCOPES**
An imaging x-ray microscope using a laser plasma source and a Schwarzchild objective
[DE90-016432] N91-10266
**MICROSTRUCTURE**
Microstructural and phase stability studies of nanometer period metal/carbon multilayer structures for x ray optics
[DE90-015307] N91-10129
A weldability study of Haynes Alloy no. 242
[DE90-013875] N91-10154
Radiation-induced microstructural development and microchemical changes in Fe-Cr-Mn-Ni solute-bearing alloys
[DE90-016359] N91-10160
Mechanical and microstructural response of Ni3Al at high strain rate and elevated temperatures
[DE90-016489] N91-10162
Shock experiments in metals and ceramics
[DE90-016613] N91-10165
Strength and toughness of single-phase and dual-phase high-temperature intermetallics
[DE90-017192] N91-10166
High-strain-rate compression and fracture of B4C-aluminum cermets
[DE90-016568] N91-10176
Theoretical calculations of the nonlinear dielectric function of inhomogeneous thin films
[DE90-017186] N91-10778
Excitons in semiconducting superlattices, quantum wells, and ternary alloys
[DE90-017287] N91-10779
Contribution to the study of MOS structures ageing
[ECL-90-04] N91-10785
**MICROWAVE OSCILLATORS**
An x band backward-wave oscillator experiment
[DE90-015119] N91-10219
**MICROWAVE POWER BEAMING**
A consideration on flight paths for microwave-powered airplanes
[NAL-TR-1051] N91-10053

Practical flight paths for microwave-powered airplanes
[NAL-TR-1052T] N91-10054
Determination of surface resistance and magnetic penetration depth of superconducting YBa2Cu3O(7-delta) thin films by microwave power transmission measurements
[NASA-TM-103616] N91-10780

**MICROWAVE REFLECTOMETERS**
An analysis of the effects of secondary reflections on dual-frequency reflectometers
[NASA-TM-102709] N91-10221

**MICROWAVE SPECTRA**
Biomedical applications on laser technology at Los Alamos
[DE90-016447] N91-10277

**MICROWAVES**
Microwave link N91-10355

**MILITARY TECHNOLOGY**
Gas turbines for main propulsion and auxiliary power systems
[PNR-90709] N91-10069

**MINERAL METABOLISM**
Space medicine considerations: Skeletal and calcium homeostasis N91-10580
Changes in mineral metabolism with immobilization/space flight N91-10581

**MINIATURIZATION**
Vibration testing of a 1/5 scale model of H-2 launch vehicle
[NAL-TR-1061] N91-10099

**MIRRORS**
Damage assessment and possible damage mechanisms to 1-meter diameter Nova turning mirrors
[DE90-016473] N91-10278
Deposition controlled uniformity of multilayer mirrors
[DE90-015906] N91-10718

**MISALIGNMENT**
Image mapping N91-10359

**MISSILE CONFIGURATIONS**
Prediction and comparison with measurements of the aerodynamic characteristics of flare-stabilized XM910 prototypes
[AD-A208099] N91-10005

**MISSILE TESTS**
Prediction and comparison with measurements of the aerodynamic characteristics of flare-stabilized XM910 prototypes
[AD-A208099] N91-10005

**MISSION PLANNING**
Multispacecraft measurement at varying scalelengths: The Cluster/Regatta opportunity N91-10418
Specific tasks of multiple scale plasma measurements in Regatta-Cluster system N91-10419
Review of the Cluster orbit and separation strategy: Consequence for measurements N91-10420

**MIXTURES**
Thermophysical properties of fluids and fluid mixtures
[DE90-016306] N91-10792

**MOBILE COMMUNICATION SYSTEMS**
A Mobile Satellite Experiment (MSAT-X) network definition
[NASA-CR-187336] N91-10105

**MOBILITY**
Mobility power flow analysis of an L-shaped plate structure subjected to distributed loading
[NASA-CR-187353] N91-10334

**MODULATORS**
WEFAX subsystem N91-10353

**MODULUS OF ELASTICITY**
Analysis of moving strong discontinuity surfaces in elastic-plastic solids including effects of inertia and finite strain N91-10323

**MOISTURE**
Analysis of tethered balloon data from San Nicolas Island on 8 July 1987 N91-10517

**MOISTURE CONTENT**
Lidar and aircraft studies of deep Cirrus systems from the 1986 FIRE IFO N91-10460
A GCM parameterization for the shortwave radiative properties of water clouds N91-10494
Estimated accuracy of ground-based liquid water measurements during FIRE N91-10508
Estimating integrated cloud liquid water from extended time observations of solar irradiance N91-10510
Thermodynamic structure of the stratocumulus-capped boundary layer on 5 July 1987 N91-10516
Turbulence measurements using tethered balloon instrumentation during FIRE 1987 N91-10518
Dependence of marine stratocumulus reflectivities on liquid water paths N91-10524

**MOLECULAR COLLISIONS**
Comparison between the null-collision and time counter direct-simulation Monte Carlo methods: Leading-edge flow
[NAL-TR-1016T] N91-10012
A sensitive test for accuracy in evaluation of molecular collision number in the direct-simulation Monte Carlo method
[NAL-TR-1050T] N91-10712

**MOLECULAR ORBITALS**
Optical properties of inorganic polymers
[DE90-017143] N91-10179
Effects of in-plane pi prime bonding on electronic transition energies for inorganic polymers
[DE90-017144] N91-10180

**MOLECULAR STRUCTURE**
Organometallic chemistry of bimetallic compounds
[DE90-017601] N91-10121
Optical properties of inorganic polymers
[DE90-017143] N91-10179

**MOLECULAR WEIGHT**
Theoretical studies of High Energy Density Matter (HEDM) molecules
[DE90-014831] N91-10706

**MOLYBDENUM CARBIDES**
Corrosion-resistant coatings for high-temperature high-sulfur activity applications
[DE90-016638] N91-10177

**MOMENTUM**
Pressure measurements on the release system and determination of jet momentum in the project BA propane field tests 1989
[FOA-E-40044-4.5] N91-10263

**MOMENTUM TRANSFER**
The scientific case for magnetic field satellites
[NASA-CR-186532] N91-10101
AFDM: An Advanced Fluid-Dynamics Model
[DE90-017536] N91-10241

**MONITORS**
Image monitor N91-10344
Telemetry subsystem N91-10345
Command subsystem N91-10346
Antenna/transmitter control unit N91-10348
Operation console N91-10350
System console N91-10351
WEFAX subsystem N91-10353
DPC telecommunication system N91-10354
A distributed control and monitor system used in laser fusion research
[DE90-013478] N91-10732

**MONKEYS**
Preliminary studies before defining a payload adapted to the primate model
[ETN-90-97581] N91-10107

**MONOMERS**
Influence of expanding monomer on carbon fiber reinforced epoxy composites
[AD-A223277] N91-10124

**MONOMOLECULAR FILMS**
Monomolecular and thin polymer films: Fabrication, characterization, applications, and models of wetting
[DE90-016415] N91-10174

**MONOTONE FUNCTIONS**
Pseudo-monotone complementarity problems in Hilbert space
[DE90-016310] N91-10660

**MONTE CARLO METHOD**
Comparison between the null-collision and time counter direct-simulation Monte Carlo methods: Leading-edge flow
[NAL-TR-1016T] N91-10012
Dijet spectroscopy at high luminosity
[DE90-016901] N91-10147
Modeling of hydrocarbon fueling
[DE90-014790] N91-10289
A sensitive test for accuracy in evaluation of molecular collision number in the direct-simulation Monte Carlo method
[NAL-TR-1050T] N91-10712
Numerical simulation of ion temperature gradient driven modes in the presence of ion-ion collisions
[DE90-017092] N91-10745
Estimation of astronomical images from the bispectrum of atmospherically distorted infrared data N91-10806

**MORPHOLOGY**
Optical and morphological properties of Cirrus clouds determined by the high spectral resolution lidar during FIRE N91-10458
Interpretation of the optical and morphological properties of Cirrus clouds from lidar measurements N91-10483
Morphological examination of rat adrenal glands following flight aboard Biosputnik Kosmos-1667 N91-10553
Protective functions of skin N91-10555

**MOTION PERCEPTION**
Role of orientation reference selection in motion sickness
[NASA-CR-186612] N91-10591

**MOTION SICKNESS**
Effects of rolling motion on the circadian rhythm of sinoatrial node N91-10558
Requirements for an ideal drug for preventing space motion sickness N91-10566
Role of orientation reference selection in motion sickness
[NASA-CR-186612] N91-10591

**MOTION SIMULATION**
Configuration, function and performance of the flight simulation test facility and its motion simulation system
[NAL-TM-575] N91-10080

**MOTION SIMULATORS**
Configuration, function and performance of the flight simulation test facility and its motion simulation system
[NAL-TM-575] N91-10080

**MSAT**
A Mobile Satellite Experiment (MSAT-X) network definition
[NASA-CR-187336] N91-10105

**MULTIGRID METHODS**
Numerical solutions of rotating disc flows using a non-linear multigrid algorithm
[PNR-90679] N91-10259

**MULTIPHASE FLOW**
AFDM: An Advanced Fluid-Dynamics Model. Volume 1: Scope, approach, and summary
[DE90-016723] N91-10239

**MULTIPLEXING**
A new method for doing flat-field intensity calibrations of multiplexed ITT streak cameras
[DE90-016475] N91-10267

**MULTIPROCESSING (COMPUTERS)**
A manual for PARTI runtime primitives
[NASA-CR-187442] N91-10599
Multiprocessors and runtime compilation
[NASA-CR-182100] N91-10600
Workshop on Massively Parallel Computing in Magnetic Fusion Energy
[DE90-018009] N91-10650

**MULTISPECTRAL PHOTOGRAPHY**
Cloud altitude determination from infrared spectral radiances N91-10474

**MULTISTAGE ROCKET VEHICLES**
Hybrid propulsion technology program: Phase 1, volume 1
[NASA-CR-183972] N91-10111

**MULTIVARIATE STATISTICAL ANALYSIS**
Density estimation using optimally quantized histograms
[PB90-190588] N91-10686
Multivariate tau-estimators for location and scatter
[REPT-90-04] N91-10688

**MUON SPIN ROTATION**
Muon SR and high T(sub c) superconductivity
[DE90-015089] N91-10760

**MUSCLES**
Work, exercise, and space flight. 3: Exercise devices and protocols N91-10579
A unique problem of muscle adaptation from weightlessness: The deceleration deficiency N91-10582
Exercise issues related to the neuromuscular function and adaptation to microgravity N91-10584
Considerations for an exercise prescription N91-10585
Cardiovascular group N91-10587

**MUSCULAR TONUS**
Cardiovascular group N91-10587

**MUSCULOSKELETAL SYSTEM**
Workshop on Exercise Prescription for Long-Duration Space Flight
[NASA-CP-3051] N91-10574
Space medicine considerations: Skeletal and calcium homeostasis N91-10580
Changes in mineral metabolism with immobilization/space flight N91-10581
Biomedical perspectives on locomotion in null gravity N91-10583
Summary and recommendations for initial exercise prescription N91-10588

## N

**N-TYPE SEMICONDUCTORS**
Ion-assisted doping of 2-6 compounds during physical vapor deposition
[DE90-000358] N91-10756

**NARROWBAND**
Fast estimation of the variance of a narrowband process
[IFSI-90-16] N91-10209

**NASA PROGRAMS**
Development and application of linear and nonlinear methods for interpretation of lightning strikes to in-flight aircraft
[NASA-CR-3974] N91-10548

**NASTRAN**
Comparison of NASTRAN analysis with ground vibration results of UH-60A NASA/AEFA test configuration
[NASA-CR-184565] N91-10333
**NATIONAL AIRSPACE SYSTEM**
DOD responsibilities on Federal aviation and national airspace system matters
[PB90-218827] N91-10001
National airspace system: In-flight assistance operational concept
[PB90-233115] N91-10032
**NATURAL GAS**
Measurements of coefficients of discharge for concentric flange-tapped square-edged orifice meters in natural gas over the Reynolds number range 25,000 to 16,000,000
[PB90-219601] N91-10231
**NAVIER-STOKES EQUATION**
User's guide to CUNIFLOW
[AD-A207606] N91-10004
Prediction and comparison with measurements of the aerodynamic characteristics of flare-stabilized XM910 prototypes
[AD-A208099] N91-10005
Numerical computation of viscous flow about unconventional airfoil shapes
[NASA-CR-187343] N91-10019
A contribution to the numerical solution of transonic flow around a delta wing by solving Navier-Stokes equations
[DLR-FB-90-13] N91-10026
Numerical investigations in three-dimensional internal flows
[NASA-CR-186958] N91-10083
A three-dimensional turbulent heat transfer analysis for advanced tubular rocket thrust chambers
[NASA-TM-103293] N91-10249
Computation of boundary layer flow using thin-layer Navier-Stokes equations with flux-vector splitting
[REPT-B-21] N91-10254
On the convergence at infinity, rate of convergence and uniqueness of solutions with finite Dirichlet integral to the exterior Dirichlet problem for the steady plane Navier-Stokes system of equations
[PREPRINT-166] N91-10257
**NEAR FIELDS**
Contribution to the study of the electromagnetic field radiation close to electronics circuits
[ECL-90-12] N91-10211
**NEAR INFRARED RADIATION**
Near infrared radiances observed by the UK C130 multi-channel radiometer during the marine stratocumulus IFO and preliminary comparison with model calculations
N91-10525
FIRE extended time/limited area observations at Palisades, New York N91-10527
**NEGATIVE ELECTRON AFFINITY**
A correlation between T(sub 3) and electronegativity difference in high-temperature superconductors
[DE90-016640] N91-10775
**NEGATIVE FEEDBACK**
First order oscillators
[ETN-90-97758] N91-10226
The effects of cloud radiative forcing on an ocean-covered planet N91-10456
**NEGATIVE IONS**
Direct extraction of a Na(-) beam from a sodium plasma
[NIFS-35] N91-10751
**NEPHANALYSIS**
VTR loop movie N91-10367
**NETHERLANDS**
Spectra and gradients of stormy winds at Cabauw, Netherlands, up to 200 meters high
[KNMI-TR-119] N91-10546
**NETWORK ANALYSIS**
Prediction and control of chaotic processes using nonlinear adaptive networks
[DE90-016505] N91-10697
**NETWORK CONTROL**
Labeling problems in truth maintenance systems
[REPT-89-90] N91-10651
**NEUMANN PROBLEM**
Quadrature imposition of compatibility conditions in Chebyshev methods
[NASA-CR-187458] N91-10251
**NEUROMUSCULAR TRANSMISSION**
Exercise issues related to the neuromuscular function and adaptation to microgravity N91-10584
**NEUTRAL ATMOSPHERES**
Neutral winds derived from IRI parameters and from the HWM87 wind model for the sundial campaign of September, 1986
[NASA-TM-103445] N91-10543
**NEUTRAL BUOYANCY SIMULATION**
The design and fabrication of the Centaur neutral buoyancy trainer and related hardware
[NASA-CR-171944] N91-10085
**NEUTRON COUNTERS**
Multiple channel programmable coincidence counter
[DE90-014681] N91-10602
**NEUTRON DIFFRACTION**
On the effects of magnetic bonding in rare earth transition metal intermetallics
[DE90-015800] N91-10156
**NEUTRON FLUX DENSITY**
Plots of the 5-minute neutron monitor intensity and multiplicities recorded by the Rome 17-NM64, March 1990
[IFSI-90-15] N91-10833
Plots of the 5-minute neutron monitor intensity and multiplicities recorded by the Rome 17-NM64, April 1990
[IFSI-90-18] N91-10834
Cosmic-ray intensity increase observed on September 29, 1989: The Chilean neutron monitor data (brief report)
[IFSI-90-4] N91-10838
**NEUTRON IRRADIATION**
Radiation-induced noise in Charge-Coupled Device (CCD) and Charge-Injection Device (CID) imagers
[DE90-016724] N91-10777
Plots of the 5-minute neutron monitor intensity and multiplicities recorded by the Rome 17-NM64, March 1990
[IFSI-90-15] N91-10833
Plots of the 5-minute neutron monitor intensity and multiplicities recorded by the Rome 17-NM64, April 1990
[IFSI-90-18] N91-10834
**NEUTRON SPECTROMETERS**
Plots of the 5-minute neutron monitor intensity and multiplicities recorded by the Rome 17-NM64, March 1990
[IFSI-90-15] N91-10833
Plots of the 5-minute neutron monitor intensity and multiplicities recorded by the Rome 17-NM64, April 1990
[IFSI-90-18] N91-10834
**NEUTRONS**
Cosmic-ray intensity increase observed on September 29, 1989: The Chilean neutron monitor data (brief report)
[IFSI-90-4] N91-10838
**NEWTON METHODS**
A potential reduction method for a class of smooth convex programming problems
[REPT-90-01] N91-10636
**NICKEL**
Brittle fracture and ductility improvement in nickel and iron aluminides
[DE90-017319] N91-10167
**NICKEL ALLOYS**
High temperature cyclic oxidation data. Part 1: Turbine alloys
[NASA-TM-83665] N91-10149
High-temperature cyclic oxidation data. Part 2: Turbine alloys
[NASA-TM-101468] N91-10150
Weldability of nickel and iron aluminides
[DE90-013498] N91-10153
A weldability study of Haynes Alloy no. 242
[DE90-013875] N91-10154
Mechanical and microstructural response of Ni3Al at high strain rate and elevated temperatures
[DE90-016489] N91-10162
Casting alloys for the jet age
[PNR-90723] N91-10168
**NIGHT**
Aircraft measurements of the mean and turbulent structure of marine stratocumulus clouds during FIRE
N91-10514
Energetics of valley and basin atmospheres during the evening transition and nighttime periods
[DE90-016356] N91-10542
**NIOBIUM ALLOYS**
Strength and toughness of single-phase and dual-phase high-temperature intermetallics
[DE90-017192] N91-10166
**NITROGEN COMPOUNDS**
Constant stress of XD (trademark) TiAl containing nitrogen
[DE90-011947] N91-10158
**NOBLE METALS**
Characterization of mono- and multi-molecular assemblies at glassy carbon and noble metals by ex situ and in situ infrared external reflection spectroscopy
[DE90-016417] N91-10144
**NOISE (SOUND)**
The development of interior noise and vibration criteria
[NASA-TM-102736] N91-10702
**NOISE GENERATORS**
Signal detection in non-Gaussian and non-white noise
N91-10200
**NOISE INTENSITY**
Properties of acoustic energy quantities
[DE90-518714] N91-10701
**NOISE MEASUREMENT**
Helicopter far-field acoustic levels as a function of reduced main-rotor advancing blade-tip Mach number
[NASA-TM-102684] N91-10699
Aeroacoustic effects of reduced aft tip speed at constant thrust for a model counterrotation turboprop at takeoff conditions
[NASA-TM-103608] N91-10703
Do we really need 57 ways of rating aircraft noise
[PNR-90720] N91-10704
**NOISE POLLUTION**
Re-engining: Real stage 3 compliance plus other benefits
[PNR-90755] N91-10075
Do we really need 57 ways of rating aircraft noise
[PNR-90720] N91-10704
**NOISE PREDICTION (AIRCRAFT)**
Rotor loads computation using singularity methods and application to the noise prediction
[ISL-PU-301/90] N91-10018
Application of flight path reconstruction algorithms for flight data of helicopter
[NAL-TM-582] N91-10031
**NOISE PROPAGATION**
Properties of acoustic energy quantities
[DE90-518714] N91-10701
**NOISE REDUCTION**
The actuator for the low-noise STOL test plane flight control system and its development test
[NAL-TM-574] N91-10038
The full-body ground vibration tests using the low-noise STOL test plane
[NAL-TM-576] N91-10077
Multiple widths yield reliable finite differences
[OUEL-1827/90] N91-10646
Structural acoustics: An applied science with many applications
[PB90-183633] N91-10698
Properties of acoustic energy quantities
[DE90-518714] N91-10701
Radiation-induced noise in Charge-Coupled Device (CCD) and Charge-Injection Device (CID) imagers
[DE90-016724] N91-10777
**NOISE SPECTRA**
Signal detection in non-Gaussian and non-white noise
N91-10200
**NONDESTRUCTIVE TESTS**
Composite heat damage. Part 1: Mechanical testing of IM6/3501-6 laminates. Part 2: Nondestructive evaluation studies of IM6/3501-6 laminates
[DE90-016207] N91-10125
Physical interpretation and application of principles of ultrasonic nondestructive evaluation of high-performance materials
[NASA-CR-180489] N91-10293
Eddy current inspection of graphite fiber components
[NASA-TM-103514] N91-10294
Structural integrity assessment of concrete slabs by nondestructive examination and Fourier transform-infrared methods
[DE90-017233] N91-10296
Evaluation of nondestructive evaluation techniques for determination of flawed conditions and the effects of flaws on the burst pressure in Kevlar-epoxy filament-wound spherical test specimens
[DE90-014839] N91-10330
**NONLINEAR EQUATIONS**
Lobe area in adiabatic Hamiltonian systems
[DE90-016566] N91-10663
**NONLINEAR FEEDBACK**
Nonlinear feedback control for high alpha flight
[NASA-CR-186545] N91-10047
**NONLINEAR OPTICS**
Polarization modulated solitary waves in an optical fiber
[DE90-015034] N91-10715
Nonlinear optics and nonlinear dynamics
[DE90-015975] N91-10716
Order and chaos in polarized nonlinear optics
[DE90-016717] N91-10721
Nonlinear optical absorption in intrinsic Stark effect superlattices
[DE90-016466] N91-10767
**NONLINEAR SYSTEMS**
Numerical solutions of rotating disc flows using a non-linear multigrid algorithm
[PNR-90679] N91-10259
Computation of maximum gust loads in nonlinear aircraft using a new method based on the matched filter approach and numerical optimization N91-10317

**NONLINEARITY**
The inviscid secondary instability of fully nonlinear longitudinal vortex structures in growing boundary layers
[NASA-CR-187455] N91-10021
The 'optimum' upwind advection on a triangular mesh
[NASA-CR-187459] N91-10250
Computation of maximum gust loads in nonlinear aircraft using a new method based on the matched filter approach and numerical optimization N91-10317
Prediction and control of chaotic processes using nonlinear adaptive networks
[DE90-016505] N91-10697
Estimation of astronomical images from the bispectrum of atmospherically distorted infrared data N91-10806
**NONUNIFORM FLOW**
User's guide to CUNIFLOW
[AD-A207606] N91-10004
**NOTCH TESTS**
A macro-micromechanics analysis of a notched metal matrix composite
[NASA-TM-102728] N91-10128
**NOTCHES**
A macro-micromechanics analysis of a notched metal matrix composite
[NASA-TM-102728] N91-10128
**NOVA LASER SYSTEM**
Damage assessment and possible damage mechanisms to 1-meter diameter Nova turning mirrors
[DE90-016473] N91-10278
**NOZZLE FLOW**
Detailed heat transfer measurements in nozzle guide vane passages in linear and annular cascades in the presence of secondary flows
[PNR-90706] N91-10260
An investigation of secondary flows in nozzle guide vanes
[PNR-90739] N91-10262
**NOZZLE GEOMETRY**
An investigation of secondary flows in nozzle guide vanes
[PNR-90739] N91-10262
**NUCLEAR EXPLOSION EFFECT**
Large blast and thermal simulator advanced concept driver design by computational fluid dynamics
[AD-A211364] N91-10230
**NUCLEAR FUELS**
Pellet injector development at ORNL (Oak Ridge National Laboratory)
[DE90-017024] N91-10742
**NUCLEAR FUSION**
Workshop on Massively Parallel Computing in Magnetic Fusion Energy
[DE90-018009] N91-10650
Theoretical atomic physics for fusion
[DE90-017280] N91-10710
**NUCLEAR MAGNETIC RESONANCE**
Copper NMR and hole depletion in the normal state of Y(1-x)Pr(x)Ba2Cu3O7
[DE90-016468] N91-10768
**NUCLEAR MODELS**
Nuclear structure calculations for astrophysical applications
[DE90-016433] N91-10818
**NUCLEAR PARTICLES**
Pre-equilibrium emission and multifragmentation in heavy ion collisions
[LUIP-8902] N91-10705
**NUCLEAR REACTIONS**
Numerical models of beam dynamics in ion induction linacs
[DE90-017043] N91-10713
**NUCLEAR REACTORS**
Statistical characterization of a mode-stirred chamber
[DE90-014860] N91-10202
Artificial intelligence, human factors, robotics, and computer simulation
[DE90-016866] N91-10653
**NUCLEAR STRUCTURE**
Nuclear structure calculations for astrophysical applications
[DE90-016433] N91-10818
**NUCLEATION**
Cirrus cloud model parameterizations: Incorporating realistic ice particle generation N91-10453
False-vacuum decay in generalized extended inflation
[NASA-CR-186419] N91-10695
**NUCLEON-NUCLEON INTERACTIONS**
Theoretical studies in few-body intermediate energy physics
[DE90-017279] N91-10709
**NUMERICAL ANALYSIS**
Boundary-layer receptivity due to a wall suction and control of Tollmien-Schlichting waves
[NASA-CR-182103] N91-10009
**NUMERICAL WEATHER FORECASTING**
Cloud motion wind N91-10365
Q-vectors: A new approach to an old problem
[PB90-235490] N91-10414
**NYQUIST DIAGRAM**
Bounded-error data, and frequency response design
[OUEL-1766/89] N91-10683

**O**

**O STARS**
Fundamental properties and mass loss in hot, near-main sequence stars N91-10821
**OBSERVATION**
Cloud information for FIRE from surface weather reports N91-10452
Models of the human observer and controller of a dynamic system
[ETN-90-97759] N91-10597
**OBSTACLE AVOIDANCE**
Planning of the paths for manipulation robots
[ETN-90-97826] N91-10291
**OCTAHEDRONS**
Generating all 3-connected 4-regular planar graphs from the octahedron graph
[MEMO-854] N91-10678
**ONE DIMENSIONAL FLOW**
A computational model for z-pinch plasma channels N91-10730
**OPERATING SYSTEMS (COMPUTERS)**
Network, system, and status software enhancements for the autonomously managed electrical power system breadboard. Volume 3: Commands specification
[NASA-CR-185882] N91-10620
Converting from VMS to ULTRIX
[PB90-220310] N91-10622
**OPERATIONS RESEARCH**
Pseudo-monotone complementarity problems in Hilbert space
[DE90-016310] N91-10660
**OPERATOR PERFORMANCE**
Operational evaluation of initial data link air traffic control services. Volume 2: Appendices
[DOT/FAA/CT-90/1-VOL-2] N91-10033
The effects of outcome and process feedback
[NASA-CR-187332] N91-10595
**OPERATORS (MATHEMATICS)**
Operator formalism of multi-pole Virasoro algebra on Riemann sphere
[DE90-627217] N91-10657
**OPTICAL COMMUNICATION**
Influence of the telescope depointing on the performances of an optical link. Correlation between depointing law and coding, concerning the computation of mean BER
[CNES-CT/DRT/TIT/TR-88/24-T] N91-10206
**OPTICAL FIBERS**
Polarization modulated solitary waves in an optical fiber
[DE90-015034] N91-10715
**OPTICAL FILTERS**
Holographic rugate structures for x ray optics applications
[DE90-017103] N91-10270
**OPTICAL MEASUREMENT**
An analysis of the effects of secondary reflections on dual-frequency reflectometers
[NASA-TM-102709] N91-10221
Design of highly concentrating solar collectors and solar collector systems
[DLR-FB-90-11] N91-10390
**OPTICAL MEASURING INSTRUMENTS**
Development, characterization, and applications of optical pH sensors supported at cellulosic film
[DE90-016416] N91-10146
Laser Doppler velocimetry using diode lasers
[ISBN-90-9002803-X] N91-10285
**OPTICAL PROPERTIES**
Characterization of mono- and multi-molecular assemblies at glassy carbon and noble metals by ex situ and in situ infrared external reflection spectroscopy
[DE90-016417] N91-10144
Evaluation of nondestructive evaluation techniques for determination of flawed conditions and the effects of flaws on the burst pressure in Kevlar-epoxy filament-wound spherical test specimens
[DE90-014839] N91-10330
Optical and morphological properties of Cirrus clouds determined by the high spectral resolution lidar during FIRE N91-10458
Subvisual Cirrus cloud properties derived from a FIRE IFO case study N91-10464
Interpretation of the optical and morphological properties of Cirrus clouds from lidar measurements N91-10483
Nonlinear optical absorption in intrinsic Stark effect superlattices
[DE90-016466] N91-10767
**OPTICAL PUMPING**
Sodium-neon resonant photoexcitation soft x ray laser experiments on Saturn
[DE90-014946] N91-10275
**OPTICAL RADAR**
A synopsis of Langley Research Center's lidar effort for the 1986 FIRE IFO N91-10457
Optical and morphological properties of Cirrus clouds determined by the high spectral resolution lidar during FIRE N91-10458
Lidar and aircraft studies of deep Cirrus systems from the 1986 FIRE IFO N91-10460
Lidar and radiometer results from the ER-2 for the FIRE field experiments N91-10468
A four-lidar view of Cirrus from the FIRE IFO: 27-28 October 1986 N91-10478
The new FIRE cloud lidar at Langley Research Center N91-10482
Interpretation of the optical and morphological properties of Cirrus clouds from lidar measurements N91-10483
Both sides now N91-10485
A study of marine stratocumulus using lidar and other FIRE aircraft observations N91-10511
Aircraft measurements of the mean and turbulent structure of marine stratocumulus clouds during FIRE N91-10514
ER-2 lidar measurements of stratocumulus cloud top structure on July 14, 1987 N91-10523
Plume mechanics and stratocumulus convection N91-10526
Comparison and calibration of NCAR electra instruments: July 5 and 7, 1987 N91-10532
**OPTICAL SCANNERS**
Preliminary results of radiation measurements from the marine stratus FIRE experiment N91-10529
**OPTICAL THICKNESS**
Multi-spectral window radiance observations of Cirrus from satellite and aircraft, November 2, 1986 Project FIRE N91-10465
Cirrus cloud statistics: Temperatures and optical depths N91-10466
Cloud optical parameters as derived from the multispectral cloud radiometer N91-10513
Horizontal variability of the marine boundary layer structure upwind of San Nicolas Island during FIRE, 1987 N91-10519
FIRE extended time/limited area observations at Palisades, New York N91-10527
**OPTICAL TRACKING**
Image motion experiments with the Oxford AGV
[OUEL-1809/90] N91-10654
**OPTICS**
Variable-coherence beam optics
[ISBN-952-90-1784-7] N91-10724
**OPTIMAL CONTROL**
Nonlinear feedback control for high alpha flight
[NASA-CR-186545] N91-10047
Discounted dynamic programming. Part 3: Successive approximation
[TW-89-14-PT-3] N91-10640
**OPTIMIZATION**
Future supersonic transport populsion optimization
[PNR-90737] N91-10071
Optimization criteria for the design of orbital replacement units
[MBB-UO-0092-90-PUB] N91-10109
Global optimization methods for engineering design N91-10310
Exponential approximations in optimal design N91-10311
Combined design of structures and controllers for optimal maneuverability N91-10314
Computation of maximum gust loads in nonlinear aircraft using a new method based on the matched filter approach and numerical optimization N91-10317
Materials analysis and device optimization of CuInSe2 solar cells
[DE90-000365] N91-10384
Fully automatic analysis in an industrial environment
[PNR-90722] N91-10647
**ORBIT TRANSFER VEHICLES**
Measured and predicted shock shapes for AFE configuration at Mach 6 in air and in CF4
[NASA-TM-100660] N91-10245
**ORBITAL LIFETIME**
Long-term orbital lifetime predictions
[NASA-TP-3058] N91-10092
**ORBITAL MECHANICS**
Review of the Cluster orbit and separation strategy: Consequence for measurements N91-10420
Configurational sensitivity of multipoint magnetic field measurements N91-10421
**ORBITS**
Lobe area in adiabatic Hamiltonian systems
[DE90-016566] N91-10663

**ORGANIC MATERIALS**
Organic getter materials for the removal of hydrogen and its isotopes
[DE90-016284] N91-10185
**ORGANOMETALLIC COMPOUNDS**
Organometallic chemistry of bimetallic compounds
[DE90-017601] N91-10121
**ORIENTATION**
Optimum orientations of the observation axes for 2-dimensional vector sensing under consideration of bias errors
[NAL-TR-1055] N91-10679
**ORIFICE FLOW**
Measurements of coefficients of discharge for concentric flange-tapped square-edged orifice meters in natural gas over the Reynolds number range 25,000 to 16,000,000
[PB90-219601] N91-10231
The 3-D laser anemometer study of compressible flow through orifice plates
[PB90-216771] N91-10273
**ORTHOGONALITY**
On q-analogues of the Fourier and Hankel transforms
[REPT-89-89] N91-10666
**ORTHONORMAL FUNCTIONS**
The development of the continuous orthonormalization and adjoint methods for solar seismology: Eigenfrequency computation and sensitivity analysis for direct and inverse problems N91-10827
**OSCILLATING FLOW**
Mass transfer in oscillating flows: Efficient drying via pulse combustors
[PB90-242389] N91-10235
**OSCILLATIONS**
The development of the continuous orthonormalization and adjoint methods for solar seismology: Eigenfrequency computation and sensitivity analysis for direct and inverse problems N91-10827
**OSCILLATORS**
Minimizing frequency pulling of quartz oscillators due to power supply variations
[DE90-014566] N91-10218
First order oscillators
[ETN-90-97758] N91-10226
**OXIDATION**
High temperature cyclic oxidation data. Part 1: Turbine alloys
[NASA-TM-83665] N91-10149
High-temperature cyclic oxidation data. Part 2: Turbine alloys
[NASA-TM-101468] N91-10150
**OXIDES**
Basic study of solid oxide fuel cells
[DE90-517069] N91-10386
**OXIDIZERS**
Hybrid propulsion technology program: Phase 1, volume 4
[NASA-CR-183975] N91-10114
**OXYGEN**
Specific impulse comparison of high density hydrocarbon fuel burned with oxygen
[NAL-TR-1053] N91-10148
A miniature inexpensive, oxygen sensing element
[DE90-014080] N91-10269
**OXYGEN TENSION**
Changes in maximum allowable supersaturation coefficient in high-altitude decompression N91-10560
**OZONE**
Global tropospheric chemistry modeling
[DE90-015908] N91-10409
**OZONE DEPLETION**
Atmospheric ozone 1985: Assessment of our understanding of the processes controlling its present distribution and change, volume 3
[NASA-TM-103462] N91-10393
Geophysical monitoring for climatic change
[PB90-222126] N91-10538

**P**

**P-TYPE SEMICONDUCTORS**
Ion-assisted doping of 2-6 compounds during physical vapor deposition
[DE90-000358] N91-10756
**PALEOMAGNETISM**
The scientific case for magnetic field satellites
[NASA-CR-186532] N91-10101
**PANEL METHOD (FLUID DYNAMICS)**
Three-dimensional viscous/inviscid coupling in subsonic flow
[REPT-B-24] N91-10023
Calculation of three-dimensional viscous/inviscid interaction in subsonic flow
[REPT-B-25] N91-10024
The numerical simulation of nonlinear gravity waves in three dimensions using a higher order panel method
[ISBN-90-9002667-23] N91-10443
**PANELS**
Test/semi-empirical analysis of a carbon/epoxy fabric stiffened panel N91-10302
Repeated buckling of composite shear panels
N91-10303
**PARABOLIC ANTENNAS**
Evaluation of alternatives for best-fit paraboloid for deformed antenna surfaces N91-10313
**PARABOLIC DIFFERENTIAL EQUATIONS**
Spectral methods for time dependent problems
[NASA-CR-187443] N91-10664
Strong maximum principles for systems
[REPT-90-37] N91-10671
**PARABOLIC REFLECTORS**
Design of highly concentrating solar collectors and solar collector systems
[DLR-FB-90-11] N91-10390
**PARALLEL COMPUTERS**
Architecture simulator of parallel computer
[NAL-TM-583] N91-10601
**PARALLEL FLOW**
Anomalous viscosity due to drift wave turbulence
[NIFS-33] N91-10752
**PARALLEL PROCESSING (COMPUTERS)**
Massively parallel computing system
[DE90-014683] N91-10648
Workshop on Massively Parallel Computing in Magnetic Fusion Energy
[DE90-018009] N91-10650
Parallel inference and communication process for Horn clause. First order extension by connection method
[ETN-90-97825] N91-10652
**PARALLEL PROGRAMMING**
A conservative approach to parallelizing the Sharks World simulation
[NASA-CR-187440] N91-10629
Parallel inference and communication process for Horn clause. First order extension by connection method
[ETN-90-97825] N91-10652
**PARAMETER IDENTIFICATION**
Flight characteristics of a modified Schweizer SGS1-36 sailplane at low and very high angles of attack
[NASA-TP-3022] N91-10079
First evaluation of the main parameters in the dynamics of the Small Expendable Deployer System (SEDS) for a tethered satellite
[NASA-CR-4319] N91-10098
**PARAMETERIZATION**
FIRE Science Results 1988
[NASA-CP-3083] N91-10448
Cirrus cloud model parameterizations: Incorporating realistic ice particle generation N91-10453
A GCM parameterization for the shortwave radiative properties of water clouds N91-10494
Dependence of marine stratocumulus reflectivities on liquid water paths N91-10524
Parameterization of cosmological scale factor during inflationary times N91-10815
**PARTIAL DIFFERENTIAL EQUATIONS**
The cousin problems in the viewpoint of partial differential equations
[DE90-627172] N91-10656
**PARTICLE ACCELERATION**
Acceleration by pulsar winds in binary systems
[NASA-TM-103451] N91-10816
**PARTICLE BEAMS**
Prompt lepton production in a proton beamdump experiment
[ETN-90-97750] N91-10711
Plasma wakefield excitation by charge particle beams
N91-10729
**PARTICLE COLLISIONS**
Pre-equilibrium emission and multifragmentation in heavy ion collisions
[LUIP-8902] N91-10705
Theoretical atomic physics for fusion
[DE90-017280] N91-10710
**PARTICLE EMISSION**
Heavy duty liquid and gaseous fuel emissions database test results from four alternative fuel configurations of the Caterpillar 3406 engine
[DE90-014783] N91-10288
Pre-equilibrium emission and multifragmentation in heavy ion collisions
[LUIP-8902] N91-10705
**PARTICLE ENERGY**
The Joint NASA/Goddard-University of Maryland Research Program in Charged Particle and High Energy Photon Detector Technology
[NASA-CR-180335] N91-10810
**PARTICLE IN CELL TECHNIQUE**
Plasma wakefield excitation by charge particle beams
N91-10729
Electromagnetic particle codes on unstructured grids
[DE90-015187] N91-10733
**PARTICLE MASS**
Dijet spectroscopy at high luminosity
[DE90-016901] N91-10147
**PARTICLE MOTION**
Theory of longitudinal adiabatic invariant in the helical torus
[NIFS-37] N91-10749
**PARTICLE SIZE DISTRIBUTION**
Cirrus microphysics and radiative transfer: A case study N91-10463
Subvisual Cirrus cloud properties derived from a FIRE IFO case study N91-10464
**PARTICLE TRACKS**
Particle displacement tracking for PIV
[NASA-TM-103288] N91-10271
**PARTICLE TRAJECTORIES**
Features of mid-tail ion trajectories during substorms
N91-10435
**PARTICLES**
A Knudsen layer theory for lattice gases
[ETN-90-97583] N91-10248
Symmetries of the three body problem
[MEMO-843] N91-10674
**PARTICULATES**
Global tropospheric chemistry modeling
[DE90-015908] N91-10409
**PASSENGERS**
The development of interior noise and vibration criteria
[NASA-TM-102736] N91-10702
**PASSIVITY**
Corrosion, passivity, and breakdown of alloys used in high energy density batteries
[DE90-016648] N91-10223
**PATTERN RECOGNITION**
Density estimation using optimally quantized histograms
[PB90-190588] N91-10686
**PATTERN REGISTRATION**
Some defects in finite-difference edge finders
[OUEL-1826/90] N91-10645
Multiple widths yield reliable finite differences
[OUEL-1827/90] N91-10646
Digital image integration technique of multiple geoscience information system and its application
[DE90-627893] N91-10801
**PAYLOADS**
Preliminary studies before defining a payload adapted to the primate model
[ETN-90-97581] N91-10107
Ground test program for new Atlas payload fairings
N91-10315
Studies of the system-environment interaction by electron beam emission from a sounding rocket payload in the ionosphere N91-10410
Specific tasks of Regatta-E measurements correlated with Cluster/Regatta-A in the ISTP and Regatta programmes N91-10436
**PCM TELEMETRY**
Telemetry subsystem N91-10345
**PEELING**
The looped adhesive strip: An example of coplanar delamination interaction N91-10306
**PELLETS**
Pellet injector development at ORNL (Oak Ridge National Laboratory)
[DE90-017024] N91-10742
**PENDULUMS**
Lobe area in adiabatic Hamiltonian systems
[DE90-016566] N91-10663
**PENETRATION**
Determination of surface resistance and magnetic penetration depth of superconducting YBa2Cu3O(7-delta) thin films by microwave power transmission measurements
[NASA-TM-103616] N91-10780
**PERFLUOROALKANE**
Evaluation of available perfluorobutane data for selected physical properties
[DE90-016516] N91-10145
**PERFORATED PLATES**
The 3-D laser anemometer study of compressible flow through orifice plates
[PB90-216771] N91-10273
**PERFORMANCE PREDICTION**
Progress in certifying F402-RR-408: The improved Pegasus engine for AV-8B and Harrier 2 plus
[PNR-90719] N91-10056
Long-term orbital lifetime predictions
[NASA-TP-3058] N91-10092
**PERFORMANCE TESTS**
Characteristics of piping interference elimination unit used in the high-speed wind tunnel test of ASUKA seven percent semi-born prototype
[NAL-TM-588] N91-10003

The establishment and performance test of PAPI (Precision Approach Path Indicator) System for NAL STOL aircraft
[NAL-TM-579] N91-10030
The actuator for the low-noise STOL test plane flight control system and its development test
[NAL-TM-574] N91-10038
Wind tunnel test of redundant vane-type flow-direction sensing systems
[NAL-TM-590] N91-10057
Specific impulse comparison of high density hydrocarbon fuel burned with oxygen
[NAL-TR-1053] N91-10148
Hydrogen maser: Results of evaluations done by the CNES from May 1986 to December 1987
[CNES-DRT/TIT/TF-88/338-T] N91-10284
Materials analysis and device optimization of CuInSe2 solar cells
[DE90-000365] N91-10364
Architecture simulator of parallel computer
[NAL-TM-583] N91-10601

**PERIODIC VARIATIONS**
Analyzing long time series of hydrological data with respect to climate variability: Project description
[WCAP-3] N91-10444

**PEROVSKITES**
Methane conversion by solid electrolyte membranes
[PB90-226341] N91-10381

**PERTURBATION THEORY**
Cosmological singularities in electrovacuum spacetimes with two-parameter spacelike isometry groups
N91-10811

**PH**
Development, characterization, and applications of optical pH sensors supported at cellulosic film
[DE90-016416] N91-10146

**PHARMACOLOGY**
JPRS report: Science and technology. USSR: Life sciences
[JPRS-ULS-90-001] N91-10551

**PHASE MATCHING**
Anomalous dispersion as a phase-matching technique for second harmonic generation
[DE90-015696] N91-10172

**PHASE SHIFT**
Theoretical studies in few-body intermediate energy physics
[DE90-017279] N91-10709

**PHASE SHIFT KEYING**
Modelization of LOCSTAR synchronisation system. Computation of non detection and false alarm probabilities. Reflections on threshold adjustment and correlator structure
[CNES-CT/DRT/TIT/TR-88/060] N91-10691

**PHASE TRANSFORMATIONS**
The influence of shock pre-strain and peak pressure on spall behavior of 4340 steel
[DE90-016612] N91-10164
About antiferromagnetic Heisenberg models
[ETN-90-97768] N91-10784

**PHASE-SPACE INTEGRAL**
On the structure of quantum phase space
[DE90-627185] N91-10786

**PHASED ARRAYS**
Cluster as a wave telescope N91-10424

**PHOSPHORIC ACID FUEL CELLS**
The physical and chemical state of Westinghouse Phosphoric Acid Fuel Cell assemblies after long term operation: Surface and near-surface analysis
[DE90-015055] N91-10382

**PHOTODISSOCIATION**
Time-resolved FTIR (Fourier Transform Infrared) emission studies of laser photofragmentation and chain reactions
[DE90-017223] N91-10722

**PHOTOMAPPING**
Cloud altitude determination from infrared spectral radiances N91-10474

**PHOTOMETERS**
Development, characterization, and applications of optical pH sensors supported at cellulosic film
[DE90-016416] N91-10146

**PHOTOMETRY**
Estimated accuracy of ground-based liquid water measurements during FIRE N91-10506
Bicolored photometry and spectral accommodation in X-ray region of mass impregnated stellar X-ray binaries
[MPE-219] N91-10808

**PHOTOMULTIPLIER TUBES**
MicroChannel Plate detectors (MCP)
[CNES-CT/DRT/TIT/OE-88/037-T] N91-10227

**PHOTONS**
The technique of Cerenkov ring image detection
[ETN-90-97747] N91-10714
Localizability in the Hamiltonian formalism and in quantum-mechanics
[DE90-628368] N91-10787
The Joint NASA/Goddard-University of Maryland Research Program in Charged Particle and High Energy Photon Detector Technology
[NASA-CR-180335] N91-10810

**PHOTOSPHERE**
Coaligned observations of solar magnetic fields at different heights: MSFC Center director's discretionary fund final report (Project No. 88-10)
[NASA-TM-103516] N91-10832

**PHYSICAL EXERCISE**
Workshop on Exercise Prescription for Long-Duration Space Flight
[NASA-CP-3051] N91-10574
The history of in-flight exercise in the US manned space program N91-10577
Work, exercise, and space flight. 1: Operations, environment, and effects of spaceflight N91-10578
Work, exercise, and space flight. 3: Exercise devices and protocols N91-10579
Changes in mineral metabolism with immobilization/space flight N91-10581
Biomedical perspectives on locomotion in null gravity N91-10583
Exercise issues related to the neuromuscular function and adaptation to microgravity N91-10584
Considerations for an exercise prescription N91-10585
Work, exercise, and space flight. 2: Modification of adaptation by exercise (exercise prescription) N91-10586
Cardiovascular group N91-10587
Summary and recommendations for initial exercise prescription N91-10588

**PHYSICAL PROPERTIES**
Evaluation of available perfluorobutane data for selected physical properties
[DE90-016516] N91-10145

**PHYSICAL WORK**
Summary and recommendations for initial exercise prescription N91-10588

**PHYSICS**
JPRS report: Science and technology. USSR: Physics and mathematics
[JPRS-UPM-90-003] N91-10694

**PHYSIOLOGICAL EFFECTS**
Preliminary studies before defining a payload adapted to the primate model
[ETN-90-97581] N91-10107
Effects of prolonged exposure to acetic acid vapors on acid-base balance in humans N91-10561
Combined effects of elevated concentrations of carbon dioxide and ambient temperature on thermal state of humans in closed chambers N91-10563

**PHYSIOLOGY**
ELF (extremely-low-frequency): Exposure levels, bioeffects, and epidemiology
[DE90-016554] N91-10573
Cardiovascular group N91-10587

**PHYTOPLANKTON**
Chesapeake Bay Basin Monitoring Program Atlas. Volume 2: Biological and living resource monitoring programs
[PB90-147943] N91-10392

**PIEZOELECTRICITY**
Piezoelectrically forced vibrations of electroded doubly rotated quartz plates by state space method N91-10318

**PILOT PERFORMANCE**
Flight characteristics of a modified Schweizer SGS1-36 sailplane at low and very high angles of attack
[NASA-TP-3022] N91-10079
Psychophysiological assessment of piloting motor habits in pilot retraining N91-10564

**PIPE FLOW**
The 3-D laser anemometer study of compressible flow through orifice plates
[PB90-216771] N91-10273

**PIPELINES**
Evaluation of candidate alloys for the construction of metal flex hoses in the STS launch environment
[NASA-TM-103808] N91-10157

**PISTONS**
Velocity measurements in piston-induced turbulent boundary layers in a shock tube
[ISL-CO-235/89] N91-10247

**PLANAR STRUCTURES**
The looped adhesive strip: An example of coplanar delamination interaction N91-10306
Generating all 3-connected 4-regular planar graphs from the octahedron graph
[MEMO-854] N91-10678

**PLANE STRAIN**
Piezoelectrically forced vibrations of electroded doubly rotated quartz plates by state space method N91-10318

**PLANE WAVES**
Electromagnetic scattering from two-dimensional thick material junctions
[NASA-CR-186976] N91-10201
Localizability in the Hamiltonian formalism and in quantum-mechanics
[DE90-628368] N91-10787

**PLANETARY BOUNDARY LAYER**
Fractional cloudiness in shallow cumulus layers N91-10498

**PLANETARY MAGNETOTAILS**
Specific tasks of multiple scale plasma measurements in Regatta-Cluster system N91-10419

**PLANETARY METEOROLOGY**
Activities report of the World Meteorological Organization
[WMO-734] N91-10547

**PLASMA CONDUCTIVITY**
Models of plasma confinement and heating in tokamaks
[DE90-016671] N91-10741

**PLASMA CONTROL**
A computational model for z-pinch plasma channels N91-10730
Confinement studies in the ZT-40M reversed field pinch
[DE90-016442] N91-10739
Models of plasma confinement and heating in tokamaks
[DE90-016671] N91-10741
Pellet injector development at ORNL (Oak Ridge National Laboratory)
[DE90-017024] N91-10742
Plasma properties
[DE90-017256] N91-10746
Theoretical studies of turbulence and anomalous transport in toroidal confinement devices
[DE90-017606] N91-10747
Theory of longitudinal adiabatic invariant in the helical torus
[NIFS-37] N91-10749

**PLASMA CURRENTS**
Multispacecraft measurement at varying scalelengths: The Cluster/Regatta opportunity N91-10418
On the possibility to support multisatellite measurements of the Cluster mission by single satellite measurements in the Regatta-Cluster project N91-10428
RF helicity injection and current drive
[NIFS-34] N91-10750
Direct extraction of a Na(-) beam from a sodium plasma
[NIFS-35] N91-10751

**PLASMA DENSITY**
On lower hybrid wave scattering by plasma density fluctuation nonlinear reflection coefficient of the fast magnetoacoustic wave
[IPPCZ-281] N91-10725
Comments on edge turbulence during lower hybrid current drive experiment on CASTOR tokamak
[IPPCZ-279] N91-10726

**PLASMA DIAGNOSTICS**
A refractive index gradient (RING) diagnostic for transient discharges or expansions of vapor or plasmas
[DE90-015840] N91-10736

**PLASMA DRIFT**
Tearing modes in tokamaks with lower hybrid current drive
[DE90-017090] N91-10743

**PLASMA DYNAMICS**
A mathematical model of the structure and evolution of small scale discrete auroral arcs
[NASA-CR-187238] N91-10734

**PLASMA EQUILIBRIUM**
Unified theory of ballooning instabilities and temperature gradient driven trapped ion modes
[DE90-017091] N91-10744
Numerical simulation of ion temperature gradient driven modes in the presence of ion-ion collisions
[DE90-017092] N91-10745
Plasma properties
[DE90-017256] N91-10746

**PLASMA FLUX MEASUREMENT**
Multispacecraft measurement at varying scalelengths: The Cluster/Regatta opportunity N91-10418
Properties of large scale plasma flow during the early stage of the plasmaspheric refilling
[NASA-TM-103446] N91-10441

**PLASMA FREQUENCIES**
Passive-filtered and active-driven probes for RF plasmas
[OUEL-1806/89] N91-10754

**PLASMA HEATING**
Comments on edge turbulence during lower hybrid current drive experiment on CASTOR tokamak
[IPPCZ-279] N91-10726
Experiments on linear high beta helical axis stellarators to study simulated toroidal effects and Alfven-wave heating
[DE90-016122] N91-10738
Tilt stability and compression heating studies of field-reversed configurations
[DE90-016443] N91-10740
Models of plasma confinement and heating in tokamaks
[DE90-016671] N91-10741

**PLASMA LAYERS**
Examination of ion acceleration in the plasma layer during magnetospheric partial gales
[MPE-218] N91-10753

**PLASMA OSCILLATIONS**
Self-consistent field error effects in reversed field pinch plasmas N91-10728

**PLASMA PHYSICS**
Plasma waves as a signature of flux transfer events
N91-10427
Theoretical analysis of a runaway electron suppression device
[DE90-015992] N91-10737
Models of plasma confinement and heating in tokamaks
[DE90-016671] N91-10741

**PLASMA RADIATION**
A computational model for z-pinch plasma channels
N91-10730

**PLASMA SHEATHS**
Stellarator theory
[DE90-017607] N91-10748

**PLASMA TURBULENCE**
Experimental constraints in the characterization of a turbulent field from several satellites N91-10425
Comments on edge turbulence during lower hybrid current drive experiment on CASTOR tokamak
[IPPCZ-279] N91-10726

**PLASMA WAVES**
Studies of the system-environment interaction by electron beam emission from a sounding rocket payload in the ionosphere N91-10410
Cluster as a wave telescope N91-10424
Plasma wave measurements on the dayside: Scale sizes and observational requirements N91-10426
Plasma waves as a signature of flux transfer events
N91-10427
On the possibility to support multisatellite measurements of the Cluster mission by single satellite measurements in the Regatta-Cluster project N91-10428
Problems of cold plasma measurements on the Regatta-A spacecraft N91-10431
Multipoint study of small-scale structures at the magnetopause N91-10432
Comments on edge turbulence during lower hybrid current drive experiment on CASTOR tokamak
[IPPCZ-279] N91-10726
Plasma wakefield excitation by charge particle beams
N91-10729
Confinement studies in the ZT-40M reversed field pinch
[DE90-016442] N91-10739

**PLASMAS (PHYSICS)**
Sodium-neon resonant photoexcitation soft x ray laser experiments on Saturn
[DE90-014946] N91-10275
Two-dimensional magnetohydrodynamic equilibria with flow and studies of equilibrium fluctuations N91-10727
Plasma puff initiation of high Coulomb transfer switches
[NASA-CR-187024] N91-10735

**PLASMASPHERE**
Specific tasks of Regatta-E measurements correlated with Cluster/Regatta-A in the ISTP and Regatta programmes N91-10436
Properties of large scale plasma flow during the early stage of the plasmaspheric refilling
[NASA-TM-103446] N91-10441

**PLASTIC PROPERTIES**
Analysis of moving strong discontinuity surfaces in elastic-plastic solids including effects of inertia and finite strain N91-10323

**PLASTICS**
An analytical solution for the elastoplastic response of a continuous fiber composite under uniaxial loading
N91-10305

**PLATES (STRUCTURAL MEMBERS)**
Compressive failure of thick-section composite laminates with and without cutouts subjected to biaxial loading N91-10304
Piezoelectrically forced vibrations of electroded doubly rotated quartz plates by state space method
N91-10318

**PLATINUM**
The physical and chemical state of Westinghouse Phosphoric Acid Fuel Cell assemblies after long term operation: Surface and near-surface analysis
[DE90-015055] N91-10382

**PLOTTERS**
Script: General purpose graphics program; user's manual
[PD-ST-9027] N91-10625

**PLUMES**
Transient characteristics of unconfined fire plume-driven ceiling jets
[PB90-227976] N91-10193
Plume mechanics and stratocumulus convection
N91-10526

**POLAR CUSPS**
Specific tasks of multiple scale plasma measurements in Regatta-Cluster system N91-10419

**POLARIZATION (WAVES)**
Polarization modulated solitary waves in an optical fiber
[DE90-015034] N91-10715

**POLICIES**
Potential effects of global climate change on the United States. Appendix J: Policy
[PB90-173188] N91-10404

**POLISHING**
Microstructural and phase stability studies of nanometer period metal/carbon multilayer structures for x ray optics
[DE90-015307] N91-10129

**POLLUTION CONTROL**
National acid precipitation assessment program. Report to the President and Congress
[PB90-185646] N91-10405
Short-rotation woody crop opportunities to mitigate carbon dioxide buildup
[DE90-016526] N91-10406
Reaction kinetics of the Ca-SO2 system in absence of inter-grain pore diffusion
[DE90-009672] N91-10781

**POLLUTION MONITORING**
Chesapeake Bay Basin Monitoring Program Atlas. Volume 1: Water quality and other physiochemical monitoring programs
[PB90-147935] N91-10391

**POLYESTER RESINS**
Evaluation of composite materials for use on launch complexes
[NASA-TM-103809] N91-10131

**POLYHEDRONS**
Probabilistic structural analysis by extremum methods
N91-10306

**POLYIMIDE RESINS**
Evaluation of two bisimide additives in LARC-TPI adhesive
[NASA-TM-102742] N91-10182

**POLYMER CHEMISTRY**
Optical properties of inorganic polymers
[DE90-017143] N91-10179

**POLYMERIC FILMS**
Development, characterization, and applications of optical pH sensors supported at cellulosic film
[DE90-016416] N91-10146
Monomolecular and thin polymer films: Fabrication, characterization, applications, and models of wetting
[DE90-016415] N91-10174

**POLYNOMIALS**
A potential reduction method for a class of smooth convex programming problems
[REPT-90-01] N91-10636
Chebyshev approximation by spline functions with free knots
[MEMO-853] N91-10677
A remark on the convexity of piecewise polynomial functions on triangulations
[MEMO-857] N91-10682

**POROSITY**
Thermochemistry of shock-induced exothermic reactions in selected porous mixtures
[DE90-016104] N91-10183

**POSITION SENSING**
Experiments and theory with a 0.5 ton mobile robot
[OUEL-1807/90] N91-10035

**POSITIONING**
Magnetic sensitivity of on-board quartz oscillators: State of the knowledge
[CNES-CT/DRT/TIT/TF-88/354] N91-10110
Specific tasks of multiple scale plasma measurements in Regatta-Cluster system N91-10419
Review of the Cluster orbit and separation strategy: Consequence for measurements N91-10420

**POSITIVE FEEDBACK**
First order oscillators
[ETN-90-97758] N91-10226

**POSTFLIGHT ANALYSIS**
Flight set 360L007 (STS-33R) field joint protection system, thermal protection system, and systems tunnel components, volume 7
[NASA-CR-184026] N91-10115
Analysis techniques for residual acceleration data
[NASA-TM-103507] N91-10191

**POTENTIAL THEORY**
A potential reduction method for a class of smooth convex programming problems
[REPT-90-01] N91-10636

**POWDER (PARTICLES)**
Thermochemistry of shock-induced exothermic reactions in selected porous mixtures
[DE90-016104] N91-10183

**POWDER METALLURGY**
Advanced materials for high-temperature solid electrolyte applications
[DE90-016328] N91-10143

**POWER SPECTRA**
On lower hybrid wave scattering by plasma density fluctuation nonlinear reflection coefficient of the fast magnetoacoustic wave
[IPPCZ-281] N91-10725

**PRASEODYMIUM**
Copper NMR and hole depletion in the normal state of Y(1-x)Pr(x)Ba2Cu3O7
[DE90-016468] N91-10768

**PRECIPITATES**
Fibre-matrix reaction zones in model silicon carbide-titanium aluminide metal-matrix composites
[PNR-90713] N91-10137

**PRECIPITATION (METEOROLOGY)**
Satellite-derived index of precipitation intensity
N91-10362
GPCP data processing N91-10370

**PREDICTION ANALYSIS TECHNIQUES**
Measured and predicted shock shapes for AFE configuration at Mach 6 in air and in CF4
[NASA-TM-100660] N91-10245

**PREDICTIONS**
Vibration testing of a 1/5 scale model of H-2 launch vehicle
[NAL-TR-1061] N91-10099
Application of generalized predictive control to a boiler turbine unit for electricity generation
[OUEL-1823/90] N91-10229
Verification of GONO wave predictions for the period October 1987 to April 1988
[KNMI-TR-118] N91-10545
Technique for human-error sequence identification and signification
[ISBN-90-353-10144] N91-10596
Robustness effects of a prefilter in generalized predictive control
[OUEL-1799/89] N91-10685

**PREFLIGHT OPERATIONS**
National Space Transportation System Reference. Volume 2: Operations
[NASA-TM-89785] N91-10100

**PREPROCESSING**
Multiprocessors and runtime compilation
[NASA-CR-182100] N91-10600

**PRESSURE**
Measurement of unsteady blade surface pressure on a single rotation large scale advanced prop-fan with angular and wake inflow at Mach numbers from 0.02 to 0.70
[NASA-CR-182123] N91-10065

**PRESSURE DISTRIBUTION**
Wall interference studies
[PD-CF-9012] N91-10232
The 3-D laser anemometer study of compressible flow through orifice plates
[PB90-216771] N91-10273

**PRESSURE DRAG**
Determination of the pressure drag of airfoils by integration of surface pressures
[NASA-TM-102722] N91-10078

**PRESSURE EFFECTS**
Evaluation of flow quality in newly constructed low-turbulence calibration wind-tunnel for laser velocimeters
[NAL-TR-1054] N91-10087
The influence of shock pre-strain and peak pressure on spall behavior of 4340 steel
[DE90-016612] N91-10164
Design methodology needs for fiber-reinforced ceramic heat exchangers
[DE90-016659] N91-10178

**PRESSURE GRADIENTS**
Two-phase flow patterns and frictional pressure gradients in a small, horizontal, rectangular channel
[DE90-014802] N91-10236
**PRESSURE MEASUREMENT**
Pressure measurements on the release system and determination of jet momentum in the project BA propane field tests 1989
[FOA-E-40044-4.5] N91-10263
**PRESSURE OSCILLATIONS**
The instability of combustion in propulsion engines
N91-10141
**PRESSURE REDUCTION**
Probability of decompression sickness during space suit testing N91-10559
Changes in maximum allowable supersaturation coefficient in high-altitude decompression N91-10560
**PRIORITIES**
Conservative parallel simulation of priority class queueing networks
[NASA-CR-187438] N91-10628
**PROBABILITY DENSITY FUNCTIONS**
Density estimation using optimally quantized histograms
[PB90-190588] N91-10686
**PROBABILITY THEORY**
Technique for human-error sequence identification and signification
[ISBN-90-353-10144] N91-10596
**PROBLEM SOLVING**
Developing a framework for qualitative engineering: Research in design and analysis of complex structural systems N91-10322
The core and the tau-value for cooperative games with coalition structures
[MEMO-848] N91-10692
The development of the continuous orthonormalization and adjoint methods for solar seismology: Eigenfrequency computation and sensitivity analysis for direct and inverse problems N91-10827
**PROCESS CONTROL (INDUSTRY)**
Introduction: Needs and approaches to reliability and quality assurance in design and manufacture
[PNR-90683] N91-10297
**PRODUCT DEVELOPMENT**
Incorporation of the operation safety in the industry and in a product development process inducting subcontractors
[ETN-90-97822] N91-10196
Engineering design: A powerful influence on the business success on manufacturing industry
[PNR-90763] N91-10197
**PRODUCTION MANAGEMENT**
An evaluation of the production processes and methods associated with Carello Cell at RISTS, Telford
[ETN-90-97578] N91-10228
Total quality management at Rolls-Royce PLC
[PNR-90759] N91-10298
**PRODUCTIVITY**
Towards a comprehensive framework for reuse: A reuse-enabling software evolution environment
[UMIACS-TR-88-92] N91-10608
Ada software productivity prototypes: A case study
N91-10613
**PROGRAM VERIFICATION (COMPUTERS)**
Static and dynamic finite element stress analysis of layered composite plates and shells N91-10326
**PROGRAMMING LANGUAGES**
Bidirectional translator between DXF and IGES formats
[DE90-016430] N91-10632
Parallel inference and communication process for Horn clause. First order extension by connection method
[ETN-90-97825] N91-10652
**PROJECT MANAGEMENT**
Multi industry application of advanced materials
[PNR-90764] N91-10139
System engineering of aerospace and advanced technology programs at an astronautics company (record of study) N91-10192
The Software Management Environment (SME)
N91-10609
The integrated scheduling system: A case study in project management
[NASA-CR-187261] N91-10793
**PROJECT PLANNING**
Industry liaison section implementation plan
[NASA-CR-177569] N91-10048
KrF laser path to high gain ICF (inertial confinement fusion) laboratory microfusion facility
[DE90-016439] N91-10282
**PROJECTILES**
Prevention of breakdown behind railgun projectiles
[DE90-014573] N91-10094
**PROP-FAN TECHNOLOGY**
Measurement of unsteady blade surface pressure on a single rotation large scale advanced prop-fan with angular and wake inflow at Mach numbers from 0.02 to 0.70
[NASA-CR-182123] N91-10065
**PROPANE**
Pressure measurements on the release system and determination of jet momentum in the project BA propane field tests 1989
[FOA-E-40044-4.5] N91-10263
**PROPELLANT COMBUSTION**
The instability of combustion in propulsion engines
N91-10141
Very high burn rate propellants
[DE90-016865] N91-10186
Combustion diagnostics of propellants with sandwich structure
[ISL-CO-212/89] N91-10189
**PROPELLANT GRAINS**
Very high burn rate propellants
[DE90-016865] N91-10186
Combustion diagnostics of propellants with sandwich structure
[ISL-CO-212/89] N91-10189
**PROPELLANT TANKS**
Filament wound metal lined propellant tanks for future Earth-to-orbit transports
[NASA-TM-100594] N91-10106
**PROPELLANTS**
Hot gas side heat transfer characteristics of LOX/H2 and LOX/HC type propellants
[NAL-TR-1062T] N91-10190
**PROPELLER BLADES**
Measurement of unsteady blade surface pressure on a single rotation large scale advanced prop-fan with angular and wake inflow at Mach numbers from 0.02 to 0.70
[NASA-CR-182123] N91-10065
**PROPELLER FANS**
Aeroacoustic effects of reduced aft tip speed at constant thrust for a model counterrotation turboprop at takeoff conditions
[NASA-TM-103608] N91-10703
**PROPELLERS**
Structural properties of laminated Douglas fir/epoxy composite material
[NASA-RP-1236] N91-10127
**PROPULSION SYSTEM CONFIGURATIONS**
Gas turbines for main propulsion and auxiliary power systems
[PNR-90709] N91-10069
Technology update of early gas turbine designs
[PNR-90710] N91-10070
Future supersonic transport populsion optimization
[PNR-90737] N91-10071
Hybrid propulsion technology program: Phase 1, volume 1
[NASA-CR-183972] N91-10111
Hybrid propulsion technology program: Phase 1, volume 2
[NASA-CR-183973] N91-10112
Hybrid propulsion technology program: Phase 1. Volume 3: Thiokol Corporation Space Operations
[NASA-CR-183974] N91-10113
Hybrid propulsion technology program: Phase 1, volume 4
[NASA-CR-183975] N91-10114
Integrated hydrogen/oxygen technology applied to auxiliary propulsion systems
[NASA-CR-185289] N91-10116
**PROPULSION SYSTEM PERFORMANCE**
Technology update of early gas turbine designs
[PNR-90710] N91-10070
Hybrid propulsion technology program: Phase 1, volume 1
[NASA-CR-183972] N91-10111
Hybrid propulsion technology program: Phase 1, volume 2
[NASA-CR-183973] N91-10112
Hybrid propulsion technology program: Phase 1. Volume 3: Thiokol Corporation Space Operations
[NASA-CR-183974] N91-10113
Hybrid propulsion technology program: Phase 1, volume 4
[NASA-CR-183975] N91-10114
Integrated hydrogen/oxygen technology applied to auxiliary propulsion systems
[NASA-CR-185289] N91-10116
**PROPULSIVE EFFICIENCY**
Progress in certifying F402-RR-408: The improved Pegasus engine for AV-8B and Harrier 2 plus
[PNR-90719] N91-10056
Hybrid propulsion technology program: Phase 1, volume 1
[NASA-CR-183972] N91-10111
Hybrid propulsion technology program: Phase 1, volume 2
[NASA-CR-183973] N91-10112
Hybrid propulsion technology program: Phase 1. Volume 3: Thiokol Corporation Space Operations
[NASA-CR-183974] N91-10113
**PROTECTIVE COATINGS**
Corrosion-resistant coatings for high-temperature high-sulfur activity applications
[DE90-016638] N91-10177
Corrosion, passivity, and breakdown of alloys used in high energy density batteries
[DE90-016648] N91-10223
**PROTOCOL (COMPUTERS)**
Network, system, and status software enhancements for the autonomously managed electrical power system breadboard. Volume 2: Protocol specification
[NASA-CR-185881] N91-10619
Conservative parallel simulation of priority class queueing networks
[NASA-CR-187438] N91-10628
Designing application software in wide area network settings
[NASA-CR-187333] N91-10633
**PROTON DENSITY (CONCENTRATION)**
Prompt lepton production in a proton beamdump experiment
[ETN-90-97750] N91-10711
**PROTON FLUX DENSITY**
Prompt lepton production in a proton beamdump experiment
[ETN-90-97750] N91-10711
**PROTON IRRADIATION**
Effects of taurine on cytogenetic corneal disturbances induced in mice by 9 GeV protons N91-10562
Effect of single impacts of heavy ions of galactic cosmic rays on lactuca sativa seeds exposed on Salyut-6 and Salyut-7 stations N91-10567
**PROTOTYPES**
Ada software productivity prototypes: A case study
N91-10613
**PSYCHOMOTOR PERFORMANCE**
Psychophysiological assessment of piloting motor habits in pilot retraining N91-10564
**PSYCHOPHYSIOLOGY**
Psychophysiological assessment of piloting motor habits in pilot retraining N91-10564
**PULLING**
Minimizing frequency pulling of quartz oscillators due to power supply variations
[DE90-014566] N91-10218
**PULSARS**
Acceleration by pulsar winds in binary systems
[NASA-TM-103451] N91-10816
**PULSE CODE MODULATION**
Telemetry subsystem N91-10345
**PULSED LASERS**
KrF laser path to high gain ICF (inertial confinement fusion) laboratory microfusion facility
[DE90-016439] N91-10282
Investigation of pulsed laser target interaction processes by high-speed diagnostic techniques
[ISL-CO-234/89] N91-10283
NIST research reports, May 1990
[PB90-244435] N91-10800
**PULSES**
Command subsystem N91-10346
**PYRANOMETERS**
Temperature sensitivity of Eppley broadband radiometers N91-10484
FIRE extended time/limited area observations at Palisades, New York N91-10527

**Q**

**QUADRATIC EQUATIONS**
Tabu-search and simulated annealing for the quadratic assignment problem
[REPT-89-028] N91-10658
**QUADRATIC PROGRAMMING**
Global optimization methods for engineering design
N91-10310
**QUADRATURES**
Quadrature imposition of compatibility conditions in Chebyshev methods
[NASA-CR-187458] N91-10251
**QUALITY CONTROL**
Incorporation of the operation safety in the industry and in a product development process inducting subcontractors
[ETN-90-97822] N91-10196
Engineering design: A powerful influence on the business success on manufacturing industry
[PNR-90763] N91-10197

An evaluation of the production processes and methods associated with Carello Cell at RISTS, Telford
[ETN-90-97578] N91-10228
Introduction: Needs and approaches to reliability and quality assurance in design and manufacture
[PNR-90683] N91-10297
Total quality management at Rolls-Royce PLC
[PNR-90759] N91-10298
Intrinsic (?) reference standards
[DE90-015714] N91-10696

**QUANTUM COUNTERS**
Prompt lepton production in a proton beamdump experiment
[ETN-90-97750] N91-10711

**QUANTUM ELECTRODYNAMICS**
Discretized light-cone quantization: Application to quantum electrodynamics
[DE90-014832] N91-10790

**QUANTUM MECHANICS**
On the structure of quantum phase space
[DE90-627185] N91-10786
Localizability in the Hamiltonian formalism and in quantum-mechanics
[DE90-628368] N91-10787

**QUANTUM THEORY**
Discretized light-cone quantization: Application to quantum electrodynamics
[DE90-014832] N91-10790

**QUANTUM WELLS**
Excitons in semiconducting superlattices, quantum wells, and ternary alloys
[DE90-017287] N91-10779

**QUARTZ**
Minimizing frequency pulling of quartz oscillators due to power supply variations
[DE90-014566] N91-10218
Piezoelectrically forced vibrations of electroded doubly rotated quartz plates by state space method
N91-10318

**QUASARS**
Core-dominated radio sources and the unified scheme
N91-10835

**QUATERNIONS**
On the rotation interpolation and animation problems in computer graphics
[REPT-90-08] N91-10637

**QUEUEING THEORY**
Conservative parallel simulation of priority class queueing networks
[NASA-CR-187438] N91-10628
Optimization of polling systems
[CWI-BS-R8932] N91-10635

**R**

**RADAR DATA**
Satellite-derived index of precipitation intensity
N91-10362

**RADAR ECHOES**
Satellite-derived index of precipitation intensity
N91-10362

**RADAR IMAGERY**
The new FIRE cloud lidar at Langley Research Center
N91-10482
Both sides now N91-10485

**RADAR MEASUREMENT**
Vertical velocities within a Cirrus cloud from Doppler lidar and aircraft measurements during FIRE: Implications for particle growth N91-10461
A four-lidar view of Cirrus from the FIRE IFO: 27-28 October 1986 N91-10478
Interpretation of the optical and morphological properties of Cirrus clouds from lidar measurements N91-10483
ER-2 lidar measurements of stratocumulus cloud top structure on July 14, 1987 N91-10523
Comparison and calibration of NCAR electra instruments: July 5 and 7, 1987 N91-10532

**RADIANCE**
ISCCP data processing N91-10363
VISSR histogram data N91-10368
GPCP data processing N91-10370
Cloud grid data N91-10371
Multi-spectral window radiance observations of Cirrus from satellite and aircraft, November 2, 1986 Project FIRE N91-10465
Cirrus cloud statistics: Temperatures and optical depths N91-10466
The radiation budget of a Cirrus layer deduced from simultaneous aircraft observations and model calculations N91-10467
Cloud parameters from GOES visible and infrared radiances during the FIRE Cirrus IFO, October 1986
N91-10473
Cloud altitude determination from infrared spectral radiances N91-10474
Cirrus cloud properties derived from coincident GOES and lidar data during the 1986 FIRE Cirrus Intensive Field Observations (IFO) N91-10476
Sub-visual Cirrus detection and characterization
N91-10486
Cloud atlas for the FIRE Cirrus Intensive Field Observation (IFO) N91-10487
Reflectivities of uniform and broken marine stratiform clouds N91-10501
Structures observed on the spot radiance fields during the FIRE experiment N91-10503
Cloud parameters derived from GOES during the 1987 marine stratocumulus FIRE Intensive Field Observation (IFO) period N91-10505
In situ measurements of ship tracks N91-10507
Near infrared radiances observed by the UK C130 multi-channel radiometer during the marine stratocumulus IFO and preliminary comparison with model calculations
N91-10525

**RADIANT HEATING**
Analysis of pulsed laser-generated impulse in an advanced airbreathing thruster N91-10062

**RADIATION ABSORPTION**
Cloud absorption properties as derived from airborne measurements of scattered radiation within clouds
N91-10512

**RADIATION COUNTERS**
Dijet spectroscopy at high luminosity
[DE90-016901] N91-10147
Prototype instrumentation and design studies — electrostatic analyzer system for the Space Shuttle
[AD-A211566] N91-10264

**RADIATION DAMAGE**
Effects of taurine on cytogenetic corneal disturbances induced in mice by 9 GeV protons N91-10562
Radiation damage in Al2O3 crystals implanted with 3.8 MeV Fe(2+)
[DE90-016038] N91-10761

**RADIATION DETECTORS**
The GAMMASPHERE
[DE90-016849] N91-10224
Design, performance, and calibration of the ALEXIS ultrasoft x-ray telescopes
[DE90-016483] N91-10720

**RADIATION DISTRIBUTION**
Radiative properties of Cirrus clouds: FIRE IFO case October 28, 1986 N91-10479
A cloud classification scheme applied to the breakup region of marine stratocumulus N91-10497

**RADIATION DOSAGE**
ELF (extremely-low-frequency): Exposure levels, bioeffects, and epidemiology
[DE90-016554] N91-10573
Statistical methods for analyzing and combining data on low-level exposures to ionizing radiation
[DE90-017193] N91-10593

**RADIATION EFFECTS**
Radiation-induced microstructural development and microchemical changes in Fe-Cr-Mn-Ni solute-bearing alloys
[DE90-016359] N91-10160
Holographic rugate structures for x ray optics applications
[DE90-017103] N91-10270
Effects of taurine on cytogenetic corneal disturbances induced in mice by 9 GeV protons N91-10562
Effect of single impacts of heavy ions of galactic cosmic rays on lactuca sativa seeds exposed on Salyut-6 and Salyut-7 stations N91-10567
ELF (extremely-low-frequency): Exposure levels, bioeffects, and epidemiology
[DE90-016554] N91-10573
Interaction of extremely low-frequency electromagnetic fields with humans
[DE90-017190] N91-10592
Radiation-induced noise in Charge-Coupled Device (CCD) and Charge-Injection Device (CID) imagers
[DE90-016724] N91-10777

**RADIATION MEASUREMENT**
Preliminary results of radiation measurements from the marine stratus FIRE experiment N91-10529

**RADIATION THERAPY**
Biomedical applications on laser technology at Los Alamos
[DE90-016447] N91-10277

**RADIATIVE TRANSFER**
Sea surface temperature N91-10372
Radiative properties of visible and subvisible Cirrus: Scattering on hexagonal ice crystals N91-10462
Cirrus microphysics and radiative transfer: A case study N91-10463
The radiation budget of a Cirrus layer deduced from simultaneous aircraft observations and model calculations N91-10467
Interpretation of satellite-measured bidirectional reflectance from Cirrus cloudy atmospheres N91-10470
FIRE Cirrus on October 28, 1986: LANDSAT; ER-2; King Air; theory N91-10480
Reflectivities of uniform and broken marine stratiform clouds N91-10501
Synthesis and inversion of Stokes spectral profiles
[PB90-214487] N91-10828

**RADIO EMISSION**
Radio wave remote sensing by Cluster and Regatta
N91-10439

**RADIO FREQUENCIES**
Passive-filtered and active-driven probes for RF plasmas
[OUEL-1806/89] N91-10754
Solar emission levels at low radio frequencies
[NASA-CR-187337] N91-10829

**RADIO FREQUENCY INTERFERENCE**
Hydrologic and meteorological operations in the 162-174 and 406.1-420 MHz bands
[PB90-207820] N91-10199

**RADIO JETS (ASTRONOMY)**
Core-dominated radio sources and the unified scheme
N91-10835

**RADIO OBSERVATION**
Vigorous star formation in galactic nuclei N91-10814

**RADIOMETERS**
Lidar and radiometer results from the ER-2 for the FIRE field experiments N91-10468
Identification of Cirrus over Wausau during the 1986 FIRE IFO from ground-based radiometer data
N91-10469
Temperature sensitivity of Eppley broadband radiometers N91-10484
Sub-visual Cirrus detection and characterization
N91-10486
Cloud absorption properties as derived from airborne measurements of scattered radiation within clouds
N91-10512
Cloud optical parameters as derived from the multispectral cloud radiometer N91-10513
Turbulence measurements using tethered balloon instrumentation during FIRE 1987 N91-10518
Winds and turbulence above San Nicolas Island during FIRE N91-10522
Dependence of marine stratocumulus reflectivities on liquid water paths N91-10524
Near infrared radiances observed by the UK C130 multi-channel radiometer during the marine stratocumulus IFO and preliminary comparison with model calculations
N91-10525

**RADON**
Rn222, Rn222 progeny and Rn220 progeny as atmospheric tracers of air masses at the Mauno Loa Observatory
[DE90-014872] N91-10539

**RAIL TRANSPORTATION**
NIST research reports, May 1990
[PB90-244435] N91-10800

**RAILGUN ACCELERATORS**
Prevention of breakdown behind railgun projectiles
[DE90-014573] N91-10094
Railgun restrike control
[DE90-015108] N91-10095

**RAMAN SPECTRA**
Measurement of air entrainment by a free jet using laser velocimetry and Raman scattering
[ISL-R-109/89] N91-10017

**RAMJET ENGINES**
Parametric assessment of propulsion system mass for airbreathing launcher configurations
[PNR-90634] N91-10063

**RANDOM ACCESS MEMORY**
Multiple channel programmable coincidence counter
[DE90-014681] N91-10602

**RANDOM ERRORS**
Optimum orientations of the observation axes for 2-dimensional vector sensing under consideration of bias errors
[NAL-TR-1055] N91-10679

**RANDOM WALK**
The difference of two renewal processes: Level crossing and the infimum
[MEMO-845] N91-10690

**RANGEFINDING**
Design for navigation: Using acoustic cats' eyes to improve sonar range and direction range finding for industrial mobile robots and AGV's
[OUEL-1812/90] N91-10036
Protective autonomy: Embedding sensor-based safety and protection mechanisms into the motion control of mobile and tele-operated robots
[OUEL-1808/90] N91-10292
Trilateration ranging subsystem N91-10347
Fundamental properties and mass loss in hot, near-main sequence stars N91-10821

**RATS**
Morphological examination of rat adrenal glands following flight aboard Biosputnik Kosmos-1667
N91-10553

**RAYLEIGH SCATTERING**
Equal eigenvalues in multicomponent diffusion: The extraction of diffusion coefficients from experimental data in ternary systems
[DE90-012074] N91-10142

**REACTION KINETICS**
Organometallic chemistry of bimetallic compounds
[DE90-017601] N91-10121
Transition state theory applying to the study of reaction processes in detonation
[DE90-016558] N91-10187
Corrosion, passivity, and breakdown of alloys used in high energy density batteries
[DE90-016648] N91-10223
Reaction kinetics of the Ca-SO2 system in absence of inter-grain pore diffusion
[DE90-009672] N91-10781
In situ transmission electron microscopy and computer simulation study of the kinetics of oxygen loss in YBa2Cu3O(z)
[DE90-014508] N91-10783
NIST research reports, May 1990
[PB90-244435] N91-10800

**REACTION PRODUCTS**
Fibre-matrix reaction zones in model silicon carbide-titanium aluminide metal-matrix composites
[PNR-90713] N91-10137

**REACTIVITY**
Collision-induced gas phase dissociation rates
[NASA-CR-185874] N91-10707

**REACTOR TECHNOLOGY**
Statistical characterization of a mode-stirred chamber
[DE90-014860] N91-10202
Artificial intelligence, human factors, robotics, and computer simulation
[DE90-016866] N91-10653
Theoretical studies of turbulence and anomalous transport in toroidal confinement devices
[DE90-017606] N91-10747

**READOUT**
Educator's guide for building and operating environmental satellite receiving stations
[NOAA-TR-NESDIS-44] N91-10093

**REAL TIME OPERATION**
Real-time safety analysis for autonomous guided vehicles
[OUEL-1833/90] N91-10037
Spacecraft Health Automated Reasoning Prototype (SHARP): The fiscal year 1989 SHARP portability evaluations task for NASA Solar System Exploration Division's Voyager project
[NASA-CR-187338] N91-10204
Interactive real time flow simulations
[NASA-CR-187325] N91-10238
Q-vectors: A new approach to an old problem
[PB90-235490] N91-10414
Representing object oriented specifications and designs with extended data flow notations N91-10617

**RECOMBINATION REACTIONS**
Theoretical atomic physics for fusion
[DE90-017280] N91-10710

**RECTANGULAR BEAMS**
A new beam theory using first-order warping functions
N91-10307

**RECURSIVE FUNCTIONS**
The digital regulator and tracker for deterministic continuous-time linear time-varying systems
[REPT-90-05] N91-10668
The digital regulator and tracker for stochastic continuous-time linear time-varying systems
[REPT-90-06] N91-10689

**REDUCED GRAVITY**
Analysis techniques for residual acceleration data
[NASA-TM-103507] N91-10191
Considerations for an exercise prescription
N91-10585
The growth of zinc selenide single crystals by physical vapor transport in microgravity
[NASA-CR-180428] N91-10755

**REDUNDANCY**
Redundancy control of a robot manipulator using a systolic array processor N91-10287

**REFERENCE ATMOSPHERES**
Neutral winds derived from IRI parameters and from the HWM87 wind model for the sundial campaign of September, 1986
[NASA-TM-103445] N91-10543

**REFLECTANCE**
Hydrometeor development in cold clouds in FIRE
N91-10459
Cirrus cloud properties derived from coincident GOES and lidar data during the 1986 FIRE Cirrus Intensive Field Observations (IFO) N91-10476
Reflectivities of uniform and broken marine stratiform clouds N91-10501
Marine stratocumulus cloud characteristics from multichannel satellite measurements N91-10502
Structures observed on the spot radiance fields during the FIRE experiment N91-10503
Estimated accuracy of ground-based liquid water measurements during FIRE N91-10508
Dependence of marine stratocumulus reflectivities on liquid water paths N91-10524
Near infrared radiances observed by the UK C130 multi-channel radiometer during the marine stratocumulus IFO and preliminary comparison with model calculations
N91-10525
A preliminary analysis of LANDSAT and UK C130 data from Mission 197-A, on 16 July 1987 N91-10535
On lower hybrid wave scattering by plasma density fluctuation nonlinear reflection coefficient of the fast magnetoacoustic wave
[IPPCZ-281] N91-10725

**REFLEXES**
Requirements for an ideal drug for preventing space motion sickness N91-10566
Role of orientation reference selection in motion sickness
[NASA-CR-186612] N91-10591

**REFRACTIVITY**
A refractive index gradient (RING) diagnostic for transient discharges or expansions of vapor or plasmas
[DE90-015840] N91-10736

**REFRACTORY MATERIALS**
Multi industry application of advanced materials
[PNR-90764] N91-10139

**REFRIGERATORS**
Design and application of gas-gap heat switches
[NASA-CR-187339] N91-10222

**REGENERATION (ENGINEERING)**
First order oscillators
[ETN-90-97758] N91-10226

**REGIONAL PLANNING**
Potential effects of global climate change on the United States. Appendix H: Infrastructure
[PB90-172313] N91-10402
Potential effects of global climate change on the United States. Appendix J: Policy
[PB90-173188] N91-10404

**REGRESSION ANALYSIS**
Satellite-derived index of precipitation intensity
N91-10362
Confidence intervals and curvature measures in nonlinear regression using the IML and NLIN procedures in SAS(tm) software
[PB90-246398] N91-10624

**REINFORCING FIBERS**
Micro-mechanical analysis of damage growth and fracture in discontinuous fiber reinforced metal matrix composites
[NASA-CR-187020] N91-10126
A macro-micromechanics analysis of a notched metal matrix composite
[NASA-TM-102728] N91-10128
Industrial applications and markets for ceramic matrix composites
[PNR-90753] N91-10138

**RELATIVITY**
Discrete gravity
[DE90-014808] N91-10789

**RELIABILITY**
Introduction: Needs and approaches to reliability and quality assurance in design and manufacture
[PNR-90683] N91-10297
Study of mixed mode stress intensity factor using the experimental method of transmitted caustics
N91-10324
Evolving impact of Ada on a production software environment N91-10607
A Markov renewal approach to an apportunistic replacement model in continuous time
[MEMO-844] N91-10675

**RELIABILITY ANALYSIS**
The difference of two renewal processes: Level crossing and the infimum
[MEMO-845] N91-10690

**RELIABILITY ENGINEERING**
Rotorcraft drivetrain life safety and reliability
[AGARD-R-775] N91-10042
Helicopter transmissions: Design for safety and reliability N91-10043
Drive system life and reliability N91-10044
Progress in certifying F402-RR-408: The improved Pegasus engine for AV-8B and Harrier 2 plus
[PNR-90719] N91-10056

**REMOTE CONTROL**
Microwave link N91-10355

**REMOTE SENSING**
The 1990 Reference Handbook: Earth Observing System
[NASA-TM-102910] N91-10378
Radio wave remote sensing by Cluster and Regatta
N91-10439
FIRE Cirrus on October 28, 1986: LANDSAT; ER-2; King Air; theory N91-10480
Cloud and boundary layer structure over San Nicolas Island during FIRE N91-10515

**RENORMALIZATION GROUP METHODS**
Renormalization from density functional theory strong coupling models for the electronic structure of La2CuO4
[DE90-015990] N91-10765

**REPLACING**
Modification in the main air blower unit for two meter times two meter transonic wind tunnel: Plan and configuration
[NAL-TM-580] N91-10081
A Markov renewal approach to an apportunistic replacement model in continuous time
[MEMO-844] N91-10675

**REPORTS**
Activities report of the World Meteorological Organization
[WMO-734] N91-10547

**REQUIREMENTS**
A practical approach to object based requirements analysis N91-10615

**RESEARCH AIRCRAFT**
Supersonic combustion engine testbed, heat lightning
[NASA-CR-187010] N91-10061

**RESEARCH AND DEVELOPMENT**
JPRS report: Science and technology. USSR: Space
[JPRS-USP-89-009] N91-10088
JPRS report: Science and technology. USSR: Space
[JPRS-USP-90-001] N91-10089
JPRS report: Science and technology. USSR: Space
[JPRS-USP-90-002] N91-10090
JPRS report: Science and technology. USSR: Electronics and electrical engineering
[JPRS-UEE-90-004] N91-10213
JPRS report: Science and technology. USSR: Electronics and electrical engineering
[JPRS-UEE-90-007] N91-10215
JPRS report: Science and technology. USSR: Electronics and electrical engineering
[JPRS-UEE-90-008] N91-10216
JPRS report: Science and technology. USSR: Electronics and electrical engineering
[JPRS-UEE-90-009] N91-10217
Laser Doppler velocimetry using diode lasers
[ISBN-90-9002803-X] N91-10285
JPRS report: Science and technology. USSR: Earth sciences
[JPRS-UES-90-006-L] N91-10376
JPRS report: Science and technology. USSR: Earth sciences
[JPRS-UES-90-007] N91-10377
JPRS report: Science and technology. USSR: Life sciences
[JPRS-ULS-90-001] N91-10551
JPRS report: Science and technology. USSR: Life sciences
[JPRS-ULS-90-013] N91-10552
JPRS report: Science and technology. USSR: Life sciences
[JPRS-ULS-90-012] N91-10556
JPRS report: Science and technology. USSR: Life sciences
[JPRS-ULS-90-011] N91-10565
JPRS Report: Science and technology. USSR: Life sciences
[JPRS-ULS-90-010] N91-10568
JPRS Report: Science and technology. USSR: Life sciences
[JPRS-ULS-90-009] N91-10569
JPRS Report: Science and technology. USSR: Life sciences
[JPRS-ULS-90-008] N91-10570
JPRS Report: Science and technology. USSR: Life sciences
[JPRS-ULS-90-006] N91-10571
JPRS report: Science and technology. USSR: Life sciences
[JPRS-ULS-90-005] N91-10572
JPRS report: Science and technology. USSR: Life sciences
[JPRS-ULS-89-008] N91-10589
JPRS report: Science and technology. USSR: Life sciences
[JPRS-ULS-89-010] N91-10590

JPRS report: Science and technology. USSR: Physics and mathematics
[JPRS-UPM-90-003] N91-10694
Bibliography of Lewis Research Center technical publications announced in 1989
[NASA-TM-102542] N91-10798
NIST research reports, May 1990
[PB90-244435] N91-10800

**RESEARCH FACILITIES**
Configuration, function and performance of the flight simulation test facility and its motion simulation system
[NAL-TM-575] N91-10080
Columbus logistics support. A conceptional definition of the operational phase
[MBB-UO-0093-90-PUB] N91-10091
Activities report of the European Southern Observatory
[ISSN-0531-4496] N91-10809

**RESEARCH MANAGEMENT**
Activities report of the Permanent Committee of the General Council
[ISSN-0524-7705] N91-10198

**RESEARCH PROJECTS**
Putting technology to work, 1990. Examples of industry-laboratory cooperation contributing to our nation's economic strength
[PB90-215187] N91-10805

**RESEARCH VEHICLES**
OVRhyp, scramjet test aircraft
[NASA-CR-187009] N91-10041
NASA transport systems research vehicle B-737 data link system and display formats
[NASA-TM-102717] N91-10058

**RESIDUAL STRESS**
Design of a triaxial residual stress measurement system using high-energy x ray diffraction
[DE90-016212] N91-10331

**RESONANCE**
Minimizing frequency pulling of quartz oscillators due to power supply variations
[DE90-014566] N91-10218

**RESONANT FREQUENCIES**
Combined design of structures and controllers for optimal maneuverability N91-10314

**RESOURCES MANAGEMENT**
Potential effects of global climate change on the United States. Appendix J: Policy
[PB90-173188] N91-10404

**RETRAINING**
Psychophysiological assessment of piloting motor habits in pilot retraining N91-10564

**RETROFITTING**
Re-engining: Real stage 3 compliance plus other benefits
[PNR-90755] N91-10075

**REUSABLE LAUNCH VEHICLES**
Filament wound metal lined propellant tanks for future Earth-to-orbit transports
[NASA-TM-100594] N91-10106

**REVERSE FIELD PINCH**
Self-consistent field error effects in reversed field pinch plasmas N91-10728
Confinement studies in the ZT-40M reversed field pinch
[DE90-016442] N91-10739
Tilt stability and compression heating studies of field-reversed configurations
[DE90-016443] N91-10740
Theoretical studies of turbulence and anomalous transport in toroidal confinement devices
[DE90-017606] N91-10747

**REYNOLDS NUMBER**
Measurements of coefficients of discharge for concentric flange-tapped square-edged orifice meters in natural gas over the Reynolds number range 25,000 to 16,000,000
[PB90-219601] N91-10231

**RICCATI EQUATION**
The digital regulator and tracker for deterministic continuous-time linear time-varying systems
[REPT-90-05] N91-10688
The digital regulator and tracker for stochastic continuous-time linear time-varying systems
[REPT-90-06] N91-10689

**RIDING QUALITY**
The development of interior noise and vibration criteria
[NASA-TM-102736] N91-10702

**RIEMANN MANIFOLD**
Operator formalism of multi-pole Virasoro algebra on Riemann sphere
[DE90-627217] N91-10657

**RIGID STRUCTURES**
Evaluation of alternatives for best-fit paraboloid for deformed antenna surfaces N91-10313

**RINGS (MATHEMATICS)**
Cohomology for Lagrangian systems and Noetherian symmetries
[DE90-628371] N91-10788

**RISK**
Structural risk assessment and aircraft fleet maintenance N91-10321

**ROBOT ARMS**
Redundancy control of a robot manipulator using a systolic array processor N91-10287
Planning of the paths for manipulation robots
[ETN-90-97826] N91-10291
Experiences with Ada in an embedded system
N91-10614

**ROBOT DYNAMICS**
Redundancy control of a robot manipulator using a systolic array processor N91-10287
Planning of the paths for manipulation robots
[ETN-90-97826] N91-10291

**ROBOTICS**
Experiments and theory with a 0.5 ton mobile robot
[OUEL-1807/90] N91-10035
Design for navigation: Using acoustic cats' eyes to improve sonar range and direction range finding for industrial mobile robots and AGV's
[OUEL-1812/90] N91-10036
Protective autonomy: Embedding sensor-based safety and protection mechanisms into the motion control of mobile and tele-operated robots
[OUEL-1808/90] N91-10292
Eddy current inspection of graphite fiber components
[NASA-TM-103514] N91-10294
Artificial intelligence, human factors, robotics, and computer simulation
[DE90-016866] N91-10653

**ROBOTS**
Redundancy control of a robot manipulator using a systolic array processor N91-10287

**ROBUSTNESS (MATHEMATICS)**
Robustness effects of a prefilter in generalized predictive control
[OUEL-1799/89] N91-10685

**ROCKET ENGINE DESIGN**
Developments in REDES: The rocket engine design expert system
[NASA-TM-103657] N91-10119

**ROCKET ENGINES**
A three-dimensional turbulent heat transfer analysis for advanced tubular rocket thrust chambers
[NASA-TM-103293] N91-10249

**ROCKET THRUST**
A three-dimensional turbulent heat transfer analysis for advanced tubular rocket thrust chambers
[NASA-TM-103293] N91-10249

**ROLL**
Boundary layer roll circulations during FIRE
N91-10521

**ROTARY WINGS**
Application of a state-space wake model to elastic blade flapping in hover N91-10006
Wake coupling to full potential rotor analysis code
[NASA-TM-102805] N91-10013
Rotor loads computation using singularity methods and application to the noise prediction
[ISL-PU-301/90] N91-10018

**ROTATING CYLINDERS**
Elastohydrodynamic lubrication: A dynamic variation method
[ISBN-90-9003079-4] N91-10290

**ROTATING DISKS**
Numerical solutions of rotating disc flows using a non-linear multigrid algorithm
[PNR-90679] N91-10259

**ROTATION**
Role of orientation reference selection in motion sickness
[NASA-CR-186612] N91-10591
On the rotation interpolation and animation problems in computer graphics
[REPT-90-08] N91-10637

**ROTOR AERODYNAMICS**
Application of a state-space wake model to elastic blade flapping in hover N91-10006
Transonic flow analysis for rotors. Part 3: Three-dimensional, quasi-steady, Euler calculation
[NASA-TP-2375] N91-10007
Wake coupling to full potential rotor analysis code
[NASA-TM-102805] N91-10013

**ROTOR BLADES (TURBOMACHINERY)**
A system design and demonstrative field test of wind turbine with a 14 m diameter rotor
[NAL-TR-1056] N91-10389

**ROTOR DYNAMICS**
Application of a state-space wake model to elastic blade flapping in hover N91-10006

**ROTOR SPEED**
A system design and demonstrative field test of wind turbine with a 14 m diameter rotor
[NAL-TR-1056] N91-10389

**ROTOR SYSTEMS RESEARCH AIRCRAFT**
Rotor systems research aircraft risk-reduction shake test
[NASA-TM-4186] N91-10045

**ROTORS**
Experimental investigation on the effect of coolant injection on turbine aerodynamic characteristics. Part 2: Effects of injection from rotor casing with 30 deg slanted holes
[NAL-TM-587-PT-2] N91-10060

**RULES**
The generalized modus ponens considered as a fuzzy relation
[REPT-90-02] N91-10687

**RUN TIME (COMPUTERS)**
A manual for PARTI runtime primitives
[NASA-CR-187442] N91-10599
Multiprocessors and runtime compilation
[NASA-CR-182100] N91-10600

## S

**S MATRIX THEORY**
Continuum states of the Klein-Gordon equations for vector and scalar interactions
[DE90-627178] N91-10693

**SABOT PROJECTILES**
Prediction and comparison with measurements of the aerodynamic characteristics of flare-stabilized XM910 prototypes
[AD-A208099] N91-10005

**SAFETY**
Real-time safety analysis for autonomous guided vehicles
[OUEL-1833/90] N91-10037
Conservative buffering of approximate nonlinear constraints N91-10312

**SAFETY FACTORS**
Rotorcraft drivetrain life safety and reliability
[AGARD-R-775] N91-10042
Helicopter transmissions: Design for safety and reliability N91-10043
Conservative buffering of approximate nonlinear constraints N91-10312

**SAMPLING**
Evaluation of nondestructive evaluation techniques for determination of flawed conditions and the effects of flaws on the burst pressure in Kevlar-epoxy filament-wound spherical test specimens
[DE90-014839] N91-10330
Rn222, Rn222 progeny and Rn220 progeny as atmospheric tracers of air masses at the Mauno Loa Observatory
[DE90-014872] N91-10539

**SANDWICH STRUCTURES**
Combustion diagnostics of propellants with sandwich structure
[ISL-CO-212/89] N91-10189
Axial compression buckling test on CFRP surface plate/aluminum honeycomb sandwiched curved surface plate
[NAL-TM-584] N91-10299

**SATELLITE ALTIMETRY**
Geoid and Doppler induced errors on the altimeter measurement and their correction
[CNES-CT/DRT/TIT/RL-88/226] N91-10380

**SATELLITE COMMUNICATION**
Space station N91-10576

**SATELLITE IMAGERY**
Image mapping N91-10359
ISCCP data processing N91-10363
Typhoon information N91-10366
Geographic display of circulation model data
[NOAA-NESDIS-27] N91-10446
Where are cirrus clouds and why are they there
N91-10450
Evidence for asymmetric inertial instability in the FIRE satellite dataset N91-10454
Analysis of stratocumulus cloud fields using LANDSAT imagery: Size distributions and spatial separations
N91-10504
In situ measurements of ship tracks N91-10507

**SATELLITE INSTRUMENTS**
Possibilities of charged particle injection from spacecraft for active diagnostics of the surrounding plasma and active spacecraft potential control N91-10437
AVHRR and VISSR satellite instrument calibration results for both Cirrus and marine stratocumulus IFO periods N91-10475

**SATELLITE OBSERVATION**

The scientific case for magnetic field satellites [NASA-CR-186532] N91-10101

ISCCP data processing N91-10363

Satellite cloud information chart N91-10374

FIRE Science Results 1988 [NASA-CP-3083] N91-10448

ISCCP results for the FIRE IFO regions and times N91-10451

Evidence for asymmetric inertial instability in the FIRE satellite dataset N91-10454

Vertical velocities within a Cirrus cloud from Doppler lidar and aircraft measurements during FIRE: Implications for particle growth N91-10461

Radiative properties of visible and subvisible Cirrus: Scattering on hexagonal ice crystals N91-10462

Interpretation of satellite-measured bidirectional reflectance from Cirrus cloudy atmospheres N91-10470

Cloud parameters from GOES visible and infrared radiances during the FIRE Cirrus IFO, October 1986 N91-10473

AVHRR and VISSR satellite instrument calibration results for both Cirrus and marine stratocumulus IFO periods N91-10475

Cirrus cloud properties derived from coincident GOES and lidar data during the 1986 FIRE Cirrus Intensive Field Observations (IFO) N91-10476

A four-lidar view of Cirrus from the FIRE IFO: 27-28 October 1986 N91-10478

Surface radiation observations for October 27-28, 1986 during the Wisconsin FIRE/SRB experiment N91-10481

Cloud atlas for the FIRE Cirrus Intensive Field Observation (IFO) N91-10487

Extended time observations of California marine stratocumulus clouds from GOES for July 1983-1987 N91-10488

Marine stratocumulus cloud characteristics from multichannel satellite measurements N91-10502

Estimated accuracy of ground-based liquid water measurements during FIRE N91-10508

NRL tethered balloon measurements at San Nicolas Island during FIRE IFO 1987 N91-10509

Aircraft measurements of the mean and turbulent structure of marine stratocumulus clouds during FIRE N91-10514

Cloud and boundary layer structure over San Nicolas Island during FIRE N91-10515

Winds and turbulence above San Nicolas Island during FIRE N91-10522

San Nicolas Island surface radiation-meteorology data N91-10531

Comparison and calibration of NCAR electra instruments: July 5 and 7, 1987 N91-10532

Aircraft/island/ship/satellite intercomparison: Preliminary results from July 16, 1987 N91-10534

**SATELLITE ORBITS**

Trilateration ranging subsystem N91-10347

**SATELLITE SOUNDING**

Comparison of NOAA-9 ERBE measurements with Cirrus IFO satellite and aircraft measurements N91-10471

Cloud altitude determination from infrared spectral radiances N91-10474

**SATELLITE TRANSMISSION**

A Mobile Satellite Experiment (MSAT-X) network definition [NASA-CR-187336] N91-10105

Outline of the GMS telecommunication system N91-10339

**SATELLITE-BORNE INSTRUMENTS**

Design, performance, and calibration of the ALEXIS ultrasoft x-ray telescopes [DE90-016483] N91-10720

**SCALARS**

Continuum states of the Klein-Gordon equations for vector and scalar interactions [DE90-627178] N91-10693

**SCALE MODELS**

Vibration testing of a 1/5 scale model of H-2 launch vehicle [NAL-TR-1061] N91-10099

**SCATTERING**

Radiative properties of visible and subvisible Cirrus: Scattering on hexagonal ice crystals N91-10462

Cloud absorption properties as derived from airborne measurements of scattered radiation within clouds N91-10512

Users manual for AUTOMESH-2D: A program of automatic mesh generation for two-dimensional scattering analysis by the finite element method [NASA-CR-186929] N91-10623

Continuum states of the Klein-Gordon equations for vector and scalar interactions [DE90-627178] N91-10693

**SCATTERING COEFFICIENTS**

Markov model of the propagation of a light wave in a heated turbulent media [ECL-90-06] N91-10723

**SCATTEROMETERS**

Impact of SASS wind data on analyses and forecasts of a fine mesh limited area model [BCRS-89-38] N91-10544

**SCHEDULING**

Software sizing, cost estimation and scheduling N91-10612

**SCHOOLS**

Educator's guide for building and operating environmental satellite receiving stations [NOAA-TR-NESDIS-44] N91-10093

**SCHROEDINGER EQUATION**

Polarization modulated solitary waves in an optical fiber [DE90-015034] N91-10715

**SCIENTIFIC SATELLITES**

Problems of cold plasma measurements on the Regatta-A spacecraft N91-10431

Specific tasks of Regatta-E measurements correlated with Cluster/Regatta-A in the ISTP and Regatta programmes N91-10436

**SCREWS**

A simple screw thread model for use in finite element stress analysis [AD-A210233] N91-10300

**SEA LEVEL**

Potential effects of global climate change on the United States. Appendix B: Sea level rise [PB90-172628] N91-10396

**SEA SURFACE TEMPERATURE**

Sea surface temperature N91-10372

The effects of cloud radiative forcing on an ocean-covered planet N91-10456

Aircraft measurements of the mean and turbulent structure of marine stratocumulus clouds during FIRE N91-10514

Horizontal variability of the marine boundary layer structure upwind of San Nicolas Island during FIRE, 1987 N91-10519

The stationary wave response to tropical and midlatitude SST anomalies N91-10536

**SEASAT PROGRAM**

Impact of SASS wind data on analyses and forecasts of a fine mesh limited area model [BCRS-89-38] N91-10544

**SEATS**

Seat dynamic performance standards for a range of sizes [DOT/FAA/CT-TN90/23] N91-10028

**SECONDARY FLOW**

Detailed heat transfer measurements in nozzle guide vane passages in linear and annular cascades in the presence of secondary flows [PNR-90706] N91-10260

An investigation of secondary flows in nozzle guide vanes [PNR-90739] N91-10262

**SECONDARY INJECTION**

Experimental investigation on the effect of coolant injection on turbine aerodynamic characteristics. Part 2: Effects of injection from rotor casing with 30 deg slanted holes [NAL-TM-587-PT-2] N91-10060

**SEDIMENTS**

Geology, geohydrology, and soils of NASA, Kennedy Space Center: A review [NASA-TM-103813] N91-10442

**SEGMENTS**

Performance characterization of a segmented anode arcjet thruster [NASA-TM-103227] N91-10116

**SEISMOLOGY**

The scientific case for magnetic field satellites [NASA-CR-186532] N91-10101

**SELF CONSISTENT FIELDS**

Self-consistent field error effects in reversed field pinch plasmas N91-10728

**SELF LUBRICATION**

Self-lubricating boric acid films for tribological applications [DE90-007805] N91-10171

**SEMICONDUCTING FILMS**

Ion-assisted doping of 2-6 compounds during physical vapor deposition [DE90-000358] N91-10756

**SEMICONDUCTOR DEVICES**

Measured silicon displacement damage ratios support the need to replace the ASTM E-722 damage function with the NJOY calculated function [DE90-016225] N91-10762

NIST research reports, May 1990 [PB90-244435] N91-10800

**SEMICONDUCTOR LASERS**

Laser Doppler velocimetry using diode lasers [ISBN-90-9002803-X] N91-10285

**SEMICONDUCTORS (MATERIALS)**

Excitons in semiconducting superlattices, quantum wells, and ternary alloys [DE90-017287] N91-10779

**SENSITIVITY**

A sensitive test for accuracy in evaluation of molecular collision number in the direct-simulation Monte Carlo method [NAL-TR-1050T] N91-10712

**SEPARATED FLOW**

Numerical computation of viscous flow about unconventional airfoil shapes [NASA-CR-187343] N91-10019

**SEQUENTIAL ANALYSIS**

Incorporation of the operation safety in the industry and in a product development process inducting subcontractors [ETN-90-97822] N91-10196

**SERVICE LIFE**

Rotorcraft drivetrain life safety and reliability [AGARD-R-775] N91-10042

Drive system life and reliability N91-10044

Thermal fatigue cycling in turbine blades [PNR-90682] N91-10067

The physical and chemical state of Westinghouse Phosphoric Acid Fuel Cell assemblies after long term operation: Surface and near-surface analysis [DE90-015055] N91-10382

**SERVICE MODULES**

Optimization criteria for the design of orbital replacement units [MBB-UO-0092-90-PUB] N91-10109

**SEYFERT GALAXIES**

Investigation of Markarian galaxies with multiple nuclei N91-10813

**SHEAR FLOW**

Bounded energy states in homogeneous turbulent shear flow: An alternative view [NASA-CR-187439] N91-10237

**SHEARING**

Repeated buckling of composite shear panels N91-10303

**SHELLS (STRUCTURAL FORMS)**

Static and dynamic finite element stress analysis of layered composite plates and shells N91-10326

**SHIFT REGISTERS**

Multiple channel programmable coincidence counter [DE90-014681] N91-10602

**SHIPS**

Gas turbines for main propulsion and auxiliary power systems [PNR-90709] N91-10069

In situ measurements of ship tracks N91-10507

Structural acoustics: An applied science with many applications [PB90-183633] N91-10698

**SHOCK**

Measured and predicted shock shapes for AFE configuration at Mach 6 in air and in CF4 [NASA-TM-100660] N91-10245

**SHOCK LAYERS**

Computation of boundary layer flow using thin-layer Navier-Stokes equations with flux-vector splitting [REPT-B-21] N91-10254

**SHOCK TUBES**

Large blast and thermal simulator advanced concept driver design by computational fluid dynamics [AD-A211364] N91-10230

Turbulent boundary layers in high enthalpy flows. Numerical code validation by shock tube experiments [ISL-CO-221/89] N91-10246

Velocity measurements in piston-induced turbulent boundary layers in a shock tube [ISL-CO-235/89] N91-10247

**SHOCK TUNNELS**

The ISL hypersonic shock tunnel and its instrumentation [ISL-CO-213/89] N91-10086

Large blast and thermal simulator advanced concept driver design by computational fluid dynamics [AD-A211364] N91-10230

**SHOCK WAVE ATTENUATION**

Wind tunnel investigations of the appearance of shocks in the windward region of bodies with circular cross section at angle of attack [DLR-FB-90-15] N91-10027

**SHOCK WAVE PROPAGATION**

Propagation of magnetoacoustic waves in the solar atmosphere with random inhomogeneities of density and magnetic fields [DE90-017616] N91-10831

**SHOCK WAVES**
Optimum hypersonic airfoil with power law shock waves
[DE90-014903] N91-10008
High strain rate deformation behavior of shocked copper
[DE90-016481] N91-10161
Shock experiments in metals and ceramics
[DE90-016613] N91-10165
Thermochemistry of shock-induced exothermic reactions in selected porous mixtures
[DE90-016104] N91-10183
Analysis of moving strong discontinuity surfaces in elastic-plastic solids including effects of inertia and finite strain N91-10323
Multiple-ion waves behind shocks N91-10429
**SHORELINES**
Potential effects of global climate change on the United States. Appendix B: Sea level rise
[PB90-172628] N91-10396
**SHORT TAKEOFF AIRCRAFT**
The establishment and performance test of PAPI (Precision Approach Path Indicator) System for NAL STOL aircraft
[NAL-TM-579] N91-10030
The actuator for the low-noise STOL test plane flight control system and its development test
[NAL-TM-574] N91-10038
The full-body ground vibration tests using the low-noise STOL test plane
[NAL-TM-576] N91-10077
**SHOULDERS**
A unique problem of muscle adaptation from weightlessness: The deceleration deficiency
N91-10582
**SHROUDS**
Experimental investigation on the effect of coolant injection on turbine aerodynamic characteristics. Part 2: Effects of injection from rotor casing with 30 deg slanted holes
[NAL-TM-587-PT-2] N91-10060
**SIGNAL ANALYSIS**
SILAGE to ELLA translation
[RSRE-MEMO-4385] N91-10639
**SIGNAL DETECTION**
Signal detection in non-Gaussian and non-white noise
N91-10200
**SIGNAL DETECTORS**
Signal detection in non-Gaussian and non-white noise
N91-10200
**SIGNAL PROCESSING**
Time/frequency analysis of vibro-acoustic behaviour of a launcher in flight
[ETN-90-97584] N91-10097
Principles of LOCSTAR system experiments
[CNES-CT/DRT/TIT/TR-88/355] N91-10207
SILAGE to ELLA translation
[RSRE-MEMO-4385] N91-10639
**SILICA GEL**
Nano-composite desiccation materials
[PB90-247388] N91-10123
**SILICATES**
XAFS analysis in the anharmonic limit: Application to HI-Tc superconductors and ferrosilicates
[DE90-016720] N91-10776
**SILICON**
Substrate temperature effects on (cubic x cubic lattice) R 30 deg domain growth of Ag on Si(111) surface
[DE90-016527] N91-10772
**SILICON CARBIDES**
Properties of reactively-deposited SiC and GeC alloys
[DE90-016363] N91-10766
**SILICON TRANSISTORS**
Measured silicon displacement damage ratios support the need to replace the ASTM E-722 damage function with the NJOY calculated function
[DE90-016225] N91-10762
**SILVER**
Substrate temperature effects on (cubic x cubic lattice) R 30 deg domain growth of Ag on Si(111) surface
[DE90-016527] N91-10772
YBa2Cu3O(x) composites with improved toughness and strength
[DE90-011180] N91-10782
**SIMULATION**
Conservative parallel simulation of priority class queueing networks
[NASA-CR-187438] N91-10628
A sensitive test for accuracy in evaluation of molecular collision number in the direct-simulation Monte Carlo method
[NAL-TR-1050T] N91-10712
**SIMULATORS**
A synopsis of Langley Research Center's lidar effort for the 1986 FIRE IFO N91-10457
**SINGLE CRYSTALS**
The growth of zinc selenide single crystals by physical vapor transport in microgravity
[NASA-CR-180428] N91-10755
Evaluation, development, and characterization of superconducting materials for space applications
[NASA-CR-187017] N91-10763
**SINGLE-PHASE FLOW**
AFDM: An Advanced Fluid-Dynamics Model. Volume 4: The AFDM heat- and mass-transfer solution algorithm
[DE90-017535] N91-10240
**SINGULARITY (MATHEMATICS)**
Rotor loads computation using singularity methods and application to the noise prediction
[ISL-PU-301/90] N91-10018
Cosmological singularities in electrovacuum spacetimes with two-parameter spacelike isometry groups
N91-10811
**SINTERING**
Advanced materials for high-temperature solid electrolyte applications
[DE90-016328] N91-10143
**SIZE DISTRIBUTION**
Analysis of stratocumulus cloud fields using LANDSAT imagery: Size distributions and spatial separations
N91-10504
Cloud absorption properties as derived from airborne measurements of scattered radiation within clouds
N91-10512
Cloud optical parameters as derived from the multispectral cloud radiometer N91-10513
**SKIN (ANATOMY)**
Protective functions of skin N91-10555
**SKY BRIGHTNESS**
Cloud grid data N91-10371
Sea surface temperature N91-10372
**SKY SURVEYS (ASTRONOMY)**
Activities report of the European Southern Observatory
[ISSN-0531-4496] N91-10809
**SLABS**
Electromagnetic scattering from two-dimensional thick material junctions
[NASA-CR-186976] N91-10201
**SLOTS**
Boundary-layer receptivity due to a wall suction and control of Tollmien-Schlichting waves
[NASA-CR-182103] N91-10009
**SMALL PERTURBATION FLOW**
Optimum hypersonic airfoil with power law shock waves
[DE90-014903] N91-10008
**SMOKE**
Structural tests of aircraft window assembly equipped with smoke evacuation valve
[DOT/FAA/CT-TN89/44] N91-10051
Airplane systems modifications for improved cabin smoke evacuation
[DOT/FAA/CT-TN90/24] N91-10052
**SMOKE ABATEMENT**
Flight testing of two Allison T56 engines modified to the ARL developed low smoke configuration
[ARL-PROP-TM-449] N91-10064
**SNOW**
Measurements of the light-absorbing material inside cloud droplets and its effect on cloud albedo
N91-10528
**SODAR**
The international sodar intercomparison experiment
[PB90-246224] N91-10416
Winds and turbulence above San Nicolas Island during FIRE N91-10522
**SODIUM**
Direct extraction of a Na(-) beam from a sodium plasma
[NIFS-35] N91-10751
**SODIUM SULFUR BATTERIES**
Corrosion-resistant coatings for high-temperature high-sulfur activity applications
[DE90-016638] N91-10177
**SOFTWARE ENGINEERING**
Proceedings of the Thirteenth Annual Software Engineering Workshop
[NASA-TM-103314] N91-10606
Evolving impact of Ada on a production software environment N91-10607
Towards a comprehensive framework for reuse: A reuse-enabling software evolution environment
[UMIACS-TR-88-92] N91-10608
The Software Management Environment (SME)
N91-10609
A communication channel model of the software process N91-10610
Software sizing, cost estimation and scheduling
N91-10612
Ada software productivity prototypes: A case study
N91-10613
A practical approach to object based requirements analysis N91-10615
A modernized PDL approach for Ada software development N91-10616
Software integration technologies in industrial applications
[MA-55] N91-10627
**SOFTWARE TOOLS**
Proceedings of the Thirteenth Annual Software Engineering Workshop
[NASA-TM-103314] N91-10606
Software sizing, cost estimation and scheduling
N91-10612
Ada software productivity prototypes: A case study
N91-10613
A modernized PDL approach for Ada software development N91-10616
**SOIL MECHANICS**
Geotechnical Engineering, 1989
[PB90-222159] N91-10415
Some recent applications of numerical methods to geotechnical analysis
[PB90-201229] N91-10655
**SOIL MOISTURE**
Documentation for Program SOILSIM: A computer program for the simulation of heat and moisture flow in soils and between soils, canopy and atmosphere
[NASA-CR-186953] N91-10379
**SOILS**
Documentation for Program SOILSIM: A computer program for the simulation of heat and moisture flow in soils and between soils, canopy and atmosphere
[NASA-CR-186953] N91-10379
Geology, geohydrology, and soils of NASA, Kennedy Space Center: A review
[NASA-TM-103813] N91-10442
**SOLAR ACTIVITY**
The importance of simultaneous monitoring of solar activity for the interpretation of solar plasma phenomena
N91-10433
Solar-geophysical data number 545, January 1990. Part 1 (Prompt reports). Data for December, November 1989 and late data
[PB90-182338] N91-10822
**SOLAR ACTIVITY EFFECTS**
The empirical geomagnetic parameter infer near-Earth interplanetary shocks
[IFSI-90-14] N91-10820
**SOLAR ATMOSPHERE**
Propagation of magnetoacoustic waves in the solar atmosphere with random inhomogeneities of density and magnetic fields
[DE90-017616] N91-10831
Coaligned observations of solar magnetic fields at different heights: MSFC Center director's discretionary fund final report (Project No. 88-10)
[NASA-TM-103516] N91-10832
**SOLAR CELLS**
Materials analysis and device optimization of CuInSe2 solar cells
[DE90-000365] N91-10384
**SOLAR COLLECTORS**
Design of highly concentrating solar collectors and solar collector systems
[DLR-FB-90-11] N91-10390
**SOLAR CONSTANT**
Third generation earth radiation budget measurements; ERBE in the context of earlier systems N91-10530
**SOLAR CORONA**
Coronal heating by nanoflares: Plasma dynamics of elementary events
[DE90-016495] N91-10830
**SOLAR ENERGY**
Third generation earth radiation budget measurements; ERBE in the context of earlier systems N91-10530
**SOLAR FLARES**
Solar-geophysical data number 548, April 1990. Part 1: (Prompt reports). Data for March, February 1990, and late data
[PB90-226028] N91-10411
Solar-geophysical data number 548, April 1990. Part 2: (Comprehensive reports). Data for October 1989 and miscellaneous
[PB90-226036] N91-10412
Solar-geophysical data number 546, February 1990. Part 1: (Prompt reports). Data for January 1990, December 1989, and late data
[PB90-195363] N91-10823
Solar-geophysical data number 546, February 1990. Part 2: (Comprehensive reports). Data for August 1989 and miscellaneous
[PB90-195371] N91-10824

Solar-geophysical data number 547, March 1990. Part 1: (Prompt reports). Data for February, January 1990, and late data [PB90-208877] N91-10825

Solar-geophysical data number 547, March 1990. Part 2: (Comprehensive reports). Data for September 1989 and miscellaneous [PB90-208885] N91-10826

Coronal heating by nanoflares: Plasma dynamics of elementary events [DE90-016495] N91-10830

Plots of the 5-minute neutron monitor intensity and multiplicities recorded by the Rome 17-NM64, March 1990 [IFSI-90-15] N91-10833

Plots of the 5-minute neutron monitor intensity and multiplicities recorded by the Rome 17-NM64, April 1990 [IFSI-90-18] N91-10834

**SOLAR FLUX DENSITY**

The importance of simultaneous monitoring of solar activity for the interpretation of solar plasma phenomena N91-10433

**SOLAR MAGNETIC FIELD**

Solar-geophysical data number 548, April 1990. Part 1: (Prompt reports). Data for March, February 1990, and late data [PB90-226028] N91-10411

Solar-geophysical data number 545, January 1990. Part 1 (Prompt reports). Data for December, November 1989 and late data [PB90-182338] N91-10822

Solar-geophysical data number 546, February 1990. Part 1: (Prompt reports). Data for January 1990, December 1989, and late data [PB90-195363] N91-10823

Solar-geophysical data number 547, March 1990. Part 1: (Prompt reports). Data for February, January 1990, and late data [PB90-208877] N91-10825

Synthesis and inversion of Stokes spectral profiles [PB90-214487] N91-10828

Coaligned observations of solar magnetic fields at different heights: MSFC Center director's discretionary fund final report (Project No. 88-10) [NASA-TM-103516] N91-10832

**SOLAR NEUTRINOS**

Intrinsic neutrino properties: As deduced from cosmology, astrophysics, accelerator, and non-accelerator experiments [DE90-016467] N91-10836

**SOLAR PHYSICS**

Solar-geophysical data number 548, April 1990. Part 1: (Prompt reports). Data for March, February 1990, and late data [PB90-226028] N91-10411

Solar-geophysical data number 548, April 1990. Part 2: (Comprehensive reports). Data for October 1989 and miscellaneous [PB90-226036] N91-10412

Solar-geophysical data number 546, February 1990. Part 1: (Prompt reports). Data for January 1990, December 1989, and late data [PB90-195363] N91-10823

Solar-geophysical data number 546, February 1990. Part 2: (Comprehensive reports). Data for August 1989 and miscellaneous [PB90-195371] N91-10824

Solar-geophysical data number 547, March 1990. Part 1: (Prompt reports). Data for February, January 1990, and late data [PB90-208877] N91-10825

Solar-geophysical data number 547, March 1990. Part 2: (Comprehensive reports). Data for September 1989 and miscellaneous [PB90-208885] N91-10826

Cosmic-ray intensity increase observed on September 29, 1989: The Chilean neutron monitor data (brief report) [IFSI-90-4] N91-10838

**SOLAR RADIATION**

Hydrometeor development in cold clouds in FIRE N91-10459

Interpretation of satellite-measured bidirectional reflectance from Cirrus cloudy atmospheres N91-10470

Estimating integrated cloud liquid water from extended time observations of solar irradiance N91-10510

Cosmic-ray intensity increase observed on September 29, 1989: The Chilean neutron monitor data (brief report) [IFSI-90-4] N91-10838

**SOLAR RADIO BURSTS**

Solar-geophysical data number 548, April 1990. Part 2: (Comprehensive reports). Data for October 1989 and miscellaneous [PB90-226036] N91-10412

Solar-geophysical data number 546, February 1990. Part 2: (Comprehensive reports). Data for August 1989 and miscellaneous [PB90-195371] N91-10824

Solar-geophysical data number 547, March 1990. Part 2: (Comprehensive reports). Data for September 1989 and miscellaneous [PB90-208885] N91-10826

**SOLAR RADIO EMISSION**

Solar-geophysical data number 548, April 1990. Part 1: (Prompt reports). Data for March, February 1990, and late data [PB90-226028] N91-10411

Solar-geophysical data number 545, January 1990. Part 1 (Prompt reports). Data for December, November 1989 and late data [PB90-182338] N91-10822

Solar-geophysical data number 546, February 1990. Part 1: (Prompt reports). Data for January 1990, December 1989, and late data [PB90-195363] N91-10823

Solar-geophysical data number 547, March 1990. Part 1: (Prompt reports). Data for February, January 1990, and late data [PB90-208877] N91-10825

Solar emission levels at low radio frequencies [NASA-CR-187337] N91-10829

**SOLAR ROTATION**

Solar-geophysical data number 546, February 1990. Part 2: (Comprehensive reports). Data for August 1989 and miscellaneous [PB90-195371] N91-10824

**SOLAR SPECTRA**

Preliminary results of radiation measurements from the marine stratus FIRE experiment N91-10529

**SOLAR TERRESTRIAL INTERACTIONS**

Neutral winds derived from IRI parameters and from the HWM87 wind model for the sundial campaign of September, 1986 [NASA-TM-103445] N91-10543

The empirical geomagnetic parameter infer near-Earth interplanetary shocks [IFSI-90-14] N91-10820

**SOLAR WIND**

Space Plasma Physics Investigations by Cluster and Regatta [ESA-SP-306] N91-10417

The importance of simultaneous monitoring of solar activity for the interpretation of solar plasma phenomena N91-10433

Energetic particles in the Earth's magnetotail or: Cluster and Regatta as a dispersiometer N91-10434

Neutral winds derived from IRI parameters and from the HWM87 wind model for the sundial campaign of September, 1986 [NASA-TM-103445] N91-10543

The Joint NASA/Goddard-University of Maryland Research Program in Charged Particle and High Energy Photon Detector Technology [NASA-CR-180335] N91-10810

The empirical geomagnetic parameter infer near-Earth interplanetary shocks [IFSI-90-14] N91-10820

**SOLID ELECTROLYTES**

Advanced materials for high-temperature solid electrolyte applications [DE90-016328] N91-10143

Methane conversion by solid electrolyte membranes [PB90-226341] N91-10381

**SOLID LUBRICANTS**

Self-lubricating boric acid films for tribological applications [DE90-007805] N91-10171

**SOLID PROPELLANTS**

Very high burn rate propellants [DE90-016865] N91-10186

**SOLID-SOLID INTERFACES**

Fibre-matrix reaction zones in model silicon carbide-titanium aluminide metal-matrix composites [PNR-90713] N91-10137

XAFS studies of interactions at transition-metal/Al interfaces [DE90-016313] N91-10159

PREGO: A simulation code for one-dimensional viscoelastic acoustics [DE90-014859] N91-10700

Physical and electronic structure of the electrolyte-solid interface through optical phenomena [DE90-015935] N91-10764

**SOLIDIFICATION**

A weldability study of Haynes Alloy no. 242 [DE90-013875] N91-10154

**SOLIDS**

Analysis of moving strong discontinuity surfaces in elastic-plastic solids including effects of inertia and finite strain N91-10323

**SOLITARY WAVES**

Polarization modulated solitary waves in an optical fiber [DE90-015034] N91-10715

**SONAR**

Design for navigation: Using acoustic cats' eyes to improve sonar range and direction range finding for industrial mobile robots and AGV's [OUEL-1812/90] N91-10036

**SONIC BOOMS**

Application of CFD to sonic boom near and mid flow-field prediction [NASA-TM-102867] N91-10015

**SOUND FIELDS**

Properties of acoustic energy quantities [DE90-518714] N91-10701

**SOUND PRESSURE**

Helicopter far-field acoustic levels as a function of reduced main-rotor advancing blade-tip Mach number [NASA-TM-102684] N91-10699

**SOUND PROPAGATION**

Fast sound propagation in binary fluid mixtures N91-10233

**SOUND RANGING**

Design for navigation: Using acoustic cats' eyes to improve sonar range and direction range finding for industrial mobile robots and AGV's [OUEL-1812/90] N91-10036

**SOUND WAVES**

Evaluation of flow quality in newly constructed low-turbulence calibration wind-tunnel for laser velocimeters [NAL-TR-1054] N91-10087

Time/frequency analysis of vibro-acoustic behaviour of a launcher in flight [ETN-90-97584] N91-10097

Structural acoustics: An applied science with many applications [PB90-183633] N91-10698

**SOUNDING**

Thermodynamic structure of the stratocumulus-capped boundary layer on 5 July 1987 N91-10516

Winds and turbulence above San Nicolas Island during FIRE N91-10522

**SOUNDING ROCKETS**

Studies of the system-environment interaction by electron beam emission from a sounding rocket payload in the ionosphere N91-10410

**SPACE COMMERCIALIZATION**

Space station N91-10576

**SPACE FLIGHT**

Time/frequency analysis of vibro-acoustic behaviour of a launcher in flight [ETN-90-97584] N91-10097

**SPACE FLIGHT STRESS**

Work, exercise, and space flight. 1: Operations, environment, and effects of spaceflight N91-10578

Work, exercise, and space flight. 3: Exercise devices and protocols N91-10579

Changes in mineral metabolism with immobilization/space flight N91-10581

Work, exercise, and space flight. 2: Modification of adaptation by exercise (exercise prescription) N91-10586

Cardiovascular group N91-10587

**SPACE INDUSTRIALIZATION**

Space station N91-10576

**SPACE LABORATORIES**

Columbus elements processing needs at KSC [MBB-UO-0092-90-PUB] N91-10108

Small Space Lab as a basic spacecraft of Regatta project N91-10423

**SPACE LAW**

JPRS report: Science and technology. USSR: Space [JPRS-USP-90-001] N91-10089

**SPACE LOGISTICS**

Columbus logistics support. A conceptional definition of the operational phase [MBB-UO-0093-90-PUB] N91-10091

**SPACE MISSIONS**

Small Space Lab as a basic spacecraft of Regatta project N91-10423

Space medicine considerations: Skeletal and calcium homeostasis N91-10580

**SPACE PLASMAS**

Space Plasma Physics Investigations by Cluster and Regatta [ESA-SP-306] N91-10417

Multispacecraft measurement at varying scalelengths: The Cluster/Regatta opportunity N91-10418

Specific tasks of multiple scale plasma measurements in Regatta-Cluster system N91-10419

Small Space Lab as a basic spacecraft of Regatta project N91-10423

Cluster as a wave telescope N91-10424

Experimental constraints in the characterization of a turbulent field from several satellites N91-10425
Plasma wave measurements on the dayside: Scale sizes and observational requirements N91-10426
Plasma waves as a signature of flux transfer events N91-10427
On the possibility to support multisatellite measurements of the Cluster mission by single satellite measurements in the Regatta-Cluster project N91-10428
Multiple-ion waves behind shocks N91-10429
Non-linear evolution of the Kelvin-Helmholtz instability: Constraints on multipoint measurements N91-10430
Possibilities of charged particle injection from spacecraft for active diagnostics of the surrounding plasma and active spacecraft potential control N91-10437
The possibility of making fast measurements of ion distribution functions N91-10438

**SPACE PROGRAMS**
Space station N91-10576
The history of in-flight exercise in the US manned space program N91-10577

**SPACE SHUTTLE BOOSTERS**
Flight set 360L007 (STS-33R) field joint protection system, thermal protection system, and systems tunnel components, volume 7
[NASA-CR-184026] N91-10115
Probabilistic failure assessment with application to solid rocket motors N91-10309

**SPACE SHUTTLE MAIN ENGINE**
Probabilistic failure assessment with application to solid rocket motors N91-10309

**SPACE SHUTTLE MISSIONS**
National Space Transportation System Reference. Volume 2: Operations
[NASA-TM-89785] N91-10100

**SPACE SHUTTLES**
National Space Transportation System Reference. Volume 2: Operations
[NASA-TM-89785] N91-10100
Computational methods for the Boltzmann equation
[BR-43] N91-10256
Prototype instrumentation and design studies --- electrostatic analyzer system for the Space Shuttle
[AD-A211566] N91-10264

**SPACE STATION PAYLOADS**
Columbus elements processing needs at KSC
[MBB-UO-0092-90-PUB] N91-10108

**SPACE STATION POWER SUPPLIES**
Network, system, and status software enhancements for the autonomously managed electrical power system breadboard. Volume 1: Project summary
[NASA-CR-185880] N91-10618
Network, system, and status software enhancements for the autonomously managed electrical power system breadboard. Volume 2: Protocol specification
[NASA-CR-185881] N91-10619
Network, system, and status software enhancements for the autonomously managed electrical power system breadboard. Volume 3: Commands specification
[NASA-CR-185882] N91-10620
Network, system, and status software enhancements for the autonomously managed electrical power system breadboard. Volume 4: Graphical status display
[NASA-CR-185879] N91-10621

**SPACE STATIONS**
Space Station Freedom Environmental Control and Life Support System (ECLSS) phase 3 simplified integrated test trace contaminant control subsystem performance
[NASA-TM-4202] N91-10103
Advanced ceramic fabric body mounted radiator for Space Station Freedom Phase O design
[DE90-018361] N91-10104
Space station N91-10576
Knowledge-based assistance in costing the space station DMS N91-10611

**SPACE SUITS**
Probabilty of decompression sickness during space suit testing N91-10559

**SPACE TRANSPORTATION SYSTEM**
National Space Transportation System Reference. Volume 2: Operations
[NASA-TM-89785] N91-10100
Flight set 360L007 (STS-33R) field joint protection system, thermal protection system, and systems tunnel components, volume 7
[NASA-CR-184026] N91-10115

**SPACEBORNE ASTRONOMY**
Space Plasma Physics Investigations by Cluster and Regatta
[ESA-SP-306] N91-10417
Accuracy of the estimate of J via multipoint measurements N91-10422
The importance of simultaneous monitoring of solar activity for the interpretation of solar plasma phenomena N91-10433
Specific tasks of Regatta-E measurements correlated with Cluster/Regatta-A in the ISTP and Regatta programmes N91-10436
Design, performance, and calibration of the ALEXIS ultrasoft x-ray telescopes
[DE90-016483] N91-10720

**SPACEBORNE EXPERIMENTS**
Possibilities of charged particle injection from spacecraft for active diagnostics of the surrounding plasma and active spacecraft potential control N91-10437

**SPACECRAFT CHARGING**
Studies of the system-environment interaction by electron beam emission from a sounding rocket payload in the ionosphere N91-10410

**SPACECRAFT COMMUNICATION**
Meteorological Satellite Center Technical Note. Special Issue (1989). Summary of GMS System. 1: Telecommunication System N91-10338
Antenna/transmitter control unit N91-10348
System console N91-10351
Microwave link N91-10355

**SPACECRAFT CONFIGURATIONS**
Configurational sensitivity of multipoint magnetic field measurements N91-10421
Accuracy of the estimate of J via multipoint measurements N91-10422
Small Space Lab as a basic spacecraft of Regatta project N91-10423
Cluster as a wave telescope N91-10424
Experimental constraints in the characterization of a turbulent field from several satellites N91-10425
Non-linear evolution of the Kelvin-Helmholtz instability: Constraints on multipoint measurements N91-10430

**SPACECRAFT DESIGN**
Optimization criteria for the design of orbital replacement units
[MBB-UO-0092-90-PUB] N91-10109

**SPACECRAFT ELECTRONIC EQUIPMENT**
Method for simulating large dimension devices submitted to electromagnetic perturbations
[ECL-90-10] N91-10210

**SPACECRAFT ENVIRONMENTS**
Protective functions of skin N91-10555

**SPACECRAFT EQUIPMENT**
Magnetic sensitivity of on-board quartz oscillators: State of the knowledge
[CNES-CT/DRT/TIT/TF-88/354] N91-10110

**SPACECRAFT MAINTENANCE**
Optimization criteria for the design of orbital replacement units
[MBB-UO-0092-90-PUB] N91-10109

**SPACECRAFT ORBITS**
Specific tasks of multiple scale plasma measurements in Regatta-Cluster system N91-10419
Review of the Cluster orbit and separation strategy: Consequence for measurements N91-10420
Configurational sensitivity of multipoint magnetic field measurements N91-10421

**SPACECRAFT SHIELDING**
Intercalated graphite fiber composites as EMI shields in aerospace structures
[NASA-TM-103632] N91-10134

**SPACECREWS**
The design and fabrication of the Centaur neutral buoyancy trainer and related hardware
[NASA-CR-171244] N91-10085
The history of in-flight exercise in the US manned space program N91-10577

**SPACING**
Review of the Cluster orbit and separation strategy: Consequence for measurements N91-10420

**SPALLING**
The influence of shock pre-strain and peak pressure on spall behavior of 4340 steel
[DE90-016612] N91-10164

**SPATIAL DEPENDENCIES**
Energetic particles in the Earth's magnetotail or: Cluster and Regatta as a dispersiometer N91-10434

**SPATIAL DISTRIBUTION**
Cloud amount distribution N91-10373
Cloud spatial structure during the FIRE MS IFO N91-10500
Analysis of stratocumulus cloud fields using LANDSAT imagery: Size distributions and spatial separations N91-10504

**SPATIAL RESOLUTION**
The technique of Cerenkov ring image detection
[ETN-90-97747] N91-10714

**SPECIFIC HEAT**
Determination of ideal-gas enthalpies of formation for key compounds: The 1988 project results
[DE90-000247] N91-10791

**SPECIFIC IMPULSE**
Specific impulse comparison of high density hydrocarbon fuel burned with oxygen
[NAL-TR-1053] N91-10148

**SPECTRAL BANDS**
Temperature sensitivity of Eppley broadband radiometers N91-10484
A GCM parameterization for the shortwave radiative properties of water clouds N91-10494

**SPECTRAL EMISSION**
Multi-spectral window radiance observations of Cirrus from satellite and aircraft, November 2, 1986 Project FIRE N91-10465

**SPECTRAL METHODS**
Spectral methods for time dependent problems
[NASA-CR-187443] N91-10664

**SPECTRAL RESOLUTION**
Optical and morphological properties of Cirrus clouds determined by the high spectral resolution lidar during FIRE N91-10458
Cloud altitude determination from infrared spectral radiances N91-10474

**SPECTROSCOPY**
Characterization of mono- and multi-molecular assemblies at glassy carbon and noble metals by ex situ and in situ infrared external reflection spectroscopy
[DE90-016417] N91-10144
Dijet spectroscopy at high luminosity
[DE90-016901] N91-10147

**SPECTRUM ANALYSIS**
Spectra and gradients of stormy winds at Cabauw, Netherlands, up to 200 meters high
[KNMI-TR-119] N91-10546

**SPECULAR REFLECTION**
Design for navigation: Using acoustic cats' eyes to improve sonar range and direction range finding for industrial mobile robots and AGV's
[OUEL-1812/90] N91-10036
Image motion experiments with the Oxford AGV
[OUEL-1809/90] N91-10654

**SPIN DYNAMICS**
Muon SR and high T(sub c) superconductivity
[DE90-015089] N91-10760

**SPIN-LATTICE RELAXATION**
Muon SR and high T(sub c) superconductivity
[DE90-015089] N91-10760

**SPIRAL GALAXIES**
Investigation of Markarian galaxies with multiple nuclei N91-10813
Vigorous star formation in galactic nuclei N91-10814

**SPLINE FUNCTIONS**
Approximation and geometric modeling with simplex B-splines associated with irregular triangles
[MEMO-842] N91-10673
Chebyshev approximation by spline functions with free knots
[MEMO-853] N91-10677
A remark on the convexity of piecewise polynomial functions on triangulations
[MEMO-857] N91-10682

**SPRAYED COATINGS**
Applications of thermally sprayed coating systems in aero engines
[PNR-90750] N91-10072

**STABILITY**
Microstructural and phase stability studies of nanometer period metal/carbon multilayer structures for x ray optics
[DE90-015307] N91-10129
A miniature inexpensive, oxygen sensing element
[DE90-014080] N91-10269
Basic study of solid oxide fuel cells
[DE90-517069] N91-10386
Stability of some stationary solutions for the forced KdV equation
[DE90-016506] N91-10662

**STABILIZATION**
Studies of the system-environment interaction by electron beam emission from a sounding rocket payload in the ionosphere N91-10410

**STANDARD DEVIATION**
The international sodar intercomparison experiment
[PB90-246224] N91-10416

**STANDARDS**
Seat dynamic performance standards for a range of sizes
[DOT/FAA/CT-TN90/23] N91-10028
NIST (National Institute of Standards and Technology) standard reference materials catalog, 1990-1991
[PB90-183310] N91-10120
A miniature inexpensive, oxygen sensing element
[DE90-014080] N91-10269
Heavy duty liquid and gaseous fuel emissions database test results from four alternative fuel configurations of the Caterpillar 3406 engine
[DE90-014783] N91-10288
Intrinsic (?) reference standards
[DE90-015714] N91-10696

**STAR FORMATION**
Investigation of Markarian galaxies with multiple nuclei N91-10813

Vigorous star formation in galactic nuclei N91-10814
**STARBURST GALAXIES**
Vigorous star formation in galactic nuclei N91-10814
**STARK EFFECT**
Nonlinear optical absorption in intrinsic Stark effect superlattices
[DE90-016466] N91-10767
**STATIC TESTS**
Differential Global Positioning System (DGPS) test plan
[DOT/FAA/CT-TN90/15] N91-10034
**STATISTICAL ANALYSIS**
Application of flight path reconstruction algorithms for flight data of helicopter
[NAL-TM-582] N91-10031
Statistical characterization of a mode-stirred chamber
[DE90-014860] N91-10202
A cloud classification scheme applied to the breakup region of marine stratocumulus N91-10497
Statistical methods for analyzing and combining data on low-level exposures to ionizing radiation
[DE90-017193] N91-10593
Activities of the Board on Mathematical Sciences
[DE90-015118] N91-10598
**STATISTICAL DISTRIBUTIONS**
Cirrus cloud statistics: Temperatures and optical depths N91-10466
Multivariate tau-estimators for location and scatter
[REPT-90-04] N91-10688
**STEADY STATE**
Direct extraction of a Na(-) beam from a sodium plasma
[NIFS-35] N91-10751
**STEADY STATE CREEP**
Finite element analysis of nonlinear creeping flows
[DE90-627189] N91-10327
**STEELS**
Radiation-induced microstructural development and microchemical changes in Fe-Cr-Mn-Ni solute-bearing alloys
[DE90-016359] N91-10160
The influence of shock pre-strain and peak pressure on spall behavior of 4340 steel
[DE90-016612] N91-10164
**STEERING**
Fast steering of the angle of attack: A contribution to the guidance of high velocity projectiles
[ISL-CO-220/89] N91-10050
**STELLAR FLARES**
A semi-analytical model of stellar flares
[DE90-016434] N91-10817
**STELLAR LUMINOSITY**
Vigorous star formation in galactic nuclei N91-10814
Fundamental properties and mass loss in hot, near-main sequence stars N91-10821
**STELLAR MODELS**
A semi-analytical model of stellar flares
[DE90-016434] N91-10817
**STELLAR RADIATION**
Acceleration by pulsar winds in binary systems
[NASA-TM-103451] N91-10816
**STELLAR SPECTRA**
Bicolored photometry and spectral accommodation in X-ray region of mass impregnated stellar X-ray binaries
[MPE-219] N91-10808
**STELLAR WINDS**
Acceleration by pulsar winds in binary systems
[NASA-TM-103451] N91-10816
**STELLARATORS**
Experiments on linear high beta helical axis stellarators to study simulated toroidal effects and Alfven-wave heating
[DE90-016122] N91-10738
Stellarator theory
[DE90-017607] N91-10748
**STIFFNESS**
Analysis of elastically tailored viscoelastic damping member N91-10319
**STIRRING**
Statistical characterization of a mode-stirred chamber
[DE90-014860] N91-10202
**STOCHASTIC PROCESSES**
Comparison between the null-collision and time counter direct-simulation Monte Carlo methods: Leading-edge flow
[NAL-TR-1016T] N91-10012
Probabilistic failure assessment with application to solid rocket motors N91-10309
Global optimization methods for engineering design
N91-10310
The difference of two renewal processes: Level crossing and the infimum
[MEMO-845] N91-10690
Prediction and control of chaotic processes using nonlinear adaptive networks
[DE90-016505] N91-10697
**STOKES THEOREM (VECTOR CALCULUS)**
Synthesis and inversion of Stokes spectral profiles
[PB90-214487] N91-10828
**STORMS (METEOROLOGY)**
Impact of SASS wind data on analyses and forecasts of a fine mesh limited area model
[BCRS-89-38] N91-10544
Spectra and gradients of stormy winds at Cabauw, Netherlands, up to 200 meters high
[KNMI-TR-119] N91-10546
**STRAIN HARDENING**
Mechanical and microstructural response of Ni3Al at high strain rate and elevated temperatures
[DE90-016489] N91-10162
Texture-induced anisotropy and high-strain rate deformation in metals
[DE90-016611] N91-10163
**STRAIN RATE**
High strain rate deformation behavior of shocked copper
[DE90-016481] N91-10161
Mechanical and microstructural response of Ni3Al at high strain rate and elevated temperatures
[DE90-016489] N91-10162
Texture-induced anisotropy and high-strain rate deformation in metals
[DE90-016611] N91-10163
High-strain-rate compression and fracture of B4C-aluminum cermets
[DE90-016568] N91-10176
**STRATEGY**
Aircraft/island/ship/satellite intercomparison: Preliminary results from July 16, 1987 N91-10534
**STRATOCUMULUS CLOUDS**
FIRE Science Results 1988
[NASA-CP-3083] N91-10448
Climate data system supports FIRE N91-10455
AVHRR and VISSR satellite instrument calibration results for both Cirrus and marine stratocumulus IFO periods N91-10475
Extended time observations of California marine stratocumulus clouds from GOES for July 1983-1987
N91-10488
Analysis of diurnal variation of SCu layer using 2 days of CLASS soundings on San Nicolas Island N91-10490
Diurnal variation of marine stratocumulus over San Nicolas Island during the FIRE IFO N91-10491
Analysis of tethered balloon, ceilometer and class sounding data taken on San Nicolas Island during the FIRE project N91-10492
Preliminary mixed-layer model results for FIRE marine stratocumulus IFO conditions N91-10495
Simulations and observations of cloudtop processes
N91-10496
A cloud classification scheme applied to the breakup region of marine stratocumulus N91-10497
Cloud spatial structure during the FIRE MS IFO
N91-10500
Marine stratocumulus cloud characteristics from multichannel satellite measurements N91-10502
Analysis of stratocumulus cloud fields using LANDSAT imagery: Size distributions and spatial separations
N91-10504
Cloud parameters derived from GOES during the 1987 marine stratocumulus FIRE Intensive Field Observation (IFO) period N91-10505
Aerosol measurements in the stratocumulus project
N91-10506
A study of marine stratocumulus using lidar and other FIRE aircraft observations N91-10511
Cloud absorption properties as derived from airborne measurements of scattered radiation within clouds
N91-10512
Cloud optical parameters as derived from the multispectral cloud radiometer N91-10513
Aircraft measurements of the mean and turbulent structure of marine stratocumulus clouds during FIRE
N91-10514
Cloud and boundary layer structure over San Nicolas Island during FIRE N91-10515
Thermodynamic structure of the stratocumulus-capped boundary layer on 5 July 1987 N91-10516
Horizontal variability of the marine boundary layer structure upwind of San Nicolas Island during FIRE, 1987 N91-10519
An overview of UK C130 observations from the FIRE marine stratocumulus IFO N91-10520
ER-2 lidar measurements of stratocumulus cloud top structure on July 14, 1987 N91-10523
Dependence of marine stratocumulus reflectivities on liquid water paths N91-10524
Near infrared radiances observed by the UK C130 multi-channel radiometer during the marine stratocumulus IFO and preliminary comparison with model calculations
N91-10525
Plume mechanics and stratocumulus convection
N91-10526
Preliminary results of radiation measurements from the marine stratus FIRE experiment N91-10529
Thermodynamic structure of the stratocumulus-capped boundary layer on 7 July, 1987 N91-10533
Aircraft/island/ship/satellite intercomparison: Preliminary results from July 16, 1987 N91-10534
**STRATUS CLOUDS**
ISCCP results for the FIRE IFO regions and times
N91-10451
Lidar and radiometer results from the ER-2 for the FIRE field experiments N91-10468
The relationship of marine stratus to synoptic conditions N91-10489
Studying marine stratus with large eddy simulation
N91-10499
Reflectivities of uniform and broken marine stratiform clouds N91-10501
In situ measurements of ship tracks N91-10507
Horizontal variability of the marine boundary layer structure upwind of San Nicolas Island during FIRE, 1987 N91-10519
Preliminary results of radiation measurements from the marine stratus FIRE experiment N91-10529
**STREAK CAMERAS**
A new method for doing flat-field intensity calibrations of multiplexed ITT streak cameras
[DE90-016475] N91-10267
**STRESS ANALYSIS**
A simple screw thread model for use in finite element stress analysis
[AD-A210233] N91-10300
Static and dynamic finite element stress analysis of layered composite plates and shells N91-10326
Design of a triaxial residual stress measurement system using high-energy x ray diffraction
[DE90-016212] N91-10331
**STRESS CYCLES**
Thermal fatigue cycling in turbine blades
[PNR-90682] N91-10067
**STRESS INTENSITY FACTORS**
Mechanical properties and fracture toughness of 8090-T651 plate and 2091 and 8090 sheet
[NRL-MP-88049-4] N91-10151
Study of mixed mode stress intensity factor using the experimental method of transmitted caustics
N91-10324
Fatigue crack propagation of coplanar semi-elliptical cracks in pure bending
[PNR-90742] N91-10337
**STRESS MEASUREMENT**
Design of a triaxial residual stress measurement system using high-energy x ray diffraction
[DE90-016212] N91-10331
**STRESS-STRAIN RELATIONSHIPS**
An analytical solution for the elastoplastic response of a continuous fiber composite under uniaxial loading
N91-10305
Analysis of moving strong discontinuity surfaces in elastic-plastic solids including effects of inertia and finite strain N91-10323
**STRONTIUM COMPOUNDS**
Advanced materials for high-temperature solid electrolyte applications
[DE90-016328] N91-10143
**STRUCTURAL ANALYSIS**
Body weight of hypersonic aircraft, part 1
[NASA-TM-101028] N91-10049
Structural tests of aircraft window assembly equipped with smoke evacuation valve
[DOT/FAA/CT-TN89/44] N91-10051
XAFS studies of interactions at transition-metal/Al interfaces
[DE90-016313] N91-10159
Probabilistic structural analysis by extremum methods
N91-10308
Exponential approximations in optimal design
N91-10311
An experimental and analytical study of structural identification N91-10325
Comparison of NASTRAN analysis with ground vibration results of UH-60A NASA/AEFA test configuration
[NASA-CR-184565] N91-10333
Mobility power flow analysis of an L-shaped plate structure subjected to distributed loading
[NASA-CR-187353] N91-10334
Experimental measurement of structural power flow on an aircraft fuselage
[NASA-CR-187352] N91-10335
**STRUCTURAL BASINS**
Energetics of valley and basin atmospheres during the evening transition and nighttime periods
[DE90-016356] N91-10542

**STRUCTURAL DESIGN**
Axial compression buckling test on CFRP surface plate/aluminum honeycomb sandwiched curved surface plate
[NAL-TM-584] N91-10299
Conservative buffering of approximate nonlinear constraints N91-10312
Analysis of elastically tailored viscoelastic damping member N91-10319
**STRUCTURAL FAILURE**
Structural integrity assessment of concrete slabs by nondestructive examination and Fourier transform-infrared methods
[DE90-017233] N91-10296
Analysis of elastically tailored viscoelastic damping member N91-10319
**STRUCTURAL WEIGHT**
Body weight of hypersonic aircraft, part 1
[NASA-TM-101028] N91-10049
**SUBSONIC FLOW**
Three-dimensional viscous/inviscid coupling in subsonic flow
[REPT-B-24] N91-10023
Calculation of three-dimensional viscous/inviscid interaction in subsonic flow
[REPT-B-25] N91-10024
Determination of the pressure drag of airfoils by integration of surface pressures
[NASA-TM-102722] N91-10078
**SUBSONIC SPEED**
Computation of boundary layer flow using thin-layer Navier-Stokes equations with flux-vector splitting
[REPT-B-21] N91-10254
Aeroacoustic effects of reduced aft tip speed at constant thrust for a model counterrotation turboprop at takeoff conditions
[NASA-TM-103608] N91-10703
**SUCTION**
Boundary-layer receptivity due to a wall suction and control of Tollmien-Schlichting waves
[NASA-CR-182103] N91-10009
**SUDDEN IONOSPHERIC DISTURBANCES**
Solar-geophysical data number 545, January 1990. Part 1 (Prompt reports). Data for December, November 1989 and late data
[PB90-182338] N91-10822
**SUDDEN STORM COMMENCEMENTS**
The empirical geomagnetic parameter infer near-Earth interplanetary shocks
[IFSI-90-14] N91-10820
**SULFUR DIOXIDES**
Reaction kinetics of the Ca-SO2 system in absence of inter-grain pore diffusion
[DE90-009672] N91-10781
**SUN**
The development of the continuous orthonormalization and adjoint methods for solar seismology: Eigenfrequency computation and sensitivity analysis for direct and inverse problems N91-10827
Propagation of magnetoacoustic waves in the solar atmosphere with random inhomogeneities of density and magnetic fields
[DE90-017616] N91-10831
Coaligned observations of solar magnetic fields at different heights: MSFC Center director's discretionary fund final report (Project No. 88-10)
[NASA-TM-103516] N91-10832
**SUPERCOMPUTERS**
Architecture simulator of parallel computer
[NAL-TM-583] N91-10601
**SUPERCONDUCTING MAGNETS**
High-temperature superconductors: Their potential for utility applications
[DE90-009704] N91-10757
Impact of high-critical-temperature superconductors on electromagnetic pump applications
[DE90-014809] N91-10759
**SUPERCONDUCTING POWER TRANSMISSION**
High-temperature superconductors: Their potential for utility applications
[DE90-009704] N91-10757
**SUPERCONDUCTING SUPER COLLIDER**
SSC dipole magnet measurement and alignment using laser technology
[DE90-014881] N91-10281
**SUPERCONDUCTIVITY**
Preparation of superconducting wire by deposition of YBa2Cu3O(x) onto fibers
[DE90-013380] N91-10758
Muon SR and high T(sub c) superconductivity
[DE90-015089] N91-10760
Evaluation, development, and characterization of superconducting materials for space applications
[NASA-CR-187017] N91-10763
Renormalization from density functional theory strong coupling models for the electronic structure of La2CuO4
[DE90-015990] N91-10765
Superconducting borides
[DE90-016484] N91-10769
Fe site occupancy and superconductivity in Y(1-z)Ca(z)Ba(z) (Cu(1-x)Fe(x))3O(6+y)
[DE90-016614] N91-10774
**SUPERCONDUCTORS**
Evaluation, development, and characterization of superconducting materials for space applications
[NASA-CR-187017] N91-10763
XAFS analysis in the anharmonic limit: Application to HI-Tc superconductors and ferrosilicates
[DE90-016720] N91-10776
**SUPERHIGH FREQUENCIES**
An x band backward-wave oscillator experiment
[DE90-015119] N91-10219
**SUPERLATTICES**
Nonlinear optical absorption in intrinsic Stark effect superlattices
[DE90-016466] N91-10767
Substrate temperature effects on (cubic x cubic lattice) R 30 deg domain growth of Ag on Si(111) surface
[DE90-016527] N91-10772
Excitons in semiconducting superlattices, quantum wells, and ternary alloys
[DE90-017287] N91-10779
**SUPERSATURATION**
Aerosol measurements in the stratocumulus project
N91-10506
**SUPERSONIC COMBUSTION RAMJET ENGINES**
OVRhyp, scramjet test aircraft
[NASA-CR-187009] N91-10041
Supersonic combustion engine testbed, heat lightning
[NASA-CR-187010] N91-10061
**SUPERSONIC COMMERCIAL AIR TRANSPORT**
Future supersonic transport populsion optimization
[PNR-90737] N91-10071
**SUPERSONIC FLOW**
Evaluation of the ZONA51D program
[REPT-B-28] N91-10025
**SUPPORT SYSTEMS**
Columbus logistics support. A conceptional definition of the operational phase
[MBB-UO-0093-90-PUB] N91-10091
Automated support of the modelling process: A view based on experiments with expert information engineers
[REPT-90-09] N91-10638
**SUPPORTS**
Thermionic converter emitter support arrangement
[DE90-015132] N91-10383
**SURFACE DEFECTS**
Holographic examination of great surface fiberbound components in industrial conditions: Resumes of final reports, April 1986 to June 1989
[MBB-Z-0306-90-PUB-KURZFASSUNG] N91-10136
**SURFACE DISTORTION**
System engineering of aerospace and advanced technology programs at an astronautics company (record of study) N91-10192
**SURFACE FINISHING**
Applications of thermally sprayed coating systems in aero engines
[PNR-90750] N91-10072
Diamond turning of optical crystals
[DE90-015909] N91-10719
**SURFACE LAYERS**
Deposition controlled uniformity of multilayer mirrors
[DE90-015906] N91-10718
**SURFACE TEMPERATURE**
Documentation for Program SOILSIM: A computer program for the simulation of heat and moisture flow in soils and between soils, canopy and atmosphere
[NASA-CR-186953] N91-10379
**SURFACE VEHICLES**
Experiments and theory with a 0.5 ton mobile robot
[OUEL-1807/90] N91-10035
Image motion experiments with the Oxford AGV
[OUEL-1809/90] N91-10654
**SURVEYS**
Applied technology center business plan and market survey
[NASA-CR-187259] N91-10794
**SWELLING**
Radiation-induced microstructural development and microchemical changes in Fe-Cr-Mn-Ni solute-bearing alloys
[DE90-016359] N91-10160
**SWEPT WINGS**
Vortex instabilities in 3D boundary layers: The relationship between Goertler and crossflow vortices
[NASA-CR-187456] N91-10022
**SWITCHES**
Railgun restrike control
[DE90-015108] N91-10095
Design and application of gas-gap heat switches
[NASA-CR-187339] N91-10222
**SWITCHING**
Plasma puff initiation of high Coulomb transfer switches
[NASA-CR-187024] N91-10735
**SYMMETRY**
On q-analogues of the Fourier and Hankel transforms
[REPT-89-89] N91-10666
Symmetries of the three body problem
[MEMO-843] N91-10674
Cohomology for Lagrangian systems and Noetherian symmetries
[DE90-628371] N91-10788
**SYNCHRONISM**
A conservative approach to parallelizing the Sharks World simulation
[NASA-CR-187440] N91-10629
Modelization of LOCSTAR synchronisation system. Computation of non detection and false alarm probabilities. Reflections on threshold adjustment and correlator structure
[CNES-CT/DRT/TIT/TR-88/060] N91-10691
**SYNOPTIC METEOROLOGY**
Q-vectors: A new approach to an old problem
[PB90-235490] N91-10414
Synoptic conditions producing cirrus during the FIRE cirrus IFO N91-10449
ISCCP results for the FIRE IFO regions and times
N91-10451
Cloud information for FIRE from surface weather reports N91-10452
Vertical velocities within a Cirrus cloud from Doppler lidar and aircraft measurements during FIRE: Implications for particle growth N91-10461
Overview of the 27-28 October FIRE Cirrus IFO case: Meteorology and cloud fields N91-10477
**SYNTHESIS (CHEMISTRY)**
Trifluoromethyl-substituted polymers
[NASA-CR-186955] N91-10170
**SYNTHETIC RESINS**
Environmental degradation of macro defect free cements. 1: Mechanical properties investigation
[AERE-R-13354-1] N91-10169
**SYSTEM FAILURES**
Automatic determination of fault effects on aircraft functionality
[NASA-CR-181352] N91-10039
Drive system life and reliability N91-10044
A representation scheme for fault diagnosis of physical systems
[DE90-016362] N91-10295
**SYSTEM IDENTIFICATION**
Function library using APL for time series analysis and system identification in structures
[NAL-TM-578] N91-10604
**SYSTEMS ANALYSIS**
Developing a framework for qualitative engineering: Research in design and analysis of complex structural systems N91-10322
**SYSTEMS ENGINEERING**
Space Station Freedom Environmental Control and Life Support System (ECLSS) phase 3 simplified integrated test trace contaminant control subsystem performance
[NASA-TM-4202] N91-10103
System engineering of aerospace and advanced technology programs at an astronautics company (record of study) N91-10192
Developing a framework for qualitative engineering: Research in design and analysis of complex structural systems N91-10322
A modernized PDL approach for Ada software development N91-10616
**SYSTEMS INTEGRATION**
System engineering of aerospace and advanced technology programs at an astronautics company (record of study) N91-10192
Knowledge-based assistance in costing the space station DMS N91-10611
Software integration technologies in industrial applications
[MA-55] N91-10627

## T

**T-56 ENGINE**
Flight testing of two Allison T56 engines modified to the ARL developed low smoke configuration
[ARL-PROP-TM-449] N91-10064
**TABLES (DATA)**
Solar-geophysical data number 545, January 1990. Part 1 (Prompt reports). Data for December, November 1989 and late data
[PB90-182338] N91-10822

**TARGETS**
Sodium-neon resonant photoexcitation soft x ray laser experiments on Saturn
[DE90-014946] N91-10275
**TEARING MODES (PLASMAS)**
Tearing modes in tokamaks with lower hybrid current drive
[DE90-017090] N91-10743
**TECHNOLOGIES**
JPRS report: Science and technology. USSR: Space
[JPRS-USP-90-001] N91-10089
JPRS report: Science and technology. USSR: Electronics and electrical engineering
[JPRS-UEE-90-004] N91-10213
JPRS Report: Science and technology. USSR: Life sciences
[JPRS-ULS-90-008] N91-10570
**TECHNOLOGY TRANSFER**
Industry liaison section implementation plan
[NASA-CR-177569] N91-10048
Artificial intelligence, human factors, robotics, and computer simulation
[DE90-016866] N91-10653
Technical Abstracts: Mechanical engineering
[DE90-014797] N91-10802
Putting technology to work, 1990. Examples of industry-laboratory cooperation contributing to our nation's economic strength
[PB90-215187] N91-10805
**TECHNOLOGY UTILIZATION**
Industry liaison section implementation plan
[NASA-CR-177569] N91-10048
Technology update of early gas turbine designs
[PNR-90710] N91-10070
Industrial applications and markets for ceramic matrix composites
[PNR-90753] N91-10138
Multi industry application of advanced materials
[PNR-90764] N91-10139
Engineering design: A powerful influence on the business success on manufacturing industry
[PNR-90763] N91-10197
High-temperature superconductors: Their potential for utility applications
[DE90-009704] N91-10757
**TELECOMMUNICATION**
Spacecraft Health Automated Reasoning Prototype (SHARP): The fiscal year 1989 SHARP portability evaluations task for NASA Solar System Exploration Division's Voyager project
[NASA-CR-187338] N91-10204
Principles of LOCSTAR system experiments
[CNES-CT/DRT/TIT/TR-88/355] N91-10207
Outline of the GMS telecommunication system
N91-10339
Outline of CDAS telecommunication system
N91-10340
DPC telecommunication system N91-10354
**TELEMETRY**
Meteorological Satellite Center Technical Note. Special Issue (1989). Summary of GMS System. 1: Telecommunication System N91-10338
Outline of CDAS telecommunication system
N91-10340
Telemetry subsystem N91-10345
Command subsystem N91-10346
**TELEOPERATORS**
Protective autonomy: Embedding sensor-based safety and protection mechanisms into the motion control of mobile and tele-operated robots
[OUEL-1808/90] N91-10292
**TELESCOPES**
Influence of the telescope depointing on the performances of an optical link. Correlation between depointing law and coding, concerning the computation of mean BER
[CNES-CT/DRT/TIT/TR-88/24-T] N91-10206
Cluster as a wave telescope N91-10424
**TEMPERATE REGIONS**
The stationary wave response to tropical and midlatitude SST anomalies N91-10536
**TEMPERATURE DEPENDENCE**
Ultra-thin vertical magneto-optical media and system for using same
[DE90-014589] N91-10603
**TEMPERATURE DISTRIBUTION**
Brightness temperature distribution N91-10369
**TEMPERATURE EFFECTS**
Numerical simulation of hypersonic flow around a space plane. Part 3: Analysis of aerothermodynamic heating
[NAL-TR-1027T] N91-10011
Composite heat damage. Part 1: Mechanical testing of IM6/3501-6 laminates. Part 2: Nondestructive evaluation studies of IM6/3501-6 laminates
[DE90-016207] N91-10125
Beryllium weldability
[DE90-014696] N91-10155
Constant stress of XD (trademark) TiAl containing nitrogen
[DE90-011947] N91-10158
Mechanical and microstructural response of Ni3Al at high strain rate and elevated temperatures
[DE90-016489] N91-10162
Design methodology needs for fiber-reinforced ceramic heat exchangers
[DE90-016659] N91-10178
System engineering of aerospace and advanced technology programs at an astronautics company (record of study) N91-10192
Overdischarge protection in high-temperature cells and batteries
[DE90-015180] N91-10220
Preparation of superconducting wire by deposition of YBa2Cu3O(x) onto fibers
[DE90-013380] N91-10758
Electronic, structural and transport properties of (almost) rare-earth-like actinide hydrides
[DE90-016491] N91-10771
Substrate temperature effects on (cubic x cubic lattice) R 30 deg domain growth of Ag on Si(111) surface
[DE90-016527] N91-10772
**TEMPERATURE GRADIENTS**
Unified theory of ballooning instabilities and temperature gradient driven trapped ion modes
[DE90-017091] N91-10744
Numerical simulation of ion temperature gradient driven modes in the presence of ion-ion collisions
[DE90-017092] N91-10745
**TEMPERATURE INVERSIONS**
Boundary layer roll circulations during FIRE
N91-10521
**TEMPERATURE MEASUREMENT**
Horizontal variability of the marine boundary layer structure upwind of San Nicolas Island during FIRE, 1987 N91-10519
Comparison and calibration of NCAR electra instruments: July 5 and 7, 1987 N91-10532
**TEMPERATURE PROFILES**
Turbulence measurements using tethered balloon instrumentation during FIRE 1987 N91-10518
Boundary layer roll circulations during FIRE
N91-10521
**TENSILE PROPERTIES**
Brittle fracture and ductility improvement in nickel and iron aluminides
[DE90-017319] N91-10167
**TENSILE STRESS**
An analytical solution for the elastoplastic response of a continuous fiber composite under uniaxial loading
N91-10305
**TENSILE TESTS**
Influence of expanding monomer on carbon fiber reinforced epoxy composites
[AD-A223277] N91-10124
Constant stress of XD (trademark) TiAl containing nitrogen
[DE90-011947] N91-10158
**TERMINOLOGY**
NASA Thesaurus supplement: A four part cumulative supplement to the 1988 edition of the NASA Thesaurus (supplement 4)
[NASA-SP-7064-SUPPL-4] N91-10804
**TERNARY ALLOYS**
Equal eigenvalues in multicomponent diffusion: The extraction of diffusion coefficients from experimental data in ternary systems
[DE90-012074] N91-10142
Excitons in semiconducting superlattices, quantum wells, and ternary alloys
[DE90-017287] N91-10779
**TERRAIN**
Terrain-induced mesoscale circulations in the Columbia Basin
[DE90-016338] N91-10541
**TERRESTRIAL RADIATION**
Radio wave remote sensing by Cluster and Regatta
N91-10439
FIRE extended time/limited area observations at Palisades, New York N91-10527
**TEST FACILITIES**
Effects of coolant injection on turbine aerodynamic characteristics. Part 1: Test turbine and apparatus
[NAL-TM-585-PT-1] N91-10059
Large blast and thermal simulator advanced concept driver design by computational fluid dynamics
[AD-A211364] N91-10230
**TEST STANDS**
Supersonic combustion engine testbed, heat lightning
[NASA-CR-187010] N91-10061
**TETHERED BALLOONS**
Analysis of tethered balloon, ceilometer and class sounding data taken on San Nicolas Island during the FIRE project N91-10492
NRL tethered balloon measurements at San Nicolas Island during FIRE IFO 1987 N91-10509
Analysis of tethered balloon data from San Nicolas Island on 8 July 1987 N91-10517
Turbulence measurements using tethered balloon instrumentation during FIRE 1987 N91-10518
**TETHERED SATELLITES**
First evaluation of the main parameters in the dynamics of the Small Expendable Deployer System (SEDS) for a tethered satellite
[NASA-CR-4319] N91-10098
**TETHERING**
First evaluation of the main parameters in the dynamics of the Small Expendable Deployer System (SEDS) for a tethered satellite
[NASA-CR-4319] N91-10098
**THEOREM PROVING**
The 'optimum' upwind advection on a triangular mesh
[NASA-CR-187459] N91-10250
On the convergence at infinity, rate of convergence and uniqueness of solutions with finite Dirichlet integral to the exterior Dirichlet problem for the steady plane Navier-Stokes system of equations
[PREPRINT-166] N91-10257
**THEORETICAL PHYSICS**
Operator formalism of multi-pole Virasoro algebra on Riemann sphere
[DE90-627217] N91-10657
**THERMAL ANALYSIS**
A weldability study of Haynes Alloy no. 242
[DE90-013875] N91-10154
**THERMAL CONDUCTIVITY**
Design and application of gas-gap heat switches
[NASA-CR-187339] N91-10222
Temporal behaviour of self generated magnetic field and its influence on inhibition of thermal flux in ICF plasma
[DE90-627478] N91-10731
**THERMAL DEGRADATION**
Thermal stability of jet fuel
[DE90-016801] N91-10188
Basic study of solid oxide fuel cells
[DE90-517069] N91-10386
**THERMAL FATIGUE**
Thermal fatigue cycling in turbine blades
[PNR-90682] N91-10067
**THERMAL PROTECTION**
Flight set 360L007 (STS-33R) field joint protection system, thermal protection system, and systems tunnel components, volume 7
[NASA-CR-184026] N91-10115
**THERMAL SIMULATION**
Large blast and thermal simulator advanced concept driver design by computational fluid dynamics
[AD-A211364] N91-10230
**THERMAL STABILITY**
Thermal stability of jet fuel
[DE90-016801] N91-10188
**THERMAL STRESSES**
Reduction of thermal stresses in continuous fiber reinforced metal matrix composites with interface layers
[NASA-CR-185302] N91-10133
**THERMIONIC CONVERTERS**
Thermionic converter emitter support arrangement
[DE90-015132] N91-10383
**THERMIONIC EMITTERS**
Thermionic converter emitter support arrangement
[DE90-015132] N91-10383
**THERMOCHEMISTRY**
Thermochemistry of shock-induced exothermic reactions in selected porous mixtures
[DE90-016104] N91-10183
**THERMODYNAMIC EFFICIENCY**
Design of highly concentrating solar collectors and solar collector systems
[DLR-FB-90-11] N91-10390
**THERMODYNAMIC EQUILIBRIUM**
Transition state theory applying to the study of reaction processes in detonation
[DE90-016558] N91-10187
**THERMODYNAMIC PROPERTIES**
Boundary layer roll circulations during FIRE
N91-10521
Thermophysical properties of fluids and fluid mixtures
[DE90-016306] N91-10792
**THERMODYNAMICS**
Monomolecular and thin polymer films: Fabrication, characterization, applications, and models of wetting
[DE90-016415] N91-10174
Proceedings of the 8th Symposium on Energy Engineering Sciences: Micro/Macro Studies of Multiphase Media
[DE90-014844] N91-10385

Aircraft measurements of the mean and turbulent structure of marine stratocumulus clouds during FIRE
N91-10514
Cloud and boundary layer structure over San Nicolas Island during FIRE N91-10515
Thermodynamic structure of the stratocumulus-capped boundary layer on 5 July 1987 N91-10516
ER-2 lidar measurements of stratocumulus cloud top structure on July 14, 1987 N91-10523
Thermodynamic structure of the stratocumulus-capped boundary layer on 7 July, 1987 N91-10533
Energetics of valley and basin atmospheres during the evening transition and nighttime periods
[DE90-016356] N91-10542
Parameterization of cosmological scale factor during inflationary times N91-10815

**THERMOMETERS**
Thin film thermometers and flowmeters for applications in liquid helium N91-10265

**THERMONUCLEAR EXPLOSIONS**
Large blast and thermal simulator advanced concept driver design by computational fluid dynamics
[AD-A211364] N91-10230

**THERMONUCLEAR REACTIONS**
Theoretical atomic physics for fusion
[DE90-017280] N91-10710

**THERMOPHYSICAL PROPERTIES**
Thermophysical properties of fluids and fluid mixtures
[DE90-016306] N91-10792

**THERMOPLASTIC RESINS**
Evaluation of two bisimide additives in LARC-TPI adhesive
[NASA-TM-102742] N91-10182

**THERMOREGULATION**
Combined effects of elevated concentrations of carbon dioxide and ambient temperature on thermal state of humans in closed chambers N91-10563

**THESAURI**
NASA Thesaurus supplement: A four part cumulative supplement to the 1988 edition of the NASA Thesaurus (supplement 4)
[NASA-SP-7064-SUPPL-4] N91-10804

**THETA PINCH**
Experiments on linear high beta helical axis stellarators to study simulated toroidal effects and Alfven-wave heating
[DE90-016122] N91-10738

**THICKNESS**
Thermodynamic structure of the stratocumulus-capped boundary layer on 5 July 1987 N91-10516

**THIN FILMS**
Characterization of mono- and multi-molecular assemblies at glassy carbon and noble metals by ex situ and in situ infrared external reflection spectroscopy
[DE90-016417] N91-10144
Anomalous dispersion as a phase-matching technique for second harmonic generation
[DE90-015696] N91-10172
Monomolecular and thin polymer films: Fabrication, characterization, applications, and models of wetting
[DE90-016415] N91-10174
Thin film thermometers and flowmeters for applications in liquid helium N91-10265
The looped adhesive strip: An example of coplanar delamination interaction N91-10306
Materials analysis and device optimization of CuInSe2 solar cells
[DE90-000365] N91-10384
Ultra-thin vertical magneto-optical media and system for using same
[DE90-014589] N91-10603
Stability of some stationary solutions for the forced KdV equation
[DE90-016506] N91-10662
Theoretical calculations of the nonlinear dielectric function of inhomogeneous thin films
[DE90-017186] N91-10778
Determination of surface resistance and magnetic penetration depth of superconducting YBa2Cu3O(7-delta) thin films by microwave power transmission measurements
[NASA-TM-103616] N91-10780

**THREADS**
A simple screw thread model for use in finite element stress analysis
[AD-A210233] N91-10300

**THREE BODY PROBLEM**
Symmetries of the three body problem
[MEMO-843] N91-10674

**THREE DIMENSIONAL FLOW**
Modeling blade/vortex interactions
[ISL-R-107/89] N91-10016
Aeroelastic analysis of wings using the Euler equations with a deforming mesh
[NASA-TM-102733] N91-10020
Three-dimensional viscous/inviscid coupling in subsonic flow
[REPT-B-24] N91-10023
Calculation of three-dimensional viscous/inviscid interaction in subsonic flow
[REPT-B-25] N91-10024
Numerical investigations in three-dimensional internal flows
[NASA-CR-186958] N91-10083

**THREE DIMENSIONAL MODELS**
Modeling blade/vortex interactions
[ISL-R-107/89] N91-10016
Multigrid solution for the Euler equations in axisymmetric flow
[REPT-B-17] N91-10253
Modeling of hydrocarbon fueling
[DE90-014790] N91-10289
The numerical simulation of nonlinear gravity waves in three dimensions using a higher order panel method
[ISBN-90-9002667-23] N91-10443
CVMAC 2D Program: A method of converting 3D to 2D
[DE90-015147] N91-10626
Some recent applications of numerical methods to geotechnical analysis
[PB90-201229] N91-10655

**THRUST**
Analysis of pulsed laser-generated impulse in an advanced airbreathing thruster N91-10062

**THRUST CONTROL**
Aero engine design factors for a low fuel price scenario
[PNR-90681] N91-10066

**THRUST MEASUREMENT**
Performance characterization of a segmented anode arcjet thruster
[NASA-TM-103227] N91-10118

**THRUST VECTOR CONTROL**
Nonlinear feedback control for high alpha flight
[NASA-CR-186545] N91-10047

**THUNDERSTORMS**
Development and application of linear and nonlinear methods for interpretation of lightning strikes to in-flight aircraft
[NASA-CR-3974] N91-10548

**TIDAL WAVES**
Verification of GONO wave predictions for the period October 1987 to April 1988
[KNMI-TR-118] N91-10545
Wind wave propagation in tidal seas
[REPT-90-1] N91-10550

**TIME DEPENDENCE**
Simulation of time-dependent compressible viscous flows using central and upwind-biased finite difference techniques N91-10234
Energetic particles in the Earth's magnetotail or: Cluster and Regatta as a dispersiometer N91-10434
The digital regulator and tracker for deterministic continuous-time linear time-varying systems
[REPT-90-05] N91-10668
The digital regulator and tracker for stochastic continuous-time linear time-varying systems
[REPT-90-06] N91-10689

**TIME LAG**
Fully automatic analysis in an industrial environment
[PNR-90722] N91-10647

**TIME MARCHING**
Simulation of time-dependent compressible viscous flows using central and upwind-biased finite difference techniques N91-10234

**TIME SERIES ANALYSIS**
Analysis techniques for residual acceleration data
[NASA-TM-103507] N91-10191
Analyzing long time series of hydrological data with respect to climate variability: Project description
[WCAP-3] N91-10444
Function library using APL for time series analysis and system identification in structures
[NAL-TM-578] N91-10604

**TIN ALLOYS**
Mechanisms of high temperature crack growth in metals and alloys
[DE90-014934] N91-10152

**TIP SPEED**
Aeroacoustic effects of reduced aft tip speed at constant thrust for a model counterrotation turboprop at takeoff conditions
[NASA-TM-103608] N91-10703

**TITANIUM ALLOYS**
Constant stress of XD (trademark) TiAl containing nitrogen
[DE90-011947] N91-10158

**TITANIUM NITRIDES**
Corrosion-resistant coatings for high-temperature high-sulfur activity applications
[DE90-016638] N91-10177

**TOKAMAK DEVICES**
Modeling of hydrocarbon fueling
[DE90-014790] N91-10289
On lower hybrid wave scattering by plasma density fluctuation nonlinear reflection coefficient of the fast magnetoacoustic wave
[IPPCZ-281] N91-10725
Comments on edge turbulence during lower hybrid current drive experiment on CASTOR tokamak
[IPPCZ-279] N91-10726
Models of plasma confinement and heating in tokamaks
[DE90-016671] N91-10741
Pellet injector development at ORNL (Oak Ridge National Laboratory)
[DE90-017024] N91-10742
Tearing modes in tokamaks with lower hybrid current drive
[DE90-017090] N91-10743

**TOLERANCES (MECHANICS)**
Introduction: Needs and approaches to reliability and quality assurance in design and manufacture
[PNR-90683] N91-10297

**TOLLMIEN-SCHLICHTING WAVES**
Boundary-layer receptivity due to a wall suction and control of Tollmien-Schlichting waves
[NASA-CR-182103] N91-10009

**TOROIDAL PLASMAS**
Self-consistent field error effects in reversed field pinch plasmas N91-10728
Theoretical analysis of a runaway electron suppression device
[DE90-015992] N91-10737
Experiments on linear high beta helical axis stellarators to study simulated toroidal effects and Alfven-wave heating
[DE90-016122] N91-10738
Theory of longitudinal adiabatic invariant in the helical torus
[NIFS-37] N91-10749

**TOROIDS**
Theoretical studies of turbulence and anomalous transport in toroidal confinement devices
[DE90-017606] N91-10747

**TRACKING (POSITION)**
Differential Global Positioning System (DGPS) test plan
[DOT/FAA/CT-TN90/15] N91-10034

**TRAINING DEVICES**
The design and fabrication of the Centaur neutral buoyancy trainer and related hardware
[NASA-CR-171944] N91-10085

**TRAJECTORIES**
The 1987 Strategic Defense Initiative Organization (SDIO) Workshop on Laser Propulsion
[DE90-013484] N91-10274

**TRAJECTORY CONTROL**
Entry vehicle performance analysis and atmospheric guidance algorithm for precision landing on Mars
[NASA-CR-185614] N91-10102
Redundancy control of a robot manipulator using a systolic array processor N91-10287

**TRANSFER FUNCTIONS**
Minimizing frequency pulling of quartz oscillators due to power supply variations
[DE90-014566] N91-10218
Casual eigenvector function approximations and the problem of scaling: An algorithm
[OUEL-1822/90] N91-10644
H 2 and H infinity approximations for eigenvalue/vector functions of transfer matrices
[OUEL-1778/89] N91-10684
Estimation of astronomical images from the bispectrum of atmospherically distorted infrared data N91-10806

**TRANSFORMATIONS (MATHEMATICS)**
Invariant measures exist under a summability condition for unimodal maps
[REPT-90-36] N91-10670
On Baecklund transformations and identities in bilinear form
[MEMO-856] N91-10681

**TRANSITION METALS**
On the effects of magnetic bonding in rare earth transition metal intermetallics
[DE90-015800] N91-10156

**TRANSITION TEMPERATURE**
Muon SR and high T(sub c) superconductivity
[DE90-015089] N91-10760
Fe site occupancy and superconductivity in Y(1-z)Ca(z)Ba(z) (Cu(1-x)Fe(x))3O(6+y)
[DE90-016614] N91-10774
A correlation between T(sub 3) and electronegativity difference in high-temperature superconductors
[DE90-016640] N91-10775

**TRANSMISSION EFFICIENCY**
Hydrologic and meteorological operations in the 162-174 and 406.1-420 MHz bands
[PB90-207820] N91-10199
**TRANSMISSION LINES**
Three-dimensional full-wave analysis of signal communications in active integrated circuits using a variable-mesh TLM method N91-10212
High-temperature superconductors: Their potential for utility applications
[DE90-009704] N91-10757
**TRANSMISSIONS (MACHINE ELEMENTS)**
Helicopter transmissions: Design for safety and reliability N91-10043
**TRANSMITTANCE**
Estimating integrated cloud liquid water from extended time observations of solar irradiance N91-10510
**TRANSMITTERS**
Antenna/transmitter control unit N91-10348
**TRANSONIC FLOW**
Transonic flow analysis for rotors. Part 3: Three-dimensional, quasi-steady, Euler calculation
[NASA-TP-2375] N91-10007
Wake coupling to full potential rotor analysis code
[NASA-TM-102805] N91-10013
A contribution to the numerical solution of transonic flow around a delta wing by solving Navier-Stokes equations
[DLR-FB-90-13] N91-10026
**TRANSONIC SPEED**
Time/frequency analysis of vibro-acoustic behaviour of a launcher in flight
[ETN-90-97584] N91-10097
**TRANSPARENCE**
Study of mixed mode stress intensity factor using the experimental method of transmitted caustics
N91-10324
**TRANSPORT AIRCRAFT**
Computation of maximum gust loads in nonlinear aircraft using a new method based on the matched filter approach and numerical optimization N91-10317
**TRANSPORT PROPERTIES**
The transport properties of activated carbon fibers
[DE90-015910] N91-10130
About the possibilities of using an air mass transformation model in Taiyuan, Shanxi Province, China
[KNMI-TR-120] N91-10540
Electronic, structural and transport properties of (almost) rare-earth-like actinide hydrides
[DE90-016491] N91-10771
**TRANSPORT THEORY**
A one-equation turbulence transport model for high Reynolds number wall-bounded flows
[NASA-TM-102847] N91-10252
INEX modeling of the Boeing ring optical resonator free-electron laser
[DE90-016488] N91-10280
About the possibilities of using an air mass transformation model in Taiyuan, Shanxi Province, China
[KNMI-TR-120] N91-10540
Plasma properties
[DE90-017256] N91-10746
The growth of zinc selenide single crystals by physical vapor transport in microgravity
[NASA-CR-180428] N91-10755
**TRAPPED PARTICLES**
Unified theory of ballooning instabilities and temperature gradient driven trapped ion modes
[DE90-017091] N91-10744
**TREADMILLS**
Work, exercise, and space flight. 3: Exercise devices and protocols N91-10579
**TREES (PLANTS)**
Short-rotation woody crop opportunities to mitigate carbon dioxide buildup
[DE90-016526] N91-10406
**TRIANGULATION**
An experimental and analytical study of structural identification N91-10325
Approximation and geometric modeling with simplex B-splines associated with irregular triangles
[MEMO-842] N91-10673
A remark on the convexity of piecewise polynomial functions on triangulations
[MEMO-857] N91-10682
**TRIAXIAL STRESSES**
Design of a triaxial residual stress measurement system using high-energy x ray diffraction
[DE90-016212] N91-10331
**TRIBOLOGY**
Self-lubricating boric acid films for tribological applications
[DE90-007805] N91-10171
**TRITIUM**
Hydrogen-tritium getters and their applications
[DE90-016282] N91-10184
Organic getter materials for the removal of hydrogen and its isotopes
[DE90-016284] N91-10185
**TROPICAL METEOROLOGY**
Radiative control on tropical convective boundary layer equilibrium N91-10493
**TROPICAL REGIONS**
The stationary wave response to tropical and midlatitude SST anomalies N91-10536
**TROPICAL STORMS**
Mariners Weather Log, Volume 34, Number 2, Spring 1990
[PB90-222324] N91-10537
**TROPOPAUSE**
Subvisual Cirrus cloud properties derived from a FIRE IFO case study N91-10464
**TROPOSPHERE**
Global tropospheric chemistry modeling
[DE90-015908] N91-10409
The effects of cloud radiative forcing on an ocean-covered planet N91-10456
**TROUGHS**
Sub-visual Cirrus detection and characterization
N91-10486
**TRUNCATION ERRORS**
The 'optimum' upwind advection on a triangular mesh
[NASA-CR-187459] N91-10250
**TRUSSES**
Analysis of elastically tailored viscoelastic damping member N91-10319
**TURBINE BLADES**
Thermal fatigue cycling in turbine blades
[PNR-90682] N91-10067
Heat transfer in aero engine gas turbines, part 1
[PNR-90754-PT-1] N91-10074
Design/development issues for high bypass ratio fans
[PNR-90758] N91-10076
**TURBINE ENGINES**
The evolution of the bypass engine
[PNR-90707] N91-10068
**TURBINES**
High temperature cyclic oxidation data. Part 1: Turbine alloys
[NASA-TM-83665] N91-10149
High-temperature cyclic oxidation data. Part 2: Turbine alloys
[NASA-TM-101468] N91-10150
**TURBOFAN ENGINES**
Re-engining: Real stage 3 compliance plus other benefits
[PNR-90755] N91-10075
**TURBOFANS**
Future supersonic transport populsion optimization
[PNR-90737] N91-10071
Re-engining: Real stage 3 compliance plus other benefits
[PNR-90755] N91-10075
Design/development issues for high bypass ratio fans
[PNR-90758] N91-10076
**TURBOJET ENGINES**
Parametric assessment of propulsion system mass for airbreathing launcher configurations
[PNR-90634] N91-10063
**TURBOMACHINERY**
Flow measurements in turbomachinery using laser anemometry and holography
[PNR-90717] N91-10261
**TURBULENCE**
Aircraft measurements of the mean and turbulent structure of marine stratocumulus clouds during FIRE
N91-10514
Theoretical studies of turbulence and anomalous transport in toroidal confinement devices
[DE90-017606] N91-10747
Anomalous viscosity due to drift wave turbulence
[NIFS-33] N91-10752
**TURBULENCE EFFECTS**
Evaluation of flow quality in newly constructed low-turbulence calibration wind-tunnel for laser velocimeters
[NAL-TR-1054] N91-10087
Static and dynamic aeroelastic characterization of an aerodynamically heated generic hypersonic aircraft configuration N91-10320
**TURBULENCE MODELS**
Numerical computation of viscous flow about unconventional airfoil shapes
[NASA-CR-187343] N91-10019
A three-dimensional turbulent heat transfer analysis for advanced tubular rocket thrust chambers
[NASA-TM-103293] N91-10249
Preliminary mixed-layer model results for FIRE marine stratocumulus IFO conditions N91-10495
Simulations and observations of cloudtop processes
N91-10496
Fractional cloudiness in shallow cumulus layers
N91-10498
**TURBULENT BOUNDARY LAYER**
Turbulent boundary layers in high enthalpy flows. Numerical code validation by shock tube experiments
[ISL-CO-221/89] N91-10246
Velocity measurements in piston-induced turbulent boundary layers in a shock tube
[ISL-CO-235/89] N91-10247
Model of gravity-wave-induced variability and turbulence in the stratified free atmosphere
[PB90-235482] N91-10413
**TURBULENT FLOW**
Turbulent flow calculations using unstructured and adaptive meshes
[NASA-CR-182102] N91-10010
Numerical computation of viscous flow about unconventional airfoil shapes
[NASA-CR-187343] N91-10019
Transient characteristics of unconfined fire plume-driven ceiling jets
[PB90-227976] N91-10193
Bounded energy states in homogeneous turbulent shear flow: An alternative view
[NASA-CR-187439] N91-10237
Turbulence measurements using tethered balloon instrumentation during FIRE 1987 N91-10518
Plume mechanics and stratocumulus convection
N91-10526
Markov model of the propagation of a light wave in a heated turbulent media
[ECL-90-06] N91-10723
**TURBULENT HEAT TRANSFER**
AFDM: An Advanced Fluid-Dynamics Model
[DE90-017537] N91-10242
A three-dimensional turbulent heat transfer analysis for advanced tubular rocket thrust chambers
[NASA-TM-103293] N91-10249
**TVD SCHEMES**
Numerical simulation of hypersonic flow around a space plane. Part 3: Analysis of aerothermodynamic heating
[NAL-TR-1027T] N91-10011
**TWO DIMENSIONAL BODIES**
User's guide to CUNIFLOW
[AD-A207606] N91-10004
Users manual for AUTOMESH-2D: A program of automatic mesh generation for two-dimensional scattering analysis by the finite element method
[NASA-CR-186929] N91-10623
**TWO DIMENSIONAL FLOW**
Modeling blade/vortex interactions
[ISL-R-107/89] N91-10016
**TWO DIMENSIONAL MODELS**
Turbulent flow calculations using unstructured and adaptive meshes
[NASA-CR-182102] N91-10010
The effects of critical layers on atmospheric cnoidal waves
[DE90-016540] N91-10440
Cirrus cloud model parameterizations: Incorporating realistic ice particle generation N91-10453
**TWO PHASE FLOW**
Two-phase flow patterns and frictional pressure gradients in a small, horizontal, rectangular channel
[DE90-014802] N91-10236
AFDM: An Advanced Fluid-Dynamics Model. Volume 4: The AFDM heat- and mass-transfer solution algorithm
[DE90-017535] N91-10240
**TYPHOONS**
Mariners Weather Log, Volume 34, Number 2, Spring 1990
[PB90-222324] N91-10537

## U

**U.S.S.R.**
JPRS report: Science and technology. USSR: Space
[JPRS-USP-89-009] N91-10088
JPRS report: Science and technology. USSR: Space
[JPRS-USP-90-001] N91-10089
JPRS report: Science and technology. USSR: Space
[JPRS-USP-90-002] N91-10090
JPRS report: Science and technology. USSR: Electronics and electrical engineering
[JPRS-UEE-90-004] N91-10213
JPRS report: Science and technology. USSR: Electronics and electrical engineering
[JPRS-UEE-90-006] N91-10214
JPRS report: Science and technology. USSR: Electronics and electrical engineering
[JPRS-UEE-90-007] N91-10215
JPRS report: Science and technology. USSR: Electronics and electrical engineering
[JPRS-UEE-90-008] N91-10216

JPRS report: Science and technology. USSR: Electronics and electrical engineering
[JPRS-UEE-90-009] N91-10217
JPRS report: Science and technology. USSR: Earth sciences
[JPRS-UES-90-006-L] N91-10376
JPRS report: Science and technology. USSR: Earth sciences
[JPRS-UES-90-007] N91-10377
JPRS report: Science and technology. USSR: Life sciences
[JPRS-ULS-90-001] N91-10551
JPRS report: Science and technology. USSR: Life sciences
[JPRS-ULS-90-013] N91-10552
JPRS report: Science and technology. USSR: Life sciences
[JPRS-ULS-90-012] N91-10556
JPRS report: Science and technology. USSR: Life sciences
[JPRS-ULS-90-011] N91-10565
JPRS Report: Science and technology. USSR: Life sciences
[JPRS-ULS-90-010] N91-10568
JPRS Report: Science and technology. USSR: Life sciences
[JPRS-ULS-90-009] N91-10569
JPRS Report: Science and technology. USSR: Life sciences
[JPRS-ULS-90-008] N91-10570
JPRS Report: Science and technology. USSR: Life sciences
[JPRS-ULS-90-006] N91-10571
JPRS report: Science and technology. USSR: Life sciences
[JPRS-ULS-90-005] N91-10572
JPRS report: Science and technology. USSR: Life sciences
[JPRS-ULS-89-008] N91-10589
JPRS report: Science and technology. USSR: Life sciences
[JPRS-ULS-89-010] N91-10590
JPRS report: Science and technology. USSR: Physics and mathematics
[JPRS-UPM-90-003] N91-10694

**U-2 AIRCRAFT**
Lidar and radiometer results from the ER-2 for the FIRE field experiments N91-10468
Thermodynamic structure of the stratocumulus-capped boundary layer on 7 July, 1987 N91-10533

**UH-60A HELICOPTER**
Comparison of NASTRAN analysis with ground vibration results of UH-60A NASA/AEFA test configuration
[NASA-CR-184565] N91-10333

**ULTRAHIGH FREQUENCIES**
Hydrologic and meteorological operations in the 162-174 and 406.1-420 MHz bands
[PB90-207820] N91-10199

**ULTRASONIC TESTS**
Physical interpretation and application of principles of ultrasonic nondestructive evaluation of high-performance materials
[NASA-CR-180489] N91-10293

**ULTRAVIOLET ASTRONOMY**
UV observations of Herbig-Haro objects associated with bipolar molecular outflows: HH 7, HH 11 and HH 29
[IFSI-90-9] N91-10819

**UNIFIED FIELD THEORY**
Unified theory of ballooning instabilities and temperature gradient driven trapped ion modes
[DE90-017091] N91-10744

**UNITED STATES**
Potential effects of global climate change on the United States. Appendix C: Agriculture, volume 1
[PB90-171588] N91-10394
Potential effects of global climate change on the United States. Appendix A: Water resources
[PB90-171968] N91-10395
Potential effects of global climate change on the United States. Appendix B: Sea level rise
[PB90-172628] N91-10396
Potential effects of global climate change on the United States. Appendix C: Agriculture, volume 2
[PB90-171596] N91-10397
Potential effects of global climate change on the United States. Appendix D: Forests
[PB90-173238] N91-10398
Potential effects of global climate change on the United States. Appendix E: Aquatic resources
[PB90-172297] N91-10399
Potential effects of global climate change on the United States. Appendix F: Air quality
[PB90-172230] N91-10400
Potential effects of global climate change on the United States. Appendix G: Health
[PB90-173881] N91-10401
Potential effects of global climate change on the United States. Appendix H: Infrastructure
[PB90-172313] N91-10402
Potential effects of global climate change on the United States. Appendix I: Variability
[PB90-173899] N91-10403
Potential effects of global climate change on the United States. Appendix J: Policy
[PB90-173188] N91-10404

**UNIX (OPERATING SYSTEM)**
Converting from VMS to ULTRIX
[PB90-220310] N91-10622

**UNSTEADY AERODYNAMICS**
Aeroelastic analysis of wings using the Euler equations with a deforming mesh
[NASA-TM-102733] N91-10020
Evaluation of the ZONA51D program
[REPT-B-28] N91-10025
Direct use of linear time-domain aerodynamics in aeroservoelastic analysis: Aerodynamic model
N91-10316

**UNSTEADY FLOW**
Boundary-layer receptivity due to a wall suction and control of Tollmien-Schlichting waves
[NASA-CR-182103] N91-10009
Measurement of unsteady blade surface pressure on a single rotation large scale advanced prop-fan with angular and wake inflow at Mach numbers from 0.02 to 0.70
[NASA-CR-182123] N91-10065
Interactive real time flow simulations
[NASA-CR-187325] N91-10238
A computational model for z-pinch plasma channels
N91-10730

**UPPER ATMOSPHERE**
Overview of the 27-28 October FIRE Cirrus IFO case: Meteorology and cloud fields N91-10477

**USER MANUALS (COMPUTER PROGRAMS)**
User's guide to CUNIFLOW
[AD-A207606] N91-10004
Users manual for AUTOMESH-2D: A program of automatic mesh generation for two-dimensional scattering analysis by the finite element method
[NASA-CR-186929] N91-10623
Script: General purpose graphics program; user's manual
[PD-ST-9027] N91-10625
Bidirectional translator between DXF and IGES formats
[DE90-016430] N91-10632

## V

**VALENCE**
Effects of in-plane pi prime bonding on electronic transition energies for inorganic polymers
[DE90-017144] N91-10180

**VALLEYS**
Energetics of valley and basin atmospheres during the evening transition and nighttime periods
[DE90-016356] N91-10542

**VALVES**
Structural tests of aircraft window assembly equipped with smoke evacuation valve
[DOT/FAA/CT-TN89/44] N91-10051

**VAPOR DEPOSITION**
Ion-assisted doping of 2-6 compounds during physical vapor deposition
[DE90-000358] N91-10756
Preparation of superconducting wire by deposition of YBa2Cu3O(x) onto fibers
[DE90-013380] N91-10758
Substrate temperature effects on (cubic x cubic lattice) R 30 deg domain growth of Ag on Si(111) surface
[DE90-016527] N91-10772

**VAPOR PHASES**
Collision-induced gas phase dissociation rates
[NASA-CR-185874] N91-10707

**VAPOR PRESSURE**
Determination of ideal-gas enthalpies of formation for key compounds: The 1988 project results
[DE90-000247] N91-10791

**VAPORIZING**
AFDM: An Advanced Fluid-Dynamics Model. Volume 4: The AFDM heat- and mass-transfer solution algorithm
[DE90-017535] N91-10240

**VAPORS**
Effects of prolonged exposure to acetic acid vapors on acid-base balance in humans N91-10561
A refractive index gradient (RING) diagnostic for transient discharges or expansions of vapor or plasmas
[DE90-015840] N91-10736

**VARIABILITY**
Potential effects of global climate change on the United States. Appendix I: Variability
[PB90-173899] N91-10403

**VECTOR QUANTIZATION**
Density estimation using optimally quantized histograms
[PB90-190588] N91-10686

**VECTOR SPACES**
Operator formalism of multi-pole Virasoro algebra on Riemann sphere
[DE90-627217] N91-10657

**VECTORS (MATHEMATICS)**
Optimum orientations of the observation axes for 2-dimensional vector sensing under consideration of bias errors
[NAL-TR-1055] N91-10679
Geometric ergodicity of the ALOHA-system and a coupled processors model
[TW-90-01-B] N91-10680

**VELOCITY DISTRIBUTION**
The possibility of making fast measurements of ion distribution functions N91-10438

**VELOCITY MEASUREMENT**
Application of Fabry-Perot velocimetry to hypervelocity impact experiments
[DE90-015612] N91-10096
Velocity measurements in piston-induced turbulent boundary layers in a shock tube
[ISL-CO-235/89] N91-10247
Particle displacement tracking for PIV
[NASA-TM-103288] N91-10271
Distortion of LDA fringe pattern by tracer particles
[SFB-210/E/59] N91-10288

**VENTILATION**
Airplane systems modifications for improved cabin smoke evacuation
[DOT/FAA/CT-TN90/24] N91-10052

**VENTURI TUBES**
Measurements of coefficients of discharge for concentric flange-tapped square-edged orifice meters in natural gas over the Reynolds number range 25,000 to 16,000,000
[PB90-219601] N91-10231

**VERTICAL AIR CURRENTS**
Q-vectors: A new approach to an old problem
[PB90-235490] N91-10414
Plume mechanics and stratocumulus convection
N91-10526

**VERTICAL DISTRIBUTION**
Satellite cloud information chart N91-10374
Overview of the 27-28 October FIRE Cirrus IFO case: Meteorology and cloud fields N91-10477

**VERY LARGE ARRAY (VLA)**
Core-dominated radio sources and the unified scheme
N91-10835

**VERY LONG BASE INTERFEROMETRY**
The scientific case for magnetic field satellites
[NASA-CR-186532] N91-10101

**VESTIBULAR TESTS**
Role of orientation reference selection in motion sickness
[NASA-CR-186612] N91-10591

**VESTIBULES**
Requirements for an ideal drug for preventing space motion sickness N91-10566

**VIBRATION**
Time/frequency analysis of vibro-acoustic behaviour of a launcher in flight
[ETN-90-97584] N91-10097
Vibration testing of a 1/5 scale model of H-2 launch vehicle
[NAL-TR-1061] N91-10099
Mobility power flow analysis of an L-shaped plate structure subjected to distributed loading
[NASA-CR-187353] N91-10334
The development of interior noise and vibration criteria
[NASA-TM-102736] N91-10702
Collision-induced gas phase dissociation rates
[NASA-CR-185874] N91-10707

**VIBRATION DAMPING**
Design of control laws for flutter suppression based on the aerodynamic energy concept and comparisons with other design methods
[NASA-TP-3056] N91-10328
Development of the force envelope for an acceleration/force extremal controlled vibration test
[DE90-015712] N91-10329

**VIBRATION MODE**
Vibro-acoustic emission rubbing sources
[PNR-90730] N91-10336

**VIBRATION SIMULATORS**
The full-body ground vibration tests using the low-noise STOL test plane
[NAL-TM-576] N91-10077

**VIBRATION TESTS**
Rotor systems research aircraft risk-reduction shake test
[NASA-TM-4186] N91-10045
The full-body ground vibration tests using the low-noise STOL test plane
[NAL-TM-576] N91-10077
Vibration testing of a 1/5 scale model of H-2 launch vehicle
[NAL-TR-1061] N91-10099
Development of the force envelope for an acceleration/force extremal controlled vibration test
[DE90-015712] N91-10329
Comparison of NASTRAN analysis with ground vibration results of UH-60A NASA/AEFA test configuration
[NASA-CR-184565] N91-10333
**VIBRATORY LOADS**
Rotor systems research aircraft risk-reduction shake test
[NASA-TM-4186] N91-10045
**VIDEO DATA**
Image data compression overview: Issues and partial solutions
[PB90-172008] N91-10796
**VIDEO TAPES**
VTR loop movie N91-10367
**VINYL POLYMERS**
Evaluation of composite materials for use on launch complexes
[NASA-TM-103809] N91-10131
**VIRTUAL MEMORY SYSTEMS**
Converting from VMS to ULTRIX
[PB90-220310] N91-10622
**VISCOELASTIC DAMPING**
Analysis of elastically tailored viscoelastic damping member N91-10319
**VISCOELASTICITY**
Analysis of elastically tailored viscoelastic damping member N91-10319
PREGO: A simulation code for one-dimensional viscoelastic acoustics
[DE90-014859] N91-10700
**VISCOSITY**
Evaluation of two bisimide additives in LARC-TPI adhesive
[NASA-TM-102742] N91-10182
Anomalous viscosity due to drift wave turbulence
[NIFS-33] N91-10752
**VISCOUS FLOW**
Numerical computation of viscous flow about unconventional airfoil shapes
[NASA-CR-187343] N91-10019
Three-dimensional viscous/inviscid coupling in subsonic flow
[REPT-B-24] N91-10023
Calculation of three-dimensional viscous/inviscid interaction in subsonic flow
[REPT-B-25] N91-10024
Simulation of time-dependent compressible viscous flows using central and upwind-biased finite difference techniques N91-10234
**VISIBLE INFRARED SPIN SCAN RADIOMETER**
VISSR demodulate and processing subsystem
N91-10342
Stretched VISSR subsystem N91-10343
Image monitor N91-10344
Telemetry subsystem N91-10345
DPC telecommunication system N91-10354
General flow of image data processing N91-10358
Image mapping N91-10359
Calibration N91-10360
Cloud motion wind N91-10365
VISSR histogram data N91-10368
Cloud grid data N91-10371
**VISUAL AIDS**
Function and performance of visual simulation unit of flight simulation test facility
[NAL-TM-581] N91-10082
**VISUAL FIELDS**
Function and performance of visual simulation unit of flight simulation test facility
[NAL-TM-581] N91-10082
**VISUAL FLIGHT**
The establishment and performance test of PAPI (Precision Approach Path Indicator) System for NAL STOL aircraft
[NAL-TM-579] N91-10030
**VISUAL OBSERVATION**
The radiation budget of a Cirrus layer deduced from simultaneous aircraft observations and model calculations N91-10467
**VISUAL PERCEPTION**
Role of orientation reference selection in motion sickness
[NASA-CR-186612] N91-10591
Image data compression overview: Issues and partial solutions
[PB90-172008] N91-10796
**VOLCANOES**
Survey of possibility for volcanic energy development
[DE90-517230] N91-10387
**VORTICES**
The inviscid secondary instability of fully nonlinear longitudinal vortex structures in growing boundary layers
[NASA-CR-187455] N91-10021
Vortex instabilities in 3D boundary layers: The relationship between Goertler and crossflow vortices
[NASA-CR-187456] N91-10022
Studying marine stratus with large eddy simulation
N91-10499
Boundary layer roll circulations during FIRE
N91-10521
**VORTICITY**
Q-vectors: A new approach to an old problem
[PB90-235490] N91-10414
**VOYAGER PROJECT**
Spacecraft Health Automated Reasoning Prototype (SHARP): The fiscal year 1989 SHARP portability evaluations task for NASA Solar System Exploration Division's Voyager project
[NASA-CR-187338] N91-10204

## W

**WALKING**
Biomedical perspectives on locomotion in null gravity
N91-10583
**WALL FLOW**
Wall interference studies
[PD-CF-9012] N91-10232
A one-equation turbulence transport model for high Reynolds number wall-bounded flows
[NASA-TM-102847] N91-10252
**WALL PRESSURE**
Wall interference studies
[PD-CF-9012] N91-10232
**WALLS**
Boundary-layer receptivity due to a wall suction and control of Tollmien-Schlichting waves
[NASA-CR-182103] N91-10009
**WATER**
Estimated accuracy of ground-based liquid water measurements during FIRE N91-10508
Estimating integrated cloud liquid water from extended time observations of solar irradiance N91-10510
**WATER POLLUTION**
National acid precipitation assessment program. Report to the President and Congress
[PB90-185646] N91-10405
**WATER QUALITY**
Chesapeake Bay Basin Monitoring Program Atlas. Volume 1: Water quality and other physiochemical monitoring programs
[PB90-147935] N91-10391
**WATER RESOURCES**
Potential effects of global climate change on the United States. Appendix A: Water resources
[PB90-171968] N91-10395
Potential effects of global climate change on the United States. Appendix E: Aquatic resources
[PB90-172297] N91-10399
Potential effects of global climate change on the United States. Appendix J: Policy
[PB90-173188] N91-10404
**WATER VAPOR**
Comparison and calibration of NCAR electra instruments: July 5 and 7, 1987 N91-10532
**WATER WAVES**
Directional response of wind waves to turning winds
[REPT-90-2] N91-10549
Wind wave propagation in tidal seas
[REPT-90-1] N91-10550
**WAVE DIFFRACTION**
Electromagnetic scattering from two-dimensional thick material junctions
[NASA-CR-186976] N91-10201
**WAVE DISPERSION**
Propagation of magnetoacoustic waves in the solar atmosphere with random inhomogeneities of density and magnetic fields
[DE90-017616] N91-10831
**WAVE EQUATIONS**
Modes of elliptical waveguides: A correction
[DE90-016647] N91-10203
**WAVE FUNCTIONS**
XAFS analysis in the anharmonic limit: Application to Hi-Tc superconductors and ferrosilicates
[DE90-016720] N91-10776
Discretized light-cone quantization: Application to quantum electrodynamics
[DE90-014832] N91-10790
**WAVE INTERACTION**
The effects of critical layers on atmospheric cnoidal waves
[DE90-016540] N91-10440
**WAVE PROPAGATION**
Effect of surface deposits on electromagnetic waves propagating in uniform ducts
[NASA-TM-103282] N91-10208
Physical interpretation and application of principles of ultrasonic nondestructive evaluation of high-performance materials
[NASA-CR-180489] N91-10293
Proceedings of the 8th Symposium on Energy Engineering Sciences: Micro/Macro Studies of Multiphase Media
[DE90-014844] N91-10385
Directional response of wind waves to turning winds
[REPT-90-2] N91-10549
Wind wave propagation in tidal seas
[REPT-90-1] N91-10550
PREGO: A simulation code for one-dimensional viscoelastic acoustics
[DE90-014859] N91-10700
Polarization modulated solitary waves in an optical fiber
[DE90-015034] N91-10715
RF helicity injection and current drive
[NIFS-34] N91-10750
**WAVE REFLECTION**
The effects of critical layers on atmospheric cnoidal waves
[DE90-016540] N91-10440
**WAVE SCATTERING**
On lower hybrid wave scattering by plasma density fluctuation nonlinear reflection coefficient of the fast magnetoacoustic wave
[IPPCZ-281] N91-10725
**WAVEFORMS**
Accuracy of the estimate of J via multipoint measurements N91-10422
**WAVEGUIDES**
Modes of elliptical waveguides: A correction
[DE90-016647] N91-10203
An x band backward-wave oscillator experiment
[DE90-015119] N91-10219
**WAVERIDERS**
Project HyBuJET
[NASA-CR-187011] N91-10040
Supersonic combustion engine testbed, heat lightning
[NASA-CR-187010] N91-10061
**WEAK INTERACTIONS (FIELD THEORY)**
Discrete gravity
[DE90-014808] N91-10789
**WEAR**
Vibro-acoustic emission rubbing sources
[PNR-90730] N91-10336
Diamond turning of optical crystals
[DE90-015909] N91-10719
**WEAR RESISTANCE**
Applications of thermally sprayed coating systems in aero engines
[PNR-90750] N91-10072
**WEAR TESTS**
Self-lubricating boric acid films for tribological applications
[DE90-007805] N91-10171
**WEATHER**
Educator's guide for building and operating environmental satellite receiving stations
[NOAA-TR-NESDIS-44] N91-10093
FAX image processing N91-10361
Mariners Weather Log, Volume 33, Number 1, Winter, 1989
[PB90-179987] N91-10447
Cloud information for FIRE from surface weather reports N91-10452
Hydrometeor development in cold clouds in FIRE
N91-10459
Multi-spectral window radiance observations of Cirrus from satellite and aircraft, November 2, 1986 Project FIRE N91-10465
Identification of Cirrus over Wausau during the 1986 FIRE IFO from ground-based radiometer data
N91-10469
**WEATHER FORECASTING**
Satellite-derived index of precipitation intensity
N91-10362
VTR loop movie N91-10367
Brightness temperature distribution N91-10369
Satellite cloud information chart N91-10374
The relationship of marine stratus to synoptic conditions N91-10489

About the possibilities of using an air mass transformation model in Taiyuan, Shanxi Province, China
[KNMI-TR-120] N91-10540
Impact of SASS wind data on analyses and forecasts of a fine mesh limited area model
[BCRS-89-38] N91-10544

**WEIBULL DENSITY FUNCTIONS**
Calculation of Weibull strength parameters, Batdorf flaw density constants and related statistical quantities using PC-CARES
[NASA-TM-103247] N91-10332

**WEIGHTLESSNESS**
Morphological examination of rat adrenal glands following flight aboard Biosputnik Kosmos-1667
N91-10553
Central and regional hemodynamics in prolonged space flights N91-10554
Workshop on Exercise Prescription for Long-Duration Space Flight
[NASA-CP-3051] N91-10574
The history of in-flight exercise in the US manned space program N91-10577
Work, exercise, and space flight. 1: Operations, environment, and effects of spaceflight N91-10578
Space medicine considerations: Skeletal and calcium homeostasis N91-10580
Changes in mineral metabolism with immobilization/space flight N91-10581
A unique problem of muscle adaptation from weightlessness: The deceleration deficiency
N91-10582
Biomedical perspectives on locomotion in null gravity
N91-10583
Exercise issues related to the neuromuscular function and adaptation to microgravity N91-10584
Work, exercise, and space flight. 2: Modification of adaptation by exercise (exercise prescription)
N91-10586

**WEIGHTLESSNESS SIMULATION**
The design and fabrication of the Centaur neutral buoyancy trainer and related hardware
[NASA-CR-171944] N91-10085

**WELDABILITY**
Weldability of nickel and iron aluminides
[DE90-013498] N91-10153
A weldability study of Haynes Alloy no. 242
[DE90-013875] N91-10154
Beryllium weldability
[DE90-014696] N91-10155

**WIENER FILTERING**
Fast estimation of the variance of a narrowband process
[IFSI-90-16] N91-10209

**WIENER HOPF EQUATIONS**
The difference of two renewal processes: Level crossing and the infimum
[MEMO-845] N91-10690

**WIND (METEOROLOGY)**
Cloud motion wind N91-10365
Boundary layer roll circulations during FIRE
N91-10521
Terrain-induced mesoscale circulations in the Columbia Basin
[DE90-016338] N91-10541
Impact of SASS wind data on analyses and forecasts of a fine mesh limited area model
[BCRS-89-38] N91-10544

**WIND DIRECTION**
The international sodar intercomparison experiment
[PB90-246224] N91-10416

**WIND EFFECTS**
Practical flight paths for microwave-powered airplanes
[NAL-TR-1052T] N91-10054
Directional response of wind waves to turning winds
[REPT-90-2] N91-10549
Wind wave propagation in tidal seas
[REPT-90-1] N91-10550

**WIND MEASUREMENT**
Cloud motion wind N91-10365
Cirrus microphysics and radiative transfer: A case study N91-10463

**WIND PROFILES**
Model of gravity-wave-induced variability and turbulence in the stratified free atmosphere
[PB90-235482] N91-10413
Aircraft measurements of the mean and turbulent structure of marine stratocumulus clouds during FIRE
N91-10514
Boundary layer roll circulations during FIRE
N91-10521
Winds and turbulence above San Nicolas Island during FIRE N91-10522

**WIND SHEAR**
Model of gravity-wave-induced variability and turbulence in the stratified free atmosphere
[PB90-235482] N91-10413

**WIND TUNNEL APPARATUS**
Characteristics of piping interference elimination unit used in the high-speed wind tunnel test of ASUKA seven percent semi-born prototype
[NAL-TM-588] N91-10003
Modification in the main air blower unit for two meter times two meter transonic wind tunnel: Plan and configuration
[NAL-TM-580] N91-10081

**WIND TUNNEL CALIBRATION**
Evaluation of flow quality in newly constructed low-turbulence calibration wind-tunnel for laser velocimeters
[NAL-TR-1054] N91-10087

**WIND TUNNEL TESTS**
Characteristics of piping interference elimination unit used in the high-speed wind tunnel test of ASUKA seven percent semi-born prototype
[NAL-TM-588] N91-10003
Euler and potential experiment/CFD correlations for a transport and two delta-wing configurations
[NASA-TM-102208] N91-10014
Wind tunnel investigations of the appearance of shocks in the windward region of bodies with circular cross section at angle of attack
[DLR-FB-90-15] N91-10027
Wind tunnel test of redundant vane-type flow-direction sensing systems
[NAL-TM-590] N91-10057
Measurement of unsteady blade surface pressure on a single rotation large scale advanced prop-fan with angular and wake inflow at Mach numbers from 0.02 to 0.70
[NASA-CR-182123] N91-10065
Measured and predicted shock shapes for AFE configuration at Mach 6 in air and in CF4
[NASA-TM-100660] N91-10245
A laser-sheet flow visualization technique for the large wind tunnels of the National Full-Scale Aerodynamics Complex
[NASA-TM-102793] N91-10268

**WIND TUNNEL WALLS**
Wall interference studies
[PD-CF-9012] N91-10232

**WIND TURBINES**
A system design and demonstrative field test of wind turbine with a 14 m diameter rotor
[NAL-TR-1056] N91-10389

**WIND VELOCITY**
Typhoon information N91-10366

**WIND VELOCITY MEASUREMENT**
The international sodar intercomparison experiment
[PB90-246224] N91-10416
Spectra and gradients of stormy winds at Cabauw, Netherlands, up to 200 meters high
[KNMI-TR-119] N91-10546

**WINDOWS (APERTURES)**
Structural tests of aircraft window assembly equipped with smoke evacuation valve
[DOT/FAA/CT-TN89/44] N91-10051

**WINDPOWER UTILIZATION**
A system design and demonstrative field test of wind turbine with a 14 m diameter rotor
[NAL-TR-1056] N91-10389

**WINDS ALOFT**
Overview of the 27-28 October FIRE Cirrus IFO case: Meteorology and cloud fields N91-10477

**WING FLAPS**
Static and dynamic aeroelastic characterization of an aerodynamically heated generic hypersonic aircraft configuration N91-10320

**WING PROFILES**
Euler and potential experiment/CFD correlations for a transport and two delta-wing configurations
[NASA-TM-102208] N91-10014

**WINGS**
Calculation of three-dimensional viscous/inviscid interaction in subsonic flow
[REPT-B-25] N91-10024
Experimental measurement of structural power flow on an aircraft fuselage
[NASA-CR-187352] N91-10335

**WINTER**
Mariners Weather Log, Volume 33, Number 1, Winter, 1989
[PB90-179987] N91-10447

**WIRE**
Preparation of superconducting wire by deposition of YBa2Cu3O(x) onto fibers
[DE90-013380] N91-10758

**WOOD**
Structural properties of laminated Douglas fir/epoxy composite material
[NASA-RP-1236] N91-10127

**WORKLOADS (PSYCHOPHYSIOLOGY)**
Cardiovascular group N91-10587

**WORLD METEOROLOGICAL ORGANIZATION**
Proceedings of the WMO Region 3/4 Training Seminar on Climate Data Management and User Services
[WCDP-1] N91-10445
Activities report of the World Meteorological Organization
[WMO-734] N91-10547

## X

**X RAY ABSORPTION**
XAFS studies of interactions at transition-metal/Al interfaces
[DE90-016313] N91-10159

**X RAY ANALYSIS**
Microstructural and phase stability studies of nanometer period metal/carbon multilayer structures for x ray optics
[DE90-015307] N91-10129

**X RAY APPARATUS**
An imaging x-ray microscope using a laser plasma source and a Schwarzchild objective
[DE90-016432] N91-10266

**X RAY ASTRONOMY**
The Joint NASA/Goddard-University of Maryland Research Program in Charged Particle and High Energy Photon Detector Technology
[NASA-CR-180335] N91-10810

**X RAY BINARIES**
Bicolored photometry and spectral accommodation in X-ray region of mass impregnated stellar X-ray binaries
[MPE-219] N91-10808

**X RAY DENSITY MEASUREMENT**
The importance of simultaneous monitoring of solar activity for the interpretation of solar plasma phenomena
N91-10433

**X RAY DIFFRACTION**
Design of a triaxial residual stress measurement system using high-energy x ray diffraction
[DE90-016212] N91-10331

**X RAY IMAGERY**
An imaging x-ray microscope using a laser plasma source and a Schwarzchild objective
[DE90-016432] N91-10266

**X RAY LASERS**
Sodium-neon resonant photoexcitation soft x ray laser experiments on Saturn
[DE90-014946] N91-10275

**X RAY SOURCES**
Design of a triaxial residual stress measurement system using high-energy x ray diffraction
[DE90-016212] N91-10331

**X RAY SPECTRA**
XAFS analysis in the anharmonic limit: Application to Hi-Tc superconductors and ferrosilicates
[DE90-016720] N91-10776

**X RAY TELESCOPES**
The importance of simultaneous monitoring of solar activity for the interpretation of solar plasma phenomena
N91-10433
Design, performance, and calibration of the ALEXIS ultrasoft x-ray telescopes
[DE90-016483] N91-10720

**X RAYS**
Holographic rugate structures for x ray optics applications
[DE90-017103] N91-10270

## Y

**YIELD STRENGTH**
High strain rate deformation behavior of shocked copper
[DE90-016481] N91-10161
YBa2Cu3O(x) composites with improved toughness and strength
[DE90-011180] N91-10782

**YTTRIUM OXIDES**
Preparation of superconducting wire by deposition of YBa2Cu3O(x) onto fibers
[DE90-013380] N91-10758
Evaluation, development, and characterization of superconducting materials for space applications
[NASA-CR-187017] N91-10763
Copper NMR and hole depletion in the normal state of Y(1-x)Pr(x)Ba2Cu3O7
[DE90-016468] N91-10768

## Z

**ZEOLITES**
Nano-composite desiccation materials
[PB90-247388] N91-10123

**ZETA PINCH**
Sodium-neon resonant photoexcitation soft x ray laser experiments on Saturn
[DE90-014946] N91-10275
A computational model for z-pinch plasma channels
N91-10730
**ZINC SELENIDES**
The growth of zinc selenide single crystals by physical vapor transport in microgravity
[NASA-CR-180428] N91-10755
**ZIRCONIUM OXIDES**
Analysis of aluminum oxide ceramic
[DE90-016517] N91-10175

# PERSONAL AUTHOR INDEX

SCIENTIFIC AND TECHNICAL AEROSPACE REPORTS VOLUME 29 NUMBER 1

### Typical Personal Author Index Listing

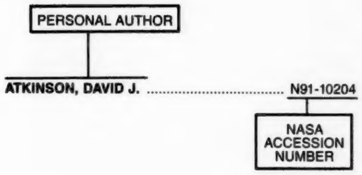
PERSONAL AUTHOR
ATKINSON, DAVID J. .................................... N91-10204
NASA ACCESSION NUMBER

Listings in this index are arranged alphabetically by personal author. The NASA accession number denotes the number by which the citation is identified.

## A

| | |
|---|---|
| ABE, T. | N91-10386 |
| ABE, TSUTOYA | N91-10340 |
| ABRAHAM, M. M. | N91-10761 |
| ACKERMAN, STEVEN A. | N91-10471 |
| ACKERMAN, THOMAS P. | N91-10463<br>N91-10466<br>N91-10467<br>N91-10529 |
| AGIM, YUSUF ZIYA | N91-10727 |
| AHMED, S. | N91-10019 |
| AHN, B. T. | N91-10783 |
| AKHTYRSKIY, V. N. | N91-10214 |
| AKIMOTO, KAZUICHIROU | N91-10347 |
| ALBRECHT, BRUCE A. | N91-10514<br>N91-10515 |
| ALDROVANDI, R. | N91-10786 |
| ALEXANDER, J. IWAN D. | N91-10191 |
| ALLEN, DANIEL T. | N91-10383 |
| ALLEN, DAVID H. | N91-10305 |
| ALLEYNE, H. ST. C. | N91-10426 |
| ALVAREZ, JOSE M. | N91-10457<br>N91-10476<br>N91-10478<br>N91-10482 |
| AMBROSIANO, JOHN J. | N91-10733 |
| AMEDURI, FRANK | N91-10720 |
| AMIN, M. R. | N91-10693 |
| ANDERSON, ELMER E. | N91-10755 |
| ANDERSON, J. A. | N91-10302 |
| ANDERSON, LARRY E. | N91-10573 |
| ANNARATONE, B. M. | N91-10754 |
| ANSAI, RYOETSU | N91-10354 |
| ANTONIAK, ZEN I. | N91-10104<br>N91-10388 |
| ARAKAWA, HARUHIKO | N91-10011 |
| ARDEMA, MARK D. | N91-10049 |
| ARDUINI, ROBERT F. | N91-10480 |
| ARENZ, R. W. | N91-10269 |
| ARGO, B. E. | N91-10742 |
| ARGO, D. | N91-10415 |
| ARKING, ALBERT | N91-10487 |
| ARMSTRONG, I. | N91-10647 |
| ARNONE, GAETANO J. | N91-10602 |
| ARORA, JASBIR S. | N91-10310 |
| ARPACI, V. S. | N91-10235 |
| ASAI, KEISUKE | N91-10003 |
| ASELAGE, TERRY | N91-10132 |
| ASH, D. I. | N91-10153 |
| ASLAN, J. | N91-10041 |
| ASO, TADASHI | N91-10374 |
| ASTONE, P. | N91-10209 |
| ASTRIDGE, DEREK G. | N91-10042<br>N91-10043 |
| ATHERTON, TIM | N91-10036 |
| ATKINSON, DAVID J. | N91-10204 |
| ATTWOOD, MIKE C. | N91-10091 |
| AUERBACH, S. | N91-10673 |
| AUREILLE, MARC | N91-10107 |
| AUSTIN, PHILIP H. | N91-10516<br>N91-10532<br>N91-10533 |
| AVANESOV, G. | N91-10423 |
| AZUMI, M. | N91-10750 |

## B

| | |
|---|---|
| BACKUS, GEORGE E. | N91-10101 |
| BADER, SAMUEL D. | N91-10603 |
| BAEDE, A. P. M. | N91-10544 |
| BAKER, C. B. | N91-10416 |
| BAKER, D. R. | N91-10137 |
| BAKER, M. B. | N91-10496 |
| BALDWIN, BARRETT S. | N91-10252 |
| BALEBANOV, V. M. | N91-10438 |
| BALIKHIN, M. A. | N91-10426 |
| BALOGH, A. | N91-10421 |
| BANDO, TOSHIO | N91-10080 |
| BARANSKA, V. | N91-10553 |
| BAREFIELD, E. K. | N91-10758 |
| BARLOW, R. | N91-10495<br>N91-10520 |
| BARNES, C. W. | N91-10697 |
| BARNES, D. C. | N91-10740 |
| BARNES, G. A. | N91-10740 |
| BARON, B. N. | N91-10384 |
| BARRERA, E. V. | N91-10159 |
| BARRETT, CHARLES A. | N91-10149<br>N91-10150 |
| BARTH, TIMOTHY J. | N91-10252 |
| BARTHELEMY, JEAN-FRANCOIS M. | N91-10301 |
| BARUCH, MENAHEM | N91-10313 |
| BASILI, V. R. | N91-10608 |
| BASSOLO, V. S. | N91-10436 |
| BASSOM, ANDREW | N91-10022 |
| BATEMAN, B. R. | N91-10231 |
| BATES, J. L. | N91-10143 |
| BATINA, JOHN T. | N91-10020 |
| BATIUK, RICHARD | N91-10391<br>N91-10392 |
| BAUMEISTER, KENNETH J. | N91-10208 |
| BAYLOR, L. R. | N91-10742 |
| BECK, HAROLD L. | N91-10539 |
| BECKMAN, A. W. | N91-10114 |
| BEERY, J. G. | N91-10382 |
| BELEGUNDU, A. D. | N91-10311 |
| BELMONT, G. | N91-10430 |
| BENDER, J. M. | N91-10300 |
| BENNER, ROBERT E. | N91-10648 |
| BENNETT, W. D. | N91-10766 |
| BENTLEY, J. | N91-10156 |
| BENTON, EDWARD R. | N91-10101 |
| BERGSMA, FELIX | N91-10711 |
| BERK, M. | N91-10705 |
| BERLIN, A. A. | N91-10555 |
| BERNARD, PETER S. | N91-10237 |
| BERRYMAN, HARRY | N91-10599<br>N91-10600 |
| BERTHIER, J. | N91-10239<br>N91-10240<br>N91-10242 |
| BETTS, ALAN K. | N91-10490<br>N91-10493<br>N91-10516<br>N91-10533 |
| BEYERS, R. | N91-10783 |
| BHASIN, K. B. | N91-10780 |
| BIEG, K. W. | N91-10736 |
| BIGELOW, C. A. | N91-10128 |
| BIGIO, IRVING J. | N91-10276<br>N91-10277 |
| BIRKMIRE, R. W. | N91-10384 |
| BIRMAN, KEN | N91-10633 |
| BISARD, T. | N91-10041 |
| BISHOP, MICHAEL | N91-10615 |
| BISHOP, PETER C. | N91-10793 |
| BLACK, F. OWEN | N91-10591 |
| BLAKE, R. A. | N91-10330 |
| BLASKOVIC, M. | N91-10491 |
| BLASS, J. J. | N91-10178 |
| BLECKI, J. | N91-10427 |
| BLOCH, JEFFREY J. | N91-10720 |
| BLOMQVIST, GUNNAR | N91-10587 |
| BLUMENTHAL, WILLIAM R. | N91-10176 |
| BOBIN, L. | N91-10017 |
| BODONYI, R. J. | N91-10009 |
| BOERS, REINOUT | N91-10516<br>N91-10523<br>N91-10532<br>N91-10533 |
| BOHL, W. R. | N91-10239<br>N91-10240<br>N91-10241<br>N91-10242<br>N91-10244 |
| BONIFAZI, P. | N91-10209 |
| BOOKER, J. R. | N91-10655 |
| BOQUET, JEAN | N91-10107 |
| BOSLOUGH, M. B. | N91-10183 |
| BOTTEGA, W. J. | N91-10306 |
| BOVERIE, B. | N91-10202 |
| BOXMA, O. J. | N91-10635 |
| BRADFORD, J. R. | N91-10632 |
| BRAGIN, L. KH. | N91-10561 |
| BRAITHWAITE, N. S. J. | N91-10754 |
| BRANDEKI, SCOTT | N91-10509 |
| BRANDON, SCOTT T. | N91-10733 |
| BREISACHER, KEVIN J. | N91-10117 |
| BRETHERTON, C. S. | N91-10496 |
| BRICARD, PIERRE | N91-10227 |
| BRIMHALL, JOHN L. | N91-10166 |
| BROERSMA, H. J. | N91-10676<br>N91-10678 |
| BROM, G. | N91-10017 |
| BROSEY, W. D. | N91-10330 |
| BROWN, ALAN C. | N91-10037 |
| BROWN, B. D. | N91-10331 |
| BROWN, D. R. | N91-10388 |
| BROWN, P. T. | N91-10655 |
| BRUEMMER, STEPHEN M. | N91-10166 |
| BRUNER, J. | N91-10802 |
| BRYSON, C. C. | N91-10294 |
| BUBE, R. H. | N91-10756 |
| BUECHNER, J. | N91-10434 |
| BUELL, JOHN | N91-10609 |
| BURMESTER, C. P. | N91-10783 |
| BUSCH, D. E. | N91-10171 |
| BUSER, JON FRANKLIN | N91-10617 |
| BUSHNELL, P. | N91-10065 |

## C

| | |
|---|---|
| CAHALAN, ROBERT F. | N91-10500 |
| CAHILL, P. A. | N91-10172 |
| CALFEE, M. T. | N91-10330 |
| CALLEN, J. D. | N91-10741 |
| CAMACHO, J. F. | N91-10219 |
| CAMASSA, ROBERTO | N91-10662 |
| CAMERON, MURRAY | N91-10819 |
| CAMPA, ALESSANDRO | N91-10233 |
| CAMPBELL, J. | N91-10278 |
| CARETTE, P. | N91-10634 |
| CARPENTER, D. A. | N91-10175 |
| CARRIERE, A. | N91-10205 |
| CARSON, J. A. | N91-10281 |
| CARTER, J. P. | N91-10655 |
| CARTER, W. B. | N91-10758 |
| CARTWRIGHT, DAVID C. | N91-10282 |
| CASEY, CHARLES P. | N91-10121 |
| CASSIDY, PATRICK E. | N91-10170 |
| CATS, G. | N91-10544 |
| CAVAGE, WILLIAM, JR. | N91-10051 |
| CAVANAGH, PETER R. | N91-10583 |
| CELMINS, ILMARS | N91-10005 |
| CEREZO, ERNESTO | N91-10199 |
| CHADOV, V. I. | N91-10560 |
| CHAN, C. K. | N91-10222 |
| CHAN, K. C. D. | N91-10279 |
| CHAN, LAI-HIM | N91-10708 |
| CHANDER, R. | N91-10318 |
| CHANG, I-CHUNG | N91-10007<br>N91-10013 |
| CHANG, ZHE | N91-10657 |
| CHANTEUR, G. | N91-10430 |
| CHARLESON, R. J. | N91-10528 |

CHAU, H. H. N91-10096
CHAU, LAI KWAN N91-10174
CHAVEZ, J. R. N91-10736
CHEADLE, WILLIAM G. N91-10612
CHEN, C. H. N91-10716
CHEN, D. W. N91-10504
CHEN, G.-S. N91-10319
CHEN, Y. N91-10761
CHENG, HAI-YUIN N91-10755
CHEUNG, SAMSON H. N91-10015
CHEW, J. W. N91-10259
CHICK, L. A. N91-10143
CHIEN, K.-F. N91-10756
CHILDS, JEFFREY D. N91-10487
CHIN, R. C. Y. N91-10661
CHIRICO, R. D. N91-10781
CHOI, E. H. N91-10735
CHRIEN, R. E. N91-10740
CHRISTIAN, TOM F. N91-10321
CHUNG, HYOSANG N91-10471
CHUNG, Y. S. N91-10758
CIESIELSKI, PAUL E. N91-10454
N91-10492
CIMMERMAN, B. N91-10334
CINLAR, ERHAN N91-10675
CLAFLIN, S. E. N91-10114
CLARKE, A. D. N91-10528
CLARKE, D. W. N91-10685
CLARKE, DAVID A. N91-10073
N91-10138
CLEVELAND, W. G. N91-10231
CLEVENSON, S. A. N91-10702
CLIFF, S. E. N91-10014
COAKLEY, JAMES A., JR. N91-10501
N91-10524
COAKLEY, JAMES E. N91-10507
COCKRELL, C. R. N91-10221
COFFEY, DERMOT N91-10770
COFFEY, H. E. N91-10411
N91-10412
N91-10823
N91-10824
N91-10825
N91-10826
COFFEY, HELEN E. N91-10822
COGGESHALL, STEPHEN V. N91-10282
COLLET, BILL N91-10040
COMBS, S. K. N91-10742
CONEY, M. H. N91-10067
CONNOLY, EDWARD N91-10228
CONRADSON, S. D. N91-10776
CONSTERDINE, IAN N91-10509
CONVERTINO, VICTOR A. N91-10585
COOK, RONALD L. N91-10381
COPENHAVER, RONALD M. N91-10188
COPLIN, JOHN F. N91-10139
N91-10197
CORDADO, E. G. N91-10838
CORNILLEAU-WEHRLIN, N. N91-10432
CORNUBERT, R. N91-10248
CORT, BARBARA N91-10771
COTTLE, RICHARD W. N91-10660
COX, LAWRENCE E. N91-10771
COX, STEPHEN K. N91-10471
N91-10479
N91-10484
N91-10492
N91-10517
N91-10531
CRAVEN, P. N91-10441
CROESSMANN, C. D. N91-10737
CROPPER, K. R. N91-10337
CROW, J. E. N91-10768
CULLY, SCOTT N91-10720
CUNEO, M. E. N91-10736
CURRAN, FRANCIS M. N91-10118
CURTIS, JAMES T. N91-10004
CUSCHIERI, J. M. N91-10334
N91-10335
CZUCHLEWSKI, STEVEN J. N91-10276

D

DALLINGA, S. N91-10041
DAMKROGER, BRIAN K. N91-10155
DAMSMA, MARTIN N91-10672
DANBERG, JAMES E. N91-10005
DAVID, D. N91-10715
DAVIDIAN, KENNETH O. N91-10119
DAVIDSON, BARRY D. N91-10309
DAVIDSON, KEN N91-10534
DAVIES, R. N91-10491
DAVIS, ROBERT B. N91-10106
DEANGELIS, R. M. N91-10447
N91-10537
DECKER, WILLIAM N91-10609
DEKONING, W. L. N91-10668
N91-10689
DELCOURT, D. C. N91-10435
DELUCA, LUIGI N91-10098
DENHERTOG, D. N91-10636
DENIS, M. N91-10427
DESBOIS, MICHEL N91-10503
DHUMIERES, D. N91-10248
DIERIAM, TODD A. N91-10102
DIVITTORIO, S. L. N91-10130
DIXON, RAYMOND D. N91-10155
DMITRIYEV, A. P. N91-10568
DO, DUNG N91-10029
DODD, D. A. N91-10296
DODD, G. C. N91-10453
N91-10464
DOLGIN, B. P. N91-10319
DOMINY, R. G. N91-10262
DOMRACHEVA, M. V. N91-10554
DOOGOOD, P. N. N91-10064
DOORBAR, P. J. N91-10137
DORAN, J. C. N91-10541
DORRER, M. N91-10380
DOWELL, D. H. N91-10280
DOYLE, RICHARD J. N91-10204
DRAINE, BRUCE T. N91-10462
DRAPER, K. N91-10041
DREHER, P. E. N91-10092
DRESSELHAUS, M. S. N91-10130
DREW, DANIEL W. N91-10615
DRIESSEN, T. S. H. N91-10692
DROST, M. K. N91-10388
DUBINSKY, R. N91-10482
DUCK, P. W. N91-10009
DUDA, DAVID P. N91-10517
DUIJVESTIJN, A. J. W. N91-10678
DUNLOP, M. W. N91-10420
N91-10421
N91-10424
DUNNETT, R. M. N91-10229
DURKEE, PHILIP A. N91-10502
DURST, F. N91-10258

E

EASTERBROOK, CALVIN C. N91-10548
EDGERTON, REGGIE N91-10584
EDMUNDS, T. N91-10647
EDWARDS, G. N91-10278
EDWARDS, G. R. N91-10153
EDWARDS, THOMAS A. N91-10015
EKLUND, THOR I. N91-10052
ELKINS, J. W. N91-10538
ELLIOTT, C. J. N91-10280
ELORANTA, EDWIN W. N91-10458
N91-10483
ELPHIC, R. C. N91-10421
EMERY, V. J. N91-10760
EMIN, DAVID N91-10132
ENDO, HIROSHI N91-10389
ENDO, M. N91-10130
ENDO, SHUJI N91-10299
ENGLAND, A. C. N91-10737
ERCK, R. A. N91-10171
ERDEMIR, A. N91-10171
ERICKSON, W. C. N91-10829
ESCH, HELMUT N91-10027
ESER, SEMIH N91-10188
ESGAR, JACK B. N91-10127
ESKER, L. N91-10607
EVEREST, A. WALLACE, III N91-10264

F

FADEEVA, N. YE. N91-10214
FAIRALL, C. W. N91-10413
N91-10510
FAIRALL, CHRISTOPHER W. N91-10515
N91-10522
FARENBRUCH, A. L. N91-10756
FARR, J. D. N91-10382
FEDOROV, A. O. N91-10438
FEDOTOV, V. N91-10423
FEHLING, D. T. N91-10742
FELICI, A. N91-10820
FENSKE, G. R. N91-10171
FERET, J. N91-10382
FERRIS, KIM F. N91-10179
N91-10180
N91-10778
FEYOCK, STEFAN N91-10039
FIELD, RICHARD T. N91-10379
FIGUEIRO, JOSEPH F. N91-10282
FILIPENKOV, S. N. N91-10559
FILIPPI, CESAR N91-10199
FINCHUM, A. N91-10131
FISENNE, ISABEL M. N91-10539
FISHER, P. W. N91-10742
FISK, Z. N91-10769
FLAKE, G. W. N91-10697
FLATAU, PIOTR J. N91-10462
FLECK, MARGARET M. N91-10645
N91-10646
FLECK, V. N91-10050
FOOT, J. S. N91-10525
FOREMAN, R. J. N91-10718
FOSTER, C. A. N91-10742
FOUST, C. R. N91-10742
FRAGASZY, R. J. N91-10415
FRAME, B. J. N91-10125
FRANCE, D. M. N91-10236
FRANCK, BRUNO M. N91-10322
FRANKS, ALAN M. N91-10245
FRANTZ, CH. E. N91-10164
FREEMAN, JOHN R. N91-10713
FREEMAN, JONATHAN DENNIS N91-10806
FREEMAN, WILLIAM T., JR. N91-10106
FREI, ALAN N91-10527
FREI, ALLAN N91-10469
FRESE, K. W. N91-10140
FREY, RICHARD N91-10474
FRIEDRICH, M. N91-10437
FROLOV, N. N. N91-10564
FROUIN, R. N91-10475
FUCHS, B. A. N91-10719
FUJIEDA, ATSUTOSHI N91-10057
FUJIMAKI, MASARU N91-10339
FUJITA, JUNJI N91-10751
FUJITA, TOSHIMI N91-10057
FUKUSHIMA, YUKIO N91-10299
FUKUYAMA, A. N91-10750
FULLER, W. H. N91-10482
FUMOUX, C. N91-10097
FURTAK, T. E. N91-10764

G

GAGUA, T. I. N91-10437
GAIER, JAMES R. N91-10134
GAINES, GEOFFREY A. N91-10720
GAISSER, T. K. N91-10816
GALETTI, D. N91-10786
GALLAGHER, J. C. N91-10581
GALLI, M. T. N91-10658
GALPERIN, YU. I. N91-10431
GARLICK, RALPH G. N91-10149
N91-10150
GARNER, F. N91-10160
GARY, G. A. N91-10832
GATHMAN, STUART N91-10509
GAUTIER, C. N91-10475
GAUTIER, CATHERINE N91-10497
GAYNOR, J. E. N91-10416
GEMMEN, R. N91-10235
GEORGE, ANDREAS C. N91-10539
GEORGE, E. P. N91-10167
GERBER, HERMAN N91-10534
GERBER, HERMANN N91-10509
GERHARDT, DAVID L. N91-10116
GEYER, GEORGE B. N91-10029
GIBSON, G. G. N91-10472
GIESE, R. F. N91-10757
GILBERT, ETHEL S. N91-10593
GILBERT, MICHAEL G. N91-10316
N91-10320
GILHAM, S. N91-10259
GILLIGAN, J. G. N91-10737
GILLIOM, LAURA R. N91-10185
GLASSMEIER, K.-H. N91-10421
N91-10424
GMELIGMEYLING, R. H. J. N91-10673
GNEMMI, P. N91-10016
GODDARD, K. N91-10075
GOEBEL, F. N91-10678
GOLDBERG, D. A. N91-10203
GOLDSTEIN, J. C. N91-10280
GOLDSTEIN, M. K. N91-10622
GOLDSTONE, JOYCE A. N91-10771
GOMPF, R. H. N91-10194
GOODSELL, A. M. N91-10014
GOPINATH, R. N91-10232
GORDON, W. L. N91-10780
GORE, WARREN J. Y. N91-10466
N91-10529
GOREE, JAMES G. N91-10126
GORETTA, K. C. N91-10782
GOSSAGE, STEVEN A. N91-10649
GOTTESFELD, S. N91-10382

GOTTLIEB, D. N91-10251
GOUGE, M. J. N91-10742
GOUGEON, MEADE N91-10127
GOUTAGNY, L. N91-10239
N91-10240
GRAHAM, R. L. N91-10406
GRAMS, G. N91-10486
GRAY, GEORGE T., III N91-10161
N91-10162
N91-10164
N91-10165
GRAY, L. J. N91-10195
GREEN, DAN N91-10147
GREENE, DAVID L. N91-10046
GRIFFIN, M. K. N91-10464
GRIFFIN, P. J. N91-10762
GRIFFITHS, M. H. N91-10168
GRIGORE, R. D. N91-10787
GRIGSBY, JAMES A. N91-10821
GRIMBERGEN, M. N91-10756
GRIMM, PETER N91-10489
GRINGAUZ, K. I. N91-10436
GRONSKY, R. N91-10783
GROPENGIESSER, F. N91-10256
GRUBER, M. N91-10065
GRUND, CHRISTIAN JOHN N91-10458
N91-10478
N91-10483
GUANGJIAN, SUO N91-10667
GUER, T. M. N91-10783
GUERREIRO, JOAO NISAN C. N91-10327
GUINN, THOMAS A. N91-10492
N91-10517
GULTEPE, ISMAIL N91-10461
GUO, HAN-YING N91-10657
GUPTA, S. K. N91-10472
GURNETT, DONALD A. N91-10439
GUSTAFSON, JOHN L. N91-10648
GYEKENYESI, JOHN P. N91-10332

## H

HAACK, TRACY N91-10521
HABIB-AGAHI, HAMID N91-10613
HAERTIG, JACQUES N91-10016
N91-10018
HAFKENSCHEID, L. M. N91-10544
HAFTKA, RAPHAEL T. N91-10313
HAGYARD, M. J. N91-10832
HAHN, CAROLE J. N91-10452
HAIRE, RICHARD G. N91-10771
HALL, EDWARD JOSEPH N91-10234
HALL, FREEMAN F. N91-10478
HALL, KENNETH R. N91-10273
HALL, PHILIP N91-10021
N91-10022
HAMAMATSU, K. N91-10750
HAMMEL, P. C. N91-10768
HAMMER, PHILIP D. N91-10529
HAMPTON, LAWRENCE N91-10029
HANAMATSU, TAKESHI N91-10030
HANIGOFSKY, J. A. N91-10758
HANSEN, C. FREDERICK N91-10707
HANSON, ANGELA K. N91-10180
HANSON, HOWARD P. N91-10526
N91-10534
HANZAWA, ASAO N91-10389
HARADA, KOICHI N91-10601
HARDING, ALICE K. N91-10816
HARDING, S. C. N91-10262
HARKINS, DAVID N91-10145
HARRAH, S. D. N91-10221
HARRIS, BERNARD A., JR. N91-10574
N91-10588
HARRIS, DAVID B. N91-10282
HARRISON, CHRISTOPHER G. A. N91-10101
HARRISON, EDWIN F. N91-10472
N91-10473
N91-10488
N91-10505
HARTROPP, S. J. N91-10066
HARVEY, N. W. N91-10260
HASHIDATE, MASATAKA N91-10389
HAUER, ALLAN A. N91-10282
HAWKE, RONALD S. N91-10094
HAYES, JUDITH N91-10576
HAYMAKER, R. W. N91-10665
HAYMAKER, RICHARD N91-10708
HEADLEY, T. J. N91-10154
HEALD, S. M. N91-10159
HEARN, C. P. N91-10221
HEASLY, PATRICIA N91-10391
N91-10392
HECK, PATRICK W. N91-10472
N91-10473
N91-10476
HEDIN, A. E. N91-10543
HEDSTROM, G. W. N91-10661
HEEG, JENNIFER N91-10317
N91-10320
HEFFNER, R. H. N91-10768
HEIFETS, V. N91-10423
HEIN, PAUL F. N91-10479
HEIRTZLER, JAMES R. N91-10101
HELLENDOORN, HANS N91-10687
HENAGER, CHARLES H., JR. N91-10166
HENNEKE, E. G. N91-10330
HENNINGER, R. J. N91-10244
HENSON, TROY N91-10611
HERMAN, LEROY N91-10471
HESLINGA, GERBEN N91-10596
HESS, KURT W. N91-10446
HEWITT, F. A. N91-10063
HEYMSFIELD, ANDREW J. N91-10459
N91-10460
N91-10461
N91-10463
N91-10467
N91-10480
HICKS, R. M. N91-10014
HIGGINS, J. D. N91-10415
HIGNETT, PHILLIP N91-10518
HIHN, JAIRUS M. N91-10613
HILGENSTOCK, ACHIM N91-10026
HILL, D. N. N91-10758
HILL, M. G. N91-10639
HILL, MARY ANN N91-10155
HINKLE, C. ROSS N91-10442
HINTON, BARRY N91-10489
HISAMATSU, T. N91-10386
HOBBS, PETER V. N91-10507
N91-10512
HODGDON, MARION L. N91-10773
HODGIN, ROBERT F. N91-10794
N91-10795
HOFFREN, JAAKKO N91-10253
HOGAN, J. T. N91-10289
HOLCOMBE, C. E. N91-10175
HOLLINGSWORTH, MICHAEL N91-10085
HOLM, DARRYL D. N91-10721
HOLMAN, RICHARD N91-10695
HOLMES, DOUGLAS SCOTT N91-10265
HOLSTE, JAMES C. N91-10273
HOLTZ, R. E. N91-10759
HORDIJK, A. N91-10640
N91-10641
N91-10642
HORSEMAN, NICOLA J. N91-10021
HORTON, LINDA L. N91-10181
HORVITZ, A. H. N91-10799
HOSOE, NOBUYUKI N91-10003
HOSSENLOPP, I. A. N91-10791
HOWARD, W. MICHAEL N91-10818
HOWELL, BARBARA F. N91-10124
HOWELL, H. B. N91-10465
HOYING, D. N91-10061
HUA, CHONGYU N91-10623
HUBER, ALAN C. N91-10264
HUBER, HELMUT B. N91-10055
HUDSON, JAMES G. N91-10506
HUFFORD, G. N91-10041
HUGENBERG, K. F. N91-10267
HUGENSCHMIDT, MANFRED N91-10283
HUGGINS, R. A. N91-10783
HUGHES, CHRISTOPHER E. N91-10703
HUNT, W. H. N91-10457
N91-10482
HUSSEY, TOM N91-10275
HUSUNG, DIETER N91-10108
HUTCHINSON, W. N91-10382
HUTTER, ADAM R. N91-10539
HYBERTSEN, MARK S. N91-10765

## I

IASCONE, DOMINICK N91-10455
IBANEZ-ESPIGA, MARIA-BLANCA N91-10652
IDOSOR, FLORENTINO N91-10333
IE, C. A. N91-10307
IGAR, KARYN N91-10040
IGNATOVA, O. V. N91-10555
IMLAY, RICHARD N91-10708
INAGAKI, TOSHIHARU N91-10030
INGRAHAM, JOHN C. N91-10739
INOUE, SHIGEO N91-10059
N91-10060
IPAVICH, F. M. N91-10810
IRELAND, P. T. N91-10260
N91-10272
ISEYEV, L. R. N91-10560
ISHIKAWA, H. N91-10386
ISKE, PAUL-LOUIS N91-10784
ISOBE, TOSHIO N91-10605
ISSI, J.-P. N91-10130
ITO, TADASHI N91-10389
ITO, TAKESHI N91-10054
ITOH, FUMIKO N91-10053
ITOH, K. N91-10750
ITOH, S.-I. N91-10750
N91-10752
IUCCI, N. N91-10833
N91-10834
N91-10838
IWASAKI, AKIHITO N91-10057

## J

JAKOBSSON, B. N91-10705
JAMES, GEORGE HENRY, III N91-10325
JAMES, JEFFREY N91-10509
JAMES, MARK L. N91-10204
JAN, DARRELL L. N91-10309
JANKE, C. J. N91-10125
JANKOWSKI, A. F. N91-10718
JANNSON, TOMASZ N91-10270
JANSSON, S. N91-10133
JAROSS, R. A. N91-10759
JENDRZEJCZYK, J. A. N91-10236
JENNISON, D. R. N91-10765
JENSEN, DOUGLAS R. N91-10519
JENSEN, JORGEN B. N91-10511
JENTINK, HENDRIK WILLEM N91-10285
JHA, L. N. N91-10731
JOHE, CH. N91-10016
JOHNSON-PASQUA, CHRISTOPHER M. N91-10517
N91-10531
JOHNSON, DEBRA STEELE N91-10595
JOHNSTON, J. W. N91-10766
JOHNSTONE, A. N91-10438
JONES, BOBBY A. N91-10732
JONES, D. G. N91-10261
JONES, R. D. N91-10697
JONES, T. V. N91-10260
JONES, THOMAS P. N91-10146
JOU, CHENGFONG JOSEPH N91-10775
JUDSON, E. A. N91-10758

## K

KABAMBA, PIERRE N91-10314
KACYNSKI, KENNETH J. N91-10249
KAIMAL, J. C. N91-10416
KAISIG, M. N91-10831
KALLENBERG, L. C. M. N91-10640
N91-10641
N91-10642
KAMINSKAYA, YE. V. N91-10567
KANAZAWA, YOSHIYUKI N91-10353
KANG, GAO N91-10540
KAPER, TASSO J. N91-10663
KARASAWA, TOSHIO N91-10003
N91-10081
KARE, JORDIN T. N91-10274
KARKISHCHENKO, N. N. N91-10566
KAUFMAN, TIM N91-10204
KAUFMAN, Y. J. N91-10475
KAWABATA, SEIJI N91-10348
KAWAHARA, HIROYASU N91-10080
N91-10082
KELBLE, C. N91-10061
KELLY, J. G. N91-10762
KENDALL, DEWAYNE N91-10040
KENNEDY, MIKE O. N91-10192
KENT, G. N91-10482
KHALSA, SIRI JODHA SINGH N91-10497
N91-10534
KIANG, C. S. N91-10407
KIM, D. N91-10756
KIMURA, TAKEO N91-10057
N91-10679
KING, MICHAEL D. N91-10512
N91-10513
KINNE, STEFAN A. N91-10463
N91-10467
KLEIN, A. C. N91-10173
KLIMOV, S. I. N91-10426
N91-10428
KLOESEL, KEVIN A. N91-10489
N91-10514
N91-10534
KNIGHT, NANCY C. N91-10459
N91-10460
KNOTT, J. F. N91-10337
KNOX, CHARLES E. N91-10058
KOBA, HIROYUKI N91-10336

KOEHNE, RAINER N91-10390
KOGAN, A. N91-10423
KOIKE, YO N91-10003
KOK, JACOBUS BERNARDUS WILHELMUS N91-10255
KOLB, EDWARD W. N91-10695
KOLESNIKOVA, E. I. N91-10438
KOMARNENI, S. N91-10123
KOMATSU, KEIJI N91-10099
N91-10604
KOMATSU, YUKIO N91-10081
N91-10389
KONDO, SAYA N91-10363
KONDRAKOV, V. M. N91-10557
KONO, H. N91-10781
KOOPMANN, H. J. C. N91-10091
KOORNWINDER, TOM H. N91-10666
KOPP, ROGER A. N91-10817
N91-10830
KOSMATKA, J. B. N91-10307
KOSSACKI, K., JR. N91-10427
KOSTAS, J. G. N91-10202
KOSTENKO, V. N91-10423
KOURA, KATSUHISA N91-10012
N91-10712
KOUVARITAKIS, B. N91-10229
N91-10644
N91-10683
N91-10684
KOVALENKO, YE. A. N91-10570
KOZHUKHOVSKY, A. I. N91-10438
KRASNOSELSKIKH, V. V. N91-10426
N91-10428
KRATZ, KARL-LUDWIG N91-10818
KRAZINSKI, J. L. N91-10759
KROEMER, H. N91-10767
KROESE, D. P. N91-10690
KROESE, DIRK P. N91-10675
KRUGER, JEROME N91-10223
KRUGLYI, A. E. N91-10428
KRYSKA, L. N91-10726
KUGLER, D. L. N91-10624
KUKLA, GEORGE N91-10527
KULLBERG, M. L. N91-10782
KUMAGAI, TATSUO N91-10148
KUMAKAWA, AKINAGA N91-10190
KUMAR, R. N91-10156
KUO, CHUN-PAO N91-10141
KUZMIN, A. S. N91-10564

L

LABAUGH, ROBERT J. N91-10614
LACKEY, W. J. N91-10758
LAINE, SEPPO N91-10023
N91-10024
N91-10254
LAKOWSKE, STEPHEN N91-10048
LANGENBAHN, A. N91-10061
LANGER, HELMAR N91-10136
LANGERVELD, DIRK N91-10714
LANGHI, R. G. N91-10014
LAPORTE, JEAN-BERNARD N91-10284
LARSEN, RICHARD J. N91-10539
LASLETT, L. J. N91-10203
LASSILA, DAVID H. N91-10161
LAUCKS, M. L. N91-10280
LAURICH, B. K. N91-10767
LAWRENCE, SCOTT L. N91-10015
LAWSON, ANDREW C. N91-10771
LEARNED, DAVID B. N91-10793
LEATHERWOOD, J. D. N91-10702
LEBLANC, MARY N91-10161
LECKIE, F. A. N91-10133
LECROY, S. R. N91-10481
LEE, E. H. N91-10624
LEE, I-YANG N91-10224
LEE, JONG-WON N91-10305
LEE, K. N91-10697
LEE, V. Y. N91-10783
LEFEUVRE, F. N91-10425
LEGG, J. IVAN N91-10710
LEIGHTON, J. N91-10520
LEMASURIER, PHILIP N91-10699
LENGSFIELD, BYRON H., III N91-10706
LENSCHOW, DONALD H. N91-10511
LEONE, STEPHEN R. N91-10722
LEONOV, N. A. N91-10437
LEU, H. J. N91-10782
LEVERMORE, D. N91-10248
LEVIN, R. N91-10475
LEVY, H. N91-10635
LEWIS, G. M. N91-10068
LEWIS, P. S. N91-10697
LICHT, H. H. N91-10189
LIN, M.-X. N91-10465
LINDSEY, E. N91-10278
LING, JER N91-10314
LIOU, K. N. N91-10470
LIPSKI, A. N91-10281
LISEAU, RENE N91-10819
LIU, C. T. N91-10167
LIU, CHIAN N91-10603
LIU, DECHANG N91-10801
LOCKNER, T. R. N91-10736
LOEHNER, RAINALD N91-10733
LOETTO, M. H. N91-10137
LONDON, JULIUS N91-10452
LOPEZ-OTERO, A. N91-10756
LOPUHAA, HENDRIK P. N91-10688
LOREE, THOMAS R. N91-10277
LOULA, ABINMAEL F. D. N91-10327
LOWELL, CARL E. N91-10149
LOWN, JOE N91-10626
LOWREY, A. R. N91-10280
LOWRIE, B. W. N91-10071
LU, BEI N91-10211
LYONS, A. T. N91-10092
LYONS, JAMIE H. N91-10507

M

MACCONOCHIE, IAN O. N91-10106
MACDOWELL, LOUIS G., III N91-10157
MACLAUGHLIN, D. E. N91-10768
MACOMB, DARYL JACK N91-10807
MAFFIOLI, F. N91-10658
MAGUIRE, M. C. N91-10153
N91-10154
MAHMOOD, RASHID N91-10326
MAIELLO, MARK L. N91-10539
MAJOT, BRUNO N91-10196
MAKOWIECKI, D. M. N91-10718
MAKPANGOU, MESAAC N91-10633
MAKSIMOVA, YE. N. N91-10567
MALHOTRA, SHAN N91-10613
MANAGADZE, G. G. N91-10437
MANSFIELD, PHILIP ANDREW N91-10811
MANZELLA, DAVID H. N91-10118
MARCHENKO, A. M. N91-10558
MARCHESINI, ROBERTO N91-10794
N91-10795
MARKS, C. H. N91-10193
MARQUETTE, G. N91-10097
MARTEL, HUGO N91-10812
MARTIN, DAVID J. N91-10056
MARTIN, P. M. N91-10766
MARTIN, PATRICK L. N91-10158
MARTIN, R. GAIUS N91-10204
MASUBUCHI, KOUZO N91-10352
MATZEN, KEITH N91-10275
MAUDLIN, P. J. N91-10163
MAVRIPLIS, DIMITRI J. N91-10010
MAZZARELLA, JOSEPH MICHAEL N91-10813
MCCANDLESS, B. E. N91-10384
MCCORMICK, M. P. N91-10457
N91-10482
MCCOWN, ANDREW W. N91-10276
MCDARMAID, D. S. N91-10151
MCDONALD, THOMAS E. N91-10282
MCDOUGAL, DAVID S. N91-10448
MCGARITY, JOHN O. N91-10264
MCGARRY, F. N91-10607
MCGUIRE, GENE N91-10275
MCHARGUE, CARL J. N91-10181
MCKEE, JAMES W. N91-10618
N91-10619
N91-10620
N91-10621
MCKEE, THOMAS B. N91-10492
MCKENZIE, R. L. N91-10120
MCKERNAN, M. A. N91-10718
MCNEIL, ROGER N91-10708
MCVEY, B. D. N91-10280
MEBIUS, J. E. N91-10637
MEIJER, R. W. M. N91-10546
MELTON, J. E. N91-10014
MERRITT, JOHN H. N91-10487
METCALF, WILLIAM N91-10708
MIKLOSOVIC, DAVE N91-10040
MILHAUD, CLAUDE N91-10107
MILLER, DONALD G. N91-10142
MILLER, GUTHRIE N91-10739
MILLER, JAMES G. N91-10293
MILLER, K. L. N91-10543
MILORA, S. L. N91-10742
MILROY, R. D. N91-10740
MINEART, GARY M. N91-10502
MINEGISHI, MASAKATSU N91-10099
MINNIS, PATRICK N91-10470
N91-10472
N91-10473
N91-10476
N91-10488
N91-10505
MINODA, MITSUHIRO N91-10059
N91-10060
MIRANDA, F. A. N91-10780
MIRIN, A. A. N91-10650
MITA, SADAO N91-10354
MITSUBORI, SUSUMU N91-10003
MIURA, SHIGETO N91-10350
MIYAJIMA, HIROSHI N91-10148
MIYATAKE, SHINICHI N91-10364
MIZUTANI, T. N91-10709
MOELLER, PETER N91-10818
MOENG, CHIN-HOH N91-10499
MONTRY, GARY R. N91-10648
MOORE, J. D. N91-10457
MOORE, NICHOLAS R. N91-10309
MOORE, THOMAS P. N91-10575
N91-10577
MORAN, SCOTT J. N91-10264
MORI, N. N91-10386
MORI, YOSHIKAZU N91-10343
MORINO, YOSHIKI N91-10099
MORISAKI, MASASHI N91-10347
MORITA, TOSHIYUKI N91-10099
MORITZ, R. R. N91-10076
MORRISON, GERALD L. N91-10273
MOSES, RONALD W. N91-10739
MOSS, T. S. N91-10758
MOTEVALLI, V. N91-10193
MOTSCHMANN, U. N91-10429
MOTTERSHEAD, TOM N91-10717
MOYER, KERRY A. N91-10514
MOYER, S. A. N91-10014
MUELLER, ARNOLD W. N91-10699
MULANSKY, B. N91-10677
MULANSKY, BERND N91-10682
MUNSON, CARTER P. N91-10739
MURAKAMI, YOSHITAKA N91-10030
MURPHY, DAVID W. N91-10835
MURPHY, G. A. N91-10828
MUSTREDELEON, J. N91-10776
MYERS, NEIL BRUBAKER N91-10410

N

NABHA, HUSSEIN N91-10785
NAFDAY, AVINASH M. N91-10308
NAHORY, R. E. N91-10779
NAIK, R. A. N91-10128
NAITO, SHIGENORI N91-10357
NAITO, SHUJI N91-10347
NAKAGAWA, KIYOSHI N91-10340
NAKAJIMA, ERUYUKI N91-10513
NAKAJIMA, TERUYUKI N91-10512
NAKAMURA, MASAYOSHI N91-10003
NAKAMURA, R. N91-10001
NANOBASHVILI, S. N91-10726
NATANZON, A. M. N91-10428
NAVARRE, GILLES ALEXANDRE HENRI N91-10135
NEAMTU, M. N91-10673
NEBEL, RICHARD A. N91-10739
NELSON, B. A. N91-10738
NELSON, TOMMY RAY N91-10408
NEMETH, NOEL N. N91-10332
NERI, FERI N91-10717
NESASA, MITSUO N91-10359
NESENBERGS, M. N91-10796
NEUBAUER, F. M. N91-10421
N91-10424
NEUNZERT, H. N91-10256
NEVZGODINA, L. V. N91-10567
NEWMAN, H. S. N91-10780
NEWMAN, LEONARD N91-10407
NGUYEN, A. N91-10791
NGUYEN, TAI D. N91-10129
NICHOLAS, D. J. N91-10076
NICHOLLS, S. N91-10495
N91-10520
N91-10535
NICHOLS, F. A. N91-10171
NICOL, DAVID M. N91-10628
N91-10629
NIELSEN, PAMELA ANN N91-10200
NIEMER, K. A. N91-10737
NINOKATA, H. N91-10239
NIRMALA, G. A. N91-10625
NISHIDA, HIROZOU N91-10349
NISSIM, ELI N91-10328
NIX, J. RAYFORD N91-10818
NIX, WILLIAM D. N91-10152
NOGUCHI, YOSHIO N91-10299
NOHARA, TOSIO N91-10389
NONAKA, OSAMU N91-10389

NOOR, AHMED K. N91-10301
NOSE, HIROYUKI N91-10059
NOUSE, HIROYUKI N91-10060
NOWICKI, TOMASZ N91-10670
NOYES, H. PIERRE N91-10789
NUCCIARONE, JEFFEREY J. N91-10514
NYREN, KENNETH N91-10263

O

OBOT, N. T. N91-10236
OBRIEN, D. F. N91-10758
OESTERREICHER, H. N91-10774
OH, BYUNG K. N91-10013
OHNUKI, S. N91-10160
OHSHIMA, TAKASHI N91-10364
N91-10365
OKABE, MASANORI N91-10080
N91-10082
OKAZAKI, TSUKASA N91-10354
OLSEN, LOLA M. N91-10455
ONIGATA, TOSHIO N91-10352
ONO, FUMIEI N91-10190
ONO, KOICHI N91-10299
ONTIVEROS, CORDELIA N91-10157
OOSAWA, KAZUHIRO N91-10369
N91-10370
N91-10373
OPALKA, KLAUS O. N91-10230
OROUKE, M. K. N91-10697
OSHER, J. E. N91-10096
OTAKE, KUNIHIKO N91-10299
OVSYANNIKOV, A. V. N91-10571
OWEN, D. A. N91-10069

P

PAFFETT, M. T. N91-10382
PAK, Z. P. N91-10555
PALILOVA, A. N. N91-10569
PALLOTTINO, G. V. N91-10209
PAN, HUACHEN N91-10254
PANTAZIS, JOHN A. N91-10264
PAPIN, P. N91-10382
PARISI, M. N91-10837
PARK, J. S. N91-10331
PARKER, F. R. N91-10239
N91-10243
N91-10244
PARKER, JERALD V. N91-10095
PARKER, LINDSAY N91-10480
PARKER, R. J. N91-10261
PARKER, STEVEN L. N91-10548
PARKS, PAUL F. N91-10710
PARROT, M. N91-10425
PARZYCH, D. N91-10065
PASE, S. N91-10837
PASQUIER, MICHEL N91-10291
PATRICK, GARY N91-10199
PATTERSON, E. N91-10486
PATTERSON, R. G. N91-10718
PAULEY, K. A. N91-10173
PAULEY, KEITH A. N91-10104
PEDRAZA, D. F. N91-10761
PEMHA, ELKANA N91-10723
PENCIL, ERIC J. N91-10118
PENG, YINGCAI N91-10665
PENNER, JOYCE E. N91-10409
PERALA, RODNEY A. N91-10548
PEREZ, JOSEPH D. N91-10710
PERISON, JANICE N91-10188
PERRY, BOYD, III N91-10317
PERRY, J. L. N91-10103
PERSELLO, L. FRANK N91-10034
PETERKA, ROBERT J. N91-10591
PETERS, M. N91-10151
PETERS, W. N91-10041
PETRZILKA, V. N91-10725
PEW, H. K. N91-10266
PHILLIPS, J. E. N91-10384
PHILLIPS, RICHARD L. N91-10803
PHILLIPS, WILLIAM H. N91-10078
PHILPOT, H. E. N91-10125
PICKARD, A. C. N91-10297
PICKRELL, MARK M. N91-10739
PINCON, J. L. N91-10425
PINDZOLA, MICHAEL S. N91-10710
PIRAUX, L. N91-10130
POEPPEL, R. B. N91-10782
POLETTO, GIANNINA N91-10817
N91-10830
POOLE, B. D. N91-10457
POOLE, B. R. N91-10219
POOLE, L. R. N91-10457
N91-10481
POPOV, I. G. N91-10555
POPP, O. T. N91-10788
PORTER, JOHN N91-10275
POSPIESZCZYK, A. N91-10289
POST, D. N91-10330
POST, G. N91-10681
POTOTZKY, ANTHONY S. N91-10317
N91-10320
POTTECK, S. N91-10206
N91-10207
N91-10691
POULOS, H. G. N91-10655
POUND, B. G. N91-10140
PRATER, E. T. N91-10414
PRATLEY, D. J. N91-10069
PRIEDHORSKY, WILLIAM C. N91-10720
PRIEM, RICHARD J. N91-10117
PRODAN, N. G. N91-10553
PROGAR, DONALD J. N91-10182
PROKHORENKO, V. I. N91-10419
PULTZ, SUSAN N91-10391
N91-10392
PUXLEY, PHILIP JOHN N91-10814
PYTLOWANY, PETER J. N91-10446

Q

QIAN, S. N91-10697
QUALLS, A. L. N91-10742
QUIMBY, K. N91-10607

R

RABADI, RAJA EL-SALEM N91-10510
RADKE, L. F. N91-10528
RADKE, LAWRENCE F. N91-10507
N91-10512
RAIZONVILLE, P. N91-10380
RAJAN, S. D. N91-10311
RAJGOPAL, J. N91-10311
RAMSAY, TOM N91-10040
RANDALL, DAVID A. N91-10456
N91-10498
RASZILLIER, H. N91-10258
RAYMOND, P. N91-10205
RE, F. N91-10833
N91-10834
REBAGAY, T. V. N91-10296
REDEY, LASZLO N91-10220
REED, R. P. N91-10696
REIFF, J. N91-10540
REIFSNIDER, K. L. N91-10330
REINATH, M. S. N91-10268
REJ, D. J. N91-10740
REMIZOV, A. P. N91-10436
RENKO, KARI N91-10025
REPH, MARY G. N91-10455
REUSS, ROBYN N91-10040
REVERCOMB, H. E. N91-10465
REYES, A. P. N91-10768
REYNOLDS, MIKE N91-10033
REZEAU, L. N91-10432
REZNIKOV, A. E. N91-10428
RHODES, ALAN N91-10070
RHYS-JONES, T. N. N91-10072
RIBE, F. L. N91-10738
RICHARD, JACQUES CONSTANT N91-10062
RICHARDS, P. G. N91-10441
N91-10543
RICHARDSON, DAVID E. N91-10126
RICOY, M. A. N91-10201
RIDGWAY, W. N91-10493
RIEDLER, W. N91-10437
RIFFE, SCOTT E. N91-10629
RIMMER, R. A. N91-10203
RINGER, MARK N91-10040
RISSER, STEVEN M. N91-10179
N91-10180
N91-10778
ROBBINS, MICHAEL J. N91-10315
ROBERT, EMMANUEL N91-10110
ROBERT, P. N91-10422
ROBERTSON, D. D. N91-10014
ROBERTSON, ERICA N91-10155
N91-10158
ROBINSON, B. D. N91-10685
ROBINSON, BRIAN A. N91-10020
ROBINSON, D. A. N91-10481
ROBINSON, DAVID A. N91-10469
N91-10527
ROBOTHAM, W. F. N91-10281
ROE, P. L. N91-10250
ROGERS, J. N91-10041
ROGERS, MELISSA J. B. N91-10191
ROGERS, STEPHEN N91-10706
ROLFE, E. J. N91-10417
ROMATE, JOHAN EGBERT N91-10443
ROMBACH, H. D. N91-10608
RONE, KYLE N91-10611
ROOS, C. N91-10636
ROSE, WILLIAM C. N91-10083
ROSEN, S. P. N91-10836
ROSENBERGER, FRANZ E. N91-10755
ROSENBLUTH, M. N. N91-10743
N91-10744
N91-10745
ROSENBURY, E. T. N91-10219
ROSENWALD, ROSS DEBNER N91-10827
ROSS, J. C. N91-10268
ROSS, R. G., JR. N91-10222
ROSSITER, J. A. N91-10229
N91-10644
N91-10684
ROSSON, R. M. N91-10538
ROSSOW, WILLIAM B. N91-10451
ROUSE, B. R. N91-10457
N91-10482
ROUSSEL-DUPRE, DIANE N91-10720
ROUX, A. N91-10422
N91-10432
ROUXEL, L. N91-10304
ROY, M. N91-10384
ROY, R. N91-10123
RUCK, B. N91-10286
RUDOLPH, TERENCE N91-10548
RUGGLES, M. B. N91-10178
RYUTOVA, M. N91-10831

S

SABONNADIERE, EMMANUEL N91-10210
SACHSENWEGER, DORIS N91-10753
SADREHAGHIGHI, I. N91-10238
SAFF, C. R. N91-10321
SAITO, KENJI N91-10030
SAITO, MASAKAZU N91-10346
SAITO, T. T. N91-10719
SAITO, TAKEO N91-10346
SAKAMOTO, HIROSHI N91-10190
SALMINEN, ESA N91-10023
N91-10024
SALTZ, JOEL N91-10599
N91-10600
SALUSTI, E. N91-10837
SAMMELLS, ANTHONY F. N91-10381
SANO, MASAAKI N91-10099
SASAKI, HIDEYUKI N91-10368
N91-10371
N91-10372
SASAKI, MASAHIRO N91-10348
SASAKI, MASAKI N91-10190
SASAKI, MASAYUKI N91-10360
SASAKI, SHUICHI N91-10031
SASAKI, YUKIO N91-10341
N91-10344
N91-10351
SASAO, MAMIKO N91-10751
SASSEN, KENNETH N91-10453
N91-10459
N91-10460
N91-10464
N91-10476
N91-10478
SATO, KAZUO N91-10190
SATO, KOJI N91-10350
SATO, MASAHIRO N91-10148
SATOH, MOTOYASU N91-10375
SAUER, K. N91-10429
SAVAGE, M. N91-10042
N91-10044
SAVANT, GAJENDRA N91-10270
SAVIN, S. P. N91-10419
SAVOLAINEN, TAPANI N91-10627
SCANLON, CHARLES H. N91-10058
SCHAEBEN, H. N91-10673
SCHAFFAR, MARTIN N91-10018
SCHEIDT, TONY N91-10040
SCHICK, CLAUS N91-10055
SCHIFERL, S. K. N91-10163
SCHLUTER, MICHAEL N91-10765
SCHMALZER, PAUL A. N91-10442
SCHMIDT, E. N91-10486
SCHMIT, L. A. N91-10312
SCHMUCK, P. N91-10240
SCHNEIDER, VICTOR B. N91-10580
SCHOBERT, HAROLD H. N91-10188
SCHOENBERG, KURT F. N91-10739
SCHRA, L. N91-10151
SCHUBERT, WAYNE H. N91-10492
N91-10515

N91-10517
SCHULER, A. L. N91-10111
N91-10112
N91-10113
SCHULMAN, L. S. N91-10659
SCHULZ, NORBERT S. N91-10808
SCHULZE, MANFRED W. N91-10109
SCHWAB, RAINER R. N91-10063
SCHWIESOW, RONALD N91-10534
SCHYOKOTOV, A. YU. N91-10428
SCIEZ, GERALD N91-10196
SCRIVENER, C. T. J. N91-10074
SEGALMAN, DANIEL J. N91-10700
SEIBLE, FRIEDER N91-10333
SEILER, F. N91-10247
SELA, I. N91-10767
SELAMET, A. N91-10235
SELCHOW, NICHOLAS J. N91-10732
SELMAN, J. ROBERT N91-10177
SENGUPTA, S. K. N91-10504
SEYLER, C. E. N91-10734
SEZE, GENEVIEVE N91-10503
SHACKELFORD, J. F. N91-10331
SHAFARMAN, W. N. N91-10384
SHAPIRO, M. J. N91-10758
SHARMA, D. K. N91-10757
SHARPS, P. N91-10756
SHEAHEN, T. P. N91-10757
SHEN, JIAN-MIN N91-10657
SHEN, YINONG N91-10323
SHEPODD, TIM J. N91-10185
SHEPODD, TIMOTHY J. N91-10184
SHINGLEDECKER, CLARK N91-10033
SHINOZUKA, SUSUMU N91-10355
SHIRAKAWA, YOSHISHIGE N91-10361
SHIRER, HAMPTON N. N91-10521
SIDIKMAN, KENNETH LEE N91-10728
SIEGMUND, OSWALD H. W. N91-10720
SIEMON, R. E. N91-10740
SIEMS, S. T. N91-10496
SIGAL, ASHER N91-10005
SIGNORETTI, F. N91-10833
N91-10834
SIIKONEN, TIMO N91-10253
N91-10254
SIM, ALEX G. N91-10079
SIMPSON, W. A., JR. N91-10125
SINDT, C. F. N91-10231
SINGER, JOSEF N91-10303
SINGER, KENNETH D. N91-10172
SINGH, J. P. N91-10782
SINGH, NAGENDRA N91-10441
SINOPALNIKOV, V. I. N91-10557
SIZEK, H. W. N91-10162
SKYLLINGSTAD, E. D. N91-10440
N91-10541
SLATER, P. N. N91-10475
SLINGO, A. N91-10494
SMALL, J. C. N91-10655
SMALLWOOD, DAVID O. N91-10329
SMEETS, G. N91-10086
N91-10246
SMITH, BARHAM W. N91-10720
SMITH, CHARLES D. N91-10699
SMITH, D. L. N91-10767
SMITH, G. N91-10475
SMITH, H. MIKE N91-10185
SMITH, HENRY M. N91-10184
SMITH, HERB, JR. N91-10321
SMITH, J. E. N91-10832
SMITH, JOEL B. N91-10394
N91-10395
N91-10396
N91-10397
N91-10398
N91-10399
N91-10400
N91-10401
N91-10402
N91-10403
N91-10404
SMITH, LEONARD N91-10503
SMITH, M. G. N91-10774
SMITH, M. J. T. N91-10704
SMITH, MIKE N91-10509
SMITH, N. K. N91-10791
SMITH, WILLIAM L. N91-10465
N91-10471
N91-10474
SMITH, WILLIAM L., JR. N91-10479
N91-10484
SNIDER, JACK B. N91-10508
N91-10510
N91-10515
N91-10517
N91-10524
N91-10534
SNYDER, ROBERT S. N91-10191
SOBOYEJO, W. O. N91-10337
SOCOLESCU, DAN N91-10257
SOLTANI, NASSER N91-10324
SOLTIS, STEPHEN N91-10028
SOMEYA, TERUO N91-10057
SON, LE HUNG N91-10656
SONG, CHUNSHAN N91-10188
SOSNOVSKIY, A. V. N91-10563
SOUTHWOOD, D. J. N91-10418
N91-10421
SPALEK, G. N91-10279
SPARNOCCHIA, S. N91-10837
SPELT, PHILIP F. N91-10653
SPERA, DAVID A. N91-10127
SPERRY, DAVID J. N91-10264
SPEZIALE, CHARLES G. N91-10237
SPIEKSMA, FLOS M. N91-10680
SPIELMAN, RICK N91-10275
SPIER, E. E. N91-10302
SPINHIRNE, JAMES D. N91-10468
N91-10480
N91-10523
STAHL, M. N91-10061
STAKENBORG, LUC N91-10651
STALFORD, HAROLD N91-10047
STARR, DAVID OC. N91-10449
N91-10453
N91-10477
STAUBER, WILLIAM T. N91-10582
STAYLOR, W. F. N91-10475
STCLAIR, TERRY L. N91-10182
STECHEL, E. B. N91-10765
STEELE, W. V. N91-10791
STEER, BARRY N91-10035
N91-10036
N91-10292
N91-10654
STEIN, HERMAN N91-10132
STELL, GEORGE N91-10792
STEPHENS, D. G. N91-10702
STEPHENS, GRAEME L. N91-10462
STEVENS, DUANE E. N91-10454
STEWART, DONALD F. N91-10574
N91-10576
N91-10588
STINNETT, R. W. N91-10736
STOECKEL, J. N91-10726
STOFFELEN, A. C. M. N91-10544
STOLE, SCOTT M. N91-10144
STORINI, M. N91-10820
N91-10837
N91-10838
STRADLING, G. L. N91-10266
STRATTON, REX C. N91-10295
N91-10631
STREETT, C. L. N91-10251
STRUCKMEIER, J. N91-10256
STURGE, M. D. N91-10779
SU, AY N91-10006
SU, JAO-JANG N91-10729
SUBBANNA, S. N91-10767
SUDO, TAKAYUKI N91-10148
SUEMATSU, KAZUYO N91-10605
SUENAGA, SYOUJI N91-10003
SUGAI, MASAAKI N91-10352
SULLIVAN, J. AL N91-10282
SUMMERS, R. JOE N91-10093
SUN, MAORONG N91-10801
SUTTLES, JOHN T. N91-10475
N91-10480
SUZUKI, HIROKAZU N91-10003
SUZUKI, HIROYUKI N91-10341
N91-10344
N91-10351
SUZUKI, KAZUFUMI N91-10362
SUZUKI, MASAMITSU N91-10081
SUZUKI, TAKAO N91-10340
SWARTTOUW, RENE F. N91-10666
SWEERS, GUIDO N91-10671
SYN, C. K. N91-10719
SYRETT, WILLIAM J. N91-10515
N91-10522
SZATMARY, STEVEN A. N91-10332

T

TADMOR, EITAN N91-10664
TAGGART, D. P. N91-10740
TAJIMA, T. N91-10831
TAKAGI, SHOHEI N91-10087
TAKAHASHI, H. N91-10160
TAKAHASHI, TAICHI N91-10358
TAKAHASHI, TATSUO N91-10346
TAKAKU, SABURO N91-10345
TAKANO, Y. N91-10470
TAKASAWA, KINGO N91-10053
TAKI, NOBUYUKI N91-10339
TAKIGAWA, M. N91-10768
TAKIZAWA, MINORU N91-10057
TALOTTA, NICHOLAS J. N91-10033
TALUKDAR, B. N91-10693
TAMARGO, M. C. N91-10779
TAMURA, HIROSHI N91-10190
TANAKA, TOSHIHARU N91-10342
TANG, ANDREW C. N91-10790
TANG, PIER K. N91-10187
TANGE, AKIHIKO N91-10345
TANNEHILL, J. C. N91-10019
TAO-GUANG, LI N91-10540
TAUSWORTHE, ROBERT C. N91-10610
TAYLOR, ANTOINETTE J. N91-10276
TAYLOR, JOHN N91-10314
TAYLOR, R. D. N91-10774
TEILLET, P. M. N91-10475
TENFORDE, T. S. N91-10592
TERLAKY, T. N91-10636
TERRY, P. W. N91-10747
TERUI, YUSHI N91-10030
TESTI, NICHOLAS N91-10649
THART, W.G. T. N91-10151
THOMAS, H. L. N91-10312
THOMPSON, J. D. N91-10768
THOMSON, DENNIS W. N91-10522
THORNTON, WILLIAM N91-10578
N91-10579
N91-10586
THORPE, ARTHUR N. N91-10763
TIJS, S. H. N91-10692
TINCHER, M. N91-10061
TING, MINGFANG N91-10536
TIRPAK, DENNIS A. N91-10394
N91-10395
N91-10396
N91-10397
N91-10398
N91-10399
N91-10400
N91-10401
N91-10402
N91-10403
N91-10404
TISONE, G. S. N91-10736
TITCHELL, I. N91-10169
TIWARI, S. N. N91-10238
TODA, NOBUHIRO N91-10081
TODOROKI, JIRO N91-10749
TOKAR, R. L. N91-10280
TOLMAN, HENDRIK LIEUWE N91-10550
TOMIOKA, KENJI N91-10099
TORKAR, K. N91-10437
TORR, D. G. N91-10441
N91-10543
TORRES, FRANCISCO J. N91-10013
TRATNIK, M. V. N91-10715
TRETMANS, JAN N91-10643
TRIMBOLI, M. S. N91-10683
N91-10684
TSUI, HERMANN Y. W. N91-10739
TURCHANINOVA, V. F. N91-10554
TURCICH, ELIZABETH N91-10084
TURHOLLOW, A. F. N91-10406
TURKO, BOJAN T. N91-10777
TURUNEN, JARI N91-10724
TUSZEWSKI, M. N91-10740
TWOHY, C. H. N91-10528

U

UCHIDA, TADAO N91-10057
UCHIYAMA, TOKUEI N91-10367
UEDA, SHUICHI N91-10148
UJINO, ISAO N91-10099
UOSUKAINEN, SEPPO N91-10701
USAVAGE, PAUL, JR. N91-10616
USUI, HIROSHI N91-10059
N91-10060

V

VADAS, SHARON L. N91-10695
VAISBERG, O. L. N91-10438
VALERO, FRANCISCO P. J. N91-10466
N91-10467
N91-10529
VALETT, JON D. N91-10609
VALNICEK, B. N91-10433
VANBEMMELEN, THEO N91-10674
VANDENHEUVEL, J. N91-10676

**VANMOERKERKEN, R. A.** N91-10545
**VANSTRIEN, SEBASTIAN** N91-10670
**VANVLEDDER, GERBRANT PHILIPPUS** N91-10549
**VANWILLIGENBURG, L. G.** N91-10668
N91-10689
**VANZUTPHEN, TOM** N91-10225
**VAUGHAN, C. M.** N91-10259
**VAUGHN, M. A.** N91-10482
**VELDMAN, H. J.** N91-10676
**VELSKO, S. P.** N91-10719
**VENABLE, D. D.** N91-10735
**VERHOEVEN, CHRISTIAAN JOHANNES MARI**
N91-10226
**VERSTAPPEN, ROELAND WILHEMUS CAROLUS**
N91-10290
**VILLORESI, G.** N91-10833
N91-10834
**VOELKER, ROBERT HETH** N91-10212
**VOGIN, RICHARD** N91-10196
**VOLAKIS, JOHN L.** N91-10201
N91-10623
**VONDERHAAR, THOMAS H.** N91-10530
**VOROZHTSOVA, S. V.** N91-10562

## W

**WADA, MOTOI** N91-10751
**WAGNER, B. A.** N91-10008
**WAGNER, H. SCOTT** N91-10448
**WAGNER, JOHN S.** N91-10713
**WAHBA, RENEE RAOUF** N91-10815
**WAKAIRO, KAORU** N91-10080
N91-10082
**WALDMAN, D. J.** N91-10288
**WALDROP, D. A.** N91-10330
**WALKER, S. N.** N91-10426
**WALSH, M.** N91-10061
**WALSH, M. J.** N91-10337
**WALSTROM, PETER** N91-10717
**WALTER, R.** N91-10424
**WAMBSGANSS, M. W.** N91-10236
**WANG, CHARLES C.** N91-10105
**WANG, GUO-JUAN** N91-10801
**WANG, S. S.** N91-10122
N91-10304
**WANG, SHI-KUN** N91-10657
**WANG, WENXING** N91-10407
**WANG, YUN** N91-10695
**WANG, Z.** N91-10260
N91-10272
**WARD, JOHN W.** N91-10771
**WARD, PAUL T.** N91-10617
**WARE, ALAN S.** N91-10085
**WARE, BRUCE E.** N91-10084
**WARNER, J. D.** N91-10780
**WARREN, JOHN** N91-10720
**WARREN, STEPHEN G.** N91-10452
N91-10528
**WASHBURN, J.** N91-10775
**WATANABE, AKIRA** N91-10080
N91-10082
**WATANABE, ATSUTARO** N91-10148
**WATKINS, D. E.** N91-10767
**WEBB, B. J.** N91-10173
**WEBB, BRENT J.** N91-10104
**WEBER, PAUL G.** N91-10739
**WEBER, W. J.** N91-10143
**WEBSTER, JOHN R.** N91-10336
**WEBSTER, R. B.** N91-10740
**WEDGE, R. H.** N91-10298
**WEIL, MELINDA L.** N91-10529
**WELCH, PETER J.** N91-10131
**WELCH, R. M.** N91-10504
**WELCH, RONALD M.** N91-10480
**WELLER, TANCHUM** N91-10303
**WELLMAN, J. BRENT** N91-10045
**WELLS, WILLIAM L.** N91-10245
**WENDELKEN, J. F.** N91-10772
**WERNET, MARK P.** N91-10271
**WESSENDORF, KURT O.** N91-10218
**WEST, E. A.** N91-10832
**WESTRATE, J. A.** N91-10635
**WEWERINKE, PAULUS HEINRICH** N91-10597
**WHALEN, B. A.** N91-10431
**WHETSTONE, J. R.** N91-10231
**WHITE, ALLEN B.** N91-10522
**WHITEMAN, C. D.** N91-10542
**WHITING, E. V.** N91-10639
**WHITLOCK, C. H.** N91-10475
N91-10481
**WHITTAKER, J. W.** N91-10330
**WIELICKI, BRUCE A.** N91-10472
N91-10480
**WIELICKI, BRUCE M.** N91-10534
**WIGGINS, STEPHEN** N91-10663
**WILCOX, L. D.** N91-10686
**WILEY, D. R.** N91-10111
N91-10112
N91-10113
**WILHELM, D.** N91-10239
N91-10242
**WILKINSON, P. J.** N91-10543
**WILLE, L. T.** N91-10783
**WILLIAMS, SHAREN L.** N91-10487
**WILSON, ANTHONY** N91-10051
**WILSON, FREDERICK C.** N91-10539
**WILSON, ROBERT** N91-10199
**WINTER, STELLAN** N91-10263
**WINTERS, G. M.** N91-10638
**WISEALL, S. S.** N91-10261
**WISLER, S.** N91-10061
**WITTEVEEN, CEES** N91-10651
**WOLFE, R.** N91-10278
**WOLSKY, A. M.** N91-10757
**WOODS, J. A.** N91-10316
**WOODWARD, RICHARD P.** N91-10703
**WOOLLISCROFT, L. J. C.** N91-10426
N91-10427
N91-10428
**WORKMAN, G. L.** N91-10294
**WORREL, WAYNE L.** N91-10381
**WRIGHT, B. L.** N91-10740
**WRIGHT, JOSEPH A.** N91-10029
**WRIGHT, L. L.** N91-10406
**WU, JANET** N91-10600
**WU, KE** N91-10657
**WU, T. YAO-TSU** N91-10662
**WURDEN, GLEN A.** N91-10739
**WYLIE, DONALD P.** N91-10449
N91-10450
N91-10471
N91-10477
N91-10485
N91-10489
N91-10534

## X

**XU, KEI-WEN** N91-10657
**XU, X. Q.** N91-10743
N91-10744
N91-10745

## Y

**YAMAKAWA, MASAKI** N91-10148
**YAMAMOTO, YUKIMITSU** N91-10011
**YAMAOKA, HITOSHI** N91-10751
**YAMASHITA, AKIFUMI** N91-10342
**YAN, TSUN-YEE** N91-10105
**YANG, HENRY T. Y.** N91-10020
**YANQIAN, YE** N91-10669
**YAO, JEN-CHIH** N91-10660
**YARTSEV, YE. I.** N91-10562
**YASAR, OSMAN** N91-10730
**YATES, GEORGE J.** N91-10777
**YATSUYANAGI, NOBUYUKI** N91-10190
**YEGOROV, A. D.** N91-10554
**YELON, W. B.** N91-10156
**YOES, CISSY A.** N91-10793
**YOKOYA, TAKESHI** N91-10345
**YOKOYAMA, SHINTARO** N91-10030
**YOSHIDA, RYUJI** N91-10011
**YOUNG, DAVID F.** N91-10472
N91-10473
N91-10476
N91-10488
N91-10505
**YOUNG, GEORGE** N91-10514
**YOUNGBLOOD, G. E.** N91-10143
**YOUNGER, STEPHEN M.** N91-10282
**YUAN, F. G.** N91-10122
**YUNUS, A.** N91-10693
**YURI, I.** N91-10386

## Z

**ZACEK, F.** N91-10726
**ZANGRILLI, N. L.** N91-10833
N91-10834
**ZELENYI, L. M.** N91-10419
**ZHANG, YEHONG** N91-10287
**ZHU, ZIQIANG** N91-10024
**ZHU, ZIQUIANG** N91-10023
**ZIEGLER, R. E.** N91-10125
**ZIMAN, JA.** N91-10423
**ZIOLKOWSKI, R. W.** N91-10659
**ZOU, JINGKE** N91-10801
**ZUO, J. K.** N91-10772
**ZUREK, A. K.** N91-10164
**ZUTECK, MICHAEL D.** N91-10127

# CORPORATE SOURCE INDEX

**SCIENTIFIC AND TECHNICAL AEROSPACE REPORTS VOLUME 29 NUMBER 1**

### Typical Corporate Source Index Listing

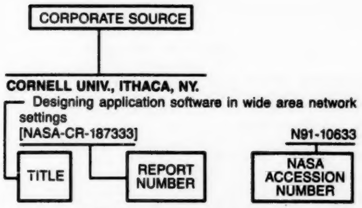
CORPORATE SOURCE
CORNELL UNIV., ITHACA, NY.
Designing application software in wide area network settings
[NASA-CR-187333]
N91-10633
TITLE
REPORT NUMBER
NASA ACCESSION NUMBER

Listings in this index are arranged alphabetically by corporate source. The title of the document provides the user with a brief description of the subject matter. The report number helps to indicate the type of document cited (e.g., NASA report, translation, NASA contractor report). The NASA accession number denotes the number by which the citation is identified. The titles are arranged under each corporate source in ascending accession number order.

## A

**ACADEMY OF SCIENCES, BERLIN (GERMAN D.R.).**

Multiple-ion waves behind shocks N91-10429

**ACADEMY OF SCIENCES, POTSDAM (GERMAN D.R.).**

Energetic particles in the Earth's magnetotail or: Cluster and Regatta as a dispersiometer N91-10434

**ACADEMY OF SCIENCES (USSR), MOSCOW.**

Specific tasks of multiple scale plasma measurements in Regatta-Cluster system N91-10419

Small Space Lab as a basic spacecraft of Regatta project N91-10423

Problems of cold plasma measurements on the Regatta-A spacecraft N91-10431

Specific tasks of Regatta-E measurements correlated with Cluster/Regatta-A in the ISTP and Regatta programmes N91-10436

Possibilities of charged particle injection from spacecraft for active diagnostics of the surrounding plasma and active spacecraft potential control N91-10437

The possibility of making fast measurements of ion distribution functions N91-10438

**ACADEMY OF SCIENCES (USSR), TROITSK.**

On the possibility to support multisatellite measurements of the Cluster mission by single satellite measurements in the Regatta-Cluster project N91-10428

**ADVISORY GROUP FOR AEROSPACE RESEARCH AND DEVELOPMENT, NEUILLY-SUR-SEINE (FRANCE).**

Rotorcraft drivetrain life safety and reliability
[AGARD-R-775] N91-10042

**AERONAUTICAL RESEARCH LABS., MELBOURNE (AUSTRALIA).**

Flight testing of two Allison T56 engines modified to the ARL developed low smoke configuration
[ARL-PROP-TM-449] N91-10064

**AEROSTRUCTURES, INC., ARLINGTON, VA.**

Piezoelectrically forced vibrations of electroded doubly rotated quartz plates by state space method
N91-10318

**AIR FORCE SPACE TECHNOLOGY CENTER, KIRTLAND AFB, NM.**

Design and application of gas-gap heat switches
[NASA-CR-187339] N91-10222

**AKRON UNIV., OH.**

Drive system life and reliability N91-10044

**ALABAMA UNIV., HUNTSVILLE.**

Network, system, and status software enhancements for the autonomously managed electrical power system breadboard. Volume 1: Project summary
[NASA-CR-185880] N91-10618

Network, system, and status software enhancements for the autonomously managed electrical power system breadboard. Volume 2: Protocol specification
[NASA-CR-185881] N91-10619

Network, system, and status software enhancements for the autonomously managed electrical power system breadboard. Volume 3: Commands specification
[NASA-CR-185882] N91-10620

Network, system, and status software enhancements for the autonomously managed electrical power system breadboard. Volume 4: Graphical status display
[NASA-CR-185879] N91-10621

The growth of zinc selenide single crystals by physical vapor transport in microgravity
[NASA-CR-180428] N91-10755

Parameterization of cosmological scale factor during inflationary times N91-10815

**ALLIED-SIGNAL AEROSPACE CO., KANSAS CITY, MO.**

Bidirectional translator between DXF and IGES formats
[DE90-016430] N91-10632

**AMES LAB., IA.**

Characterization of mono- and multi-molecular assemblies at glassy carbon and noble metals by ex situ and in situ infrared external reflection spectroscopy
[DE90-016417] N91-10144

Development, characterization, and applications of optical pH sensors supported at cellulosic film
[DE90-016416] N91-10146

Monomolecular and thin polymer films: Fabrication, characterization, applications, and models of wetting
[DE90-016415] N91-10174

**AMPTEK, INC., BEDFORD, MA.**

Prototype instrumentation and design studies
[AD-A211566] N91-10264

**AMSTERDAM UNIV. (NETHERLANDS).**

Prompt lepton production in a proton beamdump experiment
[ETN-90-97750] N91-10711

**ARGONNE NATIONAL LAB., IL.**

Self-lubricating boric acid films for tribological applications
[DE90-007805] N91-10171

Overdischarge protection in high-temperature cells and batteries
[DE90-015180] N91-10220

Two-phase flow patterns and frictional pressure gradients in a small, horizontal, rectangular channel
[DE90-014802] N91-10236

Proceedings of the 8th Symposium on Energy Engineering Sciences: Micro/Macro Studies of Multiphase Media
[DE90-014844] N91-10385

Ultra-thin vertical magneto-optical media and system for using same
[DE90-014589] N91-10603

High-temperature superconductors: Their potential for utility applications
[DE90-009704] N91-10757

Impact of high-critical-temperature superconductors on electromagnetic pump applications
[DE90-014809] N91-10759

YBa2Cu3O(x) composites with improved toughness and strength
[DE90-011180] N91-10782

**ARIZONA UNIV., TUCSON.**

Estimation of astronomical images from the bispectrum of atmospherically distorted infrared data N91-10806

The development of the continuous orthonormalization and adjoint methods for solar seismology: Eigenfrequency computation and sensitivity analysis for direct and inverse problems N91-10827

**ARNOLD ENGINEERING DEVELOPMENT CENTER, ARNOLD AIR FORCE STATION, TN.**

User's guide to CUNIFLOW
[AD-A207606] N91-10004

**ASTRIDGE (DEREK) AND ASSOCIATES, LANGPORT (ENGLAND).**

Helicopter transmissions: Design for safety and reliability N91-10043

**AUBURN UNIV., AL.**

Theoretical atomic physics for fusion
[DE90-017280] N91-10710

## B

**BALLISTIC RESEARCH LABS., ABERDEEN PROVING GROUND, MD.**

Prediction and comparison with measurements of the aerodynamic characteristics of flare-stabilized XM910 prototypes
[AD-A208099] N91-10005

Large blast and thermal simulator advanced concept driver design by computational fluid dynamics
[AD-A211364] N91-10230

A simple screw thread model for use in finite element stress analysis
[AD-A210233] N91-10300

**BELEIDSCOMMISSIE REMOTE SENSING, DELFT (NETHERLANDS).**

Impact of SASS wind data on analyses and forecasts of a fine mesh limited area model
[BCRS-89-38] N91-10544

**BERTIN ET CIE., PLAISIR (FRANCE).**

Time/frequency analysis of vibro-acoustic behaviour of a launcher in flight
[ETN-90-97584] N91-10097

Preliminary studies before defining a payload adapted to the primate model
[ETN-90-97581] N91-10107

A Knudsen layer theory for lattice gases
[ETN-90-97583] N91-10248

PROTHE: A software as a help for the studies in industrial thermal engineering
[ETN-90-97582] N91-10634

**BETTS (ALAN K.), MIDDLEBURY, VT.**

Analysis of diurnal variation of SCu layer using 2 days of CLASS soundings on San Nicolas Island N91-10490

Radiative control on tropical convective boundary layer equilibrium N91-10493

**BIONETICS CORP., COCOA BEACH, FL.**

Geology, geohydrology, and soils of NASA, Kennedy Space Center: A review
[NASA-TM-103813] N91-10442

Considerations for an exercise prescription
N91-10585

**BIRMINGHAM UNIV. (ENGLAND).**

An evaluation of the production processes and methods associated with Carello Cell at RISTS, Telford
[ETN-90-97578] N91-10228

**BROOKHAVEN NATIONAL LAB., UPTON, NY.**

XAFS studies of interactions at transition-metal/Al interfaces
[DE90-016313] N91-10159

Global and regional environmental atmospheric chemistry
[DE90-016693] N91-10407

Muon SR and high T(sub c) superconductivity
[DE90-015089] N91-10760

## C

**CALIFORNIA UNIV., BERKELEY. LAWRENCE BERKELEY LAB.**

Microstructural and phase stability studies of nanometer period metal/carbon multilayer structures for x ray optics
[DE90-015307] N91-10129

Corrosion-resistant coatings for high-temperature high-sulfur activity applications
[DE90-016638] N91-10177

Modes of elliptical waveguides: A correction
[DE90-016647] N91-10203

Corrosion, passivity, and breakdown of alloys used in high energy density batteries
[DE90-016648] N91-10223

A correlation between T(sub 3) and electronegativity difference in high-temperature superconductors
[DE90-016640] N91-10775

In situ transmission electron microscopy and computer simulation study of the kinetics of oxygen loss in YBa2Cu3O(z)
[DE90-014508] N91-10783

**CALIFORNIA UNIV., LOS ANGELES.**

Conservative buffering of approximate nonlinear constraints N91-10312

Exercise issues related to the neuromuscular function and adaptation to microgravity N91-10584

Plasma wakefield excitation by charge particle beams N91-10729

**CALIFORNIA UNIV., SAN DIEGO, LA JOLLA.**

A new beam theory using first-order warping functions N91-10307

Comparison of NASTRAN analysis with ground vibration results of UH-60A NASA/AEFA test configuration [NASA-CR-184565] N91-10333

**CALIFORNIA UNIV., SANTA BARBARA.**

Reduction of thermal stresses in continuous fiber reinforced metal matrix composites with interface layers [NASA-CR-185302] N91-10133

**CALSPAN FIELD SERVICES, INC., ARNOLD AFS, TN.**

User's guide to CUNIFLOW [AD-A207606] N91-10004

**CATERPILLAR TRACTOR CO., PEORIA, IL.**

Heavy duty liquid and gaseous fuel emissions database test results from four alternative fuel configurations of the Caterpillar 3406 engine [DE90-014783] N91-10288

**CENTER FOR MATHEMATICS AND COMPUTER SCIENCE, AMSTERDAM (NETHERLANDS).**

Optimization of polling systems [CWI-BS-R8932] N91-10635

**CENTRAL INST. OF PHYSICS, BUCHAREST (ROMANIA).**

Localizability in the Hamiltonian formalism and in quantum-mechanics [DE90-628368] N91-10787

Cohomology for Lagrangian systems and Noetherian symmetries [DE90-628371] N91-10788

**CENTRAL RESEARCH INST. OF ELECTRIC POWER INDUSTRY, TOKYO (JAPAN).**

Basic study of solid oxide fuel cells [DE90-517069] N91-10386

**CENTRE DE RECHERCHES EN PHYSIQUE DE L'ENVIRONNEMENT TERRESTRE ET PLANETAIRE, ORLEANS (FRANCE).**

Accuracy of the estimate of J via multipoint measurements N91-10422

Non-linear evolution of the Kelvin-Helmholtz instability: Constraints on multipoint measurements N91-10430

Multipoint study of small-scale structures at the magnetopause N91-10432

**CENTRE DE RECHERCHES SCIENTIFIQUES ET TECHNIQUES DE L'INDUSTRIE DES FABRICATIONS METALLIQUES, BRUSSELS (BELGIUM).**

Activities report of the Permanent Committee of the General Council [ISSN-0524-7705] N91-10198

**CENTRE NATIONAL D'ETUDES SPATIALES, TOULOUSE (FRANCE).**

Magnetic sensitivity of on-board quartz oscillators: State of the knowledge [CNES-CT/DRT/TIT/TF-88/354] N91-10110

Influence of the telescope depointing on the performances of an optical link. Correlation between depointing law and coding, concerning the computation of mean BER [CNES-CT/DRT/TIT/TR-88/24-T] N91-10206

Principles of LOCSTAR system experiments [CNES-CT/DRT/TIT/TR-88/355] N91-10207

MicroChannel Plate detectors (MCP) [CNES-CT/DRT/TIT/OE-88/037-T] N91-10227

Hydrogen maser: Results of evaluations done by the CNES from May 1986 to December 1987 [CNES-DRT/TIT/TF-88/338-T] N91-10284

Geoid and Doppler induced errors on the altimeter measurement and their correction [CNES-CT/DRT/TIT/RL-88/226] N91-10380

Modelization of LOCSTAR synchronisation system. Computation of non detection and false alarm probabilities. Reflections on threshold adjustment and correlator structure [CNES-CT/DRT/TIT/TR-88/060] N91-10691

**CENTRE NATIONAL DE LA RECHERCHE SCIENTIFIQUE, ORLEANS (FRANCE).**

Experimental constraints in the characterization of a turbulent field from several satellites N91-10425

**CERAMPHYSICS, INC., WESTERVILLE, OH.**

A miniature inexpensive, oxygen sensing element [DE90-014080] N91-10269

**CESKOSLOVENSKA AKADEMIE VED, ONDREJOV.**

The importance of simultaneous monitoring of solar activity for the interpretation of solar plasma phenomena N91-10433

**CESKOSLOVENSKA AKADEMIE VED, PRAGUE.**

On lower hybrid wave scattering by plasma density fluctuation nonlinear reflection coefficient of the fast magnetoacoustic wave [IPPCZ-281] N91-10725

Comments on edge turbulence during lower hybrid current drive experiment on CASTOR tokamak [IPPCZ-279] N91-10726

**CHINA NUCLEAR INFORMATION CENTRE, BEIJING.**

Digital image integration technique of multiple geoscience information system and its application [DE90-627893] N91-10801

**CLARKSON UNIV., POTSDAM, NY.**

Path integral asymptotics in the absence of classical paths [DE90-016213] N91-10659

**CLEMSON UNIV., SC.**

Micro-mechanical analysis of damage growth and fracture in discontinuous fiber reinforced metal matrix composites [NASA-CR-187020] N91-10126

**COLLEGE OF WILLIAM AND MARY, WILLIAMSBURG, VA.**

Automatic determination of fault effects on aircraft functionality [NASA-CR-181352] N91-10039

**COLOGNE UNIV. (GERMANY, F.R.).**

Cluster as a wave telescope N91-10424

**COLORADO SCHOOL OF MINES, GOLDEN.**

Physical and electronic structure of the electrolyte-solid interface through optical phenomena [DE90-015935] N91-10764

**COLORADO STATE UNIV., FORT COLLINS.**

Evidence for asymmetric inertial instability in the FIRE satellite dataset N91-10454

The effects of cloud radiative forcing on an ocean-covered planet N91-10456

Radiative properties of visible and subvisible Cirrus: Scattering on hexagonal ice crystals N91-10462

Radiative properties of Cirrus clouds: FIRE IFO case October 28, 1986 N91-10479

Temperature sensitivity of Eppley broadband radiometers N91-10484

Analysis of tethered balloon, ceilometer and class sounding data taken on San Nicolas Island during the FIRE project N91-10492

Fractional cloudiness in shallow cumulus layers N91-10498

Analysis of tethered balloon data from San Nicolas Island on 8 July 1987 N91-10517

Third generation earth radiation budget measurements; ERBE in the context of earlier systems N91-10530

San Nicolas Island surface radiation-meteorology data N91-10531

**COLORADO UNIV., BOULDER.**

Cloud information for FIRE from surface weather reports N91-10452

A cloud classification scheme applied to the breakup region of marine stratocumulus N91-10497

Time-resolved FTIR (Fourier Transform Infrared) emission studies of laser photofragmentation and chain reactions [DE90-017223] N91-10722

**CONSIGLIO NAZIONALE DELLE RICERCHE, FRASCATI (ITALY).**

Fast estimation of the variance of a narrowband process [IFSI-90-16] N91-10209

UV observations of Herbig-Haro objects associated with bipolar molecular outflows: HH 7, HH 11 and HH 29 [IFSI-90-9] N91-10819

The empirical geomagnetic parameter infer near-Earth interplanetary shocks [IFSI-90-14] N91-10820

**CONSIGLIO NAZIONALE DELLE RICERCHE, ROME (ITALY).**

Plots of the 5-minute neutron monitor intensity and multiplicities recorded by the Rome 17-NM64, March 1990 [IFSI-90-15] N91-10833

Plots of the 5-minute neutron monitor intensity and multiplicities recorded by the Rome 17-NM64, April 1990 [IFSI-90-18] N91-10834

On the autoregression methods applied to the hourly nucleonic-component records [IFSI-89-19] N91-10837

Cosmic-ray intensity increase observed on September 29, 1989: The Chilean neutron monitor data (brief report) [IFSI-90-4] N91-10838

**CORNELL UNIV., ITHACA, NY.**

Designing application software in wide area network settings [NASA-CR-187333] N91-10633

A mathematical model of the structure and evolution of small scale discrete auroral arcs [NASA-CR-187238] N91-10734

Large scale structures in nonzero Lambda Friedmann universes N91-10812

**COUNCIL ON ENVIRONMENTAL QUALITY, WASHINGTON, DC.**

National acid precipitation assessment program. Report to the President and Congress [PB90-185646] N91-10405

**CRANFIELD INST. OF TECH., BEDFORD (ENGLAND).**

Static and dynamic finite element stress analysis of layered composite plates and shells N91-10326

**CREIGHTON UNIV., OMAHA, NE.**

Changes in mineral metabolism with immobilization/space flight N91-10581

## D

**DARTMOUTH COLL., HANOVER, NH.**

Excitons in semiconducting superlattices, quantum wells, and ternary alloys [DE90-017287] N91-10779

**DELAWARE UNIV., NEWARK.**

Documentation for Program SOILSIM: A computer program for the simulation of heat and moisture flow in soils and between soils, canopy and atmosphere [NASA-CR-186953] N91-10379

Materials analysis and device optimization of CuInSe2 solar cells [DE90-000365] N91-10384

**DEPARTMENT OF ENERGY, NEW YORK, NY.**

Rn222, Rn222 progeny and Rn220 progeny as atmospheric tracers of air masses at the Mauno Loa Observatory [DE90-014872] N91-10539

**DEPARTMENT OF ENERGY, WASHINGTON, DC.**

Prevention of breakdown behind railgun projectiles [DE90-014573] N91-10094

Multiple channel programmable coincidence counter [DE90-014681] N91-10602

Massively parallel computing system [DE90-014683] N91-10648

**DESERT RESEARCH INST., RENO, NV.**

Aerosol measurements in the stratocumulus project N91-10506

**DEUTSCHE FORSCHUNGSANSTALT FUER LUFT- UND RAUMFAHRT, COLOGNE (GERMANY, F.R.).**

Wind tunnel investigations of the appearance of shocks in the windward region of bodies with circular cross section at angle of attack [DLR-FB-90-15] N91-10027

**DEUTSCHE FORSCHUNGSANSTALT FUER LUFT- UND RAUMFAHRT, GOETTINGEN (GERMANY, F.R.).**

A contribution to the numerical solution of transonic flow around a delta wing by solving Navier-Stokes equations [DLR-FB-90-13] N91-10026

**DEUTSCHE FORSCHUNGSANSTALT FUER LUFT- UND RAUMFAHRT, STUTTGART (GERMANY, F.R.).**

Design of highly concentrating solar collectors and solar collector systems [DLR-FB-90-11] N91-10390

**DRAPER (CHARLES STARK) LAB., INC., CAMBRIDGE, MA.**

Entry vehicle performance analysis and atmospheric guidance algorithm for precision landing on Mars [NASA-CR-185614] N91-10102

## E

**ECOLE CENTRALE DE LYON (FRANCE).**

Method for simulating large dimension devices submitted to electromagnetic perturbations [ECL-90-10] N91-10210

Contribution to the study of the electromagnetic field radiation close to electronics circuits [ECL-90-12] N91-10211

Markov model of the propagation of a light wave in a heated turbulent media [ECL-90-06] N91-10723

Contribution to the study of MOS structures ageing [ECL-90-04] N91-10785

**ECOLE POLYTECHNIQUE, PARIS (FRANCE).**

Structures observed on the spot radiance fields during the FIRE experiment N91-10503

**EDINBURGH UNIV. (SCOTLAND).**

Vigorous star formation in galactic nuclei N91-10814

**ELECTRO MAGNETIC APPLICATIONS, INC., DENVER, CO.**

Development and application of linear and nonlinear methods for interpretation of lightning strikes to in-flight aircraft [NASA-CR-3974] N91-10548

**ELTRON RESEARCH, INC., AURORA, IL.**

Methane conversion by solid electrolyte membranes [PB90-226341] N91-10381

**ENVIRONMENTAL PROTECTION AGENCY, ANNAPOLIS, MD.**

Chesapeake Bay Basin Monitoring Program Atlas. Volume 1: Water quality and other physiochemical monitoring programs
[PB90-147935] N91-10391

Chesapeake Bay Basin Monitoring Program Atlas. Volume 2: Biological and living resource monitoring programs
[PB90-147943] N91-10392

**ENVIRONMENTAL PROTECTION AGENCY, RESEARCH TRIANGLE PARK, NC.**

The international sodar intercomparison experiment
[PB90-246224] N91-10416

**ENVIRONMENTAL PROTECTION AGENCY, WASHINGTON, DC.**

Potential effects of global climate change on the United States. Appendix C: Agriculture, volume 1
[PB90-171588] N91-10394

Potential effects of global climate change on the United States. Appendix A: Water resources
[PB90-171968] N91-10395

Potential effects of global climate change on the United States. Appendix B: Sea level rise
[PB90-172628] N91-10396

Potential effects of global climate change on the United States. Appendix C: Agriculture, volume 2
[PB90-171596] N91-10397

Potential effects of global climate change on the United States. Appendix D: Forests
[PB90-173238] N91-10398

Potential effects of global climate change on the United States. Appendix E: Aquatic resources
[PB90-172297] N91-10399

Potential effects of global climate change on the United States. Appendix F: Air quality
[PB90-172230] N91-10400

Potential effects of global climate change on the United States. Appendix G: Health
[PB90-173881] N91-10401

Potential effects of global climate change on the United States. Appendix H: Infrastructure
[PB90-172313] N91-10402

Potential effects of global climate change on the United States. Appendix I: Variability
[PB90-173899] N91-10403

Potential effects of global climate change on the United States. Appendix J: Policy
[PB90-173188] N91-10404

**EQE ENGINEERING, INC., COSTA MESA, CA.**

Probabilistic structural analysis by extremum methods
N91-10308

**ERLANGEN-NUREMBERG UNIV. (GERMANY, F.R.).**

Coriolis-effect in mass flow metering
[LSTM-266/T/89] N91-10258

**ERNO RAUMFAHRTTECHNIK G.M.B.H. BREMEN (GERMANY, F.R.).**

Optimization criteria for the design of orbital replacement units
[MBB-UO-0092-90-PUB] N91-10109

**ESSEX CORP., HUNTSVILLE, AL.**

The design and fabrication of the Centaur neutral buoyancy trainer and related hardware
[NASA-CR-171944] N91-10085

**EUROPEAN SOUTHERN OBSERVATORY, GARCHING (GERMANY, F.R.).**

Activities report of the European Southern Observatory
[ISSN-0531-4496] N91-10809

**EUROPEAN SPACE AGENCY, PARIS (FRANCE).**

Space Plasma Physics Investigations by Cluster and Regatta
[ESA-SP-306] N91-10417

**EUROPEAN SPACE AGENCY. EUROPEAN SPACE RESEARCH AND TECHNOLOGY CENTER, ESTEC, NOORDWIJK (NETHERLANDS).**

Features of mid-tail ion trajectories during substorms
N91-10435

## F

**FEDERAL AVIATION ADMINISTRATION, ATLANTIC CITY, NJ.**

Tests of the general fire suppression concentrate Pyrocap B-136
[DOT/FAA/CT-TN90/21] N91-10029

Operational evaluation of initial data link air traffic control services. Volume 2: Appendices
[DOT/FAA/CT-90/1-VOL-2] N91-10033

Differential Global Positioning System (DGPS) test plan
[DOT/FAA/CT-TN90/15] N91-10034

Structural tests of aircraft window assembly equipped with smoke evacuation valve
[DOT/FAA/CT-TN89/44] N91-10051

Airplane systems modifications for improved cabin smoke evacuation
[DOT/FAA/CT-TN90/24] N91-10052

FAA air traffic operational evaluation of Automated Surface Observing System (ASOS)
[DOT/FAA/CT-TN90/42] N91-10084

**FEDERAL AVIATION ADMINISTRATION, LONG BEACH, CA.**

Seat dynamic performance standards for a range of sizes
[DOT/FAA/CT-TN90/23] N91-10028

**FEDERAL AVIATION ADMINISTRATION, WASHINGTON, DC.**

National airspace system: In-flight assistance operational concept
[PB90-233115] N91-10032

Atmospheric ozone 1985: Assessment of our understanding of the processes controlling its present distribution and change, volume 3
[NASA-TM-103462] N91-10393

**FEDERAL LAB. CONSORTIUM, WASHINGTON, DC.**

Putting technology to work, 1990. Examples of industry-laboratory cooperation contributing to our nation's economic strength
[PB90-215187] N91-10805

**FERMI NATIONAL ACCELERATOR LAB., BATAVIA, IL.**

Dijet spectroscopy at high luminosity
[DE90-016901] N91-10147

SSC dipole magnet measurement and alignment using laser technology
[DE90-014881] N91-10281

False-vacuum decay in generalized extended inflation
[NASA-CR-186419] N91-10695

**FINNISH ACADEMY OF TECHNICAL SCIENCES, HELSINKI.**

Software integration technologies in industrial applications
[MA-55] N91-10627

**FLORIDA ATLANTIC UNIV., BOCA RATON.**

Mobility power flow analysis of an L-shaped plate structure subjected to distributed loading
[NASA-CR-187353] N91-10334

Experimental measurement of structural power flow on an aircraft fuselage
[NASA-CR-187352] N91-10335

## G

**GA TECHNOLOGIES, INC., SAN DIEGO, CA.**

Thermionic converter emitter support arrangement
[DE90-015132] N91-10383

**GENERAL DYNAMICS CORP., SAN DIEGO, CA.**

Hybrid propulsion technology program: Phase 1, volume 1
[NASA-CR-183972] N91-10111

Hybrid propulsion technology program: Phase 1, volume 2
[NASA-CR-183973] N91-10112

Hybrid propulsion technology program: Phase 1. Volume 3: Thiokol Corporation Space Operations
[NASA-CR-183974] N91-10113

Ground test program for new Atlas payload fairings
N91-10315

**GENERAL ELECTRIC CO., PHILADELPHIA, PA.**

A modernized PDL approach for Ada software development N91-10616

**GEORGE WASHINGTON UNIV., HAMPTON, VA.**

First evaluation of the main parameters in the dynamics of the Small Expendable Deployer System (SEDS) for a tethered satellite
[NASA-CR-4319] N91-10098

**GEORGIA INST. OF TECH., ATLANTA.**

Application of a state-space wake model to elastic blade flapping in hover N91-10006

Nonlinear feedback control for high alpha flight
[NASA-CR-186545] N91-10047

Sub-visual Cirrus detection and characterization
N91-10486

Preparation of superconducting wire by deposition of YBa2Cu3O(x) onto fibers
[DE90-013380] N91-10758

**GOOD SAMARITAN HOSPITAL AND MEDICAL CENTER, PORTLAND, OR.**

Role of orientation reference selection in motion sickness
[NASA-CR-186612] N91-10591

**GOVERNMENT PRINTING OFFICE, WASHINGTON, DC.**

US Congressional serial set catalog: Numerical lists and schedule of volumes; 99th Congress: 1985-1986: Entries and indexes
[PB90-171737] N91-10797

## H

**HAMILTON STANDARD, WINDSOR LOCKS, CT.**

Measurement of unsteady blade surface pressure on a single rotation large scale advanced prop-fan with angular and wake inflow at Mach numbers from 0.02 to 0.70
[NASA-CR-182123] N91-10065

**HAMPTON INST., VA.**

Plasma puff initiation of high Coulomb transfer switches
[NASA-CR-187024] N91-10735

**HELSINKI UNIV. OF TECHNOLOGY, ESPOO (FINLAND).**

Variable-coherence beam optics
[ISBN-952-90-1784-7] N91-10724

**HELSINKI UNIV. TECHNOLOGY, OTANIEMI (FINLAND).**

Three-dimensional viscous/inviscid coupling in subsonic flow
[REPT-B-24] N91-10023

Calculation of three-dimensional viscous/inviscid interaction in subsonic flow
[REPT-B-25] N91-10024

Evaluation of the ZONA51D program
[REPT-B-28] N91-10025

Multigrid solution for the Euler equations in axisymmetric flow
[REPT-B-17] N91-10253

Computation of boundary layer flow using thin-layer Navier-Stokes equations with flux-vector splitting
[REPT-B-21] N91-10254

**HOUSTON UNIV., CLEAR LAKE, TX.**

The integrated scheduling system: A case study in project management
[NASA-CR-187261] N91-10793

Applied technology center business plan and market survey
[NASA-CR-187259] N91-10794

Space market model space industry input-output model
[NASA-CR-187252] N91-10795

**HOUSTON UNIV., TX.**

The effects of outcome and process feedback
[NASA-CR-187332] N91-10595

**HOWARD UNIV., WASHINGTON, DC.**

Evaluation, development, and characterization of superconducting materials for space applications
[NASA-CR-187017] N91-10763

## I

**IIT RESEARCH INST., BARTLESVILLE, OK.**

Determination of ideal-gas enthalpies of formation for key compounds: The 1988 project results
[DE90-000247] N91-10791

**ILLINOIS INST. OF TECH., CHICAGO.**

Corrosion-resistant coatings for high-temperature high-sulfur activity applications
[DE90-016638] N91-10177

**ILLINOIS UNIV., CHICAGO.**

The instability of combustion in propulsion engines
N91-10141

**ILLINOIS UNIV., URBANA.**

Analysis of delamination in fiber composite laminates out-of-plane under bending
[NASA-CR-186023] N91-10122

**ILLINOIS UNIV. AT URBANA-CHAMPAIGN, SAVOY.**

Compressive failure of thick-section composite laminates with and without cutouts subjected to biaxial loading N91-10304

**IMPERIAL COLL. OF SCIENCE AND TECHNOLOGY, LONDON (ENGLAND).**

Multispacecraft measurement at varying scalelengths: The Cluster/Regatta opportunity N91-10418

Review of the Cluster orbit and separation strategy: Consequence for measurements N91-10420

Configurational sensitivity of multipoint magnetic field measurements N91-10421

**INSTITUT FRANCO-ALLEMAND DE RECHERCHES, SAINT-LOUIS (FRANCE).**

Modeling blade/vortex interactions
[ISL-R-107/89] N91-10016

Measurement of air entrainment by a free jet using laser velocimetry and Raman scattering
[ISL-R-109/89] N91-10017

Rotor loads computation using singularity methods and application to the noise prediction
[ISL-PU-301/90] N91-10018

Fast steering of the angle of attack: A contribution to the guidance of high velocity projectiles
[ISL-CO-220/89] N91-10050

The ISL hypersonic shock tunnel and its instrumentation
[ISL-CO-213/89] N91-10086

Combustion diagnostics of propellants with sandwich structure
[ISL-CO-212/89] N91-10189

Numerical simulation of electromagnetic acceleration by induction. Part 1: Thin loops
[ISL-R-102/89-PT-1] N91-10205

Turbulent boundary layers in high enthalpy flows. Numerical code validation by shock tube experiments
[ISL-CO-221/89] N91-10246

Velocity measurements in piston-induced turbulent boundary layers in a shock tube
[ISL-CO-235/89] N91-10247

Investigation of pulsed laser target interaction processes by high-speed diagnostic techniques
[ISL-CO-234/89] N91-10283

**INSTITUT NATIONAL DES SCIENCES APPLIQUEES DE LYON, VILLEURBANNE (FRANCE).**

Study of the mechanisms of damage and failure of fiber and ceramic matrix composites
[ISAL-90-0026] N91-10135

**INSTITUT NATIONAL POLYTECHNIQUE, GRENOBLE (FRANCE).**

Planning of the paths for manipulation robots
[ETN-90-97826] N91-10291

Parallel inference and communication process for Horn clause. First order extension by connection method
[ETN-90-97825] N91-10652

**INSTITUTE FOR COMPUTER APPLICATIONS IN SCIENCE AND ENGINEERING, HAMPTON, VA.**

Boundary-layer receptivity due to a wall suction and control of Tollmien-Schlichting waves
[NASA-CR-182103] N91-10009

Turbulent flow calculations using unstructured and adaptive meshes
[NASA-CR-182102] N91-10010

The inviscid secondary instability of fully nonlinear longitudinal vortex structures in growing boundary layers
[NASA-CR-187455] N91-10021

Vortex instabilities in 3D boundary layers: The relationship between Goertler and crossflow vortices
[NASA-CR-187456] N91-10022

Bounded energy states in homogeneous turbulent shear flow: An alternative view
[NASA-CR-187439] N91-10237

The 'optimum' upwind advection on a triangular mesh
[NASA-CR-187459] N91-10250

Quadrature imposition of compatibility conditions in Chebyshev methods
[NASA-CR-187458] N91-10251

A manual for PARTI runtime primitives
[NASA-CR-187442] N91-10599

Multiprocessors and runtime compilation
[NASA-CR-182100] N91-10600

Conservative parallel simulation of priority class queueing networks
[NASA-CR-187438] N91-10628

A conservative approach to parallelizing the Sharks World simulation
[NASA-CR-187440] N91-10629

Spectral methods for time dependent problems
[NASA-CR-187443] N91-10664

**INSTITUTO DE FISICA TEORICA, SAO PAULO (BRAZIL).**

On the structure of quantum phase space
[DE90-627185] N91-10786

**INTERNATIONAL BUSINESS MACHINES CORP., HOUSTON, TX.**

Knowledge-based assistance in costing the space station DMS N91-10611

**INTERNATIONAL CENTRE FOR THEORETICAL PHYSICS, TRIESTE (ITALY).**

The cousin problems in the viewpoint of partial differential equations
[DE90-627172] N91-10656

Operator formalism of multi-pole Virasoro algebra on Riemann sphere
[DE90-627217] N91-10657

Continuum states of the Klein-Gordon equations for vector and scalar interactions
[DE90-627178] N91-10693

Temporal behaviour of self generated magnetic field and its influence on inhibition of thermal flux in ICF plasma
[DE90-627476] N91-10731

**IOWA STATE UNIV. OF SCIENCE AND TECHNOLOGY, AMES.**

Numerical computation of viscous flow about unconventional airfoil shapes
[NASA-CR-187343] N91-10019

Simulation of time-dependent compressible viscous flows using central and upwind-biased finite difference techniques N91-10234

Study of mixed mode stress intensity factor using the experimental method of transmitted caustics
N91-10324

Tests and applications of Cherenkov imaging in TeV astronomy N91-10807

**IOWA UNIV., IOWA CITY.**

Global optimization methods for engineering design
N91-10310

Radio wave remote sensing by Cluster and Regatta
N91-10439

## J

**JET PROPULSION LAB., CALIFORNIA INST. OF TECH., PASADENA.**

A Mobile Satellite Experiment (MSAT-X) network definition
[NASA-CR-187336] N91-10105

Spacecraft Health Automated Reasoning Prototype (SHARP): The fiscal year 1989 SHARP portability evaluations task for NASA Solar System Exploration Division's Voyager project
[NASA-CR-187338] N91-10204

Design and application of gas-gap heat switches
[NASA-CR-187339] N91-10222

Probabilistic failure assessment with application to solid rocket motors N91-10309

Analysis of elastically tailored viscoelastic damping member N91-10319

A communication channel model of the software process N91-10610

Ada software productivity prototypes: A case study
N91-10613

Solar emission levels at low radio frequencies
[NASA-CR-187337] N91-10829

**JOHNS HOPKINS UNIV., BALTIMORE, MD.**

Corrosion, passivity, and breakdown of alloys used in high energy density batteries
[DE90-016648] N91-10223

**JOINT OCEANOGRAPHIC INST., INC., WASHINGTON, DC.**

The scientific case for magnetic field satellites
[NASA-CR-186532] N91-10101

**JOINT PUBLICATIONS RESEARCH SERVICE, ARLINGTON, VA.**

JPRS report: Science and technology. USSR: Space
[JPRS-USP-89-009] N91-10088

JPRS report: Science and technology. USSR: Space
[JPRS-USP-90-001] N91-10089

JPRS report: Science and technology. USSR: Space
[JPRS-USP-90-002] N91-10090

JPRS report: Science and technology. USSR: Electronics and electrical engineering
[JPRS-UEE-90-004] N91-10213

JPRS report: Science and technology. USSR: Electronics and electrical engineering
[JPRS-UEE-90-006] N91-10214

JPRS report: Science and technology. USSR: Electronics and electrical engineering
[JPRS-UEE-90-007] N91-10215

JPRS report: Science and technology. USSR: Electronics and electrical engineering
[JPRS-UEE-90-008] N91-10216

JPRS report: Science and technology. USSR: Electronics and electrical engineering
[JPRS-UEE-90-009] N91-10217

JPRS report: Science and technology. USSR: Earth sciences
[JPRS-UES-90-006-L] N91-10376

JPRS report: Science and technology. USSR: Earth sciences
[JPRS-UES-90-007] N91-10377

JPRS report: Science and technology. USSR: Life sciences
[JPRS-ULS-90-001] N91-10551

JPRS report: Science and technology. USSR: Life sciences
[JPRS-ULS-90-013] N91-10552

Morphological examination of rat adrenal glands following flight aboard Biosputnik Kosmos-1667
N91-10553

Central and regional hemodynamics in prolonged space flights N91-10554

Protective functions of skin N91-10555

JPRS report: Science and technology. USSR: Life sciences
[JPRS-ULS-90-012] N91-10556

Diagnostic possibilities of inflight EKG monitoring of flight crew N91-10557

Effects of rolling motion on the circadian rhythm of sinoatrial node N91-10558

Probabilty of decompression sickness during space suit testing N91-10559

Changes in maximum allowable supersaturation coefficient in high-altitude decompression N91-10560

Effects of prolonged exposure to acetic acid vapors on acid-base balance in humans N91-10561

Effects of taurine on cytogenetic corneal disturbances induced in mice by 9 GeV protons N91-10562

Combined effects of elevated concentrations of carbon dioxide and ambient temperature on thermal state of humans in closed chambers N91-10563

Psychophysiological assessment of piloting motor habits in pilot retraining N91-10564

JPRS report: Science and technology. USSR: Life sciences
[JPRS-ULS-90-011] N91-10565

Requirements for an ideal drug for preventing space motion sickness N91-10566

Effect of single impacts of heavy ions of galactic cosmic rays on lactuca sativa seeds exposed on Salyut-6 and Salyut-7 stations N91-10567

JPRS Report: Science and technology. USSR: Life sciences
[JPRS-ULS-90-010] N91-10568

JPRS Report: Science and technology. USSR: Life sciences
[JPRS-ULS-90-009] N91-10569

JPRS Report: Science and technology. USSR: Life sciences
[JPRS-ULS-90-008] N91-10570

JPRS Report: Science and technology. USSR: Life sciences
[JPRS-ULS-90-006] N91-10571

JPRS report: Science and technology. USSR: Life sciences
[JPRS-ULS-90-005] N91-10572

JPRS report: Science and technology. USSR: Life sciences
[JPRS-ULS-89-008] N91-10589

JPRS report: Science and technology. USSR: Life sciences
[JPRS-ULS-89-010] N91-10590

JPRS report: Science and technology. USSR: Physics and mathematics
[JPRS-UPM-90-003] N91-10694

## K

**KAISERSLAUTERN UNIV. (GERMANY, F.R.).**

Computational methods for the Boltzmann equation
[BR-43] N91-10256

On the convergence at infinity, rate of convergence and uniqueness of solutions with finite Dirichlet integral to the exterior Dirichlet problem for the steady plane Navier-Stokes system of equations
[PREPRINT-166] N91-10257

**KARLSRUHE UNIV. (GERMANY, F.R.).**

Distortion of LDA fringe pattern by tracer perticles
[SFB-210/E/59] N91-10286

## L

**LABORATORIO DE COMPUTACAO CIENTIFICA, RIO DE JANEIRO (BRAZIL).**

Finite element analysis of nonlinear creeping flows
[DE90-627189] N91-10327

**LAWRENCE LIVERMORE NATIONAL LAB., CA.**

Application of Fabry-Perot velocimetry to hypervelocity impact experiments
[DE90-015612] N91-10096

The transport properties of activated carbon fibers
[DE90-015910] N91-10130

Equal eigenvalues in multicomponent diffusion: The extraction of diffusion coefficients from experimental data in ternary systems
[DE90-012074] N91-10142

High strain rate deformation behavior of shocked copper
[DE90-016481] N91-10161

Very high burn rate propellants
[DE90-016865] N91-10186

An x band backward-wave oscillator experiment
[DE90-015119] N91-10219

A new method for doing flat-field intensity calibrations of multiplexed ITT streak cameras
[DE90-016475] N91-10267

The 1987 Strategic Defense Initiative Organization (SDIO) Workshop on Laser Propulsion
[DE90-013484] N91-10274

Damage assessment and possible damage mechanisms to 1-meter diameter Nova turning mirrors
[DE90-016473] N91-10278

KrF laser path to high gain ICF (inertial confinement fusion) laboratory microfusion facility
[DE90-016439] N91-10282

Design of a triaxial residual stress measurement system using high-energy x ray diffraction
[DE90-016212] N91-10331

Global tropospheric chemistry modeling
[DE90-015908] N91-10409

CVMAC 2D Program: A method of converting 3D to 2D
[DE90-015147] N91-10626

Workshop on Massively Parallel Computing in Magnetic Fusion Energy
[DE90-018009] N91-10650

Domain decomposition: An instrument of asymptotic-numerical methods
[DE90-016478] N91-10661

Theoretical studies of High Energy Density Matter (HEDM) molecules
[DE90-014831] N91-10706

Deposition controlled uniformity of multilayer mirrors
[DE90-015906] N91-10718

Diamond turning of optical crystals
[DE90-015909] N91-10719

Design, performance, and calibration of the ALEXIS ultrasoft x-ray telescopes
[DE90-016483] N91-10720

A distributed control and monitor system used in laser fusion research
[DE90-013478] N91-10732

Electromagnetic particle codes on unstructured grids
[DE90-015187] N91-10733

Technical Abstracts: Mechanical engineering
[DE90-014797] N91-10802

Coronal heating by nanoflares: Plasma dynamics of elementary events
[DE90-016495] N91-10830

**LEIDEN UNIV. (NETHERLANDS).**

Discounted dynamic programming. Part 3: Successive approximation
[TW-89-14-PT-3] N91-10640

Discounted dynamic programming. Part 4: Accelerated successive approximation
[TW-90-03-PT-4] N91-10641

Discounted dynamic programming. Part 5: Modified policy iteration
[TW-90-04-PT-5] N91-10642

Geometric ergodicity of the ALOHA-system and a coupled processors model
[TW-90-01-B] N91-10680

The technique of Cerenkov ring image detection
[ETN-90-97747] N91-10714

**LOS ALAMOS NATIONAL LAB., NM.**

Optimum hypersonic airfoil with power law shock waves
[DE90-014903] N91-10008

Railgun restrike control
[DE90-015108] N91-10095

Beryllium weldability
[DE90-014696] N91-10155

Constant stress of XD (trademark) TiAl containing nitrogen
[DE90-011947] N91-10158

Mechanical and microstructural response of Ni3Al at high strain rate and elevated temperatures
[DE90-016489] N91-10162

Texture-induced anisotropy and high-strain rate deformation in metals
[DE90-016611] N91-10163

The influence of shock pre-strain and peak pressure on spall behavior of 4340 steel
[DE90-016612] N91-10164

Shock experiments in metals and ceramics
[DE90-016613] N91-10165

High-strain-rate compression and fracture of B4C-aluminum cermets
[DE90-016568] N91-10176

Transition state theory applying to the study of reaction processes in detonation
[DE90-016558] N91-10187

AFDM: An Advanced Fluid-Dynamics Model. Volume 1: Scope, approach, and summary
[DE90-016723] N91-10239

AFDM: An Advanced Fluid-Dynamics Model. Volume 4: The AFDM heat- and mass-transfer solution algorithm
[DE90-017535] N91-10240

AFDM: An Advanced Fluid-Dynamics Model
[DE90-017536] N91-10241

AFDM: An Advanced Fluid-Dynamics Model
[DE90-017537] N91-10242

AFDM: An Advanced Fluid-Dynamics Model
[DE90-017538] N91-10243

AFDM: An Advanced Fluid-Dynamics Model
[DE90-017539] N91-10244

An imaging x-ray microscope using a laser plasma source and a Schwarzchild objective
[DE90-016432] N91-10266

Recent advances in excimer laser technology at Los Alamos
[DE90-016441] N91-10276

Biomedical applications on laser technology at Los Alamos
[DE90-016447] N91-10277

Cumulative beam breakup of the ground-based-free-electron laser
[DE90-016485] N91-10279

INEX modeling of the Boeing ring optical resonator free-electron laser
[DE90-016488] N91-10280

The physical and chemical state of Westinghouse Phosphoric Acid Fuel Cell assemblies after long term operation: Surface and near-surface analysis
[DE90-015055] N91-10382

Stability of some stationary solutions for the forced KdV equation
[DE90-016506] N91-10662

Lobe area in adiabatic Hamiltonian systems
[DE90-016566] N91-10663

Prediction and control of chaotic processes using nonlinear adaptive networks
[DE90-016505] N91-10697

Polarization modulated solitary waves in an optical fiber
[DE90-015034] N91-10715

High-order optics of multipole magnets
[DE90-016438] N91-10717

Order and chaos in polarized nonlinear optics
[DE90-016717] N91-10721

Confinement studies in the ZT-40M reversed field pinch
[DE90-016442] N91-10739

Tilt stability and compression heating studies of field-reversed configurations
[DE90-016443] N91-10740

Nonlinear optical absorption in intrinsic Stark effect superlattices
[DE90-016466] N91-10767

Copper NMR and hole depletion in the normal state of Y(1-x)Pr(x)Ba2Cu3O7
[DE90-016468] N91-10768

Superconducting borides
[DE90-016484] N91-10769

Calculation of the static magnetism of metamagnetic La2CuO4
[DE90-016490] N91-10770

Electronic, structural and transport properties of (almost) rare-earth-like actinide hydrides
[DE90-016491] N91-10771

Computation of superconductor critical current densities and magnetization curves
[DE90-016567] N91-10773

Fe site occupancy and superconductivity in Y(1-z)Ca(z)Ba(z) (Cu(1-x)Fe(x))3O(6+y)
[DE90-016614] N91-10774

XAFS analysis in the anharmonic limit: Application to HI-Tc superconductors and ferrosilicates
[DE90-016720] N91-10776

Radiation-induced noise in Charge-Coupled Device (CCD) and Charge-Injection Device (CID) imagers
[DE90-016724] N91-10777

An interpersonal multimedia visualization system
[DE90-014974] N91-10803

A semi-analytical model of stellar flares
[DE90-016434] N91-10817

Nuclear structure calculations for astrophysical applications
[DE90-016433] N91-10818

Intrinsic neutrino properties: As deduced from cosmology, astrophysics, accelerator, and non-accelerator experiments
[DE90-016467] N91-10836

**LOUISIANA STATE UNIV., BATON ROUGE.**

Convergence of Langevin simulation for complex Gaussian integrals
[DE90-017402] N91-10665

Research in elementary particle physics
[DE90-017278] N91-10708

**LUND UNIV. (SWEDEN).**

Pre-equilibrium emission and multifragmentation in heavy ion collisions
[LUIP-8902] N91-10705

## M

**MANCHESTER UNIV. (ENGLAND).**

Core-dominated radio sources and the unified scheme
N91-10835

**MARTIN MARIETTA AEROSPACE, DENVER, CO.**

Software sizing, cost estimation and scheduling
N91-10612

Experiences with Ada in an embedded system
N91-10614

**MARYLAND UNIV., COLLEGE PARK.**

Transient characteristics of unconfined fire plume-driven ceiling jets
[PB90-227976] N91-10193

Towards a comprehensive framework for reuse: A reuse-enabling software evolution environment
[UMIACS-TR-88-92] N91-10608

Prediction and control of chaotic processes using nonlinear adaptive networks
[DE90-016505] N91-10697

The Joint NASA/Goddard-University of Maryland Research Program in Charged Particle and High Energy Photon Detector Technology
[NASA-CR-180335] N91-10810

**MASSACHUSETTS INST. OF TECH., CAMBRIDGE.**

Structural acoustics: An applied science with many applications
[PB90-183633] N91-10698

**MAX-PLANCK-INST. FUER PHYSIK UND ASTROPHYSIK, GARCHING (GERMANY, F.R.).**

Examination of ion acceleration in the plasma layer during magnetospheric partial gales
[MPE-218] N91-10753

Bicolored photometry and spectral accommodation in X-ray region of mass impregnated stellar X-ray binaries
[MPE-219] N91-10808

**MCDONNELL AIRCRAFT CO., SAINT LOUIS, MO.**

Structural risk assessment and aircraft fleet maintenance N91-10321

**MCGILL UNIV., MONTREAL (QUEBEC).**

Diurnal variation of marine stratocumulus over San Nicolas Island during the FIRE IFO N91-10491

**MESSERSCHMITT-BOELKOW-BLOHM/ENTWICKLUNG SPRING NORD, BREMEN (GERMANY, F.R.).**

Columbus logistics support. A conceptional definition of the operational phase
[MBB-UO-0093-90-PUB] N91-10091

Columbus elements processing needs at KSC
[MBB-UO-0092-90-PUB] N91-10108

**MESSERSCHMITT-BOELKOW-BLOHM G.M.B.H., MUNICH (GERMANY, F.R.).**

MBB'S BO 108 design and development
[MBB-UD-0568-90-PUB] N91-10055

Optimization criteria for the design of orbital replacement units
[MBB-UO-0092-90-PUB] N91-10109

Holographic examination of great surface fiberbound components in industrial conditions: Resumes of final reports, April 1986 to June 1989
[MBB-Z-0306-90-PUB-KURZFASSUNG] N91-10136

**METEOROLOGICAL OFFICE, LONDON (ENGLAND).**

Preliminary mixed-layer model results for FIRE marine stratocumulus IFO conditions N91-10495

An overview of UK C130 observations from the FIRE marine stratocumulus IFO N91-10520

A preliminary analysis of LANDSAT and UK C130 data from Mission 197-A, on 16 July 1987 N91-10535

**METEOROLOGICAL SATELLITE CENTER, TOKYO (JAPAN).**

Meteorological Satellite Center Technical Note. Special Issue (1989). Summary of GMS System. 1: Telecommunication System N91-10338
- Outline of the GMS telecommunication system N91-10339
- Outline of CDAS telecommunication system N91-10340
- Station control and monitor subsystem N91-10341
- VISSR demodulate and processing subsystem N91-10342
- Stretched VISSR subsystem N91-10343
- Image monitor N91-10344
- Telemetry subsystem N91-10345
- Command subsystem N91-10346
- Trilateration ranging subsystem N91-10347
- Antenna/transmitter control unit N91-10348
- Frequency standard unit N91-10349
- Operation console N91-10350
- System console N91-10351
- DCP subsystem N91-10352
- WEFAX subsystem N91-10353
- DPC telecommunication system N91-10354
- Microwave link N91-10355

Meteorological Satellite Center Technical Note. Special Issue (1989). Summary of GMS System. 2: Data Processing N91-10356
- Computer system N91-10357
- General flow of image data processing N91-10358
- Image mapping N91-10359
- Calibration N91-10360
- FAX image processing N91-10361
- Satellite-derived index of precipitation intensity N91-10362
- ISCCP data processing N91-10363
- Pre-processing of image data N91-10364
- Cloud motion wind N91-10365
- Typhoon information N91-10366
- VTR loop movie N91-10367
- VISSR histogram data N91-10368
- Brightness temperature distribution N91-10369
- GPCP data processing N91-10370

Cloud grid data N91-10371
Sea surface temperature N91-10372
Cloud amount distribution N91-10373
Satellite cloud information chart N91-10374
DCP data processing N91-10375

**METHODIST HOSPITAL, INDIANAPOLIS, IN.**
US space flight experience. Physical exertion and metabolic demand of extravehicular activity: Past, present, and future N91-10575
The history of in-flight exercise in the US manned space program N91-10577

**MICHIGAN UNIV., ANN ARBOR.**
Electromagnetic scattering from two-dimensional thick material junctions
[NASA-CR-186976] N91-10201
Three-dimensional full-wave analysis of signal communications in active integrated circuits using a variable-mesh TLM method N91-10212
Mass transfer in oscillating flows: Efficient drying via pulse combustors
[PB90-242389] N91-10235
Combined design of structures and controllers for optimal maneuverability N91-10314
Users manual for AUTOMESH-2D: A program of automatic mesh generation for two-dimensional scattering analysis by the finite element method
[NASA-CR-186929] N91-10623
Investigation of Markarian galaxies with multiple nuclei N91-10813

**MIDWEST RESEARCH INST., GOLDEN, CO.**
Materials analysis and device optimization of CuInSe2 solar cells
[DE90-000365] N91-10384
Ion-assisted doping of 2-6 compounds during physical vapor deposition
[DE90-000358] N91-10756

**MINNESOTA UNIV., SAINT PAUL.**
Developing a framework for qualitative engineering: Research in design and analysis of complex structural systems N91-10322

## N

**NATIONAL ACADEMY OF SCIENCES - NATIONAL RESEARCH COUNCIL, WASHINGTON, DC.**
Activities of the Board on Mathematical Sciences
[DE90-015118] N91-10598

**NATIONAL AERONAUTICAL LAB., BANGALORE (INDIA).**
Wall interference studies
[PD-CF-9012] N91-10232
Script: General purpose graphics program; user's manual
[PD-ST-9027] N91-10625

**NATIONAL AERONAUTICS AND SPACE ADMINISTRATION, WASHINGTON, DC.**
Aeronautical engineering: A continuing bibliography with indexes (supplement 256)
[NASA-SP-7037(256)] N91-10002
National Space Transportation System Reference. Volume 2: Operations
[NASA-TM-89785] N91-10100
Atmospheric ozone 1985: Assessment of our understanding of the processes controlling its present distribution and change, volume 3
[NASA-TM-103462] N91-10393
Aerospace medicine and biology: A continuing bibliography with indexes (supplement 341)
[NASA-SP-7011(341)] N91-10594
NASA Thesaurus supplement: A four part cumulative supplement to the 1988 edition of the NASA Thesaurus (supplement 4)
[NASA-SP-7064-SUPPL-4] N91-10804

**NATIONAL AERONAUTICS AND SPACE ADMINISTRATION. AMES RESEARCH CENTER, MOFFETT FIELD, CA.**
Transonic flow analysis for rotors. Part 3: Three-dimensional, quasi-steady, Euler calculation
[NASA-TP-2375] N91-10007
Wake coupling to full potential rotor analysis code
[NASA-TM-102805] N91-10013
Euler and potential experiment/CFD correlations for a transport and two delta-wing configurations
[NASA-TM-102208] N91-10014
Application of CFD to sonic boom near and mid flow-field prediction
[NASA-TM-102867] N91-10015
Rotor systems research aircraft risk-reduction shake test
[NASA-TM-4186] N91-10045
Industry liaison section implementation plan
[NASA-CR-177569] N91-10048
Body weight of hypersonic aircraft, part 1
[NASA-TM-101028] N91-10049
A one-equation turbulence transport model for high Reynolds number wall-bounded flows
[NASA-TM-102847] N91-10252
A laser-sheet flow visualization technique for the large wind tunnels of the National Full-Scale Aerodynamics Complex
[NASA-TM-102793] N91-10268
Cirrus microphysics and radiative transfer: A case study N91-10463
Cirrus cloud statistics: Temperatures and optical depths N91-10466
The radiation budget of a Cirrus layer deduced from simultaneous aircraft observations and model calculations N91-10467
Preliminary results of radiation measurements from the marine stratus FIRE experiment N91-10529

**NATIONAL AERONAUTICS AND SPACE ADMINISTRATION. GODDARD INST. FOR SPACE STUDIES, NEW YORK, NY.**
ISCCP results for the FIRE IFO regions and times N91-10451

**NATIONAL AERONAUTICS AND SPACE ADMINISTRATION. GODDARD SPACE FLIGHT CENTER, GREENBELT, MD.**
The 1990 Reference Handbook: Earth Observing System
[NASA-TM-102910] N91-10378
Synoptic conditions producing cirrus during the FIRE cirrus IFO N91-10449
Cirrus cloud model parameterizations: Incorporating realistic ice particle generation N91-10453
Climate data system supports FIRE N91-10455
Lidar and radiometer results from the ER-2 for the FIRE field experiments N91-10468
Overview of the 27-28 October FIRE Cirrus IFO case: Meteorology and cloud fields N91-10477
Cloud atlas for the FIRE Cirrus Intensive Field Observation (IFO) N91-10487
Cloud spatial structure during the FIRE MS IFO N91-10500
Cloud absorption properties as derived from airborne measurements of scattered radiation within clouds N91-10512
Cloud optical parameters as derived from the multispectral cloud radiometer N91-10513
Thermodynamic structure of the stratocumulus-capped boundary layer on 5 July 1987 N91-10516
ER-2 lidar measurements of stratocumulus cloud top structure on July 14, 1987 N91-10523
Comparison and calibration of NCAR electra instruments: July 5 and 7, 1987 N91-10532
Thermodynamic structure of the stratocumulus-capped boundary layer on 7 July, 1987 N91-10533
Neutral winds derived from IRI parameters and from the HWM87 wind model for the sundial campaign of September, 1986
[NASA-TM-103445] N91-10543
Proceedings of the Thirteenth Annual Software Engineering Workshop
[NASA-TM-103314] N91-10606
Evolving impact of Ada on a production software environment N91-10607
The Software Management Environment (SME) N91-10609
Acceleration by pulsar winds in binary systems
[NASA-TM-103451] N91-10816

**NATIONAL AERONAUTICS AND SPACE ADMINISTRATION. HUGH L. DRYDEN FLIGHT RESEARCH FACILITY, EDWARDS, CA.**
Flight characteristics of a modified Schweizer SGS1-36 sailplane at low and very high angles of attack
[NASA-TP-3022] N91-10079
Design of control laws for flutter suppression based on the aerodynamic energy concept and comparisons with other design methods
[NASA-TP-3056] N91-10328

**NATIONAL AERONAUTICS AND SPACE ADMINISTRATION. JOHN F. KENNEDY SPACE CENTER, COCOA BEACH, FL.**
Evaluation of composite materials for use on launch complexes
[NASA-TM-103809] N91-10131
Evaluation of candidate alloys for the construction of metal flex hoses in the STS launch environment
[NASA-TM-103808] N91-10157
Physical and chemical test results of electrostatic safe flooring materials
[NASA-TM-103501] N91-10194

**NATIONAL AERONAUTICS AND SPACE ADMINISTRATION. LYNDON B. JOHNSON SPACE CENTER, HOUSTON, TX.**
Workshop on Exercise Prescription for Long-Duration Space Flight
[NASA-CP-3051] N91-10574
Space station N91-10576
Work, exercise, and space flight. 1: Operations, environment, and effects of spaceflight N91-10578
Work, exercise, and space flight. 3: Exercise devices and protocols N91-10579
Space medicine considerations: Skeletal and calcium homeostasis N91-10580
Work, exercise, and space flight. 2: Modification of adaptation by exercise (exercise prescription) N91-10586
Summary and recommendations for initial exercise prescription N91-10588

**NATIONAL AERONAUTICS AND SPACE ADMINISTRATION. LANGLEY RESEARCH CENTER, HAMPTON, VA.**
Aeroelastic analysis of wings using the Euler equations with a deforming mesh
[NASA-TM-102733] N91-10020
NASA transport systems research vehicle B-737 data link system and display formats
[NASA-TM-102717] N91-10058
Determination of the pressure drag of airfoils by integration of surface pressures
[NASA-TM-102722] N91-10078
Filament wound metal lined propellant tanks for future Earth-to-orbit transports
[NASA-TM-100594] N91-10106
A macro-micromechanics analysis of a notched metal matrix composite
[NASA-TM-102728] N91-10128
Evaluation of two bisimide additives in LARC-TPI adhesive
[NASA-TM-102742] N91-10182
An analysis of the effects of secondary reflections on dual-frequency reflectometers
[NASA-TM-102709] N91-10221
Measured and predicted shock shapes for AFE configuration at Mach 6 in air and in CF4
[NASA-TM-100660] N91-10245
Research in Structures, Structural Dynamics and Materials, 1990
[NASA-CP-3064] N91-10301
Direct use of linear time-domain aerodynamics in aeroservoelastic analysis: Aerodynamic model N91-10316
Computation of maximum gust loads in nonlinear aircraft using a new method based on the matched filter approach and numerical optimization N91-10317
Static and dynamic aeroelastic characterization of an aerodynamically heated generic hypersonic aircraft configuration N91-10320
FIRE Science Results 1988
[NASA-CP-3083] N91-10448
A synopsis of Langley Research Center's lidar effort for the 1986 FIRE IFO N91-10457
ERBE and AVHRR Cirrus cloud fire study N91-10472
Cloud parameters from GOES visible and infrared radiances during the FIRE Cirrus IFO, October 1986 N91-10473
AVHRR and VISSR satellite instrument calibration results for both Cirrus and marine stratocumulus IFO periods N91-10475
Cirrus cloud properties derived from coincident GOES and lidar data during the 1986 FIRE Cirrus Intensive Field Observations (IFO) N91-10476
A four-lidar view of Cirrus from the FIRE IFO: 27-28 October 1986 N91-10478
FIRE Cirrus on October 28, 1986: LANDSAT; ER-2; King Air; theory N91-10480
Surface radiation observations for October 27-28, 1986 during the Wisconsin FIRE/SRB experiment N91-10481
The new FIRE cloud lidar at Langley Research Center N91-10482
Extended time observations of California marine stratocumulus clouds from GOES for July 1983-1987 N91-10488
Cloud parameters derived from GOES during the 1987 marine stratocumulus FIRE Intensive Field Observation (IFO) period N91-10505
Horizontal variability of the marine boundary layer structure upwind of San Nicolas Island during FIRE, 1987 N91-10519
Aircraft/island/ship/satellite intercomparison: Preliminary results from July 16, 1987 N91-10534
Helicopter far-field acoustic levels as a function of reduced main-rotor advancing blade-tip Mach number
[NASA-TM-102684] N91-10699
The development of interior noise and vibration criteria
[NASA-TM-102736] N91-10702

**NATIONAL AERONAUTICS AND SPACE ADMINISTRATION. LEWIS RESEARCH CENTER, CLEVELAND, OH.**
Analysis of 5 KHz combustion instabilities in 40K methane/LOX combustion chambers
[NASA-TM-101368] N91-10117

Performance characterization of a segmented anode arcjet thruster
[NASA-TM-103227] N91-10118
Developments in REDES: The rocket engine design expert system
[NASA-TM-103657] N91-10119
Structural properties of laminated Douglas fir/epoxy composite material
[NASA-RP-1236] N91-10127
Intercalated graphite fiber composites as EMI shields in aerospace structures
[NASA-TM-103632] N91-10134
High temperature cyclic oxidation data. Part 1: Turbine alloys
[NASA-TM-83665] N91-10149
High-temperature cyclic oxidation data. Part 2: Turbine alloys
[NASA-TM-101468] N91-10150
Effect of surface deposits on electromagnetic waves propagating in uniform ducts
[NASA-TM-103282] N91-10208
A three-dimensional turbulent heat transfer analysis for advanced tubular rocket thrust chambers
[NASA-TM-103293] N91-10249
Particle displacement tracking for PIV
[NASA-TM-103288] N91-10271
Calculation of Weibull strength parameters, Batdorf flaw density constants and related statistical quantities using PC-CARES
[NASA-TM-103247] N91-10332
Aeroacoustic effects of reduced aft tip speed at constant thrust for a model counterrotation turboprop at takeoff conditions
[NASA-TM-103608] N91-10703
Determination of surface resistance and magnetic penetration depth of superconducting YBa2Cu3O(7-delta) thin films by microwave power transmission measurements
[NASA-TM-103616] N91-10780
Bibliography of Lewis Research Center technical publications announced in 1989
[NASA-TM-102542] N91-10798

**NATIONAL AERONAUTICS AND SPACE ADMINISTRATION. MARSHALL SPACE FLIGHT CENTER, HUNTSVILLE, AL.**
Long-term orbital lifetime predictions
[NASA-TP-3058] N91-10092
Space Station Freedom Environmental Control and Life Support System (ECLSS) phase 3 simplified integrated test trace contaminant control subsystem performance
[NASA-TM-4202] N91-10103
Analysis techniques for residual acceleration data
[NASA-TM-103507] N91-10191
Eddy current inspection of graphite fiber components
[NASA-TM-103514] N91-10294
Properties of large scale plasma flow during the early stage of the plasmaspheric refilling
[NASA-TM-103446] N91-10441
Coaligned observations of solar magnetic fields at different heights: MSFC Center director's discretionary fund final report (Project No. 88-10)
[NASA-TM-103516] N91-10832

**NATIONAL AEROSPACE LAB., AMSTERDAM (NETHERLANDS).**
Mechanical properties and fracture toughness of 8090-T651 plate and 2091 and 8090 sheet
[NRL-MP-88049-4] N91-10151

**NATIONAL AEROSPACE LAB., TOKYO (JAPAN).**
Characteristics of piping interference elimination unit used in the high-speed wind tunnel test of ASUKA seven percent semi-born prototype
[NAL-TM-588] N91-10003
Numerical simulation of hypersonic flow around a space plane. Part 3: Analysis of aerothermodynamic heating
[NAL-TR-1027T] N91-10011
Comparison between the null-collision and time counter direct-simulation Monte Carlo methods: Leading-edge flow
[NAL-TR-1016T] N91-10012
The establishment and performance test of PAPI (Precision Approach Path Indicator) System for NAL STOL aircraft
[NAL-TM-579] N91-10030
Application of flight path reconstruction algorithms for flight data of helicopter
[NAL-TM-582] N91-10031
The actuator for the low-noise STOL test plane flight control system and its development test
[NAL-TM-574] N91-10038
A consideration on flight paths for microwave-powered airplanes
[NAL-TR-1051] N91-10053
Practical flight paths for microwave-powered airplanes
[NAL-TR-1052T] N91-10054
Wind tunnel test of redundant vane-type flow-direction sensing systems
[NAL-TM-590] N91-10057
Effects of coolant injection on turbine aerodynamic characteristics. Part 1: Test turbine and apparatus
[NAL-TM-585-PT-1] N91-10059
Experimental investigation on the effect of coolant injection on turbine aerodynamic characteristics. Part 2: Effects of injection from rotor casing with 30 deg slanted holes
[NAL-TM-587-PT-2] N91-10060
The full-body ground vibration tests using the low-noise STOL test plane
[NAL-TM-576] N91-10077
Configuration, function and performance of the flight simulation test facility and its motion simulation system
[NAL-TM-575] N91-10080
Modification in the main air blower unit for two meter times two meter transonic wind tunnel: Plan and configuration
[NAL-TM-580] N91-10081
Function and performance of visual simulation unit of flight simulation test facility
[NAL-TM-581] N91-10082
Evaluation of flow quality in newly constructed low-turbulence calibration wind-tunnel for laser velocimeters
[NAL-TR-1054] N91-10087
Vibration testing of a 1/5 scale model of H-2 launch vehicle
[NAL-TR-1061] N91-10099
Specific impulse comparison of high density hydrocarbon fuel burned with oxygen
[NAL-TR-1053] N91-10148
Hot gas side heat transfer characteristics of LOX/H2 and LOX/HC type propellants
[NAL-TR-1062T] N91-10190
Axial compression buckling test on CFRP surface plate/aluminum honeycomb sandwiched curved surface plate
[NAL-TM-584] N91-10299
A system design and demonstrative field test of wind turbine with a 14 m diameter rotor
[NAL-TR-1056] N91-10389
Architecture simulator of parallel computer
[NAL-TM-583] N91-10601
Function library using APL for time series analysis and system identification in structures
[NAL-TM-578] N91-10604
Software package for 2-dimensional graphic display unit
[NAL-TM-589] N91-10605
Optimum orientations of the observation axes for 2-dimensional vector sensing under consideration of bias errors
[NAL-TR-1055] N91-10679
A sensitive test for accuracy in evaluation of molecular collision number in the direct-simulation Monte Carlo method
[NAL-TR-1050T] N91-10712

**NATIONAL CENTER FOR ATMOSPHERIC RESEARCH, BOULDER, CO.**
Hydrometeor development in cold clouds in FIRE
N91-10459
Vertical velocities within a Cirrus cloud from Doppler lidar and aircraft measurements during FIRE: Implications for particle growth N91-10461
A GCM parameterization for the shortwave radiative properties of water clouds N91-10494
Studying marine stratus with large eddy simulation
N91-10499
Reflectivities of uniform and broken marine stratiform clouds N91-10501
A study of marine stratocumulus using lidar and other FIRE aircraft observations N91-10511
Dependence of marine stratocumulus reflectivities on liquid water paths N91-10524
Measurements of the light-absorbing material inside cloud droplets and its effect on cloud albedo
N91-10528
Synthesis and inversion of Stokes spectral profiles
[PB90-214487] N91-10828

**NATIONAL GEOPHYSICAL DATA CENTER, BOULDER, CO.**
Solar-geophysical data number 548, April 1990. Part 1: (Prompt reports). Data for March, February 1990, and late data
[PB90-226028] N91-10411
Solar-geophysical data number 548, April 1990. Part 2: (Comprehensive reports). Data for October 1989 and miscellaneous
[PB90-226036] N91-10412
Solar-geophysical data number 545, January 1990. Part 1 (Prompt reports). Data for December, November 1989 and late data
[PB90-182338] N91-10822
Solar-geophysical data number 546, February 1990. Part 1: (Prompt reports). Data for January 1990, December 1989, and late data
[PB90-195363] N91-10823
Solar-geophysical data number 546, February 1990. Part 2: (Comprehensive reports). Data for August 1989 and miscellaneous
[PB90-195371] N91-10824
Solar-geophysical data number 547, March 1990. Part 1: (Prompt reports). Data for February, January 1990, and late data
[PB90-208877] N91-10825
Solar-geophysical data number 547, March 1990. Part 2: (Comprehensive reports). Data for September 1989 and miscellaneous
[PB90-208885] N91-10826

**NATIONAL INST. FOR FUSION SCIENCE, NAGOYA (JAPAN).**
Theory of longitudinal adiabatic invariant in the helical torus
[NIFS-37] N91-10749
RF helicity injection and current drive
[NIFS-34] N91-10750
Direct extraction of a Na(-) beam from a sodium plasma
[NIFS-35] N91-10751
Anomalous viscosity due to drift wave turbulence
[NIFS-33] N91-10752

**NATIONAL INST. OF STANDARDS AND TECHNOLOGY, GAITHERSBURG, MD.**
NIST (National Institute of Standards and Technology) standard reference materials catalog, 1990-1991
[PB90-183310] N91-10120
Measurements of coefficients of discharge for concentric flange-tapped square-edged orifice meters in natural gas over the Reynolds number range 25,000 to 16,000,000
[PB90-219601] N91-10231
NIST research reports, May 1990
[PB90-244435] N91-10800

**NATIONAL OCEANIC AND ATMOSPHERIC ADMINISTRATION, BOULDER, CO.**
Model of gravity-wave-induced variability and turbulence in the stratified free atmosphere
[PB90-235482] N91-10413
Estimated accuracy of ground-based liquid water measurements during FIRE N91-10508
Plume mechanics and stratocumulus convection
N91-10526
Geophysical monitoring for climatic change
[PB90-222126] N91-10538
Converting from VMS to ULTRIX
[PB90-220310] N91-10622

**NATIONAL OCEANIC AND ATMOSPHERIC ADMINISTRATION, ROCKVILLE, MD.**
Atmospheric ozone 1985: Assessment of our understanding of the processes controlling its present distribution and change, volume 3
[NASA-TM-103462] N91-10393

**NATIONAL OCEANIC AND ATMOSPHERIC ADMINISTRATION, WASHINGTON, DC.**
Educator's guide for building and operating environmental satellite receiving stations
[NOAA-TR-NESDIS-44] N91-10093
Geographic display of circulation model data
[NOAA-NESDIS-27] N91-10446
Earth System Monitor, Volume 1, Number 1, June 1990
[PB90-215146] N91-10799

**NATIONAL OCEANOGRAPHIC DATA CENTER, WASHINGTON, DC.**
Mariners Weather Log, Volume 33, Number 1, Winter, 1989
[PB90-179967] N91-10447
Mariners Weather Log, Volume 34, Number 2, Spring 1990
[PB90-222324] N91-10537

**NATIONAL TELECOMMUNICATIONS AND INFORMATION ADMINISTRATION, ANNAPOLIS, MD.**
Hydrologic and meteorological operations in the 162-174 and 406.1-420 MHz bands
[PB90-207820] N91-10199

**NATIONAL TELECOMMUNICATIONS AND INFORMATION ADMINISTRATION, BOULDER, CO.**
Image data compression overview: Issues and partial solutions
[PB90-172008] N91-10796

**NATIONAL WEATHER SERVICE, FORT WORTH, TX.**
Q-vectors: A new approach to an old problem
[PB90-235490] N91-10414

**NAVAL POSTGRADUATE SCHOOL, MONTEREY, CA.**
Marine stratocumulus cloud characteristics from multichannel satellite measurements N91-10502

**NAVAL RESEARCH LAB., WASHINGTON, DC.**
NRL tethered balloon measurements at San Nicolas Island during FIRE IFO 1987 N91-10509

**NAVAL SHIP RESEARCH AND DEVELOPMENT CENTER, BETHESDA, MD.**
Influence of expanding monomer on carbon fiber reinforced epoxy composites
[AD-A223277] N91-10124

**NEVADA UNIV., RENO.**
Numerical investigations in three-dimensional internal flows
[NASA-CR-186958] N91-10083

**NEW ENERGY DEVELOPMENT ORGANIZATION, TOKYO (JAPAN).**
Survey of possibility for volcanic energy development
[DE90-517230] N91-10387

**NEW YORK UNIV., NEW YORK.**
Plasma properties
[DE90-017256] N91-10746

**NSI TECHNOLOGY SERVICES CORP., CORVALLIS, OR.**
Confidence intervals and curvature measures in nonlinear regression using the IML and NLIN procedures in SAS(tm) software
[PB90-246398] N91-10624

## O

**OAK RIDGE GASEOUS DIFFUSION PLANT, TN.**
Evaluation of available perfluorobutane data for selected physical properties
[DE90-016516] N91-10145

**OAK RIDGE NATIONAL LAB., TN.**
Energy efficiency improvement potential of commercial aircraft to 2010
[DE90-014767] N91-10046
Composite heat damage. Part 1: Mechanical testing of IM6/3501-6 laminates. Part 2: Nondestructive evaluation studies of IM6/3501-6 laminates
[DE90-016207] N91-10125
On the effects of magnetic bonding in rare earth transition metal intermetallics
[DE90-015800] N91-10156
Brittle fracture and ductility improvement in nickel and iron aluminides
[DE90-017319] N91-10167
Design methodology needs for fiber-reinforced ceramic heat exchangers
[DE90-016659] N91-10178
Meetings on the structure and properties of implanted ceramics
[DE90-017313] N91-10181
Electroplating corners
[DE90-017023] N91-10195
The GAMMASPHERE
[DE90-016849] N91-10224
Heavy duty liquid and gaseous fuel emissions database test results from four alternative fuel configurations of the Caterpillar 3406 engine
[DE90-014783] N91-10288
Modeling of hydrocarbon fueling
[DE90-014790] N91-10289
Short-rotation woody crop opportunities to mitigate carbon dioxide buildup
[DE90-016526] N91-10406
Research on climate change
[DE90-016726] N91-10408
Artificial intelligence, human factors, robotics, and computer simulation
[DE90-016866] N91-10653
Nonlinear optics and nonlinear dynamics
[DE90-015975] N91-10716
Pellet injector development at ORNL (Oak Ridge National Laboratory)
[DE90-017024] N91-10742
Preparation of superconducting wire by deposition of YBa2Cu3O(x) onto fibers
[DE90-013380] N91-10758
Radiation damage in Al2O3 crystals implanted with 3.8 MeV Fe(2+)
[DE90-016038] N91-10761
Substrate temperature effects on (cubic x cubic lattice) R 30 deg domain growth of Ag on Si(111) surface
[DE90-016527] N91-10772

**OAK RIDGE Y-12 PLANT, TN.**
Analysis of aluminum oxide ceramic
[DE90-016517] N91-10175
Evaluation of nondestructive evaluation techniques for determination of flawed conditions and the effects of flaws on the burst pressure in Kevlar-epoxy filament-wound spherical test specimens
[DE90-014839] N91-10330

**OFFICE OF THE UNDER SECRETARY OF DEFENSE (ACQUISITIONS), WASHINGTON, DC.**
DOD responsibilities on Federal aviation and national airspace system matters
[PB90-218827] N91-10001

**OHIO STATE UNIV., COLUMBUS.**
Project HyBuJET
[NASA-CR-187011] N91-10040
OVRhyp, scramjet test aircraft
[NASA-CR-187009] N91-10041
Supersonic combustion engine testbed, heat lightning
[NASA-CR-187010] N91-10061

**OLD DOMINION UNIV., NORFOLK, VA.**
Interactive real time flow simulations
[NASA-CR-187325] N91-10238

**OREGON UNIV., EUGENE.**
Collision-induced gas phase dissociation rates
[NASA-CR-185874] N91-10707

**OXFORD UNIV. (ENGLAND).**
Experiments and theory with a 0.5 ton mobile robot
[OUEL-1807/90] N91-10035
Design for navigation: Using acoustic cats' eyes to improve sonar range and direction range finding for industrial mobile robots and AGV's
[OUEL-1812/90] N91-10036
Real-time safety analysis for autonomous guided vehicles
[OUEL-1833/90] N91-10037
Application of generalized predictive control to a boiler turbine unit for electricity generation
[OUEL-1823/90] N91-10229
A facility for calibrating calorimeter gauges at high rates of convective heat transfer
[OUEL-1825/90] N91-10272
Protective autonomy: Embedding sensor-based safety and protection mechanisms into the motion control of mobile and tele-operated robots
[OUEL-1808/90] N91-10292
Casual eigenvector function approximations and the problem of scaling: An algorithm
[OUEL-1822/90] N91-10644
Some defects in finite-difference edge finders
[OUEL-1826/90] N91-10645
Multiple widths yield reliable finite differences
[OUEL-1827/90] N91-10646
Image motion experiments with the Oxford AGV
[OUEL-1809/90] N91-10654
Bounded-error data, and frequency response design
[OUEL-1766/89] N91-10683
H 2 and H infinity approximations for eigenvalue/vector functions of transfer matrices
[OUEL-1778/89] N91-10684
Robustness effects of a prefilter in generalized predictive control
[OUEL-1799/89] N91-10685
Passive-filtered and active-driven probes for RF plasmas
[OUEL-1806/89] N91-10754

## P

**PACIFIC NORTHWEST LAB., RICHLAND, WA.**
Advanced ceramic fabric body mounted radiator for Space Station Freedom Phase O design
[DE90-016361] N91-10104
Advanced materials for high-temperature solid electrolyte applications
[DE90-016328] N91-10143
Radiation-induced microstructural development and microchemical changes in Fe-Cr-Mn-Ni solute-bearing alloys
[DE90-016359] N91-10160
Strength and toughness of single-phase and dual-phase high-temperature intermetallics
[DE90-017192] N91-10166
Design considerations for a ceramic fabric radiator
[DE90-016342] N91-10173
Optical properties of inorganic polymers
[DE90-017143] N91-10179
Effects of in-plane pi prime bonding on electronic transition energies for inorganic polymers
[DE90-017144] N91-10180
A representation scheme for fault diagnosis of physical systems
[DE90-016362] N91-10295
Thermal energy storage for power generation applications
[DE90-016539] N91-10388
The effects of critical layers on atmospheric cnoidal waves
[DE90-016540] N91-10440
Terrain-induced mesoscale circulations in the Columbia Basin
[DE90-016338] N91-10541
Energetics of valley and basin atmospheres during the evening transition and nighttime periods
[DE90-016356] N91-10542
ELF (extremely-low-frequency): Exposure levels, bioeffects, and epidemiology
[DE90-016554] N91-10573
Interaction of extremely low-frequency electromagnetic fields with humans
[DE90-017190] N91-10592
Statistical methods for analyzing and combining data on low-level exposures to ionizing radiation
[DE90-017193] N91-10593
A representation scheme for fault diagnosis
[DE90-016291] N91-10631
Properties of reactively-deposited SiC and GeC alloys
[DE90-016363] N91-10766
Theoretical calculations of the nonlinear dielectric function of inhomogeneous thin films
[DE90-017186] N91-10778

**PENNSYLVANIA STATE UNIV., UNIVERSITY PARK.**
Nano-composite desiccation materials
[PB90-247388] N91-10123
Thermal stability of jet fuel
[DE90-016801] N91-10188
Exponential approximations in optimal design
N91-10311
Estimating integrated cloud liquid water from extended time observations of solar irradiance N91-10510
Aircraft measurements of the mean and turbulent structure of marine stratocumulus clouds during FIRE
N91-10514
Cloud and boundary layer structure over San Nicolas Island during FIRE N91-10515
Boundary layer roll circulations during FIRE
N91-10521
Winds and turbulence above San Nicolas Island during FIRE N91-10522
Biomedical perspectives on locomotion in null gravity
N91-10583

**PENNSYLVANIA UNIV., PHILADELPHIA.**
Redundancy control of a robot manipulator using a systolic array processor N91-10287

**PHYSICAL OPTICS CORP., TORRANCE, CA.**
Holographic rugate structures for x ray optics applications
[DE90-017103] N91-10270

**POLISH ACADEMY OF SCIENCES, WARSAW.**
Plasma waves as a signature of flux transfer events
N91-10427

**POLITECNICO DI MILANO (ITALY).**
Tabu-search and simulated annealing for the quadratic assignment problem
[REPT-89-028] N91-10658

**PRINCETON UNIV., NJ.**
Signal detection in non-Gaussian and non-white noise
N91-10200
The stationary wave response to tropical and midlatitude SST anomalies N91-10536

## R

**RENSSELAER POLYTECHNIC INST., TROY, NY.**
Analysis of pulsed laser-generated impulse in an advanced airbreathing thruster N91-10062

**ROCKEFELLER UNIV., NEW YORK, NY.**
Fast sound propagation in binary fluid mixtures
N91-10233

**ROCKWELL INTERNATIONAL CORP., CANOGA PARK, CA.**
Hybrid propulsion technology program: Phase 1, volume 4
[NASA-CR-183975] N91-10114

**ROCKWELL INTERNATIONAL CORP., DOWNEY, CA.**
Integrated hydrogen/oxygen technology applied to auxiliary propulsion systems
[NASA-CR-185289] N91-10116

**ROHR INDUSTRIES, INC., SAN DIEGO, CA.**
Test/semi-empirical analysis of a carbon/epoxy fabric stiffened panel N91-10302

**ROLLS-ROYCE, INC., ATLANTA, GA.**
Design/development issues for high bypass ratio fans
[PNR-90758] N91-10076

**ROLLS-ROYCE LTD., BRISTOL (ENGLAND).**
Progress in certifying F402-RR-408: The improved Pegasus engine for AV-8B and Harrier 2 plus
[PNR-90719] N91-10056
Technology update of early gas turbine designs
[PNR-90710] N91-10070
Future supersonic transport populsion optimization
[PNR-90737] N91-10071
Applications of thermally sprayed coating systems in aero engines
[PNR-90750] N91-10072
Casting alloys for the jet age
[PNR-90723] N91-10168
An investigation of secondary flows in nozzle guide vanes
[PNR-90739] N91-10262
Fully automatic analysis in an industrial environment
[PNR-90722] N91-10647

**ROLLS-ROYCE LTD., COVENTRY (ENGLAND).**
Gas turbines for main propulsion and auxiliary power systems
[PNR-90709] N91-10069
Fabrication aspects of glass matrix composites for gas turbine applications
[PNR-90752] N91-10073

**ROLLS-ROYCE LTD., DERBY (ENGLAND).**
Parametric assessment of propulsion system mass for airbreathing launcher configurations
[PNR-90634] N91-10063
Aero engine design factors for a low fuel price scenario
[PNR-90681] N91-10066
Thermal fatigue cycling in turbine blades
[PNR-90682] N91-10067
The evolution of the bypass engine
[PNR-90707] N91-10068
Heat transfer in aero engine gas turbines, part 1
[PNR-90754-PT-1] N91-10074
Re-engining: Real stage 3 compliance plus other benefits
[PNR-90755] N91-10075
Fibre-matrix reaction zones in model silicon carbide-titanium aluminide metal-matrix composites
[PNR-90713] N91-10137
Industrial applications and markets for ceramic matrix composites
[PNR-90753] N91-10138
Multi industry application of advanced materials
[PNR-90764] N91-10139
Engineering design: A powerful influence on the business success on manufacturing industry
[PNR-90763] N91-10197
Numerical solutions of rotating disc flows using a non-linear multigrid algorithm
[PNR-90679] N91-10259
Detailed heat transfer measurements in nozzle guide vane passages in linear and annular cascades in the presence of secondary flows
[PNR-90706] N91-10260
Flow measurements in turbomachinery using laser anemometry and holography
[PNR-90717] N91-10261
Introduction: Needs and approaches to reliability and quality assurance in design and manufacture
[PNR-90683] N91-10297
Total quality management at Rolls-Royce PLC
[PNR-90759] N91-10298
Vibro-acoustic emission rubbing sources
[PNR-90730] N91-10336
Fatigue crack propagation of coplanar semi-elliptical cracks in pure bending
[PNR-90742] N91-10337
Do we really need 57 ways of rating aircraft noise
[PNR-90720] N91-10704

**ROYAL AIR FORCE, CARDINGTON (ENGLAND).**
Turbulence measurements using tethered balloon instrumentation during FIRE 1987 N91-10518

**ROYAL AIRCRAFT ESTABLISHMENT, FARNBOROUGH (ENGLAND).**
Near infrared radiances observed by the UK C130 multi-channel radiometer during the marine stratocumulus IFO and preliminary comparison with model calculations
N91-10525

**ROYAL NETHERLANDS METEOROLOGICAL INST., DE BILT.**
About the possibilities of using an air mass transformation model in Taiyuan, Shanxi Province, China
[KNMI-TR-120] N91-10540
Verification of GONO wave predictions for the period October 1987 to April 1988
[KNMI-TR-118] N91-10545
Spectra and gradients of stormy winds at Cabauw, Netherlands, up to 200 meters high
[KNMI-TR-119] N91-10546

**ROYAL SIGNALS AND RADAR ESTABLISHMENT, MALVERN (ENGLAND).**
SILAGE to ELLA translation
[RSRE-MEMO-4385] N91-10639

**RUTGERS - THE STATE UNIV., NEW BRUNSWICK, NJ.**
Identification of Cirrus over Wausau during the 1986 FIRE IFO from ground-based radiometer data
N91-10469
FIRE extended time/limited area observations at Palisades, New York N91-10527

**RUTGERS - THE STATE UNIV., PISCATAWAY, NJ.**
The looped adhesive strip: An example of coplanar delamination interaction N91-10306

## S

**SANDIA NATIONAL LABS., ALBUQUERQUE, NM.**
Infrared absorption in boron carbides: Dependence on isotope and carbon concentration
[DE90-017592] N91-10132
Weldability of nickel and iron aluminides
[DE90-013498] N91-10153
A weldability study of Haynes Alloy no. 242
[DE90-013875] N91-10154
Anomalous dispersion as a phase-matching technique for second harmonic generation
[DE90-015696] N91-10172
Thermochemistry of shock-induced exothermic reactions in selected porous mixtures
[DE90-016104] N91-10183
Hydrogen-tritium getters and their applications
[DE90-016282] N91-10184
Organic getter materials for the removal of hydrogen and its isotopes
[DE90-016284] N91-10185
Statistical characterization of a mode-stirred chamber
[DE90-014860] N91-10202
Minimizing frequency pulling of quartz oscillators due to power supply variations
[DE90-014566] N91-10218
Sodium-neon resonant photoexcitation soft x ray laser experiments on Saturn
[DE90-014946] N91-10275
Development of the force envelope for an acceleration/force extremal controlled vibration test
[DE90-015712] N91-10329
Measurements of the light-absorbing material inside cloud droplets and its effect on cloud albedo
N91-10528
Software safety workshop problem
[DE90-016222] N91-10630
Performance and operational characteristics of a Fiber Distributed Data Interface (FDDI) ring
[DE90-016103] N91-10649
Intrinsic (?) reference standards
[DE90-015714] N91-10696
PREGO: A simulation code for one-dimensional viscoelastic acoustics
[DE90-014859] N91-10700
Numerical models of beam dynamics in ion induction linacs
[DE90-017043] N91-10713
A refractive index gradient (RING) diagnostic for transient discharges or expansions of vapor or plasmas
[DE90-015840] N91-10736
Theoretical analysis of a runaway electron suppression device
[DE90-015992] N91-10737
Measured silicon displacement damage ratios support the need to replace the ASTM E-722 damage function with the NJOY calculated function
[DE90-016225] N91-10762
Renormalization from density functional theory strong coupling models for the electronic structure of La2CuO4
[DE90-015990] N91-10765

**SHEFFIELD UNIV. (ENGLAND).**
Plasma wave measurements on the dayside: Scale sizes and observational requirements N91-10426

**SOCIETE EUROPEENNE DE PROPULSION, VERNON (FRANCE).**
Incorporation of the operation safety in the industry and in a product development process inducting subcontractors
[ETN-90-97822] N91-10196

**SOFTWARE DEVELOPMENT CONCEPTS, MD.**
Representing object oriented specifications and designs with extended data flow notations N91-10617

**SOUTH DAKOTA SCHOOL OF MINES AND TECHNOLOGY, RAPID CITY.**
Analysis of stratocumulus cloud fields using LANDSAT imagery: Size distributions and spatial separations
N91-10504

**SOUTHWEST TEXAS STATE COLL., SAN MARCOS.**
Trifluoromethyl-substituted polymers
[NASA-CR-186955] N91-10170

**SRI INTERNATIONAL CORP., MENLO PARK, CA.**
Electrochemical oxidation of methane at metal and metal oxide electrodes
[PB90-205196] N91-10140

**STANFORD LINEAR ACCELERATOR CENTER, CA.**
Discrete gravity
[DE90-014808] N91-10789
Discretized light-cone quantization: Application to quantum electrodynamics
[DE90-014832] N91-10790

**STANFORD UNIV., CA.**
Mechanisms of high temperature crack growth in metals and alloys
[DE90-014934] N91-10152
Pseudo-monotone complementarity problems in Hilbert space
[DE90-016310] N91-10660

**STATE UNIV. OF NEW YORK, ALBANY.**
Thermophysical properties of fluids and fluid mixtures
[DE90-016306] N91-10792

**SWEDISH DEFENCE RESEARCH ESTABLISHMENT, UMEA.**
Pressure measurements on the release system and determination of jet momentum in the project BA propane field tests 1989
[FOA-E-40044-4.5] N91-10263

**SYDNEY UNIV. (AUSTRALIA).**
Some recent applications of numerical methods to geotechnical analysis
[PB90-201229] N91-10655
Synthesis and inversion of Stokes spectral profiles
[PB90-214487] N91-10828

## T

**TECHNICAL RESEARCH CENTRE OF FINLAND, ESPOO.**
Properties of acoustic energy quantities
[DE90-518714] N91-10701

**TECHNION - ISRAEL INST. OF ENGINEERING, HAIFA.**
Evaluation of alternatives for best-fit paraboloid for deformed antenna surfaces N91-10313

**TECHNION - ISRAEL INST. OF TECH., HAIFA.**
Prediction and comparison with measurements of the aerodynamic characteristics of flare-stabilized XM910 prototypes
[AD-A208099] N91-10005
Repeated buckling of composite shear panels
N91-10303

**TECHNISCHE UNIV., DELFT (NETHERLANDS).**
An avalanche electron emitting diode in gallium arsenide
[ETN-90-97746] N91-10225
First order oscillators
[ETN-90-97758] N91-10226
Directional response of wind waves to turning winds
[REPT-90-2] N91-10549
Wind wave propagation in tidal seas
[REPT-90-1] N91-10550
Technique for human-error sequence identification and signification
[ISBN-90-353-10144] N91-10596
A potential reduction method for a class of smooth convex programming problems
[REPT-90-01] N91-10636
On the rotation interpolation and animation problems in computer graphics
[REPT-90-08] N91-10637
Automated support of the modelling process: A view based on experiments with expert information engineers
[REPT-90-09] N91-10638
Labeling problems in truth maintenance systems
[REPT-89-90] N91-10651
On q-analogues of the Fourier and Hankel transforms
[REPT-89-89] N91-10666
Existance of at most two limit cycles for the system of differential equations: dx/dt = a + summation for i+j = 2 of (a sub ij) (x sup i) (y sup j) and dy/dt =b + summation for i+j = 2 of (b sub ij) (x sup i) (y sup j)
[REPT-90-03] N91-10667
The digital regulator and tracker for deterministic continuous-time linear time-varying systems
[REPT-90-05] N91-10668
Relative position of the critical points of a certain cubic system and a generalization of the Bendixson index formula
[REPT-90-23] N91-10669
Invariant measures exist under a summability condition for unimodal maps
[REPT-90-36] N91-10670
Strong maximum principles for systems
[REPT-90-37] N91-10671
The generalized modus ponens considered as a fuzzy relation
[REPT-90-02] N91-10687
Multivariate tau-estimators for location and scatter
[REPT-90-04] N91-10688
The digital regulator and tracker for stochastic continuous-time linear time-varying systems
[REPT-90-06] N91-10689

**TELEDYNE/MCCORMICK SELPH, HOLLISTER, CA.**
Very high burn rate propellants
[DE90-016865] N91-10186

**TEXAS A&M UNIV., COLLEGE STATION.**
System engineering of aerospace and advanced technology programs at an astronautics company (record of study) N91-10192

The 3-D laser anemometer study of compressible flow through orifice plates
[PB90-216771] N91-10273
An analytical solution for the elastoplastic response of a continuous fiber composite under uniaxial loading
N91-10305
An experimental and analytical study of structural identification N91-10325
**TEXAS UNIV., AUSTIN.**
Tearing modes in tokamaks with lower hybrid current drive
[DE90-017090] N91-10743
Unified theory of ballooning instabilities and temperature gradient driven trapped ion modes
[DE90-017091] N91-10744
Numerical simulation of ion temperature gradient driven modes in the presence of ion-ion collisions
[DE90-017092] N91-10745
Propagation of magnetoacoustic waves in the solar atmosphere with random inhomogeneities of density and magnetic fields
[DE90-017616] N91-10831
**TEXAS UNIV. HEALTH SCIENCE CENTER, DALLAS.**
Cardiovascular group N91-10587
**THIOKOL CORP., BRIGHAM CITY, UT.**
Flight set 360L007 (STS-33R) field joint protection system, thermal protection system, and systems tunnel components, volume 7
[NASA-CR-184026] N91-10115
**TOLEDO UNIV., OH.**
Fundamental properties and mass loss in hot, near-main sequence stars N91-10821
**TRANSPORTATION RESEARCH BOARD, WASHINGTON, DC.**
Geotechnical Engineering, 1989
[PB90-222159] N91-10415

## U

**UNISYS CORP., HOUSTON, TX.**
A practical approach to object based requirements analysis N91-10615
**UNITED KINGDOM ATOMIC ENERGY AUTHORITY, HARWELL (ENGLAND).**
Environmental degradation of macro defect free cements. 1: Mechanical properties investigation
[AERE-R-13354-1] N91-10169
**UNIVERSITEIT TWENTE, ENSCHEDE (NETHERLANDS).**
Dynamics of gas bubbles moving through liquid
[ETN-90-97760] N91-10255
Laser Doppler velocimetry using diode lasers
[ISBN-90-9002803-X] N91-10285
Elastohydrodynamic lubrication: A dynamic variation method
[ISBN-90-9003079-4] N91-10290
The numerical simulation of nonlinear gravity waves in three dimensions using a higher order panel method
[ISBN-90-9002667-23] N91-10443
Models of the human observer and controller of a dynamic system
[ETN-90-97759] N91-10597
Test case derivation from LOTOS specifications
[MEMO-INF-90-21] N91-10643
An introduction to ultrafunctions
[MEMO-841] N91-10672
Approximation and geometric modeling with simplex B-splines associated with irregular triangles
[MEMO-842] N91-10673
Symmetries of the three body problem
[MEMO-843] N91-10674
A Markov renewal approach to an apportunistic replacement model in continuous time
[MEMO-844] N91-10675
Long cycles, degree sums, and neighborhood unions
[MEMO-851] N91-10676
Chebyshev approximation by spline functions with free knots
[MEMO-853] N91-10677
Generating all 3-connected 4-regular planar graphs from the octahedron graph
[MEMO-854] N91-10678
On Baecklund transformations and identities in bilinear form
[MEMO-856] N91-10681
A remark on the convexity of piecewise polynomial functions on triangulations
[MEMO-857] N91-10682
The difference of two renewal processes: Level crossing and the infimum
[MEMO-845] N91-10690
The core and the tau-value for cooperative games with coalition structures
[MEMO-848] N91-10692
About antiferromagnetic Heisenberg models
[ETN-90-97768] N91-10784
**UNIVERSITIES SPACE RESEARCH ASSOCIATION, HOUSTON, TX.**
Project HyBuJET
[NASA-CR-187011] N91-10040
OVRhyp, scramjet test aircraft
[NASA-CR-187009] N91-10041
Supersonic combustion engine testbed, heat lightning
[NASA-CR-187010] N91-10061
**UTAH STATE UNIV., LOGAN.**
Studies of the system-environment interaction by electron beam emission from a sounding rocket payload in the ionosphere N91-10410
**UTAH UNIV., SALT LAKE CITY.**
Lidar and aircraft studies of deep Cirrus systems from the 1986 FIRE IFO N91-10460
Subvisual Cirrus cloud properties derived from a FIRE IFO case study N91-10464
Interpretation of satellite-measured bidirectional reflectance from Cirrus cloudy atmospheres N91-10470

## V

**VIRGINIA POLYTECHNIC INST. AND STATE UNIV., BLACKSBURG.**
Theoretical studies in few-body intermediate energy physics
[DE90-017279] N91-10709

## W

**WASHINGTON UNIV., SAINT LOUIS, MO.**
Physical interpretation and application of principles of ultrasonic nondestructive evaluation of high-performance materials
[NASA-CR-180489] N91-10293
**WASHINGTON UNIV., SEATTLE.**
Simulations and observations of cloudtop processes
N91-10496
In situ measurements of ship tracks N91-10507
Measurements of the light-absorbing material inside cloud droplets and its effect on cloud albedo
N91-10528
Experiments on linear high beta helical axis stellarators to study simulated toroidal effects and Alfven-wave heating
[DE90-016122] N91-10738
**WEST VIRGINIA UNIV., MORGANTOWN.**
A unique problem of muscle adaptation from weightlessness: The deceleration deficiency
N91-10582
Reaction kinetics of the Ca-SO2 system in absence of inter-grain pore diffusion
[DE90-009672] N91-10781
**WESTINGHOUSE HANFORD CO., RICHLAND, WA.**
Structural integrity assessment of concrete slabs by nondestructive examination and Fourier transform-infrared methods
[DE90-017233] N91-10296
**WISCONSIN UNIV., MADISON.**
Organometallic chemistry of bimetallic compounds
[DE90-017601] N91-10121
Thin film thermometers and flowmeters for applications in liquid helium N91-10265
Analysis of moving strong discontinuity surfaces in elastic-plastic solids including effects of inertia and finite strain N91-10323
Where are cirrus clouds and why are they there
N91-10450
Optical and morphological properties of Cirrus clouds determined by the high spectral resolution lidar during FIRE N91-10458
Multi-spectral window radiance observations of Cirrus from satellite and aircraft, November 2, 1986 Project FIRE N91-10465
Comparison of NOAA-9 ERBE measurements with Cirrus IFO satellite and aircraft measurements N91-10471
Cloud altitude determination from infrared spectral radiances N91-10474
Interpretation of the optical and morphological properties of Cirrus clouds from lidar measurements N91-10483
Both sides now N91-10485
The relationship of marine stratus to synoptic conditions N91-10489
Two-dimensional magnetohydrodynamic equilibria with flow and studies of equilibrium fluctuations N91-10727
Self-consistent field error effects in reversed field pinch plasmas N91-10728
A computational model for z-pinch plasma channels
N91-10730
Models of plasma confinement and heating in tokamaks
[DE90-016671] N91-10741
Theoretical studies of turbulence and anomalous transport in toroidal confinement devices
[DE90-017606] N91-10747
Stellarator theory
[DE90-017607] N91-10748
**WORCESTER POLYTECHNIC INST., MA.**
Transient characteristics of unconfined fire plume-driven ceiling jets
[PB90-227976] N91-10193
**WORLD METEOROLOGICAL ORGANIZATION, GENEVA (SWITZERLAND).**
Atmospheric ozone 1985: Assessment of our understanding of the processes controlling its present distribution and change, volume 3
[NASA-TM-103462] N91-10393
Analyzing long time series of hydrological data with respect to climate variability: Project description
[WCAP-3] N91-10444
Proceedings of the WMO Region 3/4 Training Seminar on Climate Data Management and User Services
[WCDP-1] N91-10445
Activities report of the World Meteorological Organization
[WMO-734] N91-10547

## X

**XEROX PALO ALTO RESEARCH CENTER, CA.**
Density estimation using optimally quantized histograms
[PB90-190588] N91-10686

## Y

**YALE UNIV., NEW HAVEN, CT.**
Cosmological singularities in electrovacuum spacetimes with two-parameter spacelike isometry groups
N91-10811

## Z

**ZHEJIANG UNIV. (CHINA).**
Operator formalism of multi-pole Virasoro algebra on Riemann sphere
[DE90-627217] N91-10657

# CONTRACT NUMBER INDEX

SCIENTIFIC AND TECHNICAL AEROSPACE REPORTS VOLUME 29 NUMBER 1

## Typical Contract Number Index Listing

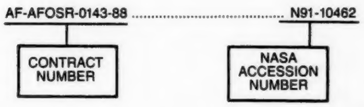

Listings in this index are arranged alphanumerically by contract number. Under each contract number the NASA accession numbers denoting documents that have been produced as a result of research done under that contract are arranged in ascending order. The NASA accession number denotes the number by which the citation is identified.

AF-AFOSR-0143-88 ........ N91-10462
BMFT-03-M-1012 ........ N91-10136
BMVG-T/R-760/H-0003/H-1763 ........ N91-10247
DA PROJ. 1L1-62618-AH-80 ........ N91-10005
DA PROJ. 1L6-62618-AH-80 ........ N91-10300
DAAG29-84-K-0069 ........ N91-10458
N91-10478
N91-10483
DE-AC02-76CH-00016 ........ N91-10159
N91-10407
N91-10760
DE-AC02-76CH-03000 ........ N91-10147
N91-10281
DE-AC02-83CH-10093 ........ N91-10384
N91-10756
DE-AC03-76SF-00098 ........ N91-10129
N91-10177
N91-10203
N91-10223
N91-10775
N91-10783
DE-AC03-76SF-00515 ........ N91-10789
N91-10790
DE-AC03-86SF-16298 ........ N91-10383
DE-AC04-76DP-00613 ........ N91-10184
N91-10185
N91-10632
DE-AC04-76DP-00789 ........ N91-10132
N91-10153
N91-10154
N91-10172
N91-10183
N91-10202
N91-10218
N91-10275
N91-10329
N91-10630
N91-10648
N91-10649
N91-10696
N91-10700
N91-10713
N91-10736
N91-10737
N91-10762
N91-10765
DE-AC05-84OR-21400 ........ N91-10046
N91-10125
N91-10156
N91-10167
N91-10178
N91-10181
N91-10195
N91-10224
N91-10288
N91-10289
N91-10406
N91-10408
N91-10608
N91-10653
N91-10716
N91-10737
N91-10742
N91-10758
N91-10761
N91-10772
DE-AC05-84OS-21400 ........ N91-10175
N91-10330
DE-AC05-84OT-21400 ........ N91-10145
DE-AC06-76RL-01830 ........ N91-10104
N91-10143
N91-10160
N91-10166
N91-10173
N91-10179
N91-10180
N91-10295
N91-10388
N91-10440
N91-10541
N91-10542
N91-10573
N91-10592
N91-10593
N91-10631
N91-10766
N91-10778
DE-AC06-87RL-10930 ........ N91-10296
DE-AC22-88PC-88827 ........ N91-10188
DE-AI01-76ET-20320 ........ N91-10127
DE-AS05-77ER-05490 ........ N91-10665
N91-10708
DE-AS05-80ER-10742 ........ N91-10159
DE-FC21-87MC-24207 ........ N91-10781
DE-FC22-83FE-60149 ........ N91-10791
DE-FG01-88CE-15401 ........ N91-10269
DE-FG02-85ER-13406 ........ N91-10121
DE-FG02-85ER-53201 ........ N91-10748
DE-FG02-86ER-5321 ........ N91-10741
DE-FG02-86ER-45253 ........ N91-10764
DE-FG02-86ER-53223 ........ N91-10746
DE-FG02-87ER-45330 ........ N91-10779
DE-FG02-88ER-13850 ........ N91-10792
DE-FG02-88ER-13860 ........ N91-10722
DE-FG02-89ER-53291 ........ N91-10747
DE-FG03-84ER-45169 ........ N91-10152
DE-FG03-86ER-13600 ........ N91-10270
DE-FG03-87ER-25028 ........ N91-10660
DE-FG03-88ER-53275 ........ N91-10745
DE-FG05-80ET-53088 ........ N91-10743
N91-10744
N91-10745
N91-10831
DE-FG05-84ER-40143 ........ N91-10709
DE-FG05-86ER-53217 ........ N91-10710
DE-FG05-89ER-25080 ........ N91-10596
DE-FG06-87ER-53242 ........ N91-10738
DRET-87-068 ........ N91-10017
ERI PROJ. 1874 ........ N91-10019
F19628-87-C-0094 ........ N91-10264
F49620-87-K-0001 ........ N91-10129
GRI-5086-260-1340 ........ N91-10273
GRI-5086-260-1424 ........ N91-10140
GRI-5087-260-1473 ........ N91-10123
GRI-5088-260-1686 ........ N91-10235
GRI-5089-260-1824 ........ N91-10381
LBL-4539610 ........ N91-10223
LBL-4559910 ........ N91-10177
MDA972-88-C-0024 ........ N91-10633
MDA972-88-J-1006 ........ N91-10783
NAGW-856 ........ N91-10101
NAGW-1340 ........ N91-10695
NAGW-1581 ........ N91-10734
NAG1-224 ........ N91-10313
NAG1-286 ........ N91-10122
NAG1-552 ........ N91-10491
NAG1-554 ........ N91-10479
N91-10484
N91-10492
N91-10517
N91-10531
NAG1-631 ........ N91-10170
NAG1-645 ........ N91-10019
NAG1-651 ........ N91-10526
NAG1-653 ........ N91-10469
N91-10527
NAG1-685 ........ N91-10334
N91-10335
NAG1-686 ........ N91-10464
NAG1-718 ........ N91-10464
NAG1-959 ........ N91-10047
NAG1-970 ........ N91-10735
NAG1-971 ........ N91-10126
NAG1-1046 ........ N91-10707
NAG1-1060 ........ N91-10629
NAG2-206 ........ N91-10452
NAG2-541 ........ N91-10201
N91-10623
NAG2-593 ........ N91-10633
NAG3-894 ........ N91-10133
NAG5-915 ........ N91-10379
NAG5-1017 ........ N91-10763
NAG8-720 ........ N91-10618
N91-10619
N91-10620
N91-10621
NAG8-767 ........ N91-10755
NAG9-117 ........ N91-10591
NAG9-398 ........ N91-10595
NASA ORDER L-08100-B ........ N91-10460
NASA ORDER L-79877-B ........ N91-10501
N91-10524
NASA ORDER L-98100-B ........ N91-10459
NAS1-17748 ........ N91-10548
NAS1-18107 ........ N91-10251
NAS1-18272 ........ N91-10465
N91-10474
NAS1-18458 ........ N91-10098
NAS1-18605 ........ N91-10009
N91-10010
N91-10021
N91-10022
N91-10237
N91-10250
N91-10251
N91-10599
N91-10600
N91-10628
N91-10629
N91-10664
NAS2-11555 ........ N91-10048
NAS3-23051 ........ N91-10065
NAS3-25266 ........ N91-10127
NAS3-25643 ........ N91-10116
NAS5-28800 ........ N91-10490
N91-10493
NAS5-30365 ........ N91-10439
NAS5-30730 ........ N91-10439
NAS7-918 ........ N91-10105
N91-10204
N91-10222
N91-10829
NAS8-30490 ........ N91-10115
NAS8-37777 ........ N91-10111
N91-10112
N91-10113
N91-10114
NAS9-17325 ........ N91-10085
NAS9-18147 ........ N91-10102
NAS10-11624 ........ N91-10442
NA86AA-D-SG089 ........ N91-10698
NCC1-68 ........ N91-10238
NCC1-122 ........ N91-10039
NCC2-507 ........ N91-10083
NCC2-598 ........ N91-10333
NCC9-16 ........ N91-10793
N91-10794
N91-10795
NGR-21-002-316 ........ N91-10810
NIST-NANB5H0551 ........ N91-10193
NSF ASC-88-19373 ........ N91-10629
NSF ASC-88-19374 ........ N91-10599
NSF AST-86-12013 ........ N91-10462
NSF ATM-83-52205 ........ N91-10454
NSF ATM-85-13975 ........ N91-10453
N91-10459
N91-10460

N91-10464
N91-10478
NSF ATM-85-19160 .......... N91-10462
NSF ATM-85-21214 .......... N91-10479
N91-10484
NSF ATM-86-05134 .......... N91-10528
NSF ATM-86-07377 .......... N91-10528
NSF ATM-86-15344 .......... N91-10507
NSF ATM-86-19854 .......... N91-10521
NSF ATM-86-20165 .......... N91-10496
NSF ATM-87-05403 .......... N91-10490
N91-10493
NSF ATM-87-09659 .......... N91-10828
NSF ATM-89-00357 .......... N91-10734
NSF DMR-88-02401 .......... N91-10768
NSF DMR-88-14783 .......... N91-10768
NSF DMS-89-13088 .......... N91-10660
NSF DMS-89-14420 .......... N91-10248
NSF STC-88-09854 .......... N91-10782
NSG-1490 .......... N91-10312
NSG-1601 .......... N91-10293
NSG-5123 .......... N91-10608
NWO-10-62-10 .......... N91-10688
N00014-84-K-0405 .......... N91-10526
N00014-85-K-0581 .......... N91-10458
N91-10478
N91-10483
N00014-86-K-06880 .......... N91-10521
N00014-87-K-0228 .......... N91-10517
N91-10531
N00014-87-K-0307 .......... N91-10608
N00014-89-J-1659 .......... N91-10660
N000014-87-K-0228 .......... N91-10492
STW-CWI44-0632 .......... N91-10443
STW-CWI47-0632 .......... N91-10443
STW-DTN33-467 .......... N91-10225
SVERDRUP-5324-85 .......... N91-10117
W-31-109-ENG-38 .......... N91-10171
N91-10220
N91-10236
N91-10385
N91-10603
N91-10757
N91-10759
N91-10782
W-7405-ENG-36 .......... N91-10008
N91-10095
N91-10155
N91-10158
N91-10162
N91-10163
N91-10164
N91-10165
N91-10176
N91-10187
N91-10239
N91-10240
N91-10241
N91-10242
N91-10243
N91-10244
N91-10266
N91-10276
N91-10277
N91-10279
N91-10280
N91-10282
N91-10382
N91-10602
N91-10662
N91-10663
N91-10697
N91-10715
N91-10717
N91-10720
N91-10721
N91-10739
N91-10740
N91-10767
N91-10768
N91-10769
N91-10770
N91-10771
N91-10773
N91-10774
N91-10776
N91-10777
N91-10803
N91-10817
N91-10818
N91-10830
N91-10836
W-7405-ENG-48 .......... N91-10094
N91-10096
N91-10130
N91-10142
N91-10161
N91-10186
N91-10219
N91-10267
N91-10274
N91-10278
N91-10331
N91-10409
N91-10626
N91-10650
N91-10659
N91-10661
N91-10706
N91-10718
N91-10719
N91-10732
N91-10733
N91-10802
W-7405-ENG-82 .......... N91-10144
N91-10146
N91-10174
073-36-00-00-72 .......... N91-10574
404-00-73-04-17 .......... N91-10829
505-03-01 .......... N91-10065
505-33-1A .......... N91-10149
505-34-13-34 .......... N91-10548
505-45-21 .......... N91-10079
505-60-00 .......... N91-10013
N91-10252
505-61-01 .......... N91-10268
505-61-21 .......... N91-10014
505-61-51 .......... N91-10007
N91-10045
N91-10048
505-62-4D .......... N91-10703
505-62-01 .......... N91-10271
505-62-21 .......... N91-10208
505-63-1B .......... N91-10332
505-63-01 .......... N91-10150
505-63-01-05 .......... N91-10128
505-63-01-07 .......... N91-10301
505-63-50-12 .......... N91-10020
505-66-01-02 .......... N91-10078
505-66-41 .......... N91-10058
505-66-71 .......... N91-10328
505-90-21-01 .......... N91-10009
N91-10010
N91-10021
N91-10022
N91-10237
N91-10250
N91-10251
N91-10599
N91-10600
N91-10628
N91-10664
506-41-41 .......... N91-10134
506-42-11 .......... N91-10119
506-42-31 .......... N91-10116
N91-10118
506-43-11-01 .......... N91-10182
506-44-20 .......... N91-10780
506-44-21-03 .......... N91-10221
506-49-11-01 .......... N91-10106
510-01-01 .......... N91-10133
532-06-01-09 .......... N91-10699
535-03-11-03 .......... N91-10702
537-03-21 .......... N91-10015
582-01-21 .......... N91-10117
583-01-11-02 .......... N91-10245
590-12-31-02-50 .......... N91-10204
591-41-21 .......... N91-10249
644-11-00-05-81 .......... N91-10222
672-22-10-70 .......... N91-10448
763-01-61 .......... N91-10049
776-33-41 .......... N91-10127
906-70-16-02 .......... N91-10098

# REPORT/ACCESSION NUMBER INDEX

### Typical Report Number Index Listing

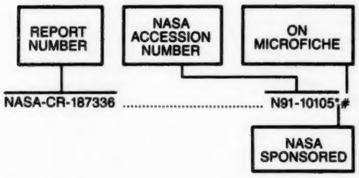
REPORT NUMBER
NASA ACCESSION NUMBER
ON MICROFICHE
NASA-CR-187336 ..................................... N91-10105*#
NASA SPONSORED

Listings in this index are arranged alphanumerically by report number. The NASA accession number denotes the number by which the citation is identified. An asterisk (*) indicates that the item is a NASA report. A pound sign (#) indicates that the item is available on microfiche.

| | | |
|---|---|---|
| A-86374-PT-3 | N91-10007* | # |
| A-88279-PT-1 | N91-10049* | # |
| A-88316 | N91-10045* | # |
| A-89197 | N91-10014* | # |
| A-90082 | N91-10268* | # |
| A-90117 | N91-10013* | # |
| A-90231 | N91-10252* | # |
| A-90246 | N91-10015* | # |
| A-90303 | N91-10048* | # |
| AD-A207606 | N91-10004 | # |
| AD-A208099 | N91-10005 | # |
| AD-A210233 | N91-10300 | # |
| AD-A211364 | N91-10230 | # |
| AD-A211566 | N91-10264 | # |
| AD-A223277 | N91-10124 | # |
| AEDC-TR-88-31 | N91-10004 | # |
| AERE-R-13354-1 | N91-10169 | |
| AGARD-R-775 | N91-10042 | # |
| AIAA-89-1212 | N91-10328* | # |
| AIAA-90-1032 | N91-10020* | # |
| AIAA-90-2582 | N91-10118* | # |
| AIAA-90-3933 | N91-10703* | # |
| ANL-90/19 | N91-10236 | # |
| ANL/MCT-90/1 | N91-10759 | # |
| AR-006-100 | N91-10064 | # |
| ARL-PROP-TM-449 | N91-10064 | # |
| AVSCOM-TR-88-A-003 | N91-10045* | # |
| BCRS-89-38 | N91-10544 | # |
| BIO-2 | N91-10442* | # |
| BNL-44434 | N91-10159 | # |
| BNL-44819 | N91-10760 | # |
| BR-43 | N91-10256 | # |
| BRL-MR-3752 | N91-10005 | # |
| BRL-MR-3773 | N91-10300 | # |
| BRL-TR-3026 | N91-10230 | # |
| BR114304 | N91-10639 | # |
| BUGRI-0005 | N91-10801 | # |
| CBP/TRS-34/89-VOL-1 | N91-10391 | # |
| CBP/TRS-35/89-VOL-2 | N91-10392 | # |
| CFD-24 | N91-10019* | # |
| CMU-HEP90-13 | N91-10695* | # |
| CNES-CT/DRT/TIT/OE-88/037-T | N91-10227 | # |
| CNES-CT/DRT/TIT/RL-88/226 | N91-10380 | # |
| CNES-CT/DRT/TIT/TF-88/354 | N91-10110 | # |
| CNES-CT/DRT/TIT/TR-88/24-T | N91-10206 | # |
| CNES-CT/DRT/TIT/TR-88/060 | N91-10691 | # |
| CNES-CT/DRT/TIT/TR-88/355 | N91-10207 | # |
| CNES-DRT/TIT/TF-88/338-T | N91-10284 | # |
| CNIC-00257 | N91-10801 | # |
| CONF-890525 | N91-10407 | # |
| CONF-891119-136 | N91-10765 | # |
| CONF-891119-137 | N91-10778 | # |
| CONF-891119-138 | N91-10180 | # |
| CONF-891119-139 | N91-10179 | # |
| CONF-900348-13 | N91-10281 | # |
| CONF-900367-2 | N91-10836 | # |
| CONF-900442-4 | N91-10173 | # |
| CONF-900450-10 | N91-10224 | # |
| CONF-900466-47 | N91-10158 | # |
| CONF-900466-79 | N91-10156 | # |
| CONF-900466-82 | N91-10166 | # |
| CONF-900489-2 | N91-10760 | # |
| CONF-900495-2 | N91-10592 | # |
| CONF-900546-13 | N91-10143 | # |
| CONF-900607-6 | N91-10295 | # |
| CONF-900619-7 | N91-10104 | # |
| CONF-900623-12 | N91-10160 | # |
| CONF-900632-1 | N91-10167 | # |
| CONF-900679-7 | N91-10573 | # |
| CONF-900751-3 | N91-10768 | # |
| CONF-900756-26 | N91-10096 | # |
| CONF-900756-35 | N91-10766 | # |
| CONF-900756-37 | N91-10267 | # |
| CONF-900756-38 | N91-10718 | # |
| CONF-900793-4 | N91-10631 | # |
| CONF-900802-5 | N91-10771 | # |
| CONF-900814-8 | N91-10762 | # |
| CONF-900818-3 | N91-10161 | # |
| CONF-900818-4 | N91-10162 | # |
| CONF-900830-1 | N91-10772 | # |
| CONF-900870-3 | N91-10769 | # |
| CONF-900870-4 | N91-10132 | # |
| CONF-900918-1 | N91-10737 | # |
| CONF-900918-3 | N91-10282 | # |
| CONF-900918-4 | N91-10742 | # |
| CONF-900936-1 | N91-10761 | # |
| CONF-900953-1 | N91-10276 | # |
| CONF-901004-1 | N91-10770 | # |
| CONF-901004-2 | N91-10773 | # |
| CONF-901004-4 | N91-10774 | # |
| CONF-901009-1 | N91-10171 | # |
| CONF-901017-1-REV-2 | N91-10732 | # |
| CONF-901025-2 | N91-10740 | # |
| CONF-901025-3 | N91-10739 | # |
| CONF-901062-1 | N91-10757 | # |
| CONF-901073-6 | N91-10382 | # |
| CONF-901088-3 | N91-10758 | # |
| CONF-901089-2 | N91-10803 | # |
| CONF-901095-2 | N91-10153 | # |
| CONF-901095-3 | N91-10154 | # |
| CONF-901095-4 | N91-10155 | # |
| CONF-901099-1 | N91-10289 | # |
| CONF-901105-2 | N91-10783 | # |
| CONF-901109-4 | N91-10782 | # |
| CONF-8710452 | N91-10274 | # |
| CONF-8909204-6 | N91-10185 | # |
| CONF-8911192-6 | N91-10278 | # |
| CONF-9002131-2 | N91-10661 | # |
| CONF-9002140-1 | N91-10721 | # |
| CONF-9004133-4 | N91-10388 | # |
| CONF-9004240-SUMM | N91-10650 | # |
| CONF-9005183 | N91-10385 | # |
| CONF-9005237-3 | N91-10715 | # |
| CONF-9005237-4 | N91-10662 | # |
| CONF-9005237-6 | N91-10663 | # |
| CONF-9005261-1 | N91-10406 | # |
| CONF-9006111-4 | N91-10541 | # |
| CONF-9006111-6 | N91-10542 | # |
| CONF-9006111-7 | N91-10440 | # |
| CONF-9006179-5 | N91-10219 | # |
| CONF-9006195-7 | N91-10733 | # |
| CONF-9006212-2 | N91-10818 | # |
| CONF-9006261-1 | N91-10830 | # |
| CONF-9006265-1 | N91-10719 | # |
| CONF-9006267-1 | N91-10147 | # |
| CONF-9006267-2 | N91-10665 | # |
| CONF-9007109-2 | N91-10296 | # |
| CONF-9007136-3 | N91-10697 | # |
| CONF-9007157-1 | N91-10720 | # |
| CONF-9007158-1 | N91-10817 | # |
| CONF-9007161-1 | N91-10195 | # |
| CONF-9007165-2 | N91-10593 | # |
| CONF-9008106-1 | N91-10142 | # |
| CONF-9008125-4 | N91-10183 | # |
| CONF-9008125-5 | N91-10176 | # |
| CONF-9008125-6 | N91-10165 | # |
| CONF-9008125-7 | N91-10164 | # |
| CONF-9008125-8 | N91-10163 | # |
| CONF-9008128-1 | N91-10275 | # |
| CONF-9008134-2 | N91-10696 | # |
| CONF-9008141-1 | N91-10159 | # |
| CONF-9008141-2 | N91-10776 | # |
| CONF-9008142-1 | N91-10277 | # |
| CONF-9008143-1 | N91-10767 | # |
| CONF-9009166-1 | N91-10279 | # |
| CONF-9009166-2 | N91-10280 | # |
| CONF-9009192-12 | N91-10736 | # |
| CONF-9009200-5 | N91-10717 | # |
| CONF-9009200-10 | N91-10713 | # |
| CONF-9009201-4 | N91-10184 | # |
| CONF-9009220-1 | N91-10218 | # |
| CONF-9009225-1 | N91-10626 | # |
| CONF-9009227-1 | N91-10789 | # |
| CONF-9009232-2 | N91-10649 | # |
| CONF-9009235-1 | N91-10266 | # |
| CONF-9009240-1 | N91-10409 | # |
| CONF-9010154-1 | N91-10008 | # |
| CONF-9010170-1 | N91-10172 | # |
| CONF-9010171-2 | N91-10630 | # |
| CONF-9010172-1 | N91-10329 | # |
| CRIE-W-89011 | N91-10386 | # |
| CS-TR-2158 | N91-10608* | # |
| CSDL-T-1053 | N91-10102* | # |
| CWI-BS-R8932 | N91-10635 | # |
| DE90-000247 | N91-10791 | # |
| DE90-000358 | N91-10756 | # |
| DE90-000365 | N91-10384 | # |
| DE90-007805 | N91-10171 | # |
| DE90-009672 | N91-10781 | # |
| DE90-009704 | N91-10757 | # |
| DE90-011180 | N91-10782 | # |
| DE90-011947 | N91-10158 | # |
| DE90-012074 | N91-10142 | # |
| DE90-013380 | N91-10758 | # |
| DE90-013478 | N91-10732 | # |
| DE90-013484 | N91-10274 | # |
| DE90-013498 | N91-10153 | # |
| DE90-013875 | N91-10154 | # |
| DE90-014080 | N91-10269 | # |
| DE90-014508 | N91-10783 | # |
| DE90-014566 | N91-10218 | # |
| DE90-014573 | N91-10094 | # |
| DE90-014589 | N91-10603 | # |
| DE90-014681 | N91-10602 | # |
| DE90-014683 | N91-10648 | # |
| DE90-014696 | N91-10155 | # |
| DE90-014767 | N91-10046 | # |
| DE90-014783 | N91-10288 | # |
| DE90-014790 | N91-10289 | # |
| DE90-014797 | N91-10802 | # |
| DE90-014802 | N91-10238 | # |
| DE90-014808 | N91-10789 | # |
| DE90-014809 | N91-10759 | # |
| DE90-014831 | N91-10706 | # |

DE90-014832 ........ N91-10790 #
DE90-014839 ........ N91-10330 #
DE90-014844 ........ N91-10385 #
DE90-014859 ........ N91-10700 #
DE90-014860 ........ N91-10202 #
DE90-014872 ........ N91-10539 #
DE90-014881 ........ N91-10281 #
DE90-014903 ........ N91-10008 #
DE90-014934 ........ N91-10152 #
DE90-014946 ........ N91-10275 #
DE90-014974 ........ N91-10803 #
DE90-015034 ........ N91-10715 #
DE90-015055 ........ N91-10382 #
DE90-015089 ........ N91-10760 #
DE90-015108 ........ N91-10095 #
DE90-015118 ........ N91-10598 #
DE90-015119 ........ N91-10219 #
DE90-015132 ........ N91-10383 #
DE90-015147 ........ N91-10626 #
DE90-015180 ........ N91-10220 #
DE90-015187 ........ N91-10733 #
DE90-015307 ........ N91-10129 #
DE90-015612 ........ N91-10096 #
DE90-015696 ........ N91-10172 #
DE90-015712 ........ N91-10329 #
DE90-015714 ........ N91-10696 #
DE90-015800 ........ N91-10156 #
DE90-015840 ........ N91-10736 #
DE90-015906 ........ N91-10718 #
DE90-015908 ........ N91-10409 #
DE90-015909 ........ N91-10719 #
DE90-015910 ........ N91-10130 #
DE90-015935 ........ N91-10764 #
DE90-015975 ........ N91-10716 #
DE90-015990 ........ N91-10765 #
DE90-015992 ........ N91-10737 #
DE90-016038 ........ N91-10761 #
DE90-016103 ........ N91-10649 #
DE90-016104 ........ N91-10183 #
DE90-016122 ........ N91-10738 #
DE90-016207 ........ N91-10125 #
DE90-016212 ........ N91-10331 #
DE90-016213 ........ N91-10659 #
DE90-016222 ........ N91-10630 #
DE90-016225 ........ N91-10762 #
DE90-016282 ........ N91-10184 #
DE90-016284 ........ N91-10185 #
DE90-016291 ........ N91-10631 #
DE90-016306 ........ N91-10792 #
DE90-016310 ........ N91-10660 #
DE90-016313 ........ N91-10159 #
DE90-016328 ........ N91-10143 #
DE90-016338 ........ N91-10541 #
DE90-016342 ........ N91-10173 #
DE90-016356 ........ N91-10542 #
DE90-016359 ........ N91-10160 #
DE90-016361 ........ N91-10104 #
DE90-016362 ........ N91-10295 #
DE90-016363 ........ N91-10766 #
DE90-016415 ........ N91-10174 #
DE90-016416 ........ N91-10146 #
DE90-016417 ........ N91-10144 #
DE90-016430 ........ N91-10632 #
DE90-016432 ........ N91-10266 #
DE90-016433 ........ N91-10818 #
DE90-016434 ........ N91-10817 #
DE90-016438 ........ N91-10717 #
DE90-016439 ........ N91-10282 #
DE90-016441 ........ N91-10276 #
DE90-016442 ........ N91-10739 #
DE90-016443 ........ N91-10740 #
DE90-016447 ........ N91-10277 #
DE90-016466 ........ N91-10767 #
DE90-016467 ........ N91-10836 #
DE90-016468 ........ N91-10768 #
DE90-016473 ........ N91-10278 #
DE90-016475 ........ N91-10267 #
DE90-016478 ........ N91-10661 #
DE90-016481 ........ N91-10161 #
DE90-016483 ........ N91-10720 #
DE90-016484 ........ N91-10769 #
DE90-016485 ........ N91-10279 #
DE90-016488 ........ N91-10280 #
DE90-016489 ........ N91-10162 #
DE90-016490 ........ N91-10770 #
DE90-016491 ........ N91-10771 #
DE90-016495 ........ N91-10830 #
DE90-016505 ........ N91-10697 #
DE90-016506 ........ N91-10662 #
DE90-016516 ........ N91-10145 #
DE90-016517 ........ N91-10175 #
DE90-016526 ........ N91-10406 #
DE90-016527 ........ N91-10772 #
DE90-016539 ........ N91-10388 #
DE90-016540 ........ N91-10440 #
DE90-016554 ........ N91-10573 #
DE90-016558 ........ N91-10187 #
DE90-016566 ........ N91-10663 #
DE90-016567 ........ N91-10773 #
DE90-016568 ........ N91-10176 #
DE90-016611 ........ N91-10163 #
DE90-016612 ........ N91-10164 #
DE90-016613 ........ N91-10165 #
DE90-016614 ........ N91-10774 #
DE90-016638 ........ N91-10177 #
DE90-016640 ........ N91-10775 #
DE90-016647 ........ N91-10203 #
DE90-016648 ........ N91-10223 #
DE90-016659 ........ N91-10178 #
DE90-016671 ........ N91-10741 #
DE90-016693 ........ N91-10407 #
DE90-016717 ........ N91-10721 #
DE90-016720 ........ N91-10776 #
DE90-016723 ........ N91-10239 #
DE90-016724 ........ N91-10777 #
DE90-016726 ........ N91-10408 #
DE90-016801 ........ N91-10188 #
DE90-016849 ........ N91-10224 #
DE90-016865 ........ N91-10186 #
DE90-016866 ........ N91-10653 #
DE90-016901 ........ N91-10147 #
DE90-017023 ........ N91-10195 #
DE90-017024 ........ N91-10742 #
DE90-017043 ........ N91-10713 #
DE90-017090 ........ N91-10743 #
DE90-017091 ........ N91-10744 #
DE90-017092 ........ N91-10745 #
DE90-017103 ........ N91-10270 #
DE90-017143 ........ N91-10179 #
DE90-017144 ........ N91-10180 #
DE90-017186 ........ N91-10778 #
DE90-017190 ........ N91-10592 #
DE90-017192 ........ N91-10166 #
DE90-017193 ........ N91-10593 #
DE90-017223 ........ N91-10722 #
DE90-017233 ........ N91-10296 #
DE90-017256 ........ N91-10746 #
DE90-017278 ........ N91-10708 #
DE90-017279 ........ N91-10709 #
DE90-017280 ........ N91-10710 #
DE90-017287 ........ N91-10779 #
DE90-017313 ........ N91-10181 #
DE90-017319 ........ N91-10167 #
DE90-017402 ........ N91-10665 #
DE90-017535 ........ N91-10240 #
DE90-017536 ........ N91-10241 #
DE90-017537 ........ N91-10242 #
DE90-017538 ........ N91-10243 #
DE90-017539 ........ N91-10244 #
DE90-017592 ........ N91-10132 #
DE90-017601 ........ N91-10121 #
DE90-017606 ........ N91-10747 #
DE90-017607 ........ N91-10748 #
DE90-017616 ........ N91-10831 #
DE90-018009 ........ N91-10650 #
DE90-517069 ........ N91-10386 #
DE90-517230 ........ N91-10387 #
DE90-518714 ........ N91-10701 #
DE90-627172 ........ N91-10656 #
DE90-627178 ........ N91-10693 #
DE90-627185 ........ N91-10786 #
DE90-627189 ........ N91-10327 #
DE90-627217 ........ N91-10657 #
DE90-627478 ........ N91-10731 #
DE90-627893 ........ N91-10801 #
DE90-628368 ........ N91-10787 #
DE90-628371 ........ N91-10788 #

DLR-FB-90-11 ........ N91-10390 #
DLR-FB-90-13 ........ N91-10026 #
DLR-FB-90-15 ........ N91-10027 #

DOD-D-5030.19 ........ N91-10001 #

DOE/CE-15401/T8 ........ N91-10269 #

DOE/ER-05490/111 ........ N91-10665 #
DOE/ER-05490/123 ........ N91-10708 #
DOE/ER-13406/5 ........ N91-10121 #
DOE/ER-13600/T1 ........ N91-10270 #
DOE/ER-13850/15 ........ N91-10792 #
DOE/ER-13860/3 ........ N91-10722 #
DOE/ER-25080/1 ........ N91-10598 #
DOE/ER-40143/7 ........ N91-10709 #
DOE/ER-45169/T1 ........ N91-10152 #
DOE/ER-45253/5 ........ N91-10764 #
DOE/ER-45330/2 ........ N91-10779 #
DOE/ER-53201/T5 ........ N91-10748 #
DOE/ER-53217/4 ........ N91-10710 #
DOE/ER-53223/145 ........ N91-10746 #
DOE/ER-53242/4 ........ N91-10738 #
DOE/ER-53291/1 ........ N91-10747 #
DOE/ET-53088/443 ........ N91-10744 #
DOE/ET-53088/444 ........ N91-10743 #
DOE/ET-53088/445 ........ N91-10745 #
DOE/ET-53088/446 ........ N91-10831 #

DOE/MC-24207/2857 ........ N91-10781 #

DOE/NASA/20320-76 ........ N91-10127* #

DOE/PC-88827/T5 ........ N91-10188 #

DOT/FAA/CT-TN89/44 ........ N91-10051 #
DOT/FAA/CT-TN90/15 ........ N91-10034 #
DOT/FAA/CT-TN90/21 ........ N91-10029 #
DOT/FAA/CT-TN90/23 ........ N91-10028 #
DOT/FAA/CT-TN90/24 ........ N91-10052 #
DOT/FAA/CT-TN90/42 ........ N91-10084 #

DOT/FAA/CT-90/1-VOL-2 ........ N91-10033 #

DTRC/SME-90/20 ........ N91-10124 #

E-1499-PT-1 ........ N91-10149* #
E-4137 ........ N91-10065* #
E-4263-PT-2 ........ N91-10150* #
E-4407 ........ N91-10117* #
E-4720 ........ N91-10127* #
E-5352 ........ N91-10798* #
E-5507-1 ........ N91-10271* #
E-5643 ........ N91-10118* #
E-5674 ........ N91-10332* #
E-5732 ........ N91-10703* #
E-5737 ........ N91-10208* #
E-5743 ........ N91-10780* #
E-5753 ........ N91-10249* #
E-5781 ........ N91-10134* #
E-5848 ........ N91-10119* #

ECL-90-04 ........ N91-10785 #
ECL-90-06 ........ N91-10723 #
ECL-90-10 ........ N91-10210 #
ECL-90-12 ........ N91-10211 #

EMA-85-R-37 ........ N91-10548* #

EML-522 ........ N91-10539 #

EPA/230/05-89/051-APP-A ........ N91-10395 #
EPA/230/05-89/052-APP-B ........ N91-10396 #
EPA/230/05-89/053-APP-C-VOL-1 ........ N91-10394 #
EPA/230/05-89/053-APP-C-VOL-2 ........ N91-10397 #
EPA/230/05-89/054-APP-D ........ N91-10398 #
EPA/230/05-89/055-APP-E ........ N91-10399 #
EPA/230/05-89/056-APP-F ........ N91-10400 #
EPA/230/05-89/057-APP-G ........ N91-10401 #
EPA/230/05-89/058-APP-H ........ N91-10402 #
EPA/230/05-89/059-APP-I ........ N91-10403 #
EPA/230/05-89/060-APP-J ........ N91-10404 #
EPA/600/D-90/069 ........ N91-10416 #
EPA/600/D-90/077 ........ N91-10624 #

ESA-SP-306 ........ N91-10417 #

ETN-90-97142 ........ N91-10063 #
ETN-90-97188 ........ N91-10151 #
ETN-90-97360 ........ N91-10658
ETN-90-97568 ........ N91-10205 #
ETN-90-97569 ........ N91-10016 #
ETN-90-97570 ........ N91-10017 #
ETN-90-97571 ........ N91-10189 #
ETN-90-97572 ........ N91-10086 #
ETN-90-97573 ........ N91-10050 #
ETN-90-97574 ........ N91-10246 #
ETN-90-97575 ........ N91-10283 #
ETN-90-97576 ........ N91-10247 #
ETN-90-97577 ........ N91-10018 #
ETN-90-97578 ........ N91-10228 #
ETN-90-97581 ........ N91-10107 #
ETN-90-97582 ........ N91-10634 #
ETN-90-97583 ........ N91-10248 #
ETN-90-97584 ........ N91-10097 #
ETN-90-97587 ........ N91-10417 #
ETN-90-97609 ........ N91-10639 #
ETN-90-97626 ........ N91-10390 #
ETN-90-97628 ........ N91-10026 #
ETN-90-97629 ........ N91-10027 #
ETN-90-97631 ........ N91-10627 #
ETN-90-97647 ........ N91-10545
ETN-90-97648 ........ N91-10546
ETN-90-97649 ........ N91-10540
ETN-90-97665 ........ N91-10635 #
ETN-90-97687 ........ N91-10544 #
ETN-90-97696 ........ N91-10666 #
ETN-90-97697 ........ N91-10651 #
ETN-90-97698 ........ N91-10636 #
ETN-90-97699 ........ N91-10687 #

ETN-90-97700 N91-10667 #
ETN-90-97701 N91-10688 #
ETN-90-97702 N91-10668 #
ETN-90-97703 N91-10689 #
ETN-90-97704 N91-10637 #
ETN-90-97705 N91-10638 #
ETN-90-97716 N91-10669 #
ETN-90-97717 N91-10670 #
ETN-90-97718 N91-10671 #
ETN-90-97727 N91-10640 #
ETN-90-97728 N91-10680 #
ETN-90-97729 N91-10641 #
ETN-90-97730 N91-10642 #
ETN-90-97731 N91-10643 #
ETN-90-97732 N91-10672 #
ETN-90-97733 N91-10673 #
ETN-90-97734 N91-10674 #
ETN-90-97735 N91-10675 #
ETN-90-97736 N91-10690 #
ETN-90-97737 N91-10692 #
ETN-90-97738 N91-10676 #
ETN-90-97739 N91-10677 #
ETN-90-97740 N91-10678 #
ETN-90-97742 N91-10681 #
ETN-90-97743 N91-10682 #
ETN-90-97746 N91-10225 #
ETN-90-97747 N91-10714 #
ETN-90-97750 N91-10711 #
ETN-90-97755 N91-10549 #
ETN-90-97756 N91-10550 #
ETN-90-97757 N91-10596 #
ETN-90-97758 N91-10226 #
ETN-90-97759 N91-10597 #
ETN-90-97760 N91-10255 #
ETN-90-97767 N91-10443 #
ETN-90-97768 N91-10784 #
ETN-90-97771 N91-10285 #
ETN-90-97776 N91-10290 #
ETN-90-97780 N91-10837 #
ETN-90-97787 N91-10838 #
ETN-90-97792 N91-10819 #
ETN-90-97796 N91-10820 #
ETN-90-97797 N91-10833 #
ETN-90-97798 N91-10209 #
ETN-90-97800 N91-10834 #
ETN-90-97805 N91-10206 #
ETN-90-97806 N91-10691 #
ETN-90-97807 N91-10207 #
ETN-90-97808 N91-10380 #
ETN-90-97810 N91-10227 #
ETN-90-97811 N91-10284 #
ETN-90-97812 N91-10110 #
ETN-90-97818 N91-10723 #
ETN-90-97819 N91-10785 #
ETN-90-97820 N91-10210 #
ETN-90-97821 N91-10211 #
ETN-90-97822 N91-10196 #
ETN-90-97823 N91-10135 #
ETN-90-97825 N91-10652 #
ETN-90-97826 N91-10291 #
ETN-90-97836 N91-10108 #
ETN-90-97837 N91-10091 #
ETN-90-97838 N91-10055 #
ETN-90-97865 N91-10256 #
ETN-90-97866 N91-10257 #
ETN-90-97871 N91-10753
ETN-90-97872 N91-10808
ETN-90-97875 N91-10809 #
ETN-90-97876 N91-10286 #
ETN-90-97883 N91-10136 #
ETN-90-97885 N91-10109 #
ETN-90-97889 N91-10258 #
ETN-90-97912 N91-10683 #
ETN-90-97913 N91-10684 #
ETN-90-97914 N91-10685 #
ETN-90-97915 N91-10754 #
ETN-90-97916 N91-10035 #
ETN-90-97917 N91-10292 #
ETN-90-97918 N91-10654 #
ETN-90-97919 N91-10036 #
ETN-90-97920 N91-10644 #
ETN-90-97921 N91-10229 #
ETN-90-97922 N91-10272 #
ETN-90-97923 N91-10645 #
ETN-90-97924 N91-10646 #
ETN-90-97926 N91-10037 #
ETN-90-97927 N91-10259 #
ETN-90-97928 N91-10066 #
ETN-90-97929 N91-10067 #
ETN-90-97930 N91-10297 #
ETN-90-97938 N91-10260 #
ETN-90-97939 N91-10068 #
ETN-90-97940 N91-10069 #
ETN-90-97941 N91-10070 #
ETN-90-97942 N91-10137 #
ETN-90-97944 N91-10261 #
ETN-90-97945 N91-10056 #
ETN-90-97946 N91-10704 #
ETN-90-97947 N91-10647 #
ETN-90-97948 N91-10168 #
ETN-90-97949 N91-10336 #
ETN-90-97950 N91-10071 #
ETN-90-97951 N91-10262 #
ETN-90-97952 N91-10337 #
ETN-90-97955 N91-10072 #
ETN-90-97956 N91-10073 #
ETN-90-97957 N91-10138 #
ETN-90-97958 N91-10074 #
ETN-90-97959 N91-10075 #
ETN-90-97960 N91-10076 #
ETN-90-97961 N91-10298 #
ETN-90-97962 N91-10197 #
ETN-90-97963 N91-10139 #
ETN-90-97973 N91-10547 #
ETN-90-97974 N91-10198 #
ETN-90-97978 N91-10724 #
ETN-90-97988 N91-10263 #

FNAL-PUB-90/147-A N91-10695* #

FNAL-TM-1671 N91-10281 #

FNAL/C-90/151 N91-10147 #

FOA-E-40044-4.5 N91-10263 #

GDSS-HPT-89-001-VOL-1 N91-10111* #
GDSS-HPT-89-001-VOL-2 N91-10112* #

GL-TR-89-0098 N91-10264 #

GMCC-17 N91-10538 #

GP-3.34:85-86 N91-10797 #

GRI-90/0026 N91-10140 #
GRI-90/0036 N91-10273 #
GRI-90/0092 N91-10123 #
GRI-90/0135 N91-10235 #
GRI-90/0136 N91-10381 #

H-86-04 N91-10085* #
H-1549 N91-10328* #
H-1563 N91-10079* #

HL88-1003-1 N91-10169

IAEA-CN-53/C-2-2(1) N91-10739 #
IAEA-CN-53/C-4-4 N91-10740 #

IC-89/144 N91-10731 #
IC-89/277 N91-10693 #
IC-90/9 N91-10656 #
IC-90/20 N91-10657 #

ICASE-IR-13 N91-10599* #
ICASE-IR-14 N91-10664* #

ICASE-90-59 N91-10600* #
ICASE-90-61 N91-10010* #
ICASE-90-62 N91-10009* #
ICASE-90-64 N91-10628* #
ICASE-90-66 N91-10237* #
ICASE-90-67 N91-10629* #
ICASE-90-71 N91-10021* #
ICASE-90-72 N91-10022* #
ICASE-90-74 N91-10251* #
ICASE-90-75 N91-10250* #

IFIN-FT-346-1989 N91-10787 #
IFIN-FT-357-1989 N91-10788 #

IFSI-89-19 N91-10837 #
IFSI-90-4 N91-10838 #
IFSI-90-9 N91-10819 #
IFSI-90-14 N91-10820 #
IFSI-90-15 N91-10833 #
IFSI-90-16 N91-10209 #
IFSI-90-18 N91-10834 #

IFSR-443 N91-10744 #
IFSR-444 N91-10743 #
IFSR-445 N91-10745 #
IFSR-446 N91-10831 #

IFT-P-29/89 N91-10786 #

IPPCZ-279 N91-10726 #
IPPCZ-281 N91-10725 #

IS-T-1484 N91-10146 #
IS-T-1486 N91-10144 #
IS-T-1487 N91-10174 #

ISAL-90-0026 N91-10135 #

ISBN-0-309-04815-X N91-10415 #
ISBN-90-353-10144 N91-10596 #
ISBN-90-9002667-23 N91-10443 #
ISBN-90-9002803-X N91-10285 #
ISBN-90-9003079-4 N91-10290 #
ISBN-92-63-10734-9 N91-10547 #
ISBN-92-835-0540-9 N91-10042 #
ISBN-92-9092-066-1 N91-10417 #
ISBN-951-22-0117-8 N91-10254 #
ISBN-951-22-0248-4 N91-10023 #
ISBN-951-22-0329-4 N91-10024 #
ISBN-951-22-0398-7 N91-10025 #
ISBN-951-666-304-4 N91-10627 #
ISBN-951-754-987-3 N91-10253 #
ISBN-952-90-1784-7 N91-10724 #

ISL-CO-212/89 N91-10189 #
ISL-CO-213/89 N91-10086 #
ISL-CO-220/89 N91-10050 #
ISL-CO-221/89 N91-10246 #
ISL-CO-234/89 N91-10283 #
ISL-CO-235/89 N91-10247 #

ISL-PU-301/90 N91-10018 #

ISL-R-102/89-PT-1 N91-10205 #
ISL-R-107/89 N91-10016 #
ISL-R-109/89 N91-10017 #

ISSN-0038-0911 N91-10822 #
ISSN-0101-6113 N91-10327 #
ISSN-0169-1708 N91-10540
ISSN-0169-1708 N91-10545
ISSN-0169-1708 N91-10546
ISSN-0169-2690 N91-10672 #
ISSN-0169-2690 N91-10673 #
ISSN-0169-2690 N91-10674 #
ISSN-0169-2690 N91-10675 #
ISSN-0169-2690 N91-10676 #
ISSN-0169-2690 N91-10677 #
ISSN-0169-2690 N91-10678 #
ISSN-0169-2690 N91-10681 #
ISSN-0169-2690 N91-10682 #
ISSN-0169-2690 N91-10690 #
ISSN-0169-2690 N91-10692 #
ISSN-0171-1342 N91-10026 #
ISSN-0171-1342 N91-10027 #
ISSN-0171-1342 N91-10390 #
ISSN-0178-0719 N91-10753
ISSN-0178-0719 N91-10808
ISSN-0281-9945 N91-10263 #
ISSN-0348-9329 N91-10705 #
ISSN-0355-2713 N91-10627 #
ISSN-0358-2620 N91-10023 #
ISSN-0358-2620 N91-10024 #
ISSN-0358-2620 N91-10025 #
ISSN-0358-2620 N91-10253 #
ISSN-0358-2620 N91-10254 #
ISSN-0379-6566 N91-10417 #
ISSN-0389-4010 N91-10011 #
ISSN-0389-4010 N91-10012 #
ISSN-0389-4010 N91-10053 #
ISSN-0389-4010 N91-10054 #
ISSN-0389-4010 N91-10087 #
ISSN-0389-4010 N91-10099 #
ISSN-0389-4010 N91-10148 #
ISSN-0389-4010 N91-10190 #
ISSN-0389-4010 N91-10389 #
ISSN-0389-4010 N91-10679 #
ISSN-0389-4010 N91-10712 #
ISSN-0452-2892 N91-10038
ISSN-0452-2982 N91-10003
ISSN-0452-2982 N91-10030
ISSN-0452-2982 N91-10031
ISSN-0452-2982 N91-10057
ISSN-0452-2982 N91-10059
ISSN-0452-2982 N91-10060
ISSN-0452-2982 N91-10077
ISSN-0452-2982 N91-10080
ISSN-0452-2982 N91-10081
ISSN-0452-2982 N91-10082
ISSN-0452-2982 N91-10299
ISSN-0452-2982 N91-10601
ISSN-0452-2982 N91-10604
ISSN-0452-2982 N91-10605
ISSN-0524-7705 N91-10198 #
ISSN-0531-4496 N91-10809 #
ISSN-0915-633X N91-10740 #
ISSN-0915-633X N91-10750 #
ISSN-0915-633X N91-10751 #
ISSN-0915-633X N91-10752 #
ISSN-0922-5641 N91-10636 #

ISSN-0922-5641 N91-10637 #
ISSN-0922-5641 N91-10638 #
ISSN-0922-5641 N91-10651 #
ISSN-0922-5641 N91-10666 #
ISSN-0922-5641 N91-10667 #
ISSN-0922-5641 N91-10668 #
ISSN-0922-5641 N91-10669 #
ISSN-0922-5641 N91-10670 #
ISSN-0922-5641 N91-10671 #
ISSN-0922-5641 N91-10687 #
ISSN-0922-5641 N91-10688 #
ISSN-0922-5641 N91-10689 #
ISSN-0923-1714 N91-10643 #

ISU-ERI-AMES-91-110 N91-10019* #

JPL-PUBL-90-19 N91-10105* #
JPL-PUBL-90-20 N91-10204* #
JPL-PUBL-90-34 N91-10829* #
JPL-PUBL-90-38 N91-10222* #

JPRS-UEE-90-004 N91-10213 #
JPRS-UEE-90-006 N91-10214 #
JPRS-UEE-90-007 N91-10215 #
JPRS-UEE-90-008 N91-10216 #
JPRS-UEE-90-009 N91-10217 #

JPRS-UES-90-006-L N91-10376 #
JPRS-UES-90-007 N91-10377 #

JPRS-ULS-89-008 N91-10589 #
JPRS-ULS-89-010 N91-10590 #
JPRS-ULS-90-001 N91-10551 #
JPRS-ULS-90-005 N91-10572 #
JPRS-ULS-90-006 N91-10571 #
JPRS-ULS-90-008 N91-10570 #
JPRS-ULS-90-009 N91-10569 #
JPRS-ULS-90-010 N91-10568 #
JPRS-ULS-90-011 N91-10565 #
JPRS-ULS-90-012 N91-10556 #
JPRS-ULS-90-013 N91-10552 #

JPRS-UPM-90-003 N91-10694 #

JPRS-USP-89-009 N91-10088 #
JPRS-USP-90-001 N91-10089 #
JPRS-USP-90-002 N91-10090 #

JTN-90-80003 N91-10038
JTN-90-80004 N91-10080
JTN-90-80005 N91-10077
JTN-90-80006 N91-10604
JTN-90-80007 N91-10030
JTN-90-80008 N91-10081
JTN-90-80009 N91-10082
JTN-90-80010 N91-10031
JTN-90-80011 N91-10601
JTN-90-80012 N91-10299
JTN-90-80013 N91-10059
JTN-90-80014 N91-10060
JTN-90-80015 N91-10003
JTN-90-80016 N91-10605
JTN-90-80017 N91-10057

K/QT-331 N91-10145 #

KCP-613-4172 N91-10632 #
KCP-613-4204 N91-10185 #
KCP-613-4410 N91-10184 #

KNMI-TR-118 N91-10545
KNMI-TR-119 N91-10546
KNMI-TR-120 N91-10540

L-16735 N91-10301* #
L-16814 N91-10448* #

LA-UR-89-2875 N91-10276 #
LA-UR-90-1552 N91-10158 #
LA-UR-90-2272 N91-10715 #
LA-UR-90-2437 N91-10008 #
LA-UR-90-2516 N91-10155 #
LA-UR-90-2538 N91-10382 #
LA-UR-90-2614 N91-10803 #
LA-UR-90-2623 N91-10768 #
LA-UR-90-2631 N91-10836 #
LA-UR-90-2632 N91-10767 #
LA-UR-90-2633 N91-10776 #
LA-UR-90-2660 N91-10721 #
LA-UR-90-2671 N91-10774 #
LA-UR-90-2677 N91-10165 #
LA-UR-90-2678 N91-10164 #
LA-UR-90-2679 N91-10163 #
LA-UR-90-2699 N91-10176 #
LA-UR-90-2708 N91-10773 #
LA-UR-90-2714 N91-10663 #
LA-UR-90-2744 N91-10662 #
LA-UR-90-2755 N91-10697 #
LA-UR-90-2764 N91-10830 #
LA-UR-90-2792 N91-10771 #
LA-UR-90-2799 N91-10770 #
LA-UR-90-2801 N91-10162 #
LA-UR-90-2809 N91-10280 #
LA-UR-90-2845 N91-10279 #
LA-UR-90-2847 N91-10769 #
LA-UR-90-2851 N91-10720 #
LA-UR-90-2854 N91-10277 #
LA-UR-90-2864 N91-10740 #
LA-UR-90-2868 N91-10739 #
LA-UR-90-2887 N91-10282 #
LA-UR-90-2888 N91-10717 #
LA-UR-90-2903 N91-10817 #
LA-UR-90-2909 N91-10818 #
LA-UR-90-2915 N91-10266 #

LA-11692-MS-VOL-1 N91-10239 #
LA-11692-MS-VOL-3 N91-10242 #
LA-11692-MS-VOL-4 N91-10240 #
LA-11692-MS-VOL-5 N91-10241 #
LA-11692-MS-VOL-7 N91-10244 #
LA-11692-MS-VOL-8 N91-10243 #
LA-11706-MS N91-10777 #
LA-11903-MS N91-10187 #

LBL-27358 N91-10783 #
LBL-28515 N91-10223 #
LBL-28702 N91-10203 #
LBL-28993 N91-10775 #
LBL-29138 N91-10177 #
LBL-29206 N91-10129 #

LC-79-640375 N91-10822 #
LC-90-5427 N91-10415 #

LNCC-044/88 N91-10327 #

LPS-90-1 N91-10734* #

LSTM-266/T/89 N91-10258 #

LUIP-8902 N91-10705 #

LUNFD6/(NFFK-7098)1-14(1988) N91-10705 #

MA-55 N91-10627 #

MBB-UD-0568-90-PUB N91-10055 #

MBB-UO-0092-90-PUB N91-10108 #
MBB-UO-0092-90-PUB N91-10109 #
MBB-UO-0093-90-PUB N91-10091 #

MBB-Z-0306-90-PUB-KURZFASSUNG N91-10136 #

MEMO-INF-90-21 N91-10643 #

MEMO-841 N91-10672 #
MEMO-842 N91-10673 #
MEMO-843 N91-10674 #
MEMO-844 N91-10675 #
MEMO-845 N91-10690 #
MEMO-848 N91-10692 #
MEMO-851 N91-10676 #
MEMO-853 N91-10677 #
MEMO-854 N91-10678 #
MEMO-856 N91-10681 #
MEMO-857 N91-10682 #

MITSG-89-33 N91-10698 #

MPE-218 N91-10753
MPE-219 N91-10808

MSAT-X-164 N91-10105* #

MTB-316-87 N91-10194* #
MTB-325-87A N91-10157* #
MTB-402-89 N91-10131* #

NAL-TM-574 N91-10038
NAL-TM-575 N91-10080
NAL-TM-576 N91-10077
NAL-TM-578 N91-10604
NAL-TM-579 N91-10030
NAL-TM-580 N91-10081
NAL-TM-581 N91-10082
NAL-TM-582 N91-10031
NAL-TM-583 N91-10601
NAL-TM-584 N91-10299
NAL-TM-585-PT-1 N91-10059
NAL-TM-587-PT-2 N91-10060
NAL-TM-588 N91-10003
NAL-TM-589 N91-10605
NAL-TM-590 N91-10057

NAL-TR-1016T N91-10012 #
NAL-TR-1027T N91-10011 #
NAL-TR-1050T N91-10712 #
NAL-TR-1051 N91-10053 #
NAL-TR-1052T N91-10054 #
NAL-TR-1053 N91-10148 #
NAL-TR-1054 N91-10087 #
NAL-TR-1055 N91-10679 #
NAL-TR-1056 N91-10389 #
NAL-TR-1061 N91-10099 #
NAL-TR-1062T N91-10190 #

NAS 1.15:4186 N91-10045* #
NAS 1.15:4202 N91-10103* #
NAS 1.15:83665 N91-10149* #
NAS 1.15:89785 N91-10100* #
NAS 1.15:100594 N91-10106* #
NAS 1.15:100660 N91-10245* #
NAS 1.15:101028 N91-10049* #
NAS 1.15:101368 N91-10117* #
NAS 1.15:101468 N91-10150* #
NAS 1.15:102208 N91-10014* #
NAS 1.15:102542 N91-10798* #
NAS 1.15:102684 N91-10699* #
NAS 1.15:102709 N91-10221* #
NAS 1.15:102717 N91-10058* #
NAS 1.15:102722 N91-10078* #
NAS 1.15:102728 N91-10128* #
NAS 1.15:102733 N91-10020* #
NAS 1.15:102736 N91-10702* #
NAS 1.15:102742 N91-10182* #
NAS 1.15:102793 N91-10268* #
NAS 1.15:102805 N91-10013* #
NAS 1.15:102847 N91-10252* #
NAS 1.15:102867 N91-10015* #
NAS 1.15:102910 N91-10378* #
NAS 1.15:103227 N91-10118* #
NAS 1.15:103247 N91-10332* #
NAS 1.15:103282 N91-10208* #
NAS 1.15:103288 N91-10271* #
NAS 1.15:103293 N91-10249* #
NAS 1.15:103314 N91-10606* #
NAS 1.15:103445 N91-10543* #
NAS 1.15:103446 N91-10441* #
NAS 1.15:103451 N91-10816* #
NAS 1.15:103462 N91-10393* #
NAS 1.15:103501 N91-10194* #
NAS 1.15:103507 N91-10191* #
NAS 1.15:103514 N91-10294* #
NAS 1.15:103516 N91-10832* #
NAS 1.15:103608 N91-10703* #
NAS 1.15:103616 N91-10780* #
NAS 1.15:103632 N91-10134* #
NAS 1.15:103657 N91-10119* #
NAS 1.15:103808 N91-10157* #
NAS 1.15:103809 N91-10131* #
NAS 1.15:103813 N91-10442* #
NAS 1.21:7011(341) N91-10594*
NAS 1.21:7037(256) N91-10002*
NAS 1.21:7064-SUPPL-4 N91-10804* #
NAS 1.26:3974 N91-10548* #
NAS 1.26:4319 N91-10098* #
NAS 1.26:171944 N91-10085* #
NAS 1.26:177569 N91-10048* #
NAS 1.26:180335 N91-10810* #
NAS 1.26:180428 N91-10755* #
NAS 1.26:180489 N91-10293* #
NAS 1.26:181352 N91-10039* #
NAS 1.26:182100 N91-10600* #
NAS 1.26:182102 N91-10010* #
NAS 1.26:182103 N91-10009* #
NAS 1.26:182123 N91-10065* #
NAS 1.26:183972 N91-10111* #
NAS 1.26:183973 N91-10112* #
NAS 1.26:183974 N91-10113* #
NAS 1.26:183975 N91-10114* #
NAS 1.26:184026 N91-10115* #
NAS 1.26:184565 N91-10333* #
NAS 1.26:185289 N91-10116* #
NAS 1.26:185302 N91-10133* #
NAS 1.26:185614 N91-10102* #
NAS 1.26:185874 N91-10707* #
NAS 1.26:185879 N91-10621* #
NAS 1.26:185880 N91-10618* #
NAS 1.26:185881 N91-10619* #
NAS 1.26:185882 N91-10620* #
NAS 1.26:186023 N91-10122* #
NAS 1.26:186419 N91-10695* #
NAS 1.26:186532 N91-10101* #
NAS 1.26:186545 N91-10047* #
NAS 1.26:186612 N91-10591* #
NAS 1.26:186929 N91-10623* #
NAS 1.26:186953 N91-10379* #

NAS 1.26:186955 N91-10170* #
NAS 1.26:186958 N91-10083* #
NAS 1.26:186976 N91-10201* #
NAS 1.26:187009 N91-10041* #
NAS 1.26:187010 N91-10061* #
NAS 1.26:187011 N91-10040* #
NAS 1.26:187017 N91-10763* #
NAS 1.26:187020 N91-10126* #
NAS 1.26:187024 N91-10735* #
NAS 1.26:187238 N91-10734* #
NAS 1.26:187252 N91-10795* #
NAS 1.26:187259 N91-10794* #
NAS 1.26:187261 N91-10793* #
NAS 1.26:187325 N91-10238* #
NAS 1.26:187332 N91-10595* #
NAS 1.26:187333 N91-10633* #
NAS 1.26:187336 N91-10105* #
NAS 1.26:187337 N91-10829* #
NAS 1.26:187338 N91-10204* #
NAS 1.26:187339 N91-10222* #
NAS 1.26:187343 N91-10019* #
NAS 1.26:187352 N91-10335* #
NAS 1.26:187353 N91-10334* #
NAS 1.26:187438 N91-10628* #
NAS 1.26:187439 N91-10237* #
NAS 1.26:187440 N91-10629* #
NAS 1.26:187442 N91-10599* #
NAS 1.26:187443 N91-10664* #
NAS 1.26:187455 N91-10021* #
NAS 1.26:187456 N91-10022* #
NAS 1.26:187458 N91-10251* #
NAS 1.26:187459 N91-10250* #
NAS 1.55:3051 N91-10574* #
NAS 1.55:3064 N91-10301* #
NAS 1.55:3083 N91-10448* #
NAS 1.60:2375 N91-10007* #
NAS 1.60:3022 N91-10079* #
NAS 1.60:3056 N91-10328* #
NAS 1.60:3058 N91-10092* #
NAS 1.61:1236 N91-10127* #

NAS-SR-1328 N91-10032 #

NASA-CP-3051 N91-10574* #
NASA-CP-3064 N91-10301* #
NASA-CP-3083 N91-10448* #

NASA-CR-3974 N91-10548* #
NASA-CR-4319 N91-10098* #
NASA-CR-171944 N91-10085* #
NASA-CR-177569 N91-10048* #
NASA-CR-180335 N91-10810* #
NASA-CR-180428 N91-10755* #
NASA-CR-180489 N91-10293* #
NASA-CR-181352 N91-10039* #
NASA-CR-182100 N91-10600* #
NASA-CR-182102 N91-10010* #
NASA-CR-182103 N91-10009* #
NASA-CR-182123 N91-10065* #
NASA-CR-183972 N91-10111* #
NASA-CR-183973 N91-10112* #
NASA-CR-183974 N91-10113* #
NASA-CR-183975 N91-10114* #
NASA-CR-184026 N91-10115* #
NASA-CR-184565 N91-10333* #
NASA-CR-185289 N91-10116* #
NASA-CR-185302 N91-10133* #
NASA-CR-185614 N91-10102* #
NASA-CR-185874 N91-10707* #
NASA-CR-185879 N91-10621* #
NASA-CR-185880 N91-10618* #
NASA-CR-185881 N91-10619* #
NASA-CR-185882 N91-10620* #
NASA-CR-186023 N91-10122* #
NASA-CR-186419 N91-10695* #
NASA-CR-186532 N91-10101* #
NASA-CR-186545 N91-10047* #
NASA-CR-186612 N91-10591* #
NASA-CR-186929 N91-10623* #
NASA-CR-186953 N91-10379* #
NASA-CR-186955 N91-10170* #
NASA-CR-186958 N91-10083* #
NASA-CR-186976 N91-10201* #
NASA-CR-187009 N91-10041* #
NASA-CR-187010 N91-10061* #
NASA-CR-187011 N91-10040* #
NASA-CR-187017 N91-10763* #
NASA-CR-187020 N91-10126* #
NASA-CR-187024 N91-10735* #
NASA-CR-187238 N91-10734* #
NASA-CR-187252 N91-10795* #
NASA-CR-187259 N91-10794* #
NASA-CR-187261 N91-10793* #
NASA-CR-187325 N91-10238* #
NASA-CR-187332 N91-10595* #
NASA-CR-187333 N91-10633* #
NASA-CR-187336 N91-10105* #
NASA-CR-187337 N91-10829* #
NASA-CR-187338 N91-10204* #
NASA-CR-187339 N91-10222* #
NASA-CR-187343 N91-10019* #
NASA-CR-187352 N91-10335* #
NASA-CR-187353 N91-10334* #
NASA-CR-187438 N91-10628* #
NASA-CR-187439 N91-10237* #
NASA-CR-187440 N91-10629* #
NASA-CR-187442 N91-10599* #
NASA-CR-187443 N91-10664* #
NASA-CR-187455 N91-10021* #
NASA-CR-187456 N91-10022* #
NASA-CR-187458 N91-10251* #
NASA-CR-187459 N91-10250* #

NASA-RP-1236 N91-10127* #

NASA-SP-7011(341) N91-10594*
NASA-SP-7037(256) N91-10002*
NASA-SP-7064-SUPPL-4 N91-10804* #

NASA-TM-4186 N91-10045* #
NASA-TM-4202 N91-10103* #
NASA-TM-83665 N91-10149* #
NASA-TM-89785 N91-10100* #
NASA-TM-100594 N91-10106* #
NASA-TM-100660 N91-10245* #
NASA-TM-101028 N91-10049* #
NASA-TM-101368 N91-10117* #
NASA-TM-101468 N91-10150* #
NASA-TM-102208 N91-10014* #
NASA-TM-102542 N91-10798* #
NASA-TM-102684 N91-10699* #
NASA-TM-102709 N91-10221* #
NASA-TM-102717 N91-10058* #
NASA-TM-102722 N91-10078* #
NASA-TM-102728 N91-10128* #
NASA-TM-102733 N91-10020* #
NASA-TM-102736 N91-10702* #
NASA-TM-102742 N91-10182* #
NASA-TM-102793 N91-10268* #
NASA-TM-102805 N91-10013* #
NASA-TM-102847 N91-10252* #
NASA-TM-102867 N91-10015* #
NASA-TM-102910 N91-10378* #
NASA-TM-103227 N91-10118* #
NASA-TM-103247 N91-10332* #
NASA-TM-103282 N91-10208* #
NASA-TM-103288 N91-10271* #
NASA-TM-103293 N91-10249* #
NASA-TM-103314 N91-10606* #
NASA-TM-103445 N91-10543* #
NASA-TM-103446 N91-10441* #
NASA-TM-103451 N91-10816* #
NASA-TM-103462 N91-10393* #
NASA-TM-103501 N91-10194* #
NASA-TM-103507 N91-10191* #
NASA-TM-103514 N91-10294* #
NASA-TM-103516 N91-10832* #
NASA-TM-103608 N91-10703* #
NASA-TM-103616 N91-10780* #
NASA-TM-103632 N91-10134* #
NASA-TM-103657 N91-10119* #
NASA-TM-103808 N91-10157* #
NASA-TM-103809 N91-10131* #
NASA-TM-103813 N91-10442* #

NASA-TP-2375 N91-10007* #
NASA-TP-3022 N91-10079* #
NASA-TP-3056 N91-10328* #
NASA-TP-3058 N91-10092* #

NCAR/CT-124 N91-10828 #

NEDO-P-8912 N91-10387 #

NIFS-33 N91-10752 #
NIFS-34 N91-10750 #
NIFS-35 N91-10751 #
NIFS-37 N91-10749 #

NIPER-422 N91-10791 #

NIST/GCR-90/574 N91-10193 #

NIST/SP-260 N91-10120 #
NIST/SP-783 N91-10800 #

NIST/TN-1270 N91-10231 #

NOAA-NESDIS-27 N91-10446 #

NOAA-TM-ERL-WPL-176 N91-10622 #
NOAA-TM-ERL-WPL-179 N91-10413 #

NOAA-TM-NWS-SR-129 N91-10414 #

NOAA-TR-NESDIS-44 N91-10093 #

NRL-MP-88049-4 N91-10151 #

NTIA-89-252 N91-10796 #
NTIA-90-259 N91-10199 #

OB-56 N91-10698 #

ORNL-6622 N91-10046 #

ORNL/ATD-33 N91-10125 #

ORNL/FTR-3709 N91-10716 #
ORNL/FTR-3714 N91-10408 #
ORNL/FTR-3715 N91-10653 #
ORNL/FTR-3720 N91-10181 #

ORNL/SUB-86-SB195/1 N91-10288 #

ORNL/TM-11012 N91-10178 #
ORNL/TM-11542 N91-10289 #

OTN-027462 N91-10136 #
OTN-027615 N91-10108 #
OTN-027616 N91-10091 #
OTN-027636 N91-10055 #
OTN-027668 N91-10109 #

OUEL-1766/89 N91-10683 #
OUEL-1778/89 N91-10684 #
OUEL-1799/89 N91-10685 #
OUEL-1806/89 N91-10754 #
OUEL-1807/90 N91-10035 #
OUEL-1808/90 N91-10292 #
OUEL-1809/90 N91-10654 #
OUEL-1812/90 N91-10036 #
OUEL-1822/90 N91-10644 #
OUEL-1823/90 N91-10229 #
OUEL-1825/90 N91-10272 #
OUEL-1826/90 N91-10645 #
OUEL-1827/90 N91-10646 #
OUEL-1833/90 N91-10037 #

PARC-EDL-89-4 N91-10686 #

PATENTS-US-A7315871 N91-10602 #
PATENTS-US-A7317389 N91-10648 #
PATENTS-US-A7336377 N91-10095 #
PATENTS-US-A7341019 N91-10094 #
PATENTS-US-A7357246 N91-10603 #
PATENTS-US-A7376071 N91-10383 #
PATENTS-US-A7384604 N91-10220 #

PB90-147935 N91-10391 #
PB90-147943 N91-10392 #
PB90-171588 N91-10394 #
PB90-171596 N91-10397 #
PB90-171737 N91-10797 #
PB90-171968 N91-10395 #
PB90-172008 N91-10796 #
PB90-172230 N91-10400 #
PB90-172297 N91-10399 #
PB90-172313 N91-10402 #
PB90-172626 N91-10396 #
PB90-173188 N91-10404 #
PB90-173238 N91-10398 #
PB90-173881 N91-10401 #
PB90-173899 N91-10403 #
PB90-179967 N91-10447 #
PB90-181504 N91-10393* #
PB90-182338 N91-10822 #
PB90-183310 N91-10120 #
PB90-183633 N91-10698 #
PB90-185646 N91-10405 #
PB90-190588 N91-10686 #
PB90-195363 N91-10823 #
PB90-195371 N91-10824 #
PB90-201229 N91-10655 #
PB90-205196 N91-10140 #
PB90-207820 N91-10199 #
PB90-208877 N91-10825 #
PB90-208885 N91-10826 #
PB90-214487 N91-10828 #
PB90-215146 N91-10799 #
PB90-215187 N91-10805 #
PB90-216771 N91-10273 #
PB90-218827 N91-10001 #
PB90-219601 N91-10231 #
PB90-220310 N91-10622 #
PB90-222126 N91-10538 #
PB90-222159 N91-10415 #
PB90-222324 N91-10537 #
PB90-226028 N91-10411 #

PB90-226036 ........ N91-10412 #
PB90-226341 ........ N91-10381 #
PB90-227976 ........ N91-10193 #
PB90-233115 ........ N91-10032 #
PB90-233305 ........ N91-10816* #
PB90-235482 ........ N91-10413 #
PB90-235490 ........ N91-10414 #
PB90-242389 ........ N91-10235 #
PB90-244435 ........ N91-10800 #
PB90-246224 ........ N91-10416 #
PB90-246398 ........ N91-10624 #
PB90-247388 ........ N91-10123 #

PD-CF-9012 ........ N91-10232 #

PD-ST-9027 ........ N91-10625 #

PNL-SA-17201 ........ N91-10173 #
PNL-SA-17225 ........ N91-10778 #
PNL-SA-17230 ........ N91-10180 #
PNL-SA-17302 ........ N91-10295 #
PNL-SA-17526 ........ N91-10104 #
PNL-SA-17536 ........ N91-10542 #
PNL-SA-17819 ........ N91-10592 #
PNL-SA-17825 ........ N91-10166 #
PNL-SA-17876 ........ N91-10766 #
PNL-SA-17987 ........ N91-10541 #
PNL-SA-17988 ........ N91-10440 #
PNL-SA-17992 ........ N91-10388 #
PNL-SA-18059 ........ N91-10179 #
PNL-SA-18090 ........ N91-10631 #
PNL-SA-18162 ........ N91-10143 #
PNL-SA-18229 ........ N91-10160 #
PNL-SA-18314 ........ N91-10573 #
PNL-SA-18391 ........ N91-10593 #

PNR-90634 ........ N91-10063 #
PNR-90679 ........ N91-10259 #
PNR-90681 ........ N91-10066 #
PNR-90682 ........ N91-10067 #
PNR-90683 ........ N91-10297 #
PNR-90706 ........ N91-10260 #
PNR-90707 ........ N91-10068 #
PNR-90709 ........ N91-10069 #
PNR-90710 ........ N91-10070 #
PNR-90713 ........ N91-10137 #
PNR-90717 ........ N91-10261 #
PNR-90719 ........ N91-10056 #
PNR-90720 ........ N91-10704 #
PNR-90722 ........ N91-10647 #
PNR-90723 ........ N91-10168 #
PNR-90730 ........ N91-10336 #
PNR-90737 ........ N91-10071 #
PNR-90739 ........ N91-10262 #
PNR-90742 ........ N91-10337 #
PNR-90750 ........ N91-10072 #
PNR-90752 ........ N91-10073 #
PNR-90753 ........ N91-10138 #
PNR-90754-PT-1 ........ N91-10074 #
PNR-90755 ........ N91-10075 #
PNR-90758 ........ N91-10076 #
PNR-90759 ........ N91-10298 #
PNR-90763 ........ N91-10197 #
PNR-90764 ........ N91-10139 #

PREPRINT-166 ........ N91-10257 #

PUBL-91190 ........ N91-10115* #

R-598 ........ N91-10655 #

REPT-B-17 ........ N91-10253 #
REPT-B-21 ........ N91-10254 #
REPT-B-24 ........ N91-10023 #
REPT-B-25 ........ N91-10024 #
REPT-B-28 ........ N91-10025 #

REPT-89-89 ........ N91-10666 #
REPT-89-90 ........ N91-10651 #
REPT-89-028 ........ N91-10658
REPT-90-1 ........ N91-10550 #
REPT-90-2 ........ N91-10549 #
REPT-90-01 ........ N91-10636 #
REPT-90-02 ........ N91-10687 #
REPT-90-03 ........ N91-10667 #
REPT-90-04 ........ N91-10688 #
REPT-90-05 ........ N91-10668 #
REPT-90-06 ........ N91-10689 #
REPT-90-08 ........ N91-10637 #
REPT-90-09 ........ N91-10638 #
REPT-90-18-VOL-1 ........ N91-10618* #
REPT-90-18-VOL-2 ........ N91-10619* #
REPT-90-18-VOL-3 ........ N91-10620* #
REPT-90-18-VOL-4 ........ N91-10621* #
REPT-90-23 ........ N91-10669 #
REPT-90-36 ........ N91-10670 #
REPT-90-37 ........ N91-10671 #
REPT-025921-14-T ........ N91-10201* #
REPT-025921-15-T ........ N91-10623* #

RI/RD89-261-VOL-4 ........ N91-10114* #

RSRE-MEMO-4385 ........ N91-10639 #

S-597 ........ N91-10574* #

SAND-89-2284C ........ N91-10762 #
SAND-89-2771C ........ N91-10765 #
SAND-89-2877C ........ N91-10696 #
SAND-90-0593 ........ N91-10700 #
SAND-90-0647C ........ N91-10183 #
SAND-90-1002C ........ N91-10736 #
SAND-90-1085C ........ N91-10218 #
SAND-90-1491C ........ N91-10713 #
SAND-90-1583C ........ N91-10329 #
SAND-90-1680 ........ N91-10202 #
SAND-90-1693C ........ N91-10154 #
SAND-90-1694C ........ N91-10153 #
SAND-90-1944C ........ N91-10275 #
SAND-90-2018C ........ N91-10737 #
SAND-90-2058C ........ N91-10172 #
SAND-90-2060C ........ N91-10132 #
SAND-90-2066C ........ N91-10649 #
SAND-90-2255C ........ N91-10630 #

SEL-88-004 ........ N91-10606* #

SERI/TP-211-3896 ........ N91-10384 #
SERI/TP-211-3907 ........ N91-10756 #

SFB-210/E/59 ........ N91-10286 #

SGD-545-PT-1 ........ N91-10822 #
SGD-546-PT-1 ........ N91-10823 #
SGD-546-PT-2 ........ N91-10824 #
SGD-547-PT-1 ........ N91-10825 #
SGD-547-PT-2 ........ N91-10826 #
SGD-548-PT-1 ........ N91-10411 #
SGD-548-PT-2 ........ N91-10412 #

SRI-PYU-2970 ........ N91-10140 #

SSRP-90/03 ........ N91-10333* #

SU-SLAC-PUB-5218 ........ N91-10789 #

SU-SLAC-351 ........ N91-10790 #

SU-SOL-90-10 ........ N91-10660 #

TR-90-1165 ........ N91-10633* #

TRB/TRR-1219 ........ N91-10415 #

TW-89-14-PT-3 ........ N91-10640 #
TW-90-01-B ........ N91-10680 #
TW-90-03-PT-4 ........ N91-10641 #
TW-90-04-PT-5 ........ N91-10642 #

TWR-17546-VOL-7 ........ N91-10115* #

UCRL-CR-104544 ........ N91-10130 #
UCRL-CR-104574 ........ N91-10331 #
UCRL-CR-104583 ........ N91-10659 #
UCRL-CR-104639 ........ N91-10186 #

UCRL-ID-103344 ........ N91-10706 #
UCRL-ID-103495-89 ........ N91-10802 #

UCRL-JC-103247 ........ N91-10142 #
UCRL-JC-103469 ........ N91-10161 #
UCRL-JC-104204 ........ N91-10626 #
UCRL-JC-104241 ........ N91-10733 #
UCRL-JC-104336 ........ N91-10267 #
UCRL-JC-104693 ........ N91-10661 #
UCRL-JC-104734 ........ N91-10409 #
UCRL-JC-104774 ........ N91-10650 #

UCRL-101768 ........ N91-10278 #
UCRL-101945-REV-2 ........ N91-10732 #
UCRL-102468 ........ N91-10096 #
UCRL-102583 ........ N91-10718 #
UCRL-102625 ........ N91-10219 #
UCRL-102807 ........ N91-10719 #

UMIACS-TR-88-92 ........ N91-10608* #

US-PATENT-APPL-SN-315871 ........ N91-10602 #
US-PATENT-APPL-SN-317389 ........ N91-10648 #
US-PATENT-APPL-SN-336377 ........ N91-10095 #
US-PATENT-APPL-SN-341019 ........ N91-10094 #
US-PATENT-APPL-SN-357246 ........ N91-10603 #
US-PATENT-APPL-SN-376071 ........ N91-10383 #
US-PATENT-APPL-SN-384604 ........ N91-10220 #

UWAERP-23 ........ N91-10738 #

UWPR-89-2 ........ N91-10741 #

VTT-TUTK-656 ........ N91-10701 #

WCAP-3 ........ N91-10444 #

WCDP-1 ........ N91-10445 #

WHC-SA-0872 ........ N91-10296 #

WMO-16-VOL-3 ........ N91-10393* #
WMO-734 ........ N91-10547 #

WMO/TD-224 ........ N91-10444 #
WMO/TD-227 ........ N91-10445 #

Y-2428 ........ N91-10330 #

Y/DW-1008 ........ N91-10175 #

# Appendix

## NASA SCIENTIFIC AND TECHNICAL INFORMATION PROGRAM PRODUCTS AND SERVICES

The NASA Scientific and Technical Information (STI) program provides for the collection and announcement of aerospace-related reports and literature obtained worldwide through agreements and exchanges. The result of the collection is the comprehensive NASA STI Database that covers aeronautics, space, and supporting disciplines.

The STI Database, documents generated or obtained by NASA, and products and services derived from or supporting the database are made available to the NASA research community and to the public. Descriptions and sources of these items are presented in the following pages.

*Scientific and Technical Aerospace Reports* (*STAR*) is an abstract journal, listing citations with abstracts for aerospace-related reports obtained from worldwide sources. *STAR* is issued on the 8th and 23rd of each month and announces current documents that have been entered into the NASA STI Database during the previous two weeks. The reports are of the following types:

- NASA, NASA contractor, and NASA grantee reports;
- Reports issued by other U.S. Government agencies, domestic and foreign institutions, universities, and private firms;
- Translations in report form;
- NASA-owned patents and patent applications;
- Other U.S. Government agency and foreign patents and patent applications;
- Domestic and foreign dissertations and theses.

Journal, book, and conference literature, journal translations, and certain foreign dissertations having the same subject scope as *STAR* are announced in a companion journal, *International Aerospace Abstracts* (*IAA*). *IAA* is issued on the 1st and 15th of each month and is available from the American Institute of Aeronautics and Astronautics, Technical Information Service, 555 West 57th Street, 12th Floor, New York, NY 10019.

## ELIGIBILITY AND REGISTRATION FOR NASA STI PRODUCTS AND SERVICES

Organizations of the type listed below that have registered with NASA can receive products and services.

- NASA offices and installations, contractors, subcontractors, grantees, and consultants;
- Other U.S. Government agencies and their contractors;
- Libraries in the United States that have arrangements with NASA to maintain collections of NASA documents for public reference;
- Other organizations in the United States having a need for NASA documents in work related to aeronautics and space research;
- Organizations abroad that have established reciprocal documents exchange arrangements with NASA.

Only the central service points or central points of document acquisition and control within qualified organizations are eligible to register for NASA STI products and services. Domestic organizations that may be eligible to receive various classes of NASA publications and services should address their requests for registration or further information to:

NASA Scientific and Technical Information Facility
ATTN: Registration Services
P.O. Box 8757
BWI Airport, MD 21240
301-621-0153

Organizations abroad should direct requests to:

National Aeronautics and Space Administration
Director, Scientific and Technical Information Divison
Code NTT
Washington, DC 20546
USA
703-271-5640

## SUBJECT SCOPE

The subject scope of *STAR* and *IAA* includes all aspects of aeronautics and space research and development, supporting basic and applied research, and applications. Aerospace aspects of Earth resources, energy development, conservation, oceanography, environmental protection, urban transportation, and other topics of high national priority are also covered.

## HOW TO USE *STAR* SUBJECT CATEGORIES

Abstracts in *STAR* are categorized by 10 major subject divisions that are divided further into 76 specific subject categories. The subject divisions and categories are listed in the Table of Contents together with a note for each that defines its scope and provides any cross-references. For example:

> **16 SPACE TRANSPORTATION**
> Includes passenger and cargo space transportation, e.g., shuttle operations; and space rescue techniques. For related information see also *03 Air Transportation and Safety* and *18 Spacecraft Design, Testing and Performance.* For space suits see *54 Man/System Technology and Life Support.*

## CROSS-REFERENCES

Individual *STAR* abstracts are not ordinarily cross-referenced, except for certain conference reports or book translations that have had separate abstracts written for their component papers or chapters. Citations and abstracts of the components follow immediately after those of the parent document. When the subject content of a component differs sufficiently from the general content of the parent, a cross-reference citation also is printed at the end of the category to which it normally would have been assigned if it were independent.

## DOCUMENTS ON MICROFICHE

Documents available on microfiche are designated by a pound sign (#) following the accession number.

## LIMITED REPRODUCIBILITY

A note of limited reproducibility appears in the citation, if there are factors affecting the reproducibility of more than 20% of the document. These factors include faint or broken type, color photographs, black and white photographs, foldouts, dot matrix print, or some other factor that limits the reproducibility of the document. This notation also appears on the microfiche header with the specific factor checked off on a list visible in the second frame.

## COLOR COPIES

An increasing number of NASA scientific and technical reports are being produced with color graphs, charts, illustrations, and photographs. An indication that a document has color pages follows the source and pricing (SAP) information in the *STAR* citation.

Registered users of the NASA Scientific and Technical Information Program will receive ordered documents with color at no additional cost, as long as stock copies of the document are available. Otherwise, an additional fee of $2.00 per color page will be charged. The NASA STI Facility staff will contact registered users to determine individual user's needs.

## NASA PATENTS AND PATENT APPLICATIONS

Patents and patent applications owned by NASA are announced in *STAR* under appropriate subject categories and are referenced in the *STAR* indexes. In the Report/Accession Number Index, patents are indexed by the NASA Case Number, and the U.S. Patent Class. Patent applications are indexed by the NASA Case Number and the U.S. Patent Application Serial Number.

Printed copies of patents (which are not microfiched) are available for purchase from the U.S. Patent and Trademark Office.

NASA patent application specifications are sold in both paper copy and microfiche by the National Technical Information Service (NTIS). The US-Patent-Appl-SN-number should be used in ordering either paper copy or microfiche from NTIS.

When ordering patents, the U.S. Patent Number should be used, and payment must be remitted in advance, by money order or check payable to the Commissioner of Patents and Trademarks. Prepaid purchase coupons for ordering are also available from the U.S. Patent and Trademark Office.

The patents and patent applications announced in *STAR* are owned by NASA and are available for royalty-free licensing. Requests for licensing terms and further information should be addressed to:

National Aeronautics and Space Administration
Associate General Counsel for Intellectual Property
Code GP
Washington, DC 20546

## SOURCES FOR DOCUMENTS

One or more sources from which a document announced in *STAR* is available to the public is given in each citation. The most commonly indicated sources and their acronyms or abbreviations are listed on page A-6. If the publication is available from a source other than those listed, the publisher and address will be displayed on the availability line or in combination with the corporate source line.

Avail: NTIS. Sold by the National Technical Information Service. Prices for hard copy (HC) and microfiche (MF) are indicated by a price code following the letters HC or MF in the *STAR* citation. Current values for the price codes are given in the tables on page A-7.

Initially distributed microfiche under the NTIS SRIM (Selected Research in Microfiche) is available at greatly reduced unit prices. For this service and for information concerning subscription to NASA printed reports, consult the NTIS Subscription Section, Springfield, VA 22161.

NOTE ON ORDERING DOCUMENTS: When ordering NASA publications (those followed by the * symbol), use the N accession number. NASA patent applications (only the specifications are offered) should be ordered by the US-Patent-Appl-SN number. Non-NASA publications (no asterisk) should be ordered by the AD, PB, or other *report number* shown on the last line of the citation, not by the N accession number. It is also advisable to cite the title and other bibliographic identification.

Avail: SOD (or GPO). Sold by the Superintendent of Documents, U.S. Government Printing Office, in hard copy. The current price and order number are given following the availability line. (NTIS will fill microfiche requests, as indicated above, for those documents identified by a # symbol.)

Avail: BLL (formerly NLL): British Library Lending Division, Boston Spa, Wetherby, Yorkshire, England. Photocopies available from this organization at the price shown. (If none is given, address inquiry to the BLL.)

Avail: DOE Depository Libraries. Organizations in U.S. cities and abroad that maintain collections of Department of Energy reports, usually in microfiche form, are listed in *Energy Research Abstracts*. Services available from the DOE and its depositories are described in a booklet, *DOE Technical Information Center - Its Functions and Services* (TID-4660), which may be obtained without charge from the DOE Technical Information Center.

Avail: ESDU. Pricing information on specific data, computer programs, and details on Engineering Sciences Data Unit (ESDU) topic categories can be obtained from ESDU International Ltd. Requesters in North America should use the Virginia address while all other requesters should use the London address, both of which are on page A-6.

Avail: Fachinformationszentrum, Karlsruhe. Sold by the Fachinformationszentrum Energie, Physik, Mathematik GMBH, Eggenstein Leopoldshafen, Federal Republic of Germany, at the price shown in deutschmarks (DM).

Avail: HMSO. Publications of Her Majesty's Stationery Office are sold in the U.S. by Pendragon House, Inc. (PHI), Redwood City, CA. The U.S. price (including a service and mailing charge) is given, or a conversion table may be obtained from PHI.

Avail: NASA Public Document Rooms. Documents so indicated may be examined at or purchased from the National Aeronautics and Space Administration, Public Documents Room (Room 126), 600 Independence Ave., S.W., Washington, DC 20546, or public document rooms located at NASA installations, and the NASA Pasadena Office at the Jet Propulsion Laboratory.

Avail: Univ. Microfilms. Documents so indicated are dissertations selected from *Dissertation Abstracts* and are sold by University Microfilms as xerographic copy (HC) and microfilm. All requests should cite the author and the Order Number as they appear in the citation.

Avail: US Patent and Trademark Office. Sold by Commissioner of Patents and Trademarks, U.S. Patent and Trademark Office, at the standard price of $1.50 each, postage free. (See discussion of NASA patents and patent applications below.)

Avail: (US Sales Only). These foreign documents are available to users within the United States from the National Technical Information Service (NTIS). They are available to users outside the United States through the International Nuclear Information Service (INIS) representative in their country, or by applying directly to the issuing organization.

Avail: USGS. Originals of many reports from the U.S. Geological Survey, which may contain color illustrations, or otherwise may not have the quality of illustrations preserved in the microfiche or facsimile reproduction, may be examined by the public at the libraries of the USGS field offices whose addresses are listed on page A-6. The libraries may be queried concerning the availability of specific documents and the possible utilization of local copying services, such as color reproduction.

Avail: Issuing Activity, or Corporate Author, or no indication of availability. Inquiries as to the availability of these documents should be addressed to the organization shown in the citation as the corporate author of the document.

## PUBLIC COLLECTIONS OF NASA DOCUMENTS

**DOMESTIC:** NASA and NASA-sponsored documents and a large number of aerospace publications are available to the public for reference purposes at the library maintained by the American Institute of Aeronautics and Astronautics, Technical Information Service, 555 West 57th Street, 12th Floor, New York, NY 10019.

**EUROPEAN:** An extensive collection of NASA and NASA-sponsored publications is maintianed by the British Library Lending Divison, Boston Spa, Wetherby, Yorkshire, England, for public access. The British Library Lending Division also has available many of the non-NASA publications cited in *STAR*.

European requesters may purchase facsimile copy or microfiche of NASA and NASA-sponsored documents, those identified by both the symbols # and * from ESA—Information Retrieval Service, European Space Agency, 8-10 rue Mario-Nikis, 75738 Paris CEDEX 15, France.

**FEDERAL DEPOSITORY LIBRARIES:** To provide the general public with greater access to U.S. Government publications, Congress established the Federal Depository Library Program under the Government Printing Office (GPO), with 51 regional depositories responsible for permanent retention of material, inter-library loan, and reference services. (These libraries are not sales outlets.) At least one copy of nearly every NASA and NASA-sponsored publication, either in printed or microfiche format, is received and retained by the 51 regional depositories. A list of the regional GPO libraries, appears on page A-8. A local library can contact a regional depository library to help locate specific reports, or direct contact may be made by an individual.

## SUBMITTING DOCUMENTS

All users of this abstract service are urged to forward reports to be considered for announcement in *STAR*. This will aid NASA in its efforts to provide the fullest possible coverage of all scientific and technical publications that might support aeronautics and space research and development. If you have prepared relevant reports (other than those you will transmit to NASA, DOD, or DOE through the usual contract- or grant-reporting channels), please send them for consideration to the NASA Scientific and Technical Information Facility, P.O. Box 8757, BWI Airport, MD 21240.

Reprints of journal articles, book chapters, and conference papers are also welcome. These will be considered for announcement in *STAR*'s companion journal, *IAA*.

You may specify a particular source to be included in a report announcement if you wish; otherwise the report will be placed on a public sale at the National Technical Information Service. Copyrighted publications will be announced but not distributed or sold.

## PURCHASE OF *STAR*

*STAR* is publicly available on annual subscription from the Superintendent of Documents, U.S. Government Printing Office, Washington, DC 20402.

*STAR* is available to registered users on annual subscription from the NASA Scientific and Technical Information Facility, ATTN: Registration Services, P.O. Box 8757, BWI Airport, MD 21240.

Microfiche of the abstract sections of *STAR* are available, on annual subscription only, from NTIS as PB91-911300, Attn: Subscriptions, 5285 Port Royal Road, Springfield, VA 22161. Annual subscription rates are $85.00 North America; $170.00 foreign. Abstract sections for previous years retroactive to 1964 are available at the current rates.

# ADDRESSES OF ORGANIZATIONS

American Institute of Aeronautics and Astronautics
Technical Information Service
555 West 57th Street, 12th Floor
New York, New York 10019

British Library Lending Division,
Boston Spa, Wetherby, Yorkshire,
England

Commissioner of Patents and Trademarks
U.S. Patent and Trademark Office
Washington, DC 20231

Department of Energy
Technical Information Center
P.O. Box 62
Oak Ridge, Tennessee 37830

European Space Agency-Information Retrieval Service
ESRIN
Via Galileo Galilei
00044 Frascati (Rome) Italy

Engineering Sciences Data Unit International
P.O. Box 1633
Manassas, Virginia 22110

Engineering Sciences Data Unit International, Ltd.
251-259 Regent Street
London, W1R 7AD, England

Fachinformationszentrum Energie, Physik, Mathematik
GMBH
7514 Eggenstein Leopoldshafen
Federal Republic of Germany

Her Majesty's Stationery Office
P.O. Box 569, S.E. 1
London, England

NASA Scientific and Technical Information Facility
P.O. Box 8757
BWI Airport, Maryland 21240

National Aeronautics and Space Administration
Scientific and Technical Information Division (NTT)
Washington, DC 20546

National Technical Information Service
5285 Port Royal Road
Springfield, Virginia 22161

Pendragon House, Inc.
899 Broadway Avenue
Redwood City, California 94063

Superintendent of Documents
U.S. Government Printing Office
Washington, DC 20402

University Microfilms
A Xerox Company
300 North Zeeb Road
Ann Arbor, Michigan 48106

University Microfilms, Ltd.
Tylers Green
London, England

U.S. Geological Survey Library National Center
MS 950
12201 Sunrise Valley Drive
Reston, Virginia 22092

U.S. Geological Survey Library
2255 North Gemini Drive
Flagstaff, Arizona 86001

U.S. Geological Survey
345 Middlefield Road
Menlo Park, California 94025

U.S. Geological Survey Library
Box 25046
Denver Federal Center, MS914
Denver, Colorado 80225

# NTIS PRICE SCHEDULES

(Effective January 1, 1991)

## Schedule A
## STANDARD PRICE DOCUMENTS AND MICROFICHE**

| PRICE CODE | NORTH AMERICAN PRICE | FOREIGN PRICE |
|---|---|---|
| A01 | $ 8.00 | $ 16.00 |
| A02 | 11.00 | 22.00 |
| A03 | 15.00 | 30.00 |
| A04-A05 | 17.00 | 34.00 |
| A06-A09 | 23.00 | 46.00 |
| A10-A13 | 31.00 | 62.00 |
| A14-A17 | 39.00 | 78.00 |
| A18-A21 | 45.00 | 90.00 |
| A22-A25 | 53.00 | 106.00 |
| A99 | * | * |
| N01 | 60.00 | 120.00 |
| N02 | 59.00 | 118.00 |
| N03 | 20.00 | 40.00 |

## Schedule E
## EXCEPTION PRICE DOCUMENTS AND MICROFICHE**

| PRICE CODE | NORTH AMERICAN PRICE | FOREIGN PRICE |
|---|---|---|
| E01 | $10.00 | $ 20.00 |
| E02 | 12.00 | 24.00 |
| E03 | 14.00 | 28.00 |
| E04 | 16.50 | 33.00 |
| E05 | 18.50 | 37.00 |
| E06 | 21.50 | 43.00 |
| E07 | 24.00 | 48.00 |
| E08 | 27.00 | 54.00 |
| E09 | 29.50 | 59.00 |
| E10 | 32.50 | 65.00 |
| E11 | 35.00 | 70.00 |
| E12 | 38.50 | 77.00 |
| E13 | 41.00 | 82.00 |
| E14 | 45.00 | 90.00 |
| E15 | 48.50 | 97.00 |
| E16 | 53.00 | 106.00 |
| E17 | 57.50 | 115.00 |
| E18 | 62.00 | 124.00 |
| E19 | 69.00 | 138.00 |
| E20 | 80.00 | 160.00 |
| E99 | * | * |

* Contact NTIS for price quote.

** Effective January 1, 1991, the microfiche copy of any new document entering the NTIS collection will be priced the same as the paper copy of the document.

## IMPORTANT NOTICE

NTIS Shipping and Handling Charges

U.S., Canada, Mexico — ADD $3.00 per TOTAL ORDER

All Other Countries — ADD $4.00 per TOTAL ORDER

Exceptions — Does NOT apply to:

ORDERS REQUESTING NTIS RUSH HANDLING
ORDERS FOR SUBSCRIPTION OR STANDING ORDER PRODUCTS *ONLY*

NOTE: Each additional delivery address on an order requires a separate shipping and handling charge.

# FEDERAL REGIONAL DEPOSITORY LIBRARIES

### ALABAMA

**AUBURN UNIV. AT MONTGOMERY LIBRARY**
Documents Department
Montgomery, AL 36193
(205) 279-9110 ext.253

**UNIV. OF ALABAMA LIBRARY**
Reference Department/Documents
Box S
Tuscaloosa, AL 35486
(205) 348-6046

### ARIZONA

**DEPT. OF LIBRARY, ARCHIVES, AND PUBLIC RECORDS**
Third Floor State Capitol
1700 West Washington
Phoenix, AZ 85007
(602) 255-4121

### ARKANSAS

**ARKANSAS STATE LIBRARY**
Documents Service Section
One Capitol Mall
Little Rock, AR 72201
(501) 371-2090

### CALIFORNIA

**CALIFORNIA STATE LIBRARY**
Govt. Publications Section
914 Capitol Mall
Sacramento, CA 95814
(916) 322-4572

### COLORADO

**UNIV. OF COLORADO**
**Norlin Library**
Government Publications Division
Campus Box 184
Boulder, CO 80309
(303) 492-8834

**DENVER PUBLIC LIBRARY**
Govt. Pub. Department
1357 Broadway
Denver, CO 80203
(303) 571-2346

### CONNECTICUT

**CONNECTICUT STATE LIBRARY**
231 Capitol Avenue
Hartford, CT 06106
(203) 566-4971

### FLORIDA

**UNIV. OF FLORIDA LIBRARIES**
Documents Department
Library West
Gainesville, FL 32611
(904) 392-0367

### GEORGIA

**UNIV. OF GEORGIA LIBRARIES**
Government Documents Dept.
Athens, GA 30602
(404) 542-8949

### HAWAII

**UNIV. OF HAWAII**
Hamilton Library
Government Documents Collection
2550 The Mall
Honolulu, HI 96822
(808) 948-8230

### IDAHO

**UNIV. OF IDAHO LIBRARY**
Documents Section
Moscow, ID 83843
(208) 885-6344

### ILLINOIS

**ILLINOIS STATE LIBRARY**
Federal Documents
Centennial Building
Springfield, IL 62756
(217) 782-5012

### INDIANA

**INDIANA STATE LIBRARY**
Serials Section
140 North Senate Avenue
Indianapolis, IN 46204
(317) 232-3686

### IOWA

**UNIV. OF IOWA LIBRARIES**
Government Publications Dept.
Iowa City, IA 52242
(319) 335-5926

### KANSAS

**UNIVERSITY OF KANSAS**
Spencer Research Library
Government Documents
Lawrence, KS 66045
(913) 864-4662

### KENTUCKY

**UNIV. OF KENTUCKY LIBRARIES**
Government Publications/Maps Dept.
Lexington, KY 40506
(606) 257-8400

### LOUISIANA

**LOUISIANA STATE UNIVERSITY**
Middleton Library
Government Documents Dept.
Baton Rouge, LA 70803
(504) 388-2570

**LOUISIANA TECHNICAL UNIV.**
Prescott Memorial Library
Government Documents Dept.
Ruston, LA 71272
(318) 257-4962

### MAINE

**UNIVERSITY OF MAINE**
Raymond H. Fogler Library
Govt. Documents & Microforms Dept.
Orono, ME 04469
(207) 581-1680

### MARYLAND

**UNIVERSITY OF MARYLAND**
McKeldin Library
Documents/Maps Room
College Park, MD 20742
(301) 454-3034

### MASSACHUSETTS

**BOSTON PUBLIC LIBRARY**
Government Documents Dept.
666 Boylston Street
Boston, MA 02117
(617) 536-5400 ext.226

### MICHIGAN

**DETROIT PUBLIC LIBRARY**
5201 Woodward Avenue
Detroit, MI 48202
(313) 833-1409

**LIBRARY OF MICHIGAN**
Government Documents
P.O. Box 30007
735 E. Michigan Avenue
Lansing, MI 48909
(517) 373-1593

### MINNESOTA

**UNIVERSITY OF MINNESOTA**
Wilson Library
Government Publications
309 Nineteenth Avenue South
Minneapolis, MN 55455
(612) 373-7813

### MISSISSIPPI

**UNIV. OF MISSISSIPPI LIB.**
Government Documents Dept.
106 Old Gym Bldg.
University, MS 38677
(601) 232-5857

### MISSOURI

**University of Missouri at Columbia Library**
Government Documents
Columbia, MO 65201
(314) 882-6733

### MONTANA

**UNIV. OF MONTANA**
Mansfield Library
Documents Division
Missoula, MT 59812
(406) 243-6700

### NEBRASKA

**UNIVERSITY OF NEBRASKA - LINCOLN**
Love Memorial Library
Documents Department
Lincoln, NE 68588
(402) 472-2562

### NEVADA

**UNIV. OF NEVADA-RENO LIB.**
Govt. Pub. Department
Reno, NV 89557
(702) 784-6579

### NEW JERSEY

**NEWARK PUBLIC LIBRARY**
U.S. Documents Division
5 Washington Street
P.O. Box 630
Newark, NJ 07101
(201) 733-7812

### NEW MEXICO

**UNIVERSITY OF NEW MEXICO**
General Library
Government Publications/Maps Dept.
Albuquerque, NM 87131
(505) 277-5441

**NEW MEXICO STATE LIBRARY**
325 Don Gaspar Avenue
Santa Fe, NM 87501
(505) 827-3826

### NEW YORK

**NEW YORK STATE LIBRARY**
Documents Sect. Cultural Educ. Ctr.
Empire State Plaza
Albany, NY 12230
(518) 474-5563

### NORTH CAROLINA

**UNIVERSITY OF NORTH CAROLINA AT CHAPEL HILL**
Davis Library 080A
BA/SS Department Documents
Chapel Hill, NC 27514
(919) 962-1151

### NORTH DAKOTA

**NORTH DAKOTA STATE UNIVERSITY LIBRARY**
Government Documents Dept.
Fargo, ND 58105
(701) 237-8352
In cooperation with Univ. of North Dakota, Chester Fritz Library Grand Forks

### OHIO

**STATE LIBRARY OF OHIO**
Documents Section
65 South Front Street
Columbus, OH 43266
(614) 644-7051

### OKLAHOMA

**OKLAHOMA DEPT. OF LIBRARIES**
Government Documents
200 NE 18th Street
Oklahoma City, OK 73105
(405) 521-2502, ext. 252

**OKLAHOMA STATE UNIV. LIB.**
Documents Department
Stillwater, OK 74078
(405) 624-0489

### OREGON

**PORTLAND STATE UNIV.**
Millar Library
934 SW Harrison - P.O. Box 1151
Portland, OR 97207
(503) 229-3673

### PENNSYLVANIA

**STATE LIBRARY OF PENN.**
Government Publications Section
Box 1601
Walnut St. & Commonwealth Ave.
Harrisburg, PA 17105
(717) 787-3752

### SOUTH CAROLINA

**CLEMSON UNIV. COOPER LIB.**
Documents Department
Clemson, SC 29634
(803) 656-5174
In cooperation with Univ. of South Carolina, Thomas Cooper Library, Columbia

### TEXAS

**TEXAS STATE LIBRARY**
Public Services Department
P.O. Box 12927 - 1201 Brazos
Austin, TX 78711
(512) 463-5455

**TEXAS TECH. UNIV. LIBRARY**
Documents Department
Lubbock, TX 79409
(806) 742-2268

### UTAH

**UTAH STATE UNIVERSITY**
Merrill Library & Learning Resources Center, UMC-30
Documents Department
Logan, UT 84322
(801) 750-2682

### VIRGINIA

**UNIVERSITY OF VIRGINIA**
Alderman Library
Government Documents
Charlottesville, VA 22903
(804) 924-3133

### WASHINGTON

**WASHINGTON STATE LIBRARY**
Document Section
Olympia, WA 98504
(206) 753-4027

### WEST VIRGINIA

**WEST VIRGINIA UNIV. LIB.**
Government Documents Section
P.O. Box 6069
Morgantown, WV 26506
(304) 293-3640

### WISCONSIN

**ST. HIST SOC. OF WISCONSIN LIB.**
Government Pub. Section
816 State Street
Madison, WI 53706
(608) 262-2781
In cooperation with Univ. of Wisconsin-Madison, Memorial Library

**MILWAUKEE PUBLIC LIBRARY**
Documents Division
814 West Wisconsin Avenue
Milwaukee, WI 53233
(414) 278-3065

### WYOMING

**WYOMING STATE LIBRARY**
Supreme Court & Library Bldg.
Cheyenne, WY 82002
(307) 777-5919

# TYPICAL CITATION AND ABSTRACT

**NASA SPONSORED**
**ON MICROFICHE**

**ACCESSION NUMBER** → **N91-10047*#** Georgia Inst. of Tech., Atlanta. School of Aerospace ← **CORPORATE SOURCE**
Engineering.
**TITLE** → **NONLINEAR FEEDBACK CONTROL FOR HIGH ALPHA**
**FLIGHT Final Report, Jan. 1989 - Apr. 1990** — **PUBLICATION DATE**
**AUTHOR** → Harold Stalford Apr. 1990 15 p
**CONTRACT OR GRANT** → (Grant NAG1-959) — **AVAILABILITY SOURCE**
**REPORT NUMBERS** → (NASA-CR-186545; NAS 1.26;186545) Avail: NTIS HC/MF A03 ← **PRICE CODE**
**COSATI CODE** → CSCL 01C

Analytical aerodynamic models are derived from a high alpha 6 DOF wind tunnel model. One detail model requires some interpolation between nonlinear functions of alpha. One analytical model requires no interpolation and as such is a completely continuous model. Flight path optimization is conducted on the basic maneuvers: half-loop, 90 degree pitch-up, and level turn. The optimal control analysis uses the derived analytical model in the equations of motion and is based on both moment and force equations. The maximum principle solution for the half-loop is poststall trajectory performing the half-loop in 13.6 seconds. The agility induced by thrust vectoring capability provided a minimum effect on reducing the maneuver time. By means of thrust vectoring control the 90 degrees pitch-up maneuver can be executed in a small place over a short time interval. The agility capability of thrust vectoring is quite beneficial for pitch-up maneuvers. The level turn results are based currently on only outer layer solutions of singular pertrubation. Poststall solutions provide high turn rates but generate higher losses of energy than that of classical sustained solutions.

Author

National Aeronautics and
Space Administration
Code NTT
Washington, D.C.
20546

Official Business
Penalty for Private Use, $300

SPECIAL FOURTH-CLASS RATE
POSTAGE & FEES PAID
NASA
PERMIT No. G27

POSTMASTER: If Undeliverable (Section 158
Postal Manual) Do Not Return